IMPERIAL INSTITUTE
OF
AGRICULTURAL RESEARCH, PUSA.

# PROCEEDINGS

OF THE

# ROYAL SOCIETY OF LONDON

## SERIES A

CONTAINING PAPERS OF A MATHEMATICAL AND
PHYSICAL CHARACTER.

VOL. CXXXIII

LONDON:
PRINTED FOR THE ROYAL SOCIETY AND SOLD B
HARRISON AND SONS, LTD., ST. MARTIN'S LANE,
PRINTERS IN ORDINARY TO HIS MAJESTY.

OCTOBER, 1931.

LONDON:
HARRISON AND SONS, LTD., PRINTERS IN ORDINARY TO HIS MAJESTY,
ST MARTIN'S LANE

# CONTENTS.

## SERIES A. VOL. CXXXIII.

### No. 821.—September 1, 1931.

PAGE

The Diffraction of Electrons by Single Crystals. By G. P. Thomson, F.R.S. (Plates 1 and 2.) ... 1

Refractive Dispersion of Organic Compounds. Part I.—Experimental Methods. Part II.—Cyclohexane. Part III.—Benzene. By T. M. Lowry, F.R.S., and C. B. Allsopp. (Plates 3 and 4.) ... 26

Quantised Singularities in the Electromagnetic Field. By P. A. M. Dirac, F.R.S. ... 60

Estimation of Metals in Solution by Means of their Spark Spectra. By F. Twyman, F.R.S., and C. S. Hitchen. (Plates 5 and 6.) ... 72

On the Definition of Distance in Curved Space, and the Displacement of the Spectral Lines of Distant Sources. By E. T. Whittaker, F.R.S. ... 93

The Cataphoresis of Suspended Particles. Part I.—The Equation of Cataphoresis. By D. C. Henry. Communicated by Professor A. Lapworth, F.R.S. ... 106

Cataphoresis. Part II.—A New Experimental Method, and a Confirmation of Smoluchowski's Equation. By C. G. Sumner and D. C. Henry. Communicated by Professor A. Lapworth, F.R.S. ... 130

Interfacial Tension and Hydrogen-ion Concentration. By R. A. Peters. Communicated by C. N. Hinshelwood, F.R.S. ... 140

The Influence of Hydrogen-ion Concentration upon the Adsorption of Weak Electrolytes by Pure Charcoal.—Part II. By H. J. Phelps. Communicated by C. N. Hinshelwood, F.R.S. ... 155

Discontinuities at the Melting Point of Bismuth. By W. L. Webster. Communicated by P. Kapitza, F.R.S. ... 162

Gaseous Combustion in Electric Discharges. Part VIII.—The Cathodic Combustion of Hydrogen-Oxygen Mixtures. By G. I. Finch and E. A. J. Mahler. Communicated by W. A. Bone, F.R.S. ... 173

The Gyromagnetic Effect for Paramagnetic Substances. II.—Results on Salts of the Iron Group. By W. Sucksmith. Communicated by A. P. Chattock, F.R.S. ... 179

The Refraction and Dispersion of Some Gaseous Compounds. By H. Lowery. Communicated by W. L. Bragg, F.R.S. ... 188

PAGE

The Band Spectrum of Yttrium Oxide (YO) With a Note on the ScO and LaO Systems. By W. L Johnson and R. C. Johnson. Communicated by O. W. Richardson, F.R.S. ...... 207

The Spark Spectra of Tellurium—Te IV and Te VI By K. R Rao. Communicated by A. Fowler, F.R.S. (Plate 7.) ...... 220

The Theory of the Effect of Resonance Levels on Artificial Disintegration. By N. T. Mott. Communicated by P. A. M. Dirac, F R.S. ...... 228

The Stellar Coefficients of Absorption and Opacity. By S. Chandrasekhar. Communicated by P. A M. Dirac, F R S ...... 241

The Quantum Theory of Dispersion in Metallic Conductors—II By R de L. Kronig Communicated by C G. Darwin, F R.S. ...... 255

A Vacuum Spectrometer for Long Wave-Length X-Rays. By R. T. W Bingham Communicated by T. H Laby, F.R S. (Plates 8 and 9.) ...... 260

The Reflection and Diffraction of X-Rays. By T. H. Laby, F.R.S, and R. T. W. Bingham ...... 274

The Reflection of Long X-Rays By C. B. O. Mohr. Communicated by T. H. Laby, F R.S. ...... 292

The Chemical Constants of the Vapours of Hydrogen and of Hydrogen Chloride, and the Entropy Change Accompanying the Reaction $H_2 + Cl_2 \rightleftarrows 2HCl$. By T. E Stern Communicated by R H Fowler, F.R.S . ...... 303

The Properties of Wave Tensors. By Sir Arthur Eddington, F.R.S. ...... 311

The Spectrum of the Hydrogen-Nitrous Oxide Flame. By A. Fowler, F R.S., and J. S Badami. (Plates 10 and 11.) ...... 325

The Nuclear Moment of the Indium Atom. By J. C. McLennan, F.R.S., E. J. Allin and K. E. Hall. (Plate 12.) ...... 333

Interpretation of the Spectra of CaF and SrF. By A. Harvey. Communicated by A Fowler, F R S. (Plates 13-15) ...... 336

## No. 822.—October 1, 1931.

Analysis of the α-Particles Emitted from Thorium C and Actinium C. By Lord Rutherford, F.R.S., C. E. Wynn-Williams and W. B. Lewis ...... 351

The β-Particle Emission of Radium D. By H. O. W. Richardson. Communicated by Lord Rutherford, F.R S. (Plate 16.) ...... 367

The Photoelectric Effect for γ-Rays. By H. R. Hulme. Communicated by P. A. M. Dirac, F.R.S. ...... 381

The Photoelectric Effect in Thin Metallic Films. By W. G. Penney. Communicated by S. Chapman, F.R.S. ...... 407

The Arc Spectrum of Iodine. By S F. Evans. Communicated by T. H. Havelock, F.R.S. ...... 417

PAGE

Absorption Spectra of the Alkyl Halides Energies of the C-I and C-Br Bonds. By T. Iredale and A. G Mills. Communicated by F D. Donnan, F.R S . . ..... 430

A Revision of the Atomic Weight of Thallium. By H. V. A. Briscoe, S Kikuchi and J B. Peel. Communicated by H. B. Baker, F.R.S. ...... ...... .. .......... .... 440

The Theory of Electronic Semi-Conductors. By A. H. Wilson. Communicated by P. A. M. Dirac, F.R S. ........ .. ............. .... ... . . .. .. ............ 458

The Specific Heats of Air, Oxygen, Nitrogen from 20° C. to 370° C By P. S. H. Henry Communicated by E. R. Rideal, F R S. . .......... ........... 492

The Sorption of Hydrogen on Copper Part I.—Adsorption and the Heat of Adsorption. By A. F H. Ward. Communicated by E. K. Rideal, F.R S ..... 506

The Sorption of Hydrogen on Copper. Part II.—The Rate of Solution By A F. H. Ward. Communicated by E K Rideal, F.R.S. . . . . . ... ..... .. .. . ..... 522

An X-Ray Analysis of the Structure of Hexachlorobenzene, using the Fourier Method. By K. Lonsdale. Communicated by Sir William Bragg, F.R.S. .... .. .. .... 536

Interferometric Measurements in the Spectrum of the Iron Arc in Air in the Region λ 3100-λ 3500. By C V Jackson Communicated by A Fowler, F.R.S .. 553

Some Investigations on the Deformation and Breaking of Water Drops in Strong Electric Fields. By W. A. Macky Communicated by C. T R. Wilson, F.R.S. (Plates 17-21.) .... ....... .. ....... ....... ... ... . ... .... .... ....... ..... 565

Studies in Membrane Behaviour Part I.—Equilibrium Conditions with Gelatine Membranes in Acetate Buffer Solutions By W L Francis. Communicated by E. K. Rideal, F.R S ....... ... .... . .. ......... ......... ................ 587

On the Value of the Cosmical Constant By Sir Arthur Eddington, F R.S............. 605

The Diffraction of Electrons in Gases. By F L Arnot. Communicated by J. Chadwick, F.R.S. ....... ...... .... ... ...... . ........ ........... .. ............... 615

✓ The Elastic Scattering of Slow Electrons in Gases.—II. By E C. Bullard and H. S. W. Massey. Communicated by Lord Rutherford, F.R.S. ..... .. ........... 637

Interpretation of Hyperfine Structure —Discussion of H.F.S. in Tl II. Relative $g$ (I) factors of Tl, Bi and Pb (207), and Nuclear Structure. By Professor J. C. McLennan, F.R.S., A. B. McLay, and M F Crawford.... ........................... 652

The Significance of the Differences between the Dipole Moments of Saturated and Unsaturated Substances. By L. E. Sutton. Communicated by R. Robinson, F.R.S. .............................. . ............................................ 668

A Simple Method of Measuring Surface Tension. By J. H. Gaddum. (Abstract.) Communicated by H. H. Dale, Sec. R.S. ............................................ 695

## OBITUARY NOTICE.

Herbert Hall Turner (with portrait) ............................................... i

Index ................................................................................ xi

PROCEEDINGS OF
THE ROYAL SOCIETY.

*Section A.—Mathematical and Physical Sciences.*

# *The Diffraction of Electrons by Single Crystals.*

By G. P. Thomson, M.A., F.R.S., Professor of Physics in the University of London.

(Received May 26, 1931.)

[Plates 1, 2.]

## *The Diffraction of Electrons by Single Crystals.*

1. The diffraction of electron waves has been observed both with single crystals and with polycrystalline aggregates. So far most of the work with single crystals has been done with slow electrons of a few hundred volts energy. While the results are in general agreement with wave mechanics, they differ considerably from the predictions of the simple theory, even when the latter is extended to include a consideration of the inner potential of the crystal. Part of the discrepancy is caused by undue simplification of the theory, and better results have been got with the more elaborate theory of Morse,* but there are a number of cases in which beams corresponding to half order spectra and reflection by "forbidden" crystal planes have been recorded,† and for these the present theory is quite unable to account.

Experiments with fast electrons on polycrystalline aggregates have shown results in full agreement with the simple theory, and it is hoped that electron diffraction will become a valuable method for the study of surface films.

---

* 'Phys. Rev.,' vol. 35, p. 1310 (1930).

† v. Laue and Rupp, 'Ann. Physik,' vol. 4, p. 1097 (1930); Farnsworth, 'Phys. Rev.,' vol. 34, p. 679 (1929), and vol. 35, p. 1131 (1930).

Clearly, however, this cannot be done satisfactorily as long as there is any doubt of the ability of the existing theory to explain the diffraction by known structures. It is therefore of importance to see whether any abnormalities exist for single crystals with fast electrons. So far the only work in this connection is that of Kikuchi and others on mica, that of Niskikawa and Kikuchi on calcite, and some work by Emslie at Aberdeen on galena and calcite.* Kikuchi's work shows complete agreement with theory, but has unusual features on account of the large spacing of mica across the cleavage face. The work on calcite is complicated by charging up of the crystal, and galena, as the present author has found,† changes under the influence of the rays, so that it is difficult to draw precise conclusions. No metals have been investigated. The present work has, therefore, been undertaken. It consists of a detailed investigation of the diffraction of electrons of from 30,000 to 50,000 volts by single crystals of rocksalt, copper and silver.

## *Method.*

2. The apparatus used was described in the 'Proceedings of the Royal Society.'‡ The principle is shown diagrammatically in fig. 1. A narrow

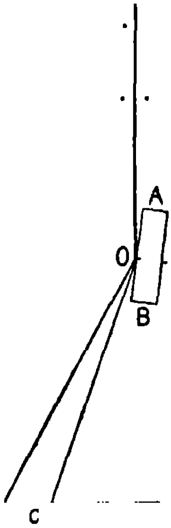

FIG. 1.

---

* Kikuchi, 'Proc. Imp. Acad. Jap.,' vol. 4, pp. 271, 275, 354, 471 (1928) and 'Jap. J. Phys.,' vol. 5, p. 83 (1928); Nishikawa and Kikuchi, 'Nature,' vol. 122, p. 726 (1928); 'Proc. Imp Acad. Jap.,' vol. 4, p. 475 (1928); Emslie, 'Nature,' p. 977 (1929).

† "Wave Mechanics of Free Electrons," McGraw Hill, p. 103.

‡ Thomson and Frazer, 'Proc. Roy Soc.,' A, vol. 128, p. 641 (1930).

beam of cathode rays is incident on the face AB of the crystal. Diffracted beams strike a willemite screen at C and produce visible fluorescence. The crystal can be rotated about an axis perpendicular to the plane of the diagram (change of incidence), and about ON the normal to the free surface (change of azimuth). It can also be moved bodily in a direction nearly parallel to ON. These movements can be made *in vacuo* with the electron beam in action. To obtain a permanent record a photographic plate (Paget process) is lowered in front of C and the rays record themselves directly by their impact on it. The exposures were of the order of 15 seconds.

### *Experiments on Copper and Silver.*

3. These have face-centred cubic lattices. The cube side $a = 3 \cdot 61$ Å. for copper and $4 \cdot 079$ for silver. I am indebted to Sir Harold Carpenter for the single crystal of copper. This was a rod about 10 cm. long and 0·6 cm. diameter In order to get a surface corresponding to a plane of simple indices it was necessary to find the directions of the axes and then cut the crystal. The first was done by the method of optical reflection as described by Bridgman.* The crystal was then cut with a fine saw, roughly to the required face, a piece mounted in a brass holder with plaster of Paris, and the face etched. The etched face was set approximately perpendicular to the axis of a lathe, the crystal being held in the toolholder so that it could be rotated through a small angle A beam of light was reflected along the axis of the lathe by a small mirror on the axis, and the reflection from the etched surface observed by an eye near the lathe axis. When the etched surface was slightly turned spots of light flashed out on it due to reflection from the crystal facets, and the crystal was clamped in position when the flashes were brightest. This makes the facets perpendicular to the lathe axis It was then ground by a wheel rotated in the lathe to give a surface perpendicular to the axis of the latter.† It is sometimes difficult to pick out the reflection from the facets against the background of diffuse reflection from the rest of the crystal surface, and the later specimens were prepared by using the electron diffraction itself to determine the direction of the axes. In this method, after the crystal had been cut approximately to the right face, it was etched and tested in the apparatus. From the patterns obtained with two settings differing by 90° in azimuth, the direction of the required face could be calculated. The crystal was then

---

* 'Proc. Amer. Acad. Sci.,' vol. 60, p. 303 (1924).

† Farnsworth, 'Phys. Rev.,' vol. 34, p. 677 (1929).

mounted in the jig shown in fig. 2 (the screws AB being set to give the calculated angle) and ground on a piece of plate glass. It was afterwards etched to remove the broken surface. The etching was sometimes done with ammonium persulphate, sometimes with 50 per cent. nitric acid. The silver crystal was made accidentally by slowly cooling a bead of molten silver. It was cut by the method last described.

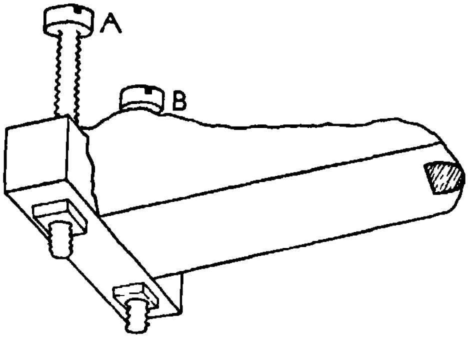

Fig. 2.

4. Both silver and copper gave in general a pattern of diffracted spots. Several orders of the same reflection were often visible at once (see Plate 1). The photographs were taken without rotation of the crystal, and so are equivalent to Laue patterns *with monochromatic rays.* One would, therefore, expect no spots to appear except for certain special settings of the crystal and then only one or two. Actually a pattern of many spots appears over a considerable range of angles. A similar effect was observed by Kikuchi with very thin sheets of mica. The explanation depends on a principle explained in " Wave Mechanics of the Free Electron," p. 72. Quite recently* Bragg and Kirchner have suggested that this is also the explanation of Kikuchi's results. In the present case it is necessary to make an assumption as to the nature of the surface. This must apparently consist of a number of lumps or ridges through which the electrons pass. Consider, for simplicity, a cubical lump with Bragg planes parallel to one pair of faces and rays incident on these at the glancing angle given by $2d \sin \theta = n\lambda$ (fig. 3). There will, of course, be reflection. The centre atoms of each line in the figure form a two-dimensional grating whose spacing in the plane of the paper is $d$. Now for a plane grating with angle of incidence $\phi$, the directions $\psi$ of the diffracted beams are

---

* 'Nature,' vol. 127, p. 738 (1931).

given by $d(\sin\psi + \sin\phi) = n\lambda$, where $\psi$, $\phi$ are positive on the same side of the normal. Hence

$$2d \sin \tfrac{1}{2}(\psi + \phi) . \cos \tfrac{1}{2}(\psi - \phi) = n\lambda.$$

If $\phi$, $\psi$ are small this is approximately $\chi d = n\lambda$, where $\chi$ is the deviation of the ray and is of the order 2°–12°. Thus as far as the centre atoms are concerned a ray will appear at the same deviation within a wide range of angle of incidence. If the incident and diffracted rays do not make equal angles with the Bragg plane, the wavelets from the different atoms in each separate plane will not be exactly in phase, but at small angles and for moderate sized pieces of crystal the discrepancy is not serious.

In fact, the path difference for atoms at the end of a row of length $l$ is

$$l(\cos\phi - \cos\psi) \simeq \tfrac{1}{2}l(\psi^2 - \phi^2).$$

The resultant for the row does not vanish until the path difference between the wavelets from the end atoms is $\lambda$. This occurs when $\psi - \phi = \pm 2d/nl$, so that the width of the diffracted beam from each row of atoms is $4d/nl$. If $l$ is not too large this may be wide enough to include values of $n$ corresponding to several orders, all of which will then appear for the same $\lambda$ and $\phi$. The same expression gives the angle through which the crystal can be rotated without destroying the spot. Notice that on this view "forbidden" planes remain forbidden, and can give rise to no reflected spots. The value of $l$ required to give patterns extending over the range of angles observed, is of the order of $2 \times 10^{-6}$ cm. for 40,000 volt electrons.

It remains to describe and explain the actual arrangement of the spots in the various patterns. Specimens of copper crystals were examined with (100), (111), (331) and (311) faces and one of silver with a (100) face, besides the plates taken to determine the angle of the final grinding in which the exposed surface of the crystal had no simple indices. In all, some 50 plates were measured. The majority show regular patterns having the following characteristics. The exceptions will be dealt with later (p. 12), but (1) applies to them also.

(1) The radial distance of each spot from the origin (undeflected beam) satisfies approximately the relation

$$\chi = \lambda\sqrt{j^2 + k^2 + l^2}\,/a,$$

where $a$ is the cube face, $(jkh)$ are possible Miller indices, and $\lambda$ is the electronic wave-length calculated from the potential of the rays by de Broglie's formula $\lambda = h/mv$.

(2) The spots in the plane of incidence correspond to reflections from the free face of the crystal. After this had been verified in one or two cases, it was used as a method of determining the orientation of the axes with respect to the crystal for the purpose of making the final cutting of the face.

(3) The spots form a portion of a two-dimensional lattice pattern of which the origin is a member

(4) The angles between the lines joining any two spots to the origin is equal to the angle between the planes to which they correspond.

(5) The distance between any two spots is equal to the deviation due to reflection from a Bragg plane whose indices are the difference of those assigned to the two spots.

(6) The indices correspond to planes of a single zone.

(7) The patterns which showed the greatest numbers of spots for (100) and (111) faces were of the forms illustrated in figs. 4–8.

(8) If experiments are made with the crystal turned through various angles about the normal to its face, the sequence of these patterns is that to be expected from the change in azimuth.

(9) The appearance on the screen changed when the angle of incidence of the beam to the free surface of the crystal was altered keeping the azimuth constant. The spots changed in intensity, some disappearing and others appearing, but they did not move, and the nature of the pattern did not change.

Some of the above are geometrically deducible from others. Thus it can be shown that if (1) and (3) are exactly true, the intervals being precisely equal at all places of the lattice pattern, (4) and (5) will inevitably follow. The truth of (7) carries with it that of (1), (3), (4), (5) and (6) and when the pattern is one of these familiar simple forms, it can easily be checked by measurements of a few of the spacings, and the indices assigned. In other cases the best method of assigning indices to the spots is a matter of experience. Thus (1) means little for the distant spots, as values of the indices can always be found to give the right radius within the error of measurements. On the other hand when

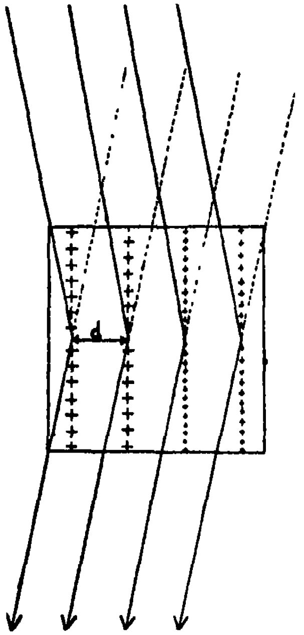

Fig. 3.

the indices have been assigned, the measurements of radial distance give a useful check. Strictly speaking, any two spots determine the zone axis and so the whole pattern, but if two spots are observed it must be possible to assign indices to satisfy (1) and (4) or (5). When the pattern is determined two co-ordinates of any kind will determine if any given spot belongs to it One of these may be the fact that it lies on a line with two other assigned spots.

5 The explanation of these laws and the assignment of indices to the spots is most shortly expressed by the use of Ewald's reciprocal lattice. This is a collection of points such that the vector to each from a common origin coincides in direction with the normal to a net plane, and is inversely proportional to the spacing between adjacent net planes parallel to it. For a face-centred cubic crystal, it is a collection of points whose rectangular cartesians co-ordinates are $(jkl)$ where $j$, $k$, $l$ are all even or all odd and the point corresponds to reflection from the plane of the same Miller indices. The axes in this case are the same as those of the crystal.

If now we have an incident beam parallel to a zone axis, the points of the reciprocal lattice corresponding to the zone planes will all lie on a plane OXY normal to the beam. The lines in which a given set of parallel net planes cut OXY form a two-dimensional grating of the kind considered above, for it can easily be seen that they contain the projections of the lattice points on OXY. The lattice points projected on OXY form in fact a two-dimensional array which can be referred to the lines OX, OY in which any two (non-parallel) planes of the zone cut OXY. The deviation due to such a grating, regarding the lattice points as diffracting centres, is inversely as the spacing of the lines, *i.e.*, of the net planes, and is $\chi = n\lambda/d = \lambda\sqrt{j^2+k^2+l^2}/a$, where $n$ is included in $(jkl)$ which are therefore not usually prime to each other. Let L be the distance of the plate from the crystal, and let all distances on the plate be measured in terms of the unit $L\lambda/a$. Then, since the plate is nearly normal to the rays and all angles are small, the distance of the spot from the origin O′ (position of the undeviated beam) is $\sqrt{(j^2+k^2+l^2)}$.

For each set of indices $(jkl)$ belonging to the zone there is one spot P on the plate, and the line O′P is normal to the planes $(hjk)$. Corresponding to the indices $(jkl)$ there is a point Q of the reciprocal lattice which lies on OXY, if $(jkl)$ belongs to the zone. Further $OQ = \sqrt{(j^2+k^2+l^2)}$ and is normal to the planes $(hjk)$. Thus the pattern formed on the plate by the spots P is identical with that formed on OXY by the points Q or the *complete pattern of diffraction spots, due to the two-dimensional array, formed on the photographic plate is identical with the section of the reciprocal lattice, by a plane normal to* *the incident beam.* We have seen in the previous paragraph that if the lumps of the crystal are not too thick the actual pattern will be identical with that due to the two-dimensional array.

The general character of the patterns is readily seen from the consideration that if any two planes $(j_1k_1l_1)$ represented by $Q_1$ and $(j_2k_2l_2)$, represented by $Q_2$, are both members of the zone then $(aj_1 + bj_2, ak_1 + bk_2, al_1 + bl_2)$ is also a member if $a$ and $b$ are integers. Thus any point of the two-dimensional lattice whose unit translations are $OQ_1$, $OQ_2$ will appear as a spot. Notice that for the face-centred cubic structure of all the substances dealt with in this paper, $(jkl)$ are all even or all odd.

These considerations enable us to determine the indices of any spot in the pattern when those of any other two spots are known, assuming, of course, that the whole pattern is due to a single crystal. The numbers found can be checked by applying the following result. The line joining any two points on the reciprocal lattice is parallel and equal to the radius vector whose indices are the difference of the indices of the first two. This is easily seen for a cubic lattice since the co-ordinates of the reciprocal lattice points are the indices of the plane. It is generally true. It follows that if indices can be assigned to any two spots, the line joining them gives the direction of the normal to a plane of the zone and is inversely proportional to the corresponding spacing.

6. In most cases the most convenient way of measuring up the pattern of spots is to use a special holder for the plate which allows the point of a needle to be brought into coincidence with the spots in succession, the needle being moved by means of two perpendicular slides with scales on each. This is equivalent to measuring rectangular cartesians co-ordinates, and the calculations can be made as follows.

Let $\alpha$, $\beta$, $\gamma$ be the direction cosines of the zone axis to which the incident beam is mostly nearly parallel. Then the spots are given by the points of the reciprocal lattice through which $\alpha x + \beta y + \gamma z = 0$ passes, *i.e.*, we have to find the solutions in integers of this equation. The points will be referred to rectangular axes $O\xi$, $O\eta$ in the plane $\alpha x + \beta y + \gamma z = 0$, $O\xi$ being in the direction of the normal $(pqr)$ to the free surface of the crystal. As explained above, the crystal was cut so as to make this a net plane. The glancing angle of the rays on the crystal surface was always small.

Then the co-ordinates $\xi$, $\eta$, corresponding to a point $(jkl)$ of the reciprocal lattice, are seen to be

$$\xi = pj + qk + rl$$

$$\eta = (q\gamma - r\beta)j + (r\alpha - p\gamma)k + (p\beta - q\alpha)l = \sqrt{j^2 + k^2 + l^2 - \xi^2}$$

by applying the usual formulæ for change of axes.

Clearly if $(\xi_1, \eta_1)$ correspond to $(j_1k_1l_1)$ and $(\xi_2, \eta_2)$ to $(j_2k_2l_2)$ the whole pattern is a lattice built up of $o \rightarrow (\xi_1, \eta_1)$ and $o \rightarrow (\xi_2, \eta_2)$ as unit translations. In particular cases the solutions are generally best found by inspection of the equation $\alpha j + \beta k + \gamma l = 0$, remembering that since the incidence is small $\alpha p + \beta q + \gamma r \simeq 0$.

*Case* 1. $p = q = r = 1/\sqrt{3}$, crystal cut to a (111) plane.

$$\sqrt{3}\xi = j + k + l$$

$$\sqrt{3}\eta = j(\gamma - \beta) + k(\alpha - \gamma) + l(\beta - \alpha)$$

$$= \sqrt{3(j^2 + k^2 + l^2) - (j + k + l)^2} = \sqrt{\Sigma(j - k)^2}$$

Simple solutions of $\alpha j + \beta k + \gamma l = 0$

$$\alpha + \beta + \gamma = 0$$

$$\alpha^2 + \beta^2 + \gamma^2 = 1$$

are $\alpha = 0$, $\beta = \mp 1/\sqrt{2}$, $\gamma = \pm 1/\sqrt{2}$, which with permutations of signs and axes occur six times in all. Also we have $\alpha = \pm 2/\sqrt{6}$, $\beta = \gamma = \mp 1/\sqrt{6}$ again ocurring six times.*

The first gives $k = l$ and $\sqrt{3}\eta = \pm \sqrt{2}(j - k)$. We can take as unit translations $o \rightarrow (\sqrt{3}, 0)$ and $o \rightarrow (1/\sqrt{3}, \sqrt{8/3})$. The second gives $2j - k - l = 0$, $\eta = \pm (k - l)/\sqrt{2}$ with unit translations $o \rightarrow (\sqrt{3}, 0)$ and $o \rightarrow (0, 2\sqrt{2})$. In both cases $\sqrt{3}\xi = j + k + l$.

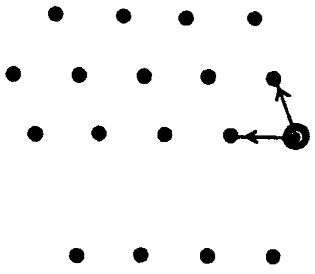

FIG. 4.

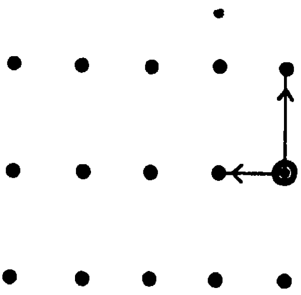

FIG. 5.

*Case* 2. $p = 1$, $q = r = 0$ crystal cut to a (100) face. Here $\alpha = 0$, $\xi = j$, $\eta = \beta l - \gamma k = \sqrt{k^2 + l^2}$ where $kl$ satisfy $\beta k + \gamma l = 0$ and $j$ is any integer. Simple cases are :—

(*a*) $\beta = 0$, $\gamma = \pm 1$, incident ray nearly parallel to a cube axis, giving $l = 0$, $\eta = \pm k$. In this case $j$, $k$ must be even. Unit translations are $o \rightarrow (2, 0)$ and $o \rightarrow (0, 2)$.

---

* There is a difference between the orientation of the whole crystal corresponding to the plus and minus signs in the latter case, but since we are now virtually only dealing with the diffraction by a plane grating it is immaterial from which side the rays come.

(*b*) $\beta = \pm \gamma = 1/\sqrt{2}$, $k = \mp l$, giving $\eta = \sqrt{2}k$. Unit translations are $o \rightarrow (2, 0)$ and $o \rightarrow (1, \sqrt{2})$.

(*c*) $\beta = 1/\sqrt{10}$, $\gamma = \pm 3/\sqrt{10}$, $k + 3l = 0$, $\eta = \sqrt{10}l$. Unit translations $o \rightarrow (2, 0)$ and $o \rightarrow (1, \sqrt{10})$.

Each of the above occurs for four different crystal settings, as is obvious from the fourfold symmetry of the (100) axis.

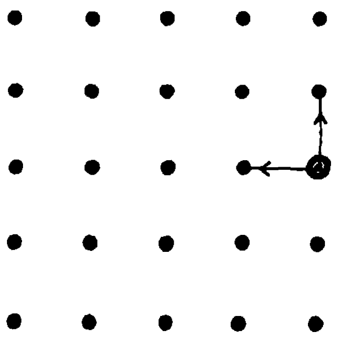

Fig. 6.

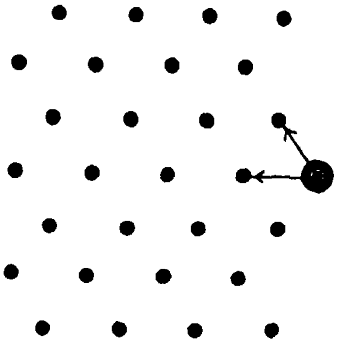

Fig. 7.

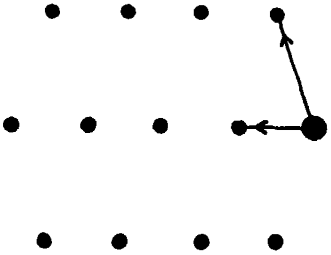

Fig. 8.

The majority of the 50 plates measured were of a regular type such as those shown in Plate 1, figs. 1-5.

While it is easy, after a little practice, to assign the correct indices to each spot of such a pattern by mere inspection, the plates were always carefully measured up, as one object of the research was to detect divergencies from theory. The degree of accuracy possible in these measurements varies greatly with the size of the spots. In some plates the spots were only about 1 mm. in diameter. These could be measured to an error of about $\pm 0{\cdot}1$ and the greatest error was in the determination of the zero which was uncertain to $\pm 0{\cdot}2$ mm. On other plates the spots were drawn out into short lines pointing to the origin, indicating that the electrons were not sufficiently homogeneous in wave-length. In some cases the spots were over-exposed and had spread owing to halation, in others they were rather fuzzy. It is probable that the last cases were due to insufficient resolving power of the crystal, the small blocks (fig. 3) not containing enough atoms in a cross section normal to the electron beam to give good resolutions. Spots about 2 mm. across are common. If 1 mm. of this width is due to the size of the crystal the width of the beam effectively used would be of the order of $0 \cdot 5 \times 10^{-6}$, which is of the same order as that found above for $l$. Thus blocks of crystal of this order of size would account for the observed effects. The measurements of the co-ordinates $\xi$, $\eta$ agreed with the theory within the limits of error of measurements in the majority of cases. In some cases the values of $\xi$ corresponding to successive orders of spots on the central line were not exactly in the ratio of the simple integers. This is almost certainly due to the error in fixing the origin (position of the undeflected beam) for it did not occur consistently.

The only consistent divergence from theory was found in the specimen of copper cut to a (111) face for which the $\eta$ co-ordinates were systematically 2 per cent. larger than would correspond to the $\xi$ values. The specimen in question was the first one prepared, and probably suffered more than the others in the process of cutting and grinding. It seems likely that the lattice had been slightly distorted by this process. After the surface had been etched several times it gave the normal ratios.

The angles between the lines of spots could be measured to about ½° in the best cases. The results were in agreement with the theory to this extent, except in the cases of the (111) specimen, where the discrepancy between $\xi$ and $\eta$ carried with it an error of the order of 1° as a necessary consequence.

When the crystal is rotated in azimuth the patterns repeat. This is easiest seen on the willemite screen where, for example, the square pattern of the (100) face of copper repeated at 90° intervals as nearly as could be measured (2°–3°). The more complicated patterns also recurred, thus, for example, for the (100) face of silver the following sequence was found from the photographs (which show up the more complicated patterns better than the screen) :—

| | | | | | | |
|---|---|---|---|---|---|---|
| Azimuth of crystal | Zero | 42°<br>44° | 73° | 87° | 102° | 133° |
| ($\alpha$, $\beta$, $\gamma$) for incident ray | (001) | (011) | (031) | (010) | (03$\bar{1}$) | (01$\bar{1}$) |
| Calculated angle (to nearest degree) | Zero | 45° | 72° | 90° | 108° | 135° |

In some cases when the setting was not exact, the upper part of the photograph showed a pattern corresponding to one simple azimuth, and the lower part that of another near it.

No attempt was made to check the de Broglie law of wave-length over a wide range of voltages, which only varied between 30,000 and 60,000 volts, but within this range the values of the unit cube found from the pattern size were consistent. The mean of 32 plates gave " $a$ " for copper as $3\cdot59 \times 10^{-8}$ against the X-ray value of $3\cdot61 \times 10^{-8}$, while for silver 10 plates gave $4\cdot05 \times 10^{-8}$ instead of $4\cdot079 \times 10^{-8}$. The relativity correction has been included in these figures. About half the plates (19) differed from the mean by 0·03 or

### *Exceptional Patterns.*

Exceptions to the rules stated on p. 5 were of four kinds :—

(1) Isolated faint spots, these were probably due to small pieces of broken crystal orientated at random. They were most common on the first specimen prepared.

(2) Cases in which portions of two regular patterns were superposed, generally in different parts of the field. This occurred when the setting was not quite right for either pattern, in such a case the angle might be more nearly right for one pattern in part of the field and for another in the rest.

(3) Various spots not forming any simple pattern, but always having some regularity.

(4) A pattern, of which the origin did not form part, often not quite correct in angles and spacing, usually faint and superposed on a normal pattern, occasionally existing alone.

In all cases the radial distances of the spots gave possible indices without the use of "forbidden" combinations or half orders. The third case occurred most often when the crystal was cut to a face other than (111) or (100), *e.g.*, (331). In such a case the possible true patterns have their spots scattered sparsely, but, on the other hand, there are a number of points of the reciprocal lattice which lie *near* a plane passing through the face normal. All these cases were carefully analysed in the hope of finding some abnormality which the theory could not explain, but none was found. The general method was to assign indices to the spots, using their radial distances and their relative positions. In most cases several lay on a line, often equally spaced or nearly so ; the difference of indices between adjacent spots is then constant. Also the angles between the lines joining two pairs of spots is, at least nearly, that between the planes denoted by the difference of indices of the members of a pair. After assigning indices the test is to see if a plane can be drawn through the reciprocal lattice such that the points corresponding to the spots all lie within a small distance of it. The ideal method would be to use least squares. It is near enough in practice to take the plane through two spots near the centre of the group.

To take a particular case, illustrated in Plate 1, fig. 6. The face was approximately (331), and there is a faint spot 1*a* on the centre line which agrees with this. The nearest bright spot 1 corresponds to $\sqrt{(j^2 + k^2 + l^2)} = \sqrt{11}$. The other five gave distances in proportion to $\sqrt{40 \cdot 8}$, $\sqrt{55}$, $\sqrt{83 \cdot 5}$, $\sqrt{116}$, $\sqrt{146}$. These numbers are too large to be sure of to a few units, so we take the differences (1–3) and (1–2) which give $\sqrt{28}$ and $\sqrt{11}$ The nearest possible indices to 40·8 are $6^2 + 2^2 + 0^2$, to 28, $5^2 + 1^2 + 1^2$ or $3^2 + 3^2 + 3^2$, and for 11 we have $3^2 + 1^2 + 1^2$. We assign (311) to spot 1 so we must permute the indices or change signs. A possible arrangement is to take (1–3) as (151) and (1–2) as $(3\bar{1}1)$. The angle between these is $93\frac{1}{3}°$, the measured value is 93° which checks. The indices of spots 2, 3 are (602) or $\sqrt{40}$ and (462) or $\sqrt{56}$ in reasonable agreement with measurement. The distance (3–5) is again $\sqrt{11}$ and (5–6) = (1–2). We assign accordingly (884) or $\sqrt{144}$ to 6 and (593) or $\sqrt{115}$ to 5 in reasonable agreement with the measured radial distances The angle between (5–3) and (3–4) should then be that between (131) and $(3\bar{1}1)$, *i.e.*, $\cos^{-1}(1/11) = 85°$, the measured value is 85°. Now let us see if these points are possible as one pattern, *i.e.*, if they lie near a plane. The plane through (462) and (753) has direction cosines proportional to $(4, 1, \overline{11})$. The angular distance between this plane and the radii vectors to the points of the reciprocal lattice, corresponding to the indices we have taken for the other spots, is never more than about 3°, which is well within the tolerance observed in the regular patterns.

Several cases were observed of a pattern resembling the main pattern of a regular plane but displaced so that no simple line passed through the origin and generally slightly distorted. When superposed, as it sometimes is, on a similar true pattern, it looks at first sight like a halving of the regular pattern. This, however, is not so. The spots all obey the law of radial distances and correspond to possible indices, but the angles are wrong and the corresponding points of the reciprocal lattice do not lie on a plane. As before, however, a plane can be drawn through two which *nearly* contains the others. The projection on this plane causes a distortion of the angles between the lines of spots. The divergence of the lattice points from the plane is sometimes greater than that given in the above example, reaching 11° in the worst case, but is usually only 4° or 5°. In such cases this pseudo-pattern contains all the points of the reciprocal lattice nearest to the assumed plane within the field covered by the main pattern. There is, of course, no essential difference between this case and case 3, except for the frequent presence of the regular pattern in addition, but the pseudo-patterns associated with regular planes are themselves unusually regular. This is to be expected if they are caused by a plane near a very simple one. In those cases when a true pattern and a pseudo-pattern are superposed the presence of the latter is presumably due to a small portion of the crystal having a somewhat different orientation from the rest. In one case it seems likely that a minute piece was slightly curved.

### *Nature of the Surface.*

Microscopic examination of the etched (100) face of copper showed that the most prominent features were a number of square-sided pyramidal pits In other cases ridges appeared. Our explanation requires the surface to consist of a series of lumps, through which the electrons can pass, of the order of $10^{-6}$ in linear dimensions. If the surface has etched into pits, and if on a sub-microscopic scale the pits are very close together, the intermediate portions can be regarded as projections and will serve the purpose of our explanation. It seemed of interest to try if the surface after etching could be made smooth, especially as it should be possible* to measure the inner potential of the metal if the electrons passed out from the same surface by which they entered, but this hope was not realised.

### *Electro-deposited Surfaces.*

With this object copper was deposited electrolytically on the etched surface of single crystals of copper with (100) and (111) faces, and one with a face cut at random. The bath contained 10 gm. copper sulphate and 10 gm. sulphuric acid in 50 c.c. of water. The current density was low, about 4 milliamps. per square centimetre for 1 hour, but as the surface was irregular in shape this could only be estimated roughly. Experiments with X-rays† have shown that in some cases copper when deposited from solution continues the crystal structure of the original surface. The results showed that :—

(1) The spacing of part at least of the added substance is larger than that of normal copper but the structure is roughly similar.

---

* "Wave Mechanics of Free Electrons," p. 95.

† Wood, 'Proc. Phys. Soc.,' vol. 43, p. 138 (1931).

(2) The deposited substance generally, but not always, follows the orientation of the original crystal.

(3) Certain spots occurred which would correspond to "forbidden" planes of copper.

The first is shown best in the photograph of Plate 2, fig. 1. Here are two sets of points corresponding to similar structures but of different scale. One is the same as the original copper, which perhaps shows through the added layer in some places, the other is a structure of larger spacing.

The spacing of the latter structure was about $4{\cdot}5 \times 10^{-8}$. Both sets of points showed a discrepancy between the $\xi$ and $\eta$ values, the latter being disproportionately large, especially in the case of the new structure. It is difficult to say if much importance is to be attached to this. The spots are unusually diffuse, they are not very exactly arranged, and in some cases appear double. Probably the portions of crystal causing them are small, giving poor resolving power, and not quite exactly aligned with the underlying structure or with each other. The structure causing the new spots, for which the effect is most marked, may not be strictly cubic but stretched along the normal to the surface.

The forbidden spots may be seen faintly on the plate at half the distance up and down of the main spots. They correspond to planes (120), (231) and (342), but since the structure from its large spacing is certainly not normal copper their appearance is no contradiction of the theory. As it seemed possible that the new structure was due to hydrogen absorbed by the copper, I tried omitting the sulphuric acid from the electrolyte. The same spacing still occurred, however, though the spots were less good and the surface had a purple tinge. Heating *in vacuo* to a very dull red turned the pattern to rings, some of which corresponded to $Cu_2O$. It is possible that the deposited copper had reacted chemically with the electrolyte while it was being washed and dried. If so, the normal structure may be due to part of the deposit which had remained unchanged, and not to the original crystal showing through.

When the (100) surface was used the patterns were less extensive, but in one or two cases definitely of the (111) form with the large spacing. The spots on the $\xi$ axis, which were always present, were in the same positions as before, corresponding to the (111) plane of the new structure. In addition one or two strong spots corresponding to the original (100) surface could be seen, and one photograph had a (100) pattern of normal spacing. One photograph also, difficult to interpret, suggested a structure of the new spacing, but arranged in conformity with the underlying (100) plane. One may conclude that the deposited copper followed the original structure in some parts of the specimen but not in others, part, at least, of the deposited substance being of the large spacing.

When the copper was deposited on a surface cut at random, the patterns showed spots due to the underlying structure unchanged in position and spacing. In addition there are short arcs due to the deposited substance. Some of these arcs lie roughly on the same radius as a spot, and have a radial distance proportional to that of the spot. They show that at least, in some places, the new structure has followed the orientation of the old but with a bigger spacing. Other arcs show no obvious relation to the underlying structure. They may be, and in some cases almost certainly are, due to planes forbidden in the case of ordinary copper, while in other cases they are due to crystals which do not follow the direction of the axes of the original specimen. The spacing from these plates is about $4 \cdot 4 \times 10^{-8}$. Silver deposited on a (100) surface followed this surface with the normal spacing

### *Lines and Rings.*

In contrast to rocksalt, the metal crystals usually show no sign of the Kikuchi lines. After repeated etching and grinding, however, a few appear, but they are never so strong or so sharply defined as those of rocksalt (see below). They are usually short and generally pass near to, or through, a spot. They are not sufficiently sharp for accurate measurement, but when they pass through a spot are roughly perpendicular to the line joining it to the origin. It seems likely that the double scattering required for the production of the lines does not have room to occur in the small lumps which usually constitute the metal surface. As the etching continues the small pits may be expected to coalesce, leaving the surface in larger lumps which may have been protected by some minute particles of insoluble impurity, *e.g.*, of grinding material. It is noticeable that the photographs which do show lines have generally only a few strong spots, which, however, are still part of a regular pattern. These photographs approximate in appearance to those given by rocksalt.

### *Rings.*

Some of the photographs with silver show faint rings, apparently due to traces of the metal in a disorientated state. One or two of the copper photographs have faint rings not due to the metal, and probably caused by a compound formed on the surface by air or an impurity in the etching liquid.

### *Low Voltage.*

A few photographs were taken at about 7000 volts with an Evershed and Vignolles generator. In one case there was a faint spot.

### *Experiments with Rocksalt.*

Some preliminary experiments were made on rocksalt in 1929.* They showed nothing abnormal and were not continued at the time. Later, a paper by v. Laue and Rupp† described the frequent occurrence of reflections by "forbidden" planes and of half order spectra, from rocksalt and a number of other ionic crystals. Although certain unexplained effects had been observed before,‡ these new divergencies from the theory were much more startling, and the experiments were therefore continued in the summer§ and autumn of last year to see if similar effects could be found with high-speed electrons.

The difficulty with experiments of this kind on an insulator is that the specimen is liable to charge up electrostatically. This happens with rocksalt to a marked extent when the incidence of the rays on the crystal is made very small. At larger angles it is not apparent, but may still be taking place to some extent. I tried several devices to diminish the charging. Bringing a red hot spiral near the surface of the crystal was effective, but also destroyed the diffracted spots, which reappeared faintly on cooling. Bombardment by electrons from a hot filament made the charging worse The charging sometimes seemed to grow worse with time, and it seemed possible that the crystal became a better insulator as it lost moisture in the vacuum. However, making the crystal into a thin plate covering a cell containing water was no very definite improvement. A beam of ultra-violet light focussed on the crystal with a quartz lens had no effect It seemed that the natural blue salt was rather better than the white, and the great majority of the experiments were done with it, but there is a good deal of difference between different specimens, and as I had no numerical measure of the effect, do not attach much weight to the difference between blue and white.

In all cases a cleaved surface (100) was used. There was a considerable fatigue effect in the production of diffraction spots. Specimens cleaved more than 2 or 3 days, and kept in a desiccator in the interval, were inferior to a fresh surface. When in use, the fatigue from any small portion of the surface is very rapid. If the crystal is set so as to give a bright spot on the willemite screen, the spot will become faint in a few minutes. By turning the crystal in azimuth the spot can be brightened again, probably because another part of the surface is used. In this way, observations can be continued for some hours. There appears to be a slight recovery if the crystal is left overnight in the vacuum, but it is by no means complete. Care was therefore taken to withdraw the crystal from the beam when not actually in use. One specimen could be made to give four or five good photographs.

---

* "Wave Mechanics of Free Electrons," p. 161.

† von Laue and Rupp, 'Ann. Physik,' vol. 4, p. 1047 (1930).

‡ Rupp, 'Ann. Physik,' vol. 3, p. 497 (1929).

§ 'Nature,' vol. 126, p. 55 (1930).

### *Diffraction Patterns.*

The structure of rocksalt is similar to that of copper and silver, but the patterns observed were markedly different in appearance. Rocksalt never gave a wide pattern containing a number of spots, only a few being visible at once Alteration of the angle of incidence which had little effect on the metals, changed the intensity of the rocksalt spots markedly and produced a quite visible shift in their position. Further, the photographs with rocksalt show strong Kikuchi lines (see Plate 2). The difference is due to the difference in surface. The rocksalt cleavage is really smooth, except possibly for steps, and the humps we have had to postulate for copper and silver are absent. We get, therefore, conditions like those in X-ray work Each spot occurs, in theory, for only one particular setting of the crystal plane from which the (monochromatic) beam is reflected to form the spot. The shift of the spot as the crystal is moved is due to the limited resolving power of the few surface layers of atoms to which alone the electrons penetrate

### *Centre Line Spots.*

The brightest spots seen on the willemite screen are generally those in the plane of incidence of the rays. These "centre line spots," due to reflection from the cleavage face (100), can be followed for several orders by altering the angle of incidence of the face. They are best investigated by visual measurement on the fluorescent screen. If $x$ is the displacement in centimetres and P the voltage of the rays, the following values were found for different specimens of blue rocksalt .—

| Date | $x\sqrt{P} \times 10^{-1}$. | | | | | |
|---|---|---|---|---|---|---|
| June 13 | 45·3 | 65·4 | 85·0 | 101 | 118 | — |
| ,, 24–25 | 46·4 | 66·1 | 85·0 | 104·5 | 122·5 | 137 |
| ,, 26 | 47·6 | 62·6 | 83·7 | 104 | 121 | 140 |
| December 3–4 | — | 65·8 | 84·1 | 104 | 123 | 146 |
| Mean | 46·4 | 65·0 | 84·6 | 103 | 121 | 141 |
| $n'$ | 5·24 | 7·33 | 9·55 | 11·7 | 13·7 | 15·9 |
| $\Phi$ *volts* | 10·1 | 12·1 | 10·7 | 8·5 | 9·4 | — |

Except in the last column each number is the mean of a large number of readings. In this table $n'$ is the number found by dividing the spacing calculated from the value of $x\sqrt{P}$ into $5 \cdot 63 \times 10^{-8}$, the (100) spacing of NaCl. If the simple theory held, the values should be even integers It will be seen that they tend to approach this law as $n'$ increases. The considerable difference of the three lower orders is well beyond the experimental error. It may be due to a charging of the crystal, but it would require a positive charge. This is not absolutely impossible, since the secondary electrons leaving the crystal might exceed in number those striking it, yet since when charging is strong it is of negative sign, this explanation seems unlikely. Also one would hardly expect the results with different crystals to be as constant as they are, since the conditions varied considerably from time to time. It seems more likely that this is an effect of inner potential, and the potentials required to account for the effect are calculated in the last line from the formula

$$\Phi = \frac{150n^2}{4a^2}$$

where $a$ is the cube side and $n$ is the integral order corresponding to $n'$. The values of $\Phi$ show tolerable agreement when it is remembered that they involve the difference of two quantities, which is small for the higher orders.

### *Depth of Penetration of the Rays.*

Unlike the spots given by the metals, those due to rocksalt show an appreciable change in position as the angle of incidence is altered by turning the crystal. The cleavage surface probably contains a large number of atoms in regular order, and the wavelets from these can only reinforce if the angle of reflection is very exactly equal to that of incidence. There will only be one angle of deviation which exactly satisfies Bragg's law

$$2d \sin \theta = n\lambda \text{ for a given } \lambda.$$

But if either $\lambda$ is variable or some latitude is allowed in Bragg's law there will be a possibility of shift. The first will give a range

$$\pm \delta\theta = \pm \theta \, . \, \delta\lambda/\lambda,$$

where $\pm \delta\lambda$ is the range of wave-length. The second case will arise if, as is probable, the number of layers affecting the electrons is limited by the penetrating power of the latter. If we denote by N the number of layers which would give a range $\pm \delta'\theta$, supposing each layer equally effective, then by the usual argument of resolving power

$$N \,.\, 2d \sin(\theta + \delta'\theta) = (n \,.\, N + 1)\lambda$$

giving $Nd = \lambda/2\delta'\theta$, taking $\cos\theta$ as unity.

We shall call $Nd$ the effective depth of penetration.

By measurements on the willemite screen I found the distance over which the centre of the spot could be moved and still remain just visible. To find $\delta'\theta$ we must subtract $\delta\theta$ from this. If the main beam is deflected magnetically, since the deflection varies as the wave-length, the spot will spread into a short spectrum whose length, for a given average $\lambda$ and given deflection, is equivalent to $\delta\theta$. Since the homogeneity of the rays varies with the potential of discharge, this experiment must be made at the same potential as the measurement of shift, but allowance can easily be made if the deflection is not the same. It was found that at the highest voltages the apparent width of the deflected beam was actually less than that of the undeflected, probably because it was much fainter, as the magnet interfered with the passage of the rays through the diaphragms defining the beam Since the spots were fainter still, this width was taken as representing the geometrical size of the beam and was subtracted from the widths found at the lower voltages to give $\delta\theta$.

The value deduced for the effective depth of penetration is $1 \cdot 2 \times 10^{-7}$ cm. for rays of 35,000 volts. The corrected shifts due to finite resolving power were of the order of 2 mm. The probable error is large, perhaps as much as 25 per cent.; no definite variation with voltage was found. It will, of course, be understood that we are dealing with a very oblique grazing angle (*circa* 4°); the normal penetration would be much larger. Since the faster the rays the smaller the angle, the effective depth would not be expected to vary rapidly with the speed of the rays

### *Photographs*

About 10 successful plates were taken showing spots and Kikuchi lines and carefully measured to look for abnormalities such as "forbidden" planes. The theory of the occurrence of spots in such a case as this is as follows. Let the principal axes of the crystal be taken as axes of co-ordinates, OZ normal to the cleavage face. Let the incident ray OC meet the plate in C (fig. 9) and $(p, q, o)$ be the indices of the zone axis nearest to the projection of OC on OXY. Then if $(jkl)$ is a plane giving rise to a spot it must pass through $(pqo)$ since the angles are small, *i.e.*, $pj + qk = 0$. Take C as the origin of co-ordinates $\xi\eta$, the axis of $\xi$ being parallel to OZ. Let the zone axis $(pqo)$ meet the plate in A, the plane OXY meet it in AB and the plane $(jkl)$ in AD. Draw CN parallel to AD. By the law of reflection, if a spot occurs due to $(jkl)$ it must be at P $(\xi\eta)$, on CN produced such that CN = NP, but it will only occur if Bragg's law is obeyed. The first condition shows that P lies on a circle through C with centre A.

If, as usual, $\xi\eta$ are measured in terms of the unit $a/L\lambda$, then as in case 2, p. 9, we have $\xi = 1$, $\eta = \sqrt{(j^2 + k^2)}$ but $(jkl)$ are integral and $pj + qk = 0$, hence $\xi$ and $\eta q/\sqrt{(p^2 + q^2)}$ must be integral, and we shall expect a spot at each point of the circle for which this is the case.

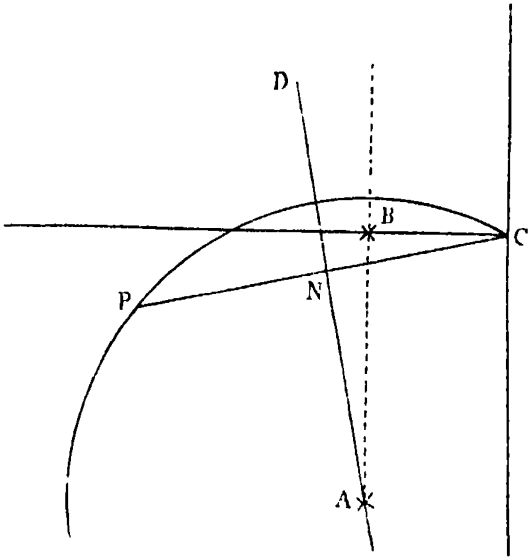

FIG. 9.

In practice the distortion of the crystal allows a little latitude in the fulfilment of the condition. The photographs which show bright spots satisfy these two rules; an example is shown in Plate 2, fig. 4. The co-ordinates of the spots in the above units are (9·90, *o*); (12·1, 3·99); (12·15, 5·98). In the case of spots for which $\xi$ is small, the co-ordinates on most of the plates are less than even integers, showing the refractive index effect in fair agreement with the willemite measurements, but as the setting was not necessarily that to make the spots brightest, the shift considered in the last paragraph prevents them being used to find $\Phi$.

### *Kikuchi Lines.*

The plates all show well-marked lines of the kind studied by Kikuchi for mica, usually showing both white and black lines, though the latter are more prominent. The distance between the white and black lines is equal on Kikuchi's theory to the deflection of a spot reflected from the corresponding planes. This is confirmed here, and the indices so assigned have been checked by measurement of the angles between the lines which should be those between the corresponding planes. The agreement is good to a degree or two, which is about the accuracy of measurement, the lines being often fuzzy. They should theoretically be affected by refraction if this exists. In fact if $\mu^2 - 1 = \Phi/P$ is small, each point $(\xi, \eta)$ of the line is moved towards the axis (if $\Phi$ is positive) to a position $(\xi', \eta)$ where $\xi'^2 = \xi^2 - \Phi L./P$. The effect gets small if the line is far out, as most of the clear ones are.

An effect noticed by Kikuchi* for mica is shown in Plate 2 (fig. 2). Here the incident beam is in a principal plane, and corresponding to this plane we have a broad strip of blackening of width corresponding to the distance between black and white lines, which themselves do not appear. Other black lines near it are also accompanied by similar strips, the white lines being faint or invisible. This effect has not so far been explained.

It shall be noticed that, as Kikuchi's theory shows, and as is observed in the experiment, there may be several black and white lines parallel to a plane and corresponding to different orders. The distance between a pair of black lines is *half* that between the spots of two adjacent orders due to the same plane. At first sight these look rather like half-order spectra or the "forbidden" odd orders of planes such as (100). The vertical lines on Plate 1, fig. 3, are due to this plane.†

*Discussion.*

Two points in the above work need further remarks : the complete absence of forbidden reflections and half orders, and the large positive potential of rocksalt.

The clearest and most certain cases of half-order reflections have been found by Rupp‡ for the (111) face of nickel and the (110) face of iron and molybdenum. These reflections occur only if the metal has been exposed to hydrogen, and can be destroyed again by heating *in vacuo*. They are undoubtedly to be explained as a pentration of the metal lattice by the hydrogen atoms in such a manner as to make alternate planes different, without appreciably altering the spacing. This explanation may also account for various cases of faint reflections by forbidden planes which have been reported, if they are not to be assigned to experimental error. The case of copper is more complicated. We have seen that no such effect occurs at high voltages. Rupp* finds half-order spectra from the (100) face which apparently depend on hydrogen, but even when these are removed the " forbidden " third order spectrum persists. Farnsworth (*loc. cit*), in a very careful and elaborate research, in which a number of azimuths are investigated, finds a large number of beams which cannot be accounted for on the simple theory, even allowing a variable $\Phi$ (7 to 30 volts) † In fact, in spite of the sharpness of the beams, his results bear only a qualitative resemblance to the requirements of the wave theory. Some of the extra beams can be assigned to half-order spectra, which in this case have a rather different significance from those in Rupp's work, since the incidence was always normal and not at an angle equal to that of reflection. In his second paper‡ he finds these beams diminished by very intense heating. Some other beams are apparently connected with the presence of hydrogen. I think that the experiments of p. 14 have a bearing on this work. They show that a structure widely different in spacing from the original copper can yet follow it in orientation. Thus beams will appear in the same azimuths as those due to copper, and will show the same fourfold symmetry round the (100) axis. Copper is easily attacked chemically, and moderate heating, such as Farnsworth used in his original work, may, if the vacuum is not quite perfect, cover the surface with a layer of a compound. Heating strong enough to vaporise the copper would probably remove the layer if the supply of gas was limited. This may also account for Rupp's result In a later paper Boas and Rupp§ find a large number of forbidden planes and half-order spectra for polycrystalline tungsten, using the method of a fixed collector and variable $\lambda$. Here a compound is unlikely ; the higher orders might be accounted for by a different assignment of indices or choice of $\Phi$, but the occurrence of the first order reflections from the (100) and (111) planes in two experiments is a definite challenge to the existing theory.

---

* Kikuchi, 'Phys. Z.,' vol. 31, p. 783 (1930).

† *Note added in proof*.—It is worth notice that when two Kikuchi lines meet at a small angle one curves into the other, which weakens before the point of tangency. The effect is shown in the centre of fig. 3, Plate 2. It seems likely that the explanation requires a complete treatment of the diffraction problem on the lines suggested by Morse.

‡ Rupp, 'Ann. Physik,' vol. 5, p. 453 (1930).

---

* *Loc. cit.*

† I wish to take this opportunity of withdrawing the criticism of Farnsworth's method of calculating $\Phi$ expressed on p. 101 of " Wave Mechanics of a Free Electron " As he has pointed out to me, the calculation is correct if the observed *voltages* are used to find $\Phi$. If the observed *angles* are used the values found are markedly different.

‡ Farnsworth, ' Phys. Rev ,' vol 35, p 1131 (1930).

§ Boas and Rupp, ' Ann. Physik,' vol. 7, p 983 (1930).

In the case of ionic crystals Rupp* reports a number of cases. The complexity of the photographs in Plate 2 shows the great difficulty of interpreting correctly experiments in which electrical observations are made, confined to a single plane of incidence and reflection, such as would correspond to exploring one of these photographs along a single line. It is not even certain in such experiments whether the actual surface is that of the original crystal or polycrystalline, as seems to have been the case for the cleaved and lightly polished surfaces of NaCl, KCl and KBr which gave reflections corresponding to planes other than the cleavage plane. In view of the theoretical importance of the point, it is very desirable that the diffraction by some ionic crystal should be measured over the whole field to see if there is really a fundamental difference between the behaviour of slow and fast electrons.

Rupp† finds —3·5 volts for the inner potential of natural rocksalt, and —2·8 for the same coloured by electron bombardment. He failed to get diffraction for the blue variety. The electrons were of the order of 100 volts energy in all cases. The large value, about 10 volts, found in the present work may be compared with 10·6 volts found by Yamaguti‡ for mica and 22 volts found by Emslie for calcite, who both used high-speed electrons. According to v. Laue's theory§ a cubic crystal should have a definite inner potential and this should be positive for NaCl. It ought to be possible to distinguish between a true inner potential, which involves a discontinuity at the surface, and a charge on the crystal as a whole, which would exert an electric intensity throughout the chamber enclosing it. The latter should produce much the same effect on all diffracted beams, while the former influences the lower orders of spectra much the most. We have seen that the different orders give values of $\Phi$ in fair agreement; this is good evidence that $\Phi$ has a real existence.

I wish to express my sincere thanks to Sir Harold Carpenter, F.R.S., for making the copper crystals for me, and to Mr. J. D. McKay and Mr. T. Riches for their most valuable assistance in working the apparatus.

## *Summary.*

(1) Experiments are described on the diffraction of electrons of 30–50 kilovolts by single crystals of copper and silver. They show a widely extended pattern of diffraction spots.

---

* *Loc. cit.*, p. 21, also 'Z. Physik,' vol. 61, p. 587 (1930).

† *Loc. cit.*

‡ Yamaguti, 'Proc Phys. Math. Soc., Japan,' vol. 12, p. 203 (1930); also quoted by Kikuchi, 'Phys. Z.,' vol. 31, p. 781 (1930).

§ v. Laue, 'Sitzungsberichten der Preuss. Acad. der Wiss.' (1930, II).

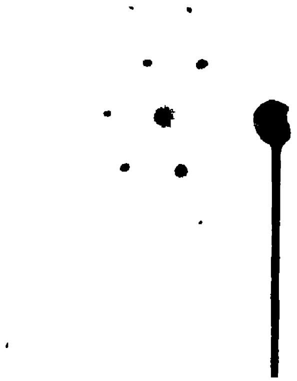

Fig. 1 Copper (111)

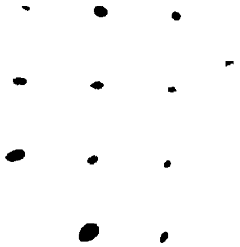

Fig. 2 Copper (100)

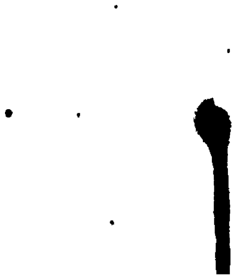

Fig. 3.—Copper (100)

Fig. 4 Copper (111)

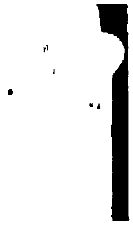

Fig. 5.—Silver (100)

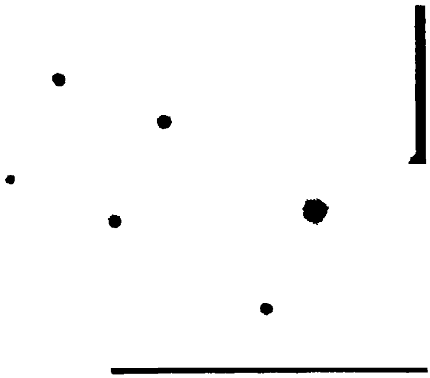

Fig. 6 Copper (331)

*Note.*—The vertical white streaks were produced by withdrawing the crystal and gradually raising the plate. They help to define the origin of co-ordinates.

FIG. 1. Electro-deposited copper

FIG. 2. Rock salt

FIG. 3.—Rock salt

FIG. 4.—Rock salt
(The cross shows the centre of a circle drawn through the spots.)

(2) The usual wave theory can be extended to account for these patterns by supposing that the etched surface of the crystal is composed of a number of lumps of dimensions of the order of $10^{-6}$ cm. These may in some cases be the portions left between adjacent etching pits.

(3) The nature of the surface prevents any effect of inner potential being detected. A detailed agreement exists between theory and experiment, even in the case of the more irregular "exceptional" patterns, the only discrepancy being probably due to a 2 per cent. distortion of the surface lattice in one specimen.

(4) No sign was found of reflection by "forbidden" crystal planes or of half-order spectra.

(5) Some experiments on copper electrolytically deposited on a single crystal of the same showed: (*a*) a strong tendency for the deposit to follow the underlying copper in orientation; (*b*) a marked difference of spacing (4·45 instead of 3·61) in some cases and the appearance of spots not characteristic of the ordinary face-centred structure of copper.

(6) Diffraction spectra are produced from a cleavage face of rocksalt, and also well-marked Kikuchi lines.

(7) The spectra of different orders are not evenly spaced. This seems to indicate an inner potential of about +10 volts for rocksalt.

(8) The depth of penetration of the rays, under the conditions of oblique incidence used, is about $10^{-7}$ cm.

(9) With the exception of (7) the position of the spots and Kikuchi lines is in excellent agreement with the simple theory. In particular, there are no "forbidden" reflections or half-order spectra.

(10) In some cases the Kikuchi lines are represented by blackened strips. The cause of this is not explained.

(11) Explanations are suggested for some of the anomalies observed by other workers.

# *Refractive Dispersion of Organic Compounds. Part* I.—*Experimental Methods. Part* II.—*Cyclohexane. Part* III—*Benzene.*

By T. M. Lowry, F.R.S., and C. B. Allsopp, M.A.

(Received May 28, 1931.)

[Plates 3, 4.]

## Part I.—Experimental Methods.

Eight years ago, in the introduction to a paper by Colonel J. W. Gifford,* attention was directed to the need for investigating the form of the curves of refractive dispersion by similar methods to those which had already been followed successfully in the investigation of curves of rotatory dispersion.† Two attempts were made to develop a programme of research on these lines, by applying (i) to the hydrocarbons, benzene and cyclohexane,* and (ii) to the optically-active base, nicotine,‡ the extremely precise methods of measurement which Gifford had used in determining the refractive indices of glass and quartz. The conditions under which the research was carried out, however, were such that an extensive programme of work became impracticable; moreover, the data then recorded suffered from two limitations, which it was important to overcome before extending the scope of the research indefinitely.

(*a*) The first of these limitations was due to the common difficulty of efficient control of temperature in optical apparatus. Thus, it has already been shown § that a gradient of temperature of 1° between the air and the water-jacket of a Pulfrich refractometer produces a cooling of 0·1° in the liquid under examination. In practice, Gifford's measurements were always made at room temperature and corrected to 15° with the help of observations at higher and lower temperatures. This is a perfectly satisfactory way of dealing with solids, which have only a small coefficient of expansion, or even with water, of which the coefficient of expansion is exceptionally small; but the much larger coefficients of expansion of organic liquids introduce a serious source of error, which makes it almost a waste of time to use the super-excellent methods (involving 36 readings for each wave-length), whereby Gifford measured the refractive indices of quartz, fluorite and amorphous silica with an accuracy that is unlikely to be surpassed during the lifetime of the present generation.

---

* Gifford, 'Proc. Roy. Soc.,' A, vol. 104, pp. 430–437 (1923).

† Lowry, 'Proc Roy Soc.,' A, vol. 81, pp. 472–474 (1908); Lowry and Vernon, 'Proc. Roy. Soc.,' A, vol. 119, pp. 706–709 (1928); Lowry and Dickson, 'Trans. Faraday Soc.,' vol. 10, pp. 96–102 (1914); Lowry and Abram, *ibid.*, pp. 103–106; Lowry, 'Trans. Faraday Soc.,' vol. 26, pp 266–271 (1930); Lowry and Owen, *ibid.*, pp. 371–376; 'Phil. Trans.,' A, vol. 212, pp. 261–297 (1912); vol. 222, pp. 249–308 (1922); vol 226, pp. 391–466 (1927); 'Trans. Chem. Soc,' vol. 103, pp. 1062–1067 (1913), *et seq.*

‡ Gifford and Lowry, 'Proc. Roy. Soc.,' A, vol. 114, pp. 592–593 (1927).

§ Lowry, 'Proc. Optical Convention' (1912), p. 296; compare Lowry and Parker, 'J. Sci. Inst,' vol. 1, p. 16 (1923).

(*b*) The second limitation was due to the thickness of the column which the light must penetrate when measurements are made of the refractive indices of a liquid in a hollow prism, where the edges are not usually available for refraction as they are in a solid prism. Since the most interesting features of refractive dispersion are to be found in and near the region of absorption, it was thought that measurements to three or four decimals in this part of the spectrum would be of greater value than readings to five or six decimals within the zone of complete transparency.

The first of these limitations was overcome as a sequel to including prussic acid amongst the liquids to be investigated. The room containing the instruments had already been provided with a system of heating-coils, controlled automatically by a regulator in the neighbourhood of a fan; but measurements with prussic acid demanded also that an efficient draught should be provided round the instruments. This was done by enclosing each instrument in a wooden case connected to an exhaust. The air of the room (already heated to about 19° by the outside heating coils) was then brought up to 20° by a supplementary heater in the inlet-pipe, controlled by a sensitive regulator inside the case The jacketed parts of the instrument were already provided with a liberal flow of water at 20° from a thermostat in the next room. By bathing the intrument in a current of air at 20° it was then possible to ensure that loss of heat by radiation or convection was reduced to a minimum, so that the temperature of the optical parts did not differ appreciably from the temperature of the circulating water.

The second limitation was removed as a result of the successful development of an interferometric method for measuring the refractive indices of a thin film of liquid enclosed between quartz plates. Readings could then be taken with equal ease in the visible and ultra-violet region, up to the limit of transparency of a film only a few wave-lengths in thickness. The apparatus used for measuring the refractive indices of the film has already been described,* but a new method of using it has now been developed, whereby the standard of accuracy has been increased at least tenfold. Refractive indices in the ultra-violet can therefore now be measured with about the same accuracy as that attained in visual readings with a refractometer.

---

* Lowry and Allsopp, 'Proc. Roy. Soc.,' A, vol. 126, pp 165–169 (1929)

Although eight years have elapsed since a programme of work on refractive indices was first set out, there is still ample scope for such an investigation. Thus, even to-day it is not possible to say which of the three relevant parameters is involved in the phenomenon of optical exaltation, which has been familiar to chemists for so many years Arrangements have been made with Dr. Kon whereby this phenomenon can be investigated with the help of pairs of isomeric compounds containing conjugated and unconjugated double bonds ; but we also propose to investigate the simpler problem of discovering how the structural changes involved in isomerism, polymerism, unsaturation and ring-closure affect the course of the curves of refractive dispersion of organic compounds. In particular, we hope to make a detailed study of the hydrocarbons in which these phenomena are displayed in such bewildering abundance, and to pay particular attention to the refractive dispersion in the neighbourhood of the region of absorption. Finally, since the method now described is even more readily applicable to vapours than to liquids, we propose to study the more volatile compounds in both states of aggregation, using for this purpose a modification of the Rayleigh interferometer, which has recently been described.*

*Apparatus.*—Refractive indices in the visible spectrum from 6707 to 4358 A.U. have been measured by means of a Pulfrich refractometer, the accuracy of which had been increased substantially by engraving a new and finer scale on the divided circle as suggested by Geffcken and Kohner.† The refractometer was calibrated against quartz for not less than 30 wave-lengths For this purpose the refractive indices $n$ of quartz for the ordinary ray for wave-length $\lambda$ were deduced from the equation :

$$n^2 = 3\cdot53445 + \frac{0\cdot008067}{\lambda^2 - 0\cdot0127493} + \frac{0\cdot002682}{\lambda^2 - 0\cdot000974} + \frac{127\cdot2}{\lambda^2 - 108},$$

which was found by Coode Adams‡ to fit the very accurate values given by Gifford. § Guild|| has pointed out that Gifford's values for the refractive index

---

* British patent 22886/30.

† Geffcken and Kohner, 'Z. Phys Chem ,' B, vol. 1, p. 457 (1927)

‡ Coode Adams, 'Proc. Roy. Soc ,' A, vol. 117, p. 209 (1927).

§ Gifford, 'Proc. Roy Soc.,' vol. 70, p. 329 (1902) ; vol. 73, p. 201 (1904) ; A, vol. 84, p. 193 (1910).

|| Guild, 'Phys. Soc. Proc.,' vol. 30, p. 157 (1917-18).

of quartz for the sodium line and for the three hydrogen lines, $H_\alpha$, $H_\beta$, $H_\gamma$, are higher by about 4 units in the fifth decimal than the weighted mean of the values recorded by other observers. These differences may be due to the presence of impurities in some samples of quartz, as is proved by their unequal transparency in the range from 2000 to 1850 Å.U.; but the errors which are thus introduced are too small to affect our readings.

For wave-lengths less than 5000 Å.U. the etalon-refractometer, shown in fig. 1 of the previous paper,* has been used, but with three modifications, as follows · (1) an image of the interference pattern formed in the film of the etalon is now thrown on to the slit of the spectrograph by means of the quartz-fluorspar doublet, $L_2$, placed in the position formerly occupied by the quartz lens, $L_3$, which is no longer used; (2) an auxiliary quartz lens of short focal length has been introduced in front of the lens, $L_1$; (3) the dispersion has been increased about fourfold by using a Hilger E.1 spectrograph in place of the E.3 instrument; but an equal density of distribution of spectral lines has been obtained by using electrodes of tungsten steel instead of iron.

*Light Sources.*—For the Pulfrich refractometer, lines from a mercury lamp, giving a steady and intense illumination of the field, were used as standards. In addition, strong lines in the arc spectra of copper and zinc (brass arc), cadmium and silver (cadmium-silver arc), sodium, lithium and barium, and the $H_\alpha$ and $H_\beta$ lines of hydrogen have been used. The instrument was also calibrated for four helium lines, but these are not suitable for measurements by the method of total reflection, since strong neighbouring lines tend to blurr the edges. Readings can be made easily and accurately in the light blue, green, and yellow regions of the spectrum. In the violet, low intensities reduce contrast in the field, and flickering of the arc becomes troublesome; but accurate values can still be obtained by taking more readings In the middle red, the edges are never quite sharp, owing to continuous radiation from the hot poles of the arc, and the readings are therefore of a lower order of accuracy.

The tungsten-steel arc, which was used as a source of light for the etalon, gives a very bright spectrum, with many sharp lines on a continuous background. In order to facilitate the recognition of the wave-lengths at which coincidences occur, a simple comparator was constructed, by means of which an image of the plate could be viewed through an eye-piece in close juxtaposition to a standard iron-arc spectrum recorded in the same spectrograph. In this way the iron lines could easily be identified, and the tungsten lines could then be recognised by their relationship to the neighbouring lines of the iron arc.

---

* Lowry and Allsopp, *loc. cit.*

*Methods of Measurement.*—In the method first employed, a real image of the etalon was thrown on to the slit of a spectrograph and recorded as a line-spectrum on a photographic plate. Measurements were then made of the number of fringes which could be counted within a section of each spectral line corresponding with the interval between two reference points near the top and bottom of the slit. Since the casual errors arose mainly in attempting to estimate the fraction of a fringe at each end of the line, the sensitiveness of this method was proportional to the number of fringes between the reference-points on the slit. It was therefore directly proportional to the sine of the angle of tilt of the plates, and independent of the distance between them. The accuracy of the method was also limited by systematic errors arising from unequal magnification of the image formed on the slit by a lens-system which had been achromatised for two wave-lengths only. Thus, when the instrument was calibrated with the help of an air-film for a series of lines in the iron-arc spectrum, variations of about 1 per cent. were observed in the values of $n\lambda$, and it was not even certain that these would be reproducible on resetting the instrument.

The method now in use was designed to eliminate both sources of error by basing the measurements of refractive indices on observations of integral numbers of wave-lengths in the total thickness of the film. A line spectrum with a continuous background was obtained with the help of a tungsten-steel arc. The interference fringes are then seen as continuous bands, running obliquely across the spectrum, instead of being recorded only as a discrete pattern on each spectral line. Reference points were provided by a number of fine fibres, stretched across the slit of the spectrograph. These are seen on the negative as a series of parallel, horizontal white lines running right across the spectrum (see Plate 3.)

For certain wave-lengths, a spectral line, a fringe, and the reference line coincide, as is shown in the enlargement (Plate 4). The essence of the present method is the accurate determination of the wave-lengths at which such coincidences occur. With the large dispersion now available, these "coincidence wave-lengths" can be measured within about 2 Å.U. over most of the spectrum. The accuracy of the measurements then depends on the number of wave-lengths included in the *total* thickness of the film instead of in the wedge which is formed by tilting the plates. This thickness can be increased indefinitely by separating the quartz plates, and within certain limits each increase of thickness now results in a corresponding increase in the precision of the readings.

Experiments were made to determine whether any error was introduced as a result of placing the reference points on the slit of the spectrograph, instead of in the film itself. For this purpose, reference lines were scribed with a fine point on the platinum film of the upper etalon plate, and a liquid film of nicotine was used to produce the interference bands. The spectra were then crossed by two sets of lines, namely white lines corresponding to reference points on the slit, and black lines to reference points on the upper plate. The results obtained from the two sets of readings were identical, but the white lines were easier to read. In all subsequent work, therefore, reference points on the slit have been used.

*Calculation of Refractive Indices*.—Let us suppose that a coincidence is found on one of the white reference lines at wave-length $\lambda_0$, where the unknown order of interference is $p$, and that there are further coincidences at shorter wave-lengths $\lambda_1$, $\lambda_2$, etc. These are separated from the first coincidence by definite numbers of fringes, $q_1$, $q_2$, etc., which can be counted directly on the plate. If $n_0$, $n_1$, $n_2$, etc., are the corresponding refractive indices, then

$$\frac{p\lambda_0}{n} = (p + q_1)\frac{\lambda_1}{n} = (p + q_2)\frac{\lambda_2}{n}, \text{ etc.}$$

The unknown order of interference at wave-length $\lambda_0$ can be calculated if the refractive indices are known for *two* of the lines at which coincidences are recorded. Now the photographic observations overlap the visual readings over a range of more than 600 Å.U., *e g.*, from 4358 Å.U. to 5000 Å.U., and this range could be increased by 3000 Å.U. or more* by using panchromatic plates. Since the refractive indices given by the Pulfrich refractometer can be represented by a continuous dispersion-curve, several pairs of coincidences are usually available from which the order of one of the fringes can be determined The order thus determined usually differs from an integer by a small fraction; but, since the order must be integral, this fraction is neglected, and the nearest integer is taken as correct. The principal objection to the previous method, arising from lack of precision in measuring fractions of a fringe-width in the height of the slit, is thus obviated.

When the integral value of $p$ is known for one wave-length, the order of interference at which the other coincidences occur is read off by counting the fringes on the plate, and the corresponding refractive indices are calculated from the preceding formula.

---

* In practice, however, the useful range is limited by the low dispersion given by a quartz spectrograph at the yellow and red end of the spectrum, as will be described later.

The most satisfactory procedure is to start with a very thin film of liquid (compare Plate 4, *e*). The fringes of low order, which are thus obtained, are not very sharp. There is therefore a relatively large possible error in the wave-lengths of the coincidences; but this is more than compensated by other considerations. For instance, a value of 30·1 for the order of interference, $p$, obviously corresponds to an integral value, $p = 30$; but, if the film were ten times as thick, there would be an ambiguity between the alternative values $p = 300$ and $p = 301$. Again, in the case of a thin film, a mistake of a unit in the order produces an obvious discontinuity at the "overlap" between photographic and visual readings, but would not necessarily do so if a thick film had been used.

The refractive indices of the thin film give a preliminary dispersion-curve, which is not usually smooth, but becomes more regular for short wave-lengths, where a higher order of interference gives rise to sharper fringes. A "thick" film (*i e.*, up to ten times as thick), giving sharp and accurately-readable fringes and many more coincidences (compare Plate 4, *d*) is then used to fix the detailed course of the dispersion-curve. Any risk of ambiguity in the order of interference can now be eliminated by the condition that, at least for the short wave-lengths, the new curve must be superposed exactly on that derived from the thin film.

It should be noted that the reflections do not occur at the surface of the etalon plates, since the rays penetrate into the platinum, giving rise to a change of phase on reflection from the metal. This may be expressed as a small fractional increment of $p$, which varies with wave-lengths, and may vary irregularly after the plates have been in use for some time, when the platinum surfaces deteriorate through repeated contact with liquids. The correction has been investigated for nickel films by Buisson and Fabry, and also by Meggers,* and corresponds to an order of 0·01 Å.U. Since the position of a coincidence can certainly not be determined to this degree of accuracy, this source of error has been ignored.

*Range of Application.*—A series of experiments was made in order to find out how far the use of the etalon could be extended in the direction of longer wave-lengths. The order of interference for a thick film of cyclohexane was deduced from refractometer measurements in the range between 4358 and 4600 Å.U. Refractive indices were then calculated from a number of coincidences in the green and red. Up to 5400 Å.U. the values fell on the same smooth curve as the refractive indices deduced from measurements with the refractometer. They also agreed closely with values calculated from a dispersion formula, based upon three refractive indices measured photographically in the violet and ultra-violet regions (see Table II, Part II). Beyond this point, however, the accurate identification of a coincidence became increasingly difficult as the dispersion of the quartz spectrograph decreased and the lines in the iron-tungsten spectrum became less crowded; the accuracy of measurements of the refractive indices therefore fell off rapidly. Better results might perhaps be obtained by using glass prisms of much higher dispersion and a light source richer in strong lines in the yellow and red; but with the methods now in use it was found to be impracticable to extend the measurements with the etalon to longer wave-lengths than those of the green region of the visible spectrum.

---

* 'Bureau of Standards Bulletin,' vol. 12, p. 198 (1915).

In the direction of shorter wave-lengths, when making use of the high dispersion of the E 1 spectrograph, good fringes could be obtained up to 2400 A.U. The fringes tended to disappear, however, before the spectral intensity began to fall off, apparently because, owing to the excessive dispersion in this region of the spectrum, the fringes were spread out over too wide an area to leave a satisfactory record on the photographic plate. This conclusion is supported by the fact that, when using the lower dispersion of the E.3 spectrograph, the corresponding fringes were much more intense.

A similar effect was observed when films of strongly absorbing liquids were used. The fringes again disappeared before the limit of transmission was reached, obviously because the twice-reflected beam was reduced in intensity to an extent which did not permit of a complete interference with the directly-transmitted beam. Weak absorption bands do not present the same difficulty, since we have been able, for instance, to make measurements of the refractive indices of benzene in the region of weak absorption which precedes the principal absorption bands.

The disappearance of the fringes on approaching a strong absorption band is a serious limitation to the usefulness of the interferometer method of measuring refractive indices, when values are wanted for wave-lengths in the region of absorption; but this limitation is not confined to the method now under consideration. Thus, interference methods of the Rayleigh type, which depend on measuring a change of path-difference, would also be vitiated by absorption of one of the interfering beams. Moreover, Guillery,* who used a total reflection method for the same purpose, found that the boundary between transmission and total reflection became indefinite when the region of strong absorption was approached. The only methods which appear to be free from this limitation depend on measuring the refraction produced by a prism of very narrow angle, as used by Feussner,* or by a series of minute parallel prisms, as used by Voellmy†, but these methods are of a lower order of accuracy, and also appear to break down in the region of absorption. The etalon method might, however, be applied to thin films of solutions of strongly absorbing substances in transparent solvents, when the refractive indices in the region of absorption could be deduced in the usual way from the observed refractive indices of the solution.

---

* Guillery, 'Phys Z.,' vol. 31, p. 700 (1930).

*Limits of Error*.—The refractive indices of the glass prism of a Pulfrich refractometer, as deduced by calibration with quartz, lie on a smooth curve within a range of accuracy of about 0·0001. This is also the maximum accuracy which can be obtained when determining the refractive index of a liquid with the help of the same instrument.‡ When, however, a curve of refractive indices is plotted from readings in the ultra-violet, and is made to show a zero error at either end of the visible spectrum, indications are obtained of systematic errors, which may be about three times as great (see Part II, p. 44).

In order to determine the degree of accuracy with which refractive indices can be measured by the etalon-interferometer, the refractive index of a thick film of air was measured over the range of wave-lengths from 2700 to 4383 Å.U., within which the variations from unity are limited to the fifth decimal place. The value of $p$ for $\lambda = 4383$ Å.U. was first determined from three pairs of coincidences, the refractive index at each wave-length being taken as unity.

*Coincidences.*

| $\lambda$ | | $p_{4383}$ |
|---|---|---|
| 3677·629 | $p_{3677} = 205$ | 172 |
| 3236·785 | $p_{3236} = 283$ | |
| 4383·548 | $p_{4383} = 172$ | 172 |
| 2754·032 | $p_{2754} = 274$ | |
| 3887·053 | $p_{3887} = 194$ | 172 |
| 3042·025 | $p_{3042} = 248$ | |

---

* Feussner, 'Z. Physik,' vol. 45, 9.10, pp. 689–716 (1927).

† Voellmy, 'Z. Phys. Chem.,' vol. 127, 5/6, p. 305 (1927); compare Henri, 'Etudes de Photochimie' (1919).

‡ *Cf.* Guild, 'Phys. Soc. Proc.,' vol. 30, p. 157 (1917–18); and Simeon, same volume, following paper.

The mean value of $p\lambda$ for these six wave-lengths was then employed for the calculation of the refractive indices for 36 "coincidence wave-lengths," as set out in Table I. The maximum deviation is $\pm 0{\cdot}0008$; the mean deviation is $\pm 0{\cdot}0003$ and the mean error $-0{\cdot}0001$. These values were obtained with an E 3 spectrograph; with the E.1 spectrograph the accuracy of the readings would be substantially greater.

Table I.—Calibration of the Etalon.

| Wave-length of coincidence * | Order of interference. | Refractive index of air. | Deviation from unity |
|---|---|---|---|
| $\lambda$. | $p$ | $n$. | $(n-1) \times 10^4$. |
| 4383·518 (B) | 172 | 0·9997 | −3 |
| 4307·910 (B) | 175 | 0·9996 | −4 |
| 4233·615 (I) | 178 | 0·9992 | −8 |
| 4143·874 (B) | 182 | 1·0000 | ± |
| 4031·968 (B) | 187 | 0·9997 | −7 |
| 3969·263 (B) | 190 | 1·0000 | ± |
| 3948·779 (B) | 191 | 1·0000 | ± |
| 3927·925 (B) | 192 | 1·0000 | ± |
| 3887·053 (B) | 194 | 1·0000 | ± |
| 3865·527 (I) | 195 | 0·9995 | −5 |
| 3825·886 (B) | 197 | 0·9994 | −6 |
| 3790·094 (B) | 199 | 1·0000 | ± |
| 3732·398 (B) | 202 | 0·9997 | −3 |
| 3677·629 (I) | 205 | 0·9997 | −3 |
| 3608·860 (B) | 209 | 1·0001 | +1 |
| 3556·881 (I) | 212 | 0·9998 | −2 |
| 3541·090 (B) | 213 | 1·0001 | +1 |
| 3476·705 (B) | 217 | 1·0003 | +3 |
| 3427·127 (B) | 220 | 0·9997 | −3 |
| 3413·140 (B) | 221 | 1·0002 | +2 |
| 3305·980 (B) | 228 | 0·9995 | −5 |
| 3265·629 (B) | 231 | 1·0002 | +2 |
| Mn 3236·785 (B) | 233 | 1·0000 | ± |
| 3196·937 (B) | 236 | 1·0004 | +4 |
| 3067·250 (B) | 246 | 1·0005 | +5 |
| 3042·025 (B) | 248 | 1·0003 | +3 |
| 3016·200 (B) | 250 | 0·9998 | −2 |
| 2969·364 (B) | 254 | 1·0001 | +1 |
| 2957·370 (B) | 255 | 0·9999 | −1 |
| 2912·157 (F) | 259 | 1·0001 | +1 |
| 2845·55 (B) | 265 | 0·9998 | −2 |
| 2823·276 (B) | 267 | 0·9995 | −5 |
| 2804·523 (B) | 269 | 1·0003 | +3 |
| 2754·032 (B) | 274 | 1·0006 | +6 |
| 2744·072 (B) | 275 | 1·0006 | +6 |
| 2720·910 (B) | 277 | 0·9994 | −6 |

Mean deviation = 0·003; mean error = − 0·0001.

---

* (I) = International Standard. (F) = Fabry and Buisson, 'C.R.,' vol. 144, p. 1155; 'J. Physique' [IV], vol. 7, p. 169 (1908). (B) = Burns, 'Z. Wiss. Photogr.,' vol. 16, p. 225 (1917).

### *Summary.*

An interference-method is described whereby the refractive indices of a thin film of liquid can be measured to four places of decimals for a range of wave-lengths from about 5000 Å.U up to the limit of transparency of the film in the ultra-violet.

## PART II.—CYCLOHEXANE.

The substances selected for the first measurements of refractive dispersion by the methods described above were identical with those which had already been supplied to Gifford for examination by the prism method, namely cyclohexane and benzene. The purpose of this choice was to make a direct comparison of the old and new methods of measurement, and especially to discover by practical experience how far the extended range of the new methods in the ultra-violet would compensate for its smaller accuracy in the visible region. It was also important to find out whether the new method could be reduced to such a simple form as to make it possible to undertake an extensive programme of work on a number of important series of organic compounds, or whether it would only be suitable for use in a few selected cases. The problems involved in the examination of these two compounds, however, are of quite different natures. Thus, while the values previously recorded for the refractive indices of cyclohexane were found to satisfy a simple dispersion-formula to an extremely high degree of accuracy, the data for benzene indicated a very much more complex dispersion Whilst cyclohexane, therefore, was an ideal substance with which to test the accuracy of the new method, the problem with benzene was rather to investigate whether the data obtained were sufficiently accurate to allow of a complete mathematical analysis of the dispersion-curve.

*Accuracy and Scope of the Measurements.*—The experiments with cyclohexane were carried out primarily in order to standardise the methods of measurement. No trouble was spared, therefore, in repeating the observations, under various conditions and with different materials, until we were satisfied that we had developed the method as far as was practicable at the present stage. As a result, we can assert that refractive indices in the green, blue and ultra-violet regions of the spectrum can be measured with the etalon-interferometer to about the same degree of accuracy as that obtained in measurements with a refractometer in the visible region only. In the region of longer wave-lengths (as has been stated in Part I) the scope of the measurements is limited by practical difficulties arising from the low dispersion of the spectrograph and the scarcity of strong spectrum lines in the red and yellow regions of the spectrum; but the measurements can be extended indefinitely in the region of shorter wave-lengths up to the limit of transparency of the medium. Thus, a single photographic plate, which can be exposed and developed in a few minutes, may provide a permanent record of some hundreds of lines from each of which the refractive index of the medium for the appropriate wave-lengths can be deduced. The time spent in reading the plate and in calculating the refractive indices depends on the number of wave-lengths for which values are wanted, but a hundred coincidences may be identified and recorded in a single day without undue fatigue. In general the total time required for a given number of wave-lengths is approximately the same, whether the measurements are made with a refractometer or with the etalon.

*Materials.*—Two samples of cyclohexane were used for the main series of experiments. The first of these, A, supplied by Professor Timmermans from the *Bureau des etalons physico-chimiques*, at Brussels, had a freezing point of 6·40° C. The other sample, B, was purified in this laboratory, as follows Commercial cyclohexane was shaken with oleum for a total of 32 hours, washed with distilled water and calcium carbonate, dried over lime and over calcium chloride and distilled It was then redistilled in an all-glass apparatus from lime (three times) and freshly fused calcium chloride (three times) until a fraction boiling constantly at 81·4° was obtained. This was then fractionally frozen until the freezing point could not be raised further The product began to freeze at 5·9° C and was completely transparent and free from incipient absorption-bands within the range of the iron arc In spite of a difference of 0·5° in freezing point, its refractive indices in the visible region, as measured with the Pulfrich refractometer, differed from those of sample A only by a few units in the fifth decimal, whereas the admitted range of errors was ten times greater. The readings with the etalon in the ultra-violet were also in good agreement down to 2900 Å.U., after which a steady though small divergence was observed On the other hand, a third sample, also obtained from abroad, which froze at 4·2°, gave refractive indices which were higher by about 0·002 throughout the visible spectrum; it was therefore rejected as being insufficiently pure for the present purpose.

*Experimental Results.*—Table II shows the refractive indices, for 9 wave-lengths in the visible spectrum, of Professor Timmermans' sample of cyclohexane, A, and for 21 wave-lengths from Li 6708 to Hg 4358 of our own sample, B, as measured by means of the Pulfrich refractometer. Although these values are only regarded as accurate to the fourth decimal, the average difference between the two series is actually only +0·00001.

## Table II.—Refractive Indices of Cyclohexane at 20° C.

### First Series: Pulfrich Refractometer.

$$\text{I.}\quad n^2 = 2{\cdot}00519 + \frac{0{\cdot}0098035}{\lambda^2 - 0{\cdot}011923}. \qquad \text{II.}\quad n^2 = 2{\cdot}00723 + \frac{0{\cdot}009264}{\lambda^2 - 0{\cdot}01582}.$$

| λ. | $n$ calculated from I | Sample A. | | Sample B. | | | Difference (A−B) × $10^4$. |
|---|---|---|---|---|---|---|---|
| | | $n$ observed | Difference (O−C) × $10^4$. | $n$ observed | Difference (O − C) × $10^4$ | | |
| | | | | | I | II | |
| Li 6707·86 | $1{\cdot}4239_3$ | $1{\cdot}4239_8$ | +0·5 | $1{\cdot}4239_6$ | +0·3 | −3·2 | +0·2 |
| $H_\alpha$ 6562·85 | $1{\cdot}4242_9$ | $1{\cdot}4242_7$ | −0·2 | $1{\cdot}4242_7$ | −0·2 | −3·6 | ± |
| Cd 6438·47 | $1{\cdot}4246_2$ | | | $1{\cdot}4244_0$ | −2·2 | −5·4 | |
| Zn 6362·34 | $1{\cdot}4248_3$ | | | $1{\cdot}4245_5$ | −2·8 | −6·0 | |
| Li 6103·6 | $1{\cdot}4256_2$ | $1{\cdot}4254_5$ | −1·7 | $1{\cdot}4254_5$ | −1·7 | −4·5 | ± |
| Na 5895·93 | $1{\cdot}4263_2$ | $1{\cdot}4263_6$ | +0·4 | $1{\cdot}4263_6$ | +0·4 | −2·3 | ± |
| Hg 5790·66 | $1{\cdot}4267_1$ | $1{\cdot}4267_8$ | +0·7 | $1{\cdot}4267_5$ | +0·4 | −2·1 | +0·3 |
| Ag 5471·51 | $1{\cdot}4280_4$ | | | $1{\cdot}4282_2$ | +1·8 | −0·3 | |
| Hg 5460·73 | $1{\cdot}4281_4$ | $1{\cdot}4283_4$ | +2·0 | $1{\cdot}4283_0$ | +1·6 | ± | +0·4 |
| Cu 5220·06 | $1{\cdot}4292_7$ | | | $1{\cdot}4295_0$ | +2·3 | +0·5 | |
| Ag 5209·04 | $1{\cdot}4293_5$ | | | $1{\cdot}4295_4$ | +2·1 | +0·4 | |
| Cu 5105·55 | $1{\cdot}4299_0$ | | | $1{\cdot}4302_4$ | +3·4 | +1·8 | |
| Cd 5085·82 | $1{\cdot}4300_1$ | | | $1{\cdot}4302_8$ | +2·7 | +1·1 | |
| $H_\beta$ 4861·33 | $1{\cdot}4313_9$ | $1{\cdot}4317_0$ | +3·1 | $1{\cdot}4317_0$ | +3·1 | +1·8 | ± |
| Zn 4810·53 | $1{\cdot}4317_3$ | | | $1{\cdot}4317_8$ | +0·5 | −0·7 | |
| Cd 4799·91 | $1{\cdot}4318_1$ | | | $1{\cdot}4319_9$ | +1·8 | −1·3 | |
| Zn 4722·16 | $1{\cdot}4323_5$ | | | $1{\cdot}4326_4$ | +2·9 | +1·8 | |
| Cd 4678·15 | $1{\cdot}4326_8$ | | | $1{\cdot}4328_6$ | +1·8 | +0·8 | |
| Li 4603·0 | $1{\cdot}4332_6$ | $1{\cdot}4334_8$ | +2·2 | $1{\cdot}4334_8$ | +2·2 | +1·3 | ± |
| Ba 4554·04 | $1{\cdot}4337_1$ | | | $1{\cdot}4337_2$ | +0·1 | −0·7 | |
| Hg 4358·31 | $1{\cdot}4353_6$ | $1{\cdot}3454_1$ | +0·5 | $1{\cdot}4354_2$ | +0·6 | ± | −0·1 |

Table III shows the refractive indices of sample A for 97 wave-lengths from Fe 5410 to Fe 2452, as deduced from photographic observations with the quartz etalon. Eight films of different thickness were used, as follows:—

$a = 18{\cdot}75\ \mu$, $b = 18{\cdot}55\ \mu$, $c = 18{\cdot}25\ \mu$, $d = 18{\cdot}65\ \mu$,

$e = 5{\cdot}37\ \mu$, $f = 5{\cdot}53\ \mu$, $g = 9{\cdot}87\ \mu$, $h = 10{\cdot}25\ \mu$,

## Table III.—Refractive Indices of Cyclohexane at 20° C. Professor Timmermans' Specimen A.

### Second Series: Photographic Method.

$$\text{I.}\quad n^2 = 2{\cdot}00519 + \frac{0{\cdot}0098035}{\lambda^2 - 0{\cdot}011923}.$$

| Wave-length of coincidence | Film | Refractive index | | Difference (O − C) × $10^4$ |
|---|---|---|---|---|
| | | *n* (observed). | *n* (calculated). | |
| Fe 5410·900 (B) | *b* | 1·4284 | 1·4283 | + 1 |
| W 5204·516 | *a* | 1·4291 | 1·4293 | − 2 |
| Fe 5202·342 (B) | *b* | 1·4294 | 1·4294 | ± |
| W 5015·334 | *a* | 1·4307 | 1·4304 | + 3 |
| Fe 4966·104 (B) | *a* & *b* | 1·4306 | 1·4307 | − 1 |
| Fe 4919·008 (B) | *b* | 1·4311 | 1·4310 | + 1 |
| Fe 4745·804 (B) | *b* | 1·4318 | 1·4322 | − 4 |
| Fe 4707·287 (B) | *b* | 1·4328 | 1·4325 | + 3 |
| W 4680·539 | *h* | 1·4328 | 1·4327 | + 1 |
| Fe 4607·665 (B) | *h* | 1·4333 | 1·4332 | + 1 |
| Fe 4595·368 (B) | *a* | 1·4331 | 1·4334 | ± |
| Fe 4556·128 (B) | *c* | 1·4338 | 1·4336 | + 2 |
| W 4535·065 | *e* | 1·4341 | 1·4338 | + 3 |
| Fe 4469·390 (B) | *h* | 1·4344 | 1·4344 | ± |
| Fe 4442·349 (B) | *c* | 1·4345 | 1·4346 | − 1 |
| Fe 4415·127 (B) | *f* | 1·4349 | 1·4348 | + 1 |
| Fe 4369·777 (B) | *c* | 1·4350 | 1·4353 | − 3 |
| Fe 4367·584 (B) | *b* | 1·4353 | 1·4353 | ± |
| W 4339·463 | *h* | 1·4355 | 1·4355 | ± |
| Fe 4307·910 (B) | *a* | 1·4356 | 1·4358 | − 2 |
| Fe 4299·254 (B) | *b* | 1·4360 | 1·4359 | + 1 |
| Fe 4242·728 (B) | *a* | 1·4365 | 1·4365 | ± |
| Fe 4233·615 (I) | *c*<br>*b* | 1·4367<br>1·4369 | 1·4366 | + 1<br>+ 3 |
| Fe 4210·362 (B) | *a* | 1·4368 | 1·4368 | ± |
| Fe 4147·676 (I) | *a* | 1·4375 | 1·4373 | + 2 |
| W 4102·713 | *h* | 1·4379 | 1·4380 | − 1 |
| W 4074·374 | *c* | 1·4383 | 1·4383 | ± |
| Fe 4070·279 (B) | *e* | 1·4385 | 1·4384 | + 1 |
| Fe 4045·822 (B) | *b* | 1·4385 | 1·4387 | − 2 |
| Fe 4044·617 (B) | *c* & *h* | 1·4385 | 1·4387 | − 2 |
| W 3092·700 | *h* | 1·4391 | 1·4393 | − 2 |
| Fe 3969·263 (B) | *a* & *e* | 1·4394 | 1·4396 | − 2 |
| Fe 3942·446 (B) | *a* | 1·4399 | 1·4400 | − 1 |
| Fe 3897·892 (B) | *c* | 1·4400 | 1·4406 | − 6 |
| Fe 3887·053 (B) | *a* | 1·4404 | 1·4407 | − 3 |
| Fe 3843·261 (I) | *g*<br>*c* | 1·4407<br>1·4409 | 1·4413 | − 6<br>− 4 |
| Fe 3833·312 (B) | *a* | 1·4410 | 1·4415 | − 5 |
| Fe 3794·341 (B) | *g* | 1·4416 | 1·4420 | − 4 |
| Fe 3790·094 (B) | *c* | 1·4417 | 1·4421 | − 4 |
| Fe 3756·940 (B) | *a* | 1·4423 | 1·4426 | − 3 |
| Fe 3738·310 (B) | *c* | 1·4424 | 1·4428 | − 4 |
| Fe 3707·048 (B) | *a* | 1·4429 | 1·4434 | − 5 |
| Fe 3693·999 (B) | *e* | 1·4430 | 1·4436 | − 6 |
| W 3688·069 | *c* | 1·4432 | 1·4437 | − 5 |
| Fe 3682·235 (B) | *a* | 1·4431 | 1·4438 | − 7 |
| Fe 3659·521 (B) | *a* | 1·4439 | 1·4442 | − 3 |
| Fe 3655·470 (B) | *h* | 1·4439 | 1·4442 | − 3 |
| Fe 3612·082 (B) | *h* | 1·4446 | 1·4450 | − 4 |
| Fe 3570·102 (B) | *e* | 1·4459 | 1·4457 | + 2 |

Table III.—(continued).

| Wave-length of coincidence | Film | Refractive index. |  | Difference (O – C) $\times 10^4$ |
|---|---|---|---|---|
|  |  | *n* (observed) | *n* (calculated) |  |
| Fe 3526·016 (B) | *g* | 1·4468 | 1·4465 | + 3 |
| Fe 3524·077 (B) | *c* | 1·4466 | 1·4466 | ± |
| Fe 3489·672 (B) | *h* | 1·4473 | 1·4473 | ± |
| Fe 3485·345 (I) | *f* | 1·4474 | 1·4473 | + 1 |
| Fe 3459·922 (B) | *a* | 1·4482 | 1·4478 | + 4 |
| Fe 3417·847 (B) | *a* | 1·4488 | 1·4487 | + 1 |
| Fe 3415·537 (B) | *c* | 1·4488 | 1·4487 | + 1 |
| W 3395·817 | *e* | 1·4497 | 1·4492 | + 5 |
| Fe 3354·068 (B) | *c* | 1·4502 | 1·4501 | + 1 |
| Fe 3303·476 (B) | *h* | 1·4517 | 1·4512 | + 5 |
| Fe 3254·372 (B) | *e* | 1·4528 | 1·4524 | + 4 |
| Fe 3246·015 (B) | *d* | 1·4534 | 1·4526 | + 8 |
| Fe 3239·449 (B) | *c* | 1·4538 | 1·4528 | +10 |
| Fe 3227·814 (B) | *d* | 1·4539 | 1·4531 | + 8 |
| Fe 3191·666 (B) | *d* | 1·4548 | 1·4540 | + 8 |
|  | *e* | 1·4545 |  | + 5 |
| Fe 3156·269 (B) | *d* | 1·4556 | 1·4550 | + 6 |
| Fe 3125·661 (F) | *g* | 1·4567 | 1·4558 | + 9 |
| W 3105·879 | *d* | 1·4573 | 1·4564 | + 9 |
| W 3094·034 | *g* | 1·4578 | 1·4568 | +10 |
| W 3089·066 | *d* | 1·4577 | 1·4569 | + 8 |
| Fe 3063·939 (B) | *g* | 1·4586 | 1·4577 | + 9 |
| Fe 3040·430 (B) | *d* | 1·4592 | 1·4584 | + 8 |
| Fe 3033·104 (B) | *g* | 1·4597 | 1·4586 | +11 |
| W 3013·796 | *c* | 1·4598 | 1·4593 | + 5 |
| W 2997·794 | *e* | 1·4602 | 1·4598 | + 4 |
| Fe 2966·902 (B) | *c* | 1·4614 | 1·4608 | + 6 |
| W 2952·298 | *e* | 1·4623 | 1·4614 | + 9 |
| Fe 2937·809 (B) | *e* | 1·4632 | 1·4618 | +14 |
| W 2934·994 | *d* | 1·4634 | 1·4619 | +15 |
| Fe 2904·163 (B) | *d* | 1·4639 | 1·4631 | + 8 |
| W 2833·634 | *d* | 1·4663 | 1·4658 | + 5 |
| Fe 2806·985 (B) | *d* | 1·4676 | 1·4669 | + 7 |
| W 2792·702 | *d* | 1·4677 | 1·4675 | + 2 |
| Fe 2754·032 (B) | *d* | 1·4694 | 1·4692 | + 2 |
| Fe 2741·833 (B) | *d* | 1·4703 | 1·4697 | + 6 |
| Fe 2666·970 (B) | *d* | 1·4730 | 1·4734 | – 4 |
| Fe 2656·154 (B) | *d* | 1·4742 | 1·4739 | + 3 |
| Fe 2644·008 (B) | *d* | 1·4745 | 1·4745 | ± |
| Fe 2632·248 (B) | *d* | 1·4750 | 1·4752 | – 2 |
| Fe 2610·759 (B) | *d* | 1·4770 | 1·4763 | + 7 |
| Fe 2599·405 (B) | *d* | 1·4775 | 1·4769 | + 6 |
| Fe 2588·016 (F) | *d* | 1·4780 | 1·4776 | + 4 |
| W 2522·060 | *d* | 1·4808 | 1·4815 | – 7 |
| Fe 2501·70 (B) | *d* | 1·4828 | 1·4828 | ± |
| W 2482·101 | *d* | 1·4841 | 1·4841 | ± |
| Fe 2473·159 (B) | *d* | 1·4853 | 1·4847 | + 6 |
| Fe 2462·652 (B) | *d* | 1·4856 | 1·4854 | + 2 |
| W 2452·020 | *d* | 1·4858 | 1·4861 | – 3 |

Table IV shows the results of a similar series of observations of sample B, for 31 wave-lengths from Fe 4308 to 2413. Three films were used, of which the thicknesses were $l = 5 \cdot 33\ \mu$, $m = 7 \cdot 25\ \mu$, $n = 5 \cdot 50\ \mu$.

The wave-lengths in Table II are taken from the International Critical Tables. The wave-lengths of the iron lines in Tables III and IV are either the International Standards, I, or the interferometer values, F, of Fabry and Buisson, when available; otherwise we have used the interpolated wave-lengths (nearly all given to three decimals) of Kayser,* K, or Burns,† B. The wave-lengths of the tungsten lines in Tables III and IV are those given by Belke.‡

Table IV.—Refractive Indices of Cyclohexane at 20° C.

Specimen B.

Third Series: Photographic Method.

$$\text{II.}\quad n^2 = 2·00723 + \frac{0·009264}{\lambda^2 - 0·011923}$$

| Wave-length of coincidence | Film. | Refractive index | | Difference (O − C) × 10⁴. |
|---|---|---|---|---|
| | | *n* (observed) | *n* (calculated) | |
| Fe 4307·910 (B) | *m* | 1·4359 | 1·4359 | ± |
| Fe 4260·489 (B) | *l* | 1·4366 | 1·4364 | + 2 |
| Fe 4147·676 (I) | *l* | 1·4374 | 1·4375 | − 1 |
| Fe 4067·277 (B) | *m* | 1·4379 | 1·4385 | − 6 |
| Fe 3956·682 (B) | *m* | 1·4388 | 1·4398 | −10 |
| Fe 3852·577 (B) | *m* | 1·4398 | 1·4412 | −14 |
| Fe 3756·940 (B) | *m* | 1·4420 | 1·4426 | − 6 |
| Fe 3669·525 (B) | *l* | 1·4436 | 1·4440 | − 4 |
| Fe 3576·762 (B) | *m* | 1·4451 | 1·4456 | − 5 |
| W 3435·724 | *l* | 1·4482 | 1·4481 | + 1 |
| Fe 3415·537 (B) | *m* | 1·4490 | 1·4488 | + 2 |
| Fe 3306·790 (B) | *l* | 1·4506 | 1·4499 | + 7 |
| Fe 3298·137 (B) | *l* | 1·4519 | 1·4515 | + 4 |
| Fe 3268·246 (B) | *m* | 1·4525 | 1·4523 | + 2 |
| Fe 3233·061 (B) | *l* | 1·4536 | 1·4531 | + 5 |
| W 3198·843 | *m* | 1·4540 | 1·4541 | − 1 |
| W 3133·895 | *m* | 1·4561 | 1·4559 | + 2 |
| W 2997·794 | *l* | 1·4601 | 1·4603 | − 2 |
| W 2946·992 | *l* | 1·4630 | 1·4621 | + 9 |
| Fe 2895·036 (B) | *l* | 1·4643 | 1·4641 | + 2 |
| W 2831·387 | *n* | 1·4664 | 1·4667 | − 3 |
| Fe 2788·108 (B) | *n* | 1·4693 | 1·4687 | + 6 |
| Fe 2744·072 (B) | *n* | 1·4711 | 1·4707 | + 4 |
| W 2702·127 | *n* | 1·4731 | 1·4728 | + 3 |
| Fe 2662·066 (B) | *n* | 1·4755 | 1·4750 | + 5 |
| W 2622·217 | *n* | 1·4772 | 1·4772 | ± |
| Fe 2584·544 (B) | *n* | 1·4795 | 1·4795 | ± |
| W 2547·155 | *n* | 1·4812 | 1·4819 | − 7 |
| W 2513·978 | *n* | 1·4848 | 1·4842 | + 6 |
| Fe 2478·14 (K) | *n* | 1·4861 | 1·4867 | − 6 |
| Fe 2413·310 (F) | *n* | 1·4911 | 1·4918 | − 7 |

---

* Kayser, "Handbuch der Spektroscopie," vol. 6.

† Burns, 'Z. Wiss. Photogr.,' vol. 12, pp 207–236 (1913).

‡ Belke, 'Z. Wiss. Photogr.,' vol. 17, p. 132 (1917) and vol. 17, p. 144 (1918).

*Calculation of Refractive Indices*—(*a*) Gifford's very exact data, for 12 visible and 10 ultra-violet wave-lengths and for a temperature of 15° C , were expressed over the range 7701 Å.U. to 3282 Å.U. by the simple dispersion equation

$$n^2 = 2\cdot011046 + \frac{0\cdot0102467}{\lambda^2 - 0\cdot013977}. \qquad \text{(III)}$$

Omitting the readings for the two shortest wave-lengths, which were abnormal, the average difference between observed and calculated values was only 0·00006 for a series of 20 wave-lengths Within this range, therefore, the formula expresses the experimental results perfectly, as may be seen by reference to the difference-curve, fig. 1 (*a*), which lies along the axis throughout its whole length, apart from the two points referred to above

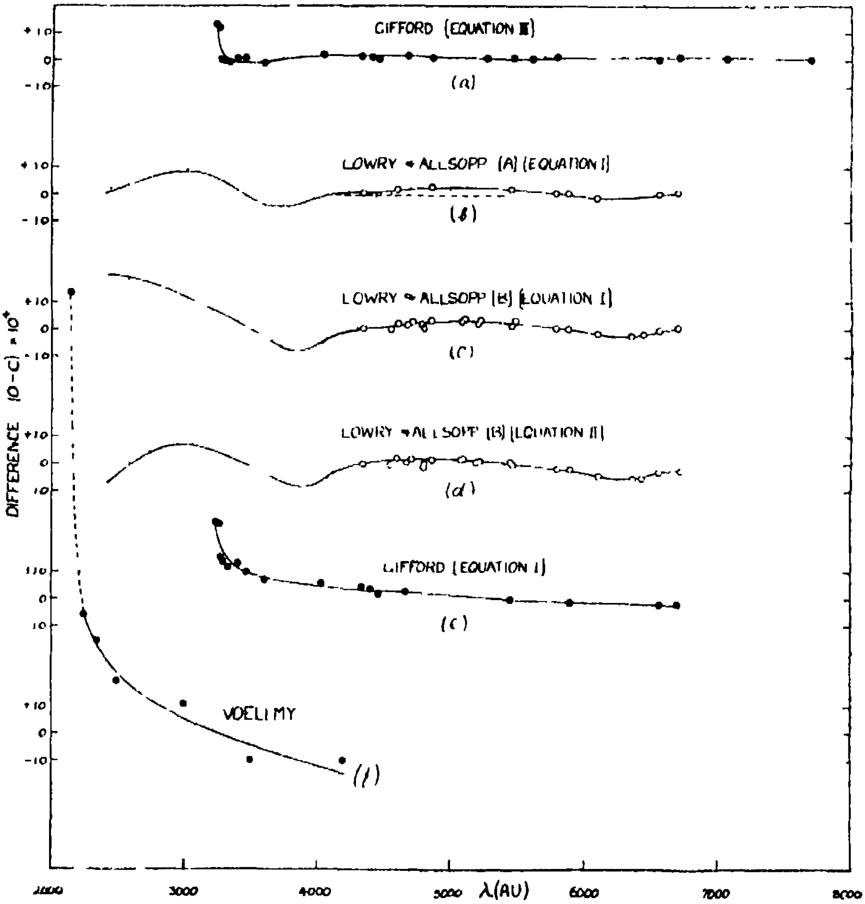

Fig 1

(*b*) The dispersion-curve now obtained for Professor Timmermans' specimen A, is reproduced in fig. 2. The refractive indices at 20° C. can be expressed over the range from 6707 to 2450 Å.U. by the equation

$$n^2 = 2\cdot00519 + \frac{0\cdot0098035}{\lambda^2 - 0\cdot011923}. \qquad \text{(I)}$$

This equation was calculated from three selected photographic readings, but is also valid in the region covered by the visual observations. The deviations from it are shown in Tables II and III, and a difference-curve has been drawn in fig. 1 (*b*). The nine visual readings in Table II show a mean deviation of ±0·00012 from the calculated values and an average error of +0·00008. The 97 photographic readings, set out in Table III, show a mean deviation of ±0·0004 and an average error of +0·00016. These averages, however, include a double loop in the curve of errors between 2800 Å.U. and 3950 Å.U.

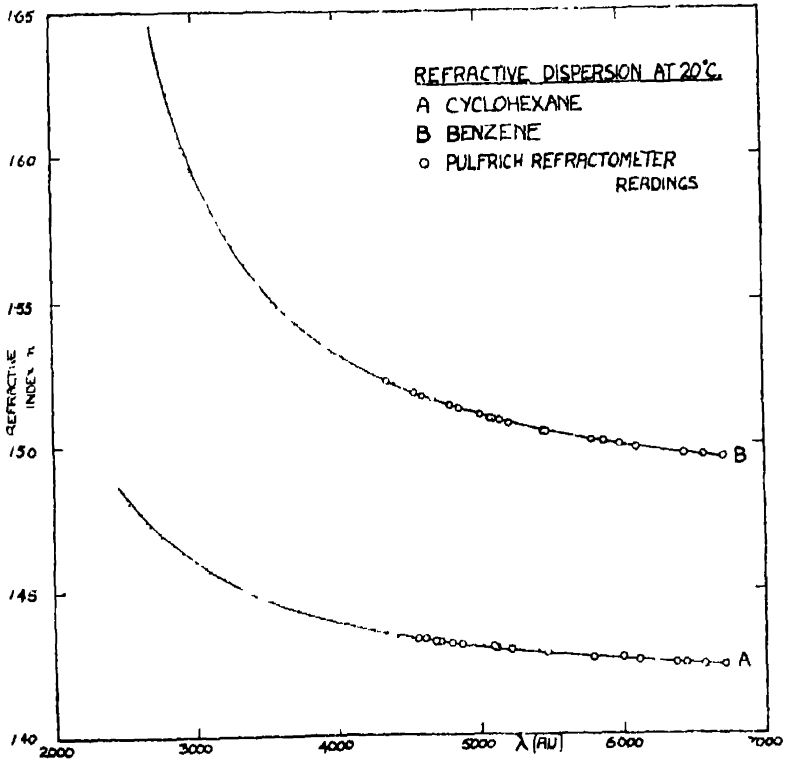

Fig. 2.

(about one-third of the range covered), where the deviations increase to 0·001. Outside this range, the mean deviation is ±0·0002, and the mean error falls to +0·00005. The origin of this loop is discussed below.

(*c*) The refractive indices of our own specimen B were investigated fully before sample A became available Table II therefore includes refractive indices for 21 wave-lengths, as compared with only 9 wave-lengths for sample A. The values recorded, however, are substantially identical (as is shown by the small differences in the last column of Table II), and the data for specimen B can therefore be expressed satisfactorily by the equation used for specimen A. The mean deviation for 21 values calculated from equation (I) is +0·00017, and the average error is +0·00010, as compared with ±0·00012 and +0·00008 for the nine lines which were specially selected as being most favourable for measurement in the case of specimen A.

The photographic readings for 31 wave-lengths for specimen B are set out in Table IV. Down to 2900 Å.U the values are similar to those obtained for specimen A; beyond this point, however, the refractive indices increase more rapidly than for specimen A, as is shown by the curve of differences reproduced in fig. 1 (*c*). Despite this deviation, however, the refractive indices for specimen B at 20° C. were found to fit a similar equation, as follows

$$n^2 = 2\cdot00723 + \frac{0\cdot009264}{\lambda^2 - 0\cdot01582}. \qquad \text{(II)}$$

The differences from this equation are plotted in fig. 1 (*d*) and are also set out in Tables II and IV The visual readings of Table II show a mean deviation of ±0·00019, and an average error of —0·00009 The photographic readings of Table IV show a mean deviation of ±0·0004 and a mean error of only —0·00003, despite the existence of the loop already recorded for specimen A.

*Systematic Errors.*—The large number of wave-lengths for which refractive indices have been calculated makes it possible to discriminate between casual and systematic errors, in a way that has been impossible hitherto. Thus an inspection of the difference-curve, fig 1 (*b*) for specimen A, discloses two series of systematic deviations, in the visible and in the ultra-violet regions respectively, which are too large in comparison with the casual fluctuations to be overlooked or ignored.

(*a*) The existence of systematic deviations was disclosed as a result of submitting the Pulfrich refractometer to an unusually severe test, by taking readings for 21 different wave-lengths. The validity of the simple dispersion-equation to express the refractive indices of cyclohexane throughout the visual and early ultra-violet regions has already been established by Gifford's measurements, the accuracy of which admittedly exceeds that attained by any other method. Since it is unlikely that the extra purity of sample A would *introduce* an anomaly into the curve of refractive dispersion, we are satisfied that deviations from the formula must be attributed to instrumental errors. This conclusion is confirmed by the fact that the deviations in question are confined to the readings taken with the refractometer. The interferometer values, on the other hand, agree closely with the formula as is shown by the contiguity to the zero line of the broken line in the difference-curve of fig. 1 (*b*).

It is perhaps surprising that such deviations should persist when the instrument was calibrated with the help of a block of quartz for each wave-length used in the subsequent measurements. The appearance of the spectrum is, however, very variable, since it depends on the difference of refractive indices between the glass and the substance placed upon it for measurement, and, whilst it may be possible under a fixed set of conditions to make duplicate readings with great precision, this is in itself no guarantee of the absence of systematic errors. In particular, the regions where the most irregular deviations occur, namely the middle-red and the blue-green, are precisely those in which the difficulties of reading are greatest, on account either of the continuous red spectrum from the arc or of the multiplicity of lines, both giving rise to a blurring of the limit of total reflection. On the other hand, systematic errors might perhaps be caused by a lack of achromatism of the telescope, the objective of which is a simple doublet, achromatised for two wave-lengths in the red and blue respectively, that is, in the regions where the systematic errors appear to vanish.

In view of these considerations, we think it necessary to admit that reproducible errors of the order of magnitude of the differences of Table II may exist, in spite of the remarkable agreement between the refractive indices now recorded for two different samples of cyclohexane. If then a maximum of accuracy were required in this region, it would be necessary to revert to the laborious procedure developed by Gifford for measuring the refractive indices of solid prisms, and to couple it with a stricter control of temperature when working with organic liquids; but we do not regard this procedure as necessary for the present purpose, since the visual readings are here used only as a preliminary to photographic readings over a much wider range of wave-lengths. The data obtained with the refractometer in the green and blue regions of the spectrum are sufficiently exact for this purpose, since the film thickness, which is used in deducing refractive indices from readings with the etalon, is derived from readings of the Pulfrich refractometer for at least half a dozen wave-lengths in the blue region of the spectrum, where the errors do not exceed 0·0001.

(*b*) The origin of the double " loop " in the middle ultra-violet is more obscure. Its real existence can scarcely be doubted, since a similar loop was observed with sample B, fig. 1 (*c*) and (*d*), which had a lower freezing point than sample A ; moreover, Gifford's last two readings, for a specimen intermediate in this respect between A and B, diverge in the same direction from the calculated values, fig. 1 (*a*), although his observations did not extend into the region covered by the positive section of the loop. If the positive branch of the loop had occurred on the side of longer wave-lengths, it would have suggested the presence in the material of an impurity with an absorption-band at about 3400 Å U., producing a slight " ripple " on the dispersion-curve. Since, however, the negative loop appears first, the effect must be due to a more complicated absorption in the medium. In this connection, it is interesting to notice that the dispersion-constants of the equations (I), (II) and (III), decrease progressively as the freezing point of the specimen rises. This suggests that purification of the material removes an impurity which is more absorptive than cyclohexane, as would be expected in view of the completely-saturated character of this hydrocarbon. This impurity cannot, however, be responsible for the " loop " in the dispersion-curve, since this is not affected substantially by the difference of 0·55° in the freezing point of samples A and B.

*Comparison with Earlier Observations.*—Previous determinations of the refractive indices of cyclohexane have been made by Eisenlohr,* Gifford and Voellmy.† Eisenlohr's measurements were for four lines only in the visible spectrum, and were probably made with a Pulfrich refractometer. Voellmy's measurements, by a modification of the method of crossed prisms described by Victor Henri,‡ cover a range of wave-lengths from 6560 to 2150 Å.U., but his data are for wave-lengths in exact multiples of 100 or 50 Å.U , and therefore appear to be interpolated values.

Comparison with these earlier observations can best be made by means of difference-curves ; and, in order to avoid casual error, the refractive indices recorded by other workers were compared with values calculated from our dispersion formula (I), instead of with individual values. Fig. 1 (*e*) shows the differences of these calculated values from those given by Gifford, when corrected to 20° C. by means of the temperature coefficients which he himself had used. Apart from the last two points, which were read with great difficulty, the concordance is quite good. On the other hand, Voellmy's values, similarly corrected, show large and irregular differences, amounting to some four units in the third decimal place, as shown in fig. 1 (*f*). It should be mentioned here that Guillery[*] has called attention to a similar divergence of about ±0·004 between Voellmy's values and the mean values of the indices recorded by other observers for glycerol, propyl alcohol and butyl alcohol, the difference in the case of glycerol increasing to 0·01 in the ultra-violet. From these facts it is clear that the data given by Gifford, which are admittedly of a higher degree of precision than we have been able to attain up to the present by any alternative method, are the only ones with which an accurate comparison can usefully be made. Since, however, the sample of cyclohexane procured from Brussels was purer than that supplied to Gifford in 1923, the refractive indices now recorded are more trustworthy than those given by Gifford, which are lower by about 0·0002 for wave-lengths in the visible spectrum, but become progressively higher in the ultra-violet by reason of the higher dispersion of the less pure sample.

---

* Eisenlohr, ' Spektrochemie Organischer Verbindungen,' p 86.

† ' Z. Phys. Chem.,' vol. 127, p. 305 (1927).

‡ ' Etudes de Photochimie,' (1919).

## *Summary.*

(1) Values for the refractive indices of highly-purified cyclohexane are given to the fourth decimal for 21 wave-lengths in the range of visual observations with a refractometer and for 97 wave-lengths in the region covered by photographic readings with an etalon.

(2) These refractive indices can be expressed within a few units in the fourth decimal by the equation

$$n^2 = 2\cdot00519 + 0\cdot0098035/(\lambda^2 - 0\cdot011923),$$

but systematic deviations rising to a maximum of one unit in the third decimal are found between 3950 and 2800 Å.U.

(3) Systematic deviations of smaller magnitude in the visual readings are attributed to instrumental errors in the refractometer, since they were not observed in measurements made with the etalon, and were absent in earlier measurements made by Gifford with a hollow prism.

[*] Guillery, *loc cit.*

## PART III.—BENZENE.

The refractive dispersion of benzene has been investigated in the visible and ultra-violet regions of the spectrum by Simon* in 1894, by Gifford† in 1923 and by Voellmy‡ in 1927. Measurements were also made in the visible and infra-red regions by Rubens§ in 1892, but in no case has the region of selective absorption in the ultra-violet between 2700 Å.U. and 2350 Å.U been penetrated. Attempts have also been made to represent the dispersion by formulæ of the Ketteler-Helmholtz type, but with much less success than in the case of cyclohexane. In particular, Coode.Adams was quite unable to express Gifford's very accurate data by an equation of the kind which represented accurately all but two of the corresponding data for cyclohexane. The most successful attempt was made some years ago by Richardson‖ who used the equation cited on p. 50 to represent the values given by Simon and by Rubens for the refractive indices of benzene over the whole available range of wave-lengths. This equation contains four arbitrary constants, and includes contributions to the refractive index from two absorption frequencies, one in the infra-red and one in the Schumann region of the spectrum.

The experiments now described were undertaken in the first instance as part of a programme for developing and standardising our new method of measuring refractive indices; but the investigation soon developed into a struggle to bring about a reconciliation between the experimental data and the theoretical formulæ for refractive dispersion. In this we had three advantages over earlier workers First, the sample of benzene supplied by Professor Timmermans from the *Bureau des etalons physico-chimiques* had a higher freezing point (5·45°) than the specimen which we had purified in our own laboratory for this research (5·29°), and was almost identical with that of the specimen which we had supplied to Colonel Gifford in 1923 (5·58°) The absolute values of our refractive indices are therefore more accurate, and the relative values are obviously more trustworthy than those recorded previously for samples which had been purified by distillation only. Second, it is impossible in work of this kind to secure a satisfactory check upon the accuracy of a formula by using a short series of readings, since half a dozen refractive indices are needed to fix the arbitrary constants of the dispersion equation, and a much longer

---

* Simon, 'Ann. Physik,' vol. 53, p. 542 (1894).

† Gifford and Lowry, 'Proc. Roy. Soc.,' A, vol. 104, p. 430 (1923)

‡ Voellmy, 'Z. Phys. Chem.,' vol. 127, p. 305 (1927).

§ Rubens, 'Ann. Physik,' vol. 45, p. 238 (1892).

‖ Richardson, 'Phil. Mag.,' vol. 31, p. 249 (1916).

*Lowry and Allsopp.* *Proc. Roy. Soc., A, vol.* 133, *Pl.* 3.

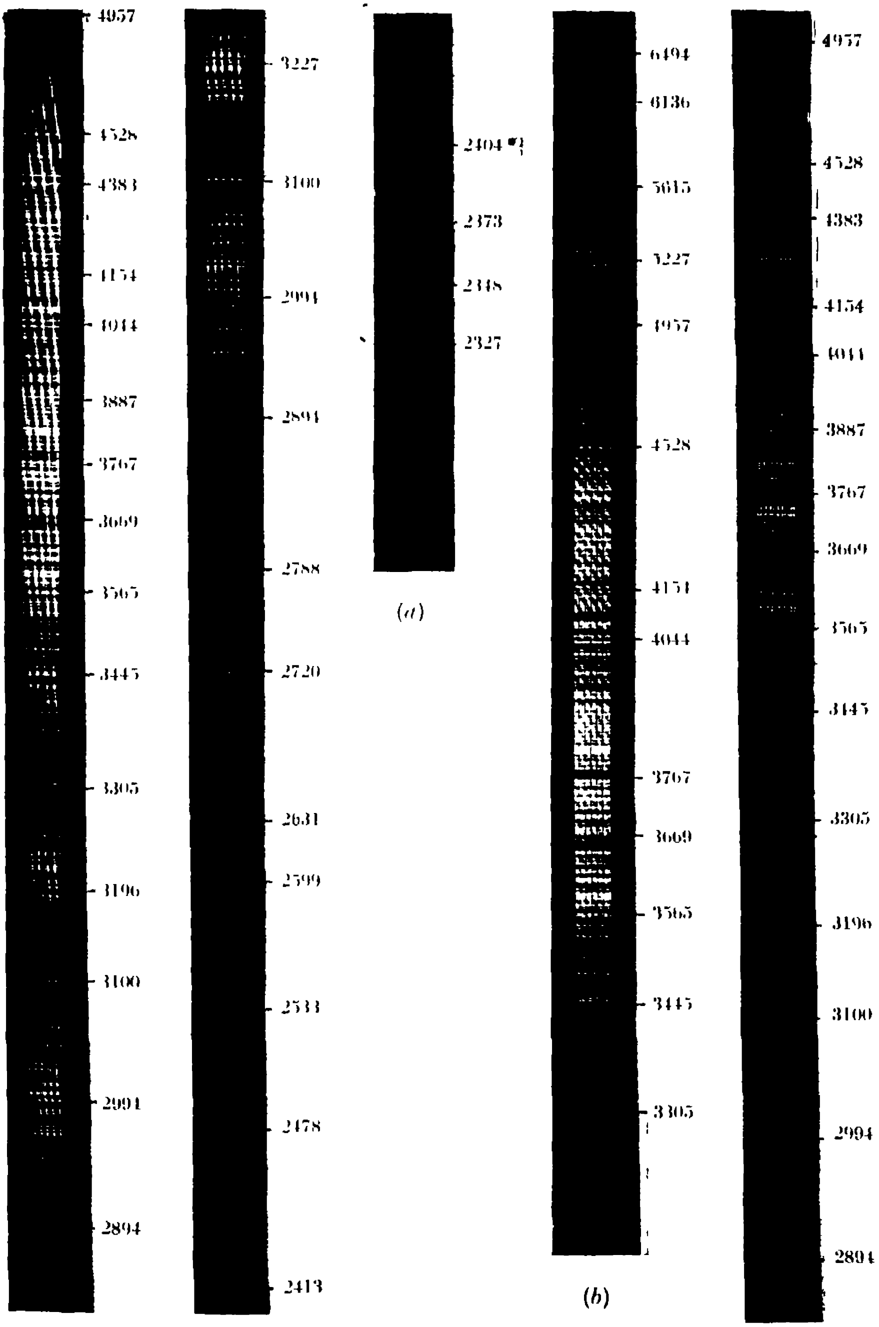

(*a*) (*a*) (*a*) (*b*) (*c*)

(*a*) Air film, thickness = 10 μ (*b*) Cyclohexane, thickness = 5·5 μ (*c*) Cyclohexane, thickness = 10·5 μ

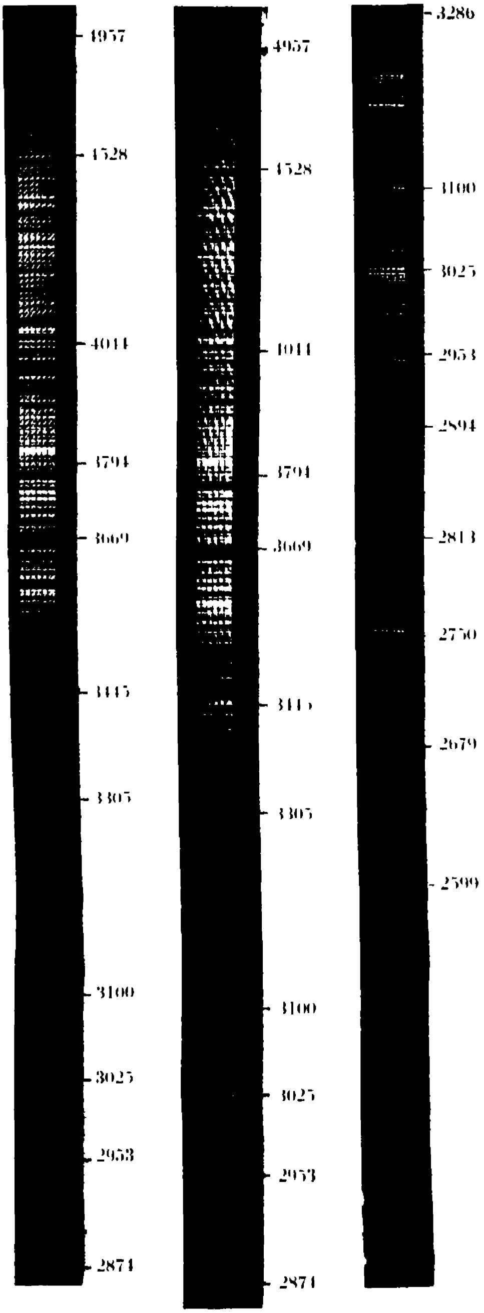

(*d*) (*e*) (*f*)

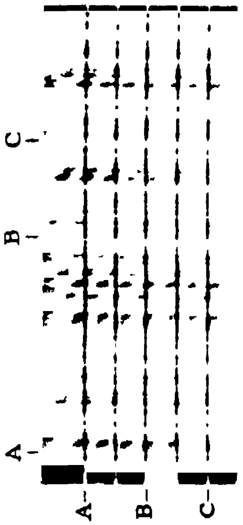

Showing coincidences at AA BB CC

(*d*) Benzene, thickness = 38 μ (*e*) Benzene, thickness = 7 μ (*f*) Benzene, thickness = 13 μ series is needed before the relative magnitude of the casual and systematic errors can be estimated. The use of the etalon therefore provides an ideal method of investigation, since refractive indices for an almost unlimited number of wave-lengths can be read from a single photographic plate, under such conditions that the only variables are the wave-length of the light and the unequal thickness of liquid at five adjacent reference points in the film. Finally, by using specially thin films of the liquid, it has been possible to penetrate further than any of the earlier workers into the region of absorption and thus to follow the curve of refractive dispersion into a range of wave-lengths where the existence of a "damping factor" becomes of dominant importance in reconciling the observed refractive indices with those calculated from a theoretical formula. The recognition of this factor increases the difficulty of the investigation but enhances very greatly the value of the work, since a formula which is valid in the region of absorption is obviously more trustworthy than any of the formulæ of the type previously used, which break down completely in this region and only become approximately correct as the wave-length recedes from those of the absorption-bands.

The experimental work, which is described in detail below, need not be cited in this introduction, except in order to note that our tables of refractive indices include values for 22 wave-lengths in the visual range from 6707 to 4358 Å.U., and for 102 wave-lengths in the photographic range from 4900 to 2700 Å.U., and that 9 of these wave-lengths fall within the region of incipient absorption, from 2850 Å U. downwards, where only two observations, by different workers, had previously been recorded.

The analysis of these data has been simplified by the use of difference-curves, such as were employed in the work on cyclohexane, in order to separate casual from systematic and instrumental errors. They now have a further application. Thus, if, as was suggested by Richardson, the effect of the ultra-violet absorption-bands of benzene is very small compared with those in the infra-red and distant ultra-violet regions, the dispersion-curve itself is unlikely to show any marked disturbance as these ultra-violet absorption-bands are approached. On the other hand, a difference-curve, showing the deviations from some simple equation, on a scale ten thousand times greater than that of the dispersion-curve, is very sensitive to the smallest anomalies This method of analysis has, in fact, led to the detection of a refraction term due to the nearer absorption-bands, which is one-hundredth times smaller than the term used to represent the influence of the gigantic bands in the Schumann region.

*Development of a New Dispersion Formula.*—(*a*) The data of Rubens include refractive indices at 12° for 10 infra-red wave-lengths extending from 0·8 to 1·8 μ, whilst those of Simon include refractive indices at 20° for 9 wave-lengths in the visible and 6 in the ultra-violet region, from 7681 to 2837 Å.U. Martens* corrected the observations of Rubens at 12° by making them coincide in the visual region with the observations of Simon at 20° and attempted to represent the refractive indices thus deduced by a 3-constant equation as follows

$$n^2 - 1 = 0\cdot4528 + 0\cdot7264\ \lambda^2/(\lambda^2 - 0\cdot03045). \qquad \text{(I)}$$

He was unable, however, to reconcile this equation with the experimental data. Richardson, using the same data deduced the equation

$$n^2 - 1 = 0\ 55695 + 0\cdot62871\ \lambda^2/(\lambda^2 - 0\cdot03294) - 0\cdot0017\ \lambda^2, \qquad \text{(II)}$$

for which a difference-curve has now been plotted in fig 3 (*a*). This curve shows that, although the average deviation for the 25 indices selected by Richardson is only ±0·0003, over the range from 2837 to 18,500 Å.U., systematic errors are present which give rise to three very unequal loops between the four points for which ± values are given by the 4-constant equation. Three of Simon's values, not used by Richardson, give similar deviations; but a fourth value, for a wave-length 60 Å.U. less than that of the shortest wave-length (2837 Å.U.) used in calculating the dispersion equation, diverges from the calculated values by 0·0068. Simon's observation has not been confirmed by our measurements, but these show clearly that Richardson's equation cannot be extended in the ultra-violet beyond his last ± value, since it then no longer represents the experimental data even approximately.

(*b*) In calculating a dispersion-formula to fit the new data set out in Tables V to VII below, care was taken to avoid the use of points lying too near to the region of absorption. The most satisfactory of the 3-constant equations is

$$n^2 = 2\cdot18753 + 0\cdot020678/(\lambda^2 - 0\cdot03197), \qquad \text{(III)}$$

where the $\lambda^2$ has been omitted from the numerator of the ultra-violet term of Martens' equation, although our dispersion-constant is of similar magnitude to his. The differences between the observed and calculated values, which are plotted in fig. 3 (*b*), give rise to three approximately equal loops, with a mean amplitude of ± 0·0004. The average deviation is only ± 0·0003, but increases rapidly to 0·005 when the region of absorption is approached.

(*c*) The 3-constant equations are remarkable in that, whilst Richardson's 4-constant equation gives rise to a difference-curve which intersects the axis of zero error at *four* points, the difference-curve for our 3-constant equation cuts the zero axis at *five* points, namely, four points in the visible and ultra-violet and one in the near infra-red. Unlike Richardson's equation (II), however, our equation (III) exhibits large deviations in the infra-red, as is shown in fig. 3 (*b*). In order to eliminate this divergence, an infra-red term of the same form as Richardson's was introduced into our equation, which (after

---

* Martens, 'Ann. Physik,' vol 6, p. 603 (1901).

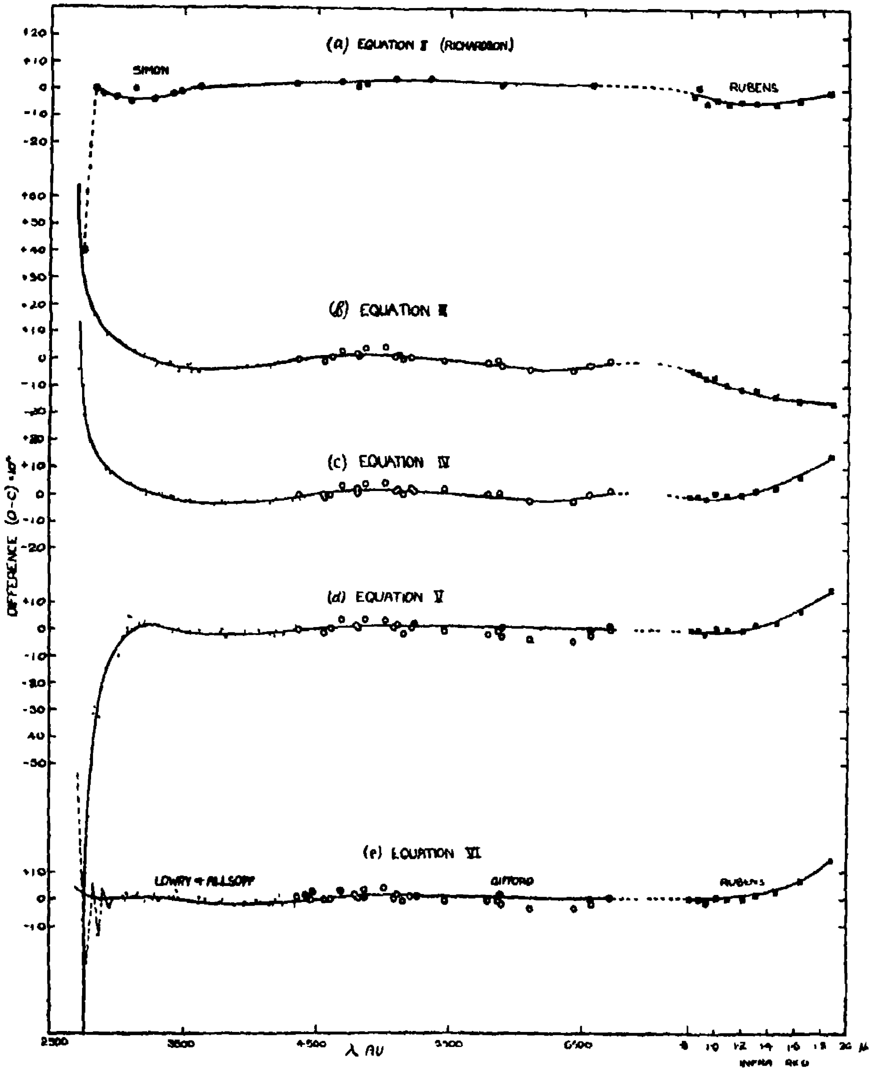

Fig. 3

restoring the $\lambda^2$ in the numerator of the ultra-violet term) assumed the following form

$$n^2 = 1\cdot54245 + 0\cdot64581\ \lambda^2/(\lambda^2 - 0\cdot03197) - 0\cdot0027\ \lambda^2. \qquad \text{(IV)}$$

In order to secure a satisfactory basis for comparison with this equation, the infra-red readings of Rubens were corrected to 20° by making them coincide with the corrected values of Gifford in the visible spectrum, and then making use of the constancy of the Lorenz-Lorentz expression to correct the data in the infra-red. The infra-red term becomes negligible for wave-lengths less than about 4800 Å U , so that the difference-curve, fig. 3 (*c*), is not substantially affected in the region covered by the photographic and visual observations. The infra-red galvanometric observations, however, show much smaller deviations, since they no longer diverge from the calculated values, except in the region covered by a weak absorption-band at $1\cdot6\ \mu$; and the differences are reduced to zero at no less than *six* points.

(*d*) After eliminating the deviations in the infra-red, by the introduction of one additional term and one more arbitrary constant, attempts were made to remove the loops in the visible and ultra-violet regions. The double loop in the visual region was similar to that recorded for cyclohexane, and was again attributed to instrumental errors, since no similar deviations are found in the very accurate values which Gifford obtained in this region with the help of a hollow prism. The loop between 3100 and 4300 Å.U., which could not be attributed to instrumental errors, was eliminated by introducing a second ultra-violet term, with two additional constants. The dispersion-constant of this additional term was $\lambda_0{}^2 = 0\cdot07017$, $\lambda_0 = 2650$ Å.U., corresponding with a wave-length lying within the region of selective absorption which extends from 2700 to 2350 Å.U. The difference-curve, fig. 3 (*d*), shows the disappearance of the ultra-violet loop when using the modified equation

$$n^2 = 1\cdot51304 + \frac{0\cdot66992\ \lambda^2}{\lambda^2 - 0\cdot030170} + \frac{0\cdot005977\ \lambda^2}{\lambda^2 - 0\cdot070171} - 0\cdot0027\ \lambda^2. \qquad \text{(V)}$$

(*e*) The preceding 6-constant equation (V) gives zero differences at *seven* different wave-lengths, but still fails to represent the data satisfactorily at the two extremes of wave-lengths. Attempts to calculate a *third* ultra-violet term gave rise to a dispersion-constant in a range of wave-lengths where no absorption is observed, and therefore contributed nothing to the solution of the problem. A clue to the origin of the remaining anomalies was provided, however, by the fact that the difference-curve for equation (V) swings off abruptly from the axis in the negative direction for wave-lengths less than

3000 Å.U., and in the positive direction for wave-lengths greater than 1·4 μ, thus suggesting that the middle ultra-violet term, and the infra-red term, had been given too large a weight within the region of absorption. This would obviously happen if a damping factor had been ignored, leaving the theoretical curve to approach asymptotically to an infinite value at the wave-lengths represented by the relevant dispersion-constants. It was then a simple matter to replace the ultra-violet term

$$\frac{A\lambda^2}{\lambda^2 - \lambda_0^2} \quad \text{by} \quad \frac{A'(\lambda^2 - \lambda_0^2)\lambda^2}{(\lambda^2 - \lambda_0^2)^2 + g\lambda^2},$$

where $g$ is a damping factor. The two arbitrary constants in this term, namely $A'$ and $g$, were deduced from two of the readings which needed correction. In this way a final equation was deduced as follows

$$n^2 = 1\cdot 51304 + \frac{0\cdot 66992\,\lambda^2}{\lambda^2 - 0\cdot 030170} + \frac{0\ 06143\,(\lambda^2 - 0\cdot 070171)\,\lambda^2}{(\lambda^2 - 0\cdot 070171)^2 + 0\cdot 0003448\,\lambda^2} - 0\cdot 0027\,\lambda^2. \qquad \text{(VI)}$$

This equation is in satisfactory agreement with the observed refractive indices over the whole range of transparency of the medium, as may be seen from the difference-curve, fig. 3 (e), which lies so close to the axis that the number of intersections has now become indeterminate. This difference-curve has been drawn through Gifford's readings in the visual region, although our readings with the Pulfrich refractometer are also shown. Where the use of a fluorescent eye-piece became necessary, Gifford's values for the refractive indices of benzene are less accurate than in the range where direct readings could be taken. Their accuracy then appears to be comparable with that of our own interferometer readings, which provide the majority of the data in the violet and ultra-violet regions. In the region of absorption beyond 2750 Å.U., the deviations are much larger than in the region of complete transparency, and it is possible that there is an oscillatory deviation due to the fine structure of the absorption; but the mean values are still very close to the calculated curve. The last two or three readings in the infra-red (where the scale of wave-lengths is ten times smaller) show a definite deviation from the calculated curve; but these readings also lie within a region of weak absorption near 1·6 μ.[*] An additional constant is obviously needed to bring the infra-red values into conformity with the experimental data, but this has not been included in our final equation. The closeness of the agreement between the observed and calculated values is illustrated by the fact that the visual readings in Table V show a mean deviation of only ± 0·0003 and a mean error of + 0·00016. Gifford's readings in the same region also show a mean deviation of ± 0·00016. Over the whole range of values, including the readings of Gifford and Rubens, the mean deviation is ±0·00037 and the mean error is —0·00008. In the central region from 3400 to 4800 Å.U., where the damping factor and the influence of the infra-red absorption-band are alike inappreciable, the dispersion can be expressed by a 5-constant equation, containing one constant term and two variable terms, *i.e.*, by equation (V) without the negative

---

[*] Henri, 'Etudes de Photochimie,' p. 113.

Table V.—Refractive Indices of Benzene at 20° C. Professor Timmermans' Specimen.

First Series : Pulfrich Refractometer

| Wave-length. | Refractive index | | Difference (O — C) × $10^4$ Equation | | |
|---|---|---|---|---|---|
| | *n* (observed) | *n* (calculated from equation V or VI) | V | III. | IV |
| Li 6707·86 | 1·4957 | 1·4957 | ± | ± | +2 |
| $H_\alpha$ 6562·85 | 1·4963 | 1·4965 | −2 | −2 | ± |
| Cd 6438·47 | 1·4968 | 1·4972 | −4 | −4 | −2 |
| Li 6103·6 | 1·4991 | 1·4994 | −3 | −3 | −1 |
| Na 5895·93 | 1·5009 | 1·5011 | 2 | −1 | ± |
| He 5875·62 | 1·5012 | 1·5012 | ± | ± | +1 |
| Hg 5790·66 | 1·5019 | 1·5020 | −1 | ± | +1 |
| Ag 5471·51 | 1·5049 | 1·5050 | −1 | + | +1 |
| Hg 5460·73 | 1·5051 | 1·5051 | ± | ± | +1 |
| Cu 5220·06 | 1·5080 | 1·5079 | +1 | +1 | +2 |
| Ag 5209·04 | 1·5081 | 1·5080 | +1 | +2 | +2 |
| Cu 5153·26 | 1·5086 | 1·5087 | −1 | ± | ± |
| Cu 5105·55 | 1·5095 | 1·5093 | +2 | +2 | +2 |
| Cd 5085·82 | 1·5097 | 1·5096 | +1 | +1 | +2 |
| He 5015·68* | 1·5110 | 1·5106 | +4 | +4 | +5 |
| $H_\beta$ 4861·33 | 1·5133 | 1·5129 | +4 | +4 | +5 |
| Zn 4810·53 | 1·5138 | 1·5137 | +1 | +1 | +2 |
| Cd 4799·91 | 1·5141 | 1·5139 | +2 | +3 | +3 |
| Cd 4678·15 | 1·5164 | 1·5160 | +4 | +4 | +4 |
| Li 4603·0 | 1·5175 | 1·5174 | +1 | +1 | +1 |
| Ba 4554·04 | 1·5184 | 1·5185 | 1 | −1 | −1 |
| Hg 4358·34 | 1·5226 | 1·5226 | ± | ± | ± |

| Equation . | V. | III. | IV. |
|---|---|---|---|
| Mean deviation | ±0·00016 | ±0·00015 | ±0·00017 |
| Mean error | +0·00003 | +0·00006 | +0·00014 |

---

* Interferometer value, P. W. Merrill, 'Bureau of Standards Bulletin,' vol. 14, p. 162 (1918–19).

term; but an additional constant is needed in order to extend the validity of the equation to wave-lengths above or below this range, so that the final equation contains seven arbitrary constants in all.

In view of the facts cited above, it is clear that no smaller number of constants than seven would suffice to represent the complete series of refractive indices. On the other hand, the data are not sufficiently precise to give correct values for seven unknowns merely by solving seven simultaneous equations. The step-by-step method of analysis is therefore probably the only one by which a solution of the problem could be reached in the particular case of benzene, or in any other similar case that may come up for analysis later. It is, however, believed that most of the cases that may be encountered in the future will prove amenable to the process of analysis which has been developed for the purposes of the present research.

## *Experimental.*

*Materials.*—The sample supplied by Professor Timmermans from the *Bureau des etalons physico-chemiques* had a density $d_4^{15} = 0{\cdot}88419$, and froze at 5·45° C. A sample purified in the same way as that supplied to Gifford in 1923 froze at 5·29° C instead of 5·58° C., and gave refractive indices which were lower throughout by four or five units in the fourth decimal; the measurements made with this sample (before the purer sample from Brussels became available) are therefore only of interest because they reproduce in minute detail all the anomalies observed in the mathematical analysis of the data for the purer sample (see fig 4, $a_1$ and $a_2$).

*Experimental Methods and Results.*—The refractive indices were measured as described in Parts I and II above. The thickness of the three films of benzene used in obtaining the photographic readings were $a = 38{\cdot}1\ \mu$, $b = 10{\cdot}3\ \mu$, $c = 13{\cdot}4\ \mu$ (compare Plate 1, *d*, *e*, *f*). Table V includes 22 refractive indices derived from visual readings with the Pulfrich refractometer between $\lambda = 6701$ and $\lambda = 4358$ Å.U. Table VI includes 52 refractive indices in the photographic range between 4886 and 3400 Å.U., whilst Table VII includes 50 more refractive indices in the photographic range from 3400 to 2700 Å.U. Each table shows also the differences between the observed refractive indices and those derived from certain of the equations set out above.

### Table VI.—Refractive Indices of Benzene at 20° C. Professor Timmermans' Specimen.

Second Series: Photographic Readings: λ = 4886 Å.U. to λ = 3400 Å.U.

| Wave-length of coincidence | Film. | Refractive index. | | Difference (O − C) × 10⁴. Equation | |
|---|---|---|---|---|---|
| | | n (observed) | n (calculated from equation V or VI). | V or VI | III or IV. |
| W 4886·922 | *a* | 1·5131 | 1·5125 | + 6 | + 7 |
| W 4509·972 | *b* | 1·5175 | 1·5174 | + 1 | + 1 |
| W 4536·068 | *b* | 1·5187 | 1·5187 | ± | ± |
| Fe 4454·387 (B) | *a* | 1·5201 | 1·5204 | − 3 | − 3 |
| Fe 4407·716 (B) | *a* | 1·5215 | 1·5215 | ± | ± |
| Fe 4375·934 (I) | *a* | 1·5220 | 1·5222 | 2 | − 2 |
| W 4345·846 | *a* | 1·5230 | 1·5229 | + 1 | + 1 |
| Fe 4315·089 (I) | *a* | 1·5235 | 1·5237 | − 2 | − 2 |
| W 4302·123 | *b* | 1·5236 | 1·5238 | − 2 | − 2 |
| W 4269·399 | *a* | 1·5242 | 1·5247 | − 5 | − 6 |
| W 4241·451 | *a* | 1·5253 | 1·5255 | − 2 | − 3 |
| Fe 4213·649 (B) | *a* | 1·5264 | 1·5262 | + 2 | + 1 |
| Fe 4184·894 (B) | *a* | 1·5270 | 1·5270 | | − 1 |
| Fe 4170·906 (B) | *a* | 1·5273 | 1·5274 | 1 | − 2 |
| Fe 4156·805 (B) | *a* | 1·5276 | 1·5278 | − 2 | − 3 |
| Fe 4143·874 (B) | *b* | 1·5279 | 1·5281 | − 2 | − 3 |
| Fe 4114·454 (B) | *a* | 1·5283 | 1·5289 | − 6 | − 8 |
| Fe 4062·451 (B) | *a* | 1·5303 | 1·5306 | − 3 | − 5 |
| Fe 4045·822 (B) | *b* | 1·5310 | 1·5310 | ± | − 2 |
| Fe 3997·398 (B) | *a* | 1·5320 | 1·5324 | − 4 | − 7 |
| | *b* | 1·5321 | | 3 | − 6 |
| Fe 3971·328 (B) | *a* | 1·5324 | 1·5335 | −11 | −14 |
| Fe 3952·606 (B) | *b* | 1·5341 | 1·5342 | − 1 | − 2 |
| Fe 3948·779 (B) | *a* | 1·5341 | 1·5343 | − 2 | − 3 |
| Fe 3935·818 (I) | *a* | 1·5342 | 1·5351 | − 9 | −10 |
| Fe 3906·482 (I) | *b* | 1·5351 | 1·5358 | − 7 | − 8 |
| Fe 3888·520 (B) | *a* | 1·5362 | 1·5364 | − 2 | − 3 |
| Fe 3865·527 (I) | *a* | 1·5373 | 1·5373 | ± | − 1 |
| W 3864·335 | *b* | 1·5373 | 1·5373 | ± | − 1 |
| Fe 3841·052 (B) | *a* | 1·5376 | 1·5382 | − 6 | − 7 |
| Fe 3821·132 (B) | *b* | 1·5384 | 1·5390 | − 6 | − 7 |
| Fe 3807·541 (B) | *a* | 1·5392 | 1·5395 | − 3 | − 4 |
| W 3796·290 | *a* | 1·5396 | 1·5400 | 4 | − 5 |
| Fe 3785·948 (B) | *a* | 1·5404 | 1·5404 | ± | − 1 |
| Fe 3774·826 (B) | *a* | 1·5408 | 1·5409 | − 1 | − 2 |
| Fe 3730·390 (B) | *a* | 1·5423 | 1·5418 | + 5 | + 4 |
| Fe 3719·938 (B) | *a* | 1·5429 | 1·5432 | − 3 | 4 |
| Fe 3647·845 (B) | *a* | 1·5465 | 1·5465 | ± | − 1 |
| Fe 3617·780 (B) | *a* | 1·5480 | 1·5480 | ± | − 1 |
| Fe 3586·115 (B) | *b* | 1·5484 | 1·5496 | −12 | −13 |
| | *a* | 1·5485 | | −11 | −12 |
| W 3575·979 | *a* | 1·5490 | 1·5501 | −11 | −12 |
| Fe 3558·522 (B) | *a* | 1·5506 | 1·5510 | − 4 | − 5 |
| Fe 3552·840 (B) | *b* | 1·5512 | 1·5513 | − 1 | − 2 |
| Fe 3540·132 (B) | *a* | 1·5519 | 1·5520 | − 1 | − 2 |
| Fe 3521·264 (B) | *a* | 1·5529 | 1·5530 | − 1 | − 2 |
| Fe 3475·653 (B) | *a* | 1·5556 | 1·5563 | − 7 | − 8 |
| W 3457·726 | *a* | 1·5567 | 1·5567 | ± | − 1 |
| W 3448·842 | *a* | 1·5570 | 1·5573 | − 3 | − 4 |
| Fe 3440·614 (B) | *a* | 1·5580 | 1·5577 | + 3 | + 2 |
| Fe 3422·665 (B) | *a* | 1·5588 | 1·5588 | ± | − 1 |
| Fe 3418·514 (B) | *b* | 1·5590 | 1·5590 | ± | − 2 |

| | Equations · | V or VI | III or IV. |
|---|---|---|---|
| Mean deviation | | ±0·00031 | ±0·00040 |
| Mean error | | −0·00024 | −0·00034 |

Table VII.—Refractive Indices of Benzene at 20° C Professor Timmermans' Specimen.

Third Series: Photographic Readings: λ = 3396 Å.U. to λ = 2708 Å.U.

| Wave-length of coincidence. | Film. | Refractive index. | | Difference $(O - C) \times 10^4$. Equation | | |
|---|---|---|---|---|---|---|
| | | *n* (observed). | *n* (calculated from equation VI) | VI | V | III. |
| Fe 3396·982 (B) | a | 1·5605 | 1·5004 | + 1 | ± | − 1 |
| Fe 3380·115 (B) | a | 1·5616 | 1·5613 | + 3 | + 3 | + 2 |
| Fe 3372·081 (B) | a | 1·5623 | 1·5621 | + 2 | + 2 | + 1 |
| Fe 3355·235 (B) | a | 1·5635 | 1·5634 | + 1 | + 2 | + 1 |
| Fe 3314·746 (B) | a | 1·5662 | 1·5662 | ± | + 1 | ± |
| Fe 3306·357 (B) | a | 1·5666 | 1·5668 | − 2 | − 1 | − 2 |
| Fe 3290·995 (B) | a | 1·5679 | 1·5679 | + | + 1 | ± |
| Fe 3286·763 (B) | c | 1·5681 | 1·5684 | − 3 | − 3 | − 3 |
| Fe 3268·246 (B) | a | 1·5700 | 1·5697 | + 3 | + 3 | + 3 |
| Fe 3265·057 (B) | c | 1·5699 | 1·5699 | ± | ± | ± |
| Fe 3253·610 (B) | a | 1·5715 | 1·5709 | + 6 | + 7 | + 7 |
| Fe 3222·070 (B) | a | 1·5732 | 1·5737 | − 5 | ± | − 1 |
| | c | 1·5733 | | − 4 | − 1 | ± |
| Fe 3207·092 (B) | a | 1·5743 | 1·5744 | − 1 | + 3 | + 4 |
| Fe 3200·847 (B) | a | 1·5753 | 1·5757 | − 4 | + 1 | + 2 |
| Fe 3193·314 (B) | a | 1·5759 | 1·5763 | − 4 | + 1 | + 2 |
| Fe 3157·877 (B) | a | 1·5792 | 1·5793 | − 1 | + 2 | + 4 |
| Fe 3151·341 (B) | a | 1·5800 | 1·5797 | + 3 | + 6 | + 8 |
| Fe 3144·488 (B) | a | 1·5807 | 1·5805 | + 2 | + 3 | + 6 |
| Fe 3134·109 (B) | b | 1·5813 | 1·5814 | − 1 | + | + 3 |
| Fe 3116·632 (B) | a | 1·5831 | 1·5830 | + 1 | ± | + 4 |
| W 3084·918 | c | 1·5864 | 1·5862 | + 2 | − 1 | + 6 |
| Fe 3083·745 (B) | a | 1·5866 | 1·5863 | + 3 | ± | + 7 |
| Fe 3057·451 (B) | a | 1·5891 | 1·5891 | ± | − 4 | + 5 |
| Fe 3047·608 (B) | c | 1·5903 | 1·5902 | + 1 | − 4 | + 6 |
| Fe 3045·082 (B) | a | 1·5906 | 1·5905 | + 1 | − 3 | + 7 |
| Fe 3025·846 (B) | a | 1·5925 | 1·5927 | − 2 | − 6 | + 5 |
| W 3011·682 | c | 1·5910 | 1·5945 | − 5 | − 9 | + 3 |
| Fe 3007·284 (B) | a | 1·5943 | 1·5949 | − 6 | −10 | + 2 |
| Fe 3000·951 (B) | a | 1·5952 | 1·5957 | − 5 | − 8 | + 4 |
| Fe 2990·394 (B) | b | 1·5959 | 1·5966 | − 7 | −11 | + 2 |
| Fe 2981·448 (B) | a | 1·5966 | 1·5980 | −14 | −18 | − 5 |
| Fe 2960·364 (B) | b | 1·5990 | 1·5996 | − 6 | −10 | + 4 |
| Fe 2959·996 (B) | a | 1·6006 | 1·6007 | − 1 | − 6 | + 9 |
| Fe 2953·943 (B) | a | 1·6012 | 1·6015 | − 3 | − 8 | + 7 |
| Fe 2947·876 (B) | b | 1·6018 | 1·6020 | − 2 | − 8 | + 8 |
| Fe 2936·903 (B) | a | 1·6036 | 1·6038 | − 2 | − 8 | +10 |
| W 2912·245 | c | 1·6065 | 1·6071 | − 6 | −15 | + 9 |
| Fe 2899·418 (B) | a | 1·6097 | 1·6094 | + 3 | − 9 | +20 |
| W 2898·252 | c | 1·6097 | 1·6095 | + 2 | −10 | +19 |
| Fe 2866·629 (B) | c | 1·6134 | 1·6145 | −11 | −33 | +11 |
| Fe 2851·800 (F) | c | 1·6156 | 1·6169 | −13 | −41 | +11 |
| W 2839·343 | c | 1·6192 | 1·6189 | + 3 | −29 | +29 |
| Fe 2825·556 (B) | c | 1·6219 | 1·6213 | + 6 | −32 | +34 |
| Fe 2794·706 (B) | c | 1·6250 | 1·6269 | −19 | −69 | +15 |
| Fe 2767·518 (B) | c | 1·6298 | 1·6321 | −23 | −142 | +13 |
| Fe 2755·736 (B) | c | 1·6332 | 1·6340 | − 8 | −157 | +29 |
| Fe 2744·072 (B) | c | 1·6364 | 1·6356 | + 8 | −174 | +40 |
| Fe 2719·037 (B) | c | 1·6418 | 1·6398 | +23 | −233 | +46 |
| Fe 2708·580 (B) | c | 1·6456 | 1·6408 | +48 | −244 | +64 |

| Equation: | VI. | V. | III. |
|---|---|---|---|
| **Mean deviation** | ±0·00056 | ±0·0027 | ±0·00077 |
| **Mean error** | −0·00007 | −0·0025 | +0·00072 |

*Comparison with previous Measurements.*—The differences between the refractive indices measured by earlier observers and those calculated from equation (VI) are set out graphically in fig. 4. The curves $a_1$, $a_2$, $a_3$ show how the values obtained by Simon ($a_3$) lie uniformly between the values found by us for the sample supplied by Professor Timmermans ($a_1$) and that prepared in this laboratory ($a_2$). Curve *b* shows the results of Gifford's* measurements, by the prism method, of the refractive indices of a sample, also purified in this laboratory, when corrected to 20° by means of his own temperature coefficients. A remarkably close agreement with our equation is found in the blue, green and red regions, where our measurements with the Pulfrich instrument exhibit

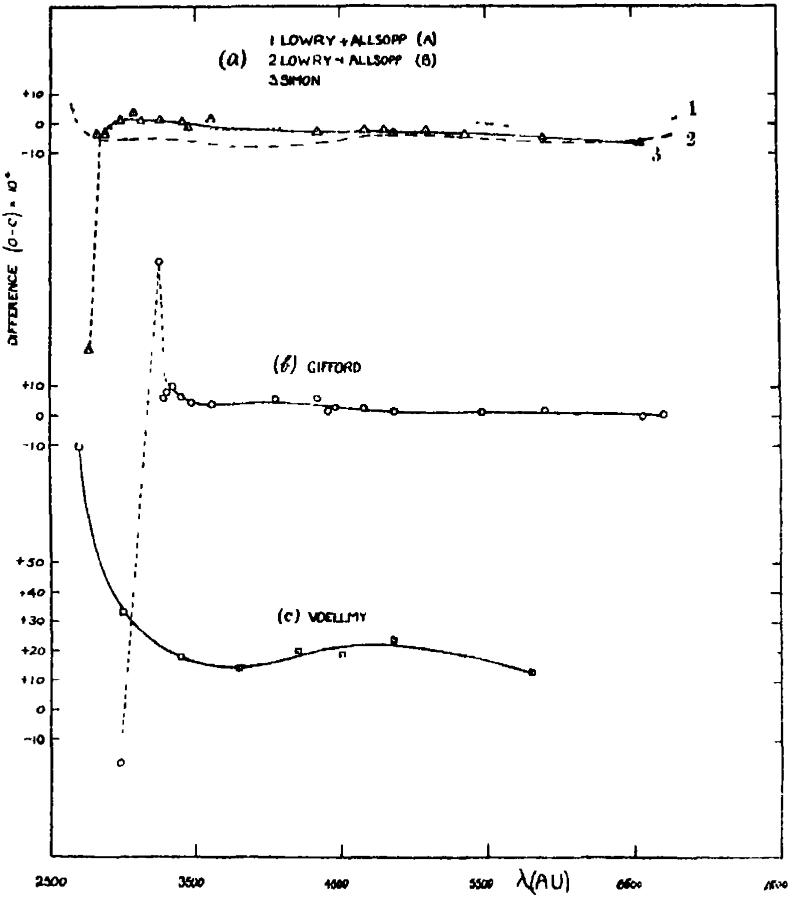

Fig 4

---

[*] Gifford, 'Proc. Roy. Soc.,' A, vol. 104, p. 430 (1923).

systematic deviations, which therefore appear once more to be due to the method of measurement and not to the properties of the material. Voellmy's* values, corrected to 20° by means of Gifford's temperature coefficients, give rise to a difference-curve *c*, which shows the same wide divergences as the difference-curve derived from his data for cyclohexane.

## *Summary.*

(1) Values are given for the refractive indices of benzene at 20° for 22 wave-lengths in the range of visual observations with a refractometer and for 122 wave-lengths in the region covered by photographic readings with an etalon.

(2) In the range of visual observations, the values deduced from observations with the refractometer are less accurate than those determined by Gifford with the help of a hollow prism, and were therefore not used in the final calculations.

(3) Gifford's data in the range of visual observations, together with our own data in the violet and ultra-violet regions, and those of Rubens in the infra-red when corrected to 20°, can be expressed by the equation

$$n^2 = 1{\cdot}51304 + \frac{0{\cdot}66992\,\lambda^2}{\lambda^2 - 0{\cdot}030170} + \frac{0{\cdot}06143\,(\lambda^2 - 0{\cdot}070171)\,\lambda^2}{(\lambda^2 - 0{\cdot}070171)^2 + 0{\cdot}0003448\,\lambda^2} - 0{\cdot}0027\,\lambda^2.$$

This equation includes one constant term, and three variable terms corresponding with frequencies in the Schumann region, in the middle ultra-violet and in the infra-red, but concordant results are only obtained when a damping factor is introduced into the middle ultra-violet term.

The authors desire to place on record their indebtedness to the Department of Scientific and Industrial Research for providing a Research Assistantship during the period in which the investigation described in the present series of papers (Parts I to III) was carried out.

---

* Voellmy, 'Z. Phys. Chem.,' vol. 127, p. 305 (1927).

# *Quantised Singularities in the Electromagnetic Field.*

By P. A. M. Dirac, F.R.S., St. John's College, Cambridge.

(Received May 29, 1931.)

## § 1. *Introduction*

The steady progress of physics requires for its theoretical formulation a mathematics that gets continually more advanced. This is only natural and to be expected What, however, was not expected by the scientific workers of the last century was the particular form that the line of advancement of the mathematics would take, namely, it was expected that the mathematics would get more and more complicated, but would rest on a permanent basis of axioms and definitions, while actually the modern physical developments have required a mathematics that continually shifts its foundations and gets more abstract. Non-euclidean geometry and non-commutative algebra, which were at one time considered to be purely fictions of the mind and pastimes for logical thinkers, have now been found to be very necessary for the description of general facts of the physical world. It seems likely that this process of increasing abstraction will continue in the future and that advance in physics is to be associated with a continual modification and generalisation of the axioms at the base of the mathematics rather than with a logical development of any one mathematical scheme on a fixed foundation.

There are at present fundamental problems in theoretical physics awaiting solution, *e.g.*, the relativistic formulation of quantum mechanics and the nature of atomic nuclei (to be followed by more difficult ones such as the problem of life), the solution of which problems will presumably require a more drastic revision of our fundamental concepts than any that have gone before. Quite likely these changes will be so great that it will be beyond the power of human intelligence to get the necessary new ideas by direct attempts to formulate the experimental data in mathematical terms. The theoretical worker in the future will therefore have to proceed in a more indirect way. The most powerful method of advance that can be suggested at present is to employ all the resources of pure mathematics in attempts to perfect and generalise the mathematical formalism that forms the existing basis of theoretical physics, and *after* each success in this direction, to try to interpret the new mathematical features in terms of physical entities (by a process like Eddington's Principle of Identification).

A recent paper by the author* may possibly be regarded as a small step according to this general scheme of advance. The mathematical formalism at that time involved a serious difficulty through its prediction of negative kinetic energy values for an electron. It was proposed to get over this difficulty, making use of Pauli's Exclusion Principle which does not allow more than one electron in any state, by saying that in the physical world almost all the negative-energy states are already occupied, so that our ordinary electrons of positive energy cannot fall into them. The question then arises as to the physical interpretation of the negative-energy states, which on this view really exist. We should expect the uniformly filled distribution of negative-energy states to be completely unobservable to us, but an unoccupied one of these states, being something exceptional, should make its presence felt as a kind of hole. It was shown that one of these holes would appear to us as a particle with a positive energy and a positive charge and it was suggested that this particle should be identified with a proton. Subsequent investigations, however, have shown that this particle necessarily has the same mass as an electron† and also that, if it collides with an electron, the two will have a chance of annihilating one another much too great to be consistent with the known stability of matter.‡

It thus appears that we must abandon the identification of the holes with protons and must find some other interpretation for them. Following Oppenheimer,§ we can assume that in the world as we know it, *all*, and not merely nearly all, of the negative-energy states for electrons are occupied. A hole, if there were one, would be a new kind of particle, unknown to experimental physics, having the same mass and opposite charge to an electron. We may call such a particle an anti-electron. We should not expect to find any of them in nature, on account of their rapid rate of recombination with electrons, but if they could be produced experimentally in high vacuum they would be quite stable and amenable to observation. An encounter between two hard $\gamma$-rays (of energy at least half a million volts) could lead to the creation simultaneously of an electron and anti-electron, the probability of occurrence of this process being of the same order of magnitude as that of the collision of the two $\gamma$-rays on the assumption that they are spheres of the same size as classical electrons. This probability is negligible, however, with the intensities of γ-rays at present available.

---

* 'Proc. Roy. Soc.,' A, vol. 126, p. 360 (1930).

† H. Weyl, 'Gruppentheorie und Quantenmechanik,' 2nd ed. p. 234 (1931).

‡ I. Tamm, 'Z. Physik,' vol. 62, p. 545 (1930); J. R. Oppenheimer, 'Phys. Rev.,' vol. 35, p. 939 (1930); P. Dirac, 'Proc. Camb. Philos. Soc.,' vol. 26, p. 361 (1930).

§ J. R. Oppenheimer, 'Phys. Rev.,' vol. 35, p. 562 (1930).

The protons on the above view are quite unconnected with electrons. Presumably the protons will have their own negative-energy states, all of which normally are occupied, an unoccupied one appearing as an anti-proton. Theory at present is quite unable to suggest a reason why there should be any differences between electrons and protons.

The object of the present paper is to put forward a new idea which is in many respects comparable with this one about negative energies. It will be concerned essentially, not with electrons and protons, but with the reason for the existence of a smallest electric charge. This smallest charge is known to exist experimentally and to have the value $e$ given approximately by*

$$hc/e^2 = 137. \tag{1}$$

The theory of this paper, while it looks at first as though it will give a theoretical value for $e$, is found when worked out to give a connection between the smallest electric charge and the smallest magnetic pole. It shows, in fact, a symmetry between electricity and magnetism quite foreign to current views. It does not, however, force a complete symmetry, analogous to the fact that the symmetry between electrons and protons is not forced when we adopt Oppenheimer's interpretation. Without this symmetry, the ratio on the left-hand side of (1) remains, from the theoretical standpoint, completely undetermined and if we insert the experimental value 137 in our theory, it introduces quantitative differences between electricity and magnetism so large that one can understand why their qualitative similarities have not been discovered experimentally up to the present.

## § 2. *Non-integrable Phases for Wave Functions.*

We consider a particle whose motion is represented by a wave function $\psi$, which is a function of $x$, $y$, $z$ and $t$. The precise form of the wave equation and whether it is relativistic or not, are not important for the present theory. We express $\psi$ in the form

$$\psi = Ae^{i\gamma}, \tag{2}$$

where A and $\gamma$ are real functions of $x$, $y$, $z$ and $t$, denoting the amplitude and phase of the wave function. For a given state of motion of the particle, $\psi$ will be determined except for an arbitrary constant numerical coefficient, which must be of modulus unity if we impose the condition that $\psi$ shall be normalised.

---

* $h$ means Planck's constant divided by $2\pi$.

The indeterminacy in $\psi$ then consists in the possible addition of an arbitrary constant to the phase $\gamma$. Thus the value of $\gamma$ at a particular point has no physical meaning and only the difference between the values of $\gamma$ at two different points is of any importance.

This immediately suggests a generalisation of the formalism. We may assume that $\gamma$ has no definite value at a particular point, but only a definite difference in values for any two points. We may go further and assume that this difference is not definite unless the two points are neighbouring. For two distant points there will then be a definite phase difference only relative to some curve joining them and different curves will in general give different phase differences. The total change in phase when one goes round a closed curve need not vanish.

Let us examine the conditions necessary for this non-integrability of phase not to give rise to ambiguity in the applications of the theory. If we multiply $\psi$ by its conjugate complex $\phi$ we get the density function, which has a direct physical meaning. This density is independent of the phase of the wave function, so that no trouble will be caused in this connection by any indeterminacy of phase. There are other more general kinds of applications, however, which must also be considered. If we take two different wave functions $\psi_m$ and $\psi_n$, we may have to make use of the product $\phi_m \psi_n$. The integral

$$\int \phi_m \psi_n \, dx \, dy \, dz$$

is a number, the square of whose modulus has a physical meaning, namely, the probability of agreement of the two states. In order that the integral may have a definite modulus the integrand, although it need not have a definite phase at each point, must have a definite phase difference between any two points, whether neighbouring or not. Thus the change in phase in $\phi_m \psi_n$ round a closed curve must vanish. This requires that the change in phase in $\psi_n$ round a closed curve shall be equal and opposite to that in $\phi_m$ and hence the same as that in $\psi_m$. We thus get the general result. – *The change in phase of a wave function round any closed curve must be the same for all the wave functions.*

It can easily be seen that this condition, when extended so as to give the same uncertainty of phase for transformation functions and matrices representing observables (referring to representations in which $x$, $y$ and $z$ are diagonal) as for wave functions, is sufficient to insure that the non-integrability of phase gives rise to no ambiguity in all applications of the theory. Whenever a $\psi_n$ appears, if it is not multiplied into a $\phi_m$, it will at any rate be multiplied into something of a similar nature to a $\phi_m$, which will result in the uncertainty of phase cancelling out, except for a constant which does not matter. For example, if $\psi_n$ is to be transformed to another representation in which, say, the observables $\xi$ are diagonal, it must be multiplied by the transformation function $(\xi\,|\,xyzt)$ and integrated with respect to $x$, $y$ and $z$. This transformation function will have the same uncertainty of phase as a $\phi$, so that the transformed wave function will have its phase determinate, except for a constant independent of $\xi$. Again, if we multiply $\psi_n$ by a matrix $(x'y'z't\,|\,\alpha\,|\,x''y''z''t)$, representing an observable $\alpha$, the uncertainty in the phase as concerns the column [specified by $x''$, $y''$, $z''$, $t$] will cancel the uncertainty in $\psi_n$ and the uncertainty as concerns the row will survive and give the necessary uncertainty in the new wave function $\alpha\psi_n$. The superposition principle for wave functions will be discussed a little later and when this point is settled it will complete the proof that all the general operations of quantum mechanics can be carried through exactly as though there were no uncertainty in the phase at all.

The above result that the change in phase round a closed curve must be the same for all wave functions means that this change in phase must be something determined by the dynamical system itself (and perhaps also partly by the representation) and must be independent of which state of the system is considered. As our dynamical system is merely a simple particle, it appears that the non-integrability of phase must be connected with the field of force in which the particle moves

For the mathematical treatment of the question we express $\psi$, more generally than (2), as a product

$$\psi = \psi_1 e^{i\beta}, \tag{3}$$

where $\psi_1$ is any ordinary wave function (*i.e.*, one with a definite phase at each point) whose modulus is everywhere equal to the modulus of $\psi$. The uncertainty of phase is thus put in the factor $e^{i\beta}$. This requires that $\beta$ shall not be a function of $x$, $y$, $z$, $t$ having a definite value at each point, but $\beta$ must have definite derivatives

$$\kappa_x = \frac{\partial\beta}{\partial x}, \qquad \kappa_y = \frac{\partial\beta}{\partial y}, \qquad \kappa_z = \frac{\partial\beta}{\partial z}, \qquad \kappa_0 = \frac{\partial\beta}{\partial t},$$

at each point, which do not in general satisfy the conditions of integrability $\partial\kappa_x/\partial y = \partial\kappa_y/\partial x$, etc. The change in phase round a closed curve will now be, by Stokes' theorem,

$$\int (\boldsymbol{\kappa},\, d\mathbf{s}) = \int (\operatorname{curl} \boldsymbol{\kappa},\, d\mathbf{S}), \tag{4}$$

where **ds** (a 4-vector) is an element of arc of the closed curve and **dS** (a 6-vector) is an element of a two-dimensional surface whose boundary is the closed curve. The factor $\psi_1$ does not enter at all into this change in phase.

It now becomes clear that the non-integrability of phase is quite consistent with the principle of superposition, or, stated more explicitly, that if we take two wave functions $\psi_m$ and $\psi_n$ both having the same change in phase round any closed curve, any linear combination of them $c_m\psi_m + c_n\psi_n$ must also have this same change in phase round every closed curve. This is because $\psi_m$ and $\psi_n$ will both be expressible in the form (3) with the same factor $e^{i\beta}$ (*i.e.*, the same $\kappa$'s) but different $\psi_1$'s, so that the linear combination will be expressible in this form with the same $e^{i\beta}$ again, and this $e^{i\beta}$ determines the change in phase round any closed curve. We may use the same factor $e^{i\beta}$ in (3) for dealing with all the wave functions of the system, but we are not obliged to do so, since only curl $\boldsymbol{\kappa}$ is fixed and we may use $\kappa$'s differing from one another by the gradient of a scalar for treating the different wave functions.

From (3) we obtain

$$-ih\frac{\partial}{\partial x}\psi = e^{i\beta}\left(-ih\frac{\partial}{\partial x} + h\kappa_x\right)\psi_1, \tag{5}$$

with similar relations for the $y$, $z$ and $t$ derivatives. It follows that if $\psi$ satisfies any wave equation, involving the momentum and energy operators **p** and W, $\psi_1$ will satisfy the corresponding wave equation in which **p** and W have been replaced by $\mathbf{p} + h\boldsymbol{\kappa}$ and $\mathrm{W} - h\kappa_0$ respectively.

Let us assume that $\psi$ satisfies the usual wave equation for a free particle in the absence of any field. Then $\psi_1$ will satisfy the usual wave equation for a particle with charge $-e$ moving in an electromagnetic field whose potentials are

$$\mathbf{A} = hc/e\ \boldsymbol{\kappa}, \qquad \mathrm{A}_0 = -h/e\,.\,\kappa_0. \tag{6}$$

Thus, since $\psi_1$ is just an ordinary wave function with a definite phase, our theory reverts to the usual one for the motion of an electron in an electromagnetic field This gives a physical meaning to our non-integrability of phase. We see that we must have the wave function $\psi$ always satisfying the same wave equation, whether there is a field or not, and the whole effect of the field when there is one is in making the phase non-integrable.

The components of the 6-vector curl $\boldsymbol{\kappa}$ appearing in (4) are, apart from numerical coefficients, equal to the components of the electric and magnetic fields **E** and **H**. They are, written in three-dimensional vector-notation,

$$\operatorname{curl}\boldsymbol{\kappa} = \frac{e}{hc}\mathbf{H}, \qquad \operatorname{grad}\kappa_0 - \frac{\partial\boldsymbol{\kappa}}{\partial t} = \frac{e}{h}\mathbf{E}. \tag{7}$$

The connection between non-integrability of phase and the electromagnetic field given in this section is not new, being essentially just Weyl's Principle of Gauge Invariance in its modern form.* It is also contained in the work of Iwanenko and Fock,† who consider a more general kind of non-integrability based on a general theory of parallel displacement of half-vectors. The present treatment is given in order to emphasise that non-integrable phases are perfectly compatible with all the general principles of quantum mechanics and do not in any way restrict their physical interpretation.

## § 3. *Nodal Singularities.*

We have seen in the preceding section how the non-integrable derivatives $\kappa$ of the phase of the wave function receive a natural interpretation in terms of the potentials of the electromagnetic field, as the result of which our theory becomes mathematically equivalent to the usual one for the motion of an electron in an electromagnetic field and gives us nothing new. There is, however, one further fact which must now be taken into account, namely, that a phase is always undetermined to the extent of an arbitrary integral multiple of $2\pi$. This requires a reconsideration of the connection between the $\kappa$'s and the potentials and leads to a new physical phenomenon

The condition for an unambiguous physical interpretation of the theory was that the change in phase round a closed curve should be the same for all wave functions. This change was then interpreted, by equations (4) and (7), as equal to (apart from numerical factors) the total flux through the closed curve of the 6-vector **E**, **H** describing the electromagnetic field. Evidently these conditions must now be relaxed The change in phase round a closed curve may be different for different wave functions by arbitrary multiples of $2\pi$ and is thus not sufficiently definite to be interpreted immediately in terms of the electromagnetic field.

To examine this question, let us consider first a very small closed curve. Now the wave equation requires the wave function to be continuous (except in very special circumstances which can be disregarded here) and hence the change in phase round a small closed curve must be small. Thus this change cannot now be different by multiples of $2\pi$ for different wave functions. It must have one definite value and may therefore be interpreted without ambiguity in terms of the flux of the 6-vector **E**, **H** through the small closed curve, which flux must also be small.

---

* H. Weyl, 'Z. Physik,' vol. 56, p. 330 (1929).

† D. Iwanenko and V. Fock, 'C. R.,' vol. 188, p. 1470 (1929); V. Fock, 'Z. Physik,' vol. 57, p. 261 (1929). The more general kind of non-integrability considered by these authors does not seem to have any physical application.

There is an exceptional case, however, occurring when the wave function vanishes, since then its phase does not have a meaning. As the wave function is complex, its vanishing will require two conditions, so that in general the points at which it vanishes will lie along a line.* We call such a line a *nodal line*. If we now take a wave function having a nodal line passing through our small closed curve, considerations of continuity will no longer enable us to infer that the change in phase round the small closed curve must be small. All we shall be able to say is that the change in phase will be close to $2\pi n$ where $n$ is some integer, positive or negative. This integer will be a characteristic of the nodal line. Its sign will be associated with a direction encircling the nodal line, which in turn may be associated with a direction along the nodal line

The difference between the change in phase round the small closed curve and the nearest $2\pi n$ must now be the same as the change in phase round the closed curve for a wave function with no nodal line through it. It is therefore this difference that must be interpreted in terms of the flux of the 6-vector **E**, **H** through the closed curve. For a closed curve in three-dimensional space, only magnetic flux will come into play and hence we obtain for the change in phase round the small closed curve

$$2\pi n + e/hc \,. \int (\mathbf{H}, \, d\mathbf{S}).$$

We can now treat a large closed curve by dividing it up into a network of small closed curves lying in a surface whose boundary is the large closed curve. The total change in phase round the large closed curve will equal the sum of all the changes round the small closed curves and will therefore be

$$2\pi \Sigma n + e/hc \,. \int (\mathbf{H}, \, d\mathbf{S}), \tag{8}$$

the integration being taken over the surface and the summation over all nodal lines that pass through it, the proper sign being given to each term in the sum. This expression consists of two parts, a part $e/hc \,. \int (\mathbf{H}, \, d\mathbf{S})$ which must be the same for all wave functions and a part $2\pi \Sigma n$ which may be different for different wave functions.

---

* We are here considering, for simplicity in explanation, that the wave function is in three dimensions. The passage to four dimensions makes no essential change in the theory. The nodal lines then become two-dimensional nodal surfaces, which can be encircled by curves in the same way as lines are in three dimensions.

Expression (8) applied to any surface is equal to the change in phase round the boundary of the surface. Hence expression (8) applied to a closed surface must vanish. It follows that $\Sigma n$, summed for all nodal lines crossing a closed surface, must be the same for all wave functions and must equal $-e/2\pi hc$ times the total magnetic flux crossing the surface.

If $\Sigma n$ does not vanish, some nodal lines must have end points inside the closed surface, since a nodal line without such end point must cross the surface twice (at least) and will contribute equal and opposite amounts to $\Sigma n$ at the two points of crossing. The value of $\Sigma n$ for the closed surface will thus equal the sum of the values of $n$ for all nodal lines having end points inside the surface. This sum must be the same for all wave functions Since this result applies to *any* closed surface, it follows that *the end points of nodal lines must be the same for all wave functions. These end points are then points of singularity in the electromagnetic field.* The total flux of magnetic field crossing a small closed surface surrounding one of these points is

$$4\pi\mu = 2\pi nhc/e,$$

where $n$ is the characteristic of the nodal line that ends there, or the sum of the characteristics of all nodal lines ending there when there is more than one. Thus at the end point there will be a magnetic pole of strength

$$\mu = \tfrac{1}{2}nhc/e.$$

Our theory thus allows isolated magnetic poles, but the strength of such poles must be quantised, the quantum $\mu_0$ being connected with the electronic charge $e$ by

$$hc/e\mu_0 = 2. \tag{9}$$

This equation is to be compared with (1). The theory also requires a quantisation of electric charge, since any charged particle moving in the field of a pole of strength $\mu_0$ must have for its charge some integral multiple (positive or negative) of $e$, in order that wave functions describing the motion may exist.

## § 4. *Electron in Field of One-Quantum Pole.*

The wave functions discussed in the preceding section, having nodal lines ending on magnetic poles, are quite proper and amenable to analytic treatment by methods parallel to the usual ones of quantum mechanics. It will perhaps help the reader to realise this if a simple example is discussed more explicitly.

Let us consider the motion of an electron in the magnetic field of a one-quantum pole when there is no electric field present. We take polar co-ordinates $r$, $\theta$, $\phi$ with the magnetic pole as origin. Every wave function must now have a nodal line radiating out from the origin.

We express our wave function $\psi$ in the form (3), where $\beta$ is some non-integrable phase having derivatives $\kappa$ that are connected with the known electromagnetic field by equations (6) It will not, however, be possible to obtain $\kappa$'s satisfying these equations all round the magnetic pole There must be some singular line radiating out from the pole along which these equations are not satisfied, but this line may be chosen arbitrarily. We may choose it to be the same as the nodal line for the wave function under consideration, which would result in $\psi_1$ being continuous. This choice, however, would mean different $\kappa$'s for different wave functions (the difference between any two being, of course, the four-dimensional gradient of a scalar, except on the singular lines). This would perhaps be inconvenient and is not really necessary We may express all our wave functions in the form (3) with the same $e^{i\beta}$, and then those wave functions whose nodal lines do not coincide with the singular line for the $\kappa$'s will correspond to $\psi_1$'s having a certain kind of discontinuity on this singular line, namely, a discontinuity just cancelling with the discontinuity in $e^{i\beta}$ here to give a continuous product.

The magnetic field **H**, lies along the radial direction and is of magnitude $\mu_0/r^2$, which by (9) equals $\frac{1}{2}hc/er^2$ Hence, from equations (7), curl $\boldsymbol{\kappa}$ is radial and of magnitude $1/2r^2$ It may now easily be verified that a solution of the whole of equations (7) is

$$\kappa_0 = 0, \qquad \kappa_r = \kappa_\theta = 0, \qquad \kappa_\phi = 1/2r \,.\, \tan \tfrac{1}{2}\theta, \tag{10}$$

where $\kappa_r$, $\kappa_\theta$, $\kappa_\phi$ are the components of $\boldsymbol{\kappa}$ referred to the polar co-ordinates. This solution is valid at all points except along the line $\theta = \pi$, where $\kappa_\phi$ becomes infinite in such a way that $\int (\boldsymbol{\kappa}, \mathbf{ds})$ round a small curve encircling this line is $2\pi$. We may refer all our wave functions to this set of $\kappa$'s.

Let us consider a stationary state of the electron with energy W. Written non-relativistically, the wave equation is

$$-h^2/2m \,.\, \nabla^2\psi = \mathrm{W}\psi.$$

If we apply the rule expressed by equation (5), we get as the wave equation for $\psi_1$

$$-h^2/2m \,.\, \{\nabla^2 + i(\boldsymbol{\kappa}, \nabla) + i(\nabla, \boldsymbol{\kappa}) - \boldsymbol{\kappa}^2\}\, \psi_1 = \mathrm{W}\psi_1. \tag{11}$$

The values (10) for the $\kappa$'s give

$$(\kappa, \nabla) = (\nabla, \kappa) = \kappa_\phi \frac{1}{r \sin\theta} \frac{\partial}{\partial\phi} = \frac{1}{4r^2} \sec^2 \tfrac{1}{2}\theta \frac{\partial}{\partial\phi}$$

$$\kappa^2 = \kappa_\phi^{\,2} = \frac{1}{4r^2} \tan^2 \tfrac{1}{2}\theta,$$

so that equation (11) becomes

$$-\frac{h^2}{2m}\left\{\nabla^2 + \frac{i}{2r^2}\sec^2\tfrac{1}{2}\theta \frac{\partial}{\partial\phi} - \frac{1}{4r^2}\tan^2\tfrac{1}{2}\theta\right\}\psi_1 = W\psi_1.$$

We now suppose $\psi_1$ to be of the form of a function $f$ of $r$ only multiplied by a function S of $\theta$ and $\phi$ only, *i.e.*,

$$\psi_1 = f(r)\, S(\theta\phi).$$

This requires

$$\left\{\frac{d^2}{dr^2} + \frac{2}{r}\frac{d}{dr} - \frac{\lambda}{r^2}\right\} f = -\frac{2mW}{h^2} f, \tag{12}$$

$$\left\{\frac{1}{\sin\theta}\frac{\partial}{\partial\theta}\sin\theta\frac{\partial}{\partial\theta} + \frac{1}{\sin^2\theta}\frac{\partial^2}{\partial\phi^2} + \tfrac{1}{2}i\sec^2\tfrac{1}{2}\theta\frac{\partial}{\partial\phi} - \tfrac{1}{4}\tan^2\tfrac{1}{2}\theta\right\} S = -\lambda S, \tag{13}$$

where $\lambda$ is a number.

From equation (12) it is evident that there can be no stable states for which the electron is bound to the magnetic pole, because the operator on the left-hand side contains no constant with the dimensions of a length. This result is what one would expect from analogy with the classical theory. Equation (13) determines the dependence of the wave function on angle. It may be considered as a generalisation of the ordinary equation for spherical harmonics.

The lowest eigenvalue of (13) is $\lambda = \frac{1}{2}$, corresponding to which there are two independent wave functions

$$S_a = \cos\tfrac{1}{2}\theta, \quad S_b = \sin\tfrac{1}{2}\theta\, e^{i\phi},$$

as may easily be verified by direct substitution. The nodal line for $S_a$ is $\theta = \pi$, that for $S_b$ is $\theta = 0$. It should be observed that $S_a$ is continuous everywhere, while $S_b$ is discontinuous for $\theta = \pi$, its phase changing by $2\pi$ when one goes round a small curve encircling the line $\theta = \pi$. This is just what is necessary in order that both $S_a$ and $S_b$, when multiplied by the $e^{i\beta}$ factor, may give continuous wave functions $\psi$. The two $\psi$'s that we get in this way are both on the same footing and the difference in behaviour of $S_a$ and $S_b$ is due to our having chosen $\kappa$'s with a singularity at $\theta = \pi$.

The general eigenvalue of (13) is $\lambda = n^2 + 2n + \frac{1}{2}$. The general solution of this wave equation has been worked out by I. Tamm.*

---

* Appearing probably in 'Z. Physik.'

## § 5 *Conclusion.*

Elementary classical theory allows us to formulate equations of motion for an electron in the field produced by an arbitrary distribution of electric charges and magnetic poles. If we wish to put the equations of motion in the Hamiltonian form, however, we have to introduce the electromagnetic potentials, and this is possible only when there are no isolated magnetic poles. Quantum mechanics, as it is usually established, is derived from the Hamiltonian form of the classical theory and therefore is applicable only when there are no isolated magnetic poles.

The object of the present paper is to show that quantum mechanics does not really preclude the existence of isolated magnetic poles. On the contrary, the present formalism of quantum mechanics, when developed naturally without the imposition of arbitrary restrictions, leads inevitably to wave equations whose only physical interpretation is the motion of an electron in the field of a single pole. This new development requires *no change whatever* in the formalism when expressed in terms of abstract symbols denoting states and observables, but is merely a generalisation of the possibilities of representation of these abstract symbols by wave functions and matrices Under these circumstances one would be surprised if Nature had made no use of it.

The theory leads to a connection, namely, equation (9), between the quantum of magnetic pole and the electronic charge It is rather disappointing to find this reciprocity between electricity and magnetism, instead of a purely electronic quantum condition, such as (1). However, there appears to be no possibility of modifying the theory, as it contains no arbitrary features, so presumably the explanation of (1) will require some entirely new idea.

The theoretical reciprocity between electricity and magnetism is perfect. Instead of discussing the motion of an electron in the field of a fixed magnetic pole, as we did in § 4, we could equally well consider the motion of a pole in the field of fixed charge. This would require the introduction of the electromagnetic potentials B satisfying

$$\mathbf{E} = \operatorname{curl} \mathbf{B}, \quad \mathbf{H} = \frac{1}{c}\frac{\partial \mathbf{B}}{\partial t} + \operatorname{grad} \mathbf{B}_0,$$

to be used instead of the A's in equations (6). The theory would now run quite parallel and would lead to the same condition (9) connecting the smallest pole with the smallest charge.

There remains to be discussed the question of why isolated magnetic poles are not observed. The experimental result (1) shows that there must be some cause of dissimilarity between electricity and magnetism (possibly connected with the cause of dissimilarity between electrons and protons) as the result of which we have, not $\mu_0 = e$, but $\mu_0 = 137/2 . e$. This means that the attractive force between two one-quantum poles of opposite sign is $(137/2)^2 = 4692\frac{1}{4}$ times that between electron and proton. This very large force may perhaps account for why poles of opposite sign have never yet been separated.

---

# *Estimation of Metals in Solution by Means of their Spark Spectra.*

By F. Twyman, F Inst.P., F.R.S , and C. Stansfield Hitchen, A.R.C.S., Ph.D

(Received May 29, 1931 —Revised August 5, 1931 )

[Plates 5, 6 ]

## *Introduction*

This paper records experiments undertaken to extend to liquids the accuracy of quantitative analysis recently attained by the spectrography of alloys. How to produce from a solution a spectrum which shall truly represent the solution, and what effect may be expected from the presence of other metals than the one under determination, are among the questions dealt with, for they must come into consideration in applying any method of quantitative spectrography of solutions.

## *The Production of the Spark.*

(*a*) *The Sparking Vessel for Liquids.*—At the outset of the investigation it became apparent that the older forms of sparking apparatus, used by Hartley, Pollok and Leonard, and others, were unsuitable for quantitative work, for it was found that, owing to incrustation of the electrodes and to decomposition of the solution around them, the spark soon became unrepresentative of the bulk of the solution

The apparatus finally devised embodies two principles which a number of trials showed to be necessary :—

(i) The spark takes place from liquid to liquid.

(ii) There is a steady feed of fresh liquid, any scum being carried away.

The apparatus consists (fig. 1) of a funnel (A) of 20 to 25 c.c. capacity, the stem of which is a long glass tube of narrow bore. Towards its lower end, the tube is bent at right angles and is sealed to a short vertical tube of larger diameter (B). The upper end of this latter tube carries a jet (C) which consists of transparent silica tubing of about 2·5 cm. length and 0·20 cm. internal diameter. The upper part of the jet is slit vertically for a distance of 0·3 cm. (see inset 1, fig. 1), the jet itself being fixed firmly in the wider tube by means of rubber tubing. Both the jet and the upper portion of the tube B are surrounded by a circular glass guard (D) which prevents dissemination of spray, and acts as a receiver. The guard has an aperture for the passage of ultra-violet rays.

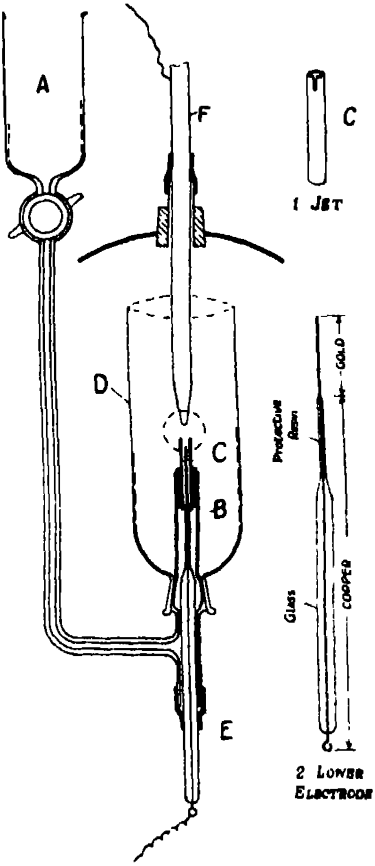

Fig. 1

The lower electrode (inset 2, fig. 1) consists of a pure gold wire, 3 cm. long and 0·7 to 1 mm. in diameter, which is welded to a copper wire of similar diameter but of greater length. Most of the latter is encased in glass tubing of such a diameter that it fits loosely within the tube B, but 3 to 4 cm. project above the glass, as shown, the exposed part being covered with bakelite up to the junction with the gold wire. The object of this arrangement is to make a short piece of gold wire suffice. Although gold is used for general work, copper, silver, or nickel can be substituted where suitable. The height of the gold electrode may be adjusted inside the jet by a short piece of rubber tubing at E, it being usual to work with the tip of the wire on a level with the base of the slit in the jet.

The upper electrode may consist of another gold wire, but latterly it has been found that a pure graphite rod (F), (0·6 cm. diameter), sharpened to a point by means of a pencil-sharpener, proves equally successful. A shield, made from a clock-glass, is attached to the upper electrode, as shown, and protects surrounding objects from spray.

The apparatus can be easily fitted to the "Gramont" form of spark stand, thus allowing the electrodes to be rapidly aligned with the spectrograph.

The mode of operation is simple and consists of turning the tap so that a slow stream of liquid passes from the funnel and gently flows over the jet into the receiver D. The spark is then applied. If the liquid is a good conductor (*e.g.*, 5 per cent. HCl), the silica jet will withstand the customary condensed spark discharge almost indefinitely; if, however, the liquid is a poor conductor the jet will usually be shattered; it is therefore necessary to render such a solution conducting by the addition of a suitable acid or alkali. The spark so formed may be expected truly to represent the bulk of the solution.

(*b*) *Electrical Equipment.*—The spark was excited by the usual transformer and auto-transformer running on A.C., voltages varying from 8000 to 15,000 (on open circuit) being obtained by suitable tappings on the auto-transformer. A condenser of 0 006 microfarad being used in parallel with the spark gap, as shown in fig 2, the arrangement produces the customary train of oscillating sparks for each alternation of the primary voltage. No additional self-induction was introduced, since, although it reduces air lines, it heats the electrodes, and also reduces the spectrographic sensitivity of an element, at least when solutions are used.

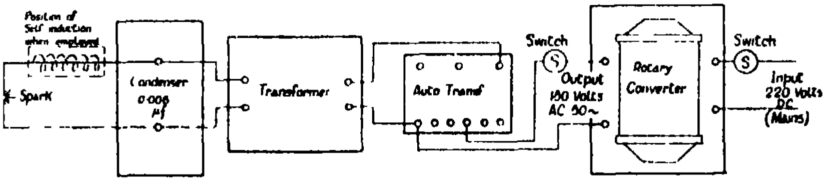

FIG 2

## *Spectrographs.*

Two quartz spectrographs were used, the dispersion of which from 8000 to 2000 A. were 67 and 24 cm. respectively.

In order that the spectrum should truly represent the whole of the radiation from the spark and that each element of the slit should be uniformly illuminated,* the following optical conditions were fulfilled.

A convex condensing lens of quartz was used to form a real image of the spark on the prism of the spectrograph, and not, as is customary, on the slit. The condensing lens was of such diameter and focal length, and was so disposed, that neither by the margin of the condensing lens nor by anything within the spectrograph were rays obstructed which by passing through each element of the slit to form the real image would thence, on being gathered by the camera lens of the spectrograph, proceed forward to form the spectrum lines on the photographic plate.

---

* Except as modified by the "wedge section" to be described later.

### *Photometric Apparatus.*

Quantitative spectrum analysis is now usually based on correlating the intensity of spectral lines with percentage composition.*

By the use of the logarithmic wedge sector, as will be seen, it is possible to determine the relative intensities of spectral lines; but, for reasons to be stated later, we have preferred to use, in plotting the graphs, not the relative intensities of the lines, but the phenomenon observed, namely, "lengths of the lines"

The next point to consider is that factors such as electrical and photographic conditions, and length of exposure, affect the intensities. In order to circumvent such difficulties we have introduced an "internal standard"† by adding to each solution to be tested a definite known amount (say 1 to 10 per cent.) of a metal that will not be liable to occur in the sample as impurity, and whose spectrum will yield lines near to the lines of the element which it is desired to estimate spectrographically. Then, following Gerlach's procedure, a line given by the latter metal is selected and measured in relationship to a suitable line given by the "internal standard" metal. If suitable line pairs are chosen small variations in exposure, or electrical or photographic conditions, affect the intensities of both lines alike, the ratio of the intensities remaining constant. Since the percentage of the standard element present is known, a correlation can be made between relative intensity and percentage composition, and this correlation is not affected by accidental variations of the factors mentioned. When a specimen contains a very large amount of one element, the addition of an internal standard can often be omitted since lines of the major constituent can then be selected as standards for comparison, as has been done for instance in determining the minor constituents in alloy steels ‡

The intensities of the lines required for quantitative spectrum analysis have been measured by various observers in a number of ways, from simple visual inspection to measurement by microphotometer.

---

* Though other methods have been, and still are, successfully used.

† The use, as a standard, of one of the lines of the main substance, is known as Gerlach's "internal standard" method (see W. Gerlach, 'Z. Anorg. Chemie,' vol. 142, p. 383 (1925); and E. Schweitzer, *ibid.*, vol. 164, p. 127 (1927).

‡ Twyman and Fitch, 'J. Iron & Steel Inst.,' 1930, No. 2, p. 289.

In planning the present investigation we have considered the relative advantages of these methods, and have actually tried four of them, those, namely, of Occhialini (*loc. cit.*), of Barratt, and of Twyman, and finally the method of wedge spectra as obtained by a rotating sector. We have chosen the last, since although the Barratt and Twyman methods, in favourable circumstances and used visually, are more accurate, yet the rotating sector not only gave good accuracy throughout all the experiments tried (whether on alloys or solutions, or, in experiments now in progress, on powders), but is simpler and much more rapid than any of the others except in certain instances where the determination consists only of finding the relative percentages present of two metals which give suitable lines in the visible spectrum.

The rotating sector has already been used in estimating the constituents of alloy steels.* Wedge spectra, first used by Mees† for rapidly measuring the colour sensitiveness of photograph plates, and the absorption of dyes, have also been employed by Merton,‡ and later by Dobson and others. The rotating sector was used by Holst and Hamburger,§ but was first applied to spectrum analysis by Scheibe and Neuhausser.‖

The sector used by us is illustrated in fig 3, and consists of a metal disc, the periphery of which is cut to conform to the equation

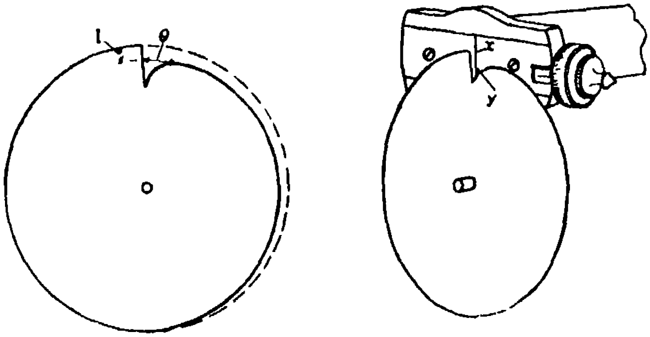

Fig. 3.

$$-\log\theta = 0{\cdot}3 + 0{\cdot}2\,l,$$

where θ represents the circumferential aperture, expressed as a fraction of a

* Twyman and Fitch, *loc. cit.*

† Mees and Wratten, 'Br. J. of Photography,' p. 384 (1907).

‡ Nicholson and Merton, 'Phil. Trans.,' A, vol. 216, p. 459 (1916).

§ 'Verh. K. Akad. Wet. Amsterdam,' vol. 20, p. 1021 (1918).

‖ Scheibe and Neuhausser, 'Z. Angew. Chem.,' vol. 41, p. 1218 (1928), Twyman and Simeon, 'Trans. Opt. Soc.,' vol. 31, p. 169 (1930); Twyman and Fitch, *loc. cit.*

complete circle at distance $l$ measured radially inwards from the outermost part of the periphery, $l$ being expressed in millimetres, while 0·3 and 0·2 are constants which are found in practice to give a convenient sector. The greatest value of $l$ is 13·5. The disc when rotated immediately in front of the spectrograph as shown in fig 3B exposes the slit to the radiation of the spark for lengths of time which vary along the length of the slit, the top portion, "$x$," receiving light from the source during half the revolution, while the bottom, "$y$," is exposed for only 1/1000 revolution. The effect of this arrangement is to produce "wedge-spectra" (illustrated in fig. 5)* in which the length of a line is a measure of its intensity, and hence of the amount of the element to which its presence is due. The sector is accordingly used to produce by spectrography, from graded standard specimens of known composition, graphs which can be referred to for the analysis of other specimens of unknown composition. Fuller details concerning the principles of its use are given by Twyman and Simeon (*loc cit*).

In their first paper on wedge-sector spectrography, Scheibe and Neuhausser took the *ratio*

$$\frac{\text{Length of line of standard}}{\text{Length of line of element to be estimated}}$$

and plotted this against percentage composition. The method employed in this present paper however, is that advocated by Twyman and Simeon, in which the *difference* between the length of the line of the standard and that of the line of the element to be estimated is plotted against percentage composition. This difference is proportional to the logarithm of the relative intensities of the lines, so that if the lengths of these lines are $l_1$ and $l_2$

$$l_1 - l_2 = \mathrm{A} \log (\mathrm{I}_1/\mathrm{I}_2),$$

A = $1/0{\cdot}2p$, where $p$ is what we may call, for brevity, the Schwarzschild constant provided we remember that we are here concerned with the threshold of blackening of the plate and with intermittent exposures. A is a constant under the experimental conditions obtaining in these experiments, except perhaps for the very low intensities †

---

* It has not been found possible to reproduce the photographs themselves in a satisfactory way. Fig. 5 has been produced by drawing to elucidate the text.

† Twyman and Simeon, *loc. cit.* The paper does not establish the relation quite conclusively, nor are we aware of any published data quite to the point. We have therefore determined A experimentally, and find that it may be taken as a constant to the limit of accuracy of these experiments, except possibly for very low intensities. A more thorough investigation of the matter is now being carried out.

## *Photography.*

Since the method depends on the observer deciding what is the precise point at which a line terminates, a photographic plate and method of development must be selected which are favourable to that purpose. We have used in these experiments rapid process panchromatic plates with a restrained caustic-hydroquinone developer. We have thought it desirable to give full details in the appendix.

In the course of their investigations on the quantitative spectrographic analysis of steels, Twyman and Fitch very carefully controlled the time and temperature of development by the use of a special tank constructed on the lines indicated by Dobson, Griffiths and Harrison; they found, however, that such precautions procured no perceptible increase of accuracy under the circumstances of their investigation. Twyman and Fitch also tried methods suggested by Merton for rendering more definite the end points of lines obtained by wedge spectra, also without advantage. Accepting the conclusions of Twyman and Fitch, we have not tried using these refinements of procedure in the present series of measurements. It may be that in any future measurements on solutions they would be worth another trial. We have found that although the sector plus spectrograph measurements on any one solution show no greater or less consistency than do those on any one alloy, yet if in series of measurements graphs are plotted of "lengths of lines" against percentage composition there is a greater irregularity in the graphs for alloys than in those for solutions, and we are inclined to attribute some at least of the irregularities to unreliability of the methods of chemical analysis in vogue.

## *General Experimental Procedure.*

The apparatus having been arranged as shown in fig. 4 (Plate 5), the electrodes and condensing lens are brought into alignment with the slit of the spectrograph, the slit adjusted to a width of 0·02 mm and the logarithmic sector placed immediately in front of it. There should be a space of 2 to 5 mm. between the top of the sector and the top of the slit. This causes a continuously exposed strip to be photographed at the bottom of the wedge spectrum, and thus provides a base for measurement of the length of the lines. The liquid to be examined is poured into the sparking apparatus, and the flow adjusted as described under "the production of the spark," the spark is applied, the sector started, and the exposure commenced and continued for a sufficient time, namely, 2 minutes for the copper, zinc, lead and bismuth, which were studied

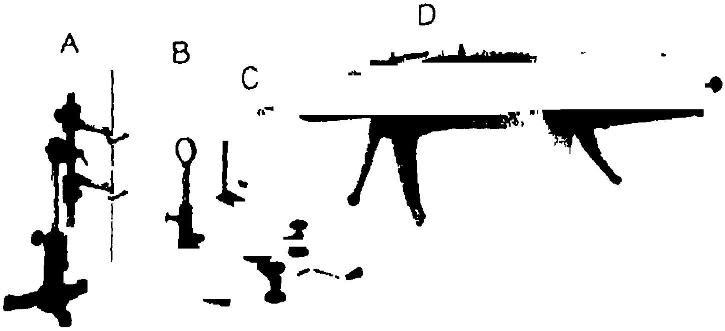

Fig. 1

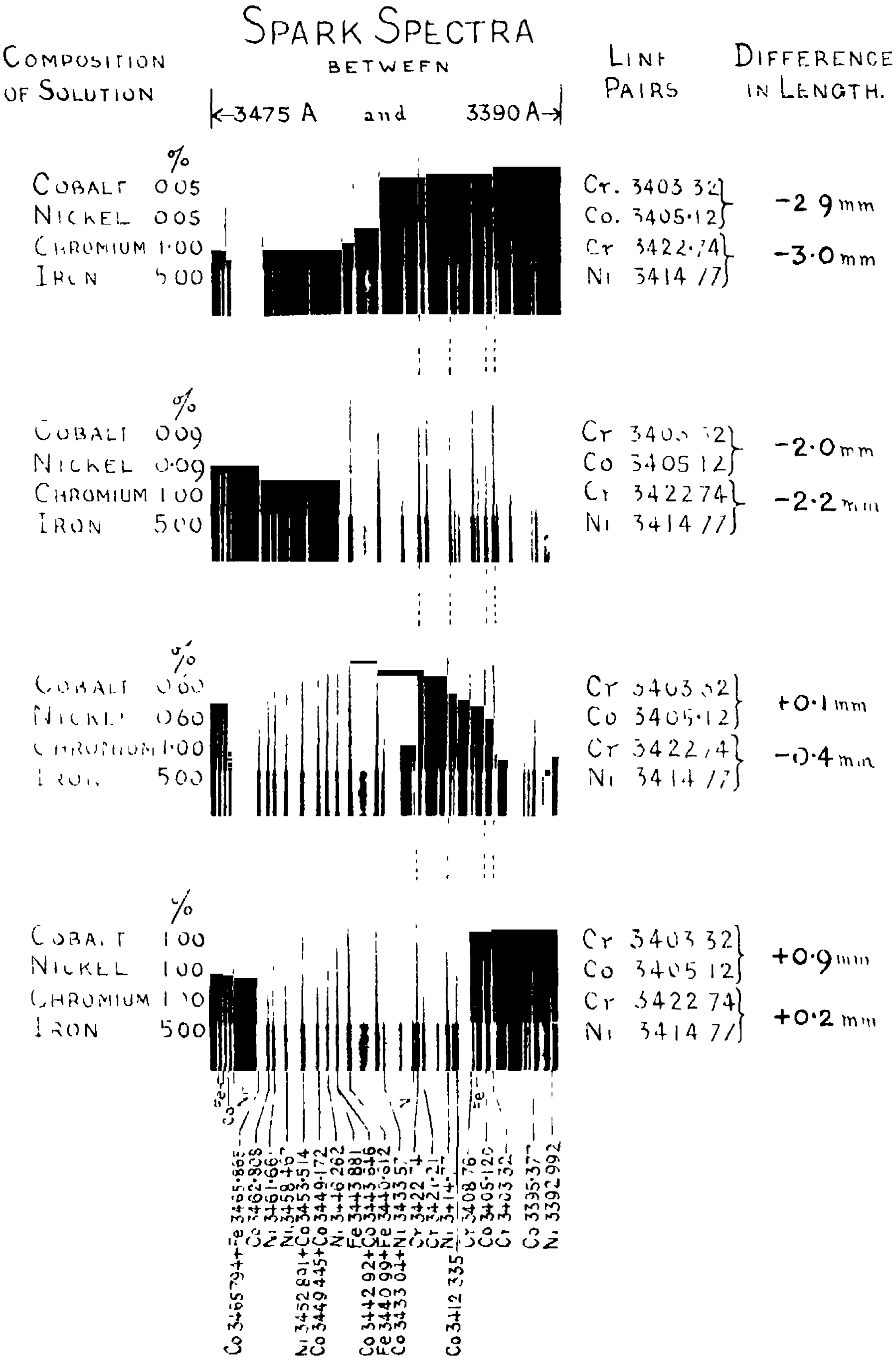
SPARK SPECTRA
BETWEEN
←3475 A and 3390 A→
COMPOSITION OF SOLUTION
LINE PAIRS
DIFFERENCE IN LENGTH.
%
COBALT 0·05
NICKEL 0·05
CHROMIUM 1·00
IRON 5·00
Cr. 3403 32
Co. 3405·12
−2·9 mm
Cr 3422·74
Ni 3414 77
−3·0 mm
%
COBALT 0·09
NICKEL 0·09
CHROMIUM 1·00
IRON 5·00
Cr 3403 32
Co 3405 12
−2·0 mm
Cr 3422 74
Ni 3414 77
−2·2 mm
%
COBALT 0·60
NICKEL 0·60
CHROMIUM 1·00
IRON 5·00
Cr 3403 32
Co 3405·12
+0·1 mm
Cr 3422 74
Ni 3414 77
−0·4 mm
%
COBALT 1·00
NICKEL 1·00
CHROMIUM 1·00
IRON 5·00
Cr 3403 32
Co 3405 12
+0·9 mm
Cr 3422 74
Ni 3414 77
+0·2 mm
Fe
Co
V
V
Fe
Co 3465 794+Fe 3465 865
Co 3462 808
Ni 3461 66
Ni 3458 467
Ni 3452 891+Co 3453 514
Co 3449 445+Co 3449 172
Ni 3446 262
Fe 3443 881
Co 3442 92+Co 3443 646
Fe 3440 99+Fe 3440 612
Co 3433 04+Ni 3433 57
Cr 3422 74
Cr 3421 21
Ni 3414 77
Co 3412 335
Cr 3408 76
Co 3405·120
Cr 3403 32
Co 3395·37
Ni 3392 992

FIG. 5.

on the smaller spectrograph, and 3 minutes for the nickel and cobalt, for which the larger spectrograph was used.

### *Selection and Measurement of Lines.*

The full advantage of the "internal standard" method is only secured if suitable lines are chosen in the spectrum of the internal standard metal and in that of the metal to be estimated. The choice of lines in the spectrum of the latter element will often be confined to its persistent lines or *raies ultimes*,* which enable it to be estimated in quantities down to its limit of spectrographic sensitivity. For the estimation of the element in larger amounts, a less intense line may be chosen. Since it is desirable that the line or lines of the internal standard should lie reasonably near to the line of the element to be estimated, it is obvious that the choice of the former is also limited. No line should be used which is not sharp and of marked intensity. Although it is difficult to lay down any definite rule as regards proximity, satisfactory results should be obtained when the lines measured are not separated by a greater distance than 2 cm. on the photographic plate, a much smaller distance is, however, desirable. In selecting lines it is of the utmost importance to see that they do not coincide with lines of any other element which is likely to be present; in ascertaining this Kayser's "Tabelle"† is invaluable.

Since in the spark spectrum the relative intensities of the lines emitted by neutral and ionised atoms are dependent on the amount of capacity and self-induction in the circuit, it is necessary to see that these remain unaltered throughout the experiments. For analytical purposes, E. Schweitzer‡ selects those pairs of lines (one of the internal standard and the other of the element) whose relative intensities are practically independent of the discharge conditions. Such lines he terms "homologous pairs" of lines. For standardising discharge conditions (*i.e.*, self-induction and capacity), Schweitzer selects two other lines of the internal standard or major constituent, one an arc line and the other a spark line, *i.e.*, lines the ratio of the intensities of which will be *most* affected by discharge conditions, and makes discharge conditions standard when these latter lines are of equal intensity. Selection of such lines for standardisation of the discharge is certainly advantageous but cannot always be complied with in practice owing to the diverse distribution of lines. When the logarithmic sector is employed, however, a constant difference of length between two non-homologous lines of the internal standard may serve as a criterion for the standardisation of discharge conditions, and a greater choice of suitable lines is thus afforded.

---

* These lines as given by various observers will be found in "Wave-length Tables for Spectrum Analysis," 2nd ed., Twyman and Smith (Adam Hilger, Ltd.)

† Kayser, 'Tabelle der Hauptlinien der Linienspektra aller Elemente,' Julius Springer, Berlin W9., 1926.

‡ 'Z. Anorg. Chemie.,' vol. 164, p 127 (1927).

The measurement of the lines is effected by examining the negative in transmitted light with an X-12 eye-piece fitted with a 20 mm. scale divided into tenths of a millimetre. Length is measured from the top of the continuously exposed spectrum to the point where the wedge line terminates (see fig. 5, Plate 6). With a little practice terminations can usually be located by any one individual within 0·2 mm., though some lines give less definite readings than this. As pointed out by Twyman and Fitch, a spectrogram in which the selected standard line differs from its customary length under similar conditions by more than 1·5 to 2·0 mm. should be discarded, since it has been observed that the differences in the lengths of the lines in such cases often prove unreliable.

### *Results.*

The experiments which have been carried out may be divided into two series. The first was conducted with a view to constructing curves connecting lengths of lines with percentages for metals having spectra of relatively few lines, and were accordingly made with the smaller spectrograph. The elements examined were in the form of chlorides and consisted of copper, zinc, bismuth, and lead, cobalt being used for the internal standard. The lead chloride was dissolved in the usual concentrated hydrochloric acid containing approximately 30 per cent HCl by weight. All the other salts were dissolved in dilute hydrochloric acid (approximately 5 per cent. HCl by weight).

The second series of experiments was carried out using the larger quartz spectrograph, the object being to construct similar curves for metals with complex spectra, and also to note how much such curves were influenced by the presence of definite amounts of other elements. The two metals selected for estimation in the second series of experiments were nickel and cobalt, chromium being used for the internal standard. The influence of 10 per cent. and 5 per cent. of iron, 5 per cent. and 2·5 per cent. of copper, and 10 per cent. of iron + 5 per cent. of copper upon the curves for nickel and cobalt was then found.

In both series of experiments the general procedure was to prepare for each metal (or mixture) a graded set of 19 solutions each of 100 c.c. and containing the elements to be investigated in amounts ranging from 0·01 per cent. to

1·00 per cent. In the second group of experiments each solution contained nickel and cobalt together in equal quantities.

The results were tabulated as shown for the range of 19 copper solutions containing from 1 per cent. down to 0·01 per cent. of copper. The remaining tables are omitted for reasons of space; but the curves are given for the whole of the solutions.

### *Results.—First Series.*

*Copper.*—Range 0·01 per cent. to 1·00 per cent. Internal standard. Cobalt, 1 per cent.; solution of chlorides in 5 per cent. HCl

| Percentage Cu | Length Co line 3405·120A | Length Cu line 3247 548A | Difference | Percentage Cu | Length Co line 3405 120A | Length Cu line 3247 548A | Difference. |
|---|---|---|---|---|---|---|---|
| | mm | mm | mm | | mm | mm | mm |
| 1·00 | 7·0 | 10·5 | +3·5 | 0·09 | 7·0 | 7·1 | +0·1 |
| 0·90 | 7·1 | 10·5 | +3·4 | 0·08 | 7·1 | 7·0 | −0·1 |
| 0·80 | 7·2 | 10·0 | +2·8 | 0·07 | 6·8 | 6·5 | 0·3 |
| 0·70 | 7·1 | 10·0 | +2·9 | 0·06 | 8·0 | 7·6 | −0·4 |
| 0·60 | 7·0 | 9·7 | +2·7 | 0·05 | 7·0 | 6·6 | −0·4 |
| 0·50 | 7·1 | 9·4 | +2·3 | 0·04 | 7·0 | 6·4 | −0·6 |
| 0·40 | 7·1 | 9·5 | +2·4 | 0·03 | 7·0 | 6·2 | −0·8 |
| 0·30 | 7·5 | 9·1 | +1·6 | 0·02 | 7·2 | 6·2 | −1·0 |
| 0·20 | 6·9 | 8·1 | +1·2 | 0·01 | 7·1 | 5·8 | −1·3 |
| 0·10 | 7·2 | 7·7 | +0·5 | | | | |

These results plotted in fig. 6

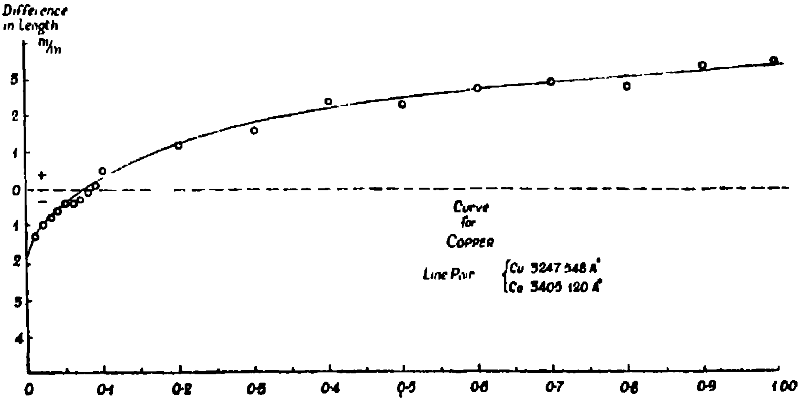

FIG. 6

*Zinc.*—Range 0·01 per cent. to 1·00 per cent. Internal standard: Cobalt, 1 per cent. Solution of chlorides in 5 per cent. HCl.

Results plotted in fig. 7.

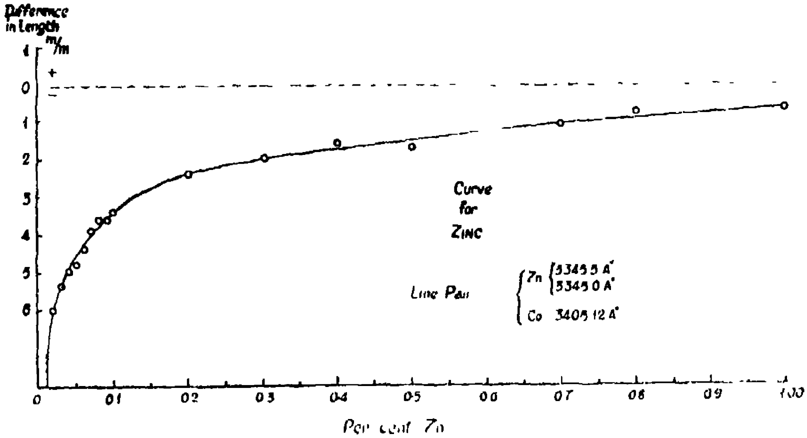

Fig. 7

*Bismuth.*—Range 0·01 per cent to 1·00 per cent. Internal standard: Cobalt, 1 per cent. Solution of chlorides in 5 per cent. HCl.

(The standard cobalt line coincides with the bismuth line 3405·23 A., but the latter does not occur in the spectra of solutions containing 1 per cent. or less of bismuth.)

Results plotted in fig. 8.

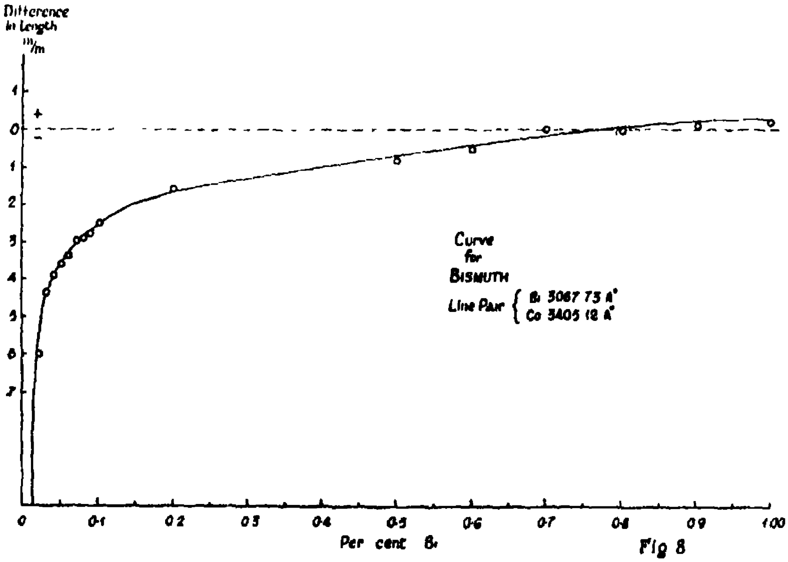

Fig. 8.

*Lead.*—Range 0·01 per cent. to 0·90 per cent. Internal standard: Cobalt, 1 per cent. Solution of chlorides in 30 per cent. HCl.

(The lead line 4057·830 A. coincides with the cobalt lines 4058·19 A. and 4057·19 A., but these do not appear under the present conditions. This lead line cannot be used in presence of large amounts of cadmium and manganese.)

Results plotted in fig. 9.

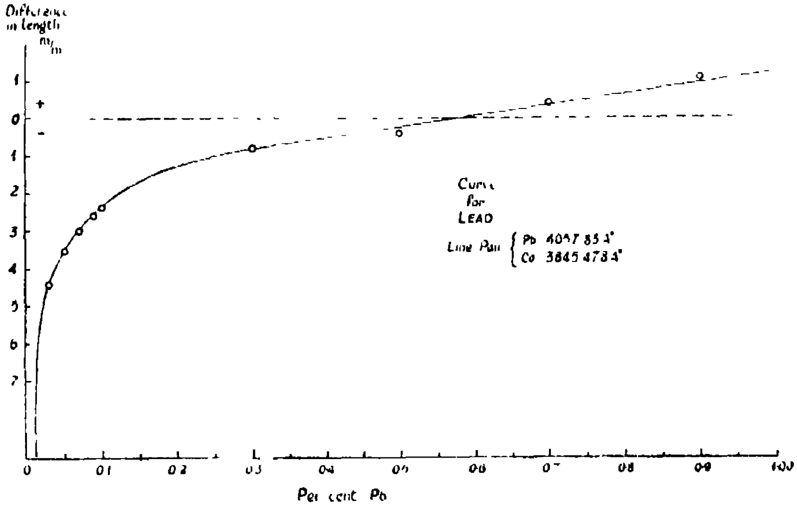

FIG. 9

## *Second Series.*

*Cobalt and Nickel.*—Range 0·01 per cent. to 1·00 per cent. Internal standard: Chromium, 1 per cent. Solutions in chlorides in 5 per cent. HCl.

*Data from which modified curves are plotted.*

*Cobalt and Nickel.*—Range 0·01 per cent. to 1·00 per cent. Internal standard 1 per cent. Chromium. Solutions of chlorides in 5 per cent. HCl, 10 per cent. of iron being present in one set of measurements and 5 per cent. in the other.

Results plotted in figs. 10 and 11.

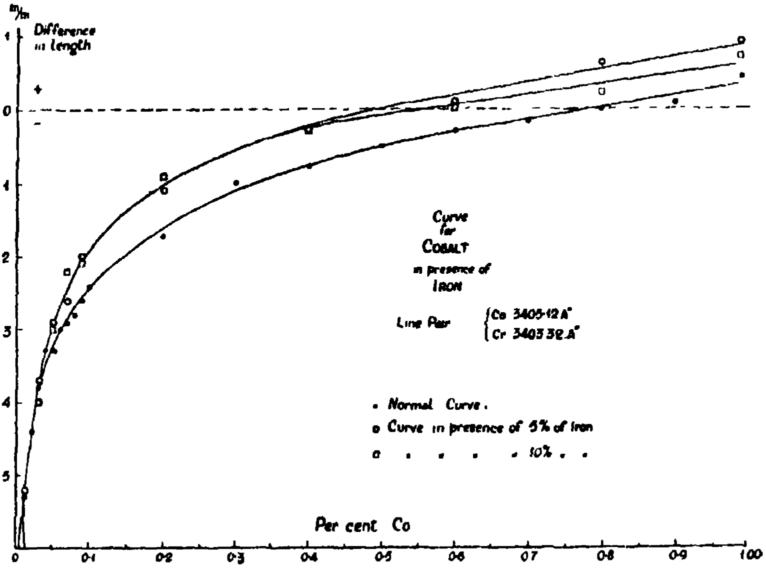

Fig. 10.

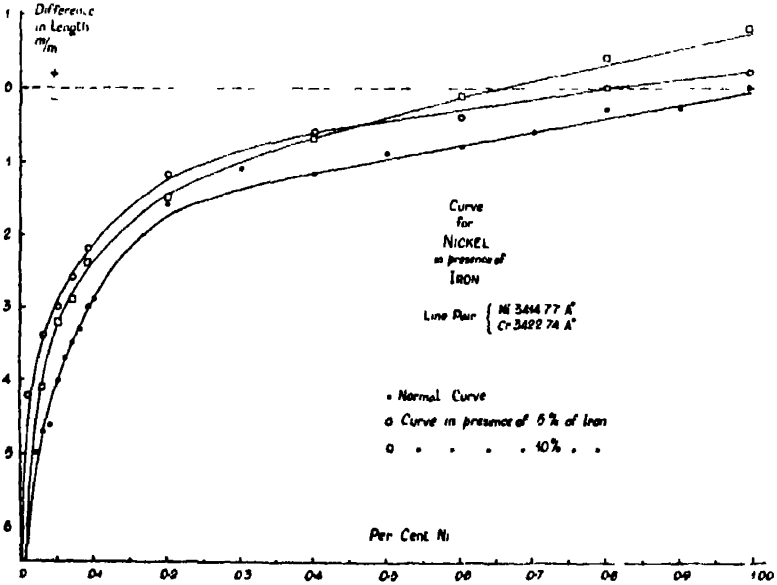

Fig. 11.

*Cobalt and Nickel.*—Range 0·01 per cent. to 0·90 per cent. Internal standard: 1 per cent. chromium. Solutions of chlorides in 5 per cent. HCl, 5 per cent. of copper being present in one set of measurements and 2·5 per cent. in the other.

Results plotted in figs. 12 and 13.

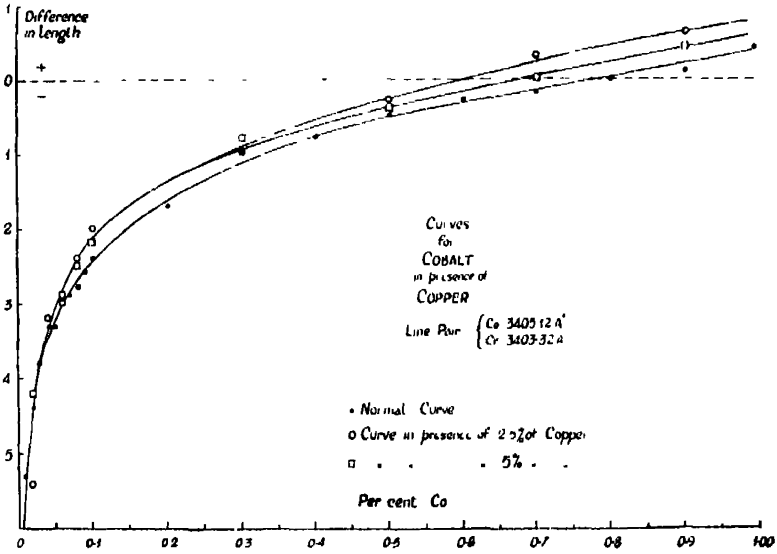

FIG. 12

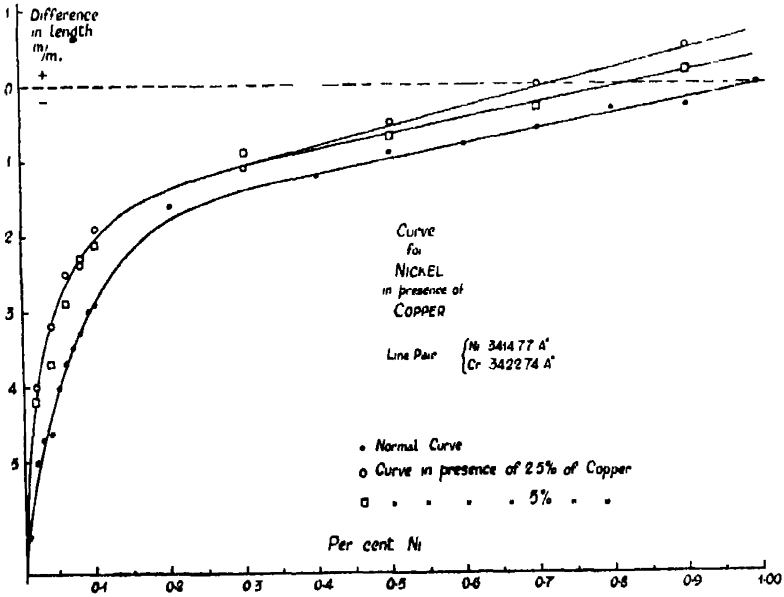

FIG. 13.

***Cobalt and Nickel*** in presence of iron and copper.

Range 0·01 per cent. to 1·00 per cent. Internal standard: chromium, 1 per cent. Solutions of chlorides in 5 per cent. HCl. 10 per cent. of iron + 5 per cent. of copper being present.

Results plotted in figs. 14 and 15.

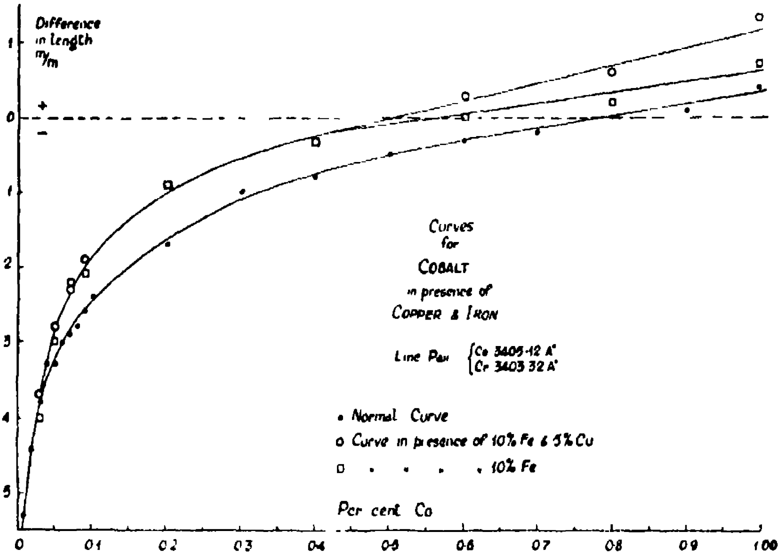

FIG 14

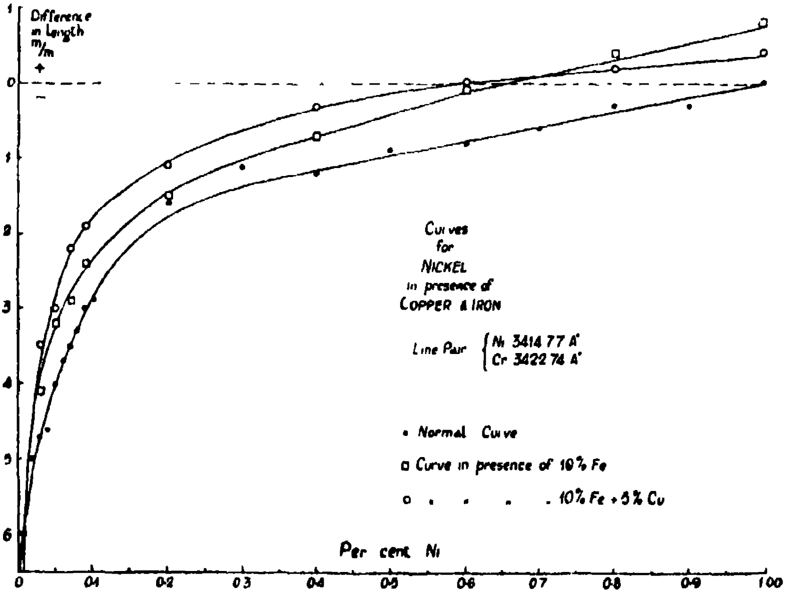

FIG. 15.

### *Discussion of Results.*

If differences of length are plotted as ordinates against log per cent. as abscissæ graphs are obtained, which in all cases are straight lines down to percentages of 0·1 to 0·2 The results for cobalt exhibit this feature very clearly (fig. 16).

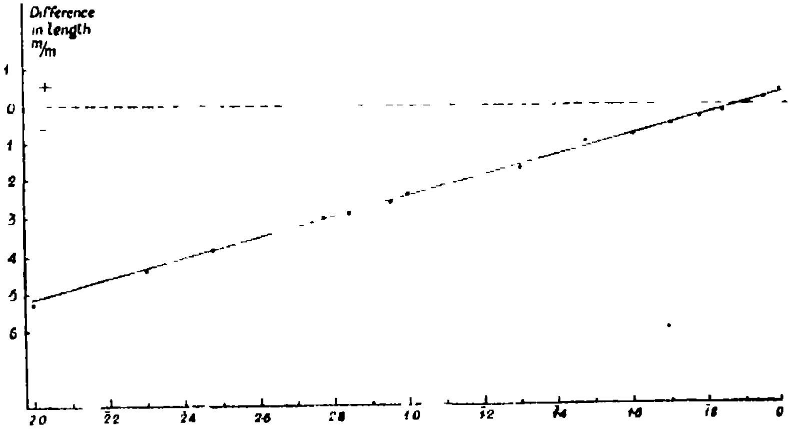

Fig. 16

The relative intensities of the lines can be found from the differences in their lengths by the formula on page 77. It has been found by us experimentally that the Schwarzschild constant, under the conditions of use of the sector described in this paper, is very close indeed to unity. We have determined these relative intensities and plotted graphs corresponding with figures 6 to 15, but in which the relative intensities are plotted against percentages as abscissæ Although all these graphs are straight lines for all the percentages except where the latter are very small (0·1 to 0·2), below this there is a departure from the straight line law which we have some reason to attribute to the Schwarzschild constant not holding for the very low intensities of illumination It is known, too, in the case of the spark spectra of solids, that for considerable percentages, and for some spectral lines (the *raies ultimes* for instance) the intensity does not increase uniformly with the percentage.

Thus, although the method here described doubtless affords data from which the relative intensities can be found, we have in the graphs here published preferred to use the observed data rather than the relative intensities determined therefrom. The degree of complexity of the relationship between percentage and intensity of spectrum line does not invalidate the empirical use of the method as a means of analysis, once the necessary graphs have been prepared under defined conditions from specimens of known composition, although where the linear relation holds it is of course advantageous since two specimens of known composition then suffice for drawing a graph.

A survey of the first four curves for copper, zinc, bismuth, and lead shows that the error does not often exceed 10 per cent. of the quantity of the element present. As far as small quantities are concerned, *i e.*, below 0·10 per cent., such an error compares very favourably with ordinary analytical methods except particularly accurate colorimetric ones In a few of the measurements, possibly where spark conditions have been somewhat variable, errors of 15 to 20 per cent. have arisen. In order to guard against such errors in practice it is advisable to take two spectrograms of each sample. The extra time required for such a precaution would only amount to 2 or 3 minutes.

Coming now to a consideration of the spectrographic estimation of nickel and cobalt, it will be observed that the curves are modified by the presence, in solution, of iron or copper. It will be further noted that in each case the modified curve lies above the normal curve.

We have made a number of observations with a view to establishing some general principles underlying the effect of the presence of various metals on the determination of other metals. We have not succeeded in establishing such general principles, and have therefore omitted these observations, partly for reasons of space, but chiefly because we see no useful purpose in connection with chemical analysis that would be served by their inclusion. Such general principles as those sought would doubtless depend in a very complex way on such factors as (1) the proportions of the vapours of the metals present in the spark-gap; (2) the ionisation potentials of the metals; and (3) the voltage of the spark and the nature of its oscillation.

That variation of the kind referred to does occur is, however, a fact of prime importance which cannot be disregarded in using spectrography for analysis. Fortunately, it is a very simple matter to determine in the way described the effect of the various metallic constituents in any class of solutions which may be of interest. A single spectrogram will then reveal in any solution of that class the whole of the metallic constituents, with the percentages present, to a first approximation. Corrections can then be applied of the amounts shown to be necessary by the first approximation.

### *General Application of the Method.*

It may be well to describe some types of analysis of metals in solution which are indicated by these experiments.

If the metal to be estimated spectrographically be called " A," the metal employed as an internal standard " B," and any other metals present in solution $C_1$, $C_2$, $C_3$, etc., then some of the cases which will normally present themselves in practice may be conveniently stated and discussed thus :—

*Case I*—The solution contains " A " alone in unknown amount from 0·01 to 3 per cent

In this case a definite quantity (say, 1 to 5 per cent.) of a selected internal standard " B " is added to the set of known solutions of " A " used in preparing the graph, and to any unknown solution of " A " thenceforward to be determined. No difficulties should present themselves either in the preparation of a graph in the manner described in this paper, or in its employment in spectrographic determinations of like solutions of " A," and an accuracy of 5 to 10 per cent. of the percentage of " A " present should normally be attained.

*Case II.*—The solution contains " A " (0·01 to 3·00 per cent.) and another element " C " (1 to 10 per cent.), this latter occurring in practically the same known amount in every sample.

In these circumstances it is possible that " C " may serve the purpose of an internal standard since it is present in constant amount. If the spectrum given by " C " is unsuitable as an internal standard, another element " B " must be added for that purpose and the graph obtained, although modified by the presence of " C," can be used for spectrographic determinations because the concentration of " C " remains the same in every sample.

*Case III.*—The solution contains " A " (0·01 to 3·00 per cent.) and another element " C " in unknown amount, which latter may vary between wide limits.

Here difficulty may be experienced in obtaining accurate results spectrographically owing to the fact that widely varying amounts of " C " will cause variation of intensity of the spark-spectrum lines due to " A " and also of those due to " B " if this latter element has been added.

It may so happen that " C," if a major constituent, will in any case be determined accurately by chemical means or that it can be quickly determined volumetrically. If " C " is thus determined, the amount of it in solution can be easily adjusted to a certain fixed concentration either by simple dilution or by addition of a standard solution of "C." The case then becomes essentially the same as Case II.

If "C" cannot be conveniently estimated, it may still be possible, in many instances, spectrographically to determine "A," although results may not be so accurate as in the simpler cases set out above. If the element "C" yields a spectrum such that it can be used as an internal standard, the preparation of the necessary graph and subsequent estimation of "A" may be effected by adding a large excess or even saturating the solution with "C" and using its persistent lines (*raies ultimes* and sensitives) as standards for comparison. This procedure is based on two facts. First, it is well known that with high concentration of an element, the intensities of the persistent lines in its spectrum remain almost unaffected by further small increments in the amount of the element present. Secondly, variation in the intensities of the lines due to "A" caused by varying amounts of "C" tends to a minimum when concentration of the latter is high. In certain cases this appears to hold good even when the intensities of the lines of "A" are compared with those of an added internal standard "B" Thus, referring to the curve for cobalt in presence of iron, fig. 10, it will be found that the results for this element, whether in presence of 5 per cent. or 10 per cent. of iron, lie on the same curve, up to a percentage of about 0·5 per cent of cobalt.

It may be added more generally that, in order to obtain the most satisfactory results by spectrographic methods, it is necessary to have some knowledge of the amounts of major constituents present in the solution so that their concentration may be controlled. Where the major constituents of a sample are first determined accurately by chemical methods (or partially removed), the spectrograph should provide convenient and rapid means of determining minor constituents, while in some cases it will be found possible to obtain results of reasonable accuracy by following such procedures as have been outlined above, without determining the major constituents.

For the sake of simplicity it has been assumed in the above statements that only one element is being estimated spectrographically; in practice, however, it should be found possible to estimate a number of minor constituents simultaneously provided the concentration of major constituents can be adjusted either to fixed standard amounts or to approximate amounts such that their presence will cause but little variation in the intensities of the lines of the estimated elements.

It may be concluded, therefore, that the method described for the spectrographic analysis of solutions of metals for minor constituents offers as great advantages as those realised in the spectrographic analysis of alloys, among such advantages being the following :—

(1) The method is rapid.

(2) The accuracy as regards amounts up to 0·50 per cent. is equal to that usually obtained by ordinary chemical methods, even where the chemical separations are easy. Further, the accuracy, unlike that of an ordinary analytical determination, when stated as a percentage of the percentage present, remains constant even when the percentage is very small. Thus, for percentages less than 0·5 the spectrographic methods could usually be substituted with advantage for the chemical ones.

(3) Where difficult or complicated separations are involved, the spectrographic methods often reveal unexpected errors in the chemical analyses, or discrepancies between the findings of independent analysts, and in such instances the spectrographic method would appear to be the more reliable even where the chemical results are ostensibly more precise.

(4) The photographed spectrum is far superior to chemical analysis in speed, certainty, and completeness, for making a qualitative analysis of the metallic constituents of a complex substance.

(5) The spectrogram is a permanent record of the analysis.

## *Conclusion.*

In conclusion, we wish to express our thanks to Professor W. W. Watts and to his successor, Professor P G H. Boswell, for their kindness in permitting this work to be carried out in the Geological Department of the Imperial College of Science and Technology, London, and for providing the necessary facilities.

## APPENDIX.

Details of the photographic procedure adopted in the present investigation are given below :—

**Plates.**—Ilford Rapid Process Panchromatic, 10 inches by 4 inches, thin glass, speed-Watkins 110, Wynne 67.

Time of Exposure.—2 to 3 minutes according to instrument and condensing lens.

Development —Caustic-hydroquinone developer, made up as follows .—

| A. | | B. | |
|---|---|---|---|
| Hydroquinone .. . . . | 25 gms | Caustic potash . . . . .. | 50 gms. |
| Potassium metabisulphite | 25 gms. | Distilled water to .. . .. .. | 1000 c.c. |
| Potassium bromide ...... | 25 gms. | | |
| Distilled water to ... .. . | 1000 c.c. | | |

| | |
|---|---|
| Temperature of developer ... .. .. .. . | 15° C. |
| Time of development .. ..... . . . ... | 2½ minutes. |
| Fixing solution :— | |
| Sodium thiosulphate . ..... | 100 gms. |
| Potassium metabisulphite .. .. .. | 10 gms. |
| Water to ................... ....... | 1000 c.c. |

The plate is developed in absolute darkness in a large dish which is rocked at a uniform rate in order to avoid the Eberhard effect,* and uneven development. After development is complete, the plate is washed in running water and transferred to the fixing bath for 10 to 15 minutes Final washing is accomplished in about an hour. Rapid washing and drying may be effected by the use of a "Hickmann" washer with subsequent drying in alcohol; it is then possible to have the plate ready for measurement in half an hour; in cases of particular urgency, however, the plate may be examined wet. In developing, it is important to guard against the formation of "ground fog" which renders accurate reading of the termination of the wedge line difficult. In this connection the following points are worthy of note .—

(*a*) The large amount of "restrainer" in the above developer is in itself a safeguard against the formation of fog. The developer should be used in the strength indicated and not diluted. It is unwise to develop much below 15° C.

(*b*) Over-development is a frequent cause of fog It is therefore advisable to carry out a few careful experiments on the influence of time and temperature upon development.

(*c*) Panchromatic plates are more susceptible to fog than ordinary plates owing to some disintegration, in the course of time, of the heavy molecule of the dyestuff with which they are impregnated. No trouble is usually experienced with plates up to an age of 4 months, they should, however, be stored in the coolest place available

---

* Local under-development often found in the darker portions of the negative, due to the developer having become locally "used up" and not replenished by agitation of the dish.

# *On the Definition of Distance in Curved Space, and the Displacement of the Spectral Lines of Distant Sources.*

By E. T. WHITTAKER, F.R.S.

(Received June 26, 1931.)

## § 1. *Introduction.*

The displacement of lines in the spectrum of a distant star, on the assumption that space-time is of constant curvature (the "de Sitter world") has been extensively studied.* The question, however, is not yet settled, different investigators reaching conclusions which are not apparently concordant. The origin of some of the discordances may be traced to the ambiguities which are involved in the use of the terms "time," "spatial distance" and "velocity," when applied by an observer to an object which is remote from him in curved space-time. The "interval" which is defined by $ds^2 = \sum_{p, q} g_{pq}\, dx^p\, dx^q$ involves space and time blended together, and although any particular observer at any instant perceives in his immediate neighbourhood an "instantaneous three-dimensional space," consisting of world-points which he regards as simultaneous, and within which the formulæ of the "restricted relativity theory" are valid, yet this space cannot be defined beyond his immediate neighbourhood; for with a general Riemannian metric, it is not possible to define simultaneity (with respect to a particular observer) over any *finite* extent of space-time.

The concept of "spatial distance between two material particles" is, however, not really dependent on the concept of "simultaneity." When the astronomer asserts that "the distance of the Andromeda nebula is a million light-years," he is stating a relation between the world-point occupied by ourselves at the present instant and the world-point occupied by the Andromeda nebula at the instant when the light left it which arrives here now; that is, he is asserting a relation between two world-points such that a light-pulse, emitted by one, arrives at the other; or in geometrical language, between two world-points which lie on the same null geodesic. The spatial distance of two material particles in a general Riemannian space-time may, then, be thought of as *a relation between two world-points which are on the same null geodesic.* It is obviously right that "spatial distance" should exist only between two world-points which are on the same null geodesic; for it is only then that the particles at these points are in direct physical relation with each other. This statement brings out into sharp relief the contrast between "spatial distance" and the "interval" defined by $ds^2 = \sum_{p,q} g_{pq}\, dx^p\, dx^q$; for between two points on the same null geodesic the "interval" is always zero. Thus "*spatial distance*" *exists when, and only when, the* "*interval*" *is zero.*

---

* The most recent publications are those of R. C. Tolman, 'Astrophys. J.,' vol. 69, p. 245 (1929); H. Weyl, 'Phil. Mag.,' vol. 9, p. 936 (1930); L. Silberstein, "The Size of the Universe" (Oxford, 1930); J. Chazy, "La Théorie de la Relativité et la Mécanique Céleste" (Paris, 1930); G. Castelnuovo, 'Lincei Rend.,' vol. 12, p. 263 (1930); M. von Laue, 'Berlin Sitz.,' p. 123 (1931).

In order to define "spatial distance" conformably to these ideas, in a general Riemannian metric, we shall translate into the language of differential geometry the principle by which astronomers actually calculate the "distance" of very remote objects such as the spiral nebulæ. The principle is this · first, the absolute brightness of the object (the "star" as we shall call it) is determined,* then this is compared with the apparent brightness (*i.e.*, the brightness as actually seen by the observer). The *distance* of the star is then defined to be proportional to the square root of the ratio of the absolute brightness to the apparent brightness.

In adopting this principle into differential geometry, we take a "star" A and an observer B, which are on the same null geodesic (so that a ray of light can pass from A to B) and we consider a thin pencil of null geodesics (rays of light) which issue from A and pass near B. This pencil intersects the observer B's "instantaneous three-dimensional space," giving a two-dimensional cross-section; the "spatial distance AB" is then defined to be proportional to the square root of this cross-section. Distance, as thus defined, is an invariant, *i.e.*, it is independent of the choice of the co-ordinate system. This invariant, however, involves not only the position of the star and the position of the observer, but also the motion of the observer, since his "instantaneous three-dimensional space" is determinate only when his motion is known. Thus the "spatial distance" of a star from an observer depends on the motion of the observer, but this is quite proper, and indeed has always been recognised in the theory of restricted relativity; for in restricted relativity the spatial distance of a star from an observer at the origin is $(X^2 + Y^2 + Z^2)^{\frac{1}{2}}$, where (T, X, Y, Z) are co-ordinates referred to *that particular inertial system with*

---

* For this purpose, astronomers in practice use the known relation between the period and absolute magnitude of Cepheid variables, or (in the method of spectroscopic parallaxes) the known relations between absolute magnitude and spectral behaviour.

*respect to which the observer is at rest*; the necessity for the words in italics shows that the distance really depends on the motion of the observer.

It will be seen that the conception of "spatial distance" here developed is totally distinct from the conception of "interval," and may be contrasted with it in almost every feature. In discussions on the relation which the displacement of spectral lines of remote objects bears to their distance, and in discussions on "expanding universes," it seems desirable that the term "distance" should be used in the sense here defined, since this corresponds to the "distance" of astronomers.

## § 2. *Spatial Distance in the de Sitter World.*

We shall now work out the analytical theory of spatial distance, as defined in § 1, for the de Sitter world

The de Sitter world* is a four-dimensional space-time of constant curvature, which can be represented as a hyper-pseudo-sphere† whose equation is

$$\xi^2 + \eta^2 + \zeta^2 + \omega^2 - \upsilon^2 = R^2 \tag{1}$$

embedded in a five-dimensional hyperspace with the pseudo-Euclidean metric

$$ds^2 = d\upsilon^2 - d\xi^2 - d\eta^2 - d\zeta^2 - d\omega^2. \tag{2}$$

Writing

$$x = \frac{\xi}{\omega}, \quad y = \frac{\eta}{\omega}, \quad z = \frac{\zeta}{\omega}, \quad u = \frac{\upsilon}{\omega},$$

the equations (1) and (2) give

$$\frac{ds^2}{R^2} = \frac{du^2 - dx^2 - dy^2 - dz^2}{1 + x^2 + y^2 + z^2 - u^2} + \frac{(u\,du - x\,dx - y\,dy - z\,dz)^2}{(1 + x^2 + y^2 + z^2 - u^2)^2} \tag{3}$$

an equation‡ which specifies the metric of the de Sitter world. The advantage of taking the metric in this form is that the geodesics are represented by linear equations

$$x = au + a', \quad y = bu + b', \quad z = cu + c',$$

---

* W. de Sitter, 'Monthly Notices R.A.S.,' vol. 78, p. 3 (1917); *Cf.* Eddington, "Math. Theory of Relativity," p. 155 (1923).

† The prefix *hyper* indicates that we are dealing with geometry of more than the usual three dimensions, and the prefix *pseudo* refers to the occurrence of negative signs in the equation.

‡ It is really due to Beltrami, 'Annali mat.,' vol. 2, p. 232 (1868–69).

so that if $(x, y, z, u)$ are mapped as co-ordinates in a Euclidean space $S_4$ of four dimensions, the geodesics are the straight lines of the space.*

The $ds$ of equation (3) is the "interval" or "proper time" between two neighbouring world-points. Equation (3) can be integrated, so that if $s$ is the "interval" between the points $(u, x, y, z)$ and $(u', x', y', z')$, measured along the geodesic connecting them, we have

$$\cosh\frac{s}{R} = \frac{1 + xx' + yy' + zz' - uu'}{(1 + x^2 + y^2 + z^2 - u^2)^{\frac{1}{2}}\,(1 + x'^2 + y'^2 + z'^2 - u'^2)^{\frac{1}{2}}} \tag{4}$$

This formula shows that our geometry is really a Cayley-Klein geometry defined by an "absolute"

$$u^2 - x^2 - y^2 - z^2 = 1. \tag{5}$$

The absolute is a real two-sheeted hyper-hyperboloid ; the de Sitter world is the region external to it, *ie.*, the region from which real tangent-cones can be drawn to it The world-lines of free particles are the parts, outside the absolute, of the straight lines which intersect it. The paths of light-pulses, that is to say, the null geodesics, are the straight lines which touch the absolute.

We have now to enquire what powers we have of choosing the co-ordinate-system so as to simplify the discussion of physical problems without loss of generality. It is clear that any collineation which transforms the absolute (5) into itself may be applied in order to bring the co-ordinate-system into a simple relation with the physical data, and from (1) and (2) it is evident that such a collineation must be a linear homogeneous transformation of the co-ordinates $\xi$, $\eta$, $\zeta$, $\upsilon$, $\omega$, which conserves the two expressions

$$(\xi^2 + \eta^2 + \zeta^2 + \omega^2 - \upsilon^2) \quad \text{and} \quad (d\xi^2 + d\eta^2 + d\zeta^2 + d\omega^2 - d\upsilon^2)$$

---

* The more usual form of the metric of the de Sitter world is obtained by making the transformation

$$\begin{cases} x = \tan\chi \sin\theta \cos\phi \operatorname{sech}\dfrac{ct}{R}, \\ y = \tan\chi \sin\theta \sin\phi \operatorname{sech}\dfrac{ct}{R}, \\ z = \tan\chi \cos\theta \operatorname{sech}\dfrac{ct}{R}, \\ u = \tanh\dfrac{ct}{R}, \end{cases}$$

when equation (3) becomes

$$ds^2 = c^2\cos^2\chi\, dt^2 - R^2\, d\chi^2 - R^2\sin^2\chi\, d\theta^2 - R^2\sin^2\chi\sin^2\theta\, d\phi^2$$

the form in which the metric of the de Sitter world has generally been represented.

that is, it must be a Lorentz transformation in the co-ordinates $(\xi, \eta, \zeta, \omega, \upsilon)$. By means of a transformation of this type we can transform any given world-line $l$ into the axis of $u$, and also any given point P on this line $l$ into the origin $u = 0$, and at the same time any other line through P, in the hyperplane orthogonal to the line $l$, can be transformed into the axis of $x$. These transformations enable us to simplify the analysis of physical problems without any real loss of generality.

We are now prepared to investigate the formula for the "spatial distance" between two material particles, in the sense explained in § 1. Suppose that we have a star A, emitting light, and an observer B receiving the light. We shall choose the co-ordinate system so that the world-line of the observer B is the line

$$x = x_0, \quad y = 0, \quad z = 0,$$

where $x_0$ is a constant, and we shall suppose the star A, at the instant when it emits the light, to be at the world-point

$$u = u_1, \quad x = x_1, \quad y = 0, \quad z = 0.$$

By what has just been said, there is no real loss of generality in making these suppositions. The line AB, being the path of a pulse of light, must be a tangent-line to the absolute (5); and it is in the plane of $ux$, it must therefore be represented by equations of the form

$$\frac{u - u_1}{\sinh \beta} = \frac{x - x_1}{\cosh \beta} = \frac{y}{0} = \frac{z}{0}, \tag{6}$$

where, since the line touches the absolute, $\beta$ satisfies the equation

$$u_1 \cosh \beta - x_1 \sinh \beta = 1,$$

so that

$$\begin{aligned} \sinh \beta &= -\frac{1 - u_1^2}{x_1 + u_1 (1 + x_1^2 - u_1^2)^{\frac{1}{2}}} = -\frac{x_1 - u_1 (1 + x_1^2 - u_1^2)^{\frac{1}{2}}}{x_1^2 - u_1^2} \\ &= -\frac{(1 + x_1^2 - u_1^2)^{\frac{1}{2}} - u_1 x_1}{u_1 + x_1 (1 + x_1^2 - u_1^2)^{\frac{1}{2}}} \\ \cosh \beta &= \frac{(1 + x_1^2 - u_1^2)^{\frac{1}{2}} + u_1 x_1}{x_1 + u_1 (1 + x_1^2 - u_1^2)^{\frac{1}{2}}} = \frac{x_1 (1 + x_1^2 - u_1^2)^{\frac{1}{2}} - u_1}{x_1^2 - u_1^2} \\ &= \frac{1 + x_1^2}{u_1 + x_1 (1 + x_1^2 - u_1^2)^{\frac{1}{2}}} \end{aligned} \tag{7}$$

The sign of the radical must be chosen so that the null geodesic represents a pulse of light *from* A *to* B. Now on the null geodesics through A, the directions which correspond to propagation *from* A are separated from the directions which correspond to propagation *to* A, by the spatial geodesics, i e., the straight lines which do not intersect the absolute quadric. This law, together with considerations of continuity, and with the convention that at the origin of co-ordinates the direction of $u$ increasing corresponds to the positive direction of time, suffice to distinguish the directions corresponding to propagation *from* A from those which correspond to progagation *to* A. If we assume for definiteness that $x_1 > x_0$, it is found that the sign of the radical we require is the positive one.

Now consider another tangent-line from A to the absolute, only very slightly inclined to the tangent-line (6), let its equations be

$$\frac{u-u_1}{\sinh\beta} = \frac{x-x_1}{\cosh\beta + l} = \frac{y}{m} = \frac{z}{n} \tag{8}$$

where $l$, $m$ $n$ are small Regarding $m$ and $n$ as small quantities of the first order, it is evident from the symmetry about the plane $ux$ that $l$ will be a small quantity of the second order.

Let us find the intersection of the line (8) with the " instantaneous three-dimensional space " of the observer at B, whose world-line is

$$x = x_0, \qquad y = 0, \qquad z = 0$$

If we consider an observer at B whose world-line has the direction

$$\frac{du}{\lambda} = \frac{dx}{\alpha} = \frac{dy}{\beta} = \frac{dz}{\gamma}$$

(where $\lambda$, $\alpha$, $\beta$, $\gamma$, are any constants), his instantaneous space is the hyperplane orthogonal to this world-line at B, or rather the region of this hyperplane which is infinitesimally near to B. But orthogonality is the same thing as conjugacy with respect to the absolute, and the hyperplane which is conjugate to the direction

$$\frac{du}{\lambda} = \frac{dx}{\alpha} = \frac{dy}{\beta} = \frac{dz}{\gamma}$$

at the point B $(u_0, x_0, 0, 0)$, with respect to the absolute (5), is the hyperplane

$$(\lambda + \lambda x_0^2 - \alpha u_0 x_0)(u - u_0) - (\alpha - \alpha u_0^2 + \lambda u_0 x_0)(x - x_0)$$
$$- \beta(1 + x_0^2 - u_0^2)y - \gamma(1 + x_0^2 - u_0^2)z = 0. \tag{9}$$

So the hyperplane orthogonal to the world-line ($x = x_0$, $y = 0$, $z = 0$) at B is (putting $\alpha = \beta = \gamma = 0$)

$$\frac{u-u_0}{u_0} - \frac{x_0(x-x_0)}{1+x_0^2} = 0. \tag{9.1}$$

By (8) and (9.1), the point of intersection of the line (8) with the instantaneous space of the observer B is given by the equations

$$x - x_0 = \text{an expression which contains } l \text{ as a factor, and is therefore of the second order of small quantities}$$

$$y = \frac{m(x_0 - x_1)}{\cosh \beta} \qquad (10)$$

$$z = \frac{n(x_0 - x_1)}{\cosh \beta}$$

The cross-section of a pencil of light sent from A to B, in B's instantaneous space, is therefore in the plane $x - x_0 = 0$, and the point of intersection of any ray with the instantaneous space is given by (10).

Now spatial distance in this instantaneous space is given by equation (3) when—

(1) the sign of $ds^2$ is reversed,
(2) $y$ and $z$ are put equal to zero,
(3) $du$ is given in terms of $dx$ by (9.1),

that is, if $ds$ denotes spatial distance in this instantaneous space,

$$\frac{ds^2}{R^2} = \frac{dx^2}{(1 + x_0^2)(1 + x_0^2 - u_0^2)} + \frac{dy^2 + dz^2}{1 + x_0^2 - u_0^2} \qquad (11)$$

so the area of the cross-section of the pencil of light in B's instantaneous space is

$$\frac{R^2}{1 + x_0^2 - u_0^2} \iint dy\, dz$$

or by (10)

$$\frac{R^2}{1 + x_0^2 - u_0^2} \frac{(x_0 - x_1)^2}{\cosh^2 \beta} \iint dm\, dn$$

or

$$\frac{R^2 (x_0 - x_1)^2}{(\sinh \beta - x_0)^2} \iint dm\, dn.$$

Now, as explained in § 1, we define the "spatial distance" of B from A as being proportional to the square root of this cross-section, and therefore the spatial distance of B from A, so far as it depends on $x_0$, is proportional to

$$\frac{x_1 - x_0}{x_0 - \sinh \beta}$$

Suppose then that the spatial distance is

$$\Delta = \frac{x_1 - x_0}{x_0 - \sinh\beta} f(u_1, x_1), \tag{12}$$

where $f(u_1, x_1)$ is a function to be determined

When $x_0$ is very near $x_1$, $\Delta$ must coincide with the spatial distance as measured in B's instantaneous three-dimensional space, and therefore, comparing (11) and (12), we have

$$\frac{dx}{x_1 - \sinh\beta} f(u_1, x_1) = \frac{\mathrm{R}\,dx}{(1 + x_1^2)^{\frac{1}{2}}(1 + x_1^2 - u_1^2)^{\frac{1}{2}}}$$

whence

$$f(u_1, x_1) = \frac{\mathrm{R}(x_1 - \sinh\beta)}{(1 + x_1^2)^{\frac{1}{2}}(1 + x_1^2 - u_1^2)^{\frac{1}{2}}} = \frac{\mathrm{R}\cosh\beta}{(1 + x_1^2)^{\frac{1}{2}}}. \tag{13}$$

From (12) and (13) we have

$$\Delta = \frac{(x_1 - x_0)\mathrm{R}\cosh\beta}{(1 + x_1^2)^{\frac{1}{2}}(x_0 \sinh\beta)^{\frac{1}{2}}}$$

and thus *the spatial distance from the point* $(u_1, x_1, 0, 0)$ *to a free particle describing the world-line* $(x = x_0, y = 0, z = 0)$, *is*

$$\Delta = \frac{\mathrm{R}(x_1 - x_0)(1 + x_1^2)^{\frac{1}{2}}}{(1 + x_0 x_1)(1 + x_1^2 - u_1^2)^{\frac{1}{2}} - u_1(x_1 - x_0)}. \tag{14}$$

We now want to free ourselves from the specialisation involved in the choice of our co-ordinate-system, so as to obtain a general formula in place of (14). We shall therefore now make no restrictions on the choice of the co-ordinate-system, except that the axis of $u$ is to be chosen parallel to the world-line of the observer Then the spatial distance $\Delta$ must be a function of the co-ordinate of the star $(u_1, x_1, y_1, z_1)$ and of the world-line of the observer $(x_0, y_0, z_0)$, which is invariant with respect to all the collineations which transform the absolute (5) into itself and which also transform lines parallel to the axis of $u$ into lines parallel to the axis of $u$.* Now we can at once write down two functions of $(u_1, x_1, y_1, z_1, x_0, y_0, z_0)$ which are invariant with respect to all such collineations, namely,

---

* *E g.*, a simple collineation of this kind is the transformation from $(u, x, y, z)$ to $(u', x', y', z')$, where

$$u' = \frac{u}{x\sin\gamma + \cos\gamma}, \quad x' = \frac{x\cos\gamma - \sin\gamma}{x\sin\gamma + \cos\gamma}, \quad y' = \frac{y}{x\sin\gamma + \cos\gamma},$$

$$z' = \frac{z}{x\sin\gamma + \cos\gamma},$$

and where $\gamma$ is any constant.

(1) The quantity

$$\frac{u_1}{(1 + x_1^2 + y_1^2 + z_1^2)^{\frac{1}{2}}} \tag{15}$$

(where the radical will be taken positively), which we shall denote by $\sin \sigma$, where $\sigma$ is defined to be between $-\pi/2$ and $\pi/2$; and

(2) The quantity

$$\frac{1 + x_0 x_1 + y_0 y_1 + z_0 z_1}{(1 + x_0^2 + y_0^2 + z_0^2)^{\frac{1}{2}} (1 + x_1^2 + y_1^2 + z_1^2)^{\frac{1}{2}}} \tag{16}$$

which we shall denote by $\cos \rho$, where $\rho$ is defined to be between 0 and $\pi$.*

In the particular case when $y_0$, $z_0$, $y_1$, $z_1$ are all zero, the formulæ (15) and (16) give

$$\left.\begin{aligned} \sin \sigma &= \frac{u}{(1 + x_1^2)^{\frac{1}{2}}}, & \cos \sigma &= \frac{(1 + x_1^2 - u_1^2)^{\frac{1}{2}}}{(1 + x_1^2)^{\frac{1}{2}}} \\ \cos \rho &= \frac{1 + x_0 x_1}{(1 + x_0^2)^{\frac{1}{2}} (1 + x_1^2)^{\frac{1}{2}}}, & \sin \rho &= \frac{x_1 - x_0}{(1 + x_0^2)^{\frac{1}{2}} (1 + x_1^2)^{\frac{1}{2}}} \end{aligned}\right\} \tag{17}$$

and comparing these with (14), we see that in this particular case

$$\Delta = \frac{R \sin \rho}{\cos (\gamma + \rho)} \tag{18}$$

But since $\Delta$, $\rho$, $\gamma$, are all invariants, and since the particular case for which we have proved this relation involves no restriction on generality,† therefore the relation (18) holds in general, that is to say, *the "spatial distance" between two material particles in de Sitter's world is given by formula* (18) *where* $\sigma$ *and* $\rho$ *are the two invariants defined by* (15) *and* (16).

## § 3. *The Observer's Proper-time.*

We have seen in § 2 that if a pulse of light emitted from a star A $(u_1, x_1, 0, 0)$ in de Sitter's world arrives at an observer B $(u_0, x_0, 0, 0)$ whose world-line is $(x = x_0, y = 0, z = 0)$, then the line AB is represented by equation (6), where $\beta$ is given by equations (7). From these we have at once

$$\begin{aligned} u_0 &= u_1 - (x_1 - x_0) \tanh \beta \\ &= u_1 - (x_1 - x_0) \cdot \frac{u_1 x_1 - (1 + x_1^2 - u_1^2)^{\frac{1}{2}}}{1 + x_1^2} \qquad \text{by (7)} \\ &= \frac{u_1 (1 + x_0 x_1) + (x_1 - x_0)(1 + x_1^2 - u_1^2)^{\frac{1}{2}}}{1 + x_1^2} \\ &= (1 + x_0^2)^{\frac{1}{2}} \sin (\sigma + \rho) \qquad \text{by (17).} \end{aligned} \tag{19}$$

---

* The invariance of $\rho$ is suggested by its being the distance between the points $(x_1, y_1, z_1)$, and $(x_0, y_0, z_0)$ in the Cayley-Klein geometry for which the absolute is $x^2 + y^2 + z^2 + 1 = 0$.

† *i.e.*, it can be transformed into the general case.

Also by (3), if $d\tau_0$ denotes the proper-time of the observer B, we have

$$\frac{d\tau_0^2}{R^2} = \frac{du_0^2}{1+x_0^2-u_0^2} + \frac{u_0^2\,du_0^2}{(1+x_0^2-u_0^2)^2}$$

or

$$\frac{d\tau_0}{R} = \frac{(1+x_0^2)^{\frac{1}{2}}\,du_0}{1+x_0^2-u_0^2}$$

so

$$u_0 = (1+x_0^2)^{\frac{1}{2}} \tanh \frac{\tau_0}{R}. \tag{20}$$

From (19) and (20) we have

$$\tanh \frac{\tau_0}{R} = \sin(\sigma + \rho). \tag{21}$$

This being a relation between invariants must be true not merely in the special case for which we have proved it, but also in the general case when the $y$ and $z$ co-ordinates of the star and observer are not zero. Thus *the proper-time of an observer, moving on the world-line* $x = x_0$, $y = y_0$, $z = z_0$, *at the instant when he receives a light-signal from a star at* $(u_1, x_1, y_1, z_1)$, *is* $\tau_0$, *then* $\tau_0$ *is expressed in terms of the invariants* $\sigma$ *and* $\rho$ *by equation* (21).

There is always a second null geodesic which passes through the star and intersects the given world-line, and which represents a signal travelling *to* the star *from* the observer. The proper-time of the observer at the world-point where this second null geodesic meets his world-line is $\tau_{-1}$, where

$$\tanh \frac{\tau_{-1}}{R} = \sin(\sigma - \rho). \tag{22}$$

## § 4. *The History of the Observation of a Star in the de Sitter World.*

As we saw in § 2, if the observed star is moving freely, then $x_1$, $y_1$, $z_1$, are linear functions of $u_1$. But we readily find that equation (18) cannot give a constant value of $\Delta$ when $x_1$, $y_1$, $z_1$, are linear functions of the variable $u_1$, and therefore a freely moving star and a freely moving observer cannot remain at a constant spatial distance apart in the de Sitter world. The nearest resemblance to a universe whose stars have a constant configuration is when, choosing the co-ordinate-system so that the world-line of the observer is parallel to the axis of $u$, the $(x, y, z)$ co-ordinates of all stars are constant, so that their world-lines are also parallel to the axis of $u$. Thus, suppose a star has the world-line

$$x = x_1, \quad y = y_1, \quad z = z_1,$$

and the observer has the world-line

$$x = x_0, \quad y = y_0, \quad z = z_0,$$

where $(x_1, y_1, z_1, x_0, y_0, z_0)$ are all constant. Then from (16) we see that $\rho$ is constant; we can call $\rho$ the *proper distance* of the star from the observer.

We shall now trace the history of the observation of a star which has a definite proper-distance from the observer. We choose the co-ordinates so that the observer's world-line is the axis of $u$ and the star's world-line is the line $x = x_1$, $y = 0$, $z = 0$, where for definiteness $x_1$ will be supposed positive. Then if F be the beginning of the star's world-line, that is the point $(-\sqrt{(1 + x_1^2)}, x_1, 0, 0)$ where the world-line meets the absolute, and if $FF_0$ be the tangent to the absolute at F, meeting the observer's world-line at $F_0\,(-(1 + x^2)^{-\frac{1}{2}}, 0, 0, 0)$, the observer will not perceive the star at all until he arrives at $F_0$, since until then, no null geodesics, representing propagation of light from the star, intersect the observer's world-line. For the positions F, $F_0$, of the star and observer, we have $\sigma = -90°$, while $\rho$ has its constant values; so the spatial distance is

$$\Delta = R\,\frac{\sin\rho}{\cos(-90^\circ + \rho)} = R.$$

Thus, when the observer first sees the star, its spatial distance is equal to the radius of curvature of the universe.

After this the star is continuously visible, its spatial distance at the observer's proper-time $\tau_0$ being given by the formula

$$\Delta = R \sin\rho \cosh\frac{\tau_0}{R}, \tag{23}$$

which follows at once from (18) and (21).

The minimum value of $\Delta$ is $R \sin\rho$, and after this it increases continually. Let $H_0$ be the point where the observer's world-line terminates on the absolute, that is, the point $(1, 0, 0, 0)$, and let $H_0H$ be the tangent to the absolute at $H_0$, meeting the star's world-line at H. Then, as the observer approaches $H_0$, his proper-time $\tau_0$ increases indefinitely, $(\sigma + \rho)$ tends to $\pi/2$, and the spatial distance $\Delta$ of the star thus increases indefinitely; that is, the star's apparent brightness decreases to zero, it becomes too faint to be seen. This happens when the star is at H, which is not the terminus of its own world-line, so the star continues to exist after it has ceased to have any relations with this particular observer.

We may remark that with the definition of spatial distance which we have adopted in this paper, de Sitter's world is *not* spatially finite; the spatial distance of a star from an observer ultimately tends to infinity.

### § 5. *The Doppler Effect in the de Sitter World.*

A formula for the Doppler effect in the de Sitter world can be obtained at once. For if as before $\tau_0$ denotes the proper-time of the observer at the instant when he perceives a light-signal which left the star at the star's proper-time $\tau$, then the Doppler effect $\delta\lambda/\lambda$ (where $\lambda$ denotes wave-length) is given by the simple equation

$$\frac{\delta\lambda}{\lambda} = \frac{d\tau_0}{d\tau} - 1. \tag{24}$$

Now from (21) we have

$$\frac{d\tau_0}{\mathrm{R}} = \frac{d(\sigma + \rho)}{\cos(\sigma + \rho)}, \tag{25}$$

and from (3) we have

$$\frac{d\tau^2}{\mathrm{R}^2} = \frac{du^2 - dx^2 - dy^2 - dz^2}{1 + x^2 + y^2 + z^2 - u^2} + \frac{(u\,du - x\,dx - y\,dy - z\,dz)^2}{(1 + x^2 + y^2 + z^2 - u^2)^2}. \tag{26}$$

Equations (24), (25), (26) are the rigorous analytical formulæ for the Doppler effect. In the case considered in the last article, where the co-ordinate system is so chosen that the observer's world-line is the axis of $u$ and the star describes a world-line parallel to this axis, formulæ (25) and (26) become respectively

$$\frac{d\tau_0}{\mathrm{R}} = \frac{d\sigma}{\cos(\sigma + \rho)}$$

and

$$\frac{d\tau}{\mathrm{R}} = \frac{d\sigma}{\cos\sigma}$$

so

$$\frac{d\tau_0}{d\tau} = \frac{\cos\sigma}{\cos(\sigma + \rho)} \tag{27}$$

Thus at the observer's instant $\mathrm{F}_0$ when the star first becomes visible (and where, as we have seen, $\sigma = -\pi/2$), $d\tau_0/d\tau$ is zero; and when the star finally fades out from visibility at $\mathrm{H}_0$, (where $\sigma + \rho = \pi/2$), $d\tau_0/d\tau$ is infinite.

A comparison of the results of astronomical observation with the formulæ obtained above would involve the discussion of questions of a different character, and may fitly be deferred to a separate paper.

### § 6. *Special Relativity as a Particular Case.*

When the radius of curvature of the world is increased indefinitely, our formulæ should pass, in the limit, into the well-known formulæ of the theory of special or restricted relativity. It is easy to see that they do so; for supposing R very large, we study the region of the pseudo-sphere (1) in the neighbourhood of the point

$$\xi = \eta = \zeta = \upsilon = 0, \quad \omega = \mathrm{R};$$

so $x$, $y$, $z$, $u$, are all very small, but if

$$\mathrm{R}x = \mathrm{X}, \qquad \mathrm{R}y = \mathrm{Y}, \qquad \mathrm{R}z = \mathrm{Z}, \qquad \mathrm{R}u = \mathrm{T},$$

then X, Y, Z, T, are all finite and are in fact the usual co-ordinates of the theory of special relativity. Equation (3) becomes

$$ds^2 = d\mathrm{T}^2 - d\mathrm{X}^2 - d\mathrm{Y}^2 - d\mathrm{Z}^2;$$

equation (15) becomes

$$\sigma = \mathrm{T}_1/\mathrm{R};$$

equation (16) becomes

$$\rho = \frac{1}{\mathrm{R}}\{(\mathrm{X}_1 - \mathrm{X}_0)^2 + (\mathrm{Y}_1 - \mathrm{Y}_0)^2 + (\mathrm{Z}_1 - \mathrm{Z}_0)^2\}^{\frac{1}{2}},$$

and formula (18) becomes

$$\Delta = \{(\mathrm{X}_1 - \mathrm{X}_0)^2 + (\mathrm{Y}_1 - \mathrm{Y}_0)^2 + (\mathrm{Z}_1 - \mathrm{Z}_0)^2\}^{\frac{1}{2}},$$

so our spatial distance $\Delta$ reduces in this case to the spatial distance of the theory of special relativity.

Formula (25) becomes

$$d\tau_0 = d\mathrm{T}_1 + d\,.\{(\mathrm{X}_1 - \mathrm{X}_0)^2 + (\mathrm{Y}_1 - \mathrm{Y}_0)^2 + (\mathrm{Z}_1 - \mathrm{Z}_0)^2\}^{\frac{1}{2}},$$

and formula (26) becomes

$$d\tau_1 = \{d\mathrm{T}_1{}^2 - d\mathrm{X}_1{}^2 - d\mathrm{Y}_1{}^2 - d\mathrm{Z}_1{}^2\}^{\frac{1}{2}}$$

so

$$\frac{d\tau_0}{d\tau_1} = \frac{1 + \dfrac{d}{d\mathrm{T}_1}\{(\mathrm{X}_1 - \mathrm{X}_0)^2 + (\mathrm{Y}_1 - \mathrm{Y}_0)^2 + (\mathrm{Z}_1 - \mathrm{Z}_0)^2\}^{\frac{1}{2}}}{\left\{1 - \left(\dfrac{d\mathrm{X}_1}{d\mathrm{T}_1}\right)^2 - \left(\dfrac{d\mathrm{Y}_1}{d\mathrm{T}_1}\right)^2 - \left(\dfrac{d\mathrm{Z}_1}{d\mathrm{T}_1}\right)^2\right\}^{\frac{1}{2}}}$$

$$= \frac{1 + \dfrac{w_r}{c}}{\sqrt{\left(1 - \dfrac{w^2}{c^2}\right)}}$$

where $w$ is the star's velocity and $w_r$ is the radial component of $w$; this is the well-known formula for the Doppler effect in special relativity.

# *The Cataphoresis of Suspended Particles. Part I.—The Equation of Cataphoresis.*

By D. C. **Henry**, M.A., Director of the Thomas Graham Colloid Research Laboratory, and Lecturer in Chemistry in the Victoria University of Manchester.

(Communicated by A. Lapworth, F.R.S.—Received March 20, 1931.)

§ 1. The theory of cataphoresis, and of the complementary phenomenon of electrosmosis, is based on the conception of an " electrical double layer " at the interface between the two phases whose relative motion is under consideration.* In the original theory, as propounded by Quincke and Helmholtz, this electrical double layer was regarded as a kind of parallel plate condenser made up of two laminar distributions of electrification, of which one —the so-called " inner sheet "—was firmly attached to the rigid phase, while the other—the " outer sheet "—resided in the mobile phase; the separation between the two was considered to be a distance of the order of molecular dimensions. The currently accepted view, initiated by Gouy, differs from that of Helmholtz chiefly in that the outer sheet of the double layer is considered to be a diffuse distribution of electrification—an " ionic atmosphere " of the type investigated by Debye and his collaborators in connection with the theory of strong electrolytes. The net electric density in the ionic atmosphere varies continuously from a maximum in the immediate neighbourhood of the fixed inner sheet, to a negligibly small value in the bulk of the liquid, over a distance which is a function of the ionic concentration, and which lies as a rule between molecular dimensions and some thousand micromillimetres.

In a deduction which appears to be completely consistent with this more modern view of the double layer, Smoluchowski† deduced the expression

$$U = DX\zeta/4\pi\eta \qquad (1)$$

for the cataphoretic velocity U; X is the applied field strength, $\zeta$ the potential difference across the double layer, D the dielectric constant and $\eta$ the viscosity of the medium. The equation is identical with that developed by Helmholtz except for the inclusion of the dielectric constant, but was deduced on a much more general basis, and is claimed by Smoluchowski to be valid for rigid electrically insulating particles of any shape, subject only to the following four restrictions :—

---

* For a general account of the subject, v. Freundlich, "Colloid and Capillary Chemistry," p. 240 *sq.*, or Smoluchowski, in Graetz' " Handbuch der Elektrizitat und des Magnetismus," vol. 2, p. 366 (1914).

† 'Bull. Acad. Sci. Cracovie,' p. 182 (1903).

(1) That the usual hydrodynamical equations for the motion of a viscous fluid may be assumed to hold both in the bulk of the liquid and within the double layer ;

(2) That the motion is "stream line motion," and slow enough for the "inertia terms" in the hydrodynamic equations to be neglected ,

(3) That the applied field may be taken as simply superimposed on the field due to the electrical double layer ; and

(4) That the thickness of the double layer (*i e* , the distance normal to the interface over which the potential differs appreciably from that in the bulk of the liquid) is small compared with the radius of curvature at any point of the surface.

Debye and Huckel* have criticised Smoluchowski's conclusions, and contend that, while the relation

$$U = c\,DX\zeta/\eta$$

is, subject to Smoluchowski's four restrictions, valid for particles of any shape, the constant $c$ is not always $1/4\pi$, but varies with the shape of the particle, and can only be determined in each case by a detailed hydrodynamic analysis of the motion of the liquid. Huckel† has published such an analysis for the case of a spherical particle, and finds that $c$ is then equal to $1/6\pi$.‡ Debye and Huckel further state that for a cylinder the constant is $1/4\pi$ , presumably this conclusion is meant to apply only to a cylinder placed axially to the applied field, as in electrosmosis through a cylindrical tube, for an analysis (by the author) of the case of a cylinder placed broadside on to the applied field leads on Huckel's assumptions to the result $1/8\pi$.

As the conclusion that the cataphoretic velocity of a particle should depend on its shape appears to be at variance with the experimental facts, the analysis given by Debye and Huckel was examined, and it was found that they assume the applied potential gradient to be everywhere parallel to the $x$-axis and to be undisturbed by the presence of the particle. This will only be the case if the electrical conductivity of the particle is identical with that of the medium, which will rarely occur in practice. With an insulating particle, the applied field will be distorted (quite apart from any effect of the electrical double layer such as is excluded from consideration by the third restriction) so that the lines of force near the interface run tangentially. It appeared likely that the discrepancy between the results of Smoluchowski and of Debye and Huckel might be due to this cause, and it was decided to repeat the theoretical deductions, employing the same analytical methods as Huckel, but allowing for a specific electrical conductivity of the particle different from that of the medium. This process has been applied to spheres and to cylinders (in both the axial and transverse positions), with the result that, subject to Smoluchowski's four restrictions, equation (1) is found to hold in each case. In view of the striking dissimilarity (to be referred to later) in the hydrodynamic behaviour of spherical and cylindrical surfaces, this result lends considerable support to the view that the same equation holds for any shape of particle, even if Smoluchowski's theoretical demonstration of this is not held to be conclusive.

---

* 'Physik. Z ,' vol. 25, p. 49 (1924).

† 'Physik. Z.,' vol. 25, p. 204 (1924).

‡ For the particular case of the sphere, Hückel finds the fourth restriction to be unnecessary.

§ 2. *The Cataphoresis of a Solid Sphere of any desired Conductivity.*—We shall consider a sphere of radius $a$ and specific conductivity $\mu'$ immersed in an infinite volume of an incompressible liquid of specific conductivity $\mu$, dielectric constant D and viscosity $\eta$. The sphere carries a fixed charge[*] $e$ which gives rise to a centrally-symmetrical distribution of electrification, $\rho$ per unit volume, in the liquid immediately surrounding the sphere. Let $\psi$ be the potential at any point outside the sphere corresponding to this distribution, and let $\psi_a$ be the value of $\psi$ on the surface of the sphere, the value at a great distance from the sphere being set equal to zero

If now an external field of strength X is applied to the system in a direction parallel to the $x$-axis of co-ordinates, the sphere will assume the steady cataphoretic velocity U in the same direction. By imposing a velocity $-$U on the whole system, the sphere is brought to rest, while the liquid streams past it and moves at infinity with a velocity $-$U in the $x$-direction. We shall employ polar co-ordinates $r$, $\theta$ and $\omega$ with the centre of the sphere as origin and the polar axis $\theta = 0$ in the $x$-direction. We shall assume the validity of the first three of Smoluchowski's restrictions; the fourth, which limits the permissible thickness of the electrical double layer, is not involved in the deduction of the general result represented by equations (16), (17) and (18), and will only be introduced for the purpose of reducing these to Smoluchowski's form. The

---

[*] It is not essential that the fixed charge should be a surface distribution, but merely that it should have central symmetry.

practical limitations imposed by the acceptance of these restrictions will be discussed later.

In the absence of the applied field, $\psi$ and all its derivatives are functions of the radial co-ordinate only, and by the third restriction this will also hold in the presence of the applied field. By the same assumption, if $\phi$ and $\phi'$ are the potentials due to the latter at points respectively outside and inside the sphere, these are unaffected by the presence of the electrical double layer, and are determined by the equations

$$\nabla^2\phi = \nabla^2\phi' = 0,$$

together with the boundary conditions $\partial\phi/\partial x = -\mathrm{X}$ for $r = \infty$, and $\phi = \phi'$, $\partial\phi/\partial\theta = \partial\phi'/\partial\theta$, $\mu . \partial\phi/\partial r = \mu' \; \partial\phi'/\partial r$ for $r = a$. The solution is easily shown to be

$$\left.\begin{aligned} \phi &= -\mathrm{X}\,(r + \lambda a^3/r^2)\cos\theta \\ \phi' &= -\mathrm{X}\,(1+\lambda) r\cos\theta \end{aligned}\right\}$$

where $\lambda$ is written for $(\mu - \mu')/(2\mu + \mu')$.

The total potential at any point is $\phi + \psi$, and the mechanical force per unit volume is $-\rho \,.\, \mathrm{grad}\,(\phi + \psi)$. The hydrodynamic equations of the fluid motion, neglecting the "inertia terms," are therefore

$$\left.\begin{aligned} \eta \,.\, \mathrm{curl}\;\mathrm{curl}\;\mathbf{v} + \mathrm{grad}\,p &= -\rho \,.\, \mathrm{grad}\,(\phi + \psi) \\ \mathrm{div}\;\mathbf{v} &= 0, \end{aligned}\right\}$$

where $\mathbf{v}$ denotes the vector velocity* and $p$ is the hydrostatic pressure. We further have, by Poisson's equation,

$$\rho = -\frac{\mathrm{D}}{4\pi}\nabla^2(\phi + \psi) = -\frac{\mathrm{D}}{4\pi}\nabla^2\psi,$$

since $\nabla^2\phi$ is everywhere zero.

Set

$$p_1 = p - \int_\infty^r \rho\,(\partial\psi/\partial r)\,dr;$$

then

$$\mathrm{grad}\,p = \mathrm{grad}\,p_1 + \mathrm{grad}\int_\infty^r \rho\,(\partial\psi/\partial r)\,dr.$$

---

* Throughout this paper vector quantities will be denoted by Clarendon type and their components by italic characters. Thus $\mathbf{v}$ is a vector with Cartesian components $v_x$, $v_y$, $v_z$. The scalar product of two vectors **a** and **b** will be denoted **a . b** and the vector product $\mathbf{a}_\wedge\mathbf{b}$.

The last term on the right has only an $r$-component, which is $\rho \,.\, \partial\psi/\partial r$; hence

$$\operatorname{grad} p = \operatorname{grad} p_1 + \rho \quad \operatorname{grad} \psi,$$

and the equations of motion can be written

$$\left.\begin{aligned} \eta \,.\, \operatorname{curl}\operatorname{curl} \mathbf{v} + \operatorname{grad} p_1 &= -\rho \,.\, \operatorname{grad} \phi \\ \operatorname{div} \mathbf{v} &= 0 \end{aligned}\right\} \qquad (2)$$

Applying the operator div to the first equation of (2), we get

$$\begin{aligned} \nabla^2 p_1 &= -\operatorname{div} (\rho \,.\, \operatorname{grad} \phi) \\ &= -\rho \,.\, \operatorname{div}\operatorname{grad} \phi - \operatorname{grad} \phi \,.\, \operatorname{grad} \rho \\ &= -\frac{\partial\phi}{\partial r}\,\frac{\partial\rho}{\partial r} \\ &= -\frac{\mathrm{DX}}{4\pi}\left(1 - 2\lambda\frac{a^3}{r^3}\right)\cos\theta \,.\, \frac{\partial}{\partial r}\nabla^2\psi \end{aligned} \qquad (3)$$

If as a trial solution we set

$$p_1 = -\frac{\mathrm{DX}}{4\pi}\cos\theta\left(\frac{\partial\psi}{\partial r} - 2\lambda a^3 \mathrm{P}_1\right) \qquad (4)$$

where $\mathrm{P}_1$ is a function of $r$ only, so that

$$\begin{aligned} \nabla^2 p_1 &\equiv \frac{1}{r^2}\frac{\partial}{\partial r}\left(r^2\frac{\partial p_1}{\partial r}\right) + \frac{1}{r^2 \sin\theta}\frac{\partial}{\partial\theta}\left(\sin\theta\frac{\partial p_1}{\partial\theta}\right) \\ &= -\frac{\mathrm{DX}}{4\pi}\cos\theta\left\{\frac{\partial}{\partial r}\nabla^2\psi - \frac{2\lambda a^3}{r}\left[\frac{\partial^2(\mathrm{P}_1 r)}{\partial r^2} - \frac{2\mathrm{P}_1 r}{r^2}\right.\right. \end{aligned}$$

we find that equation (3) is satisfied provided

$$r^2\frac{\partial^2(\mathrm{P}_1 r)}{\partial r^2} - 2\mathrm{P}_1 r = \frac{\partial}{\partial r}\nabla^2\psi. \qquad (5)$$

This is a homogeneous linear differential equation whose particular integral reduces to

$$\mathrm{P}_1 = r\int^r \frac{1}{r^4}\nabla^2\psi\, dr.$$

The complementary function, which includes the constants of integration, takes the form $c_1 r + c_2/r^2$. Here, as also in the solution of the similar equations (9) and (11), it will be more convenient to defer consideration of the respective complementary functions, introducing them all together in the solution of (13). Inserting the value of $P_1$ in equation (4) we have

$$p_1 = -\frac{DX}{4\pi}\cos\theta\left(\frac{\partial\psi}{\partial r} - 2\lambda a^3 r\int^r \frac{1}{r^4}\nabla^2\psi\,.\,dr\right).$$

Since $p_1$ must be zero for large values of $r$, we may set the lower limit of integration $\infty$, and finally obtain

$$p = \int_\infty^r \rho\frac{\partial\psi}{\partial r}dr - \frac{DX}{4\pi}\cos\theta\left(\frac{\partial\psi}{\partial r} - 2\lambda a^3 r\int_\infty^r \frac{1}{r^4}\nabla^2\psi\,dr\right). \tag{6}$$

To obtain a solution for v, we apply the operator curl to the first equation of (2), when, since curl grad $= 0$, we obtain

$$\eta\,.\,\text{curl curl}\ \mathbf{w} = -\,\text{curl}\,(\rho\,.\,\text{grad}\,\phi), \tag{7}$$

where **w** is written for curl v. Since v has zero $\omega$-component, it follows from the ordinary formulæ of vector analysis that **w** and curl curl **w** have zero $r$- and $\theta$-components, and that their respective $\omega$-components are

$$w_\omega \equiv \frac{1}{r}\left\{\frac{\partial}{\partial r}(rv_\theta) - \frac{\partial v_r}{\partial\theta}\right\},$$

and

$$\text{curl curl}_\omega\ \mathbf{w} \equiv -\frac{1}{r}\left\{\frac{\partial^2}{\partial r^2}(rw_\omega) + \frac{1}{r}\frac{\partial}{\partial\theta}\left[\frac{1}{\sin\theta}\frac{\partial}{\partial\theta}(\sin\theta\,.\,w_\omega)\right]\right\}.$$

Now curl ($\rho$ . grad $\phi$) $=$ grad $\rho$ $\wedge$ grad $\phi$ $+$ $\rho$ . curl grad $\phi$, and has $r$-, $\theta$-, $\omega$-components respectively

$$0,\ 0,\ \frac{1}{r}\,.\,\frac{\partial\rho}{\partial r}\,.\,\frac{\partial\phi}{\partial\theta}.$$

Equation (7) therefore reads

$$\text{curl curl}_\omega\ \mathbf{w} = -\frac{1}{\eta r}\,.\,\frac{\partial\rho}{\partial r}\,.\,\frac{\partial\phi}{\partial\theta} = \frac{DX}{4\pi\eta}\sin\theta\left(1 + \lambda\frac{a^3}{r^3}\right)\frac{\partial}{\partial r}\nabla^2\psi. \tag{8}$$

If as a trial solution we set

$$w_\omega = -\frac{DX}{4\pi\eta}\left(\frac{\partial\psi}{\partial r} + \lambda a^3 W_1\right)\sin\theta,$$

where $W_1$ is a function of $r$ only, curl curl$_\omega$ **w** takes the value

$$\frac{DX}{4\pi\eta}\left\{\frac{\partial}{\partial}\nabla^2\psi + \frac{\lambda a^3}{} \qquad \frac{}{\partial r^2}\right.$$

and we find that equation (8) is satisfied provided

$$r^2\frac{\partial^2(rW_1)}{\partial r^2} - 2rW_1 = \frac{\partial}{\partial r}\nabla^2\psi, \tag{9}$$

whence, as with equation (5), we have

$$W_1 = r\int^r \frac{1}{r^4}\nabla^2\psi\, dr,$$

and

$$w_\omega = -\frac{DX}{4\pi\eta}\sin\theta\left\{\frac{\partial\psi}{\partial r} + \lambda a^3 r\int_\infty^r \frac{1}{r^4}\nabla^2\psi\, dr\right\}$$

where the lower limit of integration is set $\infty$ in view of the fact that the vorticity **w** must vanish for large values of $r$.

Setting

$$\xi = \frac{\partial\psi}{\partial r} + \lambda a^3 r\int_\infty^r \frac{1}{r^4}\nabla^2\psi\, dr,$$

we now have to solve the equations

$$\left.\begin{aligned} \operatorname{curl}_\omega \mathbf{v} &\equiv \frac{1}{r}\frac{\partial}{\partial r}(rv_\theta) - \frac{1}{r}\frac{\partial v_r}{\partial\theta} = -\frac{DX\xi}{4\pi\eta}\sin\theta \\ \operatorname{div} \mathbf{v} &\equiv \frac{1}{r^2}\frac{\partial}{\partial r}(r^2 v_r) + \frac{1}{r\sin\theta}\frac{\partial}{\partial\theta}(\sin\theta\,.\,v_\theta) = 0 \end{aligned}\right\} \quad (10)$$

Setting as solutions $v_r = R_1\cos\theta$, $v_\theta = R_2\sin\theta$, where $R_1$, $R_2$ are functions of $r$ only, these equations reduce to

$$\left.\begin{aligned} \frac{1}{r}\frac{\partial}{\partial r}(rR_2) + \frac{1}{r^3}(r^2R_1) &= -\frac{DX\xi}{4\pi\eta} \\ \frac{1}{r^2}\frac{\partial}{\partial r}(r^2R_1) + \frac{2}{r^2}(rR_2) &= 0 \end{aligned}\right\} \quad (11)$$

Eliminating $rR_2$ and solving as with equation (5), we obtain

$$\left.\begin{aligned} v_r &= \frac{DX}{6\pi\eta}\cos\theta\left(\int^r \xi\, dr - \frac{1}{r^3}\int^r r^3\xi\, dr\right) \\ v_\theta &= -\frac{DX}{6\pi\eta}\sin\theta\left(\int^r \xi\, dr + \frac{1}{2r^3}\int^r r^3\xi\, dr\right) \end{aligned}\right\}. \quad (12)$$

The lower limits of integration depend on the boundary conditions, and will for the moment be left undetermined.

To achieve the complete solution of equation (2), we must add to the particular solution represented by equations (6) and (12) a general solution of the equations

$$\left.\begin{aligned} \eta\,.\operatorname{curl}\operatorname{curl}\mathbf{v} + \operatorname{grad} p &= 0 \\ \operatorname{div}\mathbf{v} &= 0 \end{aligned}\right\}. \quad (13)$$

Having regard to the symmetry of the system about the polar axis, this takes the form

$$
\begin{aligned}
p &= A_0 + (A_1 r + B_1/r^2)\cos\theta \\
v_r &= (A_1 r^2/10\eta + B_1/\eta r + A_2 + B_2/r^3)\cos\theta, \\
v_\theta &= (-A_1 r^2/5\eta - B_1/2\eta r - A_2 + B_2/2r^3)\sin\theta, \\
v_\omega &= 0.
\end{aligned}
$$

$A_0$, $A_1$, $A_2$, $B_1$ and $B_2$ are constants to be determined by the boundary conditions. Since the velocity **v** is everywhere finite, $A_1$ must be zero, and the complete solution of (2) is

$$
\begin{aligned}
p &= \int_\infty^r \rho\frac{\partial\psi}{\partial r}\,dr + A_0 + \cos\theta\left\{\frac{B_1}{r^2} - \frac{DX}{4\pi}\left(3\frac{\partial\psi}{\partial r} - 2\xi\right)\right\}, \\
v_r &= \cos\theta\left\{\frac{B_1}{\eta r} + A_2 + \frac{B_2}{r^3} + \frac{DX}{6\pi\eta}\left(\int^r \xi\,dr - \frac{1}{r^3}\int^r r^3\xi\,dr\right)\right\}, \\
v_\theta &= \sin\theta\left\{-\frac{B_1}{2\eta r} - A_2 + \frac{B_2}{2r^3} - \frac{DX}{6\pi\eta}\left(\int^r \xi\,dr + \frac{1}{2r^3}\int^r r^3\xi\,dr\right)\right\}, \\
v_\omega &= 0.
\end{aligned}
$$

The boundary conditions are –

$$
\begin{aligned}
&\text{for } r = \infty, \quad v_r = -U\cos\theta, \quad v_\theta = U\sin\theta, \quad \psi = 0, \\
&\text{and for } r = a, \quad v_r = v_\theta = 0, \qquad \psi = \psi_a.
\end{aligned}
$$

From the conditions at infinity we have

$$
-U = A_2 + \frac{DX}{6\pi\eta}\left\{\int^\infty \xi\,dr - \operatorname*{Limit}_{r\to\infty}\left(\frac{1}{r^3}\int^r r^3\xi\,dr\right)\right\}
$$

and

$$
U = -A_2 - \frac{DX}{6\pi\eta}\left\{\int^\infty \xi\,dr + \tfrac{1}{2}\operatorname*{Limit}_{r\to\infty}\left(\frac{1}{r^3}\int^r r^3\xi\,dr\right)\right\}.
$$

A solution is therefore only possible if

$$
\operatorname*{Limit}_{r\to\infty}\left(\frac{1}{r^3}\int^r r^3\xi\,dr\right) = 0.
$$

This requires that, as $r$ increases,

$$
\xi \equiv \frac{\partial\psi}{\partial r} + \lambda a^3 r\int_\infty^r \frac{1}{r^4}\nabla^2\psi\,dr
$$

should tend to zero more rapidly than $1/r$. This will in practice always be so, for if we had a charged sphere without ionic atmosphere (which is a less favourable case than the actual), $\partial\psi/\partial r$ tends to zero as $1/r^2$, while for large enough $r$

$$r\int_{\infty}^{r}\frac{1}{r^4}\nabla^2\psi\,dr < r\int_{\infty}^{r}\frac{1}{r^4}\,dr,$$

which also tends to zero as $1/r^2$. This condition being satisfied, we find

$$A_2 = -U - \frac{DX}{6\pi\eta}\int^{\infty}\xi\,dr$$

The conditions at $r = a$ then lead to the values

$$\frac{B_1}{a\eta} = \tfrac{3}{4}U - \frac{DX}{4\pi\eta}\int_{\infty}^{a}\xi\,dr,$$

and

$$\frac{B_2}{a^3} = -\tfrac{1}{4}U + \frac{DX}{12\pi\eta}\int_{\infty}^{a}\xi\,dr + \frac{DX}{6\pi\eta a^3}\int^{a} r^3\xi\,dr$$

Introducing these values of the constants, and setting $A_0$, which is merely an additive hydrostatic pressure, equal to zero, the complete solution of the equations of motion becomes

$$p = \int_{\infty}^{r}\rho\frac{\partial\psi}{\partial r}\,dr + \cos\theta\left\{\frac{3\eta a}{2r^2}U - \frac{a}{r^2}\frac{DX}{4\pi}\int_{\infty}^{a}\xi\,dr - \frac{DX}{4\pi}\left(3\frac{\partial\psi}{\partial r} - 2\xi\right)\right\},$$

$$v_r = \cos\theta\left\{-\left(1 - \frac{3a}{2r} + \frac{a^3}{2r^3}\right)U - \left(\frac{a}{r} - \frac{a^3}{3r^3}\right)\frac{DX}{4\pi\eta}\int_{\infty}^{a}\xi\,dr\right.$$
$$\left. - \frac{DX}{6\pi\eta}\left(\int_{\infty}^{r}\xi\,dr - \frac{1}{r^3}\int_{a}^{r}r^3\xi\,dr\right)\right\},$$

$$v_\theta = \sin\theta\left\{\left(1 - \frac{3a}{4r} - \frac{a^3}{4r^3}\right)U + \left(\frac{a}{2r} + \frac{a^3}{6r^3}\right)\frac{DX}{4\pi\eta}\int_{\infty}^{a}\xi\,dr\right.$$
$$\left. - \frac{DX}{6\pi\eta}\left(\int_{\infty}^{r}\xi\,dr + \frac{1}{2r^3}\int_{a}^{r}r^3\xi\,dr\right)\right\},$$

$$v_\omega = 0.$$

It remains to calculate the force on the sphere produced by this fluid motion. From symmetry it is evident that only the $x$-components of the stresses need be taken into account, as the components perpendicular to the polar axis will vanish when integrated over the surface of the sphere. A straightforward though somewhat tedious calculation shows that the $x$-component of the stress normal to any point of the surface is given by

$$p_{rx} \equiv \left(-p + 2\eta\frac{\partial v_r}{\partial r}\right)_{r=a} . \cos\theta - \left(\frac{\partial v_\theta}{\partial r} + \frac{1}{r}\frac{\partial v_r}{\partial\theta} - \frac{v_\theta}{r}\right)_{r=a} . \sin\theta$$

$$= \cos\theta\int_\infty^r \rho\frac{\partial\psi}{\partial r}dr + \cos^2\theta\left\{-\frac{3\eta}{2a}\mathrm{U} + \frac{\mathrm{DX}}{4\pi}\left[\frac{1}{a}\int_\infty^a \xi\,dr + 3\left(\frac{\partial\psi}{\partial r}\right)_a - 2\xi_a\right]\right\}$$

$$+ \sin^2\theta\left\{-\frac{3\eta}{2a}\mathrm{U} + \frac{\mathrm{DX}}{4\pi}\left[\frac{1}{a}\int_\infty^a \xi\,dr + \xi_a\right]\right\}.$$

The force required is obtained by integrating $p_{rx}$ round the surface of the sphere, and therefore equals $2\pi a^2\int_0^\pi p_{rx}\ \sin\theta\,.\,d\theta$, which reduces to

$$-6\pi a\eta\mathrm{U} + \mathrm{DX}a\int_\infty^a \xi\,dr + \mathrm{DX}a^2\left(\frac{\partial\psi}{\partial r}\right)_a \tag{14}$$

To this expression we must now add the force on the sphere due to its fixed surface charge. This amounts to $e$X, which by Gauss' theorem is equal to $-\mathrm{DX}a^2(\partial\psi/\partial r)_a$, and just cancels the last term in expression (14). The total force on the sphere is therefore $-6\pi a\eta\mathrm{U} + \mathrm{DX}a\int_\infty^a \xi\,dr$. For steady motion this must vanish, so that

$$\mathrm{U} = \frac{\mathrm{DX}}{6\pi\eta}\int_\infty^a \xi\,dr. \tag{15}$$

Inserting the value of $\xi$ and integrating by parts, we obtain

$$\mathrm{U} = \frac{\mathrm{DX}}{6\pi\eta}\left\{\psi_a + \frac{\lambda a^3}{2}\left(a^2\int_\infty^a \frac{1}{r^4}\nabla^2\psi\,.\,dr - \int_\infty^a \frac{1}{r^2}\nabla^2\psi\,.\,dr\right)\right\}. \tag{16}$$

Setting

$$\nabla^2\psi = \frac{1}{r^2}\frac{\partial}{\partial r}\left(r^2\frac{\partial\psi}{\partial r}\right)$$

and again employing integration by parts, we obtain the equivalent expressions

$$\mathrm{U} = \frac{\mathrm{DX}}{6\pi\eta}\left\{\psi_a + \lambda a^3\left(3a^2\int_\infty^a \frac{1}{r^5}\frac{\partial\psi}{\partial r}\,.\,dr - 2\int_\infty^a \frac{1}{r^3}\frac{\partial\psi}{\partial r}\,dr\right)\right\} \tag{17}$$

and

$$\mathrm{U} = \frac{\mathrm{DX}}{6\pi\eta}\left\{\psi_a(1+\lambda) + 3\lambda a^3\left(5a^2\int_\infty^a \frac{\psi}{r^6}\,dr - 2\int_\infty^a \frac{\psi}{r^4}\,dr\right)\right\}. \tag{18}$$

It should be noted that the reduction of equation (16) to these alternative forms merely requires that as $r$ tends to infinity, $\nabla^2\psi$ and $\partial\psi/\partial r$ remain finite or zero, which is evidently so.

The evaluation of the definite integrals involved in the relations (16) to (18) requires in general a knowledge of the law of the electric field in the ionic atmosphere. This question will be discussed in § 5. There are two special cases for which this knowledge is not required. The first is that of a sphere whose conductivity is the same as that of the medium, we now have $\lambda = 0$ and $U = DX\zeta/6\pi\eta$ irrespective of the thickness of the electrical double layer. This is Huckel's result. The other case is where Smoluchowski's fourth restriction may be assumed to hold, so that we can find a distance $l$, small in comparison with $a$, such that, when $r > a + l$, the absolute value of $\psi$ is less than an arbitrary positive quantity $\varepsilon$, which is negligibly small in comparison with the absolute value of $\psi_a$. We can write

$$\int_\infty^a \frac{1}{r^5}\frac{\partial\psi}{\partial r}dr = \int_\infty^{a+l}\frac{1}{r^5}\frac{\partial\psi}{\partial r}dr + \int_{a+l}^a \frac{1}{r^5}\frac{\partial\psi}{\partial r}dr = \left[\frac{\psi}{r^5}\right]_\infty^{a+l} + 5\int_\infty^{a+l}\frac{\psi}{r^6}dr + \int_{a+l}^a \frac{1}{r^5}\frac{\partial\psi}{\partial r}dr.$$

In the last expression, the first two terms are easily shown to be of order $\varepsilon/a^5$, and are therefore negligible in comparison with $\psi_a/a^5$, while the third term differs from $\psi_a/a^5$ by a quantity of order $l\psi_a/a^6$. To the order of approximation involved in our present assumption, therefore,

$$\int_\infty^a \frac{1}{r^5}\frac{\partial\psi}{\partial r}dr = \frac{\psi_a}{a^5},$$

and by similar reasoning

$$\int_\infty^a \frac{1}{r^3}\frac{\partial\psi}{\partial r}dr = \frac{\psi_a}{a^3}$$

Hence from (17)

$$U = \frac{DX\psi_a}{6\pi\eta}(1 + \lambda) = \frac{3\mu}{2\mu + \mu'}\cdot\frac{DX\zeta}{6\pi\eta} \tag{19}$$

where $\zeta$ is the potential difference of the electrical double layer. For an insulating sphere, $\mu' = 0$, and

$$U = DX\zeta/4\pi\eta$$

in agreement with Smoluchowski's result, which is thus confirmed for a rigid spherical insulating particle, subject to his four restrictions.

§ 3. *The Cataphoresis of an Infinite Cylinder in a Transverse Electric Field.*—The attempt to solve the present problem on the lines of the last section results in failure, since no solution satisfying the boundary conditions is obtainable if the "inertia terms" in the hydrodynamic equations are completely neglected. Neglect of these second order terms leads, in the case of the sphere, to a solution which, though not exact over the whole field, is so to a close approximation for the motion in the immediate neighbourhood of the spherical surface, where alone it enters into the calculation of the resistance. As first pointed out by Stokes, this does not hold in the case of the cylinder, the resistance of which can only be calculated by taking the inertia terms at least partially into account. This can be done by the method of Oseen.* Taking the axis of the cylinder and the direction of the applied field respectively as the $z$ and $x$ axes of co-ordinates, the motion of the fluid will by symmetry be confined to the $xy$ plane. Let $u$, $v$ be the $x$ and $y$ components of velocity (the cylinder being considered as at rest), and let the velocity of the liquid at a great distance from the cylinder be $-\mathrm{U}$ Then setting $u_1 = u + \mathrm{U}$, $v_1 = v$, we neglect terms of the second degree in $u_1$ and $v_1$. Since $u$ is, over most of the field, of the same order as $-\mathrm{U}$, we are in effect including in our equations a major portion of the inertia terms With the same notation as in the last section,† except that v here denotes the vector velocity whose Cartesian components are $u_1$, $v_1$ and 0, the equations of motion now read

$$\left.\begin{array}{c} \eta \,.\, \mathrm{curl\ curl\ v} + \mathrm{grad}\, p_1 + \delta \mathrm{U} \,.\, \partial \mathrm{v}/\partial x = - \rho \,.\, \mathrm{grad}\, \phi, \\ \mathrm{div\ v} = 0 \end{array}\right\} \qquad (19)$$

where

$$p_1 = p - \quad \rho \frac{\partial \psi}{\partial r}\, dr,$$

and $\delta$ is the density of the liquid , the electric density $\rho$ is, as before, assumed to be a function of the $r$-co-ordinate only.

The boundary conditions are: for $r = \infty$ , $u_1 = v_1 = 0$, and for $r = a$, $u_1 = \mathrm{U}$, $v_1 = 0$ The applied field is easily shown to be .

$$\phi = - \mathrm{X} (r + \lambda a^2/r) \cos \theta,$$

$$\phi' = - \mathrm{X} (1 + \lambda)\, r \cos \theta,$$

where

$$\lambda = (\mu - \mu')/(\mu + \mu').$$

The complete solution of equations (19) is to be obtained by the superposition of a particular solution of the equations as they stand and a general solution of the equations which result when the right-hand side is made zero. The latter is given by Lamb (*loc. cit.*) in a form which satisfies the boundary conditions at infinity, and which can be expressed, for small values of $r$, by means of a convergent series. With a trivial change of variables Lamb's solution* can be written in the form

---

* See Lamb, "Hydrodynamics," 5th ed , § 343, p. 581.

† Where the analytical methods are similar to those of § 2, the demonstration will be given in a more condensed form. Cylindrical polar co-ordinates $r$, $\theta$, $z$ will be employed, the angle $\theta$ being measured from the $x$ axis as previously defined

$$\begin{aligned} p_1 &= -\delta U\,(A_0 \cos\theta/r - A_1 \cos 2\theta/r^2 + \ldots) \\ u_1 &= -(C/2k + A_0)\cos\theta/r - \tfrac{1}{2}C\,(\gamma + \log kr/2 - \tfrac{1}{2}) \\ &\qquad\qquad\qquad + (C/4 + A_1/r^2)\cos 2\theta + \ldots \\ v_1 &= -(C/2k + A_0)\sin\theta/r \qquad + (C/4 + A_1/r^2)\sin 2\theta + \end{aligned} \tag{20}$$

$\gamma$ is Euler's constant (0·5772) and $k = \delta U/2\eta$, which is assumed to be a small quantity in comparison with $1/a$, that this condition is realised in practice will be pointed out later. All terms of the infinite series which are omitted from equation (20) are of the first or higher degree in $kr$.

A particular solution of equations (19) must now be sought which independently satisfies the boundary conditions at infinity, and which, when combined with (20), also satisfies those at the surface of the cylinder. Using the same methods as in § 2, we obtain

$$p_1 = -\frac{DX}{4\pi}\cos\theta\left(\frac{\partial\psi}{\partial r} - \lambda a^2 r\int_\infty^r \frac{1}{r^3}\nabla^2\psi\,.\,dr\right)$$

The equation

$$\text{curl curl}_z\,\mathbf{w} - 2k\;\;\partial w_z/\partial r = -\frac{1}{r}\cdot\frac{\partial\phi}{\partial\theta}\cdot\frac{\partial\rho}{\partial r}, \tag{21}$$

which arises in place of equation (8) of § 2, can be solved by a method of successive approximations. The first approximation, obtained by omitting the second term from consideration, is

$$\begin{aligned} w_z = &-\frac{DX}{4\pi\eta}\sin\theta\left(\frac{\partial\psi}{\partial r} + \lambda a^2 r\int_\infty^r \frac{1}{r^3}\nabla^2\psi\,dr\right) \\ &-\frac{DX}{4\pi\eta}\sin\theta\;\;\xi. \end{aligned} \tag{22}$$

A second approximation can be obtained by substituting this value of $w_z$ in the second term of (21) and again solving; this results in the introduction into (22) of the additional term

$$-\frac{DX}{4\pi\eta}\sin 2\theta\,.\,kr\xi_1,$$

where

$$\xi_1 = \frac{1}{r^3}\int^r r^2\xi\,dr.$$

---

* It is to be noted that the sign of Lamb's U has been reversed in the present demonstration.

In a similar manner further approximations can be obtained which introduce into (22) terms involving expressions of the type $(kr)^2\xi_2$, $(kr)^3\xi_3$, etc., where the quantities $\xi_1$, $\xi_2$, etc., are functions of $r$ of the same degree in $r$ as $\xi$. These additional terms, involving the first and higher powers of $kr$, will not enter into our calculation of the force on the cylinder, and can therefore be neglected provided that they do not invalidate the boundary condition at infinity. To secure this we must have $\underset{r\to\infty}{\text{Limit}}\, r^n\xi_n = 0$ for all values of $n$, which will only be the case if, as $r$ tends to infinity, $\psi$ ultimately tends to zero more rapidly than any inverse power of $r$. This might appear to be a drastic limitation, but when we consider that the ionic atmosphere is in all probability of the type considered in Debye and Huckel's theory of strong electrolytes, we see that it is almost certainly realised in practice. For the Debye-Huckel ionic atmosphere is, to a close approximation, defined by the equation $\nabla^2\psi = \kappa^2 . \psi$, the axially symmetrical solution of which is $\psi = AK_0(\kappa r)$, where A is a constant and $K_0(\kappa r)$ is the "modified Bessel function of the second kind and order zero." For large $r$, $K_0(\kappa r)$ tends to zero* as $e^{-\kappa r}/\sqrt{\kappa r}$, which itself tends to zero more rapidly than any inverse power of $r$. The same will, therefore, hold for the quantities $\xi$, $\xi_1$, $\xi_2$, etc., and our assumption is justified. Assuming it to hold, equation (22) leads to the desired particular solution by a method analogous to that employed in solving equation (10) of the last section, except that this time we must not defer consideration of the "complementary function terms," since our present particular solution must be made to satisfy the boundary conditions at infinity *independently* of the general solution represented by equation (20). Having regard to the requirement that v is everywhere finite, the complementary function terms reduce to two in number, and we obtain

$$\left.\begin{aligned} u_1 &= B_0 + \frac{DX}{8\pi\eta}\int^r \xi\,dr + \left(\frac{B_1}{r^2} - \frac{DX}{8\pi\eta}\cdot\frac{1}{r^2}\int^r r^2\xi\,dr\right)\cos 2\theta \\ v_1 &= \qquad\qquad\qquad\quad \left(\frac{B_1}{r^2} - \frac{DX}{8\pi\eta}\cdot\frac{1}{r^2}\int^r r^2\xi\,dr\right)\sin 2\theta \end{aligned}\right\}$$

The boundary conditions at infinity require that

$$\underset{r\to\infty}{\text{Limit}}\,\frac{1}{r^2}\int^r r^2\xi\,dr = 0,$$

which holds in view of the considerations adduced above, and that

$$B_0 = -\frac{DX}{8\pi\eta}\int^\infty \xi\,dr.$$

---

* See *e.g.*, Gray, Mathews and MacRobert, "Bessel Functions," p. 56 (1922).

Inserting this value of $B_0$, we obtain the system of equations

$$\left.\begin{aligned} p_1 &= -\frac{DX}{4\pi}\cos\theta\left(2\frac{\partial\psi}{\partial r} - \xi\right), \\ u_1 &= \frac{DX}{8\pi\eta}\int_\infty^r \xi\,dr + \left(\frac{B_1}{r^2} - \frac{DX}{8\pi\eta}\,\frac{1}{r^2}\int^r r^2\xi\,dr\right)\cos 2\theta \\ v_1 &= \qquad\qquad\qquad\quad \left(\frac{B_1}{r^2} - \frac{DX}{8\pi\eta}\,\frac{1}{r^2}\int^r r^2\xi\,dr\right)\sin 2\theta \end{aligned}\right\} \tag{23}$$

The superposition of equations (20) and (23) provides a complete solution of the equations of motion to the approximation here entertained. Applying to the combined equations the boundary conditions at $r = a$, viz., $u_1 = U$, $v_1 = 0$, we find that

$$\begin{aligned} A_0 &= -C/2k \\ -\frac{C}{2}(\gamma + \log ka/2 - \tfrac{1}{2}) + \frac{DX}{8\pi\eta}\int_\infty^a \xi\,dr &= U \\ A_1 + B_1 &= \frac{DX}{8\pi\eta}\int^a r^2\xi\,dr - Ca^2/4 \end{aligned} \tag{24}$$

Substituting these values for the constants $A_0$ and $(A_1 + B_1)$, the combined solution takes the form

$$\begin{aligned} p_1 &= \left\{\eta C/r - \frac{DX}{4\pi}\left(2\frac{\partial\psi}{\partial r} - \xi\right)\right\}\cos\theta, \\ u_1 &= -\frac{C}{2}(\gamma + \log kr/2 - \tfrac{1}{2}) + \frac{DX}{8\pi\eta}\int_\infty^r \xi\,dr \\ &\qquad\qquad + \left\{\frac{C}{4}(r^2 - a^2) - \frac{DX}{8\pi\eta}\int_a^r r^2\xi\,dr\right\}\cdot\frac{1}{r^2}\cdot\cos 2\theta, \\ &\qquad\qquad\ \ \left\{\frac{C}{4}(r^2 - a^2) - \frac{DX}{8\pi\eta}\int_a^r r^2\xi\,dr\right\}\ \frac{1}{r^2}\sin 2\theta \end{aligned}$$

The force exerted on unit length of the cylinder by the fluid motion is obtained by integrating $rp_{rx}$ between $\pm\pi$ and setting $r = a$, and reduces to the expression $-2\pi\eta C + DXa\,(\partial\psi/\partial r)_a$. The force on the cylinder due to its fixed charge is $eX$ per unit length, which by Gauss' theorem is equal to $-DXa\,(\partial\psi/\partial r)_a$, and just cancels the second term of the previous expression. For steady motion the residual force, $-2\pi\eta C$, and hence the constant C, must be zero. Substitution in (24) leads to the result that

$$U = \frac{DX}{8\pi\eta}\int_\infty^a \xi\,dr.$$

By repeated integration by parts, subject to Smoluchowski's fourth restriction, this reduces to

$$U = \frac{DX\psi_a}{8\pi\eta}(1 + \lambda) = \frac{2\mu}{\mu + \mu'}\frac{DX\zeta}{8\pi\eta}$$

For an insulating cylinder, for which $\mu' = 0$

$$U = DX\zeta/4\pi\eta$$

in agreement with Smoluchowski's formula, while if $\mu = \mu'$

$$U = DX\zeta/8\pi\eta,$$

which is the formula which results from Huckel's assumptions

§ 4. *The Electrosmotic Velocity at a Plane Surface in a Tangential Field, or at a Cylindrical Surface in an Axial Field*.—In this section it will be more natural to adopt the point of view of electrosmosis rather than that of cataphoresis, since the surfaces dealt with are treated as extending to infinity in the direction of motion. Apart from this, the surfaces are characterised solely by the fact that they are "developable surfaces" whose generators are parallel to the direction of the applied field. Under these circumstances, not only are the stream lines and the gradients of potential and pressure everywhere parallel to the boundary surfaces, but the gradients in question are both constant in magnitude. The problem of calculating the electrosmotic velocity is thereby much simplified, and a general demonstration can be given to include both the plane surface set tangentially, and the infinite cylinder (of any cross-section) set axially to the applied field.

Take the $x$-axis of co-ordinates parallel to the applied field, and let $u$ denote the velocity at any point. The equation of motion is $\eta \nabla^2 u = \partial p/\partial x - \rho X$, where the symbols have the same meaning as heretofore. Setting the constant pressure gradient equal to P, and substituting for $\rho$ by Gauss' theorem, we obtain

$$\eta \nabla^2 (u - DX\psi/4\pi\eta) = P \tag{25}$$

This equation, together with the condition $u = 0$ and $\psi = \psi_a$ at the boundary, defines the motion. If we set $w = u - DX\psi/4\pi\eta$, we obtain $\eta \nabla^2 w = P$, with $w = - DX\psi_a/4\pi\eta$ at the boundary. This is the equation of a rectilinear stream line motion under zero external field of force, subject to a constant boundary velocity $w_0 = - DX\zeta/4\pi\eta$. At all points outside the electrical double layer, $u = w$, and the actual motion is exactly equivalent to the unconstrained motion provided we assume a boundary velocity $w_0$. The velocity $w_0$ is the desired electrosmotic velocity, the magnitude of which is therefore given as before by Smoluchowski's equation. Within the double layer the equivalence ceases to hold, and if the thickness of the double layer is significant equation (25) must be solved with special reference to the actual form of the boundary. Otherwise it is sufficient to solve the problem of the unconstrained motion with the fictitious boundary condition, and, provided the point of observation is outside the double layer, no limitation need be imposed on the thickness of the latter

§ 5 *Discussion* - In the preceding sections it has been found that, subject to the four restrictions quoted in § 1, Smoluchowski's equation for the velocity of cataphoresis or electrosmosis is valid for rigid insulating surfaces of very diverse form, which lends support to the supposition that it would be found to hold under like conditions for surfaces of any form. It remains to discuss the limitations imposed by these restrictions, and to review the experimental evidence which bears on the validity of Smoluchowski's equation.

The condition that the surface should be rigid is essential since we have assumed the inner sheet of the double layer to be at rest with respect to the body which carries it. A preliminary investigation by the author of the cataphoresis of a fluid droplet indicates that the cataphoretic velocity will be considerably affected by a circulatory motion within the drop

The arguments of §§ 2 and 3 would seem to indicate that Smoluchowski's equation is only valid for insulating particles, and that the cataphoretic velocity of a particle which is a good conductor should be extremely small On the other hand, experiment shows that the mobility of particles of colloidal gold and silver is of the same order as that of insulating particles such as those of arsenious sulphide or gum mastic Abramson* has made a direct comparison of the cataphoretic mobilities of various conducting and non-conducting particles which were provided with identical surfaces by coating them with a layer of protein, and finds that the conductivity of the particle is without measurable influence on the mobility. It seems probable that under normal circumstances conducting particles behave as insulators, so far as the distribution of the applied field is concerned, in consequence of electric polarisation at the surface, and that in consequence they will conform to Smoluchowski's equation. Some experiments, carried out in the author's laboratory, on the cataphoretic deflection of fine silver fibres suspended in a solution of silver nitrate indicate that where polarisation is deliberately minimised, the cataphoretic effect with a good conductor is in fact extremely small.

---

* Abramson and Michaelis, 'J. Gen. Physiol,' vol. 12, p. 587 (1929); Abramson, 'J. Phys. Chem.,' vol. 35, p. 299 (1931).

Turning now to the "four restrictions" of § 1, the first would not appear to be serious, though it is possible that the appropriate values of the dielectric constant and coefficient of viscosity will not be those which apply to the liquid in bulk

For the problems discussed in §§ 2 and 3, the second restriction requires that $Ua\delta/\eta$ should be small in comparison with unity That this condition is as a rule amply fulfilled becomes evident when we consider that for a particle with the relatively large diameter of 20 μ, moving with the abnormally great cataphoretic velocity of 100 μ/sec. through a dilute aqueous solution, this ratio has the value 0·001. For the electrosmotic flow discussed in § 1, the limiting factor is the onset of turbulent motion, which allows even greater latitude, for example, Osborne Reynolds found that stream line motion persists in a cylindrical tube up to a value of $Ua\delta/\eta$ of over 1000. If we wish to consider particles of irregular shape, it appears possible that the existence of sharp edges or pronounced re-entrant angles would produce turbulent motion, so that the results here obtained might not be applicable to colloidal particles having a rough or echinate surface. Since, however, such particles are often strongly solvated, it is at least possible that the attached shell of solvent molecules will produce a micelle of "easy shape" to which the equations will apply. The observed fact that particles of most diverse shapes show the same cataphoretic velocity speaks in favour of this view

The third restriction raises much more serious difficulties It is certain that the application of an external field and the motion of the particle will disturb the symmetry of the ionic atmosphere, but it is not easy to estimate the magnitude of the error thus introduced. A paper has recently appeared by Mooney* in which he reports having formulated differential equations for the cataphoretic mobility which are not subject to this restriction, he says, however, that they are "too complicated to allow any hope for a complete solution." This is also the experience of the author, who has made several attempts in the same direction. At present experiment must be relied on to decide the importance of the third restriction.

For a discussion of the fourth restriction, it will be convenient to assume some probable law for the electric distribution in the outer sheet of the double layer. As already indicated, this will almost certainly be a "Debye-Huckel" ionic atmosphere. A first approximation to this distribution, for the case of spherical symmetry, is given by the equation

$$\psi = \psi_a (a/r)\, e^{-\kappa(r-a)}. \tag{26}$$

---

* 'J. Phys. Chem.,' vol. 35, p. 331 (1931).

Inserting this value of $\psi$ in equation (18), and setting $\lambda = 1/2$ for an insulating particle, we are able to derive the following alternative expressions for U:

$$U = \frac{DX\zeta}{4\pi\eta}(1 - 3/\kappa a + 25/\kappa^2a^2 - 220/\kappa^3a^3 + \ldots),$$

$$U = \frac{DX\zeta}{6\pi\eta}\left(1 + \kappa^2a^2/16 - 5\kappa^3a^3/48 - \kappa^4a^4/96 + \kappa^5a^5/96 - \frac{11}{96}e^{\kappa a}\int_{\infty}^{\kappa a}\frac{e^{-t}}{t}\,dt\right).$$

The former expression is an asymptotic series which allows U to be computed (to three significant figures) for values of $\kappa a$ not less than 25; the latter expression is convergent for all values of $\kappa a$, but is only practicable for computation when $\kappa a$ is not greater than 5. There is thus a hiatus in the series of computations, but fortunately there does not appear to be much doubt about the course of the graph. If we set $U = f(\kappa a) \cdot DX\zeta/4\pi\eta$, fig. 1 (Curve 1) shows $f(\kappa a)$ plotted against $\log_{10}\kappa a$; we find that for values of $\kappa a$ not less than 300, Smoluchowski's equation should hold to within 1 per cent. For smaller values of $\kappa a$, $f(\kappa a)$ diminishes towards the value 2/3, until for values of $\kappa a$ about 0·5 Huckel's equation in turn becomes valid to within 1 per cent. This curve, and the numerical deductions from it, are to be regarded merely as approximations to the truth, since equation (26), on which they are based, provides only an approximate representation of the "Debye-Huckel atmosphere." Its failure is most pronounced for large values of $\psi$ and therefore, for a given charge on the particle, for small values of $a$; the left-hand end of the curves of fig. 1 is therefore the least reliable. The author is at present engaged on the somewhat laborious numerical integration of the exact Debye-Huckel equation, and hopes to produce later a revised and more accurate version of fig. 1. Table I shows the values of $\kappa$ for a number of aqueous solutions of different ionic concentrations, together with the corresponding values of $1/\kappa$ (which may be regarded as a measure of the "thickness of the double layer"), and the respective minimum (S) and maximum (H) limits of particle diameter for the validity (to 1 per cent.) of the Smoluchowski and Hückel equations; these are calculated on the basis of equation (26), and will therefore almost certainly need revision. Provisionally, however, it may be inferred that particles in colloidal solutions will almost always lie in the region within which the cataphoretic mobility varies with the size, but that droplets in emulsions, and other suspended particles of microscopic (as distinct from ultramicroscopic) size should provide material for the experimental verification of Smoluchowski's equation.

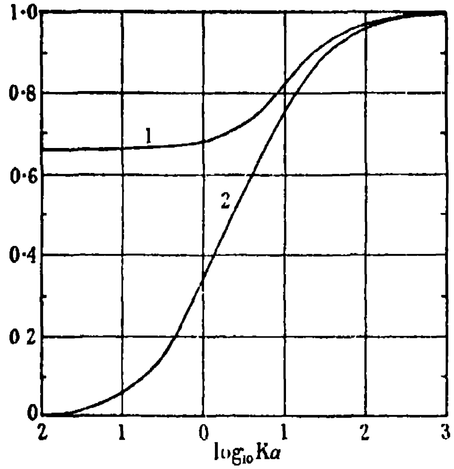

FIG 1 - Curve 1. Graph of $f(\kappa a)$ against $\log \kappa a$.

Curve 2 Graph of $\frac{\kappa a}{1 + \kappa a} f(\kappa a)$ against $\log \kappa a$.

Table I

| Electrolyte. | Concentration, N | $\kappa$ at 20° cm $^{-1}$ | $1/\kappa$ $\mu$ | Diameters ($\mu$) | |
|---|---|---|---|---|---|
| | | | | (S.) | (H.) |
| Pure water | — | $1·0 \times 10^4$ | 1·0 | 600 | 1·0 |
| Uni-univalent | $10^{-5}$ | $1·0 \times 10^5$ | 0·1 | 60 | 0·1 |
| | $10^{-3}$ | $1·0 \times 10^6$ | 0·01 | 6·0 | 0·01 |
| | $10^{-1}$ | $1·0 \times 10^7$ | 0·001 | 0·6 | 0·001 |
| Uni-bivalent | $10^{-5}$ | $1·8 \times 10^5$ | 0·056 | 34 | 0·056 |
| | $10^{-1}$ | $1·8 \times 10^7$ | 0·00056 | 0·34 | 0·00056 |
| Bi-bivalent | $10^{-5}$ | $2·1 \times 10^5$ | 0·048 | 29 | 0·048 |
| | $10^{-1}$ | $2·1 \times 10^7$ | 0·00048 | 0·29 | 0·00048 |

§ 6. *Experimental Evidence.*—The relevant evidence falls under two headings: firstly, evidence that, subject to the necessary size restrictions, the cataphoretic mobility of a particle is not dependent on its shape, and, secondly, evidence that the constant in the cataphoretic equation is actually $1/4\pi$ for particles of the necessary size.

On the first point, Abramson* has collected a considerable volume of evidence. He finds for example, that shape does not affect the cataphoretic mobility of quartz, glass and clay particles of very irregular forms and of size varying from 3 to 15 $\mu$, similar experiments by the author with glass particles led to the same conclusion. Abramson further finds that the mobility of leucocytes, blood platelets and red cells are the same as that of their respective irregularly shaped aggregates His most convincing evidence is that based on the discovery that solid particles of various materials suspended in a dilute protein solution become covered with an adsorbed layer of protein, and behave as if they had surfaces of identical nature He was thus able to compare the cataphoretic mobilities of spherical mastic particles and oil globules, from 1 to 5 $\mu$ in diameter, with those of needles of asbestos and *m*-aminobenzoic acid whose length, ranging from 12 to 150 $\mu$, was many times their diameter. In every case, irrespective of its orientation, the needle-shaped particle was found to have, within experimental error, the same mobility as the spherical particle with which it was directly compared

---

* Abramson, 'J. Exp. Med.,' vol. 41, p. 445 (1925); vol. 48, p. 677 (1928), 'J. Amer. Chem. Soc.,' vol. 50, p 390 (1928); Freundlich and Abramson, 'Z Phys Chem.,' vol. 128, p. 25 (1927), vol. 133, p 51 (1928), Abramson and Michaelis, 'J. Gen Physiol.,' vol. 12, p 587 (1929). Summarised in 'J. Phys. Chem.,' vol. 35, p 291 (1931).

The attempt to determine quantitatively the constant in the cataphoretic equation depends on a comparison of the cataphoretic velocity, $u$, of a suspended particle with the electrosmotic velocity $w_0$ at a plane surface of the same material. When the microscopic technique is used, $u$ and $w_0$ can be separately determined by measurements of the apparent velocity of particles at different depths in the cell, for details of the calculation reference may be made to Freundlich's text-book or to Smoluchowski's monograph. If the walls of the microscope cell have the same surface as the suspended particles, we should find $w_0/u$ equal to $-1$ if Smoluchowski's equation is correct, but equal to $-1 \cdot 5$ if Huckel's equation applies.

By an application of this method, van der Ginten* claims to have shown that $w_0/u = -1 \cdot 5$; he used particles made by grinding up glass of the same sort as that of which the cell was built. Abramson† criticises his technique and shows that his conclusion is not justified; he further quotes experiments to show that particles of ground-up glass have not got a surface identical with that of the sheet glass from which they were made. Experiments by the author confirm this; the ratio $w_0/u$ was found to be reasonably constant (though not equal either to $-1$ or to $-1 \cdot 5$) for a given kind of glass, but to vary outside the limits of experimental error from one kind of glass to another. Presumably the surface produced by fracture is different from that produced by fusion or polishing, and experiments carried out in this way must be inconclusive. Abramson† has overcome this difficulty by using a dilute protein solution as medium, when both particle and cell wall behave as if they were protein and are directly comparable. As the mean of 16 experiments (excluding one), carried out with two different proteins and with various applied potentials and electrolytes in the medium, he finds $w_0/u = -1{\cdot}01$ with a maximum deviation of 0·17 and an average deviation of 0·088 The particles were made of powdered glass, powdered quartz and, in one instance, of benzyl alcohol; the size is not stated, but presumably was upwards of 3 $\mu$, as it is not easy to prepare glass powder finer than this.

---

* 'J. Chem. Phys.,' vol. 23, p. 14 (1916).

† 'J. Phys. Chem.,' *loc. cit.*

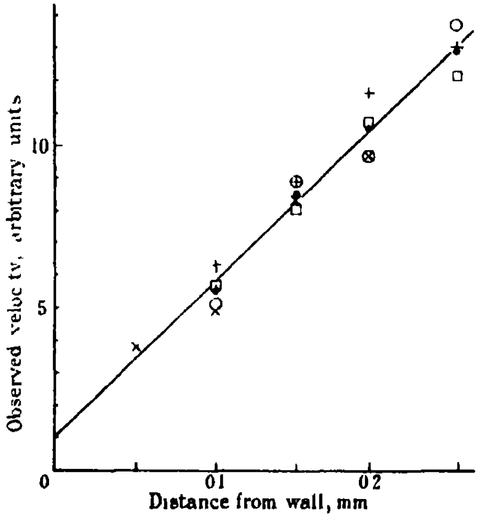

FIG. 2.—Velocity of Wax Particles near Wax Wall , experiment 1 , ⊙, experiment 2 , +, experiment 3 , ⊡, experiment 4 , ●, mean

The author has experimented with spherical particles of wax, prepared by emulsifying the molten wax in N/1000 salt solution and cooling, one wall of the cataphoresis cell was covered with a layer of the same wax, deposited by allowing the molten wax to solidify in contact with the salt solution; by this means it was hoped to secure that the wax wall and the particles should have identical surfaces. Observations were made in the neighbourhood of the centre of the wax wall, and use was made of the fact that the velocity of a particle right against the wall would be $u + w_0$; by Smoluchowski's equation this should be zero, but by Huckel's equal to $-\frac{1}{2}u$. It was neither possible nor desirable to make observations right against the wall, but the velocity which should obtain there was deduced by the extrapolation of observations made at various small distances from the wall; these were confined to a range of about one-twelfth of the thickness of the cell, which varied in different experiments between 3·1 and 3·4 mm., within this range the relation between velocity and distance could be taken as sensibly linear. Four experiments were carried out, a fresh wax wall and suspension being made for each. Each experiment consisted of 32 (in one case 31) velocity measurements made at four different distances The average deviation from their mean of each set of observations made at a given point was from 2 to 5 per cent. The distance from the wall was not easy to determine with accuracy, as the wall was not absolutely flat; the flattest portions available were, however, always selected, and the distances quoted are probably accurate to ±0·01 mm. The means of each set of observations are plotted in fig 2, which also shows the straight line drawn to give the best fit with the mean results of the whole series. Extrapolated to zero distance, it indicates a value of $u + w_0$ equal to $+1$ in the arbitrary units employed The exact values of $u$ and $w_0$ could not be determined directly, the calculations for a cell having walls of different materials not being feasible, but from an experiment with the same suspension done in an all-glass cell it was found that $u$ was of the order $30 \pm 3$ in the units employed. The experiments therefore indicate that $u = -w_0$ to within 3 or 4 per cent, and confirm Smoluchowski's equation. The diameter of the particles used was estimated to be from 2 to 6 $\mu$, giving a value of $\kappa a$ of from 100 to 300.

The above experiments, which were carried out some two years ago, were withheld from publication owing to the anomalous results obtained in similar experiments carried out by a different method, the value of $u + w_0$ as determined by extrapolation varied in an irregular manner from experiment to experiment, and frequently assumed a considerable negative value (though never as great as that demanded by Huckel's equation) At that time the limits of size necessary for the validity of Smoluchowski's equation had not been calculated, and it now appears probable that the particles were too small since the method employed involved the use of wax suspensions which had stood for considerable periods during which the larger particles would tend to settle out. It was intended to hold up publication pending the verification of this suggestion, but the conclusive nature of Abramson's evidence rendered it desirable to publish the available material without delay.

Some further evidence in favour of Smoluchowski's equation, derived from observations of the cataphoretic deflection of cylindrical fibres placed broadside on to the applied field, have been obtained by a completely different method, which will be described in the following paper. These measurements, which appear to be accurate to within about 5 per cent., supplement Abramson's work with a direct comparison of a cylindrical and a plane surface, and lend further support to the opinion that, subject to the stated conditions, Smoluchowski's equation holds for particles of all shapes.

It is highly desirable that an experimental check should be obtained of the predicted variation of cataphoretic mobility with particle size below the limit of validity of Smoluchowski's equation. For particles immersed in the same medium it would seem likely, as Abramson and Muller* suggest, that the charge per unit surface, rather than the potential $\zeta$, will be the same for all particles. If we employ the approximate Debye-Huckel equation (26), the relation between the mobility and the size of particles in the same medium would then be

$$U = \frac{X\sigma}{\kappa} \frac{\kappa a}{1 + \kappa a} f(\kappa a), \tag{27}$$

where $\sigma$ is the charge per square centimetre. The function

$$\frac{\kappa a}{1 + \kappa a} \cdot f(\kappa a)$$

is plotted as Curve 2 of fig. 1. Mooney† has observed a variation of mobility with size of droplets of various liquids suspended in water and aqueous solutions. His experimental results agree only very roughly with the predictions of equation (27). Three possible causes of this discrepancy suggest themselves; first, the approximate nature of equation (26); secondly, the probability that cataphoresis equations developed for rigid particles are not applicable to fluid droplets; and thirdly, the possibility that it is erroneous to assume a constant surface density of charge on the particle. If, as Mooney thinks probable, his droplets were not in a state of equilibrium with the medium, the last alternative seems very likely, while the first two are by no means improbable. Further work, both experimental and theoretical, will be required to enable a decision to be made.

---

* Abramson, 'J. Phys. Chem.,' vol. 35, p. 294 (1931).

† Mooney, 'Phys. Rev.,' vol. 23, p. 396 (1924); 'J. Phys. Chem.,' vol. 35, p. 331 (1931).

# *Cataphoresis. Part II.—A New Experimental Method, and a Confirmation of Smoluchowski's Equation.*

By C. G. Sumner, Ph.D., and D. C. Henry, M.A., Director of the Thomas Graham Colloid Research Laboratory, and Lecturer in Chemistry in the Victoria University of Manchester.

(Communicated by Professor A Lapworth, F R S —Received March 20, 1931 )

§ 1. In Part I of this communication it was shown that, subject to certain restrictions, the cataphoretic velocity of an insulating cylinder placed broadside on to the applied field should conform to Smoluchowski's equation

$$U = DX\zeta/4\pi\eta, \qquad (1)$$

whereas the assumptions made by Huckel* lead to the result

$$U = DX\zeta/8\pi\eta \qquad (2)$$

This conclusion has been investigated by a method depending on the static deflection of a suspended glass fibre, whose diameter is very great compared with the thickness of the electrical double layer. In principle the method derives from that of Billiter,† though the modifications and complications introduced in the effect to make it quantitative are so considerable as to render the technique in effect novel.

A fine glass fibre, some 20 cm. long, weighted at the bottom end by a glass sphere about 1 mm in diameter, is suspended from a rigid support so that some 5 cm. of its lower end hangs within a rectangular glass cell filled to the brim with a suitable liquid. The cell usually employed is a microscopists' filter cell 9·2 cm. high × 6 cm. long × 1·49 cm. thick. It is fitted with electrodes at the narrow ends and mounted on a sliding stage which can be made to traverse steadily at any desired speed in a direction parallel to the length of the cell. The suspended system may be deflected from its position of rest either by applying a potential gradient to the liquid, the cell being stationary (" electric deflection "), or by traversing the cell bodily, the applied potential being cut off (" mechanical deflection "). In either case equilibrium is reached when the restoring force due to gravity is just sufficient to inhibit the motion which would be assumed by the immersed portion of the suspension if it were floating freely.

---

* 'Physik Z ,' vol. 25, p. 204 (1924).

† 'Ann. Physik,' vol. 11, p. 902 (1903).

The original intention was to employ a comparison of the electric and mechanical deflections to measure the cataphoretic velocity of the glass sphere, the influence of the suspending fibre being taken as negligible. It was later discovered, both theoretically and by experiment, that the reverse is much more nearly true, and that approximately ten-elevenths of the total deflecting force is due to the fibre (*vide* § 3). To the order of accuracy which we have been able to attain, the influence of the sphere is therefore almost, but not quite, negligible.

In an electrical experiment, the lateral velocity $v_e$ which would be assumed by any small element of the immersed fibre if floating freely is compounded of its cataphoretic velocity $u$ in stationary liquid and the streaming velocity $w$ produced at the point in question by electrosmosis at the cell walls. $u$ is the same for all elements of the immersed fibre, but $w$ will in general vary from point to point, and must be calculated hydrodynamically in terms of the electrosmotic velocity $w_0$ at the cell wall. The usual formula*

$$\frac{w}{w_0} = -\tfrac{1}{2} + \tfrac{3}{2}\frac{y^2}{b^2}$$

(where $2b$ is the depth of the cell and $y$ the distance of the point of observation from the median plane) was derived for the case of a flat cell whose depth is so small compared with its width that the flow could be treated as taking place between infinite parallel planes. For a cell such as ours, whose width and depth are not widely different, we require a solution of the problem of the flow of a liquid through a pipe of rectangular cross section. This has been investigated by Cornish,† and takes the form

$$w = w_0 + \frac{\mathrm{P}b^2}{2\eta}\left(1 - \frac{y^2}{b^2}\right) - \frac{32}{\pi^5}\frac{\mathrm{P}b^2}{2\eta}\sum_0^\infty \frac{(-1)^n}{(2n+1)^3}\frac{\cosh(2n+1)\pi z/2b}{\cosh(2n+1)\pi c/2b} \cos(2n+1)\pi y/2b, \quad (3)$$

where P is the (constant) pressure gradient parallel to the line of flow, $2b$, $2c$ are the sides of the rectangular cross section, and $y$, $z$ are the co-ordinates of the point under consideration referred to the centre of the rectangle as origin and lines parallel to the respective sides as axes. By integration the total flow across the whole section is found to be

$$4bcw_0 + \tfrac{1}{3}\frac{\mathrm{P}}{\eta}b^3c - \frac{256}{\pi^5}\frac{\mathrm{P}}{\eta}b^4\sum_0^\infty \frac{1}{(2n+1)^5}\tanh(2n+1)\pi c/2b; \quad (4)$$

---

* Smoluchowski, in Graetz' "Handbuch der Elektrizitat und des Magnetismus," vol. 2, p. 382 (1914).

† 'Proc. Roy. Soc.,' A, vol. 120, p 691 (1928).

in a closed cell this must be zero. The elimination of P between equation (3) and the equation resulting when expression (4) is equated to zero gives the required velocity distribution, which has been verified by experiment by one of the authors. Since the flow in an open channel, such as our experimental cell, is equivalent to that in one-half of a closed cell of twice the depth, we shall have $c = 9 \cdot 2$ cm., $b = 0 \cdot 745$ cm. It is now easy to show that, for values of $z$ not greater than $5 \cdot 5$ cm., and of $y/b$ not numerically greater than $2/3$, the term in (3) involving the infinite series is over a thousand times smaller than that involving $(1 - y^2/b^2)$; since all our observations were made within these limits, we can write

$$w = w_0 + (\mathrm{P}b^2/2\eta)(1 - y^2/b^2), \tag{5}$$

which gives the same value of $w$ for each point of the fibre. Consequently we can write $v_e = u + w$ for the whole immersed portion of the fibre, where $w$ depends solely on $w_0$, the electrosmotic velocity at the walls, and on the position of the suspension in the thickness of the cell. In a mechanical experiment $v_m$ is simply the speed of the stage; if the latter is so adjusted as to produce the same deflection in both experiments, $v_e = v_m$, and the stage speed provides a measure of $u + w$.

Substituting the same values as before for $b$ and $c$ in the expression (4), the hyperbolic tangents are found to differ inappreciably from unity; the infinite series thus takes the form $\sum\limits_0^\infty 1/(2n + 1)^5 = 1 \cdot 0045$. This leads to the value $-1 \cdot 58$ for $\mathrm{P}b^2/2\eta$, which, with equation (5), gives as the relation between $w$, $w_0$ and $y/b$ the equation

$$w/w_0 = 1 \cdot 58y^2/b^2 - 0 \cdot 58.$$

Two or more pairs of experiments, carried out with different values of $y/b$, thus enable us to evaluate $u$ and $w_0$ If the cell walls and the fibre can be assumed to have the same value of $\zeta$, a discrimination between equations (1) and (2) can be made. The experiments of series I were carried out in this manner, the cell walls being lined with cover slip glass, and the suspensions made by drawing a portion of the same glass into a fibre. Since cover slip glass is manufactured by fusion, the surfaces were probably identical. As will be shown, the results definitely favour equation (1).

§ 2. *The Apparatus.*—The essential features of the apparatus are shown diagrammatically in fig. 1. The main support consists of a ¾-inch steel pillar, A, screwed into the heavy base B. The latter is supported on 15 tennis balls in a partitioned tray, and carried by a slate slab built into the laboratory wall. The suspension C hangs from an ebonite plug D in the top of the tube E which is mounted in the carriage F; the latter is provided with transverse and vertical adjustments by micrometer screw G and rack and pinion H respectively, and is carried on the pillar A by a deep collar J. The latter rides on another collar K, independent set screws being provided to both collars. Collar J can thus be rotated about the pillar without disturbing its vertical adjustment; this motion is required to bring the suspension above the vessel L into which it is lowered for cleaning. A stop is provided for collar J which ensures an accurate return to its normal position when cleaning is completed.

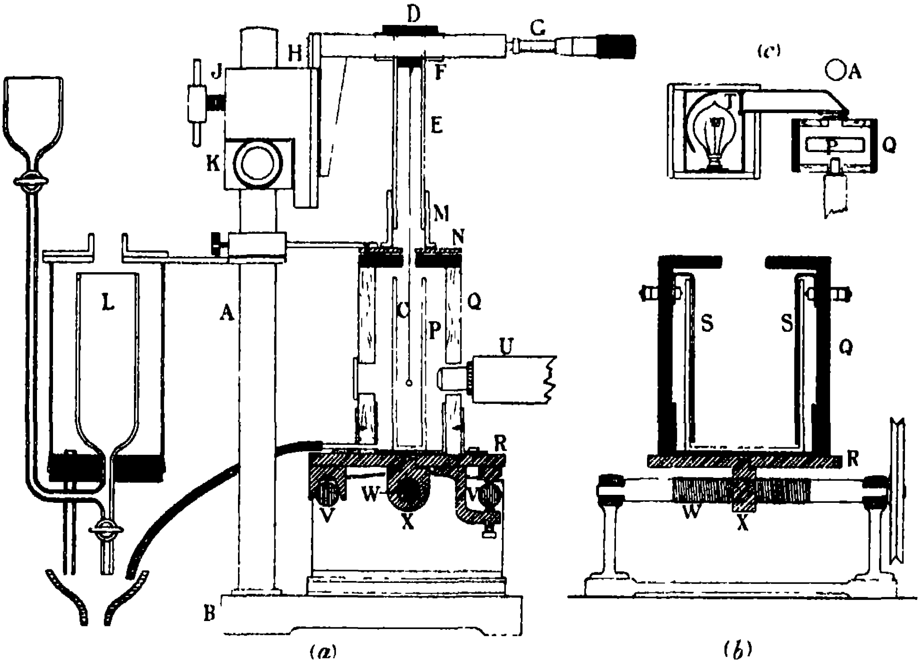

(a) (b)

FIG. 1.—(*a*) Side elevation (with some parts in section); (*b*) section, parallel to direction of traverse, of cell box and traversing mechanism; (*c*) horizontal section (on a smaller scale) in the plane of observation, to show method of illumination.

The suspension is protected from draughts by the glass tube E, which is provided with a telescopic extension M at its lower end. In use the latter rests freely on the brass plate N, which is drilled in the centre for the passage of the suspension, and is independently adjustable just clear of the moving cell box. Thus complete protection from draughts is provided without inhibiting the vertical adjustment of the carriage F.

The glass cell P is held by copper guides inside the cell box Q, the base of which is bolted to the moving platform R. The bottom of the cell box contains a zinc trough, with waste pipe, to catch liquid overflowed from the cell in filling it. The ends of the box are of ebonite and carry electrodes SS made of copper sheet. The front and back are of wood with windows for the illumination and observation of the suspension. The top of the box is of ebonite, slotted for the passage of the suspension, and is detachable in order to give access to the cell. The suspension is illuminated by reflected light from an electric bulb T, which is so placed and shielded as to prevent any appreciable amount of heat reaching the cell. The deflections are observed with an adjustable reading microscope U of usual pattern, fitted with a 1-inch objective and eyepiece micrometer.

The moving platform R slides on two guide rods V by means of two V-blocks and a point contact, and is propelled by a lead screw W of $\frac{3}{4}$-inch diameter and $\frac{1}{2}$ mm pitch; this works in a nut X so attached to the bottom of the platform as to permit vertical play, thus avoiding that vitiation of the "geometric slide" principle which would result from the introduction of a rigid constraint. The whole unit is rigidly mounted on the base B. The lead screw carries a pulley wheel at one end, and is driven by very uniform cord belting from an electric motor through two consecutive worm reduction gears. To avoid the transmission of vibration the motor and reduction gears are mounted on a table completely independent of the slab which carries the main apparatus. The motor circuit is provided with starting and reversing switches and with a continuously variable rheostat system for speed control. An electric contact attached to the first reduction gear produces one click per revolution in a telephone receiver, and provides a means for timing the stage speed by ear and stop watch.

The construction of the washing vessel L, with its concentric jacket to catch overflow, will be evident from the figure.

*The Manufacture of the Suspensions, and Preparations for Experiment.*—A glass particle, sealed by fusion to a glass fibre, was chosen for the suspension in order to facilitate the very rigorous cleaning which preliminary work showed to be essential. The manufacture of suitable fibres, and still more their attachment to the glass particles, proved to be a difficult task, the successful accomplishment of which is mainly a matter of much patience and practice. No useful purpose would be served by a detailed account of the various methods tried, and it is sufficient to record that, in the technique finally adopted, the fine fibres were drawn from thin rod with the help of a simple catapult arrangement made of rubber tubing, and that the particle was made directly on its own suspension fibre by careful fusion of the latter in a minute gas jet, used against a dark background. The completed suspension was cut to length, attached with a trace of celluloid varnish to a pin in the ebonite plug D, and carefully threaded (dry) down tube E. It was washed successively in Beckmann mixture, tap water and conductivity water in vessel L, into which it was lowered, as previously indicated, without removing it from the draught tube E. Special care was necessary to prevent the wet fibre from touching the walls of the cleaning vessel, for if this occurred it adhered and an attempt to remove it was attended by considerable risk of breakage.

Conductivity water was found unsuitable for use as the experimental liquid in consequence of the readiness with which its properties (and in particular its hydrogen-ion concentration) are affected by slight traces of impurity. A much more reproducible liquid is provided by a dilute buffer solution, and throughout the experiments recorded a M/10000 solution of disodium phosphate was employed.

For each experiment the cell was rigorously cleaned with Beckmann mixture, tap water and conductivity water, and the electrodes with rouge paper and water. Special care was taken not to touch the cleaned cell or electrodes with the fingers. The experimental liquid was run in through a cleaned thistle funnel till the cell overflowed, when the funnel was withdrawn and the level of the liquid at the top of the cell adjusted to be exactly flat; this is necessary to prevent deflection of the suspension by a curved meniscus. The cleaned suspension was then lowered to the desired depth, its position in the cell adjusted with the micrometer screw G, and the microscope focussed on the fibre just above the particle. The system was then ready for the experiment.

*Experimental Series I*—As already stated, the front and back walls of the cell were lined with sheets of microscope cover glass, the suspension being made from fused portions of the same sheet. Experiments were carried out at seven different values of $y/b$, which were correlated with the corresponding readings of the micrometer G with the help of a fine plumb line. In each experiment a succession of electric deflections, from 8 to 16 in number, was observed, deflections being made alternately to right and to left, The mean deflection was then calculated. Four mechanical deflections in each direction were then observed, the stage speed being adjusted for each observation to make the deflection equal to the mean electric deflection. The mean stage speed was then calculated and the result taken as the value of $v$ in equation (6).

In all 50 experiments of this series were carried out, of which 41 were retained as satisfactory, while 9 were rejected on observational grounds, as for instance an unsteady zero or an unduly sluggish motion (the latter a sure sign of a contaminated suspension). It should be emphasised that these experiments were rejected *before* the results were worked up; no experiment has been omitted from the record below on the ground that its results were discrepant.

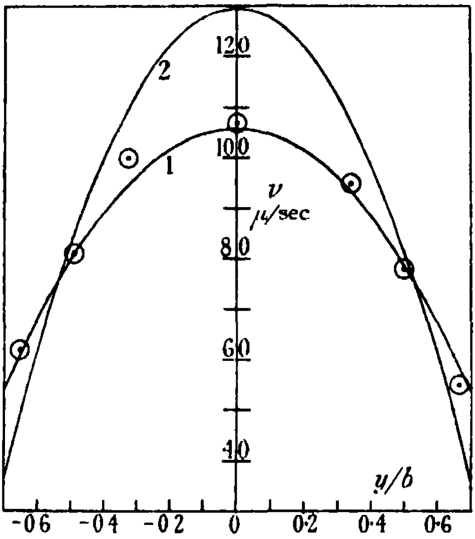

FIG. 2.—Curve 1 calculated according to equation (1), Curve 2 calculated according to equation (2) Circles denote final mean experimental values.

The observations of a typical experiment, intermediate between the best and the worst in self-concordance, are recorded in Table I, while Table II contains a summary of the whole series. The same suspension and potential gradient were used throughout; the cleaning process was, of course, carried out afresh for each experiment. No correction has been applied for the rate of the stop watch, since only relative velocities are required.

## Table I.

Experiment 21 $y/b = 0 \cdot 342$ Potential gradient, 10 3 volts per centimetre

Electrical deflections—

| | | | | | | |
|---|---|---|---|---|---|---|
| To right | 17 | 18 | 18 | 17 | 16½ | scale divisions |
| To left | 17 | 15½ | 14½ | 15½ | 14½ | ,, |
| Means | 17 | 16¾ | 16¼ | 16¼ | 15½ | ,, |

Mean of all 10 observations = 16⅜ scale divisions.

Mechanical deflections—stage speed required to give deflection of 16⅜ scale divisions:—

| | | | | | |
|---|---|---|---|---|---|
| To right | 85 | 82 | 84 | 82 | $\mu$/sec |
| To left | 82 | 79 | 83 | 84 | ,, |

Mean stage speed = 83 $\mu$/sec.

Table II.

| $y/b$: | $+0·668$ | $+0·502$ | $+0·342$ | $+0·010$ | $-0·324$ | $-0·488$ | $-0·652$ |
|---|---|---|---|---|---|---|---|
| $v$, $\mu$/sec (mean values from single experiments) | 58<br>57<br>54<br>53<br>51 | 84<br>78<br>77<br>76<br>75 | 102<br>101<br>98<br>97<br>95<br>87<br>83 | 109<br>108<br>107<br>107<br>104<br>[85] | 114<br>104<br>102<br>101<br>100<br>96<br>94<br>92 | 87<br>82<br>82<br>79<br>79 | 68<br>63<br>62<br>59<br>59 |
| $v$ (mean) $\mu$/sec | 55 | 78 | 95 | 107* | 100 | 81 | 62 |
| Mean deviation | 2·4 | 2·2 | 5·4 | 1·2* | 4·9 | 2·4 | 2·6 |
| Number of experiments rejected | 0 | 2 | 3 | 0 | 4 | 0 | 0 |

* The bracketed value of $v$ is omitted from the mean

The final means were fitted to the equation

$$v = u + w_0(1·58y^2/b^2 - 0·58) \tag{6}$$

in three different ways :—

(1) The " best values " of $u$ and $w_0$, subject to no predetermined relation, were found by the method of medians to be

$$u = 66\ \mu/\text{sec.},\ w_0 = -75\ \mu/\text{sec.},$$

giving a ratio $w_0/u$ numerically equal to 1·14.

(2) The best fit subject to the condition that $u = -w_0$, as required by equation (1), is given by

$$u = -w_0 = 67\ \mu/\text{sec.}$$

(3) The best fit subject to the condition that $u = -\frac{1}{2}w_0$, as required by equation (2), is given by

$$u = -\tfrac{1}{2}w_0 = 60\ \mu/\text{sec}$$

Table III exhibits a comparison of the experimental values of $v$ with those calculated on each of these three assumptions, together with the mean deviations. It will be seen that equation (1) represents the results much better than equation (2), and in fact deviates scarcely more than the best fit possible. The same conclusion is more strikingly demonstrated by fig. 2, where the curve corresponding to Smoluchowski's equation and to equation (2) are plotted, together with the experimental results.

Table III.

| $y/b$. | $v$ (obs.) | $v$ (calc. 1) | $\Delta$ | $v$ (calc. 2) | | $v$ (calc. 3) | $\Delta$. |
|---|---|---|---|---|---|---|---|
| 0·668 | 55 | 57 | | 59 | −4 | 45 | +10 |
| +0·502 | 78 | 80 | | 79 | −1 | 82 | −4 |
| +0·342 | 95 | 96 | | 93 | +2 | 107 | −12 |
| +0·010 | 10 | 109 | | 106 | +1 | 130 | −23 |
| −0·324 | 100 | 97 | +3 | 95 | +5 | 110 | −10 |
| −0·488 | 81 | 81 | 0 | 81 | 0 | 85 | −4 |
| −0·652 | 62 | 59 | +3 | 61 | +1 | 49 | +13 |
| Mean deviations | | | | | 2·0 | — | 11·1 |

§ 3. *The Influence of the Spherical Particle.*—In the preceding section it has been tacitly assumed that the deflecting force due to the particle is negligible in comparison with that due to the fibre. A few words must be said in justification of this

By Stokes' law the deflecting force on the sphere is given by $F_s = 6\pi a_s \eta v$, where $a_s$ is the radius of the particle and $v$ is the relative velocity of liquid and sphere. By the Oseen-Lamb* expression the corresponding force per unit length of a cylinder is given by $F_c = 4\pi\eta v/\{-0\cdot07 - \log_e (\delta v a_c/2\eta)\}$, where $a_c$ is the radius of the cylinder. For the experiments recorded above, $a_s = 0\cdot44$ mm. and $a_c = 0\cdot01$ mm (approximately) so that, for a value of $v$ equal to 100 $\mu$/sec., we have

$$F_s = 0\cdot000083 \text{ dynes and } F_c = 0\cdot000167 \text{ dynes per cm.}$$

The length of fibre immersed was 5·5 cm., and its total length 20·75 cm. The moment of the deflecting forces due to the sphere and the fibre are therefore about 0·0017 and 0·017 dyne-cm. respectively. The effect of the sphere is thus about one-tenth of that of the fibre, and though just within the limits of detection, does not materially affect our conclusions about the cataphoresis of the cylinder. The same will hold for other velocities, since the ratio $F_s/F_c$ is very insensitive to changes of $v$.

When it was first realised that the fibre plays the predominant part in producing the cataphoretic deflection, a number of experiments (Series II) were carried out in the attempt to separate the effects due to the sphere and the fibre. The idea of these experiments was to measure the electrical and mechanical deflections in the centre of the cell with varying depths of immersion of the suspension; an analysis of the deflecting forces should then lead to independent values for the respective cataphoretic effects. As might perhaps have been anticipated, the attempt failed owing to the experimental error being of the same order as the effect due to the sphere; these experiments will not be further described, except to remark that the value found for $F_c$ agreed quite well with that calculated by the Lamb-Oseen formula, as is shown by Table IV; the values found for $F_s$ were naturally very divergent. Very little weight can be attached to the results of the experiments with suspension 4, as on examination it proved to be very non-uniform.

---

* Lamb, "Hydrodynamics," 5th ed., § 343, p. 581.

Table IV.

| Suspension number. | Number of experiments. | $F_c$ | | $F_s$. | |
|---|---|---|---|---|---|
| | | Found. | Calculated | Found | Calculated. |
| 1 | 1 | 0 000189 | 0 000191 | 0 000045 | 0 000103 |
| 2 | 1 | 0 000190 | 0 000179 | 0 000092 | 0 000098 |
| 3 | 4 | 0 000166 | 0 000164 | 0 000067 | 0 000091 |
| 4 | 4 | 0 000216 | 0 000187 | -- | — |

§ 4. *Summary of Parts I and II.*—(1) By methods which, subject to certain stated restrictions, are believed to be rigorous, equations have been developed for the cataphoretic mobility of rigid spheres and cylinders of any desired electrical conductivity, and for the electrosmotic velocity at plane surfaces, or in cylindrical channels of any cross section.

(2) Provided the radius of curvature of the particle is large compared with the effective thickness of the electrical double layer, the cataphoretic mobility of an insulating particle, and the electrosmotic velocities at the surfaces considered, are found to be those given by Smoluchowski's equation $U = DX\zeta/4\pi\eta$.

(3) For particles, such as those in colloidal solutions, whose size is not large compared with the effective thickness of the electrical double layer, the cataphoretic mobility has been shown to vary with the size, tending towards the value $U = DX\zeta/6\pi\eta$ for very small particles. A provisional calculation has been made of this variation.

(4) Experimental evidence is quoted from the literature which (*a*) confirms the validity of Smoluchowski's equation for spherical particles of microscopic size, and (*b*) shows that the cataphoretic mobility of relatively large particles is independent of their shape. Further there is described in Part II an experi-

mental investigation, by a new method, which confirms Smoluchowski's equation for the cataphoresis of cylindrical fibres.

The authors' best thanks are due to Professor E. A. Milne, F.R.S., for criticisms of the mathematical sections of the paper, to Imperial Chemical Industries, Limited, a grant from whom to the Manchester University Chemistry Department has helped to defray the cost of the apparatus used; and to the Department of Scientific and Industrial Research for a maintenance grant which enabled one of them (C. G. S) to undertake this work

# *Interfacial Tension and Hydrogen-ion Concentration.*

By Rudolph Albert Peters, from the Department of Biochemistry, Oxford.

(Communicated by C N Hinshelwood, F.R S.—Received April 29, 1931 )

The object of this communication* is to extend our knowledge of the relation between the interfacial tension of long chain carbon compounds dissolved in benzene and the hydrogen-ion concentration of the aqueous phase with which they may be placed in contact. To this extent, it forms an extension of earlier work by Hartridge and Peters.† The stimulus of the work was in large part the desire to throw light upon the question of ionisable interfaces in the living cell.

## *Historical.*

It is well known in a general way that the Hydrion concentration ($C_H$) of the aqueous phase influences the interfacial tension between solutions of a fatty substance dissolved in a lipoid solvent and an aqueous solution, and that the fall in interfacial tension which takes place with increasing alkalinity is produced by the presence of soap.‡ The first experimental indication that there was a direct relation between $C_H$ and the interfacial tension (I.T.) of such a system appears to have been given by Reinders.§ This relation, highly significant so far as biochemical processes are concerned, seems to have attracted little attention. Though it is mentioned by Freundlich,* interest has been concerned in the main with emulsification. In 1920–22, Hartridge and Peters found a direct relation between $p_H$ and interfacial tension in the system olive oil in benzene-aqueous buffered solution. A fall in I.T. commenced to the alkaline side of $p_H$ 4·5†, which started rather abruptly and appeared to pursue an almost straight line to $p_H$ 9·0, the degree of fall being independent of the buffer used. The drop weight method was used for most of the experiments, but was checked against a ripple method. In accordance with expectation, with a series of pure substances, the only ones showing a change of I.T. were those containing a $-COOH$ group, but a change also appeared with $-COOH$ combined in a triglyceride. The relation was not quite simple, because the strength of the buffer solution influenced the results. Below a certain concentration of phosphate for instance, 0·005 M. in the case of a buffered solution of $p_H$ 7·6, no lowering of I.T. took place. In explanation it was suggested that the effects only appeared when sufficient alkali was present to form alkali salts of the fatty acids at the interface.

---

* A preliminary account of some of this work has already appeared, 'Trans. Faraday Soc.,' vol. 26, p. 797 (1930).

† 'Proc. Roy. Soc.,' A, vol. 101, p. 348 (1922).

‡ Donnan, 'Z. Phys. Chem.,' vol. 31, p. 42 (1899); Harkins and Humphrey, 'J. Amer. Chem. Soc.,' vol. 38, p. 242 (1915); Harkins and Zollmann, *ibid.*, vol. 48, p. 69 (1926).

§ Van Bemmelin Festschrift (1910); quoted from Freundlich "Kapillarchemie" (1922).

It is proposed to show here that with solutions of pure long chain fatty acids dissolved in benzene the fall in interfacial tension commences at $p_H$ 5·5 approximately and extends to $p_H$ 9·5 approximately, and that a reverse change occurs in the case of a long chain amine The ionisation of a $-COOH$ group occupying an oriented position in an interface therefore extends over a range of $p_H$ which covers that of significance in living matter. Using the change in interfacial tension as an indicator of change in ionisation, some idea of the dissociation constant of ionisable groups in an interface can be obtained.

### *Experimental Methods.*

The measurements have been made by a simple drop weight method, using the corrections of Harkins in the International Critical Tables. The tips used for the measurements have been of diameter approximately 2·0 mm. unless otherwise stated. The drop volumes used for calculation have been the average of several drops. The aqueous phase was run from the pipette into the benzene phase. The interfacial tension benzene-water has been taken to be 35·00 dynes/cm. at 20° C. The tips employed in some of the experiments gave theoretical values for benzene-water within the limit of experimental error.‡

---

* "Kapillarchemie" (1922).

† $p_H = \log 1/[H]$.

‡ For other tips, a correction was applied using 35·00 dynes/cm. as standard.

Measurements are believed to be subject to an error of not more than 2 per cent. of the values given as an extreme value.

Buffered solutions have been made with glass distilled water following the instructions of Clark and Lubs.* $p_H$ values were checked colorimetrically or otherwise, and may be relied upon to 0·1 $p_H$†. In the case of the glycine buffer, the corrections given by Walbum‡ have been used.

The benzene was redistilled twice from A.R. benzene. Of the substances used in the research, I am indebted to Dr. N K. Adam for specimens of palmitic acid, hexadecyl alcohol and ethyl palmitate, and to Dr. Gulland for some capric acid. Stearic acid was obtained by recrystallisation of Kahlbaum's stearic acid. Hexadecylamine hydrochloride was obtained from Kahlbaum's palmitic acid by the method of Kraft, in Adam and Dyer, 1925 § Two methods of preparing amine solutions were employed. Precaution was taken to exclude traces of $CO_2$

(*a*) The amine was prepared from the hydrochloride by distillation from slaked lime and redistillation of the distillate obtained from sodium.

(*b*) The amine hydrochloride was dissolved in alcohol, benzene added and the system repeatedly shaken with $CO_2$ free NaOH (N/10), six times with twice the volume of soda. The benzene obtained was separated and made up to a known weight of benzene by any necessary additions. The strength of the amine was checked by titration with HCl in alcoholic solution, using brom cresol purple as indicator.

In method (*a*), the product obtained was soluble to the extent of about 0·16 per cent. in benzene at room temperature; in method (*b*) more amine could be apparently obtained in solution. The values given in fig 4 were obtained by method (*a*). The carbonate was made in one case by passing $CO_2$ over the melted amine, and found to be much less soluble in benzene.

The purity of all compounds was checked by melting point, and accepted if the compound melted within 0·5° C. of the value given in Beilstein's Handbuch

---

* Clark, "Determination of the Hydrogen ion," Williams and Wilkins, 2nd ed.

† For glycine buffer $p_H$ 6 4 to 8·0, traces of NaOH were added to the standard glycine-NaCl solutions. The $p_H$ so obtained is not quite as reliable owing to the poor buffering.

‡ 'Biochem. Z.,' vol. 107, p. 219 (1920).

§ Kraft, 'Ber. Deuts. Chem. Ges.,' vol. 22, p. 812 (1889); Adam and Dyer, 'J. Chem. Soc ,' vol. 127, p. 72 (1926). I am most grateful to Dr. N. K. Adam for supplying me with precise details of his methods of preparing this substance.

The special difficulties in making some of the measurements will be described as they present themselves.

### *Experimental Results.*

*Long Chain Carbon Acids.*—It is convenient to consider first the results for long chain carbon acids dissolved in benzene. The examples of these chosen have been palmitic, stearic, lauric and capric acids, and it is believed that the concentrations of acids selected have given maximal effects. It has been shown previously (Hartridge and Peters, 1922) that as the concentration of acid dissolved in the benzene is increased, the fall in interfacial tension for a given change in $p_H$ becomes more pronounced, reaching a maximum for palmitic acid at a concentration of approximately 0·2 per cent. At this concentration presumably the interface becomes saturated with the acid In the present instance for capric and lauric acids it was found that rather more acid must be dissolved in the benzene in order to show the maximum possible lowering of interfacial tension. This is possibly correlated with the shorter chain. It was found impossible to use phthalate buffered solutions owing to the solubility of phthalic acid in benzene. A solution of palmitic acid in benzene showed a progressive fall in interfacial tension with increasing acidity to the acid side of $p_H$ 4·0 when phthalate buffered solutions were used, but this happened with benzene alone.

For the points more acid than $p_H$ 5·6 and 6·4 respectively, the phosphate or glycine buffer solutions were titrated with HCl and the $C_H$ of the solutions so obtained determined with the hydrogen or glass electrode.

Points obtained over the range in which phosphate and glycine are only acting as weak buffers are rather unreliable. For glycine this range extends from about $p_H$ 4·0 to 7·6. Figs. 1, 2 and 3 give the curves obtained for the four acids. Each point represents the mean of at least six drops.

*Palmitic, Lauric and Capric Acids.*—Some comments are necessary upon the estimations Those with palmitic acid were easy to make and gave great consistency between different sets of readings. The determinations for lauric acid were not so consistent, especially at $p_H$ more acid than $p_H$ 6·0 and with the glycine buffers.

For capric acid (fig. 3), the curve with glycine buffers is not different from the others ; that against phosphate, however, shows a variation which warrants further investigation and must be related to the increasing water solubility of the 10 carbon acid. At least 1 per cent. of capric acid is needed to saturate the interface.

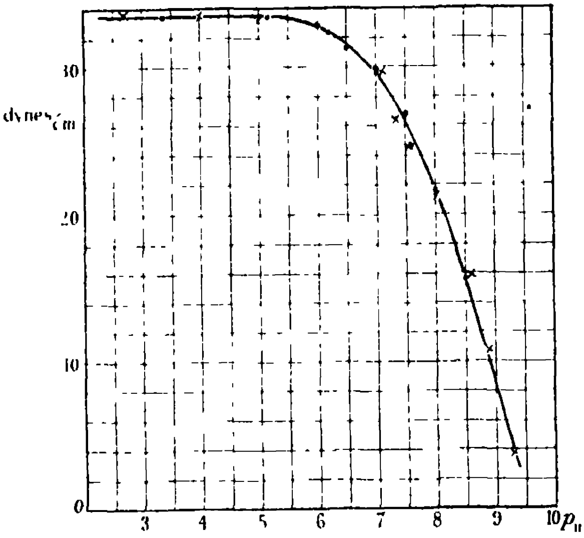

FIG. 1.—Palmitic Acid, 0·39 gm. in 100 gm benzene. Temperature 20° C ± 0·1. ● Phosphate buffers. × Glycine buffers.

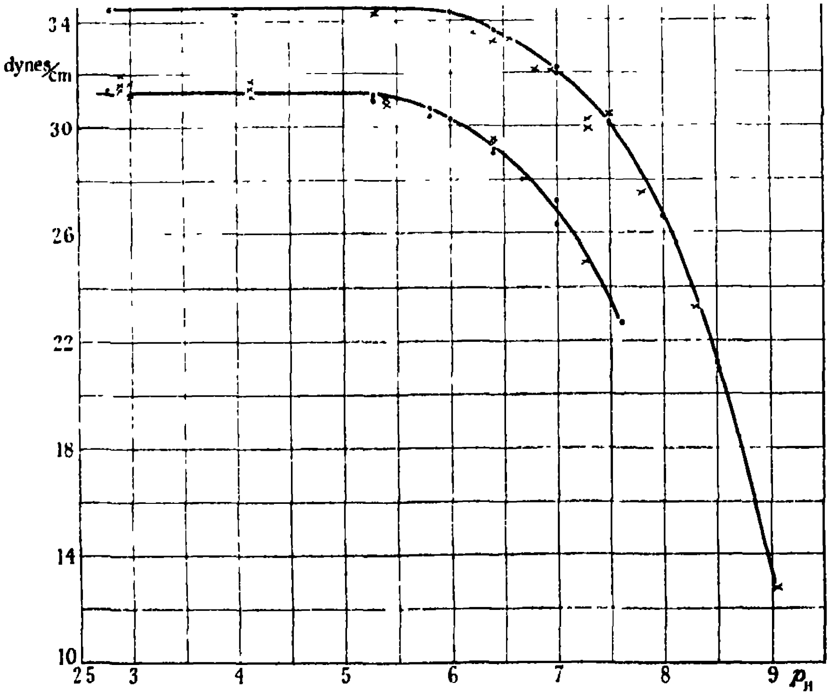

FIG. 2.—Upper curve: Stearic Acid, 0·18 gm. in 100 gm. benzene; 30° C. ± 0·2. Lower curve: Lauric Acid, 1·0 gm. in 100 gm. benzene; 20° C. ± 0·1. ● Phosphate buffers. × Glycine buffers.

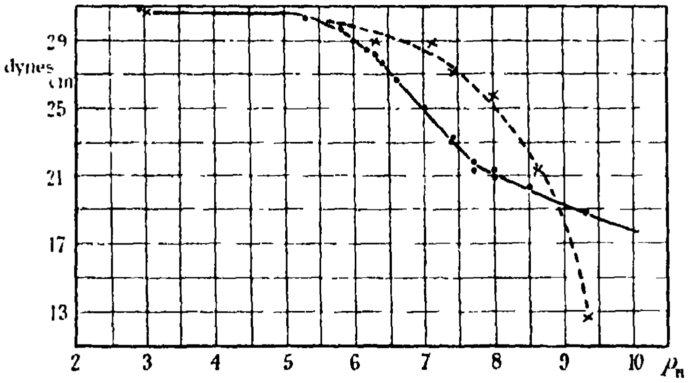

FIG. 3.—Capric Acid, 0·9 gm in 100 gm benzene, 20° C. ± 0·1. • Phosphate buffers. × Glycine buffers.

*Stearic Acid.*—The determinations with this acid were not simple. Measurements were made at both 20° and 30° C. No difficulty was experienced in obtaining satisfactory readings at $p_H$ 8·0 and to the acid side of this value. At 20° C, and $p_H$ 8·6 however, the size of the drops was found to vary with the speed of delivery, so much so as to make readings impossible. A drop of about three-quarters of the maximum size at this $p_H$ reacted strongly to the introduction of more fluid by exhibiting a kind of contraction. This rather interesting phenomenon was not pursued; the difficulties are probably related to the temperature effects observed by Adam,* in surface films (expanded films). The trouble seems to disappear in the main at 30° C. Small differences are induced by several factors, especially at the beginning of the curve. At 30° C. and a concentration of 0·2 per cent. approximately the first fall occurred at $p_H$ 6·0. At the same concentration at 20° C, there was a gradual slight fall over the range $p_H$ 5·3 to 6·1. Upon increase of the concentration to 0·5 per cent., the fall at 30° C. took place rather before $p_H$ 6·0.

With all these acids, a change in interfacial tension starts at approximately $p_H$ 5·5 and extends over the range $p_H$ 5·5 to 9·5 approximately or over 4·0 $p_H$ units.†

That the effect is essentially due to $C_H$ is proved from the remarkable coincidence of the curves for glycine and phosphate buffers in the case of lauric, palmitic and stearic acids. The variation for capric acid is not general. Since the ionisation curves for simple acids and bases extend over a range of $p_H$ very similar to the above, there seems to be little doubt that the change in interfacial tension is a direct function of the ionisation of —COOH at the interface. If this is so, then a similar change in the opposite direction should be shown by the amine of similar length to palmitic acid.

---

* 'Proc. Roy. Soc.,' A, vol. 101, pp. 452, 516 (1922).

† It is probable that for stearic acid the point is 0·3 $p_H$ more alkaline, and for lauric acid more acid than $p_H$ 5·5. Very probably there is also a variation with temperature. These, however, are minor differences in this connection.

*Hexadecylamine* —Unexpected difficulties arose in the attempt to measure the interfacial tension of this substance Phosphate and borate buffered solutions proved unsuitable, as the insoluble salt of the amine separated at the interface , this might be expected from the work of Adam.* It proved necessary to work with glycine buffers and at a temperature of 30° C. A further difficulty occurred in taking measurements to the acid side of $p_H$ 8 0, because there was a tendency for the amine to become adsorbed upon the inside rim of the glass tip. With freshly cleaned tips it was possible to get drops from the outer diameter. Much fruitless time was spent in trying to find some other material or variety of glass tip which would eliminate the trouble ; resort was eventually made to careful observation of the condition of each drop as it fell The interfacial tension for those falling from the inner rim was calculated for the inner diameter. It is probable that this does not lead to great inaccuracy as there can be seen to be substantial agreement between the values calculated from the inner and outer rim respectively.

Many experiments were made with different amine solutions at different temperatures, all of which showed a fall in interfacial tension between $p_H$ 10 and 6·0. Fig. 4 gives the points obtained in the last two experiments with approximately saturated solutions of the amine, prepared from the hydrochloride by method (*a*). It will be noticed that the ionisation curve with $\log 1/k = 7 \cdot 0$ passes through the points of the last experiment made. This is believed to have been the most accurate as especial precautions were taken to avoid the presence of $CO_2$, the amine being used immediately after the final distillation. Some uncertainty, however, still exists as to the exact position of the lower points upon the curve, owing to the feeble buffering of the glycine solutions at the more acid $C_H$. The effect of $CO_2$ can be judged from the readings for the amine carbonate, also included upon the curve. It can be seen that the values for $p_H$ 7·1 and 8·0 are substantially the same ; the more alkaline points are altered. The presence of traces of $CO_2$ therefore would not be likely to influence any fall between $p_H$ 8·0 and 7·0 ; possibly this is because any carbonate present in the interface is rapidly decomposed by the buffer solution.

---

* 'Proc. Roy. Soc.,' A, vol. 126, p. 366 (1930).

It will be noticed that the points shown upon the curve do not extend beyond $p_H$ 10·7. Readings were made with glycine buffers more alkaline than this. At $p_H$ 11·7 and 12·6, values of 30·5 dynes were obtained. These points are not indicated upon the figure as it is difficult to be certain that unrecognised errors had been excluded. Values for the interface (30° C.) benzene-glycine buffer showed no variation for $p_H$ 8·0, 9·0 and 12·0, so that the effect appeared to be introduced by the amine.

From these results it is clear that the change in interfacial tension for the amine solution takes place in the opposite sense to that for the —COOH and over approximately the same range of $p_H$. The curve occupies a position to the acid side of that for a water-soluble amine such as butylamine.

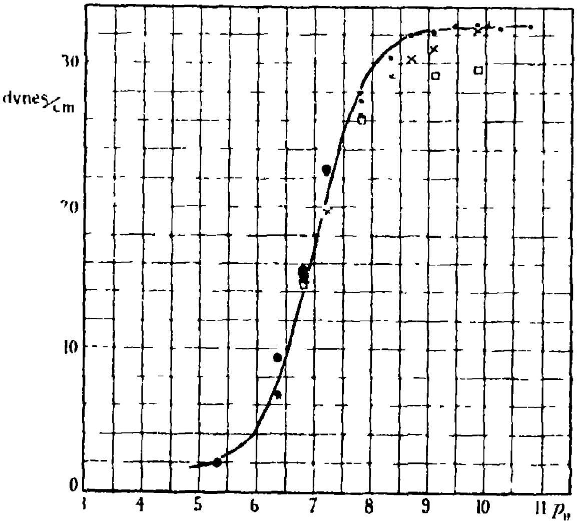

FIG. 4.—Hexadecylamine, 0·14 gm. in 100 gm. benzene. Experiment 1, ×. Experiment 2: •, outer rim of tip; ⊙, inner rim of tip. Hexadecylamine carbonate, □.

If we assume that the first drop in interfacial tension commences coincidently with the first appearance of ionisation in the groups at the interface, then this change in the case of the carboxyl head occurs about 3·0 units $p_H$ to the alkaline side, and in the case of the amine some 4·0 units $p_H$ to the acid side of the point at which the corresponding water soluble acid and base would commence to ionise when in aqueous solution.*

$$pK_a\ (= \log 1/K_a) \quad \text{and} \quad pK_b\ (= \log 1/K_b)$$

are therefore about 7·5, and 7·0 at 30° C., or $K_a = 3 \cdot 2 \times 10^{-8}$ and $K_b = 1 \cdot 0 \times 10^{-7}$. So far as I am aware, this is the first measurement of the strength of such ionisation at an interface. This paper is concerned in the first instance with a first approximation to the conditions of interfacial ionisation, and the exact detail of the curves is therefore of secondary importance. Nevertheless, some features deserve comment In fig. 4 (hexadecylamine), the curve drawn is that for the dissociation of a base of $\log K_w - \log (1/K_b) = 7 \cdot 0$. The points for experiment 2 coincide surprisingly well with this, in a way that seems to exclude a chance correspondence. When, however, we turn to the curves for the acids, we do not find the same correspondence The curve is not linear and not a simple ionisation curve ; the reason for this difference between the base and the acid is not clear yet. It is possible that it is correlated with the formation at the interface of the sodium salt of the acid in alkaline solutions. The matter is discussed below Table 1 summarises the curves.

---

* $K_a$ for butyric acid and caproic acid = $1 \cdot 5 \times 10^{-5}$ approximately.

*Other Substances.*—Observations have been made upon two substances of cognate interest to the research, namely, ethyl palmitate and hexadecyl alcohol, fig. 5. With ethyl palmitate, the changes commence some 1·5 $p_H$ units to the alkaline side of the point at which the fatty acid begins to change. This result is in general agreement with those found by Hartridge and Peters (1922) for the glycerides of fatty acids.

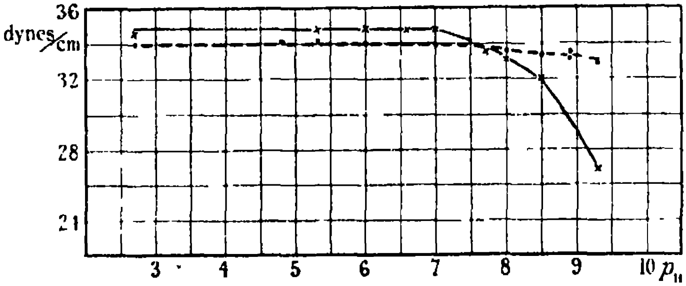

FIG. 5 — ——— Ethyl Palmitate, 2·18 gm. in 100 gm. benzene, phosphate buffers, 20° C. ± 0·1. ------ Hexadecyl Alcohol, 0·35 gm. in 100 gm. benzene, phosphate buffers $p_H$ 2·7 to 8 0, glycine buffers $p_H$ 8·88 to 9·3.

It is interesting to compare the above results with the behaviour of hexadecyl alcohol. Within the limits of error no change in interfacial tension takes place between $p_H$ 2·7 and 7·5.* The outstanding fall in interfacial tension therefore occurs only with compounds having the group R—COOH, R—$CH_2NH_2$ or with an ester of the acid, as was previously found.

* The slight fall of 1 dyne at $p_H$ 9·3 is outside the experimental error. Its cause is unknown, but it is clearly of a different order to the effects here studied.

Table I.—Approximate Values at different $p_H$ values. Dynes per centimetre.

| Substance | C. | Concentration gm./100 gm benzene | Temperature. | $p_H$ | | | | | | | | | | | |
|---|---|---|---|---|---|---|---|---|---|---|---|---|---|---|---|
| | | | | 3·0 | 5·0 | 5·5 | 6·0 | 6·5 | 7·0 | 7·5 | 8·0 | 8·5 | 9·0 | 9·5 | 10·0 |
| | Atoms | gm | °C | | | | | | | | | | | | |
| Stearic acid | 18 | 0·18 | 30 | 34·5 | 34·5 | 34·5 | 34·3 | 33·4 | 32·1 | 30·1 | 26·6 | 21·2 | 13·1 | — | — |
| Palmitic acid | 16 | 0·39 | 20 | 33·5 | 33·5 | 33·3 | 32·8 | 31·7 | 29·7 | 26·3 | 21·7 | 15·5 | 8·3 | ’ | — |
| Lauric acid | 12 | 1·0 | 20 | 31·3 | 31·3 | 31·1 | 30·3 | 28·9 | 26·7 | 23·4 | — | — | — | — | — |
| Ethylpalmitate | — | 2·18 | 20 | 34·8 | 34·8 | 34·8 | 34·8 | 34·8 | 34·8 | 34·2 | 33·0 | 31·9 | 29·0 | — | — |
| Hexadecylamine | 16 | 0·14 | 30 | — | — | 2·5 | 4·5 | 9·5 | 17·0 | 25·2 | 29·7 | 31·5 | 32·3 | 32·5 | 32·5 |

### *Discussion.*

The view has been taken throughout this work that the changes in I.T. depend upon changes occurring in a unimolecular layer at the interfaces concerned. This seems to be justified (see Donnan* for a discussion of this point). Though only one instance of a long chain amine has been investigated, there is no reason to think that the results will not prove to be general. Taken together with the determinations upon the fatty acids, they appear to prove the relation between the fall in interfacial tension and the degree of interfacial ionisation. The $C_H$ almost alone determines the state of the interfacial ionisable groups. Other effects may be superimposed in the case of a more soluble acid such as capric acid. Something further also must be invoked to explain the behaviour of the esters.

### *Cause of Fall in Interfacial Tension.*

Though there is no doubt about the general relation to ionisation, as a secondary question there arises the problem as to whether the presence of dissociable salts of the long chain compounds in the interface is sufficient to explain all the effects. On this view the degree of lowering of I.T. is due to the percentage of dissociated salt formed. This was substantially the explanation advanced by Hartridge and Peters. It is consistent with the fact that at a given $p_H$ the interfacial tension begins to rise, as the buffer solution is diluted, before there is actual change in $p_H$. For instance, at $p_H$ 7·5 in the case of the interface phosphate—palmitic acid in benzene, dilution of the phosphate to one-tenth of the normal strength does not change the $p_H$ significantly, but there is a rise of about 1 dyne in the interfacial tension. This was explained by believing that the change was a function of the concentration of sodium ion from which it follows that there is only sufficient sodium at concentrations above approximately M/200 $Na_2HPO_4$. This simple explanation unfortunately is not consistent with the present work. We have seen that identical falls of interfacial tension occur with the glycine buffer, in which the amount of NaOH for a given fall is considerably less than the limiting value for phosphate. In this case also dilution changes the I.T. more rapidly than the $p_H$ of the buffer. As the ordinary glycine buffer is made up with sodium chloride, I have performed an experiment at $p_H$ 7·6 with glycine made up without NaCl, obtaining in this case a similar fall in tension. The fall therefore does not appear to be a function of the sodium ion, but even supposing that this was remotely possible, it seems to be impossible when we come to the amines. If our conditions have been sufficiently rigorous to exclude $CO_2$, the low interfacial tension at $p_H$ 7·0 is not due to the presence at the interface of an amine salt. It seems to be unlikely that there is a compound with glycine, not only because it is known that monoaminomonocarboxylic acids are not appreciably adsorbed (Phelps and Peters*), but also because it is difficult to see how at the same $p_H$ glycine could tend to combine both with an acid and a basic group (the $C_{16}$ acid and amine). It must be remembered that the amine and its salts are practically insoluble in water, and there does not appear to be any tendency for a long chain acid such as palmitic acid to enter the aqueous phase, at any rate before an alkalinity of $p_H$ 9·0 is reached. Murray† found that in the case of the distribution of oleic acid between benzene and water, there was no oleic acid in the aqueous phase at hydrion concentrations more acid that $p_H$ 9·0 I incline to the opinion that there is a state of the polar groups at the interface, possibly connected with adsorption of ions at a polarised layer of water molecules which precedes that of true ionisation, and is reflected in the changes observed This explanation is more consistent with the fall in I.T occurring with the glycerides and esters. It is certain that here simple ionisation cannot explain the fall, as it begins before hydrolysis It is usual to believe that the fall in interfacial tension taking place with esters in contact with alkaline solutions is due to hydrolysis at the interface. This is probably true when a high degree of alkalinity is reached, but for a $p_H$ 8 0 to 9 0, I am of the opinion that hydrolysis does not explain the change. This can be shown in more ways than one. If hydrolysis occurred, we should expect to find that the successive formation of drops of alkaline buffer solution in a small volume of ethyl palmitate solution would gradually produce sufficient palmitic acid to affect the readings. This does not happen. Further, supposing that a very small amount of palmitic acid was formed, the evidence is that it would dissolve in the benzene and not affect the interfacial tension; it has been shown that some 0·07 per cent. of palmitic acid would have to be present to produce a lowering of about 3 dynes (Hartridge and Peters, *loc. cit.*, Table V). It seems that in this change in the head grouping, which appears as an interfacial tension change, we are observing some intermediate stage in the hydrolysis of the compound. Such stages have been often postulated without actual evidence for their existence. It was pointed out previously and has been made more definite here that there is a coincidence between the $p_H$ at which changes take place in the volume of fatty acids upon the surface of the Langmuir trough and the point of inflexion of these curves, suggesting an intimate relation between the two events.

---

* Address, Section B, British Association 1923.

---

* 'Proc. Roy. Soc.,' A, vol. 124, p. 554 (1929); see also Michaelis (1925), "Ions in Colloidal Systems," Williams and Wilkins

† 'J. Biol. Chem.,' vol. 56, p. 509 (1923).

### *Relation to Adsorption at the Liquid-solid Interface.*

It is interesting to compare the results with those of Phelps and Peters (*loc. cit.*) and of Phelps* for adsorption of simple acids and bases upon charcoal. For the acids, as the solubility in water decreased, the curve for variation of adsorption with $p_H$ shifted gradually towards the alkaline side though retaining a general correspondence with the dissociation curve. For caproic acid the shift amounted to 2·0 units $p_H$. The condition at the charcoal-water interface is therefore intermediate between that of the conditions here studied and that of the shortest chain acids when dissolved in water. The most recent curve for the adsorption of butylamine upon charcoal (Phelps) shows variation of adsorption between $p_H$ 7·0 to 11·0. The adsorption rises from a minimum at $p_H$ 7·0 to a maximum at $p_H$ 11·0, this is again intermediate between the $p_H$ values over which hexadecylamine exhibits its variations of interfacial tension and the simple amine ionisation curves. Taken together, the two sets of results appear to constitute the strongest evidence for the essential similarity of conditions at the liquid-solid and liquid-liquid interface.

In a recent lecture Freundlich† has drawn attention to the results of Deutsch,‡ showing that displacement of equilibrium takes place at interfaces in systems consisting of benzene–buffer solution containing some indicator such as brom thymol blue. In many cases the changes appear to indicate an increased acidity at the interface, in others, however, the change occurs in the opposite direction. The general conclusion to the experiments appears to be that a change in the direction of diminished dissociation occurs at the interface. Such a conclusion would be in harmony with the finding here. It requires a relatively more alkaline or more acid solution to ionise an acid or basic group at the interface than when in simple solution.§

---

* 'Chem Ind. Proc. Biochem. Soc.,' vol. 49, p. 55 (1930).

† 'J Chem Soc,' 1930, p. 164.

‡ 'Z Phys Chem,' vol 136, p. 353 (1928).

§ During a repetition of these experiments with Professor R. Chambers, we found that a shift of $p_H$ does not occur with phenol red under conditions which cause a shift with brom thymol blue. This indicates that phenol red does not get into the interface so readily; the results with this indicator inside cells are therefore more likely to give a true picture of the $p_H$ inside.

### *Some Biological Considerations.*

The biological application of these results deserves some comment. The effects studied here occur over the range of $p_H$ which is the mean reaction of the living cell $p_H$ 7·3. At this reaction, simple acids and bases in true aqueous solution would be completely present as salts. At the interface this should not be so, and therefore these groups might take part in dynamic actions of the cell.

It is surely significant that the curves for amine and carboxylic acid cover approximately the same $p_H$. A problem of some interest in living matter is raised by the presence of fatty substances in interfaces and their probable exposure to varying H-ion concentrations. Why do they not tear the cell to pieces ? It is likely that the living cell is buffered against changes in interfacial tension in its various parts. Such buffering must readily take place with a mixture of an amine and an acid such as the above. A few experiments with a mixture of amine and carboxylic acid in benzene indeed indicate that this is so ; such a mixture showed the following I.T. at various $p_H$ :—

| | | | | |
|---|---|---|---|---|
| $p_H$ .. .... | 5·4 | 6·3 | 8·0 | 10·42 |
| I.T. ... ........... . | 9·40 | 13·8 | 19·7 | 6·15 |

At either extreme of reaction there was definite evidence of "tension" buffer effect.

The view that muscular motion might be produced by changes in surface tension (Bernstein) has been variously treated, receiving support from Hartridge and Peters (*loc. cit.*), and adverse criticism from Harkins, Davies and Clark* and A. V. Hill.† Hartridge and Peters (*loc. cit.*) pointed out that if COOH groups formed part of the protein structure of the contractile mechanism of a muscle, their work indicated the way in which changes of interfacial tension might be caused by changes in $C_H$ Later somewhat similar views have been advanced by Garner‡ and Meyer§. Definite evidence has been here produced that $-NH_2$ as well as $-COOH$ groups can take part in such effects. The groundwork for the theory that protein structure may react to experimental variations in $p_H$ by mechanical changes therefore exists, though recent work (Meyerhof) suggests that muscular contraction may not be associated with changes in $p_H$.

---

* 'J. Amer. Chem. Soc.,' vol 39, p. 354 (1917).

† 'Proc. Roy. Soc.,' B, vol. 98, p. 506 (1925).

‡ 'Proc. Roy. Soc.,' B, vol. 99, p. 40 (1925).

§ 'Biochem. Z.,' vol. 214. p. 253, and vol. 217, p. 433 (1929).

It is well known that certain cells of the central nervous system (the so-called respiratory centre) are sensitive to changes of $p_H$ of the order of 0·02, and probably rather less. At a $p_H$ 7·4, 0·01 $p_H$ corresponds to a change of about 0·14 dyne for the amine and rather less for the acids. It is quite possible that this is sufficient to initiate the appropriate response.

## *Conclusions.*

(1) Long chain carboxylic acids dissolved in benzene show regular changes in interfacial tension against aqueous "buffered" solutions as the hydrion concentration of these is altered. A fall in interfacial tension starts at $p_H$ 5·5 and extends over the range of 4 0 $p_H$ units to $p_H$ 9·3 approximately, tending to vanish at this point The curve is not identical with a dissociation curve, though it extends over the same range of $p_H$. For a given $p_H$ the results are identical for phosphate and glycine "buffered" solutions, and for all acids investigated, except capric acid ($C_{10}$). which shows an abnormality for phosphate.

(2) Hexadecylamine shows similar changes, in the opposite sense between approximately the same $p_H$ range, which follow the dissociation curve of a weak base rather closely

(3) The $K_a$ and $K_b$ of $-COOH$ and $-NH_2$ in the interface can be calculated approximately from these results to be $3 \cdot 2 \times 10^{-8}$ and $1 \cdot 0 \times 10^{-7}$.

(4) Ethyl palmitate shows a fall of similar type to that for the carboxylic acids, but starting at a more alkaline point. Hexadecyl alcohol exhibits no change

(5) The theoretical aspects and biological application of these results are discussed.

I am indebted to the Government Grants Committee of the Royal Society for apparatus used in this research and to W. Wakelin for assistance, also to Mr. Havard and Mr Barnes for $p_H$ estimations with the glass electrode. I am further most grateful to Mr. Hinshelwood for his helpful criticism.

# *The Influence of Hydrogen-ion Concentration upon the Adsorption of Weak Electrolytes by Pure Charcoal.—Part* II.

By Harold John Phelps, B.A., B.Sc., Department of Biochemistry, Oxford, Ramsay Memorial Research Fellow.

(Communicated by C. N Hinshelwood, F R S --Received April 30, 1931.)

In a recent communication results were described which indicate that propionic, hexoic, and succinic acids are adsorbed by purified charcoal only as unionised molecules.* There was no evidence that anions of these acids were adsorbed to any measurable extent Thus the amount of these acids adsorbed from mixed solutions of any one acid and its sodium salt is proportional to the amount of unionised acid present as calculated from the known ionisation constants and the hydrogen-ion concentration of the solutions.† Further work‡ has led to the conclusion that the presence of an unionised carboxyl group is essential for adsorption to take place On the other hand, the adsorption curve for the bases *n*-propylamine and *n*-butylamine at different hydrogen-ion concentrations did not follow the ionisation curves very closely. Strong preferential adsorption of the unionised molecule was observed but there was quite considerable adsorption from solutions of such acidity that no unionised amine could exist in them. The adsorption of both bases was found to fall off gradually and continuously with increasing acidity from $p_H$ 11 to $p_H$ 3.

In view of the fact that the charcoal used in this work was Norit charcoal purified by treatment with strong halogen acids, it was thought possible that very small traces of these acids remained after the washing to which the charcoal was subjected, and that these traces of acid caused the adsorption of basic ions by direct chemical combination.

A stream of air in which a sample of the acid-treated charcoal was ignited was free from hydrogen chloride, but the retention of small quantities of hydrogen fluoride was not impossible.

It seemed desirable, therefore, to obtain a pure charcoal by some method other than acid extraction. It was found that a fairly active adsorbent charcoal could be prepared from " ashless " filter paper.

---

* Phelps and Peters, 'Proc. Roy. Soc.,' A, vol. 124, p. 584 (1929).

† It being assumed that an equilibrium exists between adsorbed molecules and those in solutions.

‡ Phelps, 'J. Chem. Soc.,' 1929, p. 1724.

### *Preparation of Purified Charcoal.*

Whatman's No. 40 "ashless" filter circles were damped and compacted as far as possible and then carbonised by gradual heating in platinum vessels. Residual organic matter was then removed and the charcoal activated by heating at 1200° C. in a reducing atmosphere in a gas furnace for half-an-hour.* The adsorbent power of this charcoal, for the substances studied, is slightly less than half that of the acid-purified Norit charcoal previously used.

### *Experimental.*

In order to make this investigation comparable with my previous work, the electrolytes investigated were: propionic acid, *n*-propylamine and *n*-butylamine. All were purified by distillation. The general technique of the adsorption experiments also exactly followed that previously employed. Various hydrogen-ion concentrations were obtained by partial neutralisation of the electrolytes with the requisite quantities of strong acids or bases. As has previously been pointed out, the resulting mixtures of the weak acids or bases and their salts are to some extent self-buffering and consequently there are no large changes of hydrogen-ion concentration during adsorption. For each experiment a total volume of 22 c.c. of solution (approximately 0·2 per cent. in each case) was shaken with 200 mg. of charcoal for about 12 hours at 20° C.

At the end of each experiment the mixture was centrifuged and the clear liquid decanted and analysed by the appropriate method, as described in Part I (*loc. cit.*) and in the 'Journal of the Chemical Society' (*loc. cit.*). The equilibrium values of the hydrogen-ion concentration were determined by the bubbling hydrogen electrode.

### *Experimental Results.*

The effect of hydrogen-ion concentration upon the adsorption of *n*-propylamine and *n*-butylamine is shown in figs. 1 and 2 respectively. It will be seen that in each case the adsorption is very exactly related to the degree of ionisation of the bases at different hydrogen-ion concentrations. The adsorption

---

* The charcoal was heated in a silica crucible 8 cm. in diameter and 11 cm. high. Above the charcoal was placed a layer of small circles of filter paper to provide a reducing atmosphere in the early stages of heating. The crucible was provided with a lid. The supply of gas and air to the furnace was adjusted for nearly complete combustion. There was probably a small amount of oxidation during the early stages of heating but this was almost certainly confined to the protective layer of paper and the charcoal immediately adjacent to it. Both the ash from the paper and the surface layers of the charcoal were rejected.

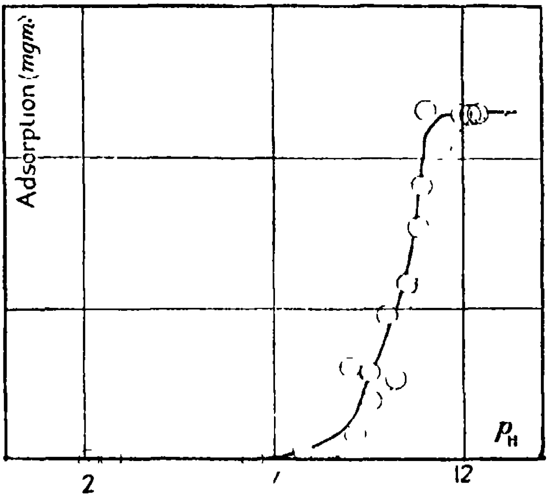

FIG. 1.—The adsorption of *n*-propylamine plotted against hydrogen-ion concentration (continuous curve) The adsorption is plotted as milligrams of base adsorbed by 200 mg. of charcoal. The dotted curve represents the approximate ionisation curve of *n*-propylamine plotted to such a scale that the maximum adsorption of the base is equivalent to zero ionisation

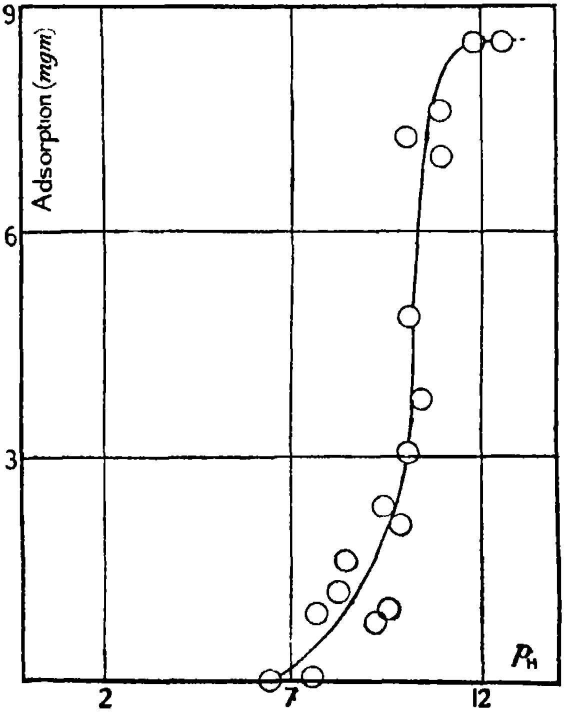

FIG. 2.—The adsorption of *n*-butylamine plotted against hydrogen-ion concentration. The adsorption is plotted as milligrams of base adsorbed by 200 mg. of charcoal.

rises from nil at $p_H$ 7–8 to a sustained maximum in solutions more alkaline than $p_H$ 11. The value of the ionisation constant of *n*-propylamine given by Ostwald* is $4 \cdot 7 \times 10^{-4}$. These results indicate that charcoal prepared from pure cellulose adsorbs the molecules of the normal amines, but that it will not adsorb their ions to any measurable degree.

The influence of hydrogen-ion concentration upon the adsorption of propionic acid is shown in fig. 3. It will be seen from the broken curve that the adsorption does not show the rapid fall with increasing alkalinity that is shown in the

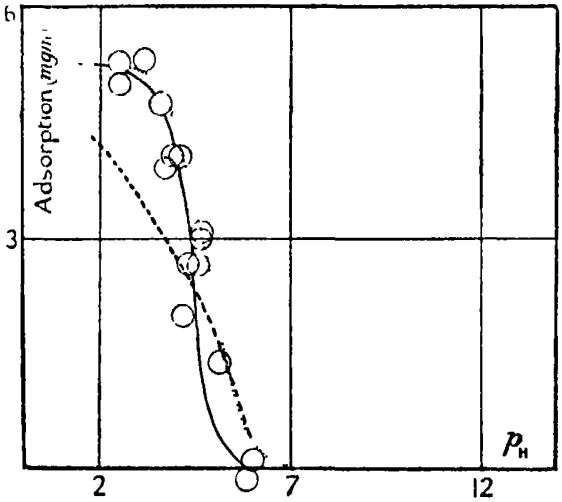

Fig. 3.—The adsorption of propionic acid by filter-paper charcoal (broken curve) and by the same charcoal after acid-treatment (continuous curve), plotted against hydrogen-ion concentration. The adsorption is plotted as milligrams of acid adsorbed by 200 mg. of charcoal. The dotted curve represents the approximate ionisation curve of propionic acid, plotted to such a scale that the maximum adsorption of the acid by acid-treated charcoal is equivalent to zero ionisation.

adsorption of this acid by purified Norit charcoal. It falls off gradually from $p_H$ 1·5 to $p_H$ 6. This can hardly be due to the adsorption of propionate ions as there is no adsorption in solutions more alkaline than $p_H$ 6, at which hydrogen-ion concentration, the concentration of propionic acid molecules, may be considered to have fallen to zero. Ostwald gives K for propionic acid as $1 \cdot 34 \times 10^{-5}$.† It seems probable that the adsorption of propionic acid is influenced by changes in hydrogen-ion concentration in solutions more acid than $p_H$ 3, on account of some ionising impurity in the charcoal itself. The results at least indicate a disturbance of the equilibrium between the solution and the surface.

---

* 'Z. Phys. Chem.,' vol. 33, p. 361 (1898).

† 'Z. Phys. Chem.,' vol. 3, p. 170 (1889).

It is well known that the most highly purified filter papers contain a certain amount of basic impurity. The nature of these impurities has been discussed by Fresenius.[*] Lange[†] has found that it is almost impossible to remove the last traces of silica, calcium and iron from celluloses of vegetable origin. It seemed reasonable to attribute the anomalous adsorption of propionic acid by filter paper charcoal to the presence of these substances.

A sample of the charcoal was, therefore, digested with a mixture of hydrochloric and hydrofluoric acids and evaporated slowly to dryness. The charcoal was then repeatedly washed with distilled water until the washings were chloride-free, and subsequently heated under reduced pressure. In this way the treatment to which the purified Norit charcoal had been subjected was exactly imitated.

After this treatment the filter-paper charcoal was found to be almost as selective an adsorbent of molecular propionic acid as the acid-purified Norit charcoal. The curve relating adsorption with hydrogen-ion concentration is shown in fig. 3 (continuous curve). In the case of acid-treated filter-paper charcoal, adsorption falls from a maximum value to nil between $p_H$ 3·2 and $p_H$ 6 In the case of acid-purified Norit charcoal the values are $p_H$ 3·8 and $p_H$ 6 respectively. The results agree as closely as can be expected with the view that only the unionised acid molecule is adsorbed.

By analogy with the results obtained with acid-purified Norit it might have been expected that the acid-treated filter-paper charcoal would have acquired the property of adsorbing propylammonium ions. This was not the case. A series of experiments with this charcoal showed that the adsorption of *n*-propylamine by it was influenced by hydrogen-ion concentration in exactly the same way as was the adsorption by untreated filter-paper charcoal. The actual amount of base adsorbed was also, within the limits of experimental error, identical in the two cases.

## *Discussion of Results.*

The hypothesis that the adsorption of basic ions by purified Norit charcoal was due to direct chemical combination between these ions and traces of acid impurity in the charcoal, seems to be justified by the results here described. Such impurities as there are in charcoal prepared from filter paper are certainly basic. This charcoal adsorbs only unionised amine molecules. The presence of basic impurities, however, in the filter-paper charcoal does not give it the property of adsorbing acid ions.

---

[*] 'Z. Analyt. Chem.,' 1883, p. 241.

[†] 'Ber. Deut. Chem. Ges.,' 1878, p. 823.

In view of the fact that propionic acid is not appreciably ionised in solutions more acid than $p_H$, one would expect that the adsorption of the acid would also remain constant with increasing acidity beyond $p_H$ 3. This does, of course, happen with acid-purified Norit charcoal and also with acid-treated filter-paper charcoal. The steady rise in the adsorption of propionic acid upon untreated filter-paper charcoal with increasing acidity up to $p_H$ 1·5 at least must, therefore, be a property of the impure charcoal itself.

It has been suggested by Rideal* that the molecular adsorption of weak acids observed with purified Norit charcoal might be apparent only. If one imagines that hydroxyl ions are expelled from the charcoal and replaced by acid anions the observed adsorption would be indistinguishable from that produced by true molecular adsorption. This argument is in essence the same as that advanced by Miller,† except in so far as Rideal would attribute the origin of the hydroxyl ions to gases adsorbed by the charcoal, while Miller postulates a layer of water molecules on the charcoal surface. If the adsorption of weak acids be regarded as proceeding by the replacement of hydroxyl-ions, it must be assumed, either that the number of available hydroxyl-ions decreases with increasing alkalinity, which seems improbable, or it must be assumed that the hydroxyl-ions are more easily displaced from the surface as the hydrogen-ion concentration in the liquid phase rises. If one imagines that the expulsion of hydroxyl-ions from the charcoal is determined by the concentration of hydrogen-ions in the liquid phase, one would expect that with any one charcoal the adsorption of all weak acids would be influenced by hydrogen-ion concentration in the same way. The results which have been described for maleic and fumaric acids, for example, show that this is not the case.

If the adsorption of the simple amines is to be explained on the same lines, it must be assumed to proceed by the displacement of hydrogen-ions from the charcoal surface by ionised base. Further it must be assumed that such hydrogen-ions are replaced progressively more readily as the hydrogen-ion concentration in the liquid phase falls from $p_H$ 7 to $p_H$ 11. Apart altogether from the complex assumptions that any ionic representation of the adsorption of weak electrolytes may demand, it is hard to imagine any ionic mechanism of adsorption, as a result of which the adsorption rises progressively as the concentration of adsorbable ions falls, and which would account for the fact that the adsorption is maintained at a maximum value in solutions of such "reaction" that the concentrations of adsorbable ions in them must be very small indeed. On the other hand, the assumption that the adsorption of the weak electrolytes studied proceeds very largely, or exclusively, through the medium of unionised molecules, adequately explains all the results so far obtained.

---

* "Surface Chemistry," 2nd ed., p. 277.

† 'J. Phys. Chem.,' vol. 28, p. 992 (1924).

There is no reason to suppose that the adsorption of strong electrolytes, in which case there is a considerable concentration of ions under practically all conditions, proceeds in a similar way. Much evidence of the ionic adsorption of strong electrolytes exists. It has been shown, also, by Schilov and his co-workers* that the adsorption of strong electrolytes by charcoal depends on the presence of adsorbed or combined gases on the charcoal surface

## *Summary*

It has been found that charcoal prepared from Whatman's No. 40 filter circles adsorbs *n*-propylamine and *n*-butylamine only as unionised molecules. The amount of base adsorbed at any given hydrogen-ion concentration is, therefore, proportional to the concentration of unionised molecules existing under the conditions.

Propionic acid is adsorbed only as unionised molecules, but some impurity in the charcoal prevents true equilibrium between the molecules in solution and those at the surface being established Acid-treatment of the charcoal removes this impurity and there is good relation between the concentration of propionic acid molecules in solution and the amount of adsorption that takes place. The acid-treatment of the charcoal has no influence on the adsorption of *n*-propylamine or *n*-butylamine.

These results justify the assumption that a sufficiently purified charcoal will present a perfectly neutral surface to a water solution of a weak electrolyte. Such a surface will adsorb weak acids and bases only as unionised molecules.

Acid-treated filter-paper seems to approximate very closely to an ideal neutral surface.

My sincere thanks are due to Professor R. A. Peters for his advice and encouragement and to the Ramsay Memorial Trustees for a Fellowship which enabled me to undertake this work. I must also express my indebtedness to the Deputy Master and Assayers of the Royal Mint in whose laboratories the filter-paper charcoal was prepared.

---

* Schilov and Tschmutov, 'Z. Phys. Chem.,' vol. 148, p. 233 (1930); Schilov, Tschmutov and Schatunovskaja, 'Z. Phys. Chem.,' vol. 149, p. 211 (1930); and also by Frumkin, 'Koll. Z.,' vol. 51, p. 123 (1930).

# *Discontinuities at the Melting Point of Bismuth.*

By W. L. WEBSTER.

(Communicated by P. Kapitza, F R.S.—Received May 5, 1931)

## § 1. *Introduction.*

During the last two or three years considerable attention has been given to the growth of single crystals of bismuth and to their physical properties. The result of this work has shown that the preparation of a good single crystal is exceedingly difficult, the process being easily disturbed in many ways, and the conclusion must be drawn that it has not yet been possible to obtain anything approaching a perfect crystal. In all cases where the grown crystal has been adequately examined, it has been necessary to admit that the supposed single crystal was full of discontinuities.

This was shown by Kapitza* in his work on the growth and magneto-resistance change of single crystals of bismuth He found it very difficult to produce a crystal rod parallel to the hexagonal axis that was flexible. Almost all the crystals grown with this orientation were apparently brittle in that a very little strain would cause a sharp fracture parallel to the principal cleavage plane. Some crystals indeed broke up into small pieces 2 or 3 mm long when dropped from a height of a few centimetres on a table. As the separate pieces proved to be fairly flexible this brittleness is not a real property of the crystal, but appears to be due to isolated cracks or discontinuities in the crystal (the word " crack " is used with the meaning defined by Kapitza in his paper, where further arguments for their existence from X-ray and resistance measurements are given). These cracks are not characteristic only of the brittle crystals, but appear to be present in many flexible crystals as well, their flexibility being due to a random distribution of a comparatively large number of cracks small in area compared to the dimensions of the rod.

In his work, while Kapitza was unable to eliminate these cracks, he did find that a very large temperature gradient was favourable to the production of flexible crystals, while a small gradient usually gave rise to the brittle variety of crystal. This difference in the method of growth seems to be sufficient to explain the difference in the distribution of the cracks in the two cases. With a steep temperature gradient the exact position of the liquid-solid surface must be very uncertain, as it will be easily affected by any change in the experimental conditions. It is probable that in the growth of crystals with a steep heat gradient, the progress of the liquid-solid surface does not take place continuously but in a very erratic manner, so that any otherwise regular discontinuity will have a great tendency to be broken up and to appear irregularly as do the cracks in the so-called flexible crystals grown by this process. In growing crystals with a small gradient of temperature, the heat flow will not be large compared to the heat capacity and latent heat of the bismuth, and the effect of small variations in the conditions must be effectively damped out, so that such discontinuities as these cracks will be able to form in a regular way and be continuous over comparatively large areas

---

* 'Proc. Roy. Soc.,' A, vol. 119, p. 358 (1928).

To explain the existence of these cracks Kapitza made the suggestion that in solidifying, bismuth, which normally has a rhombohedral structure, passes through a cubic modification The bismuth must then change structure while solid, and it would be conceivable that the strains resulting from such a process might be responsible for the development of cracks This view was based on the experiments of Curie,* who found that the anomalously large diamagnetism of solid bismuth disappeared at a temperature appreciably below the melting point.

More recently another kind of discontinuity has been discovered by Goertz.† With a very careful etching process Goertz has shown that the crystal does not react uniformly to the acid, but is dissolved more rapidly along planes parallel to the four cleavage planes of the crystal. These planes of rapid etching have a fairly definite periodicity with a spacing of the order of $10^{-3}$ mm , and have been interpreted by Zwicky as supporting his theory‡ of the mosaic structure of crystals.

The experiments to be described were designed to investigate the mechanism suggested by Kapitza to account for the cracks observed by him, and do not directly concern the discontinuities of Goertz and Zwicky, which appear on a scale a thousand times smaller, and may, therefore, be quite different in origin.

The present experiments were made in an effort to find the supposed cubic modification of bismuth, and depended on the supposition that such a structure would have a diamagnetism of the same order as that of liquid bismuth. The anomalously large diamagnetism of normal solid bismuth should then appear at a temperature appreciably below the solidification point. It has been possible to show that the temperatures at which the diamagnetic discontinuity, solidification, and the latent heat appear are coincident within an experimental error of less than 0·3° C. There is then no indication whatever of a non-magnetic solid state of bismuth such as was suggested by Curie's experiment, and it becomes necessary therefore to abandon this explanation of crack formation.

---

* 'J. Physique,' vol. 4, p. 206, footnote (1895).

† 'Proc. Nat. Acad. Sci,' vol. 16, p. 99 (1930).

‡ 'Proc. Nat Acad. Sci,' vol. 15, p. 816 (1929).

In the last section an alternative mechanism is proposed which seems capable of accounting for the cracks, in terms of processes whose existence is well known

## § 2. *The Magnetic Discontinuity at the Melting Point of Bismuth.*

The experiment described in this section was undertaken with the object of finding out if the anomalous diamagnetism of bismuth disappeared exactly at the melting point of bismuth The experiment of Curie, quoted above, suggested that this was not the case, but as his results were only qualitative, it was felt that a more exact investigation was necessary in view of the possibility of a cubic modification. Actually the experiment was done for the process of solidification. Two sets of readings were taken simultaneously, one giving a cooling curve, the other a record of the magnetic moment of the bismuth. From the simultaneous appearance of the discontinuity in both records it was obvious that the anomalous increase in susceptibility could be exactly identified with the emission of latent heat.

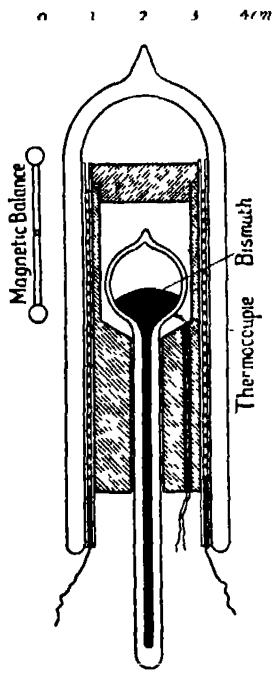

Fig. 1.

The bismuth was placed in an evacuated pyrex bulb which was in turn placed in a furnace clamped rigidly between the poles of an electromagnet giving a field of about 12,000 gauss. The susceptibility of the bismuth was measured by a new type of magnetic balance placed just beside the furnace. As an account of this balance is being given elsewhere, it will not be described in this paper. The arrangement used is shown in fig. 1, which gives a section at right angles to the magnetic field. The bismuth was placed in a pyrex bulb with a long appendix which was brought out from the furnace and by providing an always solid bismuth surface prevents supercooling. This bulb was inside a heavy copper block drilled to take the bulb and appendix and thermo-couple leads. A heating coil of nichrome wire was wound non-inductively around the copper block and insulated from it by mica. This assembly was then placed in an inverted pyrex Dewar flask which provided sufficient heat insulation, and then clamped firmly between the poles of the magnet as near the balance as possible.

The bismuth used in these experiments was supplied by Kahlbaum in the form of a cast rod This was treated with hydrochloric acid to remove any iron dust from the surface, then washed in distilled water and dried To remove as much of the adsorbed gas as possible, the bismuth was heated for a few minutes well above its melting point in an evacuated bulb to which the experimental bulb and appendix were joined by a short length of tube containing a constriction. The bismuth was poured into the latter bulb, which was then sealed off at the constriction while still evacuated This process always removed a considerable amount of gas, but it is not pretended that all the absorbed gas could have been eliminated by such a comparatively gentle treatment

There are two other points in the experimental arrangements which must be discussed. These are the magnetic variation of the furnace assembly, and the position of the thermo-couple used to measure the temperature. Both of these factors lead to apparent anomalies in the experimental curves, but their effects can easily be disentangled from the results. With the apparatus used, the magnetic moment measured is the total moment of the bismuth and furnace assembly As nichrome wire was used as the resistor element, there is a considerable variation with temperature of the magnetic moment of the furnace assembly. A blank run without bismuth showed that there were no discontinuities in the magnetic effect of the furnace near the melting point of bismuth, so that the discontinuity observed with bismuth present must be due to the bismuth itself Above the melting point the susceptibility of bismuth is very small and constant, and the magnetic variation observed is due entirely to the furnace.

The thermo-couple junction was placed outside the pyrex bulb, but pressed up against it by the leads. It, therefore, did not record the actual temperature of the bismuth, but a value between that and the temperature of the copper furnace block The actual difference between the junction and the bismuth will change as soon as the temperature difference between the bismuth and the copper alters There appears on the curves an effect, as of super-cooling, when solidification and the emission of the latent heat takes place. This is due to the readjustment of the temperature lead of the junction, corresponding to the altered temperature gradient between the bismuth and the copper, when the bismuth stops cooling. The effect becomes less when slower cooling, and consequently smaller, gradients are used.

The usual course of an experiment was as follows. The furnace was first heated to a temperature 30 or 40° higher than the melting point. The heating current was then reduced to a value which would give an equilibrium temperature 1 or 2° below the melting point, and the furnace allowed to cool down till the temperature was about 10° above the melting point (by which time the cooling had begun to follow a normal cooling curve). The taking of readings connecting the time, temperature and magnetic moment was then begun and carried on till the bismuth had completely solidified. Readings were taken at least once a minute over a period of about 2 hours. The normal error in determining the temperature at any point was about 0·05° C., and the error in the magnetic moment in the best run about 0·25 per cent. of the total magnetic discontinuity at the melting point. The error in the magnetic measurement depended on the stability of the zero of the magnetic balance; this in turn depended on various factors not entirely controllable, and for this reason was not always the same.

In fig. 2 the temperature and magnetic moment of the bismuth and furnace are shown as functions of the time for a small region near the melting point. (For this and all the other figures the temperature scale is arbitrary in that the discontinuity of the cooling curve is assumed to occur at 270° C. The scale

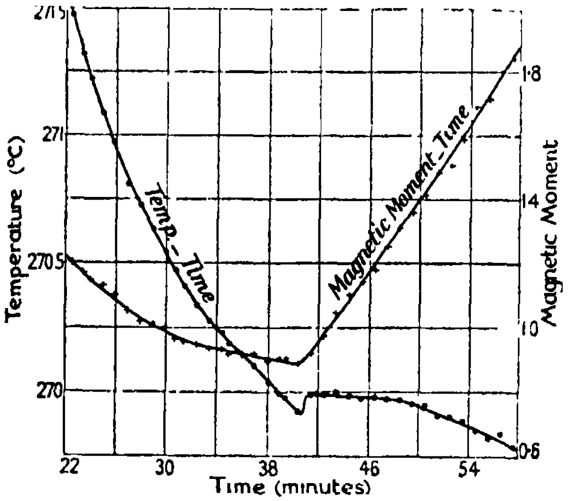

FIG. 2.

of magnetic moment is completely arbitrary and is arranged so that an increase in scale reading corresponds to an increase in diamagnetic moment.) From these two curves it can be seen that the two discontinuities appear almost simultaneously. Such difference as exists may be put down to the different way in which the first bismuth to solidify will act on the thermo-couple and magnetic balance. It is certainly possible to state that the temperature interval between the magnetic change of bismuth and the latent heat emission is not more than 0·05° C.

In fig. 3 the magnetic moment is plotted as a function of the temperature for the same region. The decreasing moment above the melting point is due to the increasing paramagnetism of the furnace, but the sharp rise in diamagnetic moment when cooling stops is clearly seen The slight diamagnetic tendency just before this point is probably due to the effect of the bismuth solidifying in the appendix of the bulb This will have a measurable effect on the magnetic balance, but not on the thermo-couple.

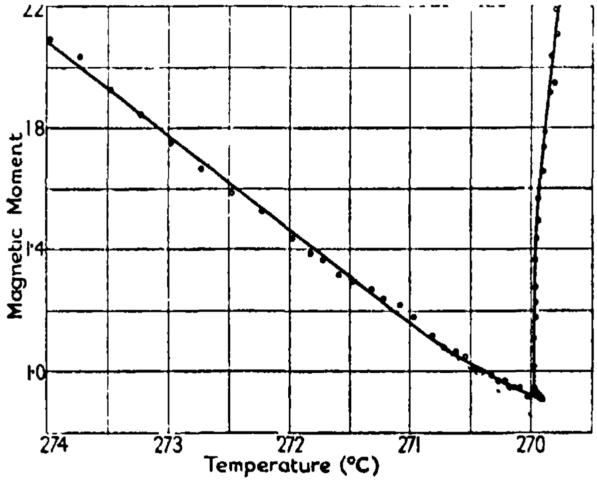

FIG. 3.

An analysis of the cooling curve showed that the rate of cooling was inversely proportional to the excess temperature down to the temperature at which the main latent heat emission sets in. There is then no appreciable emission of heat above this temperature and consequently little likelihood of a transition phase between the normal liquid and anomalously diamagnetic solid states.

## § 3 *The Solid Liquid Transition.*

The experiment just described showed that the magnetic discontinuity occurred simultaneously with the emission of the latent heat, but, as it did not define the actual solid-liquid transition point by the rigidity characteristic of the solid state, it did not definitely rule out the possibility of an intermediate phase provided that the transition from the liquid to this phase involved no great change in the internal energy of the bismuth Another experiment was made in which the temperature at which rigidity was lost or acquired was determined relative to the latent heat absorption or emission. The results showed that, within the limit of experimental error, there was again coincidence between the two discontinuities

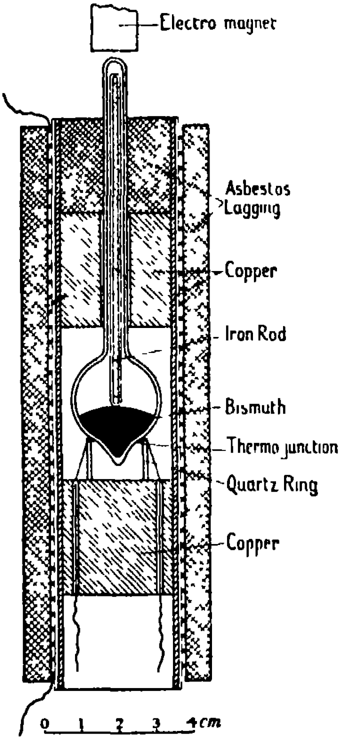

FIG 4.

Bismuth was placed inside an evacuated pyrex bulb by the same method as before. The bulb, however, was provided with a wide appendix tube which held, in this case, a plunger consisting of some soft iron wire sealed off in a pyrex tube small enough to slide easily in the appendix tube of the bulb. The plunger could then be operated electro-magnetically and the rigidity of the bismuth determined at any temperature

The bulb and appendix were placed in a well-lagged copper furnace shown in fig 4 The temperature was measured by means of a thermo-couple pressed against the outside of the bulb, and the top of the plunger was observed through a telescope

By adjusting the heating current as in the previous experiment, the bismuth was made to pass slowly through the melting point in either direction. The heating or cooling curve was recorded and also the height of the rod. The initiation of change in the latter indicated the commencement of liquefaction or solidification, and the actual height of the rod showed approximately the amount of bismuth present in a solid state.

In fig. 5, curves are shown for the process of melting Here the beginning of melting is not well defined, for there is a departure from a linear relation in the temperature-rate of heating curve several degrees below the real flattening out of the heating curve. This means that the bismuth is not homogeneous, and that melting takes place over a temperature range of several degrees.

That it is really melting which occurs is borne out by the fact that the drop in the height of the plunger begins at the same temperature as does the departure from a linear heating curve. The sudden drop observable at the end of melting is caused by the final breaking of the surface, which is the last part to melt, and which, till then, has been gradually sinking into the molten bismuth under the weight of the plunger.

In the case of the cooling curve it is impossible to determine exactly the temperature at the beginning of solidification on account of supercooling which, in spite of violent stirring with the plunger, was always present to the extent of 5° C to 10° C. But, as in the previous case, it is quite clear that the acquisition of rigidity takes place coincidently with, and proportionately to, the emission of the latent heat, for almost the whole process of solidification as defined by the rigidity takes place in a range of temperature varying by not more than 0·3° C, and, as much of this apparent change must be due to variation in the temperature gradient in which the thermo-junction is situated, consequent on the continued cooling of the outside of the furnace, any lag between the latent heat absorption and solidification must be appreciably less than this 0·3° C.

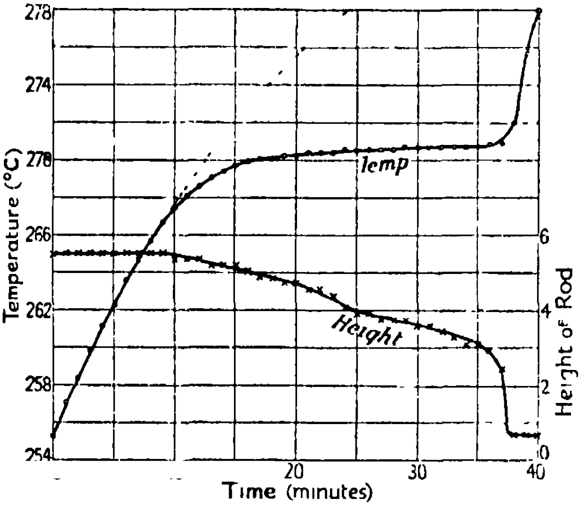

FIG. 5.

This result, combined with that of the experiment on the magnetic discontinuity, make the existence of a cubic "non-magnetic" modification of bismuth very improbable, and in any case confine it to such a small temperature range that it could scarcely account for the "cracks" in the way proposed by Kapitza.

The explanation of Curie's observations is rather difficult, as their description is very brief He showed that small lumps of bismuth retained their shape several degrees above the temperature at which the anomalous diamagnetism disappeared. But, though the shape remained the same, Curie found that the crystal axes had changed orientation, and for this reason it seems necessary to assume that the bismuth had really melted inside a rigid shell. Some experiments* of the writer have shown that an oxide layer on a bismuth rod 1 mm in diameter can support the hydrostatic pressure of 1 cm. of molten bismuth at temperatures several degrees above the melting point. It is possible that the absence of change of shape in Curie's experiments was due to the presence of sufficient oxidation to form such a rigid shell.

## § 4. *The Cracks in Bismuth.*

The heterogeneity of the melting point of bismuth found above is a phenomenon which seems capable of explaining the cracks observed by Kapitza. Further measurements of the heating curve of bismuth were made which showed that the majority of the latent heat emission took place at a well-defined temperature which formed the upper limit of the range in which the emission took place. The spread in the melting point is due to a small proportion of the bismuth having a lower melting point than this limit, which presumably corresponds to the true melting point of bismuth. These experiments are not completely satisfactory, as no precautions were taken to prevent super-cooling during the solidification of the bismuth afterwards to be melted for the heating curve. As supercooling of as much as 20° C. has been observed, and usually 5 to 10° C., not only will the bismuth be polycrystalline, but also an appreciable part may be in a strained condition resulting from its too rapid solidification. The release of the strain energy and the surface energy of the crystal inter-faces may then be responsible for the anomalies observed in the heating curves. Further experiments are being carried out to check this point.

If this mechanism proves to be inadequate to explain the apparent spread of the melting point, then it will be necessary to assume that there are regions with subnormal melting points scattered about and separating much larger volumes of normal bismuth. That such is the case is supported by the experiments of Roberts,† who found anomalies in the coefficient of thermal expansion for single crystals some 10° below the melting point, which he interpreted as a sign of a general loosening up of the crystal before melting actually occurred.

---

* See also W. B. Pietenpol and H. A. Miley, 'Phys. Rev.,' vol. 30, p. 697 (1927).

† J. K. Roberts, 'Proc. Roy. Soc.,' A, vol. 106, p. 385 (1924).

The experiments of Roberts must, however, be interpreted with due reserve in considering good single crystals, because the bismuth cylinders used by him were cut from large parent crystals, a process which must inevitably introduce strains in the crystals used.

Observations by the writer on polycrystalline bismuth which had not been outgassed, but which was heated in a vacuum, have shown that the crystal components fell apart several degrees below the melting point of the bulk of the individual components by a process of melting along the crystal boundaries. There is then definite evidence of pre-melting in bismuth in regions particularly likely to absorb impurities, in this case the crystal boundaries. And it seems quite likely that the anomalies recorded above are also due to the presence of impurities. If there are impurities present in the molten liquid, even to a small extent, then the solid in crystallising will reject the impurities, and they will eventually be concentrated at the boundaries of the crystals where they may produce an appreciable lowering of the melting point.

In the process of the growth of single crystal rods from a seed crystal placed at one end, which is that by which Kapitza's brittle bismuth was obtained, there is a simple mechanism by which this self-purification of the solid may lead to discontinuities in the structure corresponding to his "cracks" The impurities rejected at the surface of solidification must increase the concentration and lower the melting point in the liquid immediately adjacent to the solid surface. These impurities will diffuse through the melt and possibly into the surrounding atmosphere. There will exist consequently a decreasing gradient in the impurity concentration and an increasing melting point from the solid surface forward into the melt The nature of this gradient will depend on the rate of advance of the surface of crystallisation, on the rate of diffusion of the impurity in the melt, and possibly on the nature of the surface and surrounding atmosphere Its effect will be to lower the temperature at which crystallisation is proceeding below the normal freezing point of the liquid beyond the reach of the gradient This liquid will not solidify on its own since it is able to supercool much more than the lowering of the freezing point by any probable amount of impurity, and it will remain in an unstable supercooled condition.

If conditions are such as to favour a high degree of instability, it is very likely that there will occasionally occur a cataclysm during which the solidified part of the bismuth transmits a growth nucleus to the supercooled part of the liquid. Enough will then solidify in a rush to raise, by the liberation of its latent heat, the temperature of the supercooled liquid to its normal freezing point. The very impure liquid next the original surface of solidification will then be entrapped between two solid surfaces, which will prevent the escape of the impurities concentrated there, except for that part which may diffuse through the surface, until sufficient cooling of the whole has occurred to allow this impure bismuth to solidify.

The result of this will be not only that the final bismuth crystal will contain regions with a lower melting point than that of pure bismuth, but also that the crystal on account of its discontinuous growth will exhibit mechanical discontinuities These must appear as a much-reduced cohesion between the parts of the bismuth crystal which have grown homogeneously and seem therefore to correspond to the cracks observed by Kapitza.

As to the nature of the impurities, there is little information except what may be drawn from the conditions favouring the disappearance of the cracks. With the process just described, factors which prevent the accumulation of a large concentration of impurities at the surface of solidification should reduce the probability of formation of a "crack." The crystals used by Kapitza were grown open to the atmosphere and must therefore have become well oxidised on the surface. On the other hand, Goertz, growing crystals in an atmosphere of hydrogen with only slight oxidation, and the writer growing crystals in a vacuum, find little evidence of these cracks. These results suggest that the essential impurity is dissolved oxygen or nitrogen which, in the latter experiments, could diffuse without hindrance through the surface of the molten bismuth into the surrounding atmosphere, but which, in the case of well-oxidised bismuth, could not diffuse through the oxide layer at all.

## *Summary.*

The investigations described in this paper were undertaken to determine whether bismuth in solidifying passed through a transitional cubic phase—a suggestion put forward by Professor Kapitza to explain the formation of cracks during the growth of bismuth crystals. The experiments show that the temperature of emission of the latent heat of fusion, of the acquisition of rigidity, and of the anomalous diamagnetic discontinuity coincide within an experimental error of 0·3° C. This coincidence leaves no room for such a cubic phase, and another process based on the self-purification of growing crystals is suggested to account for these cracks.

In conclusion, I should like to thank Professor Kapitza, at whose suggestion this work was undertaken, for his continued interest and helpful criticism.

# *Gaseous Combustion in Electric Discharges. Part VIII.—The Cathodic Combustion of Hydrogen-Oxygen Mixtures.*

By G. I. **Finch** and E. A. J. **Mahler**, Imperial College of Science.

(Communicated by W. A. Bone, F.R.S.—Received May 5, 1931.)

## *Introduction.*

In Part I* hereof it was established that the rate of cathodic combustion of electrolytic gas is proportional to the current traversing the cathode zone. Subsequent investigations (III to IV) have shown that sputtered metal particles play an important rôle in the cathodic combustion of carbonic oxide, and that the nature of the cathode materials employed in the experiments described in (I) was therefore such as to render difficult a full interpretation of the results set forth therein, because, from the point of view of cathodic sputtering, copper occupies a position intermediate between the non-sputtering and freely sputtering classes of metals. Also, the results of recent experiments on the catalytic properties of sputtered platinum films, an account of which it is hoped will shortly be submitted to the Society, have shown that even at room temperature sputtered platinum is sometimes capable of powerfully catalysing the union of hydrogen and oxygen. These considerations clearly indicated the need for extending the study of the cathodic combustion of electrolytic gas to that occurring at electrodes such as gold, silver, tantalum and tungsten. Furthermore, with the object previously outlined in (VII), *i.e.* the elucidation of the mechanism of the combustion of hydrogen by oxygen and the rôle played by hydrogen in promoting the combustion of carbonic oxide, the scope of the present investigation was extended in order to study the effect of such diluents as oxygen, hydrogen and steam upon the cathodic combustion of electrolytic gas.

The results of our experiments, of which an account is given in what follows, have shown, *inter alia*, that the rate of combustion of electrolytic gas at a non-sputtering cathode increases rapidly on dilution with hydrogen; whereas, at a freely sputtering cathode, this effect is far less pronounced.

---

* 'Proc. Roy. Soc.,' A, vol. 129, p. 672 (1930), Part VII; wherein references are given for the preceding parts of this series. For brevity, these are referred to in the above communication by their Roman numerals within brackets.

## *Experimental.*

The circulation apparatus employed and the experimental procedure followed have been previously described in sufficient detail (III, VI and VII). Gold, silver, tantalum and tungsten cathodes were used. The conditions of gap width, gas pressure and discharge current were such as to preclude the formation of an active positive column, without at the same time giving rise to distortion of the cathode zone The cathode glow in all experiments was normal, *i e*, it never completely enveloped the cathode surface.

## *The Experimental Results*

*Series I.*—The combustion of electrolytic gas, either previously dried over purified phosphoric oxide or containing 1·6 or 3·7 mm. partial pressure of steam, at gold and tantalum cathodes was studied in these experiments over a pressure range between 90 and 25 mm. The gap width was varied between 1 and 3 mm. and the current between 1·82 and 2·55 milliamperes The results are given in Table I, wherein $c/i$ is the ratio of the rate of combustion in cubic centimetres of electrolytic gas at N.T.P. burnt per minute to the current in milliamperes.

Table I.—$c/i$ Values for the Cathodic Combustion of Electrolytic Gas.

| Total pressure in mm | Dry $(2H_2 + O_2)$ | | | | $(2H_2+O_2)$ + 1·60 mm $H_2O$ | | $(2H_2 + O_2)$ + 3·7 mm. $H_2O$. | |
|---|---|---|---|---|---|---|---|---|
| | $Wo^-$. | $Ta^-$ | $Ag^-$ | $Au^-$. | $Ta^-$. | $Au^-$. | $Ta^-$ | $Au^-$. |
| 90 | 0·38 | 0·28 | 0·27 | 0·25 | 0·32 | 0·26 | 0·34 | 0·26 |
| 60 | 0·37 | 0·27 | 0·26 | 0·24 | 0·30 | 0·26 | 0·34 | 0·25 |
| 30 | 0·36 | 0·26 | 0·25 | 0·23 | 0·29 | 0·25 | 0·33 | 0·24 |

*Series II*—In this series the effect of dilution with either oxygen or hydrogen upon the cathodic combustion of electrolytic gas was studied. Since in these experiments the product of combustion was continually removed, the percentage concentration of the diluent gas increased as the total pressure fell. The initial composition of the mixtures employed ranged between 33·3 $H_2$ + 66·7 $O_2$ and 95·1 $H_2$ + 4·9 $O_2$ and the initial pressure between 140 and 60 mm. The experimental results obtained with gold and tantalum electrodes are incorporated in the figure. Similar results were also obtained with silver and tungsten cathodes respectively.

*Series III.*—These experiments were carried out with the object of determining the amount, if any, of hydrogen peroxide formed during the cathodic combustion of hydrogen at sputtering and non-sputtering cathodes. The average volume of the circulation apparatus when carrying out the experiments of Series I and II was about 500 c.c. For the purpose of these experiments the volume of the circulation apparatus was increased to about 1200 c.c. by inserting a bulb of suitable capacity between the phosphoric oxide drying tube, Q (see diagram, Part III, p. 306) and the entrant end of the reaction vessel, and a horizontally disposed tube containing a titanous sulphate solution immediately after the combustion vessel (VI). Each experiment was carried

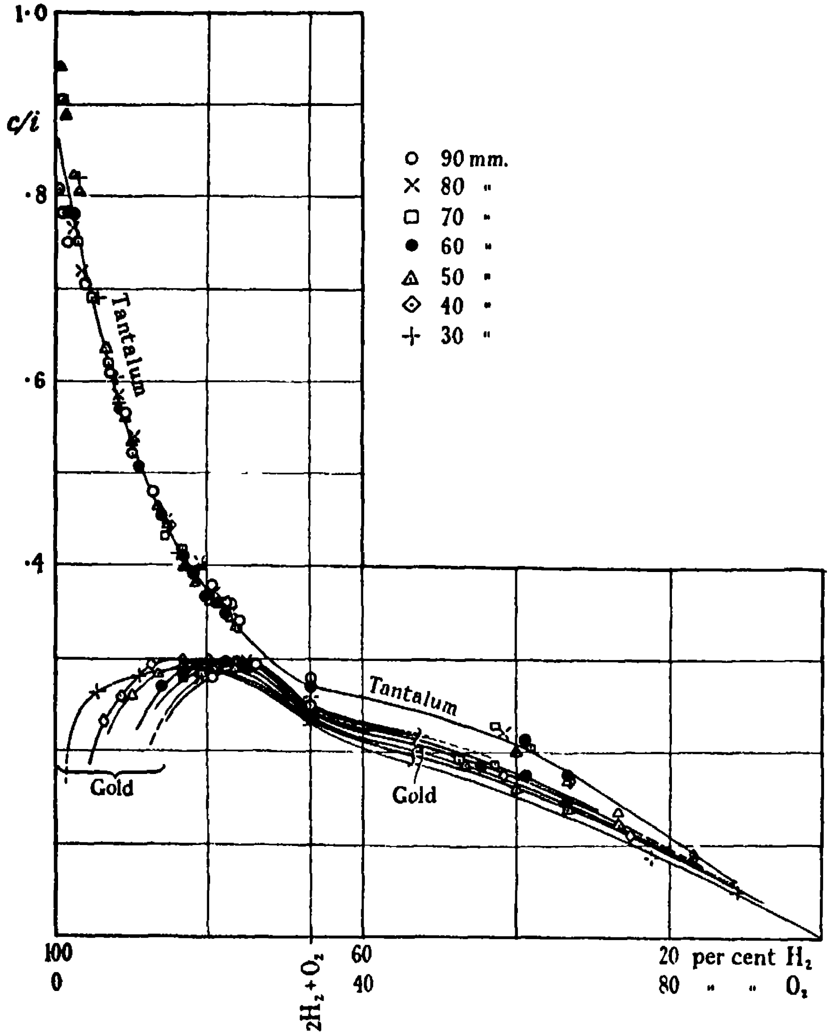

out over the comparatively narrow range of pressure between 100 and 80 mm.; thus the initial and final compositions of the mixtures differed by less than 6·5 per cent. The results are incorporated in the first four lines of the following table.

Table II—Showing the Amount of Hydrogen Peroxide formed during the Cathodic Combustion of Hydrogen-Oxygen Mixtures

| Average composition of gaseous mixture | Percentage of total oxygen burnt and recovered as peroxide oxygen at – | |
|---|---|---|
| | Ta-. | Au-. |
| 60 $O_2$ + 40 $H_2$ | 0·56 | 0·35 |
| 33 $O_2$ + 67 $H_2$ | 0·88 | 0·66 |
| 20 $O_2$ + 80 $H_2$ | 1·12 | 0·75 |
| 10 $O_2$ + 90 $H_2$ | 1·33 | 0·71 |
| 33 $O_2$ + 67 $H_2$ | 0·43 | 0·31 |

Further experiments in which undiluted electrolytic gas was burnt cathodically from an initial pressure of 120 down to 30 mm. yielded the results given in the last horizontal line of Table II.

### *Discussion of the Results.*

The experimental results set forth above directly establish the remarkable fact that dilution with hydrogen, even up to a point when the mixture contains as much as 99·5 per cent. $H_2$, results in a rapid increase in the rate of combustion of electrolytic gas at a non-sputtering cathode. It will be readily understood that, owing to limitations imposed by the apparatus employed in our experiments, it was not possible to determine in what precise mixture of $H_2$ and $O_2$ the rate of combustion at a non-sputtering cathode would have attained a maximum. The results incorporated in the figure show clearly, however, that the mixture burning most rapidly under the conditions outlined above must contain more than 99·5 per cent. $H_2$. In the case of combustion occurring at a freely sputtering cathode (Au or Ag), on dilution with hydrogen, the rate of steam formation increased comparatively slowly to a maximum beyond which further such dilution reduced the rate of combustion. The position of this maximum in relation to the composition of the mixture depends upon the gas pressure; with decrease in pressure the maximum shifts towards the region of greater hydrogen dilution. At a freely sputtering cathode, in a $H_2$-$O_2$ mixture containing between 75 and 85 per cent. $H_2$, $c/i$ reaches a maximum value of 0·30, a value which is less than one-third of that observed when a mixture much richer in hydrogen is burnt at a non-sputtering cathode. Dilution of electrolytic gas with oxygen results in an approximately proportionate reduction in the rate of combustion at either non-sputtering or freely sputtering cathodes.

It seems to us that these facts suggest that (i) the cathodic combustion of $H_2$–$O_2$ mixtures is primarily determined by a prior excitation of both constituents, (ii) while the life of the excited oxygen is short that of the excited hydrogen is long; and (iii) sputtered metal particles reduce the life of one or both excited constituents. It is improbable that sputtered metal inhibits the excitation of either constituent to an extent sufficient to account for the pronounced specific effect of such particles upon combustion, because the colour and the appearance of the cathode zone is not visibly affected by the nature of the cathode material; nor have we been able to detect any difference between spectrograms of the cathode glow in mixtures of $H_2$ and $O_2$ or in steam at different cathodes, other than that due to the presence, or otherwise, of sputtered metal atoms (V).

The results set forth in Table II show that the formation of $H_2O_2$ during the cathodic combustion is favoured by (i) dilution of the $H_2$–$O_2$ mixture by $H_2$, except in the case of a freely sputtering cathode where the amount of $H_2O_2$ recovered increases with increasing $H_2$ concentration up to about 80 per cent., but beyond this, further addition of $H_2$ results in a reduction of the $H_2O_2$ yield; by (ii) increase in pressure; and, finally, by (iii) the absence of sputtered metal particles. A comparison of the results given in Table II with those incorporated in the figure shows, further, that the amount of $H_2O_2$ formed during the cathodic combustion of $H_2$–$O_2$ mixtures is, within the probable limits of experimental error involved in the peroxide estimations, proportional to the value of $c/i$. These facts by themselves do not justify the conclusion being drawn that $H_2O_2$ is the primary product of the cathodic combustion of $H_2$–$O_2$ mixtures; particularly when it is borne in mind that, under the most favourable conditions of our experiments, the amount of $H_2O_2$ recovered was never more than a comparatively small fraction of the steam formed. It is our intention to discuss this matter in greater detail in connection with further experiments on the combustion of $H_2$ which are now in progress.

The presence of moisture results in a definite, though not pronounced, increase in the rate of combustion of electrolytic gas at a non-sputtering cathode (see Table I), but exerts practically no effect at a freely sputtering cathode. Thus a marked parallelism exists between these results and those set forth in (IV), (VI) and (VII) in which are given an account of the effect of moisture upon the cathodic combustion of $CO-O_2$ mixtures. It was then found that the rate of combustion of CO at a non-sputtering cathode was greatly accelerated by the presence of steam and still more so by $H_2$, whereas under similar conditions, but at a freely sputtering cathode, the rate of combustion was, if anything, reduced, though generally only to a slight extent. It was also shown previously (VII) that the cathodic combustion of $CO-O_2-H_2$ mixtures proceeds in such a manner that $H_2$ burns first, yielding products which in turn oxidise the CO far more readily than does oxygen These facts, in conjunction with those set forth in the first paragraph of this discussion, suggest that, in the absence of sputtered metal, steam promotes the cathodic combustion of $H_2$, but that such effect is suppressed by the presence of sputtered metal atoms In connection with this attention may be drawn to the remarkable fact brought to light in the course of these investigations to the effect that mixtures such as, amongst others, $2H_2 + O_2$, $2CO + O_2$ and $2CO + O_2 + xH_2$, whether dry or moist, all burn at a freely sputtering cathode at such a rate that the value of $c/i$ lies close to 0·25, whereas, in the absence of sputtered metal atoms these mixtures burn cathodically at such widely different rates that the value of $c/i$ may vary between 0 045 and 0·67. It may also be recalled that Güntherschultze* and von Hippel and Blechschmidt* have shown that the rate of cathodic sputtering is proportional to the current, and, further, that a simple calculation (III) showed that the number of sputtered atoms was probably approximately of the same order as the number of molecules reacting within the cathode zone. These facts suggest that sputtered metal atoms are not only powerful promoters of the cathodic combustion of $H_2$, CO and mixtures thereof by oxygen, but it seems also that at the same time these metal atoms inhibit the promotion of such combustion by either steam or the freshly formed products of combustion of $H_2$.

The results incorporated in Table I show that electrolytic gas burns much more rapidly at a tungsten than at a tantalum cathode We are unable at the moment to offer an explanation of this fact; it may be recalled, however, that the rates of combustion of electrolytic gas at copper (I) and tungsten cathodes are practically identical.

One of us (E.A J M.) wishes to thank the Department of Scientific and Industrial Research for a grant which has enabled him to devote his full time to this work. Our thanks are also due to the Government Grants Committee of the Royal Society for a grant which enabled some of the apparatus employed in this investigation to be procured.

---

* See references in Part III, p. 310.

# *The Gyromagnetic Effect for Paramagnetic Substances.* II.—*Results on Salts of the Iron Group.*

By W. Sucksmith, University of Bristol.

(Communicated by A. P. Chattock.*—Received May 7, 1931.)

In a previous paper (referred to hereafter as Part I) a method for measuring the gyromagnetic ratio for paramagnetic substances was described. Owing to the smallness of the angular moment produced by a change in the magnetic moment of a paramagnetic substance, a low frequency resonance method was employed to build up the amplitude to a measurable magnitude. An account of the method of measurement and elimination of errors was given in detail. The results of experiments on one paramagnetic substance, $Dy^{+++}$ in dysprosium oxide ($Dy_2O_3$), showed the Landé splitting factor for this ion to be 1·28, which indicates that the magnetic moment arises from both orbital and spin contributions. This agrees well with the theoretical value 1 33, corresponding to the state $^6H_{15/2}$ deduced by Hund† as the most probable ground state of this ion.

The present contribution deals with results on salts of the iron group The magnetic susceptibilities range from $10^{-5}$ to $10^{-4}$ compared with $2 \cdot 4 \times 10^{-4}$ in the case of the $Dy_2O_3$ previously used. This necessitates a greater sensitivity than that used in Part I, and the means employed to achieve this are described below.

The gyromagnetic amplitude produced‡ at resonance by an alternating square wave field $H_0$ is given by

$$\theta_M = \frac{1}{g} \cdot \frac{2m_0}{e} \cdot \frac{2\chi TMH_0}{\pi\lambda I}, \tag{1}$$

where $g$ is the Landé splitting factor; $m_0$ and $e$ the mass and charge of the electron; I the moment of inertia of the specimen used containing M grams of mass susceptibility $\chi$; T is the time of oscillation; and $\lambda$ the logarithmic decrement of the suspended system.

In Part I the factors which limit the maximum amplitude obtainable were discussed, and a compromise between the conflicting requirements had to be effected Of these, the ratio M/I should be as large as possible The maximum occurs for a radius of specimen between 0·20 and 0·25 mm, and most of the specimens used conformed to this requirement.

---

* 'Proc. Roy. Soc.,' A, vol. 128, p. 276 (1930).

† Hund, 'Z. Physik,' vol. 33, p. 855 (1925).

‡ On p. 288 in Part I there is a typographical error in the first equation. This should read $\theta_M = f/\kappa w$, the "2" being deleted. The subsequent equations are not invalidated.

Of the rest, analysis of the required conditions is facilitated if we consider the rate of growth of the gyromagnetic amplitude $\theta = \theta_M (1 - e^{-Kt})$ where the damping constant $K = 2\lambda/T$. If the time for the amplitude to grow to half the maximum value $\theta_M$ is written $\tau$, then $\lambda = 0{\cdot}345\ T/\tau$, or $T/\lambda$, which appears in equation (1), is equal to $\tau/0{\cdot}345$. In other words, the maximum amplitude is really independent of T and depends on the total time necessary for the experiment, *i e.*, the time required for the amplitude to reach a value within 1 or 2 per cent. of $\theta_M$.

Hence, in order to increase $\tau$, which in Part I was of the order 60 to 80 seconds, it is necessary to continue the experiment for a longer period With the coil used in the measurements on dysprosium oxide, it was essential to wait at least an hour between readings, as otherwise the heat developed in the magnetising coil caused error in two ways. An expansion of the coil itself causes the direction of the magnetising field to be changed, and secondly, a rise of temperature of the suspension causes a change in the period of oscillation, thus producing dissonance.* Furthermore, it was found that the temperature coefficient of the period was far in excess of that of the torsion constant of the quartz suspension, and was evidently due to yield or expansion in the shellac joints. Various attempts were made to minimise this source of trouble, but little improvement was effected.

When the experiment has to be continued for a longer period in order to increase the sensitivity, these troubles are accentuated unless the windings of the coil itself are kept sufficiently cool. For this purpose a coil based on the lines of a type used by McLennan† was constructed, and proved satisfactory. A diagram of the coil is shown in the figure.

The coil windings are totally enclosed in a brass container so that oil can be circulated through the windings. Special precautions were necessary to ensure that no sparking to the case took place at " break." Ebonite " spacers " separated each layer from the case or its neighbour, the thickness being $\frac{1}{4}$ inch between the first layer and the case and 1/32 inch between adjacent layers. The coil was wound with 10 layers of No. 18 D.S.C. enamelled copper wire, giving a mean field over the length of the specimen, 6 cm., of 91 gauss per ampere. Oil is forced through the perforated ebonite disc at the bottom, through the windings and out at the top. An oil pump was used to circulate the oil, which before entering the coil was passed through 80 feet of 1-inch diameter copper tubing immersed in cold water. During a continuous run with a current of 10 amperes, the temperature of the oil would rise 5 or 6° C, so that in order to maintain the specimen at room temperature an additional water-jacket was added (see figure), the water being forced upwards through the annular space and directed by a helical baffle A. By varying the rate of flow of this water, the temperature could be maintained for any period at room temperature. (The cold water was usually about 4° C. below room temperature.) Under these conditions it was possible to keep the temperature constant to within 1/10° C. In spite of the constant temperature the yield of the shellac joints in the specimen caused some variations in the period of oscillation, but these were of much smaller magnitude than formerly. The alteration permitted the logarithmic decrement to be halved, and the magnetising field increased from 500 to 1200 gauss, so that a fivefold increased sensitivity was obtained.

---

* In Part I, a mathematical treatment was given showing that if the oscillation was maintained in the correct *phase*, the decrease in amplitude due to a small absence from resonance was compensated by equal increase due to a disturbing couple, but such changes as would arise in the course of a long run would be too great to admit of this correction.

† McLennan, McLeod and Ruedy, 'Phil. Mag.,' vol. 6, p. 561 (1928).

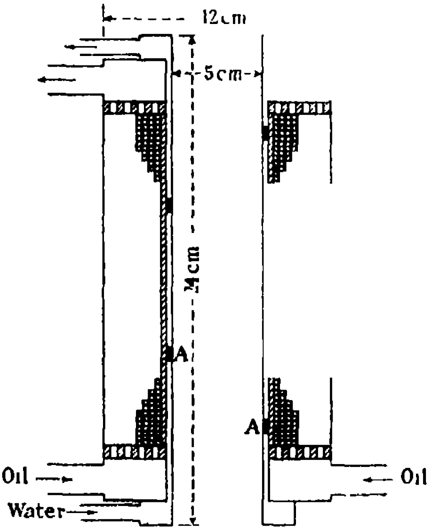

Results on some six paramagnetic substances have been obtained, but before discussing the results it is necessary to review the magnetic properties of this group in the light of the theories advanced to explain their susceptibilities.

The magnetic moment is usually expressed such that the number, *p*, of

Weiss magnetons ($\mu_W = 1123$) is given by $p = 14 \cdot 07\sqrt{C_M}$, where $C_M$ is the Curie constant per gram molecule containing 1 gram of the active metal ion. In the iron group the magneton numbers increase progressively to a maximum at the configuration $3d^5$, and then decrease to a zero value with the addition of the tenth electron.

Hund (*loc. cit.*) showed that the number of Weiss magnetons could be determined from the spectroscopic state and that

$$p = 4 \cdot 97\, g\sqrt{j\,(j+1)}, \tag{2}$$

where $g$ is the Landé splitting factor and $j$ the quantum number specifying the total angular momentum. This theory is successful in explaining the magnetic properties of the rare earth ions, but no agreement is found in the case of the iron group, with the sole exception of the configuration $3d^5$, for which the most probable ground state is $^6S$

Laporte and Sommerfeld* were led to develop explanations for the discrepancy based on the fact that whereas the S state has only one possible value, in general there would be a distribution amongst the varying $j$ levels depending upon the temperature.

Their value for the mean magnetic moment is given by

$$\bar{\mu} = \frac{\sum\limits^{j}\sum\limits^{m} mg\beta\, e^{-mg\beta H/kT}\, e^{-W/kT}}{\sum\limits^{j}\sum\limits^{m} e^{-mg\beta H/kT}\, e^{-W/kT}}, \tag{3}$$

where $\beta$ is the Bohr magneton $eh/4\pi m_0 C$ and $m$ is the magnetic quantum number which can assume values $j,\ j-1,\ \ldots,\ -j$, and $W = hc\Delta\nu$ is the difference in energy between the particular $j$ level concerned and the ground level. The overall multiplet separation is extrapolated from values of the X-ray screening constants by means of the Sommerfeld spin doublet equation.

On developing the first exponential for small values of the field H, the susceptibility is

$$\chi = \frac{N\sum\limits^{j}\{g^2\beta^2 j\,(j+1)/3kT\}\,(2j+1)\, e^{-W/kT}}{\sum\limits^{j}(2j+1)\, e^{-W/kT}}. \tag{3A}$$

This can be expressed in terms of the number of Weiss magnetons, where

$$p = \frac{4 \cdot 97\ \sqrt{\sum\limits^{j} g^2 j\,(j+1)\,(2j+1)\, e^{-W/kT}}}{\sqrt{\sum\limits^{j}(2j+1)\, e^{-W/kT}}}. \tag{3B}$$

---

* Laporte and Sommerfeld, 'Z. Physik,' vol. 40, p. 333 (1926); Laporte, *ibid.*, vol. 47, p. 761 (1928).

Some improvement on equation (2) is achieved for ions in the first half of the group, where the multiplets are erect and there are appreciable numbers of electrons in levels other than the ground level. But still no general agreement is found. In the second half, where the multiplets are inverted, practically all the electrons are in the ground state and there is little difference from the values originally calculated by Hund.

More recently Stoner* has suggested that owing to the $3d$ electrons being the outermost in these ions, the $l$ moment may be wholly or partially suppressed by intermolecular forces, and only the spin moment is effective. On the other hand, the electrons responsible for paramagnetism in the rare earth ions, the $4f$ electrons, are screened from these forces by the outer $5s$ and $5d$ completed shells. Assuming that in the case of the iron group the orbital moments are totally suppressed, then the magneton numbers are calculable from the formula

$$p = 4 \cdot 97 \sqrt{4s(s+1)}, \tag{4}$$

where $s$ is the aggregate spin moment of the $3d$ electrons present and is derived from the multiplicity $r = 2s + 1$ The calculated values are in fairly good agreement with the magneton numbers, the biggest discrepancy being for the configuration $3d^7$ which exists only in $Co^{++}$. Experiment gives $p = 24 - 26$, whereas equation (4) gives 19·3 According to Stoner, the difference is accounted for by assuming that the excess over that given by equation (4) is due to the partially effective $l$ moment.

Bose,† however, takes the following view. In the second half of the series, where these exceptions occur, there are electrons of the same $l$ moment but oppositely directed spins. The excess he assumes to be due to the fact that these pairs of electrons have not their spins exactly opposed. Thus in $Co^{++}$, to give a ${}^4F_{9/2}$ state, there are seven electrons, three with $l = 2$, $l = 1$, and $l = 0$, respectively, and parallel spins, the remaining four being two with $l = -2$ and two with $l = -1$, these pairs having opposite spins. It appears to the writer, however, that Bose's view is equivalent to an exception to the Pauli exclusion principle, and is, therefore, untenable.

Van Vleck‡ has also treated the problem on the basis of the new mechanics, and his expression for the susceptibility meets with complete success in the rare earth ions and he has applied it to the iron group. His equation for $\chi$

---

* Stoner, 'Phil. Mag.,' vol. 8, p. 250 (1929).

† Bose, 'Z. Physik,' vol. 43, p. 864 (1927).

‡ Van Vleck, 'Phys. Rev.,' vol. 31, p. 587 (1928): Van Vleck and Frank, *ibid.*, vol. 34, pp. 1494, 1625 (1929).

(below) is similar to that of Laporte and Sommerfeld, but includes a term in the numerator which is due to the component of the magnetic moment perpendicular to the angular moment vector, a term usually negligible.

$$\chi = \frac{\mathrm{N}\sum^{j}\{g^2\beta^2 j\,(j+1)/3k\mathrm{T} + \alpha\,(j)\}\,(2j+1)\,e^{-\mathrm{W}/k\mathrm{T}}}{\sum^{j}(2j+1)\,e^{-\mathrm{W}/k\mathrm{T}}}. \tag{5}$$

A further improvement in the first half of the group is effected by the above equation, but the agreement even then can by no means be regarded as satisfactory. As with equation (3B), there is no change for the second half of the group.

On the whole, therefore, it appears that susceptibility measurements are not sufficient to decide which theory holds, and a further criterion, such as is given by measurements of the gyromagnetic ratio, is desirable.

The gyromagnetic amplitude gives us a means of measuring the ratio of the magnetic moment to the angular momentum produced, *i e.*, corresponding to equation (3), this ratio is

$$\frac{\sum^{j}\sum^{m} gj\,.\,eh/4\pi mc\;\; m/j\,.\,e^{-mg\beta\mathrm{H}/k\mathrm{T}}\,e^{-\mathrm{W}/k\mathrm{T}}}{\sum^{j}\sum^{m} j\,.\,h/2\pi\,.\,m/j\,.\,e^{-mg\beta\mathrm{H}/k\mathrm{T}}\,e^{-\mathrm{W}/k\mathrm{T}}},$$

which, for small values of the field, simplifies to

$$\frac{e}{2mc}\;\frac{\sum^{j} g^2 j\,(j+1)\,(2j+1)\,e^{-\mathrm{W}/k\mathrm{T}}}{\sum^{j} gj\,(j+1)\,(2j+1)\,e^{-\mathrm{W}/k\mathrm{T}}} = \bar{g}\cdot\frac{e}{2mc} \tag{6}$$

This can be adapted or modified to suit the various theories propounded above. In the case of the expression for $\bar{g}$ corresponding to equation (5), the numerator carries an additional term corresponding to $\alpha(j)$ in the numerator, the denominator being unchanged.

*Discussion of Results.*—The experimental results which have been obtained are given in Table I. The moment of inertia and the time of oscillation of the specimen appear in the second and third columns respectively. $\lambda$ in the sixth column is the logarithmic decrement of the specimen, whilst H is the field used. Each value of $\theta_{\mathrm{M}}$ is the mean of a few runs. The values of $\bar{g}$ as calculated from equation (1) appears in the last column.

In Table II are given the values of $p$ and $\bar{g}$ by experiment and calculated according to the various equations given above.

Table I.

| Substance. | Mass $\times 10^3$ gr. | M of I $\times 10^6$. | T (seconds). | $\chi \times 10^6$. | $\lambda \times 10^3$. | H (gauss). | $\theta_M \times 10^3$. | |
|---|---|---|---|---|---|---|---|---|
| $MnCO_3$ | 13 4 | 8·52 | 2 237 | 96 | 6 15 | 929 | 1 69 | 2 16 |
| ,, | 13 4 | 8·53 | 2·516 | 96 | 7 37 | 910 | 1 77 | 1 90 |
| ,, | 10·9 | 6 77 | 2 19 | 96 | 7 37 | 910 | 1 57 | 1 91 |
| ,, | 10 9 | 6 77 | 2 19 | 96 | 5 73 | 910 | 1 90 | 2 03 |
| $MnSO_4$ | 27 0 | 19 45 | 2 55 | 93 | 6 40 | 1180 | 2 31 | ·88 |
| ,, | 27 0 | 19 82 | 2·37 | 92 | 5·70 | 1200 | 2 27 | ·97 |
| $CrCl_3$ | 26 5 | 15 75 | 3 19 | 40 | 9 05 | 910 | 0 81 | 91 |
| ,, | 26 5 | 15 50 | 2·93 | 40 | 7 56 | 910 | 0·93 | ·86 |
| ,, | 31 0 | 19 1 | 2 65 | 40 | 6 95 | 838 | 0 78 | ·91 |
| ,, | 26 5 | 15·30 | 3 03 | 40 | 7 60 | 1230 | 1·15 | 2 12 |
| $CoSO_4$ | 19·6 | 13 5 | 2·73 | 62 | 11 0 | 910 | 1·01 | 1·44 |
| ,, | 19 6 | 13·5 | 2·73 | 62 | 5 98 | 910 | 1 61 | 1 66 |
| ,, | 19·6 | 14·45 | 2 78 | 62 | 5·48 | 925 | 1·78 | 1 59 |
| ,, | 16 2 | 10 0 | 2·124 | 62 | 5 45 | 910 | 1 63 | 1·57 |
| ,, | 16·2 | 10 0 | 2 124 | 62 | 7·32 | 910 | 1·19 | 1 60 |
| $CoCl_2$ | 23 0 | 25 9 | 2·77 | 97 | 7 37 | 1180 | 1·83 | 1 50 |
| ,, | 23 0 | 25 4 | 2·71 | 96 | 7·50 | 1190 | 1·90 | 1·40 |
| $FeSO_4$ | 23 7 | 20 5 | 2 61 | 75 | 7·35 | 1220 | 1 54 | 1 75 |
| ,, | 23·7 | 20·3 | 2·69 | 75 | 7 05 | 1200 | 1·49 | 1 93 |
| ,, | 20 5 | 14 55 | 2 22 | 75 | 4·89 | 1200 | 2·30 | 1·79 |
| ,, | 20 5 | 14 70 | 2·65 | 75 | 7·77 | 1200 | 1 47 | 2 09 |

$Mn^{++}$.—This ion was used in the form of the carbonate since this substance—a finely divided non-hygroscopic powder—was found to be the most suitable salt for packing into the narrow specimen tubes. Later, in order to admit of correlation with existing susceptibility data, experiments on anhydrous $MnSO_4$ were made. The results are in agreement with those for the carbonate, and in all cases the value of $\bar{g}$ by experiment is found to be 2·0 within the limits of experimental error. All theories predict the correct magneton number

Table II.

| Ions. | $Cr^{+++}$. | | $Mn^{++}$. | | $Co^{++}$. | | $Fe^{++}$. | |
|---|---|---|---|---|---|---|---|---|
| | $p$. | $g$. | $p$. | $g$. | $p$. | $\bar{g}$. | $p$. | $\bar{g}$. |
| **Calculated** (2) | 3·9 | 0·4 | 29·4 | 2·0 | 33·2 | 1·33 | 33·6 | 1 50 |
| ,, (3*b*) | 13 0 | 1 06 | 29·4 | 2 0 | 32 8 | 1·33 | 32·3 | 1 50 |
| ,, (5) | 15·2 | 1 49 | 29 4 | 2 0 | 32·8 | 1·33 | 32 3 | 1·50 |
| ,, (4) | 19·5 | 2 0 | 29·4 | 2·0 | 19·3 | 2·0 | 24·4 | 2 0 |
| ,, (6*a*) | 25·8 | 1·39 | 29 4 | 2·0 | 25 8 | 1 39 | 27 2 | 1 66 |
| ,, (4) and (6*a*) | — | — | — | — | (25·0) | 1·42 | (26·0) | 1·78 |
| **Experiment** | 19·0 | 2 0 | 29 0 | 2·0 | 25·0 | 1·5 | 26 0 | 1·9 |

and $g = 2$ for this ion, since it has no orbital moment, the ground term being $^6S_{5/2}$.

$Cr^{+++}$.—For $Cr^{+++}$, which has a magneton number of 19 in the $CrCl_3$ used, gives an average value for $\bar{g}$ of 1·95. The scale deflections obtained were of the order 1·5 mm., so the experimental error cannot be less than 10 per cent. It is seen from Table II that the first three theories do not agree with either susceptibility measurements or with those on the gyromagnetic effect, whereas the assumption that the spin moment only is effective satisfies both the experimental results.

$Co^{++}$, which has a magneton number of 25·1 in the anhydrous $CoSO_4$ used, gives a mean value for $\bar{g}$ appreciably less than 2·0, the mean experimental value being 1·57. As a check on this result, it is desirable to make measurements on another divalent salt of cobalt. The only suitable one appears to be cobaltous chloride. This salt is easily dehydrated by heating, but on account of its extremely hygroscopic nature, it was found impossible to pack the substance even into relatively wide tubes (0·7–0·8 mm. diameter). To overcome this difficulty, a device used by Tutton* for examining deliquescent substances was employed, by means of which the tubes could be packed in a dry atmosphere. In spite of this, the specimens had usually horizontal magnetic moment 10 to 20 times greater than specimens of other materials used. (This horizontal moment is presumably due to non-uniformity in packing.) In one case, however, a satisfactory specimen was obtained, and the results agree with those obtained on the sulphate. It is worthy of note that $CoSO_4$ and $CoCl_2$ have the same magneton number, whilst the actual mass susceptibilities at room temperature are $62 \times 10^{-6}$ and $96 \times 10^{-6}$ respectively, this being due to the widely differing values of $\theta$ in the modified Curie law $\chi(T - \theta) =$ constant. The mean of all the results on $Co^{++}$ is 1·54.

The first three theories give similar results, since practically all the electrons are in the $^4F_{9/2}$ state. If we assume that the multiplet separation $\Delta\nu$ is zero in the solid state, then the Laporte-Sommerfeld theory gives 24·7 for the magneton number and 1·27 for $\bar{g}$. Whilst the former result agrees with experiment, the latter is outside the limits of error. There is the possibility that the $l$ and $s$ moments are not coupled to form a resultant $j$, but that they are quantised separately with respect to the field.† In this case the magneton number is given by

$$p = 4 \cdot 97 \sqrt{4s(s+1) + l(l+1)}, \qquad (6A)$$

---

* Tutton, "Crystallography and Practical Crystal Measurements," vol. 1, p. 630.

† Van Vleck, *loc. cit.*

giving $p$ for $Co^{++} = 25 \cdot 8$. If, on the other hand, the moment were totally suppressed, the calculated magneton number is 19·3. The values of $\bar{g}$ corresponding to the above two cases are 1·39 and 2·0 respectively. If we assume that the experimental magneton number of 25·1 to be made up of a mixture of ions corresponding to equations (1) and (6A) or, that the spin moment is fully effective, the $l$ moment being partly suppressed, then we can calculate the corresponding $\bar{g}$ value, which is 1·42. The experimental mean is 1·54, the scale deflections being 2·5–3·5 mm, so that this value lies within the errors of experiment. Other types of coupling between the angular moment vectors are possible, but it does not seem profitable to discuss these in the absence of more exact information.

$Fe^{++}$.—This ion was used as the anhydrous sulphate, the salt being dehydrated by heating *in vacuo* at 150° C The susceptibility at 18° C was $75 \times 10^{-6}$,[*] in good agreement with Ishawara's results,[†] which gives 26 for the magneton number. The mean experimental $\bar{g}$ value was found to be 1·89 If spin moment only is effective, then the magneton number should be 24·4 with $\bar{g} = 2$. On the other hand, according to equation (6A), which is the case for spin and orbital moments quantised separately relative to the field, the magneton number is 27·2 and $\bar{g} = 1 \cdot 66$. If we assume, as with $Co^{++}$ above, that the orbital moment is only partly effective, then the $\bar{g}$ value, calculated on the assumption that the magneton number is 26·0, is about 1·78. This theoretical value agrees within the limits of error with the mean experimental value 1·89. (Consideration of existing susceptibility data on $FeSO_4$ leads to the conclusion that the magneton number may be incorrect by at least 2½ per cent.)

## *Summary.*

In a previous paper a description of an apparatus used for the measurement of the gyromagnetic ratio for paramagnetic substances was given, together with results on dysprosium oxide. The apparatus here is used for similar measurements on some salts in the iron group and an account is given of the means employed to obtain the necessary increased sensitivity.

The mean value of $g$, the Landé splitting factor, for the ions $Cr^{+++}$ and $Mn^{++}$ is deduced from the experimental results and is found to be 2·0 within the limits of experimental error. For $Co^{++}$ and $Fe^{++}$ the values of $g$ are 1·5 and

---

[*] I am indebted to Dr. L. C. Jackson for the measurements of the susceptibility of the $FeSO_4$ used.

[†] Ishawara, 'Sci. Rep. Tôhoku,' vol. 3, p. 303 (1914).

1·9 respectively. These results give a criterion for the theories advanced to explain the paramagnetism in this group, and show that the Hund theory, even with the modifications introduced by Sommerfeld and Laporte, and later by Van Vleck, is untenable. They agree only with the view put forward by Stoner, *i e*, that the spin and orbital moments are quantised separately relative to the field axis, and that further, the orbital moment may be wholly or partially suppressed by the fields of neighbouring ions.

This work was carried out in the H. H. Wills Physical Laboratory of the University of Bristol, and my thanks are due to the Colston Research Society of the University of Bristol for a grant towards the expenses of the investigation.

# *The Refraction and Dispersion of Some Gaseous Compounds.*

By H. Lowery, Ph.D., F.Inst.P., Head of the Department of Pure and Applied Physics, College of Technology, University of Manchester.

(Communicated by W. L. Bragg, F.R S.—Received May 8, 1931.)

## I.—Introduction.

In the present paper, results are given of measurements which have been made by the author on the refraction and dispersion of the following substances in the gaseous state :—

(1) Silicon tetrachloride, $SiCl_4$ ; (2) silicon tetrabromide, $SiBr_4$ ; (3) boron trichloride, $BCl_3$ ; (4) boron tribromide, $BBr_3$ ; (5) phosgene, $COCl_2$ ; (6) acetone, $(CH_3)_2CO$ ; (7) ethyl ether, $(C_2H_5)_2O$ ; (8) acetylene, $C_2H_2$ ; (9) ethylene, $C_2H_4$ ; (10) ethane, $C_2H_6$ ; (11) methyl chloride, $CH_3Cl$ ; (12) methylene chloride, $CH_2Cl_2$ ; (13) methylene bromide, $CH_2Br_2$.

The gaseous refractivities of six of these compounds (viz., silicon tetrachloride, silicon tetrabromide, boron trichloride, boron tribromide, methylene chloride, methylene bromide) have not been previously determined and the recorded data for the remaining substances are either so meagre or discordant that further determinations were obviously called for.

The investigation of which this forms a part was commenced in 1924, and the results for several substances have already been published.*

## II.—EXPERIMENTAL.

### 1. *Determination of Refractive Index.*

The refractive index of each substance in the gaseous state was determined for the green mercury line, λ 5461, by means of a Jamin interferometer in conjunction with a Hilger monochromatic illuminator and a mercury vapour lamp as source of light.

For the admission of gas to the refraction tube one or other of two methods was used, the particular method adopted depending on the nature of the substance under test.

*Method I.*—A pair of glass refraction tubes, together with a density bulb, were mounted in a tank of water situated between the interferometer plates. One refraction tube remained evacuated throughout the experiments. The other tube received the gas under examination, the quantity of gas entering the tube being determined by means of the density bulb. Observations of the displacement of the interference fringes due to the entry of the gas to the refraction tube were made visually by means of a telescope having cross-wires and a micrometer scale in the eye-piece.

In the case of ether the substance was introduced, as liquid, into a reservoir communicating with one of the refraction tubes. The liquid was then frozen and the reservoir, refraction tube and density bulb were thoroughly exhausted of air. On removing the freezing agent and allowing the temperature of the reservoir to rise, vapour ultimately passed into the refraction tube and density bulb. The gases phosgene, acetylene, ethylene, ethane and methyl chloride were, of course, admitted to the refraction tube and density bulb direct from their containers.

Taps were placed at suitable points in the apparatus in order to control the rate of flow of gas into the refraction tube. Mercury manometers were also connected to both refraction tubes, though they could readily be cut off from communication with the tubes when necessary.

This method is unsuitable for use with silicon tetrachloride, silicon tetrabromide, boron trichloride, boron tribromide, acetone, methylene chloride and methylene bromide, either because greased taps and joints are inadmissible or because the vapour pressure at approximately room temperature is not high enough to allow of a large number of interference bands being counted. Accordingly, another method was adopted with these substances which not only dispensed with taps and ground joints but permitted heating of the refraction tubes, thereby enabling comparatively high vapour pressures to be used.

---

* 'Proc. Phys. Soc.,' vol. 38, p. 470 (1926), vol. 39, p. 421 (1927), and vol. 40, p. 23 (1927).

*Method II.*—A small sealed and weighed bulb of the substance (in the liquid state) was placed in one of the refraction tubes. The tube was next evacuated and sealed, the small bulb of substance being then broken so that the test substance escaped into the refraction tube. By means of a suitable freezing agent the substance was solidified. Both refraction tubes were mounted between the interferometer mirrors and the displacement of fringes in the observing telescope was noted as the substance was allowed gradually to vaporise completely. Since the weight of substance taken and the volume of the refraction tube were known, the density of the amount of vapour producing retardation of the light could be determined. This method of experiment is essentially that described by C. and M. Cuthbertson* in connection with their experiments on the refraction and dispersion of steam.

The number of interference bands counted varied with the substance under examination, but it was never less than 600 and in many cases exceeded 900 bands. No difficulty was experienced in reading to a tenth of a band

### 2. *Determination of Dispersion.*

The dispersion of each substance was determined in the region of the visible spectrum by obtaining the refractive indices for certain selected wave-lengths in relation to the refractive index already accurately found for λ 5461. The method adopted was similar to that described by C. and M. Cuthbertson,† a rough dispersion curve being obtained first of all by using for the dispersion points narrow bands of wave-lengths selected from a continuous spectrum. Afterwards the accurate values of the refractivities corresponding to the wave-lengths of the dispersion points were found by counting a large number of fringes (*e.g.*, 600–900) for λ 5461, observing the relative positions of the fringes for the chosen wave-lengths and utilising the rough dispersion curve to determine the number of fringes which would have been displaced originally had the light been of these wave-lengths instead of λ 5461.

Since for a given quantity of gas in the refraction tube at constant temperature and pressure, the refractivity, $(\mu - 1)$, is proportional to the number of interference fringes counted and to the corresponding wave-length, and since also the refractivity has already been accurately found for λ 5461, the above procedure enables the refractivities for all the dispersion wave-lengths to be calculated.

---

* 'Phil. Trans.,' A, vol. 213, p. 15 (1913).

† 'Proc. Roy. Soc.,' A, vol. 83, p. 152 (1909).

Ten experiments were made to find the rough dispersion curve for each substance and a further 10 to obtain the accurate values of the refractivities corresponding to the dispersion wave-lengths.

Monochromatic illumination for the dispersion measurements was obtained by passing the light from the following sources in turn through the Hilger monochromatic illuminator. (1) mercury vapour lamp for λ 5770, λ 5461, λ 4358, λ 4047; (2) arc between cadmium poles for λ 6438, λ 5086, λ 4800; (3) arc between carbon poles which had been drilled axially and packed with lithium chloride for λ 6708, λ 6104, λ 4602.

## III.—RESULTS.

As mentioned in a previous paper,* the method adopted for representing the results of the experiments is that which shows the refractivities of the respective gaseous substances for the same number of molecules per unit volume as hydrogen contains at N.T.P., the reduction being effected by means of the expression:—

$$(\mu - 1) = (\mathrm{N}\lambda \times \text{standard density})/(l \times \text{experimental density}),$$

where $(\mu - 1)$ is the required refractivity, N the number of interference bands counted, $l$ the length of the refraction tubes and λ the wave-length of the light employed. Refractivity determinations thus expressed in relation to the densities of the substances may readily be converted to the corresponding values under N.T.P. conditions, if required, by altering them in the ratio:

$$(\text{Experimental density at N.T.P.})/(\text{Standard density}).$$

In the results stated below, the expression $(\mu - 1)_d$ always represents the refractivity reduced from density considerations as mentioned above; similarly $(\mu - 1)_{\mathrm{ntp}}$ denotes the refractivity under N.T.P. conditions, thus:

$$(\mu - 1)_d = [(\mu - 1)_{\mathrm{ntp.}} \times \text{standard density}]/(\text{experimental density at N.T.P.})$$

The Sellmeier dispersion formula has been used to summarise the dispersion measurements and in all cases a single term has proved sufficient, viz.,

$$(\mu - 1) = \mathrm{C}/(\nu_0^2 - \nu^2),$$

---

* 'Proc. Phys. Soc.,' vol. 38, p. 471 (1926). *Cf.* C. and M. Cuthbertson, 'Proc. Roy. Soc.,' A, vol. 97, p. 152 (1920) and references.

where C is a constant, $\nu_0$ is the frequency of the free vibration in the molecule and $\nu$ is the frequency of the incident radiation $= c/\lambda$. The velocity of light, $c$, is assumed to be $3 \times 10^{10}$ cm. per second.

### 1. *Silicon Tetrachloride*, $SiCl_4$.

Pure *liquid* silicon tetrachloride was obtained for the experiments from Messrs. British Drug Houses In filling the bulb by which the substance was introduced into the refraction tube, care was taken to exclude all possible trace of moisture, the various operations being carried out under high vacuum.

Ten determinations of the refractive index for λ 5461 yielded the following results :—

$(\mu - 1)_d \times 10^6$ .... 1967, 1971, 1968, 1970, 1969, 1972, 1969, 1966, 1967, 1970.

Mean ............ 1969.

Using the data Si = 28·06, Cl = 35·457 and the density of hydrogen = 0·08985 grams per litre at N.T.P., the standard density of silicon tetrachloride vapour is 7·5691 grams per litre.

The mean experimental density $d$, of silicon tetrachloride vapour at N.T.P. was found to be 7·590 grams per litre, the reduction being effected by means of the expression

$$d = [d_0 \times (t + 273) \times 760]/(273 \times p),$$

where $d_0$ is the observed density at pressure $p$ mm. of mercury and temperature $t°$ C. Dumas and Regnault give the vapour density of silicon tetrachloride as 5·939 and 5·86 (air = 1), which correspond to 7·679 and 7·58 grams per litre respectively.

The results of the dispersion measurements are shown in Table I. The second column contains the results actually obtained in the experiments from which the constants in the Sellmeier dispersion formula were obtained, the resulting expression being

$$(\mu - 1)_d = 17{\cdot}213 \times 10^{27}/(9044{\cdot}3 \times 10^{27} - \nu^2).$$

The values in the third column have been calculated from this expression.

### 2. *Silicon Tetrabromide*, $SiBr_4$.

The specimen of silicon tetrabromide employed was of Kahlbaum manufacture. As with the tetrachloride, precautions were taken to ensure that no traces of moisture should be present in the apparatus.

Table I.—Dispersion of Gaseous Silicon Tetrachloride

| λ in Å.U. | $(\mu - 1)_d \times 10^6$ |  | Difference. |
|---|---|---|---|
|  | Observed. | Calculated. |  |
| Li 6708 | 1946, 6 | 1946, 2 | −0, 4 |
| Cd 6438 | 1950, 2 | 1950, 0 | −0, 2 |
| Li 6104 | 1955, 5 | 1955, 4 | −0, 1 |
| Hg 5770 | 1961, 7 | 1961, 8 | +0, 1 |
| Hg 5461 | 1969, 0 | 1968, 9 | −0, 1 |
| Cd 5086 | 1980, 3 | 1979, 3 | −1, 0 |
| Cd 4800 | 1989, 9 | 1989, 1 | −0, 8 |
| Hg 4602 | 1997, 0 | 1997, 0 | 0, 0 |

The refractive index for λ 5461 was measured in 10 determinations which gave the following results —

$(\mu - 1)_d \times 10^6$ .. 2723, 2726, 2723, 2724, 2728, 2725, 2726, 2725, 2728, 2723.

Mean ..... 2725.

The mean density of silicon tetrabromide vapour at N T P was found to be 15·56 grams per litre, the corresponding standard density being 15 50 grams per litre.

Table II shows the results of the dispersion experiments, the corresponding Sellmeier expression being

$$(\mu - 1)_d = 12{\cdot}940 \times 10^{27}/(5050{\cdot}1 \times 10^{27} - \nu^2).$$

Table II.—Dispersion of Gaseous Silicon Tetrabromide.

| λ in Å.U. | $(\mu - 1)_d \times 10^6$. |  | Difference |
|---|---|---|---|
|  | Observed. | Calculated |  |
| Li 6708 | 2668, 1 | 2668, 0 | −0, 1 |
| Cd 6438 | 2677, 2 | 2677, 4 | +0, 2 |
| Li 6104 | 2691, 2 | 2691, 0 | −0, 2 |
| Hg 5770 | 2707, 7 | 2707, 2 | −0, 5 |
| Hg 5461 | 2725, 0 | 2725, 2 | +0, 2 |
| Cd 5086 | 2752, 1 | 2751, 9 | −0, 2 |
| Cd 4800 | 2776, 2 | 2777, 1 | +0, 9 |

### 3. *Boron Trichloride*, $BCl_3$.

A specimen of pure boron trichloride of Kahlbaum preparation was used. Before introduction to the refraction tube this was fractionally distilled in high vacuum in the manner described by Stock and Priess.*

Measurements of the refractive index for λ 5461 were as follows –

$(\mu - 1)_d \times 10^6$ ... 1406, 1403, 1404, 1402, 1405, 1405, 1404, 1402, 1405, 1406

Mean ... .. .... 1404

The second column of Table III shows the results of the dispersion measurements. The corresponding Sellmeier formula is

$$(\mu - 1)_d = 9\cdot5829 \times 10^{27}/(7127\cdot5 \times 10^{27} - \nu^2)$$

The results in the third column have been calculated from this expression.

Table III.—Dispersion of Gaseous Boron Trichloride.

| λ in Å.U. | $(\mu - 1)_d \times 10^6$ | | Difference. |
|---|---|---|---|
| | Observed. | Calculated. | |
| Li 6708 | 1383, 2 | 1383, 3 | +0, 1 |
| Cd 6438 | 1387, 0 | 1386, 7 | −0, 3 |
| Li 6104 | 1391, 6 | 1391, 7 | +0, 1 |
| Hg 5770 | 1397, 8 | 1397, 5 | −0, 3 |
| Hg 5461 | 1404, 0 | 1403, 9 | −0, 1 |
| Cd 5086 | 1413, 4 | 1413, 5 | +0, 1 |
| Cd 4800 | 1422, 2 | 1422, 5 | +0, 3 |
| Li 4602 | 1429, 9 | 1429, 7 | −0, 2 |
| Hg 4358 | 1440, 0 | 1440, 3 | +0, 3 |

Cuthbertson† has calculated the refractive index of gaseous boron trichloride by means of the Lorentz-Lorenz rule, viz., $(n^2 - 1)/[(n^2 + 2) \times d]$ = a constant for the liquid and the gaseous state, $n$ denoting refractive index and $d$ denoting density. The value of the constant was found by using Ghira's‡ determinations of the refractive indices of *liquid* boron trichloride for different wave-lengths. The calculated gaseous index for λ 5461 is thus found to be 1·001420, the corresponding experimental value above being 1·001404.

---

* 'Ber. Wien. Akad.,' vol. 47, p. 3112 (1914).

† 'Phil. Trans.,' A, vol. 204, p. 347 (1905).

‡ 'Rend. Lincei,' vol. 2, p. 312 (1893).

### 4 *Boron Tribromide*, $BBr_3$.

Pure boron tribromide of Kahlbaum manufacture was employed, the mode of experiment being similar to that used in the case of boron trichloride above.

Ten measurements of the refractive index for λ 5461 gave the following results —

$(\mu - 1)_d \times 10^6$ .... 2010, 2013, 2014, 2012, 2009, 2013, 2012, 2015, 2011, 2010.

Mean ............ 2012.

The results of the dispersion experiments appear in Table IV, the values in the second column leading to the Sellmeier expression

$$(\mu - 1)_d = 12\cdot247 \times 10^{27}/(6388\cdot7 \times 10^{27} - \nu^2)$$

Table IV —Dispersion of Gaseous Boron Tribromide.

| λ in Å U | $(\mu - 1)_d \times 10^6$ Observed. | $(\mu - 1)_d \times 10^6$ Calculated | Difference |
|---|---|---|---|
| Li 6708 | 1978, 9 | 1978, 9 | 0, 0 |
| Cd 6438 | 1984, 7 | 1984, 4 | −0, 3 |
| Li 6104 | 1992, 2 | 1992, 4 | +0, 2 |
| Hg 5770 | 2001, 4 | 2001, 7 | +0, 3 |
| Hg 5461 | 2012, 0 | 2012, 0 | 0, 0 |
| Cd 5086 | 2027, 1 | 2027, 4 | +0, 3 |
| Cd 4800 | 2041, 5 | 2041, 8 | +0, 3 |
| Hg 4602 | 2053, 7 | 2053, 6 | 0, 1 |
| Hg 4358 | 2071, 1 | 2070, 6 | −0, 5 |

As in the case of the trichloride, Cuthbertson (*loc cit.*) has calculated the gaseous refractive index of boron tribromide by the Lorentz-Lorenz rule and found the value 1·002025, which is in close agreement with the experimental value 1·002012.

### 5. *Phosgene*, $COCl_2$.

The only previous recorded determination of the refractive index of phosgene is that by Dulong.* He found that, for white light, the refractivity of the gas in relation to that of air is 3·936. This observation has been reduced by Dufet† so as to give the value of the refractive index at N.T.P., the result being 1·001153. (The refractive index of air was assumed to be 1·000293.)

---

* 'Ann. Chim. Phys.,' vol. 31, p. 154 (1826).

† "Recueil des Données Numériques," vol. 1 (1898).

For the present experiments pure liquid phosgene prepared by Kahlbaum was used. Before admission to the apparatus, the specimen was fractionally distilled several times. The results of 10 determinations of the refractivity for λ 5461 are as follows :—

$(\mu - 1)_d \times 10^6$ .... 1150, 1147, 1148, 1151, 1149, 1149, 1152, 1150, 1148, 1149.

Mean ...... .... 1149.

Dispersion results are given in Table V., the values in the second column of which lead to the Sellmeier expression

$$(\mu - 1)_d = 9{\cdot}2574 \times 10^{27}/(8358 \times 10^{27} - \nu^2)$$

Table V.—Dispersion of Phosgene.

| λ in Å U. | $(\mu - 1)_d \times 10^6$ Observed. | $(\mu - 1)_d \times 10^6$ Calculated. | Difference. |
|---|---|---|---|
| Li 6708 | 1135, 0 | 1134, 8 | −0, 2 |
| Cd 6438 | 1136, 9 | 1137, 2 | +0, 3 |
| Li 6104 | 1140, 6 | 1140, 6 | 0, 0 |
| Hg 5770 | 1144, 9 | 1144, 6 | −0, 3 |
| Hg 5461 | 1149, 0 | 1149, 1 | +0, 1 |
| Cd 5086 | 1155, 2 | 1155, 7 | +0, 5 |
| Cd 4800 | 1162, 1 | 1161, 9 | −0, 2 |
| Li 4602 | 1167, 2 | 1166, 9 | −0, 3 |
| Hg 4358 | 1173, 7 | 1174, 2 | +0, 5 |

The mean experimental density of phosgene was found to be 4·525 grams per litre, the theoretical value being 4·408 grams per litre.

## 6. *Acetone.*

In a previous paper* the refractive index of gaseous acetone in relation to the density was given as 1·001096, the wave-length being λ 5461. The mean experimental density was 2·594 grams per litre.

Assuming the value of the refractive index for λ 5461 already found, the dispersion of gaseous acetone has now been determined with the results shown in Table VI.

The Sellmeier equation corresponding to the results in the second column, and from which the values in the third column have been calculated, is

$$(\mu - 1)_d = 15{\cdot}089 \times 10^{27}/(14069 \times 10^{27} - \nu^2).$$

---

* 'Proc. Phys. Soc.,' vol. 40, p. 27 (1927).

Table VI.—Dispersion of Gaseous Acetone.

| λ in Å.U. | $(\mu - 1)_d \times 10^6$ | | Difference. |
|---|---|---|---|
| | Observed | Calculated | |
| Li 6708 | 1087, 9 | 1088, 0 | +0, 1 |
| Cd 6438 | 1089, 4 | 1089, 3 | −0, 1 |
| Li 6104 | 1091, 4 | 1091, 2 | −0, 2 |
| Hg 5770 | 1093, 5 | 1093, 5 | 0, 0 |
| Hg 5461 | 1096, 0 | 1096, 0 | 0, 0 |
| Cd 5086 | 1099, 6 | 1099, 7 | +0, 1 |
| Cd 4800 | 1103, 2 | 1103, 1 | −0, 1 |
| Li 4602 | 1106, 0 | 1105, 9 | −0, 1 |
| Hg 4358 | 1109, 8 | 1109, 9 | +0, 1 |

The value of the refractive index of gaseous acetone for sodium light (λ 5893) and N.T.P. conditions may readily be obtained. Thus the above Sellmeier expression gives $(\mu - 1)_d$ for λ 5893 as 0·001093. Since the mean experimental density at N.T.P. = 2·594 grams per litre and the theoretical density is 2·587 grams per litre, hence

$$(\mu - 1)_{\text{n t p.}} = (0{\cdot}001093 \times 2{\cdot}594)/2{\cdot}587$$
$$= 0{\cdot}001096.$$

The corresponding refractivity values of Mascart and Prytz are 0·001093 and 0·001085 respectively.

### 7. *Ethyl Ether.*

Table VII shows the results of dispersion measurements on gaseous ethyl ether assuming the value of the refractivity previously found* for λ 5461, viz., $(\mu - 1)_d \times 10^6 = 1509$.

Table VII.—Dispersion of Gaseous Ethyl Ether.

| λ in Å.U. | $(\mu - 1)_d \times 10^6$. | | Difference. |
|---|---|---|---|
| | Observed. | Calculated | |
| Li 6708 | 1498, 9 | 1498, 8 | −0, 1 |
| Cd 6438 | 1500, 7 | 1500, 6 | −0, 1 |
| Li 6104 | 1502, 8 | 1503, 1 | +0, 3 |
| Hg 5770 | 1505, 9 | 1506, 1 | +0, 2 |
| Hg 5461 | 1509, 0 | 1509, 5 | +0, 5 |
| Cd 5086 | 1514, 2 | 1514, 3 | +0, 1 |
| Cd 4800 | 1519, 1 | 1518, 9 | −0, 2 |
| Li 4602 | 1523, 0 | 1522, 6 | −0, 4 |
| Hg 4358 | 1528, 4 | 1527, 9 | −0, 5 |

---

* *Loc. cit.*, p. 28.

The Sellmeier expression corresponding to the third column is

$$(\mu - 1)_d = 21 \cdot 575 \times 10^{27}/(14595 \times 10^{27} - \nu^2).$$

The calculated value of the refractivity for λ 5893 from this expression is 0·001505. The theoretical density of gaseous ethyl ether is 3·298 grams per litre and the mean experimental density was found to be 3·342 grams per litre, hence the refractive index for λ 5893 and N.T.P. conditions is 1·001525. Mascart and Prytz found respectively the values 1·001534 and 1·001524

### 8. *Acetylene*, $C_2H_2$

Both the refraction and dispersion of acetylene have been determined previously. Mascart, working at 12° C. found the refractivity (for sodium light) relative to that of air to be 2·075, the corresponding value of the refractive index being 1·000610 according to Loria.*

The dispersion was studied over the range of the visible spectrum by Loria and Stuckert,† respectively, with the results shown in Table VIII (adapted from Loria, *loc. cit.*).

Table VIII.—Dispersion of Acetylene

| λ in Å U. | $(\mu - 1)_{ntp}\ 10^7$ | |
|---|---|---|
| | Loria. | Stuckert. |
| 6708 | 5604 | 5977 |
| 6375 | 5627 | — |
| 5896 | 5651 | — |
| 5461 | 5698 | 6051 |
| 4359 | — | 6190 |

Loria notes the incompatibility of these values and, in remarking upon similar disagreements between the results of the various observers for *ethylene* and *ethane*, mentions that the need for revision of the measurements on these hydrocarbons is distinctly recognised. He further points out that the large differences in the recorded values can scarcely be due to systematic error in experimental procedure. In his own case, he made a determination of the dispersion of air with the same apparatus as was employed in his work on acetylene, ethylene and ethane, obtaining results which compare favourably with those of other observers. He therefore attributes the disagreements between the results of the various experimenters to the materials actually employed in the work and emphasises that as much care as possible should be taken in the process of purification when future measurements are made on these hydrocarbons. In this latter connection it is interesting to note that Mascart states of his own experiments on acetylene that N. Thenard placed at his disposal several flasks of acetylene in an *absolutely pure state.*

---

* "Die Lichtbrechung in Gasen," p. 67 (1914).

† 'Z. Elch.,' vol. 16, p. 37 (1910).

The acetylene for the present work was prepared by the action of water on calcium carbide, purification* being effected by passing the gas successively through sugar solution, a weak solution of sodium hypochlorite, a solution of silver nitrate and a tower of sodium hydrate After drying with calcium chloride the gas was liquefied and distilled several times.

Measurements of the refractive index for λ 5461 gave the following results —

| | |
|---|---|
| $(\mu - 1)_d \times 10^7$ . | 5938, 5939, 5935, 5936, 5935, 5937, 5933, 5934, 5939, 5935. |
| Mean . . | 5936 |

The results of the dispersion experiments are given in Table IX

Table IX —Dispersion of Acetylene

| λ in Å U | $(\mu - 1)_d \times 10^7$ Observed | $(\mu - 1)_d \times 10^7$ Calculated | Difference |
|---|---|---|---|
| Li 6708 | 5843, 9 | 5843, 5 | −0, 4 |
| Cd 6438 | 5859, 3 | 5858, 9 | −0, 4 |
| Li 6104 | 5880, 8 | 5880, 9 | +0, 1 |
| Hg 5770 | 5906, 7 | 5907, 0 | +0, 3 |
| Hg 5461 | 5936, 0 | 5935, 9 | −0, 1 |
| .. 5086 | 5978, 4 | 5978, 7 | +0, 3 |
| Cd 4800 | 6018, 5 | 6018, 8 | +0, 3 |
| Li 4602 | 6051, 6 | 6051, 5 | −0, 1 |
| Hg 4358 | 6098, 8 | 6098, 8 | 0, 0 |
| Hg 4047 | 6172, 8 | 6173, 2 | +0, 4 |

The results in the second column are fitted by the Sellmeier formula

$$(\mu - 1)_d = 3 \cdot 824 \times 10^{27}/(6744 \times 10^{27} - \nu^2)$$

For the purpose of comparison with the results of Mascart, Loria and Stuckert, the values of the refractive index for λ 5893 and λ 5461 may be reduced to what they would have been under N.T.P. conditions. Thus the theoretical density of acetylene is 1·159 grams per litre (assuming C = 12·000, H = 1·008 and the density of hydrogen = 0·08985 grams per litre). The mean experimental density at N T P. was 1·176 grams per litre. Taking $(\mu - 1)_d$ for λ 5461 to be 0·0005936 and altering this in the ratio:

---

* *Cf.* Travers, "Experimental Study of Gases," p 53 (1901), and Lewes, "Acetylene," p. 60 (1900).

(Experimental density at N.T.P.)/(Standard density),

the value $(\mu - 1)_{ntp} = 0\cdot0006023$ is obtained. Similarly, by calculating the value of $(\mu - 1)_d$ for λ 5893 from the Sellmeier formula and employing the same process of reduction, the refractivity for λ 5893 is found to be $(\mu - 1)_{ntp} = 0\cdot0005983$.

### 9. *Ethylene* $C_2H_4$.

The refraction and dispersion of ethylene have been determined previously by several investigators but, as Loria has remarked, the same uncertainty prevails among the results as in the case of acetylene.

Dufet* quotes determinations by Arago and Dulong for *white* light, both observers having obtained the same result, viz., $\mu_{ntp} = 1\cdot000674$; also he gives Mascart's value for sodium light as $\mu_{ntp} = 1\cdot000719$

Table X (adapted from Loria†) summarises previous dispersion measurements.

Table X -Dispersion of Ethylene.

| λ in A U | $(\mu - 1)_{ntp} \times 10^7$ | | |
|---|---|---|---|
| | Loria. | Stuckert. | Kessler ‡ |
| 6708 | | 7168 | |
| 6677 | 6516 | | |
| 6435 | — | | 7131 |
| 6185 | 6531 | | |
| 5896 | 6571 | | |
| 5790 | 6588 | | 7169 |
| 5770 | - | - | |
| 5461 | 6614 | 7315 | 7203 |
| 5230 | 6620 | | |
| 4359 | | 7428 | 7394 |

Diss Halle ' (1909).

For the present experiments, the ethylene was obtained from the action of sulphuric acid on ethyl alcohol. The gas was passed through wash bottles containing water, caustic soda solution and concentrated sulphuric acid. It was then dried by means of calcium chloride, subsequent purification being effected by the procedure detailed by Travers.*

---

* "Recueil de Données Numériques" (1898)

† *Loc. cit.*, p. 67.

Refractivity measurements for λ 5461 were as follow:—

$(\mu - 1)_d \times 10^7$ .... 7191, 7193, 7190, 7195, 7191, 7192, 7190, 7195, 7192, 7194

Mean ............ 7192.

Table XI gives the dispersion results, the Sellmeier formula corresponding to the second column being

$$(\mu - 1)_d = 5\cdot3564 \times 10^{27}/(7749\cdot7 \times 10^{27} - \nu^2)$$

Table XI.—Dispersion of Ethylene.

| λ in Å U | $(\mu - 1)_d \times 10^7$. | | Difference. |
|---|---|---|---|
| | Observed. | Calculated. | |
| Li 6708 | 7094, 8 | 7094, 9 | +0, 1 |
| Cd 6438 | 7110, 7 | 7111, 0 | +0, 3 |
| Hg 5770 | 7161, 5 | 7161, 6 | +0, 1 |
| Hg 5461 | 7192, 0 | 7191, 8 | −0, 2 |
| Cd 5086 | 7236, 4 | 7236, 6 | +0, 2 |
| Cd 4800 | 7278, 8 | 7278, 6 | −0, 2 |
| Hg 4358 | 7363, 1 | 7361, 9 | −1, 2 |

For comparison with the results of previous work, the values of the refractivities for λ 5461 and λ 5893 under N.T.P. conditions have been calculated as in the case of acetylene; they are as follow:—

$$(\mu - 1)_{ntp} = 0\cdot0007261\ (\lambda\ 5461);$$
$$(\mu - 1)_{ntp} = 0\cdot0007220\ (\lambda\ 5893).$$

In the reduction, the standard density was taken as 1·249 grams per litre, the mean experimental density at N.T.P. being 1·261 grams per litre.

## 10. *Ethane*, $C_2H_6$.

Table XII (from Loria) exhibits the results of previous work on the refraction and dispersion of ethane.

The method adopted for the preparation and purification of ethane in the

---

* *Loc. cit.*, p. 211 (1909).

Table XII.—Dispersion of Ethane.

| λ in Å.U. | $(\mu - 1)_{n.t.p.} \times 10^7$ | |
|---|---|---|
| | Loria | Stuckert. |
| 6708 | — | |
| 6677 | 7478 | |
| 6185 | 7509 | |
| 5896 | 7528 | |
| 5790 | 7542 | — |
| 5461 | 7566 | 7690 |
| 5230 | 7568 | – |
| 4359 | — | 7824 |

present work was that employed by Maass and McIntosh* in their experiments on the determination of some physical properties of liquid ethane

The gas was obtained by the action of a zinc-copper couple on methyl iodide. It was washed with caustic soda solution, dried over phosphorus pentoxide, passed through spirals cooled to —78° C., twice distilled, the middle portions being retained for experiment.

Ten determinations of the refractivity for λ 5461 gave the following values :—

$(\mu - 1)_d \times 10^7$ .... 7648, 7651, 7646, 7649, 7650, 7651, 7646, 7649, 7648, 7644

Mean . 7648.

Table XIII shows the dispersion determined in relation to the value of the refractivity for λ 5461.

Table XIII —Dispersion of Ethane

| λ in Å.U. | $(\mu - 1)_d \times 10^7$. | | Difference |
|---|---|---|---|
| | Observed | Calculated. | |
| Li 6708 | 7578, 6 | 7578, 7 | +0, 1 |
| Cd 6438 | 7589, 8 | 7590, 3 | +0, 5 |
| Hg 5770 | 7626, 0 | 7626, 6 | +0, 6 |
| Hg 5461 | 7648, 0 | 7648, 2 | +0, 2 |
| Cd 5086 | 7680, 2 | 7680, 2 | 0, 0 |
| Cd 4800 | 7709, 8 | 7710, 0 | +0, 2 |
| Hg 4358 | 7769, 2 | 7768, 7 | −0, 5 |

---

* 'J. Am. Chem. Soc.,' vol. 36, p. 737 (1914).

The Sellmeier expression corresponding to the second column is :—

$$(\mu - 1)_d = 8{\cdot}4851 \times 10^{27}/(11396 \times 10^{27} - \nu^2).$$

The third column has been calculated from this expression. Values of $(\mu - 1)_{ntp}$ for λ 5461 and λ 5893 are as follows :—

$$(\mu - 1)_{ntp} = 0{\cdot}0007745 \ (\lambda\, 5461);$$
$$(\mu - 1)_{ntp} = 0{\cdot}0007716 \ (\lambda\, 5893).$$

These may be compared directly with the results of previous workers as shown in Table XII above.

The experimental and theoretical densities are respectively 1·356 and 1·339 grams per litre

## 11 *Methyl Chloride*, $CH_3Cl$

Since methyl chloride is a gas at ordinary temperatures (vapour pressure at 0° C. = 2·5 atmospheres), it is remarkable that its refractivity has been studied by one previous worker only Mascart, working at 12° C., found the ratio of the refractivity of methyl chloride to that of air to be 2·96 (sodium light), from which Dufet (*loc cit.*) deduces the refractive index, $\mu_{ntp}$ as 1·000865.

For the present determination methyl chloride was obtained from a cylinder supplied by Messrs Griffin & Tatlock. Before admission to the refraction tube the gas was liquefied and fractionated several times.

Determinations of the refractivity for λ 5461 are as follows .—

$(\mu - 1)_d \times 10^7$ . 7803, 7799, 7805, 7802, 7807, 7804, 7807, 7803, 7801, 7806.

Mean . ... .... 7804

Assuming the value of the index for λ 5461, the dispersion was measured with the results shown in Table XIV

Table XIV. -Dispersion of Methyl Chloride

| λ in Å U. | $(\mu - 1)_d \times 10^7$. Observed. | $(\mu - 1)_d \times 10^7$. Calculated. | Difference |
|---|---|---|---|
| Li 6708 | 7699, 3 | 7699, 5 | +0, 2 |
| Cd 6438 | 7716, 9 | 7716, 9 | 0, 0 |
| Li 6104 | 7742, 1 | 7741, 8 | -0, 3 |
| Hg 5770 | 7771, 5 | 7771, 4 | −0, 1 |
| Hg 5461 | 7804, 0 | 7804, 0 | 0, 0 |
| Cd 5086 | 7852, 6 | 7852, 3 | −0, 3 |
| Cd 4800 | 7897, 9 | 7897, 6 | −0, 3 |
| Hg 4602 | 7934, 4 | 7934, 2 | −0, 2 |
| Hg 4358 | 7987, 5 | 7987, 3 | −0, 2 |

The values in the third column are calculated from the formula :—

$$(\mu - 1)_d = 5\cdot8524 \times 10^{27}/(7801 \times 10^{27} - \nu^2),$$

which was derived from the results of the second column.

The mean experimental density was found to be 2·305 grams per litre, which is in good agreement with Baume's* value of 2·3045 grams per litre. Assuming the values C = 12·000, H = 1·008, Cl = 35·457, and the density of hydrogen = 0·08985 grams per litre, the theoretical density of methyl chloride is 2·2499 grams per litre.

From the Sellmeier formula, the value of $(\mu - 1)_d$ for λ 5893 is 0·0007760 and by altering this in the ratio (Experimental density)/(Standard density) = 2·305/2·250 the value of $(\mu - 1)_{n\,t\,p}$ is found to be 0·0007950. This value does not agree with that of Mascart noted above, viz., $(\mu - 1)_{n\,t\,p}$ = 0·000870 (λ 5893), and it is difficult to give any explanation of the discrepancy as Mascart provides no indication of the source of the methyl chloride he employed. The present measurement, however, was confirmed by Mr. T. S. Hartley, M.Sc. Tech.

### 12. *Methylene Chloride*. $CH_2Cl_2$.

The refraction and dispersion of gaseous methylene chloride have not been previously measured.

For the purpose of the present experiments pure liquid methylene chloride supplied by Messrs. British Drug Houses was employed.

Refractive index determinations for λ 5461 were as follow :—

| | |
|---|---|
| $(\mu - 1)_d \times 10^6$ .... | 1110, 1113, 1108, 1109, 1116, 1113, 1117, 1111, 1108, 1114. |
| Mean ............ | 1112. |

Table XV shows the results of the dispersion measurements which lead to the Sellmeier equation

$$(\mu - 1)_d = 9\cdot1881 \times 10^{27}/(8565\cdot6 \times 10^{27} - \nu^2).$$

The theoretical density of methylene chloride is 3·785 grams per litre and the experimental density was found to be 3·799 grams per litre.

### 13. *Methylene Bromide*. $CH_2Br_2$.

There are no recorded data for the refraction and dispersion of gaseous methylene bromide.

---

* 'J Chim Phys.,' vol. 6, p. 1 (1908).

Table XV.—Dispersion of Methylene Chloride.

| λ in Å.U. | $(\mu - 1)_d \times 10^6$ | | Difference. |
|---|---|---|---|
| | Observed. | Calculated. | |
| Li 6708 | 1098, 4 | 1098, 3 | −0, 1 |
| Cd 6438 | 1100, 4 | 1100, 7 | +0, 3 |
| Li 6104 | 1103, 7 | 1103, 8 | +0, 1 |
| Hg 5770 | 1107, 6 | 1107, 6 | 0, 0 |
| Hg 5461 | 1112, 0 | 1111, 8 | −0, 2 |
| Cd 5086 | 1118, 4 | 1118, 1 | −0, 3 |
| Cd 4800 | 1124, 0 | 1123, 9 | −0, 1 |
| Hg 4602 | 1128, 6 | 1128, 7 | +0, 1 |

Pure liquid methylene bromide supplied by Messrs British Drug Houses was used in the experiments.

The following are the results of the determinations of the refractivity for λ 5461 —

$(\mu - 1)_d \times 10^6$.... 1437, 1438, 1434, 1437, 1432, 1435, 1431, 1437, 1434, 1431.

Mean ........... 1435.

Table XVI.—Dispersion of Methylene Bromide.

| λ in Å.U. | $(\mu - 1) \times 10^6$. | | Difference. |
|---|---|---|---|
| | Observed. | Calculated. | |
| Li 6708 | 1418, 0 | 1418, 0 | 0, 0 |
| Cd 6438 | 1420, 9 | 1420, 8 | −0, 1 |
| Li 6104 | 1425, 0 | 1424, 9 | −0, 1 |
| Hg 5770 | 1429, 7 | 1429, 7 | 0, 0 |
| Hg 5461 | 1435, 0 | 1435, 0 | 0, 0 |
| Cd 5086 | 1442, 3 | 1442, 8 | +0, 5 |
| Cd 4800 | 1449, 6 | 1450, 1 | +0, 5 |
| Hg 4602 | 1455, 8 | 1456, 0 | +0, 2 |
| Hg 4358 | 1464, 9 | 1464, 6 | −0, 3 |

The dispersion measurements shown in Table XVI lead to the formula

$$(\mu - 1)_d = 12 \cdot 215 \times 10^{27}/(8814 \cdot 1 \times 10^{27} - \nu^2).$$

The mean value of the density of gaseous methylene bromide was found to be 7·846 grams per litre, the theoretical value being 7·748 grams per litre. No values of the density of the gas are given in the usual reference books.

## IV. REMARKS.

In carrying out the present work, the choice of substances for measurement was made with the general aim of rendering the recorded data on refraction complete for well-defined groups of compounds, for example, the chlorine derivatives of methane. C. and M. Cuthbertson* have measured the refraction and dispersion of methane ($CH_4$). The present writer has already given corresponding results for carbon tetrachloride,† ($CCl_4$), and chloroform‡ ($CHCl_3$) The results given above for methylene chloride ($CH_2Cl_2$) and methyl chloride ($CH_3Cl$), now complete this particular series of compounds.

Methylene bromide has proved a convenient starting point for similar experiments on the bromine derivatives of methane

The series acetylene ($C_2H_2$), ethylene ($C_2H_4$) and ethane ($C_2H_6$), is interesting on account of the increment of two atoms of hydrogen as we pass from one member to the other, not to speak of the interest due to the differences in the nature of the linkages between the carbon and hydrogen atoms in the three compounds.

## V.—SUMMARY OF EXPERIMENTAL RESULTS.

For convenience of reference, the various results which have been found are arranged in Table XVII. The second column of the table contains the values of the refractivities for λ 5461 determined in relation to the densities of the

Table XVII.—Summary.

| Substance. | $(\mu - 1)_d$ for λ 5461. | $C \times 10^{-27}$ | $\nu_0^2 \times 10^{-27}$. |
|---|---|---|---|
| Silicon tetrachloride | 0·001969 | 17·213 | 9044·3 |
| Silicon tetrabromide | 0·002725 | 12·940 | 5050·1 |
| Boron trichloride | 0·001404 | 9·5829 | 7127·5 |
| Boron tribromide | 0·002012 | 12·247 | 6388·7 |
| Phosgene | 0·001149 | 9·2574 | 8358·0 |
| Acetone | 0·001096 | 15·089 | 14069 |
| Ethyl ether | 0·001509 | 21·575 | 14595 |
| Acetylene | 0·0005936 | 3·824 | 6744 |
| Ethylene | 0·0007192 | 5·3564 | 7749·7 |
| Ethane | 0·0007648 | 8·4851 | 11396 |
| Methyl chloride | 0·0007804 | 5·8524 | 7801 |
| Methylene chloride | 0·001112 | 9·1881 | 8565·6 |
| Methylene bromide | 0·001435 | 12·215 | 8814·1 |

---

* 'Proc. Roy. Soc.,' A, vol. 97, p. 156 (1920).

† 'Proc. Phys. Soc.,' vol. 39, p. 421 (1927).

‡ 'Proc. Phys. Soc.,' vol. 40, p. 23 (1927).

substances; the third and fourth columns show the values of C and $\nu_0^2$ in the Sellmeier formula

$$(\mu - 1)_\nu = C/(\nu_0^2 - \nu^2)$$

My thanks are due to Professor W. L. Bragg, F.R.S., and Mr. C. Cuthbertson, F.R.S., for the loan of certain apparatus for some of the experiments, and to the Government Grant Committee of the Royal Society for a grant in aid of the research. I also wish to thank Mr. T. S. Hartley, M.Sc. Tech. for assistance in checking several sets of calculations.

---

# *The Band Spectrum of Yttrium Oxide (YO). With a Note on the ScO and LaO Systems.*

By L. W. Johnson, M.A., and R. C. Johnson, M.A., D.Sc., University of London, King's College.

(Communicated by O. W. Richardson, F.R.S.—Received May 12, 1931.)

## *Introduction.*

Our attention was drawn to these bands during a perusal of the 'Collected Papers' of Eder and Valenta. Eder* has given measurements of a large number of bands due to yttrium oxide which appear in the flame of a carbon arc when fed with the oxide, chloride, or sulphate of this metal. He gives also some good reproductions of these bands from grating photographs. So far as we are aware, no quantum analysis of this spectrum has hitherto been published. In the present paper we give new data for the band heads which we have obtained from photographs taken in the first order of a 21-foot Rowland grating. About 100 heads have been measured, each having been evaluated from three independent plates. On the whole there is reasonably good agreement with Eder's measurements. The experimental procedure found most satisfactory was to burn a carbon arc with 10–15 amps., the positive being cored and packed with a mixture of yttrium oxide and a little sodium carbonate. In the extensive yellow flame which rose some 2 or 3 inches above the arc the bands of yttrium oxide were strongly developed, and good grating photographs were obtainable with from 15 to 30 minutes exposure.

---

* 'Sitz. K. Akad. Wien.,' Abt. IIa, vol. 125 (1916).

The band systems of the YO molecule are of considerable interest when considered in relation to those of the scandium oxide and lanthanum oxide molecules. The series ScO, YO, LaO should have similar external electronic structures* and analogous band systems may, therefore, be anticipated. The systems of scandium oxide have been only partially recorded Mecke† has analysed but one system completely The systems of lanthanum oxide have recently been dealt with by Mecke‡ and Jevons.§ The latter gives a good summary of these in his paper. During the course of the present investigation of yttrium oxide a brief summary of work by Meggers and Wheeler was published in the 'Bulletin of the American Physical Society'|| on the band spectra of all three oxides. We hope that this information may subsequently be published in full. The published summary is sufficient to show that there is—as one would anticipate—a very close resemblance between the band systems of these three molecules.

The electronic structures of these molecules should, moreover, closely resemble CaF, SrF and BaF respectively, and a comparison with the band systems of these three molecules¶ bears out the expected similarity.

All the observed systems of yttrium oxide lie in the visible part of the spectrum, and all are degraded to the less refrangible side.

## *The Systems in the Yellow-orange-red Region.*

The data of these are given in Tables I, II and III. Without implying that these are four independent systems we have for convenience of reference labelled them as four "systems" I, II, III and IV. Systems I and II are the dominating feature. In particular the (0, 0) sequences of these two systems are the outstanding features of the yttrium oxide spectrum, and persist even on a considerably under-exposed plate In Tables IV and V is given the vibrational quantum analysis of these systems. It is at once noticed that each of them is characterised by three long attenuated sequences corresponding to $\Delta v = 1, 0, -1$. This feature, found similarly in the spectra of the alkaline earth fluorides (*loc. cit.*), is a consequence of the proximity of the vibration

---

* See 'Proc. Roy. Soc.,' A, vol. 122, p 164 (1929) and 'Proc. Phys. Soc.,' vol. 41, p. 531 (1929).

† 'Z. Physik,' vol. 42, p 390 (1927).

‡ 'Naturwiss.,' vol 17, p. 84 (1929).

§ 'Proc. Phys. Soc.,' vol. 41, p. 520 (1929).

|| November, 1930, Abstract 32.

¶ Johnson, 'Proc. Roy. Soc.,' A, vol. 122, p. 161 (1929); Harvey and Jenkins, 'Phys. Rev.,' vol. 36, p. 1413 (1930).

Table I —Experimental Data of System I.

| Int | λ (air) | ν (vac.) | $v'$ | $v''$ | Int | λ (air) | ν (vac.) | $v'$ | $v''$ |
|---|---|---|---|---|---|---|---|---|---|
| 0*d* | 6717·78 | 14881·77 | 5 | 7 | 10 | 6019·96 | 16606·82 | 3 | 3 |
| 0 | 6414·13 | 15513·71 | 9 | 10 | 10 | 6003·63 | 16651·98 | 2 | 2 |
| 2 | 6421·23 | 15561·77 | 8 | 9 | 10 | 5987·72 | 16696·24 | 1 | 1 |
| 3 | 6405·74 | 15606·70 | 7 | 8 | 10 | 5972·17 | 16739·71 | 0 | 0 |
| 4 | 6387·12 | 15652·19 | 6 | 7 | 4 | 5876·18 | 17013·14 | 11 | 10 |
| 7 | 6369·935 | 15694·42 | 5 | 6 | 4 | 5838·10 | 17124·11 | 9 | 8 |
| 7 | 6352·45 | 15737·62 | 4 | 5 | 6 | 5818·63 | 17181·42 | 8 | 7 |
| 4 | 6335·95 | 15778·60 | 3 | 4 | 6 | 5800·04 | 17236·48 | 7 | 6 |
| 6 | 6127·46 | 16315·46 | 9 | 9 | 5 | 5781·80 | 17290·86 | 6 | 5 |
| 8 | 6107·87 | 16367·76 | 8 | 8 | 7 | 5764·29 | 17313·39 | 5 | 4 |
| 9 | 6089·44 | 16417·35 | 7 | 7 | 8 | 5746·97 | 17395·67 | 4 | 3 |
| 7*c* | 6071·17 | 16466·74 | 6 | 6 | 7 | 5730·15 | 17446·71 | 3 | 2 |
| 10 | 6053·85 | 16513·86 | 5 | 5 | 6 | 5713·87 | 17496·44 | 2 | 1 |
| 10 | 6036·68 | 16560·86 | 4 | 4 | 5 | 5697·80 | 17545·77 | 1 | 0 |

Table II —Experimental Data of System II

| Int | λ (air) | ν (vac.) | $v'$ | $v''$ | Int | λ (air) | ν (vac.) | $v'$ | $v''$ |
|---|---|---|---|---|---|---|---|---|---|
| 4 | 6572·60 | 15210·49 | 6 | 7 | 10 | 6199·88 | 16124·89 | 4 | 4 |
| 5 | 6553·89 | 15253·91 | 5 | 6 | 10 | 6182·26 | 16170·85 | 3 | 3 |
| 6 | 6535·86 | 15295·98 | 4 | 5 | 10 | 6165·13 | 16215·79 | 2 | 2 |
| 7 | 6518·36 | 15337·15 | 3 | 4 | 10 | 6148·43 | 16259·82 | 1 | 1 |
| 7 | 6501·27 | 15377·36 | 2 | 3 | 10 | 6132·13 | 16303·04 | 0 | 0 |
| 7 | 6481·60 | 15416·90 | 1 | 2 | [illegible] | 5969·80 | 16746·35 | 8 | 7 |
| 4 | 6359·59 | 15719·95 | 12 | 12 | [illegible] | 5950·04 | 16801·96 | 7 | 6 |
| 5 | 6338·21 | 15772·96 | 11 | 11 | 5 | 5931·13 | 16855·56 | 6 | 5 |
| 8 | 6316·32 | 15827·65 | 10 | 10 | 6 | 5912·25 | 16909·35 | 5 | 4 |
| 9 | 6295·51 | 15879·97 | 9 | 9 | 4 | 5876·18 | 17013·14 | 3 | 2 |
| 10 | 6275·02 | 15931·82 | 8 | 8 | 5 | 5858·88 | 17063·40 | 2 | 1 |
| 10 | 6236·73 | 16029·62 | 6 | 6 | 4 | 5841·96 | 17112·82 | 1 | 0 |
| 10 | 6217·98 | 16077·97 | 5 | 5 | | | | | |

Table III —Systems III and IV

| System III | | | | | System IV | | | | |
|---|---|---|---|---|---|---|---|---|---|
| Int. | λ (air). | ν (vac.) | $v'$ | $v''$ | Int | λ (air) | ν (vac.) | $v'$ | $v''$. |
| 8 | 5939·12 | 16832·85 | 0 | 0 | 8 | 6096·83 | 16397·44 | 0 | 0 |
| 7 | 5956·41 | 16783·91 | 1 | 1 | 7 | 6114·76 | 16349·35 | 1 | 1 |
| | — | — | 2 | 2 | - | - | - | 2 | 2 |
| 7*c* | 5992·10 | 16684·02 | 3 | 3 | [illegible] | 6151·82 | 16250·86 | 3 | 3 |

frequencies, and therefore of the binding forces of the initial and final electronic states. Upon examination of the first differences between two given rows or columns—which are usually approximately constant—a very rapid variation

## Table IV.

| $v'$ \ $v''$ | 0 | | 1 | | 2 | | 3 | | 4 | | 5 | | 6 | | 7 | | 8 | | 9 | | 10 |
|---|---|---|---|---|---|---|---|---|---|---|---|---|---|---|---|---|---|---|---|---|---|
| 0 | 16739·71 | | | | | | | | | | | | | | | | | | | | |
| | 806·1 | | | | | | | | | | | | | | | | | | | | |
| 1 | 17545·77 | 849·6 | 16696·24 | | | | | | | | | | | | | | | | | | |
| | | | 800·2 | | | | | | | | | | | | | | | | | | |
| 2 | | | 17496·44 | 844·5 | 16651·98 | | | | | | | | | | | | | | | | |
| | | | | | 794·7 | | | | | | | | | | | | | | | | |
| 3 | | | | | 17446·71 | 839·9 | 16606·82 | 828·2 | 15778·60 | | | | | | | | | | | | |
| | | | | | | | 788·9 | | 782·3 | | | | | | | | | | | | |
| 4 | | | | | | | 17395·67 | 834·8 | 16560·86 | 823·2 | 15737·62 | | | | | | | | | | |
| | | | | | | | | | 782·5 | | | | | | | | | | | | |
| 5 | | | | | | | | | 17343·39 | 830·5 | 16513·86 | 819·4 | 15694·42 | 812·65 | 14881·77 | | | | | | |
| | | | | | | | | | | | 777·0 | | 772·3 | | 770·42 | | | | | | |
| 6 | | | | | | | | | | | 17290·86 | 824·2 | 16466·74 | 814·55 | 15652·19 | | | | | | |
| | | | | | | | | | | | | | 769·8 | | 765·16 | | | | | | |
| 7 | | | | | | | | | | | | | 17236·48 | 819·1 | 16417·35 | 810·65 | 15606·70 | | | | |
| | | | | | | | | | | | | | | | 764·07* | | 761·06 | | | | |
| 8 | | | | | | | | | | | | | | | 17181·42 | 813·66 | 16367·76 | 806·0 | 15561·77 | | |
| | | | | | | | | | | | | | | | | | 756·35 | | 753·69 | | |
| 9 | | | | | | | | | | | | | | | | | 17124·11 | 808·65 | 16315·46 | 801·75 | 15513·71 |
| 10 | | | | | | | | | | | | | | | | | | | — | | — |
| | | | | | | | | | | | | | | | | | | | | | 17013·14 |

* Value smoothed in computation

## Table V.

| $v'$ \ $v''$ | 0 | | 1 | | 2 | | 3 | | 4 | | 5 | | 6 | | 7 | | 8 | 9 | 10 |
|---|---|---|---|---|---|---|---|---|---|---|---|---|---|---|---|---|---|---|---|
| 0 | 16303 04 | | | | | | | | | | | | | | | | | | |
| | | 853 0 | 16259 82 | 842 0 | 15416 | | | | | | | | | | | | | | |
| | | | 903 6 | | 793 | | | | | | | | | | | | | | |
| | | | 17063 40 | 847 6 | 16215 '9 | 828 4 | 5377 36 | | | | | | | | | | | | |
| | | | | | | | 793 5 | | | | | | | | | | | | |
| | | | | | 4 | 834 1 | 6170 85 | 833 7 | | | | | | | | | | | |
| | | | | | | | )bserved | | 124 89 | 828 0 | 5295 98 | | | | | | | | |
| | | | | | | | | | 785 5 | | (782 0) | | | | | | | | |
| | | | | | | | | | 35 | 832 4 | 6077 97 | 824 1 | | | | | | | |
| | | | | | | | | | | | 778 6 | | | | | | | | |
| | | | | | | | | | | | 6855 56 | 825 0 | | 819 1 | 15210 49 | | | | |
| | | | | | | | | | | | | | 3 | | | | | | |
| | | | | | | | | | | | | | 96 | | | | | | |
| | | | | | | | | | | | | | | | 16746 35 | 814 5 | | | |
| | | | | | | | | | | | | | | | | | | 58 | |

is actually observed. Such a feature is accounted for empirically by a term $cv'v''$ (using the Old Quantum Theory) in

$$\nu = \nu_0 + (a'v' - b'v'^2) - cv'v'' - (a''v'' - b''v''^2) \qquad (1)$$

Physically the term arises on account of the variation of the interval ($\nu_{\text{head}} - \nu_{\text{origin}}$) of the bands of the system. The first differences are in this case given by

$$\Delta F'_v = F'_{v+1} - F'_v = a' - b' - 2b'v' - cv'' \qquad (2)$$

$$\Delta F''_v = F''_v - F''_{v+1} = a'' - b'' - 2b''v'' + cv' \qquad (3)$$

Thus equation (2) becomes

$$\left.\begin{aligned} \Delta F'_v &= a' - b' - (2b' + c)\,v' && \text{using the (1, 0) and (0, 0) sequences} \\ \text{and} \quad \Delta F'_v &= a' - b' - c - (2b' + c)\,v' && \text{using the (0, 0) and (0, 1) sequences} \end{aligned}\right\} \qquad (2\text{A})$$

Similarly equation (3) becomes

$$\left.\begin{aligned} \Delta F''_v &= a'' - b'' + c - (2b'' - c)\,v'' && \text{using the (1, 0) and (0, 0) sequences} \\ \Delta F''_v &= a'' - b'' - (2b'' - c)\,v'' && \text{using the (0, 0) and (0, 1) sequences} \end{aligned}\right\} \qquad (3\text{A})$$

If we apply equations (2A) to the data of Table IV we obtain :

$$\Delta F'_v = 806{\cdot}7 - 6{\cdot}25\,v',$$

and

$$= 799{\cdot}2 - 5{\cdot}59\,v',$$

from which $c = 7{\cdot}5$ and $b'$ actually becomes negative. It is clear that a term $cvv'$ of this magnitude cannot be considered satisfactory, and hence an expression such as (1) is unsuitable for the expression of the data. The variation of the interval ($\nu_{\text{head}} - \nu_{\text{origin}}$) between the different sequences must here be unusually large—so large indeed that no great weight can be attached to the constants obtained by fitting the data of the band *heads* to any formula. We have decided finally to form the first differences using firstly the (1, 0) and (0, 0) sequences, and secondly the (0, 0) and (0, 1) sequences, and fit them independently to formulæ. As the expression for the first differences seemed in some cases to depart slightly from the linear form, a quadratic was adopted where necessary, thus making F a cubic. The formulæ of the New Quantum Theory have been adopted throughout the paper so that the vibrational term takes the form

$$F^v = \omega_e (v + \tfrac{1}{2}) - x_e\omega_e (v + \tfrac{1}{2})^2 - y_e\omega_e (v + \tfrac{1}{2})^3 \qquad (4)$$

The data of systems I and II have been analysed in this way and the constants of the above formulæ are collected in Table VI.

Table VI.

| System | Sequences | $\omega'_e$ | $x'_e\omega'_e$ | $y'_e\omega'_e$ | $\omega''_e$ | $x''_e\omega''_e$ | $y''_e\omega''_e$ | $\nu_e$ |
|---|---|---|---|---|---|---|---|---|
| I | (1, 0) & (0, 0) | 812·09 | 2·885 | 0·0160 | 854·15 | 2·427 | 0·0094 | 16761·0 |
| | | (or using a quadratic only) | | | | | | |
| | (1, 0) & (0, 0) | 812·96 | 3·125 | — | 854·97 | 2·567 | — | 16760·8 |
| | (0, 0) & (0, 1) | 804·77 | 2·793 | — | 845·70 | 2·391 | — | 16760·8 |
| II | (1, 0) & (0, 0) | 815·61 | 3·006 | 0·0087 | 857·53 | 2·270 | 0·0386 | 16324·2 |
| | (0, 0) & (0, 1) | 809·82 | 2·589 | 0·0055 | 851·82 | 2·168 | 0·0160 | 16324·2 |
| III | (0, 0) | Same as I ? | | | Same as I ? | | | 16854·1 ? |
| IV | (0, 0) | Same as II ? | | | Same as II ? | | | 16418·6 |

The marked differences in the vibrational constants deduced from the two different pairs of sequences will be observed. This feature must inevitably remain in an unsatisfactory condition until data of the band origins are available. This will not be easy to obtain as it will require very high resolving power. It makes a little difficult the recognition with certainty of those electronic states which are held in common by the different band systems. This same difficulty was found also by Jevons in the case of lanthanum oxide (*loc. cit.*).

The systems labelled III and IV have only been recorded fragmentarily in Table III, viz., the first few members of what are presumably the (0, 0) sequences.

### *Interpretation of Systems I–IV.*

It will be borne in mind that as ScO, YO and LaO are molecules with an even number of electrons we should expect the most prominent transitions to be of the type $^2\Pi \rightarrow {}^2\Sigma$ and $^2\Sigma \rightarrow {}^2\Sigma$. Our view is that the so-called "systems" I–IV are probably one band system corresponding to the transition $^2\Pi \rightarrow {}^2\Sigma$. The above "systems" I–II are thought to be $^2\Pi_{\frac{1}{2}} \rightarrow {}^2\Sigma$ and $^2\Pi_{1\frac{1}{2}} \rightarrow {}^2\Sigma$ respectively (the $^2\Pi$ level, we think, may be inverted). The doublet separation is about 436·7ν. While this identification looks uncertain from the constants of Table VI (for the reasons mentioned above, viz., the large variation in the intervals between the band heads and origins) it appears very plausible if the wave-number intervals between corresponding bands of the two (0, 0) sequences are formed. The following series of differences arise from I and II: 436·7, 436·4, 436·2, 436·0, 435·9, etc., which leave little room for doubt as to the correctness of this interpretation. "Systems" III and IV (see Table III) give the following intervals between corresponding bands. 435·4, 434·6, —, 433·2, a separation which must probably be identified with that obtained from I and II. The possibility that the heads of III were associated with those of I (and the heads of IV with those of II) in the relation of R branches to Q branches does not at first sight commend itself for two reasons. Firstly, the interval 93–94ν is particularly large and secondly, although the fine structure is but imperfectly resolved, the intensity distribution in the leading band of I (ν 16739·7) shows approximately the location of an "origin" so that we should argue that the band must have both P and R branches (and presumably Q branches also), the R branch or branches producing its head. If we adopt this view, however, we are driven to postulate another pair of $^2\Pi$ levels some 93–94ν above those already found, and of the same separation This seems most unlikely. Another alternative can also be dismissed—that the system (III, IV) corresponds to a transition $^2\Sigma \rightarrow {}^2\Pi$, from a higher $^2\Sigma$ level down to the known $^2\Sigma$ levels. Against this is the probability that such a system would be degraded to the more refrangible side, and further that a system ($^2\Sigma \rightarrow {}^2\Sigma$) which would be expected to exist in the region about λ 3000 is not found

On the whole it seems most probable that III is constituted of branches which are related to I, each head possibly being an R branch with an $^RQ$ branch. The heads of I would be Q branches possibly with $^QP$ or $^QR$ branches in addition. The observed intensity minimum would lie between the early members of these branches and the normal P branch The expected fine structure for this type of electronic transition has been discussed in detail by Mulliken *

### *The Blue-Green Bands. System V, etc.*

There is a well-developed system of bands in the blue-green region degraded also to the less refrangible side. The band heads are doublets having a separation of some 3 to 4ν. The observational data are given in Table VII and a vibrational analysis is made in Table VIII. Although a well-developed system, it is by no means as strong as the very intense orange-red bands we have already considered. It will be noted that Table VII is divided into two parts. In the lower part are a number of bands of which the interpretation is somewhat doubtful. They may be a part of system V, and have been shown as such in Table VIII, where they occupy the lower half of the table. Alternatively, they may be an independent system. The two alternative assignments of vibrational quantum numbers are given in Table VII If regarded as an independent system the distribution of intensities is rather unusual. The system would be approximately expressed by

---

* 'Reviews of Modern Physics,' vol. 3, No. 1, p. 128 (1931).

Table VII.

| Int | $\lambda_{air}$. | $\nu_{vac}$ | $v'$ | $v''$ | Int | $\lambda_{air}$ | $\nu_{vac}$ | $v'$ | $v''$. |
|---|---|---|---|---|---|---|---|---|---|
| 1 | 5304 49<br>5303 75 | 18846 72<br>18849 35 | 2 | 4 | 7 | 4842 79<br>4841 90 | 20643 5<br>20647 3 | 1 | 1 |
| 2 | 5275 12<br>5274 15 | 18950 58<br>18954 07 | 1 | 3 | 10 | 4818 15<br>4817 36 | 20749 08<br>20752 47 | 0 | 0 |
| 1 | 5249 49<br>5248 32 | 19044 2<br>19048·4 | 0 | 2 | 1* | —<br>4704 35 | —<br>21250 99 | 3 | 2 |
| 4 | 5078 63<br>5077 90 | 19684 89<br>19687 72 | 2 | 3 | 7 | 4676 39<br>4675 79 | 21378 07<br>21380 81 | 2 | 1 |
| 5 | 5050 56<br>5049 66 | 19791 31<br>19797 81 | 1 | 2 | 9 | 4650 13<br>4649 47 | 21498·78<br>21501 82 | 1 | 0 |
| 6 | 5025 21<br>5024 25 | 19894 13<br>19897 92 | 0 | 1 | 2* | —<br>4523 94 | —<br>22098 3 | 3 | 1 |
| 1* | —<br>4898 79 | —<br>20407 51 | 3 | 3 | | | | | |
| 3 | 4869 85<br>4869 16 | 20528 78<br>20531 68 | 2 | 2 | | | | | |

| Int | $\lambda_{air}$ | $\nu_{vac}$ | $v'$ | $v''$ | $v'$ | $v''$ | Int | $\lambda_{air}$ | $\nu_{vac}$ | $v'$ | $v''$ | $v'$ | $v''$ |
|---|---|---|---|---|---|---|---|---|---|---|---|---|---|
| 1* | —<br>4898 79 | —<br>20407 51 | 3 | 3 | 0 | 2 | 2 | 4646 78<br>— | 21514 2 | 6 | 4 | 3 | 3 |
| 0 | 4788 15<br>4787 91 | 20879 08<br>20880 14 | 5 | 4 | 2 | 3 | 3 | 4603 58<br>— | 21716 2<br>— | 5 | 3 | 2 | 2 |
| 4 | 4744 89<br>4744 53 | 21069 43<br>21071 03 | 4 | 3 | 1 | 2 | 6 | 4562 13<br>4561 85 | 21913 46<br>21914 81 | 4 | 2 | 1 | 1 |
| 1* | —<br>4704 35 | —<br>21250 99 | 3 | 2 | 0 | 1 | 2* | —<br>4523 94 | —<br>22098 44 | 3 | 1 | 0 | 0 |

$$\nu = \left.\begin{matrix} 22191\cdot0 \\ 22189\cdot9 \end{matrix}\right\} + [678\cdot2\,(v'+\tfrac{1}{2}) - 7\cdot85\,(v'+\tfrac{1}{2})^2] - \begin{bmatrix} 854\cdot64\,(v''+\tfrac{1}{2}) - 2\cdot71\,(v''+\tfrac{1}{2})^2 \\ 855\cdot04\,(v''+\tfrac{1}{2}) - 2\cdot81\,(v''+\tfrac{1}{2})^2 \end{bmatrix} \qquad (5)$$

The progression $v' = 3$ of Table VIII is then a blend of two progressions, one belonging to each of the two different systems. The alternative interpretation finds a place for these bands as a part of the main system—but appears to indicate a definite discontinuity in the vibration frequency at $v' = 3$. This is at once apparent upon examination of the first differences of the initial electronic state in Table VIII. A similar type of phenomenon has been noted by Birge* in the case of $O_2$ and other molecules. It is, however, unusual in this case in that the discontinuity appears for so low a value of the vibrational quantum number as $v' = 3$ Using the main part of the system (upper half of Table VIII) the vibrational constants are as given in Table IX.

Table VIII Blue-Green System ($^2\Sigma \rightarrow {}^2\Sigma$)

| $v'$ \ $v''$ | 0 | | 1 | | 2 | | 3 | | 4 |
|---|---|---|---|---|---|---|---|---|---|
| 0 | 20752 47<br>20749 08 | 854 5<br>854 0 | 19897 92<br>19894 13 | 849 5<br>849 9 | 19048 4<br>19044 2 | | | | |
| | 749 3<br>749 7 | | 749 4<br>749 4 | | 749 4<br>750 1 | | | | |
| 1 | 21501·82<br>21498·78 | 854 5<br>855 3 | 20647 3<br>20643 5 | 849 5<br>849 2 | 19797 8<br>19794 3 | 843 7<br>843 7 | 18954 07<br>18950 58 | | |
| | | | 733 5<br>734 6 | | 733 0<br>734 5 | | 733 6<br>734 3 | | |
| 2 | | | 21380 81<br>21378 07 | 849 1<br>849 3 | 20531 68<br>20528 78 | 844 0<br>843 9 | 19687 72<br>19684 89 | 838 4<br>838 2 | 18849 35<br>18846 72 |
| | | | 717 5<br>— | | 719 3<br>— | | 710 8<br>— | | |
| 3 | → (Discontinuity) | | 22098 2<br>— | 847 3 | 21251 0<br>— | 843 5 | 20407 5<br>— | | |
| | | | | | 663 8<br>— | | 663 5<br>— | | |
| 4 | | | | | 21914 8<br>21913 5 | 843 8<br>844 1 | 21071 0<br>21069 4 | | |
| | | | | | | | —<br>646 8 | | |
| 5 | | | | | | | —<br>21716 2 | 837 1<br>— | 20880 1<br>20879 1 |
| | | | | | | | | | 634 1(?) |
| 6 | | | | | | | | | 21514 2(?) |

---

* Birge, " Molecular Spectra and Molecular Structure," a General Discussion held by the Faraday Society, 1929, p. 710.

Table IX.—Constants of the $^2\Sigma \rightarrow {}^2\Sigma$ Transition

| | $\omega'_e$ | $x'_e\omega'_e$ | $\omega''_e$ | $x''_e\omega''_e$ | $\nu_e$ |
|---|---|---|---|---|---|
| More refrangible head | 765·08 | 7·865 | 860·05 | 2·707 | 20801·2 |
| Less refrangible head | 764·98 | 7·63 | 860·67 | 2·813 | 20798·1 |

The final electronic state of this system is undoubtedly identical with the final state of the $^2\Pi \rightarrow {}^2\Sigma$ system, and it is certain that it represents the transition $^2\Sigma \rightarrow {}^2\Sigma$. In this type of transition the resultant bands should have two P branches, $P_1$ and $P_2$, and two R branches, $R_1$ and $R_2$. The possible $^PQ$ and $^RQ$ branches are usually weak and fade out early. The two components should theoretically be of equal strength. There can be little doubt that the observed double heads are $R_1$ and $R_2$ branches and they are of approximately the same strength. It is scarcely necessary to remark that the observed doublet interval is, of course, the difference of the electronic intervals of the two $^2\Sigma$ levels, and in any case as it is determined from the heads of the R branches it will not be a precise determination of the electronic difference. The true electronic $^2\Pi$ interval will also differ from 436·7ν by an amount equal to the interval of the lower $^2\Sigma$ level. Whether it will be greater or less than this seems to us uncertain in the absence of detailed analysis. Our interpretation of the yttrium oxide spectrum is summarised, with the above reservation, in fig. 1 (which is not, however, a scale diagram). The observed bands can all be accounted for by two electronic transitions to the ground state $^2\Pi_{1\frac{1}{2},\frac{1}{2}} \rightarrow {}^2\Sigma$, and $^2\Sigma \rightarrow {}^2\Sigma$. There is some evidence of bands degraded to the violet side; these are presumably members of a $^2\Sigma \rightarrow {}^2\Pi$ system. We may mention in passing that the CaF and SrF systems are precisely analogous to these of YO discussed. (An error of interpretation originally made by one of us (R.C.J.) in regard to these fluoride spectra has been recently corrected by Harvey and Jenkins, *loc. cit.*)

## *Note on Scandium Oxide Systems.*

In the summary of their work (*loc. cit.*) Meggers and Wheeler give the (0, 0) bands of five "systems." These are so similarly placed compared with the YO bands which we have discussed, that they may at once be interpreted. Their system I at λλ 4857·79, 4858·09 is $^2\Sigma \rightarrow {}^2\Sigma$, while their II, III, IV and V at λλ 6017·07, 6036·17, 6064·31 and 6079·30 are the $^2\Pi_{1\frac{1}{2},\frac{1}{2}} \rightarrow {}^2\Sigma$ system.

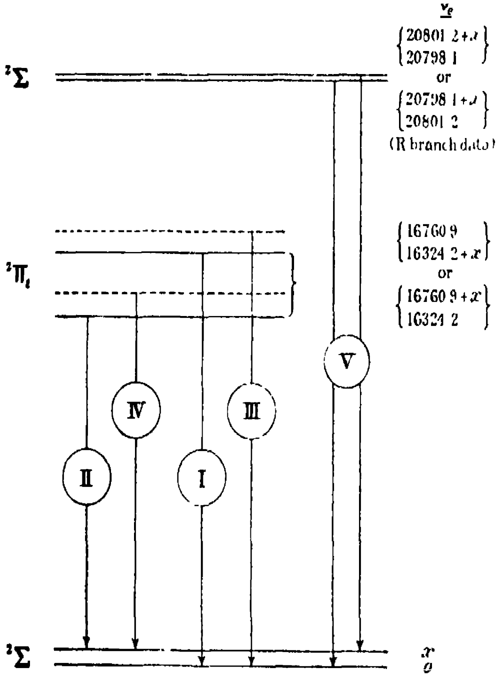

Fig. 1.—YO Electronic Levels.

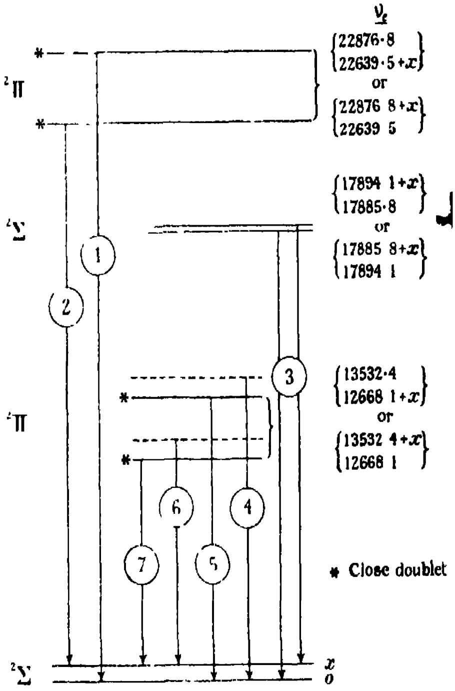

Fig. 2.—LaO Electronic Levels.

### *Note on the Lanthanum Oxide Systems*

In a paper by Jevons (*loc. cit.*) an analysis of the various band systems of LaO has been made. It is of some interest to compare these with the yttrium oxide systems already discussed. As a result of such a comparison our interpretation of the LaO systems is given in fig. 2.

It is clear in the first place that the extensive system 3 of Jevons corresponds to a $^2\Sigma \rightarrow {}^2\Sigma$ transition. The doublet separation of about 8·3ν is not the interval between Q and R heads but between $R_2$ and $R_1$ heads, just as an interval of 3·1ν was found in the analogous system of YO (and an interval of about 1·27ν occurs in ScO).

The " systems " 4, 5, 6 and 7 undoubtedly form the one system corresponding to $^2\Pi \rightarrow {}^2\Sigma$. This possibility was discussed and considered unlikely by Jevons in view of the two Q–R doublet intervals between 4 and 5 and between 6 and 7, being so large as 44ν and 53ν, compared with the supposed Q–R interval of 8ν discussed above. But we have interpreted the latter interval of 8ν differently so that Jevons' objections to Q-R intervals of 44ν and 53ν no longer hold good.

Systems 1 and 2 are considered to be the strong Q heads of a transition from a higher $^2\Pi$ level down to the common ground state $^2\Sigma$. This new level thus has a separation of about 237ν, which is a reasonable value. It is interesting to note that both components of each electronic doublet have a minor doublet separation of approximately 0·5ν. Frl. Querbach observed this in "system" 7 and Kellner and Okubu in systems 1 and 2. This is probably due to the existence of a normal Q branch and a Q-form P or R branch ($^QP$ or $^QR$).

The above interpretations we regard as fairly certain; we mention in conclusion one or two views. These are, of course, tentative only. The ultra-violet bands mentioned by Jevons in his Table IX are thought to be possibly ($^2\Sigma \rightarrow {}^2\Pi$) from a higher $^2\Sigma$ level (in the region 40000–41000ν) to the lowest $^2\Pi$ level. The band groups (*d*) and (*a*) with their continuous spectra of Jevons' Table VII may be the (0, 0) and (1, 0) sequences from this same $^2\Sigma$ level down to the $^2\Sigma$ level which is the initial state of system 3. The associated continuous spectrum is suggestive of molecular dissociation.

## *Summary*

The molecules ScO, YO and LaO are a homologous series having band spectra of considerable similarity. In this paper are given details of the band spectrum of yttrium oxide. About 100 band heads have been measured from plates taken in the first order of a 21-foot grating. These have been assigned to two systems $^2\Pi \rightarrow {}^2\Sigma$ and $^2\Sigma \rightarrow {}^2\Sigma$ having a common ground state. A full vibrational analysis is given, and the molecular constants evaluated for these states within limits of error which are discussed. The band spectra of YO are compared with those of ScO and LaO and on the basis of this comparison an interpretation of the band systems of both molecules is given.

# *The Spark Spectra of Tellurium—Te IV and Te VI.*

By K. R. Rao, D.Sc., Madras Government Research Scholar, Imperial College of Science, London.

(Communicated by A. Fowler, F.R.S.—Received May 12, 1931.)

Plate 7.

## *Introductory*

Of the spectra of the elements of the sixth group of the Periodic Table, our knowledge of the series regularities in the spectra of tellurium appears to be the most meagre. McLennan, McLay and McLeod* have suggested, in part tentatively, a few of the deepest combinations of the arc spectrum, and Gibbs and Vieweg† have discovered the triplets and a few of the singlets of the spectrum of quadruply-ionised tellurium. Besides these, so far as the author is aware, there are no published records of the analysis of the various spectra of this element.

In a former communication‡ the doublet system characteristic of selenium IV has been described. Following this work it was considered that the doublet system of the corresponding spectrum of tellurium of the same chemical group could be easily identified. The present paper gives an analysis, as so far obtained, of the third and fifth spectra of the element.§

Besides the early work, summarised in Kayser's 'Handbuch,' vol. 6, the experimental investigations of the spectrum consist chiefly of two contributions. Lacroute‖ has photographed the spectrum of a discharge through tellurium vapour in the region λ 2300 to λ 1250. L. and E. Bloch¶ have measured the spectrum between λ 7250 and λ 2200 and assigned all the lines to the various stages of ionisation of the element—Te I to Te IV. The general experimental method adopted in the course of the present work was the same as that described in detail in the previous investigations on selenium. The spark spectrum was photographed with a Siegbahn vacuum spectrograph in the region λ 1500 to λ 500 with and without self-inductance. By a close scrutiny of these plates, the lines could be easily assigned to the successive stages of ionisation of the atom The excitation was found to be violent enough to elicit lines up to Te VI. These plates, which were taken by the writer last autumn at Upsala, have since been supplemented by others taken at the Imperial College with large dispersion quartz instruments (Hilger's $E_1$ and $E_2$) in the region λ 4000 to λ 2200. The source used in these latter experiments consisted of a strong discharge through vapour of tellurium. Owing to the higher melting and boiling points of this element, the production of the discharge was found to be more difficult than in the case of selenium. By the use of a large X-ray coil, plates were obtained which indicated that lines of Te IV were easily excited under the conditions of the experiment

---

* 'Phil. Mag.,' vol. 4, p. 486 (1927).

† 'Phys. Rev.,' vol. 34, p. 400 (1929).

‡ K. R. Rao and J. S. Badami, 'Proc. Roy. Soc.,' A, vol. 131, p. 154 (1931).

§ A preliminary report of the results has been published in 'Nature,' vol. 127, p. 236 (1931).

‖ 'J. Physique,' vol. 9, p. 183 (1928).

¶ 'Ann. Physique,' vol. 13, p. 233 (1930).

### *The Spectrum* Te VI.

The spectrum Te VI, being the simplest, is considered first. From theoretical considerations, this should be of the "stripped-atom" type, all the terms being doublets resembling those of Ag I. Following the method of Millikan and Bowen, the deepest combinations of the isoelectronic spectra, Ag I to Sb V,* have been already traced. In extending this scheme further to Te VI, Lang has suggested the following pair .—

$$\begin{array}{lcccc} & & \lambda & \nu & \\ 5s\,S_{\frac{1}{2}} - 5p\,P_{\frac{1}{2}} & = & 1077\cdot91\ (8) & 92772 & \\ & & & & 11988 \\ S_{\frac{1}{2}} - \quad P_{1\frac{1}{2}} & = & 954\cdot57\ (5) & 104760 & \end{array}$$

The present experiments, however, have shown definitely (*cf.* Plate 7) that one of these lines, 1077·91, belongs to Te VI and the other, 954·54, to Te V, both being classified accordingly.†

The new identifications are given in Table I. They are quite unambiguous, the lines being the only selections supported by their behaviour with insertion of self-inductance in series with the vacuum spark.

The irregular doublet law applies quite well to the transitions $5s\,S$—$5p\,P$

---

* Lang, 'Proc. Nat. Acad. Sci.,' vol. 13, p. 341 (1927). In Sb V a modification of the group $5p\,P$—$5d\,D$ has been made later in the light of experimental work, *cf.* Gibbs and others, 'Phys. Rev.,' vol. 34, p. 406 (1929), and also J. S. Badami, 'Phy. Soc. Proc.' (*in course of publication*)

† *Cf.* later section on Te IV, and Gibbs and Vieweg, *loc cit.* on Te V.

### Table I.—Classifications in Te VI.

| Classification | λ (int.) | ν | Δν |
|---|---|---|---|
| $5s\ S_{\frac{1}{2}} - 5p\ P_{\frac{1}{2}}$ | 1071 40 (10) | 93336 | 11815 |
| $S_{\frac{1}{2}} - P_{1\frac{1}{2}}$ | 951 01 (8) | 105151 | |
| $5p\ P_{\frac{1}{2}} - 6s\ S_{\frac{1}{2}}$ | 540 24 (5) | 185103 | 11814 |
| $P_{1\frac{1}{2}} - S_{\frac{1}{2}}$ | 577 07 (6) | 173289 | |
| $5p\ P_{1\frac{1}{2}} - 5d\ D_{1\frac{1}{2}}$ | 752 27 (6) | 132931 | 1644 |
| $P_{1\frac{1}{2}} - D_{2\frac{1}{2}}$ | 743 08 (9) | 134575 | 11814 |
| $P_{\frac{1}{2}} - D_{1\frac{1}{2}}$ | 690 87 (8) | 144745 | |
| $5D_{1\frac{1}{2}} - 6p\ P_{\frac{1}{2}}$ | *1313 90 (3) | 76109 | 4399 |
| $D_{2\frac{1}{2}} - P_{1\frac{1}{2}}$ | 1268 01 (3) | 78864 | 1644 |
| $D_{1\frac{1}{2}} - P_{1\frac{1}{2}}$ | 1242 11 (0) | 80508 | |
| $6s\ S_{\frac{1}{2}} - 6p\ P_{\frac{1}{2}}$ | [2797 13] | [35751] | 4399 |
| $S_{\frac{1}{2}} - P_{1\frac{1}{2}}$ | [2490 66] | [40150] | |

* This member has been suggested by the corresponding one in Sb V located by Mr. Badami (*loc. cit.*) The bracketed lines in the above table are calculated positions

and $5p$ P—5D and also to $5p$ P—$6s$ S, in which there is a change of the total quantum number The data are as follows :—

Irregular Doublet Law Applied to the Transition $5p\ P_{\frac{1}{2}}$—$6s\ S_{\frac{1}{2}}$.

| Spectrum | ν<br>$5p\ P_{\frac{1}{2}} - 6s\ S_{\frac{1}{2}}$ | $\nu' = \nu - 1341\ (z - N)^2$ | Difference | Second difference. |
|---|---|---|---|---|
| Ag I | 13004 | 11663 | 21826 | |
| Cd II | 38853 | 33489 | 24139 | 2313 |
| In III | 69697 | 57628 | 25488 | 1349 |
| Sn IV | 104572 | 83116 | 26376 | 888 |
| Sb V | 143017 | 109492 | 27335 | |
| Te VI | 185103 | 136827 | | |

The doublet intervals in this sequence of spectra give very regular screening constants in the case of $5p$ P term, but they show an irregularity in $5d$ D which has been pointed out previously.*

An approximate estimate of the absolute values of the terms can be made by the use of a simple Rydberg formula applied to the two members of the series $5p$ P—$ms$ S; the limit $5p$ $P_{1\frac{1}{2}}$ thus obtained is 477340 cm.$^{-1}$. Extrapolation from the values of $\sqrt{\nu/R}$ for the spectra Ag I to Sn IV (in which the terms† are derived either from long series of members, or by assuming the $5g$ G term) also leads to an almost equal value, namely, 479340 cm.$^{-1}$. In Table II the terms are evaluated by taking a mean of these two estimates. The largest term, $5s$ $S_{\frac{1}{2}}$ = 583490 cm.$^{-1}$, gives an ionisation potential of about 72·0 volts.

Table II.—Term Values in Te VI.

| Term | Term value | Term | Term value |
|---|---|---|---|
| $5s$ $S_{\frac{1}{2}}$ | 583490 | $6s$ $S_{\frac{1}{2}}$ | 305051 |
| $5p$ $P_{\frac{1}{2}}$ | 490154 | $6p$ $P_{\frac{1}{2}}$ | 269300 |
| $P_{1\frac{1}{2}}$ | 478340 | $P_{1\frac{1}{2}}$ | 264901 |
| $5d$ $D_{1\frac{1}{2}}$ | 345409 | | |
| $D_{2\frac{1}{2}}$ | 343765 | | |

## *The Spectrum* Te IV.

The trebly ionised atom of tellurium, like that of selenium, has three outermost electrons and is iso-electronic with In I, Sn II, Sb III. The chief spectral terms characteristic of this atom are listed in Table III. Except in this table the numeral denoting the multiplicity is omitted

Table III.—Predicted Terms of Te IV

| $4_1$ | $4_2$ | $4_3$ | $4_4$ | $5_1$ | $5_2$ | $5_3$ | $6_1$ | $6_2$ | $6_3$ | Term prefix | Terms |
|---|---|---|---|---|---|---|---|---|---|---|---|
| 2 | 6 | 10 | | 2 | 1 | | | | | $5p$ | $^2$P |
| 2 | 6 | 10 | | 2 | | | 1 | | | $6s$ | $^2$S |
| 2 | 6 | 10 | | 2 | | 1 | | | | $5d$ | $^2$D |
| 2 | 6 | 10 | | 1 | 2 | | | | | $5p^2$ | $^4$P $^2$P $^2$D $^2$S |

---

* K. R. Rao, 'Proc. Phys Soc.,' vol. 29, p 408 (1927); also Lang, *loc. cit.*

† Ag I: Fowler, 'Report.' Cd II: v. Salis, 'Ann der Phys.,' vol. 76, p. 145 (1925). In III and Sn IV: K R. Rao, A. L. Narayan and A. S. Rao: 'Ind. Journ. Phys.,' vol. 2, p. 467 (1928).

The first indication of regularities was the discovery of the recurrence of the frequency interval 9223 cm.$^{-1}$ among the lines which, from an examination of the several plates, could be confidently assigned to Te IV. The separation is what might be expected for $5p\ P_{\frac{1}{2}}$—$5p\ P_{1\frac{1}{2}}$ of Te IV by comparison with that of Se IV or In I, SnII* and Sb III.† The pairs could be easily ascribed to the various combinations among the terms indicated in Table III. The details of the scheme are presented in Table IV in which the wave-lengths above λ 2000, as usual, are in air and the others *in vacuo*, and the intensities are on the scale of 10 for maximum

Table IV.- Classifications in Te IV.

| Classification. | λ (int.) | ν (vac.) | Δν |
|---|---|---|---|
| $5p\ P_{1\frac{1}{2}}$ — $6s\ S_{\frac{1}{2}}$ | 804·92 (7) | 124236 | 9220 |
| $P_{\frac{1}{2}}$ — $S_{\frac{1}{2}}$ | 749·31 (5) | 133456 | |
| $5p\ P_{1\frac{1}{2}}$ — $5d\ D_{1\frac{1}{2}}$ | 845·85 (6) | 118224 | 771 |
| $P_{1\frac{1}{2}}$ — $D_{2\frac{1}{2}}$ | 840·37 (9) | 118995 | 9226 |
| $P_{\frac{1}{2}}$ — $D_{1\frac{1}{2}}$ | 784·62 (8) | 127450 | |
| $5p\ P_{1\frac{1}{2}}$ — $5p^2\ P_{\frac{1}{2}}$ | 910·88 (7) | 109784 | 947 |
| $P_{1\frac{1}{2}}$ — $P_{1\frac{1}{2}}$ | 903·09 (9) | 110731 | 9225 |
| $P_{\frac{1}{2}}$ — $P_{\frac{1}{2}}$ | 840·27 (8) | 119009 | |
| $P_{\frac{1}{2}}$ — $P_{1\frac{1}{2}}$ | 833·64 (7) | 119956 | |
| $5p\ P_{1\frac{1}{2}}$ — $5p^2\ S_{\frac{1}{2}}$ | 996·85 (4) | 100316 | 9220 |
| $P_{\frac{1}{2}}$ — $S_{\frac{1}{2}}$ | 912·94 (6) | 109536 | |
| $5p\ P_{1\frac{1}{2}}$ — $5p^2\ D_{1\frac{1}{2}}$ | 1196·89 (2) | 83550 | 2039 |
| $P_{1\frac{1}{2}}$ — $D_{2\frac{1}{2}}$ | 1168·38 (10) | 85589 | 9222 |
| $P_{\frac{1}{2}}$ — $D_{1\frac{1}{2}}$ | 1077·91 (8) | 92772 | |
| $5p^2\ D_{1\frac{1}{2}}$ — $6p\ P_{\frac{1}{2}}$ | 1458·34 (5) | 68571 | 2619 |
| $D_{2\frac{1}{2}}$ — $P_{1\frac{1}{2}}$ | 1446·11 (6) | 69151 | 2039 |
| $D_{1\frac{1}{2}}$ — $P_{1\frac{1}{2}}$ | 1404·70 (4) | 71190 | |

---

* A. L. Narayan and K. R. Rao, 'Z. Physik,' vol. 45, p. 350 (1927).

† R. J. Lang, 'Phys. Rev.,' vol. 35, p. 445 (1930).

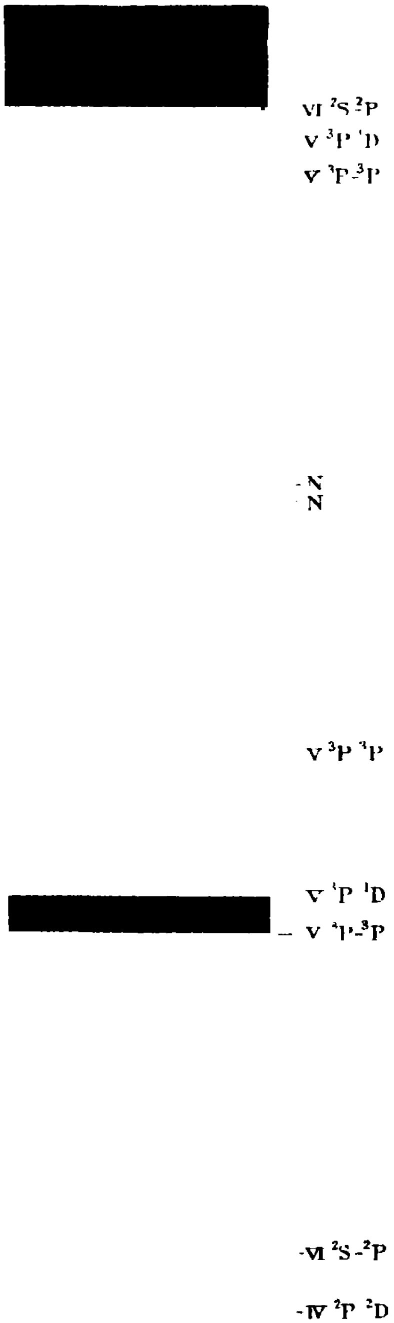

(*b*) (*a*)

Spark spectrum of Tellurium taken with a Siegbahn vacuum spectograph
(*a*) Without inductance, (*b*) with inductance

Table IV—(continued).

| Classification. | λ (int.). | ν (vac.). | Δν. |
|---|---|---|---|
| $6s\,\mathrm{S}_{\frac{1}{2}}$ — $6p\,\mathrm{P}_{\frac{1}{2}}$ | 3585 27 (10) | 27884·0 | 2619·0 |
| $\mathrm{S}_{\frac{1}{2}}$ -- $\mathrm{P}_{1\frac{1}{2}}$ | 3277·43 (10) | 30503 0 | |
| | | | |
| $5d\,\mathrm{D}_{1\frac{1}{2}}$ -- $6p\,\mathrm{P}_{\frac{1}{2}}$ | 2949·47 (10) | 33894·5 | 2619·5 |
| $\mathrm{D}_{2\frac{1}{2}}$ - $\mathrm{P}_{1\frac{1}{2}}$ | 2796·96 (10) | 35742·5 | 771 5 |
| $\mathrm{D}_{1\frac{1}{2}}$ — $\mathrm{P}_{1\frac{1}{2}}$ | 2737·87 (5) | 36514 0 | |
| | | | |
| $6p\,\mathrm{P}_{1\frac{1}{2}}$ -- $6d\,\mathrm{D}_{1\frac{1}{2}}$ | 2564·58 (9) | 38981 0 | 411·4 |
| $\mathrm{P}_{1\frac{1}{2}}$ — $\mathrm{D}_{2\frac{1}{2}}$ | 2537·80 (10) | 39392·4 | 2621·0 |
| $\mathrm{P}_{\frac{1}{2}}$ — $\mathrm{D}_{1\frac{1}{2}}$ | 2403 00 (8) | 41602 0 | |
| | | | |
| $6p\,\mathrm{P}_{\frac{1}{2}}$ — $7s\,\mathrm{S}_{\frac{1}{2}}$ | 2271·80 (5) | 44004 3 | 2619·4 |
| $\mathrm{P}_{1\frac{1}{2}}$ - $\mathrm{S}_{\frac{1}{2}}$ | 2415·63 (7) | 41384·9 | |

There are a few interesting points in the proposed scheme which deserve to be noticed. In this, as in most other spectra of atoms having three outermost electrons, the most predominant pair corresponds to the combination $5p\,\mathrm{D}$—$5p^2\,\mathrm{D}$ which has been the easiest to identify. The satellite $5p\,\mathrm{P}_{1\frac{1}{2}}$—$5p^2\,\mathrm{D}_{1\frac{1}{2}}$ is, however, of relatively very low intensity when compared with what might be expected in a normal $^2\mathrm{P}-{}^2\mathrm{D}$ combination. Of the doublet intervals (*cf.* Table V) of the terms in the In I-like spectra, $5p\,\mathrm{P}_{\frac{1}{2}}$—$5p\,\mathrm{P}_{1\frac{1}{2}}$ and $5p^2\,\mathrm{D}_{1\frac{1}{2}}$—$5p^2\,\mathrm{D}_{2\frac{1}{2}}$ progressively increase with increasing atomic number, but the difference $5d\,\mathrm{D}_{1\frac{1}{2}}$—$5d\,\mathrm{D}_{2\frac{1}{2}}$ is considerably smaller than one might have anticipated in Te IV. It was at first thought that the line λ 830·93 might be alternatively chosen to be $5p\,\mathrm{P}_{1\frac{1}{2}}$—$5d\,\mathrm{D}_{2\frac{1}{2}}$, giving the difference $5d\,\mathrm{D}_{1\frac{1}{2}}$—$5d\,\mathrm{D}_{2\frac{1}{2}}$, a value of 2123 cm.$^{-1}$, which would be in keeping with the other corresponding values But this line is seen to belong to Te V, and such a choice is not supported by the members of the secondary series in the quartz region. A similar irregularity is noticeable also in the Ga I-like spectra and seems to be characteristic of the series of *m*D terms when *m* is small, for the succeeding term intervals are again markedly regular.

With regard to the multiplet $mp\,\mathrm{P}$—$mp^2\,\mathrm{P}$, the Ga I-like spectra show a progressive variation, but in the other group it must be said that this member has only been tentatively suggested in Sn II and the agreement between the members identified in Sb III and Te IV is probably not satisfactory.

Table V.—Doublet Intervals in In I-like and Ga I-like Spectra.

| Spectrum. | $5p\ \mathrm{P}_{\frac{1}{2}}-5p\ \mathrm{P}_{1\frac{1}{2}}$. | $5p^2\ \mathrm{D}_{1\frac{1}{2}}-5p^2\ \mathrm{D}_{2\frac{1}{2}}$ | $5d\ \mathrm{D}_{1\frac{1}{2}}-5d\ \mathrm{D}_{2\frac{1}{2}}$. | $6d\ \mathrm{D}_{1\frac{1}{2}}-6d\ \mathrm{D}_{2\frac{1}{2}}$. | $5p^2\ \mathrm{P}_{\frac{1}{2}}-5p^2\ \mathrm{P}_{1\frac{1}{2}}$. |
|---|---|---|---|---|---|
| In I | 2212 6 | — | 23 5 | 49·9 | — |
| Sn II | 4247 | 625 5 | 647 4 | 113 1 | — |
| Sb III | 6576 | 1270 | 1567 | 237 | 5392 |
| Te IV | 9223 | 2039 | 771 | 411 4 | 947 |
| | $4p\ \mathrm{P}_{\frac{1}{2}}-4p\ \mathrm{P}_{1\frac{1}{2}}$. | $4p^2\ \mathrm{D}_{1\frac{1}{2}}-4p^2\ \mathrm{D}_{2\frac{1}{2}}$. | $4d\ \mathrm{D}_{1\frac{1}{2}}-4d\ \mathrm{D}_{2\frac{1}{2}}$. | $5d\ \mathrm{D}_{1\frac{1}{2}}-5d\ \mathrm{D}_{2\frac{1}{2}}$. | $4p^2\ \mathrm{P}_{\frac{1}{2}}-4p^2\ \mathrm{P}_{1\frac{1}{2}}$. |
| Ga I | 826 | — | 6 0 | 8 4 | — |
| Ge II | 1764 | 169 0 | 176 4 | 42 0 | 1107 |
| As III | 2940 | 321 | 91·2 | 84 5 | 1487 |
| Se IV | 4376 | 496 | 388 9 | 151 7 | 2220 |

### *Term Values.*

Two members of each of the diffuse and sharp series are available for an evaluation of the absolute term values. The limits for these series are :—

(1) Diffuse series—

$$6p\ \mathrm{P}_{1\frac{1}{2}}-5d\ \mathrm{D}_{2\frac{1}{2}} = -\ 35742{\cdot}5$$
$$-6d\ \mathrm{D}_{2\frac{1}{2}} = \quad 39392{\cdot}4$$
$$\text{limit } 6p\ \mathrm{P}_{1\frac{1}{2}} = 141417.$$

(2) Sharp series—

$$6p\ \mathrm{P}_{1\frac{1}{2}}-6s\ \mathrm{S}_{\frac{1}{2}} = -\ 30503{\cdot}0$$
$$-7s\ \mathrm{S}_{\frac{1}{2}} = \quad 41384{\cdot}9$$
$$\text{limit } 6p\ \mathrm{P}_{1\frac{1}{2}} = 140846.$$

The agreement between the limits is very close. In Table VI a mean value of 141132 cm.$^{-1}$ has been adopted for $6p\ \mathrm{P}_{1\frac{1}{2}}$ on which the remaining terms are based.

Table VI.—Term Values in Te IV.

| Term | Term value. | Term | Term value. |
|---|---|---|---|
| $5p\ \mathrm{P}_{\frac{1}{2}}$ | 305091 | $6d\ \mathrm{D}_{1\frac{1}{2}}$ | 102149·6 |
| $\mathrm{P}_{1\frac{1}{2}}$ | 295868 | $\mathrm{D}_{2\frac{1}{2}}$ | 101738·2 |
| $5d\ \mathrm{D}_{1\frac{1}{2}}$ | 177646 0 | $5p^2\ \mathrm{D}_{1\frac{1}{2}}$ | 212319 |
| $\mathrm{D}_{2\frac{1}{2}}$ | 176874·5 | $\mathrm{D}_{2\frac{1}{2}}$ | 210280 |
| $6s\ \mathrm{S}_{\frac{1}{2}}$ | 171635 0 | $\mathrm{S}_{\frac{1}{2}}$ | 195555 |
| $6p\ \mathrm{P}_{\frac{1}{2}}$ | 143751·6 | $\mathrm{P}_{\frac{1}{2}}$ | 186082 |
| $\mathrm{P}_{1\frac{1}{2}}$ | 141132 0 | $\mathrm{P}_{1\frac{1}{2}}$ | 185135 |
| $7s\ \mathrm{S}_{\frac{1}{2}}$ | 102366·7 | | |

Comparison* with the term values of In I, Sn II, Sb III and Te IV (Table VII) shows that the error in the adopted values of Te IV probably does not exceed about 3000 cm.$^{-1}$.

Table VII.—Comparison of Term Values in In I-like Spectra.

| Spectrum. | $5p\ \mathrm{P}_{\frac{1}{2}}$ | $6p\ \mathrm{P}_{\frac{1}{2}}$. | $6s\ \mathrm{S}_{\frac{1}{2}}$. | $5d\ \mathrm{D}_{1\frac{1}{2}}$ | $6d\ \mathrm{D}_{1\frac{1}{2}}$ | $5p^2\ \mathrm{D}_{1\frac{1}{2}}$. |
|---|---|---|---|---|---|---|
| In I | 46668 | 14811 | 22295 | 13775 | 7620 | — |
| Sn II | 29420 | 11540 | 15192 | 11572 | 6854 | 14712 |
| Sb III | 22252 | 9506 | 11924 | 11272 | 6176 | 13749 |
| Te IV | 19068 | 8984 | 10727 | 11103 | 6384 | 13270 |

The largest term, $5p^2\ \mathrm{P}_{\frac{1}{2}} = 305091$ cm.$^{-1}$, leads to an ionisation potential of about 37·7 volts for Te IV.

## *Summary.*

The spark spectrum of tellurium has been examined by means of a vacuum grating spectrograph in the region λ 1500 to λ 500 with and without inductance; photographs have also been taken with quartz instruments of discharges through tellurium vapour in capillary tubes.

With the aid of these data, the doublet system of Te IV has been identified and a term scheme has been suggested, by applying a Rydberg formula (with 16R constant) to two members of each of the sharp and diffuse secondary series. The largest term, $5p\ \mathrm{P}_{\frac{1}{2}} = 305091$ cm.$^{-1}$, gives an ionisation potential of about 37·7 volts for Te IV.

Three pairs with $\Delta\nu = 11814$ cm.$^{-1}$ have also been identified as being the combinations between the deep $5s$ S, $5p$ P, $5d$ D and $6s$ S terms of Te VI. An approximate term scheme is proposed. The ionisation potential is found to be about 72·0 volts.

---

[*] It may not be out of place here to hazard a suggestion regarding the term values in Sb III. It is evident from Table VII that while $5d\ \mathrm{D}_{1\frac{1}{2}}$ terms gradually diminish in passing from In I to Te IV, the terms $6d\ \mathrm{D}_{1\frac{1}{2}}$ show an irregularity (if the terms in Te IV are correctly estimated). It might be more plausible to assume such irregularities in the D terms of lower rather than of higher total quantum number. The writer is, therefore, tempted to suggest an increase of about 3000 cm.$^{-1}$ in the term values of Sb III. This change would shift the irregularity to the $5d$ D terms and the scheme then compares very favourably with the corresponding sequence in Ga I-like spectra (Rao and Badami, *loc. cit.*). This would also make the $5g$ G term in Sb III more hydrogenic, while the term calculated by Lang ($5g$ G = 35966) is perhaps a little too low and shows a rather large departure.

As already mentioned, the present work was started at Upsala in the laboratory of Professor M. Siegbahn and completed at the Imperial College in the laboratory of Professor A. Fowler. The writer desires to express his very sincere and grateful thanks to them for their kind and stimulating interest and encouragement. He is indebted to the Andhra University and the Madras Government for the award of a scholarship.

---

## *The Theory of the Effect of Resonance Levels on Artificial Disintegration.*

By N. F. Mott, M.A., Fellow of Gonville and Caius College, Cambridge.

(Communicated by P. A. M. Dirac, F.R.S.—Received May 14, 1931.)

### *Section* 1.—*Discussion of previous Investigations.*

According to the theory first proposed by Gamow, and by Gurney and Condon, the emission of $\alpha$-particles by radio active nuclei is to be explained by the assumption that there exists in the nucleus a " virtual " level of positive energy, which is occupied by an $\alpha$-particle. According to the wave mechanics, such levels are necessarily unstable, and there exists a definite probability that the $\alpha$-particle will escape in a given interval of time. The theory has been discussed by a great many authors; we shall need to refer in particular to the calculations of Fowler and Wilson,* who have given the exact wave function that describes the emission from a simplified one-dimensional nucleus.

We shall need the following result, which may be found in Fowler and Wilson's paper or elsewhere. Let $\tau$ be the natural period of the $\alpha$-particle in the nucleus, *i.e.*, the time taken for a particle moving with velocity of about $10^9$ cm./sec. to travel a distance of about $3 \times 10^{-13}$ cm., so that

$$\tau \sim 10^{-22} \text{ seconds.}$$

Let T be the time of decay of an $\alpha$-particle in a given level. Let us define a quantity $\zeta^2$ by the equation

$$\zeta^2 = \mathrm{T}/\tau.$$

---

* 'Proc. Roy. Soc.,' A, vol. 124, p. 493 (1929).

Then the α-particles emitted by the nucleus will have their energies distributed in a range ΔE given by

$$\frac{\Delta E}{E} \sim \frac{1}{\zeta^2}. \tag{1}$$

The quantity $\zeta^2$ is thus a measure of the breadth of the virtual level.

Now it was first pointed out by Gurney* that there might exist in the lighter nuclei similar virtual energy levels that are *not* normally occupied by an α-particle, and that if a nucleus were bombarded by α-particles having just the energy of one of these levels, the probability that an α-particle would penetrate into the nucleus would be much greater than would be the case for α-particles of other energies. It would follow that the number of H-particles produced should show strong maxima for certain velocities of the incident α-particle. It is, of course, supposed that these virtual levels are much broader than those that occur in the radioactive nuclei, the quantity $\zeta^2$ being, perhaps, of the order of magnitude 50; for a radioactive element $\zeta^2$ is $10^{20}$ or $10^{30}$. Recently the existence of such "resonance" levels has been demonstrated by Pose, who finds levels in aluminium at $3 \cdot 9 \times 10^6$ and $4 \cdot 8 \times 10^6$ volts. The breadth of these levels is not known; we shall make an estimate of it in section 4.

In this paper we shall be concerned with the effect that the resonance levels may be expected to have on the artificial disintegration and on the anomalous scattering. We shall express our results in terms of cross sections, calculating the effective area that an α-particle must hit to eject a proton, being itself captured, and the area that it must hit in order that it shall be scattered into a given solid angle $d\omega$.

We shall denote the cross section for capture by $a$ (E), and the cross section for scattering into a solid angle $d\omega$ by $I_\theta \, d\omega$. We shall investigate the circumstances under which a resonance level should occur, and estimate its breadth ΔE. We shall find an expression (equation (15)) for the maximum value of $a$ (E) within the resonance level. We shall also investigate the deviations of $I_\theta$ from the inverse square form, $(ZZ'\varepsilon^2/2mv^2 \sin^2 \frac{1}{2}\theta)^2$, that are to be expected for energies of the incident α-particle lying in the resonance range. None of the results of this paper depend on the form assumed for the interaction between the α-particle and the proton.

The effect of resonance levels on artificial disintegration has been considered by Fowler and Wilson,† Atkinson,‡ and Guido Beck.§ The first two authors discuss a one-dimensional nucleus, and they consider only the probability that the $\alpha$-particle will be captured, *i e*, that it will remain in the nucleus after collision for a time comparable with the time of decay. They do not investigate the probability of a transference of energy from the $\alpha$-particle to a proton. They find that if the $\alpha$-particle has energy equal to a resonance level of the nucleus, the probability of capture is of the order of magnitude unity; otherwise it is negligible. They do not generalise their results to apply to three degrees of freedom.

---

* 'Nature,' vol. 123, p. 565 (1929).

† *Loc. cit.*

‡ 'Z. Physik,' vol. 64, p. 507 (1930).

§ 'Z. Physik,' vol. 64, p. 22 (1930).

Beck has investigated the probability that the $\alpha$-particle should lose energy to a proton, and thus be captured into a stable level. He assumes a Coulomb interaction between the $\alpha$-particle and the proton, and obtains the probability for capture by treating this interaction as small. This method, however, gives misleading results unless the interaction energy is very small, as we shall see in this paper.

### *Section* 2.

We shall now consider what will happen when a beam of $\alpha$-particles falls on a nucleus. Let the potential energy $V(r)$ of the $\alpha$-particle in the field of the nucleus be a function of the usual type, giving Coulomb repulsion at large distances and attraction at small distances. We assume that this field has a virtual level $E_0$ of breadth* $E_0/\zeta^2$. We assume that for energies just above and below this range the chance of penetration is negligible. We assume further that $E_0$ is the energy of an S level, *i.e*, that the wave function associated with it is spherically symmetrical.

Let us consider first what will happen if the $\alpha$-particle has not enough energy to eject a proton, or to knock it into an excited state. Then, since all particles eventually escape, all that could be observed would be anomalous scattering. This we shall now investigate.

The wave equation for an $\alpha$-particle in the field $V(r)$ is

$$\nabla^2\psi + \frac{8\pi^2 m}{h^2}(E - V)\psi = 0. \tag{2}$$

The general solution of (2) is

$$\psi = \sum_{n=0}^{\infty} A_n P_n(\cos\theta) L_n(r), \tag{3}$$

where the $A_n$ are arbitrary constants, and $L_n$ is the solution, bounded at the origin, of

$$\frac{d^2L}{dr^2} + \frac{2}{r}\frac{dL}{dr} + \left\{\frac{8\pi^2 m}{h^2}(E - V) - \frac{n(n+1)}{r^2}\right\} L = 0. \tag{4}$$

---

* The order of magnitude of $\zeta^2$ may be about 100.

The constants $A_n$ must be chosen so that (3) represents an incident wave of unit amplitude, together with a scattered wave. This can be done by the method of Faxén and Holtzmark* for any given field V ($r$).

For the case of the Coulomb field, when V ($r$) is equal to $ZZ'\epsilon^2/r$, the constants $A_n$ have been found by Gordon.† We shall need certain of his results, and give them here, writing $L_n{}^c$, $A_n{}^c$, etc., for the forms that these functions take for this particular V ($r$). If $L_n{}^c(r)$ be suitably normalised, it has the asymptotic form

$$L_n{}^c(r) \sim r^{-1}\cos(kr - (n+1)\pi/2 - \alpha\log 2kr + \sigma_n), \tag{5}$$

where

$$k = 2\pi mv/h = 2\pi\sqrt{2mE}/h,$$

$$\alpha = 2\pi ZZ'\epsilon^2/hv = \frac{2Z}{137}\frac{c}{v},$$

$$\sigma_n = \arg\Gamma(i\alpha + n + 1).$$

Gordon finds for $A_n{}^c$

$$A_n{}^c = \frac{1}{k} i^n (2n+1) e^{i\sigma_n} \tag{6}$$

and finds for (3) a wave function $\psi^c$ with the asymptotic form

$$\psi^c \sim I + f^c(\theta) S,$$

where I the incident wave is given by

$$I = \exp(ikz + i\alpha\log k(r-z))$$

and for the scattered we have

$$S = \exp(ikr - i\alpha\log 2kr)$$

$$f^c(\theta) = \frac{2Z\epsilon^2}{2mv^2}\operatorname{cosec}^2\tfrac{1}{2}\theta \,.\, \exp(-i\alpha\log\sin^2\tfrac{1}{2}\theta + 2i\sigma_0 + i\pi).$$

Now if E does not lie in the neighbourhood of $E_0$, then the solution of the equation (4) for the actual nuclear field V ($r$) will be practically the same as for a Coulomb field. If, on the other hand, E lies in the resonance range, then this will still be the case, except when $n = 0$. This follows from our assumption that the virtual level is an S level. If we denote the solution of (4) for the case $n = 0$ by $L_0{}^N(r)$, then the asymptotic form of $L_0{}^N(r)$ will be

$$L_0{}^N(r) \sim r^{-1}\cos(kr - \tfrac{1}{2}\pi - \alpha\log 2kr + P + \sigma_0),$$

where P is some function of E that depends on the precise form of V($r$), and which becomes zero outside the resonance range. The wave function corresponding to (3) that describes the scattering will be

---

* Faxén and Holtzmark, 'Z. Physik,' vol. 45, p. 307 (1927).

† Gordon, 'Z. Physik,' vol. 48, p. 180 (1928).

$$\psi^{\mathrm{N}} = \mathrm{A}_0{}^{\mathrm{N}}\,\mathrm{L}_0{}^{\mathrm{N}}(r) + \sum_{n=2}^{\infty} \mathrm{A}_n{}^c\,\mathrm{L}_n{}^c\,\mathrm{P}_n(\cos\theta), \tag{7}$$

where $\mathrm{A}_0{}^{\mathrm{N}}$ is a constant which must be chosen so that $\psi^{\mathrm{N}}$ represents an incident wave and a scattered wave. From (7) we obtain

$$\psi^{\mathrm{N}} = \psi^c - \mathrm{A}_0{}^c\,\mathrm{L}_0{}^c + \mathrm{A}_0{}^{\mathrm{N}}\,\mathrm{L}_0{}^{\mathrm{N}}.$$

Since $\psi^c$ denotes an incident wave and a scattered wave, we must choose $\mathrm{A}_0{}^{\mathrm{N}}$ so that

$$\mathrm{A}_0{}^{\mathrm{N}}\,\mathrm{L}_0{}^{\mathrm{N}} - \mathrm{A}_0{}^c\,\mathrm{L}_0{}^c$$

represents a scattered wave only. This gives

$$\mathrm{A}_0{}^{\mathrm{N}} = e^{\mathrm{P} + i\sigma_0}/k,$$

and for the scattered wave

$$\left\{f^c(\theta) + \frac{1}{2ik}\left[e^{2i\mathrm{P}} - 1\right]\right\}\mathrm{S}. \tag{8}$$

The scattered intensity is given by the square of the modulus of this, and is most conveniently expressed as the ratio of the scattered intensity to the intensity given by the Rutherford formula; we obtain for this ratio

$$\left\{\cos(\alpha\log\sin^2\tfrac{1}{2}\theta) - \frac{1}{\alpha}\sin^2\tfrac{1}{2}\theta\sin 2\mathrm{P}\right\}^2 + \left\{\sin(\alpha\log\sin^2\tfrac{1}{2}\theta) + \frac{1}{\alpha}\sin^2\tfrac{1}{2}\theta\,(1-\cos 2\mathrm{P})\right\}^2$$

where

$$\alpha = \frac{2\pi\,.\,2\mathrm{Z}\epsilon^2}{h\mathrm{V}} = \frac{2\mathrm{Z}}{137}\,\frac{c}{v},$$

For scattering* at 180°, this takes the simple form

$$\left\{1 - \frac{1}{\alpha}\sin 2\mathrm{P}\right\}^2 + \left\{\frac{1}{\alpha}(1-\cos 2\mathrm{P})\right\}^2.$$

Although it is not possible, for a given value of the energy E of the incident $\alpha$-particle, to calculate the phase P unless we know the exact form of $\mathrm{V}(r)$, it is easy to see that as E passes over the range in which there is resonance, P increases through an amount equal to $\pi$. This may be seen as follows. Let $f_1$, $f_2$ be two solutions of (4) (for the case $n = 0$) in the region where $\mathrm{V} > \mathrm{E}$. Let $f_1$ be the solution that *decreases* as $r$ increases, and $f_2$ a solution that increases exponentially; both solutions are taken everywhere positive in the region considered. Such solutions clearly exist.

---

* The recoil of the nucleus is neglected.

Now let us integrate (4) outwards. If we take E equal to $E_0$, then in the range $V > E$, the solution will be $Af_1$. For any other value of E, it will be of the form

$$A(f_1 + af_2). \tag{9}$$

It is clear that as E passes through the value $E_0$, $a$ changes sign; it is further clear that for $E < E_0$, $a$ is positive and for $E > E_0$, $a$ is negative.

Now let us consider the wave function outside the nucleus, it will have the form of a sine curve, and to find the phase, we have to fit it on to the solution (9) at the point where $E - V$ becomes positive. If E is not near to $E_0$ (*i.e.*, not in the resonance range) $af_2$ will be very much greater than $f_1$. Thus the wave function for values of E slightly less than $E_0$, but not in the resonance range, is equal and opposite to the wave function for E slightly greater than $E_0$. In other words, as E increases through the resonance range, P increases from 0 to $\pi$.

We can thus form an idea of the form of the anomalous scattering curve in the neighbourhood of a resonance level, if artificial disintegration does not take place. Unfortunately, the anomalous scattering has not been investigated experimentally for any element that cannot be disintegrated, except H and He, in which cases it is not likely that there would be a resonance level. Fig. 1

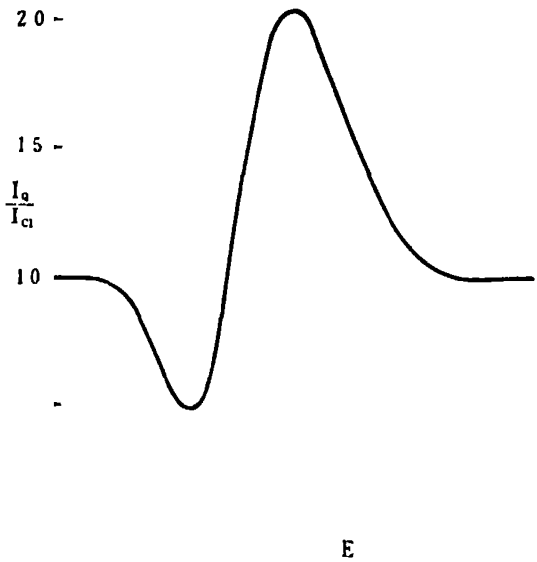

FIG. 1.

shows the type of curve that should occur. The scattering at 180°, divided by the inverse square law value is plotted against E. We have taken $Z = 8$ (oxygen) and $v = 1 \cdot 5 \times 10^9$ cm/sec. The breadth of the whole curve will depend on the breadth of the resonance level. We do not suggest that there actually is a virtual level in oxygen for this energy.

It might be thought that it would be incorrect to treat the scattering in this way, because we have assumed that the wave is in a steady state, and the time taken to reach a steady state is comparable with $T = \zeta^2\tau$ (the time of decay from the level considered), and this is much greater (say 100 times) than the time taken for the $\alpha$-particle to pass the nucleus. The objection is not valid. If the energy of the $\alpha$-particle is known with an error much less than the breadth of level, so that our scattering formula can be applied, then the position of the $\alpha$-particle is described by a wave packet of so great a length that the time taken for it to pass the nucleus is much greater than T, so that after a time shorter than this we may consider the wave to be in a steady state.

### *Section* 3.

We now pass on to the case when the proton can be knocked out of the nucleus. Let us denote by $\mathbf{r}$, or by $r\theta\phi$, the position of the $\alpha$-particle in the nucleus, and by $\mathbf{r}'$ the position of the proton. Let us further denote by $\psi(r')$ the wave function that describes a proton bound in the nucleus, and by $\chi(r)$ the wave function that describes the $\alpha$-particle in the stable state into which it is supposed to fall. Let $2\pi/k$, $2\pi/k'$ denote the wave-lengths of the incident $\alpha$-particles and the emitted protons respectively. Then to describe the collision we want a wave function with the following asymptotic form:

$$[1 + f(0)\, r^{-1} e^{ik\rho}]\, \psi(r') + cr'^{-1} e^{ik'\rho'} \chi(r). \tag{10}$$

Here $k\rho$ is written for $kr - i\alpha \log kr$, etc. With this wave function $|f(0)|^2 d\omega$ is the effective cross section for scattering into a solid angle $d\omega$, and $4\pi \dfrac{k'}{k} |c|^2$ is the effective cross section for disintegration. These are what we want to find.

As before, it is only particles of zero angular momentum (*i.e.*, those described by the first term of (3)), that are affected by the resonance level. All but the first term of (3) must be multiplied by $\psi(r')$ simply; the first term must be replaced by a solution $\Psi$ of the (unknown) wave equation for $\alpha$-particle and proton; for large $r$ or $r'$ this solution must have the form

$$\Psi(\mathbf{r}, \mathbf{r}') \sim D\,[r^{-1}(b\, e^{ik\rho} + e^{-ik\rho})\, \psi(r') + dr'^{-1} e^{ik'\rho'} \chi(r)], \tag{11}$$

*b* and *d* depend on the wave equation ; D is arbitrary and must be chosen as follows. In order that (10) shall be of the required form,

$$\Psi(\mathbf{r}, \mathbf{r}') - \mathrm{L}_0{}^c(r)\,\psi(r')$$

must represent outgoing waves only. That means that it must contain no term of the type $r^{-1}e^{-ik\rho}$. This determines D. We obtain

$$\mathrm{D} = -\mathrm{A}_0{}^c e^{-i\sigma_0}/2i = -1/2ik. \tag{12}$$

Further, for the cross section for capture we have, since by (10) and (11), *c* is equal to D*d*

$$a(\mathrm{E}) = 4\pi\frac{k'}{k}|\mathrm{D}d|^2.$$

Now (11) is a solution of the wave equation for the α-particle and the proton in the field of the nucleus, although it is not the particular solution that describes the physical process, the incident α-particle not being represented by a plane wave. (11) describes a spherical wave of α-particles converging on the nucleus, a reflected wave, and an outgoing proton wave Since (11) is a solution of the wave equation, it is subject to the conservation theorem ; the number of α-particles falling on the nucleus, *minus* the number of particles reflected, is equal to the number of protons emitted. That is to say,

$$4\pi|\mathrm{D}|^2\{1 - |b|^2\} = 4\pi|d|^2\frac{k'}{k}|\mathrm{D}|^2. \tag{13}$$

Now this gives us an upper limit to the number of protons that can be emitted ; for the right-hand side of equation (13) is the number of protons actually emitted, or more exactly the effective cross section that must be struck for disintegration. The left-hand side of (13) has no simple physical interpretation, since it refers to just one component of a plane wave. D is, however, known ; thus we can give the right-hand side an upper limit which it reaches when $b = 0$. We see that the effective cross section for capture, *a* (E) cannot be greater than

$$4\pi|\mathrm{D}|^2 = \pi/k^2 = \lambda^2/4\pi, \tag{14}$$

where λ is the wave-length of the α-particle. It is to be remembered that this result applies only when the energy of the α-particle lies within the resonance range. The cross section for capture does *not* therefore increase indefinitely for increasing sharpness of the resonance level.

If the level is not an S level, but one with azimuthal quantum number *n*, (14) must be replaced by

$$a(\mathrm{E}) \leqslant (2n + 1)\lambda^2/4\pi. \tag{15}$$

For comparison we state here that the effective area that must be hit for scattering through an angle greater than 90° is, with Coulomb forces

$$\left(\frac{2Ze}{137v}\right)^2 \frac{\lambda^2}{4\pi}.$$

We must now consider under what circumstances the quantity $a$ (E) is likely to attain, for some value of E in the neighbourhood of the resonance level, the maximum value (15). We shall obtain the result, that if the interaction energy between the proton and the $\alpha$-particle is large, then, provided that energetic relations allow of a proton being expelled at all, $a$ (E) will only show a broad and weak maximum, and never rise to a value approaching (15). The condition that $a$ (E) should show a sharp maximum and approach the value (15) is that the average value of the interaction energy between the $\alpha$-particle and the proton, for all positions of the $\alpha$-particle in the nucleus, should be small, of the order of magnitude of $E/\zeta$, where E is the energy of the $\alpha$-particle. If the interaction is greater than this, the maximum of $a$ (E) becomes broad and weak, if it becomes less, then the maximum remains sharp, but does not rise to the value (15).

The reason for this is that the breadth of the resonance level is inversely proportional to the time that the $\alpha$-particle stays in that level. If the interaction between the $\alpha$-particle and the proton is large, this time will be determined more by the probability of the $\alpha$-particle dropping into a stable level than by the probability of the $\alpha$-particle escaping. Therefore, the breadth of the resonance level will be very much greater than $E/\zeta^2$.

This may be proved as follows. We shall make calculations using the potential field shown by the line SABCDER in fig. 2, though our results are true for any other field of the usual type assumed for a nucleus. It will simplify our argument if we assume that $\psi(r')$, the wave function for a proton bound in the nucleus, vanishes outside a sphere of radius OA, OA being less than OB in fig. 2. We shall also assume that for distances greater than OA the forces acting on the proton are negligible. Both these assumptions could be dispensed with, but their introduction shortens the proof.

Consider the function $\Psi(\mathbf{r}, \mathbf{r}')$ (equation (11)) that describes an incident spherical wave falling on the nucleus, a reflected wave and an outgoing proton wave. If $r$ or $r'$ lies in the region AB, then $\Psi$ will have the form

$$G\,[r^{-1}\,(\beta\, e^{ikr} + e^{-ikr})\,\psi(r') + r'^{-1}\,\delta\, e^{ik'r'}\,\chi(r)].$$

G must be so chosen so that for large $r$, outside the potential barrier, the amplitude of the incident wave is $-1/2ik$—*cf.* equation (12). G therefore depends on the height of the potential barrier, *i.e.*, on $\zeta$. $\beta$ and $\delta$, however, do not depend on the height of the potential barrier, but only on the interaction between the $\alpha$-particle and the proton. They are connected by an equation similar to (13), namely,

$$1 - |\beta|^2 = \frac{k'}{k} |\delta|^2.$$

If the interaction is small, $|\delta|$ is small; if it is large, $|\delta|$ is of order of magnitude unity. $a$ (E) is equal to

$$4\pi k'/k \, |G\delta|^2.$$

We shall now show that unless $\delta$ is small, G must be small, and so $a$(E) is much less than (15); but that for a certain optimum small value of $\delta$, $a$(E) may approach this value.

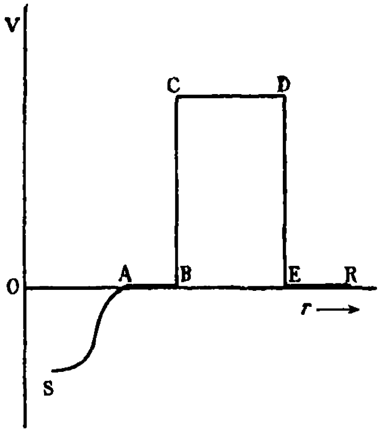

Fig. 2.

Let us denote the length OB by $R_1$ and the length OE by $R_2$. The height BC of the potential wall will be denoted by K.

To find G we have only to write down the forms of the $\alpha$-particle wave in $\Psi(\mathbf{r}, \mathbf{r}')$ in the three regions AB, BE and ER, and put in the boundary conditions, that the function and its differential coefficient must be continuous at B and E. We have for this wave,

$$\begin{array}{ll} r^{-1} G (\beta e^{ikr} + e^{-ikr}) & r < R_1, \\ r^{-1} (pe^{\gamma r} + qe^{-\gamma r}) & R_1 < r < R_2 \\ -r^{-1}/2ik \, . \, (be^{ikr} + e^{-ikr}) & R_2 < r. \end{array}$$

Here

$$\gamma^2 = 8\pi^2 m\,(\mathrm{K} - \mathrm{E})/h^2.$$

$p$, $q$ are constants; for $b$ see equation (11).

Solving for G as a function of $k$, $\gamma$ and $\beta$ we obtain

$$|\,\mathrm{G}\,| = \frac{2\zeta/\gamma}{(1 + k^2/\gamma^2)\,|\,\zeta^2(\beta' + e^{-i\alpha}) - (\beta' + e^{i\alpha})\,|}$$

where

$$e^{i\alpha} = (1 + ik/\gamma)/(1 - ik/\gamma), \qquad \beta' = \beta e^{2ikR_1},$$

and $\zeta$ denotes $e^{\gamma(R_2 - R_1)}$, the (large) constant that determines the time taken for an $\alpha$-particle to escape from the nucleus.

It will be seen that G is small, of the order of magnitude of $\zeta^{-1}$, unless $|\,\beta' + e^{-i\alpha}\,|$ is small. But this implies that $|\,\beta\,|$ is nearly equal to unity, and thus that $|\,\delta\,|$ is much less than unity. Thus resonance can only occur if the interaction between the $\alpha$-particle and the proton is small.

Let us consider the case when $|\,\beta\,|$ is nearly equal to unity, so that resonance can occur. We put $\beta'$ equal to $(1 - \varepsilon)\,e^{i\pi - i\alpha}$, $\varepsilon$ being real and small. Then to a sufficient approximation we have for $|\,\mathrm{G}\,|$,

$$|\,\mathrm{G}\,| = \frac{2\zeta/\gamma}{1 + k^2/\zeta^2}\,|\,\varepsilon\zeta^2 + 1 - e^{2i\alpha}\,|^{-1}$$

and for $|\,\delta\,|$,

$$\frac{k'}{k}\,|\,\delta\,|^2 = 2\varepsilon$$

For $a\,(\mathrm{E})$ we have, therefore,

$$a\,(\mathrm{E}) = \frac{8\lambda^2}{\pi}\left|\frac{k/\gamma}{1 + k^2/\gamma^2}\right|^2 \frac{\varepsilon\zeta^2}{(\varepsilon\zeta^2 + 1 - \cos 2\alpha)^2 + \sin^2 2\alpha}.$$

It is clear that if $\varepsilon \sim \zeta^{-2}$ then this function is of order of magnitude $\lambda^2$; otherwise it is much smaller. Thus for resonance we must have $\delta$ of order of magnitude $\zeta^{-1}$.

If this theory of the resonance levels is correct, it is difficult to reconcile the results of Pose, who finds quite sharp resonance levels in Al, with the results of experiments on $\alpha$-particles of sufficient energy to pass over the top of the potential wall. These latter experiments show that $a\,(\mathrm{E})$ is of the order of magnitude of the cross section of the nucleus. Thus the interaction between the $\alpha$-particle and proton must be large. To explain the occurrence of resonance levels, on the other hand, one must assume that for rather lower energies of the $\alpha$-particle, this interaction is small. This seems difficult to explain.

We shall now investigate the anomalous scattering of α-particles for energies near a resonance level, assuming that all the α-particles that go in are captured, so that $a\,(\mathrm{E})$ rises to its maximum value. Actually this may not be the case For the amplitude of the scattered wave in (10) we have, if the level is of angular momentum $n$,

$$f\,(\theta) = f^c\,(\theta) - (2n+1)\,e^{2i\sigma_n}/2ik.$$

We have, therefore, that the ratio of the number scattered to the number given by the inverse square law formula should *rise* to the value

$$1 + (2n+1)^2/\alpha^2, \qquad \alpha = \frac{2\mathrm{Z}}{137}\,\frac{c}{v}.$$

This formula refers to scattering at 180°. The scattering at other angles may be found in the same way.

### *Section* 4.—*Comparison with Experiment.*

From the number of protons (10 per $10^6$) observed by Pose, and our expression for the maximum value possible for $a\,(\mathrm{E})$, we can form an estimate of the minimum breadth that the levels in aluminium can have.

We first require an expression for the number of protons produced per million α-particles. Let $a\,(\mathrm{E})$ be the effective cross section that an α-particle of energy E must hit in order to eject a proton. Then the probability that an α-particle will eject a proton, while travelling a distance $dx$ through a substance containing $n$ atoms per unit volume is

$$n\,a\,(\mathrm{E})\,dx.$$

The probability $p$ therefore that it will produce a proton during the whole length of its path is

$$p = n\int_{v_0}^{0} a\,(\mathrm{E})\,\frac{d\mathrm{X}}{dv}\,dv,$$

$v_0$ being the initial velocity of the α-particle. Now if $x_0$ be the total distance that the α-particle travels, we have, by the Thomson-Whiddington law

$$v^3 = k\,(x_0 - x),$$

and therefore

$$p = \frac{n}{k}\int_0^{v_0} a\,(\mathrm{E})\,3v^2\,dv. \tag{16}$$

Now $n/k$ is independent of the number of atoms per unit volume, and is proportional to the atomic stopping power of the substance in question. For Al we have

$$n/k = 3{\cdot}35 \times 10^{-8}.$$

From (16), therefore, we obtain the number of protons per particle. Pose finds about 10 protons per $10^8$ α-particles. (16) must, therefore, be equated to $10^{-7}$. We obtain

$$\int_0^{v_0} a(\mathrm{E})\, v^2\, dv \sim 0\cdot 9. \tag{17}$$

Now if we assume that $a(\mathrm{E})$ is equal to $\lambda^2/4\pi$ in a range of velocities $\Delta v$ and zero elsewhere, (17) may be replaced by $v^2 \Delta v \lambda^2/4\pi$. If we take the velocity corresponding to the resonance level at $3\cdot 9 \times 10^6$ volts ($v = 1\cdot 37 \times 10^9$ cm./sec.), then for $a(\mathrm{E})$ in the resonance level we find

$$\begin{aligned} a(\mathrm{E}) &= 4\cdot 15 \times 10^{-26}\,(\mathrm{cm.})^2 \\ &= \pi\,(1\cdot 15 \times 10^{-13}\,\mathrm{cm.})^2. \end{aligned} \tag{18}$$

For $\Delta v/v$ we find $0\cdot 03$, and therefore

$$\Delta \mathrm{E}/\mathrm{E} \sim 0\cdot 06$$

and

$$\Delta \mathrm{E} \sim 2 \times 10^5 \quad \text{electron volts.} \tag{19}$$

The ejected protons, therefore, should have energies distributed in a range of at least this amount. This is 2 or 3 times as much as is likely from Pose's experiments; however, the value (18) for $a(\mathrm{E})$ is calculated on the assumption that level is an S level. If it were a P level then $a(\mathrm{E})$ would be three times this, and $\Delta \mathrm{E}$ therefore one-third of the value given by (19).

In Blackett's experiments on the artificial disintegration the cross section for capture, averaged over the whole path of the α-particle, is about

$$\pi\,(2 \times 10^{-13}\,\mathrm{cm.})^2.$$

This is about one-third of the total cross section of the nucleus. Of course, in this case more than one term in the expansion of the incident wave will be "responsible" for the disintegration. A rough calculation shows that an α-particle with impact parameter $3 \times 10^{-13}$ cm. has four "quanta of angular momentum." We should expect, therefore, that the disintegration is due to about four terms of the series (3).

# *The Stellar Coefficients of Absorption and Opacity.*

By S. CHANDRASEKHAR

(Communicated by P A. M. Dirac, F R S —Received May 14, 1931 )

1. The evaluation of the atomic absorption and opacity coefficients* due to atomic nuclei in an enclosure containing free electrons distributed according to the Fermi-Dirac statistics, apart from its theoretical interest, has of late gained some physical importance since Professor Milne's recent analysis of stellar structure has disclosed the possibility of *all* the stars possessing at least a zone of complete degeneracy. It is proposed, therefore, to examine this question in this paper. The formulæ here arrived at for the degenerate case are true only for high degeneracy. It has not been found possible to evaluate them for " incipient " degeneracy.

2. *Absorption by an Atomic Nucleus in an Electron-gas obeying the Fermi-Dirac Statistics.*—We shall define $a_0(\mathrm{E}, \nu)$ to be the rate of absorption of energy from radiation of frequency $\nu$ and unit intensity, by electrons of energy E, and unit mean density. Then it is known from the work of Kramers and Gaunt† that

$$a_0(\mathrm{E}, \nu) = 4\pi Z^2 e^6 / 3\sqrt{3} hcm^2 \nu^3 v, \tag{1}$$

where $Ze$ is the charge of the atomic nucleus, and $v$ the velocity of the electrons, the other symbols having their usual significance. Let this nucleus be in an enclosure of unit volume containing $\mathrm{N}_e$ free electrons distributed according to the Fermi-Dirac statistics. We want then the total absorption of energy $\mathrm{Q}_v$ from the incident radiation by all the electrons with velocity $v$, in the enclosure, in unit time. On the classical theory we should have clearly

$$\mathrm{Q}_v \, dv = a_0(\mathrm{E}, \nu) \, \mathrm{N}_v \, dv. \tag{2}$$

This, however, is not true on the Fermi-Dirac statistics. On this theory the probability of an encounter depends also on the density of the phase space in the region in which the electron finds itself after the collision. If, for instance, this region is fully packed—*i.e.*, all the phase cells are occupied—then the collision simply cannot occur. This is a consequence of Pauli's exclusion principle (as applied to the statistical mechanics) which prevents more than two electrons occupying the same phase cell. (There must, therefore, be in (2) an extra factor depending on the energy $E + h\nu$ of the electron *after* the absorption of the quantum $h\nu$). The extra factor (in general), as has been shown by Pauli and Nordheim,* is

---

* In conformity with the definitions due to A. S. Eddington, " The Internal Constitution of Stars," p. 119. For a very neat exposition of the general theory of the stellar absorption coefficient see S. Rosseland, 'Handbuch der Astrophysik,' Band III/1, p. 412, *et seq.*

† 'Phil. Trans.,' A, vol. 229, p. 163 (1930), equation (6.10).

$$(1 - N_{E'}/P_{E'}), \tag{3}$$

where $N_{E'}$ and $P_{E'}$ are the number of electrons and phase cells corresponding to the energy $E'$ of the electron after the encounter. We have, therefore, for the total absorption due to all the electrons with velocity $v$

$$Q_v \, dv = a_0 (E, \nu) \, N_E \, (1 - N_{E+h\nu}/P_{E+h\nu}) \, dv. \tag{4}$$

Now, on the Fermi-Dirac statistics

$$N_E \, dv = \frac{4\pi G m^3}{h^3} \cdot \frac{v^2 \, dv}{\frac{1}{A} e^{E/kT} + 1}, \tag{5}$$

where G is the "spin-weight" which for the case of an electron-gas equals two, and A is determined by the "normalisation condition"

$$N_e = \frac{G (2\pi m k T)^{3/2}}{h^3} \cdot \frac{2}{\sqrt{\pi}} \int_0^\infty \frac{u^{1/2} \, du}{\frac{1}{A} e^u + 1}. \tag{6}$$

The precise value of A will depend on the state of the gas—degenerate or otherwise—but we will leave it for the present unspecified. Also, it is easily seen that

$$1 - \frac{N_{E+h\nu}}{P_{E+h\nu}} = \frac{\frac{1}{A} e^{(E+h\nu)/kT}}{\frac{1}{A} e^{(E+h\nu)/kT} + 1}. \tag{7}$$

Hence by (4), (5), (6) and (7) we have for the total absorption $\alpha_\nu$ due to *all* the electrons in the enclosure,

$$\alpha_\nu = \int_0^\infty Q_v \, dv = \frac{16\pi^2 Z^2 e^6 m G}{3\sqrt{3}\, c h^4 \nu^3} \int \frac{\frac{1}{A} e^{(E+h\nu)/kT} \, v \, dv}{\left(\frac{1}{A} e^{E/kT} + 1\right)\left(\frac{1}{A} e^{(E+h\nu)/kT} + 1\right)}$$

$$\frac{16\pi^2 Z^2 e^6 G k T}{3\sqrt{3}\, c h^4 \nu^3} \, \frac{1}{A} e^{h\nu/kT} \int_1^\infty \frac{dx}{\left(\frac{1}{A} x + 1\right)\left(\frac{1}{A} e^{h\nu/kT} x + 1\right)} \tag{8}$$

---

* Nordheim, 'Proc. Roy. Soc.,' A, vol. 119, p. 689 (1928). Also R. H. Fowler, "Statistical Mechanics," pp. 556 *et seq.*

by an obvious change in the variable. We have therefore

$$\alpha_\nu = \frac{16\pi^2 Z^2 e^6 G k T}{3\sqrt{3}\, c h^4 \nu^3} \cdot \frac{e^{h\nu/kT}}{e^{h\nu/kT} - 1} \log \left[ \frac{e^{h\nu/kT}(A + 1)}{e^{h\nu/kT} + A} \right] \tag{9}$$

3. *Absorption in a Non-degenerate Gas.*—A non-degenerate gas corresponds to the " A " in (6) being a small constant. The value of A is then given by

$$A \sim \frac{N_e h^3}{G} (2\pi m k T)^{-3/2} \ll 1 \tag{10}$$

Also,

$$\begin{aligned} \log \left[ \frac{e^{h\nu/kT}(A + 1)}{e^{h\nu/kT} + A} \right] &= (1 - e^{-h\nu/kT}) \log (A + 1) \\ &\qquad - (1 - e^{-h\nu/kT}) \frac{A^2}{2} e^{-h\nu/kT} + \ldots \\ &\qquad (1 - e^{-h\nu/kT}) A, \end{aligned} \tag{11}$$

using (10) and (11) in our equation (9) for the absorption coefficient $\alpha_\nu$, we have

$$_M\alpha_\nu = N_e \frac{16\pi^2 Z^2 e^6}{3\sqrt{3}\, h c \nu^3} \cdot \frac{1}{(2\pi m)^{3/2} (kT)^{1/2}}. \tag{12}$$

Milne* gives, working from the beginning on the Maxwell-distribution law,

$$_M\alpha_\nu = N_e \frac{16\pi^2 Z^2 e^6}{3\sqrt{3}\, h c \nu^3 (2\pi m)^{3/2} (kT)^{1/2}} (1 - e^{-h\nu/kT}), \tag{13}$$

which differs from (12) by an extra-factor $(1 - e^{-h\nu/kT})$. As Gaunt† has already pointed out, this extra-factor in Milne's expression is not justifiable. It would be correct if Kramer's expression for the emission included the stimulated emission also. This, however, is not the case.‡

---

* 'M.N.R.A.S.,' vol. 85, p. 750 (1925), equation (2).

† *Loc. cit.*, p. 197.

‡ S. Rosseland (*loc. cit.*) also evaluates $_M\alpha_\nu$. His equation (377) is exactly the same as (12) but with an extra-factor $(1 + h\nu/kT)$. This is clearly an oversight. Again, his equation (389) contains an extra-factor $e^{h\nu/kT}$. This extra-factor arises because, working on Kramer's theory of emission, to calculate the total *emission* in the frequency range $\nu$ and $\nu + d\nu$ he integrates over all the *initial* velocities of the electrons from 0 to $\infty$. This he does because, according to him, this takes into account the contribution to the absorption by the " bound-free " transitions also. Rosseland, however, recognises that this is a " gross-exaggeration." *If* Rosseland is right in including the " bound-free " transitions in this way, a comparison of (23) and (24) shows that in the Maxwellian case the greater part of the total absorption is due to the " bound-free " transitions. This result is known to be true from the researches of Professor Milne. But it will be seen that in the degenerate case the " bound-free " transitions can be neglected (see § 8).

4. *The Coefficients of Absorption and Opacity in a Non-degenerate Electron-gas.*—As all the existing treatments for the evaluation of the atomic-opacity coefficient contain some error or other, it seems worth while to give a derivation of it free from such errors.* As is well known, there are two quantities of interest in astrophysical calculations: (i) the *atomic absorption coefficient* defined as the "straight mean," *i.e.*,

$$\alpha_a = \int_0^\infty \alpha'_\nu \mathrm{I}_\nu \, d\nu \Big/ \int_0^\infty \mathrm{I}_\nu \, d\nu, \tag{14}$$

and (ii) the *atomic opacity coefficient* defined as the Rosseland mean, *i.e.*,

$$\alpha_0^{-1} = \int_0^\infty \frac{1}{\alpha'_\nu} \frac{\partial \mathrm{I}_\nu}{\partial \mathrm{T}} d\nu \Big/ \int_0^\infty \frac{\partial \mathrm{I}_\nu}{\partial \mathrm{T}} d\nu. \tag{15}$$

Further, as has been explained by Rosseland,† it is not the pure absorption coefficient $\alpha_\nu$ that has to be introduced in (15). It is the absorption coefficient $\alpha_\nu$ multiplied by $(1 - e^{-h\nu/k\mathrm{T}})$, *i.e.*,

$$\alpha'_\nu = \alpha_\nu (1 - e^{-h\nu/k\mathrm{T}}). \tag{16}$$

This is necessary to take into account properly the stimulated emission process. "This result is brought about by the fact that the stimulated emission process will show exactly the same asymmetry as the field of radiation, and this fact entails the consequence that the outward flow of radiation will be reinforced by a stimulated emission in its own direction." Though Rosseland makes this remark in connection with the evaluation of the coefficient of opacity, it is clear, however, that the same arguments will also apply to the "straight-mean" giving the atomic absorption coefficient.‡ For, an incident radiation in a given direction will stimulate emission in a direction exactly parallel to itself, and what is essential in the evaluation of the absorption is the random (and *therefore* the unstimulated) emission. Hence, even in (14) we use $\alpha_\nu'$ defined by (16), and not merely $\alpha_\nu$. Thus we are effectively working with Milne's expression (13) though the extra-factor now owes its origin to an entirely different reason and is not due to the assumption that the Kramers' expression for the emission includes the stimulated emission also.

---

* The treatment in Eddington's book is not without errors. In his equation (156 3 *for the emission in the frequency range* $\nu$ *and* $\nu + d\nu$, *he replaces* $1/v$ by the mean harmonic-velocity. This clearly should not be done since $1/v$ should be averaged only from $\infty$ to $v_0$ where $\frac{1}{2} mv_0^2 = h\nu$, and not from $\infty$ to $0$ as Eddington does. Neither does Eddington make clear that this effectively means (according to Rosseland) taking into account the "bound-free" *transitions also*, and is a "gross-exaggeration."

† *Loc. cit.*, pp. 456 and 469.

‡ I owe this remark to Dr. Dirac. See Rosseland, *loc. cit.*, equation (352).

*Case I. The Rosseland Mean.*—We have, therefore, by (12), (15) and (16)

$${}_{\mathrm{M}}\alpha_o = \mathrm{N}_e \frac{16\pi^2 \mathrm{Z}^2 e^6}{3\sqrt{3}\, hc\, (2\pi m)^{3/2}\, (k\mathrm{T})^{1/2}} \cdot \frac{\partial}{\partial \mathrm{T}} \int_0^\infty \mathrm{I}_\nu \, d\nu \Big/ \frac{\mathrm{B}h}{k\mathrm{T}^2} \int_0^\infty \frac{\nu^3 e^{h\nu/k\mathrm{T}}}{e^{h\nu/k\mathrm{T}} - 1} \cdot \frac{\nu^4 e^{h\nu/k\mathrm{T}}\, d\nu}{(e^{h\nu/k\mathrm{T}} - 1)^2}, \tag{17}$$

where $\mathrm{I}_\nu$ is the usual Planck function

$$\mathrm{I}_\nu = \mathrm{B}\nu^3/(e^{h\nu/k\mathrm{T}} - 1). \tag{18}$$

Now

$$\frac{\mathrm{B}h}{k\mathrm{T}^2} \int_0^\infty \frac{\nu^7 e^{2h\nu/k\mathrm{T}}}{(e^{h\nu/k\mathrm{T}} - 1)^3} = \frac{\mathrm{B}}{\mathrm{T}} \left(\frac{k\mathrm{T}}{h}\right)^7 7\,!\ \vartheta_1 \tag{19}$$

where

$$\vartheta_1 = \tfrac{1}{2} \left\{ \sum_{n=1}^{\infty} \frac{1}{n^6} + \sum_{n=1}^{\infty} \frac{1}{n^7} \right\} = 1 \cdot 0128. \tag{20}$$

Also

$$\frac{\partial}{\partial \mathrm{T}} \int_0^\infty \mathrm{I}_\nu \, d\nu = \frac{\mathrm{B}}{\mathrm{T}} \left(\frac{k\mathrm{T}}{h}\right)^4 4\,!\ \vartheta_2, \tag{21}$$

where

$$\vartheta_2 = \sum_{n=1}^{\infty} \frac{1}{n^4} = \frac{\pi^4}{90} = 1 \cdot 0823. \tag{22}$$

Hence we have finally

$${}_{\mathrm{M}}\alpha_o = \frac{8\pi^2 \vartheta_2}{315\sqrt{3}\vartheta_1} \cdot \frac{\mathrm{Z}^2 e^6 h^2}{c\, (2\pi m)^{3/2}} \cdot \frac{\mathrm{N}_e}{(k\mathrm{T})^{7/2}}. \tag{23}$$

*Case II. The Straight Mean.*—We calculate now the straight mean giving the atomic absorption coefficient. By (12), (14) and (16) we have

$$\begin{aligned} {}_{\mathrm{M}}\alpha_a &= \mathrm{N}_e \cdot \frac{16\pi^2 \mathrm{Z}^2 e^6}{3\sqrt{3}\, hc\, (2\pi m)^{3/2}\, (k\mathrm{T})^{7/2}} \cdot \frac{\mathrm{B} \displaystyle\int_0^\infty e^{-h\nu/k\mathrm{T}}\, d\nu}{\mathrm{B} \displaystyle\int_0^\infty \frac{\nu^3\, d\nu}{e^{h\nu/k\mathrm{T}} - 1}} \\ &= \frac{80}{\pi^2\sqrt{3}} \cdot \frac{\mathrm{Z}^2 e^6 h^2}{c\, (2\pi m)^{3/2}} \cdot \frac{\mathrm{N}_e}{(k\mathrm{T})^{7/2}}. \end{aligned} \tag{24}$$

which agrees with Milne's formula (*loc. cit.*, equation (3)). A comparison of (23) and (24) shows the effect of averaging by the two different methods. The difference in the numerical factors in (23) and (24) (which amounts to a factor 30), is almost incredible, but I have been unable to detect any mistake in my algebra.

5. *The Coefficients of Absorption and Opacity in a Degenerate Gas.*—We proceed now to the evaluation of the atomic absorption and opacity coefficients in a degenerate gas, *i.e.*, corresponding to "A" in (6) being a large positive

constant. The first step is to obtain a suitable approximation to the log-factor in (9), consistent with our assumption that the gas is degenerate. Now

$$\log \frac{e^{h\nu/kT}(A+1)}{e^{h\nu/kT}+A} = \log\left(1+\frac{1}{A}\right) + \frac{h\nu}{kT} - \log\left(1+\frac{1}{A}e^{h\nu/kT}\right). \tag{25}$$

The following argument shows that

$$\frac{1}{A}e^{h\nu/kT} \ll 1$$

for the range of frequencies, about which the greater part of the radiant energy is distributed according to the Planck's law, provided the electron-gas is sufficiently degenerate

Let $\lambda_m$ be the wave-length at which there is the maximum of energy in the black-body spectrum corresponding to the temperature T. Then we have

$$\lambda_m\, T = \frac{ch}{4{\cdot}965k} \text{ (" Wien's displacement law ") or } \frac{h\nu_m}{kT} = 4{\cdot}965. \tag{26}$$

Also if

$$\frac{1}{A}e^{h\nu/kT} \ll 1$$

then

$$\log A \gg h\nu/kT. \tag{27}$$

Also the degeneracy condition is

$$\log A = \frac{h^2}{2mkT}\left(\frac{3N_e}{4\pi G}\right)^{2/3} \gg 1. \tag{28}$$

Now log A is for a highly degenerate gas of the order 20 or 30.* Hence comparing (26), (27) and (28), it can be concluded that for the main part of the Planck's curve where most of the radiant energy is concentrated, we can when working to the first order neglect not only 1/A but also $\frac{1}{A}e^{h\nu/kT}$. Hence by (25) we have with this understanding

$$\log \frac{e^{h\nu/kT}(A+1)}{e^{h\nu/kT}+A} \sim \frac{h\nu}{kT} \tag{29}$$

Using (29) in (9) we have simply,

$$_{\mathrm{D}}\alpha_\nu = \frac{16\pi^2 Z^2 e^6 G}{3\sqrt{3}\,ch^3} \cdot \frac{e^{h\nu/kT}}{\nu^2\left(e^{h\nu/kT}-1\right)}. \tag{30}$$

---

* For $n = 10^{30}$, $T = 10^{8}$, $\log A = 4{\cdot}2 \times 10^{-11}$. $N^{2/3}/T = 42$.

*Case I. The Rosseland Mean.*—By (30), (15) and (16) we have for the atomic-opacity coefficient in a highly degenerate electron-gas

$$ {}_{D}\alpha_0 = \frac{32\pi^2 Z^2 e^6}{3\sqrt{3}\, ch^3} \frac{\frac{\partial}{\partial T}\int_0^\infty I_\nu \, d\nu}{\frac{Bh}{kT^2}\int_0^\infty \frac{\nu^6 e^{h\nu/kT} d\nu}{(e^{h\nu/kT}-1)^2}} . \tag{31} $$

Since

$$ \frac{Bh}{kT^2}\int_0^\infty \frac{\nu^6 e^{h\nu/kT} d\nu}{(e^{h\nu/kT}-1)^2} = \frac{B}{T}\left(\frac{kT}{h}\right)^6 6\,! \frac{\pi^6}{945} \tag{32} $$

We have by (22), (31) and (32)

$$ {}_{D}\alpha_0 = \frac{56}{15\sqrt{3}} \frac{Z^2 e^6}{ch\,(kT)^2}. \tag{33} $$

*Case II. "The Straight Mean."*—We have for the atomic-absorption coefficient in a degenerate gas by (30), (14) and (16)

$$ {}_{D}\alpha_a = \frac{32\pi^2 Z^2 e^6}{3\sqrt{3}\, ch^3} \cdot \frac{B\int_0^\infty \frac{\nu d\nu}{e^{h\nu/kT}-1}}{B\int_0^\infty \frac{\nu^3 d\nu}{e^{h\nu/kT}-1}} $$

$$ \frac{80}{3\sqrt{3}} \frac{Z^2 e^6}{ch\,(kT)^2}. \tag{34} $$

Here again we find a large difference between the straight and the Rosseland means.

6. *The Degenerate-atomic-absorption Coefficient Formula.*—(34) then is our atomic-absorption-coefficient for a highly degenerate gas (on the assumption of the validity of the equation (1) for $a_0$ (E, $\nu$)). The most striking point about (33) and (34) is that they are independent of the electron-concentration and therefore of the density. But the following shows that this result is a natural consequence of the properties of a highly degenerate gas and the *form* of our expression for $a_0$(E, $\nu$).

An idealisation is necessary to explain the result simply. In a highly degenerate gas the distribution of energy is as shown in the figure. Or algebraically

$$ \left. \begin{aligned} N(E) &= \frac{4\pi (2m)^{3/2}}{h^3} E^{1/2} = KE^{1/2} \text{ (say)} \quad (E \leq E^*) \\ &= 0 \qquad\qquad\qquad\qquad\qquad\qquad (E > E^*) \end{aligned} \right\}, \tag{35} $$

where

$$E^* = \frac{h^2}{8m}\left(\frac{3N_e}{\pi}\right)^{2/3}. \tag{36}$$

Now, an electron with energy E′ can absorb a quantum $h\nu$ *only when*

$$E' + h\nu > E^* \tag{37}$$

for otherwise the energy of the electron after the absorption of the quantum $h\nu$ is less than E*, and the phase-cells here are all occupied. But it can absorb quanta of energy-magnitudes greater than $h\nu_0 (= E^* - E')$ since it then goes into a region of phase-space which is completely vacant.† If we now increase the electron-concentration we merely increase E*, and no alteration is made in the distribution of the electrons with energy less than E*. We merely add a few more electrons, *all* of which can have energies only greater than the original E*. From (35) we have obviously

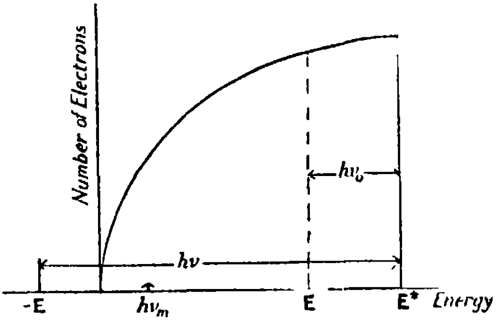

$$N_{E^*} = KE^{*1/2}. \tag{38}$$

Also from (1) we have

$$a_0\,(E^*, \nu) \propto N_{E^*}/E^{*1/2} = K.$$

Hence

$$\delta\alpha, = \delta\,(a_0\,(E,^*\,\nu)) = 0 \qquad \text{for } \mathit{all}\ \nu. \tag{39}$$

Hence our result that the atomic absorption (or opacity) coefficient is independent of density, is understood as a very natural consequence of the properties of a highly degenerate-gas and the form for our expression for the rate of absorption of energy.

---

† Similar reasoning (but not exactly the same) has been employed by R. H. Fowler ('Proc. Roy. Soc.,' A, vol. 118, p. 229 (1928)) to explain the sharp photoelectric threshold frequency.

In this connection we can on this highly idealised picture of a degenerate-gas obtain the atomic absorption coefficient also. Now by (1) we have

$$a_0(\mathrm{E}, \nu) = \frac{4\pi \mathrm{Z}^2 e^6}{3\sqrt{3} hcm^{3/2}\nu^3 \sqrt{2\mathrm{E}}} \tag{40}$$

To find the total absorption $\alpha_\nu$ due to all the electrons we must multiply (40) by $\mathrm{N_E}d\mathrm{E}$ and integrate only from $\mathrm{E}^*$ to $(\mathrm{E}^* - h\nu)$ as is clear from equation (37) and the diagram.

We find using (35) that

$$\begin{aligned} \alpha_\nu &= \frac{32\pi^2 \mathrm{Z}^2 e^6}{3\sqrt{3}\ h^4 c\nu^3} \int_{\mathrm{E}^* - h\nu}^{\mathrm{E}^*} d\mathrm{E} \\ & \frac{32\pi^2 \mathrm{Z}^2 e^6}{3\sqrt{3}\, h^3 c\nu^2}, \end{aligned} \tag{41}$$

which is exactly the same as (30) but with the factor $(1 - e^{-h\nu/k\mathrm{T}})^{-1}$ missing.† That this is not inconsistent with our assumption of degeneracy in § 5 can be seen by using (41) to find the absorption coefficient. We find readily (using the " Rosseland correction factor " also)

$$\begin{aligned} {}_{\mathrm{D}}\alpha_a &= \frac{32\pi^2 \mathrm{Z}^2 e^6}{3\sqrt{3}\, h^3 c} \frac{\mathrm{B}\displaystyle\int_0^\infty \nu e^{-h\nu/k\mathrm{T}} d\nu}{\mathrm{B}\displaystyle\int_0^\infty \frac{\nu^3 d\nu}{e^{h\nu/k\mathrm{T}} - 1}} \\ &= \frac{160}{\pi^2\sqrt{3}} \cdot \frac{\mathrm{Z}^2 e^6}{ch\,(k\mathrm{T})^2}. \end{aligned} \tag{42}$$

Similarly for $\alpha_\nu$ given by (42) the atomic-opacity coefficient is easily found to be

$$_{\mathrm{D}}\alpha_0 = \frac{16\pi^2\vartheta_2}{45\sqrt{3}\vartheta_3} \cdot \frac{\mathrm{Z}^2 e^6}{ch\,(k\mathrm{T})^2} \tag{42'}$$

where $\vartheta_2$ is defined in (22) and

$$\vartheta_3 = \tfrac{1}{2}\left\{ \sum_{n=1}^{\infty} \frac{1}{n^6} + \sum_{n=1}^{\infty} \frac{1}{n^5} \right\} = 1{\cdot}0271.$$

The atomic absorption coefficients given by (42) and (34) are exactly the same, but for a difference in the numerical factors amounting to $\pi^2/6$ or 1·6. The difference, however, between the Rosseland means (42′) and (33) is almost negligible, the ratio of the two numerical factors in the two equations being 1 : 1·01.†

---

† The approximation (35) is the one corresponding to " $\mathrm{T} \to 0$." It is clear that $(30) \to (41)$ as $\mathrm{T} \to 0$.

Presumably (34) and (33) are the more reliable ones, because the approximations used there are derived from a less idealised picture and take account of the partial vacancy in the region below E* and the non-vacancy beyond E* as well.

7. *Application of one of Gaunt's Formulæ to the case of Absorption by a Degenerate Gas.*—So far we have based our discussion exclusively on the "Kramers' approximation" for the continuous absorption. This, however, is not likely to be valid for *extreme* degeneracy, for then it is only the electrons of very high velocity that take part in the absorption-process, and since the condition that the electron-gas is very highly degenerate provides for the maximum of the Planck-curve falling well within the "threshold" energy, a better approximation (than Kramers') would appear to be the one corresponding to $E \gg h\nu$. Now, Gaunt‡ gives for this case

$$a_0(E, \nu) = \frac{4Z^2e^6}{3hcm^2v\nu^3} \log \frac{E}{h\nu}. \tag{43}$$

Since

$$\alpha_\nu = \int_{E^*-h\nu}^{E^*} a_0(E, \nu)\, N_E\, dE$$

we have by (35) and (43)

$$\begin{aligned} \alpha_\nu &= \frac{32\pi Z^2e^6}{3h^4c\nu^3} \int_{E^*-h\nu}^{E^*} \log \frac{E}{h\nu}\, dE \\ &= \frac{32\pi Z^2e^6}{3h^4c\nu^3} \left[ h\nu \log\left(\frac{E^*}{h\nu} - 1\right) - E^* \log\left(1 - \frac{h\nu}{E^*}\right) - h\nu \right], \end{aligned} \tag{44}$$

or to the same order of accuracy as (43)

$$\alpha_\nu \sim \frac{32\pi Z^2e^6}{3h^3c\nu^2} \log \frac{E^*}{h\nu}, \tag{45}$$

---

† In deriving (42) and (42′) we have not averaged $\alpha_\nu$ given by (41) but

$$\alpha_\nu' = \alpha_\nu (1 - e^{-h\nu/kT}).$$

One cannot definitely say whether the use of $\alpha_\nu$ or $\alpha_\nu'$ is more consistent when working with the highly idealised picture of a degenerate gas. For (41) is true only when $h\nu > kT$, in which case we cannot differentiate between $\alpha_\nu$ and $\alpha_\nu'$. If however, we had used $\alpha_\nu$ (given by (41)) as such, to obtain the "means," the atomic-absorption and opacity coefficients so derived would have been identical with (33) and (34).

‡ Gaunt, *loc. cit.*, equation (5.39).

(45) immediately gives a value for the atomic absorption coefficient. We have by (14), (16) and (45)

$$_{\mathrm{D}}\alpha_a = \frac{32\pi Z^2 e^6}{3h^3 c} \frac{\mathrm{B}\int_0^\infty \nu \log \frac{\mathrm{E}^*}{h\nu} e^{-h\nu/k\mathrm{T}} d\nu}{\mathrm{B}\int_0^\infty \frac{\nu^3 d\nu}{e^{h\nu/k\mathrm{T}} - 1}}. \tag{46}$$

Now

$$\int_0^\infty \nu \log \frac{\mathrm{E}^*}{h\nu} e^{-h\nu/k\mathrm{T}} d\nu = \left(\frac{k\mathrm{T}}{h}\right)^2 \int_0^\infty x \log \frac{\mathrm{E}^*}{k\mathrm{T}x} e^{-x} dx$$

$$= \left(\frac{k\mathrm{T}}{h}\right)^2 \left[\log \frac{\mathrm{E}^*}{k\mathrm{T}} + \gamma - 1\right], \tag{47}$$

where $\gamma$ is the Euler-Mascheroni's constant $= 0{\cdot}5772$. Hence we have by (46) and (47)

$$_{\mathrm{D}}\alpha_a = \frac{160}{\pi^3} \cdot \frac{Z^2 e^6}{ch(k\mathrm{T})^2} \left[\log \frac{\mathrm{E}^*}{k\mathrm{T}} - 0{\cdot}4228\right] \tag{48}†$$

which differs from the formula (42) derived on the Kramers' approximation by a factor

$$g = \frac{\sqrt{3}}{\pi}\left[\log \frac{\mathrm{E}^*}{k\mathrm{T}} + \gamma - 1\right], \tag{49}$$

so that $_{\mathrm{D}}\alpha_a = g\ _{\mathrm{D}}\alpha_a$. $g$ can appropriately be called the *Gaunt-factor.* Also

$$\frac{\mathrm{E}^*}{k\mathrm{T}} = \frac{h^2}{8mk\mathrm{T}}\left(\frac{3\mathrm{N}e}{\pi}\right)^{2/3} = \log \mathrm{A} \tag{50}$$

in our previous notation. Thus the Gaunt-factor for the atomic absorption coefficient is

$$g = \sqrt{3}\,[\log\log \mathrm{A} + \gamma - 1]/\pi. \tag{51}‡$$

---

† In deriving (48) we have averaged $\alpha_\nu'$ ($= \alpha_\nu(1 - e^{-h\nu/k\mathrm{T}})$). As was pointed out earlier, when working with the ideal picture of a degenerate gas, we cannot be certain as to which is more correct to use $\alpha_\nu$ or $\alpha_\nu'$. If we had used $\alpha_\nu$ given by (45) as such, then we would have obtained

$$_{\mathrm{D}'}\alpha_a = \frac{80}{\pi\,.\,3} \cdot \frac{Z^2 e^6}{ch(k\mathrm{T})^2}\left[\log \frac{\mathrm{E}^*}{k\mathrm{T}} + \gamma - 1\right], \tag{48'}$$

which differs from (48) by a factor $\pi^2/6$. Since, however, (43) itself is valid only for extreme degeneracy, it is likely that (48) is the more reliable one.

‡ In deriving (51) we have compared (48) with (42), since both these are derived from the same ideal picture of a degenerate gas But, as was pointed out earlier, (34) is the more reliable one. The Gaunt-factor is then given by

$$g' = 6\sqrt{3}\,[\log\log \mathrm{A} + \gamma - 1]/\pi^3 = 0{\cdot}6081g. \tag{51'}$$

If, however, we had used (48′) instead of (48), $g$ would then be given by (51).

Now, for $T = 10^8$ and $N_e = 10^{30}$ we have $\log A = 42$. The Gaunt-factor then amounts to 1·87. Also $\log_e \log A = 3\cdot78$. Thus it appears that even for this not too high a degeneracy, it would have been a good enough approximation if instead of (45) we had merely used

$$\alpha_\nu = \frac{32\pi Z^2 e^6}{3h^3 c\nu^3} \log \frac{E^*}{kT} \tag{45'}$$

in which case the Gaunt-factor would have been simply

$$g \sim \frac{\sqrt{3}}{\pi} \log \log A, \tag{51''}$$

and would mean the neglect of — 0·4228 in (51). Now, the previous sections fully illustrate the extreme sensitiveness of the Rosseland mean to the structure of $\alpha_\nu$, and we cannot rely on (45′) as a valid approximation to evaluate the atomic-opacity coefficient, though we could depend on it (as it now appears) to evaluate the atomic absorption coefficient. If, however, (45′) is a valid approximation,† then it would follow that the Gaunt-factor for the atomic-absorption as well as the opacity coefficients is given by (51″).

From the nature of the approximations which Gaunt makes in deriving his formula (43), it appears *not* quite safe to use (48) even for the degeneracy contemplated by $T = 10^8$ and $N_e = 10^{30}$. It is, however, satisfactory that the Gaunt-factor is not very large and that log log A is a slowly increasing function of $N_e$. Though it was shown in § 6 that the atomic absorption and opacity coefficients (derived on the basis of the Kramers' approximation) being independent of density could be inferred from first principles, yet it is physically rather hard to conceive of how this could be so. The introduction of the Gaunt-factor removes incidentally this difficulty.

8. *General Discussion and possible Applications.*—In the evaluation of the opacity and absorption coefficients we have considered only the "free-free" transitions, *i.e.*, the contribution to the total absorption due to the electron transitions from one occupied phase-cell of positive energy to another unoccupied phase-cell of positive energy. Now it is known‡ that in the classical Maxwell case most of the absorption is photoelectric, even in a highly ionised gas. It arises from the absorption by the very few electrons bound to atoms

---

† I am unable to see any *a priori* justification for (45′), and it is not an easy matter in any case to evaluate the Rosseland mean corresponding to the correct form for the $\alpha_\nu$ given by (45).

‡ Milne, 'M.N.R.A.S.,' vol. 85, p. 750 (1925), also Rosseland, 'Astrophys. J.,' vol. 61, p. 424 (1925).

at any one instant of time. However high the degree of ionisation, there is a large photoelectric absorption from just those very few electrons. The question which now arises is as to how important the " bound-free " transitions are in the degenerate case. The following arguments show that the contribution to the total absorption by the " bound-free " transitions must be negligible.

Firstly, it is to be noted that even the " free-electrons " can in a sense be regarded as " bound." For, an electron with energy $E'$ can absorb a quantum $h\nu$ only if

$$h\nu > E^* - E', \tag{37}$$

which is the same thing as saying that the $E'$ electrons are " bound electrons " with an " ionisation energy " $\chi = E^* - E'$. In this sense, it is only the $E^*$ electrons that deserve to be called free!

Now, an electron in an orbit with a *negative* energy E, if it has to become a " free electron," must " switch off " only to states of positive energy greater than $E^*$, *i.e.*, quanta of magnitude $h\nu > E^* + E$, alone are effective in causing transitions Also, even towards the contribution to the absorption by the " free-free " transitions, it is only the electrons with energies near the threshold energy that are operative. Further (as has been pointed out earlier) the condition that the gas is degenerate provides for the maximum of the Planck curve falling fairly well inside the threshold energy (see figure). All these considerations make clear that the " bound-free " transitions contribute very little, if at all, to the total absorption.

Now, we will briefly discuss some possible applications of the degenerate opacity formula.

Neglecting the Gaunt-factor, we have for the coefficient of opacity per unit mass $\kappa$ for a degenerate gas,

$$\kappa \propto T^{-2}. \tag{52}$$

Now in a collapsed star the central regions are degenerate, and the temperature law is[†]

$$T \propto \rho^{5/12}$$

or by (52)

$$\kappa \propto \rho^{-5/6}. \tag{53}$$

On account of the fair degree of homogeneity of the Emden polytrope " $n=3/2$," and since we can also expect the small decrease in the opacity towards the central regions to be compensated by a corresponding increase in the average rate of liberation of energy $\varepsilon_r$, we can reasonably be sure that $\kappa_r \varepsilon_r$ is fairly constant. Hence we can feel confident that the standard model equations for the degenerate core of a collapsed star are likely to be a very good approximation.

---

[†] Milne, 'M.N.R.A.S.,' vol. 91, p. 4 (1930) (especially § 24).

We cannot, however, apply our formulæ immediately to the case of the white dwarfs. The "astronomical value" for $\kappa_c \varepsilon_c$ is extremely sensitive to what we assume the effective temperature to be. Thus in the case of $O_2$ Eridani B the assumed effective temperature is 11,200 degrees. Also a Te $\sim$ 11,750 degrees would make the star *completely* of the collapsed type, *i.e.*,

$$1 - \beta = \kappa L/4\pi cGM = 0$$

This, combined with the fact that Professor Milne has raised strong doubts against the derived effective temperatures of these stars,* makes it clear that the white dwarfs in any case cannot form a test of the opacity question.

## *Summary.*

(1) A general expression for the atomic absorption coefficient $\alpha_\nu$, due to atomic nuclei in an enclosure containing free electrons distributed according to the Fermi-Dirac statistics, is derived (equation (9)).

(2) The atomic absorption coefficient (the "straight mean") and the atomic opacity coefficient (the "Rosseland mean") are evaluated both for the cases of degeneracy and non-degeneracy. The two means are found to differ more considerably than what has hitherto been thought they would.

(3) The "degenerate" opacity and absorption coefficients based on the Kramers' approximation are found to be independent of density and inversely proportional to the square of the temperature. A simple explanation for these results is given based on an idealised picture of a degenerate gas.

(4) Certain correction factors called "Gaunt-factors" are defined, the introduction of which makes the absorption and the opacity coefficients of a degenerate gas slowly increasing functions of the electron concentration.

(5) The bearing of these results to Milne's theory of stellar structure is indicated.

In conclusion, I wish to express my thanks to Dr. P. A. M. Dirac, F.R.S., for many valuable suggestions and helpful criticisms.

---

* 'M.N.R.A.S.,' vol. 91, p. 39, footnote (1930).

# *The Quantum Theory of Dispersion in Metallic Conductors.—II.*

By R. de L. Kronig, Natuurkundig Laboratorium der Rijks-Universiteit, Groningen.

(Communicated by C. G. Darwin, F.R.S.—Received May 19, 1931.)

1. *Introduction.* - In a previous paper* the optical properties of metals were discussed on the basis of Bloch's theory of metallic conduction † According to this theory the action on a given conduction electron of the other conduction electrons and the ions of the metallic lattice is replaced by a periodic field of potential. In its stationary states the electron travels freely through the metal, but when the temperature agitation of the lattice is taken into account, the electron will make transitions to other stationary states due to the collisions which then take place. In Part I it was shown that the optical constants of a metal can be expressed by the well-known formulæ of Drude in terms of its electrical conductivity $\sigma_0$ for constant electric fields, provided the period of the incident radiation is large compared with the time of relaxation of the conduction electrons or, what comes to the same thing, large compared with the average time between two collisions of such an electron and the metallic lattice. In the other limiting case of a period small compared with this time of relaxation the theory also took a simple form since then the collisions could be entirely neglected. It was further shown that the transitional region of the spectrum where the period of the radiation is comparable with the time of relaxation in general lies in the neighbourhood of a wave-length $\lambda = 10\,\mu$ at ordinary temperatures and shifts toward longer wave-lengths as the temperature gets lower since the chance of collision is thereby reduced and the time of relaxation increased.

In section 2 of this paper we shall consider once more the optical behaviour of a metal under circumstances where we may neglect the collisions of the electrons with the lattice. Some points which were still rather obscure when Part I was written will be explained more fully in this connection. In section 3 the theory will be extended to include the transitional region of the spectrum spoken of above, and in section 4 a comparison with the experimental data will be given.

---

* Kronig, 'Proc. Roy. Soc.,' A, vol. 124, p. 409 (1929), quoted as Part I.

† 'Z. Physik,' vol. 52, p. 555 (1928).

2. *The Optical Properties in the Absence of Collisions.*—In Part I we have considered the propagation of a plane electromagnetic wave of frequency $\nu$ in a cubical metal lattice in the direction of one of the crystallographic axes, say the $z$-axis, the radiation being taken as linearly polarised along one of the other two axes, say the $x$-axis. We had imagined a cube cut out of the lattice with its edges of length L also parallel to the crystallographic axes, and we had chosen L as a large integral multiple $Ga$ of the lattice constant $a$ and as small compared with the wave-length and the distance in which on account of extinction the amplitude of the incident radiation decreases appreciably; two conditions which in general can be satisfied quite well simultaneously. According to the theory of Bloch (*loc. cit.*) the solutions of the wave equation of an electron in the periodic field of potential representing the metal have the form

$$\psi(x, y, z) = u(x, y, z)\, e^{i(\alpha_1 x+\alpha_2 y+\alpha_3 z)}, \quad \alpha_1 = \frac{2\pi l_1}{L}, \quad \alpha_2 = \frac{2\pi l_2}{L}, \quad \alpha_3 = \frac{2\pi l_3}{L}, \quad (1)$$

if we subject them to the requirement that they be periodic with the period L in the direction of each of the co-ordinate axes. Here $l_1$, $l_2$, $l_3$ take all integral values from $-\infty$ to $\infty$, while $u$ is a function periodic in the $x$-, $y$-, and $z$-directions with the period $a$.

On account of the assumption regarding the size of the cube we supposed in Part I that the electric field of the radiation everywhere inside is given by

$$E_x = F\cos 2\pi\nu t, \qquad E_y = E_z = 0. \qquad (2)$$

If for brevity we denote the stationary state of an electron in the cube by $r$ (energy $W_r$) and any other stationary state by $s$ (energy $W_s$), then it was shown that the part of the current density in the $x$-direction which vibrates with the frequency $\nu$, due to this electron, is given by

$$I_x = \frac{e^2 F}{2\pi m\nu L^3}\left[1 + \frac{2}{hm}\sum_s \frac{\nu_{rs}\,|p_x(rs)|^2}{\nu_{rs}^2 - \nu^2}\right]\sin 2\pi\nu t, \qquad (3)$$

where $e$ and $m$ are the electronic charge and mass respectively while $h$ is Planck's constant. $\nu_{rs}$ is the transition frequency from the state $r$ to the state $s$,

$$h\nu_{rs} = W_r - W_s \qquad (4)$$

and

$$p_x(rs) = \frac{h}{2\pi i}\int \psi_r^* \frac{\partial \psi_s}{\partial x}\, dx\, dy\, dz$$

is the matrix element of the linear momentum of the electron in the $x$-direction, the wave functions being normalised in the cube and the integration also extending over it.

In place of (3) we may write

$$\Sigma' \frac{|p_x(rs)|^2}{} \Big| \frac{1}{\nu} \;\Big|\; \frac{2}{hm} \sum_s{}' \frac{\nu\,|p_x(rs)|}{\nu_{rs}(\nu_{rs}^2 - \nu^2)} \sin 2\pi\nu t, \qquad (5)$$

the summations now extending over all stationary states $s$ different from $r$ as indicated by the primes at the summation signs. The expression $I_xL^3$ represents the time derivative of that part of the electric polarisation of the cube in the $x$-direction, due to the electron considered, which has a frequency $\nu$. Let us compare it with the time derivative of the dipole moment of a harmonic oscillator with charge $fe$, mass $fm$, and natural frequency $\nu_0$ performing forced vibrations under the influence of the same radiation field on the classical theory, given by

$$\frac{fe^2F\nu}{2\pi m(\nu_0^2 - \nu^2)} \sin 2\pi\nu t.$$

We see then that the electron behaves like a system of such oscillators, one of them having the natural frequency zero and the strength

$$f_r = 1 + \frac{2}{hm} \Sigma' \frac{|p_x(rs)|^2}{\nu_{rs}}, \qquad (6)$$

the others having the frequencies $\nu_{rs}$ and the strengths

$$f_{rs} = -\frac{2}{hm} \frac{|p_x(rs)|^2}{\nu_{rs}}, \qquad (7)$$

so that in accordance with a general theorem due to Kuhn* and Thomas and Reiche† the total strength $\Sigma f$ of all the oscillators is unity. We may also say that the spectrum of an electron in the state $r$ consists of a line at the frequency $\nu = 0$ with a strength $f_r$ and lines at the frequencies $\nu_{rs}$ with strengths $f_{rs}$.

We proceed next to investigate more closely the resonance frequencies $\nu_{rs}$ and their $f$-values, a question not treated quite correctly in Part I. Instead of distinguishing the stationary states of the electron by means of the integers $l_1$, $l_2$, $l_3$, we shall use for this purpose the quantities $\alpha_1 a$, $\alpha_2 a$, $\alpha_3 a$, which, according to (1), have the advantage of being practically continuously variable when the edge L of the cube is large compared with the lattice constant $a$. Now the energy $W(\alpha_1 a, \alpha_2 a, \alpha_3 a)$, considered as a function of these quantities, is in general discontinuous on the surfaces $\alpha_1 a = n_1\pi$, $\alpha_2 a = n_2\pi$, $\alpha_3 a = n_3\pi$ $(n_1, n_2, n_3 = \pm 1, \pm 2, \ldots)$.* These surfaces divide the domain of $\alpha_1 a$, $\alpha_2 a$, $\alpha_3 a$ into regions inside which W is a continuous function of them in the simplest case that the potential of the lattice is separable in the $x$-, $y$- and $z$-directions. The region in which the energy takes its lowest value and which for brevity we shall call the first region is the one bounded by the surfaces $\alpha_1 a = \pm \pi$, $\alpha_2 a = \pm \pi$, $\alpha_3 a = \pm \pi$, containing according to (1) $2G^3$ stationary states, if we remember that on account of its spin the electron has two possible orientations in an outside field. If there is one conduction electron per cell of the lattice, as we shall assume here for simplicity, then, since there are $G^3$ cells in the cube, we have enough stationary states inside the first region to accommodate all the conduction electrons, and we shall in general find them nearly all in this region if the temperature is not too high.

---

* 'Z. Physik,' vol. 33, p. 408 (1925).

† 'Naturw.,' vol. 13, p. 627 (1925); 'Z. Physik,' vol. 34, p. 510 (1925); see also London, 'Z. Physik,' vol. 39, p. 322 (1926).

Taking a particular conduction electron in a stationary state $r(\alpha_1 a, \alpha_2 a, \alpha_3 a)$ of the first region, we shall inquire for which stationary states $s(\alpha_1' a, \alpha_2' a, \alpha_3' a)$ the quantity $f_{rs}$ is different from zero, *i.e.*, which of the transition frequencies $\nu_{rs}$ function as true resonance frequencies. As shown in Part I and as mentioned again by Kronig and Penney (*loc. cit.*), the conditions $\alpha_1' a = \alpha_1 a + 2n_1\pi$, $\alpha_2' a = \alpha_2 a + 2n_2\pi$, $\alpha_3' a = \alpha_3 a + 2n_3\pi$ ($n_1$, $n_2$, $n_3$ integers) must be satisfied for this purpose since only then $p_x(rs)$ does not vanish. This means that for a stationary state $r$ in the first region none of the transitions to other stationary states in the same region have values of $f_{rs}$ different from zero, while in each of the other regions there is just one stationary state $s$ giving non-vanishing $f_{rs}$. The electron in the stationary state $r$ of the first region has hence besides the resonance frequency $\nu = 0$ a number of discrete spectral lines separated by considerable intervals. These lines are absorption lines since the state $r$ lies in the lowest energy region so that the quantities $\nu_{rs}$ are negative according to (4) and the quantities $f_{rs}$ positive according to (7). From the investigations of Kronig and Penney (*loc. cit.*) it appears that the order of magnitude of the frequency $\nu_{rs}$ belonging to a state $r$ in the first region and the state $s$ in a neighbouring region for which the requirements mentioned above are fulfilled is given by $h/8ma^2$, since the discontinuity of W divided by $h$ is of this order of magnitude, and furthermore that the transitions to the states in the more remote regions have higher frequencies and in general much smaller values of

---

* See Kronig and Penney, 'Proc. Roy. Soc.,' A, vol. 130, p. 499 (1931), and Brillouin, 'J. Physique,' vol. 11, p 377 (1930), where the non-separable case is also discussed.

$f_{rs}$. The smallest of the frequencies $\nu_{rs}$ are hence about $10^{15}$ sec.$^{-1}$, lying in the visible part of the spectrum or the near ultra-violet. In Part I the discontinuities of W at the boundary of the regions were not clearly recognised, so that it seemed worth while to discuss these points more explicitly

We have until now considered the spectrum of a particular electron in the stationary state $r$. In the metal the conduction electrons will be distributed over the different stationary states according to the statistics of Dirac and Fermi. Each electron will have its own sequence of absorption lines, and since the frequencies $\nu_{rs}$ of two electrons in stationary states with only slightly different values of $\alpha_1 a$, $\alpha_2 a$, $\alpha_3 a$ lie close to each other, the spectrum of all the electrons taken together will consist of bands, each band containing as many lines as there are electrons in the cube. When the cube is made large, the lines fuse together and the bands become continuous. Of the various bands, according to what has been said above, the one corresponding to transitions from states $\alpha_1 a$, $\alpha_2 a$, $\alpha_3 a$ in the first region to the states $\alpha_1' a$, $\alpha_2' a$, $\alpha_3' a$ in the neighbouring regions such that one of the $\alpha' a$'s differs from the unprimed value by $2\pi$ while the other two are identical with the unprimed values, is the one lying furthest to the red and having the greatest intensity. In general it will be the only one to be taken into account when studying the optical properties of metals in the visible region of the spectrum and the near ultra-violet.

Since every electron has in addition to the frequencies $\nu_{rs}$ the frequency $\nu = 0$ as resonance frequency, the assemblage of electrons in the metal will also have, besides the absorption bands just discussed, a sharp spectral line at this frequency. The existence of the resonance frequency $\nu = 0$ is equivalent to the fact that the electrons can move freely through the lattice when we disregard its deformation on account of thermal agitation, so that the metal has an infinite conductivity for constant field.

As mentioned already in Part I, the electrons in the periodic field of potential are thus seen to combine the characteristic properties of free and bound electrons. They are capable of free translatory motion and they can perform transitions to other stationary states under absorption of radiation. Herein lies the great advantage of Bloch's theory of metallic conduction over the theory which treats the conduction electrons as free particles when we attempt to interpret the optical properties of metals.

A calculation of the optical constants of a metal in the visible and ultra-violet region of the spectrum, where we may neglect the temperature agitation of the metallic lattice and base our considerations on the results of this section, would be possible only if we knew the precise form of the periodic field of potential to which the conduction electrons are subjected. Taking into account the discontinuities of the energy function $W(\alpha_1 a, \alpha_2 a, \alpha_3 a)$ which we disregarded in Part I does not alter the general qualitative results there obtained so that we shall not consider the problem here any further. The question also arises as to the connection between the transitions giving rise to the absorption bands and the photoelectric emission of a metal This problem has been investigated by Tamm and Schubin.* They showed that at the frequencies for which measurements usually are made, the photoelectric yield can be entirely accounted for by the surface effect recently investigated by Frohlich,† which results even when the conduction electrons are treated as free particles The reason why the volume effect corresponding to the true absorption processes ordinarily does not contribute to this yield is explained by the fact that only the electrons in the lower stationary states can be ejected thereby, while in the surface effect also the electrons in the highest states contribute. The photoelectric threshold for the volume effect is thus higher than that for the surface effect. Unpublished calculations by Penney based on the model considered by Kronig and Penney (*loc. cit.*) confirm these results.

3. *The Optical Properties in the Transitional Region of the Spectrum.*—We had seen that in the absence of temperature agitation the spectrum of the electrons in the cube considered consists of the sharp resonance frequency $\nu = 0$ and continuous (or practically continuous) absorption bands. The effect of the collisions with the lattice which take place when we introduce the temperature agitation is most easily described by saying that the spectral lines of the system are broadened. On the continuous bands such a broadening will have practically no influence in accordance with the fact that in the visible region of the spectrum, where these bands play a predominant rôle, the optical properties are practically independent of the temperature unless this gets very high. The optical properties in the infra-red, however, where the resonance frequency $\nu = 0$ is the determining factor, will be markedly affected by the broadening which this line undergoes.

As shown in Part I, the transitional region of the spectrum at ordinary temperatures extends from about $1 \cdot 5\ \mu$ onward into the infra-red. In this region the influence of the optical absorption bands is already quite small, so that we shall neglect it entirely in this section, treating the metal there as if it had only the resonance frequency $\nu = 0$. Instead of the relation between current density and field

---

* 'Z. Physik,' vol. 68, p. 97 (1931).

† 'Ann. Physik,' vol. 7, p. 103 (1930).

$$I_x = \frac{f_r e^2 F}{2\pi m L^3} \frac{1}{\nu} \sin 2\pi\nu t,$$

which follows from (5) and (6) under this assumption, we have then for the electron in the state $r$, on taking account of the broadening,

$$I_x = \frac{f_r e^2 F}{2\pi m L^3}\left(\frac{\delta_r}{\nu^2 + \delta_r^2} \cos 2\pi\nu t + \frac{\nu}{\nu^2 + \delta_r^2} \sin 2\pi\nu t\right),$$

where $\delta_r$ is the half-breadth of the line $\nu = 0$ for this electron. In a rigorous theory the dependence of $\delta_r$ on the stationary state $r$ would have to be investigated, but as we know too little about the potential field inside the metal, we shall suppose that $\delta$ is the same for all the stationary states, which probably is roughly true. The total current density due to all electrons is then given by

$$\overline{I}_x = \frac{\sigma_0}{u^2 + 1} F \cos 2\pi\nu t + \frac{\sigma_0 u}{u^2 + 1} F \sin 2\pi\nu t, \tag{8}$$

where we have introduced the abbreviations

$$\sigma_0 = \frac{e^2}{2\pi m \delta L^3} \sum_r f_r \qquad u = \frac{\nu}{\delta} \tag{9}$$

the summation extending over all the stationary states of the cube in which there are electrons.

Introducing the quantities $\sigma$ and $\varepsilon$ occurring in the equations of Part I for the optical constants, we can write the current density of frequency $\nu$ under the influence of the radiation field (2) as

$$\overline{I}_x = \sigma F \cos 2\pi\nu t - \tfrac{1}{2}(\varepsilon - 1)\, \nu F \sin 2\pi\nu t.$$

Comparison with (8) gives us

$$\sigma = \frac{\sigma_0}{u^2 + 1}, \qquad \varepsilon = 1 - \frac{2\sigma_0 u}{\nu\,(u^2 + 1)} \tag{10}$$

From this we see that $\sigma_0$ as defined in (9) has the significance given to this symbol in the introduction, viz., that of the conductivity for constant field.

The expressions (10) are to be introduced into (6) and (7) of Part I in order to obtain the optical constants. We find

$$+ \frac{4\sigma^2}{\nu^2} = 4\frac{\sigma_0}{\nu} \frac{(\sigma_0/\nu) - u}{u^2 + 1} + 1.$$

Now for good conductors at ordinary temperatures, and even more so at low temperatures, $\sigma_0/\nu u = \sigma_0\delta/\nu^2$ in the region considered is at least 50, since as we shall see later, $\sigma_0\delta$ is about $2 \,.\, 10^{30}$. We may, therefore, write

$$\varepsilon^2 + \frac{4\sigma^2}{\nu^2} = 4\left(\frac{\sigma_0}{\nu}\right)^2 \frac{1}{u^2+1}$$

With the same approximation we have

$$\frac{2\sigma_0 u.}{\nu\,(u^2+1)}.$$

We thus obtain

$$n^2 = \frac{\sigma_0}{\nu}\left(\frac{1}{\sqrt{(u^2+1)}} - \frac{u}{u^2+1}\right), \tag{11}$$

$$\kappa^2 = \frac{\sigma_0}{\nu}\left(\frac{1}{\sqrt{(u^2+1)}} + \frac{u}{u^2+1}\right) \tag{12}$$

These expressions must be introduced into (8) of Part I in order to obtain the coefficient of reflexion R. We have

$$\mathrm{R} = 1 - \frac{4n}{n^2+\kappa^2+2n+1}.$$

When we may consider $\sigma_0/\nu$ as large compared with $u$ we can neglect $2n+1$ in the denominator and find then from (11) and (12)

$$\mathrm{R} = 1 - 2\sqrt{\frac{\nu}{\sigma_0}}\sqrt{\sqrt{u^2+1} - u}. \tag{13}$$

For small values of $u$, *i.e.*, in the far infra-red, (11), (12) and (13) go over into the classical expressions of Drude.

We must finally consider the first of the relations (9). Since the $f_r$'s are constants characteristic for the periodic field of potential in which the conduction electrons move and hence do not depend upon the temperature, the product $\sigma_0\delta$ must also be independent of temperature so that we have

$$\delta = \mathrm{const.}/\sigma_0. \tag{14}$$

Moreover, the values $f_r$ according to (6) are all smaller than unity, the $\nu_{r,s}$'s being negative as mentioned in section 2. Since there are $ZG^3$ terms in the sum of (6) if there are Z electrons in each cell of the lattice, one term for every electron in the cube, and since $L = Ga$, we must have

$$\sigma_0\delta < Ze^2/2\pi m a^3. \tag{15}$$

4. *Comparison with Experiment.*—The only measurements of $n$ and $\kappa$ in the infra-red are those of Forsterling and Freedericksz.* They were made with the elements Cu, Ag, Au, Pt and Ir. Cu was used in two forms, electrolytically deposited and sputtered, Ag was chemically, Au electrolytically deposited and Pt and Ir again sputtered. In Table I the values of $n$ and $\kappa$ observed by them are given for wave-lengths $\lambda$ greater than 1·5 $\mu$. For each value of $\lambda$ $\sigma_0$ and $\delta$ have been calculated from them by means of the relations (11) and (12).

It appears that $\kappa$ in this region of the spectrum is greater than, and usually several times as great as, $n$, while according to the classical formulæ of Drude the two quantities ought to be equal The relations (11) and (12) make it possible to interpret such a difference. Table I shows that the values of $\sigma_0$

Table I.

| Element | $\lambda$. | $n$. | $\kappa$. | $\sigma_0 . 10^{-17}$. | $\delta . 10^{-14}$ |
|---|---|---|---|---|---|
| Cu (electrolytically) | 3·11 | 4·74 | 8·1 | 0·046 | 1·72 |
| | 3·60 | 7·12 | 9·2 | 0·045 | 3·22 |
| | 4·61 | 7·61 | 9·9 | 0·052 | 2·44 |
| Cu (sputtered) | 1·53 | 0·53 | 8·0 | 0·48 | 0·263 |
| | 1·77 | 0·73 | 9·5 | 0·50 | 0·259 |
| | 2·28 | 0·68 | 11·4 | 0·73 | 0·156 |
| | 3·05 | 0·90 | 14·0 | 0·86 | 0·120 |
| | 3·25 | 1·08 | 16·4 | 1·02 | 0·113 |
| | 3·59 | 1·39 | 18·9 | 1·04 | 0·122 |
| | 4·20 | 1·92 | 22·8 | 1·12 | 0·121 |
| Au (chemically) | 2·10 | 1·00 | 14·3 | 1·06 | 0·201 |
| | 2·89 | 1·39 | 19·0 | 1·30 | 0·152 |
| | 3·38 | 2·06 | 22·9 | 1·31 | 0·161 |
| | 4·04 | 2·98 | 28·8 | 1·52 | 0·155 |
| | 4·37 | 4·34 | 32·6 | 1·40 | 0·186 |
| Au (electrolytically) | 1·69 | 0·40 | 11·4 | 1·65 | 0·125 |
| | 2·11 | 0·50 | 14·3 | 2·09 | 0·100 |
| | 2·87 | 0·73 | 16·5 | 1·66 | 0·093 |
| | 3·14 | 0·80 | 18·9 | 2·02 | 0·112 |
| | 3·50 | 0·96 | 22·6 | 2·59 | 0·073 |
| | 4·13 | 1·60 | 28·8 | 2·73 | 0·081 |
| | 4·83 | 1·83 | 33·0 | 3·07 | 0·069 |
| Pt (sputtered) | 1·52 | 4·71 | 8·3 | 0·103 | 3·32 |
| | 1·97 | 5·92 | 9·8 | 0·112 | 2·90 |
| | 3·29 | 7·50 | 12·2 | 0·104 | 1·80 |
| | 3·41 | 8·82 | 13·8 | 0·130 | 1·90 |
| | 4·65 | 10·9 | 15·5 | 0·123 | 1·80 |
| Ir (sputtered) | 1·57 | 5·16 | 7·96 | 0·094 | 4·26 |
| | 2·77 | 6·55 | 9·36 | 0·075 | 2·97 |
| | 3·36 | 8·80 | 11·28 | 0·081 | 5·02 |
| | 4·60 | 12·28 | 14·61 | 0·121 | 3·72 |

---

* 'Ann. Physik,' vol. 40, p. 20 (1913).

and $\delta$ computed for various wave-lengths are approximately the same, and taking into account the difficulty of the measurements and the simplifying assumptions made in the theoretical derivation, the constancy of these quantities must be regarded as satisfactory, particularly as it seems to improve, the further we get away from the influence of the optical absorption bands.

In Table II are given the average values of $\sigma_0$ and $\delta$ for the different elements. It is interesting to note that the values of $\sigma_0$ are in all cases less than the values of the conductivity $\sigma_0'$ as determined by resistance measurements. This is probably due to the fact that the optical constants depend upon the properties of a very thin surface layer of the metal, and it is quite possible that on account of the distortion of the metallic lattice in the surface region and the occlusion or adsorption of gases the conductivity is much diminished. The results with the two forms of copper are noteworthy in this connection, the electrolytically deposited copper having apparently a particularly bad conducting surface

Table II.

| Element. | $\sigma_0 . 10^{-17}$ | $\sigma_0' . 10^{-17}$. | $\delta$ $10^{-14}$ | $\sigma_0\delta . 10^{-30}$ | $\frac{Ze^2}{2\pi m a^3}$ $10^{-30}$. |
|---|---|---|---|---|---|
| Cu (electrolytically) | 0·048 | 5·3 | 2·45 | 1·18 | 3·45 |
| Cu (sputtered) | 0·82 | | 0·165 | 1·35 | |
| Ag (chemically) | 1·32 | 5·7 | 0·171 | 2·25 | 2·41 |
| Au (electrolytically) | 2·25 | 4·2 | 0·093 | 2·09 | 2·37 |
| Pt (sputtered) | 0·115 | 0·85 | 2·35 | 2·71 | — |
| Ir (sputtered) | 0·093 | 1·7 | 3·99 | 3·72 | — |

The values of $\sigma_0\delta$ are also shown in Table II as well as $Ze^2/2\pi m a^3$ for Cu, Ag and Au For these elements each cell contains four atoms, and as each of these furnishes one conduction electron Z = 1, while the values of $a$ are respectively $a_{Cu} = 3{\cdot}66 . 10^{-8}$ cm., $a_{Ag} = 4{\cdot}06 . 10^{-8}$ cm., $a_{Au} = 4{\cdot}08$ $10^{-8}$ cm We see that (15) is satisfied in all three cases. In addition, it is interesting that $\sigma_0\delta$ for the two forms of copper is practically the same, although the values of $\sigma_0$ and $\delta$ taken individually differ widely from each other.

Equations (11) and (12) together with the relation (14) give us also the temperature dependence of $n$ and $\kappa$ if we assume that $\sigma_0$ varies with T in the same way as $\sigma_0'$. Unfortunately, no experimental data are available on this point.

Forsterling and Freedericksz (*loc. cit.*) have calculated the value of the coefficient of reflexion R at perpendicular incidence from (8) of Part I with their values of $n$ and $\kappa$. As shown by them, the computed values agree quite well with the directly measured values of R so that the experimental material concerning R is also in conformity with the theory he reproposed. Measurements of R extend to about 10 $\mu$, which is further than the measurements of $n$ and $\kappa$, but beyond $\lambda = 5\ \mu$ the reflexion in general is so good that the accuracy of the quantity $1 - R$, which is the one usually determined, is not great. Data on the temperature dependence of R in the infra-red are thus far not available, but it is hoped that measurements in progress at this laboratory will furnish evidence in this regard.

### *Summary.*

(1) The theory of dispersion in metallic conductors developed in Part I of this paper is formulated more precisely for the case that the temperature agitation of the metallic lattice may be neglected The absorption bands which dominate the optical behaviour of metals in the visible and ultra-violet part of the spectrum are discussed in detail

(2) An extension of the theory for the infra-red region of the spectrum, where the average time between two collisions of an electron with the metallic lattice is comparable with the period of the radiation is given, explicit formulæ for the index of refraction and the coefficients of extinction and reflection being derived which go over into the classical expressions of Drude in the limit $\nu = 0$

(3) The experimental data are compared with the theoretical results and found to give a satisfactory agreement. The possibility of obtaining valuable information about the surface layers of metals from the optical constants is pointed out, as well as the desirability of measuring the temperature dependence of these constants in the infra-red

# *A Vacuum Spectrometer for Long Wave-Length X-Rays.*

By R. T. W Bingham, M.Sc., University of Melbourne.

(Communicated by T H Laby, F R.S —Received May 26, 1931 )

[Plates 8, 9.]

## *Summary.*

The instrument described was designed to give a high intensity of radiation at the photographic plate and to be capable of accurate angular measurements of crystal reflection. The Seeman form of spectrometer, in which a single slit is placed between the crystal (or ruled grating) and the photographic plate, was used together with a method of measuring angles on a single accurate circle. Both spectrometer and X-ray tube were placed in a common vacuum to allow the focal spot to be brought close to the crystal.

The instrument has been used with a method similar to Rowland's coincidence method to measure the wave-length of the $AlK\alpha_{12}$ line relative to the fifth and sixth orders of the $CuK\alpha_{12}$ doublet, using a sugar crystal. The result obtained, after correction for deviation from the Bragg law, is 8315 X.U. relative to 1539·23 X U. for the copper doublet, the results being reproducible to 1 X.U.

The instrument has also been used to study the reflection and diffraction of X-rays, the results obtained being reported in the preceding paper in this journal. The spectrometer has been proved to have a high speed for studying reflection and diffraction phenomena.

## *General Description.*

The instrument to be described was designed by Professor T. H. Laby for accurate measurements of long wave-length X-rays with a crystal. To make it effective for this purpose, it was designed for two main characteristics, namely (1) that it should be capable of measuring angles of crystal reflection accurately, and (2) that the X-ray beam should be of high intensity at the photographic plate to give a high line density with short exposures. Although these were the objects of the design, the spectrometer has also been used as a ruled grating spectrometer for measuring wave-lengths and intensities in the spectral region from 1 to 900 Å., and for studying the reflection of X-rays from copper and carbon targets by mirrors of glass, quartz and stainless steel.

In order that the instrument should have the above features, the Larsson[*] form of the Seeman[†] X-ray spectrometer is used. In this design, as shown in fig. 1, a single slit is placed near a fixed crystal and between it and the photographic film. The use of a fixed crystal appears to give spectra of higher intensity than a rotating crystal Bragg spectrometer, and it has the considerable advantage for a vacuum spectrometer that a vacuum-tight bearing for rocking the crystal is unnecessary. As evidence of the intensity of the radiation incident on the crystal, the observation may be mentioned that a calcite crystal was seen in the darkened room to be glowing with a reddish yellow light for about 5 minutes after the X-ray discharge was stopped. The X-ray tube had been working for 20 minutes at 23 KV and 3 mA. The high intensity of the radiation proved to be a very great advantage when working with this instrument It should be added that, on account of the diverging nature of the beam incident on the crystal or grating, it does not give accurate absolute measurements of wave-lengths when used with a grating, but this is a use for which it was not designed.

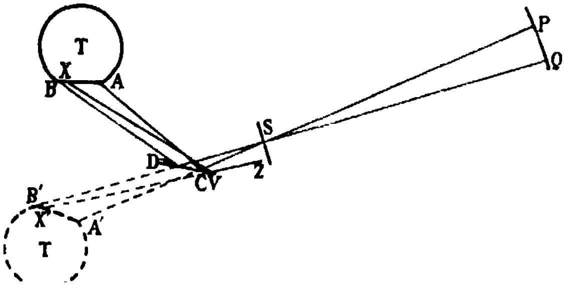

*Fig. 1*—*Range of Angles with Stationary Crystal*

The intensity of the radiation incident on the crystal was made high by placing the X-ray tube and spectrometer in a common vacuum, and bringing the focal spot close to the crystal. This has the disadvantage that the whole apparatus must be maintained at an X-ray vacuum, and, since the apparatus is constructed of metal, a very high speed pumping system is needed. The vacuum attained limited the power input of the X-ray tube which rarely exceeded 100 watts. The exposures, however, were quite reasonable, being rarely longer than 20 minutes. This difficulty could be obviated by a change in design of the X-ray tube and its method of evacuation.

---

[*] 'Phil. Mag.,' vol. 3, p. 1136 (1927).

[†] 'Phys. Z.,' vol. 20, p. 55 (1919).

The use of the instrument as a crystal spectrometer is the only one described below. Its use with a ruled grating and for studying the reflection of X-rays is described in the preceding paper in this journal.

### *Principle of the Spectrometer.*

A pencil of X-rays diverging from the focal spot AB of the target T is incident on the crystal CD at a range of angles as shown in fig. 1. If these rays satisfy the Bragg condition $n\lambda = 2d \sin \theta$, they are reflected at the face of the crystal (and in planes parallel to it) and pass through the slit S forming a spectrum on the photographic film PQ. With the long wave-lengths used, the penetration of the crystal is small, and the reflection may be described as though it took place wholly at the crystal face In the figure the rays ACP and BDQ are the limiting rays of the beam which is reflected through the slit S. Any other ray such as the ray XYZ may be reflected but will not pass through the slit. In every case the rays appear to come from an image A′B′ of the focal spot in the crystal face.

### *Outline of Design*

It will be seen from fig. 2 and Plate 8 that (1) the crystal is mounted on a bearing AA so that it can rotate relative to the camera D and the angle θ between its face and the axis of the camera can be read on an accurate circle C, and (2) the crystal and camera, which may be clamped together, are mounted on a second bearing FF and can rotate relative to the base and the focal spot, the angle 4θ being read on a second circle G graduated to 20′ of arc.

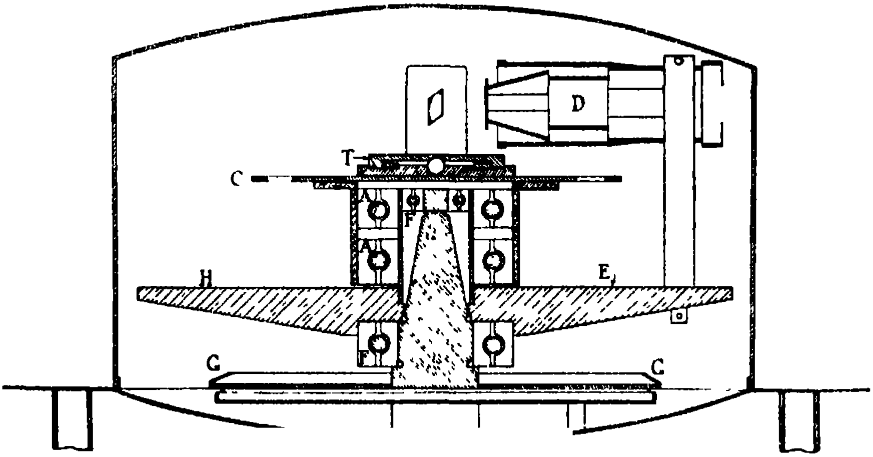

FIG. 2.—Diagrammatic Sketch of Spectrometer.

Larsson's method of determining angles of crystal reflection has been used as it has the following advantage. In the determination of a wave-length only two readings on the same circular scale plus or minus a correction for position are necessary and, since the angle measured is that between the crystal and the camera axis, the accuracy is dependent only on the crystal table bearing, whereas in the ordinary method both bearings must be accurately concentric. The method consists in taking two observations with the crystal and camera in the positions shown in fig 3 Keeping the incident beam fixed, the angle between the two positions of the crystal is $2\theta$ To get the crystal from one position to the other, it must be rotated through 180° + $2\theta$, the angle of 180° being necessary to change from the zero for one position to the zero for the other position. The crystal and camera are then clamped together and moved through an angle $4\theta$ measured on the rough circle to make the incident beam fall on the crystal at the angle $\theta$. Thus if $R_1$ and $R_2$ are the readings on the accurate circle corresponding to the two positions of the same X-ray line, the angle of reflection is given by

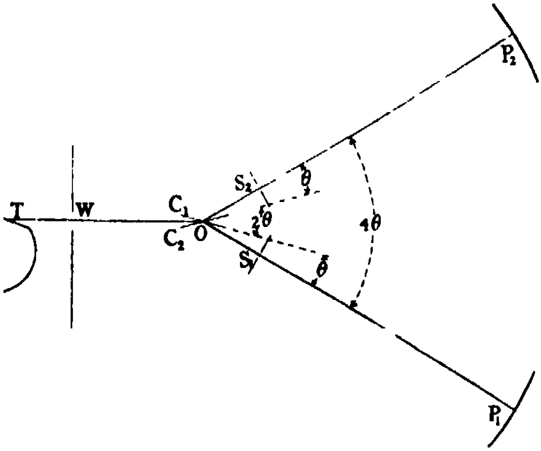

Fig 3. Method of Measuring Reflection Angles

$$\theta = \tfrac{1}{2}(R_1 - R_2 - 180)^\circ.$$

It will be noticed that in this expression the readings of the rough circle do not appear. The work of this circle is to point the spectrometer towards the focal spot at the correct angle, thus determining what range of angles is reflected. It has no effect on the position of any X-ray line on the photographic film.

The above expression assumes that $\theta$ is the angle between the crystal face and the axis of the camera, *i.e.*, the line through the centre of the slit and the junction of the crosswires on the back of the camera. In practice, however, the lines are made to fall close to the vertical crosswire and the angular readings are corrected for the divergence as shown in fig. 4. SW is the axis of the camera

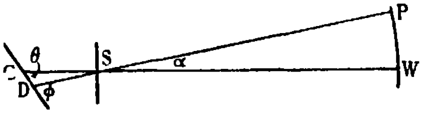

FIG. 4.—Correction of Angle for displacement from Crosswire

and SP the path of the beam forming the X-ray line. The correction of the angular reading is then $\alpha = d/r$, where $d$ is the arc WP whose centre is at S and $r$ is the camera length. In the instrument described $r$ is 7·884 cm. The final expression for the angle of reflection is therefore

$$\theta = \tfrac{1}{2}(R_1' - R_2' - 180)^\circ,$$

where $R_1'$ and $R_2'$ are the corrected angular readings of the accurate circle. Well-defined spectral lines may be measured by this method to an accuracy of at least 0·002 mm., which is equivalent to an angle of 4″. The micrometers read to 2″.

### *Description and Adjustment of Spectrometer.*

The instrument is so designed that the following adjustments may be made in the relative positions of the spectrometer parts —

(1) The camera axis to intersect the rotation axis.
(2) The camera axis perpendicular to the rotation axis.
(3) The slit and vertical crosswire parallel to the rotation axis.
(4) The centre of the accurate circle in the rotation axis.
(5) The reading microscopes 180° apart, and
(6) The face of the crystal in the rotation axis.

The general arrangement of the parts of the instrument is shown in Plate 9. The crystal table, camera, bearings and graduated circles are carried by the base, which is a square sheet of iron dished outwards to stand the vacuum and supported by a pillar at each corner. The lid is a cylinder of sheet iron with a convex end carrying the cathode in its side and the target in its top. Small glass windows are set in its side for viewing the X-ray tube and sighting along the direction of the X-ray beam. The three-stage Gaede diffusion pump, supported between two of the pillars as shown and connected to the base of the spectrometer through a liquid air trap, is backed by a Cenco Hyvac. The lid registers to the base and is sealed with soft wax.

A simple and easily removable shield of sheet iron, which has in it a circular hole of 0·3 cm. diameter to allow the X-rays to pass from target to crystal, protects the parts of the spectrometer from being sputtered with metal from the X-ray tube.

The cathode was taken from a defective Muller radiological tube. The tungsten filament was replaced by a platinum wire coated with barium and strontium oxides. In this way the light from the filament is of such colour and intensity as to have no effect on the photographic film. This was tested for exposures much longer than those actually used. This cathode works best for low potentials when brought further forward than in the original tube. The water-cooled target is a straight brass tube with a larger cylindrical cap milled flat on one face and is insulated by a glass tube 3 mm. thick in the wall. This will stand potentials up to 30 KV.

The crystal table shown in fig. 2 and Plate 8 has (1) a horizontal traversing motion controlled by a screw of fine pitch, and (2) a tilting motion about a horizontal axis controlled by a micrometer working against a spring. These adjustments enable the crystal to be moved until its face lies in the rotation axis. The 5-inch crystal circle made by Messrs. E. R. Watt is read by two micrometer readers with graduated drums reading to 2″.

The camera D carried by the arm E (fig. 2) is shown in section in fig. 5. At one end it has a symmetrical slit with stainless steel jaws carried by the two halves of a truncated cone. The construction of the slit system will be evident from the figure. The other end of the camera, see figs. 5 and 6A, is a square metal block, shaped on one side into a cylinder whose axis is the slit. A window is cut in the block and vertical and horizontal crosswires of fine tungsten wire stretched across it. The dark slide, shown in figs. 5 and 6B, presses the film against the cylindrical end of the camera in contact with the vertical crosswire. The whole camera system has proved very convenient in use.

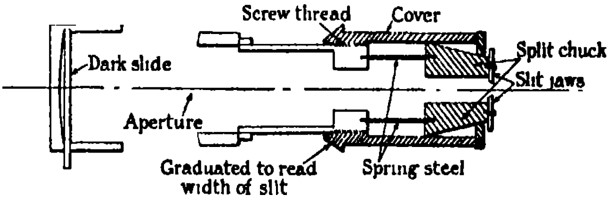

Fig. 5.—Section along axis of Camera.

To make the adjustments given above, a level is placed on the crystal table and the rotation axis adjusted to be vertical by means of four screws at the bottom base plate (see Plate 9). The slit and crosswires are then made vertical and the axis of the camera made to intersect the rotation axis defined by a plumbob. The crystal face is then placed in the rotation axis by means of a microscope.

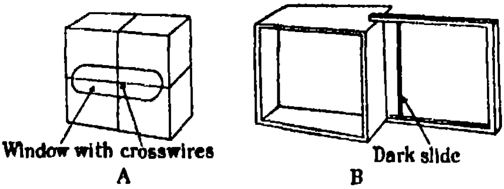

FIG. 6.—Perspective Drawing of Back of Camera and Film Holder.

The distances on the films were measured on the projector in general use in this laboratory and which has been described elsewhere.* For measuring faint lines this projector is superior to a measuring microscope both in convenience and accuracy.

### *The Wave-length of the* $\mathrm{AlK}\alpha_{12}$ *Line.*

The method finally adopted for the measurement of the wave-length of the $\mathrm{AlK}\alpha_{12}$ line consists in measuring the interval on the photographic film of the aluminium line from the $\mathrm{CuK}\alpha_{12}$ line in the fifth and sixth orders. The angle corresponding to the aluminium line was also measured.

Then

$$\theta_{5\mathrm{Cu}} = \theta_{\mathrm{Al}} - \alpha x,$$

and

$$\theta_{6\mathrm{Cu}} = \theta_{\mathrm{Al}} + \beta x,$$

where $\theta_{\mathrm{Al}}$ is the measured angle for the aluminium line, $\alpha$ and $\beta$ are the film intervals and $x$ is a constant depending on the curvature of the film.

Since

$$n\lambda = 2d \sin\theta,$$

$$\sin(\theta_{\mathrm{Al}} - \alpha x)/\sin(\theta_{\mathrm{Al}} + \beta x) = 5/6.$$

---

* Rogers, 'Proc. Roy. Soc., Victoria,' vol. 34, p. 196 (1922).

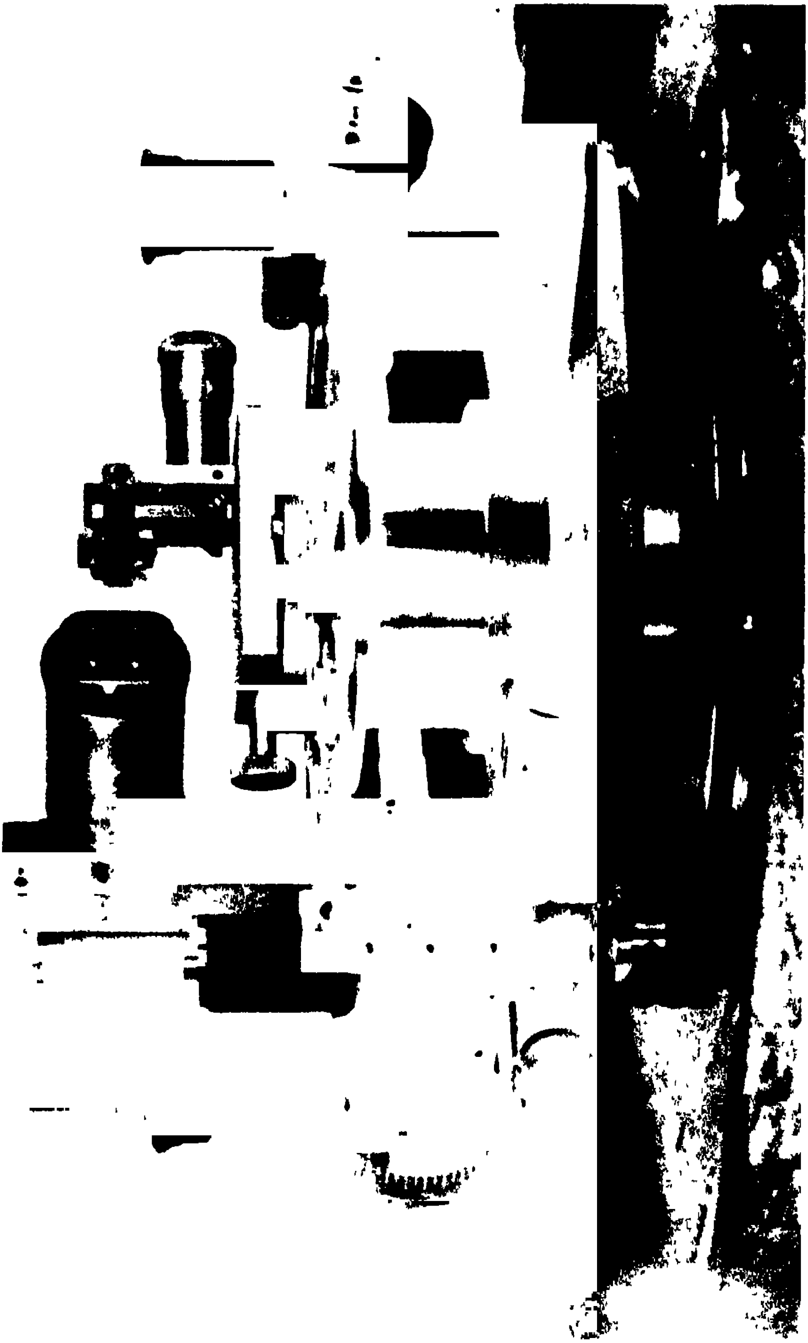

The spectrometer.

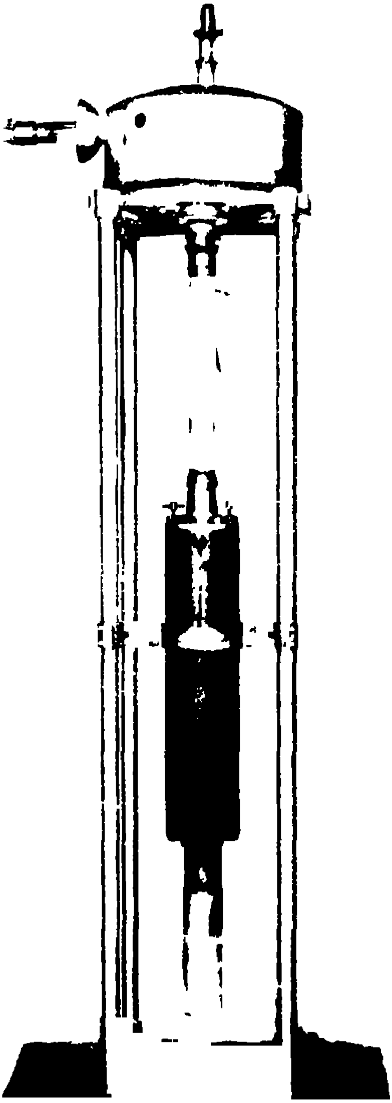

Spectrometer assembly. (The casing shown is of cast metal. Sheet iron was later substituted for this.)

The separations on the film of the AlK$\alpha_{12}$ line from the fifth and sixth orders of the CuK$\alpha_{12}$ lines are respectively

| AlK$_{12}$–CuK$_{12}$ V. | | AlK$_{12}$–CuK$_{12}$ VI | |
|---|---|---|---|
| Film. | Separation. | Film. | Separation. |
| | mm. | | mm |
| 84 | $2\ 569_5$ | 93 | 3 800 |
| 91 | $2\ 570_5$ | 95 | 3 800 |
| 94 | 2 570 | 70 | 3 795 |
| 96 | 2 570 | | |
| Mean | 2 570 | Mean | 3 800 |

and the measured angle $\theta_{Al}$ taken as a mean from 20 films is 23° 10′. This is only given correct to the nearest minute, but this is sufficient for the purpose since a high degree of accuracy in this angle is not required.

Substituting these values in the above formula

$$\sin(23^\circ\ 10' - 257x)/\sin(23^\circ\ 10' + 380x) = 5\cdot 6.$$

Solving by successive approximations, the value 25·710″ for $x$ is found to satisfy the equation to about 1 in 40,000. The angles for the fifth and sixth orders of the copper line may then be calculated and the wave-length of the aluminium line from the formula

$$\lambda_{Al} = \lambda_{5Cu} \sin\theta_{Al}/\sin\theta_{5Cu}.$$

The result, in terms of $\lambda$ CuK$\alpha_{12}$ = 1539·23 X.U., is

$$\lambda_{Al} = 8323\cdot 5 \text{ X.U.}$$

The wave-lengths of all three lines used should be corrected for deviation from the Bragg law, but the aluminium line is the only one affected appreciably as the orders of the copper lines are high. The insertion of the corrected wave-lengths of the copper lines in the above work does not alter the final value within the limits of accuracy of the calculation. The correction for the aluminium line was calculated from the formula*

$$\lambda = \lambda_B (1 - 5\cdot 4 \times 10^{-6} d^2\rho/n^2),$$

where $\lambda$ and $\lambda_B$ are the corrected and uncorrected wave-lengths, $d$ the crystal grating space, $\rho$ the density, and $n$ the order of the spectrum. Substituting the appropriate values for the sugar crystal used, the final corrected result is

---

* Siegbahn, "The Spectroscopy of X-rays," Oxford, 1926.

$$\lambda_{Al} = 8315 \cdot 4 \text{ X.U.},$$

relative to $CuK\alpha_{12} = 1539 \cdot 23$ X.U.

The accuracy of the length measurements is believed to be not quite so high as the concordance of the above measurements would indicate. This error is probably of the order of 0·002 mm., and the error introduced into the final result by an error of this magnitude has a maximum value of 0·7 X.U.

# *The Reflection and Diffraction of X-Rays.*

By Professor T H. Laby, M.A., Sc.D., F.R.S , and R. T. W. Bingham, M.Sc.,
University of Melbourne.

(Received May 26, 1931 )

## *Summary.*

The agreement between the theories of the reflection of X-rays by solids and observations is discussed Generally the observations so far obtained are not in close agreement with each other or with theory.

The writers find that X-rays of wave-lengths 13·3 Å. (Cu Lα) and 44·7 Å. (C Kα) are reflected by glass, quartz and stainless steel at angles considerably greater than the calculated critical angles. The radiation from carbon has been focussed by a spherical mirror for an angle of incidence of 45°. The ratio of the intensity of the reflected to the incident beam, when X-rays from a carbon target are incident on a glass mirror, has been determined approximately by a photographic method and is found to agree with the Fresnel electromagnetic theory provided a higher absorption of the X-rays occurs than has been previously supposed.

This evidence of reflection for angles of incidence greater than the critical angle, which is 6° for glass at a wave-length of $\lambda = 44 \cdot 7$ Å., is confirmed by observations with a glass diffraction grating with which the $\lambda = 44 \cdot 7$ Å. line has been observed for angles of incidence on a plane grating up to 19°. A new plane ruled grating spectrometer is described by means of which the C Kα line has been obtained with short exposures in all orders from the 18th negative

to the 13th positive. Microphotometer curves of the wave-length distribution of the energy in the grating spectrum of carbon radiation are given, and these indicate that it consists almost entirely of the Kα line, $\lambda = 44 \cdot 7$ Å.

Using Rowland's method of coincidences the wave-length λ C Kα is found to be $44 \cdot 7_5$ Å. relative to λ Cu Lα = $13 \cdot 32$ Å.

## *Introduction.*

When X-rays are propagated through matter, the theory of Drude and Lorentz* gives a refractive index, $n$, which is less than unity. If the electrons make forced oscillations of frequency, $\nu$, that of the incident X-rays, the refractive index is

$$n = 1 + \frac{1}{\pi} \cdot \frac{e^2}{m} \cdot \sum_{1}^{N} \frac{N_s}{\nu_s^2 - \nu^2} \tag{1}$$

where $N_s$ is the number of resonance electrons per cm.$^3$ of natural frequency $\nu_s$, and $e/m$ E.S.U. is the specific charge on the electron. When a beam of X-rays is incident on the plane surface of a solid, for which $n$ is less than 1, at a glancing angle less than a certain critical angle, $\theta_c$, the beam is totally reflected. The refraction of X-rays was first observed by Stenstrom in 1919, and total reflection by Compton in 1922. Many aspects of the optical properties of X-rays have since been studied, including the diffraction of the rays by ruled gratings.

While the simple resonance theory has been modified to take into account absorption of the radiation which occurs in all media, it is important to note the essential features of the resonance theory neglecting absorption and to see under what conditions the simple equation (2) below, which neglects resonance effects, is applicable. Both on account of the presence of electrons of several resonance frequencies within the observable range and the large amount of experimental data available for glass, we calculate its refractive index by equation (1). It is to be remembered, however, that the observed values of $n$ are for glasses of varying chemical compositions. The refractive index is calculated for a glass assumed to have the composition given below, and the K, L, M, N electrons in the Ca, Si, Na and O atoms composing it are taken as the resonance electrons.

---

* See Compton's "X-rays and Electrons," chap. 7, Macmillan, London, 1927, for this theory and for reference not given in this paper.

Table I.—Data assumed for Glass.

| Element. | Ca. | Si. | Na | O. |
|---|---|---|---|---|
| Concentration (gm./cm.$^3$) | 0·3 | 1·0 | 0·3 | 1·4 |
| Resonance wave-length for K, L, electrons | 3, 33 | 7, 100 | 12 | 25 Å |
| Number of K, L, M, N, electrons per atom | 2, 8, 8, 2 | 2, 8, 4 | 2, 8, 1 | 2, 6 |

The composition and the wave-lengths are in round numbers, but nevertheless they are sufficiently accurate to give the essential features of the dispersion curve. The resonance frequencies of the L and M absorption edges, with the exception of the L edges of the Ca and Si atoms, have no appreciable effect over the range of wave-lengths (0 to 100 Å.) considered.

Equation (1) is equivalent to

$$1 - n^2 = \frac{e^2}{\pi m}\,\frac{\lambda^2}{c^2}\cdot\frac{1}{m_{\mathrm{H}}}\sum_1^{\mathrm{N}}\frac{\mathrm{N}_a\lambda_s^2}{\lambda^2-\lambda_s^2}\cdot\frac{\rho}{\mathrm{A}}$$

where $\lambda = c/\nu$, $\lambda_s = c/\nu_s$, $n_a$ the number of K, L, ..., electrons in an atom of relative mass A ($\mathrm{H} \equiv 1{\cdot}008$), and $m_{\mathrm{H}}$ gm. is the mass of the H atom. Inserting the values of the various quantities this becomes,

$$1 - n^2 = 5{\cdot}40\,.\,10^{-6}\lambda^2\sum_1^{\mathrm{N}}\frac{\mathrm{N}_a\lambda_s^2}{\lambda^2-\lambda_s^2}\cdot\frac{\rho}{\mathrm{A}},$$

where λ is in Å. The summation is made for all the electrons mentioned. The values thus found for $1 - n^2$ for a range of values of λ are shown in fig. 1, where for compactness the logarithms of these quantities are plotted. The terms of the summation are also shown. There is, of course, a discontinuity at each resonance frequency (in the case of glass at the approximate wave-lengths 3, 7, 12, 25, 33, 100 Å.). It is important to notice that it is only over the restricted ranges of wave-length shown by the figure that the refractive index is approximately given by the simple relation

$$n^2 = 1 - \frac{1}{\pi}\cdot\frac{e^2}{m}\cdot\frac{\mathrm{N}_s}{\nu^2}, \tag{2}$$

in which form (1) may be written when $\nu_s^2 \gg \nu^2$. This gives

$$\delta \equiv 1 - n \doteqdot 4{\cdot}47\,.\,10^{-30}\mathrm{N}_s\lambda^2$$

from (2) and it follows that the critical angle of total reflection for is

$$\theta_c \doteqdot \sqrt{2\delta} \doteqdot 3{\cdot}10^{-15}\sqrt{\mathrm{N}_s}\,\lambda$$

and

$$\delta/\lambda^2 \doteqdot 4{\cdot}5\,.\,10^{-30}\,\mathrm{N}_s.$$

In fig. 1, the straight line AB represents equation (2), and the heavy line equation (1). It will be seen that these lines intersect for six values of λ, and the values of *n* given by the two equations for values of $\lambda > 25$ Å. are generally quite different.

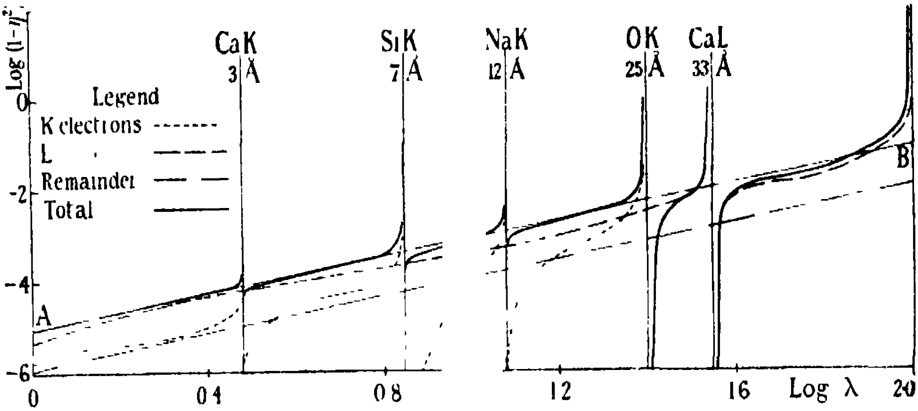

FIG. 1.—The Drude-Lorentz Dispersion Formula for Glass.

A number of observers have tested this approximation for a variety of solids, including glass, mica, calcite, barytes, pyrites, silver iron zinc and aluminium, the range of wave-lengths being 0·5 to 6·5 Å. Observations on anomalous dispersion with longer wave-lengths will be mentioned later The different observers are not in good agreement as is shown clearly in a diagram given by Larsson,* in which the observed values of $\delta/\lambda^2$ range from about 40 per cent. below to 80 per cent. above the theoretical as just given.

When the frequency, ν, of the incident radiation approximates to that of the resonance electrons, anomalous dispersion occurs. The type of curve is shown in fig. 2, where *n* is plotted against ν. A discontinuity of this type has not been observed experimentally for X-rays. It has been assumed that the

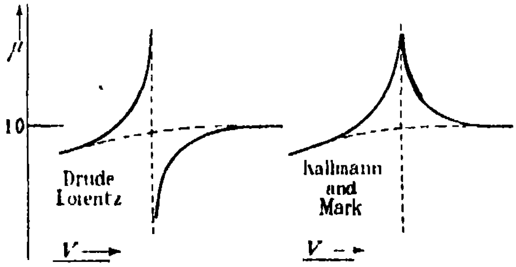

FIG. 2.—Form of the Resonance Discontinuity.

---

* 'Diss. Uppsala Univ. Ars.,' p. 20 (1929).

frequency of the resonance electron is that of the X-ray absorption edge, but the prediction of wave mechanics[*] in this respect is that the frequencies of the emission lines must be considered instead of the frequency of the absorption edge. There is no certain evidence for this in the experimental data available.

In 1924 Kramers[†] and later Kallmann and Mark[‡] assumed a number of resonators so distributed with respect to frequency as to take into account the empirical $\lambda^3$ law of X-ray absorption. The latter obtained the expression

$$n^2 = 1 - \frac{1}{\pi}\,\frac{e^2}{m}\sum_1^N \frac{N_s}{\nu_s}\left(1 + \frac{\nu_s^2}{\nu^2}\cdot\log\frac{\nu_s^2 - \nu^2}{\nu_s^2}\right)$$

The form of this expression is also shown in fig. 2. Of several attempts to obtain experimentally the form of the discontinuity only Larsson's[§] observations on calcite appear to have been successful, his curve being of the same shape as that of Kallmann and Mark.

The fraction of the energy and an X-ray beam which will be reflected by an absorbing medium has been calculated by Forster[||] on the basis of the Fresnel expressions. He shows that a sharp critical angle only exists for media whose absorption coefficients are small, and that as the absorption increases there is an increasing intensity of radiation reflected at angles greater than the critical angle. This effect on the critical angle has been observed by Forster, Prins,[¶] Schon,[**] Dershem[††] and Thibaud.[‡‡] In 1927 the writers and Shearer[§§] observed a considerable intensity of reflection for angles of incidence much greater than the critical angle as calculated by equation (3).

### *The Reflection of X-rays.*

We found that heterogeneous X-rays incident on glass at glancing angles up to 45°, and on quartz up to 40°, were reflected. The most intense component of the radiation used was the K$\alpha$ line of carbon of wave-length 45 Å. These angles are very much larger than are to be expected from the Drude-Lorentz theory, the critical angle for the glass mentioned above (see Table I and fig. 1) and this wave-length being approximately 6°, a value has been experimentally confirmed by Dershem (*loc. cit.*). As previously stated, the effect of absorption is to diminish the sharpness of the critical angle but not to such an extent that reflection would be expected at 39° beyond it unless the absorption is much greater than has hitherto been supposed. The reality of the reflection at the large angles mentioned is of interest not only as a test of the theories of dispersion just outlined, but also because the phenomena imply that the ruled grating may be used to diffract X-rays incident at larger glancing angles than is usually assumed.

---

[*] Sommerfeld, " Wave Mechanics," Methuen, London, p. 169 (1930).

[†] 'Nature,' vol. 113, p. 673 (1924).

[‡] 'Ann. Physik,' vol. 82, p. 585 (1927).

[§] *Loc. cit.*, p. 3.

[||] 'Helv. Phys. Acta.,' vol. 1, p. 18 (1928).

[¶] 'Nature,' vol. 120, p. 188 (1927); 'Z. Physik,' vol. 47, p. 479 (1928).

[**] 'Z. Physik,' vol. 58, p. 165 (1929).

[††] 'Phys. Rev.,' vol. 34, p. 1015 (1929).

[‡‡] 'J. Physique,' vol. 1, p. 37 (1930).

[§§] 'Nature,' vol. 122, p. 96 (1928), and 'Proc. Roy. Soc., Victoria,' vol. 41, p. 55 (1928).

In what follows experiments are described which verify the existence of reflection at angles greater than the calculated critical angle. The spectrometer (for description see Bingham, *supra* p 266) used by the writers did not allow the isolation of a monochromatic beam in the study of X-ray reflection and diffraction phenomena, but evidence is given that certain of the radiations used were effectively monochromatic. Messrs. Mohr and Massey at the suggestion of the senior author have made experiments on X-ray reflection, which are described in a paper by Mr. Mohr, in which a monochromatic beam was used. The latter method has the advantage that the radiation is undoubtedly monochromatic, but its intensity is small. In the former the radiation is not so definitely monochromatic, but it is of much greater intensity and effects can be observed which escape recognition in the former method

*Copper Radiation.*—The large angles of reflection referred to were first observed in attempting to use a film of an organic acid on glass as a crystal grating. To find the range of angles over which reflection occurred the radiation from a copper target with 10 kv. applied to the X-ray tube was reflected from a glass mirror. The photograph showed a laterally inverted slit image of the focal spot. Table II and fig. 3 summarises the results which are only qualitative in respect to intensity.

Table II —Intensity of Reflection of Copper Radiation.

| Angle | 4½° | 4½° | 10° | 10° | 15° | 15° | 20° | 25° | 30° |
|---|---|---|---|---|---|---|---|---|---|
| Exposure (ma. sec ) | 36 | 120 | 30 | 360 | 360 | 720 | 800 | 1200 | 2400 |
| Intensity | *s.* | *vs.* | *f.* | *m.* | *s.* | *s.* | *m.* | *m* | *f.* |

*s* = strong ; *m* = medium ; *f* = faint.

In the graph the reciprocal of the exposure for a constant photographic density as estimated visually is taken as a rough measure of the intensity of the reflected radiation. On p. 288 it is shown that the radiation from a copper target consists of the K and L spectra of copper plus a background of general radiation. The intensity at 4½° is larger than is to be expected since the theoretical critical angle for glass and $\lambda$ (Cu L$\alpha$) = 13·3 Å. is approximately 2°.

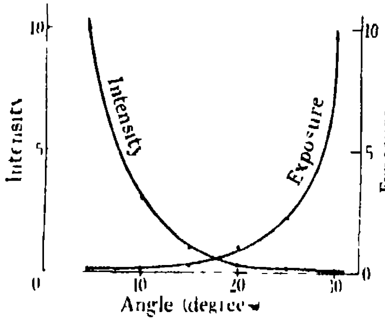

Fig. 3.—Intensity of Copper Radiation.

*Carbon Radiation.*—As the radiation reflected in the foregoing experiments might be general radiation of long wave-length, it was decided to use a carbon target. On account of its low atomic number, such a target should only emit a weak general radiation and its K radiation should be of high intensity relative to the general radiation. This proved to be the case.

Using a graphite target with 400 volt on the X-ray tube, the results given in Table III were obtained.

Table III.—Reflection of Carbon Radiation.

| Mirror. | Glass. | | | | | | | | | | Quartz | | Stainless steel. | |
|---|---|---|---|---|---|---|---|---|---|---|---|---|---|---|
| Angle | 5° | 6½° | 10° | 12½° | 15° | 17½° | 20° | 25° | 30° | 45° | 15° | 40° | 10° | 40° |
| Intensity | s | s. | s | s. | m. | m. | m. | m. | m | f. | s. | f. | s. | f. |

s = strong, m = medium; f = faint.

The exposure for all these films was 1200 m. sec. The above results for glass show that the reflected intensity falls off for angles greater than the critical angle, 6° more slowly than is to be expected (see fig. 5) except for a large absorption of the radiation by the reflector.

### *Intensity of Reflection of Carbon Radiation from Glass.*

To enable the intensity of reflection of carbon radiation from a glass mirror to be studied quantitatively up to large angles, it is necessary to photograph as wide a range of angles as possible per exposure. A mirror of glass of the same composition as that of the grating used in the experiments described later—kindly lent by Mr Z. A. Merfield—was placed on the crystal table in the rotation axis of the spectrometer and the face of the target turned to give a fine line focus. The spectrometer slit was removed and a sharp edge placed parallel to the rotation axis and close to the face of the mirror, the edge and its image in the mirror face acting as the slit. This arrangement is shown in fig. 4, in which G is the mirror, F the focal spot and F′ its image in the mirror face. S is the sharp edge, S′ its image, and PQ is the photographic film.

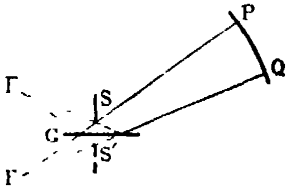

Fig. 4.—Intensity of Reflection from Mirror.

Photographs were taken with the exposures and at the angles given in Table IV. The exposures are in milliamperes per minute at 10 kv., and the angles in degrees

Table IV.—Exposures for different Angles of Incidence

| Angle | 2½° | 5° | 7½° | 10° | 12½° | 15° | 17½° | 20° | 22½° | 25° |
|---|---|---|---|---|---|---|---|---|---|---|
| Exposure | 2 | 5 | 10 | 10 | 10 | 20 | 20 | 20 | 40 | 40 |

The films were developed carefully at a controlled temperature and photometered with a Moll recording microphotometer. The photographic densities so obtained were corrected to constant exposure and plotted against the angle of reflection. Discrepancies occurred in the overlapping of the first three films due to the difficulty of measuring accurately such short exposures, so no great numerical accuracy is claimed for the results up to 12°. The densities were less than 0·7 and for values below this the intensity of the radiation is proportional to the photographic density.* In the photometry of the films only the central portion of the band of reflected radiation was used in calculating the densities, the density being irregular at the edges of the band. The photographic densities are plotted against the glancing angles of incidence in fig. 5.

---

* Eddy and Laby, 'Proc. Roy. Soc.,' A, vol. 127, p. 20 (1930).

On one of the films the density due to the direct ray was 1·3 and of the ray reflected at 6° was 0·6. Using the density-intensity curve previously referred to,* this gives 116/49 for the ratio of the intensities of these rays, and this is equivalent to 42 per cent. of energy reflected. This estimate assumes that the form of the density-intensity curve is independent of the wave-length, evidence for which is given on p. 288.

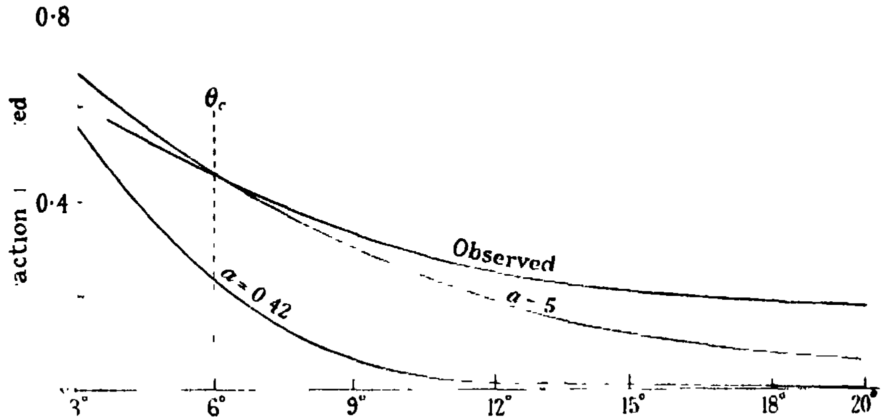

Fig. 5.—Intensity of Reflection of Carbon Radiation from a Glass Mirror.

## *Electromagnetic Theory of Reflection.*

As is well known, Fresnel's equations for the intensity of reflection at a plane separating transparent media have been incorporated into the electromagnetic theory of light, including the modification of that theory for the case of metallic reflection. Prins† and Forster‡ have applied this theory to the reflection of X-rays. Their expressions are only valid when the glancing angle of incidence and the absorption in the reflecting medium are both small. As our observations of the intensity of reflection have been made for glancing angles up to 20°, and as the absorption for a wave-length of 45 Å. appears to be large, neither of these expressions would be correct for these conditions. General expressions for the reflection of an electromagnetic wave at an absorbing (metallic) surface have been obtained by Chr. Pfeiffer based on Drude's treatment of metallic reflection.§ A very clear exposition of this subject is given by W. König in the 'Handbuch der Physik,' and the following, in which König's notation is used, indicates how the general expression is obtained.

---

* *Loc. cit.*

† 'Z. Physik,' vol. 47, p. 479 (1927).

‡ 'Helv. Phys. Acta,' vol. 1, p. 18 (1927).

§ There appear to be two misprints in Forster's paper. On p. 22 (4) should be $\kappa = \mu\lambda/4\pi$ and in expression (12) $\sin^2 \frac{1}{2}\rho$ should be $2\sqrt{(p^2 + k^2)}\sin^2 \frac{1}{2}\rho$. The latter error was noticed by Dr. Hercus of this laboratory. The following table compares the percentage

The fundamental equations are

$$\epsilon\mu\frac{\partial^2 X}{\partial t^2}+4\pi\mu\sigma\frac{\partial X}{\partial t}=c^2\Delta X$$

$$\epsilon\mu\frac{\partial^2 H}{\partial t^2}+4\pi\mu\sigma\frac{\partial H}{\partial t}=c^2\Delta H_x,$$

and similar equations for the electric vectors Y and Z, and for the magnetic vectors $H_y$ and $H_z$, where $\epsilon$ is the dielectric constant and $\mu$ the magnetic permeability. For a polarised plane wave propagated in the Z-direction

$$X = Ae^{i(pt-qz)},\quad Y = 0,\quad Z = 0,$$

and

$$\mu\epsilon p^2 - \iota\, 4\pi\mu\sigma p = c^2q^2,$$

where $\sigma$ is the conductivity of the medium.

Either $p$ or $q$ is complex, so putting $q = q' - \iota q''$, the wave may be put in the form

$$X = Ae^{-q''z}\,.\,\sin 2\pi\left(\frac{t}{\tau}-\frac{z}{\lambda}\right).$$

The refractive index of the medium is given by

$$n = c/c' = \lambda_0/\lambda,$$

where $c$ and $\lambda_0$ are the velocity and wave-length for a vacuum and $c'$ and $\lambda$ for the medium. The absorption is given by $\kappa$ where

$$\kappa = q''/q' = q''\lambda/2\pi.$$

of the incident energy reflected (for the values of $k$ and $i$ stated) as calculated by the formulæ of Pfeiffer, Forster (as corrected above), and of Forster as modified by Thibaud. ($\theta = 90° - \iota$).

Percentage of Incident Energy Reflected.

| $\theta$. | $k$. | Pfeiffer. | Forster. | Thibaud. |
|---|---|---|---|---|
| ° | | | | |
| 6 | 0·424 | 23·8 | 17·6 | 17·3 |
| 6 | 5·0 | 45·1 | 42·2 | 42·2 |
| 12 | 0·424 | 1·4 | 3·3 | 3·3 |
| 12 | 5·0 | 18·9 | 17·9 | 19·0 |

The equation for the absorption of light

$$J_1 = Je^{-2a''d} = Je^{-4\pi\kappa d/\lambda},$$

may be compared with that for the absorption for X-rays, namely,

$$J_1 = Je^{-\mu d}$$

so that

$$\mu = 4\pi\kappa/\lambda.$$

Fresnel's method is applied to find the division of energy of the incident wave between the reflected and refracted waves. This has to be done for polarised light and the ratio $(R_p/E_p)$ of the amplitude of the reflected to the incident radiation when the electric vector is parallel and the ratio $(R_s/E_s)$ when it is perpendicular to the surface of separation may be found To extend the electromagnetic theory to include metals as well as trasparent media, Drude expressed the electric and magnetic vectors in the form $e^{ipt}$ and introduced the complex quantity, $n'$, into the law of refraction as follows:—

$$\sin i/\sin r' = n'$$

and

$$n' = n_0(1 - i\kappa_0)$$

so that

$$\cos r' = \sqrt{(n'^2 - \sin^2 i)}/n'$$

$$n' \cos r' = a - ib,$$

where $i$ is the angle of incidence.

Combining the equations obtained by Fresnel's method for intensity of reflection with the electromagnetic wave equations for metals, Pfeiffer* obtained the following expression for the fraction of the energy of the incident (unpolarised) light which is reflected for an angle of incidence $i$,

$$J_1 = (R_s^2 + R_p^2)/(E_s^2 + E_p^2)$$
$$= \frac{a^2 + b^2 - 2a\cos i + \cos^2 i}{a^2 + b^2 + 2s\cos i + \cos^2 i} \cdot \frac{a^2 + b^2 + \sin^2 i \tan^2 i}{a^2 + b^2 + 2a\sin i \tan i + \sin^2 i \tan^2 i}$$

where

$$a^2 + b^2 = \sqrt{[n_0^2(1 - \kappa_0^2) - \sin^2 i]^2 + 4n_0^4\kappa_0^2}$$

and

$$a^2 = \tfrac{1}{2}\{\sqrt{[n_0^2(1 - \kappa_0^2) - \sin^2 i]^2 + 4n_0^4\kappa_0^2} + n_0^2(1 - \kappa_0^2) - \sin^2 i\}.$$

*Comparison with Observation.*—These expressions may be evaluated numerically almost as readily as the approximate ones already referred to. The values given by the above expression for $1 - n = \delta = 0 \cdot 007$ and $4\pi\kappa/\lambda = 0 \cdot 424$

---

* 'Diss. Giessen' (1912).

and $4\pi\kappa/\lambda = 5$ are plotted in fig. 5, the observed values being given on the same graph. It will be seen that for $4\pi\kappa/\lambda = 5$ the curve has the same general form and direction as that of the observed values.

The value of the quantity* $4\pi\kappa/\lambda$ may also be calculated from the observed value of the X-ray absorption. Extrapolating from Jonsson's† value for the mass absorption coefficient of aluminium, $\mu/\rho = 767$ for $\lambda = 11{\cdot}4$ Å., on the assumption that $\mu/\rho \propto N^4\lambda^3$ the value obtained for $\mu/\rho$ is $1{\cdot}3 \times 10^5$ for glass and $\lambda = 45$ Å. This corresponds to the value $0{\cdot}424$ for $4\pi\kappa/\lambda$, the curve being shown on fig. 5.

The observations which we have made, both on the reflection of the carbon K radiation and with a ruled grating, show that X-rays are reflected for angles of incidence much larger than the critical angle, which can only be accounted for on the theory just given if the value of $4\pi\kappa/\lambda$ is much greater‡ than $0{\cdot}424$, the value corresponding to $\mu/p = 1{\cdot}3 \times 10^5$.

*Reflection by a Spherical Mirror.*—To determine whether the carbon radiation could be brought to a focus by means of a spherical mirror at a large glancing angle of incidence, a concave glass surface of 6 cm. radius was fixed to the crystal table and the camera slit removed so that the X-rays from the focal spot after reflection by this spherical mirror formed an image on the photographic film. The glancing angle of incidence was set at 45°. The photographs obtained showed a diffuse image of the focal spot, whose intensity was considerably greater than that of the direct beam at the same distance from the focal spot. It is to be expected from this that in this region of the X-ray spectrum a concave grating can be used for angles of incidence up to the above value.

The photographs obtained showed a diffuse image of the focal spot, whose density was considerably greater than that due to the direct beam at the same distance from the focal spot and for the same exposure. It is to be expected from this that in the X-ray region a concave grating may be used for angles of incidence up to the above value.

---

* This is *k* of Forster's paper.

† 'Diss. Uppsala Univ. Ars.' (1929).

‡ Since the above was written H. W. Edwards ('Phys. Rev.,' vol. 37, p. 342, February, 1931) has determined the intensity of reflection of X-rays of wave-length 0·69 Å from glass for various angles of incidence. His values require a higher value of the absorption than that found by direct observation.

## *The Diffraction of X-rays.*

*Adjustment of the Grating.*—A plane grating with 4250 lines per centimetre, 2·0 cm. by 1·3 cm., ruled on glass in this University on the Grayson* ruling engine as modified by Sir Thomas Lyle and Mr. Z. A. Merfield, has been used in these observations. Owing to the great perfection of the original screw, and to improvements which have been made since in this engine, its rulings are exceptionally free from error. From the shape of the diamond used in ruling the grating, and the behaviour of other rulings with light, there is reason to expect that if in fig. 6 AC is parallel to the undisturbed surface of the glass, a part of each ruling consists of an approximately plane surface, such as AB, CD, .., inclined at a small angle to AC. The ruled face of the grating was placed accurately in the axis of rotation of the spectrometer. The cathode rays were brought to a focus about 3 mm. wide on the plane face of the target, which was turned until the focal strip, as seen from the rotation axis, was a narrow and intense line source about 3 mm. high, the final adjustment being carried out photographically. Such a line source makes the use of a slit before the grating unnecessary.

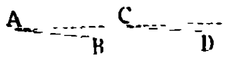

Fig. 6.

The paths of the reflected and a diffracted ray are shown in fig. 7. GHK is the grating, F the focal spot, S the spectrometer slit and PQ the photographic film. GP is the reflected beam and HQ the diffracted beam. To determine the wave-length of the rays forming the diffracted beam HQ, giving the spectral line at Q, the glancing angle of incidence, $i$, and angle of diffraction, that is the angles FHG and KHG, must be determined. To calculate the angle of incidence, which is variable, the distances $l_1 = \mathrm{SP}$, $l_2 = \mathrm{SG}$, $l_3 = \mathrm{FG}$, must be known. These distances could only be measured approximately, and consequently the absolute values of the wave-lengths found in this way were only approximate, but they were sufficiently accurate to identify with certainty a spectral line as being Cu K$\alpha$, Cu L$\alpha$, C K$\alpha$, etc., in a given order of the spectrum. This identification was verified by a graphical method (see fig. 10) which is described below. The graphical method and the measurements involved in it were such that they enabled a determination of the ratio $\lambda_{\mathrm{C\,K}\alpha}/\lambda_{\mathrm{Cu\,L}\alpha}$ to be made to an accuracy

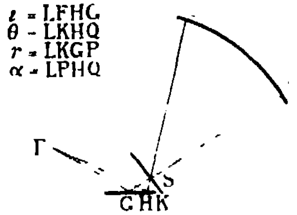

Fig. 7.—Path of Diffracted Beam.

---

* 'Proc. Roy. Soc., Victoria,' vol. 30, p. 44 (1917).

estimated to be 1 in 500, which compares favourably with recent measurements of X-ray wave-lengths with plane gratings where accuracy has been the main object and exposures have been very prolonged.

In fig. 7

$$\theta = r + \alpha$$

$$GH = l_2 \sin(r + \alpha)/\sin\alpha$$

$$= l_2 \sin\theta/\sin\alpha.$$

Also

$$GH = l_3 \sin(r - i)/\sin i$$

$$\cot i = l_2 \sin\theta/(l_3 \sin\alpha \,.\, \sin r) + \cot r.$$

In this expression $l_1 = 7 \cdot 88$ cm., $l_2 = 2 \cdot 11$ cm., and $l_3 = 3 \cdot 7$ cm. The $n\lambda$ of a spectral line was calculated by the expression

$$n\lambda = d(\cos i \sim \cos\theta),$$

where the angles $i$ and $\theta$ are the glancing angles of reflection and diffraction respectively.

*Analysis of Carbon Radiation.*—To analyse the wave-lengths present in the carbon radiation used in the reflection experiments described above, the radiation was excited by attaching a graphite plate to the face of the target, and photographs of its grating spectrum were taken for a range of angles of incidence

The carbon K line has been identified up to the 13th positive order in the positive spectrum and the 18th negative order. No other lines were found. If any other characteristic radiation is present, it must be present in very small amount, as the intensity of the lines of the spectra given by this spectrometer are high on account of the small distance from the focal spot to the photographic film. Table V shows the lines obtained, the exposures being from 8 to 40 ma. minute at 10 kv.

Table V.—Summary of Lines in Carbon Spectra.

| Film. | Angle of reflection. | Orders present. | | Range of angles of incidence. |
|---|---|---|---|---|
| | | Positive. | Negative. | |
| 15<br>17 | 4° 51′ | 2, 3, 4, 6, 8, 9, 10, 11, 13 | 1, 2, 5, 9, 10, 11 | 2° 31′ to 3° 4′ |
| 16<br>18 | 8 37 | 1–9, 11 | 1, 2, 3 | 6 57 to 8 11 |
| 19<br>20<br>21 | 10 36 | — | 1, 3, 5–7, 9–18 | 11 30 to 19 28 |

The last column of the table gives the range of angles of incidence of the rays with the surface of the grating before it is ruled, which are diffracted to give the lines of the spectra tabulated. These angles are calculated from the formula given on p. 284.

From the elementary theory of the reflection grating diffraction cannot occur unless there is reflection, and consequently the angles of incidence for the diffracted rays are of special interest. It will be seen that rays incident at angles as high as 19° 28′ were reflected enough to give a diffraction spectrum. Since the theoretical critical angle for the C Kα line is about 6°, this confirms the results previously given on the reflection of the C Kα radiation at large angles of incidence. Photometer measurements of the intensities of these lines and of the general radiation are described later.

*Analysis of Copper Radiation.*—Table VI contains a summary of the lines obtained with a copper target.

Table VI.—Summary of Lines in Copper Spectra.

| Film. | Angle of reflection. | Positive spectrum. | Negative spectrum | Range of angles of incidence |
|---|---|---|---|---|
| | ° ′ | | | ° ′ ° ′ |
| 54 | 0 11 | Cu K V | — | 0 5 |
| 53 | 0 41 | Cu K VI<br>Cu Ll I, Cu L II | — | 0 18 to 0 22 |
| 52 | 1 41 | Cu K III and IV<br>Cu L I, II and IV<br>Cu Ll I, II and IV<br>Cu K I | — | 1 13 to 2 36 |
| 50 | 2 41 | Cu L I and IV<br>Cu Ll I | Cu L II<br>Cu Ll II | 2 26 to 3 24 |
| 51 | 3 41 | Cu L I, IV and V | Cu L III, V and VI | 3 30 to 4 42 |

In the above table the Roman numbers represent the orders. In addition to these lines there were four very faint lines which were not identified. Thus the copper spectrum consists almost entirely of the Cu Kα, Cu Lα and Cu Ll lines. Any other lines present must be so weak as not to contribute anything appreciable to the total intensity of the radiation. The theoretical critical angle for the Cu Kα line is about 15′ and for the Cu Lα about 2° for a glass mirror. It will be seen from the above table that the intensity of the Cu L spectrum formed by rays incident at 4½° is sufficient to produce a diffraction pattern.

*Measurement of Intensity in the Carbon Spectrum.*—To measure the intensity of the carbon radiation, two photographs of its grating spectrum, films 16 and 17 mentioned above, were photometered in the Moll microphotometer. One of these records is shown in fig. 8. The photographic density was calculated from these records and the resulting density curves of films 16 and 17 are shown in figs. 9A and 9B It is known that up to a value of about 0·7 the density* of an X-ray photograph is proportional to the exposure I$t$, where I is the number of X-ray quanta per unit area and $t$ is the time. As previously

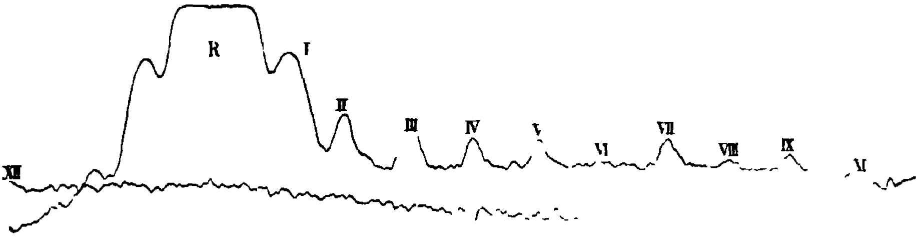

Fig. 8.—Photometer Record of Grating Spectrum of Carbon. Film 16 Angle of Incidence, 8° 37′. The lower trace is the continuation of the upper

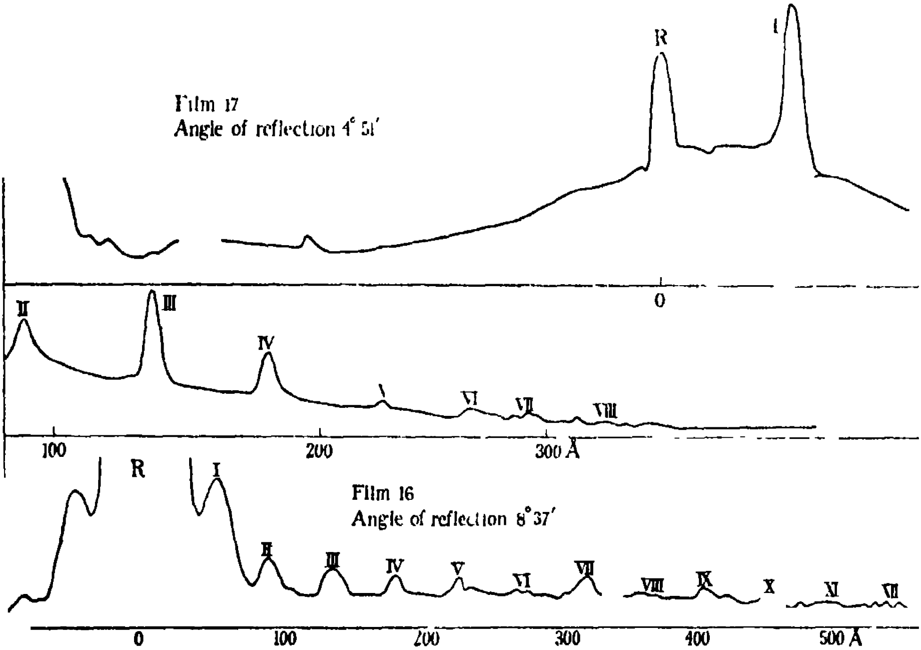

Fig. 9 —Photographic Density *v*. Wave-length for the Grating Spectrum of Carbon. R, reflected beam ; D, direct beam ; I, II, .... spectral orders.

---

* Eddy and Laby, *loc. cit*

mentioned, the validity of measuring the intensity of X-rays in this way has been tested in this laboratory for wave-lengths from that of γ-rays to that for the C Kα line at 45 Å.

The density of the greater part of the curves is less than 0·7 and consequently they are curves which give the distribution of energy in the grating spectrum of carbon. It will be seen that in film 16 the greatest part of the energy is in the reflected beam, which is reflected at an angle of 8° 37′, that the energy in the first to the ninth order C Kα lines is much less, and that these lines fall slowly in intensity as the order increases. The dotted lines represent the background of radiation due to the continuous spectrum and to scattering. There is some difficulty in separating their intensities, but if the intensity of the background in the negative orders is taken as giving the upper limit to the intensity of the continuous spectrum, then it falls off rapidly as λ increases, being zero at $\lambda = 100$ Å. for film 16. The background is of much higher density in 17 than in 16, but this is to be expected if it is mainly due to rays scattered from the grating, as the angles to the incident beam at which the rays are scattered is approximately double in 16 to 17. In accordance with the law found by Kaye that the intensity of the continuous radiation is proportional to the atomic number of the target emitting it, we conclude that the intensity of the general radiation will be quite small. Further, the intensity of the characteristic radiation is some function of $(V - V_k)$, possibly $(V - V_k)^2$ where V is the potential applied to the tube and $V_k$ is the minimum excitation potential of the Kα line, which for $\lambda = 45$ Å. is 274 volt. Thus $V - V_k$ in these experiments is about 10,000, and if the C Kα line intensity is proportional to $(V - V_k)^2$, it will be large compared with that of the continuous radiation. These considerations are confirmed by the grating observations.

*A Coincidence Method of Measuring Wave-lengths.*—The presence of the C Kα line in the copper spectrum of film 52 suggested the possibility of measuring the wave-length of the carbon line by comparison with the wave-length of the Cu Lα line. As a test of the method using this film, the displacements from the reflected beam of the I, II and IV orders of the Cu Lα line were plotted against $n\lambda$ for these lines, $\lambda = 13\cdot32$ Å.* being assumed for this line. The straight line through these three points cut the wave-length axis at $n\lambda = -3\cdot4$ Å., the line through the negative orders also cutting it at the same point. The wave-length of the C Kα line read from this graph (shown

---

* Howe, 'Nat. Acad. Sci. Proc.,' vol. 15, p. 251 (1929) found with a grating 13·31 Å., Kellstrom, 'Z. Physik,' vol. 58, p. 511 (1929) found 13·32 Å. relative to λ Al Kα = 8·323; Soderman, 'Phil. Mag.,' vol. 10, p. 600 (1920) quotes 13·301 Å. as having been found by Larsson.

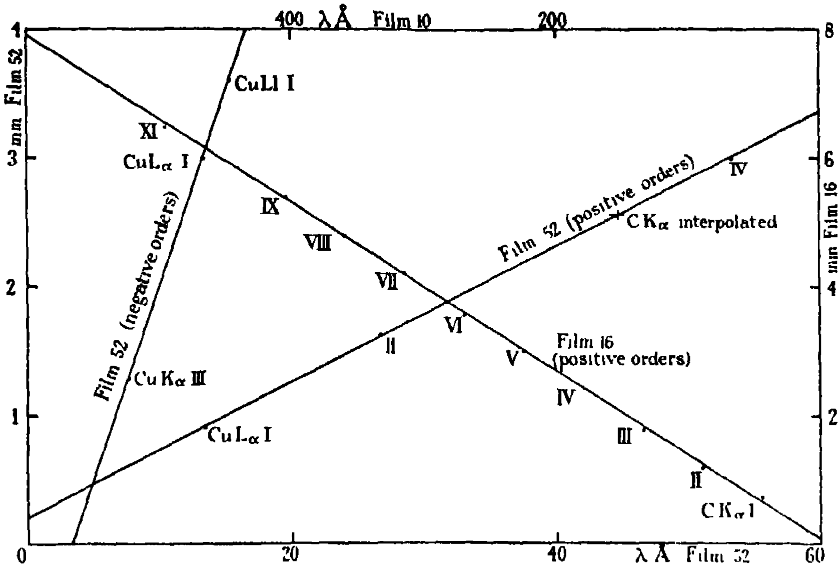

Fig. 10.—Coincidence Method with Copper and Carbon Spectra. I, II, .., spectral orders.

in fig. 10) is 44·7 Å. The deviations in λ of the points of the graph from the line are as follows:—

| Line | Cu Ll I | Cu L l | Cu K V | Cu K III | Cu K IV | Cu L I, II, IV |
|---|---|---|---|---|---|---|
| Deviation | 0 | 0·1 | 0 | 0 | 0 8 | 0 |

the deviations being expressed in Angstrom units.

A second film was obtained by rubbing graphite on the face of the copper target, the setting of the instrument being the same as for film 52. The graph for this film gave the value of the wave-length of the C Kα line as 44·8 Å. relative to the wave-length 13·32 for the Cu Lα line. The mean of these values is $\lambda$ C K = $44 \cdot 7_5$ Å.

These observations were made to test the possibility of the method for accurate determinations of wave-lengths. The writers have pointed out elsewhere* the advantages of such relative determinations over absolute determinations of X-ray wave-lengths. Using a large vacuum spectrometer with a plane grating, Howe† finds for $\lambda$ C Kα/$\lambda$ Cu Lα = 44·6/13·3 = 3·353, whereas we obtain 3·359 for this ratio, showing the accuracy obtainable by the coincidence method with a small spectrometer. The exposure with the larger instrument was 300 to 600 times as great as that used by the writers.

---

* 'Nature,' vol. 126, p. 915 (December, 1930).

† 'Rev. Sci. Inst.,' vol. 1, p. 749 (December, 1930).

# *The Reflection of Long X-Rays.*

By C. B. O. MOHR, B.A., M Sc.,* Kernot Research Scholar, Natural Philosophy
Laboratory, University of Melbourne.

(Communicated by T. H. Laby, F.R S —Received May 29, 1931.)

*Introduction.*—For X-rays passing through matter, theory and experiment give a refractive index $\mu$ slightly less than unity, so that if a beam of X-rays falls on the plane surface of a solid at a small glancing angle less than the critical glancing angle, it is totally reflected.

Determinations of the refractive indices of short wave X-rays by the total reflection method have been carried out by a considerable number of observers. The work of Forster[†] and of Doan[‡] is of particular importance in that determinations have been made with many refinements of technique for various substances over a range of wave-lengths.

The results in general are in rough accord with the theoretical values as given by the classical dispersion theory of Drude and Lorentz. In many cases, however, more or less serious divergences occur between theory and experiment, for example, in four of the thirteen refractive indices obtained by Doan, there are discrepancies with theory of 19, 24, 32 and 66 per cent. respectively.

A definite comparison between the results of various observers is difficult, for, with the exception of glass which is commonly used, few have investigated the same substance for the same wave-length. In the case of glass, the value obtained for the refractive index depends on the density of the glass, and to a lesser extent on its composition. In the few cases where comparison is possible, there occasionally occur striking and inexplicable discrepancies. Thus, for the value of $\delta = 1 - \mu$ for the wave-length $1 \cdot 537$ Å.U., with a silver reflector Doan obtains $30 \cdot 0 \pm 1 \cdot 5$, while Forster obtains $26 \cdot 64 \pm 0 \cdot 1$, and with a copper reflector Doan obtains $17 \cdot 74 \pm 0 \cdot 3$, while Forster obtains $21 \cdot 45 \pm 0 \cdot 1$, the disagreement being many times the experimental error.

---

[*] While the determinations of the critical angles given in this paper were made independently, the author wishes to acknowledge the assistance received in the early stages of the work from Mr. H. S. W. Massey, B.A., M.Sc. For some months the setting up of the apparatus and the development of the method was carried out with Mr. Massey, and some preliminary results obtained with his assistance.

[†] 'Helv. Phys. Acta,' vol. 1, p. 18 (1928).

[‡] 'Phil. Mag.,' vol. 4, p. 100 (1927).

For X-rays of longer wave-length a vacuum spectrograph is necessary and other difficulties arise. Owing to the effect of absorption, the change in the intensity of the reflected ray at the critical angle is no longer sharp, but becomes less and less abrupt with increasing absorption and thus with increasing wave-length, as indicated by the Fresnel theory.

When this work was undertaken, no results had been published on the total reflection of long homogeneous X-rays. Since then, however, Dershem* has investigated anomalous dispersion in the range 2 to 7 Å.U., using reflectors of platinum, silver, calcite, and glass, the homogeneous radiation being isolated by reflection from a gypsum crystal; his results indicate a more rapid increase of the critical angle with wave-length than expected from theory, this being particularly noticeable in the range 6 to 7 Å.U. Dershem has also studied the reflection from mirrors of glass,† quartz,‡ and gold§ of carbon K$\alpha$ radiation (45 Å U.), isolated by a ruled grating, and found that while the glass and quartz mirrors gave results in accord with theory, the gold mirror gave discordant results.

Schon‖ has measured critical angles for mirrors of glass, diamond, quartz, and aluminium at several wave-lengths in the range 3 to 13 Å U, heterogeneous radiation, however, being used; the values obtained for the critical angle were in agreement with the dispersion theory within the limits of experimental error, and qualitative evidence for the Fresnel theory found.

*Theory.*—The Drude-Lorentz theory of dispersion gives for the refractive index $\mu = 1 - \delta$ the value

$$\mu = 1 + \frac{e^2}{2\pi m} \Sigma_s \frac{n_s}{\nu_s^2 - \nu^2} \tag{1}$$

where $e$ and $m$ are the charge and mass of the electron, $\nu$ the frequency of the incident radiation of wave-length $\lambda$, $n_s$ the number of resonance electrons per unit volume of natural frequency $\nu_s$. For X-rays it is usual to associate $\nu_s$ with the critical frequencies of the K, L, - - - -, absorption edges.¶

---

* 'Phys. Rev.,' vol. 33, p. 659 (1929).

† 'Phys. Rev.,' vol. 34, p 1015 (1929).

‡ 'Phys. Rev.,' vol. 35, p. 292 (1930).

§ 'Phys. Rev.,' vol. 35, p. 128 (1930).

‖ 'Z. Physik,' vol. 58, p. 165 (1929)

¶ A similar formula to (1) is furnished by the new mechanics if each $n_s$, "the number of dispersion electrons," is replaced by certain integrals; it is easily shown, however, that the sum of all such expressions reduces to N, the classical number of electrons per unit volume. Also in the wave mechanical formula, the $\nu_s$ appears as the frequencies of the K, L, - - - - emission lines. See Sommerfeld, "Wave Mechanics," Methuen, London, p. 169 (1930).

Except near a resonance frequency (*i.e.*, in the range of normal dispersion), since $\nu_s \ll \nu$ we have approximately the following simple relations

$$\mu = 1 - \frac{e^2}{2\pi m}\frac{N}{\nu^2}, \tag{2}$$

giving

$$\delta = \frac{e^2}{2\pi mc^2} N\lambda^2, \tag{3}$$

where N is the total number of electrons per unit volume, and $c$ is the velocity of light.

The glancing angle of total reflection $\theta_c$ is given by

$$\cos\theta_c = \mu,$$

and since the quantities $\theta_c$ and $\delta$ are small, we have to a first approximation

$$\theta_c = \frac{e}{\pi^{\frac{1}{2}} m^{\frac{1}{2}} c} N^{\frac{1}{2}}\lambda. \tag{4}$$

Hence, except near an absorption edge, the critical angle is proportional to—

(*a*) the wave-length of the incident X-rays ;

(*b*) the square root of the number of electrons per unit volume, and hence approximately to the square root of the density of the substance.

In the long wave-length region it is necessary to take account of absorption, which results in a less abrupt change in the intensity of the reflected radiation near the critical angle ; for the treatment of this problem one has to resort to the Fresnel formulæ. This is discussed in detail in the previous papers* by Professor T. H. Laby and Mr. R. A. Bingham. The accompanying curves (fig. 1) show the fraction of the radiation reflected at various angles of incidence for different values of $a$ where

$$a = \eta\lambda/8\pi\delta, \tag{5}$$

$\eta$ being the absorption coefficient of radiation of wave-length $\lambda$.

*Apparatus.*—A diagram of the apparatus is shown in fig. 2, the main principles of the design being due to Professor T. H. Laby, and based on experience gained in the use of a vacuum spectrograph for investigating the reflection of X-rays by a different method.

The optical parts are arranged on a circular base plate 1 foot in diameter, the disposition of the parts being on broad lines so as to permit the use of the apparatus for long wave reflection work in general.

---

* V. *supra*, pp. 266, 274.

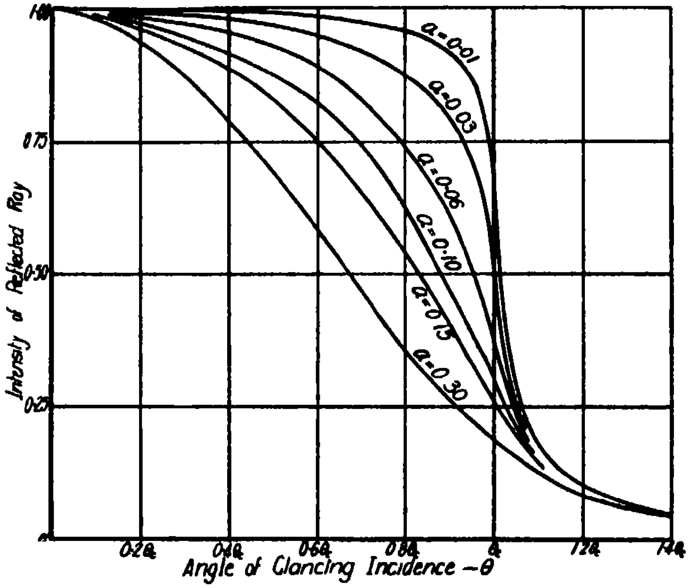

FIG. 1.

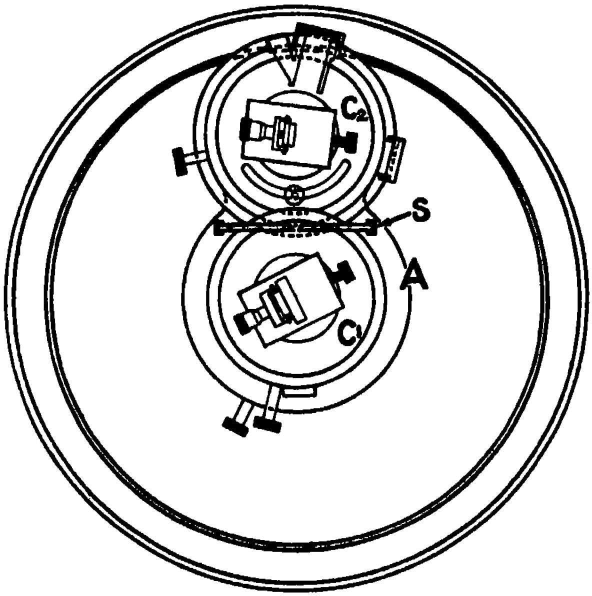

FIG. 2.

The two circles, $C_1$ and $C_2$, both 4 inches in diameter, are graduated to read minutes of arc, and are mounted in ball bearings on the arm A which rotates about the same axis as the circle $C_1$. The outer end of the arm passes over a rough circle graduated in tenths of a degree. The slit S is mounted on the arm between the centres of the circles $C_1$ and $C_2$. Upon the circle $C_1$ is mounted a holder which carries either a crystal or a plane grating to analyse the radiation from the target, while the circle $C_2$ carries in similar manner a plane mirror, rays incident on which are reflected into the camera or film holder P. This camera is attached to a circular disc which rotates about the same axis as, but independently of, the circle $C_2$; a vernier is attached to this disc enabling the position of the cross-wires on the back of the camera to be determined to 1 minute of arc.

If a crystal is used on the circle $C_1$, homogeneous rays pass in any particular direction through the slit S. If a grating is used, the face of the anticathode is turned at a small grazing angle, and as the filament gives a thin line focal spot parallel to the slit S, the use of another slit is rendered unnecessary, so that again homogeneous rays pass in any particular direction through the slit This method of using the grating with the slit system described is due to Professor T. H. Laby and Mr. R. A. Bingham of this laboratory.

Over the base plate fits a coverlid which contains the filament and target of the X-ray tube which is water cooled. The tube and apparatus are thus contained in a common vacuum, and as an oxide-coated (Wehnelt) filament is used, the usual window can be dispensed with without experiencing trouble with light from the filament.

A light metal shield is fastened to the lid and surrounds the elements of the X-ray tube in order to prevent light from the filament and scattered X-radiation from entering the apparatus; the radiation from the target passes out through a small hole in this shield.

The main advantage of this design lies in that the target is placed close to the centre of the apparatus, giving a large solid angle of X-rays and hence an extremely high intensity Thus, strong diffraction spectra were obtained with the grating with exposures of 5 milliampere minutes There is a disadvantage, however, in that as only one slit is used, the amount of scattered background on the film is liable to become comparatively high, and tends to fog the film, if the exposure is raised above a certain amount.

Owing to the high absorption of the wave-lengths used, it was necessary to use uncovered film. The film was enclosed in a small rectangular metal box with a light-tight shutter, the box just fitting on to the camera P. When about to take an exposure, the room was darkened, the camera shutter pulled aside, and the coverlid placed in position. It was thus necessary to remove the coverlid between each exposure; the process of complete evacuation, however, takes only about 10 minutes, a three-stage Gaede mercury pump backed by a Hyvac oil pump being used. A liquid air trap was used to condense vapours.

About 10 kilovolts, R.M.S., was applied to the X-ray tube from a small A.C. transformer, the tube being self rectifying.

Agfa duplitised X-ray film was used throughout, and found to be very satisfactory and sensitive even for wave-lengths as long as 45 Å.U. Development was carefully carried out for 5 minutes at 18° C. with a standard metol-hydroquinone developer.

*Procedure.*—The circle $C_1$ and the arm A were set in such a position that the characteristic radiation to be used passed along the axis of the arm through the slit S. The mirror was mounted on its holder so that the edge furthest from the X-ray tube was in the axis of rotation of the circle $C_2$, and so did not move appreciably during rotation.

The procedure frequently adopted by other workers was followed of splitting the beam of characteristic X-rays at the edge of the mirror furthest from the slit S; one part of the beam thus falls on the mirror at a small glancing angle while the other part passes by the edge of the mirror, both parts of the split beam finally entering the camera as in fig. 3. The angle of incidence of the beam on the mirror was then obtained by dividing the separation of the edges X and Z of the two lines on the film by twice the distance XV of the film from the nearer edge of the mirror.

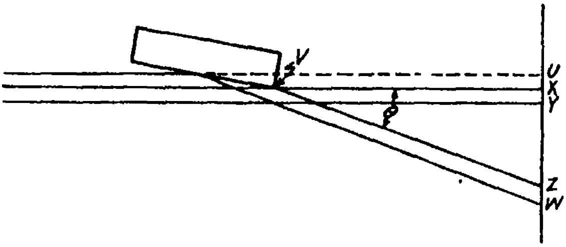

FIG 3

The difficulty of measuring to the edge of the reflected line when this was not perfectly sharp was obviated by measuring instead to the middle of the reflected line WZ, and deducting half the width of the beam UX incident on the mirror; this width was obtained by setting the mirror somewhat high up in its holder, so that part of the incident beam passed underneath it to the lower part of the film.

The method of finding the critical angle was to advance the mirror in steps of increasing angles of glancing incidence, using constant exposures, until the intensity of the reflected ray had fallen to a fraction of its original intensity. The intensity of reflection at various angles close to the critical angle was determined by measuring the density of the reflected line on each film with a Moll recording microphotometer. The curve of variation of reflected intensity with angle was drawn and compared with the various theoretical curves shown in fig. 1. The curve for zero absorption falls abruptly at the critical angle, and so the required critical angle is obtained.

The accuracy of the determinations of critical angles in this work is chiefly dependent on the distance between the mirror and film. If this distance is large, the separation between the lines XY and WZ is correspondingly large, and can be measured more accurately; on the other hand, a larger space has to be evacuated, and longer exposures are required In the apparatus used the distance from camera to mirror edge was 5 cm., and the accuracy of the critical angle determinations was about 2 or 3 per cent, which is quite satisfactory for this work.

The photographic action of long X-radiation on the film was investigated with the Moll microphotometer as follows A spectrum of carbon Kα radiation (45 Å.U.) in several orders was obtained by means of a ruled grating placed on circle $C_1$. Half the film was covered by a shutter which was pulled aside half way through the exposure, virtually giving two sets of lines, one set being half the intensity of the other. Several films were obtained in this manner with different exposure times, and from measurements of the densities of the lines it was found that the density was nearly proportional to the intensity for the densities used, which were below 0·5. As this proportionality between density and intensity is well known to hold for short X-rays, it was assumed to hold for the intermediate wave-lengths.

It was also found that if constant exposures were given, it was possible to reproduce the measured density of a given line to within a few per cent., inclusive of all slight deviations in the running of the tube and in the development and photometry of the films

*Reflection of* Al Kα (8·32 *Å.U.) and* Cu Lα (13·3 *Å.U.) from various Mirrors.*—The Al Kα radiation from an aluminium target was isolated by a gypsum or mica crystal, and the Cu Lα radiation from a copper target by a ruled grating with 10,800 lines per inch. The grating was ruled on glass, and was kindly lent by Sir Thomas Lyle and Mr. Z. A. Merfield. In both cases a single aluminium foil 0·00006 cm. thick was placed over the window to cut out background due to scattered radiation of longer wave-length.

Mirrors of quartz, calcite, glass, stainless steel, silver, and gold (22 carat) were used at 8·32 Å.U., and mirrors of quartz, glass, and stainless steel at 13·3 Å.U.

The reflections from quartz, calcite, and glass were sharp and strong, but became increasingly diffuse and weak for the denser mirrors. The densities of the lines due to the direct and reflected beams were measured with the photometer for films obtained at angles inside the critical angle ; it was found that the quartz, calcite, and glass mirrors reflected from 25 to 30 per cent. of the incident radiation, the steel mirror about 15 per cent., while the silver and gold mirrors reflected only about 5 per cent. The reflecting power of substances for X-rays thus seems to diminish considerably with increasing density of the reflector ; this appears to be one reason for the superiority of gratings ruled on glass to those ruled on metal for X-ray work.*

The exposures used for the light mirrors were about 20 or 30 milliampere minutes, while for the densest mirrors 100 milliampere minutes were necessary.

In fig. 4 are given typical curves obtained for the fall of intensity of the reflected ray with increasing angle of glancing incidence near the critical angle.

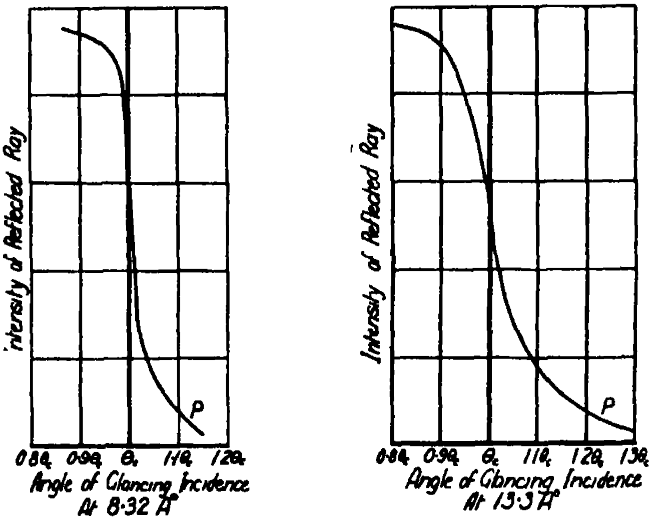

FIG. 4.

In order to ascertain which of the theoretical curves in fig. 1 should fit the results, it is necessary to determine the value of $a$ from the relation (4) using the value of the absorption coefficient $\eta$.

At 8·32 Å.U. Jonnson† finds for the mass absorption coefficient $\eta/\rho$ for aluminium the value 344.

* See Osgood, 'Rev Mod. Phys.,' vol. 1, p. 228 (1929).

† 'Diss. Upsala,' 1928.

A subsidiary experiment was performed to determine the value of $\eta/\rho$ at 13·3 Å.U. photographically. The Cu L line was isolated with the grating, and various numbers of aluminium foils of thickness 0·000061 cm. were placed in turn over half the film, the other half giving the unabsorbed intensity. The films were carefully photometered and in this way a mean value of 1220 was obtained for the mass absorption coefficient $\eta/\rho$. This value is probably correct to 5 per cent. and lies close to the value expected from extrapolation of the values found by Jonnson at 8·32, 9·87 and 11·88 Å.U. Assuming a certain composition for the glass and taking the $Z^4$ law of absorption, the value of $\eta$ for glass and quartz can be calculated at the two wave-lengths 8·32 and 13·3 Å.U., and hence the corresponding values of $a$. The approximate values thus obtained are given in the following table. -

| $\lambda$ in Å U | Mirror | $\eta$ | $\theta_c$ | $a$ (calc ). |
|---|---|---|---|---|
| 8·32 | Glass | 970 | 0·023 | 0·012 |
| | Quartz | 1430 | 0·023 | 0·018 |
| 13·3 | Glass | 3400 | 0·037 | 0·026 |
| | Quartz | 5100 | 0·037 | 0·039 |

The curves in fig 1 for $a = 0·01$ and 0·03 are seen to fit the experimental curves obtained (fig. 4) fairly satisfactorily, so that there is rough agreement between the calculated and observed values of $a$ within the experimental error. One interesting fact now appears. The values of $\eta/\rho$ given by Jonnson at 8·32 and 9·87 Å.U. for nickel, copper, silver and platinum are from 5 to 10 times as large as for aluminium. As $\delta/\rho$ is approximately constant for a given wave-length, as previously pointed out, it follows that the value of $a$ for the mirrors of steel, silver, and gold will be from 5 to 10 times that for quartz and glass, resulting in a much less rapid fall of intensity near the critical angle. No such effect was found experimentally, the intensity curve obtained being very little different for all the mirrors used.

Having superposed an experimental curve on to the theoretical curve which best fits it, the position of the critical angle is given by the ordinate at which the theoretical curve for zero absorption falls abruptly.

The following are the values of the critical angle so obtained and those computed from the formulæ (2) and (1), *i.e.*, with neglect of and taking account of absorption edges. In the latter case, the Stoner distribution of electrons was taken.

| λ in Å U. | Mirror. | Density | Observed $\theta_c$. | Calculated $\theta_c$ | |
|---|---|---|---|---|---|
| | | | | Equation (1), without absorption edges. | Equation (2), with absorption edges. |
| | | | ′ ′ | ′ | ′ |
| Al K 8·32 | Quartz | 2·63 | 80 ± 2 | 76 | 65 |
| | Calcite | 2·70 | 79 ± 2 | 77 | 76 |
| | Glass | 2·97 | 79 ± 2 | 81 | 76 |
| | Steel | 7·78 | 119 ± 2 | 126 | 127 |
| | Silver | 10·6 | 108 ± 6 | 142 | 126 |
| | Gold | 17·3 | 134 ± 6 | 181 | 132 |
| Cu L 13·3 | Quartz | 2·63 | 119 ± 3 | 123 | 117 |
| | Glass | 2·97 | 130 ± 3 | 131 | 128 |
| | Steel | 7·78 | 152 ± 3 | 152 | 258 |

*Discussion.*—The work of Forster and of Schon indicates that for any particular substance the critical angle is proportional to the wave-length over a range of wave-lengths, even fairly close to an absorption edge, and that at and just around the absorption edge there is no large deviation but merely a comparatively small kink in the straight line. These observers thus find that the simple formula (2) represents the observed facts rather than the Drude-Lorentz formula in the form (1), or the Kallman-Mark* modification of the dispersion formula.

The values obtained for the light mirrors, quartz, calcite, and glass are in good agreement with the value calculated from formula (2), a conclusion also reached by Schon who used mirrors of low density. Moreover, in the one case where the calculated value for the light mirrors differs appreciably according as formula (2) or (1) is used, namely, in the first result in the table, formula (2) is supported in agreement with Forster and Schon.

Deviations from theory, however, are seen to appear for substances of greater density. Thus the results for steel at 8·32 and 13·3 Å U. have begun to deviate from the theoretical values by an amount several times larger than the probable experimental error. The results obtained for silver and gold at 8·32 Å.U. are seen to deviate still further from the theoretical values given by relation (2), the value for silver being less than for steel, although its density is greater.

This falling below the calculated value for the heavier mirrors, not only in the critical angle, but also in the value of $a$ required to fit the experimental results, is in agreement with the results obtained by Dershem for the reflection of carbon K$\alpha$ (45 Å.U.) from gold. Dershem found that in order to get a good fit with the theoretical curves either $a$ or $\delta$ or both must have smaller values than the calculated values.

---

* 'Ann. Physik,' vol. 82, p. 585 (1927).

Comparison with the results of Schon and Dershem is possible only in two cases. Dershem worked in the range 3 to 7 Å.U., and the only mirrors in the above list that were also used by Schon are glass and quartz. For glass, however, comparison is not possible with the results of Schon, as the latter does not give the density of the glass or the theoretical values expected. For quartz, Schon obtains at 8·32° Å.U. critical angles of 71′ and 77′ as compared with 80′ above, and at 13·3 Å.U. 115′ as compared with 119′ above. This agreement seems quite satisfactory.

While the critical angles given above were all obtained with the photometer, it is of interest to note here that previous estimates of the critical angles were made by mere inspection of the films, and selecting as the critical angle that angle at which the intensity of the reflected line seemed to become suddenly weaker. Using this visual method, it was found that for the light mirrors where the reflected lines were fairly strong, the critical angle had been over-estimated—for example in the case of glass by about 10 per cent. at 8·32 Å.U., and about 20 per cent. at 13·3 Å.U. This shows the unreliability of the unaided eye for such work, particularly if the densities are high.

Dershem in his experiments selected as the critical angle that angle at which the reflected line on the film suddenly seemed to disappear; this would give too large a value for the critical angle. Thus from inspection of the reproduction of the specimen film given by Dershem, the density of the reflected line at the point taken as corresponding to the critical angle is surely only a small fraction of the density of the reflected line at the smaller angle. This would correspond to a point P in fig. 4. As seen in fig. 4, the intensity of the reflected ray falls away more slowly to a small value past the critical angle with increasing wave-length, so that the value of the critical angle is being increasingly overestimated. This would explain the larger increase of $\delta$ with wave-length obtained by Dershem than expected by theory.

In conclusion, I wish to thank Professor T. H. Laby for suggesting the problem and for his continued assistance and encouragement throughout the progress of the work. My thanks are also due to Dr. C. E. Eddy for suggestions and criticisms.

### *Summary.*

(1) The refractive indices of long wave-length X-rays is investigated by the total reflection method, a vacuum spectrograph being used, and the characteristic X-rays isolated by either a crystal or ruled grating.

(2) The critical angles were determined for quartz, calcite, glass, steel, silver, and gold at 8·32 Å.U (Al K$\alpha$), and for quartz, glass, and steel at 13·3 Å.U. (Cu L$\alpha$), and compared with the values given by the classical Drude-Lorentz dispersion formula.

(3) For the light mirrors, quartz, calcite, and glass, agreement was found within the limits of experimental error between the observed and calculated values of the critical angle, and for the rate of fall of intensity of reflection near the critical angle. For the denser mirrors, steel, silver, and gold, however, increasingly large discrepancies were found to occur with increasing density of the reflector.

---

# *The Chemical Constants of the Vapours of Hydrogen and of Hydrogen Chloride; and the Entropy Change Accompanying the Reaction $H_2 + Cl_2 \rightleftarrows 2HCl$.*

By T. E. STERN, Trinity College, Cambridge.

(Communicated by R. H. Fowler, F R.S —Received June 3, 1931 )

## § 1. *The Chemical Constant of Hydrogen Vapour.*

In a paper called " The Chemical Constant of Hydrogen Vapour, and the Entropy of Crystalline Hydrogen,"* the writer has investigated the vapour pressure of crystalline hydrogen at very low temperatures. He used the Einstein-Bose statistics for the hydrogen gas, and obtained results slightly different from those of Fowler,† who had used the classical statistics for the vapour phase. The result found by the writer for the chemical constant $i'$ was in slightly better agreement with experiment than Fowler's result, being larger than Fowler's by $\log_{10} 1\cdot04 = 0\cdot02$ at the temperatures of Eucken's experiments.‡ Also, the writer found that when hydrogen gas was condensed to the solid phase at these very low temperatures, the ratio of the number of orthohydrogen molecules to the number of para-hydrogen molecules in the crystalline phase, provided that most of the molecules were in the gaseous phase, was not 3 : 1 but instead about $3\frac{1}{8}$ : 1.

---

* 'Proc. Roy. Soc.,' A, vol. 130, p. 367 (1931).

† 'Proc. Roy. Soc.,' A, vol. 118, p. 52 (1928).

‡ 'Z. Physik,' vol. 29, p. 1 (1924).

However, there was a mistake in the writer's calculations. He carelessly omitted, from equations (5) and (5′) of his paper on hydrogen, the factors involving the work of evaporation $\chi$ at the absolute zero, per molecule. The equations (5) and (5′) should read, when these factors are included,

$$(5)\quad \bar{\mathrm{N}} = \xi \frac{\partial}{\partial \xi} \frac{(2\pi m k\mathrm{T})^{3/2}\,\mathrm{V}e^{-\chi/k\mathrm{T}}}{h^3} \sum_{n=1}^{\infty} \frac{\xi^n e^{-(n-1)\chi/k\mathrm{T}}}{n^{5/2}} \sum_{j=0,2,4,}^{\infty} (2j+1)\, e^{-\frac{nj(j+1)\epsilon}{k\mathrm{T}}}$$

and

$$(5')\quad \bar{\mathrm{N}}' = \xi' \frac{\partial}{\partial \xi'} \frac{(2\pi m k\mathrm{T})^{3/2}\,\mathrm{V}e^{-\chi/k\mathrm{T}}}{h^3} \sum_{n=1}^{\infty} \frac{\xi^{n'} e^{-(n-1)\chi/k\mathrm{T}}}{n^{5/2}} \sum_{j=1,3,5,}^{\infty} 3\,(2j+1)\, e^{-\frac{nj(j+1)\epsilon}{k\mathrm{T}}}.$$

The result, which can be deduced from these correct equations, for the chemical constant $\iota'$ of hydrogen vapour at very low temperatures, is to our order of accuracy exactly the same as Fowler's result; instead of being larger than his by 0·02. Further, if we use the correct equations (5) and (5′) we find that the ratio of ortho-hydrogen to para-hydrogen molecules in the crystalline phase is 3 : 1 to our order of accuracy; and not $3\frac{1}{8}$ : 1 at 17° K. as we found from the incorrect equations (5) and (5′) in the writer's paper on hydrogen. The remaining conclusions of the writer, in articles 4, 5 and 6 of that paper, remain unaltered by this correction.

## § 2 *The Chemical Constant of Hydrogen Chloride Vapour.*

The normal state of the gaseous hydrogen chloride molecule is almost certainly a $^1\Sigma$. Further, the nuclear vibrational energy levels higher than the ground level are so high that in a treatment of the vapour pressure of hydrogen chloride at ordinary temperatures they may be neglected entirely. The pure rotation absorption spectrum, in the extreme infra-red, and the lowest rotation-vibration spectrum in the infra-red, have both been investigated by Czerny,* so that our knowledge of the energy levels relevant to the evaluation of the partition functions for gaseous hydrogen chloride molecules is quite complete. More recently still, the two lowest absorption bands have been investigated by Meyer and Levin† and the results have been analysed by Colby,‡ who fitted them to the equations derived theoretically by Fues,* for the oscillating rotator. It appears that owing to Colby's somewhat unusual, though undoubtedly correct, analysis it is simpler in calculating the rotational partition functions to use the value for the "moment of inertia" of the molecule of hydrogen chloride obtained by Czerny, namely, $2 \cdot 656 \times 10^{-40}$ CGS units; rather than to use the correct moment of inertia of the hydrogen chloride molecule at rest obtained by Colby For we should have to apply just those corrections to the latter value, if we used it, which would give us Czerny's value. When we make calculations for the moments of inertia of the $HCl_{35}$ and $HCl_{37}$ molecules, we find that the difference between their moments of inertia is trivial, owing to the fact that the centres of mass are in both cases very close to the chlorine nuclei These calculations are confirmed by Colby's actual values of the moments of inertia obtained from his analysis of the experiments of Meyer and Levin. In calculating the gaseous partition functions we may therefore neglect the differences in the moments of inertia. We must, however, consider the differences in the masses in calculating the translational factors in the gaseous partition functions.

---

* 'Z. Physik,' vol. 44, p. 252 (1927).

† 'Phys. Rev.,' vol. 34, p. 44 (1929).

‡ 'Phys. Rev.,' vol. 34, p. 53 (1929).

We are not concerned with the Pauli exclusion principle. Just as in the case of chlorine,† the actual values of the nuclear spins are without importance when we calculate the vapour pressure of hydrogen chloride. And further, this time it does not matter to our result whether the molecules of hydrogen chloride rotate in the crystalline phase or oscillate about directions of minimum potential energy; provided that if they oscillate there is but one orientation of minimum potential energy for each molecule which is an absolute minimum, without any other minima of nearly the same value. If the molecules of hydrogen chloride in the crystal oscillate, this condition is probably fulfilled; since we should expect the orientation of minimum potential energy of a molecule like hydrogen chloride with a permanent electric moment to be in the direction of the electric field at the place where the molecule is, and in one sense only along it. For such an oscillating molecule, we can show by a perturbation method, in which the unperturbed case is a plane oscillator, that apart from nuclear spins the lowest quantum state has a statistical weight of unity. Taking account of nuclear spins, and denoting the maximum $z$ component of angular momentum of the chlorine nucleus in a particular molecule of hydrogen chloride by $nh/2\pi$, we find that the lowest oscillational state of such a molecule can be represented by $2(2n + 1)$ linearly independent wave functions. If the molecule rotates instead of oscillating in the crystal then the statistical weight of the lowest quantum state is still $2(2n+1)$. And since this is also the statistical weight of the lowest quantum state of such a molecule in the gaseous phase, we find that the molecules must have the same statistical weight, in any case, in their lowest quantum states in the crystal as in the gas

---

* 'Ann. Physik,' vol. 80, p. 367 (1926), and vol. 81, p. 281 (1926).

† Stern, 'Proc. Roy. Soc.,' A, vol. 131, p. 339 (1931).

We have assumed in this discussion that hydrogen chloride forms a molecular lattice Strong evidence for this comes from the persistence in the crystalline phase, with but a small change in wave-length, of the absorption band observed in gaseous absorption at about 3·46 microns.*

We can now calculate the chemical constant of hydrogen chloride vapour by the usual methods. We find for the chemical constant, at ordinary temperatures,

$$i = \mathrm{A}i_{\mathrm{A}} + \mathrm{B}i_{\mathrm{B}},$$

where

$$i_r = \log \frac{(2\pi m_r)^{3/2} k^{7/2} 8\pi^2 \mathrm{I}_r}{h^5}, \qquad r = \mathrm{A}, \mathrm{B}.$$

As we have indicated, both I's may be taken to be the same. We take for the molecular weights of the molecules, with sufficient accuracy, 36 and 38 respectively; the symbols A and B denote here the mole fractions of $\mathrm{HCl}_{35}$ and $\mathrm{HCl}_{37}$ respectively, and their values are† $\mathrm{A} = 0\cdot760$ and $\mathrm{B} = 0\cdot240$. We find for the chemical constant of hydrogen chloride vapour, if we use atmospheres and common logarithms, the value

$$i' = -0\cdot42\,,$$

in fair, though not very satisfactory, agreement with Eucken's old experimental‡ value

$$i' = -0\cdot26 \pm 0\cdot04,$$

but in excellent agreement with the value

$$i' = -0\cdot450$$

given by Eucken§ more recently as obtained from the experiments of Giauque and Wiebe,‖ and in excellent agreement also with the value

$$i' = -0\cdot40 \pm 0\cdot03$$

accepted by Eucken¶ as the most probably correct one, in 1930.

---

* Unpublished work of the late Fraulein G. Laski at the Reichsanstalt. The writer is indebted to F. I. G. Rawlins for this information.

† Stern, *loc. cit.*

‡ Eucken, *loc. cit.*

§ 'Phys. Z.,' vol. 30, p. 818 (1929)

‖ 'J. Amer. Chem. Soc.,' vol. 50, p. 101 (1928).

¶ 'Phys. Z.,' vol. 31, p. 361 (1930).

The existence of the transition point at 99° K. in the crystalline phase of hydrogen chloride in no way diminishes the validity of the above investigations. There does not seem to be any way of explaining, at present, the rather poor agreement of the two values, if Eucken's estimate of his experimental uncertainty is at all accurate.

### § 3. *The Entropy of Crystalline Hydrogen Chloride at the Absolute Zero.*

Consider a gram molecule of crystalline hydrogen chloride at the absolute zero of temperature. The total number of linearly independent wave functions capable of representing the crystal, corresponding to all possible distributions of the molecules $HCl_{35}$ and $HCl_{37}$ among the lattice points is

$$C = 12^{AN}\,[2\,(2n_2 + 1)]^{BN}\,\frac{N\,!}{(AN)\,!\,(BN)\,!}$$

where N is Avogadro's number. Hence, the entropy at the absolute zero, per gram molecule, is found by the use of Stirling's asymptotic formula for factorials to be

$$\begin{aligned} S_0 &= k \log C \\ &= R\,[A \log 12 + B \log 2 + B \log (2n_2 + 1) - A \log A - B \log B, \end{aligned}$$

if we suppose that Elliott's conclusions,* that the nucleus of the $Cl_{35}$ atom has a 5/2 quantum spin, is correct; and denote the spin of the $Cl_{37}$ nucleus by $n_2$. If we use the values given in the last section for A and B we find that

$$S_0 = 5\cdot19 + 0\cdot48 \log (2n_2 + 1) \text{ cal}/^\circ\text{C}.$$

### § 4. *The Entropy Change Accompanying the Reaction* $H_2 + Cl_2 \rightleftarrows 2HCl$ *between the Crystalline Phases at the Absolute Zero.*

Using the values for the entropies at the absolute zero of gram molecules of hydrogen, chlorine, and hydrogen chloride given in previous papers and above by the writer, we can calculate the change in entropy when a gram molecule of crystalline chlorine at the absolute zero reacts with a gram molecule of crystalline hydrogen at the absolute zero and yields 2 gram molecules of crystalline hydrogen chloride at the absolute zero. To a sufficient accuracy we have that

$$a = A^2,\ b = 2AB,\ c = B^2,$$

where the $a$, $b$ and $c$ are the symbols denoting the mole fractions of the three sorts of chlorine in ordinary chlorine. Hence we find that the change of entropy is a diminution, amounting numerically to

---

* 'Proc. Roy. Soc.,' A, vol. 130, p. 638 (1930).

$$\Delta S_0 = \tfrac{3}{4}R \log 3 = 1 \cdot 63 \text{ cal.}/^\circ \text{C}. \qquad (4.0)$$

The reader should refer to the note in § 6 of the writer's paper on chlorine (*loc. cit.*), and should bear in mind that the writer's "entropies at the absolute zero" are not really the entropies at precisely the absolute zero. The latter would be of but little practical importance. Our entropies are instead the entropies calculated by means of the integrals $\int (Cp/T)\, dT$ from the entropies of the substances at higher temperatures, when as indicated in the note the $Cp$'s are extrapolated (by the $T^3$ law) to the absolute zero from temperatures of a few degrees absolute. Our entropies belong to the states to which physical chemists are by this method extrapolating. To be more definite, if $\Delta S_{T'}$ is the observed diminution in entropy when the reaction occurs at a temperature T′, then

$$\tfrac{3}{4}R \log 3 = \Delta S_{T'} + 2\int_0^{T'} \frac{(Cp)_{HCl}}{T}\, dT - \int_0^{T'} \frac{(Cp)_{H_2}}{T}\, dT - \int_0^{T'} \frac{(Cp)_{Cl_2}}{T}\, dT,$$

where those contributions to the specific heats $Cp$ are neglected which are due to the resolution of the lowest energy states of the molecules for different spin configurations, or to the separating out of the constituents of our mixed crystals if such separation occurs.* By our treatment we avoid the theoretical and experimental difficulties of having to consider the states of crystals at temperatures lower than a small fraction, perhaps, of a degree absolute

The change in entropy which we have given in (4.0) does not depend upon the particular value used, namely, $\tfrac{5}{2}h/2\pi$, for the maximum value of the $z$ component of angular momentum of the $Cl_{35}$ nucleus. Nor does it depend upon the proportions of the isotopes in chlorine We have been led to this value simply because we supposed that hydrogen molecules were able to rotate quite freely in crystalline hydrogen at the lowest temperatures, while we supposed that molecules of chlorine were able only to oscillate about orientations of equilibrium in crystalline chlorine, at the lowest temperatures.

---

* *Note added August* 5, 1931 —In the case of crystalline hydrogen, Simon, Mendelssohn, and Ruhemann have found (' Naturw ' vol 18, p. 34 (1930) ) anomalies in the specific heat below 11° K which correspond probably to such separation, and possibly to the resolution of the three nuclear rotational levels with $j$ equal to 1 in the case of orthohydrogen, above 11° K. the specific heat corresponds closely to a Debye function with a characteristic temperature of 91° K. The $(C_p)_{H_2}$ to be used in the integral in the text above is therefore that given down to 11° K. by experiment, and given from 11° K. to 0° K by the Debye function with characteristic temperature 91° K. The temperatures below which it is necessary to extrapolate and to ignore the actual specific heats are probably much lower than this value of 11° K in the cases of HCl and $Cl_2$, since there are no non-combining rotational terms for the former and since molecules of the latter probably oscillate in the crystal. Anomalies in the specific heats due to separation of the isotopes probably do not occur except at even lower temperatures still.

### § 5. *The Constant in the Equation for the Equilibrium Constant. A Check.*

We may check the consistency of all of our theoretical calculations in this discussion of vapour pressures and entropies as follows · If $K_p$ is the equilibrium constant in a homogeneous gas reaction, then*

$$\log K_p = \log \{\Pi_t p_t^{q_t}\}$$

$$= -\frac{(Q_p)_0}{RT} + \frac{\sum_t q_t (C_p^t)_0}{R} \log T + \int_0^T \frac{dT'}{RT'^2} \int_0^{T'} \sum_t q_t (C_p^t)_1 \, dT'' + I. \quad (5.0)$$

In this equation $q_t$ is the number of gram molecules of the $t$'th species reacting, with a negative sign for those that disappear when the reaction takes place, and $p_t$ is the partial pressure of the $t$'th species $(Q_p)_0$ is the work which must be done to make the reaction go in this sense at constant pressure at the absolute zero, and $(C_p^t)_0$ and $(C_p^t)_1$ are the constant and variable parts of the specific heat at constant pressure of the $t$'th species I is a constant of integration, which is not to be confused in this section with the use of I, in previous sections, to denote moments of inertia. Then it follows from Fowler's equation (452), *loc. cit.*, if atmospheres and common logarithms are used, that

$$I' = \sum_t q_t (i_t' + S_0^t)/2 \cdot 3026 \, R), \quad (5.1)$$

where $S_0^t$ is the entropy at the absolute zero of a gram molecule of the $t$'th species in the crystalline form, and where the $i'$'s are the chemical constants which we have investigated in this and in previous papers. Fowler's " log K(0)" is to be distinguished from our log K(0) ; and if common logarithms are used, Fowler's " log K (0) " is equal to our $S_0/R \log_e 10$.

Using the values for $i'$ and $S_0$ found theoretically in this and previous papers, we find for the reaction $H_2 + Cl_2 - 2HCl$ the value

$$I' = -1 \cdot 15.$$

This is in excellent agreement with the value found experimentally by Eucken (1924, *loc. cit.*), namely,

$$I' = -1 \cdot 12 \pm 0 \cdot 20.$$

---

* R. H. Fowler, " Statistical Mechanics," § 7.2.

The agreement is to be regarded as a check upon the internal consistency of our calculations rather than upon the correctness of our calculated chemical constants. The high precision of the agreement is really not surprising, since the constant in the equation for the equilibrium constant is capable of calculation in terms only of the partition functions of the gases involved, and these latter are, of course, known to a great accuracy

If we use the "observed," and not the calculated chemical constants in equation (5.1), namely*

$$i'_{H_2} = -3\cdot68 \pm 0\cdot03,$$
$$i'_{Cl_2} = 1\cdot51 \pm 0\cdot16,$$
$$i'_{HCl} = -0\cdot40 \pm 0\cdot03,$$

we then find for the constant I′ the value $-1\cdot01 \pm 0\,18$, which is in fair agreement with experiment.

It is interesting to note that Fowler,† acting more or less by guess-work, applied the correction $\frac{3}{4}\log_{10}3$, which is the same that we had to apply to the $\sum_t q_t i_t'$ in attempting to calculate I′. He considered that it was to be applied because of the peculiarities of hydrogen. We have had to apply it because we supposed that hydrogen molecules rotated and that chlorine molecules did not, in the crystalline phases. The correction followed definitely from these two assumptions.

The writer wishes to thank Mr. Fowler for his helpful criticism during the course of these investigations of vapour pressures and entropies.

---

* Eucken, 1924 and 1930, *loc. cit*

† *Loc. cit*, 7.5.

# *The Properties of Wave Tensors.*

By Sir Arthur Eddington, F.R.S.

(Received July 4, 1931.)

1. In wave-mechanics there occur in addition to the ordinary physical vectors and tensors the four-valued quantities $\psi$, $\psi^*$ introduced by Dirac. In this combination certain relations of invariance in regard to transformation appear which had escaped the ordinary tensor calculus. If we call the new type of quantity involving $\psi$ and its combinations a $\psi$-tensor, the position is that we cannot reach $\psi$-tensors from the calculus of ordinary space tensors, but we can reach space tensors from a calculus of $\psi$-tensors. I have shown that although $\psi$-vectors cannot be expressed in terms of space vectors, mixed $\psi$-tensors can be immediately resolved into space vectors.†

The present paper contains a simplification and systematisation of my earlier work on the $\psi$-tensor calculus as well as a number of new results. The particular point round which the new results centre is as follows. The $\psi$-tensors occurring in wave-mechanics are the product of two $\psi$-vectors ($\psi$, $\psi^*$), and apparently the primary reason for introducing the unobservable quantity $\psi$ rather than working with physical tensors throughout is to impose this condition. I therefore examine the question: If we impose the condition that a wave tensor is the product of two $\psi$-vectors, what is the corresponding restriction on the physical tensors equivalent to it? The answer is (§ 7) that whatever is described by two $\psi$-vectors $\psi$, $\psi^*$ can equivalently be described by two space vectors of equal length at right angles to one another. One of these is the momentum vector; the other (generally ignored in current investigations) presumably represents positional relations (co-ordinates or distance); or rather I would regard it as the source of positional relations, which can only become explicit in more complicated developments involving many particles. The ordinary wave equation for one particle is obtained as an *identity*.

This investigation was made in connection with the theory of the charge and masses of electrons and protons which I have been trying to develop; but for the most part I refrain from comment on this application, as I am not yet ready to treat it definitively. I do, however, deal at some length with the question why the complete five-dimensional relativity admitted in the analytical formulæ and believed to hold good in general dynamical theory is cut down to four dimensions in applications to practical problems in our actual universe.

---

† The earlier papers are 'Proc. Roy. Soc.,' A, vol 121, p. 524; vol. 122, p. 358, vol. 126, p. 696 (1928–30). These are hereinafter quoted as I, II and III.

I have found it advisable to change my definition of the matrices $E_\mu$, so that now $E_\mu^2 = -1$, instead of $+1$ in my former papers.

2. We take four anticommuting matrices $E_1$, $E_2$, $E_3$, $E_4$, which satisfy

$$E_\mu^2 = -1 \qquad E_\mu E_\nu = -E_\nu E_\mu. \tag{2.1}$$

Let

$$E_5 = iE_1E_2E_3E_4. \tag{2.2}$$

Then it is easily verified that $E_5$ also satisfies (2.1). We introduce 10 more matrices by the definition

$$E_{\mu\nu} = E_\mu E_\nu = -E_{\nu\mu} \qquad (\mu, \nu = 1, 2, 3, 4, 5\,;\ \mu \neq \nu)$$

The properties of these 15 matrices can be exhibited more symmetrically by introducing an alternative designation of the original 5 matrices, viz.,

$$E_{0\mu} = E_\mu = -E_{\mu 0},$$

so that they may all be treated as double-suffixed and antisymmetrical. The following rules of multiplication are found to hold

$$\left.\begin{aligned} &E_{\mu\nu}^2 = -1 \\ &E_{\mu\nu}E_{\mu\sigma} = -E_{\mu\sigma}E_{\mu\nu} = E_{\nu\sigma} \\ &E_{\mu\nu}E_{\sigma\tau} = E_{\sigma\tau}E_{\mu\nu} = \pm iE_{\lambda\rho} \end{aligned}\right\} \tag{2.3}$$

where $\mu$, $\nu$, $\sigma$, $\tau$, $\lambda$, $\rho$ form any permutation of the suffixes 0, 1, 2, 3, 4, 5. Matrices anticommute or commute according as they have or have not one suffix in common.

The pentads, *i.e.*, sets of five mutally anticommuting matrices, are obtained by fixing one of the two suffixes, *e.g.*, $E_{30}$, $E_{31}$, $E_{32}$, $E_{34}$, $E_{35}$. Each matrix is a member of two pentads corresponding to its two suffixes.

We introduce a sixteenth matrix $E_{16} = i$, *i.e.*, $i$ times the unit matrix. Then $E_1, E_2, \ldots, E_{16}$ is called a *complete set* or in physical applications a *frame of matrices*. Any fourfold matrix can be expressed in one and only one way as a linear function of $E_1, E_2, \ldots, E_{16}$.

Let $E_\mu'$ be another complete set in one-to-one correspondence with $E_\mu$ and fulfilling the same equations. (We now use a single suffix notation $\mu = 1, 2, \ldots, 16$.) It can be shown that there exists a transformation.*

$$E_\mu' = P'E_\mu P \tag{2.4}$$

---

* *Cf.* G. Temple, 'Proc. Roy. Soc.,' A, vol. 127, p. 342 (1930).

where

$$P = \tfrac{1}{4}\sum_{1}^{16} E_\mu E_\mu' \qquad P' = \tfrac{1}{4}\sum_{1}^{16} E_\mu' E_\mu \tag{2.5}$$

and $PP' = P'P = 1$. Since by (2.5) P is a matrix, (2.4) is the ordinary transformation of a mixed tensor (III, equation (3.13)). Thus all possible complete sets of matrices are obtained by applying the general transformation of a mixed tensor to an original set $E_\mu$. We therefore take the $E_\mu$ to be mixed tensors, and thereby avoid reference to any particular set

I denote the contracted tensor, *i e.*, the diagonal sum of the matrix, by $\{E_\mu\}$. This is an invariant for tensor transformations. I have found a complete set consisting of four-point matrices in I, §§ 7, 8; in these it is evident by inspection that

$$\{E_\mu\} = 0 \quad \text{except } \{E_{16}\} = 4i. \tag{2.6}$$

This invariant equation must be true for all complete sets.

3. When a matrix T is expressed as a linear function of a complete set

$$T = \sum_{1}^{16} t_\mu E_\mu \tag{3.1}$$

we call the numerical coefficients $t_\mu$ the *matrix components* of T. The formula for determining $t_\mu$ was obtained in my earlier paper (I, § 14), but the following is a simpler derivation. Multiply both sides of (3.1) by $E_\nu$ and contract

$$\{TE_\nu\} = \sum_\mu t_\mu \{E_\mu E_\nu\}.$$

For the 16 values of $\mu$, $E_\mu E_\nu$ gives the original matrices $E_\mu$ in a different order by (2.3), except that there may be a factor $-1$, or $\pm i$. By (2.6) all except one vanish on contraction. The exception is $\{E_\nu E_\nu\} = \{-1\} = -4$. Hence $\{TE_\nu\} = t_\nu(-4)$, or

$$t_\nu = -\tfrac{1}{4}\{TE_\nu\}. \tag{3.2}$$

An important case is when the matrix is the product of two vectors Let $j_\mu$ be the matrix components of J where

$$J = \psi\psi^* \tag{3.3}$$

By (3.2)

$$j_\mu = -\tfrac{1}{4}\{\psi\psi^* E_\mu\}.$$

Inserting row-and-column suffixes $\psi\psi^* E_\mu$ means $(\psi\psi^*)_{\alpha\beta}(E_\mu)_{\beta\gamma} = \psi_\alpha\psi_\beta^*(E_\mu)_{\beta\gamma}$. To contract we set $\gamma = \alpha$, so that $\{\psi\psi^* E_\mu\}$ means $\psi_\alpha\psi_\beta^*(E_\mu)_{\beta\alpha} = \psi_\beta^*(E_\mu)_{\beta\alpha}\psi_\alpha$. The suffixes, being now in chain order, can be omitted according to the usual convention of matrix notation. Hence

$$j_\mu = -\tfrac{1}{4}\psi^* E_\mu \psi. \tag{3.4}$$

It may be explained that the asterisk is used to distinguish an "initial vector," *i.e.*, one which can start but cannot close a chain-product. With this understanding there is no ambiguity as to whether inner or outer multiplication is intended. Thus $\psi^*\psi$ is an inner product, $\psi\psi^*$ is an outer product. I use the summation convention for row-and-column suffixes, but not for any other suffixes.

4. When an exponential involves matrices it is understood to be defined by the exponential series. It follows from the definition that since $E_\mu^2 = -1$

$$e^{E_\mu \theta} = \cos\theta + \sin\theta \,.\, E_\mu. \tag{4.1}$$

Exponentials involving two or more non-commuting non-infinitesimal matrices do not as a rule admit of simple interpretation

Considering the general transformation of a mixed tensor

$$T' = qTq', \tag{4.2}$$

where $q$ is any matrix and $q'$ its reciprocal, let $q = e^{\frac{1}{2}E_{12}\theta}$; then by (3.1)

$$\begin{aligned} \Sigma\, E_\mu t_\mu' &= e^{\frac{1}{2}E_{12}\theta}(\Sigma\, E_\mu t_\mu)e^{-\frac{1}{2}E_{12}\theta} \\ &= \Sigma_\alpha\, E_\mu t_\mu + \Sigma_\beta\, E_\mu t_\mu e^{-E_{12}\theta} \end{aligned} \tag{4.3}$$

where $\Sigma_\alpha$ denotes summation over the eight terms $E_\mu$ which commute with $E_{12}$ and $\Sigma_\beta$ over the eight terms which anticommute. The eight terms which anticommute are the remaining members of the two pentads which contain $E_{12}$. As an example of the latter take $E_1t_1 + E_2t_2$ which contributes to (4.3).

$$\begin{aligned} &(E_1t_1 + E_2t_2)(\cos\theta - \sin\theta \,.\, E_{12}) \\ &= (E_1t_1 + E_2t_2)\cos\theta - (-E_2t_1 + E_1t_2)\sin\theta \\ &\quad = E_1(t_1\cos\theta - t_2\sin\theta) + E_2(t_1\sin\theta + t_2\cos\theta). \end{aligned}$$

Since the $E_\mu$ cannot satisfy any linear identity† we may equate coefficients of $E_\mu$ on both sides of (4.3). Hence

$$t_1' = t_1\cos\theta - t_2\sin\theta \qquad t_2' = t_1\sin\theta + t_2\cos\theta. \tag{4.4}$$

Three other pairs are similarly rotated. The remaining eight terms (comprised in $\Sigma_\alpha$) are unchanged.

Consider five components $t_1, t_2, t_3, t_4, t_5$ corresponding to a pentad. The above transformation leaves $t_3, t_4, t_5$ unchanged; so that, regarding $(t_1, t_2, t_3, t_4, t_5)$ as an ordinary vector in five-dimensional space, the transformation $q = e^{\frac{1}{2}E_{12}\theta}$ gives a simple rotation of the axes through an angle $\theta$ in the plane $x_1, x_2$. Similar rotations in all 10 co-ordinate planes are obtained by using the appropriate matrix in $q$. We therefore call $t_1, t_2, t_3, t_4, t_5$ a space vector, since all possible transformations which a space vector possesses in the elementary vector theory are included in the general tensor transformation (4.2). This would not be true of components which do not form a pentad, *e g*, a mutual rotation of $t_1$ and $t_{23}$ does not correspond to any transformation included in (4.2) It is easily shown that when the five-dimensional space is rotated the components $t_{12}, t_{13}, \ldots, t_{45}$ transform as a 10-vector (analogous to a 6-vector in four dimensions); $t_{16}$ is always an invariant Thus the tensor T is replaceable by a space vector, a 10-vector and an invariant in a five-dimensional space.

---

† See I, § 3. A general proof has been given by Temple, *loc. cit.*

5 In practice we limit space vectors to four dimensions and this leads to a somewhat different grouping of the terms $t_\mu$. The reason for this distinction of the fifth dimension (proper time) from the other four is considered in § 13.

In four dimensions the 16 components $t_\mu$ constitute

$$\left.\begin{array}{l} (a)\ \text{Two invariants } t_5 \text{ and } t_{16} \\ (b)\ \text{Two space vectors } t_1, t_2, t_3, t_4 \text{ and } t_{15}, t_{25}, t_{35}, t_{45} \\ (c)\ \text{A 6-vector } t_{23}, t_{31}, t_{12}, t_{14}, t_{24}, t_{34} \end{array}\right\}. \qquad (5.1)$$

That is to say, when any of the six tensor transformations which correspond to the possible rotations of four-dimensional space are applied, each of these behaves (independently of the others) as a space tensor of the class stated. The two vectors in (*b*) are of indistinguishable character so long as we confine the transformations to four-dimensional rotations.

I have shown that when the $E_\mu$ are four-point matrices three members of any pentad are imaginary and two are real.* I have since been able to show that this is true generally, but the proof is too long to insert here. (I admit only matrices which are wholly real or wholly imaginary.) We shall take $E_1$, $E_2$, $E_3$ to be the imaginary matrices and $E_4$, $E_5$ real. Assuming that for real phenomena the primitive tensor T is real, we see by (3.2) that the two space vectors have components

$$\left.\begin{array}{l} t_1, t_2, t_3 \text{ imaginary, } t_4 \text{ real} \\ t_{15}, t_{25}, t_{35} \text{ imaginary, } t_{45} \text{ real} \end{array}\right\}. \qquad (5\ 2)$$

Thus in the real world one dimension will be different from the other three in the same way that time is differentiated from space, viz., imaginary time must be associated with real space in order to obtain an isotropic rotatable continuum of four dimensions.

If we had taken $E_5$ to be one of the imaginary matrices we should have been left with two real and two imaginary matrices to form a continuum with two space-like and two time-like dimensions. I cannot say why this alternative is rejected, but it evidently depends on the theory of the singling out of the fifth dimension discussed in § 13

---

* I, § 8; since the $F_\mu$ were there defined so that $E_\mu^2 = 1$, real and imaginary matrices are interchanged.

As in Paper III, I will call the original tensors of our calculus (such as T and $E_\mu$) $\psi$-tensors in order to distinguish them from the space vectors and tensors which are derived from them in the way here described

6. Consider a $\psi$-tensor T with the following special properties .—

(*a*) It is the product of two $\psi$-vectors.

(*b*) Its diagonal sum vanishes.

Both properties persist when T undergoes any tensor transformation; they are therefore an absolute specialisation not referring to any particular frame of matrices. I call a tensor which satisfies these two conditions a *wave tensor* and denote it by J

The question now arises, What is the corresponding specialisation of the space tensors (§ 5 (*a*), (*b*), (*c*)) into which T can be resolved? So far as condition (*b*) is concerned the answer is immediate; by (3.2) it requires that

$$j_{16} = 0. \tag{6.1}$$

We shall defer imposing this condition since it is easily introduced at any stage, and find the conditions imposed by (*a*).

I have shown (I, § 8) that the following matrices constitute a pentad

$$\begin{matrix} 0 & i & 0 & 0 \\ i & 0 & 0 & 0 \\ 0 & 0 & 0 & i \\ 0 & 0 & i & 0 \end{matrix} \quad \begin{matrix} i & 0 & 0 & 0 \\ 0 & -i & 0 & 0 \\ 0 & 0 & i & 0 \\ 0 & 0 & 0 & -i \end{matrix} \quad \begin{matrix} 0 & 0 & 0 & i \\ 0 & 0 & -i & 0 \\ 0 & -i & 0 & 0 \\ i & 0 & 0 & 0 \end{matrix}$$

$$\begin{matrix} 0 & 1 & 0 & 0 \\ -1 & 0 & 0 & 0 \\ 0 & 0 & 0 & -1 \\ 0 & 0 & 1 & 0 \end{matrix} \quad \begin{matrix} 0 & 0 & 0 & 1 \\ 0 & 0 & -1 & 0 \\ 0 & 1 & 0 & 0 \\ -1 & 0 & 0 & 0 \end{matrix} \tag{6.2}$$

(This is the pentad $iS_\alpha$, $iD_\beta$, $iS_\gamma D_\gamma$, $S_\alpha D_\gamma$, $S_\gamma D_\beta$ in the notation of Paper I). Denoting them by $E_1$, $E_2$, $E_3$, $E_4$, $E_5$, it is not difficult to prove by straightforward verification that, if $\psi_\alpha$ is any set of four numbers,

$$(E_1\psi)_\alpha(E_1\psi)_\beta + (E_2\psi)_\alpha(E_2\psi)_\beta + (E_3\psi)_\alpha(E_3\psi)_\beta + (E_4\psi)_\alpha(E_4\psi)_\beta \\ + (E_5\psi)_\alpha(E_5\psi)_\beta - (E_{16}\psi)_\alpha(E_{16}\psi)_\beta = 0. \tag{6.3}$$

By using the transformation (2.4) we can deduce that any other matrices forming a pentad satisfy the same identity, so that (6.3) is true generally.

Multiply (6.3) by any four-valued quantity $\psi_\alpha^*$ (inner multiplication) and let

$$\psi\psi^* = J = \Sigma j_\mu E_\mu. \tag{6.4}$$

Then since

$$\psi_\alpha^*(E_1\psi)_\alpha = \psi^* E_1 \psi = -4j_1 \quad \text{by (3.4)}$$

the result is

$$(j_1E_1 + j_2E_2 + j_3E_3 + j_4E_4 + j_5E_5 - j_{16}E_{16})\psi = 0 \tag{6.51}$$

We find similarly

$$\psi^*(j_1E_1 + j_2E_2 + j_3E_3 + j_4E_4 + j_5E_5 - j_{16}E_{16}) = 0. \tag{6.52}$$

We call (6.51) and (6.52) the *wave equations*. They are equations to determine the wave vectors $\psi$, $\psi^*$ (factors of the wave tensor) when certain components of the wave tensor are prescribed. They have an infinity of solutions since the wave tensor is not fully determined by the six components occurring in (6.51) and (6.52).

7. Multiply (6.51) by initial $\psi^*$ and use (3.4); we obtain

$$j_1^2 + j_2^2 + j_3^2 + j_4^2 + j_5^2 - j_{16}^2 = 0. \tag{7.1}$$

Since any pentad can be used in (6.3) we have similarly

$$j_{15}^2 + j_{25}^2 + j_{35}^2 + j_{45}^2 + j_5^2 - j_{16}^2 = 0. \tag{7.2}$$

Again multiply (6.51) by initial $\psi^*E_5$, this gives

$$\psi^*(-j_1E_{15} - j_2E_{25} - j_3E_{35} - j_4E_{45} - j_5 - ij_{16}E_5)\psi = 0.$$

Hence by (3.4)

$$j_1j_{15} + j_2j_{25} + j_3j_{35} + j_4j_{45} = 0. \tag{7.3}$$

Let $X = (j_1, j_2, j_3, j_4)$ and $P = (j_{15}, j_{25}, j_{35}, j_{45})$ be the two space vectors contained in the wave tensor. By (7.3) they are at right angles and by (7.1) and (7.2) they have the same length $R = \sqrt{(j_{16}^2 - j_5^2)}$.

Given any two equal vectors X and P at right angles, it is always possible to find a wave-tensor containing them. For taking any solutions of (6.51) and (6.52), $\psi\psi^*$ will contain the required vector X, but in general $(j_{15}, j_{25}, j_{35}, j_{45})$ will be a vector P′ different from the prescribed P. Since P′ and P are of the same length (both equal to X) and at right angles to X, P′ is transformed into P by a rotation of four-dimensional space about X which leaves X unchanged. Since rotations of space correspond to transformations of $\psi$-tensors, we have only to make the corresponding transformation of $\psi$, $\psi^*$ in order to obtain the required wave tensor.

To prescribe P and X is equivalent to imposing six conditions, the eight components of the two vectors being reduced to six independent quantities by the conditions of equality and perpendicularity. A tensor of the form $\psi\psi^*$ contains seven independent constants, one constant being lost because, if $\psi$ is multiplied by a number $a$ and $\psi^*$ by $b$, only the product $ab$ is involved. Hence only one further condition can be imposed on $\psi\psi^*$ This condition may take the form of assigning $j_{16}$, and as stated in our definition we take $j_{16} = 0$ for a wave tensor

Hence a wave tensor is completely specified by two equal space vectors at right angles to one another. Any physical system described by $\psi\psi^*$ can alternatively be described by such a pair of space vectors.

8. The vector $\iota$P is generally called the momentum vector. We write

$$\iota(j_{15}, j_{25}, j_{35}, j_{45}, j_5) = p_1, p_2, p_3, p_4, \beta \qquad j_{16} = 0. \tag{8.1}$$

Using the other pentad $E_{15}$, $E_{25}$, .. in (6 51), the momentum wave equation is

$$(E_{15}p_1 + E_{25}p_2 + E_{35}p_3 + E_{45}p_4 + E_5\beta)\psi = 0 \tag{8.21}$$

$$\psi^*(E_{15}p_1 + E_{25}p_2 + E_{35}p_3 + E_{45}p_4 + E_5\beta) = 0. \tag{8.22}$$

Multiplying (8 21) by initial $E_5$ and (8.22) by final $E_5$, we obtain

$$H\psi \equiv (E_1p_1 + E_2p_2 + E_3p_3 + E_4p_4 - \beta)\psi = 0 \tag{8.31}$$

$$\psi^*H' \equiv \psi^*(E_1p_1 + E_2p_2 + E_3p_3 + E_4p_4 + \beta) = 0 \tag{8.32}$$

which will be taken as the standard form of the wave equation.

By straightforward multiplication

$$HH' = H'H = -(p_1^2 + p_2^2 + p_3^2 + p_4^2 + \beta^2) = 0 \tag{8.4}$$

by (7.2) and (8.1) Writing $p_4 = \iota p_0$ so that $p_0$ is the real energy (or mass) component, we have

$$\beta^2 = -p_1^2 - p_2^2 - p_3^2 + p_0^2, \tag{8.5}$$

so that $\beta$ is the corresponding *proper mass* or proper energy. For real wave-vectors $j_5$ is real and therefore $\beta$ is imaginary. Since the particles dealt with in physics have real proper mass some kind of modification of the primitive real wave tensor must have been introduced in connection with the singling out of the fifth dimension from the others. The fact that $\beta$ is real involves the introduction of complex wave tensors.

Solutions of the wave equation are found as follows. If $\chi$ is an arbitrary four-valued quantity, $HH'\chi = 0$ by (8.4). Hence $\psi = H'\chi$ is a solution of $H\psi = 0$. Inserting row-and-column suffixes, $\psi = H'\chi$ gives

$$\psi_{\cdot} = H'_{\cdot 1}\chi_1 + H'_{\cdot 2}\chi_2 + H'_{\cdot 3}\chi_3 + H'_{\cdot 4}\chi_4.$$

Since $\chi$ is arbitrary this is an arbitrary linear combination of four elementary solutions of the wave equation $H'_{\alpha 1}$, $H'_{\alpha 2}$, $H'_{\alpha 3}$, $H'_{\alpha 4}$. If the second suffix corresponds to rows, the elementary solutions are simply the four columns of $H'$; similarly the elementary solutions for $\psi^*$ are simply the four rows of H. Actually only three of the elementary solutions are independent.

Using the pentad (6.2) we have by (8 31)

$$
\begin{array}{rlllll}
-iH = & p_2 + i\beta, & p_1 - ip_4. & 0, & p_3 \\
& p_1 + ip_4, & -p_2 + i\beta, & -p_3, & 0 \\
& 0, & -p_3, & p_2 + i\beta, & p_1 + ip_4 \\
& p_3, & 0, & p_1 - ip_4, & -p_2 + i\beta.
\end{array}
$$

To obtain $H'$ we reverse the sign of $\beta$. Thus, taking the first column of $H'$ and the first row of H, particular solutions are

$$\psi = (p_2 - i\beta\ ,\ p_1 + ip_4\ ,\ 0\ ,\ p_3) \qquad \psi^* = (p_2 + i\beta,\ \ p_1 - ip_4,\ \ 0,\ \ p_3)$$

Although these are formally conjugate complex quantities they are not actually so, since in real problems $p_4$ is imaginary. If it is desired to employ genuinely conjugate wave vectors this can only be managed by making a *non-relativity* transformation of $\psi$. For our purposes there is nothing to be gained by insisting on conjugate wave vectors, or even by pairing the solutions for $\psi$ and $\psi^*$ in one-to-one correspondence To require that $\psi$ and $\psi^*$ shall be conjugate does not ensure that the physically interesting quantities $\psi^* E_\mu \psi$ shall be non-complex, and the reality conditions for these physical vectors are best introduced directly.

9. Equations (8.31) and (8.32) are not quite identical with Dirac's wave equation; he gives $\beta$ the same sign in both. We should have obtained his form if we had set $j_5 = 0$ instead of $j_{16} = 0$ in (6.51) and (6 52) and identified the coefficients correspondingly. We did not do this because $j_5 = 0$ is not an invariant condition (except for a limited class of transformations), and it involves choosing a particular frame of reference. Or we can obtain Dirac's form by setting

$$\psi = e^{\frac{1}{2}\pi E_5}\chi \qquad\qquad \psi^* = \chi^* e^{\frac{1}{2}\pi E_5} \tag{9 1}$$

in (8.21) and (8.22) and multiplying the equations by initial and final $e^{\frac{1}{2}\pi E_5}$ respectively. The equations are then simplified since

$$e^{\frac{1}{2}\pi E_5}\, E_{15}\, e^{\frac{1}{2}\pi E_5} = E_{15} \qquad\qquad e^{\frac{1}{2}\pi E_5}\, E_5\, e^{\frac{1}{2}\pi E_5} = -1.$$

This is a *non-relativity* transformation and the quantities $\chi$, $\chi^*$ are unsuitable for use in general relativity theory.

I do not know whether there is any particular advantage in using $\chi$, $\chi^*$ in practical problems rather than $\psi$, $\psi^*$. If so, we can change over at any time by equation (9.1). But if, following Dirac, we use $\chi$, $\chi^*$, the wave equation is relativistic in four dimensions only, and rotations involving the fifth dimension (proper time) are no longer permitted. This has an important bearing on the supposed difficulty with regard to negative energies, but I cannot enter into the question here.

We have

$$\left.\begin{aligned} -4j_\mu = \psi^* \mathrm{E}_\mu \psi &= \chi^* e^{\frac{1}{4}\pi \mathrm{E}_5} \mathrm{E}_\mu e^{\frac{1}{4}\pi \mathrm{E}_5} \chi \\ &= \chi^* \mathrm{E}_\mu \chi \quad \text{if } \mathrm{E}_\mu \text{ and } \mathrm{E}_5 \text{ anticommute} \\ &= \chi^* \mathrm{E}_\mu \mathrm{E}_5 \chi \quad \text{if } \mathrm{E}_\mu \text{ and } \mathrm{E}_5 \text{ commute} \end{aligned}\right\} \tag{9.2}$$

Thus the vectors P and X are the same whether calculated from $\psi$ or $\chi$, but the invariants and the 6-vector are changed. Since $\mathrm{E}_{12}\mathrm{E}_5 = -i\mathrm{E}_{34}$ by (2.2), the "magnetic" components $j_{23}$, $j_{31}$, $j_{12}$ become interchanged with the "electric" components $ij_{14}$, $ij_{24}$, $ij_{34}$. It is for this reason that in Dirac's theory the spin appears to be purely magnetic, although the corresponding 6-vector in our theory is, as shown in the next section, of purely electric type $j_{14}$ (see (10.2)).

10. We may choose our space-time axes so that of the two space vectors P is along $x_4$ and X is along $x_1$. If their common length is unity I find the following solution

$$\psi^* = (i, \ 1, \ i, \ -1) \qquad \psi = (i, \ 1, \ -i, \ 1) \tag{10.1}$$

the matrices being as in (6.2). By (3.4) we find

$$j_1 = 1 \qquad j_{45} = 1 \qquad j_5 = i \qquad j_{41} = -i \tag{10.2}$$

and all the other components vanish.

This shows the relation of the other space tensors to P and X. The invariant $j_5$ is $i$ times their common length, as is also apparent from (7.1) or (8.4). If we extend the vector X to five dimensions $(j_1, j_2, j_3, j_4, j_5)$ it is always a null vector. The 6-vector has only one non-vanishing component $j_{41}$, so that it lies wholly in the plane $x_4$, $x_1$, *i.e.*, the plane of P and X. If S is the 6-vector and I the invariant $(j_5)$ we have

$$\mathrm{IS} = [\mathrm{PX}], \tag{10.3}$$

where the bracket indicates vector product. Evidently (10.3) is independent of our special choice of axes.

The additional tensors I and S are redundant as part of a physical description of the system since they are determined by P and X; but the interaction of their components with P and X must be taken into account when we apply relativity transformations other than the six rotations of space-time.

The following relativity transformation is important. Let

$$\psi' = e^{\frac{1}{2}E_{15}\theta}\,\psi \qquad \psi^{*\prime} = \psi^* e^{-\frac{1}{2}E_{15}\theta} \tag{10.4}$$

As in (4.4) we have

$$\begin{aligned} j_1' &= j_1\cos\theta - j_5\sin\theta & \qquad j_{41}' &= j_{41}\cos\theta - j_{45}\sin\theta \\ j_5' &= j_1\sin\theta + j_5\cos\theta & \qquad j_{45}' &= j_{41}\sin\theta + j_{45}\cos\theta \end{aligned}$$

Applying this to (10 2) we have

$$j_1' = e^{-i\theta} \qquad j_{45}' = e^{-i\theta} \qquad j_5' = ie^{-i\theta} \qquad j_{41}' = -ie^{-i\theta}$$

and the other components remain zero. This result is simply

$$j_\mu' = j_\mu e^{-i\theta} \tag{10 5}$$

or $J' = Je^{-i\theta}$.

The transformation

$$\psi' = e^{\frac{1}{2}E_4\theta}\,\psi \qquad \psi^{*\prime} = \psi^* e^{-\frac{1}{2}E_4\theta} \tag{10.6}$$

also gives the same result (10.5).

The generalisation of (10.4) when the space vector X is not along $x_1$ is

$$\left.\begin{aligned} \psi' &= \exp\{\tfrac{1}{2}\theta\,(E_{15}X_1 + E_{25}X_2 + E_{35}X_3 + E_{45}X_4)/R\}\,\psi \\ \psi^{*\prime} &= \psi^*\exp\{-\tfrac{1}{2}\theta\,(E_{15}X_1 + E_{25}X_2 + E_{35}X_3 + E_{45}X_4)/R\} \end{aligned}\right\} \tag{10.7}$$

where $R^2 = X_1^2 + X_2^2 + X_3^2 + X_4^2$. Since the square of $(E_{15}X_1 + \ldots + E_{45}X_4)/R$ is $-1$, its occurrence in the exponential does not create any difficulty of interpretation although it contains non-commuting matrices. As already proved for special axes, (10.7) gives $J' = Je^{-i\theta}$.

11. Provisionally we may suppose that X represents a positional vector of some kind (displacement) as distinguished from momentum represented by P. Then the conjugated quantities, co-ordinate and momentum, will be represented in two distinct domains (as in a phase-space representation), viz., $(x_1, x_2, x_3, x_4)$ and $(x_{15}, x_{25}, x_{35}, x_{45})$, which, however, rotate together in the ordinary relativity rotations of space-time. It is interesting to note that the method of wave vectors provides no way of obtaining positional relations X without a momentum P attached, so that a purely geometrical space without momentum content is unthinkable from its standpoint. The dynamical effects of position (interaction energy) are associated with position at the start.

The fact that X is at right angles to P seems to imply that for a state of definite momentum, *i.e.*, an eigenstate, positional relation is limited to the three-dimensional section of the world at right angles to P. This section may be called a *simultaneous instant* for the eigenstate in question. We can thus recognise simultaneity of different parts of a system in a way which does not contradict the principle of relativity, for the simultaneity is relative to a particular eigenstate and not to an absolute direction in the world.

I think it probable (though I have not proved it) that in the wave equation for two electrons (III, equation (16 5) ) the co-ordinates ($x_\mu$, $x_\mu'$) and the proper distance $r$ of the two electrons must correspond to a simultaneous instant for the eigenstate in question. In particular, if we are seeking solutions in which the centre of gravity of the system is at rest we must set $t = t'$. If this is right it removes the difficulty as to the dual time.

The argument is that positional relation except in a plane at right angles to the momentum vector is not expressible by wave-mechanics and is therefore presumably non-existent; so that positional relation in four dimensions is only possible when the momentum vector is indeterminate. This is evidently connected with the Uncertainty Principle which asserts that when a momentum component is determinate the corresponding co-ordinate is completely indeterminate and therefore meaningless; but it is not an immediate consequence since it has reference to positional relations internal to the system.

12. A five-dimensional representation of phenomena is inevitable if we adopt Dirac's conception of dynamical states of a system enduring from $t = -\infty$ to $t = +\infty$, which are nevertheless continually undergoing change by perturbations due to other systems or subjectively by the observer becoming aware of additional data. This evidently postulates an independent variable outside the four dimensions of the state, to which the changes can be referred. This variable $s$ is called proper time, and the changes occur throughout the state at instants of $s$. There can be only one co-ordinate $s$ referring to the whole system, for it is contrary to the conception of a four-dimensional state for the state to change in part and not as a whole. Thus, if the system is described as consisting of a number of particles, each particle will in general have its own co-ordinates ($x_1$, $x_2$, $x_3$, $t$), but one value of $s$ will apply to them all. If two systems are combined into one their separate proper times must be replaced by one proper time for the combination. It is for this reason that we cannot combine wave functions (or probabilities) for two systems by a simple multiplicative law; a transformation is required to eliminate the redundant proper time of one of them and the elimination introduces the terms recognised as interaction energy.

In non-relativity theory proper time is represented within the four-dimensional world and not as a separate variable; in particular, if the system is at rest, it is regarded as identical with co-ordinate time $t$. Changes of state which occur throughout the system at an instant of $s$ are therefore supposed to occur at an instant of $t$. This is, of course, a flat contradiction of relativity which cannot allow world-wide instants of $t$ to be distinguished in this way. In comparing our results with Dirac's formulæ we have to remember that he does not generally make any distinction between the fourth and fifth dimensions, so that $E_4$ and $E_5$ are liable to be interchanged. He minimises the discrepancy by choosing a special set of matrices such that $E_{45}$ is a diagonal matrix $(\rho_3)$ which is unity for two components of $\psi$ and $-1$ for the other two, thus $E_4 = E_5$ for two components of $\psi$ and $E_4 = -E_5$ for the other two. The failure to discriminate between proper time and co-ordinate time must therefore occasionally lead to an error of sign, and I think this is the root of the supposed difficulty as to negative energies.

13. The complete sets of matrices which form the starting point of our analytical calculus are *equivalent*; we distinguish them relatively to one another by the transformation P which changes one into the other, but there is no absolute specification of the set that we start from. This is perhaps more easily seen in G. Temple's work, in which the $E_\mu$ are not even identified with matrices but are perfectly general symbols obeying the same laws and transformations as our matrices.* The frames of matrices should, therefore, in physical problems connote systems of reference which are *a priori* equivalent. In a purely statistical theory, such as the modern quantum theory, this equivalence is necessarily a statistical equivalence. A transformation to an equivalent frame must not alter the *a priori* probability; that essentially is the form of the general principle of relativity which I adopt in my theory. In particular, rotations of the five-dimensional space found in § 4 do not affect the *a priori* probability of a configuration.

This principle of relativity is in a sense a truism, for the only meaning that I would attach to *a priori* probability is that we are (conventionally) allowed to assume that it applies unless information to the contrary is given. It need not apply and the solver of the problem may thus reach wrong conclusions, but in that case he is entitled to complain that he was kept in ignorance of important conditions of the problem (*e.g.*, the existence of an electric or gravitational field). It is, however, the task of the complete theory to find the effects of possible deviations from *a priori* probability of the unspecified parts of the system on the behaviour of the specified particles, and to indicate what kind of information should be supplied.

---

* 'Proc. Roy. Soc.,' A, vol. 127, p. 349 (1930).

If *a priori* probability applied to the actual world in accordance with our principle of relativity, all orientations of a system in five dimensions would be statistically equivalent and there would be no way of separating the fifth dimension from the four-dimensional world. The fact that we can separate it uniquely implies that actual probability deviates from *a priori* probability. It is well known that for the universe as a whole it does deviate; and by the second law of thermodynamics the deviation tends to diminish with the lapse of proper time. Since this deviation of actual from *a priori* probability affects all practical problems, we do not treat it as a special modification but as a permanent transformation of our basis of *a priori* probability. With this transformation there is no longer statistical equivalence of orientations at different inclinations to the axis of proper time, and rotations in the fifth dimension are inadmissible (unless we make complicated corrections for the non-isotrophy).

Against this view it might be urged that, whilst any reference frame of macroscopic space and time and proper time must be defined by reference to the states of the universe (or at least of a vast number of unspecified particles), and any absoluteness attributed to a particular frame must come from the non-uniform relation of actual to ideal probability of these states, yet the "states" here referred to correspond to a broad classification which can scarcely take cognisance of condition in regard to thermodynamic equilibrium. To this there is, I think, the conclusive answer that it is well known that direction of proper time is distinguished by reference to deviation from thermodynamic equilibrium (entropy) and by nothing else.

I conclude that there is not really a misfit between the analytical theory with its five-dimensional relativity and the practical problems in which the fifth dimension is kept distinct and unrotatable. The contrast arises from something characterising the actual universe which is generally acknowledged to be exceedingly improbable *a priori*. As regards dynamical theory of simple systems and the interactions of electrons and protons, we shall have no such fixity of the fifth dimension and all the relativity transformations will be applicable. This point is important in justifying my enumeration of 136 relativity rotations of a system consisting of two particles, the results of which I have treated in other papers.

# *The Spectrum of the Hydrogen-Nitrous Oxide Flame.*

By A. Fowler, D.Sc., F.R.S., Yarrow Research Professor of the Royal Society, and J. S. Badami, B.Sc., Imperial College, South Kensington.

(Received July 7, 1931.)

[Plates 10, 11.]

## *Introductory.*

The present investigation was undertaken on the suggestion of Mr. H. T. Tizard, F.R.S., arising out of some experiments in progress at the National Physical Laboratory. Previous observations of the spectrum of the hydrogen-nitrous oxide flame have not been very complete, and it was hoped that more extended observations, in connection with our present knowledge of the constitution of the molecules associated with certain band spectra, might throw further light on the process of combustion. Observations have accordingly been made over the range λ8225 to λ2250, with the result that the spectrum in question has been found to be identical with that of the flame of ammonia burning in oxygen, apart from differences in intensities of certain bands in the two spectra.

The spectrum of the ammonia-oxygen flame has previously been described, but it may be useful to give an account of the experiments which have been made, and to state the modern interpretation of the spectra observed. As the results may be of interest to some who are not spectroscopists, it has been thought desirable to include a brief account of the spectra which form the basis of the conclusions reached.

## *Reference Spectra.*

"*Water Vapour*" *Bands* (HO).—Emission bands attributed to water vapour were discovered simultaneously by Liveing and Dewar[*] and by Huggins.[†] Liveing and Dewar observed these bands to be well developed in the flames of hydrogen or hydrocarbons burning in oxygen, and less strongly in the flames of non-hydrogenous gases, such as carbonic oxide and cyanogen, if burnt in moist oxygen. The same bands were also observed in uncondensed discharges in vacuum tubes containing moist gases, but they disappeared when the gas and apparatus had been thoroughly dried. A more complete description was given later by the same authors.*

---

[*] 'Proc. Roy. Soc.,' vol. 30, pp. 498 and 580 (1880).

[†] 'Proc. Roy. Soc.,' vol. 30, p. 576 (1880).

The spectrum consists of a number of bands degraded towards the red, of which one at λ 3064 is especially conspicuous. Other band heads are at λλ 3472, 3428, 2811 and 2608, but band lines were found by Liveing and Dewar to extend as far as λ 4100 towards the violet and to λ 2268 in the ultra-violet.

The analysis of this spectrum, in the light of the modern theory of band spectra, has resulted in its definite assignment to HO molecules †

"*Ammonia*" *Bands.*—Three groups of bands are associated with the spectrum of ammonia. The first was observed by Schuster‡ as a broad yellowish-green band, about λ 5635, in the spectrum of a vacuum tube through which a continuous stream of ammonia gas was passed. It was noted that the band at once disappeared when the supply of ammonia was cut off. Schuster's band was subsequently found by Lecoq§ to be double, with components about λλ 5643 and 5681.

The second and most characteristic band associated with ammonia, having its strongest part about λ 3360, was first described by Eder,‖ who observed it in the ammonia-oxygen flame, and designated it the β band This band was afterwards observed by Lewis¶ in the spectra of vacuum tubes containing mixtures of hydrogen and nitrogen, and a more detailed investigation of the band, and of its occurrence in the solar spectrum, was given by Fowler and Gregory.** Lewis observed that, unlike the Schuster bands, the β band persisted after the supply of ammonia was stopped.

The third system of bands, extending over the whole of the visible spectrum, was also observed by Eder in the ammonia-oxygen flame, and was distinguished by him as the α band. As a result of an investigation of the structure and chemistry of the ammonia-oxygen flame, it was concluded by A. Reis†† that this band belonged to the spectrum of ammonia.

The α band was investigated in greater detail in Professor Fowler's laboratory by W. B. Rimmer,‡‡ who found that it could also be observed in the uncondensed discharge in vacuum tubes containing ammonia at suitable pressures. Photographs taken with high resolution showed this part of the spectrum to be of great complexity, consisting of about 3000 band lines extending from red to violet, but showing no distinct heads of bands. It was further noted by Rimmer, in agreement with Eder, that with a small supply of oxygen the α band was stronger with respect to the ultra-violet band than when the supply of oxygen was abundant.

---

* 'Phil. Trans.,' vol. 179, p 27 (1888).

† *Cf* D. Jack, 'Proc. Roy. Soc,' A, vol. 115, p. 373 (1927).

‡ 'Rep. Brit. Assoc.,' p. 38 (1872).

§ 'C. R. Acad. Sci.,' Paris, vol. 101, p. 42 (1885).

‖ 'Denkschr. Wien. Akad,' vol. 60, p. 1 (1893).

¶ 'Astrophys. J.,' vol. 40, p. 154 (1914).

** 'Phil. Trans.,' A, vol. 218, p. 351 (1919).

†† 'Z. Phys. Chem.,' vol. 76, p. 560 (1911).

‡‡ 'Proc. Roy. Soc.,' A, vol. 103, p. 696 (1923).

Rimmer considered that his observations supported the suggestion of Lewis that the Schuster bands represent the true spectrum of ammonia, while the ultra-violet λ 3360 band is probably due to a more stable compound of hydrogen and nitrogen. Rimmer's investigation suggested, in addition, that the α band originates in an emission centre which represents the first stage of dissociation of the normal ammonia molecule, and that the β band represents a further stage of dissociation which precedes the final breaking up of the molecules into atoms.

Analysis of the structure of the β band, λ 3360, has been made by Hulthén and Nakamura,* from which it results that this band originates in NH molecules.

No analysis has yet been made of the α band, but Hulthén and Nakamura have expressed the opinion that this complicated system is emitted by excited $NH_3$ or $NH_2$ molecules, or a mixture of both. $NH_3$, however, appears to be ruled out by the experimental evidence, and if the Schuster bands have been correctly attributed to $NH_3$, it may provisionally be supposed that the α bands represent $NH_2$ molecules It may be noted that a recent investigation by Lavin and Bates† on the gases flowing from the exit of an ammonia discharge tube have indicated the presence of an active gas, probably consisting of atomic hydrogen and NH or $NH_2$.

"*Third Positive Nitrogen Bands*" (NO).—Five bands in the ultra-violet, extending from λ 2718 to λ 2262, were observed by Eder in the spectrum of the ammonia-oxygen flame, and were assigned the names γ–η. These were afterwards found to be identical with the well-known double-double bands, degraded to the more refrangible side, which had been designated the "Third Positive" bands of nitrogen by Deslandres, who had shown, nevertheless, that the simultaneous presence of nitrogen and oxygen was necessary for their production. Analysis of this spectrum has resulted in its assignment to NO molecules.‡

---

* 'Nature,' vol. 119, p. 235 (1927).

† 'Proc. Nat. Acad. Sci.,' vol. 16, p. 804 (1930).

‡ R. T. Birge, 'Bull. Nat. Res. Co.,' vol. 11, No. 57, p. 69 (1926); M. Guillery, 'Z. Physik,' vol. 42, p. 121 (1927).

### *Previous Observations.*

In connection with their experiments on the ignition points of gases, Dixon and Higgins* studied the ignition of several gases in an atmosphere of nitrous oxide. In the case of a hydrogen flame it was observed, as had previously been noted by Priestley and by Davy in the burning of a candle or taper, that an atmosphere of nitrous oxide produced a remarkable increase in the size and luminosity of the flame. The jet of unburnt gas was seen to be surrounded by a bright apricot-coloured zone, which appeared to give a continuous spectrum, while outside this was a thick sheath of a greenish-grey colour. A photograph obtained with a quartz spectrograph showed an apparently continuous spectrum from red to violet, and beyond this the ultra-violet "steam" (HO) bands.

Dixon and Higgins also recorded that when a jet of hydrogen was burnt in nitrous oxide at normal pressure in a wide glass tube, a red colouration due to the formation of nitrogen peroxide was seen stretching upwards from the level of the flame. Also, that when the hydrogen-nitrous oxide flame was divided in a Smithell's separator, no peroxide could be detected in the interconal gases, though it was formed in the outer flame. The general outcome of these experiments was to show that the ignition points of hydrogen in nitrous oxide, at corresponding pressures, were always lower than those in oxygen.

The hydrogen-nitrous oxide flame had previously been observed by S. Barratt† in connection with an investigation of the origin of cyanogen bands in the violet and ultra-violet. The presence of the β band of ammonia and the bands of water vapour was recorded, but no reference was made to the α band.

### *Structure of the Flames.*

*Mixed Jet.*—In the first of the present series of experiments, nitrous oxide and hydrogen were mixed by passing the gases through the two horizontal arms of a ⊥ tube, and were then burnt at a small jet on the upright arm, as in the corresponding experiment at the National Physical Laboratory. Afterwards, it was found convenient to use a mixed-jet blowpipe, which gave a flame of the same character.

The main part of the flame was only feebly luminous, but in the lower part there was a more luminous zone which varied in appearance and brightness with varying proportions of nitrous oxide. With a supply of nitrous oxide such that a hydrogen flame about 1½ inches in height (I*a*)* was extended to about 7 inches, the inner zone was conical in shape (I*b*), but with a suitable reduction in the supply of nitrous oxide, this inner cone was enlarged and became a semi-elliptical arch surmounted by a bright yellowish cap; the outer flame was then much reduced in length, and was of greater width (I*c*). Surrounding the inner zone there was a fairly bright yellowish-white region extending to more than half the height of the flame, and beyond this a feeble dull red portion which was of a somewhat smoky appearance

---

* 'Mem. Manchester Lit. Phil. Soc.,' vol. 71, p. 15 (1926).

† 'Proc. Roy. Soc.,' A, vol. 98, p. 44 (1920).

*Two-way Blowpipe.*—Experiments were also made with a two-way blowpipe in which hydrogen was passed through the outer, and nitrous oxide through the inner, tube, so that the gases were not mixed until they reached the orifice where they were burnt. In this case (I*d*) the structure of the flame was somewhat similar to that obtained with the mixed jet when there was a relatively large supply of $N_2O$ (I*b*) The inner cone, however, was somewhat less prominent, and its upper part was surrounded by a zone of considerable brightness, as shown by the enlargement in the lower part of I*d* No bright cap could be made to appear at the summit of the cone, and it would seem that the bright cap of I*c* was here represented by the bright zone which surrounds the inner cone.

*Hydrogen Flame Surrounded by $N_2O$.*—Further experiments were made by surrounding a flame of hydrogen with an atmosphere of nitrous oxide. This was done by enclosing the flame in a glass chimney into which nitrous oxide was passed, or by passing the hydrogen through the inner tube and nitrous oxide through the outer tube of a two-way blowpipe. Under these conditions the hydrogen flame was enlarged and much brightened, especially near the base (I*e*). No definite inner cone, however, was observed.

## *Spectroscopic Observations.*

*Mixed-jet Flame.*—Visual observations of the bright cone or cap (I *b, c*) with a pocket spectroscope showed six fairly distinct bands, three on each side of the D lines, superposed on a continuous spectrum of moderate intensity. Photographs taken with a small quartz spectrograph (Hilger's E 31) showed these and other bands, and experiments with vacuum tubes containing compounds of nitrogen were undertaken with a view to tracing their origin. The bands were not obtained in discharges through $N_2O$, either alone or when mixed with hydrogen or oxygen, but were eventually found to be identical with the α bands of ammonia occurring rather feebly in tubes containing ammonia. The identification was afterwards fully confirmed by photographs of the ammonia-oxygen flame, in which the α bands are very conspicuous (II*a*). With large dispersion, as in the photographs taken by Rimmer, the bands in question become unrecognisable as such.

---

* This and similar references are to the photographic reproductions, Plates 10 and 11.

It is possible that the apparent band heads, when the spectrum is viewed with small dispersion, may give a clue to the structure of this spectrum, and it may accordingly be useful to record the following roughly approximate positions :—

| λ | ν | λ | ν |
|---|---|---|---|
| *6652 | 15,029 | *5713 | 17,499 |
| 6470 | 15,452 | 5575 | 17,932 |
| *6302 | 15,864 | *5436 | 18,391 |
| *6042 | 16,546 | 5384 | 18,568 |
| 5807 | 17,216 | 5265 | 18,988 |

In this table the brighter bands are marked with an asterisk.

Visual observations of the flame above the inner cone revealed no bands, but only a continuous spectrum. The outermost part of the flame was too faint for spectroscopic observation.

A photograph of the spectrum of the inner cone of the $H_2 - N_2O$ flame (I *b*), which is identical with that of the bright cap of I c, is reproduced in II *b*. The D lines of sodium appear near the less refrangible end, and the α bands of ammonia extend from the red side of this to the near ultra-violet. The β band at λ 3360 (NH), with the wings of band-lines on each side of the central band, is very prominent. The bands of HO are also conspicuous and in the further ultra-violet there are the double bands of NO.

The spectrum of the ammonia-oxygen flame is shown in II *a* for comparison. It will be seen that this shows the same bands as the $H_2 - N_2O$ flame, but with a somewhat different distribution of intensities. Thus, the β band being of about the same intensity in the two photographs, the HO and NO bands are decidedly stronger in the $H_2 - N_2O$ flame and the α bands of ammonia ($NH_2$ ?) somewhat weaker. The weak band at λ 3883 in the $H_2 - N_2O$ flame is due to "cyanogen" (CN) and was doubtless introduced by a slight impurity of a carbon compound either in the hydrogen or nitrous oxide.

The third photograph, II *c*, was taken with an image of the bright cap of the $H_2 - N_2O$ flame (I *c*) focussed on the slit of the spectrograph, and shows very clearly that while the α and β bands of ammonia and the NO bands were almost entirely restricted to the bright flame cap, the HO bands and continuous spectrum extended through the outer flame with but little diminution of intensity. Eder similarly observed that the characteristic bands of "ammonia" appeared only in the inner cone of the ammonia-oxygen flame, while the outer flame yielded the "water-vapour" bands.

*Two-way Blowpipe Flame* --When the flame was produced with the two-way blowpipe, with nitrous oxide passing through the inner tube (I *d*), visual observations of the inner cone showed only a strong continuous spectrum In the zone immediately surrounding the inner cone, however, the continuous spectrum was much weaker and the α bands were distinctly visible Photographs also showed a continuous spectrum, and apparent discontinuities in its intensity were proved to be due to varying sensitivity of the plates, for different wave-lengths, by comparison with the spectrum of a white-light source. In the ultra-violet, the bands of HO were very strong, the NH band of moderate intensity, and the NO bands rather feeble.

The blow-through flame thus differed from the mixed-jet flame chiefly in the greater diffusion of the luminous cap of the latter, and in the increased brightness of the continuous spectrum shown by the inner cone.

*Hydrogen Flame Surrounded by $N_2O$* —Visual observations of this flame (Ie) showed only a bright continuous spectrum, as noted by Dixon and Higgins. Photographs of the spectrum also showed a strong continuous spectrum extending from red to violet, together with bands of HO, and sometimes traces of the NH band at λ 3360. The spectrum of the hydrogen flame was thus scarcely affected by the substitution of nitrous oxide for ordinary air outside the flame, except as regards the greatly increased intensity of the continuous spectrum.

## *Summary.*

Observations of the bright cap or cone, which appears near the base of the hydrogen-nitrous oxide flame in a mixed jet have shown that the spectrum is closely similar to that of the ammonia-oxygen flame. Each of these flames shows bands due to the molecules NH, HO and NO, and the so-called "α bands" of ammonia, which have been provisionally attributed to $NH_2$ molecules on the basis of experimental evidence. The Schuster bands, probably due to $NH_3$ molecules, were not observed. The hydrogen-nitrous oxide flame differs from the ammonia-oxygen flame in the greater intensity of the NH and HO bands, and the lower intensity of the $NH_2$ ? bands, the

NH band at λ 3360 being about the same in both. The outer cones of both these flames appear to exhibit nothing but the bands of HO and a continuous spectrum

## DESCRIPTION OF PLATES 10, 11.

### PLATE 10.

(*a*) Hydrogen flame.
(*b*) $H_2$ flame with large supply of $N_2O$. Mixed jet.
(*c*) $H_2$ flame with small supply of $N_2O$. Mixed jet.
(*d*) $H_2$ flame with $N_2O$ blown through. The lower photograph is an enlarged view of the inner cone from the same negative.
(*e*) $H_2$ flame surrounded by $N_2O$

### PLATE 11

(*a*) Spectrum of ammonia-oxygen flame ; oxygen passed through inner tube and ammonia through outer tube of blowpipe.
(*b*) Spectrum of $H_2$-$N_2O$ flame, inner cone (I, *b*).
(*c*) Spectrum of $H_2$-$N_2O$ flame, bright cap and flame above it (I, *c*). The apparent bands on the red side of the Na lines and the patch from λ 5000 to λ 4000, which extend across the spectrum, represent continuous spectrum as photographed with small dispersion on a plate of varying sensitivity The dark lines on the upper edge of the spectrum are due to daylight which accidentally entered the slit.

d

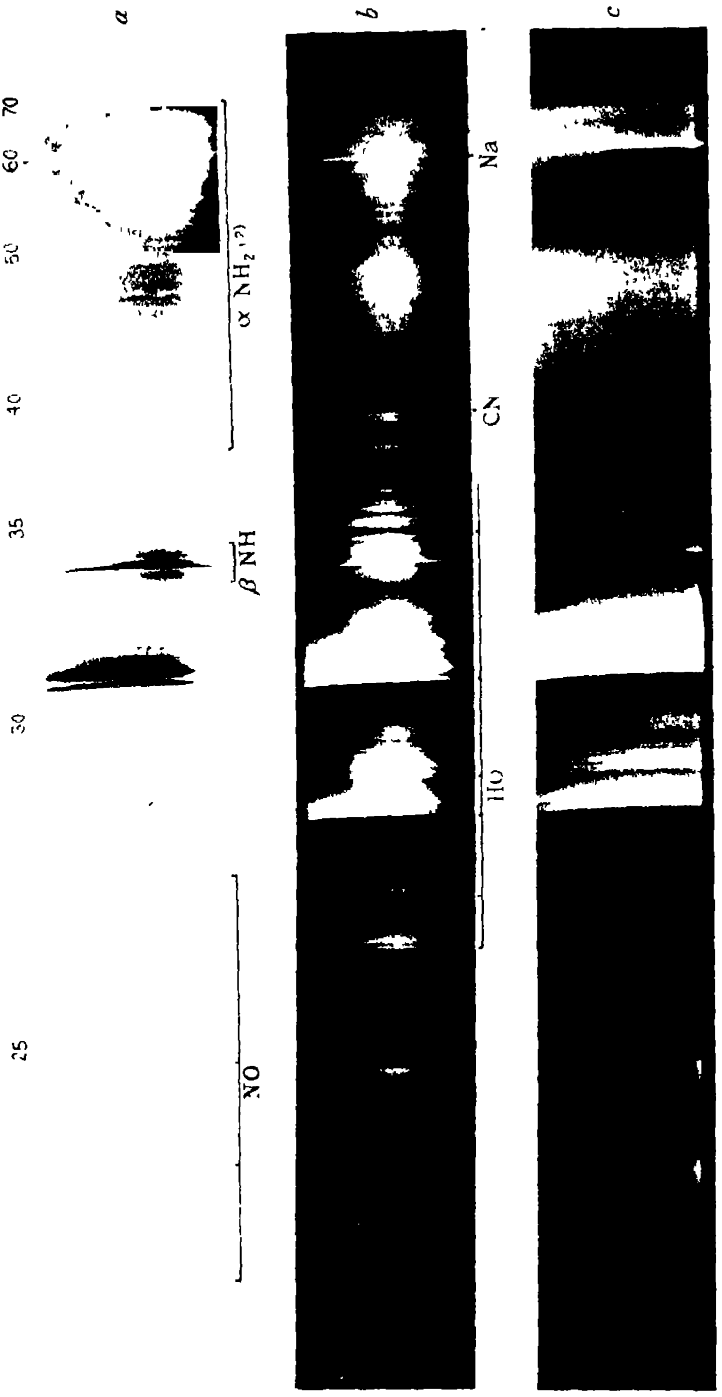

II.

# *The Nuclear Moment of the Indium Atom.*

By Professor J. C. McLennan, F.R.S., Elizabeth J. Allin and K. E. Hall.*

(Received July 13, 1931.)

(Plate 12.)

The investigation described here is a continuation of an earlier one† carried out by two of the authors in which certain lines in the first spark spectrum of indium were studied and the conclusion drawn that the nuclear moment of that atom was probably $\frac{1}{2}\ h/2\pi$. During the time that elapsed between the completion of this work and its publication there appeared a paper by Jackson‡ describing an examination of certain lines in the arc spectrum which led to an I value of unity. Two of the lines λ 4511, λ 4102 observed by him had appeared on our plates and been measured by us, the structure recorded in the two cases being quite different. In proceeding with the research it was therefore decided first to revise the work on these lines and then to direct our attention to lines in the ultra-violet region of the arc spectrum.

The discharge tube used was very similar to Jackson's. It was made from quartz and consisted of two wide portions 8 cm. in length and 2·5 cm. in diameter joined by a narrower one 4 cm. in length and 0·8 cm. in diameter. The electrodes were made of sheet copper wrapped around the wide parts of the tube and were coupled inductively to an oscillating circuit with a frequency range of 10,000 to 14,000 cycles. Two U.V. 861 General Electric screen grid radio frequency power amplifier tubes operating in parallel were used. A small amount of indium trichloride (Hilger's H.S. brand) was introduced into the tube, which was then evacuated. It was usually necessary to heat the tube slightly by means of a bunsen to start the discharge, but once this was done no further heating was necessary.

As in the earlier experiments the lines λ 4511, λ 4102 were studied by means of a transmission echelon grating of 45 plates 1·476 cm. in thickness and having steps 0·1 cm. in width used in conjunction with a constant deviation prism. For work in the ultra-violet this apparatus was, of course, unsuitable and was replaced by a quartz Lummer plate. The one used was 13 cm. in length, 1·45 cm. in width and 0·496 cm. in thickness and was mounted in an almost horizontal position but in such a way that its inclination could be adjusted. The light from the source was rendered parallel by a lens, then passed through a Foucault prism and thence through an achromatic lens which focussed it on the prism of the Lummer plate. On emerging from the latter it was focussed by means of a second achromatic lens on the vertical slit of a small Hilger quartz spectrograph. Thus interference patterns of all the lines (including λ 4511, λ 4102) were obtained in a single exposure. An alternative method was also used for the lines λ 4511, λ 4102 A quartz monochromatic illuminator was placed between the source and the plate, the light on leaving the interferometer being focussed directly on the photographic plate. These two lines were in addition investigated in the third order of a 21-feet concave grating which, however, was found inadequate to resolve them.

---

* Mr. Hall was enabled to take part in this investigation by the award of a National Research Council of Canada Bursary.

† 'Proc. Roy. Soc.,' A, vol. 129, p. 208 (1930).

‡ 'Proc. Roy. Soc.,' A, vol. 128, p. 508 (1930).

Fig 1*a* (Plate 12) shows an enlargement of a photograph of the line λ 4511 taken with the echelon grating, the slit, the step edges and the refracting edge of the prism all being vertical. Photographs were also taken with two crossed slits and the step edges of the echelon horizontal, but these are not shown.

Fig. 1*b* (Plate 12) is an enlarged reproduction of the Lummer plate pattern of this line using the second method outlined above. In both cases the line is seen to consist of two components of comparable intensity. Referring to the results previously given by us, it will be noted that in the earlier work three such components were observed, two of which correspond to the two of the present pattern. It seems probable that the third was the line listed as a weak spark line by Eder and Valenta, although this was not thought likely at the time since it did not undergo the same variation in intensity with excitation as the other spark lines under consideration. It is therefore probably due to a transition between high levels of In. I, a fact which would also explain the discrepancy between the intensities recorded in the two cases, since the excitation used by Eder and Valenta was considerably greater than that used by us as attested by the non-appearance on our plates of the indium III lines λ 5248, λ 5645 reported as strong by the latter. In place of this strong line a very weak line may now be distinguished in the position of a satellite at $+0\cdot306$ cm.$^{-1}$ Owing to its extremely low intensity it is not considered to be a part of the same pattern as the other lines.

Figs. 2*a* and *b* (Plate 12) show the corresponding patterns for λ 4102. It is seen to possess three almost equally spaced components, the central one being most intense.

Figs. 3–6 (Plate 12) shows the patterns of the lines λ 3039, λ 2933, λ 2837, λ 2754 as obtained with the Lummer plate and quartz spectrograph. All

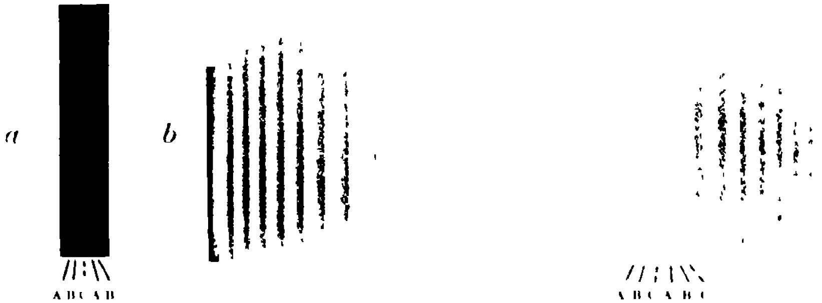

Fig. 1. $5p\ ^2P_{3/2}$ — $6s\ ^2S_{1/2}$ *a*, Echelon grating *b*, Lummer-Gehrcke plate

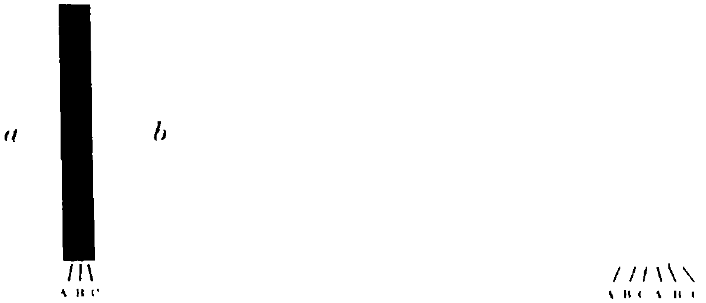

Fig. 2. $5p\ ^2P_{1/2}$ — $6s\ ^2S_{1/2}$ *a*, Echelon grating *b*, Lummer-Gehrcke plate.

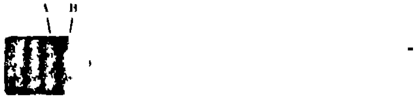

Fig. 3. $5d\ ^2D_{3/2}$ — $5p\ ^2P_{1/2}$. Lummer-Gehrcke plate

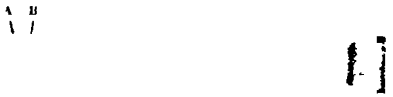

Fig. 4. $7s\ ^2S_{1/2}$ — $5p\ ^2P_{3/2}$ Lummer-Gehrcke plate

Fig. 5. $a\ ^2P_{3/2}$ - $b\ ^4P_{5/2}$ Lummer-Gehrcke plate.

Fig. 6. $7s\ ^2S_{1/2}$ — $5p\ ^2P_{1/2}$ Lummer-Gehrcke plate.

of these lines appear as doublets. In the case of λ 2933, however, the two components did not maintain a constant intensity ratio as the conditions in the source varied. Hence it was concluded that the two were due to transitions between quite different pairs of levels. The one component (that marked A on the plate) showed the same variations from plate to plate as the line λ 2754, and is therefore the line due to the transition $7s\,^2S_{1/2} - 5p\,P_{3/2}$, which is thus not double, as might at first appear, but single.

The line λ 2837 is of particular interest since Uhler and Tanch give for it six components with separations well within the possibilities of our own instrument, but there is no indication of more than two such components on our plates.

Owing to the small dispersion of the spectrograph, the patterns of the lines λ 3256 and λ 3257 and of λ 2714 and λ 2710 overlapped.

The quantitative results are tabulated below :—

| Unresolved line | | | Resolved line. | | |
|---|---|---|---|---|---|
| λ in A U | Intensity | Classification | λ in A U | in cm $^{-1}$ | Intensity. |
| 4511·31 | 10 | $5p\,^2P_{3/2} - 6s\,^2S_{1/2}$ | 0 | 0 | 8 |
| | | | −0·047 | 0·232 | 10 |
| 4101·76 | 8 | $5p\,^2P_{1/2} - 6s\,^2S_{1/2}$ | 0·053 | −0·313 | 6 |
| | | | 0 | 0 | 10 |
| | | | −0·057 | 0·343 | 6 |
| 3039·35 | 10 | $5p\,^2P_{1/2} - 5d\,^2D_{3/2}$ | 0 | 0 | 10 |
| | | | −0·036 | 0·394 | 8 |
| 2932·63 | 6 | $5p\,^2P_{3/2} - 7s\,^2S_{1/2}$ | Single | — | — |
| 2836·91 | 8 | $a\,^2P_{3/2} - b\,^4P_{5/2}$ | 0 | 0 | 5 |
| | | | −0·028 | 0·348 | 10 |
| 2753·89 | 6 | $5p\,^2P_{1/2} - 7s\,^2S_{1/2}$ | 0 | 0 | 10 |
| | | | −0·029 | 0·382 | 8 |
| 2560·16 | 8 | $5p\,^2P_{1/2} - 6d\,^2D_{3/2}$ | 0 | 0 | 10 |
| | | | −0·023 | 0·351 | 8 |

The intensities quoted for the lines λ 4511, λ 4102 were estimated from the echelon patterns, and for the other lines from the Lummer plate patterns.

The number of components and their separations are what would be expected if the levels involved were double with the following separations :—

| | |
|---|---|
| $5p\,^2P_{1/2}$ | 0·343 cm.$^{-1}$ |
| $5p\,^2P_{3/2}$ | 0·081 |
| $6s\,^2S_{1/2}$ | 0·313 |
| $5d\,^2D_{3/2}$ | −0·06 |
| $7s\,^2S_{1/2}$ | 0·10 |
| $6d\,^2D_{3/2}$ | 0 |

These considerations alone would not be sufficient to determine the value of I, but if, in addition, account is taken of the relative intensities of the components it at once becomes evident that the best value is $\frac{1}{2}$, as previously suggested.

# *Interpretation of the Spectra of CaF and SrF.*

By A. **Harvey**, Ph D , B Sc., Commonwealth Fund Fellow, Department of Physics, University of California.

(Communicated by A. Fowler, F R.S —Received June 6, 1931.)

[Plates 13-15 ]

## *Introduction.*

The structure of the band spectra of the diatomic alkaline earth fluorides has been considered in the light of the quantum theory by Mecke,* Jevons,† Johnson,‡ and Jenkins § Because of the closeness of the rotational structure it has proved impossible to obtain sufficient resolution for the application of the combination principle to the individual band lines except for BeF, which molecule has the smallest moment of inertia (Jenkins, *loc. cit.*). With the heavier molecules, assignments of vibrational quantum numbers were made from the positions and intensities of the band heads, and designations of the electronic terms were given, based on the evident similarity of certain band systems in this group of molecules. The $^2\Pi \rightarrow {}^2\Sigma$ system, which lies in the ultra-violet for BeF and MgF, and in the visible for CaF, SrF and BaF, was shown in the case of BeF to possess the expected rotational structure. The system designated $^2\Sigma \rightarrow {}^2\Sigma$ by Johnson‡ is known only in CaF, SrF and BaF, and has a slightly higher frequency than $^2\Pi \rightarrow {}^2\Sigma$.

In the course of a search for isotope effects in the spectra of CaF and SrF I have obtained plates with the 21-foot concave grating showing the two systems mentioned above in both emission and absorption. For the absorption the method of Walters and Barratt|| was used. Although the study of these plates gave evidence of isotopes only in the case of SrF, certain observations on the modifications in structure between emission and absorption are important for the interpretation of the rotational structure of the bands of both molecules, a question which apparently can only be cleared up by indirect evidence of this kind.

---

* 'Z. Physik,' vol. 42, p. 390 (1927).

† 'Proc. Roy. Soc.,' A, vol. 122, p. 211 (1929).

‡ 'Proc. Roy. Soc.,' A, vol 122, pp. 161, 189 (1929).

§ 'Phys. Rev.,' vol. 35, p 315 (1930).

|| 'Proc. Roy. Soc.,' A, vol. 118, p. 120 (1928).

### $^2\Pi \rightarrow {}^2\Sigma$ *Systems.*

The two stronger heads of the (0, 0) band of this system lie at λλ 6037, 6064 for CaF and λλ 6512, 6633 for SrF. These are evidently the $Q_2$ and $Q_{12}$ heads, in the notation of Mulliken.[*] The associated $P_2$ and $P_{12}$ heads are well developed in emission, with intensities indicated by the vertical lines drawn below them in fig. 1. In absorption at 1100° C.–1200° C. the $P_{12}$ heads are entirely absent in the case of CaF (Plate 14, fig. 7, *a*) and are very faint in SrF (Plate 15, fig. 12, *a*) whilst the $P_2$ heads are much weaker in both cases. This is evidently a consequence of the extremely high values of the rotational quantum numbers at which these heads are formed, since in both cases structure lines can be seen extending towards the red from the $Q_{12}$ head and fading out before they reach the position of the $P_{12}$ head. This behaviour is consistent with the type of structure illustrated in fig. 1, which was drawn according to approximate constants obtained for CaF by a method described in the following paragraph. The change in the Boltzmann distribution from the arc to the absorption tube is adequate to account for these modifications if the rotational quantum numbers are as shown.

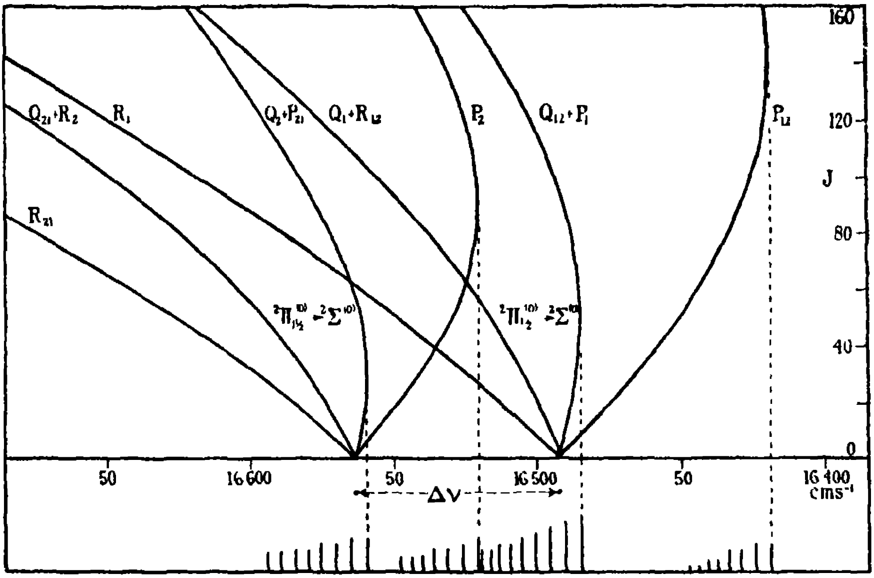

FIG. 1.—Fortrat diagram of $^2\Pi^{(0)} \rightarrow {}^2\Sigma^{(0)}$ CaF band on basis of constants obtained from the analysis; the positions of the heads of the $(v' - v'' = 0)$ sequence are shown on the bottom line.

---

[*] 'Phys. Rev.,' vol. 32, p. 411 (1928).

Qualitatively, it is to be expected that $J_{P\,\mathrm{head}}$ should be great, because of the near equality of the rotational constants in the ${}^2\Pi$ and ${}^2\Sigma$ states. The close spacing of successive bands of the sequences shows that the vibration frequencies are nearly the same in the two states ($\omega' \sim \omega''$), and when this is the case, the moments of inertia also differ only slightly, so that $B' \sim B''$. A more quantitative consideration has been made in the case of CaF by estimating these constants in the following way. Utilising the theoretical term formulæ*

$$ {}^2\Pi : \ F'(J) = B'[J(J+1) - \Omega^2] + D[J(J+1) - \Omega^2]^2 \qquad (1)$$

$$ {}^2\Sigma : \ F''(K) = B'' . K(K+1) + D . K^2(K+1)^2 \qquad (2)$$

expressions for the frequency differences $Q_{12}$ head–$P_{12}$ head and $Q_2$ head–$P_2$ head were derived in terms of $B'$, $B''$, $D$ and the J values of the heads concerned. To obtain the latter a further relation was required For this, the value of $B_1' - B''$ was computed from measurements of the resolved structure in the $Q_{12}$ branch on a second-order arc plate. These fitted closely the formula

$$\nu(M) = 16484 \cdot 92 + 0 \cdot 00334\, M^2, \qquad (3)$$

M being the ordinal number of the line from the head, ranging from 74 to 104. Applying a small correction for the effect of the D term we find $B_1' - B'' = 0 \cdot 00306$. The value of $D(D' \sim D'')$ may be found from the approximate relation $D = 4B^3/\omega^2$, using a preliminary value of B obtained from the equation

$$Q_{12}\ \text{head} - P_{12}\ \text{head} = 2B'B''/B' - B'', \qquad (4)$$

and the value of ω (583 cm.$^{-1}$) obtained by Johnson (*loc. cit.*) from the Q heads. Applying successive approximations, these estimates may be considerably improved. The final results of this calculation of constants for the (0, 0) band of CaF were

| ${}^2\Pi_{\frac12} \rightarrow {}^2\Sigma$. | ${}^2\Pi_{1\frac12} \rightarrow {}^2\Sigma$. |
|---|---|
| $B_1' = 0 \cdot 3246$ cm.$^{-1}$ | $B_2' = 0 \cdot 3268$ cm.$^{-1}$ |
| $B_1' - B'' = 0 \cdot 00306$ cm.$^{-1}$ | $B_2' - B'' = 0 \cdot 00531$ cm.$^{-1}$ |
| $J_{Qh} = 52$ | $J_{Qh} = 29$ |
| $J_{Ph} = 137$ | $J_{Ph} = 86$ |

$$B'' = 0 \cdot 3215 \text{ cm.}^{-1}$$

$$D' = D'' = -0 \cdot 38 \times 10^{-6} \text{ cm.}^{-1}.$$

The origins, $\nu_1^0$ and $\nu_2^0$, of the ${}^2\Pi_{\frac12} \rightarrow {}^2\Sigma$ and ${}^2\Pi_{1\frac12} \rightarrow {}^2\Sigma$ bands are found to be, respectively, 16493·6 and 16565·8 cm.$^{-1}$, giving as the doublet separation in the Π state $\Delta\nu^0 = 72 \cdot 2$ cm.$^{-1}$. This may be compared with the separation of the Q heads, 75·03 cm.$^{-1}$, and of the P heads, 98·06 cm.$^{-1}$. The differences result from the inequality in the distance of the two Q heads from the origins (8·5 and 5·6 cm.$^{-1}$) and of the P heads (69·4 and 43·6 cm.$^{-1}$). The larger distance in each case refers to the ${}^2\Pi_{\frac{1}{2}} \rightarrow {}^2\Sigma$ component, and is a consequence of the requirement that $B_2 \geq B_1$, which invariably holds for case (*a*) doublet states where the difference in B arises from the rotational distortion.*

---

* R. S. Mulliken, 'Rev. Mod. Phys.,' vol. 2, p. 60 (1930).

The estimates of constants may be extended to the other observed sequences, $(v' - v'' = -1)$, by applying the empirical rule†

$$\frac{2x\mathrm{B}^{(0)}}{\alpha} = 1 \cdot 4 \pm 0 \cdot 2 \tag{5}$$

to obtain $\alpha$ in the equation‡ $\mathrm{B}^{(v)} = \mathrm{B}^{(0)} - \alpha v$. One obtains $\alpha_1' = 0 \cdot 0026$, $\alpha_2' = 0 \cdot 0024$, $\alpha'' = 0 \cdot 0020$. These values lead to a ready explanation of the

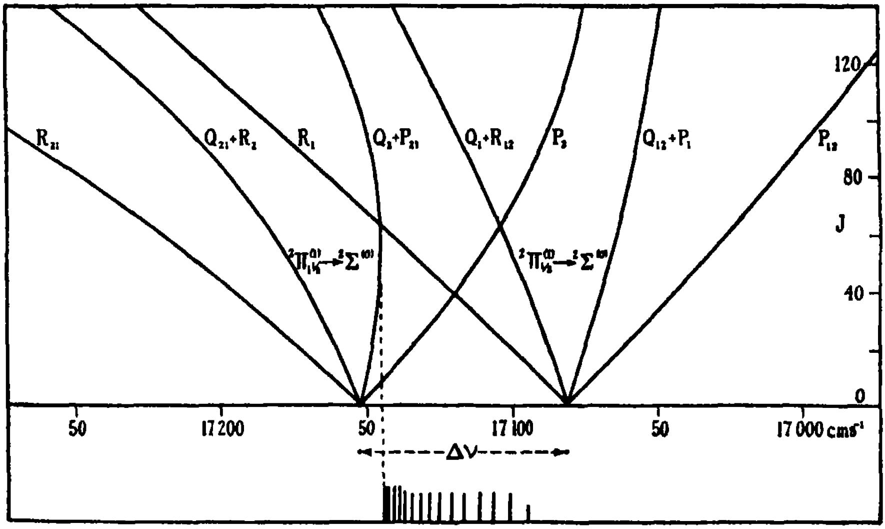

FIG. 2.—Fortrat diagram of ${}^2\Pi^{(1)} \rightarrow {}^2\Sigma^{(0)}$ CaF band based on constants obtained; the positions of the heads of the $(v' - v'' = +1)$ sequence are shown on the bottom line.

---

* R. S. Mulliken, 'Phys. Rev.,' vol. 32, p. 390 (1928).

† This rule was given by R. T. Birge at a meeting of the American Physical Society in Berkeley, 1928. Only an abstract of this paper has appeared—R. T. Birge, 'Phys. Rev.,' vol. 31, p. 919, abstract 30 (1928).

‡ In general $v$ is used as a subscript to B. In this case, however, it is more convenient to use it as a superscript in parentheses to avoid confusion. The use of $v$ as a subscript is not an essential part of the standard notation, and it is more in conformity with the other notation employed here to use the subscripts to differentiate between the two values of B.

remarkable appearance of the ($v' - v'' = +1$) sequence (Plate 14, fig. 9, *b*). This contains only one series of heads, the $Q_2$ heads (see fig. 2), in which the earlier heads are in approximate coincidence. The absence of other series of heads follows from the result that $B_2^{(1)'} - B^{(0)''}$ is very small, and $B_1^{(1)'} - B^{(0)''}$ practically zero, thus requiring the heads to be formed at very high J values. That the ${}^2\Pi_{\frac{1}{2}} \rightarrow {}^2\Sigma$ component is really present, though no heads of any strength are visible, is indicated by a diffuse double maximum with its centre at 17076·6 cm.$^{-1}$, as measured on an emission plate. The microphotometer record of fig. 3 (Plate 13) makes this more apparent, and shows that its integrated intensity is at least as great as that of the ${}^2\Pi_{1\frac{1}{2}} \rightarrow {}^2\Sigma$ component. The modification of this sequence in absorption is significant; the double maximum is still evident, but is shifted slightly to the violet. This is to be expected if the observed maxima are due to the integrated effect of a number of such symmetrical bands approximately superposed. The separation of the central minimum from the calculated origin of the ${}^2\Pi_{1\frac{1}{2}}{}^{(1)} \rightarrow {}^2\Sigma^{(0)}$ is 78·5 cm.$^{-1}$, and this is slightly greater than the value $\Delta\nu^0 = 72{\cdot}2$ cm.$^{-1}$ already obtained. But this is to be expected, since the effect of bands with higher $v$ would be to shift the minimum towards the red.

A new set of heads shaded in the opposite direction (*i.e.*, to the red) was observed on a very heavily exposed arc plate† (Plate 14, fig. 9, *a*). The wave-numbers are listed in Table I. They may be interpreted as the $Q_1$ heads of

Table I.—New CaF Heads of the ${}^2\Pi_{1\frac{1}{2}}{}^{(v+1)} \rightarrow {}^2\Sigma^{(v)}$ Sequence.

| Intensity. | Wave-length (I.A.) air. | $\nu$ (cm $^{-1}$) vac. |
|---|---|---|
| 1 | 5866·88 | 17040·12 |
| 2 | 69·93 | 031·27 |
| 1 | 72·86 | 022·77 |
| 2 | 76·03 | 013·59 |
| 2 | 79·17 | 004·50 |
| 2 | 82·38 | 16995·22 |
| 1 | 85·61 | 985·89 |
| — | — | —* |
| 0 | 92·37 | 966·41 |
| — | — | —* |
| 0— | 99·46 | 946·02 |
| 0— | 5903·16 | 935·40 |

* Masked by D-lines.

---

† This was one of a number of plates kindly lent for the purpose of this investigation by Dr. A. S. King, of the Mount Wilson Observatory.

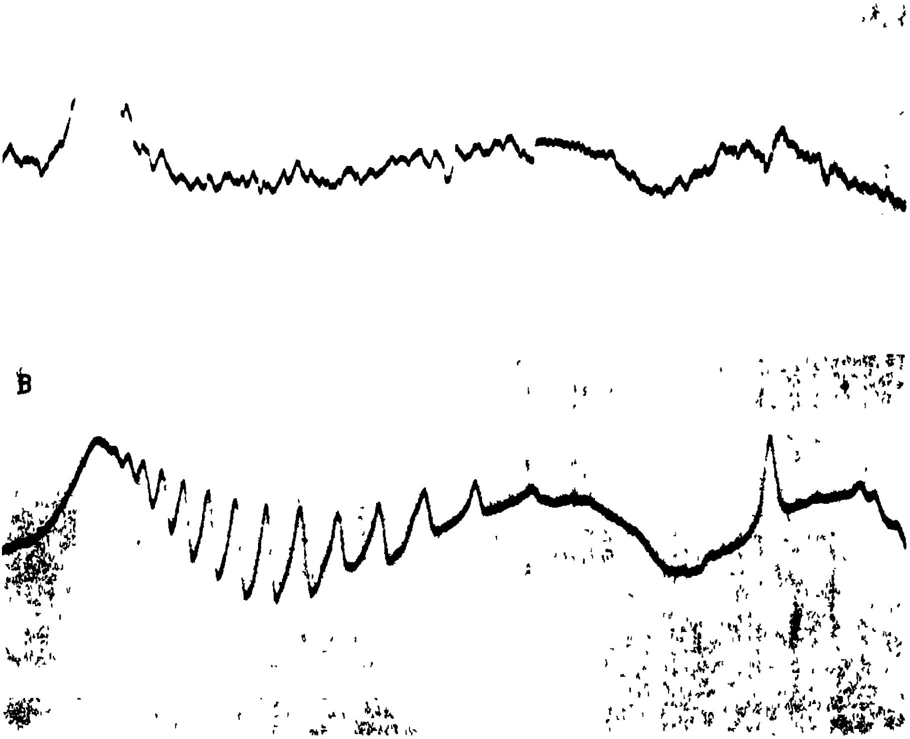

FIG 3 —Microphotometric traces of the $^2\Pi^{(a)} \rightarrow {}^2\Sigma^{(a)}$ sequence of CaF (A) In absorption. (B) In emission

bands with very high $v$. That they are shaded to the red follows from the reversal of sign of $B_1^{(v+1)'} - B^{(v)''}$ which probably takes place for high values of $v$. Similarly, the sudden breaking off of the sequence of $Q_2$ heads after that at λ 5846 does not require any assumption as to dissociation of the molecule, as made by Johnson (*loc. cit.*), but is a natural consequence of the fact that the heads are formed at higher and higher values of J as we proceed down the sequence, combined with the normal fall of intensity with increasing $v$.

The $(v' - v'' = -1)$ sequence behaves normally in absorption; the heads are formed at lower values of J than in the main sequence. The Q heads in this case are well separated, and measurements of their relative intensities in emission and absorption were made with the microphotometer.. The results are given in Table II, using as a measure of the intensity the electrometer deflection when the head passes the microphotometer slit. As a result of the lower temperature in absorption a definite shift of intensity towards lower $v$'s is observed. The same effect is easily seen visually in the reproductions of the other two sequences.

Table II.—Microphotometer Deflections for Q Heads of $^2\Pi^{(v)} \rightarrow {}^2\Sigma^{(v+1)}$ Sequence.

| Band. | (0, 1). | (1, 2). | (2, 3). | (3, 4). | (4, 5). | (5, 6). | (6, 7). | (7, 8). | (8, 9). |
|---|---|---|---|---|---|---|---|---|---|
| $Q_{12}$ head | λ6285·3 | λ6280·9 | λ6276·5 | λ6272·4 | λ6268·4 | λ6264·5 | λ6260·9 | λ6257·4 | λ6254·1 |
| Emission deflection | 3·0 | 7·2 | 10·4 | 9·7 | 9·5 | 9·0 | 8·0 | 8·1 | 7·2 |
| Absorption deflection | 2·5 | 3·5 | 3·1 | 2·6 | 2·2 | 0·8 | — | — | — |
| $Q_2$ head | λ6256·6 | λ6252·2 | λ6247·8 | λ6243·7 | λ6239·8 | λ6236·0 | λ6232·3 | λ6228·9 | λ6225·7 |
| Emission deflection | 3·2 | 4·5 | 6·6 | 4·8 | 5·2 | 4·8 | 3·8 | 3·5 | 3·3 |
| Absorption deflection | 2·1 | 2·6 | 1·8 | 2·1 | 1·4 | 0·9 | — | — | — |

The large, and variable, distance from heads to origins—even for Q branches—indicated above, vitiate any attempt to apply the combination principle to measurements of the heads for determining the vibrational term differences, and renders very inexact any constants obtained therefrom. The assignments of $v$ made by Johnson were chosen to make the discrepancies a minimum, but this method is not trustworthy in the present instance, and it seems best to base assignments of $v$ on the intensity relations alone. Since the first few $Q_2$ heads of the $(v' - v'' = +1)$ sequence are superposed, the value of $v$ must remain uncertain to one or two units. In the $(v' - v'' = -1)$ sequence the first $P_{12}$ head was overlooked by Johnson, but appears clearly at λ 6301·10, $\nu = 15865 \cdot 97$ on one of my heavily exposed arc plates (Plate 15, fig. 10). It is definitely the first head of this sequence and hence belongs to the (0, 1) band. The assignment given by Johnson for these heads should be lowered by two units. The best values of the vibrational constants, in default of a complete correction of all heads to origins, are evidently obtained by combining the $Q_2$ heads in the $(v' - v'' = 0)$ and $(v' - v'' = -1)$ sequences, since the corrections involved here are the smallest.

The $^2\Pi \rightarrow {}^2\Sigma$ system of SrF (Plate 15, fig. 12) is somewhat more regular in its behaviour ; apparently the constants B′ and B″ are not so nearly equal in this case. No attempt has been made to estimate the rotational constants as was done for CaF, since the structure is finer and a sufficiently accurate determination of $B' - B''$ did not seem feasible. The separation of the $^2\Pi$ level is greater than for CaF, being approximately 277 cm.$^{-1}$, correcting the $Q_2 - Q_{12}$ separation of 279·2 cm.$^{-1}$ by the same proportion as in CaF. In the $(v' - v''=0)$ sequence both sets of P heads appear in absorption, though $P_{12}$ is very faint and is seen only in the case of the (0, 0) band. The $(v' - v'' = +1)$ sequence, in contrast to CaF, proceeds to the violet ; in emission the Q heads are present for both components, the $P_2$ heads are faint whilst the $P_{12}$ heads are not formed. In absorption the P heads were not detected, but two or three of the earlier members of both Q sequences are visible. The $(v' - v'' = -1)$ sequence showed only the $Q_2$ heads in absorption, and by analogy with CaF this is to be expected because of the low J value of the head. The other heads would probably be observed if a higher density of the absorbing vapour were used, since this sequence is weak as a whole.

### $^2\Sigma \rightarrow {}^2\Sigma$ *Systems.*

The bands of this system have double heads and are shaded to the red, the (0, 0) heads falling at λλ 5293, 5291 for CaF and λλ 5779, 5772 for SrF. Only two sequences of heads occur in each case, these being the $(v' - v'' = 0)$ and $(v' - v'' = +1)$ sequences. The presence of double heads of wide separation in a $^2\Sigma \rightarrow {}^2\Sigma$ system is unusual, and the components are attributed by Johnson (*loc. cit.*) to R and Q branches. It is well known, however, that in bands having $\Lambda' = \Lambda'' = 0$ the Q branch is very weak, if present at all.* That the doubling is of a type which increases in magnitude with increasing J is definitely shown by the fact that in the $(v' - v'' = +1)$ sequence the doublet separation of the heads is smaller than in the $(v' - v'' = 0)$ sequence, whilst at the same time the heads must be formed at lower J's (since $B^{(1)'} < B^{(0)'} < B^{(0)''}$). It is therefore not analogous to the doubling in BeF, where just the opposite behaviour is found.* The only possibility of doubling in the branches of $^2\Sigma \rightarrow {}^2\Sigma$ bands is the separation of the component levels $J = k \pm 1/2$, known as " ρ-type " doubling. Doubling of heads due to this cause is known, and in certain cases (such as HgH), the separation of the rotational levels may reach a considerable magnitude. We may note here that in the two cases under discussion this doubling must be confined chiefly to the upper state, since no evidence for a doubling of the heads was found in the $^2\Pi \rightarrow {}^2\Sigma$ systems.

---

* R. S. Mulliken, 'Phys. Rev.,' vol. 30, p. 138 (1927).

A very remarkable feature of this system is its appearance in absorption, as first shown by Walters and Barratt (*loc. cit.*). The whole appearance of the ($v' - v'' = 0$) sequence is altered, the clear succession of double heads being replaced by a broad region of fine-line absorption, with occasional accumulations of intensity apparently bearing no evident relation to the heads in emission. Seen under high dispersion, however, the absorption spectrum shows a definite correlation with the emission spectrum. In fact, over the region λλ 5310 to 5330 in CaF, there is an emission line in exact coincidence with every absorption line, and a similar effect occurs in SrF. An examination of the spacing of the rotational structure of this sequence in emission shows that most of the strong lines must belong to the (0, 0) band, which is therefore considerably stronger than the succeeding ones. The small decrement in intensity of the heads in passing down the sequence is probably due to two factors—first, to a spurious enhancement by overlying structure from the preceding bands, and second, to the fact that the value of J head decreases with increasing $v$. The latter is evidenced by the decreasing doublet separation. We would expect the predominance of the (0, 0) band to be even greater in absorption, an effect which has already been noted in the $^2\Pi \rightarrow {}^2\Sigma$ system.

Other points of resemblance between the absorption and emission are: (1) the first pair of heads, belonging to the (0, 0) band, appear very faintly in absorption with CaF. With SrF only the second (low-frequency) component of the first pair is observed, and the same component of the second and third pairs is also faintly visible (Plate 15, fig. 13, *b*). (2) A pronounced minimum which occurs in the arc spectrum near the (3, 3) heads with a centre at λ 5308 for CaF, and at λ 5792 for SrF, becomes a very prominent feature of the absorption spectrum. In view of the fact that practically all of the intensity in absorption should be concentrated into the (0, 0) band, and that only P and R branches are expected, the simplest explanation of this minimum is that it represents the approximate position of the origin of the (0, 0) band. This would place the origin of this band 60·7 and 53·8 cm.$^{-1}$ from the two R heads in the case of CaF, and 59·1 and 36·7 cm.$^{-1}$ in SrF. These large separations of heads from origin are not unreasonable in view of the near equality of rotational constants in the upper and lower states; that the vibrational constants differ only slightly is again attested by the crowding of the bands into close sequences. Furthermore, the suppression of most of the heads in absorption is evidence for the formation of heads at very high rotational quantum numbers. An important piece of evidence for the double heads *both* being formed at high J's is found in the fact that for CaF the components of the (0, 0) double head as seen in absorption, though faint, are still of almost equal intensity. If, as Johnson suggests, the second component were formed by a Q branch, this behaviour could not be explained, for the Q head should be greatly enhanced relative to the R at the lower temperature. As mentioned above, an effect of this sort does appear in SrF, but here the ρ-type doubling has become so large that the two R heads must turn at considerably different values of J.

---

* W. Jevons, *loc. cit.*

Satisfactory confirmation of this interpretation of the structure is obtained by actual measurement of certain groups of fine lines which are clearly resolved on the absorption spectrograms of CaF. These groups are regularly spaced on either side of the origin, the spacing of the lines in each group, and of the groups themselves, increasing toward the red. Their probable origin is the

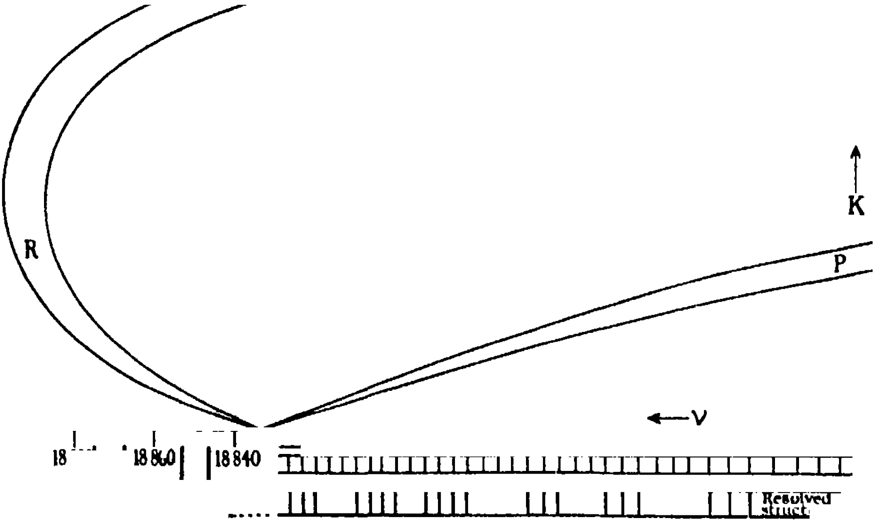

FIG. 4.—Diagrammatic representation of the ${}^2\Sigma^{(0)} \rightarrow {}^2\Sigma^{(0)}$ CaF band. On the left side of the bottom line are plotted the heads of the earlier members of the ($v' - v'' = 0$) sequence—this illustrates the appearance in emission. On the right is indicated the manner in which the two P branches of the (0, 0) band form groups of fine structure lines—this is typical of the appearance in absorption.

periodic coincidence and non-coincidence of the two series of lines with slightly different spacing which make up the two P and the two R branches, *i.e.*, the components of the ρ-type doublets (see fig. 4). Only the groups formed by the P branches were well resolved, and the measurements of these are given in Table III. In fig. 5 is plotted the mean separation in each group against

Table III.—${}^2\Sigma^{(o)} \rightarrow {}^2\Sigma^{(o)}$ P-branch Fine Structure Absorption Groups.

| Centre of group. | Number of lines observed. | Mean separation. |
|---|---|---|
| cm.$^{-1}$. | | cm.$^{-1}$. |
| 18831·9 | 4 | 0·67 |
| 821·9 | 8 | 0·71 |
| 809·5 | 13 | 0·75 |
| 795·2 | 17 | 0·79 |
| 778·2 | 12 | 0·84 |
| 760·9 | 8 | 0·88 |

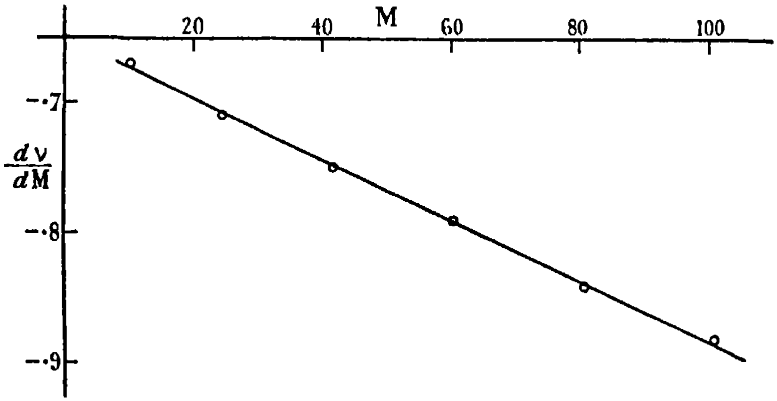

Fig. 5.—Plot of $d\nu/dM$ against M for the P branches of the ${}^2\Sigma^{(0)} \rightarrow {}^2\Sigma^{(0)}$ CaF band.

integral numbers M assigned in such a way that the frequencies of the lines in all the groups are a smooth function of M. (M thus represents the approximate rotational quantum number, apart from an unknown additive constant.)

By extrapolation of the spacing of these lines to the origin it is possible to determine the spacing at that particular point. However, owing to the uncertainty in M we plot the spacings against their frequencies and extrapolate to the known position of the origin, finding the spacing there to be 0·66 cm.$^{-1}$. This is in agreement with the expected spacing at the origin, which should be B′ + B″. We have found, from the less refrangible system, that for the lower

$^2\Sigma$ state $B'' = 0{\cdot}3215$. Furthermore, $B' - B''$ can be found from fig. 5; it is half the slope of the line (assumed straight) and amounts to $-0{\cdot}0012$. Hence $B' + B'' = 0{\cdot}64$ cm.$^{-1}$, and, the measured value being $0{\cdot}66$ cm.$^{-1}$, we thus have good support for our assignment of the position of the origin. Fine structure groups are also apparent in the corresponding SrF sequence in absorption (Plate 15, fig. 13, *b*). These are much more closely spaced, however, and contain fewer lines in each. This is to be expected, since the "beat frequency" should be greater, corresponding to the greater $\rho$-type doubling.

On the best second order CaF arc plate, 14 lines forming a regular series were resolved between the two R heads of the (0, 0) band. These fitted closely the formula

$$\nu(M) = 18894{\cdot}73 - 0{\cdot}00394\, M^2, \qquad (6)$$

where M represents the ordinal number of the line, counting from the head That the coefficient of the quadratic term is considerably larger than the value of $2(B' - B'')$ found above from the P branches is not surprising, because these heads must be formed at extremely high J values (probably over 100), and the effect of the higher power terms will have become large. The deviation is in the proper direction if the cubic term containing the coefficient D, which is invariably negative, were alone responsible.

It is rather surprising, as remarked by Johnson, to find only one of the side sequences $(v' - v'' = +1)$ represented by heads, the $(v' - v'' = -1)$ sequence being apparently absent. This dissymmetry in the vibrational intensity distribution, however, is not real, because the region in which the $(v' - v'' = -1)$ sequence is expected shows heavy structure on the emission plates at least equalling in intensity that of the $(v' - v'' = +1)$ sequence—although no heads are formed. The latter effect is really to be expected, since we have $B^{(0)'} < B^{(0)''}$, while $B^{(1)''} < B^{(0)''}$. Hence the value of $B^{(0)'} - B^{(1)''}$ must be small, all the values of $\alpha$ found earlier being of the same order of magnitude as the difference $B^{(0)''} - B^{(0)'}$.

With regard to the assignment of vibrational quantum numbers, we must again rely on intensity relations alone, in view of the large and variable contribution of the rotational energy change to the frequency of a band head. In SrF the allocation of $v$ is straightforward—both the sequences $(v' - v'' = +1)$ and $(v' - v'' = 0)$ begin abruptly with the (1, 0) and (0, 0) heads respectively. In CaF, however, the designation by Johnson of the first band in the $(v' - v'' = +1)$ sequence as (2, 1) certainly requires revision. On a very heavy exposure (Plate 15, fig. 11) it is clear that this band is the first member of the sequence and hence should be denoted (1, 0). Although this makes the correspondence of the vibrational differences for the lower state with those derived from the Q heads of the $^2\Pi \rightarrow {}^2\Sigma$ system less exact, the deviation is, in the correct sense, being caused primarily by the smaller separation ν head–ν origin in the $^2\Sigma^{(v+1)} \rightarrow {}^2\Sigma^{(v)}$ sequence as compared with $^2\Sigma^{(v)} \rightarrow {}^2\Sigma^{(v)}$.

From the value of $B^{(0)''}$ already obtained, and the relation $B = h/8\pi^2 Ic$, we find the moment of inertia of CaF to be $86 \times 10^{-40}$ g. cm.$^2$, and the internuclear distance $r_0 = \sqrt{I_0/\mu}$ to be $2 \cdot 0 \times 10^{-8}$ cm. That no large error has been committed in determining these constants is proved by the application of an empirical rule, according to which the product

$$\omega r^3 = 3000 \text{ cm.}^{-1} \text{Å}^3 \tag{8}$$

for molecules in which the nuclei are nearly equal in mass, and somewhat greater for those in which the masses are unequal. An extreme case is that of the hydrides, where the product may be as high as 6000* In the present case $\omega r^3 = 573 \times 2^3 \cong 4600$, a very reasonable result. This rule can be applied to show definitely that Johnson's interpretation of the double heads in the green CaF system as R and Q heads is untenable. Were the heads R and Q type then a fairly reliable value of B should be obtained by using the equation

$$\nu_{\text{R head}} - \nu^\circ = \overline{B}^2/B' - B'', \tag{9}$$

in which $B' - B''$ can be taken as $- 0 \cdot 0039$ (from equation (6)), and $\nu^\circ$. should be very closely the frequency of the Q head. For the (0, 0) band we have

$$- 6 \cdot 55 = \overline{B}^2/- 0 \cdot 0039 \quad \text{or} \quad \overline{B} = 0 \cdot 16.$$

This leads to $r_0 = 2 \cdot 8 \times 10^{-8}$ cm, and $\omega r^3 = 12600$—an impossibly high value. We may take this as effectively disposing of the possibility that the second heads are Q heads.

### *Isotope Effects.*

Calcium has isotopes of mass-number 40 and 44, of which $Ca^{44}$ comprises $2 \cdot 7$ per cent. of the whole, as calculated from the atomic weight $40 \cdot 07$ with allowance for the packing fraction and for the existence of the oxygen isotopes $O^{17}$ and $O^{18}$.† The small abundance of the $Ca^{44}F$ molecule would not prohibit its detection in the band spectrum, since recently isotopes present to the extent of less than 0·1 per cent. have been detected by this method.* Unfortunately, however, a computation of the positions where the $Ca^{44}F$ heads should lie shows that in all cases they would fall in such places as to be completely masked by the band structure due to the stronger system of $Ca^{40}F$. Verification of the isotope effect in calcium will probably be more successful in the spectrum of some other molecule than the fluoride.

---

* R. S. Mulliken, 'Rev. Mod. Phys.,' vol. 2, p. 81 (1930).

† S. M. Naudé, 'Phys. Rev.,' vol. 36, p. 333 (1930).

In the SrF bands the situation is more favourable. Here, again, two isotopes are known, $Sr^{88}$ and $Sr^{86}$, of which $Sr^{86}$ has an abundance of 14·5 per cent Because of the small difference from unity of the isotope coefficient, $\rho = \sqrt{\mu_1/\mu_2} = 1{\cdot}00207$, the detection of the isotope heads in the sequences $v' - v'' = 0$ is not possible. In the sequences ${}^2\Pi^{(v)} \rightarrow {}^2\Sigma^{(v+1)}$ and ${}^2\Sigma^{(v+1)} \rightarrow {}^2\Sigma^{(v)}$ the separations, as calculated from the simplified relation†

$$\nu_i - \nu = (\rho - 1)\nu_v \tag{10}$$

should be of the order of 1 cm.$^{-1}$, and we would thus expect the weaker $Sr^{86}F$ heads to be resolved. In the first case four weak companion heads were identified on the arc plates accompanying the first four $Q_2$ heads, and having the proper separation. It is to be remarked, however, that these isotope heads have an unexpectedly great relative intensity, having regard to the calculated abundance, and that no companions could be detected for the corresponding $Q_{12}$ heads. Hence no insistence is made that this effect is real here, although no alternative explanation of the extra heads is obvious.

In the ${}^2\Sigma^{(v+1)} \rightarrow {}^2\Sigma^{(v)}$ sequence of SrF the isotope effect is clearly marked (Plate 15, fig. 14). The heads of this sequence, with the exception of the first, are very close doublets, with a separation increasing towards the red. This is due to a somewhat fortuitous coincidence—the second R head of one band is nearly superposed on the first R head of the following band in the sequence. The coincidence is exact for the first two bands. In addition to these heads of the main band system of $Sr^{88}F$, there is present to the violet of each a corresponding faint head, which can be measured accurately and agrees exactly in position with that expected for $Sr^{86}F$. Only six heads could be measured, but the isotope heads are visible well beyond the (7, 6) band, although somewhat masked by the fine structure from the preceding bands. The isotope heads of the less refrangible component were not detected, but this was due to their being masked by the more refrangible heads. In Table IV the measured shifts in cm.$^{-1}$ are compared with those calculated by equation (10), using 17257 cm.$^{-1}$ for the system-origin in computing $\nu_v$. The isotope heads are indicated by dots in the enlargement (Plate 15, fig. 14). Finally, the plates show that no isotopes lighter than 86 can be present with an abundance of more than about 1/5 of Sr$^{86}$ itself.

---

* H. D. Babcock, 'Proc. Nat. Acad. Sci.,' vol. 15, p. 471 (1929), estimates the abundance of $O^{16}/O^{18}$ to be 1250 : 1. The $O^{17}$ isotope is still less abundant than the $O^{18}$ isotope.

† F. W. Loomis, chap. V of "National Research Council Report on Molecular Spectra in Gases."

Table IV.—Sr$^{86}$F Heads. $^2\Sigma^{(v+1)} \rightarrow {^2\Sigma^{(v)}}$ Sequence of SrF.

| $(v', v'')$. | Sr$^{88}$F. | Sr$^{86}$F. | Observed shift | Calculated shift, cm$^{-1}$. |
|---|---|---|---|---|
| (1, 0) | 17783 07 | — | | 1 09 |
| (2, 1) | 771 28 | 17772 32 | 1 04 | 1 06 |
| (3, 2) | 759 56 | 760 48 | 0 92 | 1·04 |
| (4, 3) | 747 83 | 748·69 | 0 86 | 1 02 |
| (5, 4) | 735 97 | 736 91 | 0 94 | 0 99 |
| (6, 5) | 724 05 | 725 05 | 1 00 | 0 97 |
| (7, 6) | 712 02 | 712 93 | 0 91 | 0·94 |

It gives me great pleasure to record my gratitude for the generous assistance of Professor F. A. Jenkins at every stage of this investigation. I have also to thank the Commonwealth Fund for the Fellowship which rendered possible this work.

## *Summary.*

(1) The designations $^2\Sigma \rightarrow {^2\Sigma}$ and $^2\Pi \rightarrow {^2\Sigma}$ for the more, and less, refrangible band systems of CaF and SrF are supported by a comparison of the spectra in absorption and emission under high dispersion.

(2) The different appearance of the bands in absorption and in the arc is shown in all cases to be a natural consequence of the difference in temperature, the main effects of lowering the temperature being (*a*) to shift the intensity toward lower vibrational quantum numbers in each sequence, (*b*) to lower the value of the rotational quantum number at which the intensity reaches a maximum in a given branch.

(3) Approximate values of the rotational constants of CaF are estimated by combining measurements of the fine structure with theoretical equations for the separations of the heads. For the lower $^2\Sigma$ state

$$I_0'' = 86 \times 10^{-40} \text{ g. cm.}^2, \; r_0'' = 2\cdot0 \times 10^{-8} \text{ cm.}$$

(4) A re-interpretation of the heads in the $^2\Sigma \rightarrow {^2\Sigma}$ bands is proposed, in which the double heads are ascribed to two R branches resulting from a large $\rho$-type doubling.

(5) Discrepancies previously found in the vibrational constants, as well as the apparent absence of certain sequences, are shown to be consequences of the extremely large value of the rotational quantum number at which most of the heads are formed. Alterations in the previous assignment of vibrational quantum numbers in the sequences $^2\Pi^{(v)} \rightarrow {}^2\Sigma^{(v+1)}$ and $^2\Sigma^{(v+1)} \rightarrow {}^2\Sigma^{(v)}$ are made.

(6) The isotope effect for $Sr^{88}$, $Sr^{86}$ is found in the $^2\Sigma^{(v+1)} \rightarrow {}^2\Sigma^{(v)}$ sequence of the SrF bands.

## DESCRIPTION OF PLATES 14, 15.

FIG. 6.—Self-reversal of the CaF $^2\Pi^{(v)} \rightarrow {}^2\Sigma^{(v)}$ sequence.

FIG. 7.—CaF $^2\Pi^{(v)} \rightarrow {}^2\Sigma^{(v)}$ sequence, (*a*) in absorption, (*b*) in emission.

FIG. 8.—Light exposure of the CaF $^2\Pi^{(v)} \rightarrow {}^2\Sigma^{(v)}$ sequence in emission

FIG. 9.—CaF $^2\Pi^{(v+1)} \rightarrow {}^2\Sigma^{(v)}$ sequence, (*a*) very heavy exposure showing new heads degraded to red, (*b*) normal exposure of the "tail" sequence.

FIG. 10.—$P_{12}$ heads of the CaF $^2\Pi^{(v)} \rightarrow {}^2\Sigma^{(v+1)}$ sequence in emission.

FIG. 11.—First members of the CaF $^2\Sigma^{(v+1)} \rightarrow {}^2\Sigma^{(v)}$ sequence in emission.

FIG. 12.—SrF $^2\Pi^{(v)} \rightarrow {}^2\Sigma^{(v)}$ sequence, (*a*) in absorption, (*b*) in emission.

FIG. 13.—SrF $^2\Sigma^{(v)} \rightarrow {}^2\Sigma^{(v)}$ sequence, (*a*) in emission, (*b*) in absorption.

FIG. 14.—SrF $^2\Sigma^{(v+1)} \rightarrow {}^2\Sigma^{(v)}$ sequence in emission.

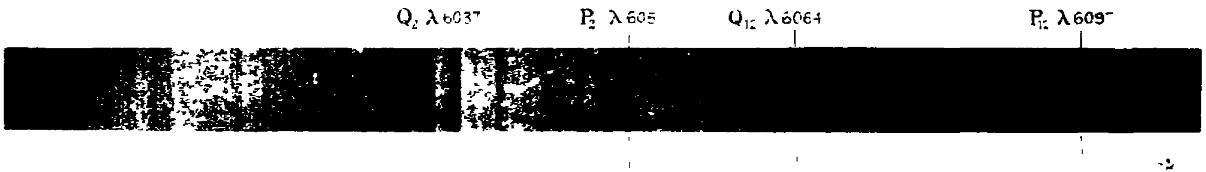

FIG. 6

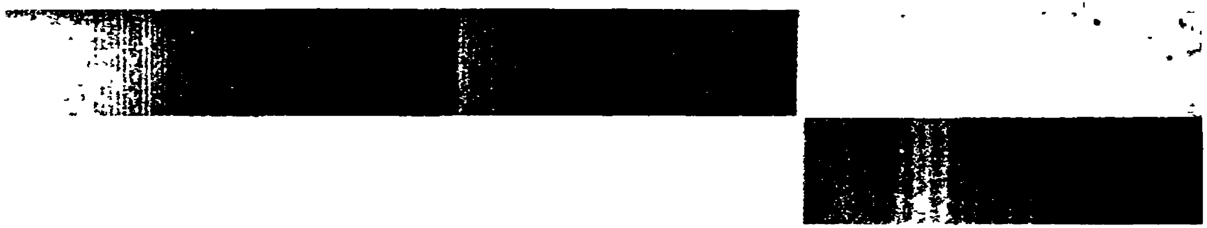

FIG. 7

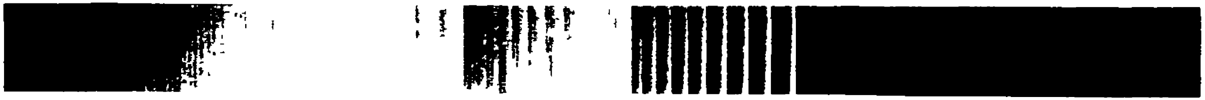

FIG. 8

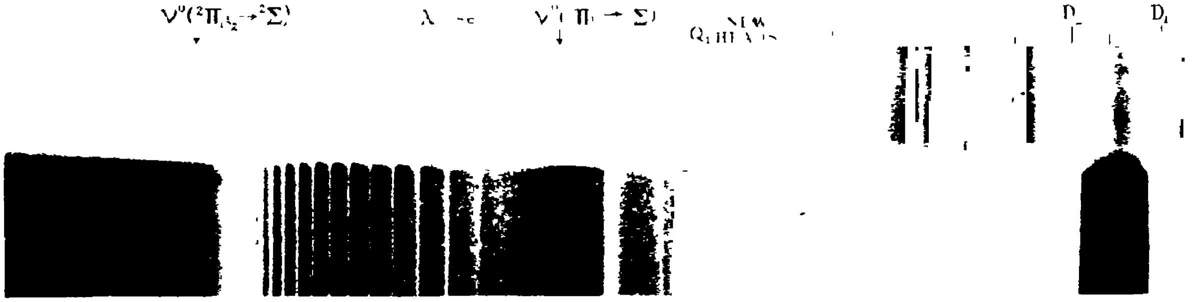

FIG. 9

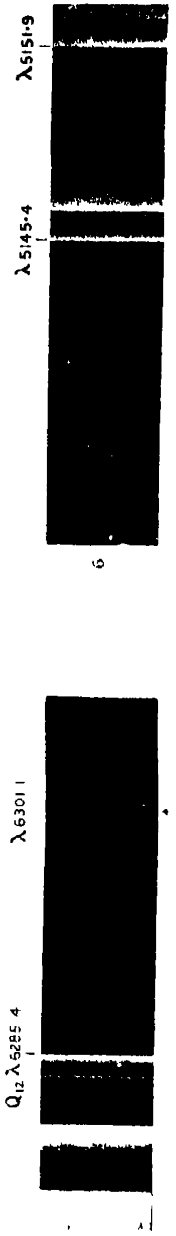

FIG 10

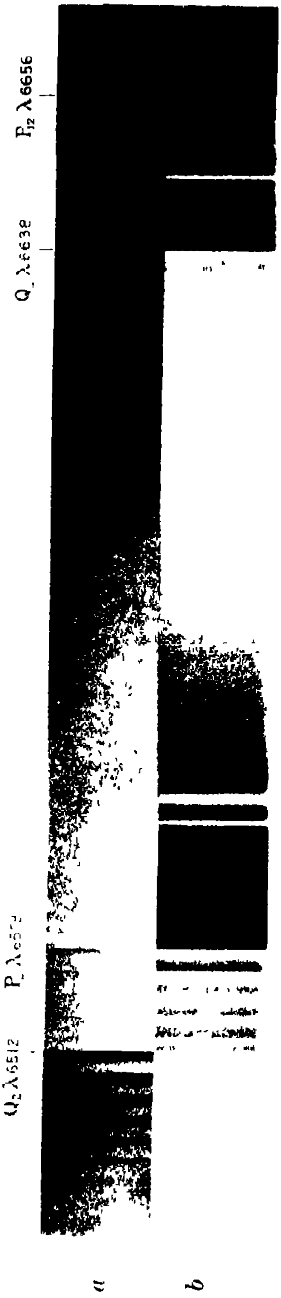

FIG 11

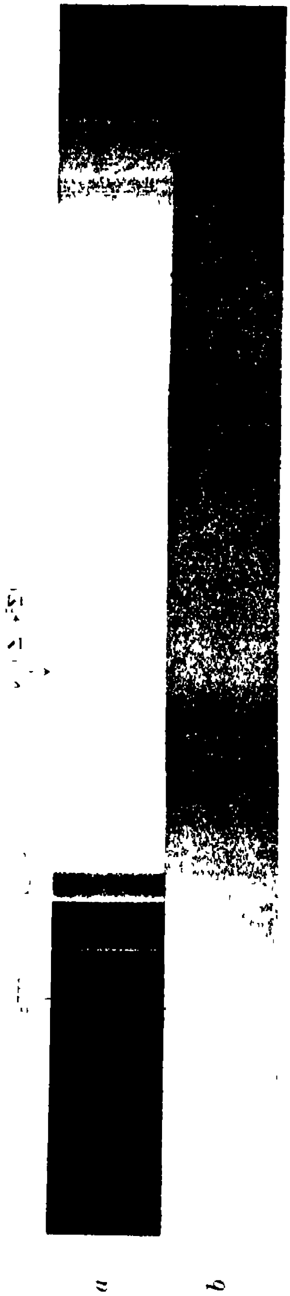

FIG 12

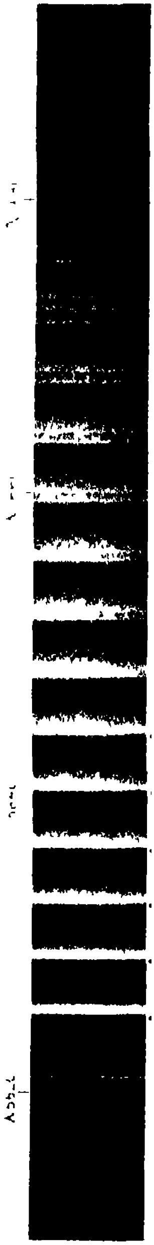

FIG 13

# *Analysis of the α-Particles Emitted from Thorium C and Actinium C.*

By Lord RUTHERFORD, O.M., F.R.S., C. E. WYNN-WILLIAMS, Ph.D., Exhibition of 1851 Senior Student, and W. B. LEWIS, B.A.

(Received August 5, 1931.)

In a recent paper,* an account has been given of the analysis of the long range α-particles emitted by radium C. Nine distinct groups of α-particles were detected varying in range between 7·8 and 11·6 cm. in air. Evidence was given that the emission of γ-rays from radium C is intimately connected with the occurrence of these groups of long range α-particles, and it was concluded that the γ-rays arise from the transition of an α-particle in an excited nucleus between two levels of different energies. This question has been discussed in more detail by Rutherford and Ellis,† who have advanced a tentative theory to account for the relation between the energies of the γ-rays emitted from radium C.

In the present paper we give the results of a corresponding analysis of the long range α-particles from thorium C and an analysis of the groups of α-particles emitted from actinium C. In these experiments the differential method of analysis was used, as in the experiments with radium C. In the present experiments, however, instead of recording the α-particles photographically on a moving film, we have mainly employed the automatic method of counting, using thyratrons in place of the oscillograph. This method, which has been developed by one of us (C. E. Wynn-Williams), has been fully discussed in a recent paper.‡ Here it suffices merely to refer to one or two points of special interest in connection with the present research.

The thyratron circuits were used in place of the oscillograph employed in the radium C experiments. Amplified potential surges from the valve amplifier (caused by the entry of particles into the differential ionisation chamber) were applied to a "thyratron ring" of four thyratrons.§ By this means two particles entering the chamber within even one five-hundredth of a second could be separately registered, the final number counted being directly recorded on a mechanical dial indicator. It can be shown that with this "resolution" of 1/500th second the probable number of particles missed by the counter (owing to the random arrival of the particles) is 1·3 per cent. at a counting speed of 400 particles per minute, and 2·6 per cent. at a speed of 800 per minute. In our experiments, counting speeds of 400 particles per minute were seldom exceeded.

---

* Rutherford, Ward and Lewis, 'Proc. Roy. Soc.,' A, vol. 131, p. 684 (1931).

† Rutherford and Ellis, 'Proc. Roy. Soc.,' A, vol. 132, p. 667 (1931).

‡ Wynn-Williams, 'Proc. Roy. Soc.,' A, vol. 132, p. 295 (1931).

§ See fig. 4, 'Proc. Roy. Soc.,' A, vol. 132, p. 302 (1931).

In interpreting the photographic records of the radium C experiment, it was necessary, for reasons already given, to count only deflections of magnitudes lying between an upper and lower limit. In the automatic counting circuit, the lower counting limit was defined by a negatively biased diode rectifier which preceded the thyratron ring; the upper limit was defined by a second single thyratron counter associated with a more heavily biased rectifier, working simultaneously with the first, which indicated the number of particles to be " rejected." The counting limits were measured electrically by the application of artificial potential surges of known magnitudes, so that it was possible to adjust the automatic recorder to count on the same basis as that normally used in analysing the photographic records of α-particles.

The sources employed in the present work were relatively weak, and there was no serious disturbance due to the γ-rays. The automatic counter worked excellently, and made the work of analysis much easier and quicker. It was possible to plot the resulting distribution curve while the experiment was in progress, and doubtful points could be re-examined at once.

### *Long Range α-particles from Thorium C.*

In 1916, Rutherford and Wood,* using the scintillation method, observed that the active deposit of thorium (thorium B + C) emitted a few α-particles of long range about 11·3 cm. in air. The number was about 1 in $10^4$ of the main group of α-particles of range 8·6 cm. From observations of the absorption of the α-particles, they concluded that the group of α-particles was complex. This was confirmed by the experiments of Meitner and Freitag† by observation of the length of the α-ray tracks in an expansion chamber, and by Philipp‡ by the scintillation method. Two distinct groups of α-particles were found, of ranges about 9·5 cm. and 11·5 cm. in air. The ratio of the numbers of α-particles in the two was found to be about 1 to 3, the longer range being more numerous.

---

* Rutherford and Wood, 'Phil. Mag.,' vol. 31, p. 379 (1916).

† Meitner and Freitag, 'Z. Physik,' vol. 37, p. 481 (1926).

‡ Philipp, 'Z. Physik,' vol. 37, p. 518 (1926).

In 1929 Nimmo and Feather* re-examined the question, using the expansion chamber method. The tracks of 550 long range α-particles were photographed, the active deposit of thorium being used as a source. They concluded that two distinct groups of α-particles were present, of mean ranges 9·82 cm. and 11·62 cm. corresponding to extrapolated ranges of 9·90 cm. and 11·70 cm. in air under standard conditions. The α-particles in the longer range group were found to be about five times as numerous as in the group of shorter range. A few tracks were observed of range greater than 13 cm , but, as we shall see later, it is clear that these must have been due to protons liberated by the main α-rays.

The method of analysis of the long range α-particles was similar to that used in the experiments with radium C. The active deposit of thorium obtained by exposure to the emanation of thorium was used as a source. The activity in the various experiments was equivalent to from 1 to 10 milligrammes of radium when measured by the γ-rays through a thickness of 6 mm. of lead Discs of nickel, or of non-magnetic stainless steel, were used as collectors. When strong sources were used, there was sometimes a slight tarnish of the metal disc, which slightly reduced the measured range of the α-particles, but with the best sources the tarnish was only just perceptible on close examination. As in the radium C experiments, the active matter was removed from the edges of the disc.

The results of the analysis are shown in fig. 1, where the ordinates† represent the number of α-particles per milligramme per minute counted for different ranges in air. It is seen that, in confirmation of other observers, two distinct groups of α-particles are present. The shape of the straggling curves was carefully determined to test the homogeneity of the α-rays in each group. Making allowance for the straggling of the rays for the two groups, the shape of the curves agreed very closely with that to be expected for a homogeneous group of α-particles. In illustration of the accuracy of the observations, the curve obtained for the longer range group of mean range 11·55 cm. is shown

---

* Nimmo and Feather, 'Proc. Roy. Soc.,' A, vol. 122, p. 668 (1929).

† The scale of ordinates used for the thorium curves is such that using a source of radium C of one milligramme equivalent, measured through 6 mm. of lead, the number of particles per minute in the main 7 cm. group of α-particles would be $10^6$. Shenstone and Schlundt ('Phil. Mag.,' vol. 43, p. 1038 (1922)) found that sources of thorium C and radium C of equal γ-ray activity when measured through 6 mm. of lead, emit respectively 738 α-particles of the 8·6 cm. range, and 1000 α-particles of the 7 cm. range in a given time. On our scale of ordinates, therefore, the total number of α-particles in the 8·6 cm. group would be 738,000.

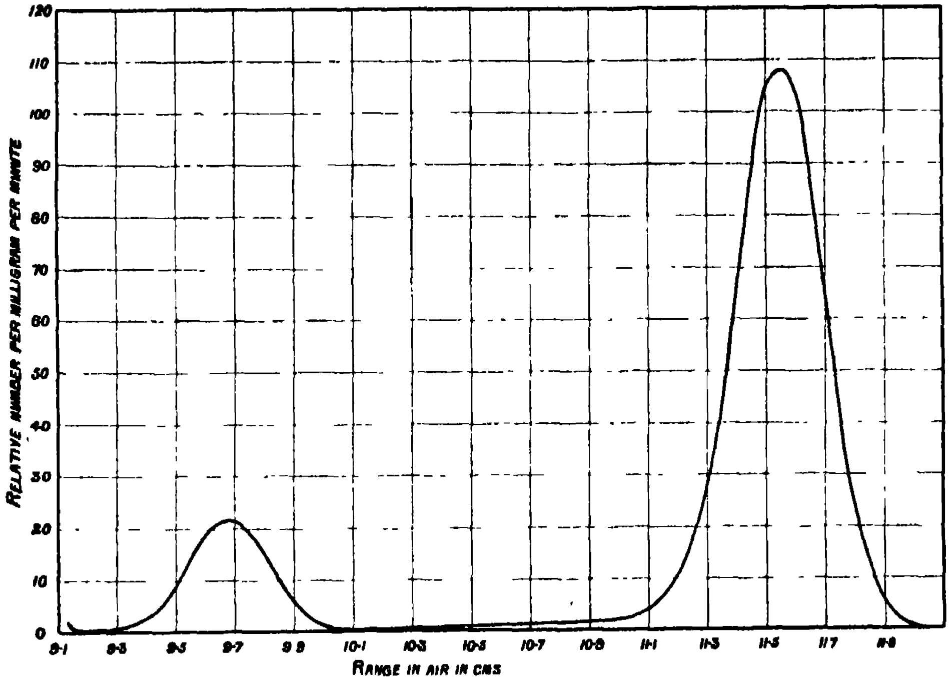

Fig. 1.—Analysis of long range α particles from Thorium C.

in fig. 2, in which the experimental points obtained using two sources on different days are plotted. The curve fitted is of correct shape and size, in drawing which the only variable not predetermined is the effective slit width. The total number of particles of the group was counted by the single chamber method, and the curve is drawn to be consistent with this. The height and breadth of the curve would both be changed by any alteration in the value assumed for the effective slit width. The position of the curve is adjusted to fit the experimental points, thus fixing the mean range.

A careful search was made to see if any other weak groups of α-particles were present corresponding to those observed from radium C. Between the two main groups of fig. 1, the number counted fell to 1/300 of the longer range group, but not the slightest evidence was obtained of the presence of additional groups. Between the 9·8 cm. group and the main group of 8·6 cm. particles, the ordinates of the curve fell to less than 1/300 of the 11·7 cm. group.

Special experiments were made to settle whether any particles of range longer than 11·7 cm. were emitted. For this purpose, strong sources were used close to the single counting chamber of low natural effect. It was concluded that if any α-particles were present, the number was certainly less

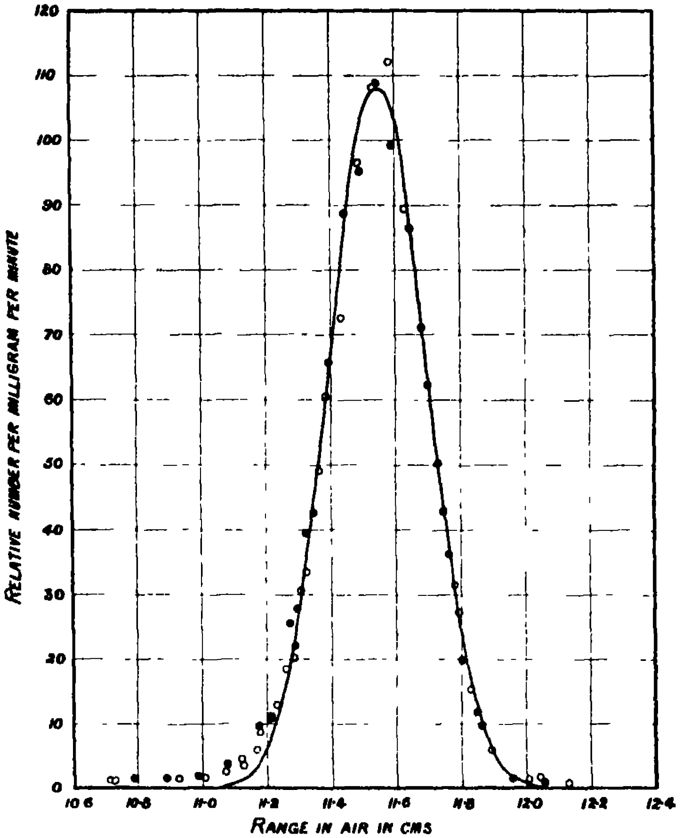

FIG 2.—Group of long range α-particles from Thorium C′, showing points obtained in two experiments.

than 1/10,000 of the number in the 11·7 cm. group. It is of interest to note that both in the case of radium C and thorium C, the swiftest α-particles emitted have nearly the same speed. For example, the highest extrapolated range for the α-particles from radium C is 11·64 cm., and for thorium C, 11·66 cm. There is no *a priori* reason to suppose that they should be identical.

In the course of these experiments, careful observations were made to test whether any additional groups of α-rays could be detected between the two main groups of thorium C, of ranges 4·8 and 8·6 cm. The ordinates of the curve just above the 4·8 cm. group was only 1/4000 of the ordinate of the main 8·6 cm. group, and increased to about 1/1000 for a range of 7·5 cm., and to 1/300 for a range of 7·9 cm. No trace of any additional groups in this region was observed.

All of the groups of α-rays from thorium C appear to be single except the

4·8 cm. peak, which is too broad. The complexity of this group first noted by Rosenblum* was illustrated in a previous paper,† and was confirmed in the present experiments.

The velocity and energy of each of the groups of α-particles from thorium C and C′ are given in the following table. As our apparatus is not suitable for the direct determination of ranges with precision, it is necessary to refer all the measurements to one standard range. After full consideration of the data, the value 8·533 cm. for the mean range of the 8·6 cm. group at 760 mm. and 15° C has been taken.

| Mean range in cm of air at 760 mm. and 15° C. | Extrapolated range in cm of air at 760 mm. and 15° C. | Velocity of α-particle in terms of $V_0$ | Energy of α-particle in electron volts $\times 10^{-6}$ | Relative number of α-particles |
|---|---|---|---|---|
| 4·670‡ | 4·713 | 0·8876 | 6·050 | $5 \cdot 4 \times 10^5$ |
| 8·533 | 8·620 | 1·0693 | 8·788 | $10^6$ |
| 9·683 | 9·781 | 1·1124 | 9·512 | 33·6 |
| 11·547 | 11·662 | 1·1754 | 10·624 | 189 |

‡ On account of the complexity of the α-particles emitted directly from thorium C, the range 4·670 cm. refers to the weighted mean of the two main groups directly measured in our experiments.

Measurements of range could be, and always were repeated to within 0·005 cm., with one notable exception. When strong sources of thorium C were used, it was impossible by our methods to determine the range of the 8·6 cm. group until the source had decayed to a minute fraction of its original strength. Under these conditions, the observed mean range was always about 0·02 cm. shorter than the value measured for fresh weak sources. This effect is attributed to a change in the surface conditions of the source. It is not believed that this difference arises when a strong source is used immediately after it is prepared.

The extrapolated ranges were deduced from the observed mean ranges.

The velocities of the long range α-particles were deduced from an extrapolation curve discussed in the previous paper (*loc. cit.*), with a slight alteration to take account of the difference between the 8·6 and the 4·8 cm. ranges determined in these experiments. The velocities are expressed in terms of $V_0$ ($1 \cdot 922 \times 10^9$ cm/sec.), the velocity of the main group of α-particles from radium C, which is taken as a standard for comparison. The energy of the α-particle corrected for relativity is given in the fourth column, expressed in electron-volts, the energy of the standard α-particle from radium C being $7 \cdot 683 \times 10^6$ volts.

---

* Rosenblum, 'C.R. Acad. Sci. Paris,' vol. 188, p. 1401 (1929), and vol. 190, p. 1124 (1930).

† Rutherford, Ward and Wynn-Williams, 'Proc. Roy. Soc.,' A, vol. 129, p. 211 (1930).

It is seen that the mean ranges found by us for the long range particles are in fair agreement with the values found by Nimmo and Feather (*loc. cit.*), viz., 9·82 cm. and 11·62 cm. Similarly the relative numbers of α-particles in the two groups, namely, 1 : 5·6, is in good accord with the ratio of 1 : 5·1 which they found.

It is estimated that for $10^6$ α-particles of range 8·6 cm., 189 are emitted of range 11·7 cm., and 33·6 of range 9·8 cm. The number in the longer range is in fair accord with previous data.

### *Discussion of Results.*

In our previous paper, it was concluded that the emission of γ-rays from radium C′ was intimately connected with the appearance of the long range α-particles. In consequence of the emission of a β-particle from radium C, it is supposed that the resulting radium C′ nucleus is left in an excited state. Some of the α-particles are raised to a higher level of energy than the normal, and after a very short interval fall back to the ground level, emitting their surplus energy in the form of a γ-ray of definite frequency. In the short time the α-particle or particles remain in a level of higher energy, there is a finite probability that an α-particle will escape through the potential barrier of the nucleus and appear as a long range α-particle of energy equal to its energy in the excited state. On this view the energies of the individual α-particles in the various groups of long range α-rays represent the energies of possible α-rays levels in the excited nucleus. In their paper,* Rutherford and Ellis discuss this hypothesis in more detail, and suggest that in the case of radium C′ more than one α-particle can occupy a given energy level, and in this way, try to connect the observed energies of the individual γ-rays. It is of much interest to see whether a similar explanation can be given for the appearance of the long range α-particles from thorium C.

It is necessary first of all to consider carefully the source of these long range α-particles. It has been generally supposed that each of the three products, radium C, thorium C and actinium C breaks up in two distinct ways. The general scheme of transformation and the notation employed is easily seen from the diagram (fig. 3).

---

* Rutherford and Ellis, 'Proc. Roy. Soc.,' A, vol. 132 p. 667 (1931).

Some of the "C" atoms break up with the emission of an α-particle, others with the emission of a β-particle, but the relative probability of the α and β

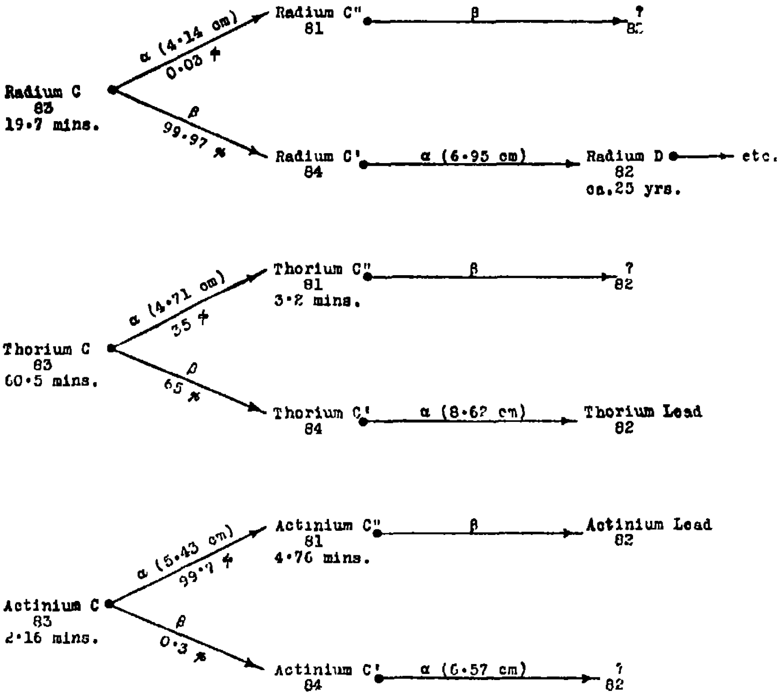

FIG 3

types of transformation varies markedly for the C bodies. For radium C, thorium C, and actinium C, the relative proportions of the C atoms which emit α-particles are approximately 0·03, 35, and 99·7 per cent. respectively.

It has been generally assumed that the long range α-particles from radium C come from the branch product radium C′ and accompany the normal 7 cm. range α-particles. In a similar way it is supposed that the long range α-particles from thorium C come from the product thorium C′, which emits the normal α-particles of range 8·6 cm. Stahel* has shown that the β-ray product thorium C″ (half value period 3·20 minutes) does not emit the long range α-particles, while thorium C is believed to emit only the complex group of α-particles of range about 4·8 cm. On account of the very rapid transformation of thorium C′, of average life estimated to be about $10^{-8}$ sec., it has not been found possible to give a direct experimental proof of the origin of the long range α-particles, but from analogy with radium C, it will be provisionally assumed that they arise from the transformation of thorium C′.

---

* Stahel, 'Z. Physik,' vol. 60, p. 595 (1930), and vol. 63, p. 149 (1930).

It is important to note that while the strong γ-rays, ordinarily observed from radium C are believed to come directly from the radium C′ nucleus, the corresponding product thorium C′ is believed to give little if any γ-radiation. The main part of the strong γ-radiation from thorium C is emitted from the β-ray product thorium C″, formed by the α-ray disintegration of thorium C. On the other hand, the product radium C″ exists in too small a quantity relative to radium C′ to give detectable γ-rays.

On the views outlined to account for the long range α-particles from radium C′, it may be supposed that there are two excited levels in the thorium C′ nucleus, of energies corresponding to the long range particles, viz., $9 \cdot 69 \times 10^6$ and $10 \cdot 38 \times 10^6$ electron volts. If these are transition levels, the energies of the γ-rays (or corresponding β-rays) emitted in the fall of the α-particle from the higher level to the ground level of energy $8 \cdot 96 \times 10^6$ volts should be $7 \cdot 4 \times 10^5$ and $18 \cdot 7 \times 10^6$ electron volts. A correction has been made for the recoil of the nucleus as in our previous paper.*

Unfortunately, owing to experimental difficulties, the magnetic spectra of thorium C′ and thorium C″ have not been separately measured. It has generally been supposed that the stronger lines in the complicated β-ray spectrum, due to thorium C in equilibrium with its products, are to be ascribed to thorium C″. Black† was unable to detect any β-ray lines in the neighbourhood of $18 \times 10^5$ volts, although strong lines of higher energy were observed due to the well-known γ-ray $26 \cdot 49 \times 10^5$ volts.

Corresponding to a γ-ray of energy $7 \cdot 4 \times 10^5$ volts, we should expect to observe in the β-ray spectrum a β-ray of energy $6 \cdot 5 \times 10^5$ volts, resulting from the conversion of the γ-ray in the K level. A weak line has been observed in the β-ray spectrum of approximately the right energy, viz., $6 \cdot 397 \times 10^5$ volts. It is to be noted that this appears to be an isolated β-ray line,‡ but it is quite possible that it may arise from thorium C″ and not from thorium C′, and have another interpretation.

While the β-ray evidence is either negative or inconclusive, it is of interest to see whether further information can be obtained by comparing the long range α-particles from thorium C′ with those obtained from radium C′ The two most marked differences are the relative simplicity of the groups of $\alpha$-particles from thorium C′ and the much greater proportion of particles in each of the two groups. In their discussion of the relation of the long range $\alpha$-particles of radium C′ with the $\gamma$-rays, Rutherford and Ellis introduced the conception of an *interaction coefficient*, $b$, which measures the probability of the transfer of the energy released in an $\alpha$-ray transition to an outer K electron of the atom. Such a coefficient applies equally to a transition in which a $\gamma$-ray may be emitted, or to a radiationless transition.

---

* Rutherford, Ward and Lewis (*loc. cit.*).

† Black, 'Proc. Roy. Soc.,' A, vol. 109, p. 166 (1925).

‡ See "Radiations from Radioactive Substances" (Rutherford, Chadwick and Ellis), 'Camb. Univ. Press,' 1930, p. 369.

It is easily seen that if $n_a$ is the average number of long range $\alpha$-particles per atom escaping during the transition, $n_e$ the number of K electrons liberated per atom, then $n_e/n_a = b/a$ where $a$ sec$^{-1}$ is the ordinary transformation constant of the $\alpha$-particle in the level and $b$ the interaction coefficient. The values of $b$ were estimated for some of the stronger $\gamma$-rays from radium C′ and found to be $6 \cdot 7 \times 10^{11}$ and $5 \cdot 2 \times 10^{13}$ for the $\gamma$-rays of energies $6 \cdot 12$ and $22 \cdot 19 \times 10^5$ electron volts respectively.

If we assume corresponding values for the thorium C transition and calculate the values of $a$, the ratio $n_e/n_a$ can be deduced. The values of the transformation constant $a$ can be calculated from the formulæ given by Gamow and Houtermans* and also Atkinson and Houtermans.† From the data given by Gamow it can be estimated that the value $a$ for the normal group of $\alpha$-particles of thorium C′ of range $8 \cdot 6$ cm. is about $2 \cdot 7 \times 10^7$ sec$^{-1}$ and for the two long range groups of ranges $9 \cdot 8$ and $11 \cdot 7$ cm., $1 \cdot 3 \times 10^9$ and $2 \cdot 1 \times 10^{11}$ sec$^{-1}$ respectively.

For a $\gamma$-ray of energy $7 \cdot 4 \times 10^5$ volts corresponding to a transition of the shorter range group we take $b = 7 \times 10^{11}$ and $a = 1 \cdot 3 \times 10^9$, consequently $n_e/n_a = 5 \cdot 4 \times 10^2$. Now $n_a = 3 \cdot 4 \times 10^{-5}$, consequently $n_e = 1 \cdot 8 \times 10^{-2}$. Now Ellis and Aston‡ found the value of $n_e$ for much the strongest line in the $\beta$-ray spectrum of radium C′ to be $4 \times 10^{-3}$. On these assumptions we should consequently expect the $\beta$-ray line arising from this transition to be very strong. If it exists at all, it is a weak line and certainly less than one-tenth of the calculated intensity.

Next consider the second group of range $11 \cdot 7$ cm. for which the energy released in the transition should be $18 \cdot 7 \times 10^5$ volts. Taking $b = 4 \cdot 6 \times 10^{13}$, $a = 2 \cdot 1 \times 10^{11}$, $n_e/n_a = 2 \cdot 2 \times 10^2$. Now $n_a = 1 \cdot 9 \times 10^{-4}$ in this case, consequently $n_e = 4 \cdot 2 \times 10^{-2}$, while the value corresponding to the easily measurable γ-ray of radium C′ of energy $22 \cdot 19 \times 10^5$ volts is only $9 \times 10^{-6}$ or 400 times smaller. Since not even a weak β-ray line corresponding to the transition under consideration has been detected, it is clear that the value of $n_e$, estimated on these views, is of the wrong order of magnitude.

---

* Gamow and Houtermans, 'Z. Physik,' vol. 52, p. 496 (1928–9).

† Atkinson and Houtermans, 'Z. Physik,' vol. 58, p. 478 (1929).

‡ Ellis and Aston, 'Proc. Roy. Soc.,' A, vol. 119, p. 145 (1930).

If the emission of the long range α-particles from thorium C′ is to be accounted for in the same general way as in the case of radium C′, we are thus driven to the conclusion that the interaction coefficient in the thorium C′ nucleus is much smaller than that estimated from the γ-ray transitions in the radium C′ nucleus and for the higher level is several hundred times smaller. This suggests that the transitions in thorium C′ are of a somewhat different type from those exhibited by radium C′. In their paper on the origin of the γ-rays from radium C′, Rutherford and Ellis conclude that the strongest group of long range particles from radium C′ of transition energy about $14 \cdot 6 \times 10^5$ electron volts is connected with a radiationless transition of the type discussed by R. H. Fowler,* in which there is a direct transfer of the nuclear energy to the outer K, L, - - -, electrons of the atom without the emission of a γ-ray. For such a radiationless transition the value of the interaction coefficient appears to be at least ten times smaller than for an ordinary γ-ray transition, and may be much smaller for higher nuclear levels Such an explanation seems not unlikely, but of course it is always possible that the levels in the thorium C′ nucleus, in which the α-particles of the two long range groups originate, are stable for the times under consideration ($10^{-9}$ sec.), and that all the α-particles escape in the normal way without any emission of energy in the form of β or γ-radiation. In such a case we should regard the long range groups of α-particles as analogous to the main group of 8·6 cm. particles, the number of particles in each level being on the average only $3 \cdot 4 \times 10^{-5}$ and $1 \cdot 9 \times 10^{-4}$ of the number in the main level.

No definite conclusion can be reached at this stage, but it is obviously of importance to examine closely whether thorium C′ emits any β-rays of the energy required by the α-ray transitions. The point is of much interest and theoretical importance in regard to the behaviour of nuclear levels.

### *Analysis of the α-particles from Actinium C.*

The scheme of dual transformation supposed to take place with actinium C is similar to that of radium C and thorium C, and is shown in the diagram (fig. 3). While with both radium C and thorium C, the β-ray branch predominates, with actinium C the reverse holds, and most of the atoms follow the α-ray branch.

---

* R. H. Fowler, 'Proc. Roy. Soc.,' A, vol. 129, p. 1 (1930).

The presence of the product actinium C′ was first inferred by Marsden and Perkins,* who found that about 1/650 of the α-particles from actinium C had a range of about 6·4 cm. in air, nearly 1 cm. greater than the range 5·5 cm. of the main group of α-rays. This group of 6·4 cm. particles was supposed to be emitted from actinium C′ and in this respect actinium C′ was analogous in behaviour to the corresponding products radium C′ and thorium C′.

Bates and Rogers,† who examined the ranges by the scintillation method, concluded that the α-particles from actinium C′ had a range of 6·5 cm and numbered 1/300 of the main group.

In a previous paper,‡ it has been shown that the ordinary group of α-particles from actinium C is complex, consisting of two distinct groups of estimated ranges 5·51 and 5·09 cm. In the present investigation we were able to obtain sources of actinium C, by exposure to the actinium emanation, about ten times stronger than those used in the earlier experiments referred to. It was thought desirable to investigate again the complexity of the main α-ray groups in order to test whether any further groups of α-rays could be detected. The curves obtained are shown in fig. 4 As before, we were only able to detect two groups, for which the mean ranges were accurately measured. The shape of the straggling curve for each group was carefully examined, and no evidence of further complexity in either group was found. It should be noted that we were definitely able to detect the complexity of the chief 4·7 cm. group of thorium C, which, according to the data given by Rosenblum (*loc cit.*), consists of two groups in the proportion 1 : 3, differing in range by 0·43 mm. Any complexity of the two main actinium C groups which may exist must certainly be less marked than this.

Our experiments thus confirm the previous conclusion that the α-rays of actinium C consist of two main groups and that 16 per cent. of the atoms of actinium C emit α-particles of the shorter range. In the experiments recorded in our previous paper, the range of the main group of α-particles was not directly measured, but assumed from the experiments of Geiger§ to be 5·511 cm. under standard conditions. The range of the other group was determined by the difference in the mean ranges. In our present experiments the mean ranges of the α-particles in the two groups were determined. Taking as standard the mean range of the 8·6 cm. particles from thorium C′ to be 8·533 cm., we find the mean ranges of the two actinium C groups to be 4·925 cm. and 5·373 cm., and the corresponding extrapolated ranges 4·972 cm. and 5·426 cm., the difference in ranges being in good accord with the previous determination.

---

* Marsden and Perkins, 'Phil. Mag.,' vol. 27, p. 690 (1914); see also Varder and Marsden, 'Phil. Mag.,' vol. 28, p. 818 (1914).

† Bates and Rogers, 'Proc. Roy. Soc.,' A, vol. 105, p. 97 (1924).

‡ Rutherford, Ward and Wynn-Williams, 'Proc. Roy. Soc.,' A, vol. 129, p. 211 (1930).

§ Geiger, 'Z. Physik,' vol. 8, p. 45 (1921).

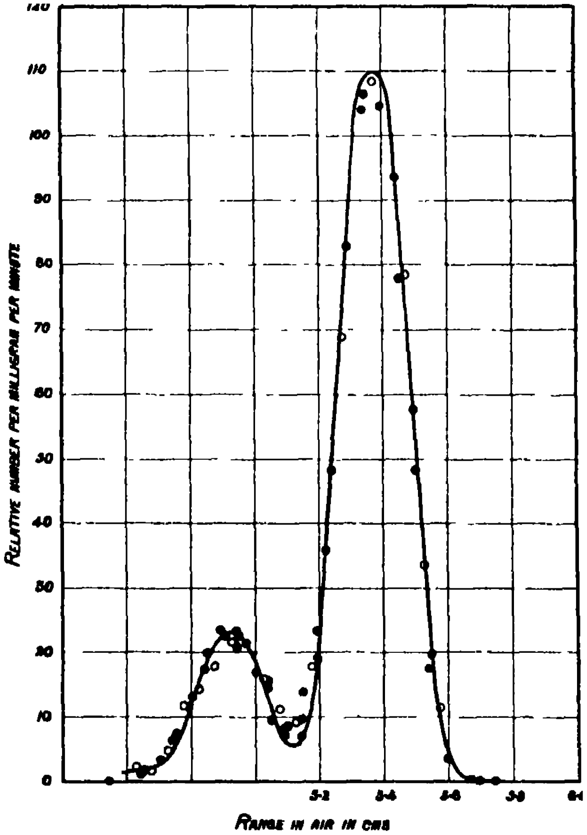

FIG 4.—Groups of α-particles from Actinium C, showing points obtained in four experiments.

The longer range α-particles (range about 6·6 cm.) were carefully examined. The straggling curve obtained is shown in fig. 5, and is of the shape to be expected if this group of α-rays is homogeneous. The region between ranges of 5·8 and 6·25 cm. was carefully examined for other groups, but with no success. The number of α-particles counted in the region of the tail of the

6·6 cm. group was down to one per cent. of the number in the 6·6 cm. group at 6·0 cm. and fell gradually to about 0·7 per cent. at 5·83 cm.

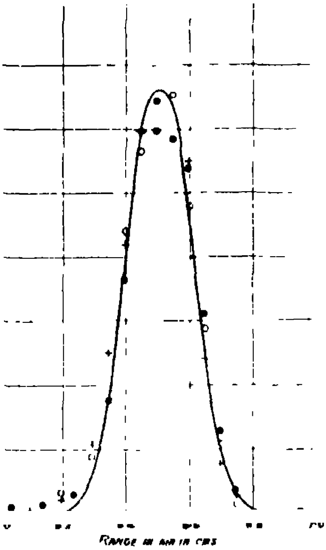

Fig. 5—Group of α-particles from Actinium C′, showing points obtained in four experiments.

The number of α-particles in the 6·6 cm. group was found to be 1/310 of the main group—a value in good agreement with the results of Bates and Rogers

A careful search was made for α-particles of range greater than 6·6 cm. For this purpose the single counting chamber of low natural effect was used, the source of actinium C being placed close to the opening of the chamber. The experiments were complicated by a small trace of thorium emanation which was released from the actinium preparation. The relative activity due to the thorium C on the collecting disc was much reduced by passing a slight current of air over the actinium preparation, and by reducing the time of exposure. In this way, the α-rays due to thorium C were reduced to less than 1/300 of the number of the 6·6 cm. particles. No evidence was obtained of any groups of α-particles of ranges between 7·1 and 12 cm., the number of particles, if any, being less than 1 in 300,000 of the number emitted in the main group of range 5·4 cm. We were unable to carry the experiment further for lack of a sufficiently strong source. The strongest source in our experiments corresponded in α-ray activity to about 1/70 milligramme of radium. Sources at least 10 to 100 times stronger would be required to investigate the presence of any group of long range particles containing less than one millionth of the number of the main group. This, as we have seen in a former paper,* is of the order of the number in the weaker groups of long range α-particles emitted from radium C′.

The data obtained from our measurements are comprised in the following table, where the velocity and energy of the α-particles in the various groups have been estimated as in the corresponding table for the products of thorium C.

---

* Rutherford, Ward and Lewis, 'Proc. Roy. Soc.,' A, vol. 131, p. 684 (1931).

| Product. | Mean range in cm. of air at 760 mm. 15° C. | Extrapolated range in cm. of air at 760 mm. 15°C | Velocity of α-particle in terms of $V_0$. | Energy of α-particle in electron volts $\times 10^{-6}$ | Relative number of α-particles |
|---|---|---|---|---|---|
| Actinium C | 4·925<br>5 373 | 4 972<br>5 426 | 0·9024<br>0·9268 | 6 254<br>6 597 | 19<br>100 |
| Actinium C′ | 6·506 | 6 572 | 0·9829 | 7 421 | 0 32 |

Taking the velocity of the main group of α-particles from actinium C as unity, the velocity of the α-ray group of range 4·97 cm. is 0·9737, and the velocity of the 6·57 cm. group 1·0605.

After these observations had been completed, a paper was published by I. Curie and Rosenblum* in which the constitution of the α-rays from actinium C was examined with the large electromagnet of the Academie des Sciences at Paris, using the focussing method. Strong sources were used, and the α-ray spectrum was photographed. The three groups of α-rays shown in the table were alone observed, and the relative velocities estimated to be 0·973 : 1 : 1·062, in close accord with our observations by the counting methods.

It should be noted that the difference of energy between the two groups of range 5·0 and 5·4 cm. is $3{\cdot}43 \times 10^5$ volts. Applying to this case the hypothesis proposed by Gamow† to account for the complex groups of α-rays from thorium C, we should expect to obtain a strong γ-ray of energy (correcting for recoil) of $3{\cdot}50 \times 10^5$ volts. Actually, Hahn and Meitner‡ observed from a preparation of actinium B + C a strong β-ray of energy $2{\cdot}646 \times 10^5$ volts. Assuming that this comes from actinium C″, and is converted in the K shell of an atom number 81, the energy of the corresponding γ-ray is $3{\cdot}50 \times 10^5$ volts. This agreement is not, however, substantiated by the other β-ray lines to be expected corresponding to conversions in the L and M levels of an atom of this atomic number. For these reasons, the apparent agreement between theory and observation should be regarded with caution, until we have further accurate data of the β-ray spectrum.

---

* Curie and Rosenblum, 'C.R.,' vol. 193, p. 33 (1931).

† Gamow, 'Nature,' vol. 126, p. 397 (Sept., 1930).

‡ Hahn and Meitner, 'Z. Physik,' vol. 34, p. 795 (1925).

## *Summary.*

The long range α-particles from thorium C have been analysed, using a differential ionisation chamber and a valve amplifier operating an automatic counter. The particles were found to consist of only two definite groups of extrapolated ranges 9·781 cm. and 11·662 cm. in general agreement with previous observations. The relative numbers of the two groups are 1 : 5·6, and the estimated number in the long range group is $1 \cdot 9/10^4$ of the main group of α-particles of range 8·620 cm. There was no indication of the presence of other groups such as we had previously observed for the case of radium C′. The question of the origin of the long range α-particles is discussed.

The α-particles emitted from actinium C have also been analysed. We have confirmed the earlier conclusions on the complexity of the main group of range about 5·4 cm., and have carefully determined the range and number of the 6·6 cm. group which are supposed to arise by the transformation of actinium C′. The group of α-rays appears to be homogeneous, and the values found in fair agreement with previous observations. No evidence was found of additional groups between the ranges 4·5—12 cm. In particular, a careful analysis was made to test whether any long range α-particles were emitted corresponding to the well-marked groups of long range α-particles found in the case of radium C and thorium C.

No evidence of such particles was obtained, but, owing to the weakness of the sources available, we should have been unable to detect a group of particles of number less than 1/300,000 of the main group of range 5·4 cm. or 1/1000 of the 6·6 cm. group.

We wish to acknowledge the help of Dr. F A. B. Ward, who assisted us with the earlier part of this work. We also express our thanks to Mr. G. R. Crowe for his help throughout the experiments, and to the Department of Scientific and Industrial Research for a grant to one of us (W.B.L.).

# *The β-Particle Emission of Radium D.*

By H. O. W. Richardson, B.Sc., King's College, London.

(Communicated by Lord Rutherford, F.R.S.—Received June 10, 1931.)

[Plate 16.]

The main object of this investigation was to obtain an energy distribution curve for the electrons emitted by radium D during its disintegration. Such a distribution curve may be expected to be made up by the electrons coming from the nucleus, which have a continuous distribution of energy, together with secondary particles forming groups of homogeneous energy, produced by the action of the single γ-ray of radium D The nuclear electrons are of great interest because owing to their very low energy they have never been identified with any certainty. The energy distribution finally obtained is shown in fig. 4, each point on the curve representing the number of particles having energies lying within 1000 volts on either side of the point.

A secondary object of the work was to attempt to estimate the absolute number of particles emitted per disintegration, which number should, of course, be unity for the nuclear particles and some fraction less than unity for the secondary groups The latter are due to the ejection of electrons from the L and outer atomic levels only, since the energy of the γ-ray, 47,200 volts, is insufficient to ionise the K level.

The method used was to photograph the tracks formed by the particles in a Wilson expansion chamber. The ranges of the tracks, which consisted of lines of drops formed on the ions produced by the passage of the particle, were measured using a stereoscopic method. By measuring sufficient ranges it is possible to obtain an approximately accurate range distribution curve and by calculation an energy distribution could be deduced.

With an expansion chamber of given dimensions it is only possible to measure tracks whose ranges lie between certain limits. Fortunately, a particle of given energy will have a range which depends greatly on the nature of the gas through which it passes and by varying the composition of the gas in the chamber it is possible to bring particles forming different parts of the energy distribution within the ranges which can be conveniently measured. In the present work three gas mixtures were used resulting in three energy distribution curves, valid over different regions. These are shown in fig. 3, and are combined to give the complete distribution in fig. 4.

The lowest energy which could be investigated by the method was, for reasons which will be discussed later, about 6000 volts, corresponding to a track of 5 mm. range in the gas of least stopping power used.

### *Experimental Method.*

The radioactive material must be deposited on some solid surface into which necessarily half of the β-particles will pass. If this mounting is thick a fairly large fraction of these particles will be scattered back so as to form tracks in the chamber indistinguishable from those due to particles which have not suffered such reflection. The presence of these reflected particles, which have lost an unknown amount of energy, will cause distortion in the low energy end of a distribution curve though it would not affect the determination of the energies of β-ray lines in the magnetic spectrograph. In order to avoid this difficulty, Feather* introduced a mounting of great thinness, through which all but the slowest particles could pass with little loss of energy. This consisted of a double thickness of gold leaf wrapped round two fine horizontal wires. The source used in the present work was of this type, the fine wires, of copper, were soldered into a frame of thicker wire which held the gold leaf with its plane vertical in the centre of the chamber, as shown in fig. 1.

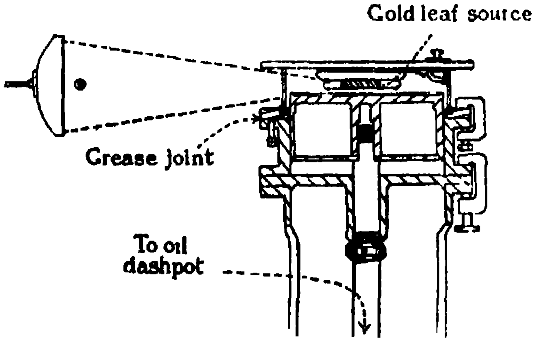

*Fig. 1.—The General Arrangement of Source and Chamber.*

The gold leaf was activated by placing it for a short time in a tube containing radon and was then left for 2 weeks to allow traces of the latter to escape by diffusion. The area of the gold leaf, which was 2·5 cm. × 0·8 cm. high, was so large that one could reasonably hope to distinguish pairs of tracks due to a nuclear and a secondary electron starting from the same atom. The results of such a search are discussed later.

---

* 'Proc. Camb. Phil. Soc.,' vol. 25, p. 522 (1929).

The leaf had a mass of 0·16 mgm. per square centimetre which, for a double thickness, gives a stopping power for $\alpha$-particles equivalent to 0·8 mm. of air.

Owing to the size and central position of the source it would have been difficult to arrange a shutter device to limit the time of entry of the particles. The shutter in any case would have caused considerable eddies in the gas, thus destroying the shorter tracks. Such a shutter, with a source at the side of the chamber, was used by Petrova* who, though using air at quite low pressures in the chamber to increase the ranges, was unable to measure tracks of such low energy as can be reached by the present method. The absence of a shutter might introduce a possible source of error which must now be considered. If a particle passes before the expansion is complete the range of the track it forms will be lower than that corresponding to the minimum density of the gas in the chamber at the end of the expansion, which density is used in calculating the energy of the track. It was thought that this source of error could be reduced by applying a strong electric field to the chamber, thus driving away all ions in a small fraction of a second after their formation. An early track would have its ions pulled apart by the field and would appear diffuse. In fact a potential of 200 volts was applied between the source and the floor of the chamber and the number of such early tracks observed was small. The great majority of the tracks were perfectly sharp, having been produced during the period of supersaturation and thus instantly fixed as lines of drops. Any error due to this source would be small in comparison with the ordinary straggling of the ranges.

The expansion chamber used in the present work was designed by R. R. Nimmo on the basis of a chamber used by Auger in which the final velocity of the piston was absorbed by an oil-dash pot. The air release-valve of large diameter was designed to allow the air to escape rapidly from beneath the piston thus causing the latter to fall suddenly without oscillation. The interior of the chamber, as shown in fig. 1, was made accessible by mounting the glass top and walls in a brass ring forming the top half of a ground grease joint.

The photographs were taken with a stereoscopic camera with the lenses generally at F8 and the planes of the plates inclined. The axis of each component of the camera made an angle of about 30° with the vertical in order to increase the light entering the lens by decreasing the angle through which it was scattered by the track. Imperial Eclipse Soft ¼-plates were used. The necessary illuminating flash was provided by discharging a 0·05 mfd. condenser charged to about 40,000 volts through two electrically heated quartz mercury lamps in series. Each lamp was provided with a parabolic reflector, which was found to give a better distributed and stronger horizontal field of illumination than the usual cylindrical lens.

---

* ‘Z. Physik,’ vol. 55, p. 628 (1929).

It was necessary to make many slow expansions between successive photographs in order to remove small drops left over after a fast expansion. In spite of this a number of drops, referred to as general cloud, were always present, uniformly distributed throughout the chamber. The effect of this cloud, which is easily seen in Plate 16, will be discussed later.

Some tracks were noticed not starting from the source which were attributable to the absorption of soft X-radiation in the gas and to stray $\gamma$-rays.

The measurement of the tracks was carried out by the method and apparatus described by Williams and Terroux.* The plates were put back in the camera and illuminated from behind. The full-size solid image thus formed was viewed through a magnifying lens and pin points were placed on suitable parts of each track. The range was the sum of the distances between adjacent points, the effect of rapid curvature being allowed for by eye. The lengths of all visible side branches were measured.

The method is obviously laborious, but it must give more accuracy and resolving power than can be obtained by merely measuring the images of the projections of tracks in single photographic plates.

### *Discussion of the Track Measurements.*

In order to investigate the particles of lowest energy a mixture of oxygen with 91 per cent. of hydrogen was used, in which a range of 1 cm. corresponded to an energy of 9400 volts. The results, expressed as a distribution of ranges, are shown in fig. 2, in which each point gives the number of tracks whose range lies within 1 mm. on either side of that point. This method of expressing the results is unsatisfactory because it cannot represent tracks with large branches and because its physical meaning is not obvious.

The energy of each track allowing for all visible branches was therefore calculated and the resulting energy distribution is shown in fig. 3, curve $A_1$, which is based on 160 observed tracks. To make this calculation the formula used was $E_0^2 - E_x^2 = nKx$, where $E_0$ is the initial energy of the particle and $E_x$ its energy after travelling a distance $x$ centimetres. $n$ is proportional

---

* 'Proc. Roy. Soc.,' A, vol. 126, p. 289 (1930).

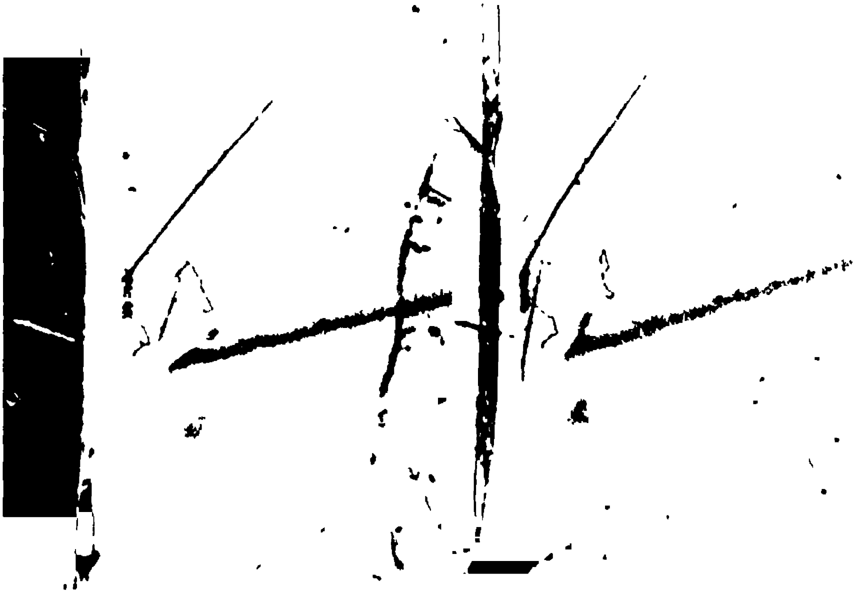

A Series (91 per cent. Hydrogen). A stereoscopic pair showing three measured tracks of range 0·99, 3·58 and 3·27 cm. The drop free layer and the drops of general cloud can be seen.

C Series (Air). The confusion caused by old α-tracks can be seen.

to the number of extranuclear electrons per cubic centimetre in the gas traversed This formula, expressing the Whiddington-Thomson law, has been verified

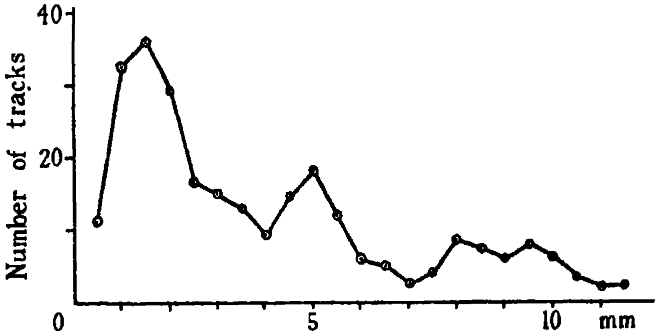

FIG. 2.—Number of Tracks against Range in millimetres of Oxygen at 0° C. and 760 mm.

for slow β-particles by Nuttall and Williams,* using an expansion chamber containing various gases.

The value for the constant K which was used in the present work is that deducible from the value of 0·709 cm. given recently by Williams† as the mean range of tracks of 20,440 volts initial energy in oxygen at 0° C. and 760 mm. This value is based on 300 tracks and leads to 24,260 volts as the energy of tracks of 1 cm. mean range.

The upper curve $A_2$ and $A_3$ was obtained from curve $A_1$ by the application of certain corrections in an attempt to counteract the selective loss of long and very short tracks in parts of the chamber in which they could not be photographed.

The first correction, which produced the part of the curve marked 2, allowed for the loss of long tracks which, it was found, were only photographed if they remained within a centrally placed horizontal layer extending nearly to the walls of the chamber. This layer was found experimentally to be about 2 cm. deep. The fraction of tracks whose end-points lay within this layer was calculated on the basis of the solid-angle available for points on the gold leaf. Loss of tracks because portions passed outside the layer was neglected and it was assumed that the straight line joining the start and end of a track was, on the average, equal to two-thirds of the range. For tracks of 1 cm. start to end length, *i.e.*, 1·5 cm. range, the fraction photographed was found to be 90 per cent. For longer tracks of range R and energy $E_0$ the fraction photographed would be $0\cdot9 \times 1\cdot5/R$, or $0\cdot9 \times E_c^2/E_0^2$, where $E_c$ is the energy of tracks of 1·5 cm. range.

---

* 'Phil. Mag.,' vol. 2, p. 1109 (1926)

† 'Proc. Roy. Soc.,' A, vol. 130, p. 318 (1931). Williams, after considering the available data, concludes that there is a departure from the Whiddington-Thomson law which is definitely outside the experimental error in the case of oxygen. The law is more nearly that $\bar{R} \propto E_0^{1.83}$ where $\bar{R}$ *is the mean range. It is to be noted that no accurate direct* information is available about the ranges of tracks above 22,130 volts energy.

The second correction attempts to allow for the loss of very short tracks which failed to emerge from a layer surrounding the source in which no drops were formed. This was probably due to the heating effect of the metal which reduced the supersaturation of the gas in contact with it. On this view it should be possible to reduce the layer by using higher piston speeds in making the expansion. This layer was found to be about 4 mm. thick in the mixture rich in hydrogen and to be less in the other gases owing perhaps to their lower conductivity. It gave a lower limit of about 6000 volts to the energy range which could be investigated and would cause the loss of many short tracks not emitted normally from the gold leaf.

The fraction of straight lines of length $x$ coming with random directions from an infinite plane and extending a distance $h$ beyond that plane is $1 - h/x$, where $x \geqslant h$. The application of the correction is difficult for several reasons. First, the size of the gold leaf makes it likely that the correction applies to only about half the tracks emitted with range more than 1·2 cm. Second, there is considerable uncertainty as to the points of origin of short tracks which appear as sharp heads just emerging from the drop-free layer, owing to the large scattering at the end of all tracks. This makes it easy to underestimate the range of such tracks For tracks above 1 cm. range this uncertainty has become negligible.

For these reasons the actual increase in the ordinates of the curve A1 which produced the corrected curve A3 was only about half that obtainable by an unrestricted application of the formula. The part of the distribution curve below 10,000 volts must thus be regarded with caution, but there is little doubt that the rise shown is real. This reality is further strengthened by the fact that particles of energy below 9000 volts will be unable to pass through the leaf and form visible tracks on the other side. There is thus bound to be an additional reduction of the number of low energy particles observed, with some distortion of the distribution. This could be avoided by a method which activated one side of the source only.

The A2 curve rises up to 25,000 volts after which it falls steeply, only two tracks being observed above 30,000 volts. This cutting off was due to many of the longer tracks reaching to within a few centimetres of the chamber walls, near which no drops were formed. This extra source of loss of long tracks is

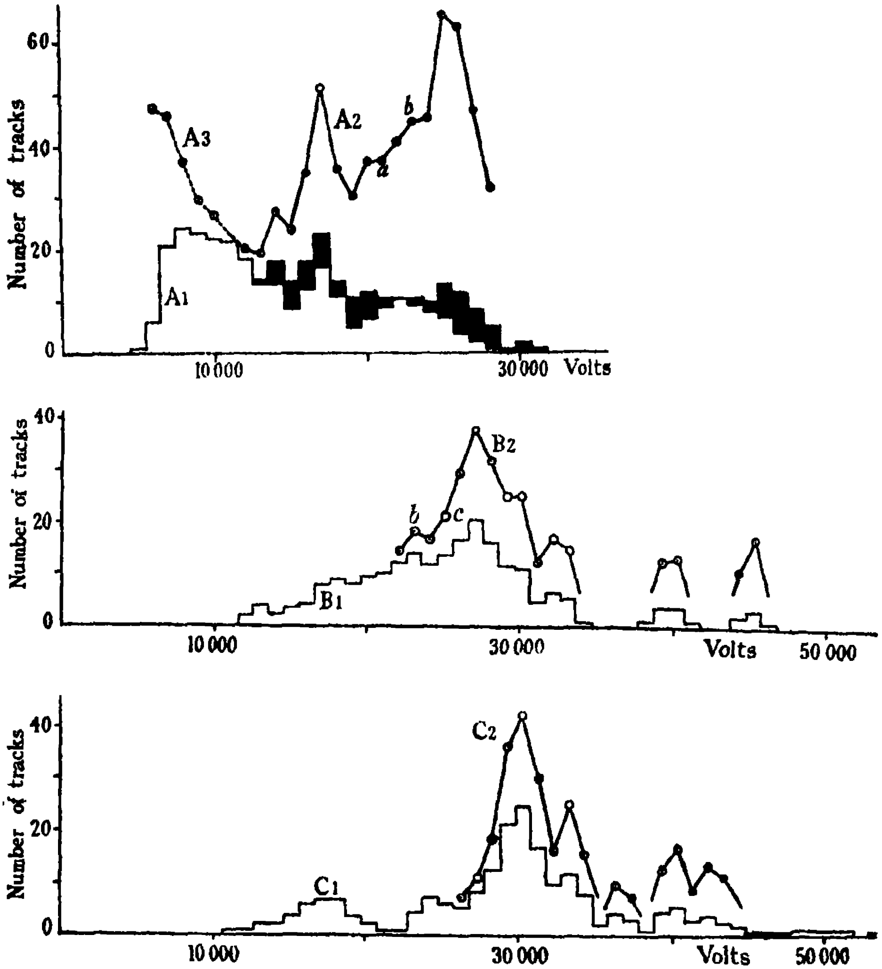

Fig. 3.—The three Energy Distribution Curves.

Series A.—160 tracks in Oxygen with 91 per cent. Hydrogen in which 1 cm. range means 9,400 volts energy. Series B.—108 tracks in Oxygen with 39 per cent. Hydrogen in which 1 cm. range means 16,400 volts energy. Series C.—109 tracks in air in which 1 cm. range means 19,200 volts energy.

illustrated by the increase above 25,000 volts in the proportion of tracks shortened by large branches. These tracks are represented by the blackened part of curve A1. Thus the corrected curve cannot be expected to be reliable above 24,000 volts and, in order to obtain data above this region, a gas of larger stopping power, containing only 39 per cent. hydrogen, was put in the chamber.

The resulting track measurements gave the curve B1 which, after correction for the loss of long tracks, gave the distribution B2. In order to obtain a reasonable number of tracks above 30,000 volts the stopping power was further increased by using air in the chamber, resulting in the corrected distribution C2.

There are many obvious differences, the causes of which must be examined in order to decide over what region each curve gives a valid representation of the energy distribution It is likely that many of the differences are due to probability fluctuations caused by the small number of observed tracks represented by a point.

The correction for the loss of short tracks was not applied to the B and C series owing to the greater thinness of the drop-free layer. The larger number of tracks ending close to the source and the greater linear density of ionisation of all tracks caused the loss by confusion of a considerable number of the shorter tracks in the B and C series. In the latter series further confusion was caused by the presence of an increased number of α-particles due to the greater age of the source.

For these reasons the B curve is considered to be invalid below about 22,000 volts and the C curve below about 27,000 volts. Above this region both curves are valid in proportion to the number of observed tracks which they contain.

A very rough independent check on the numbers of tracks lost by confusion, and by passage into regions where they could not be photographed, was obtained by counting the number of unmeasurable tracks and classifying them into energy groups by their appearance. Thus a straight track with few drops represents a fast particle probably due to the disintegration product radium E. In the A series a weakly curved and ionised track reaching near to the walls of the chamber has an energy above 25,000 volts. In the C series a curly densely ionised track will probably be due to a particle below 25,000 volts. Unfortunately such tracks are often mere fragments, but on the whole their numbers confirmed the interpretation of the measurements adopted.

The appearance of the drop-free layer in the A series can be judged from the stereoscopic pair of pictures shown in the plate. The single photograph gives an idea of the confusion caused by the more numerous α-particles in the C series.

### *The Deduction of the Final Distribution.*

The three curves have now to be combined. An obvious way of doing this, for example, would be to reduce the ordinates of the A2 curve by the factor required to fit its ordinate at the point marked *b* to that of the B2 curve at that point, which lies in a region in which both curves are probably valid. Owing to the rather small number of tracks on which each point is based it was felt that probability variations would detract from the value of this method. Fortunately an independent way of fitting the curves is made available by the presence of polonium, a disintegration product which emits α-particles and which grew in amount throughout the work in a way which could be calculated from its life period. By counting the number of α-particles observed it was possible to deduce the number of disintegrations of polonium photographed in each expansion and to estimate from this the number of radium D disintegrations photographed. This estimation requires a knowledge of the relative time intervals during which α- and β-particles form recognisable tracks during an expansion.

Consider a track which enters the chamber a short time before the end of the expansion. The electric field and heat motion of the gas will cause its ions to become drawn apart and when supersaturation occurs they will appear as a diffuse cloud of drops ultimately separating into positive and negative layers. Owing to the unavoidable presence of general cloud in the chamber such old tracks will tend to merge into the cloud, and the less the linear density of ionisation in the track the more rapid the merging and consequent loss. Thus, old α-tracks can be seen even when they have been drawn out vertically more than on 1 cm., while very fast β-tracks are lost as soon as their ions have passed out of their original straight line.

The slow β-particles which were measured in the present work ionise densely at the end of the track and their permanence was considered comparable with that of an α-particle. By observing the diffuseness of an α- or β-track its age can be estimated and no α-tracks were included whose diffuseness exceeded that of the older β-tracks measured. This estimation, despite its large personal element, was considered to be correct to within about 20 per cent. and was assisted in the case of the A series by the fact that the sharpness of the δ-projections from an α-track could often be compared with that of the end of a β-track.

The results of this counting are given in Table I, which shows that the time during which tracks were recorded did not vary greatly with the gas in the chamber.

The most probable number of disintegrations represented by the A, B and C curves thus appear to be 394, 194 and 235 respectively. The final distribution in fig. 4 was obtained by raising the ordinates of the B and C curves until each corresponded to 394 disintegrations and then averaging in the following way. Up to the point marked *a* the corrected A curve alone was used. From

Table I.—The Deduction of the Number of Disintegrations.

| Number of expansions. | Gas mixture. | Percentage polonium activity. | Sharp α-tracks per expansion at 100 per cent. activity. | Sharp and fairly diffuse α-tracks per expansion. | Number of disintegrations deduced from that of sharp α-tracks. |
|---|---|---|---|---|---|
| 99 | A 91 per cent $H_2$ | 25 7 | 4 1 | 6 55 | 394 |
| 58 | B 39 per cent $H_2$ | 6 3 | 3 35 | 5 6 | 194 |
| 43 | C Air | 38 5 | 5 45 | 6 45 | 235 |

*a* up to *c* the mean of the A and B curves was taken. At *c* the B curve alone was valid while above this point the mean of the B and C curves was used, weighted in proportion to the number of observed tracks forming the same point in each curve. It can be seen that the positions of the main peak in the B and C curves do not agree very closely. This was thought to be due to probability variations and confusion losses rather than to some defect in the method of deducing the energies from the ranges. Support for this view can be obtained from the excessive sharpness of the peaks in the separate curves, the broadness of the peak at 29,000 volts in the final distribution being more in accord with the known straggling of β-particles.

## *Discussion.*

1. *Interpretation of the distribution curve.*—In passing along the continuous curve of fig. 4 from right to left, a maximum is seen at about 41,000 volts followed by a much higher one at 29,000 volts. The first of these is interpreted as made up by the unresolved secondary groups coming from the M and N levels and known from the magnetic spectrum to have energies of 43,300 and 46,100 volts respectively. The second peak is due to particles coming from the L level, the great majority being known (by visual intensity estimation of the magnetic spectrum) to come from the $L_1$ level with 30,900 volts energy. The position of this second peak agrees well with the peak of 1·58 cm. range in air which Petrova (*loc. cit.*) found and attributed to the M secondary electrons. Attribution to the L secondaries was suggested by Feather and is confirmed by the agreement between the known energies of the β-ray lines and the energies here deduced for the peaks from the range measurements of Williams.*

---

* It is of interest to note that the slight discrepancy between the positions of the peaks and the energies of the β-ray lines is much reduced by using the law $R \propto E_0^{1\cdot82}$ to deduce the energies of the peaks. That shown at 29,000 volts is given an energy of 30,500 volts and that at 41,000 volts becomes 44,500 volts.

The accepted energies of the β-ray lines with the rough visual estimates of their intensity, are shown in Table II and their positions are also marked in fig. 4.

Table II.—The Numbers per Disintegration.

| Type of particle. | Secondary. | | | | | Tertiary. | Nuclear. |
|---|---|---|---|---|---|---|---|
| Level of origin | $L_I$. | $L_{II}$. | $L_{III}$ | $M_I$ | $N_I$. | Various | — |
| Energy of line in magnetic spectrum in volts | 30,900 | 31,500 | 33,800 | 43,300 | 46,100 | Various | — |
| Rough visual estimate of intensity of line | 50 | 2 | 0·5 | 20 | 10 | — | — |
| Number per disintegration in area between peak and broken curve | Unresolved<br>0·38 | | | Unresolved<br>0·29 | | 0·19 | 0·86 |

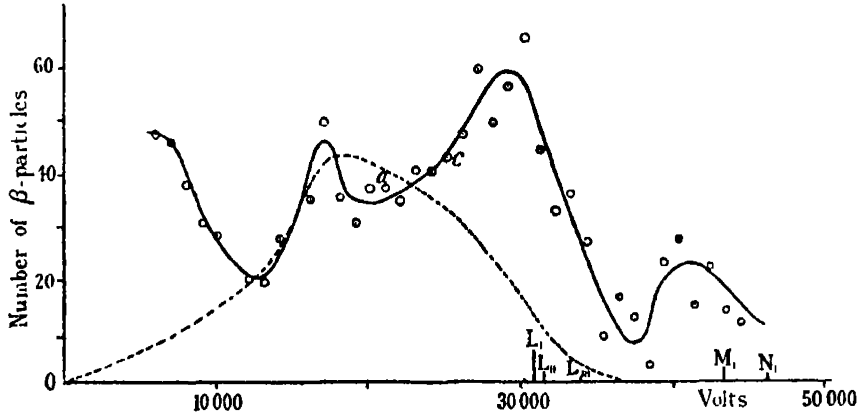

FIG. 4.—The Final Energy Distribution

In interpreting the remainder of the distribution curve it would be useful to know the way in which the energies of the L secondaries will appear spread out owing to straggling. The straggling of the ranges of β-particles of equal initial energy has been shown by Williams to be very large and to be roughly expressed by saying that the probable error of a single range measurement is 20 per cent. The probable error in calculating the energy of a track from its range will therefore be of the order of 10 per cent. and few particles of energy 31,000 volts will appear to have less than 25,000 volts. This conclusion is strengthened by the method of measuring the energy used in the present work, in which the energy lost in all visible side-spurs was added when calculating that of the track. This process should reduce the number of tracks straggled so as to have low apparent energies. Returning to the complete distribution, it is thus apparent that there are many tracks with too little energy to be L secondaries which must, therefore, be due either to nuclear particles or to further secondary groups.

The sharp peak at 18,000 volts might be thought to suggest the presence of such a homogeneous group of intensity less than that at 29,000 volts, but no evidence for this explanation has been provided by magnetic spectra and it is therefore probably correct to regard it as a large probability fluctuation in a continuous distribution.

The curve falls to a minimum at 13,000 volts and then rises up to 6000 volts below which no information was obtainable. The final rise may be accounted for by tertiary electrons. Black* has measured the complex magnetic spectrum of these electrons ejected from radium B, an isotope of radium D. The stronger lines are at 10,400 volts and 8,200 volts. No lines occur below 7,000 volts. This part of the curve cannot be due to δ-rays ejected from the source by the α-particles present as their maximum energy is too small for them to form separate tracks

As a test of the assumption that the energy distribution for the nuclear electrons has its maximum near 20,000 volts, it would be of interest to see if there were room to draw a smooth curve, of shape similar to that found for the nuclear electrons of other β-ray bodies, beneath the main curve of fig. 4. Such a distribution is shown by the broken curve. From the area below this curve the number of electrons per disintegration which it represents on the scale adopted can be found. In the curve shown this number is 0·86, which is sufficiently near to unity to show that the position drawn is a possible one. In order to reach unity a slight spreading of the curve to higher energies would be necessary.

The region between the two curves above 22,000 volts is attributed to the secondary electrons from the L, M, and N levels. The numbers of these have been estimated in the same way from the areas. The resulting numbers per disintegration which are shown in Table II must be regarded as lower limits because of losses due to confusion; also the ranges of the N secondaries are so large that many will reach near to the chamber walls.

Certain results of Gray and O'Leary† bear on this question. They measured the ionisation due (1) to the L X-radiation of radium D; (2) to those of the 47,200 volts nuclear γ-rays which are not absorbed in the parent atom; and (3) to the fast β-particles of radium E present in known relative amount. The third measurement gave the number of disintegrations and the final result was that 11/43 L quanta and 5/43 γ-rays are emitted per disintegration.

---

* 'Proc. Camb. Phil. Soc.,' vol. 22, p. 838 (1925).

† 'Nature,' vol. 123, p. 568 (1929).

The L radiation is emitted as a consequence of the ejection of an L secondary electron, but there is an unknown probability that the L quantum will be absorbed in the parent atom giving rise to one of the tertiary electrons investigated by Black. It is therefore not possible to deduce the number of L secondaries per disintegration from the results of Gray and O'Leary unless the number of these tertiaries is known. The results of Auger* for xenon suggest that it may be a fairly large fraction of the number of L secondaries. The number of the latter in the final distribution curve appears to be definitely more than of the L quanta (11/43 per disintegration) measured by Gray and O'Leary. By assuming that about 30 per cent. of these quanta are internally absorbed the present results can be explained and about 0·12 tertiary electrons per disintegration are to be expected. The data are not adequate to test the latter number.

The balance of the evidence is in favour of the conclusion that the nuclear particles occupy some such position as that shown by the broken curve with a maximum between 18,000 and 20,000 volts, starting from a very low energy value and becoming few in number above, say, 36,000 volts. The possibility that the nuclear particles are mainly below 10,000 volts cannot be completely disproved. But it would require some new explanation for the curve between 10,000 and 25,000 volts and would lead to an exceedingly high figure for the number of L secondaries per disintegration.

2. *Pairs of tracks.*—A careful search was made for tracks coming from the same atom, particularly in the A series of pictures. The strong stereoscopic effect made it easy to produce fairly long tracks back to their origins on the leaf, but for short ones the scattering occurring in the drop-free layer makes the origin uncertain. About 28 groups were found in the A series which consisted in all of 400 disintegrations. About five corresponded to an L secondary and a tertiary electron and perhaps six more could be attributed to a secondary and a nuclear electron with lower energy. The rest, as might be expected, appeared to be random combinations. A small number of pairs which could be classed as nuclear + secondary were seen in the other series.

It cannot be said that the evidence from pairs of tracks either disputes or confirms the conclusions reached in the proceeding section. The result of Kikuchi* who looked for pairs of tracks coming from a silk fibre, activated with radium D, in an expansion chamber, is not confirmed. He failed to find any indubitable pairs and therefore concluded that all the particles which he observed were secondary in origin and that the nuclear electrons had insufficient energy to form tracks. The silk fibre had a stopping power equivalent to 1 cm. of air which would cause the loss of most pairs in which one of the components entered the fibre. Further, the large stopping power of the gas used, carbon dioxide, would make the nuclear tracks short and hard to separate from the secondaries.

---

* 'Ann. Physique,' vol. 6, p. 183 (1926).

## *Summary.*

(1) Stereoscopic photographs of the tracks of the β-particles of radium D were taken using an expansion chamber.

(2) The ranges of 377 tracks, formed in gas mixtures of three different stopping powers, were measured.

(3) A possible complete energy distribution curve is constructed for the particles emitted.

(4) In this distribution the secondary electronic groups are identified and the extent to which the continuous spectrum is represented is discussed.

In conclusion, I wish to thank Lord Rutherford for his interest and encouragement throughout the work, and Drs. J. Chadwick and C. D. Ellis for many very helpful discussions and suggestions.

---

* 'Jap J. Phys,' vol. 4, p 143 (1927).

# *The Photoelectric Effect for γ-Rays.*

By H. R. Hulme, Gonville and Caius College, Cambridge.

(Communicated by P. A. M. Dirac, F R.S.—Received June 2, 1931.)

§ 1. *Introduction.*—A discussion of the photoelectric effect for hydrogen-like atoms has been given by many authors. In the simplest case it is assumed that the wave-length of the incident radiation is large compared with the "radius of the atom." If $z$ be a co-ordinate measured from the centre of the atom, the axes may be chosen so that the perturbing vector potential involves the factor exp. $(\pm 2\pi i z/\lambda)$, where $\lambda$ is the wave-length of the radiation. For very large wave-lengths we put this equal to unity, or we may use the first two terms of the expansion. For very short wave-lengths, however, the expansion is illusory, and we must use some other method For γ-rays the "radius of the atom" is large compared with the wave-length of the rays. A knowledge of the wave-function near the nucleus is therefore necessary. Further, the photo-electrons emitted have velocities comparable to that of light. In view of these two circumstances it is necessary to use a relativistic theory of the atom, and in the following we shall endeavour to apply the theory of the Dirac electron.

In § 2 we develop a normalised solution of the equations for the hydrogen-like atom, when the total energy, E, is greater than $mc^2$, the rest energy of an electron. Next we consider the perturbation theory, which gives the total number of electrons emitted and their resultant forward momentum, in terms of the matrix elements representing transitions from the ground state to states where the electron is free. The chief difficulty is the evaluation of these matrix elements, which is only carried through when the atomic number Z is small, and the wave-length of the incident light is such that the energy of one quantum is comparable to $mc^2$, corresponding to wave-lengths of the order $10^{-10}$ cm. The first restriction is very unsatisfactory, since the photoelectric effect is best observed in heavy atoms. The results obtained are, however, in qualitative agreement with the experimental results for heavy atoms, if we exclude the variation with atomic number.

§ 2. *Solution of the Wave-equation for States of Positive Energy.*—We may write the wave-equation of the electron* as

$$\left[\frac{E}{c} + \frac{e}{c}A_0 + \rho_1\left(\sigma, p + \frac{e}{c}A\right) + \rho_3 mc\right]\psi = 0, \qquad (1)$$

---

* Dirac, 'Proc. Roy. Soc.,' A, vol. 117, p. 610 (1928).

where E is the energy of the system, $A_0$ and A the scalar and vector potentials, **p** the momentum vector $(p_x, p_y, p_z)$ and $\sigma$ the vector $(\sigma_x, \sigma_y, \sigma_z)$. The quantities $\sigma_x, \sigma_y, \sigma_z, \rho_1, (\rho_2)$ and $\rho_3$ do not commute with each other, and may be conveniently represented by certain matrices of four rows and columns which obey the same non-commutability relations. In this representation the wave function $\psi$ has four components. We have further

$$p_x = -\frac{ih}{2\pi}\frac{\partial}{\partial x}, \quad p_y = -\frac{ih}{2\pi}\frac{\partial}{\partial y}, \quad p_z = -\frac{ih}{2\pi}\frac{\partial}{\partial z}.$$

Let us consider a hydrogen-like atom, that is an electron under the influence of a central charge $Ze$. We have $\mathrm{A} = 0$, $\mathrm{A}_0 = \mathrm{V} = Ze/r$, and adopting the representation of the $\sigma$'s and $\rho$'s given by Dirac, we find equation (1) becomes on writing out in full :—

$$\left.\begin{aligned}
\frac{2\pi i}{h}\left(\frac{\mathrm{E}+e\mathrm{V}}{c}+mc\right)\psi_1+\left(\frac{\partial}{\partial x}-i\frac{\partial}{\partial y}\right)\psi_4+\frac{\partial}{\partial z}\psi_3=0\\
\frac{2\pi i}{h}\left(\frac{\mathrm{E}+e\mathrm{V}}{c}+mc\right)\psi_2+\left(\frac{\partial}{\partial x}+i\frac{\partial}{\partial y}\right)\psi_3-\frac{\partial}{\partial z}\psi_4=0\\
\frac{2\pi i}{h}\left(\frac{\mathrm{E}+e\mathrm{V}}{c}-mc\right)\psi_3+\left(\frac{\partial}{\partial x}-i\frac{\partial}{\partial y}\right)\psi_2+\frac{\partial}{\partial z}\psi_1=0\\
\frac{2\pi i}{h}\left(\frac{\mathrm{E}+e\mathrm{V}}{c}-mc\right)\psi_4+\left(\frac{\partial}{\partial x}+i\frac{\partial}{\partial y}\right)\psi_1-\frac{\partial}{\partial z}\psi_2=0
\end{aligned}\right\}. \qquad (2)$$

To solve these equations we transform to polar co-ordinates, $\theta$ being the angle between the $z$-axis and the radius vector. The solutions are then of two types*

$$\left.\begin{aligned}
\psi_1 &= -i\mathrm{F}_k\mathrm{P}^u_{k+1} & \psi_2 &= -i\mathrm{F}_k\mathrm{P}^{u+1}_{k+1}\\
\psi_3 &= (k+u+1)\,\mathrm{G}_k\mathrm{P}^u_k & \psi_4 &= (-k+u)\,\mathrm{G}_k\mathrm{P}^{u+1}_k
\end{aligned}\right\}, \qquad (3\mathrm{A})$$

and

$$\left.\begin{aligned}
\psi_1 &= -i(k+u)\,\mathrm{F}_{-k-1}\mathrm{P}^u_{k-1} & \psi_2 &= -i(-k+u+1)\,\mathrm{F}_{-k-1}\mathrm{P}^{u+1}_{k-1}\\
\psi_3 &= \mathrm{G}_{-k-1}\mathrm{P}^u_k & \psi_4 &= \mathrm{G}_{-k-1}\mathrm{P}^{u+1}_k
\end{aligned}\right\}, \qquad (3\mathrm{B})$$

where $\mathrm{F}_k$, $\mathrm{G}_k$ satisfy

$$\left.\begin{aligned}
\frac{2\pi}{h}\left(\frac{\mathrm{E}+e\mathrm{V}}{c}+mc\right)\mathrm{F}_k+\frac{d\mathrm{G}_k}{dr}-\frac{k}{r}\mathrm{G}_k=0\\
-\frac{2\pi}{h}\left(\frac{\mathrm{E}+e\mathrm{V}}{c}-mc\right)\mathrm{G}_k+\frac{d\mathrm{F}_k}{dr}+\frac{k+2}{r}\mathrm{F}_k=0
\end{aligned}\right\} \qquad (4)$$

and $\mathrm{P}^u_k$ is the associated Legendre function given by

$$\mathrm{P}^u_k = (k-u)!\,\sin^u\theta\left(\frac{d}{d\cos\theta}\right)^{k+u}\frac{(\cos^2\theta-1)^k}{2^k k!}\,e^{iu\phi}, \qquad (5)$$

---

* C. G. Darwin, 'Proc. Roy. Soc.,' A, vol. 118, p. 654 (1928).

$u$ and $k$ being any numbers such that the Legendre functions involved have a meaning (see Darwin, *loc. cit.*). We shall write

$$\left.\begin{aligned} &\frac{2\pi}{h}\left(mc+\frac{\mathrm{E}}{c}\right)=\mathrm{A}^2 \\ & \qquad\qquad\qquad\qquad \gamma = 2\pi e^2\mathrm{Z}/ch = \mathrm{Z}/137 \text{ approx.} \\ &\frac{2\pi}{h}\left(mc-\frac{\mathrm{E}}{c}\right)=\mathrm{B}^2 \end{aligned}\right\} . \tag{6}$$

The equations (4) then become

$$\left.\begin{aligned} &\left(\mathrm{A}^2+\frac{\gamma}{r}\right)\mathrm{F}_k+\frac{d\mathrm{G}_k}{dr}-\frac{k}{r}\mathrm{G}_k=0 \\ &\left(\mathrm{B}^2-\frac{\gamma}{r}\right)\mathrm{G}_k+\frac{d\mathrm{F}_k}{dr}+\frac{k+2}{r}\mathrm{F}_k=0 \end{aligned}\right\} . \tag{7}$$

When $\mathrm{E} < mc^2$, suitable solutions of (7) can be obtained in the form of polynomials for a set of discrete values of the energy. Any positive value of $(\mathrm{E} - mc^2)$ will yield a permissible solution representing a diverging wave for large $r$, corresponding to a hyperbolic orbit on the older theory. For our purposes we require a normalised solution valid for all values of $r$, and such a solution may be obtained in the form of a contour integral.

Equations (7) may be transformed into a standard form by writing

$$\left.\begin{aligned} \mathfrak{F}_k &= \mathrm{AF}_k-\mathrm{BG}_k \\ \mathfrak{G}_k &= \mathrm{AF}_k+\mathrm{BG}_k \end{aligned}\right\} , \tag{8}$$

and we obtain

$$\left.\begin{aligned} r\frac{d\mathfrak{F}_k}{dr} &= \{(ib-1)+iar\}\,\mathfrak{F}_k+\{-ic-(k+1)\}\,\mathfrak{G}_k \\ r\frac{d\mathfrak{G}_k}{dr} &= \{ic-(k+1)\}\,\mathfrak{F}_k+\{(-ib-1)-iar\}\,\mathfrak{G}_k \end{aligned}\right\} , \tag{9}$$

where

$$\left.\begin{aligned} \mathrm{AB} &= ia \\ \frac{\gamma}{2}\left(\frac{\mathrm{A}}{\mathrm{B}}-\frac{\mathrm{B}}{\mathrm{A}}\right) &= -ib \\ \frac{\gamma}{2}\left(\frac{\mathrm{A}}{\mathrm{B}}+\frac{\mathrm{B}}{\mathrm{A}}\right) &= -ic \end{aligned}\right\} \tag{10}$$

and $a, b, c$ are real and positive and $b > c$. Since $\mathrm{E} > mc^2$ we see from equations (6) that A is real and B is imaginary. $\mathfrak{F}_k$ and $\mathfrak{G}_k$ are therefore conjugate quantities.

Let us now try to satisfy (9) by a set of Laplace integrals

$$\left.\begin{aligned}\mathfrak{F}_k &= \int e^{r\zeta} v_1(\zeta)\,d\zeta \\ \mathfrak{G}_k &= \int e^{r\zeta} v_2(\zeta)\,d\zeta\end{aligned}\right\}. \tag{11}$$

On substituting in the equations (9) we find that the conditions to be satisfied are

$$(-ib-1)\int e^{r\zeta}v_2(\zeta)\,d\zeta + \{ic-(k+1)\}\int e^{r\zeta}v_1(\zeta)\,d\zeta = \int re^{r\zeta}(\zeta+ia)\,v_2(\zeta)\,d\zeta$$

$$= [e^{r\zeta}(\zeta+ia)\,v_2(\zeta)] - \int e^{r\zeta}\left\{v_2(\zeta)+(\zeta+ia)\,\frac{dv_2(\zeta)}{d\zeta}\right\}d\zeta$$

on integrating by parts, together with a conjugate condition for $v_1(\zeta)$ and $v_2(\zeta)$ interchanged. These conditions can be fulfilled if we take $v_1(\zeta)$ and $v_2(\zeta)$ to satisfy the Laplace transformed system

$$\left.\begin{aligned}(\zeta-ia)\frac{dv_1}{d\zeta} &= \qquad\qquad -ib\,v_1 + \{(k+1)+ic\}\,v_2 \\ (\zeta+ia)\frac{dv_2}{d\zeta} &= \{(k+1)-ic\}\,v_1 + \qquad\qquad ib\,v_2\end{aligned}\right\} \tag{12}$$

and choose the contours so that the terms

$$[e^{r\zeta}(\zeta-ia)\,v_1(\zeta)] \quad \text{and} \quad [e^{r\zeta}(\zeta+ia)\,v_2(\zeta)]$$

vanish identically in $r$. Since $r$ is necessarily positive, one solution of our equations is a contour starting from $-\infty$, encircling the point $\zeta = ia$ and returning to $-\infty$. A similar contour encircling $\zeta = -ia$ gives a second and independent solution, but in order to obtain a convenient form we shall take a combination of the two—a contour which encircles both points (see figure). We shall now find integrals for $v_1(\zeta)$ and $v_2(\zeta)$. Eliminating $v_1(\zeta)$ from equations (12) we obtain

$$(\zeta^2+a^2)\frac{d^2v_2}{d\zeta^2} + (\zeta - ia - 2ab)\frac{dv_2}{d\zeta} + (\gamma^2-(k+1)^2)\,v_2 = 0, \tag{13}$$

using the fact that $\gamma^2 = b^2 - c^2$. This is of standard form, the solution being

$$v_2(\zeta) = \int_C (t-ia)^{-(\lambda+ib+1)}\,(t+ia)^{-(\lambda-ib+2)}\,(t-\zeta)^{\lambda+1}\,dt,$$

where $\lambda = -1 \pm \sqrt{[(k+1)^2-\gamma^2]}$, and the contour C is chosen so that

$$\int_C d\,[(t-\zeta)^{\lambda}\,(t-ia)^{-(\lambda+ib)}\,(t+ia)^{-(\lambda-ib+1)}] = 0 \tag{14}$$

independently of $\zeta$. If we choose $\lambda = -1 - \sqrt{[(k+1)^2 - \gamma^2]}$, then $\lambda$ and $\lambda + 1$ are negative for all $k \geqslant 0$, and we may take the contour C from $-ia$ to $+ia$. We obtain $v_1(\zeta)$ in a similar manner. We then find

$$v_1(\zeta) = \mathrm{S} \int_{-ia}^{+ia} (t - ia)^{-(\lambda+ib+2)} (t + ia)^{-(\lambda-ib+1)} (t - \zeta)^{\lambda+1} \, dt,$$

$$v_2(\zeta) = \mathrm{T} \int_{-ia}^{+ia} (t - ia)^{-(\lambda+ib+1)} (t + ia)^{-(\lambda-ib+2)} (t - \zeta)^{\lambda+1} \, dt,$$

where S and T are some constants and $|\arg(t \pm ia)| \leqslant \pi$ at the lower limit to make the solution definite. By substitution in equations (12) we find

$$\frac{\mathrm{S}}{\mathrm{T}} = -\frac{(k + \lambda + 2) + i(b + c)}{(k + \lambda + 2) - i(b + c)}. \tag{15A}$$

We now have

$$\left.\begin{aligned} \mathfrak{F}_k &= \mathrm{S} \int_{\mathrm{C}'} e^{r\zeta} \int_{-ia}^{+ia} (t - ia)^{-(\lambda+ib+2)} (t + ia)^{-(\lambda-ib+1)} (t - \zeta)^{\lambda+1} \, dt \, d\zeta \\ \mathfrak{G}_k &= \mathrm{T} \int_{\mathrm{C}'} e^{r\zeta} \int_{-ia}^{+ia} (t - ia)^{-(\lambda+ib+1)} (t + ia)^{-(\lambda-ib+2)} (t - \zeta)^{\lambda+1} \, dt \, d\zeta \end{aligned}\right\}, \tag{16}$$

where the contour C′ is shown in the figure.

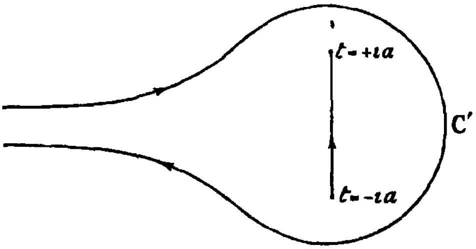

$\lambda + 1$ is negative, so that provided $(t - \zeta)$ is never equal to zero, we may interchange the order of integration. This is realised if we choose the contours as above, and we find on integrating with respect to $r$

$$\mathfrak{G}_k = \mathrm{T}\,(-)^{\lambda+1}\, 2i \sin[(\lambda + 2)\pi]\, \Gamma(\lambda + 2)\, r^{-\lambda+2} \times \int_{-ia}^{+ia} e^{rt} (t - ia)^{-(\lambda+ib+1)} (t + ia)^{-(\lambda-ib+2)} \, dt,$$

and a similar expression for $\mathfrak{F}_k$. Now we are only interested in the ratios of

$\mathfrak{F}_k$ and $\mathfrak{G}_k$, but we must choose the values of S and T so that the functions $\mathfrak{F}_k$ and $\mathfrak{G}_k$ are conjugate complex. We may take as a solution

$$\left.\begin{aligned} \mathfrak{F}_k &= -[(k-s)+i(b+c)]r^s \int_{-ia}^{+ia} (t-ia)^{s-ib}(t+ia)^{s+ib+1} e^{rt}\,dt \\ \mathfrak{G}_k &= [(k-s)-i(b+c)]r^s \int_{-ia}^{+ia} (t-ia)^{s-ib+1}(t+ia)^{s+ib} e^{rt}\,dt \\ \text{where} \quad s &= -(\lambda+2) = \sqrt{[(k+1)^2-\gamma^2]}-1 \end{aligned}\right\}. \tag{17A}$$

For the second form of solution, given by equations (3B), we must replace $k$ by $-k-1$ in equations (7). We then find in a similar way

$$\left.\begin{aligned} \mathfrak{F}_{-k-1} &= -[(b-c)-i(k-1-s')]r^{s'} \int_{-ia}^{+ia} (t-ia)^{s'-ib}(t+ia)^{s'+ib+1} e^{rt}\,dt \\ \mathfrak{G}_{-k-1} &= [(b-c)+i(k-1-s')]r^{s'} \int_{-ia}^{+ia} (t-ia)^{s'-ib+1}(t+ia)^{s'+ib} e^{rt}\,dt \\ \text{where} \quad s' &= -(\lambda'+2) = \sqrt{(k^2-\gamma^2)}-1. \end{aligned}\right\}. \tag{17B}$$

There are no solutions of this type for $k=0$, so that the condition (14) can always be fulfilled.

For the purposes of normalisation, we shall require the forms of $F_k$ and $G_k$ when $r$ is large. To find these we deform the contour into three parts and put

$$\int_{-ia}^{+ia} f(r,t)\,dt = \int_{-ia}^{-ia-R} f(r,t)\,dt + \int_{-ia-R}^{+ia-R} f(r,t)\,dt + \int_{+ia-R}^{+ia} f(r,t)\,dt.$$

On allowing R to tend to $\infty$, the middle integral tends to zero, and we are left with the other two. In the first one we put $t = -ia - x$, and in the second $t = ia - x$. This gives

$$\begin{aligned} \int_{-ia}^{+ia} (t-ia)^{s-ib+1}(t+ia)^{s+ib} e^{rt}\,dt = &-(e^{i\pi})^{s+ib} e^{-iar} (2a)^{s-ib+1} \left(e^{-\frac{i\pi}{2}}\right)^{s-ib+1} \\ &\times \int_0^\infty x^{s+ib}\left(1+\frac{x}{2ia}\right)^{s-ib+1} e^{-rx}\,dx \\ &-(e^{-i\pi})^{s-ib+1} e^{iar} (2a)^{s+ib} \left(e^{\frac{i\pi}{2}}\right)^{s+ib} \int_0^\infty x^{s-ib+1}\left(1-\frac{x}{2ia}\right)^{s+ib} e^{-rx}\,dx. \end{aligned}$$

When $r$ is large, the important part of the integral occurs when $x$ is small.

We may therefore expand in powers of $x$ and integrate term by term, obtaining, since the second integral gives $r^{-(ib+2)}$,

$$\mathfrak{G}_k = i^{s+1}[(k-s) - i(b+c)]\,e^{-\frac{3\pi b}{2}}(2a)^{s+1}\,\Gamma(s+ib+1) \\ \times e^{-iar}\,r^{-(ib+1)}\left(1 + 0\left(\frac{1}{r}\right)\right), \quad (18)$$

which gives asymptotic forms of $\mathrm{F}_k$ and $\mathrm{G}_k$,

$$\left.\begin{aligned} \mathrm{F}_k &= \frac{1}{\mathrm{A}}\sqrt{[(k-s)^2+(b+c)^2]}\,|\Gamma(s+ib+1)| \\ &\qquad \times e^{-\frac{3\pi b}{2}}(2a)^{s+1}\frac{1}{r}\cos(ar + b\log r + \delta_a) \\ \mathrm{G}_k &= \frac{1}{|\mathrm{B}|}\sqrt{[(k-s)^2+(b+c)^2]}\,|\Gamma(s+ib+1)| \\ &\qquad \times e^{-\frac{3\pi b}{2}}(2a)^{s+1}\frac{1}{r}\cos(ar + b\log r + \delta'_a) \end{aligned}\right\}, \quad (19)$$

where $\delta_a$ and $\delta'_a$ are independent of $r$. We have corresponding asymptotic forms for $\mathrm{F}_{-k-1}$ and $\mathrm{G}_{-k-1}$.

We may write the normalising and orthogonality conditions as follows

$$\int \sum^{4} \psi_r(\mathrm{E}, k, u)\,\psi_r^*(\mathrm{E}', k', u')\,d\,\mathrm{vol} \\ = \left\{\begin{matrix} \delta_{\mathrm{EE}'}\,\delta_{kk'}\,\delta_{uu'} \quad \text{for discrete states} \\ \frac{1}{h}\,\delta(\mathrm{E}-\mathrm{E}')\,\delta_{kk'}\,\delta_{uu'} \ \text{for continuous states} \end{matrix}\right\}, \quad (20)$$

using the $\delta$ function, the integral being taken over all space. It is easily verified in the usual way that the solutions are orthogonal. We have further

$$\int_0^{\pi}\int_0^{2\pi} p_k^u p_k^{u*} \sin\theta\,d\theta\,d\phi = \frac{4\pi}{2k+1}(k+u)!\,(k-u)!, \quad (21)$$

which gives for the solution (3A)

$$4\pi(k+u+1)!\,(k-u)!\int_0^\infty (\mathrm{F}_k(\mathrm{E})\,\mathrm{F}_k^*(\mathrm{E}') + \mathrm{G}_k(\mathrm{E})\,\mathrm{G}_k^*(\mathrm{E}'))\,r^2\,dr = \frac{1}{h}\,\delta(\mathrm{E}-\mathrm{E}')$$

as the normalisation condition.

We shall employ the method of normalisation used by Gaunt,† which is equivalent to taking a special form of the $\delta$ function. It is easily adapted to the case when $\psi$ has four components, and for convenience we shall express the normalising factor, $\xi(\mathrm{E}, k, u)$, as the product of $\xi(\mathrm{E}, k)$, the normalising factor of the radial part of the wave function, and $\xi(k, u)$, that of the angular part. We obtain for the solutions (3A)

---

† Gaunt, 'Phil. Trans.,' A, vol. 229, p. 163 (1930).

$$\left.\begin{aligned} &\xi(\mathrm{E}, k) = \left(\frac{2\pi\mathrm{E}}{hc^2a}\right)^{\frac{1}{2}} \frac{\mathrm{A}\,|\mathrm{B}|}{\mathrm{A}^2 + |\mathrm{B}|^2}\,\mathrm{K}^{-1} \\ \text{with}\quad &\mathrm{K} = \tfrac{1}{2}\sqrt{[(k-s)^2 + (b+c)^2]}\,|\Gamma(s + ib + 1)|\,e^{-\frac{3\pi b}{2}}(2a)^{s+1} \\ \text{and}\quad &\xi(k, u) = \sqrt{[4\pi\,(k+u+1)!\,(k-u)!]} \end{aligned}\right\}. \tag{22A}$$

To obtain $\xi(\mathrm{E}, -k-1)$ and $\xi(-k-1, u)$, the normalising factors for solutions of type (3B), we replace $k$ by $k-1$, $s$ by $s'$ and $c$ by $-c$ in the above.

§ 3. *Perturbation Theory.*—Let us now consider the case of a hydrogen-like atom in the field of a train of plane waves travelling in a direction parallel to the $z$-axis and represented by

$$\left.\begin{aligned} &\mathrm{A}_y = b_0\,[e^{2\pi i\nu_0(t-z/c)} + e^{-2\pi i\nu_0(t-z/c)}], \\ &\mathrm{A}_x = \mathrm{A}_z = 0, \qquad \mathrm{A}_0 = 0 \end{aligned}\right\}. \tag{23}$$

From (1), the wave equation is

$$\left[\frac{\mathrm{E}}{c} + \frac{e}{c}\mathrm{A}_0 + \rho_1(\boldsymbol{\sigma}, \mathbf{p}) + \rho_3\,mc\right]\psi = -\frac{e}{c}\mathrm{A}_y\rho_1\sigma_y\psi. \tag{24}$$

If $\mathrm{A}_0 = \mathrm{Z}e/r$, the equation obtained by equating the left-hand side to zero gives the equation for the undisturbed atom. We shall assume $\mathrm{A}_y$ to be small, and treat the right-hand side as a small perturbation. Put

$$\mathrm{V} = -\frac{e}{c}\mathrm{A}_y\rho_1\sigma_y \tag{25}$$

and try as a solution

$$\psi = \sum_{\substack{\mathrm{E}' < mc^2,\\ k',\,u'}} a_{\mathrm{E}',k',u'}\,\psi_{\mathrm{E}',k',u'}\,e^{-2\pi i\mathrm{E}'t/h} + \sum_{k',\,u'}\int_{mc^2}^{\infty} a(\mathrm{E}', k', u')\,\psi(\mathrm{E}', k', u') \times e^{-2\pi i\mathrm{E}'t/h}\,d\mathrm{E}'/h, \tag{26}$$

where $\psi_{\mathrm{E}',k',u'}$ and $\psi(\mathrm{E}', k', u')$ are solutions of the equation for the undisturbed atom, and the $a$'s are functions of the time. In this section we are assuming the $\psi$'s to be normalised, and labelling the final state with $\mathrm{E}'$, $k'$, $u'$, and the initial with $\mathrm{E}''$, $k''$, $u''$. When $\mathrm{A}_y$ is small, $\psi$ changes slowly, and if the time $t$ be not too great we may replace $\psi$ by $\psi_{\mathrm{E}'',k'',u''}\exp.(-2\pi i\mathrm{E}''t/h)$ on the right-hand side of (24), which involves an error of the second order since V is already small. Substituting (25) and (26) in equation (24) we have

$$\sum_{\substack{E'<mc^2,\\ k',\,u'}} a_{E',k',u'}\,\psi_{E',k',u'}\,e^{-2\pi i E't/h}+\sum_{k',u}\int_{mc^2}^{\infty} a\,(E',k',u')\,\psi\,(E',k',u')\,e^{-2\pi i E\,t/h}\,dE'/h$$

$$=\frac{2\pi c}{ih}V\psi_{E'',k'',u''}\,e^{-2\pi i E''t/h}, \qquad (27)$$

whence we obtain

$$\dot{a}\,(E',k',u')=\frac{2\pi c}{ih}(E',k',u'\mid V\mid E'',k'',u''). \qquad (28)$$

Putting

$$E'-E''=h\nu, \qquad (29)$$

and taking the time factor outside, we obtain on integration

$$a\,(E',k',u')=\frac{2\pi c}{ih}\left[\begin{array}{l}\left(E',k',u'\left|-b_0\rho_1\sigma_\nu\frac{e}{c}e^{2\pi i\nu_0 z/c}\right|E'',k'',u''\right)\dfrac{e^{2\pi i(\nu-\nu_0)t}-1}{2\pi i\,(\nu-\nu_0)}\\ +\left(E',k',u'\left|-b_0\rho_1\sigma_\nu\frac{e}{c}e^{2\pi i\nu_0 z/c}\right|E'',k'',u''\right)\dfrac{e^{2\pi i(\nu+\nu_0)t}-1}{2\pi i\,(\nu+\nu_0)}\end{array}\right]. \qquad (30)$$

The first term is important in the region $\nu\simeq\nu_0$, or $E'\simeq E''+h\nu_0$, and concerns the absorption of radiation. The second is only important when $\nu\simeq-\nu_0$, or $E'\simeq E''-h\nu_0$, and concerns the stimulated emission. We shall therefore neglect the second term as we are considering the absorption of radiation leading to a transition from a state where $E<mc^2$, to one where $E>mc^2$, that is, the emission of an electron. Practically all the electrons are emitted with energies $E'\simeq E''+h\nu_0$, and the total number transferred to energies in this neighbourhood is given by

$$\sum_{k',u'}\int\mid a\,(E',k',u')\mid^2 dE'/h \qquad (E'\simeq E''+h\nu_0). \qquad (31)$$

Since the integrand is only important when $E'\simeq E''+h\nu_0$, we may use the first term of (30) and take the matrix element outside the integral. On writing $x=2\pi(\nu-\nu_0)$, we see that the limits of the integral are immaterial provided they enclose the region $x\simeq 0$. We take then from $-\infty$ to $+\infty$, and the expression for the total number of electrons emitted becomes

$$\sum_{k',u'}\left(\frac{2\pi e b_0}{h}\right)^2\mid(E',k',u'\mid-\rho_1\sigma_\nu e^{2\pi i\nu_0 z/c}\mid E'',k'',u'')\mid^2\int_{-\infty}^{+\infty}\frac{2\,(1-\cos x)}{x^2}\frac{t}{2\pi}dx$$

$$=\sum_{k'u'}\left(\frac{2\pi e b_0}{h}\right)^2\mid(E',k',u'\mid-\rho_1\sigma_\nu e^{2\pi i\nu_0 z/c}\mid E'',k'',u'')\mid^2 t, \quad (32)$$

which is proportional to $t$, as it must be. For the validity of the above, $t$ must be large compared with the periods of the atomic oscillations, but not too large, or else we cannot replace $\psi$ by $\psi_{E'', k'', u''} \exp. (-2\pi i E'' t/h)$ in (27). Both these conditions can be realised provided the transition probability is small compared with unity. If we multiply (32) by $h\nu_0$ and divide by $t$ we obtain the rate of absorption of energy. The intensity of the radiation is $2\pi\nu_0{}^2b_0{}^2/c$, so that the rate of absorption from a beam of unit intensity is

$$\frac{2\pi ce^2}{h\nu_0} \sum_{k'u'} \left| (E', k', u' \,|\, -\rho_1\sigma_y e^{2\pi i\nu z/c} \,|\, E'', k'', u'') \right|^2, \tag{33}$$

which we shall define as the absorption coefficient

§ 4. *Space Distribution of Photo-electrons.*—The distribution of the initial directions of the photo-electrons relative to the direction of the incident beam is usually called the "longitudinal distribution." In our case this is the dependence on $\theta$, the angle between the direction of the wave and that of the velocity of the electron emitted. The "lateral distribution," which is that relative to $\phi$, is not of very great interest, and we shall not consider it, except to remark that it is uniform for a non-polarised beam.

For very long wave-lengths, experiment shows that the density is proportional to $\sin^2 \theta$, whilst for shorter wave-lengths there is greater emission in a forward direction. If $\lambda$, the wave-length, be not too small, the theory yields the following variation of the density J with $\theta$,

$$J \sim (1 + \varepsilon \cos \theta) \sin^2 \theta. \tag{34}$$

The first calculations of the quantity $\varepsilon$ were incorrect because insufficient distinction was drawn between the wave-function and its component parts representing converging and diverging waves. This is corrected in a paper by Sommerfeld and Schur* who obtain a value

$$\varepsilon = 4v/c, \tag{35}$$

where $v$ is the velocity of the photo-electron, the treatment being non-relativistic. The quantities usually measured experimentally are (1) the ratio of the number of photo-electrons emitted in a forward to those emitted in a backward direction; (2) the value of the bipartition angle, which is the semi-angle at the apex of a cone having the incident beam as its axis and dividing the photo-electron beam into two equal parts; and (3) the average value of the forward momentum of an electron. We shall consider the last as being the most convenient for our purposes and also the most significant. To find the actual dependence on $\theta$ would be more difficult and without any special interest. It would certainly not obey the simple law of equation (34).

---

* Sommerfeld and Schur, 'Ann. Phys.,' vol. 4 (1930).

Considering first the case of fairly long wave-lengths, we have

$$J \sim (1 + 4v\cos\theta/c)\sin^2\theta, \qquad (36)$$

which gives

$$\overline{\cos\theta} = 4v/5c.$$

Thus the average forward momentum is

$$4mv^2/5c = \tfrac{8}{5}h\nu_0/c, \qquad (37)$$

where we neglect the work required to liberate the electron, which is small compared with $h\nu_0$ when $\epsilon$ is appreciable. Now $h\nu_0/c$ is the momentum of the light quantum, so that the photo-electrons have an average forward momentum which is 8/5 times that of the light quantum liberating them. The statement on p. 410 of the paper just quoted, that the average momentum of the photo-electrons is $2h\nu_0/c$, does not seem to be correct. In the calculation on pp. 427–429, the authors assume a distribution $J \sim \sin^2\theta$, and then add on to the momentum of each photo-electron a quantity $h\nu_0/c$ in the direction of the light ray, obtaining a distribution

$$J \sim (1 + 2v\cos\theta/c)\sin^2\theta.$$

As the actual distribution is given by equation (36), it is inferred that the average momentum of the electrons is $2h\nu_0/c$. This procedure, however, is incorrect† because the resultant velocities of the electrons do not satisfy the Einstein law, $h\nu_0 = mv^2/2$. Actually if the initial momenta are so chosen that when compounded with $h\nu_0/c$, the resultant momenta all correspond to velocities $v$ given by $h\nu_0 = mv^2/2$, then it can be shown that the average forward momentum is $4h\nu_0/5$.

Let us consider the average forward momentum for very short wave-lengths, using relativistic theory. Neglecting as before the work required to liberate the electron we have

$$h\nu_0 + m_0c^2 = m_0c^2\beta'.$$

$$\text{Momentum of electron} = m_0v\beta',$$

where

$$\beta' = \sqrt{(1 - v^2/c^2)}.$$

---

† Williams, Nutall and Barlow, 'Proc. Roy. Soc.,' A, vol. 121, p. 611 (1928).

This gives for the ratio of the average forward momentum of an electron to that of the light quantum a value

$$\left.\begin{aligned} &\frac{v}{c}\,\frac{\beta'}{\beta'-1}\,\overline{\cos\theta} \\ &= \frac{1}{\tau}\,\overline{\cos\theta}, \\ \text{where}\qquad &\tau^2 = (1+2mc^2/h\nu_0)^{-1} \end{aligned}\right\}. \tag{38}$$

The average forward momentum of the electrons is therefore equal to

$$\frac{h\nu_0}{c\tau}\,\overline{\cos\theta}. \tag{39}$$

If $\psi$ be the wave function of the final state, we have

$$\overline{\cos\theta} = \frac{\int_0^\pi\int_0^{2\pi}\psi\psi^*\cos\theta\sin\theta\,d\theta\,d\phi}{\int_0^\pi\int_0^{2\pi}\psi\psi^*\sin\theta\,d\theta\,d\phi}. \tag{40}$$

We may use the asymptotic form of $\psi$ since we are only interested in the distribution at large distances from the nucleus. Here the contributions of the discontinuous spectrum tend to zero very rapidly and we therefore put

$$\psi = \sum_{k,u'}\int_{mc^2}^{\infty} a\,(\mathrm{E}', k', u')\,\psi\,(\mathrm{E}', k', u')\,e^{2\pi i \mathrm{E}' t/h}\,d\mathrm{E}'/h. \tag{41}$$

Each $\psi\,(\mathrm{E}', k', u')$ involves functions of the type given by equations (19), and therefore represents both converging and diverging waves. The quantity $a(\mathrm{E}', k', u')$ involves the matrix element

$$(\mathrm{E}', k', u' \,|\, -\rho_1\sigma_y e^{2\pi i\nu_0 z/c} \,|\, \mathrm{E}'', k'', u''),$$

but it is only important when $\mathrm{E}' \simeq \mathrm{E}'' + h\nu_0$, so that we may put in this value and take it outside the integral. On integrating over this range, the part representing the converging wave vanishes, and we are left with a diverging wave, which is the only physically significant solution.† For sufficiently large $t$ we find that the denominator in the expression (40) for $\overline{\cos\theta}$ is equal to the expression (32) for the total number of electrons emitted, which is what we should expect. We write $m^a_{u',k'}$, $m^b_{u',k'}$, for the matrix elements

$$(\mathrm{E}', k', u' \,|\, -\rho_1\sigma_y e^{2\pi i\nu_0 z/c} \,|\, \mathrm{E}'', k'', u'')$$

---

† See Bethe, 'Ann. Phys.,' vol. 4, p. 443 (1930).

in (32), according as the final state is of type (3A) or (3B). Taking into account the values of $\delta_a$, $\delta'_a$, etc., at the resonance point $E' = E'' + h\nu_0$, we obtain finally for $\overline{\cos\theta}$ the value

$$\frac{2\sum\limits_{u,k'}\left[\frac{\sqrt{(k'+u'+2)(k'-u'+1)}}{2k'+3}m^a_{u',k'}m^a_{u',k'+1}+\frac{\sqrt{(k'+u'+1)(k'-u')}}{2k'+1}m^b_{u',k'}m^b_{u',k'+1}+\frac{2u'+1}{2(2k'+1)(2k'+3)}m^a_{u',k'}m^b_{u',k'+1}\right]}{\sum\limits_{u',k'}\left[(m^a_{u,k'})^2+(m^b_{u',k})^2\right].} \qquad (42)$$

Actually the last term vanishes on summation, owing to equalities between the matrix elements. In this expression, as well as in the expression (33) for the absorption coefficient, only $(m_{u',k'})^2$ or $(m_{u',k'}\,m_{u',k'+1})$ occur. These decrease rapidly with $k'$, so that in the region of wave-length $\lambda = h/mc$, about 10 terms suffice to give an accuracy of one in one hundred.

§ 5. *Calculation of the Matrix Elements.*—We have

$$-\rho_1\sigma_y = \begin{pmatrix} 0 & 0 & 0 & i \\ 0 & 0 & -i & 0 \\ 0 & i & 0 & 0 \\ -i & 0 & 0 & 0 \end{pmatrix},$$

so that the matrix element $m^a_{u',k'}$ is really the sum of four elements

$$\left.\begin{aligned} &(\psi_1' \mid ie^{2\pi i\nu_0 z/c} \mid \psi_4'') + (\psi_2' \mid -ie^{2\pi i\nu_0 z/c} \mid \psi_3'') \\ +\,&(\psi_3' \mid ie^{2\pi i\nu_0 z/c} \mid \psi_2'') + (\psi_4' \mid -ie^{2\pi i\nu_0 z/c} \mid \psi_1'') \end{aligned}\right\}. \qquad (43)$$

We shall assume that the atom is initially in the state of lowest energy. The forms of the wave functions are obtained from equations (3A) and (3B). For $k = 0$ there are two solutions of type (3A) but none of type (3B). They correspond to $u = 0$ and $u = -1$. Thus the initial state is a combination of two states, corresponding to two different directions of spin. If we write

$$a_0 = \frac{h^2}{4\pi^2 mZe^2} \quad \text{(radius of the atom on the Bohr theory)},$$

$$\beta = \sqrt{(1-\gamma^2)} - 1,$$

we have†

$$\left.\begin{array}{ll} \psi_1 = -\dfrac{i\gamma}{1+\sqrt{(1-\gamma^2)}}\, r^{\beta} e^{-r/a_0} \cos\theta & \psi_2 = -\dfrac{i\gamma}{1+\sqrt{(1-\gamma^2)}}\, r^{\beta} e^{-r/a_0} \sin\theta e^{i\phi} \\ \psi_3 = \qquad r^{\beta} e^{-r/a_0} & \psi_4 = \qquad 0 \end{array}\right\} \quad (44)$$

and

$$\left.\begin{array}{ll} \psi_1 = \dfrac{i\gamma}{1+\sqrt{(1-\gamma^2)}}\, r^{\beta} e^{-r/a_0} \sin\theta e^{-i\phi} & \psi_2 = -\dfrac{i\gamma}{1+\sqrt{(1-\gamma^2)}}\, r^{\beta} e^{-r/a_0} \cos\theta \\ \psi_3 = \qquad 0 & \psi_4 = \qquad -r^{\beta} e^{-r/a_0} \end{array}\right\}. \quad (45)$$

We shall label these states $a_1$ and $a_2$. The energy in both cases is equal to $mc^2\sqrt{(1-\gamma^2)}$. These wave functions are easily normalised according to the rule for discrete states, and, if $\xi(\mathrm{E}_0)$ be the normalising factor, we have in both cases

$$[\xi(\mathrm{E}_0)]^2\, 4\pi \left(\frac{a_0}{2}\right)^{1+2\sqrt{(1-\gamma^2)}} \Gamma[1+2\sqrt{(1-\gamma^2)}]\, \frac{2}{1+\sqrt{(1-\gamma^2)}} = 1. \quad (46)$$

We take our initial state to be

$$\frac{1}{\sqrt{2}}\,\xi(\mathrm{E}_0)\,(\psi(k=0, u=0)\, e^{ip} + \psi(k=0, u=-1) e^{ip'}), \quad (47)$$

where $p$ and $p'$ are arbitrary phase factors. In our result we must then average over all values of $p$ and $p'$.

The matrix elements in (43) now take one of the following forms

$$\int_0^{\pi}\!\!\int_0^{2\pi}\!\!\int_0^{\infty} e^{-r/a_0} r^{\beta} \left\{\begin{array}{c} 1 \\ \cos\theta \\ \sin\theta e^{i\phi} \\ \sin\theta e^{-i\phi} \end{array}\right\} e^{i2\pi r\cos\theta/\lambda}\, \mathrm{P}_n^m(\cos\theta) f(r)\, r^2 \sin\theta\, d\theta\, d\phi\, dr, \quad (48)$$

where $\mathrm{P}_n^m(\cos\theta)$ is one of the wave functions of the final state. We write

$$e^{i2\pi r\cos\theta/\lambda} = \sum_{j=0}^{j=\infty} (2j+1)\, \frac{i^j}{j\,!} \sqrt{\left(\frac{\pi}{2r\,.\,2\pi/\lambda}\right)}\, \mathrm{J}_{j+\frac{1}{2}}(2\pi r/\lambda) \mathrm{P}^0{}_j \cos\theta, \quad (49)$$

where $\mathrm{J}_n(x)$ is Bessel's function of order $n$. The expression (48) now takes the form

$$\int_0^{\pi}\!\!\int_0^{2\pi}\!\!\int_0^{\infty} \left\{\begin{array}{c} 1 \\ \cos\theta \\ \sin\theta e^{i\phi} \\ \sin\theta e^{-i\phi} \end{array}\right\} \mathrm{P}_n^m(\cos\theta) \left\{\sum_{j=0}^{j=\infty} f_j(r)\, \mathrm{P}_j^0(\cos\theta)\right\} r^2 \sin\theta d\theta d\phi dr. \quad (50)$$

---

† Darwin, *loc. cit.*

The integration with respect to θ and $\phi$ yields a selection rule for $u$. All the integrals of type (50), involving three Legendre functions, vanish; excepting those below. For these we have

$$\left.\begin{aligned}\int_0^\pi\int_0^{2\pi} \mathrm{P}_k^{u*} \cos\theta\, \mathrm{P}_{k+1}^{u} \sin\theta\, d\theta\, d\phi &= \frac{4\pi (k+u+1)!\,(k-u+1)!}{(2k+1)(2k+3)}\\ \int_0^\pi\int_0^{2\pi} \mathrm{P}_k^{u*} \sin\theta\, e^{-i\phi}\, \mathrm{P}_{k+1}^{u+1} \sin\theta\, d\theta\, d\phi &= \frac{4\pi (k+u+2)!\,(k-u)!}{(2k+1)(2k+3)}\\ \int_0^\pi\int_0^{2\pi} \mathrm{P}_k^{u*} \sin\theta\, e^{i\phi}\, \mathrm{P}_{k+1}^{u-1} \sin\theta\, d\theta\, d\phi &= -\frac{4\pi (k+u)!\,(k-u+2)!}{(2k+1)(2k+3)}\end{aligned}\right\}, \quad (51)$$

together with the conjugate equations.

We may represent the possible values of $u$ in the scheme below. In the first row we place the $(0, \phi)$ part of the initial wave function, in the second row, that of the two possible types of final wave function—(3A) and (3B). The latter we write in inverted order so that $\psi_4$ (final) is under $\psi_1$ (initial), and then form products in the same column. In the third row we have a term $\mathrm{P}_n^0$ from the expansion of $e^{i2\pi r\cos\theta/\lambda}$. In the fourth row we place those Legendre functions which give an integral $\neq 0$ when combined with the initial function and $\mathrm{P}_n^0$. When $n$ and $u$ have values such that a term in row two is equal to a corresponding term in the last row, we have a possible final state with a given value of $u$, and the values of $n$ show what terms in the expansion (49) contribute towards the integral.

| Initial state | | | $-\mathrm{P}_1^0 e^{ip}$, $-\mathrm{P}_1^{-1} e^{ip'}$ | $-\mathrm{P}_1^1 e^{ip}$, $-\mathrm{P}_1^0 e^{ip'}$ | $\mathrm{P}_0^0 e^{ip}$ | $-\mathrm{P}_0^0 e^{ip'}$ |
|---|---|---|---|---|---|---|
| Final state | | | $\mathrm{P}_k^{u+1*}$ | $\mathrm{P}_k^{u*}$ | $\mathrm{P}_{k\pm1}^{u+1*}$ | $\mathrm{P}_{k\pm1}^{u*}$ |
| Term in expn of $e^{i2\pi r\cos\theta/\lambda}$ | | | $\mathrm{P}_n^0$ | $\mathrm{P}_n^0$ | $\mathrm{P}_n^0$ | $\mathrm{P}_n^0$ |
| Possible value of Legendre function in final state | | | $\mathrm{P}_{n\pm1}^{0*}$, $\mathrm{P}_{n\pm1}^{-1*}$ | $\mathrm{P}_{n\pm1}^{1*}$, $\mathrm{P}_{n\pm1}^{0*}$ | $\mathrm{P}_n^{0*}$ | $\mathrm{P}_n^{0*}$ |
| Possible values of $u$. | $u = 0$ | $n = k-1$ | | $a_2$ and $b_2$ | | $b_2$ |
| | | $n = k+1$ | | $a_2$ and $b_2$ | | $a_2$ |
| | $u = 1$ | $n = k-1$ | | $a_1$ and $b_1$ | | |
| | | $n = k+1$ | | $a_1$ and $b_1$ | | |
| | $u = -1$ | $n = k-1$ | $a_1$ and $b_1$ | | $b_1$ | |
| | | $n = k+1$ | $a_1$ and $b_1$ | | $a_1$ | |
| | $u = -2$ | $n = k-1$ | $a_2$ and $b_2$ | | | |
| | | $n = k+1$ | $a_2$ and $b_2$ | | | |

We label the combination $a$, $b$, when the final state is of type (3A), (3B) respectively, and with suffix 1, 2, when the initial wave function which contributes to the integral is of type $a_1$, $a_2$, respectively.

We shall consider wave-lengths in the region of $10^{-10}$ cm., corresponding to hard $\gamma$-rays. For these rays the electron emitted has an energy E such that $E - mc^2$ is comparable to $E + mc^2$. Hence $A/|B|$ and $F/G$ are of order unity. It might now appear that the order of magnitude of the matrix elements in (43) depended on the initial state alone, so that we could neglect those involving the $\psi_1$ and $\psi_2$ of the initial state, since they are multiplied by a factor $\gamma$. We shall find, however, that the others are also of the same order, so that we must take all four elements of (43) into consideration. When we average the result over all phases of the initial state we find that the square of the matrix element

$$|(\psi\,(\text{final})\,|\,P\,|\,\psi\,(k=0,\,u=0)e^{i\nu} + \psi\,(k=0,\,u=-1)\,e^{i\nu'})\,|^2$$

splits up into

$$|(\psi\,(\text{final})\,|\,P\,|\,\psi\,(k=0,\,u=0))\,|^2 + |(\psi\,(\text{final})\,|\,P\,|\,\psi\,(k=0,\,u=-1))\,|^2.$$

From the table of combinations it now follows that after applying this, each square in (33) reduces to the sum of three integrals for $u = 0$ or $-1$, and two integrals when $u = 1$ or $-2$. Certain exceptions occur when $k = 0$ or 1, which are indicated in the following pages. Similar remarks apply to the expression (42) for $\overline{\cos\theta}$.

We now restrict ourselves to an atom for which the atomic number Z is small, so that $\gamma = Z/137$ approximately, is small compared with unity. In this case

$$\xi(E_0) = (\pi a_0{}^3)^{-\frac{1}{2}} \text{ approximately.} \tag{52}$$

Let us now consider the integrals represented by $a_2$, $b_2$, etc., in the table, taking the combinations column by column.

I. *Combinations in the First Column.*

The matrix element is

$$(\psi_4\,(\text{final})\,|\,-ie^{2\pi ir\cos\theta/\lambda}\,|\,\psi_1\,(\text{initial})).$$

We shall calculate this for the various initial and final states, with the genera value for the suffix $k$ of the final state.

(A) *Initial $a_1$ state, $u = -1$ in final state.*

We have for the integrand

$$\left[\frac{1}{\sqrt{2}}(\pi a_0{}^3)^{-\frac{1}{2}}\frac{\gamma}{1+\sqrt{(1-\gamma^2)}}\right].\left[-ir^{\beta}e^{-r/a_0}\,P_1^0\right].\left[-ie^{2\pi ir\cos\theta/\lambda}\,\psi_4{}^*\,(\text{final})\right].$$

(1) *Final a state.*

Expand the exponential and choose one term, say the term in $P_n^0$. This gives, on putting $\sqrt{(1-\gamma^2)} = 1$,

$$\left[(\pi a_0)^{-3/2}\frac{\Upsilon}{4}r^{\beta}e^{-r/a_0}\sqrt{\left(\frac{\pi}{2\pi r/\lambda}\right)}\right]\left[P_1^0 \,.\, P_k^{0*} \,.\, P_n^0\right]$$
$$\times\left[-\xi(E, k)\,\xi(k, u)\,(-k+u)\,G_k{}^*\,\frac{2n+1}{n\,!}\,i^n\,J_{n+\frac{1}{2}}(2\pi r/\lambda)\right].$$

Denote the first bracket by $M/\sqrt{4\pi}$. On multiplying the above by $\sin\theta\, d\theta\, d\phi$, and integrating over the sphere, we obtain the following results, using (51) :—

$n = k + 1$

$$\frac{k+1}{2k+1}\sqrt{(k+1)}\,i^{k+1}\,M \,.\, J_{k+1+\frac{1}{2}}(2\pi r/\lambda) \,.\, G_k{}^* \,.\, \xi(E, k)\,.$$

$n = k - 1$

$$\frac{k}{2k+1}\sqrt{(k+1)}\,i^{k-1}\,M \,.\, J_{k-1+\frac{1}{2}}(2\pi r/\lambda) \,.\, G_k{}^*\quad \xi(E, k).$$

For all other values of $n$ the term is zero. The integrand with respect to $r$ is therefore the sum of these two.

The following results are obtained in a similar way :—

(2) *Final b state.* $k \geqslant 1$

$n = k + 1$

$$-\frac{k+1}{2k+1}\sqrt{k}\,i^{k+1}\,M \,.\, J_{k+1+\frac{1}{2}}(2\pi r/\lambda)\,G^*{}_{-k-1}\,\xi(E, -k-1)\,.$$

$n = k - 1$

$$-\frac{k}{2k+1}\sqrt{k}\,i^{k-1}\,M \,.\, J_{k-1+\frac{1}{2}}(2\pi r/\lambda)\,G^*{}_{-k-1}\,\xi(E, -k-1).$$

(B) *Initial $a_2$ state, $u = -2$ in final state.*

(1) *Final a state.* $k \geqslant 1$.

$n = k + 1$

$$-\frac{\sqrt{[k(k+1)(k+2)]}}{2k+1}\,i^{k+1}\,M \,.\, J_{k+1+\frac{1}{2}}(2\pi r/\lambda)\,G_k{}^*\,\xi(E, k).$$

$n = k - 1$

$$\frac{\sqrt{[k(k+1)(k+2)]}}{2k+1}\,i^{k-1}\,M \,.\, J_{k-1+\frac{1}{2}}(2\pi r/\lambda)\,G_k{}^*\,\xi(E, k).$$

(2) *Final b state.* $k \geqslant 2$.

$n = k + 1$

$$\frac{\sqrt{[(k-1)\,k\,(k+1)]}}{2k+1}\, i^{k+1}\mathrm{M} \,.\, \mathrm{J}_{k+1+\frac{1}{2}}(2\pi r/\lambda)\, \mathrm{G}^{*}_{-k-1}\, \xi\,(\mathrm{E}, -k-1).$$

$n = k - 1$

$$-\frac{\sqrt{[(k-1)\,k\,(k+1)]}}{2k+1}\, i^{k-1}\mathrm{M} \,.\, \mathrm{J}_{k-1+\frac{1}{2}}(2\pi r/\lambda)\, \mathrm{G}^{*}_{-k-1}\, \xi\,(\mathrm{E}, -k-1).$$

In a similar way we can find the combinations occurring in the second column; they differ only in the first factor. These expressions have then to be multiplied by $r^2$, and integrated from $r = 0$ to $r = \infty$.

Let us first consider the integrals for $\mathrm{G}_k$ and $\mathrm{G}_{-k-1}$. Putting $t = iau$ in the expression (17A) for $\mathfrak{G}_k$, we find

$$\mathfrak{G}_k = [(k-s) - i\,(b+c)]\, r^s a^{2s+2} e^{-\pi b} \int_{-1}^{+1} (1-u)^{s-ib+1} (1+u)^{s+ib} e^{iaru}\, du. \tag{53}$$

We write the integral itself, omitting the factors outside

$$\mathrm{I} = \int_{-1}^{+1} (1-u)\,(\mathrm{P} + i\mathrm{Q})\, du.$$

On changing $u$ to $-u$ this gives

$$\mathrm{I} = \int_{-1}^{+1} (1+u)\,(\mathrm{P} - i\mathrm{Q})\, du,$$

so that

$$\int_{-1}^{+1} \mathrm{P}\, du \neq 0, \quad \int_{-1}^{+1} u\mathrm{P}\, du = 0, \quad \int_{-1}^{+1} u\mathrm{Q}\, du \neq 0, \quad \int_{-1}^{+1} \mathrm{Q}\, du = 0. \tag{54}$$

We find therefore

$$\left.\begin{aligned} \Re\mathrm{I} &= \int_{-1}^{+1} (1-u)^{s-ib} (1+u)^{s+ib} e^{iaru}\, du \\ \Im\mathrm{I} &= -\int_{-1}^{+1} u\,(1-u)^{s-ib} (1+u)^{s+ib} e^{iaru}\, du \end{aligned}\right\}, \tag{55}$$

where

$$\mathrm{I} = \Re\mathrm{I} + i\Im\mathrm{I}.$$

On integrating by parts the expression

$$\int_{-1}^{+1} (1-u)^{s-ib+1} (1+u)^{s+ib+1} e^{iaru}\, du,$$

we obtain

$$\left.\begin{aligned}\mathfrak{I} = &-\frac{iar}{2(s+1)}\int_{-1}^{+1}(1-u)^{s-ib+1}(1+u)^{s+ib+1}e^{iaru}\,du\\ &-\frac{ib}{(s+1)}\int_{1}^{+1}(1-u)^{s-ib}(1+u)^{s+ib}e^{iaru}\,du\end{aligned}\right\}. \qquad (56)$$

For short wave-lengths we shall see that $b$ is of the order $\gamma$, and also that the two integrals in (56), apart from the factor $b$, contribute quantities of the same order to the radial integral The presence of $b$, therefore, enables us to neglect the second integral in (56) Remembering also that $k - s \simeq \gamma^2/k \leqslant b + c$, we have finally

$$G_k = -r^s a^{2s+2} e^{-\pi b}\frac{(b+c)}{|B|}\int_{-1}^{+1}(1-u)^{s-ib}(1+u)^{s+ib}e^{iaru}\,du. \qquad (57)$$

Similarly we find

$$G_{-k-1} = -r^{s'+1}a^{2s'+3}e^{-\pi b}\frac{(b-c)}{2(s'+1)|B|}\int_{-1}^{+1}(1-u)^{s'+1-ib}(1+u)^{s'+1+ib}e^{iaru}\,du. \qquad (58)$$

The radial integrals are of the forms

$$\left.\begin{aligned}&\int_0^\infty J_{k\pm1+\frac{1}{2}}(2\pi r/\lambda)\,G_k^*\,\xi(E,k)\,.\,M\,.\,r^2\,dr\\ \text{and}\quad&\int_0^\infty J_{k\pm1+\frac{1}{2}}(2\pi r/\lambda)\,G^*_{-k-1}\,\xi(E,-k-1)\,.\,M\,.\,r^2\,dr\end{aligned}\right\}. \qquad (59)$$

Further we have

$$\left.\begin{aligned}s &= k + O(\gamma^2/k),\\ s' &= k - 1 + O(\gamma^2/k),\\ \text{and}\quad |\Gamma(k+ib+1)| &= \Gamma(k+1)[1+O(b^2)]\end{aligned}\right\} \qquad (60)$$

We shall neglect quantities of order $b^2$ or $\gamma^2$. On substituting for M, $\xi(E, k)$, $G_k$, etc., in (59), we find that both integrals reduce to

$$L\frac{a^{k+3+\beta}}{\Gamma(k+1)2^k}\int_0^\infty r^\beta e^{-\frac{r}{a_0}}\frac{r^{k+2}}{\sqrt{(2\pi r/\lambda)}}J_{p+\frac{1}{2}}(2\pi r/\lambda)$$
$$\times\int_{-1}^{+1}(1-u)^{k-ib}(1+u)^{k+ib}e^{iaru}\,du\,dr, \qquad (61)$$

where

$$\left.\begin{aligned}L &= -\left(\frac{2\pi E}{hc^2a}\right)^{\frac{1}{2}}\frac{A}{(A^2+|B|^2)^{\frac{1}{2}}}\frac{e^{\frac{\pi b}{2}}\sqrt{\pi}\,\gamma a_0^{-\frac{1}{2}}}{2\,.\,a^{\beta+2}}\\ \text{and}\quad p &= k \pm 1\end{aligned}\right\}. \qquad (62)$$

Let us consider the values of the constants involved. Firstly we have

$$a = \mathrm{A}\,|\mathrm{B}| = \frac{2\pi}{hc}(\mathrm{E}^2 - m^2c^4)^{\frac{1}{2}}.$$

Since the energy required to liberate an electron is small compared with $h\nu_0$ in the region we are considering, $\mathrm{E} = mc^2 + h\nu_0$, and so

$$a = \frac{2\pi\nu_0}{c}\left|1 + \frac{2mc^2}{h\nu_0}\right|^{\frac{1}{2}},$$

giving

$$a = \frac{2\pi}{\lambda\tau} \text{ (equation (38)).} \tag{63}$$

Also $\beta = \sqrt{(1-\gamma^2)} - 1 = \mathrm{O}(\gamma^2)$ and is therefore small. We put $r/a_0 = \delta ar$, where $\delta = 1/aa_0$ and is also of order $\gamma$ Lastly

$$b = \frac{\gamma}{2}\,\frac{|\mathrm{B}|^2 + \mathrm{A}^2}{|\mathrm{B}|\,.\,\mathrm{A}} = \mathrm{O}(\gamma).$$

In (61) we now change the variable of integration by writing $r$ instead of $ar$, and making use of the formula

$$\mathrm{J}_{p+\frac{1}{2}}(\tau r) = \frac{(\tau r)^{p+\frac{1}{2}}}{\Gamma(p+1)\,2^{p+\frac{1}{2}}\sqrt{\pi}}\int_{-1}^{+1}(1-t^2)\,e^{i\tau rt}\,dt, \tag{64}$$

we find for (61) the expression

$$\left.\begin{aligned} &\mathrm{Q}\int_0^\infty dr\int_{-}^{+1}du\int_{-1}^{+1}dt\,e^{-r(\delta - iu - i\tau t)}\,r^{k+p+2+\beta}(1-t^2)^p(1-u)^{k-ib}(1+u)^{k+ib}\\ &\text{where}\\ &\qquad\mathrm{Q} = \frac{\mathrm{L}\tau^p}{\sqrt{\pi}\,\Gamma(p+1)\,\Gamma(k+1)\,2^{k+p+\frac{1}{2}}}\end{aligned}\right\}. \tag{65}$$

Integrating with respect to $r$ we obtain

$$\mathrm{Q}\Gamma(p+k+\beta+3)\int_{-1}^{+1}du\int_{-1}^{+1}dt\,\frac{(1-t)^p(1+t)^p(1-u)^{k-ib}(1+u)^{k+ib}}{[\delta - i(\tau t + u)^{p+k+\beta+3}]}. \tag{66}$$

This can be expressed as a hypergeometric function of two variables.* If we put $(1+u) = 2u'$ and $(1+t) = 2t'$, we find for (66) the value

$$\frac{\mathrm{Q}\Gamma(p+k+\beta+3)\,2^{2(k+p+1)}}{[\delta + i(\tau+1)]^{k+p+\beta+3}}\int_0^1 du'\int_0^1 dt'\,\frac{t'^p(1-t')^p\,u'^{k+ib}(1-u')^{k-ib}}{\left(1 - \dfrac{2\tau}{1+\tau-i\delta}t' - \dfrac{2}{1+\tau-i\delta}u'\right)^{k+p+\beta+3}}$$

---

* P. Appell et J. Kampé de Feriet, " Fonctions Hypergeometriques et Hyperspheriques," p. 28.

giving,* on neglecting β

$$\left.\begin{aligned} &\mathrm{K}\,.\,\mathrm{F}_2\left(k+p+3, p+1, k+ib+1, 2p+2, 2k+2\,;\,\frac{2\tau}{1+\tau-i\delta}, \frac{2}{1+\tau-i\delta}\right)\\ &\text{where}\\ &\quad\mathrm{K}=\frac{\mathrm{L}\tau^{p}\,2^{p+k+\frac{1}{2}}}{\sqrt{\pi}\,[\delta+i\,(\tau+1)]^{k+p+3}}\cdot\frac{\Gamma\,(p+1)\,\Gamma\,(k+1)\,\Gamma(k+p+3)}{\Gamma(2p+2)\,\Gamma(2k+2)}\end{aligned}\right\}. \qquad (67)$$

Hence for the integral (61) we have the following—

$$p=k+1$$

$$\frac{\mathrm{L}}{\sqrt{2\pi}}\,\frac{\Gamma\,(k+1)\,\Gamma\,(k+2)2^{2k+3}\,\tau^{k+1}}{\Gamma\,(2k+2)\,(i\,(\tau+1)+\delta)^{2k+4}}\,\mathrm{F}_2\,(2k+4,\,k+2,\,k+1+ib,\,2k+4,\,2k+2\,;\;x,\,y), \qquad (68\text{A})$$

$$p=k-1$$

$$\frac{\mathrm{L}}{\sqrt{2\pi}}\,\frac{\Gamma\,(k)\,\Gamma\,(k+1)2^{2k+1}\,\tau^{k-1}}{\Gamma\,(2k)\,(i\,(\tau+1)+\delta)^{2k+2}}\,\mathrm{F}_2\,(2k+2,\,k,\,k+1+ib,\,2k,\,2k+2\,;\;x,\,y), \qquad (68\text{B})$$

where

$$x=\frac{2\tau}{\tau+1-i\delta} \quad\text{and}\quad y=\frac{2}{\tau+1-i\delta}$$

These may be transformed by the following relations*

$$\left.\begin{aligned} &\mathrm{F}_2\,(\alpha,\,\beta,\,\beta',\,\gamma=\alpha,\,\gamma',\;x,\,y)\\ &\qquad\qquad=(1-x)^{-\beta}\,\mathrm{F}_1\,(\beta',\,\beta,\,\alpha-\beta,\,\gamma'\,;\;y/(1-x),\,y)\\ &\mathrm{F}_2\,(\alpha,\,\beta,\,\beta',\,\gamma,\,\gamma'=\alpha\,;\;x,\,y)\\ &\qquad\qquad=(1-y)^{-\beta}\,\mathrm{F}_1\,(\beta,\,\alpha-\beta',\,\beta',\,\gamma\,;\;x,\,x/(1-y))\end{aligned}\right\} \qquad (69)$$

Leaving aside the factor outside $\mathrm{F}_2$ for the moment, these give respectively

$$(1-x)^{-(k+2)}\,\mathrm{F}_1\,(k+1+ib,\,k+2,\,k+2,\,2k+2\,;\;y/(1-x),\,y) \qquad (70\text{A})$$

and

$$(1-y)^{-(k+1+ib)}\,\mathrm{F}_1\,(k,\,k+1-ib,\,k+1+ib,\,2k\,;\;x,\,x/(1-y)). \qquad (70\text{B})$$

Consider first (70A) and apply the following relation

$$\begin{aligned}\mathrm{F}_1\,(\alpha,\,\beta,\,\beta',\,\gamma\,;\;u,\,v)=&\frac{(\gamma-\alpha)\,(\gamma-\alpha+1)u^2}{\gamma\,(\gamma+1)\,(u-1)^2}\,\mathrm{F}_1\,(\alpha,\,\beta,\,\beta',\,\gamma+2,\;u,\,v)\\ &-\frac{2\,(\gamma-\alpha)u}{\gamma\,(u-1)^2}\,\mathrm{F}_1\,(\alpha,\,\beta-1,\,\beta',\,\gamma+1\,;\;u,\,v)\\ &+\frac{1}{(u-1)^2}\,\mathrm{F}_1\,(\alpha,\,\beta-2,\,\beta',\,\gamma\,;\;u,\,v),\end{aligned}$$

---

* See Appell, *loc. cit.*, for these and others.

giving

$$\frac{(1-x)^{-k}}{(x+y-1)^2}\left\{\begin{aligned} &\frac{(k+1-ib)(k+2-ib)}{(2k+2)(2k+3)}\frac{y^2}{(1-x)^2}F_1(k+1+ib,\\ &\qquad\qquad k+2,k+2,2k+4;\ y/(1-x),y)\\ &-\frac{2(k+1-ib)}{2k+2}\frac{y}{1-x}F_1(k+1+ib,\\ &\qquad\qquad k+1,k+2,2k+3;\ y/(1-x),y)\\ &+F_1(k+1+ib,k,k+2,2k+2;\ y/(1-x),y)\end{aligned}\right\}.$$

We now use

$$F_1(\alpha,\beta,\beta',\beta+\beta';\ u,v)=(1-u)^{-\alpha}F(\alpha,\beta',\beta+\beta';\ (u-v)/(u-1))$$

and then transform the middle term by the formula

$$\begin{aligned}(\gamma-\alpha)zF(\alpha,\beta,\gamma+1;\ z)=\gamma F(\alpha,\beta-1,\gamma;\ z)&\\ -\gamma(1-z)F(\alpha,\beta,\gamma;\ z).&\end{aligned}\qquad(71)$$

We obtain

$$\frac{(-)^k(x-1)^{1+ib}}{(x+y-1)^{k+3+ib}}\left\{\begin{aligned} &\frac{(k+1-ib)(k+2-ib)}{(2k+2)(2k+3)}\frac{y^2}{(1-x)^2}F(k+1+ib,\\ &\qquad\qquad k+2,2k+4;\ z)\\ &-\frac{2y}{(1-x)z}F(k+1+ib,k+1,2k+2;\ z)\\ &+\frac{2y-z}{z}F(k+2,k+1+ib,2k+2;\ z)\end{aligned}\right\},\qquad(72)$$

where

$$z=\frac{xy}{x+y-1}.$$

We transform the hypergeometric series by a formula of Kummer*

$$\begin{aligned}F(\alpha,\beta,2\beta;\ z)=\left(\frac{2}{1+\sqrt{(1-z)}}\right)^{2\alpha}&\\ \times F\left[\alpha,\alpha-\beta+\tfrac{1}{2},\beta+\tfrac{1}{2};\left(\frac{1-\sqrt{(1-z)}}{1+\sqrt{(1-z)}}\right)^2\right].&\end{aligned}\qquad(73)$$

We have

$$\left.\begin{aligned}z&=\frac{4\tau}{(\tau+1)^2+\delta^2}\\ \text{and}\qquad\frac{1-\sqrt{(1-z)}}{1+\sqrt{(1-z)}}&=\tau\end{aligned}\right\}.\qquad(74)$$

---

* Kummer, 'Crelle,' vol. 15. The formula is given wrongly owing to a slip in the derivation.

The transformed series converge much more rapidly, about six terms being sufficient for an accuracy of one in one hundred. We may therefore neglect the $ib$ in the hypergeometric functions as well as outside. (For the third function we must transform to $F(\alpha, k+1, 2k+2\,;\ z)$ first, using a relation similar to (71), and the result then follows). We also neglect $\delta$, though not $k\delta$, compared with unity, and on applying (73) and substituting for $x$, $y$ and $z$ we finally obtain for (68A)

$$\frac{L\Gamma(k+1)\,\Gamma(k+2)\,2^{2k+3}\,\tau^{k+1}}{\sqrt{2\pi}\,\Gamma(2k+2)\,(\tau+1)^3}\left\{\begin{array}{l} \overline{2(2k+3)}\ \overline{1-\tau} \\ \qquad \times F(k+1, -\frac{1}{2}, k+\frac{5}{2}\,;\ \tau^2) \\ -\dfrac{(1+\tau)^2}{\tau} \\ \qquad \times F(k+1, \frac{1}{2}, k+\frac{3}{2}\,;\ \tau^2) \\ +\dfrac{1}{\tau(1-\tau)} \\ \qquad \times F(k, -\frac{1}{2}, k+\frac{1}{2}\,; \end{array}\right\}. \quad (75)$$

In a similar way we may show that $ib$ may be neglected in the function (68B), and we may therefore obtain a result for this by replacing $k$ by $k-1$ and interchanging $x$ and $y$ in (72) This follows from equations (68) since $F_2$ is symmetrical in $\beta$, $x$; and $\beta'$, $y$. The result for (68B) is the expression (75) with $k$ replaced by $k-1$, and the first and last hypergeometric functions multiplied by $-\tau$.

In finding the expressions (57) and (58) for $G_k$ and $G_{-k-1}$ we neglected certain integrals which are multiplied by $b$. These lead to expressions similar to (66), which, however, cannot be reduced in the same way. We may show that they do not involve an extra factor $b$ or $\delta$ in the denominator, as follows. They are finite as $b \to 0$, and become integrals involving the product of two Bessel functions, which are again finite as $\delta \to 0$. Thus they may be neglected since they are multiplied by $b$.

In the combinations occurring in the last two columns, the integral no longer contains a factor $\gamma$, but we shall find that it contains factors $b$ or $\delta$, so that we must retain the first powers of these in evaluating it.

For the third column of the table given we find as before

*Initial $a_1$ state, $u = -1$ in final state.*

(1) *Final a state.*

$n = k + 1$

$\sqrt{k+1}\, i^{k+1}\, I_u.$

(2) *Final b state.* $k \geqslant 1$

$$n = k - 1$$

$$-\sqrt{k}\, i^{k-1} I_b,$$

where

$$\left.\begin{aligned} I_a &= \int_0^\infty a_0^{-3/2} F^*_k\, r^\beta e^{-r/a_0} \xi(E, k) \sqrt{\left(\frac{\pi}{2\pi r/\lambda}\right)} J_{k+1+\frac{1}{2}}(2\pi r/\lambda)\, r^2\, dr, \\ I_b &= \int_0^\infty a_0^{-3/2} F^*_{-k-1}\, r^\beta e^{-r/a_0} \xi(E, -k-1) \sqrt{\left(\frac{\pi}{2\pi r/\lambda}\right)} J_{k-1+\frac{1}{2}}(2\pi r/\lambda)\, r^2\, dr \end{aligned}\right\} \quad (76)$$

Similar results, involving $I_a$ and $I_b$ are obtained for column four.

We now take $F_k^*$ ($= F_k$) as the real part of $\mathfrak{G}_k/A$, and similarly for $F^*_{-k-1}$. In evaluating the integrals (76) we shall keep the first powers of $b$ and $\delta$, so that it is more convenient to keep $\mathfrak{G}_k$ in the form given by (53). We find by a procedure similar to the one used to evaluate (59)

$$\left.\begin{aligned} I_a &= \Re \,.\, \frac{L}{\sqrt{2\pi}} \frac{(-)^{k+1}[(k-s) - i(b+c)]\tau^{k+2}[\Gamma(k+1)]^2(k+1-ib)\, 2^{2k+4}}{\gamma(b+c)\,\Gamma(2k+2)(\tau+1-i\delta)^{2k+1}} F_{2a}, \\ I_b &= \Re \,.\, \frac{L}{\sqrt{2\pi}} \frac{(-)^{k+1}[(k-1-s') - i(b-c)]\,\tau^k[\Gamma(k)]^2(k-ib)\, 2^{2k+2}}{\gamma(b-c)\,\Gamma(2k)(\tau+1-i\delta)^{2k+1}} F_{2b}, \end{aligned}\right\} \quad (77)$$

where

$$F_{2a} = F_2(2k+4, k+2, k+1+ib, 2k+4, 2k+3\,,\; x, y),$$

$$F_{2b} = F_2(2k+1, k, k+ib, 2k, 2k+1\,;\; x, y)$$

Since $(k - s) \ll (b + c)$, we must retain the imaginary parts of $F_{2a}$ and $F_{2b}$. We transform these functions as before, and retaining the relevant powers of $b$, $\delta$ and $\gamma$ we find

$$I_a' = -\frac{W(k+1)}{(b+c)} \Re \,.\, \left| \begin{array}{l} [(b+c)b - (k+1)(k-s) + i(b+c)(k+1)]\,.\,(1-\tau^2)^{ib} \\ \times \left\{ \begin{array}{l} \dfrac{2}{(2k+3)(\tau+1)^2}(k+2-ib)(\tau+1+i\delta) \\ \qquad\qquad \times F(k+1+ib, ib-\frac{1}{2}, k+\frac{5}{2}\,;\; \tau^2) \\ -\dfrac{1}{2\tau} F(k+ib, ib-\frac{1}{2}, k+\frac{3}{2}\,;\; \tau^2) \\ +\dfrac{(1-\tau)^2}{2\tau} F(k+1+ib, ib+\frac{1}{2}, k+\frac{3}{2}\,;\; \tau^2) \end{array} \right\} \end{array} \right. \quad (78\text{A})$$

and

$$I_b = \frac{W(k)}{(b-c)} \mathfrak{R} \cdot \left[ \begin{array}{l} [(b-c)\,b - k\,(k-1-s') + i\,(b-c)\,k] \\ \qquad\qquad\qquad\qquad \times (1-\tau^2)^{-ib} \\ \times \left\{ \begin{array}{l} \dfrac{(1-\tau)^2}{2\tau}\, F\left(k-ib, \tfrac{1}{2}-ib, k+\tfrac{1}{2};\ \tau^2\right) \\ \dfrac{(1-\tau^2)^{2ib}\,(1-\tau^2+2i\delta)}{2\tau\,(1+\tau)^2} \\ \quad \times F\left(k-1+ib, ib-\tfrac{1}{2}, k+\tfrac{1}{2};\ \tau^2\right) \end{array} \right\} \end{array} \right], \quad (78\text{B})$$

where

$$W(k) = \frac{L\,[\Gamma(k)]^2\, 2^{2k+2}\, \tau^{k+1}}{\sqrt{2\pi}\,\Gamma(2k)\,(1-\tau)^2}$$

These results, together with the analogous ones, (75), for the first two columns, enable us to calculate all the matrix elements.

In carrying out the numerical calculations we note that only two types of hypergeometric functions occur—

$$F\left(k+ib, ib-\tfrac{1}{2}, k+\tfrac{3}{2};\ \tau^2\right) \qquad (\alpha)$$

and

$$F\left(k+ib, ib+\tfrac{1}{2}, k+\tfrac{1}{2};\ \tau^2\right) \qquad (\beta)$$

Half-a-dozen terms are quite sufficient to calculate the real and imaginary parts of (α) and the real part of (β). For the imaginary part of (β) we use the formula

$$F(\alpha, \beta, \gamma;\ z) = (1-z)^{\gamma-\alpha-\beta}\, F(\gamma-\beta, \gamma-\alpha, \gamma;\ z),$$

which gives us the ratio of the real to the imaginary part of (β) in terms of $\tau^2$ only.

§ 6. *Numerical Results.*—For the coefficient of absorption, I, we obtain the following results :—

| $\lambda$ | $6·08 \times 10^{-11}$ cm. | $1·22 \times 10^{-10}$ cm | $2·43 \times 10^{-10}$ cm | $6·08 \times 10^{-10}$ cm. | $9·73 \times 10^{-10}$ cm. |
|---|---|---|---|---|---|
| $I \times Z^{-5}$ | $4·89 \times 10^{-34}$ | $1·87 \times 10^{-33}$ | $9·92 \times 10^{-33}$ | $1·68 \times 10^{-31}$ | $8·01 \times 10^{-31}$ |
| $n$ | 1·9 | 2·4 | 3·1 | 3·3 | |

Between any two wave-lengths, we may express the mean variation of I by the formula

$$I \sim \lambda^n \,.\, Z^5.$$

Under each wave-length we have put that value of $n$ which expresses the mean variation of I between that wave-length and the one following. The value of

$n$ increases with $\lambda$, which is experimentally observed in the case of heavy atoms. It should be emphasised, however, that these results are only applicable to very light atoms—where $Z/137$ may be considered small compared with unity. A comparison with experiment is therefore not yet possible, as it is extremely difficult to measure the photoelectric effect in light atoms.

If R denote the ratio of the average forward momentum of an electron to that of the light quantum liberating it, we have the following results .—

| $\lambda$ | $\lambda \to 0$ | $1\cdot22 \times 10^{-10}$ cm | $2\cdot43 \times 10^{-10}$ cm | $6\cdot08 \times 10^{-10}$ cm | $9\cdot73 \times 10^{-10}$ cm | $\lambda \to \infty$ |
|---|---|---|---|---|---|---|
| R | 1 | 1·15 | 1·20 | 1·48 | 1·57 | 1·6 |

The first result may be inferred from a graph of the values, or by noting that as $\lambda \to 0$, $\tau \to 1$ and the matrix elements in (42) vary very slowly with $k$, so that $\overline{\cos\theta} \to 1$. The result for $\lambda \to \infty$ is obtained from the non-relativistic calculations.

The theoretical value of $n$ for long waves is 3·5, so that it is interesting to note that the deviations of $n$ and R, from their values for large wave-lengths, first become serious in the region of the Compton wave-length, given by $\lambda = h/mc = 2\cdot43 \times 10^{-10}$ cm.

I wish to express my thanks to Dr. P. A. M. Dirac and Mr. R. H. Fowler for suggesting the problem, and for valuable discussion and advice

# *The Photoelectric Effect in Thin Metallic Films.*[*]

By W. G. Penney, Imperial College of Science.

(Communicated by S. Chapman, F R S.—Received June 12, 1931.)

In spite of the many attempts to obtain a mathematical treatment of the photoelectric effect it cannot be said that a satisfactory account has yet been given. The problem is not made any easier by the discordance which exists between the results of various observers. Although there is no doubt that Einstein's law of photoelectric emission holds with extreme accuracy, many other features seem to defy certainty, among which may be mentioned the dependence of the current from a thin film on the thickness and on the direction of polarisation of the incident light. Perhaps the most puzzling feature of the whole effect, however, is the extreme inefficiency of the light in producing photoelectrons, the very best result ever obtained in practice being about 100 quanta for each photoelectron emitted, while usually it takes very many more. This means that any electron stimulated by the light has a very poor chance of ever escaping from the metal and it is only by estimating this chance that agreement with experiment can be obtained. It seems certain that any theory which does not take into account such things as the damping of the light wave or the absorption of the electrons in trying to escape from the metal (although the relative importance of these two is by no means clear), cannot hope to represent adequately the experimental material.

Frohlich[†] has given a treatment of the photoelectric effect from a thin metallic film, considering it as a potential trough, the electrons being perfectly free. On the basis of this model he calculates the dependence of the current on the frequency and finds that the emerging electrons have a velocity distribution. No account was taken either of the absorption of the light, or of the inelastic collisions of the electrons with the other particles of the lattice. The surprising feature emerged that the current was independent of the thickness of the film. This was because free electrons in a field of constant potential have no absorption frequencies (other than zero), and he assumed that the light wave was undamped. An independent treatment of the same problem has been given by Tamm and Schubin,[‡] who first consider the electrons as free to get the surface effect, and then as bound to get a volume effect, the photoelectric yield being the sum of the two. The following investigation was undertaken in the hope of improving on these models by taking into account the absorption of the light and to represent, in some measure, the fact that the electrons are not free, but must be considered as partially bound. With this improvement of the model, there is a considerable gain in agreement with experiment, although in some points the model still fails. This may be because we have taken no account of the electrons being absorbed in the film itself, or of the surface layer of impurities which always seems to be present and whose influence is considerable.

---

[*] Part of thesis for which was approved the degree of Doctor of Philosophy in the University of London.

[†] 'Ann. Physik,' vol. 7, p. 103 (1930).

[‡] 'Z. Physik,' vol. 68, p. 97 (1931).

Following on from a paper by Kronig and Penney,[*] we represent the potential field of the particles of the metallic film by a potential function of the form shown in fig. 1, in which we later make $b \rightarrow 0$ and $V_0 \rightarrow \infty$ in such a way that $bV_0$ remains finite and represents the binding force of the electrons Here $n(a+b)$ and in the limit $na$, represents the thickness of the metallic film so that $a$ is the lattice constant of the metal. The wave equation of an electron in the region $0 \leqslant x - k(a+b) \leqslant a$, $k = 0, 1, \quad (n-2)$ is

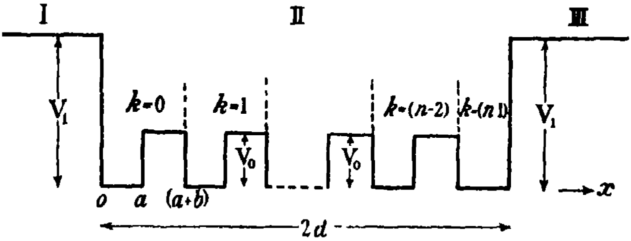

FIG. 1

$$d^2\psi/dx^2 + \beta^2\psi = 0, \qquad \beta^2 = 8\pi^2 m/h^2 W = \kappa^2 W, \tag{1A}$$

while in the region $0 \leqslant x - k(a+b) - a \leqslant b$, it is

$$d^2\psi/dx^2 - \gamma^2\psi = 0, \quad \gamma^2 = \kappa^2(V_0 - W), \tag{1B}$$

and we can take $\gamma^2 > 0$ without loss of generality since in the limit $V_0 \rightarrow \infty$. The solutions in the two regions are

$$\left.\begin{aligned} \psi &= Ce^{i\beta x} + De^{-i\beta x} \\ \psi &= Ae^{\gamma x} + Be^{-\gamma x} \end{aligned}\right\}.$$

At each potential surface of discontinuity $\psi$ and $\partial\psi/\partial x$ must be continuous, leading to a long chain of equations. By a mathematical artifice we can reduce this chain to four equations; we introduce a parameter $\alpha$ such that the wave functions have the form

---

[*] 'Proc. Roy. Soc.,' A, vol. 130, p. 499 (1931).

$$\psi = \mathrm{U}(x)\, e^{i\alpha x},$$

where the function $\mathrm{U}(x)$ and its first derivative are to be continuous and periodic with the period $(a+b)$. The four equations of continuity and periodicity of U and $\partial \mathrm{U}/\partial x$ give four linear homogeneous equations, which cannot be satisfied unless

$$\frac{\gamma^2-\beta^2}{2\beta\gamma}\sinh\gamma b \sin\beta a + \cosh\gamma b\cos\beta a = \cos\alpha(a+b)$$

Proceeding to the limit $b \to 0$, $\mathrm{V}_0 \to \infty$ in such a way that

$$\lim_{\substack{b\to 0\\ \mathrm{V}_0\to\infty}} \frac{\gamma^2 ab}{2} = \mathrm{P},$$

this becomes

$$\frac{\mathrm{P}}{\beta a}\sin\beta a + \cos\beta a = \cos\alpha a. \tag{2}$$

We adopt the convention that if $n\pi \leqslant \beta a \leqslant (n+1)\pi$, then that value of $\alpha$ must be associated with $\beta$ such that $n\pi \leqslant \alpha a \leqslant (n+1)\pi$. There is then just one value of $\alpha$ associated with each value of $\beta$ and we can use either of these symbols to denote the energy level we are considering. We find as the wave functions of an electron in the lattice in the region $ka \leqslant x \leqslant (k+1)a$,

$$\psi_\beta{}^+ = e^{i\beta x + ik(\alpha-\beta)a} + \mathrm{C}e^{-i\beta x + ik(\alpha+\beta)a},$$

$$\psi_\beta{}^- = \psi_\beta{}^{+*},$$

where

$$\mathrm{C} = -(1 - e^{i(\alpha-\beta)a})/(1 - e^{-i(\alpha+\beta)a}),$$

the asterisk denoting the conjugate complex quantity. $\psi_\beta{}^+$ corresponds to an electron moving in the positive $x$-direction, while $\psi_\beta{}^-$ corresponds to an electron moving in the negative $x$-direction, through the lattice.

We have now to find a wave function, which besides satisfying the conditions specified in the metal, will pass on continuously to a wave function outside the metal belonging to the same energy value of the electron. We assume in the various regions

$$\left.\begin{aligned} &\text{I.} \quad \psi = \mathrm{K}e^{ipx} + \mathrm{L}e^{-ipx},\\ &\text{II.} \quad \psi = \mathrm{E}(\psi_\beta{}^+ + \mathrm{F}\psi_\beta{}^-),\\ &\text{III.} \quad \psi = \mathrm{M}e^{ip(x-na)} + \mathrm{N}e^{-ip(x-na)},\end{aligned}\right\}$$

where $p^2 = \kappa^2 (W - V_1)$. If $p^2 < 0$ the condition that $\psi$ should remain finite at infinity requires $K = N = 0$. From the four conditions of continuity of $\psi$ and $\partial\psi/\partial x$ at the two boundary surfaces of the metal, we obtain a relation between $\alpha$ and $\beta$. In the case $p^2 < 0$, we find that there are two possible solutions

$$\left.\begin{aligned} &L = M, \qquad F = e^{ni\alpha a}\, e^{-i(\alpha-\beta)a}, \\ &(|pa| - P)\sin\beta a = \beta a \sin\alpha a \tan\frac{n}{2}\alpha a, \end{aligned}\right\} \qquad (3\text{A})$$

$$\left.\begin{aligned} &L = -M, \qquad F = -e^{n} \\ &(|pa| - P)\sin\beta a = -\beta a \sin\alpha a \cot\frac{n}{2}\alpha a, \end{aligned}\right\} \qquad (3\text{B})$$

normalisation requiring

$$EE^* = \frac{1}{8d}\,\frac{1 - \cos(\alpha+\beta)a}{1 - \cos\alpha a\cos\beta a + \frac{1}{P}(\cos\alpha a - \cos\beta a)^2}$$

$$= \tfrac{1}{8}\,\frac{1 - \cos(\alpha+\beta)a}{\sin^2\beta a\cos^2\alpha d}\,LL^*, \qquad (4)$$

in case (3A) while a similar result holds in case (3B) except that $\sin^2\alpha d$ must be written for $\cos^2\alpha d$ in (4). This equation is not quite exact, the order of the error not exceeding $1/n$. In the case $p^2 > 0$ there is no further restriction on $\alpha$ and $\beta$. Since in the unperturbed state the electrons are confined in the metal, it follows that their energy $W < eV_1$, and hence from equations (2), (3A), (3B), that the unperturbed energy levels are discrete. By the artifice of introducing $\alpha$ we have obtained the eliminant of the $4n$ equations of continuity in the constant coefficients as a pair of simultaneous equations In the case of mono-valent metals there will be $n$ of these discrete levels occupied if we disregard the spin, while if we take the spin into account there will be only $n/2$. For the purpose of our problem the spin can be neglected. For the higher energy levels, only the restriction (2) applies, and the energy spectrum is continuous in regions separated by finite intervals. Those values of the energy which make $\alpha$ imaginary correspond to electrons impinging on the film and being almost totally reflected. The thicker the film the better the reflecting power until for the semi-infinite crystal they are totally reflected. For the calculation of the photoelectric effect we are not interested in these solutions. In order to normalise the continuous spectrum we adopt the condition†

$$\frac{1}{0}\Big| = \int_{-\infty}^{\infty} dx \int_{\Delta} \psi(E)\,\psi^*(\epsilon)\,dE.$$

---

† See for example E. Fues, 'Ann. Physik,' vol. 81, p. 281 (1926); G. Wentzel, 'Phys. Z.,' vol. 29, p. 321 (1928).

If $E \neq \epsilon$ the equation is satisfied but trouble arises when $E = \epsilon$ on account of the degeneracy corresponding to the two possible directions of motion along the $x$-axis. It is found that a suitable pair of wave functions in the various regions are

$$\left.\begin{array}{ll} \text{I} & \frac{R}{S}\left[g e^{iqx} + h e^{-iqx} \pm F'\left(g^* e^{-iqx} + h^* e^{iqx}\right)\right], \\ \text{II.} & \frac{R}{S}\left[\psi_{\beta_1}{}^{+} \pm F'\psi_{\beta_1}{}^{-}\right], \\ \text{III} & \frac{R}{S}\left[j e^{iqx} + k e^{-iqx} \pm F'\left(j^* e^{iqx} + k^* e^{iqx}\right)\right] \end{array}\right\}$$

where to save confusion we have written $q^2 = \kappa^2(W' - V_1)$, and have used primes to denote that we are dealing with a higher continuous level. Here

$$j = F'g^*, \quad k = F'h^*, \quad F' = e^{i\mu\alpha' a}\, e^{-i(\alpha' - \beta')a},$$

$$2g = (1 + C) + \frac{\beta'}{q}(1 - C), \quad 2h = (1 + C) - \frac{\beta'}{q}(1 - C).$$

and the normalising condition becomes

$$\frac{R^2}{S^2}\left[gg^* + hh^* \pm ghF'^* \pm g^*h^*F'\right] = \frac{\kappa^2}{4\pi q}$$

In order to make clear the appearance of the energy spectrum of a thin film we give a figure which is for a film eight molecules thick, the value assumed for P being $3\pi/2$. For reasons discussed later it seemed necessary to assume that the outside potential lies somewhere between the second and third groups of energy levels.

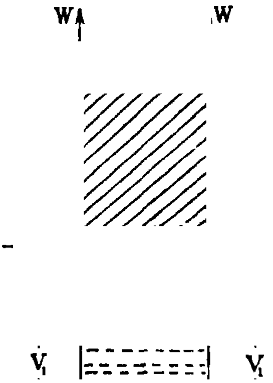

Fig. 2.

### *The Interaction of the Radiation and the Electrons.*

The most satisfactory method of treating the problem of the interaction of the radiation and the electrons would be to take account of the reaction of all the particles on the radiation field and on each other, obtaining in this way the reflected beam and the exact manner in which the incident wave is damped out, expelling photoelectrons as it passes on. Unfortunately, however, this is far too difficult a problem, and we are forced to take over an experimental result which seems to be fairly well established, that the intensity of the exciting radiation can be represented by the real part of $E_0 e^{-\frac{\mu x}{a} + \frac{2\pi i \nu x}{v}}$ where $\mu = \frac{2\pi k a}{\lambda}$ and is directly proportional to the extinction coefficient $k$ and the lattice constant $a$. $E_0$ is the component of the electric intensity of the refracted beam at the surface of the metal, and $v$ is the velocity of light in the metal. Since we are concerned with films of thickness $10^{-6}$ cm. or less (which are quite thick enough to absorb the light almost completely), it is not necessary to consider any phase effects and the time factor may be neglected.

In order to calculate the current on either side of the film, it is only necessary to estimate how many electrons are being lifted each second from the discrete energy levels to the higher continuous levels, from whence they may escape. To calculate this quantity we need the matrix elements

$$p(\alpha,\alpha') = \underset{\Delta_n \to 0}{\mathrm{Lt}} \frac{1}{\Delta_n} \int_{-\infty}^{\infty} \psi_\beta{}^* \left( \frac{\partial}{\partial x} \Delta_n \psi_{\beta_1} \right) e^{-\frac{\mu x}{a}} \, dx,$$

where

$$\Delta_n \psi_{\beta_1} = \int_{W_n}^{W_n + \Delta_n} \psi_{\beta_1} \, dW,$$

is the eigen-differential of the $n$th region of the continuous spectrum. The quantity $|p(\alpha,\alpha')|^2$ is a measure of the probability of an electron being lifted from the level $\alpha$ to the higher level $\alpha'$. It is necessary now to fix the position of the external potential in terms of the energy spectrum of the film. It appears that the correct position is somewhere in the space between the second and third groups of energy levels, for unless it is taken about there, the dependence of the current from the film on the frequency of the light is quite different from reality, while with this position, it is in quite good agreement with experiment. The amount of experimental data is more than sufficient to fix the constants of the film and it does not seem possible to fit all the experimental results with one set of constants. For example, where from experiments on the reflecting powers of electrons the external potential would seem to be about 10 volts, from the photoelectric effect it would seem to be about 5 volts. However, as we are considering only a one-dimensional model, we must expect such discrepancies as these. Indeed, one must be agreeably surprised to find that such a simple model exists which accounts for so many of the finer points of the experimental material. The very interesting feature emerges that the discrete level characterised by the quantum number $\alpha$ has a much better chance of combining with the energy levels just around $\alpha' a = \alpha a + 2\pi$ (*i.e.*, in the third allowed energy region), than with any others. This gives the film certain absorption frequencies on account of which the light will excite only those levels whose natural frequencies coincides with its own frequency, and according to this view the photoelectric effect should show a fine structure. As no actual film is absolutely uniform in thickness or perfect in other ways, it is clear that to correspond with experiment we must average over this fine structure. On account of these absorption frequencies the emerging photoelectrons should all have the same velocity. Lukirsky and Prilezaev* have measured the velocity distribution of the photoelectrons for three thicknesses of film $10^{-6}$, $3 \times 10^{-6}$ cm. and the solid metal. They found that as the films became thinner the emerging electrons became much more uniform in velocity. It would seem that the electrons all start off with the same velocity but, owing to their various experiences in the film, those that escape have all velocities up to the maximum.

Using the method of Dirac† to calculate the number of electrons $\Delta N$ excited per second from the level $\alpha$ to the level $\alpha'$, we find in our notation

$$\Delta N = \frac{e^2 E^2 h}{4\pi^2 \nu^2 m^2} \left| p(\alpha, \alpha') \right|^2,$$

where $h\nu = \frac{1}{\kappa^2}(\beta'^2 - \beta^2)$. Remembering that $|p(\alpha, \alpha')|^2$ is much greater in the region $\alpha' a = \alpha a + 2\pi$, than anywhere else, it is found possible to add the effects due to neighbouring discrete levels and average over the fine structure caused by the normalising factors $R^2$ and $S^2$ On making certain minor approximations we obtain, after considerable manipulation, the current on either side of the film as

$$S_0 = \frac{256\pi^3 m e^3 E_0{}^2 (1 - e^{-2n\mu}) \left(\frac{1}{\mu} + n e^{-n\mu}\right) \beta^2 \beta'}{h^3 a^3 (\beta'^2 - \beta^2)^4} \frac{\sin \alpha a (\cos \beta' a - \cos \beta a)^2}{\sin \beta' a \left[1 - \cos \alpha a \cos \beta a + \frac{1}{P} (\cos \alpha a - \cos \beta a)^2\right]}, \tag{5}$$

except just near the threshold, where the formula must be slightly modified. $\beta'$ is that value associated with $\alpha' a = \alpha a + 2\pi$, such that $h\nu = \frac{1}{\kappa^2}(\beta'^2 - \beta^2)$, $\nu$ being the frequency of the light. $E_0$ is the component of the electric intensity in the refracted beam at the surface of the metal, perpendicular to the surface of the film. At first sight it may seem strange that the quantity $q$ which depends on the outside potential, does not appear, but in fact it has disappeared in averaging over the fine structure already mentioned. In order to make the meaning of equation (5) clearer, we give in fig. 3 the current (in Coulombs per second) per calorie of incident radiation againt the frequency of the light for the solid metal, adopting the values $P = 3\pi/2$, $V_1 = 4$ volts, $a = 4 \times 10^{-8}$ cm., $\mu = 1/50$. To show how the magnitude of the effect can be controlled we have given also the curves for $P = \pi/2$ and $P = 5\pi$. The values are in good agreement with experiment In fig. 4 we have plotted the current against the thickness; the shape of the curve is the same for all frequencies although the magnitude of the current does depend on the frequency. As will be seen, by varying P it is possible to obtain a large variation in the sensitivity without changing the threshold by more than a factor two, corresponding *to the experimental fact that sodium, for example, is about 100 times* as sensitive as platinum By making P infinite (the case of firmly bound electrons) the current falls to zero. The case $P = 0$ is that of Frohlich (*loc. cit.*), the electrons being free, but then formula (5) breaks down, corresponding to the fact that free electrons have no absorption frequencies other than zero.

---

* 'Z. Physik,' vol 49, p. 247 (1926).

† 'Proc. Roy. Soc.,' A, vol. 112, p. 661 (1926), "The Principles of Quantum Mechanics," § 52, 54.

As far as the variation of the current with thickness is concerned, the result (5) agrees quite well with experiment and shows two maxima. Although the second of these is not very pronounced, it is very interesting that theoretically there should be two maxima, as all observers seem to agree that experimentally there are two. In our model they arise in the following way: we have seen that the higher energy levels are continuous and degenerate, the corresponding wave functions being even and odd respectively. Transitions occur from the discrete to these continuous levels, but when the film is a certain thickness, transitions to the even levels are specially favoured, while there is another thickness especially suitable to transitions to the odd levels. If we had taken into account the absorption of the electrons and the increasing reflecting power of the film as it gets thicker, the effect would have been to bring the curve down more steeply from the maxima to a lesser asymptotic value, and this would agree better with the experimental results.* Experimentally the maxima occur at thicknesses of about 25 and 35 molecules, while with our model at about 75 and 125 molecules. We really could not expect better agreement than this as we have considered only a one-dimensional model.

The way in which the current depends on the frequency is similar to that found by Frohlich (*loc. cit.*), but with a certain modification. According to our view the photoelectric effect should occur in bands. The first band covers part of the visible and ultra-violet, the next lies in the region of soft X-rays, etc. Between the bands the effect should be very small, the width of these non-sensitive regions depending on the binding constant P, and decreasing as the frequency is increased. Richardson and Young* in the case of potassium have found a strong falling off in the effect between 5000 A.U. and 4000 A.U., but, unfortunately, the measurements were not carried quite far enough to see if the yield really did decrease to a very small value and then rise again. For the heavier metals, the energy spectrum is much more distended and the maximum sensitivity occurs in the far ultra-violet

---

* See for example, K. T. Compton and L. W. Ross, 'Phys. Rev.,' vol 13, p. 374 (1919), O. Stuhlmann, 'Phys. Rev.,' vol. 20, p. 65 (1922); Goldschmidt u. Dember, 'Z. Tech Physik,' vol. 7, p. 137 (1926).

### *Extension to Three-dimensional Case*

All the models for which the photoelectric effect has been calculated fail in one point, they are one-dimensional, and the photoelectric current is caused only by that component of the electric intensity of the exciting radiation perpendicular to the surface This is certainly not true for actual metals and it seems desirable to extend the model until it agrees better on this point. Although we have made all our calculations for a model in which the potential varies in one dimension only, very similar analysis would apply in a three-dimensional case, provided the wave equation were separable into three equations of the form (1), the only difference being a different normalising condition in the $y$ and $z$ directions. The interesting point emerges that, with good approximation, each of the three components of the electric intensity causes transitions only in its own direction. The electrons stimulated by the components of the intensity parallel to the surface of the film will move off parallel to the surface and, although with this perfect model they could never emerge, in an actual metal they would soon be deflected by the metallic ions and could then escape. We find as the current which would arise in this way per unit incident energy

$$S_1 = \frac{256\pi^4 e^3 m\,(1 - e^{-2n\mu})}{\mu c h^3 a^3 (\beta'^2 - \beta^2)^4} \cdot \frac{\beta^2 \beta'^2}{\left(\beta' \dfrac{d\beta'}{d\alpha} - \beta \dfrac{d\beta}{d\alpha}\right)}$$
$$\times \frac{\sin^2 \alpha a\,(\cos \beta' a - \cos \beta a)^2}{\left[1 - \cos \alpha a \cos \beta a + \dfrac{1}{P}(\cos \alpha a - \cos \beta a)^2\right]\left[1 - \cos \alpha a \cos \beta' a + \dfrac{1}{P}(\cos \alpha a - \cos \beta' a)^2\right]}.$$

---

* 'Proc. Roy. Soc.' A, vol 107, p 377 (1925).

$S_0$ is given by (5) and the total current is $S = S_0 + S_1$. Fig. 5 gives $S_0$ and $S_1$ against the frequency for $P = 3\pi/2$. It will be noticed that this model shows

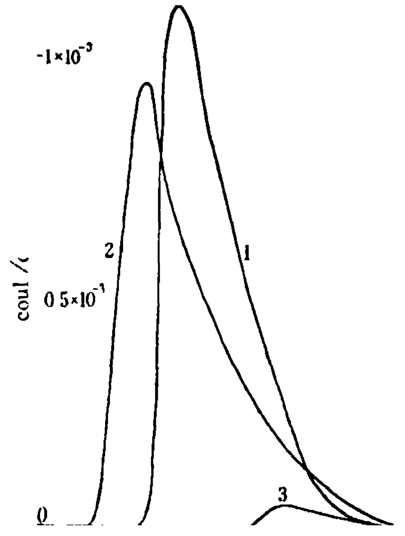

Fig. 3.—Curve 1, P = $\frac{3}{2}\pi$; Curve 2, P — $\frac{1}{2}\pi$, Curve 3, P $5\pi$

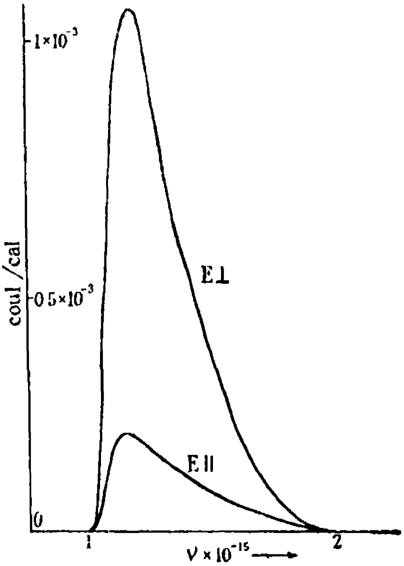

Fig

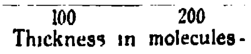

Fig. 4.

an appreciable selective photoelectric effect for all thicknesses of the film, the current obtained when the electric intensity is normal to the surface being about five times that obtained when the electric intensity lies in the plane of the film.

In conclusion, I would like to thank Dr. R. de L. Kronig for his help and encouragement during the course of this work.

### *Summary.*

The photoelectric current from a thin metallic film has been calculated on the assumption that the metal can be considered as a potential trough containing a number of infinitely high, infinitely narrow, potential barriers, one for each layer of ions It seemed necessary to take into account the damping of the incident light wave, which was assumed to decrease exponentially It is shown that this model has certain natural absorption frequencies, on account of which the emerging photoelectrons should all have the same velocity, a feature approximately satisfied in the case of thin films. The magnitude of the effect may easily be controlled by the strength of the barriers, while the threshold varies only by a factor two An extension to the three-dimensional case is made, and it appears that this model shows a selective effect. There is good agreement with the experimental results for the variation of the current with the thickness of the film and with the frequency of the light.

# *The Arc Spectrum of Iodine.*

By S. F. Evans, M.Sc , Armstrong College, Newcastle-on-Tyne.

(Communicated by T H. Havelock, F R S —Received June 19, 1931 )

## 1. *Introduction.*

Although a great deal of work has been done on the spectra associated with iodine, very little information concerning the arc spectrum is available. Wood and Kimura* give the wave-lengths of a large number of iodine lines in the visible, and separate arc from spark lines. Turner† has measured the wave-lengths of arc lines in the Schumann region and Robertson and Findlay‡ and Landau-Ziemecki§ have observed iodine spectra in the near ultra-violet under various conditions of excitation. MM. Bloch|| and Kerris¶ have extended accurate measurements up to λ 7500, but their lists contain almost

* ' Astrophys. J.,' vol. 46, p. 181 (1917).

† ' Phys. Rev.,' vol. 27, p. 397 (1926).

‡ ' Trans. Roy. Soc. Canada,' vol. 21, p. 89 (1927).

§ ' Phil. Mag.,' vol. 44, p. 651 (1922)

|| ' Ann Physique,' vol. 11, p. 141 (1929).

¶ ' Z. Physik,' vol. 60, p. 20 (1930).

entirely spark lines. Very recently Iwama* has extended observations of the arc spectrum into the infra-red, but his wave-lengths are only approximate and it has been found that many of his lines are spark lines.

The only progress that has been made with the analysis is the identification by Turner (*loc. cit.*) of the fundamental $^2P_{1/2,\,3/2}$ difference from the Schumann lines and other papers by the same author,† in which suggestions are made as to the origin of some of the Schumann lines. The work of analysis has presumably been impeded by the uncertain classification of arc and spark lines and the absence of accurate measurements in the infra-red. In the present work it has been found that the multiplet intervals are very wide and the spacing between the electronic levels is relatively small, so that many significant lines lie in the infra-red, and there is reason to believe that there are many more lines of still higher wave-length, beyond the reach of the sensitised photographic plate. The uncertainty regarding the classification of arc and spark lines is, in all probability, due to the ease with which iodine vapour may be excited to give complex spark spectra and the resultant difficulty of obtaining a reasonably pure arc spectrum of sufficient intensity to photograph on high dispersion.

## II. *Experimental Procedure.*

The high frequency discharge in iodine vapour was used as source in view of the ease with which the conditions of the discharge may be controlled to give a pure arc spectrum; a further advantage is the absence of internal electrodes. Experiments were made with a direct discharge in iodine vapour applied by internal electrodes, but it was found that the tubes had a very short life owing to the chemical activity of iodine, and that it was very difficult to maintain steady conditions or to differentiate between arc and spark lines. The quartz discharge tube, which had a plane window fused on one end, was 10 cm. long, 2·2 cm. diameter and had a central capillary 2 cm. long and 0·3 cm. internal diameter. It was exhausted with a Cenco Hyvac oil pump and charcoal cooled in liquid air, and was then baked out at a bright red heat. A few milligrams of iodine, purified by successive resublimations and dried over $P_2O_5$ were distilled into the tube which was then sealed off. After many hours running, no trace of impurity has been observed. The high frequency energy was applied by external electrodes, consisting of strips of tinfoil wrapped round the wide ends of the tube and connected to a valve maintained oscillator working at a frequency of the order of 3 × $10^7$ cycles per second, a description of this instrument has been given by the writer.* A higher power oscillator, with 400 watts input to the plates of the valves and working at a frequency of the order of $1 \cdot 5 \times 10^7$ cycles per second was used when photographing on high dispersion.

---

* 'Sci. Pap. Inst. Phys. Chem. Res. Tokyo,' No. 295, vol 15, p. 163 (1931).

† Turner and Compton, 'Phys. Rev.,' vol. 25, p. 791 (1925); 'Phys. Rev.,' vol. 31, p. 983 (1928); Turner and Samson, 'Phys. Rev.,' vol. 37, p. 1023 (1931).

At room temperature the discharge is yellow and shows strong arc lines, emission bands and weak spark lines. Raising the temperature of the tube to about 40° C. causes the discharge to become pink; under these conditions the arc lines are very strong, the bands weaker, and the spark lines almost entirely absent. The accompanying tables set out the wave-lengths and intensities of arc lines observed under these conditions. A few weak spark lines were still present, but these were identified by comparison with plates taken with the tube at room temperature, under which conditions spark lines were very much stronger. The use of the high power oscillator tends to bring up spark lines; the same effect is produced by cooling the tube and hence lowering the pressure of iodine vapour. As it was found impossible to eliminate emission bands in the region λλ 6600–5200 under the conditions necessary for the production of the arc spectrum, some weak lines may have been masked. Heating the capillary removes all trace of the band spectrum but brings up strong spark lines, presumably owing to a local lowering of density The strong spark line λ 5161 is one of the first to appear as conditions vary and its absence may be taken as a criterion of the purity of the spectrum.

The spectrum was photographed in the first order of a concave grating of 21 feet radius of curvature, the property of Dr Wilfred Hall, of Tynemouth. Iron arc comparison spectra were partially superposed; above λ 6700 second order standards were used Exposures ranged from 4 hours for the strong lines in the blue-green to 25 hours for the far infra-red lines. Ilford Golden Iso Zenith, Ilford Special Rapid Panchromatic, Kodak Extreme Red Sensitive, and Kodak Infra-red Sensitive plates were used to cover the region λλ 4000–10000. Before use plates were hypersensitised by immersion for 45 seconds in a bath containing 3½ c.c. of 0·880 ammonia in 100 c.c. water, and were then quickly dried in a current of hot air from an electric hair dryer.

It is well known that the high-frequency discharge tends to drive substances into the walls of the discharge tube; this effect was very pronounced in the present work. The inner surface of the tube became coated with a reddish film, and after running for something like 100 hours all the iodine was driven into the walls and it was no longer possible to produce a discharge in the tube.

---

* 'J. Sci. Inst.,' vol. 7, p. 261 (1930).

Some of the iodine was recovered by heating to a bright red heat, but it has not been found possible to remove the reddish film. The quartz window has also become opaque below λ 3300. The quartz capillary where the discharge was most intense does not appear to have been affected, and is still transparent down to λ 1850. Similar effects have been noted in a quartz bromine tube excited with the high frequency discharge.

## III. *Results.*

Strong arc lines were found between λ 4700 and the infra-red limit of the sensitised photographic plate. The line of highest wave-length recorded on the grating plates was λ 9731 ; on a two-prism Littrow instrument of 240 cm. focal length, two lines were observed of wave-length, determined by extrapolation λλ 10245, 10481 These lines must be very intense as they can be photographed on a Hilger Constant Deviation Spectrograph in half-an-hour, and might be of use as standards in this region if their wave-lengths were accurately determined. Although exposures up to 25 hours were given, they were not obtained on the grating plates, but it is thought that this may be due to the fact that the only infra-red plates available were some months old and were considerably less sensitive than freshly coated plates. Many of the strong infra-red lines reported by Iwama (*loc. cit*.) were found to be spark lines. No strong lines were observed between the well-known lines λ 4763 and λ 2062. An unsuccessful search was made for the lines reported by Robertson and Findlay (*loc. cit.*) and Landau-Ziemecki (*loc cit.*) in this region. The former authors have found pairs of lines showing the fundamental $^2P_{1/2,\,3/2}$ difference of 7600 cm.$^{-1}$ given by Turner, but as no trace of these lines was found in the present work it is thought that these must be spark lines and the appearance of the significant difference therefore fortuitous. There is also no sign of the " lines of low energy " λλ 3135, 2537 reported by Fruth* while investigating the spectra excited by low voltage arcs in iodine vapour. It should be noted, however, that these lines, unlike the line λ 2062, disappeared when the energy of excitation increased. The present work throws no light on the origin of these lines.

In the red and far-red there are a number of lines which, with high dispersion are seen to be close doublets or groups of lines having separations of the order of one or two wave-numbers. Their behaviour in the discharge suggests that they belong to the arc spectrum, but they do not appear to arise from combinations with any of the terms which have been identified in this analysis.

---

* 'Phys. Rev.,' vol. 31, p. 614 (1928).

Typical examples are the double lines λλ 6661, 6698, 6339 or the group of lines λ 6244.

The plates were measured on a Hilger L13 comparator. Unfortunately, it was found impossible to eliminate shifts during the exposures, and wave-lengths of lines determined from different plates differ considerably, by as much as 0·13 Å. in some cases. This cannot be due to errors in reduction, as successive determinations of the wave-length of a line using different standards on the same plate agreed to 0·01 Å. An attempt has been made to correct all the lines to a common standard, so that the relative accuracy is probably greater than the absolute accuracy. Another factor which tends to introduce errors into the measurements is the hyperfine structures of the lines These have been investigated by Mr. S. Tolansky in this laboratory, and it is found that many of the lines are unsymmetrical and have a width of the order of 0·25 Å. The intensities given, being visual estimates of blackening of the plate, can only be compared over a narrow range owing to the large and rapid changes of photographic sensitivity in this region The plates used had a pronounced minimum from λ 6700 to λ 7000 and fell off rapidly above λ 9000.

Table I.—Wave-lengths in the Arc Spectrum of Iodine.

| Intensity | $\lambda_{air}$. | $\nu_{vac}$. | Transition. |
|---|---|---|---|
| 1 | 10481 | 9538 | |
| 1 | 10245 | 9758 | |
| 2 | 9731·57 | 10272·9 | |
| 1 | 9652·88 | 10356·7 | |
| 2 | 9335·99 | 10708·3 | 6s $^2P_{3/2}$ 7p $h_{3/2}$ |
| 6 | 9113·88 | 10969·2 | 6s $^4P_{3/2}$—6p $b_{3/2}$ |
| 0 | 9098·81 | 10987·4 | |
| 7 | 9058·38 | 11036·4 | |
| 4 | 9022·43 | 11080·5 | 6s $^4P_{1/2}$—7p $i_{3/2}$ |
| 5 | 8898·44 | 11234·9 | 6s $^4P_{3/2}$—7p $g_{3/2}$ |
| 4 | 8857·46 | 11286·8 | |
| 4 | 8853·39 | 11292·0 | |
| 2 | 8700·80 | 11490·0 | |
| 6 | 8664·93 | 11537·6 | |
| 1 | 8545·56 | 11698·7 | |
| 4 | 8488·16 | 11781·2 | |
| 7 | 8393·42 | 11910·9 | 6p 6—5d 1 |
| 7 | 8240·13 | 12132·4 | 6p 7—5d 3 |
| 5 | 8222·05 | 12158·3 | 6s $^4P_{1/2}$—7p $g_{3/2}$ |
| 7 | 8169·51 | 12237·2 | 6p 7—5d 4 |
| 1 | 8093·32 | 12352·5 | 6p 8—5d 7 |
| 10 | 8043·74 | 12428·6 | 6s $^4P_{5/2}$—6p $b_{7/2}$ |
| 5 | 8003·70 | 12490·8 | 6p 6—5d 2 |
| 2 | 7969·54 | 12546·0 | 6p 8—5d 8 |
| 8 | 7700·20 | 12983·1 | 6p 5—5d 2 |
| 3 | 7588·70 | 13173·8 | |
| 5 | 7536·69 | 13229·6 | 6s $^2P_{3/2}$—7p $e_{3/2}$ |
| 6 | 7554·25 | 13234·0 | 6p 3—5d 1 |
| 5 | 7490·58 | 13346·6 | |
| 9 | 7469·04 | 13385·0 | 6p 6—5d 3 |
| 4 | 7418·55 | 13479·7 | |

Table I—(continued).

| Intensity. | $\lambda_{\text{air}}$. | $\nu_{\text{vac}}$. | Transition. |
|---|---|---|---|
| 1 | 7414·61 | 13483·1 | $6s\ ^4P_{3/2}$—$7p\ c_{1/2}$ |
| 3 | 7413·64 | 13485·0 | |
| 4 | 7411·25 | 13489·3 | $6p\ 6$—$5d\ 4$ |
| 8 | 7402·10 | 13505·9 | $6p\ 6$—$5d\ 5$ |
| 1 | 7305·47 | 13684·7 | |
| 0 | 7258·11 | 13773·9 | |
| 7 | 7236·80 | 13814·5 | $6p\ 3$—$5d\ 2$ |
| 2 | 7231·86 | 13824·0 | |
| 1 | 7227·34 | 13832·7 | |
| 1 | 7191·73 | 13901·1 | $6p\ 6$—$5d\ 8$ |
| 4 | 7164·82 | 13953·3 | |
| 3 | 7148·63 | 13981·9 | $6p\ 7$—$5d\ 12$ |
| 6 | 7142·09 | 13997·6 | $6p\ 5$—$5d\ 5$ |
| 5 | 7122·09 | 14036·9 | |
| 2 | 7120·11 | 14040·9 | |
| 4 | 7063·60 | 14153·1 | $6s\ ^4P_{1/2}$—$7p\ e_{3/2}$ |
| 4 | 7018·32 | 14244·4 | |
| 1 | 6993·45 | 14295·1 | $6s\ ^4P_{1/2}$—$7p\ d_{1/2}$ |
| 3 | 6989·84 | 14302·5 | |
| 2 | 6986·35 | 14309·7 | |
| 1 | 6958·83 | 14366·3 | |
| 1 | 6941·02 | 14403·1 | $6p\ 4$—$5d\ 3$ |
| 0 | 6939·26 | 14406·8 | $6s\ ^4P_{1/2}$—$7p\ c_{1/2}$ |
| 3 | 6928·86 | 14428·4 | |
| 0 | 6899·85 | 14489·1 | |
| 2 | 6856·82 | 14580·0 | |
| 0 | 6845·62 | 14603·9 | |
| 4 | 6812·19 | 14675·5 | $6p\ 2$—$5d\ 2$ |
| 4 | 6789·32 | 14725·0 | $\left\{\begin{array}{l} 6s\ ^4P_{1/2}\text{—}7p\ b_{3/2} \\ 6p\ 4\text{—}5d\ 7 \end{array}\right.$ |
| 0 | 6784·62 | 14735·2 | |
| 4 | 6741·56 | 14829·3 | $6p\ 3$—$5d\ 5$ |
| 4 | 6739·50 | 14833·8 | $6s\ ^2P_{3/2}$—$7p\ a_{5/2}$ |
| 5 | 6738·12 | 14836·9 | |
| 4 | 6736·60 | 14840·2 | |
| 7 | 6732·10 | 14850·1 | |
| 5 | 6727·00 | 14861·4 | |
| 4 | 6698·53 | 14924·6 | |
| 6 | 6697·33 | 14927·3 | |
| 6 | 6662·14 | 15006·1 | |
| 6 | 6661·16 | 15008·1 | |
| 3 | 6650·81 | 15031·6 | $6p\ 3$—$5d\ 7$ |
| 10 | 6619·69 | 15102·2 | $6p\ 4$—$5d\ 9$ |
| 6 | 6585·34 | 15181·0 | |
| 7 | 6583·80 | 15184·4 | |
| 4 | 6582·95 | 15186·5 | |
| 2 | 6580·58 | 15192·0 | |
| 1 | 6577·67 | 15198·7 | |
| 9 | 6566·53 | 15224·4 | $6p\ 3$—$5d\ 8$ |
| 3 | 6560·87 | 15237·6 | $6p\ 6$—$5d\ 12$ |
| 7 | 6488·18 | 15408·3 | $6p\ 3$—$5d\ 9$ |
| 0 | 6479·94 | 15428·2 | $6p\ 4$—$5d\ 10$ |
| 1 | 6479·32 | 15429·5 | |
| 0 | 6477·48 | 15433·8 | |
| 1 | 6454·08 | 15489·7 | |
| 0 | 6434·60 | 15536·7 | |
| 0 | 6433·35 | 15539·7 | |
| 3 | 6415·79 | 15582·2 | |
| 3 | 6411·29 | 15593·2 | |
| 3 | 6378·80 | 15672·6 | |
| 6 | 6371·76 | 15689·9 | $6p\ 2$—$5d\ 5$ |

Table I—(continued).

| Intensity. | $\lambda_{air}$ | $\nu_{vac}$ | Transition |
|---|---|---|---|
| 5 | 6367 34 | 15700 8 | 6*p* 4—5*d* 11 |
| 7 | 6359 19 | 15720 9 | |
| 2 | 6355·66 | 15729 7 | 6*p* 5—5*d* 12 |
| 0 | 6353 55 | 15734 9 | 6*p* 3—5*d* 10 |
| 8 | 6339 52 | 15769 7 | |
| 6 | 6338 02 | 15773 5 | |
| 3 | 6333 58 | 15784 5 | |
| 4 | 6330 45 | 15792 3 | |
| 0 | 6321 70 | 15814 2 | |
| 0 | 6320 84 | 15816 3 | |
| 2 | 6313 20 | 15835 5 | |
| 1 | 6312 55 | 15837 1 | 6*p* 2—5*d* 6 |
| 3 | 6297 08 | 15876 0 | |
| 8 | 6294 08 | 15883 7 | 6*s* ${}^4P_{3/2}$—7*p* $t_{3/2}$ |
| 1 | 6290 68 | 15892 1 | 6*p* 2—5*d* 7 |
| 2 | 6246 26 | 16005 1 | |
| 0 | 6245 72 | 16006 5 | |
| 1 | 6245 41 | 16007 4 | 6*p* 3—5*d* 11 |
| 3 | 6244 55 | 16009 5 | |
| 2 | 6244 11 | 16010 2 | |
| 1 | 6243 75 | 16011 6 | |
| 2 | 6243 28 | 16012 8 | |
| 3 | 6242 81 | 16014 0 | |
| 2 | 6240 93 | 16018 9 | |
| 2 | 6233·59 | 16037 7 | |
| 5 | 6213 17 | 16090 4 | 6*p* 1—5*d* 6 |
| 7 | 6191 97 | 16145 5 | 6*p* 1—5*d* 7 |
| 1 | 6147 50 | 16262 2 | |
| 2 | 6115 04 | 16348 6 | |
| 10 | 6082 46 | 16436 2 | 6*s* ${}^4P_{3/2}$—7*p* $h_{5/2}$ |
| 3 | 6056 10 | 16507 7 | |
| 2 | 6055 13 | 16510 3 | |
| 2 | 6054 16 | 16513 0 | |
| 3 | 6053 56 | 16514 7 | |
| 3 | 6042 78 | 16544 1 | |
| 8 | 6024 13 | 16595 3 | 6*p* 2—5*d* 10 |
| 2 | 6005 09 | 16647 9 | |
| 3 | 5985 03 | 16703 7 | |
| 3 | 5984 36 | 16705 6 | |
| 3 | 5981 42 | 16713 8 | |
| 3 | 5980 96 | 16715 1 | |
| 3 | 5968 41 | 16750 2 | |
| 2 | 5690 86 | 16754 6 | |
| 3 | 5956 98 | 16782 3 | |
| 2 | 5954 49 | 16789 4 | |
| 3 | 5950 38 | 16801 2 | |
| 10 | 5894 10 | 16961 4 | 6*s* ${}^4P_{3/2}$—7*p* $g_{3/2}$ |
| 2 | 5882 33 | 16995 3 | |
| 1 | 5843 35 | 17108 7 | |
| 2 | 5780 74 | 17294 0 | |
| 9 | 5764 42 | 17342 9 | 6*s* ${}^4P_{5/2}$—7*p* $i_{3/2}$ |
| 0 | 5761 14 | 17352 8 | |
| 7 | 5586 75 | 17895 7 | 6*s* ${}^4P_{5/2}$—7*p* $h_{5/2}$ |
| 6 | 5427 09 | 18420 9 | 6*s* ${}^4P_{5/2}$—7*p* $g_{3/2}$ |
| 7 | 5234 63 | 19098 2 | 6*s* ${}^4P_{3/2}$—7*p* $d_{1/2}$ |
| 6 | 5204 20 | 19209 9 | 6*s* ${}^4P_{3/2}$—7*p* $c_{1/2}$ |
| 10 | 5119 35 | 19528 3 | 6*s* ${}^4P_{3/2}$—7*p* $b_{3/2}$ |
| 6 | 4917 01 | 20331 9 | 6*s* ${}^4P_{5/2}$—7*p* ${}^4D_{7/2}$ |
| 5 | 4896 80 | 20415·8 | 6*s* ${}^4P_{5/2}$—7*p* $e_{3/2}$ |
| 10 | 4862 38 | 20560 3 | 6*s* ${}^4P_{3/2}$—7*p* $a_{5/2}$ |
| 7 | 4763·38 | 20987·6 | 6*s* ${}^4P_{5/2}$—7*p* $b_{3/2}$ |

## IV. *Structure of the Spectrum.*

The theoretical term scheme for iodine is shown in Table II. The terms based on $^3$P of the ion may be expected to be very much more prominent than those based on $^1$D and $^1$S.

Table II.—Term Scheme of Iodine.

| Electron configuration | Basic term of the ion. | | | | | | | | | | | | |
|---|---|---|---|---|---|---|---|---|---|---|---|---|---|
| | $^3$P | | | | | | $^1$D. | | | | | $^1$S |
| $5p^4\,5p$ | | $^2$P | | | | | | | | | | |
| $5p^4\,5d$ | $^2$P, | $^4$D, | $^2$F, | $^4$P, | $^4$D, | $^4$F | $^2$S, | $^2$P, | $^2$D, | $^2$F, | $^2$F, | $^2$D |
| $5p^4\,6s$ | | $^2$P, | | | $^4$P, | | | | $^2$D | | | $^2$S |
| $5p^4\,6p$ | $^2$S, | $^2$P, | $^2$D, | $^4$S, | $^4$P, | $^4$D | | $^2$P, | $^2$D, | $^2$F | | $^2$D |
| $5p^4\,6d$ | $^2$P, | $^4$D, | $^2$F, | $^4$P, | $^4$D, | $^4$F | $^2$S, | $^2$P, | $^2$D, | $^2$F, | $^2$G | $^2$D |
| $5p^4\,7s$ | | $^2$P, | | | $^4$P, | | | | $^2$D | | | $^2$S |
| $5p^4\,7p$ | $^2$S, | $^2$P, | $^2$D, | $^4$S, | $^4$P, | $^4$D | | $^2$P, | $^2$D, | $^2$F | | $^2$P |

In chlorine and bromine Kiess and de Bruin* have shown that the strongest lines in the Schumann region investigated by Turner (*loc. cit.*) arise from transitions corresponding to $6s \rightarrow 5p$ in iodine The first clues to the structure of the spectrum were therefore sought in Turner's lines. The lines arising from this transition were readily found; they are set out in the form of a super-multiplet in Table III. The arrangement is in agreement with Turner's observation that the only resonance lines above λ 1640 were λλ 1830, 1782, 1642. Six lines are reported by Turner to be greatly reduced in intensity when CO bands appeared Four of these are included in Table III and have been marked with an asterisk; it will be noted that they all have the stable level $5p\,^2P_{3/2}$ as the final state. This effect is somewhat obscure since these lines have a common lower level. It is probable, however, that it is in some way connected with self-absorption as the lines involved are resonance lines.

From consideration of the structures of the arc spectra of chlorine and bromine the transition $6p \rightarrow 6s$ may be expected to give a number of strong lines in the infra-red and $7p \rightarrow 6s$ another set of strong lines of higher frequency. A search was therefore made for the characteristic 6*s* differences amongst the visible and infra-red arc lines.

It is found that the 6*s* differences occur prominently among the strong lines in the visible region. As these lines are the lines of highest frequency, excluding

---

* Chlorine :—'Bur. Stan. J. Res.,' vol. 2, p. 1117 (1929). Bromine :—'Bur. Stan. J. Res.,' vol. 4, p. 667 (1930).

Table III.—Multiplet from Transition $6s \rightarrow 5p$. Wave-lengths from Turner.

| 5P | $^3P$ | $\Delta$ 7600 | $^2P_{\frac{1}{2}}$ |
|---|---|---|---|
| $^4P_{5/2}$ | (10) 54632* | | |
| $\Delta\nu = 1459$ 2 | | | |
| $^4P_{3/2}$ | (9) 56089* | | (10) 48494 |
| $\Delta\nu = 4803$ 3 | | | |
| $^4P_{1/2}$ | (7) 60885* | | (7) 53293 |
| $\Delta\nu = 923$ 7 | | | |
| $^2P_{3/2}$ | (6) 61809* | | (9) 54216 |
| $\Delta\nu = 4530$ | | | |
| $^2P_{1/2}$ | (3) 66342 | | (8) 58744 |

* Greatly reduced in intensity when CO bands appeared

the Schumann lines, it is concluded that they arise from the transition $7p \rightarrow 6s$. This identification is supported by the fact that a pair of very strong lines in the infra-red are separated by the $6s\,^4P_{5/2,\,3/2}$ interval. It may reasonably be assumed, therefore, that these two lines belong to the $6p \rightarrow 6s$ supermultiplet, the remainder of the lines lying in the inaccessible far infra-red region.

In Table IV the $7p \rightarrow 6s$ lines and the pair of $6p \rightarrow 6s$ lines are set out in the form of a supermultiplet. Possible $j$ values have been assigned to the $7p$ terms, but in view of the fact that these terms may be expected to show very abnormal intervals and intensities and no Zeeman effect data is available it has been deemed inadvisable to assign $l$ values with the exception of the term "$f$" which, having $j = 7/2$ must be $^4D_{7/2}$ The intensity of a line is given in brackets in front of the frequency. The number of hyperfine components, as determined by Tolansky, is given, where known, by a Roman numeral following the frequency. It is satisfactory that in every case except one, the hyperfine structure observations are consistent with the proposed allocation in that all lines having $6s\,^4P_{5/2}$ as final state have six components, whereas lines based on $6s\,^4P_{3/2}$ have four, although in some of the sextets the last two components are not fully resolved. The exception is the line λ 5119, ν 19528, which has two; the explanation of this anomaly has not yet been found.

There are a large number of strong lines in the far-red and infra-red which could not be fitted into the above scheme. Considerable difficulty was experienced in establishing regularities amongst these lines as they appear to arise from the combination of two extensive and unknown families of terms. Many

Table IV.—Multiplets from Transition $7p \rightarrow 6s$.

| $6s$ / $7p$ | $^4P_{5/2}$ | $\Delta\nu$ 1459·2 | $^4P_{3/2}$ | $\Delta\nu$ 4803·3 | $^4P_{1/2}$ | $\Delta\nu$ 923·7 | $^2P_{3/2}$ |
|---|---|---|---|---|---|---|---|
| $a_{3/2}$ | (22019·5) | | (10) 20560·3 (IV) | | | | (3) 14833·8 |
| $\Delta\nu = 1032·2$ | | | | | | | |
| $b_{3/2}$ | (7) 20987·6 (VI) | | (10) 19528·3 (II) | | (4) 14725·0 | | (13801·3) |
| $\Delta\nu = 318·3$ | | | | | | | |
| $c_{1/2}$ | | | (6) 19209·9 (IV) | | (0) 14406·8 | | (1) 13483·1 |
| $\Delta\nu = 111·7$ | | | | | | | |
| $d_{1/2}$ | | | (7) 19098·2 (IV) | | (1) 14295·1 | | (13371·4) |
| $\Delta\nu = 141·8$ | | | | | | | |
| $e_{3/2}$ | (5) 20415·8 (VI) | | (18956·6) | | (4) 14153·1 | | (5) 13229·6 |
| $\Delta\nu = 83·9$ | | | | | | | |
| $f_{7/2}$ | (6) 20331·9 (VI) | | | | | | |
| $\Delta\nu = 1911·0$ | | | | | | | |
| $g_{3/2}$ | (6) 18420·9 (VI) | | (10) 16961·4 (IV) | | (5) 12158·3 | | (5) 11234·9 |
| $\Delta\nu = 525·2$ | | | | | | | |
| $h_{5/2}$ | (7) 17895·7 (VI) | | (10) 16436·2 (IV) | | | | (2) 10708·3 |
| $\Delta\nu = 552·7$ | | | | | | | |
| $i_{3/2}$ | (9) 17342·9 (VI) | | (8) 15883·7 | | (4) 11080·5 | | (10156·8) |
| $6p\ b_{3/2}$ | (10) 12428·6 (VI) | | (6) 10969·2 | | | | |

Lines which are predicted, but not observed, are shown in brackets The term $6s\ ^4P_{1/2}$ is not included, combinations with it will give lines far in the infra-red beyond the limit of photographic sensitivity

of these lines are included in Table V and it appears fairly certain that this supermultiplet must be of physical significance in view of the large number of recurring differences involved. It is very probable that these lines arise from the transition $5d \rightarrow 6p$; it will be seen from the term scheme given in Table II that the transition will give rise to a very complex supermultiplet. The fact that no other combination with either of these families is observed would then be due to the closeness of the electronic levels; $5d \rightarrow 7p$ lines will, like the $6p \rightarrow 6s$ lines, lie far in the infra-red. Lines arising from $5d \rightarrow 5p$ should be observed in the Schumann region, but cannot be detected with any degree of certainty owing to the inaccuracy of wave-length determinations in this region. This identification is supported by hyperfine structure evidence. Five of the strong lines in question have been examined and are found to be single, diffuse to the red. In bromine the analogous $4d \rightarrow 5p$ lines have a similar structure, single, diffuse to the red. The family of terms which has the larger intervals has been assumed to be the $6p$ terms, but it has not been found possible to identify $6p\ b_{3/2}$ amongst them. From comparison with the other halogens $6p$ has been taken as the lower level.

## Table V.—Multiplets from Transition 5*d* → 6*p*.

| 5*d* \ 6p | 1 | *253·3* | 2 | *860·6* | 3 | *306·5* | 4 | *525·0* | 5 | *492·0* | 6 | *1253·3* | 7 | *102·8* | 8 |
|---|---|---|---|---|---|---|---|---|---|---|---|---|---|---|---|
| 1 | | | | | (6) 13234·0 | | | | | | (7) 11910·9 | | | | |
| *580·2* | | | | | | | | | | | | | | | |
| 2 | | | (4) 14675·5 | | (7) 13814·5 | | | | (8) 12983·1 | | (5) 12490·8 | | | | |
| *894·2* | | | | | | | | | | | | | | | |
| 3 | | | | | | | (1) 14403·1 | | | | (9) 13385·0* | | (7) 12132·4 | | |
| *104·5* | | | | | | | | | | | | | | | |
| 4 | | | | | | | | | | | (4) 13489·3 | | (7) 12237·2 | | |
| *16·6* | | | | | | | | | | | | | | | |
| 5 | | | (6) 15689·9 | | (4) 14829·3 | | | | (6) 13997·6 | | (8) 13505·9* | | | | |
| *147·2* | | | | | | | | | | | | | | | |
| 6 | (5) 16090·4* | | (1) 15837·1 | | | | | | | | | | | | |
| *55·1* | | | | | | | | | | | | | | | |
| 7 | (7) 16145·5* | | (1) 15892·1 | | (3) 15031·6 | | (4) 14725·0 | | | | | | | | (1) 12352·5 |
| *193·1* | | | | | | | | | | | | | | | |
| 8 | | | | | (9) 15224·4 | | | | | | (1) 13901·1 | | | | (2) 12546·0 |
| *183·9* | | | | | | | | | | | | | | | |
| 9 | | | | | (7) 15408·3 | | (10) 15102·2* | | | | * | | | | |
| *326·3* | | | | | | | | | | | | | | | |
| 10 | | | (8) 16595·3 | | (0) 15734·9 | | (0) 15428·2 | | | | | | | | |
| *272·5* | | | | | | | | | | | | | | | |
| 11 | | | | | (1) 16007·4 | | (5) 15700·8 | | | | | | | | |
| *553·9* | | | | | | | | | | | | | | | |
| 12 | | | | | | | | | (2) 15729·7 | | (3) 15237·6 | | (3) 13984·9 | | |

* Hyperfine structure single, diffuse to red.

## V. *Ionisation Potential.*

The term $7p\,b_{3/2}$ combining with the $6s$ term (see Table IV) gives rise to a pair of strong lines separated by 1459 cm.$^{-1}$; these are also the pair of lines of highest frequency which show this difference. The two infra-red lines which involve this difference may thus arise from the corresponding $6p$ term. If this assumption is made the interval $6p\,b_{3/2}$, $7p\,b_{3/2}$ is obtained, and by application of the Rydberg formula the ionisation voltage may be derived as set out below.

From Table IV, frequency of line $6s\,{}^4P_{5/2}$—$7p\,b_{3/2}$ = 20987·6 cm.$^{-1}$
„ „ „ $6s\,{}^4P_{5/2}$—$6p\,b_{3/2}$ = 12428·6 cm.$^{-1}$.

Therefore interval $6p\,b^{3/2}$—$7p\,b_{3/2}$ = 8559·0.

From Rydberg's Interpolation Table as given in Fowler's Report on Line Spectra the absolute values of the terms $6p\,b_{3/2}$, $7p\,b_{3/2}$ may be estimated. They are

$$6p\,b_{3/2} = 17500 \text{ cm.}^{-1}$$
$$7p\,b_{3/2} = 8940 \text{ cm.}^{-1}.$$

The observed term combinations enable the value of the deepest term $5p\,{}^2P_{3/2}$ to be deduced and hence the ionisation potential is calculated

$$5p\,{}^2P_{3/2} = 84560 \text{ cm.}^{-1}$$
$$\text{Ionisation potential} = 84560 \times 1\cdot2345 \times 10^{-4} \text{ volts}$$
$$= 10\cdot44 \text{ volts.}$$

This value is in surprisingly good agreement with Foote and Mohler's value of 10·4 volts determined by electrical methods.* It should be noted that the above estimate may be gravely in error due to the fact that different terms tend to different components of the deepest $^3P$ term of the ion. Kiess and de Bruin (*loc. cit.*) have shown that the separations of the fundamental $^3P$ term of the halogen ion are approximately 1·75 times as great as the separations of the fundamental $^3P$ term of the iso-electronic oxygen-like atom. McLennan, McLay and McLeod† have found that the fundamental $^3P$ term of Te I is partially inverted, the extreme separation being 4750 cm.$^{-1}$. Hence iodine terms may be expected to converge to limits having an extreme separation of the order of 8000 cm.$^{-1}$, and the value for the ionisation potential may be in error by a corresponding amount. The agreement with Foote and Mohler's value suggests that it is the true value, and the position of the deepest term determined above has been made the basis of the list of terms in Table VI

---

* 'Phys. Rev.,' vol. 21, p. 382 (1923).

† 'Phil. Mag.,' vol. 4, p. 486 (1927).

Table VI —List of Observed Terms.

Table A

| Term | Value (cm $^{-1}$) |
|---|---|
| $5p\ {}^2P_{3/2}$ | 84500 |
| $5p\ {}^2P_{1/2}$ | 76900 |
| $6s\ {}^4P_{5/2}$ | 29868 |
| $6s\ {}^4P_{3/2}$ | 28408·8 |
| $6s\ {}^4P_{1/2}$ | 23605·5 |
| $6s\ {}^2P_{3/2}$ | 22681·8 |
| $6s\ {}^2P_{1/2}$ | 18157 |
| $6p\ b_{3/2}$ | 17439·4 |
| $7p\ i_{3/2}$ | 12525·1 |
| $7p\ h_{5/2}$ | 11972·4 |
| $7p\ g_{3/2}$ | 11447·2 |
| $7p\ f_{7/2}$ | 9536·2 |
| $7p\ e_{3/2}$ | 9452 |
| $7p\ d_{1/2}$ | 9310·5 |
| $7p\ c_{1/2}$ | 9198·8 |
| $7p\ b_{3/2}$ | 8880·5 |
| $7p\ a_{5/2}$ | 7848·3 |

Table B.

| Term | Value (cm $^{-1}$) |
|---|---|
| $6p$ 1 | 21000 |
| $6p$ 2 | 20746·7 |
| $6p$ 3 | 19886·1 |
| $6p$ 4 | 19579·6 |
| $6p$ 5 | 19054·6 |
| $6p$ 6 | 18562·6 |
| $6p$ 7 | 17310·3 |
| $6p$ 8 | 17207·5 |
| $5d$ 1 | 6052·4 |
| $5d$ 2 | 6072·2 |
| $5d$ 3 | 5178·0 |
| $5d$ 4 | 5073·5 |
| $5d$ 5 | 5056·9 |
| $5d$ 6 | 4909·7 |
| $5d$ 7 | 4854·6 |
| $5d$ 8 | 4601·5 |
| $5d$ 9 | 4477·6 |
| $5d$ 10 | 4151·3 |
| $5d$ 11 | 3878·8 |
| $5d$ 12 | 3324·9 |

The values in Table A are based on the value 84500 cm.$^{-1}$ for $5p\ {}^2P_{3/2}$. The values in Table B are based on the arbitrary value 21000 cm.$^{-1}$ for $6p$ 1. This is probably of the right order of magnitude as the $6p\ b_{3/2}$ term in Table A should be one of the highest of the $6p$ terms and its most probable value, 17439·4 cm.$^{-1}$ is near the arbitrary value for $6p$ 8, 17207·5 cm.$^{-1}$.

## VI *Conclusion and Acknowledgments.*

The term scheme here presented accounts for the great majority of the strong arc lines, but is nevertheless unsatisfactory in some respects. A large number of lines, particularly in the red, remain unallocated; it is only possible to identify a few of the terms with certainty; the positions of the $6p$ and $5d$ terms relative to the deepest term are unknown, with the exception of the term $6p\ b_{3/2}$, and hence the ionisation potential can only be roughly estimated. The term $6s\ {}^2P_{1/2}$, which should be prominent and easy to detect as the other $6s$ terms are known, has not been established with any degree of reliability. These weaknesses are almost entirely due to the number of lines which lie in inaccessible regions; the $6p \rightarrow 6s$ lines, for instance, should prove an invaluable link in the setting up of a comprehensive term scheme. Zeeman effects would enable many of the terms here presented to be identified with certainty and work on this subject should lead to valuable results.

In conclusion, the author would like to record his indebtedness to Dr. Wilfred Hall for access to his private laboratory at Tynemouth and the use of his grating and comparator. The author also wishes to thank Professor W. E. Curtis for constant advice during the progress of the work, Mr S. Tolansky for use of his unpublished hyperfine structure data, and the Research Fund of Armstrong College for a grant which made this investigation possible.

---

# *Absorption Spectra of the Alkyl Halides: Energies of the C-I and C-Br Bonds.*

By T. Iredale, D.Sc., and A. G Mills, B Sc., University of Sydney

(Communicated by F. G Donnan, F R S —Received June 23, 1931.)

It is to be expected that the alkyl halides will dissociate on absorption of light into alkyl residues and excited halogen atoms. Their absorption spectra are continuous,* as is also the case with phenyl iodide,† which liberates iodine under identical conditions The C-I and C-Br linkages are certainly homopolar in the gas state. On Franck's theory‡ the long-wave limit of the absorption continuum should correspond to the heat of binding of C-I together with the excitation energy of the halogen atom. We would expect the alkyl halides to resemble the halogen hydrides in their behaviour, although with HI and HBr the long-wave limits are not very happily situated § The limit for HI is at 3320 Å., corresponding to a heat of dissociation of 65,000 calories (the thermochemical heat is 69,000 calories) and the limit for HBr at 2640 Å. (97,000 calories, the thermochemical being 85,000). It is doubtful if these disagreements are entirely due to inaccuracy in the thermochemical data. The determination of these absorption limits seems to be a difficult matter. However, in the case of some of the alkyl halides we have been successful in obtaining very satisfactory agreement between the two sets of data, and have thought it worth while to give a brief account of our experimental method, and to reproduce at least one of our photometric records.

---

* Herzberg and Scheibe, 'Z. Phys. Chem., B, vol. 7, p. 390 (1930); Iredale and Wallace, 'Phil. Mag.,' vol. 8, p. 1093 (1929).

† Pauer, 'Ann. Physik,' vol. 60, p. 363 (1897); Purvis, 'J Chem. Soc.,' vol. 99, p. 2319 (1911).

‡ 'Trans. Faraday Soc.,' vol. 21, p. 536 (1926); 'Z. Physik,' vol. 43, p. 155 (1927).

§ Bonhoeffer and Steiner, 'Z. Phys. Chem.,' vol. 122, p. 287 (1926); Tingey and Gerke, J. Amer. Chem. Soc.,' vol. 48, p. 1838 (1926): Coehn and Stuckhardt, 'Z. Phys. Chem.,' vol. 91, p. 722 (1916).

### *The Significance of the Absorption Limit.*

If the length of a column of the absorbing gas is kept constant and the pressure increased it is found that the long wave edge of the absorption band shifts towards the red and then remains fixed as the gas pressure is still further increased. As pointed out by Tingey and Gerke (*loc. cit.*), it is not really the pressure which decides the absorption limit but the product of the pressure and the length of the gas column. The limit is therefore dependent on the molecular thickness traversed by the light beam. This phenomenon must be different from the widening of a line or band due to interatomic or intramolecular effects at high pressures, such has been found recently with xenon.*

The method adopted by Tingey and Gerke was to plot the pressure against the wave-length of the band edge (a purely arbitrary proceeding), the curve becoming asymptotic to the wave-length limit at high pressures. Herzberg and Scheibe (*loc. cit.*) determined the extinction coefficients for different wave-lengths, and extrapolated to a wave-length corresponding to a very small extinction coefficient. This procedure may not give the absorption limit very accurately, unless the curve is quite linear at the long wave end.

The region where the absorption ends may be examined visually or by means of a recording microphotometer. We have found that the visual method is not very accurate, and the photometric method fails if the density of the photographic image is too great, the thermopile not being able to respond to small changes in the density.

### *Purity of Materials.*

In a number of cases minute traces of impurities are found to shift the edge of an absorption band toward the long-wave side, and even to give rise to additional bands. This constitutes a great difficulty in determining absorption limits. The alkyl halides used were liquids at ordinary temperatures, and the greatest care was taken to obtain pure products. The liquids were redistilled until there was no change in the vapour absorption limit. These stipulations apply with even greater force to measurements carried out on the liquids themselves, and it is doubtful if the results obtained in this way are always reliable. Some organic iodine compounds develop a slight yellow colour which is exceedingly difficult to remove.

---

* McLennan and Turnbull, 'Proc. Roy. Soc.,' A, vol. 129, p. 266 (1930).

## *Experimental.*

The apparatus used in the study of the light absorption was of the simplest type (fig. 1). The column of vapour was contained in a glass tube 100 cm. long, with quartz plates cemented on the ends. The pressure of the vapour was read on a mercury manometer. The liquids were introduced into the apparatus through a side tube and were cooled with liquid air while sealing off and evacuating to as low a pressure as possible ($10^{-4}$ mm.). Dissolved gases were finally removed by vapourising the liquid in a preliminary expansion chamber, cooling and re-evacuating, repeating the process if necessary. Although neither dissolved gases nor the presence of minute amounts of water vapour appeared to have any influence on the absorption, the liquid could be distilled at room temperature into another side tube through a column of phosphoric oxide. No objectionable impurities were found to arise from the samples of $P_2O_5$ used.

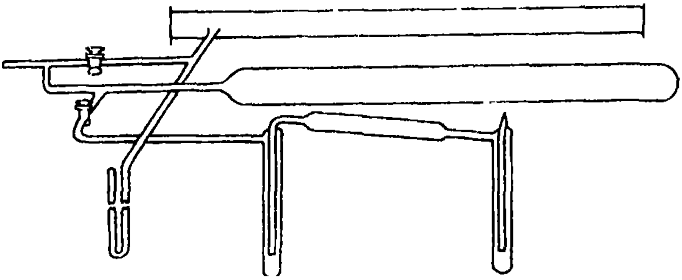

FIG 1

As sources of light we used the aluminium under-water spark, the condensed cadmium spark, and the iron arc (reference standards). In the case of the aluminium spark we followed the method of Henri and Lazlo,* but were unable to obtain exactly similar electrical conditions. The spectrum was mainly continuous with one or two lines, which, however, did not fall in the region of our absorption convergence Photographs were obtained with the Hilger E3 quartz spectrograph. The spectra of the light source were recorded in pairs on the photographic plate, one with the empty and the other with the gas-filled absorption tube, the duration of the spark being the same in each case.

---

* 'Proc. Roy. Soc.,' A, vol. 105, p. 662 (1924).

Slight fluctuations in intensity of the source were sometimes unavoidable, but where the intensities of the spectra agreed in the non-absorbable region it was considered possible to make an estimation of the absorption convergence.

The negatives were examined by purely visual and photometric methods. A narrow beam of light was passed through the negative and focussed on to a thermopile, the intensity of the unabsorbed light being registered by the galvanometer deflection. This is the principle of the Moll recording microphotometer, which we also used in some instances. The line records of the two spectra come together at the absorption limit (fig. 2).

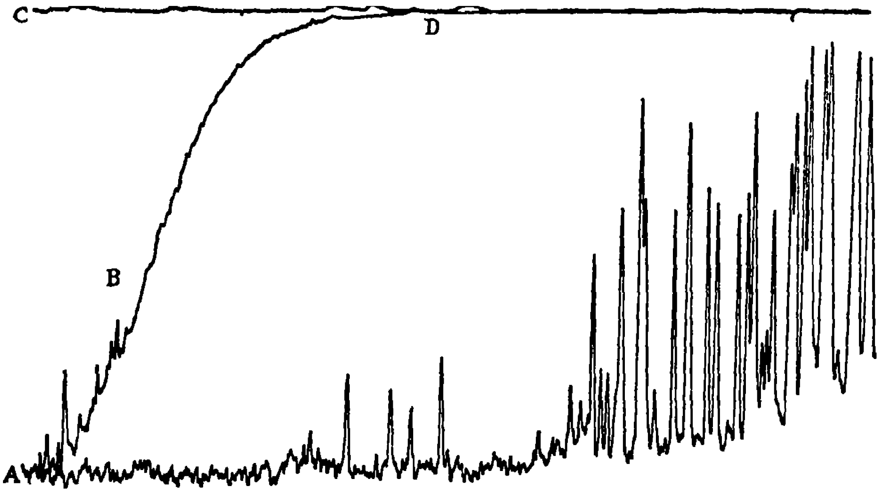

FIG. 2 —A, Comparison spectrum B, Absorption spectrum (methyl iodide) C, Continuous spectrum D, Absorption band edge.

## *Thermochemical Data.*

The energies of the C-I and C-Br bonds can be calculated from the heats of combustion of the alkyl iodides and bromides if the energy of the C-H bond is known. As pointed out by Mecke,* previous estimations of this energy are incorrect, as no account was taken of the energy necessary to excite the carbon atom from the divalent ($^3P$) to the tetravalent ($^5S$) state. This applies also to the heat of sublimation of carbon which must refer to the divalent atoms. Kohn and Guckel's value (now universally accepted) for this constant is 139 kcals. per gram-atom,† but it would appear to be something like 150 kcals. if we start from the hitherto accepted dissociation energies of CO (240 kcals.)

---

* 'Z. Phys. Chem.,' B, vol. 7, p. 108 (1930); 'Z Elekt.,' vol. 36, p. 589 (1930).

† 'Z. Physik,' vol. 27, p. 305 (1924).

and $O_2$ (128 kcals.). However, the first of these is not known very accurately, and the dissociation energy of $O_2$ is now calculated to be 117 kcals.*

The excitation energy ($x$) of the carbon atom can be calculated from the heats of combustion of carbon to CO and $CO_2$:

$$C_{solid} = C(^3P) - 139 \text{ kcals.}$$
$$C(^3P) = C(^5S) - x$$
$$C_{solid} + O_2 = CO_2 + 94$$
$$O_2 = O + O - 117$$
$$C(^5S) + 2O = CO_2 + 94 + 117 + 139 + x \qquad (a)$$
$$C_{solid} + \tfrac{1}{2}O_2 = CO + 26$$
$$C(^3P) + O = CO + 26 + 139 + 58{\cdot}5 \qquad (b)$$
$$a = 2b, \text{ whence } x = 97 \text{ kcals.}$$

Since the heat of combustion of methane is 211 kcals. and $H_2 = H + H - 101$, and $C_{solid} = C(^5S) - (139 + 97)$, $CH_4 = C + 4H - 460$ kcals. and the energy of the C-H bond = 115 kcals.

The heat of combustion of $CH_3I$ is 201 kcals. (Berthelot), $I_{2\,(solid)} = I + I - 50{\cdot}2$, so that the energy of the C-I bond is $211 - 201 + 115 - 34 - 50{\cdot}5 + 25{\cdot}1 =$ *65 kcals.* The heat of combustion of ethane is 368 kcals., of $C_2H_5Br$ is 329 (Berthelot), and $Br_2 = Br + Br - 45$, whence the energy of the C-Br bond is *92 kcals.*

These data are taken from the International Critical Tables (1929).

## *Discussion of Results.*

The absorption spectra of methyl, ethyl and iso-amyl iodide, and of ethyl bromide in the near ultra-violet are entirely continuous, as Herzberg and Scheibe† also found for $CH_3I$ and $CH_3Br$. The absorption maximum in the iodides lies at about 2550 Å. The long-wave edge of the band shifts towards the red with increasing pressure and then remains constant (absorption limit) (fig. 3). At higher temperatures the curve seems to be a little flatter, but the absorption limit does not shift very much for a temperature change of 20° C. We have not experimented with very high temperatures, but doubtless the band edge would move further towards the red owing to the increase in the number of vibrating molecules.

---

* Herzberg, 'Z. Phys. Chem.,' B, vol. 10, p. 189 (1930).

† 'Z. Phys. Chem.,' B, vol. 7, p. 390 (1930).

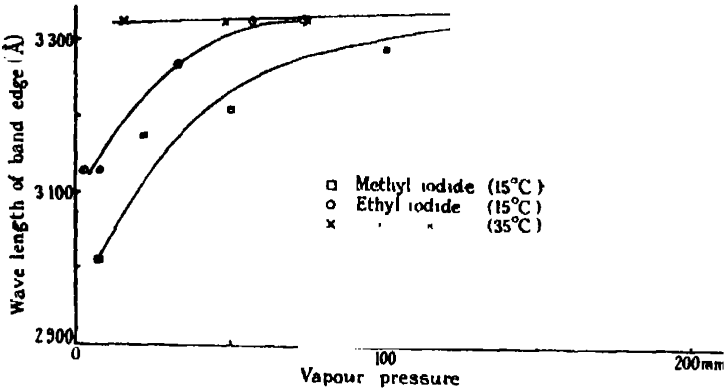

Fig 3

## Table I.

| Vapour pressure | Wave-length of band edge. |
|---|---|
| **Methyl Iodide at 15° C** | |
| mm Hg. | Å |
| 7·5 | 3010 |
| 15 | 3175 |
| 23 | 3175 |
| 50 | 3210 |
| 100 | 3290 |
| 146 | 3330 |
| 185 | 3340 |
| 264 | 3360 |
| **Ethyl Iodide at 15° C.** | |
| 3 | 3130 |
| 8 | 3130 |
| 22 | 3130 |
| 33 | 3270 |
| 56·5 | 3330 |
| 75 | 3330 |
| **Ethyl Iodide at 35° C.** | |
| 15 | 3327 |
| 48 | 3325 |
| 75 | 3330 |
| 124 | 3330 |
| 150 | 3340 |
| 178 | 3360 |

For the iodides whose absorption limit is at 3360 Å. the dissociation energy will be *64 kcals.* X, allowing 21 kcals. for the excitation energy (${}^2P_{1/2} - {}^2P_{3/2}$) of the I atom. This agrees very well with the thermal figure (65 kcals.) if the process of dissociation is simply $CH_3I = CH_3 + I^*$. If, however, the change is $CH_3I = CH_2$ (C divalent) $+ H + I^*$, the energy of the C-I bond would be $64 - 115 + 97 = 46$ kcals., which does not agree with the thermal value. It is highly improbable that this latter photochemical change takes place.

For ethyl bromide whose limit is at 2860 Å. the energy of the C-Br bond comes out to be *90 kcals.* (allowing 10 kcals for the excitation energy of the Br atom). This agrees very well with the thermal value. Both sets of data are probably only accurate to within 4 kcals., and the agreement is satisfactory.

## Table II.

Vapour pressure. Wave-length of band edge.

### Ethyl Bromide at 15° C.

| mm Hg | Å |
|---|---|
| 7 | 2500 |
| 25.5 | 2630 |
| 50 | 2640 |
| 75 | 2735 |
| 123 | 2820 |
| 200 | 2860 |
| 220 | 2860 |
| 242 | 2860 |

### Ethyl Bromide at 35° C.

| mm Hg | Å |
|---|---|
| 57 | 2735 |
| 115 | 2735 |
| 233 | 2820 |
| 305 | 2860 |
| 372 | 2860 |
| 405 | 2860 |

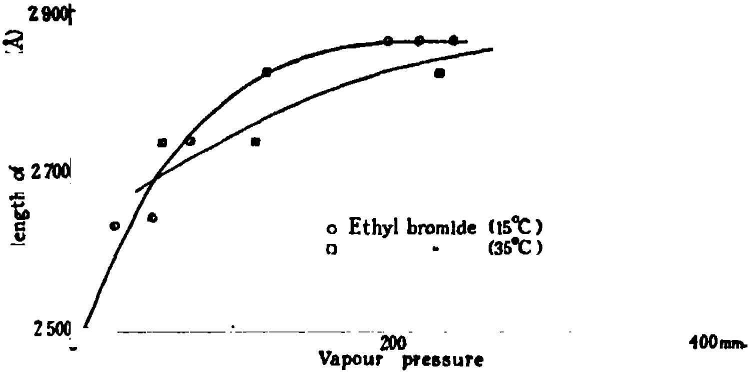

FIG 4.

## *The Liquid State.*

The absorption limit shifts toward the red when the alkyl halides are liquefied. In the case of ethyl iodide the beginning of the absorption has been found beyond 4000 Å. (Iredale and Wallace, *loc. cit.*). With liquid ethyl bromide it lies between 3050 and 3150 Å. These limits are probably not very accurately known, as minute traces of impurities dissolved in the liquid have a great influence on the band edge. With the iodides the absorption maximum appears to be much the same in the two states, but in the liquid, as may be found by using very thin films, a new region of absorption sets in on the short-wave side of 2290 Å., in addition to the new long-wave region. The unaltered position of the maximum shows that the bulk of the molecules in the liquid have the same ground state, internuclear distance, etc., as in the gas. But a percentage of them must be altered to some extent, so that the probability of absorption becomes greater in certain regions, due to the alteration in the ground state, and probably also in the energy of dissociation. The energy corresponding to the long-wave limit is certainly less than that required for dissociation into normal and excited components, but if we assume that only normal components are formed, we must also assume that the liquid molecule in the excited state cannot quantise itself satisfactorily. A re-arrangement of the internal energy therefore occurs, the molecule returning to the ground state with enough vibrational energy to dissociate it. Increased collision frequency and other disturbing factors might be held responsible for this as for the lack of rotational quantisation observed in some cases. This explanation, however, is not very satisfactory, as it does not account for the increased *probability of absorption* in the long-wave region, which, on the Franck theory, is intimately bound up with the internuclear distances in the ground and excited states. Undoubtedly these distances are affected in some way by molecular association, and in the case of the alkyl halides we must, in spite of certain evidence to the contrary,* assume that association takes place to some extent. Nevertheless, the association need not always be of the same type. One form may give rise to a new ground state with less potential energy (referred to the old ground state) and with smaller internuclear distance, and another form may have associated molecules with greater internuclear distance, greater potential energy, etc., than the normal molecules. Such types may be represented in the following way:—

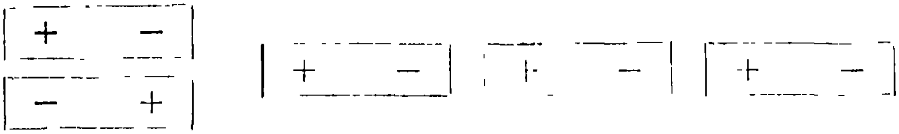

These changes in potential energy which occur in condensation processes are made known through the so-called "latent heat," but this heat effect must only be the average result of all the van der Waals forces, and it does not indicate that all molecules in passing into the liquid state have less potential energy than in the gas.

When the associated molecule passes into the excited state its electric moment will alter and there will be a profound modification in the forces responsible for the association. If the excitation makes the molecule a good deal less "polar," the excited state may differ little from the excited state of the gas molecule. But the gain or loss of potential energy which occurred during the association is now compensated for in the energy requirement for dissociation. Reference to the potential energy diagram (fig. 5) will make these points clear. The hypothetical ground states (B and C) are shown with their potential energies referred to the normal ground state as zero. The location of these states explains qualitatively at least the increases in the absorption on the short- and long-wave sides respectively of the absorption maximum.

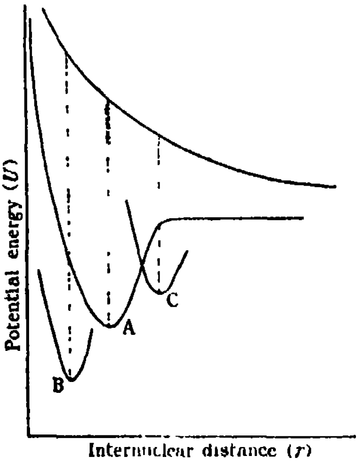

Fig 5.

---

* Turner, 'Molecular Association,' vol. 70, p. 101 (1915).

The shifting of an absorption continuum towards the long- or short-wave region should not be likened to the broadening of a line or band at high pressures. The two phenomena are related, but must be interpreted differently.

## *Summary.*

Satisfactory agreement has been found between the thermal energies of the bonds C-I and C-Br and the spectroscopic energies calculated from the long-wave limits of the continuous absorption bands of the alkyl halides in the near ultra-violet.

Dissociation into alkyl residues and excited halogen atoms undoubtedly takes place.

If this is correct there must be an excitation energy of the carbon atom from the divalent ($^3P$) to the tetravalent ($^5S$) state of 90–100 kcals.

A tentative explanation is given of the shift of the absorption limits when the halides are liquefied as related to the changes in energy levels due to some form of molecular association.

We are indebted to the Trustees of the Commonwealth Science and Industry Endowment Fund for a grant of money for the purchase of certain apparatus used in this work

# A Revision of the Atomic Weight of Thallium.

By Henry Vincent Aird Briscoe, Suetaro Kikuchi, and John Buttery Peel, Armstrong College, Newcastle upon Tyne, University of Durham.

(Communicated by H. B Baker, F.R S.—Received June 6, 1931.)

Since T. W. Richards in 1888 first devised the method of nephelometric titration and applied it to the precise determination of the ratios of soluble halides to silver, it has been the mainstay of atomic weight determinations in all countries. This is proof enough of the great advance he thus made in the accurate measurement of the fundamental ratios of chemistry. Yet, valuable as the method of nephelometric titration has been, it is, as many who have used it will admit, both extremely tedious and liable to uncertainties much greater than would appear from the results which are published. Despite the most careful observance of the conditions laid down by Richards and subsequent workers, it is a common experience to find that even after standing for the normal time, 7–14 days, a liquor showing on the first test approximate equivalence of silver and chloride, will, on adding small quantities of precipitant behave quite erratically, so that in extreme cases addition of chloride may, in subsequent tests, produce apparently an increase in dissolved silver, and *vice versa.* Thus, even where nephelometric tests proceed normally, there is always a fear that apparent equivalence of silver and halide may be illusory; and a considerable experience of such tests has given us the impression that in a normal titration, involving 5–10 grams of silver in, say, 4–6 litres of solution, the resulting uncertainty in the weight of silver is of the order of 0·0005–0·0002 gm. It is, further, no slight disadvantage that a nephelometric titration can hardly be completed in less than 2½–3 weeks and usually extends over a period of 4–6 weeks.

One of the principal objects of the present work has been, therefore, to devise and test a method of titrating halides with silver which shall be more rapid and precise. A good trial of any such method is afforded by the determination of the atomic weight of a heavy element of small valency, for which, evidently, the ratio of the halide to silver is unfavourable to the attainment of precise results. It was in part for this reason that the case of thallium was chosen. Apart from any question of method, moreover, there was good reason for a new determination of this atomic weight.

Among the heavier elements, thallium is one of the very few for which the positive ray method has, so far, failed to give any indication whether or no isotopes exist,‡‡ hence the difference of its atomic weight from a whole number has considerable theoretical significance. Yet, as is apparent from a study of the available data outlined in Table I, the atomic weight of thallium has been until quite recently uncertain by the greater part of a unit. Most of the ratios determined by the earlier investigators, notably that of thallous sulphate to barium sulphate and those involving thallic oxide, are obviously unsuited to precise work. Even in cases where the ratio is unobjectionable, for example

Table I.—Previous Determinations of the Atomic Weight of Thallium.

| Author | Ratio | Number of determinations | Atomic weight Tl = | |
|---|---|---|---|---|
| | | | Extremes. | Mean. |
| A Lamy* | $Tl_2SO_4$ $BaSO_4$ | 1 | — | 205 14 |
| | TlCl AgCl | 3 | 203 238<br>204 583 | 203 80 |
| Hebberling† | $Tl_2SO_4$ $BaSO_4$ | 3 | 205 523<br>204 445 | 204 88 |
| | TlCl AgCl | 2 | 203 357<br>202 941 | 203 16 |
| Werther‡ | TlI AgI (2 series) | 5 | 203 47<br>205 05 | 203 81 |
| | | 3 | 203 38<br>203 19 | - |
| Lepierre§ | $Tl_2O_3$ 2Tl | 2 | 204 28<br>204 03 | 204 15 |
| | $2Tl(NO_3)$ $Tl_2O_3$ | 1 | -- | 204 03 |
| | $Tl_2SO_4$ Tl | 3 | 204 04<br>204 43 | 204 150 |
| Wells and Penfield‖ | TlCl : AgCl | 2 | 204 403<br>204 406 | 204 40 |
| Crookes¶ | Tl : $TlNO_3$ | 10 | 204 06<br>204 02 | 204 04 |
| Hönigschmid** | TlCl . Ag | 12 | 204 35<br>204 42 | 204 39 |
| Birckenbach and Kothe** | TlCl AgCl | 12 | 204 36<br>204 44 | 204 39 |
| Hönigschmid and Striebel†† | TlBr · Ag | 11 | 204 36<br>204 42 | 204 39 |

* 'Ann. Chim. Phys.,' vol 67, p 410 (1862)

† 'Liebig's Ann.,' vol. 134, p. 12 (1865).

‡ 'J. Prakt. Chem., vol 92, p. 197 (1864).

§ 'Bull Soc Chim.,' vol. 9, p. 166 (1893)

‖ 'Amer. J. Sci.,' vol 47, p. 466 (1894).

¶ 'Phil. Trans.,' A, vol. 163, p 277 (1873).

** Sitzb. Bayer Akad. Wiss.,' p 179 (1922).

†† Hönigschmid and Striebel, 'Z Anorg. Allgem. Chem.,' vol. 194, p. 293 (1930)

---

‡‡ Aston, 'Phil. Mag.,' vol. 45, p. 934 (1923).

in Lamy's or Hebberling's determinations of the ratio of thallous and silver chlorides, the wide variation within the series clearly suggests that the result is untrustworthy.

For nearly 50 years the classical work of Crookes on the ratio of thallium to thallous nitrate was the only considerable and concordant series of analyses on which an acceptable value could be based and in Clarke's "Recalculation of the Atomic Weights" this series completely outweighed all others. Though the analyses of Wells and Penfield seemed to have weight as the work of skilled experimenters using a well-tried and trustworthy method, they were but two in number and incidental to another investigation. Thus great importance attaches to the results of Honigschmid and his collaborators, who in 24 very concordant determinations of the ratios of thallous chloride to silver and silver chloride obtained a value differing from that of Crookes by one-third of a unit. This disagreement between the two chief series of determinations for thallium may be held to justify the further work here recorded, in which the atomic weight of thallium has been redetermined by measurement of the ratio TlCl : Ag, and Crookes ratio, Tl : $TlNO_3$, has been subjected to a critical investigation.

### *Purification of Reagents.*

*Water.*—Laboratory distilled water, free from appreciable traces of halogens, was redistilled from caustic soda and potassium permanganate in a copper still having a vertical spray-trap packed with glass beads. It was condensed in pure tin, rejecting large head and tail fractions in each distillation, and the main distillate was collected and stored in 20-litre stoppered resistance glass bottles which had been used for some years for the storage of the purest water.

*Ammonia.*—The gas liberated by warming the purest commercial ammonia solution was dissolved in pure water, in an apparatus constructed of resistance glass with ground joints.

*Sulphur Dioxide.*—This gas, used for the precipitation of silver by Stas's method, was distilled from the middle fraction of a syphon of the liquid.

*Nitric Acid.*—The purest commercial nitric acid was thrice redistilled in an apparatus constructed of "Duro" resistance glass with ground joints, rejecting large head and tail fractions in each distillation. The final main distillate was stored in a resistance glass bottle.

*Formic Acid.*—Pure reagent formic acid was twice redistilled from a silica flask fitted with a ground-in silica condenser and adapter. Considerable head and tail fractions were rejected in each distillation and the final main fraction was stored in a stoppered silica flask.

*Hydrochloric Acid.*—The acid used for generating hydrogen was commercial reagent acid freed from arsenic by treatment with a copper-tin couple and distillation from copper gauze.* That used for making thallous chloride was further purified by two successive redistillations in a resistance glass apparatus.

*Sulphuric Acid.*—The purest reagent acid was used without further purification, since it was free from lead and arsenic and on dilution gave no precipitate with hydrogen sulphide.

*Zinc.*—Electrolytic zinc, free from arsenic, was used for the preparation of hydrogen

*Hydrogen.*—This gas, used in silver fusions, was prepared from hydrochloric acid and zinc in a Kipps' apparatus and passed, in an all-glass train, through a 12-inch column of 50 per cent. potassium hydroxide solution, over 24 inches of solid potassium hydroxide and through two 10-inch columns packed with phosphoric oxide distributed on glass wool The hydrogen used in the fusion of pure thallium was drawn from a cylinder of the compressed gas, passed slowly over a 3-foot length of red-hot copper gauze and then through concentrated potassium hydroxide solution and through a 4-foot column of phosphoric oxide.

*Nitrogen*, also used in the fusion of thallium, was drawn from a cylinder and purified precisely as described above for hydrogen.

*Magnesia.*—Magnesium nitrate was thrice precipitated from a saturated aqueous solution by excess of nitric acid, filtered on porcelain, dissolved in water and precipitated with ammonia. The hydroxide thus obtained was washed by decantation, filtered, dried at 100°, ignited in air in platinum and finally heated at 1000° for some hours in a current of moist pure hydrogen. This last treatment eliminates as hydrogen sulphide any minute traces of sulphur still retained (probably as sulphate) by the magnesia. Boats of this material were moulded by moistening the mass with dilute nitric acid and ignited at 1000° on a silica support.

*Silver.*—Three samples of silver were used in this work, prepared at different times and from different samples of commercial silver nitrate. Ammonium bisulphite, prepared by saturating aqueous ammonia with sulphur dioxide, was warmed and added to a hot filtered aqueous solution of silver nitrate with about 10 per cent. of copper nitrate.† The crystalline precipitated silver was digested six times with dilute ammonia, washed very thoroughly and dried at 100°. In certain cases this precipitation by the method of Stas was repeated, and in others the silver was further purified by dissolving 100 gm. portions in pure nitric acid and precipitating it from a hot solution by ammonium formate prepared by saturating pure formic acid with pure ammonia gas. After thorough washing with ammonia solution and with water the silver was dried first at 100° and then at 300° in an electrically heated covered beaker.

---

* Thorne and Jeffers, 'Analyst,' vol. 31, p. 101 (1906).

† Briscoe, 'J. Chem. Soc.,' vol. 107, p. 69 (1915).

Before use, the silver, in a magnesia boat, was fused and cooled in an atmosphere of hydrogen in an electrically heated silica tube furnace. The buttons of silver were etched with pure nitric acid diluted with an equal volume of water, and then washed well with water, dried at 300° for 12-24 hours, cooled in a desiccator over solid potassium hydroxide and transferred to the balance for weighing.

Small pieces of pure silver for adjustment of the quantity weighed were prepared by drawing a large button of silver into wire or by rolling it into thin sheet, the wire or sheet being subsequently cut into convenient fragments. In this mechanical working of the silver, care was taken after each contact with steel to etch the metal with nitric acid and thus remove any superficial contamination which might otherwise have been worked into the mass of silver in subsequent operations.

### *Weighing.*

The balance used for this work was made by Oertling and resembles in general design the standard type known as "No. 7, S.W." It is exceptional in having a beam of Firth's 36 per cent nickel steel, of very low coefficient of thermal expansion, pan suspensions of special design, and a separate beam enclosure with a floor of thick aluminium sheet, in general accordance with the design recommended by Manley.* A balance case of larger size than is usual provides ample room for even large objects to stand prior to weighing. The air in the case is dried by solid potassium hydroxide, and a piece of pitchblende ionises the air sufficiently to ensure the dissipation of any electric charge on objects, especially glass or silica vessels, before weighing.

During the present work this balance was housed in a dark room, centrally situated in the building and receiving no direct heat, so that changes of temperature were very gradual and limited to a narrow range, actually about 5° as between summer and winter. Six-inch rolled steel joists built into a 3-foot main wall carried a heavy concrete slab covered with a 1-inch layer of felt and a sheet of ¼-inch plate glass, on which the balance rested. This situation gave complete freedom from vibration, and the zero and sensibility of the balance remained constant throughout the investigation, the sensibility being 40 scale divisions per milligram. Recalibration of the gold-plated brass weights also made by Oertling, gave results agreeing almost exactly with a previous calibration in 1925.

---

* 'Phil. Trans.,' A, vol. 210, p. 387 (1910).

Corrections to be applied to ascertain relative weight in vacuum were calculated using the density of air at the temperature and pressure observed during the weighing and the following densities for the solid weighed: silver 10·49, thallous chloride 7·00, thallium 11·85, thallous nitrate 5·55

Silver was weighed directly on the balance pan, thallous chloride was weighed in a silica crucible using as tare another silica crucible similar in weight and dimensions, thallium and thallous nitrate were weighed in silica against a tare as described in detail later.

There is every reason to believe that the error of weighing did not in any case exceed 0·02 mgm., and in most cases was probably less than 0 01 mgm.

### *The Ratio of Thallous Chloride to Silver.*

*Preparation of Thallous Chloride.*—Having urged previously* the importance of using for atomic weight determinations only materials of definite and known origin, we naturally endeavoured to obtain samples of thallium complying with this requirement. Unfortunately, this proved extremely difficult the known thallium minerals, apparently, are so rare as to be useless as sources of thallium and of the origins of commercial supplies of thallium we could learn very little.

Eventually we had to use thallium from two sources :—

(*a*) " English " thallium, purchased, as metal, from Messrs. Johnson & Matthey, Ltd , who state that they " do not know the origin of the raw material from which this actual metal was produced."

(*b*) " German " thallium, purchased as oxide from " Sachtleben " Aktiengesellschaft fur Bergbau und Chemische Industrie, of Koln and Homberg, who were good enough to inform us that the thallium was obtained as a by-product in the burning of pyrites derived from their own mines at Meggers in Westphalia.

From these materials, thallous chloride for the several series of analyses was prepared as follows.

*Preliminary Series.*—English thallium was dissolved in diluted sulphuric acid and the solution was filtered, concentrated and crystallised. The thallous sulphate was thrice recrystallised by concentrating a dilute, filtered solution and was then redissolved to a dilute solution from which thallous chloride was precipitated by addition of a slight excess of hydrochloric acid. After thrice washing with water, the chloride was recrystallised five times from hot water, and kept in an evacuated desiccator over solid potassium hydroxide.

---

* **Briscoe and Robinson**, ' J. Chem. Soc.,' vol. 127, p. 720 (1925).

*Main Series. English A.*—The thallium was converted to sulphate as previously described, and the sulphate was twice recrystallised from water, the crystals being on each occasion drained for 30 minutes in a 25 cm. diameter porcelain centrifuge running at 1500 r.p m From a dilute solution of the sulphate the chloride was then precipitated with a slight excess of hydrochloric acid, well washed by decantation and converted to sulphate by warming with sulphuric acid. This sulphate was thrice recrystallised from water with centrifugal drainage of the crystals, and then dissolved in hot water and again treated with hydrochloric acid in slight excess. The precipitated thallous chloride was thrice recrystallised from water with centrifugal drainage and kept *in vacuo* over solid potassium hydroxide.

*Main Series. English B.*—The method of purification was similar to that adopted for English A except that the thallous sulphate was on each occasion recrystallised five times from water before being converted to chloride. In every case crystals during centrifuging were wrapped in chemically clean surgical linen which, after thorough washing in the usual way, had been boiled successively in dilute hydrochloric acid, dilute nitric acid, dilute caustic soda solution and several changes of water.

*Main Series. German.*—The original thallic oxide supplied was treated with sulphuric acid, and from the diluted solution thallium was obtained by electrolysis in the manner described by Richards and Smyth.* The metal, after being washed and boiled in air-free water, was converted to sulphate and this in turn to chloride by precipitation from a dilute aqueous solution with hydrochloric acid. The chloride, after washing by decantation and centrifuging, was reconverted to thallous sulphate, and this was thrice recrystallised from water. Finally, thallous chloride prepared as before from this sulphate was well washed by decantation, centrifuged and thrice recrystallised from water.

## *Method of Analysis.*

Preliminary experiments showed that thallous chloride fused either in platinum or in silica, in a dry atmosphere of nitrogen, with or without hydrogen chloride, acquired a distinct brown colour, and quite evidently underwent some change likely to affect its weight. In platinum, in presence of hydrogen chloride this change was very marked. The darkening may be due to one or both of two causes: decomposition, probably accompanied by hydrolysis or oxidation, and the formation of a higher chloride. In any case it was clearly desirable to avoid this change.

---

* 'J. Amer. Chem. Soc.,' vol. 44, p. 524 (1922).

Fortunately, it was found that by fusing the dried crystalline chloride in silica in pure dry air, it melted to a clear colourless liquid which resolidified to a pure white solid. To test this method some 5 grams of thallous chloride was fused in silica and held for about an hour just above its melting point whilst a steady current of pure dry air was passed over it and then through a Drechsel bottle containing dilute aqueous silver nitrite. No trace of opalescence was observed in this solution and it appears, therefore, that thallous chloride, like silver chloride, but in contrast with most metallic halides, can be fused in air without decomposition or hydrolysis.

In each determination, 5–10 grams of dry pure thallous chloride was placed in a small silica crucible which had been weighed against a similar crucible as tare, after both had been heated some hours at 400° and cooled in a desiccator over solid caustic potash. The crucible and tare were heated slowly in an electrically heated silica furnace until the chloride melted to a clear transparent liquid, and then, as soon as the chloride had solidified, were transferred to the desiccator After cooling to room temperature and standing for about 30 minutes in the balance case, the crucible with the fused chloride was again weighed against the tare.

The crucible containing the thallous chloride was now placed in a 2-litre pyrex beaker containing 1½ litres of water, and the chloride was slowly dissolved at 90° C. After cooling to about 40° C. the solution was carefully poured down a glass rod into 2 litres of water at 50° C in a 7-litre resistance glass bottle.

Meanwhile the necessary silver, having been etched in nitric acid, washed with water and dried at 350° C., was weighed out, taking about 2–3 milligrams more than that required to react completely with the thallous chloride This was dissolved in a slight excess of nitric acid diluted with its own bulk of water in a solution flask of the form previously described.*

Usually about 1 c c. of nitric acid was used to dissolve 1 gm. silver, and when solution was complete 50 c.c. water was added and the solution boiled to expel nitrous fumes.

---

* Briscoe, 'J Chem. Soc.,' vol. 107, p. 69 (1915).

The silver solution was then diluted to 500 c.c. and added to the thallous chloride solution in the bottle, followed by six washings of the solution flask, making a total bulk of about 6 litres. During the addition of silver solution the contents of the bottle were swirled, and afterwards the stoppered bottle was vigorously shaken and allowed to stand about 7 days, being shaken about 10 times each day.

In the course of the first five preliminary analyses it was found that the transference of 1½–2 litres of hot thallous chloride solution from a beaker to the bottle involved too great a strain on the operator's attention and might, therefore, quite possibly lead to accidental loss of material. Accordingly, in the remaining preliminary analyses and in all analyses of the main series the solution of thallous chloride was effected in a pyrex flask similar to that used for silver but of about 3 litres capacity. These solution flasks have angles between the pouring neck, the main neck and the side of the flask such that after the flask has been completely drained into a bottle, on tilting it back a little a stream of washwater directed into the main neck will wash residual traces of solution either out through the pouring neck or back into the flask. The main neck has a suitable stopper with a bulb-trap ground in, and the pouring neck, when not in use, is covered with a ground-on glass cap.

### *Estimation of Excess Silver.*

Attempts to avoid the difficulties and uncertainties of nephelometric titration were first made by concentrating the solution to small bulk and titrating the silver content with a chloride solution using chromate as indicator. This method failed entirely in presence of relatively large amounts of thallous nitrate. It was found, however, that titration with potassium thiocyanate, using ferric alum as indicator, gave sharp and reproducible end-points even with traces of silver in nearly saturated solutions of thallous nitrate.

An N/1000 silver nitrate solution was prepared by dissolving exactly the amount of silver required in the least quantity of nitric acid in the solution flask and diluting to 2 litres. Two litres of an approximately N/1000 of A.R. potassium thiocyanate solution was also prepared and exactly standardised against the silver nitrate.

To simulate the conditions of an analysis, 2 c.c. N/1000 $AgNO_3$ solution was placed in a Nessler glass containing 50 c.c. water and 1 c.c. ferric alum and titrated with the thiocyanate solution. A reference solution, usually a previous titration turned white by addition of silver nitrate, was always used to show, by contrast, the development of colour in the titration vessel. Under these conditions and with practice it was found possible, as in the standardisation, to determine the end-point with an error not exceeding 2 drops of the thiocyanate solution, provided that the total bulk contained not more than 1 c.c. free nitric acid and not more than 2 c.c. 10 per cent ferric alum. Moreover, the titration was found to be equally precise in a nearly saturated solution of thallous nitrate. In either case the brown colour produced at the end-point was liable to disappear in a short time in presence of silver chloride, and for this reason care was taken in all titrations to ensure that the solution was as free as possible from suspended precipitate.

### *Recovery of Excess Silver.*

It remained then to ensure that 2 or 3 mgm. of excess silver, present with 5–10 grams of thallous nitrate in 6 or 7 litres of solution, could be concentrated, completely and with certainty, in about 50 c.c. of liquor; and a considerable number of experiments were made with this object.

A series of experiments were made by diluting 2 c.c. N/1000 $AgNO_3$ in 2 litres of water and concentrating the solution to about 20 c.c. Concentration in a large silica basin on a hot plate in such a manner that the solution did not boil and there was no disturbance of its surface, always resulted in an appreciable loss of silver. This appeared to be due to the spreading of traces of silver salt over the surface of the basin. To avoid this difficulty, the evaporation of the solution was carried out by boiling in a round-bottomed pyrex flask of about 2 litres capacity, fitted with a ground-in spray trap consisting of 2 feet of wide glass tubing bent twice at right angles so that there was always a partial condensation of steam by which any spray was washed back into the flask.

In six experiments by this method the whole of the silver taken was completely recovered in the concentrate and estimated by titration.

In the actual atomic weight determinations, after the precipitation of silver chloride had been completed by standing with frequent agitation during 7–10 days, the clear supernatant liquor was decanted from the precipitate and concentrated in the manner just described, in several lots of about 1½ litres each. In the final evaporation the liquor was concentrated to about 20 c.c., which then contained the whole of the soluble material present in the original bulk. On cooling this concentrate, thallous nitrate crystallised out and the clear solution was decanted from this into a Nessler glass, followed by three washings of the crystals with water, making a total bulk of 45–50 c.c. for titration.

Since, in the preparation of the silver nitrate solution, care had been taken to use the minimum amount of nitric acid, the excess acid, even when concentrated, had no adverse effect on the thiocyanate titration.

For use in the Main English Series a fresh N/1000 silver nitrate solution was accurately made up from weighed silver, and against this a fresh N/1000 potassium thiocyanate solution was standardised. To minimise any risk of error the new thiocyanate solution was standardised also against the silver nitrate solution used in the previous series.

Similarly, silver nitrate and thiocyanate solutions were prepared anew for the German series and were standardised against each other and against the solutions used in the previous series.

### *Statement of Results.*

The experimental data for the four series, 22 determinations in all, are given in Table I, with the calculated ratios of thallous chloride to silver and the corresponding atomic weights for thallium, using as antecedent data Ag = 107·880 and Cl = 35·456.

The maximum variation in the ratio TlCl/Ag in the 22 analyses is from 2·22234 to 2·22305, a range of 0·00071 or about 7 parts in 10,000, corresponding with a variation in the atomic weight from 204·29 to 204·36, a range of 7 in 20,400.

In any series the maximum deviation of the atomic weight from the mean is 0·04 unit and the average deviation is 0·012 unit except in the series English A. As the mean values for the four series do not, in any case, differ from the general mean by more than 0·01 unit, there is a high probability, apart from systematic errors, that the value 204·34 is within 0·01 unit of the true value.

It is hardly necessary to repeat here the reasons which have previously been advanced to justify the use of silver titrations alone for such a determination as this. There is ample evidence to show that, with a given material, silver and silver chloride ratios give substantially identical results.

In only one experiment was the excess silver estimated nephelometrically and it is unfortunate that, as not infrequently happens with this method, the estimation proceeded in an erratic manner. The thallous chloride, identical with that used in the Main Series English B, was precipitated with a quantity of silver almost exactly that required were the atomic weight of thallium 204·30. After standing for a week with vigorous agitation each day, the solution was allowed to settle and 200 c.c. of the clear supernatant liquor was withdrawn and equally divided among eight nephelometer tubes. To one tube of each pair 1 c.c. N/10 sodium chloride was added, and to the other 1 c.c.

## Table I.

| Number of analysis. | Sample Ag. | Vacuum weight Ag taken. | Excess Ag in liquor. | Vacuum weight Ag used. | Vacuum weight TlCl. | Ratio TlCl/Ag. | Atomic weight Tl = (Ag = 107·880) (Cl = 35·456) | Difference from mean. |
|---|---|---|---|---|---|---|---|---|
| Preliminary Series— | | | | | | | | |
| 1 | III | 1·09755 | 0·00894 | 1·08861 | 2·41969 | 2·22273 | 204·33 | 0 |
| 2 | III | 2·24292 | 0·00235 | 2·24057 | 4·97940 | 2·22234 | 204·29 | −0·04 |
| 3 | II | 2·20928 | 0·00242 | 2·20686 | 4·90541 | 2·22280 | 204·34 | +0·01 |
| 4 | III | 2·20852 | 0·00244 | 2·20608 | 4·90351 | 2·22272 | 204·33 | 0 |
| 5 | I | 2·20860 | 0·00245 | 2·20615 | 4·90391 | 2·22283 | 204·34 | +0·01 |
| 6 | I | 2·82777 | 0·00244 | 2·82533 | 6·27962 | 2·22261 | 204·32 | −0·01 |
| | | | | | | Means | 204·33 | ±0·012 |
| Main Series. German— | | | | | | | | |
| 1 | I | 2·27816 | 0·00262 | 2·27554 | 5·05837 | 2·22293 | 204·35 | +0·01 |
| 2 | I | 2·36804 | 0·00197 | 2·36607 | 5·25891 | 2·22264 | 204·32 | −0·02 |
| 3 | I | 4·29351 | 0·00364 | 4·28987 | 9·53621 | 2·22296 | 204·35 | +0·01 |
| 4 | III | 4·51131 | 0·00343 | 4·50788 | 10·01985 | 2·22274 | 204·33 | −0·01 |
| 5 | I | 3·26528 | 0·00274 | 3·26254 | 7·25159 | 2·22268 | 204·33 | −0·01 |
| | | | | | | Means | 204·34 | ±0·012 |
| English A— | | | | | | | | |
| 1 | I | 4·52440 | 0·00230 | 4·52210 | 10·04965 | 2·22234 | 204·29 | −0·04 |
| 2 | I | 5·20042 | 0·00319 | 5·19723 | 11·55090 | 2·22251 | 204·31 | −0·02 |
| 3 | II | 4·77567 | 0·00356 | 4·77211 | 10·60756 | 2·22282 | 204·34 | +0·01 |
| 4 | II | 4·46491 | 0·00345 | 4·46146 | 9·91726 | 2·22288 | 204·35 | +0·02 |
| 5 | II | 4·29437 | 0·00414 | 4·29023 | 9·53722 | 2·22300 | 204·36 | +0·03 |
| 6 | I | 5·34893 | 0·00370 | 5·34523 | 11·88154 | 2·22283 | 204·34 | +0·01 |
| | | | | | | Means | 204·33 | ±0·022 |
| English B— | | | | | | | | |
| 1 | I | 4·27404 | 0·00313 | 4·27091 | 9·49327 | 2·22277 | 204·34 | −0·01 |
| 2 | III | 4·46539 | 0·00334 | 4·46205 | 9·91925 | 2·22302 | 204·36 | +0·01 |
| 3 | III | 4·69719 | 0·00390 | 4·69329 | 10·43230 | 2·22281 | 204·34 | −0·01 |
| 4 | II | 4·53079 | 0·00411 | 4·52668 | 10·06308 | 2·22305 | 204·36 | +0·01 |
| 5 | I | 4·08407 | 0·00333 | 4·08074 | 9·07037 | 2·22272 | 204·33 | −0·02 |
| | | | | | | Means | 204·35 | ±0·012 |
| | | | | | General mean . . | | 204·34 | ±0·015 |

N/10 silver nitrate. The turbidities of these solutions compared in the usual manner with the nephelometer gave a mean figure Ag : Cl :: 100 : 90. If this be taken to indicate equivalence of chloride and silver we have :—

| Vacuum weight Ag. | Vacuum weight TlCl. | Ratio TlCl/Ag. | Atomic weight of Tl. |
|---|---|---|---|
| 3·27760 | 7·28533 | 2·22276 | 204·34 |

The titration was, however, continued with the following results :—

| | Nephelometric ratio. | |
|---|---|---|
| | Ag . | Cl |
| Original liquor | 100 . | 90 |
| After adding 2 c.c. N/1000 NaCl | 100 | 65 |
| ,, 2 c.c. ,, | 100 . | 65 |
| ,, 2 c.c. ,, | 100 | 55 |
| ,, 4 c.c. ,, | 95 | 100 |

If the last observation be held to show equivalence we have :—

| Vacuum weight Ag | Vacuum weight TlCl | Ratio TlCl/Ag | Atomic weight Tl. |
|---|---|---|---|
| 3·27626 | 7·28533 | 2·22366 | 204·43 |

This affords a good example of the nature and extent of the uncertainty of the nephelometric method, as it is evidently largely a matter of choice whether 204·34 or 204·43 is taken as the result. Nevertheless, although this result, approximately 204·4, is rejected, it may be regarded as a rough confirmation of the figure already reported.

Considering the possible sources of error in the results, it appears that errors in weighing and in the titration of excess silver, which do not exceed about 0·02–0·03 mgm. at most, may be dismissed as insignificant by comparison with the observed deviations from the mean, the mean deviation of 0·012 unit in atomic weight corresponding with errors of about 1·0 mgm. and 0·5 mgm. in the weight of thallium chloride and silver respectively.

The silver chloride precipitate was always washed six or seven times with water, the washings being concentrated with the mother liquor, and even were the uncertainty in the titration of excess silver taken at as much as 0·2 c.c. N/1000 thiocyanate, the corresponding uncertainty in the weight of silver is under 0·03 mgm.

Systematic errors may result from impurity in the silver or thallous chloride, but, having regard to the considerable variations among the methods by which the four samples of thallous chloride and the three samples of silver were prepared, the absence of any systematic variation in the values of the atomic weight according to the samples of reagent used for their determination affords strong evidence that any impurity in these materials was insufficient to affect the result appreciably. It has been shown that the methods used for the purification of silver yield a product in which the impurities do not exceed about 1 part in 300,000,* and it seems probable that the thallium chloride was of a corresponding degree of purity.

It is believed that the methods used for dissolving and transferring the reagents excluded any possibility of loss of material. Therefore, it is suggested, that the differences actually observed are probably due, in the main, to varying occlusion and adsorption of reagents by the precipitate.

### *The Ratio Thallium to Thallous Nitrate*

Numerous attempts were made to work out a trustworthy method for determining the ratio of thallium or thallous chloride to thallous perchlorate, but these failed because it was never possible to obtain the latter salt in a suitable condition for weighing. An elevated temperature is necessary to cause solution of thallium in perchloric acid, and when the solution becomes concentrated fumes of chlorine or chlorine oxides are evolved in small quantity. These chlorine-containing fumes react with thallous perchlorate to form certain thallic salts, as is shown by work to be published later. It was decided, therefore, to reinvestigate the ratio of thallium to thallous nitrate employed by Crookes.

### *The Preparation of Pure Thallium.*

Commercial thallium was dissolved in 50 per cent. sulphuric acid, and the resulting thallous sulphate was recrystallised from water and then converted to chloride in the manner already described. This chloride was then dissolved in pure sulphuric acid, excess acid was evaporated, and the sulphate thus separated was washed and recrystallised five times from water.

A dilute solution of the sulphate was then electrolysed in the manner described by Richards and Smythe (*loc. cit.*) using platinum electrodes. The thallium deposited at the cathode as a fine spongy mass was boiled in successive quantities of air-free water and, after being kept under water for several hours, was melted in a silica furnace in a current of dry hydrogen. Subsequently it was kept in a stoppered bottle until required.

---

* Briscoe and Little, 'J. Chem. Soc.,' vol. 105, p. 1320 (1914).

### *The Weighing of Pure Thallium.*

Freshly prepared pure thallium before exposure to air possesses a fine metallic lustre. Access of air, even for a short time, rapidly tarnishes the surface of the metal, and if a piece be exposed to air and immediately dropped into air-free water it is possible to detect a small quantity of thallous oxide in solution although the surface of the metal may still appear untarnished.

It is evident, therefore, that a precise weight of pure thallium could only be obtained by etching, drying and weighing the metal in an inert atmosphere. For this purpose an apparatus of transparent silica of small internal volume, together with a tare of similar dimensions and weight, was used. As is shown in fig. 1, it consisted essentially of a small cylindrical vessel 3 inches long and ¾ inch diameter, fitted at each end with hollow ground glass stoppers carrying inlet and outlet tubes ¼ inch bore and 1 inch long. The stoppers were so smoothly polished that they could be easily turned without the use of lubricant and each had a perforation communicating with a slight indentation in the female cone so that by simple rotation the stoppers served as stopcocks.

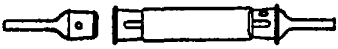

Fig. 1.

Attempts were made to obtain the pure metal by etching it with nitric acid in the silica apparatus and washing it with boiling air-free water in a counter-current of nitrogen. After this treatment and whilst kept cold in nitrogen the thallium possessed a bright lustre, but on drying it by heating in nitrogen it tarnished markedly and suddenly as the last traces of water were disappearing. Though it seemed improbable that the nitrogen could be contaminated with traces of oxygen, similar experiments were made using as the inert atmosphere a mixture of hydrogen and nitrogen which had passed over red-hot copper. Similar results were thus obtained, and so it was concluded that the production of traces of oxide under these conditions must be due to the interaction of the thallium with water.

Therefore thallium was etched with nitric acid, well washed with air-free water, dried and polished with chamois leather and placed in a transparent silica boat about ½ inch by ½ inch by ¼ inch, which was in turn placed in the silica apparatus. A current of dry hydrogen was passed through the apparatus, and after all air was expelled the thallium was slowly heated with a small flame until it melted. After cooling in hydrogen the apparatus was filled with nitrogen and then sealed by rotation of the stoppers. The thallium, which then presented a bright surface closely resembling that of mercury, was weighed in the silica apparatus against the tare, which had been treated in the same way as the weighing tube and was also filled with nitrogen.

## *The Conversion of Thallium to Thallous Nitrate.*

The apparatus, shown in fig 2, consisted of a flat bottomed "Duro" resistance glass flask of about 150 c.c. capacity, fitted with a ground stopper and also a spray trap. The silica boat containing the thallium was placed in the flask, the least possible amount of nitric acid required to dissolve the metal was added (7 c.c. for 10 gm. of metal) and the spray trap was fitted. On gently warming the flask on an electric hot plate, the metal dissolved and nitrous fumes were copiously evolved. When all reaction had ceased, the flask was allowed to cool, the spray trap was rinsed into it, and after a time thallous nitrate separated from the solution in white crystals. The apparatus was then placed in an electrically heated air bath constructed of nickel sheet and the solution was slowly evaporated to dryness at 90° C., leaving a white residue of the nitrate, which on heating slowly to about 210° melted to a clear colourless liquid. On cooling, the product, which was cream or pale brown in colour, was weighed.

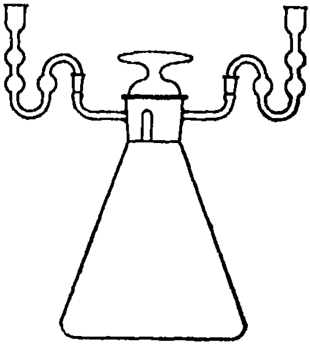

FIG. 2.

The nitrate was then dissolved in water, a trace of pure oxalic acid was added and the solution was again evaporated to dryness and the thallous nitrate fused, cooled and weighed as before. The product was still slightly brown in colour, and although this process of treating with oxalic acid, fusing and weighing was repeated several times, the thallous nitrate never became pure white in colour and its weight varied over a range of several milligrams.

In several experiments the thallium was dissolved in very dilute nitric acid, but the product on melting always possessed a slight brown colour and on solution in water left an appreciable residue of brown specks suspended in the liquid. Crookes (*loc. cit.*) also mentions the production of this brown substance, attributed to the decomposition of traces of thallic nitrate always formed by the action of nitric acid on thallium, but whereas in his experiments this colour disappeared on fusion with a trace of oxalic acid, in our experiments it always persisted. Repeated solution of the nitrate, with subsequent melting, gave no constancy of weight, as is exemplified in the following experiments :—

| Experiment A. | | Experiment B. | |
|---|---|---|---|
| $TlNO_3$. Relative weight in air. | Flask + $TlNO_3$ excess weight over tare relative weights in air | $TlNO_3$ Relative weight in air | Flask + $TlNO_3$ excess weight over tare relative weights in air |
| 16 07992 | 35 87770 | 15 74551 | 35 54735 |
| 16 07685 | 35 87463 | 15 74479 | 35 54663 |
| 16 07635 | 35 87413 | 15 74506 | 35 54690 |
| 16 07622 | 35 87400 | 15 74482 | 35 54666 |
| 16 07602 | 35 87380 | 15 74680 | 35 54864 |
| 16 07533 | 35 87311 | | |

The results, taking the last weight in each case, are :—

| Experiment | Vacuum weight thallium | Vacuum weight $TlNO_3$ | Atomic weight of thallium. |
|---|---|---|---|
| A | 12 08412 | 15 74910 | 204 42 |
| B | 12 33736 | 16 07846 | 204·46 |

With the quantity of thallium used in these experiments an uncertainty of 1 mgm. in the weight of thallous nitrate produces a corresponding uncertainty in the atomic weight of about 0·05 unit. This uncertainty, and the obvious impurity of the product, seem to make the ratio of thallium to thallous nitrate entirely unsuitable as a means of obtaining precise values of the atomic weight.

## *Conclusion.*

Evidently the results here reported are closely comparable with the data of Honigschmid, Birckenbach and Kothe, both in the value of the atomic weight deduced and in the deviation of individual analyses from the mean. Their final value, deduced from 24 analyses, is Tl = 204·39, with an average deviation from the mean ±0·012 ; our final mean value is *Tl = 204·34* with an average deviation ±0·015.

It seems clear that these two determinations considered together must completely outweigh all earlier values, including that of Crookes. Much as one must regret the eclipse of a determination so long and justly regarded as a classical research of its kind, it is no longer possible to attach serious weight to Crookes' value Tl = 204·04.

We incline to prefer our method of simply fusing thallous chloride to the rather more drastic method of sublimation adopted by Honigschmid and his collaborators. Otherwise we can see no reason to prefer either our own or Honigschmid's value We suggest, finally, that it may fairly be concluded that the atomic weight of thallium lies a little below 204·40 and most probably within one or two hundredths of a unit of the mean value 204·37.

Accepting the available evidence as to the probable value of the "packing fractions" of the heavier elements,* it is clear that were thallium a "simple" element its atomic weight should approximate closely to a whole number. In the absence of any direct evidence by the positive ray method as to the existence of isotopes of thallium† it may be concluded, therefore, that the fractional value here deduced for the atomic weight of the element indicates that thallium is very probably a mixture of two or more isotopes.

Grateful acknowledgment is made of a grant from the Department of Scientific and Industrial Research, which has enabled one of us (J.B.P.) to take part in this work.

---

* Aston, 'Proc. Roy Soc.,' A, vol. 115, p 487 (1927).

† Aston, 'Phil Mag.,' vol 45, p. 934 (1923).

# *The Theory of Electronic Semi-Conductors.*

By A. H. Wilson, Emmanuel College, Cambridge.

(Communicated by P. A. M. Dirac, F R S.—Received June 18, 1931.)

## *Introduction.*

The application of quantum mechanics to the problem of metallic conduction has cleared up many of the difficulties which were so apparent in the free electron theories of Drude and Lorentz. Sommerfeld* assumed that the valency electrons of the metallic atoms formed an electron gas which obeyed the Fermi-Dirac statistics, instead of Maxwellian statistics, and, using in the main classical ideas, showed how the difficulty of the specific heat would be removed. He was, however, unable to determine the temperature dependence of the resistance, as his formulæ contained a mean free path about which little could be said.

F. Bloch† took up the question of the mechanics of electrons in a metallic lattice, and showed that if the lattice is perfect an electron can travel quite freely through it. Therefore so long as the lattice is perfect the conductivity is infinite, and it is only when we take into account the thermal motion and the impurities that we obtain a finite value for the conductivity. On this view all the electrons in a metal are free, and we cannot assume, as we do in the classical theory, that only the valency electrons are free. This does not give rise to any difficulty in the theory of metallic conduction, as the direct proportionality between the conductivity and the number of free electrons no longer holds when the Pauli principle is taken into account. If there is no external electric field, the number of electrons moving in any direction is equal to the number moving in the opposite direction. The action of a field is to accelerate or retard the electrons, causing them to make transitions from one set of energy levels to another. This can only happen if the final energy levels are already unoccupied, and therefore only those electrons whose energies are near the critical energy of the Fermi distribution can make transitions and take part in conduction, as it is only in the neighbourhood of the critical energy that the energy levels are partly filled and partly empty. These electrons are few in number compared with the valency electrons, and are what should be called the conduction electrons. On the classical theory alone are the valency electrons, the free electrons and the conduction electrons the same.

---

* 'Z. Physik,' vol. 47, p. 1 (1928)

† 'Z. Physik,' vol. 52, p. 555 (1928).

Bloch has shown that for very tightly bound electrons the energy levels of the lowest states have the same distribution as for free electrons, the only difference being that the constants have different meanings in the two cases. This is not surprising if we rid ourselves of the false correlation between free electrons and conduction electrons, and it merely means that electrons in a metal have a dual aspect. For some phenomena the electrons behave as if they were bound, and for others as if they were free, corresponding to the particle and to the wave properties respectively of the electrons.

By applying these ideas Bloch arrives at a temperature dependence of the conductivity* which is in very satisfactory agreement with the measurements.† He finds that for high temperatures the resistance varies as T, the absolute temperature, and for low temperatures as $T^5$. Here, however, certain difficulties arise. How are we to explain the non-conductivity of insulators and the temperature dependence of the resistance of electronic semi-conductors? On the classical theory the answer is quite simple We merely postulate that there are no free electrons in an insulator, and that the number of free electrons in a semi-conductor varies rapidly with temperature. When we use quantum mechanics, we are no longer at liberty to take this easy way out, as all the electrons in a perfect lattice are free to move through the lattice, and it would seem at first sight that on Bloch's theory all substances should have infinite conductivity at absolute zero temperature. If this were a rigorous consequence of the theory it would be a very serious objection against it, and it is therefore necessary to see if we cannot find a place in the theory for insulators and semi-conductors.

It is not possible to maintain that the difference between good and bad conductors is one of degree only, the electrons in poor conductors being more tightly bound than in metals, and giving rise to a smaller current. There is an essential difference between a semi-conductor, such as germanium, and a good conductor, such as silver, which must be accounted for by any theory which attempts to deal with semi-conductors. In the first place there is the effect of impurities, which always increase the resistance of good conductors and generally decrease the resistance of poor conductors. Then there is the effect of temperature, which is still more marked. The resistance of a good conductor falls rapidly with falling temperature, while that of a poor conductor rises and becomes very large as the temperature approaches the absolute zero.

---

* 'Z. Physik,' vol. 59, p. 208 (1930).

† E. Gruneisen, 'Leipziger Vorträge' (1930).

We have already seen that on the classical theory there is a confusion between free and conduction electrons, and it may be that we have allowed this confusion to slip once more into the theory. We shall therefore examine it more carefully. First of all we may ask how it is possible to obtain a model of an insulator or a semi-conductor. To do this it is necessary to have a perfect lattice in which all the electrons are free, and in which there are no conduction electrons at the absolute zero. Now, if we confine ourselves to Sommerfeld's picture of electrons moving in a region of uniform potential, it is impossible to obtain no conduction electrons. Fortunately, the model of a lattice is not quite so simple, and actually the potential in which the electrons move is periodic in three dimensions and not constant. The problem of an electron moving in a one-dimensional periodic potential has been studied by several authors,* and it appears that the energy levels break up into a number of bands of allowed energies, separated by bands of disallowed energies, which may be of considerable width. When we consider more than one dimension the problem is not quite so simple, for although there are discontinuities in the energy it is sometimes possible for the energy to take every value between a minimum value and infinity. This introduces a new complexity which is of importance for the theory of conduction. Leaving aside this complexity for the moment, it is possible to see from the one-dimensional case how we can have no conduction electrons at the absolute zero. Suppose the number of electrons is just sufficient to fill up the lowest band of allowed energies when all the electrons are in their lowest possible states. Then in the absence of an external field there is, of course, no resultant current. If a field is applied, it will be impossible on account of the Pauli principle for any electron to increase its stream without making a transition to the second band of allowed energies. This it will be unable to do provided the field is small enough, owing to the finite energy difference between the two bands.

In this case, therefore, we have no conduction electrons, and we have the rather curious result that not only is it possible to obtain conduction with bound electrons, but it is also possible to obtain non-conduction with free electrons.

When the temperature is different from zero there will be a few electrons in the second band and a few vacant places in the first band, and conduction can take place. The increase in the number of conduction electrons with rise of temperature will tend to increase the conductivity, while the excitation of the thermal vibrations of the lattice will tend to decrease it. At low temperatures the first effect must predominate, and so the resistance will have a negative temperature coefficient. At higher temperatures the effect of the thermal vibrations will be the more important, and the resistance will obey the normal law. This is just what is observed for semi-conductors.* The problem has to be formulated a little differently when we deal with three dimensions, but it is possible to construct a model which reproduces the properties of semi-conductors.

---

* R. Peierls, 'Ann. Physik,' vol. 4, p. 121 (1930); P. M. Morse, 'Phys. Rev.,' vol. 35, p. 1310 (1930); L. Brillouin, 'J. Physique,' vol. 1, p. 377 (1930); R. Kronig and W. G. Penney, 'Proc. Roy. Soc.,' A, vol. 130, p. 499 (1931).

In the following sections these ideas are elaborated in some detail. We first discuss the energy levels of electrons in a lattice and show that, although the electrons are free in the sense that they can move from one atom of the lattice to another, yet there exist closed sub-groups which do not necessarily correspond to the closed sub-groups of the isolated atoms. Then the theory of the Fermi distribution is modified slightly so as to take account of possible discontinuities in the energy values, and applied to the problem of the paramagnetism of semi-conductors. Finally the temperature dependence of the electrical resistance of semi-conductors is worked out. The calculations are very rough, and it is not pretended that anything more is done than to show that a place can be found in the theory for insulators and semi-conductors. The question as to why certain elements form metallic lattices, and others non-metallic lattices, is a difficult one, and would require much more elaborate calculations than are possible at the moment. At present only qualitative conditions can be given. It is, however, highly satisfactory that the same model should give the properties of both metallic conductors and semi-conductors.

## *The Motion of an Electron in a Lattice.*

1. As is usual in the discussion of this problem, we only deal with a simple cubic crystal with lattice constant $a$. This means that we cannot properly apply our results to metals, that is to say quantitatively, as no metal or semi-metal has this crystal structure. However, any other assumption would make the calculations much more complicated, and, as we are only interested in general results, we may expect this simplifying assumption to give the broad outlines of the phenomena. Only in discussing the finer details of conduction, such as the anomalous thermoelectric and magnetic properties of certain

---

* *Cf.* E. Gruneisen, "Handbuch der Physik," vol. 13, p. 60.

metals, will it be necessary to include the effect of the actual crystal structure. If it is possible to obtain a division of the elements into metals and non-metals on the assumption of a cubic lattice, it is *a fortiori* possible when more complicated structures are considered.

Although the problem of the motion of an electron in a periodic field has been treated at length by the authors mentioned above, it has been thought advisable, on account of the importance of the results relative to the present problem, to review the subject once more. Exact methods are not used, perturbation methods being preferred as giving a much better insight into the problem. Two methods of approximation are employed, one starting from entirely free electrons, and the other starting from tightly bound electrons, the two methods giving very similar results. In this way it is possible to obtain the characteristics of the energy levels not only of the valency electrons but also of the inner, core, electrons.

### *Nearly Free Electrons.*

1.1. It is not convenient to consider a finite crystal, and we therefore suppose an infinite crystal to be divided up into cubes whose sides are of length G$a$, where G is a large number. All these cubes are supposed to have identical properties, which means that all the properties of the crystal have a three-dimensional periodicity with period G$a$. The potential has the smaller period $a$.

Let the mean value of the potential energy of an electron be $V_0$. Then the potential energy V can be expanded as a Fourier series

$$V = V_0 + \sum_{n_1=-\infty}^{\infty} \sum_{n_2=-\infty}^{\infty} \sum_{n_3=-\infty}^{\infty} V_{n_1 n_2 n_3}\, e^{\frac{2\pi i}{a}(n_1 x + n_2 y + n_3 z)}, \qquad (1)$$

where the axes are rectangular ones along the edges of the cube, and the combination $n_1 = n_2 = n_3 = 0$ does not occur. As zero approximation we consider an electron moving with the constant potential energy $V_0$. The wave function characterising the motion is given by

$$\psi^0_{\xi\eta\zeta} = (aG)^{-3/2}\, e^{\frac{i}{a}(\xi x + \eta y + \zeta z)}, \qquad (2)$$

where the possible values of $\xi$, $\eta$, $\zeta$ are

$$2\pi/G\,(0, \pm 1, \pm 2 \ldots). \qquad (3)$$

If $m$ is the mass of the electron, the corresponding energy values are

$$E_0 = \omega\,(\xi^2 + \eta^2 + \zeta^2) + V_0, \qquad (4)$$

$\omega$ being

$$h^2/(8\pi^2 m a^2). \qquad (5)$$

Treating the departure of the potential from uniformity as causing a small perturbation, it is easily seen that the diagonal elements of the perturbing energy are all zero, and that the non-diagonal elements $(\xi\eta\zeta \mid V \mid \xi'\eta'\zeta')$ are also zero unless $\xi'$, $\eta'$, $\zeta'$ differ from $\xi$, $\eta$, $\zeta$ respectively by multiples of $2\pi$. These non-diagonal elements are only of importance in the first approximation provided $E_0$ is nearly equal to $E_0'$, and in this case the unperturbed state is nearly degenerate. Accordingly we put

$$\psi = c\psi^0_{\xi\eta\zeta} + c'\psi^0_{\xi'\eta'\zeta'} \tag{6}$$

and

$$E = \tfrac{1}{2}(E_0 + E_0') + \varepsilon. \tag{7}$$

The secular equation to determine $\varepsilon$ is easily found to be

$$\begin{vmatrix} \tfrac{1}{2}(E_0 - E_0') - \varepsilon & (\xi \mid V \mid \xi') \\ (\xi \mid V \mid \xi') & \tfrac{1}{2}(E_0' - E_0) - \varepsilon \end{vmatrix} = 0$$

giving

$$\varepsilon^2 = \tfrac{1}{4}(E_0 - E_0')^2 + (\xi \mid V \mid \xi')^2. \tag{8}$$

This makes E a multivalued function of $\xi$, which is due to the fact that the state given by (6) is a mixture of the $(\xi, \eta, \zeta)$ state and the $(\xi', \eta', \zeta')$ state. It is convenient to have single valued functions, and we therefore adopt the convention that E is an increasing function of each of $\xi$, $\eta$, $\zeta$, which suffices to fix E completely.

Consider fixed values of $\eta$ and $\zeta$ lying between $\pm\pi$, and not being nearly equal to either of these values Then if the difference $(E_0 - E_0')$ is to be small it is necessary that $\eta = \eta'$, $\zeta = \zeta'$ and $\xi$ must be nearly $\pm\pi$. Putting $\xi = \pi - u$, then $\xi'$ must be given by $\xi' = -\pi - u$, and then

$$(\xi\eta\zeta \mid V \mid \xi'\eta'\zeta') = V_{100}.$$

Also

$$E_0 = V_0 + \omega\{(\pi - u)^2 + \eta^2 + \zeta^2\}$$

and

$$E_0' = V_0 + \omega\{(\pi + u)^2 + \eta^2 + \zeta^2\},$$

giving

$$E = V_0 + \omega(\pi^2 + u^2 + \eta^2 + \zeta^2) \pm (\pi^2\omega^2u^2 + V_{100}^2)^{\frac{1}{2}}. \tag{9}$$

On expanding the square root we have approximately

$$E = V_0 + \pi^2\omega - V_{100} - u^2\left(\frac{\pi^2\omega^2}{V_{100}} - \omega\right) + \omega(\eta^2 + \zeta^2) \tag{10A}$$

by taking the negative sign, and

$$E = V_0 + \pi^2\omega + V_{100} + u^2\left(\frac{\pi^2\omega^2}{V_{100}} + \omega\right) + \omega(\eta^2 + \zeta^2) \tag{10B}$$

by taking the positive sign. The expression (10A) is valid when $u$ is positive, and (10B) when $u$ is negative, since this satisfies the convention that E is an increasing function.

If we plot the variable part of E against $\xi$, keeping $\eta$ and $\zeta$ constant, we obtain a curve of the type given below. At the points $\xi = \pm\pi$ the energy is discontinuous, and in addition the derivative of E becomes zero. These discontinuities were first noticed by Peierls (*loc. cit.*), whose treatment we have given here. It is often convenient to treat $\xi$ as a continuous variable. This is equivalent to making G tend to infinity, and when there is no ambiguity caused by this process we shall talk about $\xi$ as if it were continuous.

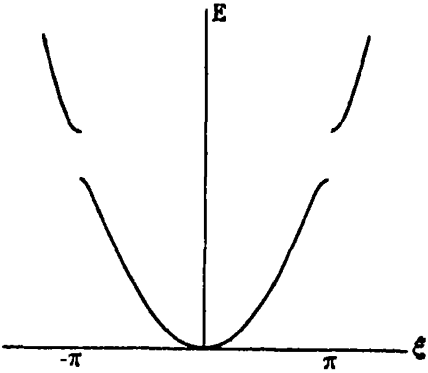

FIG 1.

1.11. It is obvious that there will be similar discontinuities whenever one of $\xi$, $\eta$, $\zeta$ passes through a multiple of $\pi$. In this way we get zones of energies, which have been exhaustively studied by Brillouin (*loc. cit.*). The first zone occurs when each of $\xi$, $\eta$, $\zeta$ lies between $-\pi$ and $\pi$, giving $G^3$ energy levels in all. The second zone consists of six separate portions in which two of $\xi$, $\eta$, $\zeta$ lie between $\pm\pi$, while the third is either greater than $\pi$ or less than $-\pi$. These six portions together give $G^3$ energy values. The third and higher zones are more complicated, and reference may be made to Brillouin's paper. They all have the property of comprising exactly $G^3$ energy levels.

As soon as we deal with more quantum numbers than one, there appears a property which is not brought out in the figure, but which may be readily seen by drawing a similar diagram for two independent variables. The highest energy levels in the first zone are given by $\xi = \pm\pi$, $\eta = \pm\pi$, $\zeta = \pm\pi$, all of which have the same energy, while the lowest energy levels in the second zone are given by $\xi = \pm\pi$, $\eta = 0$, $\zeta = 0$, and $\xi = 0$, $\eta = \pm\pi$, $\zeta = 0$ and $\xi = 0$, $\eta = 0$, $\zeta = \pm\pi$. Now there is no need for $E_{\min}$ (2) to be greater than

$E_{max}$ (1), where (1) and (2) denote that the energies belong to the first and second zones respectively. Of course, $E_{min}$ (2) must be greater than E $(\pi, 0, 0)$, (1), but E $(\pi, \pi, \pi)$ (1) is also greater than E $(\pi, 0, 0)$ (1), and so $E_{min}$ (2) may be either greater or less than $E_{max}$ (2), depending on the magnitude of the discontinuities. In fact, for nearly free electrons the coefficients $V_{n_1n_2n_3}$ will all be small, and in this case $E_{min}$ (2) will certainly be less than $E_{max}$ (1), the condition for this being that $\pi^2\omega$ is greater than $V_{100}$. The assumption of nearly free electrons, therefore, leads to the result that the energy does not show the forbidden ranges which appear in the one-dimensional case, the discontinuities only playing a rôle when we consider the energy as a function of one quantum number, the other two being considered fixed.

### *Tightly Bound Electrons.*

1.2. We shall now consider the problem starting from the opposite limiting case of tightly bound electrons. This has already been partly treated by Bloch (*loc. cit.*). This method of treatment is more logical than that just given, in that it enables the assumptions to be clearly seen, and, though at the moment it is impossible to obtain any better or more detailed results from this model, any further advance in the theory of conduction will have to be made by taking into account the various effects here neglected.

Bloch has shown by a general argument that the wave function of an electron in a cubic lattice must have the form

$$\psi_{klm} = e^{\frac{2\pi i}{K}(kx + ly + mz)} u_{klm}(xyz), \tag{11}$$

where $K = aG$; $k$, $l$, $m$ are positive or negative integers, but not zero, and $u_{klm}(xyz)$ is a periodic function of $x$, $y$, $z$ with period $a$. It is not possible to obtain a general formula for the corresponding energy levels.

If we suppose that the potential energy of an electron in the crystal is very large and negative in the neighbourhood of each lattice point, and is elsewhere nearly constant, it is possible to derive approximate formulæ for the energy levels. As zero approximation we consider the electron to be in the neighbourhood of a lattice point, and we neglect the influence of the other atoms. The energy is then that of the free atom. This state is degenerate, as placing the electron in a similar orbit round any other lattice point gives a state with the same energy. The degeneracy is of order $G^3$, and is removed when we introduce the forces due to the neighbouring atoms. Here we meet a difficulty. It is not possible even in the zero approximation to neglect entirely the interactions of the electrons, as the Coulomb forces due to the nuclei would then give an infinite potential at every point. We must suppose that the lattice is electrically neutral, and that the interactions of the electrons are partly taken into account in some way by a "self-consistent field," so that the potential, expressed as a sum over the lattice points, converges to a finite value. The exchange forces between the electrons are, however, neglected, as it is only in this case that the electrons can be treated independently of one another. With these assumptions, together with the further one that the presence of the neighbouring atoms causes an energy change small compared with the energy differences between the various energy levels of the isolated atom, it is possible to solve the problem.

Using Bloch's notation, let the integers $g_1$, $g_2$, $g_3$ characterise the various lattice points, and let the potential energy of an electron due to one lattice point be

$$U_{g_1 g_2 g_3}(xyz) = U(x - g_1 a, y - g_2 a, z - g_3 a), \tag{12}$$

which is a function of the distance of the electron from the lattice point only. The potential energy of an electron in the crystal is then given by

$$V(xyz) = \sum_{g_1 g_2 g_3 = -\infty}^{\infty} U_{g_1 g_2 g_3}(xyz), \tag{13}$$

and the Schrodinger equation is

$$\nabla^2 \psi + \frac{8\pi^2 m}{h^2}(E - V)\psi = 0, \tag{14}$$

while the Schrodinger equation for an isolated atom is

$$\nabla^2 \phi_{g_1 g_2 g_3} + \frac{8\pi^2 m}{h^2}(E - U_{g_1 g_2 g_3})\,\phi_{g_1 g_2 g_3} = 0. \tag{15}$$

This last equation has various solutions which may or may not be degenerate, and the subsequent work differs slightly in the two cases.

1.21. First let us consider an *s* state, which is the only case treated by Bloch. In this case $\phi_{g_1 g_2 g_3}$ is spherically symmetrical. If $E_1$ is the corresponding energy value, we solve equation (14) by setting

$$E = E_1 + \varepsilon_1 \quad \text{and} \quad \psi = \sum_{g_1 g_2 g_3} a_{g_1 g_2 g_3}\,\phi_{g_1 g_2 g_3}. \tag{16}$$

The equations determining $\varepsilon_1$ and the *a*'s to the first order are easily found to be

$$\sum_{g_1 g_2 g_3} a_{g_1 g_2 g_3} \int_0^K \int_0^K \int_0^K (\varepsilon_1 - U'_{g_1 g_2 g_3})\,\phi_{g_1 g_2 g_3}\,\phi_{h_1 h_2 h_3}\,dx\,dy\,dz = 0 \tag{17}$$

for all integral values of $h_1$, $h_2$, $h_3$, and where

$$U'_{g_1 g_2 g_3} = V - U_{g_1 g_2 g_3}.$$

For tightly bound electrons we assume

$$\int \phi_{g_1g_2g_3}\,\phi_{h_1h_2h_3}\,d\tau = \delta^{h_1}_{g_1}\,\delta^{h_2}_{g_2}\,\delta^{h_3}_{g_3},$$

and also since $\phi$ and U are both spherically symmetrical we put

$$\int \mathrm{U}'_{g_1g_2g_3}\,\phi_{g_1g_2g_3}\,\phi_{h_1h_2h_3}\,d\tau$$

equal to $\alpha_1$ if $g$ and $h$ are the same, equal to $\beta_1$ if $g$ and $h$ refer to lattice points which are nearest neighbours, and zero otherwise The assumption of tightly bound electrons means that $\alpha_1$ and $\beta_1$ are essentially positive.

Equations (17) reduce to the triply infinite set

$$(\varepsilon_1 - \alpha_1)\,a_{g_1g_2g_3} + \beta_1\,(a_{g_1+1,\,g_2,\,g_3} + a_{g_1-1,\,g_2,\,g_3} + a_{g_1,\,g_2+1,\,g_3}$$
$$+ a_{g_1,\,g_2-1,\,g_3} + a_{g_1,\,g_2,\,g_3+1} + a_{g_1,\,g_2,\,g_3-1}) = 0. \qquad (18)$$

There is in addition the condition that $\psi$ is periodic with period K. The equations (18) are satisfied by

$$a^{klm}_{g_1g_2g_3} = e^{\frac{2\pi i}{\mathrm{G}}(kg_1+lg_2+mg_3)}$$

giving

$$\psi_{klm} = \sum_{g_1g_2g_3=-\infty} e^{\frac{2\pi i}{\mathrm{G}}(kg_1+lg_2+mg_3)}\,\phi_{g_1g_2g_3}, \qquad (19)$$

and

$$\mathrm{E}_{klm} = \mathrm{E}_1 + \alpha_1 - 2\beta_1\left(\cos\frac{2\pi k}{\mathrm{G}} + \cos\frac{2\pi l}{\mathrm{G}} + \cos\frac{2\pi m}{\mathrm{G}}\right) \qquad (20)$$

These results are only valid for values of $k$, $l$, $m$ lying between ± ½G, higher values merely giving repetitions.

1.22. We next consider a $p$ state. Here the level is triply degenerate, but it will not split up in a cubic crystal * This is much more easily seen than in Bethe's paper if we use Cartesian co-ordinates instead of spherical polars. We then see immediately that the independent wave functions of the $p$ state can be chosen to be $xf(r)$, $yf(r)$ and $zf(r)$, where $f(r)$ is a function of $r$ only, and these three functions will give the same energy in a field with cubical symmetry. In view of Bethe's result we need only consider the levels derived from one of these wave functions, the others being obvious from symmetry.

Let $\chi_{g_1g_2g_3} = x_g f(r_g)$ be a wave function of the isolated atom corresponding to the energy value $\mathrm{E}_2$. Then we solve equation (14) as before by

$$\mathrm{E} = \mathrm{E}_2 + \varepsilon_2 \quad \text{and} \quad \psi = \sum_{g_1g_2g_3} b_{g_1g_2g_3}\,\chi_{g_1g_2g_3}, \qquad (16\text{A})$$

---

* H. Bethe, 'Ann. Physik,' vol. 3, p. 133 (1929).

obtaining a set of equations similar to (17). Here, however, the equations involve more than two constants $\alpha$ and $\beta$, since $\chi$ is not spherically symmetrical. As before we set

$$\int U'_{g_1g_2g_3}\,\chi_{g_1g_2g_3}\,\chi_{h_1h_2h_3}\,d\tau$$

equal to $\alpha_2$ if $g$ and $h$ refer to the same point. Among the other non-vanishing integrals we must distinguish two types. Firstly the type

$$\int U'_{g_1g_2g_3}\,\chi_{g_1g_2g_3}\,\chi_{g_1,g_2+1,g_3}\,d\tau.$$

This we set equal to $\beta_2$, which is essentially positive, since the only factor which makes it differ in form from the integral for $\beta_1$ is $x_g^2$, which is positive. Then there is the type

$$\int U'_{g_1g_2g_3}\,\chi_{g_1g_2g_3}\,\chi_{g_1+1,g_2,g_3}\,d\tau.$$

This we set equal to $-\gamma_2$, where $\gamma_2$ is positive, since in the integrand there occurs a factor $x_{g_1}\,x_{g_1+1}$. Little can be said about $\beta_2$ and $\gamma_2$ except that they are both positive and of the same order of magnitude. The equations corresponding to (18) are

$$(\epsilon_2-\alpha_2)\,b_{g_1g_2g_3}-\gamma_2\,(b_{g_1+1,g_2,g_3}+b_{g_1-1,g_2,g_3}) \\ +\beta_2\,(b_{g_1,g_2+1,g_3}+b_{g_1,g_2-1,g_3}+b_{g_1,g_2,g_3+1}+b_{g_1,g_2,g_3-1})=0. \quad (18\text{A})$$

This is solved as before by

$$b^{klm}_{g_1g_2g_3}=e^{\frac{2\pi i}{G}(kg_1+lg_2+mg_3)},$$

giving

$$E_{klm}=E_2+\alpha_2+2\gamma_2\cos\frac{2\pi k}{G}-2\beta_2\left(\cos\frac{2\pi l}{G}+\cos\frac{2\pi m}{G}\right). \quad (21)$$

This is valid for $l$ and $m$ lying between $\pm\frac{1}{2}G$, and $k$ lying between either $\frac{1}{2}G$ and $G$ or $-\frac{1}{2}G$ and $-G$. There are also two similar expressions obtained by permuting $k$, $l$ and $m$.

1.23. Similar results could also be obtained for $d$ and $f$ states, but the work would be more complicated, not only on account of the larger degeneracy, but also because the degeneracy is partly removed by the crystalline field. For example, for $d$ terms the harmonics may be taken to be $xy$, $yz$, $zx$, $x^2-y^2$ and $y^2-z^2$. The first three taken together will not split as they obviously give the same energy in a cubic field, but there will be an energy difference between these terms and the last two. As it is not the object of this paper to investigate the properties of special structures any further than is necessary to explain the general outlines of semi-conduction, these questions will not be further discussed here.

1.24. In the expressions for the energy levels put

$$\xi = \frac{2\pi k}{G}, \qquad \eta = \frac{2\pi l}{G}, \qquad \zeta = \frac{2\pi m}{G}.$$

Then for small values of $\xi$, $\eta$, $\zeta$ equation (20) becomes

$$E_{\xi\eta\zeta} = E_1 + \alpha_1 - 6\beta_1 + \beta_1 (\xi^2 + \eta^2 + \zeta^2),$$

which is of exactly the same form as (4) with $\beta_1$ instead of $\omega$. Also putting $\xi = \pi - u$, and supposing $u$, $\eta$, $\zeta$ small, we have

$$E_{\xi\eta\zeta} = E_1 + \alpha_1 - 2\beta_1 - \beta_1 u^2 + \beta_1 (\eta^2 + \zeta^2),$$

which is of the same form as (10A). We therefore conclude that the energy levels derived from an *s* state correspond exactly to those in the first zone of the free electron picture.

Further, treating $\eta$ and $\zeta$ as small in the expression (21) and putting $\xi = \pi + u$, we have approximately

$$E_{\xi\eta\zeta} = E_2 + \alpha_2 - 4\beta_2 - 2\gamma_2 + \gamma_2 u^2 + \beta_2 (\eta^2 + \zeta^2),$$

which is of exactly the same form as (10B) We conclude that the energy levels derived from *p* levels correspond to those in the second zone of the free electron picture. We therefore see that the discontinuities in the energy occur both for nearly free and for strongly bound electrons.

For our perturbation method to be valid it is necessary that the unperturbed energy levels of the isolated atom should be far apart. Therefore if (20) gives the states derived from a term *ns*, and (21) those derived from a term *np* it is necessary that the energy difference between these two systems should be large. Now the greatest of the energies (20) is given by putting $\xi = \eta = \zeta = \pi$ and is $E_1 + \alpha_1 + 6\beta_1$, while the least of the energies (21) is given by putting

$$\xi = \pi, \quad \eta = \zeta = 0 \quad \text{and is} \quad E_2 + \alpha_2 - 4\beta_2 - 2\gamma_2.$$

We must therefore have

$$E_2 + \alpha_2 - 4\beta_2 - 2\gamma_2 > E_1 + \alpha_1 + 6\beta_1. \tag{22}$$

In this case all the energies of the second zone lie above those of the first zone, and there are forbidden ranges of the energy, in contradistinction to the case of nearly free electrons, where, in spite of the discontinuities, the energy can take all values from $V_0$ to infinity.

### *The Internal State of a Metal.*

1.3. By using the results established above for the two limiting cases of nearly free and of tightly bound electrons, it is possible to see qualitatively the energy levels in a metal, even of the inner electrons, in so far as the exchange forces can be neglected. This is a very serious restriction—how serious further investigation must show.

The innermost electrons in a metal must be in levels derived from the 1*s* state. The energy levels must therefore be given by a formula of the same form as (20), there being $G^3$ such levels in all. On account of the spin of the electron, these levels are double and can accommodate $2G^3$ electrons, that is two per atom, and so in a metal the 1*s* or K electrons will just fill up the lowest allowed band of energies. The 1*s* level is peculiar in that the next higher state is also an *s* level, and so the second band of allowed energies is also of the type (20). There is no doubt that in all metals the K electrons are strongly bound, and do not interfere with the 2*s* levels at all. They can therefore be omitted entirely from the discussion. The groups other than the first are not peculiar and it will be sufficient to discuss an element with $(n - 1)$ completed groups, but with the *n*th incomplete.

The states derived from the *ns* level are of the type (20), and these are the lowest states whether the electrons are nearly free or strongly bound. These levels can accommodate $2G^3$ electrons. For the alkalis which have a single *ns* electron we should expect that the $G^3$ valency electrons should all go into this level, half filling it. The alkaline earths having two *ns* electrons, we might expect that their $2G^3$ valency electrons would just fill up the band of states derived from the *ns* level. This is not necessarily true, since if the electrons are nearly free the lowest levels derived from the *np* state have lower energy than the highest levels derived from the *ns* state, as was pointed out in section 1.11. In this case not all the $2G^3$ levels in the first band would be filled, some electrons being in the second band. If, on the other hand, the electrons are strongly bound, then all the levels derived from the *np* state have higher energies than those derived from the *ns* state, and in this case all the $2G^3$ valency electrons would just fill up the $2G^3$ levels of the first band. In the first case the alkaline earths would be metals, and in the second case at most semi-conductors. We thus see that it might be possible for the alkaline earths to be non-metallic, while for the alkalis there is no such possibility. The fact that the alkaline earths are metallic shows that their valency electrons must be considered as nearly free, and that the first and second bands of energies overlap. It therefore appears that electrons which form a closed sub-group in an atom need not necessarily do so in a metal.

The above discussion is sufficient to show the properties which are required to make an element a semi-conductor It is necessary that the electrons which do not form a complete group should exactly fill up one of the bands of allowed energies, and further that these electrons should be tightly bound. The first condition is a qualitative one and involves the number of electrons per atom being even. If the crystal structure were the simple cubic one which is considered here, it would also be necessary that the number of electrons should be just sufficient to complete a sub-group of the isolated atom, but this is not necessary for more complicated structures, as in these the degeneracy of the $p$ terms is removed by the crystalline field Thus, electrons which form a closed sub-group in a metal do not necessarily do so in the isolated atom. This is the converse of the statement at the end of the last paragraph. It is to be noted that we define a closed group in a metal as consisting of the electrons occupying all those levels which belong to a band of allowed energies, irrespective of whether there are discontinuities or not, the only condition being that the energy takes all values between its upper and lower bounds The second of the conditions for a semi-conductor is a quantitative one, and is the condition expressed by the inequality (22). The further investigation of this condition would necessitate the consideration of the actual crystal structure as well as the atomic levels, and would require calculations which are impossible at the moment.

To determine the properties of a semi-conductor we shall consider a cubic lattice in which both the above conditions are satisfied. The model is a very rough one and is much simplified, but ought to give the broad outlines of the phenomena.

### *The Model of a Semi-Conductor.*

2.1. We assume that we have a simple cubic lattice, consisting of atoms which have just enough electrons to fill up one of the zones discussed above, and that the electrons are tightly bound. For simplicity we shall only discuss the case when each atom has two $s$ electrons outside a closed group. To obtain semi-conducting properties it is necessary to assume that all the energy levels derived from the $p$ terms lie higher than those derived from the $s$ terms.

The $2G^3$ levels derived from the $s$ terms have energies given by

$$E_{\xi\eta\zeta} = E_1 + \alpha_1 - 2\beta_1 (\cos \xi + \cos \eta + \cos \zeta), \qquad (20)$$

and the next terms are those derived from the $p$ terms, having energies given by

$$E_{\xi\eta\zeta} = E_2 + \alpha_2 + 2\gamma_2 \cos\xi - 2\beta_2 (\cos\eta + \cos\zeta), \tag{21}$$

and by two other expressions obtained by permuting $\xi$, $\eta$, and $\zeta$. The condition (22) must also be satisfied, so

$$E_2 + \alpha_2 - 4\beta_2 - 2\gamma_2 > E_1 + \alpha_1 + 6\beta_1.$$

At the absolute zero all the $2G^3$ valency electrons will be in the $2G^3$ levels given by (20), but at any higher temperature some of the electrons will be in the upper levels. The number of electrons with quantum numbers lying between $(\xi, \eta, \zeta)$ and $(\xi + d\xi, \eta + d\eta, \zeta + d\zeta)$ is given by $(2G^3/8\pi^3)\, n_0\, (\xi\eta\zeta)\, d\xi\, d\eta\, d\zeta$, where $n_0\, (\xi\eta\zeta)$ is the Fermi function and is given by

$$n_0\, (\xi\eta\zeta) = \frac{1}{\frac{1}{A} e^{\frac{E}{kT}} + 1}. \tag{23}$$

The energy E is given by (20) for values of $\xi$, $\eta$, $\zeta$ lying between $\pm\pi$, and by (21) when two of $\xi$, $\eta$, $\zeta$ lie between $\pm\pi$ and the third lies either between $\pi$ and $2\pi$ or between $-\pi$ and $-2\pi$. The higher levels are of no interest in the present discussion. Even with these simple forms for the energy levels the subsequent calculations are very complicated. A great simplification is introduced if we suppose $\beta_2 = \gamma_2$, and we therefore assume this. The two quantities are of the same order of magnitude and it would not be worth while treating them as unequal unless we also took into account the correct crystal structure of the semi-conductor. This assumption gives E a simple form in the neighbourhood of the critical energy of the Fermi distribution, and in this case alone has it so far been found possible to carry out the calculations completely

It is first necessary to determine the value of the constant A, which is fixed by the number of electrons present. We set for convenience

$$E_1 + \alpha_1 + 6\beta_1 = W_1,$$

$$E_2 + \alpha_2 - 4\beta_2 - 2\gamma_2 = W_2 \tag{24}$$

and

$$\log A = W_0/kT.$$

In order that the effect of the discontinuity may be observable at ordinary temperatures it is necessary to assume that $(W_2 - W_1)$ is small compared with $\beta_1$. The electrons are therefore to be thought of as neither tightly bound nor nearly free, but in an intermediate condition. For insulators $(W_2 - W_1)$ is not small compared with $\beta_1$, and the conductivity will only become appreciable for exceedingly high temperatures.

In the ordinary theory of the Fermi distribution $W_0$ is constant so long as T lies below the temperature of degeneracy, which is some thousands of degrees. Here, however, the theory is not so simple and $W_0$ is constant only if $kT$ is not large compared with $(W_2 - W_1)$. In this case it is easily seen that $W_0$ must lie between $W_1$ and $W_2$, for only if this condition is satisfied are all the levels in the first zone occupied at the absolute zero, and all those in the second zone unoccupied. Ordinarily $W_0$ is the null-point energy of the electrons, but this is no longer necessarily true if there are bands of forbidden energies, and if $W_0$ happens to be a forbidden energy the null-point energy is the highest allowed energy less than $W_0$. If $kT$ is large compared with $(W_2 - W_1)$ the effect of the discontinuity is negligible and the substance behaves as a metal. For a semi-conductor this temperature range usually lies below the temperature of degeneracy. To determine $W_0$ we have the equation

$$2G^3 = \frac{2G^3}{8\pi^3}\int_{-\infty}^{\infty}\int_{-\infty}^{\infty}\int_{-\infty}^{\infty}\frac{d\xi\, d\eta\, d\zeta.}{e^{\frac{E-W_0}{kT}}+1}\,. \tag{25}$$

To evaluate the integral we split it up into parts. Consider first the contribution which is given by restricting all the variables of integration to lie between $\pm\pi$. The index of the exponential is then negative, and so the integrand is nearly unity, the deviation from unity being greatest near the points $(\pm\pi, \pm\pi, \pm\pi)$. The next contributions arise from restricting two of $\xi$, $\eta$, $\zeta$ to lie between $\pm\pi$, and the third to lie either between $-\pi$ and $-2\pi$ or between $\pi$ and $2\pi$. Since there are three such ranges of integration there will be three equal contributions. The remaining contributions are negligible for small values of T. Equation (25) can therefore be written

$$\int_{-\pi}^{\pi}\int_{-\pi}^{\pi}\int_{-\pi}^{\pi}\left(\frac{1}{e^{\frac{E-W_0}{kT}}+1}-1\right)d\xi\, d\eta\, d\zeta + 3\int_{-2\pi}^{-\pi}d\xi\int_{-\pi}^{\pi}\int_{-\pi}^{\pi}\frac{d\eta\, d\zeta}{e^{\frac{E-W_0}{kT}}+1}$$

$$+\,3\int_{\pi}^{2\pi}d\xi\int_{-\pi}^{\pi}\int_{-\pi}^{\pi}\frac{d\eta\, d\zeta}{e^{\frac{E-W_0}{kT}}+1} = 0 \tag{26}$$

Taking the terms of the first integral together, the integrand is effectively zero except in the neighbourhood of the eight points $(\pm\pi, \pm\pi, \pm\pi)$. As the expression for E given by (20) is periodic in $\xi$, $\eta$, $\zeta$ with period $2\pi$, we may replace the contributions from the regions in the neighbourhoods other than that near $(\pi, \pi, \pi)$ by equivalent integrations in the neighbourhood of $(\pi, \pi, \pi)$, of course still using the expression (20) for the energy. Using new variables defined by

$$\xi = \pi - u, \qquad \eta = \pi - v, \qquad \zeta = \pi - w,$$

the integration takes place in a cube centre $u = v = w = 0$, the length of the sides being $2\pi$. For small values of $u$, $v$, $w$ the energy is given by

$$\mathrm{E} = \mathrm{W}_1 - \beta_1 (u^2 + v^2 + w^2), \tag{27}$$

and with this expression for the energy we may take the limits of integration to be infinite with negligible error, as the integrand vanishes exponentially for large values of the variables. The first integral therefore reduces to

$$-\int_{-\infty}^{\infty}\int_{-\infty}^{\infty}\int_{-\infty}^{\infty} \frac{du\,dv\,dw}{e^{\{\mathrm{W}_0 - \mathrm{W}_1 + \beta_1 (u^2 + v^2 + w^2)\}/k\mathrm{T}} + 1}. \tag{28}$$

The integrand of the second integral is only different from zero near $(-\pi, 0, 0)$ and that of the third integral near $(\pi, 0, 0)$. By substituting $\xi = -\pi - u$, $\eta = v$, $\zeta = w$ and $\xi = \pi + u$, $\eta = v$, $\zeta = w$ respectively, these two integrals may be combined together in much the same way as for the first integral, and they finally reduce to

$$+\int_{-\infty}^{\infty}\int_{-\infty}^{\infty}\int_{-\infty}^{\infty} \frac{du\,dv\,dw}{e^{\{\mathrm{W}_2 - \mathrm{W}_0 + \beta_2 (u^2 + v^2 + w^2)\}/k\mathrm{T}} + 1}. \tag{29}$$

Equating the sum of the expression (28) and (29) to zero gives an equation for $\mathrm{W}_0$. It is impossible to obtain an explicit value for $\mathrm{W}_0$ which is valid for all values of T, but it is easy to do so if T is small For other ranges of T the evaluation is more difficult.

For small values of T we expand the denominators of the integrands and retain only the first terms. This gives

$$(\beta_1)^{-3/2}\, e^{-\frac{\mathrm{W}_0 - \mathrm{W}_1}{k\mathrm{T}}} = 3\,(\beta_2)^{-3/2}\, e^{-\frac{\mathrm{W}_2 - \mathrm{W}_0}{k\mathrm{T}}},$$

or

$$\mathrm{W}_0 = \tfrac{1}{2}(\mathrm{W}_1 + \mathrm{W}_2) - \tfrac{1}{2}k\mathrm{T}\log 3\,(\beta_1/\beta_2)^{3/2}. \tag{30}$$

The last term may be either positive or negative since $\beta_1 < \beta_2$, the *s* electrons being more tightly bound than the *p* electrons. In general this term is negligible unless $k\mathrm{T}$ is comparable with $(\mathrm{W}_2 - \mathrm{W}_1)$.

### *The Specific Heat of the Electrons.*

2.2. The specific heat of the electron gas has been calculated by Sommerfeld and by Bloch, the former using free electrons and the latter tightly bound electrons. Bloch assumes that the variable part of the energy is given by

$$\mathrm{E} = -2\beta(\cos\xi + \cos\eta + \cos\zeta),$$

and finds that the specific heat is proportional to the temperature if $T < T_0$, and falls off as $T^{-2}$ if $T > T_0$, where $T_0$ is the temperature $2\beta/k$, the maximum specific heat per gram-molecule of the metal being of the order R. For the model we are treating here the temperature dependence will be rather different, on account of the discontinuity in the energy, and for temperatures low compared with $(W_2 - W_1)/k$ the specific heat must fall off exponentially to zero.

If we choose $G^3 = L$, Loschmidt's number, the energy of the electrons per gram-molecule of metal is

$$U = \frac{2L}{8\pi^3} \iiint \frac{E\, d\xi\, d\eta\, d\zeta}{e^{\frac{E - W_0}{kT}} + 1}. \tag{31}$$

To evaluate this we split the integral up into parts, exactly as was done in the last section, and transform to the variables $u$, $v$, $w$. It is impossible to carry out the calculation exactly so we discuss two limiting cases.

(1) We first of all assume that T is very small, so small that $(W_2 - W_1)$ is large compared with $kT$.

Consider the contribution to (31) coming from the first zone of allowed energies. It is

$$\frac{2L}{8\pi^3} \int_{-\pi}^{\pi} \int_{-\pi}^{\pi} \int_{-\pi}^{\pi} \frac{E\, du\, dv\, dw}{e^{\frac{E - W_0}{kT}} + 1}$$

where

$$E = W_1 - 6\beta_1 + 2\beta_1 (\cos u + \cos v + \cos w)$$

Since $W_0 > W_1$ the index of the exponential is always large and negative, and so the exponential term is small compared with unity. We may therefore expand the denominator and take the first two terms only. The first term gives

$$\frac{2L}{8\pi^3} \iiint E\, du\, dv\, dw = 2L(W_1 - 6\beta_1).$$

The second term is more difficult to evaluate. We shall, however, only make a very small error if we expand the cosines, and, instead of integrating through the cube, integrate through a sphere of the same volume. If, further, we integrate through an infinite sphere we make negligible error since the integrand vanishes exponentially. With these approximations the second term gives

$$-\frac{2L}{8\pi^3} \iiint \{W_1 - \beta_1 (u^2 + v^2 + w^2)\}\, e^{-\frac{W_0 - W_1}{kT} - \frac{\beta_1}{kT}(u^2 + v^2 + w^2)}\, du\, dv\, dw,$$

which reduces to

$$-\frac{L\sqrt{\pi}}{8\pi^2} \left\{ 2W_1 \left(\frac{kT}{\beta_1}\right)^{3/2} - 3\beta_1 \left(\frac{kT}{\beta_1}\right)^{5/2} \right\} e^{-\frac{W_0 - W_1}{kT}}.$$

The contribution to (31) coming from the second zone of allowed energies is given by

$$\frac{6L}{8\pi^3}\iiint\frac{E\,du\,dv\,dw}{e^{\frac{E-W_0}{kT}}+1},$$

where

$$E = W_2 + 6\beta_2 - 2\beta_2(\cos u + \cos v + \cos w).$$

Since $W_2 > W_0$ the index of the exponential is always large and positive, and so we need only retain the exponential term in the denominator and omit the 1. This gives on using the same approximations as before

$$\frac{3L\sqrt{\pi}}{8\pi^2}\left\{2W_2\left(\frac{kT}{\beta_2}\right)^{3/2} + 3\beta_2\left(\frac{kT}{\beta_2}\right)^{5/2}\right\}e^{-\frac{W_2-W_0}{kT}}.$$

Finally we have for U, after using (30) to combine the exponential terms,

$$U = 2L(W_1 - 6\beta_1) + \frac{L\sqrt{\pi}}{4\pi^2}\left\{(W_2 - W_1)\left(\frac{kT}{\beta_1}\right)^{3/2} + 3\beta_1\left(\frac{kT}{\beta_1}\right)^{5/2}\right\}e^{-\frac{W_0-W_1}{kT}}. \tag{32}$$

We now make the approximation $W_0 = \frac{1}{2}(W_1 + W_2)$, and, putting $k\Theta_u = W_0 - W_1$, and $kT_0 = \beta_1$, we have for the specific heat

$$C_v = \frac{\partial U}{\partial T} = \frac{R\sqrt{\pi}}{8\pi^2}\left(\frac{T}{T_0}\right)^{3/2}\left\{4\left(\frac{\Theta_u}{T}\right)^2 + 12\frac{\Theta_u}{T} + 15\right\}e^{-\frac{\Theta_u}{T}}, \tag{33}$$

R being the gas constant.

(2) The second limiting case of interest occurs for values of T such that $(W_2 - W_1) \ll kT \ll \beta_1$. In this case the calculations are not so easy to carry out with any degree of accuracy, but it would seem a reasonable approximation to expand the integrals in powers of $\Theta_u/T$, and neglect all terms but the first. This is equivalent to putting $W_1 = W_2 = W_0$. A calculation almost identical with the one above leads to the approximate result

$$C_v = \frac{R15\sqrt{\pi}}{16\pi^2}\left\{1 + 3\left(\frac{\beta_1}{\beta_2}\right)^{3/2}\right\}\left(\frac{T}{T_0}\right)^{3/2}, \tag{33A}$$

the next term, involving $\Theta_u/T$, being negative. This value is practically identical with (33) for large values of T ($< T_0$), and it is probable that in a more exact calculation the numerical factor in the bracket would be replaced by 2, which would render the two expressions (33) and (33A) identical for large values of T. We therefore see that the specific heat increases steadily from zero according to the exponential law (33) until T becomes of the same order as $\Theta_u$. It then increases as $T^{3/2}$, there being no maximum in the curve. The order of magnitude of the specific heat is the same as that calculated by Sommerfeld, and seems well below the limit of observation.

### *The Paramagnetism of the Electrons.*

2.3. One of the first applications of the Fermi statistics was made by Pauli* to explain the small constant paramagnetism of the alkalis. For semi-conductors the paramagnetism will be constant at ordinary temperatures and will decrease exponentially to zero as the temperature is lowered.

The paramagnetic susceptibility is due to the effect of an external magnetic field in orienting the electrons, each electron possessing a magnetic moment of one Bohr magneton,

$$\mu_0 = \frac{eh}{4\pi mc}$$

Under the influence of an external magnetic field H each electronic energy level is split up into two, the energies of the states being $E(\xi\eta\zeta) \pm \mu_0 H$. Since the degeneracy of the electronic states is removed we can no longer use (23) for the distribution function, and we must distinguish between the two directions of spin. The number of electrons with quantum numbers lying between $(\xi, \eta, \zeta)$ and $(\xi + d\xi, \eta + d\eta, \zeta + d\zeta)$ is now given by

$$(G^3/8\pi^3)\, n_0(\xi\eta\zeta, \pm \mu_0 H)\, d\xi\, d\eta\, d\zeta,$$

where

$$n_0(\xi\eta\zeta, \pm \mu_0 H) = \frac{1}{\frac{1}{A} e^{\frac{E \pm \mu_0 H}{kT}} + 1}.$$

The parameter A has the same value as before to the first order in H The total magnetic moment is

$$\begin{aligned} M &= \frac{\mu_0 G^3}{8\pi^3} \iiint \left[ \frac{1}{\frac{1}{A} e^{\frac{E - \mu_0 H}{kT}} + 1} - \frac{1}{\frac{1}{A} e^{\frac{E + \mu_0 H}{kT}} + 1} \right] d\xi\, d\eta\, d\zeta \\ &= \frac{2\mu_0^2 H G^3}{8\pi^3 kT} \iiint \frac{d\xi\, d\eta\, d\zeta}{\left(\frac{1}{A} e^{\frac{E}{kT}} + 1\right)\left(\frac{1}{A} e^{\frac{-E}{kT}} + 1\right)} \end{aligned} \tag{34}$$

to the first order in H. We split the integral up into parts as before, and a short calculation shows that the paramagnetic susceptibility $\kappa$ is given by

$$\kappa = \frac{\mu_0^2 \sqrt{\pi}}{\pi^2 a^3 \beta_1} \left(\frac{T}{T_0}\right)^{\frac{1}{2}} e^{-\frac{\Theta_u}{T}}, \tag{35}$$

provided $T \ll \Theta_u$, $a$ being the lattice constant.

---

* 'Z. Physik,' vol. 41, p. 81 (1927).

This is of the same order as the constant value found for the alkalis by Pauli, and also by Bloch,* the latter obtaining

$$\kappa \sim \frac{\mu_0^2}{a^3\beta}.$$

It is doubtful whether there is any reliable experimental evidence with which to test the formula (35), though for some substances, notably carbon, an increase of diamagnetism with falling temperature has been observed, which might be attributed to the falling off of the paramagnetism of the outer electrons, the diamagnetism of the closed shells remaining constant.

## *The Calculation of the Conductivity.*

3 The combined influence of a constant electric field and of the thermal motion of the lattice on the distribution of electrons in a metal has been studied in great detail by Bloch in the papers mentioned above. In the main we shall follow the same method here, but as we shall need to use some refinements later, it has been thought advisable first to give Bloch's calculations in a modified form and afterwards to apply them to a semi-conductor.

The problem is to determine the form of the distribution function $n(\xi\eta\zeta)$ under the combined action of a constant electric field F, parallel to the $x$-axis, and the thermal vibrations. We assume that the elastic vibrations of the lattice are split up into their normal modes and that the vector displacement of a typical lattice point is given by

$$\mathbf{u}_{l_1l_2l_3} = \sum_{f',g',h'=1}^{G} \sum_{j=1}^{3} a_{f'g'h'j}\, e^{\frac{2\pi i}{G}(l_1f'+l_2g'+l_3h')}\, \mathbf{v}_{f'g'h'j},$$

where $\mathbf{v}_{f'g'h'j}$ is a unit vector giving the direction of the displacement, the $a_{f'g'h'j}$ being the normal co-ordinates, $j = 1$ giving the longitudinal vibrations and $j = 2$, $j = 3$ the transverse. The corresponding frequencies are given by

$$\nu_{fghj} = \frac{\mathfrak{b}_j}{2\pi a}\sqrt{(f^2 + g^2 + h^2)}, \tag{36}$$

where $\mathfrak{b}_j$ is the velocity of propagation and $f = 2\pi f'/\mathrm{G}$, $g = 2\pi g'/\mathrm{G}$, $h = 2\pi h'/\mathrm{G}$. By the introduction of these normal co-ordinates the problem is reduced to the interaction of the valency electrons with a number of simple harmonic oscillators characterised by the integers $f'$, $g'$, $h'$, $j$. Bloch shows that if an electron jumps from a state ($\xi$, $\eta$, $\zeta$) to a state ($\xi'$, $\eta'$, $\zeta'$), while the oscillator ($f$, $g$, $h$) emits or absorbs a quantum of energy, then it is necessary that,

$$\xi - \xi' = \pm f \pmod{2\pi}, \tag{37}$$

---

* 'Z. Physik,' vol. 53, p. 216 (1929).

with two similar conditions for $g$ and $h$. He also shows that only the longitudinal vibration is of importance, and we shall therefore omit $j$ in future.

3.1. The alteration in the distribution function $n(\xi\eta\zeta)$ due to the electric field is given by

$$-\frac{2\pi a e F}{h}\frac{\partial n}{\partial \xi}, \tag{38}$$

and the alteration due to collisions with the lattice is given by*

$$\sum_{\xi f} \overset{+}{A}_{\xi\xi' f}\left[n_{\xi'}(1 - n_{\xi})(N_f + 1) - n_{\xi}(1 - n_{\xi'}) N_f\right]$$
$$+ \sum_{\xi' f} \bar{A}_{\xi\xi' f}\left[n_{\xi'}(1 - n_{\xi}) N_f - n_{\xi}(1 - n_{\xi'})(N_f + 1)\right]. \tag{39}$$

Only one of each set of quantum numbers has been written explicitly, but this will cause no confusion The meaning of the various quantities is as follows.

$$\overset{+}{A}_{\xi\xi' f} = \frac{hC^2(f^2 + g^2 + h^2)}{8\pi^2 M a^2 \mu^2 \nu}\frac{\partial}{\partial t}\frac{1 - \cos 2\pi t(E_{\xi} - E_{\xi'} + h\nu)/h}{(E_{\xi} - E_{\xi'} + h\nu)^2}, \tag{40}$$

where M is the mass of the crystal cube, C is a quantity of the order of the square of the reciprocal of the radius of the atom, and $\mu = 8\pi^2 m/h^2$ $\bar{A}_{\xi\xi' f}$ only differs from $\overset{+}{A}_{\xi\xi' f}$ by having $(E_{\xi} - E_{\xi'} - h\nu)$ in the time factor instead of $(E_{\xi} - E_{\xi'} + h\nu)$ Further, the three conditions (37) must be satisfied.

The expression for $N_f$ varies somewhat with the assumptions we make If we assume that the lattice vibrations are always in thermal equilibrium—a state of affairs which can be brought about by a minute quantity of impurity in the crystal—then we have

$$N_f = \frac{1}{e^{\frac{h\nu_f}{kT}} - 1} \tag{41}$$

Otherwise $N_f$ takes a slightly different form which has been discussed by Peierls. This question is of little importance for semi-conductors and we accordingly take $N_f$ to be given by (41). In this case it is sufficient to consider transitions which satisfy

$$\left.\begin{array}{l} \xi - \xi' = \pm f \\ \eta - \eta' = \pm g \\ \zeta - \zeta' = \pm h \end{array}\right\}. \tag{37A}$$

The other transitions allowed by (37) would not change the temperature dependence of the resistance, but would only affect its magnitude.

Under the combined influence of the electric field and of collisions with the lattice, the distribution of electrons must be steady. We therefore obtain an integral equation for $n(\xi\eta\zeta)$ by equating to zero the sum of (38) and (39). We try to solve this by putting

---

* R. Peierls, 'Ann. Physik,' vol. 4, p. 121 (1930), equation (12), corrected.

$$n(\xi\eta\zeta) = n_0(\xi\eta\zeta) + n_1(\xi\eta\zeta), \tag{42}$$

where $n_0(\xi\eta\zeta)$ is the Fermi distribution (23), and $n_1$ is small and proportional to F. We use the abbreviations

$$\frac{E_{\xi} - W_0}{kT} = \varepsilon, \qquad \frac{E_{\xi'} - W_0}{kT} = \varepsilon', \qquad \frac{h\nu_f}{kT} = x. \tag{43}$$

Owing to the presence of the time factor, the expression for $A^{+}_{\xi\xi'f}$ is only sensibly different from zero when $\varepsilon - \varepsilon' + x = 0$, and we may substitute this value for $x$ in any terms multiplying $A^{+}_{\xi\xi'f}$ Similarly $A^{-}_{\xi\xi'f}$ is only different from zero when $\varepsilon - \varepsilon' - x = 0$. We now take as our unknown

$$\chi(\xi\eta\zeta) = n_1(\xi\eta\zeta)(e^{\varepsilon} + 1)(e^{-\varepsilon} + 1), \tag{44}$$

and then, neglecting squares of F, we have

$$\frac{2\pi aeF}{h}\frac{\partial n_0}{\partial \xi} = \sum_{\xi'} A^{+}_{\xi\xi'f}\frac{1}{(e^{\varepsilon} + 1)(e^{-\varepsilon} + 1)(e^{x} - 1)}\{\chi_{\xi'} - \chi_{\xi}\}$$
$$+ \sum_{\xi'} A^{-}_{\xi\xi'f}\frac{1}{(e^{-\varepsilon'} + 1)(e^{\varepsilon'} + 1)(e^{x} - 1)}\{\chi_{\xi'} - \chi_{\xi}\}. \tag{45}$$

It is important to note that changing $\xi$ into $\xi'$ changes the factor by which $(\chi_{\xi} - \chi_{\xi'})$ is multiplied in the first term into the factor occurring in the second term, and *vice versa*. The variables $f$, $g$ and $h$ do not occur explicitly in (45), being given by (37A).

Now let us write the equation (42) for shortness in the following form

$$\chi(\xi\eta\zeta)\,\phi(\xi\eta\zeta) - \iiint K(\xi\eta\zeta, \xi'\eta'\zeta')\,\chi(\xi'\eta'\zeta')\,d\xi'\,d\eta'\,d\zeta'$$
$$= -\frac{2\pi aeF}{h}\frac{\partial n_0}{\partial \xi}. \tag{45A}$$

We have here replaced the summation by an integration, which is allowable as we may make $\xi$, $\eta$, $\zeta$ continuous variables by allowing G to tend to infinity. As remarked above, $K(\xi, \xi')$ is symmetrical between the dashed and the undashed letters, and from the form of (45) we must have

$$\phi(\xi\eta\zeta) = \iiint K(\xi\eta\zeta, \xi'\eta'\zeta')\,d\xi'\,d\eta'\,d\zeta'. \tag{46}$$

To solve (45A) is very difficult, and we have to make approximations which will be better appreciated if we treat a special case first. The approximations are not easy to justify mathematically, and rest rather on physical arguments. Accordingly, in this section we treat the case of ordinary metals and assume that the variable part of the energy is given by

$$E_\xi = \beta(\xi^2 + \eta^2 + \zeta^2),$$

reserving the general case for consideration later.

The right-hand side of (45A) involves $\xi\partial n_0/\partial E$, that is $\xi$ multiplied by a factor which is symmetrical in $\xi$, $\eta$, $\zeta$. This suggests that we try a function of the same form for $\chi$. Further, in order that our expressions for $A_{\xi\xi'}$ may be correct, it is necessary to assume that the lattice vibrations are equivalent to a small perturbation of the electronic motion. Actually, unless the temperature is exceedingly high, an electron only loses a very small fraction of its energy or of its momentum in a collision, and we therefore suppose that $(\xi - \xi')/\xi'$ is small compared with unity. From these considerations we write (45A) in the form

$$\chi_\xi\phi_\xi - \int K(\xi, \xi')\frac{\xi}{\xi'}\chi_{\xi'}\,d\xi'\,d\eta'\,d\zeta' = -\frac{2\pi aeF}{h}\frac{\partial n_0}{\partial \xi} - \int K(\xi, \xi')\frac{\xi - \xi'}{\xi'}\chi_{\xi'}\,d\xi'\,d\eta'\,d\zeta' \qquad (47)$$

If we put the right-hand side of (47) equal to zero, the resulting homogeneous equation has the solution

$$\chi_\xi = \xi$$

on account of (46) We therefore solve (47) by successive approximations, putting

$$\chi_\xi = \alpha\xi + \chi_2,$$

where $\alpha$ is at present an arbitrary constant and $\chi_2$ is supposed small compared with the first term. We then obtain the following equation for $\chi_2$, omitting terms of the order $\chi_2(\xi - \xi')/\xi'$

$$\chi_2\phi_\xi - \int K(\xi, \xi')\frac{\xi}{\xi'}\chi_2\,d\xi'\,d\eta'\,d\zeta' = -\frac{2\pi aeF}{h}\frac{\partial n_0}{\partial \xi} - \alpha\int K(\xi, \xi')(\xi - \xi')\,d\xi'\,d\eta'\,d\zeta'.$$

The essential difference between this equation and (47) is that here the unknown function only occurs on the left-hand side of the equation, and the corresponding homogeneous equation can be solved exactly. In order that this equation may be soluble it is necessary that the right-hand side should be orthogonal to the solution of the homogeneous equation obtained by transposing the left-hand side. This condition gives an equation for $\alpha$. If we take $\chi_2\phi_\xi$ as a new unknown, it is easily seen that the solution of the homogeneous transposed equation is

$$\chi_2\phi_\xi = \xi^{-1},$$

and so the orthogonality condition is

$$\frac{2\pi a e F}{h}\int \frac{1}{\xi}\frac{\partial n_0}{\partial \xi}\,d\xi\,d\eta\,d\zeta + \alpha\iint K(\xi, \xi')\,\frac{\xi - \xi'}{\xi}\,d\xi\,d\eta\,d\zeta\,d\xi'\,d\eta'\,d\zeta' = 0 \qquad (48)$$

We therefore finally obtain an approximate solution of the form

$$n(\xi\eta\zeta) = n_0(\xi\eta\zeta) + \frac{\alpha\xi}{(e^{\epsilon}+1)(e^{-\epsilon}+1)},$$

which is Bloch's solution. The equation (48) for $\alpha$ differs slightly from that given by Bloch, who did not formulate the orthogonality condition properly. However, within the accuracy to which we are working the two equations give the same final result

3.11. We now evaluate the parameter $\alpha$ under the conditions which probably obtain in the alkali metals, the energy being given by $E = \beta(\xi^2 + \eta^2 + \zeta^2)$. The first term in (48) is

$$-\frac{2\pi a e F}{h}\,\frac{2\beta}{kT}\int \frac{d\xi\,d\eta\,d\zeta}{(e^{\epsilon}+1)(e^{-\epsilon}+1)} \qquad (49)$$

and presents no difficulty The sextuple integral is, however, extremely difficult to calculate, mainly owing to the presence of the time factor. The corresponding time factors which occur in dispersion or collision problems do not cause any trouble because there are no relations such as (37A) to be satisfied, and a simple integration over $E_{\xi'}$ suffices to eliminate the time factor. Here $\nu$ is not independent of $\xi$ and $\xi'$, and this introduces a complication which renders the evaluation of the sextuple integral a matter of some delicacy.

We first of all use polar co-ordinates $\rho$, $\theta$, $\phi$ and $\rho'$, $\theta'$, $\phi'$, so that we have $\xi^2 + \eta^2 + \zeta^2 = \rho^2$ and $\xi'^2 + \eta'^2 + \zeta'^2 = \rho'^2$, the axis of $\xi$ being $\theta = 0$. Then instead of $\rho'$, $\theta'$, $\phi'$ we use polar co-ordinates R, $\vartheta$, $\varpi$ in the $f$, $g$, $h$ space, and finally instead of R we use the equivalent variable $\nu$, which is connected with R by equation (36),

$$\nu = \frac{\mathfrak{b}}{2\pi a}R.$$

The line joining ($\xi$, $\eta$, $\zeta$) to the origin is taken as $\vartheta = 0$, and $\vartheta$ is therefore the angle between the direction of propagation of the incident electronic wave and that of the elastic vibration, the direction cosines being proportional to $(\xi, \eta, \zeta)$ and to $(f, g, h)$ respectively.

First let us consider the factor involving the time. It is

$$\frac{2\pi}{h}\frac{\sin 2\pi t\,(E_\xi - E_{\xi'} \pm h\nu)/h}{E_\xi - E_{\xi'} \pm h\nu} = \frac{2\pi}{h}\frac{\sin 2\pi t y/h}{y},$$

where

$$y = \beta\left(\frac{4\pi^2 a^2}{\mathfrak{b}^2}\nu^2 + \frac{4\pi a}{\mathfrak{b}}\nu\rho\cos\vartheta\right) \mp h\nu.$$

If $t$ is large this expression oscillates very rapidly, and in any integral involving it the only effective contributions will be from small values of $y$. We therefore change variables from $\vartheta$ to $y$, and in any expression which varies slowly we put $y = 0$. Now

$$dy = -\frac{4\pi a\beta}{\mathfrak{b}}\nu\rho\sin\vartheta\,d\vartheta$$

and so

$$\int_0^\pi \frac{\sin 2\pi t\,(E_\xi - E_{\xi'} \pm h\nu)/h}{E_\xi - E_{\xi'} \pm h\nu}\sin\vartheta\,d\vartheta = -\int_{\vartheta=0}^{\vartheta=\pi}\frac{\mathfrak{b}}{4\pi a\beta\nu\rho}\frac{\sin 2\pi t y/h}{y}\,dy.$$

Further, putting $z = 2\pi t y/h$ the integral becomes

$$\frac{\mathfrak{b}}{4\pi a\beta\nu\rho}\int_{\vartheta=\pi}^{\vartheta=0}\frac{\sin z}{z}\,dz,$$

the upper limit of integration being

$$z = \frac{2\pi t}{h}\left\{\beta\left(\frac{4\pi^2 a^2}{\mathfrak{b}^2}\nu^2 + \frac{4\pi a}{\mathfrak{b}}\nu\rho\right) \mp h\nu\right\}$$

and the lower limit being

$$z = \frac{2\pi t}{h}\left\{\beta\left(\frac{4\pi^2 a^2}{\mathfrak{b}^2}\nu^2 - \frac{4\pi a}{\mathfrak{b}}\nu\rho\right) \mp h\nu\right\}.$$

If these limits of integration are of opposite sign, then for large $t$ the last integral is effectively

$$\int_{-\infty}^{\infty}\frac{\sin z}{z}\,dz,$$

that is $\pi$, and if the limits are of the same sign the integral is zero. It is therefore necessary to consider the limits of integration carefully.

Taking first the upper sign for $h\nu$, which corresponds to the absorption of a "sound quantum" by the electrons, we see that the upper limit becomes negative if

$$\nu < \frac{h\mathfrak{b}^2}{4\pi^2 a^2 \beta} - \frac{\mathfrak{b}\rho}{\pi a}, \tag{50}$$

and the lower limit becomes positive if

$$\nu > \frac{h\mathfrak{b}^2}{4\pi^2 a^2 \beta} + \frac{\mathfrak{b}\rho}{\pi a}. \tag{51}$$

These ranges are therefore to be excluded.

Taking next the lower sign for $h\nu$, corresponding to an emission of a "sound quantum," we see that the upper limit is always positive, but that the lower limit becomes positive if

$$\nu > \frac{\mathfrak{b}\rho}{\pi a} - \frac{h\mathfrak{b}^2}{4\pi^2 a^2 \beta}. \tag{52}$$

This range is therefore to be excluded, as giving zero contribution. Further, any other factors containing $\vartheta$ are to be replaced by their values when $y = 0$, that is when

$$\cos\vartheta = \pm \frac{h\mathfrak{b}}{4\pi a\beta\rho} - \frac{\pi a \nu}{\mathfrak{b}\rho}. \tag{53}$$

We next carry out the integration over $\varpi$, which presents no difficulty as the only factor involving $\varpi$ is $(\xi - \xi')/\xi$. From (37A) we have

$$\int_0^{2\pi} \frac{\xi - \xi'}{\xi} d\varpi = -\frac{\mathrm{R}}{\rho}\int_0^{2\pi} \frac{\cos\theta_1}{\cos\theta} d\varpi,$$

where $\theta_1$ is the angle which the line joining $(\rho, \theta, \phi)$ and $(\rho', \theta', \phi')$ makes with the line $\theta = 0$. The definition of $\vartheta$ and $\varpi$ gives

$$\cos\theta_1 = \cos\theta\cos\vartheta + \sin\theta\sin\vartheta\cos\varpi.$$

and so we have

$$\int_0^{2\pi} \frac{\xi - \xi'}{\xi} d\varpi = -\frac{\mathrm{R}\cos\vartheta}{\rho} \tag{54}$$

By these integrations the sextuple integral has been reduced to the following form, from which a constant multiplying factor has been omitted.

$$\int \frac{1}{\rho^3} d\xi\, d\eta\, d\zeta \int \frac{\nu^2 d\nu}{e^x - 1}\left[\left(\nu^2 - \frac{h\mathfrak{b}^2}{4\pi^2 a^2\beta}\nu\right)\frac{1}{(e^\epsilon + 1)(e^{-\epsilon - x} + 1)} + \left(\nu^2 + \frac{h\mathfrak{b}^2}{4\pi^2 a^2\beta}\nu\right)\frac{e^x}{(e^\epsilon + 1)(e^{-\epsilon + x} + 1)}\right], \tag{55}$$

the limits of integration being determined by (50), (51) and (52). With these limits of integration the integral is finite, as it must be, though, if we had taken the limits of integration for $\rho$ to be 0 and $\infty$, the integral would have been logarithmically infinite at the lower limit However, only small values of $x$ contribute appreciably and from this it also follows that only values of $\rho$ in the neighbourhood of the critical point of the Fermi distribution are effective, as was to be expected on physical grounds The integrand is, therefore, only appreciable for small values of $x$ and of $\varepsilon$, and in this case the exact limits of integration do not affect the result We take $\nu$ to vary from 0 to $\nu_m$, the maximum Debye frequency, or equivalently we take $x$ to vary from 0 to $\Theta/T$, where $\Theta$ is the Debye characteristic temperature. The integral over $\rho$ need only be taken over a range including $\varepsilon = 0$, sufficiently large for the integrand to have become inappreciable. The equation (48) for $\alpha$ becomes

$$\left(\frac{T}{\Theta}\right)^3 \frac{\alpha}{\lambda}\int \frac{1}{\rho^3}\, d\xi\, d\eta\, d\zeta \int_0^{\Theta/T} \frac{x^2\, dx}{e^x-1}\left[\left\{\left(\frac{T}{\Theta}\right)^2 x^2 - \gamma\left(\frac{T}{\Theta}\right) x\right\}\frac{1}{(e^{\varepsilon}+1)(e^{-\varepsilon-x}+1)}\right.$$
$$\left. + \left\{\left(\frac{T}{\Theta}\right)^2 x^2 + \gamma\left(\frac{T}{\Theta}\right) x\right\}\frac{e^x}{(e^{\varepsilon}+1)(e^{-\varepsilon+x}+1)}\right] = \frac{2\beta F}{kT}\int \frac{d\xi\, d\eta\, d\zeta}{(e^{\varepsilon}+1)(e^{-\varepsilon}+1)}. \tag{56}$$

The definitions of the constants are

$$\gamma = \frac{1}{\beta k\Theta}\left(\frac{h\mathfrak{v}}{2\pi a}\right)$$

and

$$\lambda = \frac{4e\mathfrak{v}a^2M\mu^2\beta}{\pi^3G^3hC^2}\left(\frac{h\mathfrak{v}}{ak\Theta}\right)^5. \tag{57}$$

Since only small values of $x$ contribute effectively to the integral we may, in terms involving both $\varepsilon$ and $x$, expand in powers of $x$ and invert the orders of integration. The terms involving $\gamma$ disappear, and on changing the variable to E we obtain

$$\left(\frac{T}{\Theta}\right)^5 \frac{2\alpha\beta^{3/2}}{\lambda}\int \frac{dE}{E\,(e^{\varepsilon}+1)(e^{-\varepsilon}+1)}\int_0^{\Theta/T}\frac{x^4\, dx}{e^x-1} = \frac{2\beta F}{kT}\int \frac{\sqrt{E}\, dE}{(e^{\varepsilon}+1)(e^{-\varepsilon}+1)}. \tag{58}$$

The ratio of the two E integrals is found to be $W_0^{3/2}$ on using the formulæ given by Sommerfeld, while the $x$ integral is easily evaluated in the two limiting cases of T very large or very small compared with $\Theta$.

For $T \gg \Theta$ we develop the integrand in powers of $x$, obtaining for $\alpha$

$$\alpha = \frac{4F\lambda}{\sqrt{\beta}}\frac{\Theta}{T}\frac{W_0^{3/2}}{kT}.$$

For $T \ll \Theta$ the integration may be taken to $\infty$ with negligible error, and we obtain

$$\alpha = \frac{F\lambda}{125\sqrt{\beta}}\left(\frac{\Theta}{T}\right)^5\frac{W_0^{3/2}}{kT}.$$

The distribution function therefore takes the form

$$n(\xi\eta\zeta) = n_0(\xi\eta\zeta) - \mathrm{F}\lambda_1 \frac{\Theta}{\mathrm{T}} \frac{\partial n_0}{\partial \xi} \quad \text{for} \quad \mathrm{T} \gg \Theta, \tag{59A}$$

and

$$n(\xi\eta\zeta) = n_0(\xi\eta\zeta) - \frac{\mathrm{F}\lambda_1}{500} \left(\frac{\Theta}{\mathrm{T}}\right)^5 \frac{\partial n_0}{\partial \xi} \quad \text{for} \quad \mathrm{T} \ll \Theta, \tag{59B}$$

where

$$\lambda_1 = 2\left(\frac{\mathrm{W}_0}{\beta}\right)^{3/2} \lambda \tag{57A}$$

This is equivalent to Bloch's result, and gives a conductivity which varies as $\mathrm{T}^{-5}$ for low temperatures and as $\mathrm{T}^{-1}$ for high temperatures.

3.2 We now consider the general case when we do not assume E to have the simple form used in the last section. The solution of equation (45), which is valid independent of the form assumed by E, is suggested by the way in which we have written the expressions (59) Instead of (47) we use the following equation, which reduces to (47) under the conditions assumed in section 3.1.

$$\chi_\xi \phi_\xi - \int \mathrm{K}(\xi, \xi') \frac{\partial \mathrm{E}/\partial \xi}{\partial \mathrm{E}/\partial \xi'} \chi_\xi \, d\xi' \, d\eta' \, d\zeta'$$

$$= -\frac{2\pi a e \mathrm{F}}{h} \frac{\partial n_0}{\partial \xi} - \int \mathrm{K}(\xi, \xi') \frac{\partial \mathrm{E}/\partial \xi - \partial \mathrm{E}/\partial \xi'}{\partial \mathrm{E}/\partial \xi'} \chi_\xi \, d\xi' \, d\eta \, d\zeta'. \tag{47A}$$

The argument follows exactly the same lines as before, a solution of the equation with the right-hand side replaced by zero being

$$\chi_\xi = \frac{\partial \mathrm{E}}{\partial \xi}$$

We therefore solve (47A) by putting

$$\chi_\xi = \alpha' \frac{\partial \mathrm{E}}{\partial \xi} + \chi_2,$$

$\alpha'$ being given by an orthogonality condition, which is easily found to be

$$\frac{2\pi a e \mathrm{F}}{h} \int \frac{1}{\partial \mathrm{E}/\partial \xi} \frac{\partial n_0}{\partial \xi} \, d\xi \, d\eta \, d\zeta + \alpha' \iint \mathrm{K}(\xi, \xi') \frac{\partial \mathrm{E}/\partial \xi - \partial \mathrm{E}/\partial \xi'}{\partial \mathrm{E}/\partial \xi}$$

$$d\xi \, d\eta \, d\zeta \, d\xi' \, d\eta' \, d\zeta' = 0. \tag{48A}$$

3.21. It only remains to solve this equation for $\alpha'$ In the general case it is not possible to carry out the integrations as completely as above, but there is little doubt that a similar result will be obtained. Here we shall carry out the calculation for our model of a semi-conductor. We shall only treat the case of low temperatures, as all theories give the same law for high temperatures, and so the interesting region is that of low temperatures.

Our model of a semi-conductor consists in having a large number of electrons in the first zone of energy values, and a few electrons in the second, there being a finite energy difference between the two zones At low temperatures only the thermal vibrations of small energy will be excited, and the probability of the transition of an electron from the first to the second zone will be small. In calculating the conductivity we may therefore neglect such transitions as they form a very small fraction of the total number of transitions Further in evaluating (48A) we restrict $\xi$, $\eta$, $\zeta$ and $\xi'$, $\eta'$, $\zeta'$ to lie between $\pm\pi$, that is in the first zone. If we restrict them to lie in the second zone we obtain a value for $\alpha'$ which is the same as the first one, as it must be, on account of the relation (30)

As in section 2 the integrands are only effectively different from zero in the neighbourhood of the points $(\pm\pi, \pm\pi, \pm\pi)$ We therefore transform to the variables, $u$, $v$, $w$ used in section 2 The first term in (48A) then becomes

$$-\frac{2\pi a e \mathrm{F}}{h}\frac{1}{k\mathrm{T}}\int\frac{du\,dv\,dw}{(e^{\epsilon}+1)(e^{-\epsilon}+1)}, \tag{49A}$$

where

$$k\mathrm{T}\epsilon = \mathrm{E}-\mathrm{W}_0 = \mathrm{W}_1-\mathrm{W}_0-\beta_1(u^2+v^2+w^2) \qquad (\mathrm{W}_0 > \mathrm{W}_1) \tag{60}$$

The treatment of the second term follows exactly the same lines as in the last section and, omitting a constant multiplying factor, we again obtain the expression (55) There is, however, a great difference, since here $\epsilon$ is always negative and decreases as $\rho$ increases, where $\rho^2 = u^2+v^2+w^2$. Small values of $\rho$ are therefore the most important, and so the exact limits of integration must be used. From (50), (51), (52) and from the fact that neither $\rho$ nor $\nu$ can be negative we see that the expression (55) must be written

$$\begin{aligned}&4\pi\int_0^{\rho_0}\frac{1}{\rho}\,d\rho\int_{\frac{\mathfrak{b}}{\pi a}(\rho_0-\rho)}^{\frac{\mathfrak{b}}{\pi a}(\rho_0+\rho)}\frac{(\nu-\mathfrak{b}\rho_0/\pi a)\,\nu^3\,d\nu}{(e^{\epsilon}+1)(e^{-\epsilon-x}+1)(e^{x}-1)}\\&+4\pi\int_{\rho_0}^{\infty}\frac{1}{\rho}\,d\rho\int_0^{\frac{\mathfrak{b}}{\pi a}(\rho_0+\rho)}\frac{(\nu-\mathfrak{b}\rho_0/\pi a)\,\nu^3\,d\nu}{(e^{\epsilon}+1)(e^{-\epsilon-x}+1)(e^{x}-1)}\\&+4\pi\int_{\rho_0}^{\infty}\frac{1}{\rho}\,d\rho\int_0^{\frac{\mathfrak{b}}{\pi a}(\rho-\rho_0)}\frac{(\nu+\mathfrak{b}\rho_0/\pi a)\,\nu^3\,d\nu}{(e^{\epsilon}+1)(e^{-\epsilon-x}+1)(e^{x}-1)},\end{aligned} \tag{61}$$

where $\rho_0 = h\mathfrak{b}/4\pi a\beta_1$. To carry the integrations further is not easy, and we therefore make approximations which are valid when we use those numerical values of the various constants which actually occur. If we put $\mathfrak{b} = 10^5$ cm.

per second, $a = 10^{-8}$ cm. and $\beta_1 = 10^{-12}$ erg, $\rho_0$ comes out to be of the order $10^{-3}$. Further, the integrand is negligible for values of $\rho$ which are much greater than $\rho_1$, where $\beta_1\rho_1^2 = k\mathrm{T}$. The value of $\rho_1$ is of the order $10^{-2}\sqrt{\mathrm{T}}$, and this may be taken as the maximum value of $\rho$ which occurs in the $\nu$ integrals. The corresponding value of $x(= h\nu/k\mathrm{T})$ is of the order $\mathrm{T}^{-\frac{1}{2}}$. From these numerical results we see that except for extremely small values of T of the order of a fraction of a degree it is permissible to expand the integrand in powers of $x$, and we therefore replace the factor $(e^x - 1)$ by $x$. Also on account of its smallness we put $\rho_0$ equal to zero, the resulting error being negligible. We then have for (61)

$$\frac{2\pi k\mathrm{T}}{h}\left(\frac{\mathfrak{b}}{\pi a}\right)^4 \int_0^\infty \frac{\rho^3\, d\rho}{(e^\epsilon + 1)(e^{-\epsilon} + 1)}, \tag{62}$$

and so we have for $\alpha'$ the equation

$$\frac{\alpha'}{\lambda'}\,\frac{k\mathrm{T}}{\beta_1}\int_0^\infty \frac{\rho^3\, d\rho}{(e^\epsilon + 1)(e^{-\epsilon} + 1)} = \frac{\mathrm{F}}{k\mathrm{T}}\int_0^\infty \frac{\rho^2\, d\rho}{(e^\epsilon + 1)(e^{-\epsilon} + 1)}, \tag{63}$$

where

$$\lambda' = \frac{2\pi \mathrm{M}ae\mathfrak{b}^2\mu^2}{\mathrm{C}^2\mathrm{G}^3}. \tag{64}$$

On integration by parts we find

$$\alpha' = \frac{\sqrt{\pi}}{2}\left(\frac{\beta_1}{k\mathrm{T}}\right)^{3/2}\frac{\mathrm{F}\lambda'}{k\mathrm{T}}, \tag{65}$$

which gives for the distribution function

$$n(\xi\eta\zeta) = n_0(\xi\eta\zeta) - \frac{\sqrt{\pi}}{2}\quad \mathrm{F}\lambda'\left(\frac{\beta_1}{k\mathrm{T}}\right)^{3/2}\frac{\partial n_0}{\partial\xi}. \tag{66}$$

3 22. To evaluate the conductivity we use the general result that the stream of an electron is given by

$$s_x = \frac{2\pi ea}{h}\,\frac{\partial \mathrm{E}\,(\xi\eta\zeta)}{\partial\xi}. \tag{67}$$

This has been proved by Bloch for tightly bound electrons by direct evaluation of the stream, and by Peierls* for the case when $u_{klm}\,(xyz)$, defined in equation (11), does not vary rapidly with $k$, that is, for nearly free electrons. This relation also holds in the neighbourhood of the discontinuities in the energy, as may be seen by writing equation (6) in the form

$$\begin{aligned}\psi &= c\overset{0}{\psi}_{\xi\eta\zeta} + c'\overset{0}{\psi}_{\xi'\eta'\zeta'}\\ &\alpha\; ce^{i\xi x/a} + c'e^{i(\xi-2\pi)x/a}\\ &= e^{i\xi x/a}\left(c + c'e^{-2\pi ix/a}\right).\end{aligned}$$

---

* 'Z. Physik,' vol. 53, p. 255 (1929).

The expression in the bracket is $u_k(x)$ and is independent of $k$, so Peierls' proof still holds.

The total current is

$$J_x = \int n(\xi\eta\zeta)\, s_x\, d\xi\, d\eta\, d\zeta,$$

and so depends on evaluating the expression

$$\int \frac{\partial E}{\partial \xi} \frac{\partial n_0}{\partial \xi}\, d\xi\, d\eta\, d\zeta. \tag{68}$$

This we do by splitting up the integral in the usual way and considering the contributions from the different regions

Introducing the variables $u, v, w$ used in section 2, $\partial E/\partial \xi$ for the first zone becomes $2\beta_1 u$ and the corresponding contribution to the integral (68) is

$$-\int 2\beta_1\, u\, \frac{\partial n_0}{\partial u}\, du\, dv\, dw,$$

or

$$-\frac{4\beta_1{}^2}{kT}\int \frac{u^2\, du\, dv\, dw}{(e^{\{W_1-W_0-\beta_1(u^2+v^2+w^2)\}/kT}+1)\,(e^{\{W_1-W_0-\beta_1(u^2+v^2+w^2)\}/kT}+1)}.$$

If we write $kT\varepsilon_1 = \beta_1(u^2+v^2+w^2)$ this becomes

$$-\frac{8\pi\,(kT)^{3/2}}{3\,\beta_1{}^{1/2}}\int_0^\infty \frac{\varepsilon_1{}^{3/2}\, d\varepsilon_1}{(e^{\varepsilon_1+(W_0-W_1)/kT}+1)\,(e^{-\varepsilon_1-(W_0-W_1)/kT}+1)}$$

$$= -\frac{4\pi\,(kT)^{3/2}}{\beta_1{}^{1/2}}\int_0^\infty \frac{\sqrt{\varepsilon_1}\, d\varepsilon_1}{e^{\varepsilon_1+(W_0-W_1)/kT}+1}. \tag{69}$$

For small values of T we may omit the 1 in the denominator since $W_0 > W_1$, obtaining

$$-\pi^{3/2}\, kT\,(kT/\beta_1)^{1/2}\, e^{-\frac{W_0-W_1}{kT}}. \tag{70}$$

The second zone gives a similar contribution, and the two may be combined together by using (30) and we find

$$-\pi^{3/2}\, kT\left(\frac{kT}{\beta_1}\right)^{1/2}\left(1+\frac{\beta_2}{\beta_1}\right)e^{-\frac{W_0-W_1}{kT}}.$$

Introducing the temperature $\Theta_u$ defined in section 2.2, the conductivity $\sigma$ is given by

$$\sigma = \sigma_0\, e^{-\frac{\Theta_u}{T}}, \tag{71}$$

where $\sigma_0$ is a constant. This formula is only valid for $T \ll \Theta_u$. If $T \gg \Theta_u$ the discontinuity is unimportant, the substance behaves as a metal and for sufficiently high temperatures must have $\sigma$ inversely proportional to the temperature.

### *Comparison with Experiment*

4. The experimental results on semi-conductors are not easy to interpret. In the first place there are two main types of semi-conductors. The first type consists of ionic conductors in which heavy ions are transported through the crystal by a process akin to electrolysis. The second type consists of purely electronic conductors, while there is a third class in which the current is carried partly by ions and partly by electrons. The theory developed here only applies to electronic conductors. Further, we have considered the crystal to be atomic, and the theory must not be expected to apply to molecular crystals without considerable modification. The greatest difficulty in the interpretation arises, however, because there is no general agreement as to which substances are to be classified as metals and which as semi-metals Gruneisen, in his article on conductivity in the "Handbuch der Physik," cites a number of elements as semi-conductors Unfortunately, the resistance curves are often completely changed by the presence of small quantities of impurities For example, titanium is cited by Gruneisen as a semi-conductor, and in certain states it shows a pronounced negative temperature coefficient, whereas recent measurements have shown that titanium is a superconductor. Germanium exhibits a very curious resistance curve with two minima, and impure silicon shows several discontinuities in resistance, with the result that silicon shows no minimum at ordinary temperatures On the other hand, Gudden* is inclined to the view that no pure substance is ever a semi-conductor. This view is supported by the superconductivity of titanium and by the fact that a positive temperature coefficient has been found for silicon.† Recent measurements by Meissner‡ did not confirm the metallic character of silicon, though this is almost certainly due to the presence of oxygen in his single crystal From the experimental side, therefore, the existence or non-existence of semi-conductors remains an open question, and neither the measurements of specific heat nor those of susceptibility are sufficiently accurate to supply additional evidence. Theoretically there is no reason why semi-conductors should not exist, the main difference between semi-conductors and insulators being that for the former $\Theta_u$ is so small that the substance has a measurable conductivity at ordinary temperatures, while

---

* "Ergebnisse der Exakten Naturwissenschaften," vol 3, p. 116 (1924).

† H. J. Seemann, 'Phys. Z.,' vol. 28, p. 765 (1927) and vol. 29, p. 94 (1928).

‡ W. Meissner and B. Voigt, 'Ann. Physik,' vol. 7, pp. 761 and 892 (1930).

for the latter $\Theta_u$ is extremely large. Experimentally, however, the only substances which show undoubted semi-conducting properties are very impure, and it may be that they have no intrinsic conductivity. If this is so, the theory would have to be extended to take account of the effect of impurities in increasing the conductivity of poor conductors.* Under the circumstances the value of $\Delta W$ ($= W_2 - W_1$) cannot be fixed, not only because of the doubtful nature of the experimental evidence, but also because the formula for the resistance is not known over the whole range of temperature. However, a minimum resistance often occurs at a few hundred degrees absolute, and this must be due to $\Delta W$ and $kT$ becoming of the same order. $\Delta W$ is therefore usually a few hundredths of a volt, while it may be as much as a few tenths of a volt. This seems quite reasonable and indicates that, though there are many points still to be cleared up, the theory is on the right lines.

This work was carried out at the Institut fur Theoretische Physik, Leipzig. I wish to thank Professor Heisenberg for permitting me to work in his Institute, and I am indebted to him and to Dr Bloch for many interesting discussions and criticisms.

---

* [*Note added in proof*.—It has been found possible to do this to a certain extent, and the results will be published in a further paper.]

# *The Specific Heats of Air, Oxygen, Nitrogen from 20°C. to 370°C.*

By P. S. H. Henry, Coutts Trotter Student, The Laboratory of Physical Chemistry, Cambridge.

(Communicated by E. K. Rideal, F.R.S.—Received June 19, 1931.)

Some time ago a new flow method for comparing the specific heats of gases was described by P. M. S. Blackett, E. K. Rideal, and the author.* It is the purpose of this paper to give an account of further developments of the method, and of the results which have been obtained by it from room temperature up to 370° C. for air, oxygen, nitrogen.

## 1. *The Apparatus.*

The chief improvements in the apparatus over that described previously have been a different construction of the calorimeter, ensuring more uniform temperature surroundings for the tube; potentiometric measurement of the temperature differences; double glands to the pump, eliminating leakage or contamination of the gas; and automatic control of the pumping speed and heating current.

A section through the calorimeter is shown in fig. 1. The fine iron tube AA through which the gas flows has an external diameter of 2 mm. and a wall-thickness of about 0·3 mm. It is surrounded by the massive iron tube BB which has conical holes at the ends to fit the conical steel plugs CC. These are held in place by the screwed collars DD and are electrically insulated from B by thin mica, which, however, allows of easy heat transfer between B and C. The conical plugs in their turn carry the cylindrical plugs EE which are adjusted to a good sliding fit in them, and which fit tightly on to the gas tube AA. The fine constantan wires which, with the tube, form the thermocouples are arranged

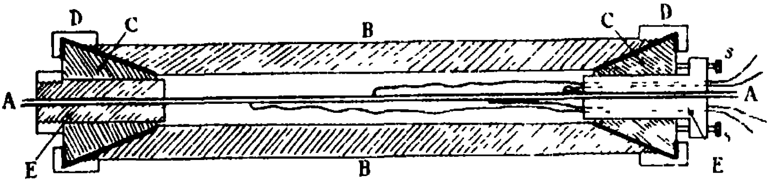

Fig. 1.

---

* Blackett, Henry and Rideal, 'Proc. Roy. Soc.,' A, vol. 126, p. 319 (1930).

as before and pass through holes in one of the plugs E, being insulated by small porcelain tubes. The tube AA and the wires and plugs can be slid out without disturbing anything else. The screws SS serve to adjust the position of the tube and thermocouples to symmetry so that there is no galvanometer deflection when the gas is not flowing. The gas-tube is heated, as before, by passing an alternating electric current from a transformer through it. The whole is placed inside an iron tube-furnace wound with a nichrome strip and well packed with asbestos wool. The temperature of the jacket B is measured by means of an iron-constantan thermocouple which was calibrated by means of the melting points of ice, tin, lead, zinc and aluminium. The cool junctions of all thermocouples are kept in oil in a Dewar flask, whose temperature is measured by means of a mercury thermometer. It was found possible to regulate the temperature of the furnace by hand to within a degree or two. The improvement over the calorimeter described previously lies in the more complete uniformity in temperature of the surroundings of the gas tube, better thermal contact between the ends of the gas tube and the jacket, and increased protection from air currents Also the new calorimeter is of a shape and size to fit into the tube of an electric furnace, and being made of iron instead of copper, can be used up to 400° C

Instead of measuring the thermal e.m.fs. by means of the galvanometer deflections, the greater parts of them are balanced out by means of a potentiometer, and the small residual galvanometer deflections are read. This procedure obviates the necessity for accurate determinations of the galvanometer sensitivity, and renders negligible any errors due to variations in this sensitivity or to non-linearity of the scale. It also enables the galvanometer to be used in a more sensitive state, so that slower rates of gas-flow can be employed. The thermojunctions which measure the difference in temperature between the centre of the tube and the ends are connected straight to the potentiometer; whilst the symmetrical thermojunctions, whose e m.f. may be only one-fortieth of that of the other pair, are connected to the potentiometer through a potential divider. At the start of an experiment the potentiometer is adjusted so that the central temperature difference e.m.f. ($\theta_m$) is as nearly as possible balanced out. The potentiometer is not again touched during the whole experiment, the small variations in central temperature being deduced from the residual galvanometer deflections. The potential divider is then adjusted so that for a given rate of flow the e.m.f. of the symmetrical thermojunctions ($\Theta$) is nearly cancelled out. The potential divider reading, corrected for the residual galvanometer deflections, thus gives directly the ratio $\Theta/\theta_m$ which is the quantity required, for, as is shown in the previous papers (pp. 327–328) the sensitivity, *i.e.*, $\Theta$ divided by the rate of gas flow, is proportional to $\theta_m$ *ceteris paribus*. A reading of $\theta_m$ is taken between every three readings of $\Theta$, which are taken with the gas flow in alternate directions. It will be seen that any slow changes in $\theta_m$ or in the potentiometer current produce no effect on $\Theta/\theta_m$, for they affect both $\Theta$ and $\theta_m$ equally. The sliding contact of the potentiometer is never moved during the whole experiment, so that no variations in its resistance need be feared, nor does the accuracy of the potentiometer affect the results. The potential divider, however, must be accurate.

Since the A.C. mains showed considerable variations in voltage, it was necessary to devise some means of regulating automatically the current which is passed through the gas tube. A fixed solenoid was connected in series with the tube and with the secondary of the transformer, and a piece of soft iron rod was suspended so that it could swing in and out of the solenoid. The whole can be tilted and the iron rod takes up a position in which the pull due to the solenoid balances that due to gravity. If the mains voltage rises the rod is pulled further into the solenoid, and the inductance of the latter is increased, thus partially compensating for the increase in voltage. In practice it was found possible to adjust the instrument so that a variation in voltage of 5 per cent. either way produced a variation in current of only ¼ per cent. The period of the regulator is about half-a-second and it is damped by means of a vane in an oil pot. The current can be varied by varying the tilt.

In order to keep the flow rate constant a differential gear system was constructed as shown in fig. 2, the two bevel wheels A and B being driven in opposite directions by the pump motor and by a Tinsley phonic motor

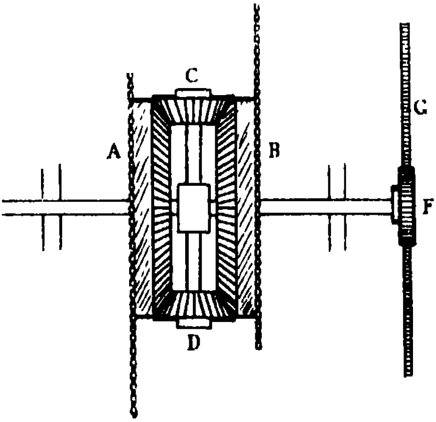

FIG. 2.

respectively. The speed of the latter is maintained constant by means of a tuning fork. A and B rotate loosely on the main axle, and as long as A is driven round at the same speed as B, the cross axle which carries the small bevel wheels C and D remains stationary, but as soon as A gains or loses on B, the cross axle moves round, carrying with it the main axle and the pinion wheel F. This moves the slider of a rheostat in the armature circuit of the driving motor by means of the rack G, and this goes on until the difference in speed is corrected Any difference in speed is reduced to half value in a second or two, which is fast enough, since the calorimeter has a much longer period. Different speeds of pumping are obtained by different gear ratios

With the gas pump described in the previous paper (p 326) it was impossible to prevent a slight leakage in of air when the apparatus was being filled with a new gas by evacuation This was prevented in the present series of experiments by constructing a new pump similar to the first, but provided with double glands. The space between the glands is connected separately to the Hyvac pump during filling and is kept exhausted so that any leakage past the inner gland is outwards and produces no contamination The space is finally filled with the same gas as the rest of the apparatus, and serves as a guard ring to prevent diffusion in of air during an experiment. The glands are packed with asbestos and graphite steam packing and are nearly sufficiently gas tight to serve without the double glands

The pump cylinders are surrounded by a thick layer of cotton wool to obviate quick changes of temperature, and thermocouples are fastened in contact with the outer surfaces of the cylinders and with the inner surfaces of the plungers. Small corrections are applied to the results if the temperature varies during an experiment.

Great care has been taken to avoid stray thermal e.m fs at connections by using stout brass wire to connect brass terminals and by wrapping all external connections in cotton-wool.

## 2. *The Experimental Procedure.*

A complete experiment consists of a comparison of the specific heats of air and another gas, and to this end a run is first done with air, then a run with the other gas, and then again one with air, so as to eliminate as far as possible effects due to any small and slow changes in, *e g.*, temperature distribution in the furnace The deflections obtained in the first and second air runs sometimes differ by as much as 1 per cent., but a few trial experiments in which air was used the whole time showed that these changes were probably slow and progressive, and not dependent upon disturbances due to changing the gas. Hence it is unlikely that errors greater than ½ per cent. at most would be introduced thus, and at present no greater accuracy than this is claimed for the experiment.

Each run with air usually consists of three determinations of the e.m.f. produced by the symmetrical thermocouples, two with a flow rate of about 11 c.c. per minute and one at 22 c.c per minute. The run with the other gas usually comprises three determinations at the slow rate and one at the fast.

Each determination of the e.m.f. involves three strokes of the pump in alternate directions, a reading of the galvanometer being taken towards the end of each stroke. The double galvanometer deflection is obtained by subtracting the second reading from the mean of the first and third, so that slow changes in the galvanometer zero are allowed for Between each determination of the e m.f. from the symmetrical thermocouples ($\Theta$) readings are taken of the e.m.fs. from the couples which give the central temperature difference ($\theta_m$) and from those which indicate the temperature of the pump cylinders and plungers. The e.m fs. corresponding to $\Theta$ and $\theta_m$ are calculated from the settings of the potentiometer and of the potential divider and from the residual galvanometer deflections obtained as above

The potentiometer current is reversed between each stroke of the pump to correspond with the sign of the e m f The sensitivities of the galvanometer in two circuits which measure $\Theta$ and $\theta_m$ are determined at the start of an experiment by noting the galvanometer readings for various settings of the potentiometer

Though the e.m fs are given to the nearest hundredth of a microvolt in the sample set of readings below, it is not claimed that this degree of accuracy was attained in their measurement. The probable error in the measurement of a given e.m.f., as judged from the agreement between successive readings of the galvanometer, was of the order of 1/20th of a microvolt. It will be seen that the method of taking alternate readings with the gas flow in opposite directions eliminates the effect of any but rapidly varying parasitic e m.fs., since the electrical circuit was not disturbed between readings except to reverse the potentiometer current, and any e.m.f at the reversing switch is reduced to about 1/100,000th before it reaches the galvanometer.

The value of $\theta_m$ corresponding to each value of $\Theta$ is taken as the mean of $\theta_m$ values found immediately before and after, and $R\Theta/\theta_m$ is worked out for each value of $\Theta$, where R is the gear ratio employed in the pump drive and is inversely proportional to the flow rate. This is then corrected for variations in the mean pump temperature on the assumption that the mass of gas passing per second is inversely proportional to the absolute temperature, since the pressure in the apparatus is kept constant and equal to the atmospheric pressure. This correction is usually only just appreciable.

Corrections are then applied to the values of $R\Theta/\theta_m$ for the slight curvature of the relation connecting $\Theta/\theta_m$ and the flow rate (see pp. 323 and 349 of the previous communication, where it is shown that it is the *initial* slope of the graph which is proportional to the specific heat) This correction is deduced from the difference between $R\Theta/\theta_m$ for the fast flow rate and for the slow flow rate, obtained from the mean of several experiments, on the assumption that the curvature is due to a cubic term (see the previous papers, *loc cit*) Thus if the fast flow rate is twice the slow, the corrections required to the fast and slow values of $R\Theta/\theta_m$ are 4/3 and 1/3 of their mean difference respectively, and amounted to 0·7 per cent and 0·2 per cent respectively in the case of air. The ratio of the corrected values of $R\Theta/\theta_m$ now gives the ratio of the specific heats at constant pressure of the two gases concerned

The temperature of the calorimeter as a whole, and of the cool junction in the Dewar flask, are noted at the beginning and end of the run with each gas. The former seldom varies more than a degree or two during the course of an experiment.

The gas is changed by evacuating the whole apparatus with a Hyvac pump, shutting off the apparatus from the Hyvac except for the spaces between the glands, waiting for a minute to see that there is no leakage, and finally letting the new gas in slowly, first to the main part of the apparatus and then to the space between the glands

After a run has been done with any gas other than air, a sample is withdrawn for analysis into a modified Haldane apparatus Contamination with air during the process of withdrawal is avoided by evacuating the connection to the analysis apparatus and washing out with the gas to be analysed once or twice. Further details of the analysis are given later.

The probable fortuitous error of a given experiment, as estimated from the differences between the several values of $R\Theta/\theta_m$ obtained in a single day's run, is about ½ per cent at the lower temperatures, and 1 per cent. at the higher temperatures, when conditions were less steady. A somewhat condensed set of readings is given on next page.

Experiment of March 17, 1931. Comparison of Air and Helium at about 350° C

Galvanometer sensitivity in $\theta_m$ circuit = 0·40 cm./$\mu$V

Galvanometer sensitivity in $\Theta$ circuit = 0·59 cm./$\mu$V. (for double deflections).

Potentiometer setting, 320 $\mu$V. (This corresponds to a central temperature difference of about $5\frac{1}{2}$° C.)

Barometer, 761 mm.

| | 1st air run | | He run. | | 2nd air run. | |
|---|---|---|---|---|---|---|
| | ° | ° | ° | ° | ° | ° |
| Furnace temperatures........ | 351 | 350 | 350 | 351 | 351 | 349 |
| Cool junction temperatures .. . | 12·6 | 12·8 | 12·9 | 13·2 | 13·2 | 13·3 |

Gear ratios of 4 : 1 and 2 : 1 correspond to flow rates of 11·3 and 22·6 c.c./min. respectively.

| Gas and gear ratio. | $\theta_m$ deflections. | $\theta_m$ | $\theta_m$ | Mean pump temperature. | $\Theta$ deflections | Residual e.m.f. | Potential divider setting | Potential divider e.m.f. | $\Theta$ | $\Theta$ | Corrected $R\Theta/\theta_m$. |
|---|---|---|---|---|---|---|---|---|---|---|---|
| | cm. | $\mu$V | °C | °C | cm. | $\mu$V | | $\mu$V | $\mu$V | °C | |
| Air 4 : 1 | −0·4 | 319 | 5·50 | 14·4 | −0·15 | −0·25 | 1·41 | 7·80 | 7·55 | 0·130 | 0·0951 |
| Air 2 : 1 | −0·4 | 319 | 5·50 | 14·6 | −0·03 | +0·05 | 1·21 | 15·23 | 15·28 | 0·264 | 0·0962 |
| Air 4 : 1 | −0·3 | 319 | 5·50 | 14·7 | +0·17 | +0·29 | 1·43 | 7·43 | 7·12 | 0·128 | 0·0974 |
| Helium 4 : 1 | −0·3 | 319 | 5·50 | 14·8 | −0·33 | −0·56 | 1·56 | 5·71 | 5·15 | 0·0889 | 0·0650 |
| Helium 2 : 1 | +0·2 | 320 | 5·52 | 15·0 | −0·07 | +0·12 | 1·31 | 10·32 | 10·44 | 0·180 | 0·0656 |
| Helium 4 : 1 | +0·1 | 320 | 5·52 | 15·2 | +0·03 | +0·05 | 1·62 | 5·16 | 5·21 | 0·0899 | 0·0656 |
| Helium 4 : 1 | 0·0 | 320 | 5·52 | 15·3 | −0·05 | −0·08 | 1·61 | 5·24 | 5·16 | 0·0891 | 0·0650 |
| Air 4 : 1 | +0·1 | 320 | 5·52 | 15·3 | +0·02 | +0·03 | 1·42 | 7·62 | 7·65 | 0·132 | 0·0965 |
| Air 2 : 1 | +0·5 | 321 | 5·54 | 15·3 | −0·47 | +0·80 | 1·22 | 14·53 | 15·33 | 0·264 | 0·0963 |
| Air 4 : 1 | +0·8 | 322 | 5·55 | 15·5 | −0·15 | −0·25 | 1·41 | 7·80 | 7·55 | 0·130 | 0·0947 |

The figures in the last column have been corrected for the variations in pump temperature, but not for curvature.

| Gas. | Flow rate | $R\Theta/\theta_m$. | Means | Corrected for curvature | Weighted means. |
|---|---|---|---|---|---|
| | c.c./min. | | | | |
| Air | 11·3 | 0·0951 | 0·0959 | 0·0961 | 0·0964 |
| | | 0·0974 | | | |
| | | 0·0965 | | | |
| | | 0·0947 | | | |
| | 22·6 | 0·0962 | 0·0962 | 0·0960 | |
| | | 0·0963 | | | |
| Helium | 11·3 | 0·0650 | 0·0652 | 0·0652 | 0·0653 |
| | | 0·0656 | | | |
| | | 0·0650 | | | |
| | 22·6 | 0·0656 | 0·0656 | 0·0656 | |

The analysis showed that the helium contained 0·48 per cent. of oxygen. If this came from the water, there will be 0·96 per cent. of nitrogen The specific heat of the impure helium will thus be 5·00 cals /mol °C. Thus at 350° C. we have .—

$$C_p \text{ for air} = 5\cdot00 \times \frac{0\cdot0964}{0\cdot0653} \text{ cals /gm. mol. °C}$$

$$= 7\cdot38 \text{ cals /gm. mol. °C}$$

and

$$C_v \text{ for air} = 5\cdot39 \text{ cals./gm mol. °C. at } 350° \text{ C.}$$

### 3. *The Results.*

(*a*) *Comparison of Air with Argon and Helium.*—The two latter gases serve as the standards, but as they were not available in large quantities, the comparison with air was made so that the latter could be used as a substandard in finding the specific heats of other gases. The air used in all experiments was freed from carbon dioxide by passage through a long soda-lime tube and then dried by means of calcium chloride. It received further drying during the run by the phosphorus pentoxide tubes included in the apparatus The argon and helium were obtained from the British Oxygen Company, and their compositions as given by the Company were argon 99·0 per cent., oxygen 0·4 per cent., nitrogen 0·6 per cent., and helium 98 per cent., neon 2 per cent. The argon was discarded after each run, and a sample was analysed for oxygen by absorption with alkaline pyrogallol, care being taken to obviate errors due to solution of the argon in the reagent. In most cases the oxygen found agreed nearly with the composition given by the Company, but on a few occasions more was found, and this was assumed to be due to admixture of air during the filling process. A correction was applied for the impurities on this assumption. This amounted to 2·4 per cent. in one case (the experiment at 345°), but in all other cases it was less than 1 per cent. The helium was used several times over for economy's sake, and had to be stored over water. The water was boiled under reduced pressure for 5 or 6 hours before it was used, to get rid of dissolved gases. It was impossible to prevent slight contamination of the helium in the later runs, however. This was allowed for by analysing the gas for oxygen before each run, and assuming that the oxygen had come from the water and was accompanied by twice its volume of nitrogen. In five cases no correction was required and in the remaining three the corrections were 0·6 per cent., 1·2 per cent. and 0·8 per cent., for the runs at 348°, 190° and 18° respectively. There was no possibility of air getting in during filling in this case. The values obtained for the molecular heat at constant volume of air, on the assumption that those of argon and helium are equal to 4·97 cals. per degree per gram molecule are shown in fig. 3. It will be seen that the values obtained with argon and helium do not differ by more than the fortuitous error of the measurements in spite of the widely different thermal conductivities of the gases concerned. The conductivities of helium, argon and air at 0° C. are about 34 × $10^{-5}$, 4 × $10^{-5}$, and 5 × $10^{-5}$ units respectively. Moreover, such difference as there is between the specific heat values is in the opposite direction to that which one would expect if the conductivity were to affect the measurements; for argon, having a lower conductivity than helium,

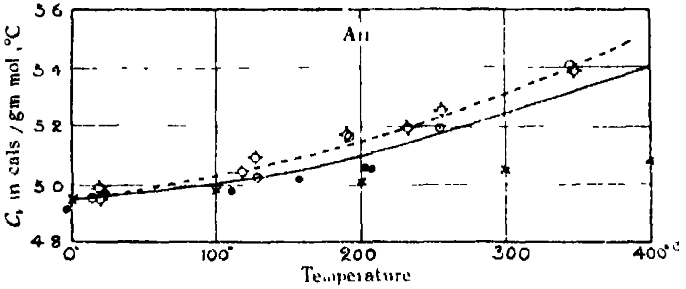

FIG. 3.

♢ by comparison with helium } The author's results
○ by comparison with argon }
× Shilling and Partington's results.
● Eucken and Lüde's results
—— Theoretical curve
- - - - Curve used in calculating $C_v$ for other gases.

would in this case appear to have a lower specific heat, and would thus give a high value for air. A reference to the figure will show that, on the whole, the opposite is the case. This should dispose of any suspicion that the results of the method used depend upon the conductivity of the gas, a criticism which is often levelled at constant flow methods. The dotted line gives the values which have been assumed in calculating the specific heats of nitrogen, oxygen and methane from comparisons of these gases with air. The significance of the full line will be discussed later.

(*b*) *Comparison of Oxygen with Air*.—Four of the oxygen values were obtained with commercial oxygen from a cylinder, and the remaining six with oxygen prepared by the electrolysis of a solution of caustic soda. The commercial oxygen contained 4½ per cent. of nitrogen which was estimated by absorbing the oxygen in alkaline pyrogallol. The correction to the specific heat required on this account varied from zero at room temperature (when the specific heats of oxygen and nitrogen are nearly equal) to 0·3 per cent. at 400° C. The electrolytic oxygen did not contain enough impurity to require a correction. The results are shown in fig. 4.

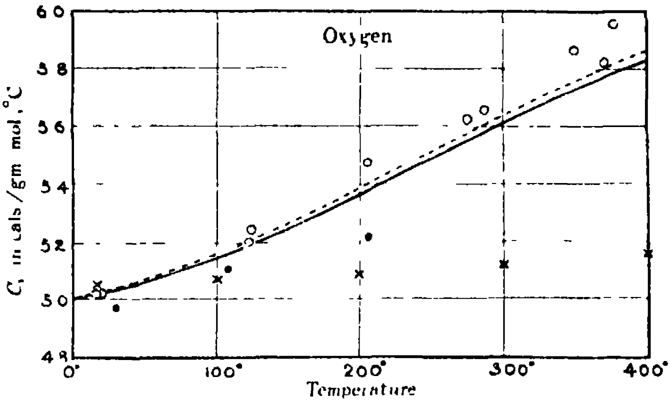

FIG. 4.

○ The author's results.
× Shilling and Partington's results
● Eucken and Lude's results
—— Planck curve using spectroscopic frequency.
- - - - Curve deduced from spectra

(*c*) *Comparison of Nitrogen with Air.*—The nitrogen employed was commercial nitrogen containing 2 per cent. of oxygen, as shown by absorption with alkaline pyrogallol in the Haldane apparatus. This, however, involved a correction of only 0·1 per cent. at the higher temperatures, and none at all below 200° C. The results are shown in fig. 5.

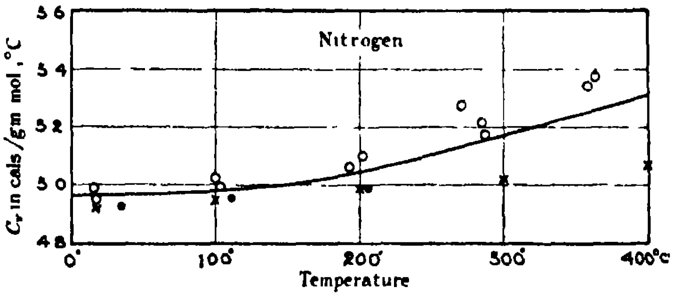

Fig. 5.

○ The author's results.
× Shilling and Partington's results.
● Eucken and Lüde's results.
—— Theoretical curve.

### 4. *Discussion of Results.*

Few experimental values are available for comparison above room temperature, but at room temperatures the specific heats of the simple gases are fairly well established. Values taken from the International Critical Tables are compared below with the author's values at 15° C. in calories per ° C. per gram molecule.

| | I.C.T. | Author. |
|---|---|---|
| Air . . . | 4·95 | 4·97 |
| Nitrogen . . | 4·95 | 4·97 |
| Oxygen . . | 4·98 | 5·02 |

It will be seen that the differences are less than 1 per cent., which is about the degree of accuracy which is claimed for these experiments.

It is also worth noting that the author's oxygen-air and nitrogen-air ratios are compatible with each other within the experimental error. This is shown by the table below, where the smoothed experimental values of $C_v$ for air are compared with those calculated from the smoothed experimental values for oxygen and nitrogen and the assumed value for argon by means of the relation:

$$100\, C_v\,(\text{air}) = 78\cdot 1\, C_{v(N_2)} + 21\cdot 0\, C_{v(O_2)} + 0\cdot 9\, C_{v(A)}.$$

There is no reason to suspect the accuracy of the additive law where, as here, it is known that the corrections to zero pressure for $C_v$ are negligible both for the constituents and for the mixture.

| | 15° C. | 200° C. | 350° C. |
|---|---|---|---|
| $C_v$ for air—found . . . . . . . . . | 4·97 | 5·14 | 5·38 |
| $C_v$ for air—calculated . . | 4·97 | 5·14 | 5·40 |

The only results between room temperatures and 350° C with any claim to accuracy, so far as the author is aware, are a number of sound velocity experiments, in particular those of Shilling and Partington* and of Dixon,† and the adiabatic expansion experiments of Eucken and Lude.‡ These are shown on the diagrams for comparison with the author's results. In the case of nitrogen there are also available the results of Holborn and Austin,§ though these have been subjected to considerable criticism on account of the uncertainty of the amount of heat conducted from their heater to their calorimeter. The two sets of sound velocity experiments gave identical results for air and nitrogen and are not shown separately. It will be seen that the author's results, whilst agreeing with the others at room temperatures, indicate a much more rapid increase of specific heat with temperature The difference rises to as much as 14 per cent for oxygen at 370° C It is worth noting that, whilst the sound velocity experiments agree well together, they are alone in the small values which they indicate for air, nitrogen and oxygen at high temperatures. This may be seen from the following table, which compares the values of $C_v$ for air and nitrogen at 1000° C, obtained by sound velocity methods, by explosion methods, and by the method of mixtures —

| | Nitrogen | Air |
|---|---|---|
| Sound velocity— | | |
| Shilling and Partington . | 5·32 | 5·32 |
| Dixon, Campbell and Parker . | 5·32 | — |

---

* Shilling, 'Phil. Mag.,' vol. 3, p. 273 (1927), Shilling and Partington, 'Phil Mag.,' vol. 6, p. 920 (1928). See also King and Partington, 'Phil Mag,' vol. 9, p. 1020 (1930)

† Dixon, Campbell and Parker, 'Proc. Roy. Soc.,' A. vol 100, p 1 (1921)

‡ Eucken and Lude, 'Z. Phys. Chem.,' B. vol. 5, p. 413 (1929).

§ Holborn and Austin, 'Abh. Phys Tech. Reich,' vol 2, p. 133 (1905). Their results show a value of 4 59 cals./gm mol ° C. for nitrogen at 0° C., which is recognised as being about 7 per cent. too low, so that it does not seem worth while comparing their absolute values with the others. It may be noted, however, that they obtained a value for the temperature coefficient much in excess of that indicated by the sound-velocity experiments.

| | Nitrogen. | Air. |
|---|---|---|
| Explosion— | | |
| Pier,[*] recalculated by Siegel[†] . . | 5·81 | — |
| Womersley[‡] . . . | — | 6·00 |
| Mixtures— | | |
| Holborn and Austin[§] . . . | 5·65 | — |

The values of $C_v$ for the explosion and mixture methods given above were obtained by applying the relation

$$C_v = \frac{d}{dt}(t \, . \, \bar{C}_v)$$

to the values of the mean specific heats between temperatures 0 and $t$ given by the authors quoted. It may be pointed out that the sound velocity method suffers from two considerable difficulties, these being the uncertainty of the tube correction,[‖] which may amount to a considerable percentage on the specific heat, and the accuracy with which the temperature of the gas must be measured. This latter necessity is due to the fact that the velocity of sound varies as the square root of the absolute temperature if the ratio of the specific heats remains constant. Now an error of 1 per cent. in the velocity produces an error of about 7 per cent. in $C_v$ in the case of air so that the mean temperature of the gas in that part of the sounding tube used in the measurements must be found with a percentage accuracy at least three or four times that desired for $C_v$. With tubes over a metre in length whose ends have to be kept cool this must be a matter of considerable difficulty, and it does not seem to the author that the method of assuming the temperature of the piston head to be that of the gas, which was adopted by Shilling and Partington, is sufficiently accurate.

The full lines shown in the diagrams are the values for the specific heats deduced from spectroscopic data on the assumption that the rotational specific heats have their "classical" values and that the vibrational specific heats are independent of the rotation, and are given by Planck terms using the spectroscopic frequencies. Thus for oxygen and nitrogen the curves are given by

---

[*] Pier, 'Z Phys. Chem.,' vol. 66, p. 759 (1909); 'Elektrochem.,' vol. 15, p. 536 (1909) and vol. 16, p. 897 (1910).

[†] Siegel, 'Z. Phys. Chem.,' vol. 87, p. 641 (1914).

[‡] Womersley, 'Proc. Roy. Soc.,' A, vol. 100, p. 483 (1921).

[§] Holborn and Austin, 'Abh. Phys. Tech. Reich.,' vol. 2, p. 133 (1905).

[‖] See Henry, 'Proc. Phys. Soc.,' vol. 43, p. 340 (1931).

$$C_v = \frac{5}{2} R + R \frac{x^2 e^x}{(e^x - 1)^2}$$

where

$$x = \frac{hc\omega_0}{kT}$$

and $\omega_0$, the vibration frequency of the molecule in wave numbers for small amplitudes of vibration, is taken as 1565 for oxygen and 2345 for nitrogen.* The curve for air was calculated from those for oxygen and nitrogen, and the constant value for argon by means of the formula given on p. 502. The dotted line on the diagram for oxygen is the curve calculated direct from the spectroscopic data in the manner used for hydrogen by McCrea,† thus allowing for the stretching effect of the rotation and the anharmonic nature of the vibration. The normal state of the oxygen molecule is the $^3\Sigma$, which fact introduces a multiplicity in the rotational states McCrea showed, however, that it was sufficient to assume that the rotations of the hydrogen molecule were classical, and this approximation will be even more close to the truth with the oxygen molecule with its greater moment of inertia, so that the multiplicity of the rotational states need not trouble us. The calculations were based on the assumption that the vibrational and rotational energy of the molecule is given by

$$\frac{E_n}{hc} = 1565n - 11{\cdot}37n^2 + (1 - 0{\cdot}013n)\,E_{r_0}$$

where $E_{r_0}$ is the energy of rotation which the molecule would have if there were no vibration The anharmonic term was obtained from tables given by Birge,‡ and the stretching term from a paper by Dieke and Babcock.§

Below is given a table of smoothed values of $C_v$ in calories per gram-molecule °C. for air, oxygen and nitrogen They should not be trusted further than about 1 per cent., except at 20° C., where they are probably correct to ½ per cent. at least.

---

* See, *e.g.*, Birge, 'Bul. Nat. Res. Coun. Wash.,' vol. 11, p. 233 (1926)

† McCrea, 'Proc. Camb. Phil Soc.,' vol 24, p 80 (1928)

‡ See, *e.g*, Birge, 'Bul. Nat Res. Coun.,' vol 11, p. 233 (1926).

§ Dieke and Babcock, 'Proc. Nat. Acad. Sci.,' vol 13, p. 670 (1927).

| Temperature. | Air | Oxygen. | Nitrogen |
|---|---|---|---|
| ° | | | |
| 0 | 4·95 | 5·00 | 4·96 |
| 20 | 4·97 | 5·02 | 4·97 |
| 50 | 4·99 | 5·07 | 4·98 |
| 100 | 5·03 | 5·17 | 5·00 |
| 150 | 5·08 | 5·29 | 5·04 |
| 200 | 5·14 | 5·43 | 5·09 |
| 250 | 5·21 | 5·57 | 5·15 |
| 300 | 5·30 | 5·71 | 5·23 |
| 350 | 5·41 | 5·85 | 5·33 |

It is hoped to extend the range and accuracy of these experiments during the next few years by the use of a new and improved calorimeter which is now being constructed of platinum, and by certain modifications in the procedure which will be described later.

Finally, I wish to place on record my thanks to Professor E. K. Rideal and Mr. P. M. S. Blackett for their unfailing encouragement and advice during the course of this work, and to Imperial Chemical Industries, Ltd., for defraying the cost of the apparatus.

---

# *The Sorption of Hydrogen on Copper. Part I.—Adsorption and the Heat of Adsorption.*

By A. F. H. Ward, M.A., Ph D.

(Communicated by E. K Rideal, F.R.S.—Received June 19, 1931 )

## *Introduction.*

A knowledge of the adsorption of gases on solid surfaces and the energy changes resulting is of great value in investigating the structures of surfaces and understanding their catalytic action. Evidence about the energy changes is usually acquired from experimental determinations of the heat of adsorption, but it must be clearly understood that this will only equal the total energy of adsorption if the adsorbed molecule is in the same condition on the surface as it was in the gas phase, which, in general, will not be true. If the molecule is distorted when adsorbed, the energy of adsorption will be the sum of the energy of distortion and the heat liberated. It is probable that an increasing total energy of adsorption will correspond to an increasing heat of adsorption, and that the heat liberated may be taken as a rough indication of the activity of the surface, but it must be wrong to use the two terms as quantitatively equivalent Lennard-Jones and Dent* have calculated the field outside the 100 plane of a crystal of KCl, and estimated the energy of adsorption of argon to be 2000–2500 cals per gram-molecule If it were possible to extend this type of theoretical treatment to the more heterogeneous catalytic surfaces where heats of adsorption are known, the amount of distortion of the adsorbed molecules could be readily determined

Much attention has been directed to the variation of the heat of adsorption of successive amounts of gas For charcoal adsorbents it seems well established that earlier portions of gas produce a greater heat evolution † The evidence as to the initial heats of adsorption with metals is less complete. Foresti‡ found 11,431 cals per gram-molecule for hydrogen on activated nickel, and for CO on copper Beebe§ found an initial high heat of from 20,000 to 30,000 cals. per gram-molecule which fell after about 2–3 c c adsorbed to about 9000 cals. per gram-molecule. Fryling‖ with different copper catalysts found heats varying from 8000 to 30,000 cals. per gram-molecule and for smaller amounts of gas adsorbed than gave the initial high heat, he found in some of his promoted catalysts an initial low heat before the region of high heat. Taylor and Kistiakowsky¶ and Kistiakowsky, Flosdorf and Taylor** repeated the work and also found a low heat, which they explained by saying that the most active portion of the surface has sufficient energy to distort the hydrogen molecule endothermically

It seemed of interest, therefore, to study in some detail the heat evolutions for initial small quantities of adsorbed gas To anticipate the results given in the following pages, it may be stated here that using a sensitive microcalorimeter capable of measuring heats over the range of low pressure, and applying several important corrections which were found to be necessary, no low initial heats were found but in all cases the heat of adsorption of hydrogen was independent of the amount of gas already on the copper surface.

---

* Lennard-Jones and Dent, 'Trans Faraday Soc.,' vol. 24, p. 92 (1927).

† Titoff, 'Z. Phys. Chem.,' vol. 74, p. 641 (1910), Magnus and Kalberer, 'Z. Anorg. Chem.,' vol. 164, p 345 and p 357 (1927); Blench and Garner, 'J. Chem. Soc.,' vol 125, p. 1288 (1924), Ward and Rideal, 'J Chem Soc,' vol. 129, p. 311 (1927).

‡ 'Gazz. Chim. Ital.,' vol. 53, p. 487 (1923).

§ 'J. Phys. Chem.,' vol. 30, p. 1538 (1926)

‖ 'J. Phys. Chem.,' vol. 30, p. 818 (1926).

¶ 'Z. Phys. Chem.,' vol. 125, p. 341 (1927).

** 'J. Amer. Chem. Soc.,' vol. 49, p. 2200 (1927).

### *Experimental.*

*Apparatus.*—Since small traces of foreign substances influence considerably the catalytic activity of a copper surface,* special precautions were taken to ensure the purity of the materials used. Electrolytic copper was dissolved in nitric acid, and the copper nitrate formed heated at 350° to 400° C. to convert to copper oxide. This was reduced by electrolytic hydrogen, re-oxidised with oxygen, again reduced, and the process repeated many times at successively lower temperatures to produce an active copper with a large surface. The sample of copper A underwent five reductions at temperatures from 300° initially to 150° finally, and B eight reductions with the same temperature limits Subsequent baking of the copper *in vacuo* had to be below 150° to avoid sintering the surface. At this low temperature several days' evacuation were necessary before the hot copper was in equilibrium with a gas pressure of $10^{-4}$ mm Hg.

The apparatus used in making adsorption measurements is shown in fig. 1. All joins were glass seals. The copper powder was placed in the tube F. This adsorption vessel had a tube running down the centre with numerous perforations to allow free passage of the gas from the centre to the copper in the annular space between the two tubes The copper was protected from poisoning by mercury vapour by a liquid air trap between it and the mercury vapour diffusion pump, and also a trap of cadmium turnings and a bulb into which sodium had been distilled on to glass wool. This latter was in the system of known volume, and was intended not to increase the dead space unnecessarily Pressure measurements were made by the McLeod gauge E over the lowest range, or the rotating gauge D This was built on the lines described by Hamlin,† but was modified in design so that there were two ranges of pressure measurement Pressures could be measured from 0·001 cm. Hg to 3·0 cm. Hg with an accuracy of about 0·0002 cm. on the lower range and 0·002 on the higher range It was connected to the rest of the apparatus by a special ground-glass joint 2 inches in length which held a perfect vacuum even on rotation. The mechanical strain was taken by metal bearings. The volume was small (50 c c ), it was very quick reading (about 10 seconds sufficed), and pressures could be read directly on the circular scale.

Before the copper was put into the apparatus, the volumes of the various parts were determined. Known volumes of hydrogen from the burette were introduced (through the three-way tap $T_1$) into the vessel A. The level of the mercury was then raised to the mark B, and the pressure read on the scale C.

---

* Hurst and Rideal, 'J. Chem Soc ,' vol 125, p 694 (1924).

† 'J. Amer. Chem. Soc.,' vol. 47, p. 709 (1925).

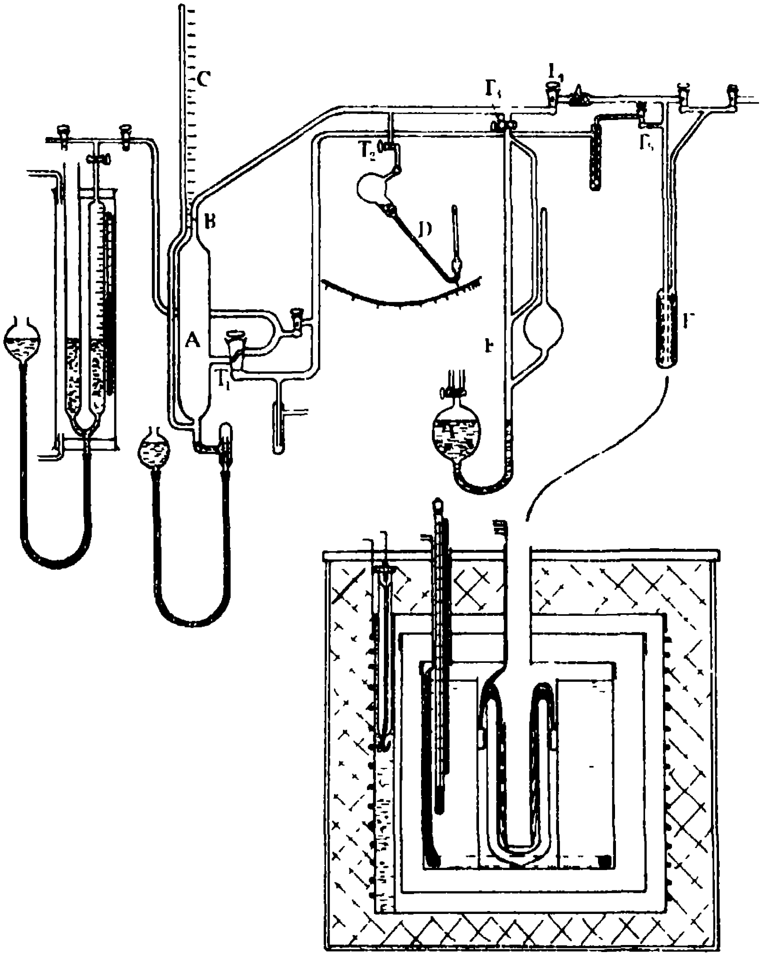

FIG 1

In this way the volumes from B to the taps $T_2$, $T_3$, $T_4$, beyond $T_4$ to the adsorption bulb, and beyond $T_2$ to the rotating gauge were found

The adsorption bulb was then cut down, filled quickly with a known weight of copper and sealed on again without altering the volume. A final treatment with hydrogen *in situ* at 150° C. reduced any copper oxide formed during the transfer. Previously the density of the copper had been determined by opening under water specimens sealed in glass after a prior exhaustion with a diffusion pump for several hours, the copper having been heated at 150° during the process of exhaustion. A value of 8·40 gm. per cubic centimetre was taken as the mean of four experiments

The volume occupied by the copper was therefore known, and consequently the volume of the dead space This volume has usually been calibrated with nitrogen, on the assumption that the adsorption of this is negligible. But experiments made here with nitrogen indicate a slight though measurable adsorption, so it appears preferable to use the absolute method

When the copper had been outgassed at 150° C. for several days, hydrogen was let into the apparatus from the mark B to the taps $T_3$ and $T_4$, and the pressure measured on the rotating gauge The tap $T_4$ was then opened and the hydrogen allowed to come into contact with the copper There was an immediate pressure fall which, owing to the adsorption, was greater than that calculated from the known volumes By equating the sum of the values of PV/T for the various parts of the system before and after the expansion of the gas, the excess gas which apparently occupied no volume in the adsorption bulb was found and hence the amount of adsorbed gas was calculated. After one adsorption, $T_4$ was closed and more gas introduced into the space between B and $T_4$. This in turn was expanded into the adsorption vessel and the process continued till a sufficient pressure was reached.

### *Measurement of Heats*

The heats of adsorption were measured by a microcalorimeter (shown in fig 1) which was mounted on a platform so that it could be raised to surround the adsorption bulb This made close sliding contact with a copper tube (enclosed in a Dewar flask) to whose outer surface were attached the junctions of 31 iron-constantan thermocouples, tied firmly to give good thermal connection, but electrically insulated from the tube and from each other by oiled silk coated with shellac. The other set of junctions of the thermocouples was kept at a constant temperature by being held in holes in a ring of brass in a thermostat. The thermocouples were connected in series with a sensitive moving coil galvanometer, whose readings were plotted against time. The heat evolution corresponding to an adsorption of gas was found from the rise in temperature of the system inside the Dewar flask, making allowance for the cooling correction. The apparatus was calibrated electrically by passing known heating currents. This calorimeter could detect a heat evolution of 0·0005 calories, and with a water equivalent of about 50 gm. this was equivalent to a temperature elevation of 0·00001° C. To get reliable results, the thermostat controlling the temperature of the cold junctions of the thermocouple had to be constant at least to within this amount. The apparatus used was the thermostat with multiple walls, designed by Professor Tian, of Marseilles* (for whose advice on many details in the construction of the microcalorimeter I am very grateful), which was found to have a constancy of rather better than two-millionths of a degree centigrade. A more detailed account of the construction, calibration and method of using this microcalorimeter has already been published.†

### *Heat of Compression of Gas.*

In calibration experiments, with no copper in the adsorption tube, heat was evolved when gas entered the tube, and a corresponding cooling occurred on decreasing the pressure. Both hydrogen and nitrogen were used, and it was found that the heat liberated was proportional to the increase in pressure. In fig. 2 the total heat evolution is plotted against the gas pressure and a straight line obtained with the same slope for both hydrogen and nitrogen. On decreasing the pressure and removing the gas, exactly the reverse process

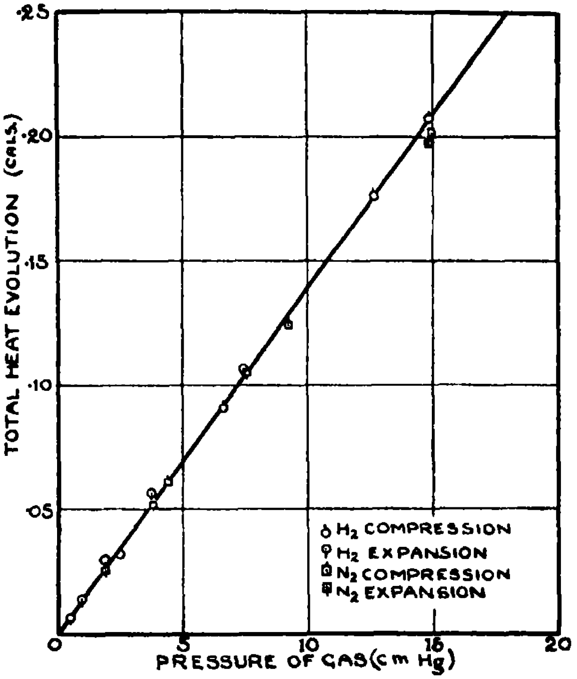

Fig. 2.

---

* 'J. Chim. Phys.,' vol. 20, p. 132 (1923).

† Ward, 'Proc. Camb. Phil. Soc.,' vol. 26, p. 278 (1930).

occurred, and the points for the cooling lie on the same line down to the origin. This linear relationship can be explained if the gas is assumed to be compressed adiabatically by the onrushing stream of gas behind, and the heat produced communicated to the calorimeter. The heat liberated in that part of the system inside the calorimeter only will be detected. On integrating $-pdv$ for the continually increasing amount of gas in the adsorption tube, it is found that for an increase in pressure from $p_1$ to $p_2$,

$$\text{Heat liberated} = 0\cdot000350\ (p_2 - p_1) \text{ cals. per cubic centimetre.}$$

The value found experimentally was 0·000321 cals. per cubic centimetre. This explanation of the heat evolution is probably correct, for, as soon as the maximum temperature was reached, cooling occurred at first more rapidly than would be expected for the exhausted bulb. This was evidently due to an extra loss of heat by conduction through the gas, as the effect was much more marked with hydrogen (which has a high conductivity) than with nitrogen. Similarly, an excess conduction of heat into the system occurred after a cooling by expansion, but on evacuating to zero pressure the heating rate was normal, as there was no gas to conduct the heat. In all cases, the higher the pressure, the more conduction through the gas.

The correction to the heats of adsorption made necessary by this heat of compression was only a small fraction at low pressures where the gas adsorbed might be large compared with the amount in the gas phase, but at higher pressures where the slope of the adsorption isotherm was not so great it was very important.

### *Solution.*

When the hydrogen had been expanded into the chamber containing the copper, the pressure did not remain at the value to which it fell initially, but continued to decrease. It seemed evident that after adsorption on the surface, the hydrogen dissolved in the copper. The simultaneous existence of adsorption and solution has also been noted for hydrogen and charcoal by McBain.* Sameshima† also found solution. McBain used the word "sorption" as an inclusive term for all the ways in which the gas was removed by the solid. "Adsorption" referred only to the gas on the surface, and "absorption" or solution to the gas inside the solid. This nomenclature will be used here.

When sorption had continued for some time, the gas pressure was suddenly reduced. This caused an immediate decrease in the amount of gas sorbed, as the amount of adsorbed gas on the surface fell to the value in equilibrium with the lower gas pressure. The layer of solid just under the surface was now supersaturated with gas, so some of this would diffuse into the still unsaturated interior, and some escape into the gas phase. A small gradual decrease in sorption was therefore found to follow the immediate surface desorption. As gas continued to diffuse into the interior of the copper, the layer under the surface would become unsaturated, and more gas would be taken up from the gas phase. This is shown in fig. 3, where the total sorption and the pressure are plotted against time. It is seen that, in spite of frequent desorptions by pressure reduction, the sorption continued to increase, but with small temporary decreases after every desorption. At room temperatures the copper continued to take up gas for several months.

---

* 'Phil. Mag.,' vol. 18, p. 916 (1909).

† 'Bull. Chem. Soc. Jap.,' vol. 2, p. 1 (1927).

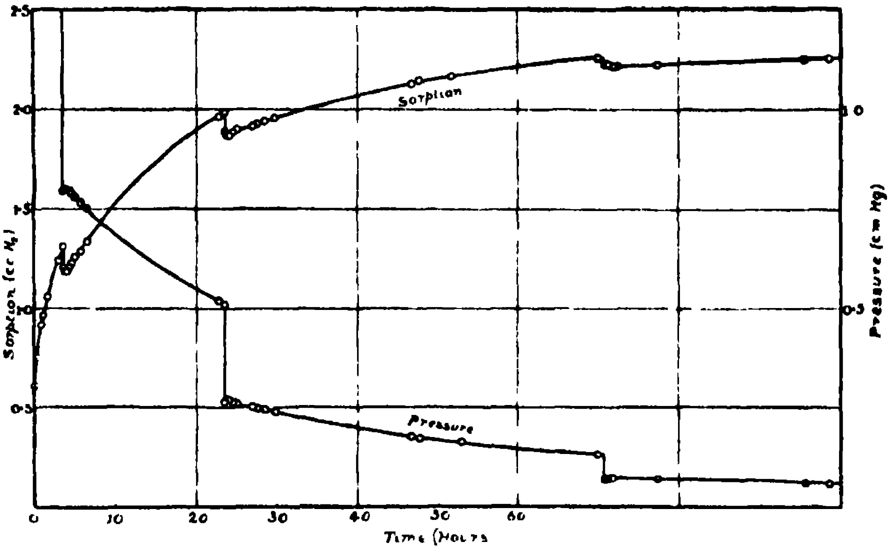

FIG. 3

It has been suggested by Taylor* that the slow sorption occurring over long periods is really a continuation of the adsorption process, which he suggests may be much slower than has previously been supposed. But in the paper following this, the investigation in greater detail of the slow sorption over a wide range of temperatures and pressures makes it quite certain that it is solution which is occurring, and gives ample support to the views expressed above.

---

* 'J. Amer. Chem. Soc.,' vol. 53, p. 578 (1931).

### *The Adsorption Isotherm.*

On account of the great difference in speed between adsorption and absorption, the two processes could be separated, and the increase on the surface only found for any increase in pressure. Thus the true adsorption isotherm could be determined. The total amount of gas on the surface was not, however, given simply by the sum of the amounts adsorbed instantaneously, since between each inlet of gas some was dissolved with an accompanying pressure fall in the system. As the pressure fell, the amount of gas in equilibrium with it on the surface also decreased, and this decrease could be read from the isotherm and subtracted from the next instantaneous adsorption to give the true increase on the surface since the previous reading. The method of making this calculation is shown in the following table

Table I.

| Experiment. | Pressure immediately after adsorption in cm Hg | Gas adsorbed immediately (= A) in c.c | Decrease in gas on surface since previous adsorption (= *d*) | A − *d* | Sum of (A−*d*) equals amount on surface in c.c. |
|---|---|---|---|---|---|
| 1 | 0·019 | 0·042 | — | 0·042 | 0·042 |
| 2 | 0·066 | 0·124 | 0·028 | 0·096 | 0·138 |
| 3 | 0·110 | 0·063 | 0·030 | 0·033 | 0·171 |
| 4 | 0·0965 | 0·162 | 0·170 | −0·008 | 0·163 |
| 5 | 0·265 | 0·100 | 0·007 | 0·093 | 0·256 |
| 6 | 0·750 | 0·160 | 0·005 | 0·155 | 0·411 |
| 7 | 0·555 | 0·140 | 0·180 | −0·040 | 0·371 |
| 8 | 1·195 | 0·140 | 0·040 | 0·100 | 0·471 |
| 9 | 1·755 | 0·080 | 0·001 | 0·079 | 0·550 |
| 10 | 0·815 | −0·125 | 0·004 | −0·129 | 0·421 |
| 11 | 0·405 | −0·100 | 0·000 | −0·100 | 0·321 |
| 12 | 0·190 | −0·070 | −0·030 | −0·100 | 0·221 |
| 13 | 0·101 | −0·060 | 0·000 | −0·060 | 0·161 |

The adsorption isotherm determined by this means is exactly reversible on decreasing the pressure, whereas the sorption which does not come to equilibrium during the time of the experiment does not retrace the same path on lowering the pressure. The method adopted of partitioning the measured sorption into adsorption and absorption is therefore entirely justified.

### *Results.*

A large number of experiments were done on each sample of copper, and the effects that heating the copper had on the adsorption isotherm and the heat of adsorption were investigated. In fig. 4 a series of adsorption isotherms is shown. The curves III and IV were obtained from the copper A, and I and II, where more hydrogen is adsorbed, from the copper B. This latter received more initial oxidations and reductions than A, and would be expected to have a larger area. It was always found that if the copper was baked out at a temperature below 150° C. the temperature of final reduction, any sintering produced by this baking did not cause any reduction in the gas adsorbed. The isotherm III, for example, was found for the copper A in all the experiments, but after a long series of experiments on the rate of diffusion of hydrogen at temperatures up to 200°, involving about 90 hours' baking between 150° and 200°, the isotherm IV was obtained. During experiments with the copper B, the tube cracked and the copper had to be transferred to another. The reduction and baking made necessary by this caused the change in the isotherm from I to II.

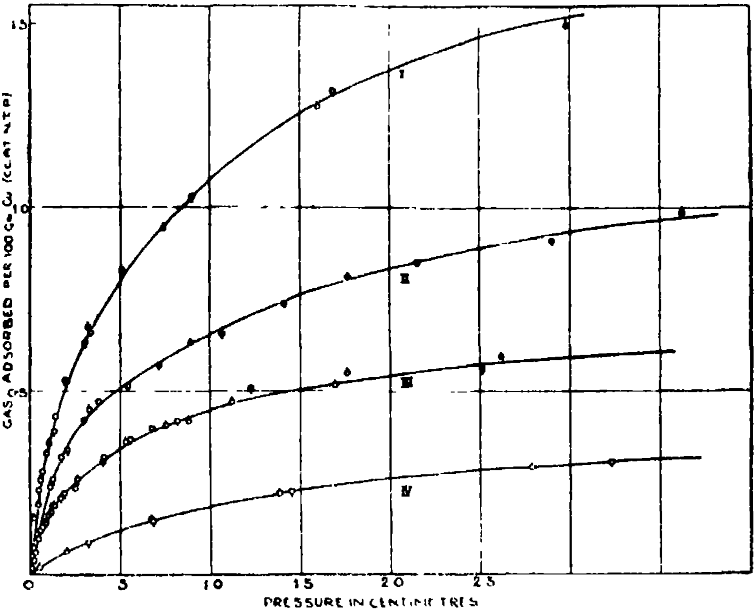

Fig. 4.

In most cases, both heats of adsorption and desorption were measured and were found to agree. In Table II the readings are shown for a typical experiment.

The results for all the experiments are collected in fig. 5, where the sums of the various heats are plotted against the sums of the amounts of gas adsorbed. It is seen that in all cases straight lines are obtained, which means that the

Table II.

| Experiment. | Pressure in cm Hg | c c $H_2$ adsorbed instantaneously per 100 gm Cu | Sum of gas adsorbed instantaneously | Heat evolved in cals | Heat of compression of gas | Corrected heat per 57 gm. Cu. | Heat per 100 gm Cu. | Sum of heats per 100 gm Cu. |
|---|---|---|---|---|---|---|---|---|
| 1 | 0 105 | 0 239 | 0 239 | 0 0510 | 0 0011 | 0 0499 | 0 0875 | 0 0875 |
| 2 | 0 325 | 0 320 | 0 559 | 0 0735 | 0 0028 | 0 0707 | 0 1240 | 0·2115 |
| 3 | 0 890 | 0 202 | 0 761 | 0 0540 | 0 0060 | 0 0480 | 0 0842 | 0 2957 |
| 4 | 1·765 | 0·180 | 0 941 | 0 0465 | 0 0091 | 0 0374 | 0 0656 | 0 3613 |
| 5 | 3 62 | 0 180 | 1 121 | 0 0600 | 0 0190 | 0 0410 | 0 0720 | 0 4333 |
| 6 | 7 45 | 0 160 | 1·281 | 0 0750 | 0 0390 | 0 0360 | 0 0632 | 0 4965 |
| 7 | 20·48 | 0 190 | 1 471 | 0 1725 | 0·1320 | 0 0405 | 0 0710 | 0 5675 |
| 8 | 9 58 | −0 170 | 1 300 | −0 1500 | −0 1110 | −0 0390 | - 0 0684 | 0 4991 |
| 9 | 4 51 | −0 140 | 1 160 | 0 0795 | −0 0510 | −0 0285 | −0 0500 | 0 4491 |
| 10 | 2 15 | −0 165 | 0 995 | −0 0585 | −0 0240 | 0 0345 | −0 0605 | 0 3886 |
| 11 | 1 065 | −0 195 | 0 800 | −0 0585 | −0 0110 | −0 0475 | −0 0835 | 0 3051 |
| 12 | 0 540 | −0 141 | 0 659 | - 0 0375 | −0 0053 | −0 0322 | −0 0565 | 0 2486 |
| 13 | 0 295 | −0 095 | 0 564 | -9 0240 | −0 0025 | −0 0215 | −0 0377 | 0 2109 |
| 14 | 0 170 | -0 100 | 0 464 | −0 0255 | - 0 0013 | −0 0232 | −0 0407 | 0 1702 |

heat of adsorption of hydrogen was independent of the concentration already on the surface. The general tendency was for the heat to fall from one experiment to the next, and that this is to be attributed to the baking out between runs and not to any "ageing" effect of the copper is shown by one experiment (curve No. I) where the adsorption and desorption were continued for several weeks and the heat (32,900 cals. per gram-molecule) remained constant.

In the first experiment on the copper A the meaning of the solution effect had not been realised, and insufficient pressure readings were taken to give the instantaneous adsorptions. The heat cannot, therefore, be found accurately for this, but must lie between the limits 60,000 and 80,000 cals. per gram-molecule. After baking out at 150° C. the heat fell to 32,900 cals. per gram-molecule in the next experiment (curve I, fig. 5). After more baking it was down to 12,000 cals. per gram-molecule and later to 9800 cals. per gram-molecule (curve IV). The copper was next used with nitrogen where the amount of gas adsorbed was extremely small, and the heat measurements equalled the heat of compression of the gas within experimental error. Then, after a long series of experiments on the rates of diffusion of hydrogen, where sintering had the effect of lowering the isotherm to curve IV, fig. 4, no further change in the heat of adsorption was found, which stayed at 9800 cals. per gram-molecule.

With the copper B, the decrease in the heats from one experiment to the next was also found, though the first heat measured was not as high as with A.

At first the heat of adsorption of hydrogen on B was 12,750 cals. per gram-molecule (curve II, fig. 5). After baking at 150° C. this fell to 11,900 cals per gram-molecule (curve III, fig. 5) and later to 8620 cals. per gram-molecule (curve V, fig. 5). Another baking failed to bring it any lower, and the heats still fit curve V.

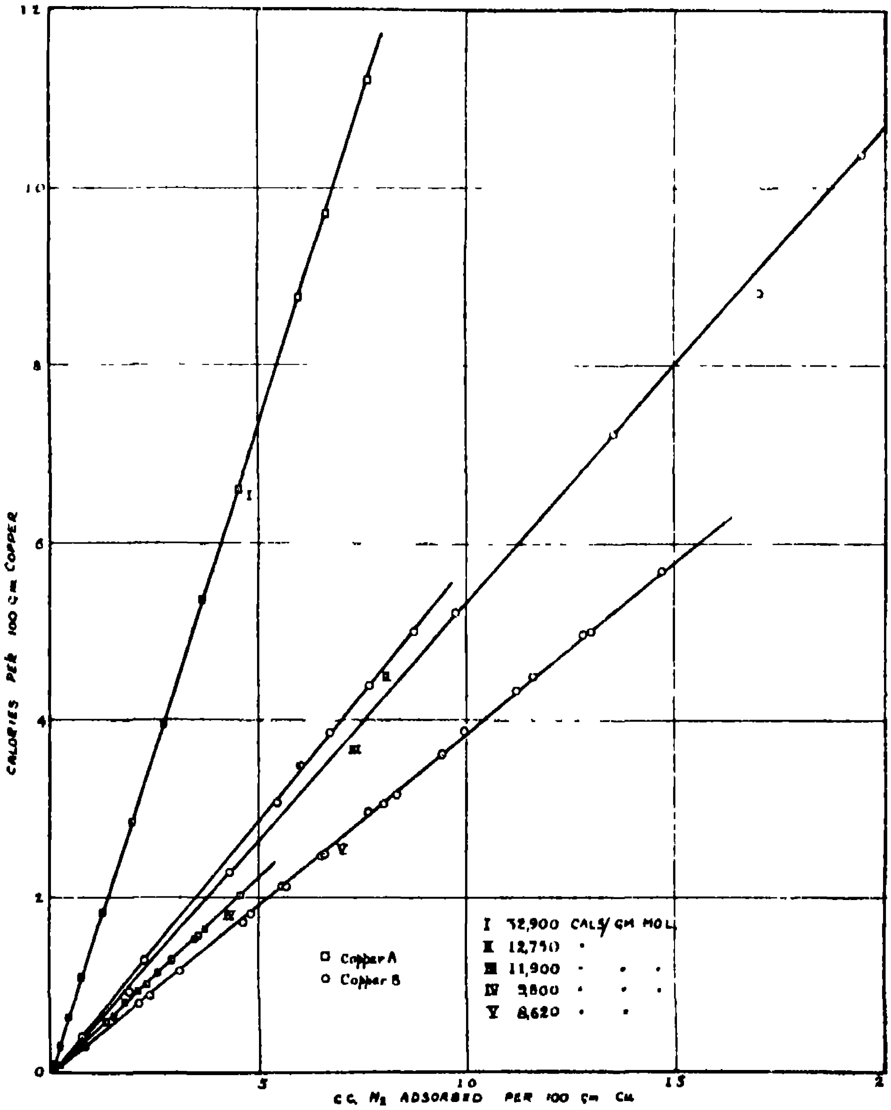

FIG 5

### *Discussion*

As a result of its method of preparation, the copper surface is not uniform and plane but contains many irregularities. The experiments of Valeton,* Niggli,* and Tertsch* on the rates of growth of crystal faces have shown that different energies are associated with different crystal faces. Higher energies are also associated with edges.† It is therefore to be expected that different parts of the copper surface will have different energies, and a simple picture of this is given by Taylor‡ who pictures groups of unsaturated metal atoms raised above the level of the surface. In general, any surface atom will have excess potential energy if it can liberate energy in being brought down to a stable position in the lattice. A study of the catalysis of the electrode position of hydrogen by various activated cathodes has shown§ that the principal effect of activation by oxidation and reduction was to increase the surface area, but that at the same time an increase in catalytic activity of the surface was produced, which decreased with time, probably due to sintering.

The effect of poisons on decreasing rates of catalysis without substantially decreasing adsorption has been attributed to poisoning the "active patches." In cases where high initial heats of adsorption are found, the gas has been supposed to be adsorbed first on the "active patches."

Since in the present work a constant heat is found throughout any one experiment, but falling steadily after each baking to a final minimum value, the effect of the heterogeneity of the surface must be regarded in a slightly different way. The question is to what extent can the potential energy of the whole surface be raised by spots of high energy. Obviously, if the Langmuir mechanism of adsorption and a rigid surface are postulated, the points of high energy will remain localised. The phenomenon of lateral diffusion of gas over the solid surface supplies an explanation of how the energy of the surface can be distributed.

Movement of substances along the surfaces of crystals of the same material was shown by Volmer and Adhikari‖ for benzophenone and by Volmer and Estermann¶ for mercury. Similarly Volmer and Adhikari** showed that benzophenone could diffuse along a glass surface, and Moll* found the same thing for phthalic anhydride, cumarin and diphenylmethane. For gas adsorbed on a nickel surface, Davisson and Germer† found the gas to occupy definite positions on the nickel surface at room temperature, but at 150° C. the gas moved about. It is probable that at low temperatures movement also occurs, but the mean life of the gas in the positions of minimum energy is large compared with the time of movement from one to another. The work of Wilkins‡ on the oxidation of copper at high pressures gives definite evidence for lateral diffusion of oxygen on the copper oxide surface. It is shown by Wilkins and Ward,§ who discuss the complete evidence for the lateral diffusion of gases, that the temperature coefficient of the adsorption maximum can be explained most accurately if lateral diffusion occurs.

---

* Valeton, 'Phys. Rev.,' vol. 21, p. 106 (1920); Niggli, 'Z. Anorg Chem.,' vol. 110, p 55 (1920); Tertsch, 'Z. Anorg. Chem.,' vol. 136, p. 205 (1924).

† Lennard-Jones and Taylor, 'Proc. Roy. Soc.,' A, vol. 102, p. 496 (1925).

‡ 'J. Phys. Chem.,' vol. 30, p 145 (1926).

§ Bowden and Rideal, 'Proc. Roy. Soc.,' A, vol. 120, p. 80 (1928).

‖ 'Z. Physik,' vol. 35, p. 170 (1925).

¶ 'Z. Physik,' vol. 7, p. 13 (1921).

** 'Z. Phys. Chem.,' vol. 119, p. 46 (1926).

It is easy to see that with the copper used lateral diffusion is geometrically possible, for with the maximum amounts of gas on the surface a unimolecular layer is not nearly complete The copper particles were measured under the microscope by comparison with blood corpuscles (diameter = 7 μ). They were extremely irregular in shape and varied in size between 6 μ and 21 μ, most of them having a diameter of 12 μ. In many cases larger particles were formed by the loose adhesion of small ones If a spherical shape is assumed for simplicity in calculation, 100 gm. of copper would have an area of about $6 \times 10^4$ cm.$^2$. It has been shown by Bowden and Rideal|| that a nickel electrode activated by oxidation and reduction had an accessible area 46 times its apparent area, though the appearance was little altered. If a metal sponge is formed, as in the case of platinum black, the area can be increased some thousand times. In the present case, the ratio is probably large on account of the irregular shape of the copper particles and the great amount of oxidation and reduction. As a rough estimate, assume the value of 100 for the ratio in this case (probably an under-estimate), giving $6 \times 10^6$ cm $^2$ as the true area of the copper. If the molecules in 1·2 c.c. of hydrogen (the maximum on the surface) were closely packed, one molecule for every copper atom, they would occupy $4 \cdot 2 \times 10^4$ cm.$^2$ of surface (assuming 3·60 A.U. as the separation of the copper atoms in the lattice), which is very much less than a complete unimolecular layer.

---

* 'Z. Phys. Chem.,' vol. 136, p 183 (1928).

† Davisson and Germer, 'Phys. Rev.,' vol. 30, p 705 (1927), Germer, 'Z. Physik,' vol. 54, p. 408 (1929).

‡ 'Proc. Roy. Soc.,' A, vol 128, p. 407 (1930).

§ 'Z. Phys. Chem.,' vol. 144, p. 259 (1929).

|| 'Proc. Roy. Soc.,' A, vol. 120, p. 80 (1928).

As a gas molecule moves over the surface it will come successively into contact with copper atoms of different potential energy, so that there will be frequent increases and decreases in the energy of the copper-gas complex. If it be assumed that different heats of adsorption correspond to the different total energies of adsorption, there will be a succession of heat evolutions and absorptions for any one gas molecule. The resultant effect of these for all the molecules on the surface will be a complete cancellation and the energy of adsorption for a given amount of gas on the copper surface will depend on some average of the potential energies of all the copper atoms on the surface. On this view it is easy to see why the heat should be reduced as a result of baking the copper. This will naturally sinter the copper and decrease the potential energy of atoms with a high energy, so that the average energy will decrease, and presumably the heat also will decrease.

It is less easy to account satisfactorily for the independence of the heat of adsorption with the amount of gas on the surface. If there is a distribution of all possible energies in the surface atoms the mean life of a gas molecule on the most active copper atoms would be expected to be greater than on the less active ones.* That is, at any given time, the copper atoms with high energy would be covered to a relatively larger extent than the copper atoms of low energy. A high initial heat of adsorption, falling off with increased concentration of gas on the surface would therefore be expected. This is generally found for the adsorption of gases on charcoal. It is conceivable that in some cases this falling off might be too small to be detected.

But this difficulty, caused by assuming the truth of Frenkel's hypothesis of longer life on an atom of solid with higher energy is merely a part of a very grave difficulty. Frenkel† gives the expression

$$\tau = \tau_0 e^{u_0/kT}$$

to show how the mean life of an adsorbed molecule on the surface varies with the energy of adsorption $u_0$. $\tau_0$ is the period of thermal vibration of the adsorbed molecule perpendicular to the surface. $\tau$ is involved in the constant $c_2$ which determines the initial slope of the Langmuir isotherm

$$x = c_1 c_2 p/(1 + c_2 p).$$

Suppose that the energy of the surface were decreased from 20,000 to 10,000 cals. per gram-molecule. Then $e^{u_0/kT}$ would decrease in the ratio

---

* Frenkel, 'Z. Physik.' vol. 26, p. 117 (1924).

† Frenkel, *loc. cit.*, p. 125.

$e^{(20,000 - 10,000)/2 \times 298} = 10^{7 \cdot 3}$ at 25° C. The increase in $\tau_0$ could be assumed proportional to the square of the binding force, so would be four times for this reduction in energy, but this would be negligible compared with the effect of the $e^{u_0/kT}$ term. The constant $c_1$ of the Langmuir isotherm would not be affected, so that the same maximum would eventually be reached, though with an initial slope $10^{7 \cdot 3}$ times less steep. There is no experimental evidence that these enormous variations can be produced in the isotherm by such alterations in the energy of the surface; in fact, the particular experiments described here show that the isotherm remains exactly the same while the heat changes Frenkel's conclusions about the variation of the mean life with the energy, though apparently based on reasonable hypotheses, are therefore not in accord with experiment.

It is hard to see why the Frenkel equation should not be generally applicable. It is possible that if the surface is not rigidly unchanging the energy of each surface atom will be continually varying, and the limiting factor for the mean life of a molecule will not be the energy of the atom but the period of its activation if this is small compared with the mean life of the gas molecule on the surface.

If the mean life of a gas molecule on a copper atom were independent of the activity of the latter, as these results indicate, the constancy of the heat of adsorption with increasing surface concentration (which owed its difficulty of explanation to the assumption of the Frenkel hypothesis) is no longer an inconsistency.

## *Summary.*

(1) The sorption and heats of adsorption of hydrogen on activated copper catalysts have been measured at 25° C for successive additions of gas.

(2) The instantaneous adsorption on the surface was followed by solution which occurred very gradually. The difference in speed allowed these processes to be separated and the true adsorption isotherm found. This was exactly reversible on decreasing the pressure.

(3) After correcting for gas in solution and the heat of compression of the gas, the heats of adsorption and desorption were found to be independent of the concentration of gas on the surface, but decreased after each baking of the copper till they reached a final value of about 9000 cals. per gram-molecule.

(4) The isotherms were not affected by baking below the temperature of preparation of the copper (150° C.), but after sintering above this temperature the amount of gas adsorbed was decreased.

(5) The effect of points of high energy on the activity of the whole surface is discussed.

The work described here was carried out in the Laboratory of Physical Chemistry, Cambridge. It is a pleasure to take this opportunity of thanking Professor E. K Rideal for his valuable suggestions and encouragement throughout the course of the work I wish also to thank Professor T. M. Lowry for his continual interest.

I am very grateful to the following for scholarships and research grants held while this work was being done—Jesus College, Cambridge; the Amy Mary Preston Read Scholarship Fund, and the Department of Scientific and Industrial Research, who provided a special grant to allow me to act as assistant to Professor Rideal. My thanks are also due to the Chemical Society for a grant from the Research Fund, which defrayed a large part of the cost of the apparatus.

# *The Sorption of Hydrogen on Copper. Part* II.—*The Rate of Solution.*

By A. F. H Ward, M.A., Ph.D.

(Communicated by E K. Rideal, F.R.S —Received June 19, 1931.)

## *Introduction.*

Before attention was directed to the adsorption of gases on the surfaces of solids much work was done on the " occlusion " at higher temperatures. Above 400° C. solution usually occurs rapidly,* and because of the decrease in surface by sintering, the adsorption is negligible compared with the absorption. In this paper, investigations on the sorption of hydrogen on copper are described at temperatures intermediate between 25° C. when adsorption is the principal phenomenon and 200° C. when solution has become important. Over this range of temperature both adsorption and absorption have been measured. On bringing the hydrogen into contact with the copper there was always an immediate fall in pressure attributable to adsorption, followed by a slower fall as absorption proceeded. This latter process, of course, became quicker at higher temperatures.

---

* Sieverts, 'Z. Phys. Chem.,' vol. 77, p 591 (1911).

### *Experimental.*

*Apparatus.*—The apparatus used was almost exactly the same as that described in the previous paper. The only difference was that instead of the thermostat at 25° C. a furnace was used. A copper tube about 50 cm. long and 5 cm. in diameter, wound with nichrome wire, had placed inside it, for half its length, a tightly fitting iron tube with thick walls (1 cm.). The adsorption bulb went into this half, and the low conductivity and large thermal capacity of the iron hindered fluctuations in temperature from reaching the bulb. In the lower half of the furnace, where the absence of the iron tube allowed the temperature to vary promptly with a changed heating current, was a thermoregulator bulb containing air, connected by capillary tubing to a U-tube in which mercury made contact with a tungsten point. On the other side of the U-tube a system of the same volume, with a bulb immersed in a thermostat, counteracted the effect of alterations of room temperature. An extra U-tube of mercury enclosed nitrogen around the spark gap to prevent dirtying the mercury surface by oxidation. With this arrangement the temperature could be kept constant to within half a degree for any length of time. Temperatures were measured by a chromel-alumel thermocouple calibrated at the boiling points of suitable liquids.

### *Results and Discussion.*

Before diffusion into the interior of the copper can occur, the hydrogen must first be adsorbed on the surface. Gas will evaporate from the surface both into the gas phase and into the copper, and at the steady state the concentration on the surface will be maintained by bombardment from the gas phase. Since the rate of attaining absorption equilibrium is extremely slow compared with that for adsorption, for any gas pressure the surface concentration will be constant and equal to the value it would have when the interior was saturated.

These conditions are similar to those found by Wilkins* for the oxidation of copper at pressures above 10 mm. Hg He showed that when the rate of diffusion of oxygen through the protective cuprous oxide layer was the factor controlling the rate of oxidation, the rate was proportional to the amount of gas adsorbed on the surface. This has been tested here for the rates of diffusion, and is found to hold for the complete range of pressures and temperatures investigated.

At equilibrium the rate of diffusion of gas from the surface into the interior

---

* 'Proc. Roy. Soc.,' A, vol. 128, p. 407 (1930).

(proportional to the surface concentration) will equal the rate in the opposite direction (proportional to the solution concentration). The equilibrium amount of gas in solution should therefore be proportional to the amount on the surface, so an isotherm of the same type should apply to each. Since at ordinary temperatures the solution equilibrium is only reached after several months it was impracticable to test the relation in this way, but measurements were made of the rate of solution at the beginning of the process.

Assume that for any given pressure (and therefore a fixed amount adsorbed on the surface) the maximum concentration in solution is $c_0$. Then at any time before equilibrium is reached, the concentration will decrease from a value $c_0$ at the surface to a smaller value, possibly zero, in the interior. If the rate of diffusion across any plane ($\partial S/\partial t$) is supposed proportional to the concentration gradient ($\partial c/\partial x$), the general differential equation describing the diffusion is

$$\frac{\partial c}{\partial t} = D \cdot \frac{\partial^2 c}{\partial x^2}, \tag{1}$$

where D is the diffusion coefficient. This equation has different solutions depending on the conditions of the diffusion, but if the distance of diffusion be infinite—that is, only such a short time considered that the interior of the metal is still free from dissolved gas—and the concentration is kept constant at $c_0$ at the surface, then

$$c = c_0 \left(1 - \frac{2}{\sqrt{\pi}} \int_0^{t} e^{-u^2}\, du\right), \tag{2}$$

where

From this it can be calculated that the rate of diffusion across an area $a$ inwards from the surface is

$$\left(\frac{\partial S}{\partial t}\right)_{x=0} = ac_0 \cdot \sqrt{\frac{D}{\pi}} \cdot \frac{1}{\sqrt{t}}. \tag{3}$$

This gives the total amount in solution at the time $t$

$$S = 2ac_0\sqrt{Dt/\pi}. \tag{4}$$

At a constant temperature and surface concentration, S is proportional to $\sqrt{t}$. In figs. 1 and 2 these are plotted for various temperatures and pressures and straight lines are obtained initially. Two factors cause a falling away from the straight line. Firstly, as the sorption occurs in a closed system it will be accompanied by a fall in pressure which will cause a decrease in the gas adsorbed on the surface which will in turn produce a slower diffusion rate. This effect should be most marked at low pressures where the amount of gas sorbed is comparable with that in the gas phase and causes a relatively large pressure fall. It is seen in fig. 1 that at 25° C., for example, the graph at the highest pressure, 7·6 cm., remains linear for a longer time than at the lowest

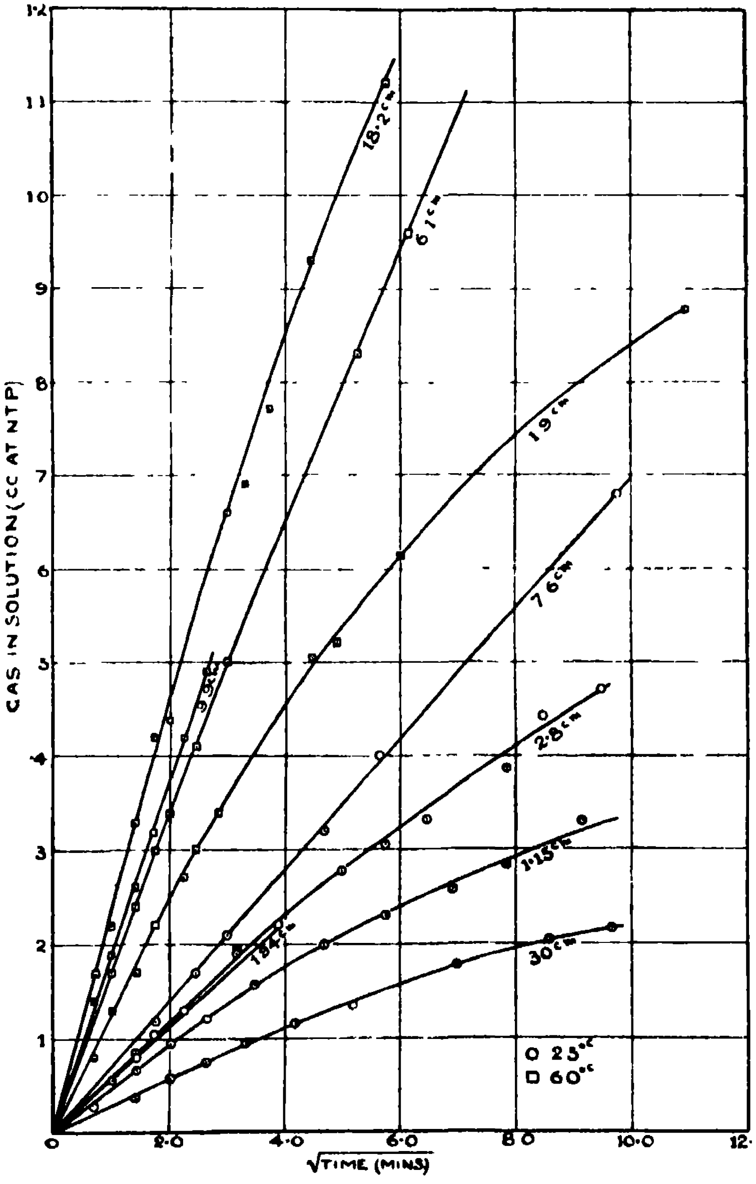

FIG. 1.

pressure, 0·30 cm. Similarly at 60° C. the 18·2 cm. curve is straighter than that at 1·9 cm. pressure. Secondly, since the linear relationship is only true while the interior of the copper is completely free from hydrogen, the graph will fall off as soon as this ceases to be true. The higher the temperature, the more quickly does the hydrogen penetrate completely into the copper, so the sooner does the graph begin to bend. This is best seen by comparing the high pressure curves where the first-mentioned departure from straightness does not occur. About 85° C this begins to be noticeable.

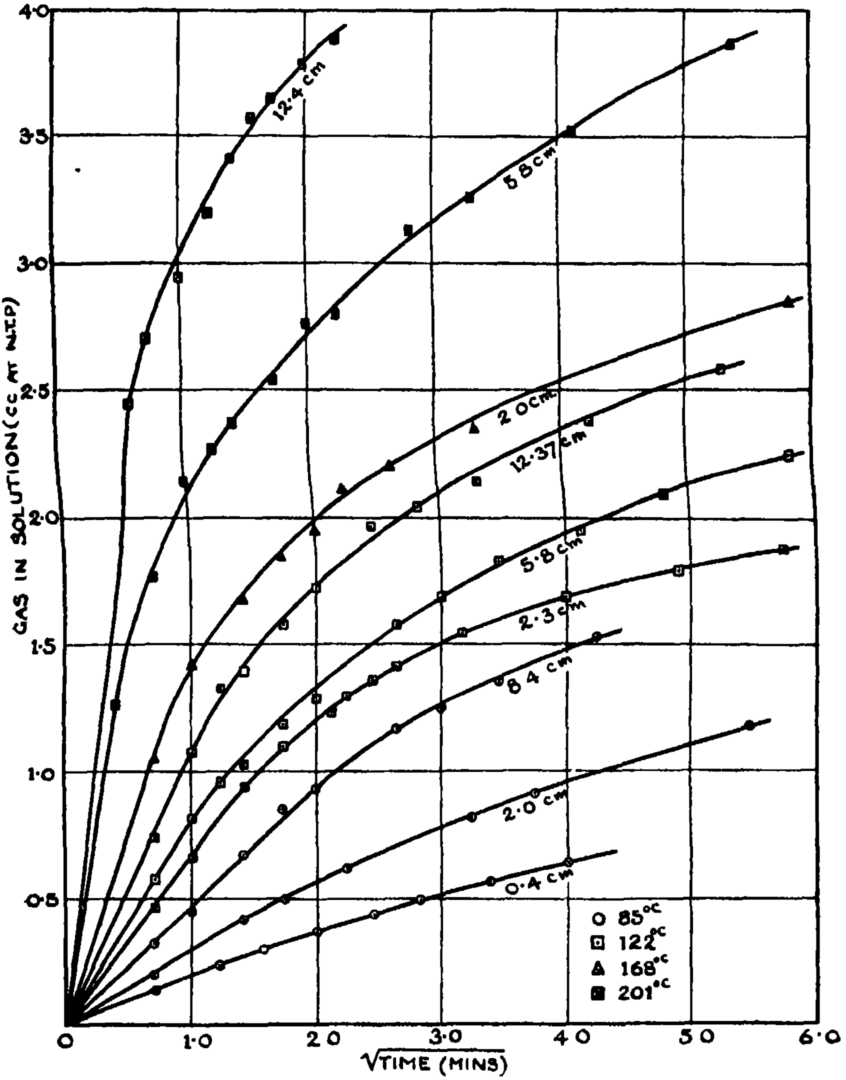

Fig. 2.

At any one temperature, $s/\sqrt{t}$ should be proportional to $c_0$, the saturated solution concentration just inside the surface, and consequently to $q(=kc_0)$, the adsorption concentration. ($k$ should be independent of temperature, since it merely involves the ratio of the rates of diffusion in and out of the copper, as mentioned above, and both these will be affected equally by temperature change.)

The values of $s/\sqrt{t}$ from the initial slopes of the curves in figs. 1 and 2 are shown in Table I, together with $q$, the gas adsorbed on the surface (cubic centimetres $H_2$ per 100 gm. copper). The adsorptions were found by the method described in the previous paper and, of course, become increasingly more difficult to determine and less accurate the higher the temperature on account of the increased rate of diffusion It was not possible to measure the isotherms above 122° C. The isotherms are shown in fig 3 Table I gives the ratios of $s/\sqrt{t}$ to $q$ and for any single temperature they are constant, confirming the theory described above.

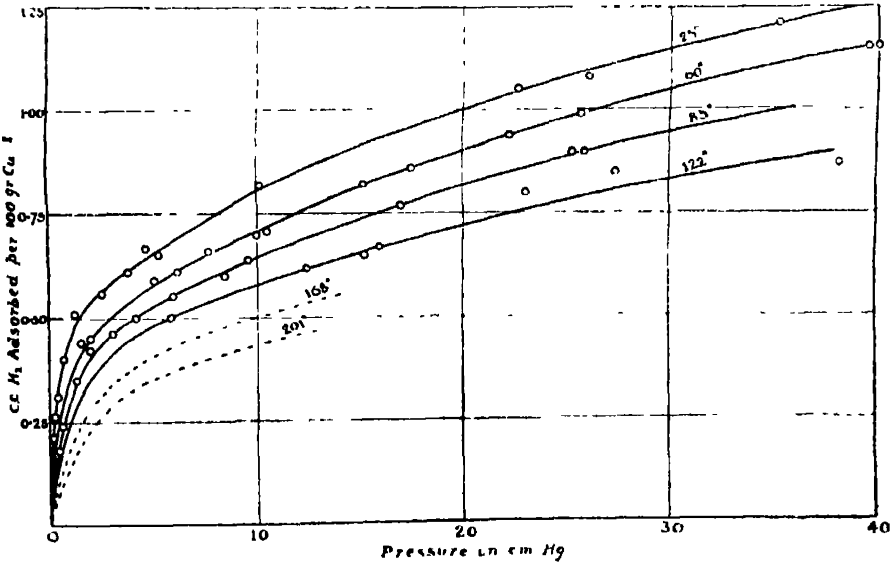

FIG. 3.

Further confirmation of the theory may be obtained from the general solution of the diffusion equation (1). The solution given (equation (4)) is only true while the interior of the metal is still free from gas. If a sphere of radius $a$ is considered, initially free from gas, and a constant surface concentration $c_0$ is kept. the gas will continue to diffuse inwards until the

Table I.

| Temperature | Pressure in cm. Hg | $q$. | $s/\sqrt{t}$ | $\frac{s/\sqrt{t}}{q}$. | Average $\frac{s/\sqrt{t}}{q}$ | $\frac{s^2}{q^2t}$. |
|---|---|---|---|---|---|---|
| °C. | | | | | | |
| 25 | 0·30 | 0·280 | 0·028 | 0·100 | 0·098 | 0·0096 |
| | 1·15 | 0·480 | 0·047 | 0·098 | | |
| | 1·94 | 0·500 | 0·056 | 0·100 | | |
| | 2·8 | 0·595 | 0·059 | 0·099 | | |
| | 7·6 | 0·750 | 0·070 | 0·094 | | |
| 60 | 1·9 | 0·45 | 0·125 | 0·28 | 0·275 | 0·0757 |
| | 6·1 | 0·61 | 0·170 | 0·28 | | |
| | 9·9 | 0·70 | 0·190 | 0·27 | | |
| | 18·2 | 0·87 | 0·235 | 0·27 | | |
| 85 | 0·4 | 0·27 | 0·20 | 0·74 | 0·76 | 0·577 |
| | 2·0 | 0·40 | 0·30 | 0·75 | | |
| | 8·4 | 0·60 | 0·47 | 0·78 | | |
| 122 | 2·3 | 0·38 | 0·67 | 1·76 | 1·71 | 2·925 |
| | 5·8 | 0·50 | 0·82 | 1·64 | | |
| | 12·37 | 0·62 | 1·08 | 1·74 | | |
| 168 | 2·0 | 0·30 | 1·50 | 5·00 | 5·00 | 25·00 |
| 201 | 5·8 | 0·38 | 3·20 | 8·42 | 8·69 | 75·50 |
| | 12·4 | 0·47 | 4·20 | 8·95 | | |

concentration is uniformly $c_0$, at an infinite time The amount of gas in solution after a time $t$ is then given by*

$$s = c_0\left[\tfrac{4}{3}\pi a^3 - \frac{8a^3}{\pi}\sum_1^\infty \frac{1}{n^2}\,e^{-kn^2\pi^2t/a^2}\right],$$

or

$$s = s_0\left[1 - 0\cdot609\sum_1^\infty \frac{1}{n^2}\,e^{-kn^2t}\right]. \qquad (5)$$

The first term of this is, of course, the saturation amount in solution. Although the copper particles absorbing hydrogen are not perfect spheres, an equation of this form would be expected to hold over a longer time than the straight line relationship of equation (4). In fig. 4 the amounts in solution in the experiments at 60° C. are plotted against time. The continuous lines represent the equation (5), where the constants have been given the values $k = 0\cdot0118$ in all cases, and

| | | | |
|---|---|---|---|
| $s_0 =$ 1·14 for solution curve at pressure | | | 1·9 cm. |
| 1·56 | ,, | ,, | 6·1 cm. |
| 1·74 | ,, | ,, | 9·9 cm. |
| 2·15 | ,, | ,, | 18·2 cm. |

---

* For the deduction of this equation I am greatly indebted to Rev. C. D. Waddams, of St. Catharine's College.

These constants were calculated from some experimental points and the derived curves are seen to fit all the points. According to the theory given,

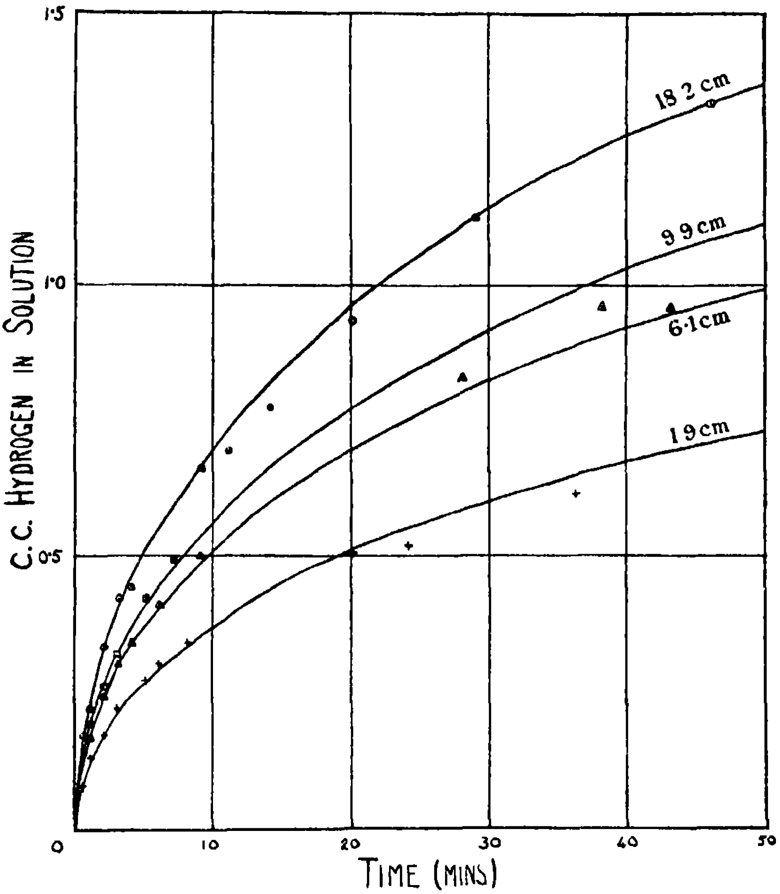

Fig. 4.

the values of $s_0$, the saturation amount in solution, should be proportional to the adsorption on the surface, $q$, given in the third column of Table I. The values obtained for the ratio $s_0/q$ are respectively 2·54, 2·56, 2·49 and 2·48, in agreement with the theory.

More information can be found as to the alteration of the diffusion coefficient with temperature. $s/q\sqrt{t}$ is proportional to $\sqrt{D}$, so the values of $s^2/q^2t$ are proportional to D at the various temperatures. Dunn* found from the rates of oxidation of metals which depended on the diffusion rate of oxygen through the oxide layer that the diffusion coefficient increased with temperature according to

---

* 'Proc. Roy. Soc.,' A, vol. 111, p. 203 (1926).

$$\frac{d \log D}{dT} = \frac{E}{RT^2},$$

where E was the "energy of activation" of the diffusion process. In fig. 5

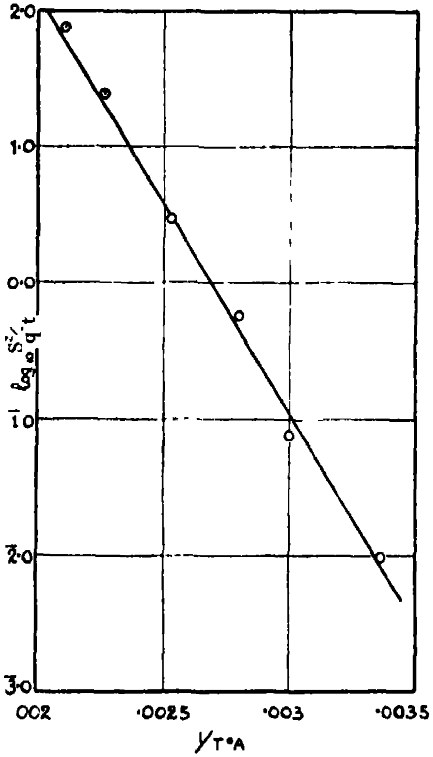

Fig. 5.

og$_{10}$ $s^2/q^2t$ is plotted against 1/T°A and a straight line is obtained whose slope is proportional to E. This gives a value of E = 14,100 cals. per gram-molecule. At the two temperatures 168° and 201° C. the isotherm could not be measured, so the values of the adsorption concentration are taken from the broken curves in fig. 3, which appear probable extrapolations from the others. But compared with the large difference in the rate of diffusion, any error introduced in this way is negligible. The temperature 201° was the highest at which diffusion could be measured, as above this the linear part of the $s/\sqrt{t}$ curve was over in too short a time.

### *The Validity of the usual Explanation of the Variation of Diffusion Rate with Pressure.*

This method of explaining the variation of the diffusion rate with pressure is different from the generally accepted theory Both the solution concentration and the diffusion rate for many gases in metals have been shown to be proportional to the square root of the pressure at high temperatures.* This has been interpreted to mean that the gas is dissociated to atoms inside the metal, so that the partition law for the case when the molecular weight of the solute in one phase is twice its value in the other would hold. Although this might occur with diatomic gases it is less probable for a solution of sulphur dioxide in liquid copper,† where the square root relationship is also found experimentally.

But the value of the heat of activation found here for the diffusion of hydrogen in copper renders dissociation to atoms very unlikely. If this occurred, the heat of activation should be of the order of 90,000 cals. per gram-molecule (the heat of dissociation), instead of which only 14,100 cals. per gram-molecule is found.

But the experimental facts on which the dissociation theory was based are not inconsistent with the theory developed here. It would mean that over the range where diffusion was measured the adsorption isotherm must also be in the form $x = k\sqrt{p}$. Although this is not true over wide ranges at ordinary temperatures for the gas-solid system, it gives practically the same curve as the Langmuir equation if the range of pressures is not too large.

Table II gives the values found by Sieverts (*loc. cit.*) for the solution of hydrogen in nickel at 822° and 923°. These values are calculated both according to a Langmuir equation and a square root equation, and it is seen that both equations fit the experimental figures equally well.

All diffusion experiments which give the square root relationship have been done at high temperatures where the expression $x = k\sqrt{p}$ can also be deduced for the adsorption isotherm as a special case of the Langmuir isotherm if it be assumed that molecules evaporate into the gas phase in pairs Since there is lateral mobility on the surface, a collision of two molecules might result in evaporation. Then the rate of evaporation is proportional to $x^2$, and at

---

* Sieverts, 'Z. Phys. Chem.,' vol. 77, p. 591 (1911); Sieverts and Hagenacker, 'Ber. Deuts. Chem. Ges.,' vol. 42, p. 338 (1909); Richardson, Nicol and Parnell, 'Phil. Mag.,' vol. 8, p. 1 (1904); Johnson and Larose, 'J. Amer. Chem. Soc.,' vol. 46, p. 1377 (1924) and vol. 49, p. 312 (1927); Lombard, 'C. R.,' vol. 177, p 116 (1923).

† Sieverts and Krumbhar, 'Ber. Deuts. Chem. Ges.,' vol. 43, p. 893 (1910).

Table II.

| Temperature. | Pressure in mm Hg. | Gas dissolved (c.c. $H_2$ per 27 gm. Ni) | | |
|---|---|---|---|---|
| | | Observed. | Calculated | |
| | | | $c_0 = \dfrac{0{\cdot}00728p}{1 + 0{\cdot}00199p}$ | $c_0 = 0{\cdot}0794\sqrt{p}$. |
| °C. | | | | |
| 822 | 764 | 2·20 | 2·20 | [2·20] |
| | 660 | 2·08 | 2·08 | 2·04 |
| | 583 | 1·93 | 1·96 | 1·92 |
| | 529 | 1·85 | 1·87 | 1·83 |
| | 447 | 1·71 | 1·72 | 1·68 |
| | 318 | 1·41 | 1·41 | 1·42 |
| | 165 | 1·01 | 0·91 | 1·02 |
| | 132 | 0·88 | 0·76 | 0·92 |
| | | | $c_0 = \dfrac{0{\cdot}00948p}{1 + 0{\cdot}00231p}$ | $c_0 = 0{\cdot}0953\sqrt{p}$. |
| 923 | 764 | 2·63 | 2·62 | [2·63] |
| | 663 | 2·50 | 2·48 | 2·46 |
| | 584 | 2·39 | 2·36 | 2·30 |
| | 448 | 2·06 | 2·09 | 2·02 |
| | 319 | 1·62 | 1·74 | 1·70 |
| | 164 | 1·11 | 1·13 | 1·22 |
| | 129 | 0·98 | 0·95 | 1·08 |

equilibrium equals the rate of condensation which is proportional to $p$ (since the surface is almost entirely bare at the high temperatures considered). This gives the isotherm $x = k\sqrt{p}$. There are not sufficient experimental data on the adsorption of gases at high temperatures to discriminate between different suggested isotherms, but, as the temperature rises and lateral mobility of adsorbed molecules increases, there is a greater probability that evaporation should occur in this way. This would explain the square root relationship obtained by Richardson, Nicol and Parnell* accurately over a wide range of pressures for the diffusion of hydrogen through platinum at high temperatures.

Experiments on the diffusion of a gas into a solid have been carried out in similar conditions to the work described here by Steacie and Johnson† for the case of oxygen and silver. Although they interpreted their results differently, it seemed of interest to calculate from their experimental figures in the same way as has been done for hydrogen and copper in figs. 1 and 2. For the temperature 310° C., when diffusion was measured at several pressures, the amount of oxygen in solution was plotted against the square root of the time, and the resulting curves were found to be straight lines initially similar to figs. 1 and 2, the slopes of which ($s/\sqrt{t}$), on the theory developed here, are proportional to the gas adsorbed on the surface In the following table (III) the ratio of $\sqrt{p}$ to these slopes ($s/\sqrt{t}$) is given in column 3, and the definite absence of constancy shows that the square root isotherm is not obeyed. The fourth column shows the value of $s/\sqrt{t}$ calculated according to the Langmuir expression $\dfrac{0\cdot00048p}{1+0\cdot00383p}$. These agree over the whole range with the experimental figures. These experiments, therefore, give a strong confirmation for the mechanism which has been shown to hold for the diffusion of hydrogen into copper.

---

* 'Phil. Mag.,' vol. 8, p. 1 (1904).

† 'Proc. Roy. Soc.,' A, vol. 112, p. 542 (1926).

Table III.

| Pressure in cm Hg. | $s/\sqrt{t}$ | $\dfrac{\sqrt{p}}{s/\sqrt{t}}$ | Calculated $s/\sqrt{t}$. |
|---|---|---|---|
| 7·55 | 0·0035 | 785 | 0·00352 |
| 13·94 | 0·0064 | 584 | 0·00635 |
| 31·34 | 0·0133 | 421 | 0·0134 |
| 39·55 | 0·0181 | 347 | 0·0165 |
| 55·18 | 0·0215 | 345 | 0·0218 |
| 57·52 | 0·0230 | 329 | 0·0226 |

### *The Nature of the Solution.*

There are two ways in which gas can diffuse into the copper—either through the copper lattice or along grain boundaries. There is much evidence that metals contain minute fissures* and that these extend to the surface.† This is supported by the evidence of Kapitza‡ that the conductivity of bismuth crystals increases on compression. On this view, the gas would move from the surface into the interior by lateral diffusion along the internal surfaces. Various reasons are discussed below why this method is more probable than lattice diffusion at ordinary temperatures.

Copper has a face-centred cubic lattice with side 3·60 A.U.,§ so that a hydrogen molecule of diameter 2·72 A.U. would not pass through easily. But, on raising the temperature, lattice diffusion would become increasingly easier.

---

* Smekal, 'Z. Elektrochem.,' vol. 34, p. 477 (1928).

† Zwicky, 'Proc. Nat. Acad. Sci.,' vol. 15, pp. 253, 816 (1929).

‡ 'Proc. Roy. Soc.,' A, vol. 119, p. 358 (1928).

§ Bragg, 'Phil. Mag.,' vol. 28, p. 355 (1914) and vol. 40, p. 169 (1920).

Dunn's work* on the oxidation of copper showed that the method of diffusion of oxygen through the cuprous oxide layer was different at higher temperatures. On plotting log D against 1/T (*v. supra*) to get the energy of activation, two straight lines were obtained. Below 650° C. the energy was 9200 cals. per gram-molecule and above it was 15,200 cals. per gram-molecule. This has been interpreted by Wilkins (*loc. cit.*) to mean that on the lower range of temperature the diffusion was along the grain boundaries and at higher temperatures lattice diffusion was occurring. The temperatures used in the experiments here were well below this limiting temperature.

Evidence from heats measured during sorption also supports grain boundary diffusion rather than lattice diffusion. If the former is the correct view, the gas, on moving from the part of the surface directly accessible to gas bombardment to the internal surfaces, should not undergo much change of energy. Accordingly as the gas diffuses gradually inwards and more from the gas phase takes its place on the surface, a further heat of adsorption will be slowly liberated. On the other hand, if lattice diffusion occurs, the same energy changes would not be expected. Evidence as to the true heat of solution (in the lattice) is rather meagre, but an approximate value can be calculated from the solution maxima measured by Sieverts† from about 400° C. to the melting point. The solubility of hydrogen in copper increases with the temperature, indicating a negative heat of solution. If the logarithm of the saturation maximum is plotted against the inverse of the absolute temperature, the heat of solution can be found from the slope of the curve. In fig 6 these heats

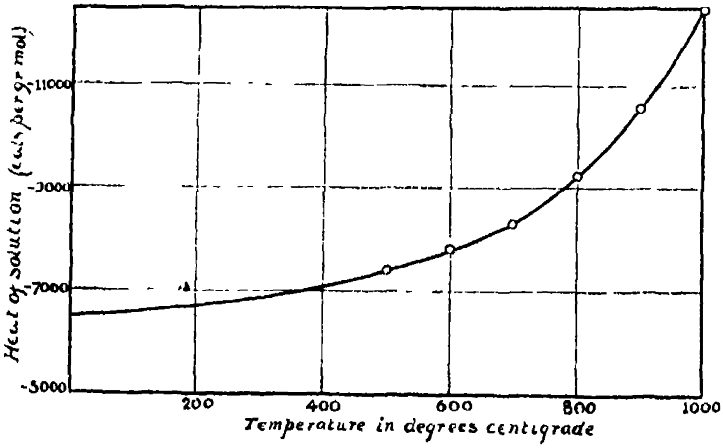

FIG. 6.

---

* 'Proc. Roy. Soc.,' A, vol. 111, p. 203 (1926).

† 'Z. Phys. Chem.,' vol. 77, p. 591 (1911).

are shown at various temperatures and extrapolation to room temperature gives a negative heat of solution of between 6000 and 7000 cals. per gram-molecule.

After the first addition of hydrogen, where adsorption was followed by an appreciable solution, the heat evolution corresponding to the adsorption was followed by a more gradual heat evolution due to the solution. This subsequent heating instead of cooling is further evidence in favour of grain boundary diffusion from the external surface to the internal surfaces of the copper, rather than lattice diffusion. By external surface is meant that part of the surface directly exposed to bombardment from the gas phase This will reach saturation almost instantaneously and gas will then begin to flow away along the surface to those parts which are not directly bombarded by the gas

## *Summary.*

(1) The adsorption of hydrogen on copper and the rates of diffusion into the interior of the metal have been measured at various pressures over a temperature range 25° to 200° C.

(2) It is shown that for any temperature the rate of diffusion into the metal is proportional to the amount of gas adsorbed on the surface The rate of diffusion is therefore related to the gas pressure by the same form of equation as the adsorption isotherm.

(3) The variation of the rate of diffusion with temperature gives an energy of activation for the diffusion process of 14,100 cals. per gram-molecule.

(4) The previously accepted theory that the diffusing molecules are split up into atoms, since diffusion rates are proportional to the square root of the pressure, is criticised and shown to be improbable.

(5) Calculations from the figures of other workers are in agreement with the theory developed here.

(6) Reasons are given why it is probable that grain boundary diffusion is occurring, rather than lattice diffusion.

# *An X-ray Analysis of the Structure of Hexachlorobenzene, using the Fourier Method.*

By KATHLEEN LONSDALE, D.Sc. (London).

(Communicated by Sir William Bragg, F.R.S.—Received June 26, 1931.)

## *Introduction.*

A recent analysis of $C_6(CH_3)_6$* showed that the benzene nucleus in that compound is similar, both in structure and in dimensions, to the plane ring of six carbon atoms, each of diameter 1·42 A., previously known to exist in graphite.†

That being so, it was clear that other benzene compounds should be examined as carefully as possible, to see whether the benzene nucleus is always of the same shape and size. The fully substituted derivatives seemed most likely to give the information desired.

The present paper is concerned with the structure of one such derivative, $C_6Cl_6$, whose crystals are sufficiently large and stable at room temperatures to be examined in detail by the X-ray ionisation spectrometer and other methods.

A few previous measurements are recorded. H. Mark‡ quotes a dissertation by W. Schneefusz (Berlin) giving the dimensions of the unit cell, and the molecular symmetry, for $C_6Cl_6$ and also for $C_6Br_6$. W. G. Plummer§ found approximately the same dimensions, using the powder method, for both these compounds, and comes to similar conclusions concerning the number and symmetry of the molecules. The results obtained, however, were quite inadequate to provide any indication of the detailed structure of the unit cell.

## *Experimental Details.*

The material for the present investigation was very kindly given to me by Professor C. K. Ingold. Slow recrystallisation gave small needle-shaped crystals, extended along the [010] direction, but with good side faces {100} {001} {10$\bar{2}$}, and end faces {11$\bar{1}$}. As recorded by P. Groth|| the (001) is a good cleavage plane and secondary cleavage occurs also on (100) and (10$\bar{2}$), while

---

* K. Lonsdale, 'Proc. Roy. Soc.,' A, vol. 123, p. 494 (1929); 'Trans. Faraday Soc.,' vol. 25, p. 352 (1929).

† O. Hassel and H. Mark, 'Z. Physik,' vol. 25, p. 317 (1924); J. D. Bernal, 'Proc. Roy. Soc.,' A, vol. 106, p. 749 (1924).

‡ 'Ber. Deuts. Chem. Ges.,' vol. 57, p. 1826 (1924).

§ 'Phil. Mag.,' vol. 50, p. 1214 (1925).

|| 'Chem. Krist.,' vol. 4, p. 9 (1910).

bent or curved crystals are common, owing to easy slipping along $(11\bar{1})$ planes. Groth also mentions the occasional occurrence of forms $\{30\bar{7}\}$ and $\{702\}$. These planes were not visually observed in the present investigation; $(30\bar{7})$ gave a small second order reflection, but (702) was not found even on the ionisation spectrometer.

The crystal density is 2·044 gr per cubic centimetre.

The unit cell is simple monoclinic prismatic, with

$$a = 8{\cdot}07 \qquad b = 3{\cdot}84 \qquad c = 16{\cdot}61 \text{ A.}$$
$$\beta = 116^\circ\, 52',$$

and it contains two molecules of $C_6Cl_6$.

The space-group is most probably $C^5_{2h}(P2_1/c)$. From the $\{h0l\}$ planes 80 reflections were observed and measured on the ionisation spectrometer (Mb anticathode). For all these $l$ was even. Careful search failed to reveal any reflection from a plane having an odd index $l$ Also, although (020) gave a small reflection, no reflection could be found from (010), (030) or any other order of the symmetry plane. This plane, however, forms the cross section of the needle-shaped crystals and is in a most unfavourable position for examination on the ionisation spectrometer. Mr. Pelton, of the Davy Faraday Laboratory, very kindly examined the $(0k0)$ planes by the oscillation photographic method, using Cu radiation and a cylindrical camera. He found no trace of any reflection except from the (020) plane, which gave a weak reflection, thus confirming the ionisation spectrometer results.

### *Structure Determination by Trial and Error.*

The 12 carbon and 12 chlorine atoms in the unit cell may therefore be divided each into three sets of four, having the co-ordinates :—

C atoms—

| | | | |
|---|---|---|---|
| $x_1\, y_1\, z_1$ | $-x_1\, -y_1\, -z_1$ | $x_1\; \tfrac{1}{2}-y_1\; \tfrac{1}{2}+z_1$ | $-x_1\; \tfrac{1}{2}+y_1\; \tfrac{1}{2}-z_1$ |
| $x_2\, y_2\, z_2$ | $-x_2\, -y_2\, -z_2$ | $x_2\; \tfrac{1}{2}-y_2\; \tfrac{1}{2}+z_2$ | $-x_2\; \tfrac{1}{2}+y_2\; \tfrac{1}{2}-z_2$ |
| $x_3\, y_3\, z_3$ | $-x_3\, -y_3\, -z_3$ | $x_3\; \tfrac{1}{2}-y_3\; \tfrac{1}{2}+z_3$ | $-x_3\; \tfrac{1}{2}+y_3\; \tfrac{1}{2}-z_3$ |

Cl atoms—

| | | | |
|---|---|---|---|
| $X_1\, Y_1\, Z_1$ | $-X_1\, -Y_1\, -Z_1$ | $X_1\; \tfrac{1}{2}-Y_1\; \tfrac{1}{2}+Z_1$ | $-X_1\; \tfrac{1}{2}+Y_1\; \tfrac{1}{2}-Z_1$ |
| $X_2\, Y_2\, Z_2$ | $-X_2\, -Y_2\, -Z_2$ | $X_2\; \tfrac{1}{2}-Y_2\; \tfrac{1}{2}+Z_2$ | $-X_2\; \tfrac{1}{2}+Y_2\; \tfrac{1}{2}-Z_2$ |
| $X_3\, Y_3\, Z_3$ | $-X_3\, -Y_3\, -Z_3$ | $X_3\; \tfrac{1}{2}-Y_3\; \tfrac{1}{2}+Z_3$ | $-X_3\; \tfrac{1}{2}+Y_3\; \tfrac{1}{2}-Z_3$ |

There are 18 unknown parameters to be determined.

In the case of $C_6(CH_3)_6$ a definite lead was given in this direction :—

(*a*) By the pseudo-hexagonal structure of the [001] zone, revealed by the observed structure factors in that zone (*i.e.*, intensities of reflection corrected for angle). In particular, the intense reflections from certain small-spacing planes helped to "place" the atoms with considerable certainty.

(*b*) By the intense reflection from the main cleavage (001) plane, and by the independence of "*l*" of the observed structure factors for all planes $\{hkl\}$.

Obviously it is necessary to seek some similar indications, if possible, in the case of $C_6Cl_6$. The needle-shaped crystals are themselves pseudo-hexagonal in form, since

$$d_{100} = 7\cdot20 \qquad d_{10\bar{2}} = 6\cdot98 \qquad d_{002} = 7\cdot41 \text{ A}$$

and

$$100 : 10\bar{2} = 56° \, 59' \qquad 10\bar{2} : 001 = 59° \, 53' \qquad 001 : 100 = 63° \, 8'.$$

The relative intensities of reflection from all possible $\{h0l\}$ planes were carefully measured and divided into three groups :—

(1) Those lying in the acute angle between (001) and (100).

(2) Those lying in the acute angle between (100) and $(10\bar{2})$.

(3) Those lying in the acute angle between $(10\bar{2})$ and (001).

These are plotted in fig. 1.

The high absorbing power of Cl for Mb radiation has a noticeable influence on the resulting graphs. The crystal used (that giving the best reflections) was of the cross section shown in fig. 2 (*a*), the distance AB being 1·3 mm., whereas CD was about 0·6 mm. The absorption therefore, was least in the region of the (001) plane, the crystal as a whole being bathed in the X-ray beam, and greatest in the region of $(10\bar{1})$. A smaller, but much more evenly developed crystal (fig. 2 (*b*)) in which approximately AB = CD = EF = 0·75 mm., gave reflections of very nearly equal intensity from the planes $(10\bar{6})$, $(30\bar{4})$ and (202), these reflections being the largest actually observed. Using this fact, it was not difficult to make an approximate correction for absorption in the larger crystal. This was done, and the usual corrections were also applied to the observed intensities to obtain "experimental" values of the structure factors for the different planes.

These are shown in fig. 3. Here allowance has also been made for the falling off of atomic scattering power with angle, using an F curve for chlorine based on that given by James and Firth,* but modified to take account of the

---

* 'Proc. Roy. Soc.,' A, vol. 117, p. 62 (1927).

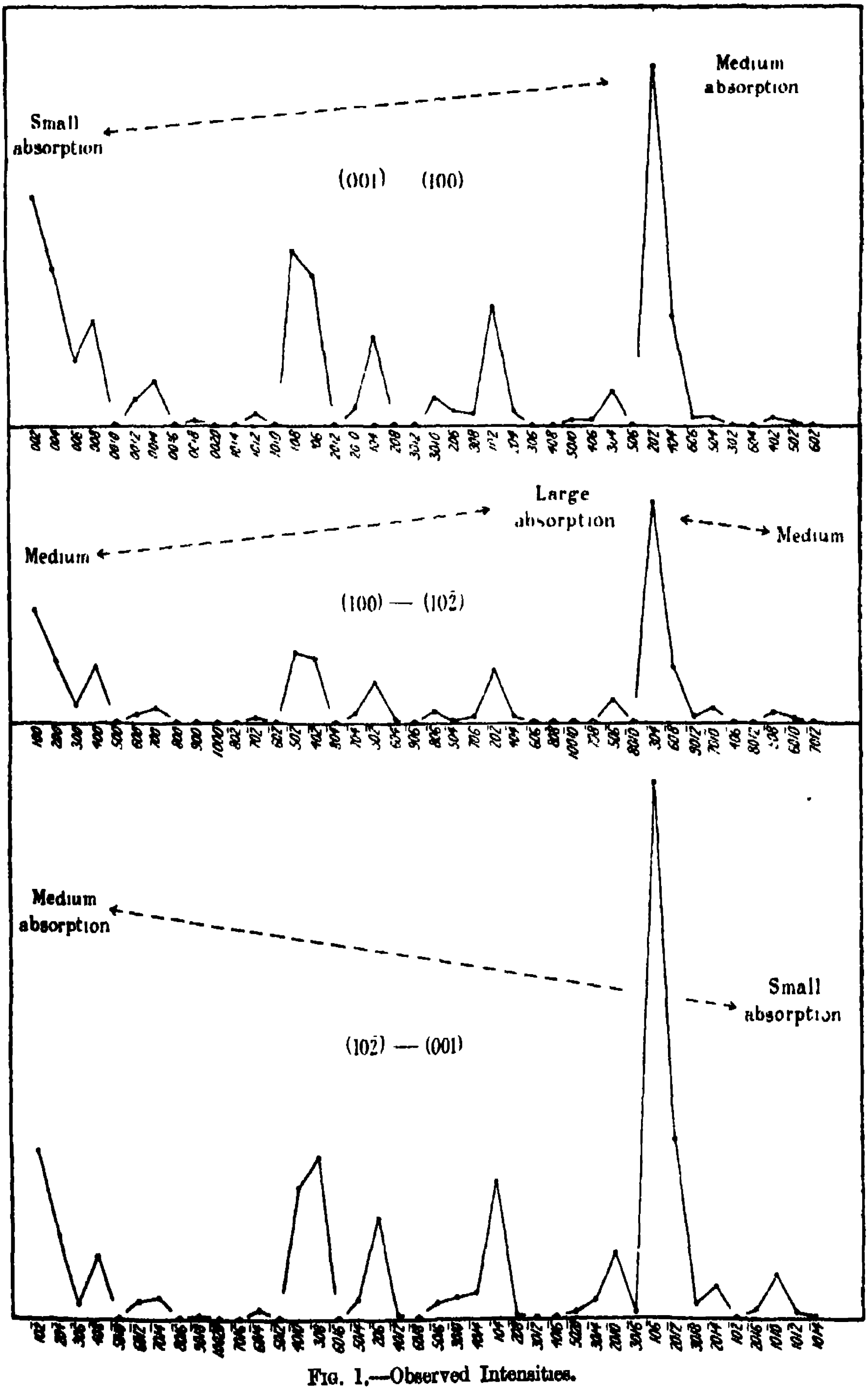

FIG. 1.—Observed Intensities.

probability that the atoms are not ionised; and an F curve for carbon similar to that adopted in the $C_6(CH_3)_6$ investigation (*loc. cit.*). This correction need only be approximate, since it has only to be used in the preliminary determination of the structure factor signs.

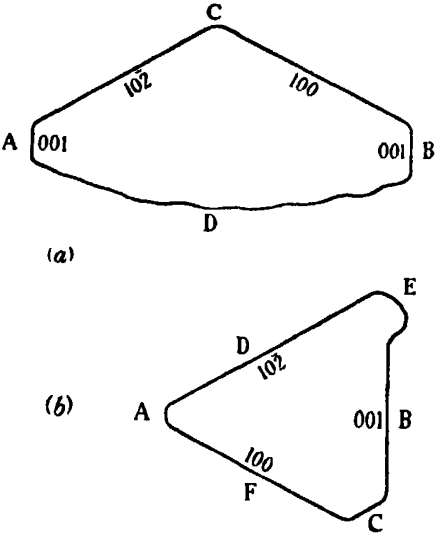

FIG. 2 (*a*) and (*b*).

Fig. 3 shows that in $C_6Cl_6$, as in $C_6(CH_3)_6$, one zone has a distinctly hexagonal structure. The correspondence between the three sets of structure factors is well marked. This considerably simplifies the problem of determining the unknown parameters, since if $x_1$, $z_1$, $X_1$, $Z_1$ can be found, the corresponding parameters for the remaining five carbon and five chlorine atoms are known at any rate approximately. A further simplification follows from the fact that the scattering power of chlorine is nearly three times as great as that of carbon, so that the exact location of the carbon atoms is not essential for a first estimate of the structure factors.

The problem of finding $X_1$ and $Z_1$ (and hence the positions of all chlorine atoms in the [010] projection) was tackled as follows. Attention was first concentrated on the various even orders of reflection from the (001) plane, to see if agreement could be obtained between observed and calculated structure factors for these 10 orders. This would give $Z_1$, $Z_2$ and $Z_3$. Since the carbon atoms are relatively unimportant, it was merely assumed, as a first approximation, that these are distant 1·42 A. from the origin, along lines making angles

$$\pm\theta, \quad \pm\left(\frac{\pi}{3}+\theta\right), \quad \pm\left(\frac{2\pi}{3}+\theta\right)$$

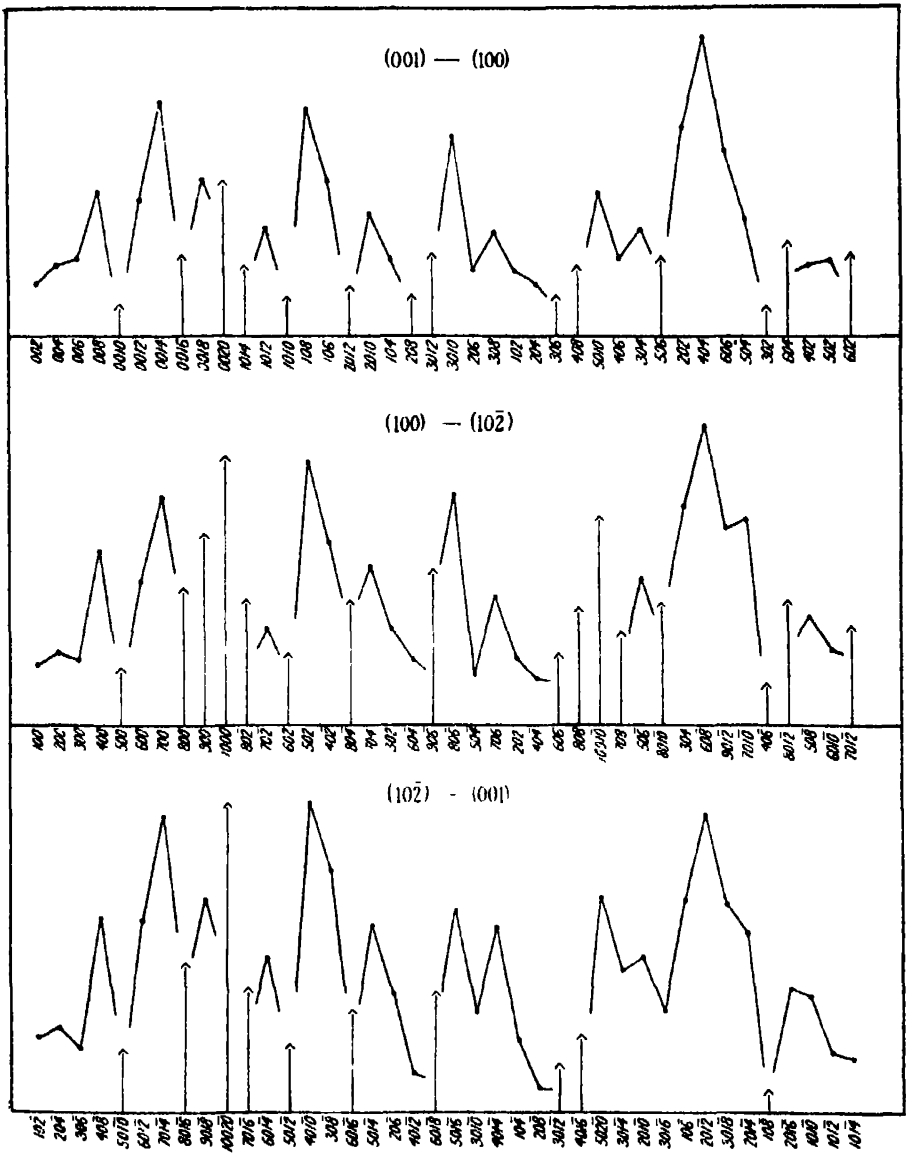

FIG. 3.

with the *a* axis. Then if the chlorine atoms are distant R from the origin along the same directions,

$$X_1 = \frac{R \sin (\beta - \theta)}{\sin \beta} \qquad Z_1 = \frac{R \sin \theta}{\sin \beta}, \text{ etc.}$$

Thus R, θ have become the two independent variables in place of X, Z.

The calculated structure factor for any even order (00*l*), assuming both Cl and C atoms to be not ionised, is given by

$$
\begin{aligned}
S \propto \Bigg[ 6\Bigg\{ & \cos 2\pi \left[\frac{l \,.\, 1{\cdot}42}{c \sin \beta} \,.\, \sin \theta\right] + \cos 2\pi \left[\frac{l \,.\, 1{\cdot}42}{c \sin \beta} \,.\, \sin \left(\frac{\pi}{3} + \theta\right)\right] \\
& + \cos 2\pi \left[\frac{l \,.\, 1{\cdot}42}{c \sin \beta} \,.\, \sin \left(\frac{2\pi}{3} + \theta\right)\right]\Bigg\} \\
+ 17\Bigg\{ & \cos 2\pi \left[\frac{l \,.\, \mathrm{R}}{c \sin \beta} \,.\, \sin \theta\right] + \cos 2\pi \left[\frac{l \,.\, \mathrm{R}}{c \sin \beta} \,.\, \sin \left(\frac{\delta\pi}{3} + \theta\right)\right] \\
& + \cos 2\pi \left[\frac{l \,.\, \mathrm{R}}{c \sin \beta} \,.\, \sin \left(\frac{2\pi}{3} + \theta\right)\right]\Bigg\} \Bigg].
\end{aligned}
$$

$\theta$ *was varied from* 0° *to* 30° by 5° *at a time*, and R varied from $(2 \times 1{\cdot}42)$ A. to $(2{\cdot}7 \times 1{\cdot}42)$ A. by $(0{\cdot}05 \times 1{\cdot}42)$ A. at a time, the latter range being taken as likely to cover all possible values of the chlorine atom radius. Subsequently the range was limited still further until finally it was found that the values $\theta = 19°$ and $\mathrm{R} = 2{\cdot}18 \times 1{\cdot}42 = 3{\cdot}10$ A. gave the best agreement for all the 10 orders in question.

| | (002) | (004) | (006) | (008) | (0010) | (0012) | (0014) | (0016) | (0018) | (0020) |
|---|---|---|---|---|---|---|---|---|---|---|
| Obs. .... | 37 | 49 | 54 | 100 | <23 | 96 | 164 | <56 | 110 | <110 |
| Calc. .... | 33 | 59 | 64 | 100 | 19 | 102 | 203 | 63 | 125 | 11 |

The higher orders were particularly sensitive to small changes either in $\theta$ or in R. It is fairly certain therefore that the value of Z is fixed to within a few per cent. for the chlorine atoms. The above test does not, of course, decide the value of X, but this is fixed by a corresponding comparison for the various orders of reflection from the (100) plane. The close correspondence between the observed structure factors for (002) .. (0020) and for (100) .. (1000) implies that $2\mathrm{Z}/c$ and $\mathrm{X}/a$ cannot greatly differ. The above values of R, $\theta$ give for $2\mathrm{Z}_1/c$, etc., the values $\pm 49{\cdot}0°$, $\pm 98{\cdot}7°$, $\pm 147{\cdot}5°$, when expressed in angular measure. The best agreement for (100) .. (1000) is obtained for $\mathrm{X}/a = \pm 46{\cdot}2°, \pm 100{\cdot}2°, \pm 146{\cdot}5°$.

| | (100) | (200) | (300) | (400) | (500) | (600) | (700) | (800) | (900) | (1000) |
|---|---|---|---|---|---|---|---|---|---|---|
| Obs. .... | 35 | 41 | 37 | 100 | <32 | 83 | 132 | <79 | <110 | <156 |
| Calc. .... | 31 | 47 | 40 | 100 | 34 | 96 | 173 | 62 | 97 | 65 |

A similar test was carried out for 10 orders of reflection from $(10\bar{2})$, and agreement was found to be best when the angular distances of the Cl atoms from the plane ($10\bar{2}$) were also $\pm 46 \cdot 2°$, $\pm 100 \cdot 2°$, and $\pm 146 \cdot 5°$.

| | ($10\bar{2}$) | ($20\bar{4}$) | ($30\bar{6}$) | ($40\bar{8}$) | ($50\overline{10}$) | ($60\overline{12}$) | ($70\overline{14}$) | ($80\overline{16}$) | ($90\overline{18}$) | ($100\overline{20}$) |
|---|---|---|---|---|---|---|---|---|---|---|
| Obs..... | 38 | 36 | 32 | 100 | < 32 | 99 | 154 | <80 | 110 | < 162 |
| Calc. .. | 31 | 47 | 40 | 100 | 34 | 96 | 173 | 62 | 97 | 65 |

These conclusions are shown graphically in fig. 4.

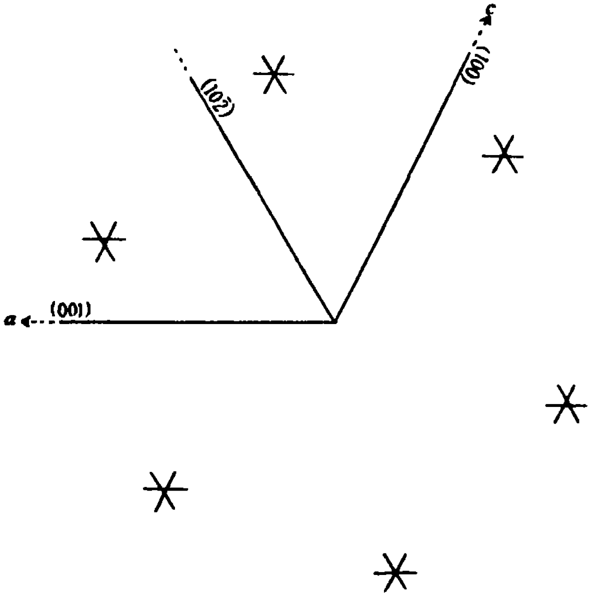

FIG 4.

It is clear that the chlorine atoms have been satisfactorily located, since the three sets of parameters very nearly intersect.

Taking as mean values

$$X_1 = 3 \cdot 225 \qquad X_2 = 2 \cdot 26 \qquad X_3 = 1 \cdot 14$$

and

$$Z_1 = 1 \cdot 155 \qquad Z_2 = 3 \cdot 46 \qquad Z_3 = -2 \cdot 26$$

fig. 5 gives the resulting structure factors for all the planes (002) .. (102) .. (100), still assuming as before that the carbon atoms are distant 1·42 A. from the origin along the lines joining the origin to the chlorine atoms, *i.e.*, that

$$x_1 = 1 \cdot 435 \qquad x_2 = 1 \cdot 01 \qquad x_3 = 0 \cdot 515$$

and

$$z_1 = 0 \cdot 51 \qquad z_2 = 1 \cdot 525 \qquad z_3 = -1 \cdot 015.$$

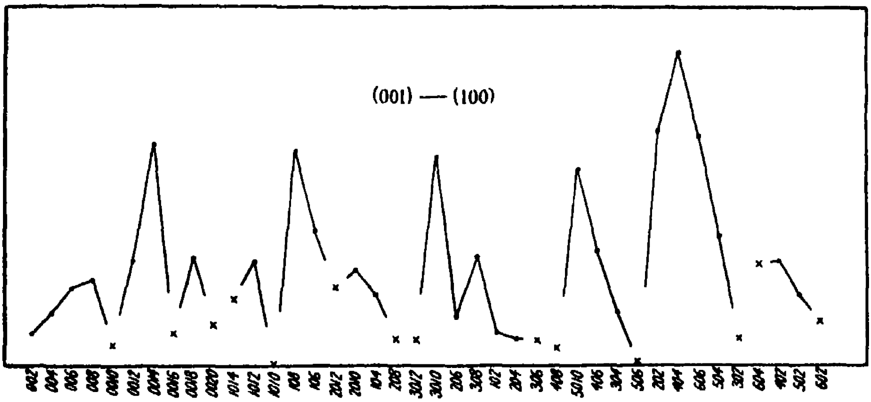

Fig 5.—Calculated Structure Factors, (001)—(100).

The correspondence between figs. 3 and 5 shows that we are justified in adopting these parameters as a means of determining the *signs* of the experimentally found structure factors. A knowledge of these signs is, of course, necessary before a Fourier analysis of the results can be carried out.*

## *Fourier Analysis of the* {*h*0*l*} *zone.*

Table I shows the experimental structure factors, with their determined signs.

Table I.—Values of F(*h*0*l*). *l* is always even. F(*h*0*l*) = F($\bar{h}$0*l*).

| Index *h* ↓ \ *l* → | $\bar{20}$ | $\bar{18}$ | $\bar{16}$ | 14 | $\bar{12}$ | $\bar{10}$ | 8 | $\bar{6}$ | 4 | $\bar{2}$ | 0 | 2 | 4 | 6 | 8 | 10 | 12 | 14 | 16 | 18 | 20 |
|---|---|---|---|---|---|---|---|---|---|---|---|---|---|---|---|---|---|---|---|---|---|
| 0 | | | | | | | | | | | \|K\| | 15 | 17 | 14 | $\bar{21}$ | 0 | 14 | 21 | 0 | $\bar{10}$ | 0 |
| 1 | | | 0 | $\bar{5}$ | 7 | $\bar{16}$ | 0 | 42 | 19 | 21 | 16 | 16 | 16 | 24 | 30 | 0 | $\bar{10}$ | 0 | | | |
| 2 | | | $\bar{10}$ | 18 | 34 | 21 | $\bar{4}$ | 23 | $\bar{21}$ | 17 | 17 | 42 | $\bar{9}$ | 9 | 0 | $\bar{12}$ | 0 | | | | |
| 3 | | 15 | 9 | 14 | 0 | $\bar{14}$ | 37 | $\bar{11}$ | 42 | 18 | 11 | 0 | 15 | 0 | 11 | 17 | 0 | | | | |
| 4 | 0 | | 0 | 18 | $\bar{4}$ | 39 | $\bar{27}$ | 0 | $\bar{7}$ | 28 | 25 | $\bar{10}$ | 35 | 8 | 0 | | 0 | | | | |
| 5 | 14 | | 17 | $\bar{18}$ | 0 | 0 | 13 | $\bar{19}$ | 7 | 33 | 0 | 8 | 11 | 0 | | $\bar{10}$ | | | | | |
| 6 | 0 | 0 | 0 | 14 | $\bar{18}$ | 8 | 33 | 0 | 8 | 0 | $\bar{14}$ | 0 | 0 | 14 | 0 | | | | | | |
| 7 | | | 0 | 24 | 0 | 19 | 0 | $\bar{12}$ | $\bar{15}$ | 9 | 19 | 0 | | | | | | | | | |
| 8 | | | 0 | 0 | 0 | 0 | 0 | 19 | 0 | 0 | 0 | | | | | | | | | | |
| 9 | | $\bar{12}$ | | | 14 | | | 0 | | | 0 | | | | | | | | | | |

---

* W. L. Bragg, 'Proc. Roy. Soc.,' A, vol. 123, p. 537 (1929), and subsequent papers.

Table II.

|  |  |  |  |  |  |  |  |  |  |  |  |  |  |  |  |  |  |  |  |  |  |  |  |  |  |  |  |  |  |  |
|---|---|---|---|---|---|---|---|---|---|---|---|---|---|---|---|---|---|---|---|---|---|---|---|---|---|---|---|---|---|---|
| 13 | 16 | 28 | 38 | 34 | 34 | 42 | 31 | 12 | 18 | 29 | 21 | 20 | 33 | 32 | 25 | 32 | 33 | 20 | 21 | 29 | 18 | 12 | 31 | 42 | 34 | 34 | 38 | 28 | 16 | 13 |
| 22 | 20 | 23 | 31 | 35 | 29 | 31 | 40 | 29 | 10 | 14 | 30 | 32 | 30 | 28 | 19 | 29 | 38 | 27 | 28 | 63 | 79 | 45 | 18 | 27 | 34 | 28 | 33 | 40 | 31 | 22 |
| 33 | 29 | 32 | 35 | 37 | 33 | 23 | 25 | 37 | 33 | 22 | 30 | 44 | 42 | 34 | 29 | 28 | 32 | 30 | 41 | 90 | 146 | 128 | 35 | 22 | 26 | 29 | 23 | 31 | 39 | 33 |
| 35 | 26 | 24 | 28 | 34 | 38 | 36 | 26 | 28 | 40 | 36 | 25 | 28 | 36 | 37 | 35 | 38 | 36 | 29 | 34 | 76 | 143 | 167 | 112 | 42 | 26 | 36 | 27 | 20 | 32 | 35 |
| 35 | 35 | 30 | 18 | 12 | 16 | 33 | 39 | 31 | 27 | 31 | 26 | 18 | 17 | 23 | 25 | 31 | 36 | 35 | 29 | 39 | 76 | 110 | 103 | 63 | 39 | 38 | 31 | 18 | 23 | 35 |
| 32 | 50 | 68 | 69 | 42 | 8 | 5 | 27 | 38 | 29 | 23 | 28 | 29 | 23 | 20 | 22 | 23 | 27 | 32 | 32 | 27 | 29 | 41 | 47 | 42 | 40 | 43 | 37 | 24 | 21 | 32 |
| 29 | 41 | 89 | 136 | 136 | 72 | 12 | 5 | 25 | 33 | 30 | 33 | 41 | 40 | 31 | 28 | 34 | 34 | 29 | 30 | 31 | 29 | 29 | 31 | 27 | 29 | 42 | 48 | 40 | 32 | 29 |
| 31 | 25 | 47 | 112 | 168 | 137 | 58 | 12 | 15 | 23 | 29 | 34 | 40 | 38 | 30 | 24 | 27 | 37 | 38 | 28 | 29 | 34 | 38 | 44 | 46 | 38 | 35 | 45 | 48 | 40 | 31 |
| 29 | 26 | 25 | 49 | 99 | 114 | 71 | 28 | 24 | 27 | 16 | 22 | 33 | 25 | 17 | 22 | 28 | 28 | 29 | 28 | 28 | 35 | 38 | 38 | 50 | 61 | 52 | 42 | 41 | 37 | 29 |
| 38 | 37 | 40 | 36 | 37 | 49 | 46 | 29 | 31 | 37 | 24 | 19 | 32 | 29 | 10 | 28 | 70 | 73 | 45 | 27 | 28 | 36 | 40 | 33 | 35 | 61 | 78 | 62 | 43 | 39 | 38 |
| 58 | 63 | 58 | 51 | 36 | 26 | 28 | 32 | 33 | 37 | 33 | 26 | 38 | 44 | 17 | 18 | 89 | 147 | 119 | 57 | 31 | 34 | 38 | 36 | 33 | 47 | 77 | 80 | 54 | 44 | 57 |
| 56 | 81 | 74 | 53 | 44 | 35 | 27 | 31 | 36 | 34 | 30 | 26 | 33 | 45 | 30 | 7 | 49 | 140 | 166 | 103 | 43 | 33 | 38 | 47 | 40 | 60 | 51 | 63 | 51 | 37 | 56 |
| 36 | 64 | 77 | 57 | 42 | 45 | 39 | 24 | 24 | 31 | 33 | 28 | 26 | 31 | 33 | 17 | 17 | 70 | 124 | 107 | 50 | 31 | 47 | 57 | 58 | 50 | 36 | 31 | 33 | 30 | 36 |
| 29 | 37 | 55 | 56 | 41 | 43 | 51 | 36 | 17 | 30 | 37 | 39 | 29 | 23 | 27 | 29 | 24 | 31 | 59 | 71 | 47 | 26 | 40 | 66 | 79 | 74 | 47 | 17 | 14 | 25 | 29 |
| 25 | 22 | 31 | 47 | 46 | 36 | 42 | 45 | 33 | 24 | 32 | 38 | 32 | 23 | 22 | 27 | 29 | 27 | 30 | 39 | 40 | 31 | 29 | 43 | 66 | 79 | 63 | 27 | 7 | 16 | 25 |
| 20 | 14 | 15 | 39 | 58 | 52 | 36 | 33 | 36 | 35 | 83 | 31 | 28 | 25 | 24 | 24 | 24 | 25 | 28 | 31 | 33 | 35 | 36 | 33 | 36 | 52 | 58 | 39 | 15 | 14 | 20 |

$\frac{c}{4}$

$a$

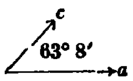

K {S (x, z) + arbitrary constant.}

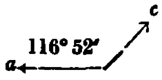

These factors are, of course, not now corrected for falling off of atomic scattering power with angle. No " temperature factor " has been added, which may account for the fact that the higher terms, which will terminate the Fourier series, are still relatively large.

A complication is introduced into the summation of the Fourier series

$$S(x, z) = \Sigma \Sigma F(h0l) \cos 2\pi (hx/a + lz/c),$$

because the experimental structure factors given in Table I are not *absolute*, but only *relative*. In other words F(000), the first and constant term of the series, is not known. This will necessarily limit the amount of information that can be obtained from the resulting contour diagram. It will not, however, affect either the positions of the atomic centres, or the shapes of the contours. If the Fourier series were complete, S(x, z) would be positive everywhere.

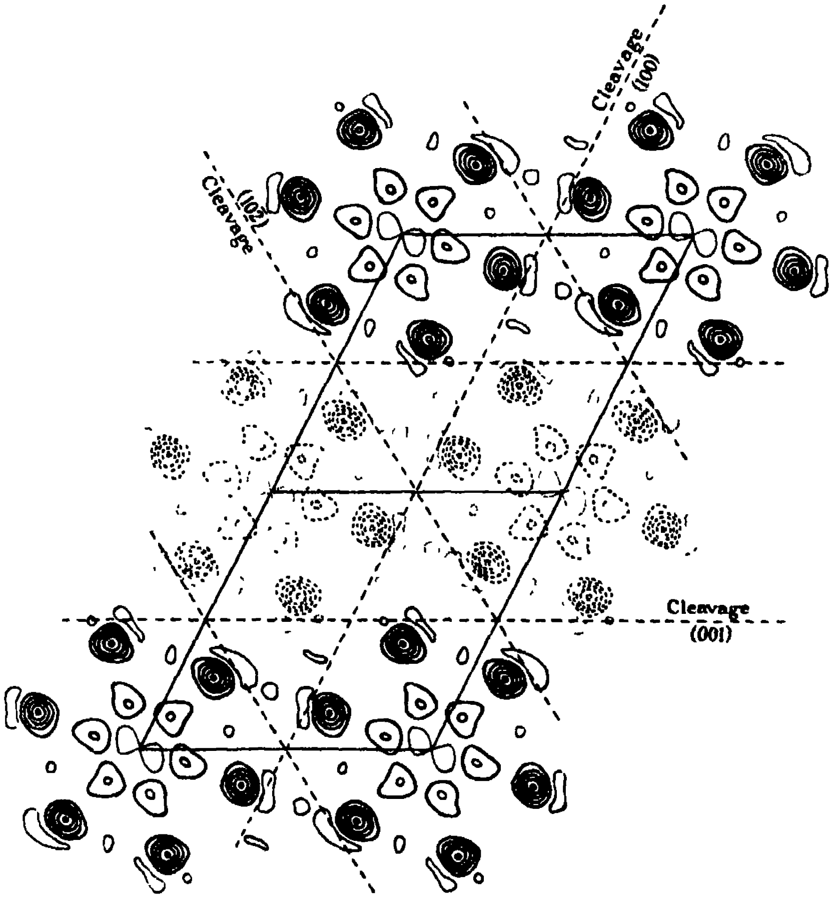

Fig. 6.—Projection on (010) Plane.

F(000) was therefore arbitrarily given such a value as to bring this about, and Table II shows the values of S($x$, $z$) so obtained.

It must be remembered, however, that these values are measured in arbitrary units and are subject to the addition of an unknown constant. Any attempt at electron counting, for example, is out of the question.

The contour diagrams shown in figs. 6 and 7 are drawn for values of S($x$, $z$) of 20, 50, 80, 110, 140, 170; also (in fig. 7) for 30 and 40 within the benzene ring.

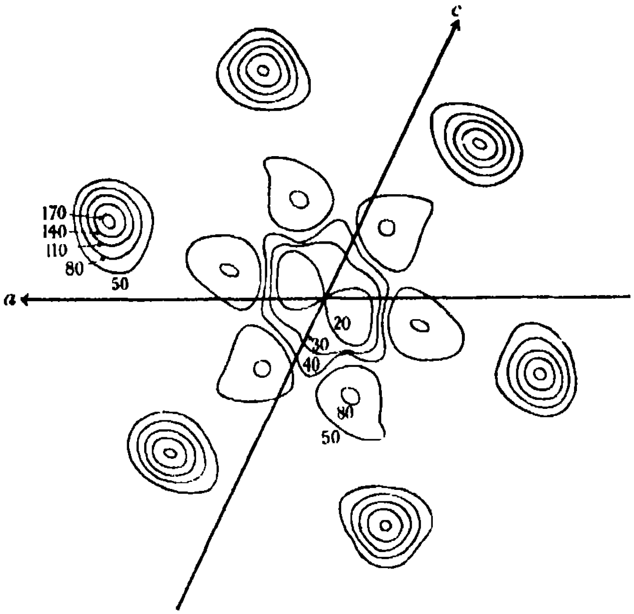

Fig 7.—Projection of $C_6 Cl_6$ Molecule.

Certain features are at once apparent

(1) The molecule is quite clearly defined, the positions of the atoms being not far from those used in the preliminary sign determination.

Table III.

| Trial and error parameters | | | | Fourier analysis parameters. | | | |
|---|---|---|---|---|---|---|---|
| $X_1$ | 3·225 | $Z_1$ | 1·155 | $X_1$ | 3 325 | $Z_1$ | 1·17 |
| $X_2$ | 2·265 | $Z_2$ | 3 46 | $X_2$ | 2 245 | $Z_2$ | 3·40 |
| $X_3$ | 1·145 | $Z_3$ | −2 26 | $X_3$ | 1·075 | $Z_3$ | −2·285 |
| $x_1$ | 1·435 | $z_1$ | 0 51 | $x_1$ | 1·46 | $z_1$ | 0·44 |
| $x_2$ | 1·01 | $z_2$ | 1 525 | $x_2$ | 0·95 | $z_2$ | 1·45 |
| $x_3$ | 0·515 | $z_3$ | −1 015 | $x_3$ | 0 39 | $z_3$ | −1·035 |

(2) Each carbon atom is roughly triangular, thus appearing to be definitely polarised in the direction of its appropriate chlorine atom and of the two neighbouring carbon atoms. No polarisation towards the centre of the benzene ring is indicated. On the other hand, there seems to be no corresponding polarisation of the chlorine atoms.

(3) Outside each chlorine atom there is a kind of buffer region of low electron density. It is probable, however, that these (20) contours would not appear if the Fourier series were completed and that they are part of a diffraction effect due to the termination of the series while the separate terms are still large.* Similarly, no reliance can be placed on the curious shape of the (20) contour within the benzene ring, unless it is found to be repeated in the analysis of other benzene derivatives.

### *Shape of the Molecule.*

The positions of the Cl and C atoms, as given by the Fourier analysis, are most easily described in terms of polar co-ordinates.

| Chlorine atoms. | | Carbon atoms. | |
|---|---|---|---|
| $R_1 = 2\cdot985$ | $\theta_1 = \pm 20° 25'$ | $r_1 = 1\cdot32$ | $\omega_1 = \pm 17° 20'$ |
| $R_2 = 3\cdot115$ | $\theta_2 = \pm 76° 55'$ | $r_2 = 1\cdot325$ | $\omega_2 = \pm 77° 15'$ |
| $R_3 = 2\cdot935$ | $\theta_3 = \mp 44° 0'$ | $r_3 = 1\cdot26$ | $\omega_3 = \mp 47° 5'$ |

It will be seen from these numbers that the distances of the carbon atoms from the origin are about 8 per cent. less than was assumed in the first approximation. Neither they nor the chlorine atoms are arranged on a regular hexagon in the [010] projection.

The intensities of reflection from planes in zones other than the {*h*0*l*}, though incomplete, show conclusively that, unlike $C_6(CH_3)_6$, the atoms do not all lie in the one axial plane. As was explained in the paper on $C_6(CH_3)_6$, the consequence of any such arrangement of plane layers of atoms parallel to an axial plane would be that the structure factors of all planes {*hkl*} would be independent of one index. Thus, in the case of $C_6(CH_3)_6$ the structure factors for the series of planes {*hk*0} showed exactly the same variations as those for the series {*hk*1}, {*hk*2}, etc. Also, the (001) plane was an excellent reflector, and showed a " normal " falling off of intensities from its various orders ; a further indication that the atoms were arranged in sheets parallel to that plane.

For $C_6Cl_6$ the (020) plane, as far as can be judged, is not a good reflector at all, and the (040) intensity is less than would be expected for the "normal" falling off.

---

* W. L. Bragg and J. West, 'Phil. Mag.,' vol. 10, p. 823 (1930).

The following are the remaining "observed" structure factors, corrected for falling off of atomic scattering power with angle, etc., but not for absorption.

Table IV.

Absorption maximum for (002), minimum for $(11\bar{1})$.

| (*hkl*) | S | (*hkl*) | S | (*hkl*) | S | (*hkl*) | S |
|---|---|---|---|---|---|---|---|
| 110 | 128 | 112 | 50 | 002 | 100 | 112 | 79 |
| 220 | 28 | 224 | <21 | | | $22\bar{4}$ | <20 |
| 330 | <21 | 336 | <22 | $11\overline{11}$ | 29 | $33\bar{6}$ | <21 |
| 440 | <24 | 113 | 32 | $11\overline{10}$ | 41 | $11\bar{1}$ | 48 |
| 111 | 30 | 226 | <21 | $11\bar{9}$ | 49 | $22\bar{2}$ | 34 |
| 222 | 24 | 114 | 58 | 118 | <19 | $33\bar{3}$ | <21 |
| 333 | <22 | 228 | <21 | | | $44\bar{4}$ | <24 |

Absorption maximum for (002).

| | | | | | | | |
|---|---|---|---|---|---|---|---|
| 002 | 100 | 012 | 160 | 020 | 64 | 120 | 84 |
| 015 | 43 | 024 | 45 | 040 | <50 | 240 | <39 |
| 014 | ? 30 | 036 | <50 | — | — | 122 | 58 |
| 013 | 39 | 011 | 68 | $21\bar{2}$ | 50 | $24\bar{4}$ | <39 |
| | | 022 | <45 | — | — | | |

Many other planes in these zones were examined but no other reflections were found. The needle-like shape of the crystals, however, made measurements in any but the $\{h0l\}$ zone exceedingly difficult.

The two centrosymmetrical molecules in the unit cell are reflections of one another in the (010) plane (fig. 8 (*a*)). If the component atoms all lay actually in that plane, the molecules would be, in effect, identical, and all planes $\{hkl\}$ having $(k + l)$ odd would disappear (fig. 8 (*b*)).

This is quite obviously not the case, as the presence of such reflections as (112), (114), (012), etc., shows.

We are therefore faced with the further problem of finding the "$y$" parameters for all the atoms. Without more data this cannot be done, but certain general conclusions may be stated :—

(1) The projections of the C atom centres on the (010) plane lie on an ellipse, of semi-major axis 1·355 A., and semi-minor axis 1·26, the major axis making an angle of 51° 34′ with the crystallographic *a* axis.

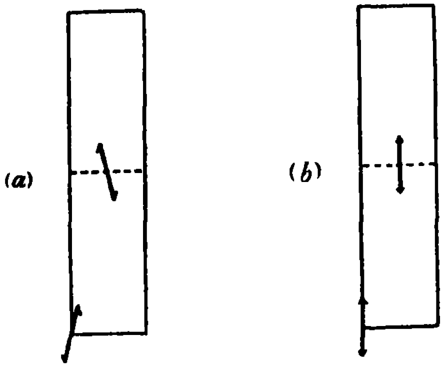

FIG. 8 (*a*) and (*b*).

(2) This projection is not compatible with any arrangement of the C atoms in a plane regular hexagon. There is, moreover, *only one* plane arrangement of C atoms, equidistant from one another, which would give the required projection. This plane ring, ABCA′B′C′, shown in fig. 9, would be inclined to the (010) plane at an angle of 32° 20′, and would involve

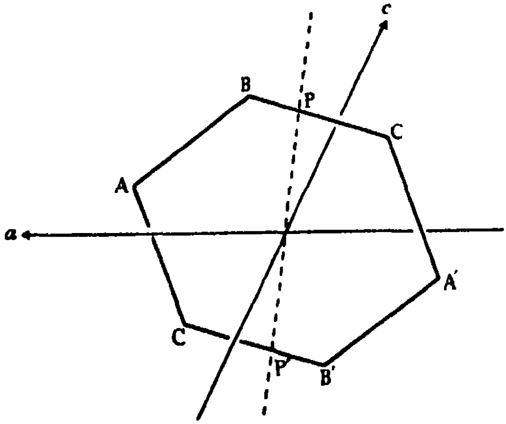

FIG. 9.

$$AB = BC' = AC = 1{\cdot}42 \text{ A.}$$

$$OA = 1{\cdot}555 \qquad OB = 1{\cdot}36 \qquad OC = 1{\cdot}34$$

$$\angle\, AOC = 58^\circ\, 20' \quad \angle\, AOB = 58^\circ\, 0' \quad \angle\, BOC' = 63^\circ\, 40'.$$

The plane of the ring would be tilted about the line PP′, which makes an angle of 97° 40′ with the *a* axis, and the *y* parameters would be

$$(A)\ y_1 = \pm\,0{\cdot}82 \qquad (B)\ y_2 = \pm\,0{\cdot}295 \qquad (C)\ y_3 = \pm\,0{\cdot}455$$

Figs. 10 (*a*) and (*b*) show the projections of such a ring on the planes (100) and (001).

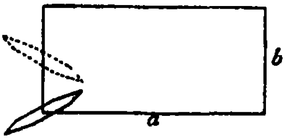

Fig. 10 (*a*).—(001).

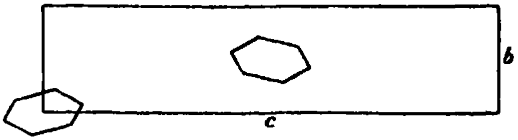

Fig. 10 (*b*).—(100).

If the Cl atoms also lay in the same plane, then their Y parameters would be ±1·83, ±0·70, ±1·135 respectively, and the actual C—Cl distances would be 1·95, 1·835 and 1·81, giving a mean Cl radius of about 1·155

(3) On the other hand, the projection on (010) might result from a puckered benzene ring for which

$$AB = BC' = AC = 1{\cdot}54\ \text{A}.$$

$$(A)\ y_1 = \pm\,0{\cdot}265 \qquad (B)\ y_2 = \mp\,0{\cdot}545 \qquad (C)\ y_3 = \mp\,0{\cdot}43.$$

Again the ring would be an irregular one, except for the constant distance apart of the atoms. The angles would not be tetrahedral, but only very approximately so (figs. 11 (*a*) and (*b*)).

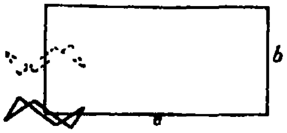

Fig. 11 (*a*).—(001).

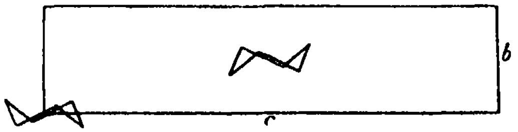

Fig. 11 (*b*).—(100).

(4) There are, of course, an infinite number of other possible arrangements, all of which would give the same projection on (010). No adequate means of deciding on the true arrangement are available at present.

It is, however, significant that the only *plane* ring which would account for the results, actually involves a C—C distance of 1·42 A., the distance found in graphite and in $C_6(CH_3)_6$.

There is no possibility of a regular arrangement (either tetrahedral or coplanar) of the three carbon valencies, which at the same time preserves a constant interatomic distance either from carbon to carbon or from carbon to chlorine.

### *Cleavage.*

The full contour diagram (fig. 6) readily explains the course of the cleavages. There are bands of low electron density between the molecules in directions parallel to (001), which is the best cleavage plane, and also parallel to (100) and (10$\bar{2}$), the secondary cleavage planes. The slipping on (11$\bar{1}$) is related to the tilt and general arrangement of the molecules relative to that plane, and cannot be explained from the limited data available.

### *Conclusions.*

It is clear that the original intention of the research has not been adequately fulfilled One projection of the molecule has been found with some certainty, but it is not possible to state whether the benzene ring in this compound is plane or not. If, however, it is plane, then the distance between adjacent carbon atoms in the ring must be 1·42 A. The distances from C to Cl atoms in the projection are 1·675, 1·665 and 1·79. These distances therefore constitute a lower limit for the actual C—Cl distances in the molecule.

### *Acknowledgments.*

The writer's grateful thanks are due to the Council of Bedford College, London, for a scholarship enabling her to work in the Physics Laboratories of the University of Leeds, to the Royal Society for a grant covering the cost of some of the apparatus employed, and to the Managers of the Royal Institution for a subsequent grant which permitted the completion of the work.

# *Interferometric Measurements in the Spectrum of the Iron Arc in Air in the Region* λ 3100 — λ 3500.

By C. V. JACKSON, Imperial College of Science and Technology.

(Communicated by A Fowler, F R S —Received July 16, 1931.)

## *Introduction.*

In a previous paper[*] I gave the results of a set of wave-length measurements in the spectrum of the iron arc in the region λ 2300 to λ 3100. These measurements were carried out because it was found that previous measurements in this region were all rather unsatisfactory and gave results considerably higher than those calculated from levels determined from the wave-lengths recommended by the International Astronomical Union[†] in 1928. My results confirm the values calculated from the I.A.U. Standards very satisfactorily, and also agree very well with the recent measurements of the vacuum arc by Burns and Walters.[‡] The apparatus was also used to measure a few lines in the visible part of the iron spectrum, and was shown to give results in excellent agreement with the values adopted by the I.A U. in 1928.

It was recommended by the I.A.U. that observations should be made in the region below λ 3400 for which there were no good modern measurements available. Accordingly the present work was undertaken to fill up the gap remaining and a set of 46 lines has been measured in the region λ 3100–λ 3500. The results are in very good agreement both with the I A U. calculated values and with the observed standards adopted by the I A.U. in 1928, the mean systematic difference (J — I.A.) being only —0·0001 A. for 8 lines, while the mean accidental difference is ±0·0006 A. The agreement with the measurements of Babcock[§] in the region λ 3370–λ 3500 is equally good, the mean systematic difference (J — B) being +0·0001 A for eight lines, while the mean accidental difference is ±0·0006 A.

The agreement with the measurements in the vacuum arc by Burns and Walters[||] over the whole range observed is also quite satisfactory, but the mean systematic difference, (J — B) = + 0·0015 A., is naturally considerably greater than that found in the extreme ultra-violet part of the spectrum on account of the pressure shift, while the mean accidental difference is about ±0·001 A.

---

[*] 'Proc. Roy. Soc.,' A, vol. 130, pp. 395–410 (1931).

[†] 'Trans. Inter. Astron. Union,' vol. 3 (1929).

[‡] Burns and Walters, 'Pub. Allegheny Obs.,' vol. 6, No. 11.

[§] Babcock, 'Astrophys. J.,' vol. 66, p. 256 (1927).

[||] *Burns and Walters, loc. cit.*

The observations and measurements were made with the apparatus used for my previous work.*

## *Experimental.*

Most of the measurements were made from the plates used for the work on the spectrum in the region below λ 3100, and in the violet, described in the previous paper, but four additional plates were taken since some of the weaker lines were too faint for satisfactory measurements on the earlier plates. For these, however, the apparatus and procedure were exactly the same as that described before and it is therefore thought unnecessary to repeat the description. It is perhaps worthy of note that there is no systematic difference between the results found from the earlier plates and those from the later plates.

The phase correction of the interferometer plates, which were lightly coated with platinum, was verified and found not to have changed in a period of rather over a year, which was the time intervening between the two sets of exposures. Moreover, the plates remained quite as good as when they were originally sputtered. As mentioned before, the phase correction was quite small and the values relative to λ 5852, for a 5-mm. étalon are given below in Table I.

Table I.

| λ. | Phase correction | λ | Phase correction. |
|---|---|---|---|
| A. | A. | A | A. |
| 6500 | +0 0010 | 2900 | −0 0043 |
| 6000 | −0 0002 | 2800 | −0 0045 |
| 5500 | −0 0005 | 2700 | −0 0049 |
| 5000 | −0 0011 | 2600 | −0 0054 |
| 4500 | −0 0018 | 2500 | −0 0059 |
| 4000 | −0 0026 | 2400 | −0 0065 |
| 3500 | −0 0034 | 2300 | −0 0071 |
| 3000 | −0 0041 | | |

The measurements were carried out in exactly the same way as that described before, it being customary to measure the diameters of the first, the second and the seventh rings, from which the fractional part of the order of interference at the centre of the ring system was calculated from the relation

$$a + e = n^2_{\kappa}/(n^2_{\kappa+1+a} - n^2_{\kappa}),$$

---

* Jackson, ‘Proc. Roy. Soc.,’ A, vol. 130, p. 395 (1931).

where $n_k$ is the diameter of the *k*th ring and $n_{k+1+a}$ is the diameter of the $n_{k+1+a}$th ring.

Only the diameters of the two innermost rings were used for the evaluation of the numerator of the expression (2), but the diameters of the outer rings were used in evaluating the denominator. In order to reduce the effect of accidental errors in the measurement of the ring diameters, the denominators were plotted on graph paper against the wave-lengths and a smooth curve was drawn through them. In evaluating the fractional value, the denominator read from the curve was used, but it only differed by a very small amount from that given by the means of the direct measurements of a single ring system, except in the case of a few diffuse lines where it occasionally differed by as much as 1 or 2 per cent. It was gratifying that throughout the course of the work no systematic difference between the fractions yielded by the first and those yielded by the second rings was detected.

The temperature and pressure were noted at the time when an exposure was made, and the wave-lengths were corrected to N.T.P. (15° C., 760 mm. pressure) by means of a table calculated from the data given by Meggers and Peters* on the refractive index of air. Since this may be of use to other workers in this field the figures are given below in Table II.

### Table II.

Temperature Correction.

Standard assumed at 6000 A. and 15° C.

| λ. | 30° C. | 22° C. | 20° C. | 10° C. |
|---|---|---|---|---|
| A. | A | A | A | A. |
| 2000 | $-0\cdot0051_2$ | −0·0024 | −0·0017 | +0·0017 |
| 2400 | $-0\cdot0035_1$ | −0·0017 | −0·0012 | +0·0012 |
| 2700 | $-0\cdot0028_0$ | −0·0013 | −0·0009 | +0·0009 |
| 3000 | $-0\cdot0021_7$ | −0·0010 | −0·0007 | +0·0007 |
| 4000 | $-0\cdot0011_2$ | −0·0005 | −0·0004 | +0·0004 |
| 5000 | $-0\cdot0004_7$ | −0·0002 | −0·0002 | +0·0002 |
| 7000 | $+0\cdot0003_7$ | +0·0002 | +0·0001 | −0·0001 |

---

* Meggers and Peters, 'Sci. Papers Bur. Stds.,' No. 327 (1918).

Table II—(continued).

Pressure Correction

Standard assumed at 6000 A. and 760 mm

| λ | 740 | 750. | 770. |
|---|---|---|---|
| 2000 | +0 0026$_0$ | +0 0013 | −0 0013 |
| 2400 | +0 0018$_6$ | 0 0009 | −0 0009 |
| 2700 | +0 0014$_1$ | 0 0007 | −0 0007 |
| 3000 | +0 0011 | 0 0005 | −0 0005 |
| 4000 | +0 0006 | 0 0003 | −0 0003 |
| 5000 | +0 0002$_6$ | +0 0001 | −0 0001 |
| 7000 | +0 0001$_8$ | −0 0001 | +0 0001 |

The wave-lengths were measured against the primary standard or against the neon secondary standards and no systematic difference was detected between the iron wave-lengths determined from the cadmium line and those that were determined from the neon lines

Most of the measurements were made from plates taken with a 5-mm. étalon, but a few were made from plates taken with 2½- and 10-mm. étalons

The accuracy of the results is similar to that of those given in the region λ 2400 to λ 3100. The systematic error appears from the agreement of the results from different plates to be less than 0·0005 A. and the possible error introduced by the phase correction in this region (λ 3100–λ 3500) is even smaller than that in the extreme ultra-violet and probably very small compared with the other errors. It is thought that the systematic error is not greater than 1 part in 10,000,000, and this seems to be supported by the agreement of the results with other recent work.

The iron arc observed was of the type recommended by the I.A U. in 1928, the negative pole, an iron rod of about 7 mm. diameter, being placed on top, while the positive pole consisted of an iron oxide bead resting on an iron support of about 2 cm. diameter. The upper pole was cooled by means of a large iron bush, and was always kept free from small drops of iron oxide. The arc was maintained with a current of from 3½ to 4 amperes on the ordinary D C. 200 volt mains. Only the light from an area of about 1 mm. square in the centre of the arc was allowed to fall on the étalon.

The lines were chosen so that, if possible, there were no gaps of much more than 10 A. between them, but in a few cases this was not possible, as in this part of the iron spectrum many of the lines are diffuse and unsuitable for wave-length standards. Only a small proportion of the lines chosen as standards were in Lang's* list of lines considered unsuitable for use as standards and these appeared to have reasonably constant wave-lengths in the arc used in this investigation.

Although all the calculations in wave-lengths were carried out to the fourth decimal place, it has been thought advisable to print the results only to the third decimal place, since it is probable that the fourth figure has no very great significance in the case of iron lines, on account of the thickness of the lines themselves and a possibility of hyperfine structure. Moreover, it was not possible to make any correction for the humidity of the atmosphere since there are no data about its effect on the refractive index of air in this region.

The wave-lengths of the 46 iron lines and the nickel line are given in the first column of Table III. The second column gives the number of plates on which the line was measured The third column gives the values recommended by the I.A.U. in 1928, while the fourth gives the values in arc *in vacuo* found by Burns and Walters A letter c after a wave-length in these two columns denotes that wave-length is calculated from term values, and not directly measured The interferometric values found by Burns and Meggers in 1915 appear in the fifth column, those of Buisson and Fabry in the sixth, of Babcock in the seventh, and those of Pressentin in the eighth column. The references to the work of these observers are given later in the paragraph on the comparison with other measurements. A letter L in the ninth column indicates that Lang found this line unsuitable for use as a standard in a short iron arc. The tenth column gives King's† temperature classification, and the next his intensity estimations. The twelfth gives the term classification of the line, and is taken from Burns and Walters' paper. The last column gives the wave number *in vacuo* calculated from the eight figure wave-lengths found in the present investigation. These figures were found with the aid of Kayser's "Tabelle der Scwingungsgahlen," and checked by a calculating machine.

## *Comparison with other Measurements.*

The earliest interferometric measurements in this region are those of Buisson and Fabry.‡ It was shown in my previous paper that their measurements seemed to be systematically too high, and the cause of this error was probably attributable mainly to an incorrect determination of the phase correction of their interferometer plates. It was, therefore, to be expected

* Lang, 'Z. Wiss. Phot.,' vol. 15, pp. 223–292 (1915).

† A. S. King, 'Astrophys. J.,' vol 56, pp. 318–339 (1922).

‡ Buisson and Fabry, 'Astrophys. J.,' vol. 28, p. 169 (1908).

## Table III.

| λ (Jackson). | N. | I.A., 1928 | Burns. Vac arc. | Burns, 1915 Inter-fer | Fabry and Buisson. | Babcock, 1927 | Pressentin, 1930 | Lang | Temp | Int | Classification | Wave number (Jackson). |
|---|---|---|---|---|---|---|---|---|---|---|---|---|
| 3116·633 | 7 | 632c | 633 | 638 | | | | | III | 12 | $a\ ^5F_1—c\ ^5D_2*$ | 32,076 632 |
| 25 658 | 7 | | | | 661 | | | | III | 15 | | 31,983 003 |
| 34·111 | 7 | 111c | 109c | 115 | | | | | III | 10 | $a\ ^5F_3—c\ ^5D_4*$ | 897 765 |
| 57 042 | 2 | | 036c | 043 | | | | L | IV | 8 | $a\ ^7D_4*—13\ W_3$ | 666 079 |
| 60 657 | 2 | | 659 | 660 | | | | L | IV | 10 | $a\ ^7D_4*—16\ W_4$ | 629 866 |
| 75·447 | 7 | | 446 | 450 | | | | L | IV | 12 | $a\ ^7D_5*—25\ W_5$ | 482 552 |
| 78 016 | 7 | | — | 014 | | | | L | IV | 10 | | 455 698 |
| 84 896 | 7 | 895c | 895 | 900 | | | | | IA | 7 | $a\ ^5D_3—a\ ^3F_3*$ | 389·153 |
| 91·660 | 7 | | 660c | 664 | | | | | IA | 7 | $a\ ^5D_4—a\ ^3D_3*$ | 322 635 |
| 96 930 | 8 | | 927 | — | | | | | II | 20 | $a\ ^7D_4*—25\ W_5$ | 271 000 |
| 3199·525 | 7 | | 499c<br>529c | 527 | | | | L | II | 15 | $a\ ^5D_1—a\ ^3F_2*$<br>$a\ ^7D_4*—27\ W_4$ | 245 639 |
| 3200·474 | 7 | | — | 478 | | | | L | IV | 15 | | 236 121 |
| 05 400 | 7 | | 399 | 401 | | | | L | IV | 15 | $a\ ^7D_1*—43\ W_1$ | 188 372 |
| 15·940 | 7 | | 938c | 944 | | | | L | IV | 3 | $a\ ^7D_2*—20\ W_2$ | 086 160 |
| 17 381 | 7 | | 376c | 385 | | | 386 | L | IV | 10 | $a\ ^7D_5*—33\ W_4$ | 072 266 |
| 22 069 | 7 | | 068 | 072 | | | 071 | L | III | 20 | $a\ ^7D_5*—34\ W_5$ | 31,027 043 |
| 25·790 | 7 | | 787 | 792 | 790 | | | L | III | 25 | $a\ ^7D_5—53\ W_6$ | 30,991·240 |
| 36·222 | 7 | 223c | 221 | 227 | | | | | IA | 8 | $a\ ^5D_3—a\ ^3F_4*$ | 891·338 |
| 39·437 | 7 | | | | | | | L | IV | 15 | | 860 593 |
| 44 190 | 7 | | 186 | 189 | | | 189 | L | IV | 15 | $a\ ^7D_4*—34\ W_5$ | 815 476 |
| 54·362 | 5 | | 362 | 367 | | | | | IV | 10 | | 719·167 |
| 57·592 | 5 | | 594 | 598 | | | | | IV | 8 | $a\ ^5P_3—4\ R_2*$ | 688·701 |
| 71·001 | 7 | | 000 | 005 | 003 | | | L | III | 15 | $a\ ^5P_2—e\ ^5P_1*$ | 562·914 |
| 80·261 | 5 | | 258 | 264 | | | | | IV | 8 | | 476·622 |
| 84·587 | 5 | | 586c | 593 | | | | | IV | 5 | $a\ ^5P_2—e\ ^5P_2*$ | 436·465 |

| | | | | | | | | | | | | |
|---|---|---|---|---|---|---|---|---|---|---|---|---|
| 86·754 | 6 | | 754 | 760 | | | | | III | 20 | $a\,{}^5P_3$—$e\,{}^5P_3$* | 416 427 |
| 3298 131 | 6 | | 131 | 136 | | | | | IV | 6 | $a\,{}^5P_1$—$4\,R_2$* | 311 507 |
| 3314·741 | 4 | | 742 | 746 | | | | | IV | 7 | | 159·619 |
| 23 737 | 4 | | — | 741 | 739 | | | | IV | 7 | | 077 997 |
| 28 866 | 4 | | 866 | 870 | | | | | IV | 5 | | 30,032 650 |
| 37·667 | 4 | | — | 670 | | | | | IV | 6 | | 29,952 460 |
| 40 566 | 4 | | 564c | 570 | | | | | IV | 6 | $a\,{}^3P_2$—$2\,R_2$* | 926 472 |
| 47 928 | 4 | | 925 | 932 | | | | | IV | 6 | $a\,{}^3P_2$—$4\,R_2$* | 859 654 |
| 55·229 | 4 | | — | 232 | | | | | IV | 6 | | 795 698 |
| 56 407 | 4 | | — | — | | | | | IV | 3 | | 785 034 |
| 69 553 Ni | 4 | | | 653 | | | | | | | | 668 768 |
| 70 786 | 4 | 787 | 782 | 782 | 789 | 787 | | | IV | 10 | | 658 159 |
| 3399 337 | 4 | | 332 | 338 | 337 | 336 | | | III | 15 | $a\,{}^5P_2$—$d\,{}^5D_2$* | 409 093 |
| 3401 522 | 4 | | 518c | 524 | | — | | | III | 6 | $a\,{}^5F_4$—$b\,{}^5P_3$* | 390 208 |
| 3427 121 | 5 | | 119c | 122 | | 120 | | | III | 20 | $a\,{}^5P_3$—$18R_4$* | 170 677 |
| 43 878 | 3 | | 876 | — | | 878 | | | I | 50*r* | $a\,{}^5D_2$—$a\,{}^5P_1$* | 028 749 |
| 45 150 | 2 | | 148c | — | 155 | 151 | | | III | 20 | $a\,{}^5P_2$—$19_5R_3$* | 29,018 030 |
| 65 863 | 3 | 863 | 861 | — | | — | | | I | 60*r* | $a\,{}^5D_1$—$a\,{}^5P_1$* | 28,844 618 |
| 76·703 | 1 | 705 | 704 | 707 | | | | | I | 40 | $a\,{}^5D_0$—$a\,{}^5P_1$* | 754 680 |
| 85 342 | 4 | | 340 | 343 | 344 | 341 | 343 | | IV | 7 | | 683 410 |
| 90 575 | 3 | — | 574 | — | | 575 | | | I | 100*r* | $a\,{}^5D_3$—$a\,{}^5P_3$* | 640 000 |
| 3497·843 | 3 | 844 | 841 | 847 | | 843 | | | I | 40 | $a\,{}^5D_1$—$a\,{}^5P_2$* | 580 908 |

that there would be a similar, most likely smaller, error in their observations in the region λ 3100 to λ 3500, and an examination of Table III shows that this is the case. The mean systematic difference (B. & F. — J.) for eight lines is +0·002 A., which is about the amount to be expected. If their measurements are corrected by this amount the mean accidental difference is ±0·001 A., which is in very satisfactory agreement, when it is remembered that the observations of Buisson and Fabry were made on the spectrum of a short iron arc, which probably showed pole effect, and that their measurements were made only with an étalon 2½ mm. thick.

The measurements of the lines in the iron arc by Burns and Meggers,* which extend from λ 2860 to λ 3700 A., were made with the nickel sputtered interferometer plates used previously by Buisson and Fabry,† and in the region λ 2850 to λ 3100 were found to be systematically higher than those of the author in this region. This difference was attributed to the use of an incorrect phase correction by Burns and Meggers. Dr. Burns agreed with this conclusion, and when the lines were corrected for this error the agreement with my values was quite satisfactory. The same applies to the wave-lengths in the region λ 3100 to λ 3500, the mean systematic difference (J. — B. & M.) being —0·004 A. for 36 lines, which, as was expected, is slightly smaller than the value (—0·005 A.) for the region λ 2851 to λ 3100. Apart from this the mean accidental difference is ±0·0015 A. It can be seen from Table III that for wave-lengths greater than about λ 3350 the systematic difference becomes abruptly smaller, being only slightly greater than —0·001 A. This is interesting in view of the fact that Burns‡ remarked that there appeared to be a discontinuity in the differences between his measurements and those of Buisson and Fabry at almost exactly this point. Moreover, the amount was 0·0028 A, which is almost exactly the amount of the discontinuity in the differences between my measurements and those of Burns and Meggers. But, as Burns remarked, it is very difficult to see how this systematic error could have entered his measurements, since they were all made on the same set of plates, nevertheless, it appears to be real. If it is treated as such, the mean accidental difference between my measurements and those of Burns and Meggers is only ±0·001 A., almost exactly the amount in the region λ 2850 to λ 3100.

---

* Burns and Meggers, 'Sci. Papers Bur. Stds.,' No. 251 (1925).

† Buisson and Fabry, 'Astrophys. J.,' vol. 28, p. 169 (1908).

‡ Burns and Meggers, *loc. cit.*, pp. 193–194.

In 1927 Babcock* made a very careful examination of the wave-lengths of the lines emitted by an iron arc in air, of the type subsequently recommended by the I.A.U in 1928. In the region λ 3370–λ 3500 there are eight lines common to his list and mine. The mean systematic difference (J. — B.) is only +0·0001 A., *i.e.*, practically nil, while the mean accidental difference is ±0·0006 A This agreement is extremely gratifying and indicates that in this region the type of iron arc recommended by the I.A.U. should form a satisfactory source of wave-length standards

The agreement with the standards adopted by the I.A.U. in 1928 in the region λ 3370 to λ 3500 and with the calculated values recommended in the region λ 3100 to λ 3336 is equally satisfactory since, neglecting the line 3476·70. which I measured on one plate only, the mean systematic difference (J. — I A.) is only —0·0001 A. for eight lines, while the mean accidental difference is ±0·0005 A.

In the region above λ 3370 there are eight lines whose revised interpolated wave-lengths were given by the I A.U. in 1928, which are also in good agreement with the results found in this investigation. The mean systematic difference (J. — R.I.) is —0 0002 A., and the mean accidental difference is ±0·0005 A.

Burns and Walters† have published a very complete list of lines in the vacuum iron arc spectrum which were observed interferometrically, or calculated from levels derived from the observed lines. The measurements were carried out with a very high degree of accuracy. The comparison between their measurements and mine shows that the two are in good agreement. It is to be expected that the systematic difference (J. — B. & W.) will be considerably greater than that in the extreme ultra-violet, on account of the greater effect of pressure shift. Its value is +0·0015 A., including all the lines measured. Since some of the lines involved levels rather sensitive to pressure effect, this amount is about that which is to be expected. The mean accidental difference is about ±0·001 A.

Pressentin‡ has measured a few lines in the ultra-violet part of the spectrum of the iron arc in air by means of the interferometer. It was concluded in my previous paper§ that his measurements were systematically too high, the error decreasing approximately linearly from about 0·005 A. at λ 3100 to zero at λ 3500. This conclusion is confirmed by the present work, but, apart from the systematic differences, the accidental differences between my values and those of Pressentin are not very great, being ±0·001 A. There are only six lines common to both sets of measurements.

---

* Babcock,' Astrophys. J.,' vol. 66, p. 256 (1927).

† Burns and Walters, ' Pub. Alleghany Obs.,' vol. 6, No. 11.

‡ Pressentin, ' Z. Physik,' vol. 60, pp. 125–136 (1930).

§ Jackson, *loc. cit.*, p. 408.

### *The Neon Line at* λ 5852 *and the Red Line of Cadmium in the Vacuum Arc.*

In the course of the work described in this paper and the previous one, a considerable amount of data on the wave-lengths of the neon lines in the red was obtained There was very good agreement with the values adopted by the I.A.U , but it was found that the line λ 5852 A. was better expressed by the value 5852·4875 than 5852·488, which is the value recommended by the I.A.U. This value was obtained both from measurements relative to the primary standard and from measurements relative to the other neon standards. The line was measured on fifteen different plates and it is thought that the wave-length is correct to 1 part in 20 million. This result is interesting in view of the fact that both Monk and Babcock* find the value λ 5852·487 A. for the wave-length of this line.

The wave-length of this line has also been determined by Wallerath,† by Burns, Meggers and Merrill,‡ and by Meissner. The mean of the determinations and those of Monk and Babcock is 5852·4875, which is in exact agreement with my value. Priest found 5852·4862 A., but this is almost certainly too low. This line is now known to have a satellite from the fainter isotope of neon, but this does not seem to affect the constancy of the wave-length of the line. The wave-length of a very heavily exposed line was compared directly with that given by a very lightly exposed one and there was no difference great enough to be detected, *i.e.*, greater than about one part in 20 million. This line is very intense and when produced by a Hilger G.E C. neon lamp, which runs directly off the 200-volt mains, requires an exposure of only 3 minutes with étalon and E(1) spectrograph. It is thought that it would form a more useful standard of length than the red line of cadmium given by the arc *in vacuo*, in cases where it is not convenient to use a Michelson tube.

Various types of quartz cadmium vacuum arc lamp were tried as a source for the red line of cadmium but none was found very satisfactory. The least troublesome contained an alloy of mercury, cadmium and gallium. Gallium was present to an extent of about 1 per cent. while there was about 20 per cent. of cadmium. This lamp gave the red line with reasonable intensity and sharpness, and could be sealed off and used without pumping. However, it was short-lived and it was necessary to melt the alloy with the aid of a Bunsen burner before the arc could be started.

---

* Monk, 'Astrophys J.,' vol. 62, p. 375 (1925); Babcock, 'Astrophys. J.,' vol. 66, p. 256 (1927).

† P. Wallerath, 'Ann. Physik,' vol. 75, p. 37 (1924).

‡ Burns, Meggers and Merrill, 'Sci. Papers Bur. Stds.,' No. 329 (1918); Meissner, 'Ann. Physik,' vol. 51, p. 115 (1916).

The wave-length of the red line of cadmium emitted by a vacuum arc lamp containing pure cadmium was found to be identical with that given by the Michelson tube to within one part in 10 million. It was also compared with the neon secondary standards and found to have a wave-length identical with that of the primary standard within experimental error

A preliminary comparison of the line emitted by the amalgam lamp indicated that it gave too great a wave-length for this line and it therefore seems that this lamp should not be used as a source of the primary standard. Dr Burns, in a private communication, stated that he found that amalgam lamps always gave too high a wave-length for the cadmium red line

A quartz mercury vapour lamp of slightly modified form which had 4 per cent. of zinc added to the mercury was found to give the zinc blue triplet with good intensity with a current of only 3½ amperes The zinc lines, moreover, are very sharp and it seems that this type of lamp may be a very convenient source for the accurate determination of the thickness of étalons Some preliminary measurements of the wave-lengths of the lines have been made, and the results are very satisfactory, but it is thought advisable not to publish any wave-lengths for the three lines until they have been measured with long interference paths by means of one of the new Hilger adjustable étalons. This work is now in progress. The lamp has the additional advantage of providing at the same time a very convenient light source for the adjustment of the parallelism of the étalon plates

The wave-length of the bright ultra-violet line of neon was measured on seven plates and found to be 3520·4733 A. This value is thought to be correct to about one part in 10 million and agrees satisfactorily with 3520·4737 found by Burns, Meggers and Merrill

The line 6402·2 A. in the spectrum of neon appears to be unsuitable for use as a standard, as different observers* have obtained rather widely discordant values. The wave-length found in this investigation was 6402·245 A., but the results from individual plates differed very much more than those for the other neon lines.

---

* See Burns, Meggers and Merrill, *loc. cit.*, p. 770.

In the previous paper on the wave-lengths of iron below λ 3100, there are a few errors which are here corrected.

The majority of the lines between λ 2327 and λ 2628 are due to the spark spectrum of iron, not to the arc spectrum as was implied by the title.

*For* λ 2337·002 *read* λ 2338·002.

I am indebted to Professor Babcock and Miss Moore for drawing my attention to the following additions and corrections to the ninth column of Table IV :—

| λ | |
|---|---|
| 2584·535 | $a\ {}^5F_5 - c\ {}^5G_6{}^*$ |
| 2635·807 | $a\ {}^5F_2 - c\ {}^5G_3{}^*$ |
| 2644·005 | $a\ {}^5F_1 - c\ {}^5G_2{}^*$ |
| 2813·288 | $a\ {}^5F_4 - b\ {}^5G_5{}^*$ |
| 2823·276 | $a\ {}^5F_3 - b\ {}^5G_3{}^*$ |

## *Summary*

Forty-six lines in the spectrum of the iron arc in air, between λ 3100 and λ 3500, have been measured by interferometric comparison with the red line of cadmium or with the secondary standards of neon. The results for lines in common are in very good agreement with observed and calculated values recommended by the I.A.U. in 1928, the mean systematic difference (J — I.A.) being —0·0001 A., while the mean accidental difference is ±0·0005 A. The agreement with the measurements of Babcock is equally good, the mean systematic difference (J. — B.) being +0·0001 A., while the mean accidental difference is ±0·0006 A.

The line at λ 5852, which is the brightest line in the neon spectrum, has been measured against the primary standard and the other neon secondary standards and found to have the wave-length 5852·4875 A.

The wave-length of the red line of cadmium given by a vacuum arc lamp has been found to be identical with that given by the Michelson tube within one part in 10 million.

The wave-length of the brightest of the lines in the ultra-violet group in the neon spectrum has been measured and found to be 3520·4733 A.

In conclusion, it is a great pleasure to thank Professor A. Fowler for his great interest and encouragement throughout the course of the work.

# *Some Investigations on the Deformation and Breaking of Water Drops in Strong Electric Fields.*

By W. A Macky, M Sc, Ph D., Cavendish Laboratory, Cambridge;
1851 Scholar of the University of New Zealand.

(Communicated by C T R Wilson, F R S --Received July 2, 1931)

[Plates 17 21]

## I *Introduction*

It is obvious that for a complete comprehension of the phenomena connected with thunderstorms we must understand the behaviour of free water drops in strong electric fields such as exist in these storms

While no direct experiments have been recorded, there are several papers which give results bearing on the problem Zeleny* made very careful observations on water drops suspended from capillary tubes and showed how filaments of various shapes are formed, but his results are not directly applicable to free drops. Experiments on the breaking of soap bubbles have been made by Wilson and Taylor† and by the writer,‡ which showed that for a given bubble there is a definite field strength at which the bubble becomes unstable. Allowing for the difference in surface tensions deductions were made of the fields required to produce instability in water drops

Nolan§ investigated water drops falling through a horizontal field, measured the fields required to break various sizes of drops, and found that the values agreed with those deduced from the experiments with soap bubbles He further looked for a charging of drops by the Lenard effect, in consequence of their breaking by the electric field, but he was unable to obtain consistent results With water drops at the approximate fields for instability deduced from the soap bubble results, Professor Wilson, in some unpublished observations, noticed the appearance of a glow which presumably was connected with the instability of the drop.

Hence, the present experiments were begun with the intention of studying as fully as possible the deformation of different-sized drops in varying fields both photographically and by eye observations, together with the attendant luminous phenomena.

---

* Zeleny, 'Phys Rev.,' vol. 16, p. 102 and earlier (1920).

† Wilson and Taylor, 'Proc Camb Phil Soc,' vol. 22, p. 728 (1925)

‡ Macky, 'Proc. Camb. Phil Soc.,' vol. 26, p. 421 (1930).

§ Nolan, 'Proc. Roy. Irish Acad.,' vol. 37, A, p. 28 (1926).

It is important to know the maximum fields which can be attained in thunderclouds. and these, presumably, are determined by the drops present. The deformation of drops may alter their rate of fall under gravity, causing an increase in vertical and a decrease in horizontal fields, and the breaking up of drops into smaller ones would cause a large decrease in the rate of fall. Another important question is the amount of ionisation which might be produced by glowing drops, for very intense ionisation might possibly be usual in thunderstorms in consequence. In thunderclouds large drops are few compared with the number of cloud particles, and the presence of a cloud might largely alter the behaviour of a drop. These questions have all been studied in the present experiments

In thunderclouds the electric field is probably more often fairly vertical rather than horizontal, and consequently the behaviour of drops in vertical fields is the more important. With a horizontal field, however, the effects of gravity and of the field are separated , and also, it is possible to subject the drops to the horizontal field for a much longer time, for the drop falls parallel to the field plates, which can be made as long as desired, whereas in a vertical field the drop is exposed to the field only during the time taken to fall the distance between the plates, and this must be small with the limited maximum potentials available in the laboratory. Consequently, both vertical and horizontal fields have been used in the present experiments.

As most thunderstorm phenomena occur at a height in the atmosphere, the effect of reduction of air pressure is important, and experiments have been made to study this also.

## II *Experimental Details.*

The main apparatus used for experiments in a vertical field is shown in Fig. 1. Two brass discs 32 cm. diameter are separated by three ebonite rods, and two saucer-shaped metal basins A and B, 6 cm. deep and 27 cm. diameter, are fastened one to each disc. The drops fell through central holes 2 cm. diameter in basins and discs. The edges of the holes in the basins were as round and smooth as possible to eliminate sparking. The two basins used were specially made ; before they were obtained other basins with less rounded corners were employed, and caused much trouble by sparking from the corners. The water reservoir C had a needle valve to regulate the flow and fitted with a conical joint on to the brass cylinder D, which was fixed centrally on the upper plate. A glass dropper was fastened to the orifice of C by a rubber connection and made to hang centrally by passing through a support E. With these arrangements the drops entered the field uncharged.

The distance between the field plates A and B was 10·3 cm in most of the experiments, but for some of the smaller drops this was reduced to 7·8 cm in order to obtain a sufficiently large field.

For experiments with a horizontal field, two aluminium basins 31 cm. diameter were used as field plates. These were supported by ebonite rods from a wooden framework on the upper cross-piece of which the brass disc and reservoir from the vertical field apparatus was placed, so that the drops fell down between the plates.

For reduced pressures both sets of apparatus were modified and are described later

A potential was generated by a Wimshurst machine, and the value adjusted by a metal point discharge The total potential was measured by a sphere gap calibrated from Kaye and Laby's tables

The water droppers were made from thin-walled glass tubing drawn out to various sizes If the water is run through rapidly, smaller drops are obtained, but the splashing of drops produces difficulties, so the water must run sufficiently slowly to keep the drops well apart. All droppers were well washed, and distilled water used throughout The diameter of the drops was determined by measuring the number required to fill a 10-c.c. vessel A check was made by photographing drops without a field, and the results agreed by the two methods.

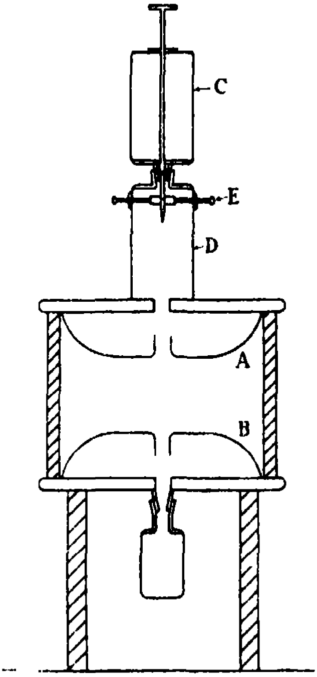

FIG. 1.

### III.—*Nature of the Observations.*

To observe the deformation of the drops, in addition to viewing them against a bright background, discontinuous illumination was used. A bright background was obtained by means of a strong electric lamp and a large condensing lens covered with a sheet of paper. For discontinuous light a mercury vapour lamp was substituted for the electric lamp. The secondary of an induction coil, with capacity in parallel, was connected directly across the lamp so that sparks passed at a frequency of about 50 per second governed by the coil make and break. The drop viewed against this light was seen in instantaneous positions and changes in shape could be readily followed.

The same lens and mercury vapour lamp was used to take photographs by discharging through the lamp a battery of Leyden jars previously charged by the induction coil through a rectifier The drops fell in the beam converging on the camera from the condensing lens and thus appeared dark against a bright background.

As the drops do not fall from the dropper at regular intervals, it was not possible to take photographs automatically and each photograph had to be taken separately. The drops were viewed through an opening in the tube D arranged so that if the observer closed the switch to the lamp as soon as he saw the drop pass the opening, the spark passed when the drop was between the plates, and with the camera shutter open, it was photographed. With practice it was possible to catch at least 60 per cent. of the drops in this manner.

The luminous phenomena connected with the breaking of drops were observed by completely darkening the room and observing the falling drops directly.

## IV.—*The General Behaviour of a Drop in an Electric Field*

When drops fall through an increasing field they become elongated in the direction of the field, but even with the largest drops this is not noticeable until a field of some 5000 volts per cm. is reached. Once the deformation is noticeable it increases rapidly until the length becomes three or four times as great as the diameter. With a slight increase in field beyond this there is a large and very sudden change, the drop becoming unstable It becomes pointed at both ends, and filaments are drawn out from its two ends towards the field plates. The formation of filaments is accompanied by a discharge between the plates , either a glow or a spark is seen in the dark and the small droplets from the filaments collect on the field plates, thus reducing the size of the drop. A much longer filament develops on the positive end of the drop than on the negative, that on the negative end being usually very short, and very little water is deposited on the positive plate in consequence.

These phenomena all occur whether the field is horizontal or vertical and in the latter case whether positive or negative. Owing, however, to the varying conditions, they are manifested in different ways in the several cases.

Nolan (*loc. cit*) has described cases of large drops in a horizontal field which "appear to have divided into a number of distinct parts, which fall

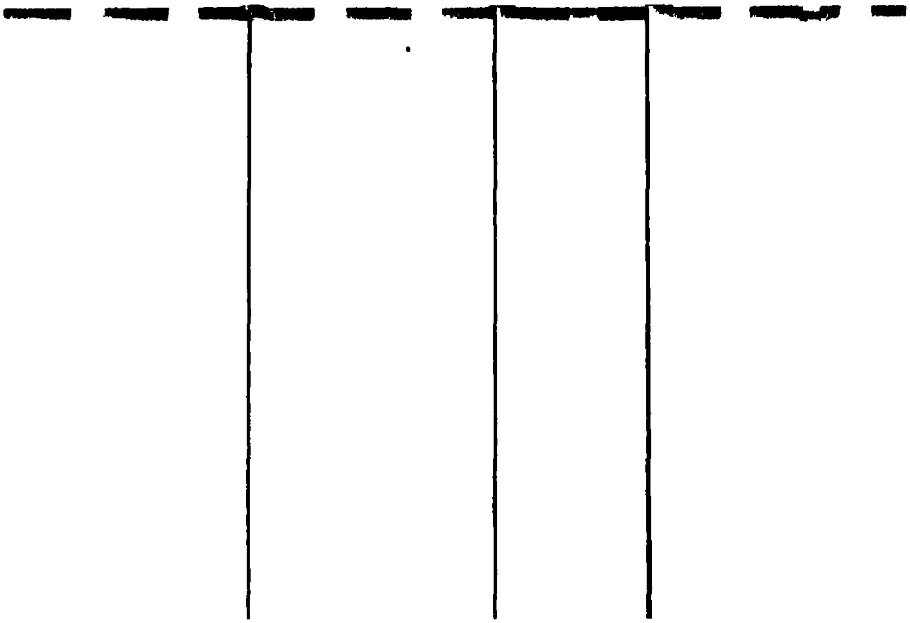

Fig. 2.

Fig. 3.

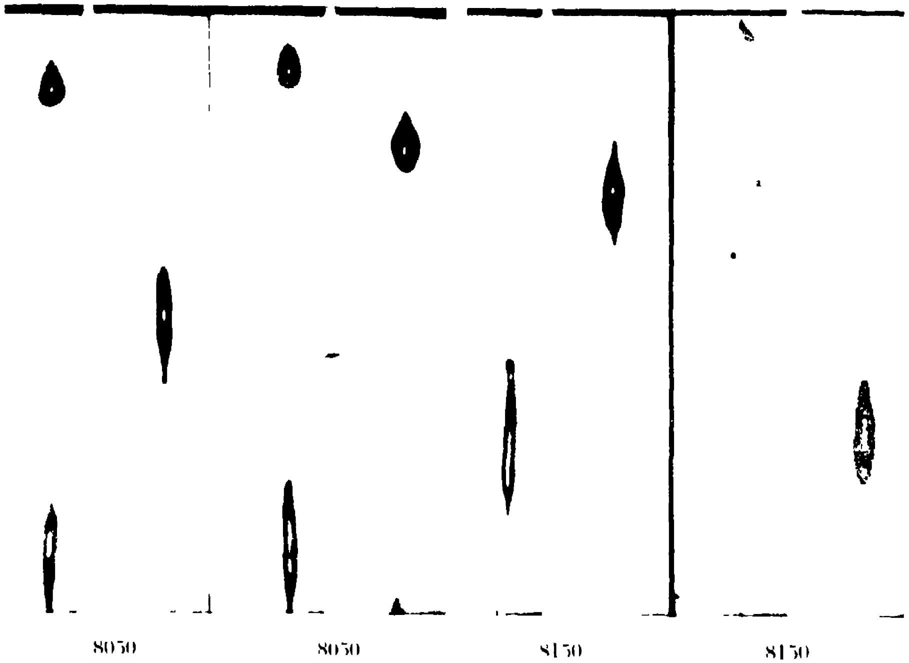

FIG. 4

FIG. 5

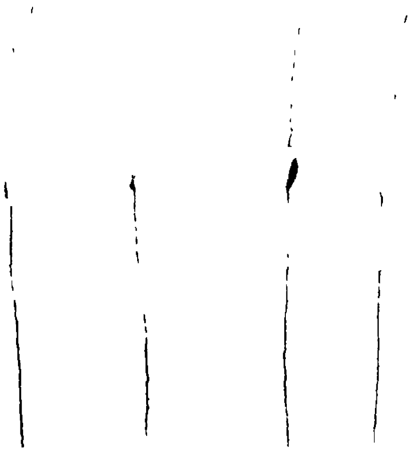

FIG. 10

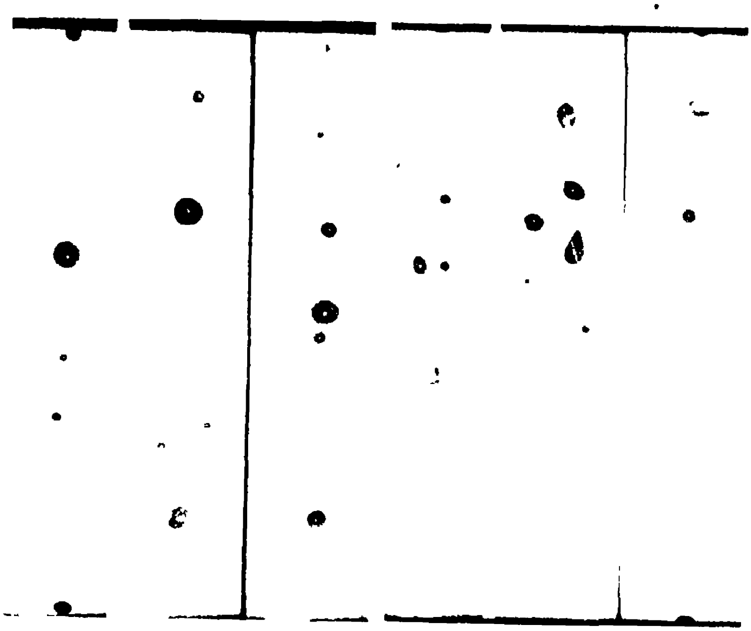

Fig. 6

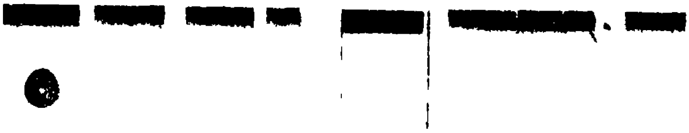

Fig. 7

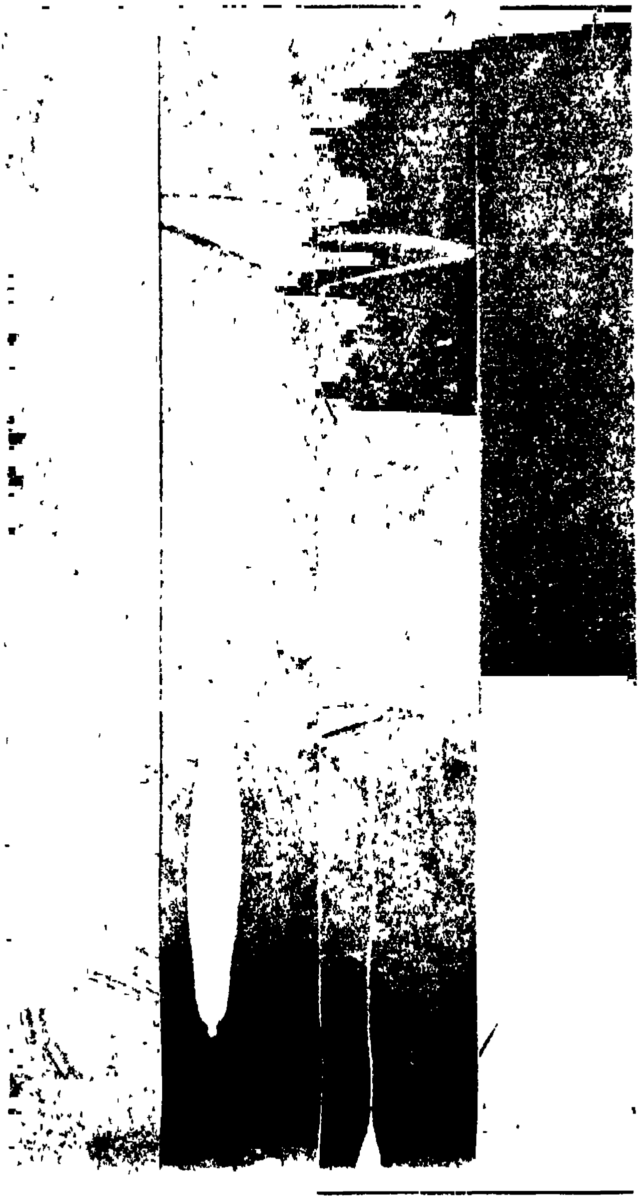

FIG. 8

FIG. 9

FIG. 14

FIG. 21

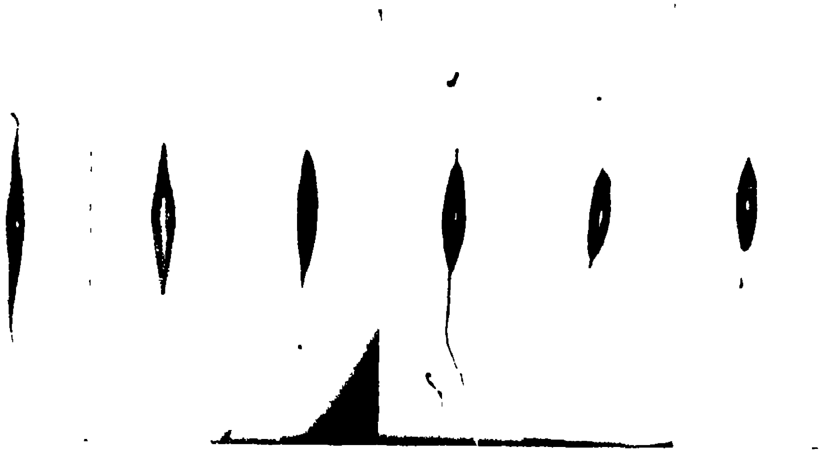

FIG. 13

together without much lateral separation" In the present experiments there was no sign of breaking of drops before filaments appear, and breaking such as Nolan's occurred only when a spark passed, and in this case the resulting droplets usually flew apart and mainly became attached to the field plates

### V.—*The Behaviour of a Drop in a Vertical Field.*

In a vertical field there is a difference according as the field is positive or negative Throughout this paper a positive vertical field is defined, in the usual manner, as one with the upper field plate positive so that the field is of the same direction as the normal atmospheric field.

In a positive field the drop is gradually elongated as described above and the sudden formation of filaments is accompanied by a faint glow in the dark, just before the drop passes out of the field This glow increases in size as the field increases and at its maximum extends from the lower, negative, plate, two-thirds or more of the distance towards the upper positive plate. It is conical in shape, with the base towards the lower plate, where it may be 3 or 4 cm diameter. This glow is very bright and distinct when fully developed. With the larger drops the breaking can be heard as a sound similar to that made when water is forced in a fine spray from a nozzle

With a field in which a bright glow is developed, as the drop enters the field, the upper end becomes more pointed than the lower, but has very little actual filament Lower down the upper filament is diminished, while a filament develops from the lower end of the drop and is continually increased as the drop falls. The bright cone-shaped glow is obviously a discharge from the positive filament.

In fig. 2 (Plate 17) are given photographs of drops in increasing positive fields. They show how in every case a certain amount of time is necessary to produce the deformation, which increases with increasing fields until instability sets in. Natural size.

In fig. 3 (Plate 17) are shown the stages through which a drop passes in a positive field. The field was 8700 volts per cm., and the drop of 0·25 cm. radius was showing a bright conical glow extending from the lower plate two-thirds of the way to the upper plate. Natural size.

Fig. 4 (Plate 18) shows large drops falling in a positive field with the interval between successive drops sufficiently short for two to be in the field at the same time. On the left, drops are shown in a field of 8050 volts per cm., which was causing a bright continuous glow, and on the right, with the same drops in a field of 8150 volts per cm., sparks were passing very frequently.

The drops show the same effects as when falling at longer intervals, namely, a small filament developing at first towards the upper positive plate and then disappearing, while a longer filament extends to the lower negative plate. Natural size.

With drops falling at long intervals, as the field is increased above that required to produce the initial glow, a spark passes with occasional drops instead of a glow, and with a given size of drop there is a small range of field in which either a spark or a glow is possible, the propoition of sparks increasing until at higher fields a spark passes with every drop These sparks pass over the surface of the drop as shown in fig. 5, Plate 18 When a spark passes larger portions are broken from the drop and collect on the two field plates. The smaller the drop, the less is the difference between the fields required to cause a glow and a spark, until with drops of about 0·11 cm. radius sparks pass in almost every case and there are no glows.

Fig. 5 (Plate 18) shows photographs of sparks by their own light with drops of 0·173 cm. radius in the field The field was positive, 12,800 volts per cm., and the plates 7·8 cm. apart. The photographs show how the spark passes over the surface of the drop and also that the drops are considerably elongated and have traversed approximately the same distance in each case. Natural size

Fig. 6 (Plate 19) shows drops from the same dropper as in fig. 4, but the drops are falling much more rapidly so that both large and small drops are present. On the left are drops without a field, and on the right in a positive field of 6800 volts per cm , causing glows and occasional sparks. The track of a spark can be seen in one photograph There is a great amount of distortion with the field and the drops are being broken although no filaments can be seen from the large drops. It is of interest to notice one case where a very small drop, close to a large one, has a filament drawn out joining the two drops together Natural size.

With a negative field there is the same gradual elongation in increasing fields until suddenly filaments are drawn out, but in this case there is even less filament from the negative end than in a positive field, and the filament from the positive end becomes longer and much more distinct as the drop falls away from it, and may extend almost the entire distance between the plates. With a negative field, however, there is no initial period in which a glow is seen and as the field is increased the first discharge when filaments form is usually a spark. Occasionally glows are seen which are as bright and as large as the fully developed ones in a positive field and have their base towards the negative plate, *i.e.*, the cone is inverted. There is no sign at all of a small glow at lower fields and the effect begins suddenly at its maximum. Sparks are much more frequent than glows, but sometimes two or three successive drops will each cause a glow although it is not possible to adjust the field to produce a glow every time

Fig 7 (Plate 19) shows the stages in the deformation of a drop of 0·25 cm. radius in a negative field. The field of 8250 volts per cm. was just causing a spark with each drop and the manner in which filaments are drawn out from the upper positive end of the drop is clearly seen. Natural size.

Fig. 8 (Plate 20) shows the same drops as in fig. 7 but in a slightly bigger field, namely 8300 volts per centimetre. Sparks were passing with every drop and the photographs have been enlarged in order to show more clearly the long filaments which are drawn out from the positive end of the drop Magnification, 2·3.

Fig. 9 (Plate 20) shows on a yet larger scale the filament of the second photograph in fig 8. The mode in which the filament is drawn out thinner and thinner until it finally breaks into drops can be clearly seen. Magnification, 3·4.

Fig. 10 (Plate 18) shows photographs of sparks in a negative field by their own light The drops were 0·173 cm in radius and the field of 12,800 volts per centimetre was causing a spark with each drop. The photographs show how the spark passes over the surface of the drop Comparing with fig. 5 for the similar case in a positive field, it is noticeable that the sparks pass in a more direct line between the plates with the negative field and also that the drops are less elongated in the negative than in the positive field. Natural size.

## VI. *The Behaviour in a Horizontal Field.*

In a horizontal field there is the same elongation as in a vertical field and then the sudden appearance of filaments at a definite field strength, which is the same in both horizontal and vertical fields. The drop being elongated in a horizontal direction, when viewed in continuous light, gives the appearance of being broken into many pieces even when it is still one mass with filaments drawn out. As in a vertical field, the positive filament is much longer than the negative, and frequently extends to the negative plate. It breaks off, collecting on the negative plate as small droplets, while a new filament develops.

In the dark a sheet of glow is seen from the positive end of the drop to the negative plate and, as the field is increased so that filaments extend right to the plate, they appear as dark lines crossing the glow. The drop itself appears as a dark space and on its negative end there is a faint glow, which appears as a line of glow owing to the fall of the drop. The appearance is shown in fig. 11.

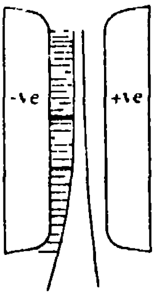

FIG 11.

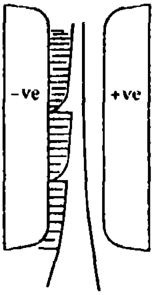

FIG. 12.

When several filaments form and break off while a drop falls through the field, the glow presents a serrated appearance as shown in fig. 12

In a field little larger than that necessary to produce the serrated appearance, a spark passes and usually no glow is seen Sometimes, however, when a spark passes as soon as the drop enters the field, a glow will occur lower down, presumably due to the field being momentarily reduced by the spark but not to a value less than that required to produce a filament and consequently a glow , the effect may also be partly due to reduction of the size of the drop by the spark. With a spark no filament can be seen and the drop appears little more elongated than before the initial glow It usually breaks up into three or more large portions with many smaller drops immediately after the spark, and of the larger portions one is drawn to the positive and one to the negative plate, while the main central part falls straight down

In fig. 13 (Plate 21) are shown drops giving very bright glows and occasional sparks in horizontal fields between 9700 and 10,800 volts per centimetre. The negative plate is on the left, and in every case there is a much longer filament on the positive than on the negative end of the drop. In several cases it reaches right to the negative plate. Magnification, 1·37.

In all the above cases the drop was falling centrally between the plates ; if, when a glow was visible, the drop was made to fall near the negative plate no great change occurred in the discharge, but if the drop fell within 1 or 1½ cm. of the positive plate, then a spark passed with each drop and no glow was seen, although the field to cause the spark remained the same as for the initial glow.

Fig. 14 (Plate 21) shows two cases of drops falling near the positive plate so that a spark passed with every drop. The photographs illustrate the strange shapes which a drop may assume owing to its vibrations after the passage of a spark. Magnification, 1·37.

When the drop fell close to the plate a large amount of water collected on the positive plate, and in most cases was sufficient to cause a spark from the plate itself after the passage of one drop, and so prevent further observations. The collection of drops on the positive plate and consequent sparking without reference to the falling drops was a constant source of trouble in all experiments, both with vertical and horizontal fields, and it was frequently necessary to stop the observations in order to dry the plates.

When a drop collected on either field plate large enough to give a discharge in fields less than required to break the falling drop, it was frequently noticed that a drop falling straight through would receive a charge in passing through the stream of ions, and consequently would be deflected towards the opposite plate. This showed how readily a drop can receive a large charge under such conditions.

### VII. *The Nature of the Luminous Discharges.*

When a steel ball 6 mms. diameter (*i.e.*, larger than any drop used) was mounted on an insulating rod between the plates, a field of 19,000 volts per cm. was necessary to cause a discharge; this was always a spark. A drop of this size would glow in a field of half this value, so it is clear that the glow is due to the deformation of the drop.

With a small double-ended metal cone 1·5 cm. long and 4-mm. maximum diameter the discharge is as shown in fig. 15. A bright glow extends from the positive end to the negative plate, and on the negative end there is a very much smaller glow almost confined to the surface of the cone. With increase of field the glow extends further from the negative point, while the positive discharge develops brighter streaks until eventually a spark passes.

If the cone is moved nearer the negative plate when a glow is passing there is no appreciable change, but if it is put within a centimetre of the positive plate a spark passes which becomes stronger the closer the cone is to the plate. With the cone, as there are no filaments to form, the same effects are observed in horizontal or vertical fields.

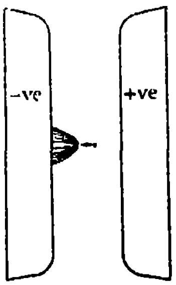

FIG. 15.

Thus it is obvious that the discharges from falling drops are of the nature of those from a metal cone, and the difference in the discharges from the two ends are merely the differences between discharges from positive and

The passage of a spark in a negative vertical field without an initial glow is most probably due to the fact that when the drop falls near to the positive plate before a discharge passes, then the discharge is a spark. The photographs show that it takes an appreciable time for a drop to be drawn out, and hence in the lowest fields causing instability the drop will not become unstable until it has nearly reached the lower plate Hence when this plate is positive a spark passes, and when negative a glow results Consequently, this observed difference is possibly due entirely to the presence of field plates, and in the free atmosphere there may be no appreciable difference in the behaviour of a drop in positive or negative fields

Another factor, however, which may be of some importance is flattening of the drop due to its motion through the air. The lower surface will tend to be more flattened than the upper, and this difference might be a factor in causing a spark in a negative field without the initial glow discharge found in a positive field.

## VIII. *The Fields necessary to Cause Instability in Drops of Various Sizes*

Observations were made of the field required to cause instability in drops of various sizes in both horizontal and vertical fields The onset of instability was determined by the passage of a glow in horizontal and positive vertical fields and a spark in a negative vertical field. The results are given in Tables I and II, and plotted in fig. 16 The values of the product of Instability Field

Table I —Glowing and Sparking Fields for Drops of different radii in a Vertical Field.

| Radius | Positive field. |  | Negative field spark | F × √(Radius) |
|---|---|---|---|---|
|  | Glow F. | Spark |  |  |
| cm. | volts/cm | volts/cm | volts/cm. |  |
| 0·117 | 11,400 | 11,600 | 11,350 | 3900 |
| 0·122 | 11,350 | 11,650 | 11,400 | 3960 |
| 0·132 | 10,700 | 11,200 | 10,700 | 3890 |
| 0·136 | 10,500 | 10,900 | 10,500 | 3870 |
| 0·139 | 10,450 | 10,900 | 10,400 | 3900 |
| 0·143 | 10,250 | 10,800 | 10,300 | 3880 |
| 0·144 | 9,950 | 10,500 | 9,950 | 3780 |
| 0·147 | 9,850 | 10,450 | 9,850 | 3780 |
| 0·153 | 9,700 | 10,400 | 9,800 | 3790 |
| 0·160 | 9,400 | 10,350 | 9,400 | 3760 |
| 0·165 | 9,350 | 10,150 | 9,350 | 3800 |
| 0·185 | 9,100 | 10,000 | 9,100 | 3920 |
| 0·188 | 8,950 | 10,000 | 8,950 | 3880 |
| 0·193 | 8,750 | 10,000 | 8,750 | 3830 |
| 0·205 | 8,750 | 10,000 | 8,750 | 3960 |
| 0·226 | 8,350 | 9,500 | 8,400 | 3970 |
| 0·253 | 8,050 | 9,500 | 8,050 | 4050 |

Table II.—Glowing and Sparking Fields for Drops in a Horizontal Field.

| Radius drop. | F, Field necessary to cause glow | Field necessary to cause spark | F × √(Radius). |
|---|---|---|---|
| cm. | volts/cm | volts/cm. | |
| 0·085 | 13,200 | 13,200 | 3840 |
| 0·106 | 11,900 | 11,900 | 3880 |
| 0·128 | 10,900 | 11,000 | 3900 |
| 0·131 | 10,650 | 11,000 | 3860 |
| 0·134 | 10,450 | 11,000 | 3820 |
| 0·143 | 10,100 | 10,700 | 3820 |
| 0·154 | 9,750 | 10,100 | 3810 |
| 0·174 | 9,100 | 9,900 | 3790 |
| 0·202 | 8,750 | 9,700 | 3930 |
| 0·228 | 8,200 | 9,200 | 3910 |
| 0·254 | 8,000 | 8,800 | 4030 |

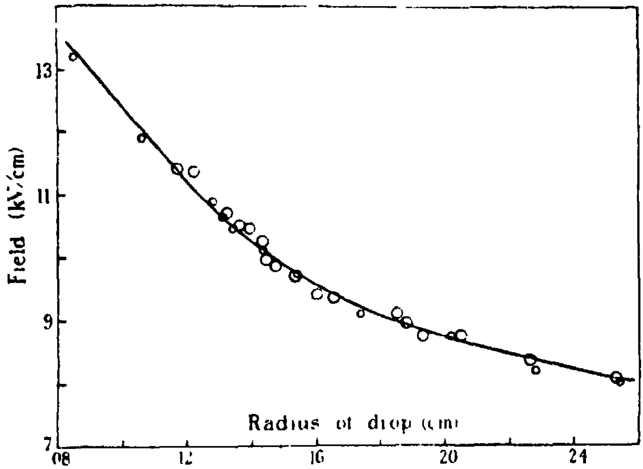

FIG. 16.—Fields causing a Discharge with Drops of Different Radii. Large circles are in a vertical field, small circles in a horizontal field.

and Square Root of Radius have been worked out and have a mean value of 3875 in Vertical Fields and 3870 in Horizontal Fields, which is very good agreement also with Nolan's value of 3880 for breaking of drops in a Horizontal Field.

## IX. *The Effect of Increased Velocity of Fall.*

In the majority of experiments with a vertical field, the drops fell about 23 cm. before reaching the centre of the field, and their velocity at this point would not be greater than 2 m. per second. In the atmosphere the drops will be, in general, at their terminal velocity, which for the largest drops is 8 m. per second; there will, therefore, be considerable deformation of these drops.

In order to see if the rate of fall influenced the commencement of instability, an extended tube support was made for the water reservoir, so that the drops fell 110 cm. before reaching the centre of the field and would therefore be falling more rapidly.

A great deal of difficulty was caused by splashing of the drops on the plates and consequent erratic sparking.

Measurements were made of the glow and sparking fields as before, and the results are given in Table III and also plotted in fig. 17 with the normal curve for comparison

With the smaller drops of less than 0·14 cm. radius the increased fall had no effect, but with larger drops the positive glow did not begin until a higher field with the increased fall, and the negative spark also required a larger field, though not so great as the positive glow

Table III.—Glowing and Sparking Fields for Drops after a fall of 110 cm.

| Radius. | Positive field. | | Negative field. |
|---|---|---|---|
| | Field to cause glow. | Field to cause spark | Field to cause spark. |
| cm. | volts/cm. | volts/cm. | volts/cm. |
| 0·128 | 10,900 | 12,400 | 10,900 |
| 0·130 | 10,800 | 12,400 | 10,800 |
| 0·132 | 10,700 | 12,300 | 10,700 |
| 0·134 | 10,600 | 12,300 | 10,600 |
| 0·137 | 10,600 | 12,400 | 10,450 |
| 0·143 | 10,500 | 12,400 | 10,450 |
| 0·144 | 10,400 | 12,250 | 10,350 |
| 0·158 | 10,400 | 12,300 | 10,150 |
| 0·178 | 10,150 | 12,500 | 9,900 |
| 0·201 | 9,950 | 12,200 | 9,250 |
| 0·225 | 9,700 | 12,500 | 8,900 |

The smaller drops were probably near their terminal velocity in both cases, and hence there was no difference.

With the large drops it is probable that the main difference from the case of slower-falling drops is due to the smaller time during which the drops are under the influence of the field. This is borne out by the results in a horizontal field, where the drops fell a distance of 55 cm. before reaching the centre of the field and the values obtained agreed with those for the slower drops in a vertical field.

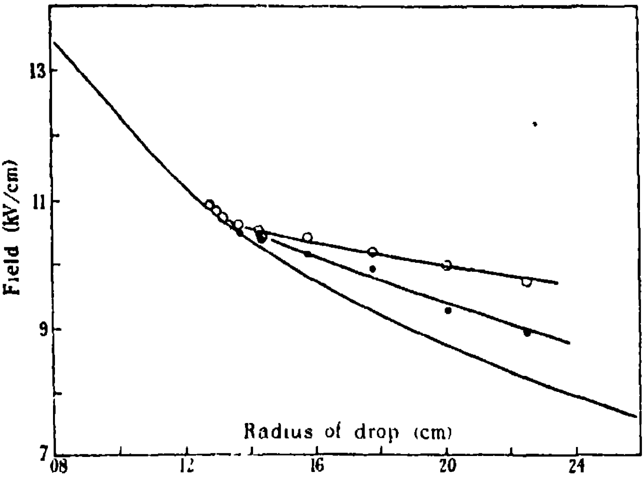

FIG. 17.—Fields causing a Discharge in a Vertical Field, after drops have fallen 110 cm. The smooth curve gives discharge fields in vertical fields after a short fall or in a horizontal field. Circles give fields for a glow in a positive field after a 110 cm. fall. Dots give fields for a spark in a negative field after a 110 cm. fall where the value differs from that for a glow in a positive field.

Another effect which might increase the discharge fields is the increased flattening of the drop due to its motion through the air, as mentioned in Section 7. The lower surface will tend to be much more flattened than the upper, and this difference might be a factor in producing a spark in a negative field at a lower field than required to give a glow in a positive field.

### *X —The Field Necessary to Cause Instability in a Free Drop of any Liquid.*

Wilson and Taylor showed theoretically that the field required to make any drop unstable is given by

$$F = \text{Constant} \times \sqrt{(\text{Surface Tension/Radius})}.$$

Taking the mean value of $F\sqrt{r}$ for water drops as 3875 and 75 c.g.s units as the surface tension of water, then the constant in the equation equals 447.

Similarly, if we take the value for soap bubbles given in the earlier paper, *i.e.*, $F\sqrt{r} = 3400$, and 58 c.g.s. units as the effective surface tension on both sides of the film, then the value of the constant comes as 446.

These two values are in very good agreement, so it is probable that the field required to produce instability in any drop is given by the expression

$$F = 447\sqrt{(\text{Surface Tension/Radius})}$$

### XI.—*The Behaviour of a Drop in a Cloud of Smaller Ones.*

It will usually be the case in a thunderstorm that large drops are relatively few in number, and are surrounded by a large number of smaller ones. Hence it is of interest to observe the behaviour of a large drop falling through a cloud.

The enclosed apparatus as used for low pressures was arranged so that it could be suddenly connected to an evacuated vessel, thus producing a thick cloud between the field plates. The cloud itself produced practically no diminution in the discharge field, and when larger drops passed through the cloud the same fields were required to deform and break them, and produce a discharge as without the cloud. Similar results were found with drops falling through a fine-water spray projected between the plates from a nozzle.

From these experiments it is reasonable to assume that in the atmosphere the fields at which a discharge begins will depend upon the largest drops present, and will be independent of the smaller ones.

### XII.—*The Effect of Reduction in Pressure of the Surrounding Air.*

As most thunderstorm phenomena take place at a height in the atmosphere it is necessary to consider the behaviour of drops at lower than normal air pressures. Although reduction of pressure is unlikely to alter the fields required to produce instability in the drops, it was possible that at the lower pressures a discharge would pass before filaments were drawn out from the drops. Observations have therefore been made as to the fields causing discharges at lower pressures.

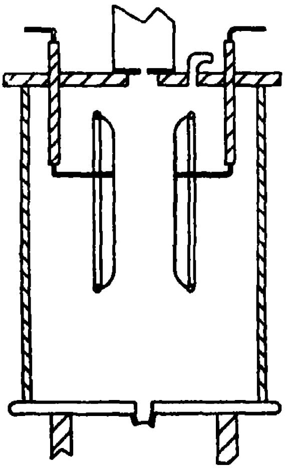

Fig. 18.

In the vertical field apparatus a glass cylinder 20·5 cm. long and 31 cm. diameter was substituted for the ebonite insulators between the field plates, and the apparatus used exactly as before. For a horizontal field the apparatus shown in fig. 18 was used, the field plates consisting of two aluminium basins with flat bottoms 20 by 10 cm.

In both cases the glass was covered with shellac, but the splashing of water destroyed the insulation and necessitated frequent drying of the inside of the glass.

The effect of pressure is found to be the same with both horizontal and vertical fields. Measurements of the field required to produce a discharge at

50 cm. pressure (which corresponds to a height of 3·5 kms in the atmosphere) were made with different drops in a vertical field, and the results are given in Table IV. They show that a discharge passes at the same field strength at 50 cm. pressure as at normal atmospheric pressure. With each particular size of drop the discharge field was measured at normal atmospheric pressure immediately after the measurement at 50 cm., and in no case was there any difference. Eye observations in discontinuous light showed that the passage of a discharge was accompanied by breaking of the drops just as at normal pressures.

Table IV.—Vertical Fields Required to Cause a Discharge with Different Drops at an Air Pressure of 50 cm

| Radius of drop. | Positive field causing glow | Negative field causing spark | Instability field $\times\sqrt{(\text{Radius})}$ |
|---|---|---|---|
| cm. | volts/cm | volts/cm | |
| 0·133 | 10,650 | 10,600 | 3875 |
| 0·141 | 10,250 | 10,350 | 3870 |
| 0·149 | 9,650 | 9,750 | 3745 |
| 0·159 | 9,600 | 9,600 | 3830 |
| 0·178 | 9,050 | 9,150 | 3840 |
| 0·185 | 9,150 | 9,200 | 3945 |
| 0·192 | 8,600 | 8,600 | 3770 |
| 0·205 | 8,550 | 8,650 | 3895 |
| 0·227 | 8,350 | 8,400 | 3990 |

Observations of the field at which a discharge passes were made with a drop of 0·227 cm. radius down to pressures of 16 cm in a vertical field. For comparison the fields were measured at which discharges passed between the same field plates at the lower air pressures in the absence of water drops.

The results obtained are given in Tables V and VI, and plotted in fig. 19.

Table V.—Fields at which a Drop of 0·227 cm. radius Causes a Discharge at Various Air Pressures.

| Air pressure | Field to cause discharge | Nature of discharge |
|---|---|---|
| cm. | volts/cm. | |
| 76·9 | 8450 | Glow. |
| 50·0 | 8400 | Bright glow. |
| 36·5 | 8350 | Very bright glow |
| 27·2 | 8400 | Very bright glow. |
| 25·8 | 8400 | Very bright glow, almost an arc |
| 24·9 | 8150 | Very bright glow, almost an arc. |
| 24·1 | 8050 | Very bright glow, almost an arc. |
| 21·5 | 7450 | Arc through drop. |
| 20·0 | 7250 | Arc, sometimes not via drop |
| 19·2 | 7200 | Arc, sometimes not via drop |
| 17·8 | 6750 | Arc direct, only sometimes via drop. |
| 16·4 | 5900 | Arc direct and never via drop |

Table VI.—Fields at which Discharge Passes between the Same Field-plates without Drops at Various Air Pressures.

| Air pressure. | Field to cause discharge. |
|---|---|
| cm. | volts/cm. |
| 27·7 | 9400 |
| 26·4 | 9250 |
| 24·9 | 8850 |
| 21·0 | 7900 |
| 18·6 | 6800 |

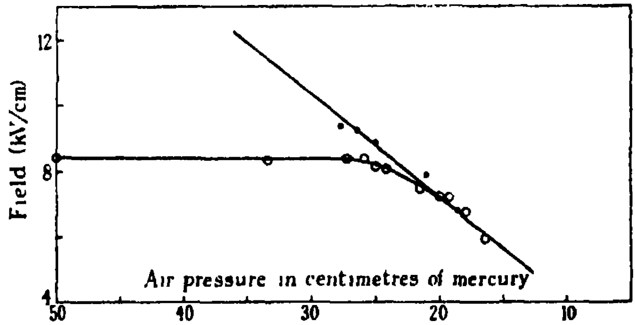

FIG. 19.—Fields causing a Discharge between the Plates. Circles, with water drops of 0·227 cm. radius falling through. Dots, without water drops.

It can be clearly seen from the graph that the field necessary to cause a discharge remains constant as the air pressure is reduced, until the pressure is nearly reached at which a discharge would pass in the absence of a drop. There is a short range of pressure where the presence of the drop causes a slight diminution in the discharge field ; and then at pressures below this the discharge passes directly between the plates and the drop has no apparent influence on the discharge.

The values given were obtained in a positive vertical field, but the same effect occurred in a negative vertical field and in a horizontal field.

Observations were also made at various pressures with a drop of 0·14 cm. radius, and they gave exactly similar results.

The most marked effect produced by reduction of air pressure was that a glow at atmospheric pressure became brighter, and eventually became a spark as the pressure was reduced. The effect is noticed in both vertical and in horizontal fields, but is more pronounced with a horizontal field.

The pressure at which transition from glow to spark takes place varies with the size of the drop, a glow persisting to a lower pressure the larger the drop. The extent of the effect is shown by Table VII.

Table VII.—Air Pressures in Centimetres Mercury at which a Discharge Changes from a Glow to a Spark at Constant Field.

| Radius of drop. | Always a spark at pressures below | Alway a glow at pressures above |
|---|---|---|
| cm. | cm | cm. |
| 0·139 | 56 | 65 |
| 0·173 | 54 | 60 |
| 0·254 | 50 | 53 |

When viewed in instantaneous illumination, it is seen that whenever a glow passes the positive filament is quite distinct, and the negative filament is also present, although very much shorter No filaments at all, however, are visible when a spark passes, and the drop, although considerably elongated, has rounded ends. Immediately after a spark the drop assumes various shapes, and smaller drops break away, sometimes completely breaking up the main drop.

Presumably at lower pressures, the field at the small rounded end of the drop reaches a value sufficient to cause a spark before a filament is formed. Thus a spark passes, and there is no initial glow discharge.

## XIII. *The Rate of Loss of Water from a Drop in an Electric Field.*

An approximate measurement was made of the rate of loss in a vertical field by comparing the sizes of drops which had and had not fallen through the field.

It was found in this way that a drop of 0·160 cm. radius when glowing in a field of 9750 volts per cm , which exceeds the critical instability field by 350 volts per cm., lost 0·00077 grams in passing through the field. At this rate it would lose half its mass in a time of approximately one-half second.

In a horizontal field the water removed from the falling drops collected on the field plates, and the amount deposited from a definite number of drops was measured with weighed pieces of blotting-paper.

The results are given in Table VIII, and, estimating that the drop is in the field for 1/20 second, they show that the larger drop when just beginning to glow loses half its mass in 1½ second ; when nearly sparking only one-half second is required. The smaller drop when nearly sparking also loses half its mass in one-half second. The rate of loss is very much greater with a spark than with a glow. The breaking up of a drop by a spark is possibly due to sudden oscillations of the elongated drop when the field is momentarily removed, and heating by the actual current passing may have some effect.

Table VIII.—Mass Lost by Drops falling through a Horizontal Field.

| Radius. | Mass. | Type of discharge | Field | Mass deposited per drop on positive plate. | Mass deposited per drop on negative plate. |
|---|---|---|---|---|---|
| cm | grm | | volts/cm | grm | grm |
| 0·156 | 0·0157 | Glow | 10,000 | 0·00006 | 0·00060 |
| | | Spark | 10,000 | 0·00080 | 0·00140 |
| 0·225 | 0·0476 | Glow | 8750 | 0·00015 | 0·00060 |
| | | Glow | 8900 | 0·00036 | 0·00167 |
| | | Glow | 9000 | 0·00082 | 0·00182 |
| | | Spark | 9400 | 0·00600 | 0·00700 |

Zeleny* states that alcohol was ejected from a drop of 0·0189 cm. radius at the end of a tube at the rate of $10^{-4}$ c.c. per second. This corresponds to a loss of half its mass in 1/7 second, which is comparable with the present results.

The values in Table VIII show clearly that with a glowing drop the amount of water ejected from the positive end is many times greater than the amount from the negative end. This difference between the amounts of water ejected from the positive and the negative ends of a drop explains the difference observed between the breaking of positive and negative soap bubbles. It was found (*loc. cit.*) that a positive bubble always bursts very soon after becoming unstable, whereas a negative bubble frequently vibrates for a considerable time before bursting. The reason is that the rate of ejection of solution is small from a negative discharge and sufficient solution can be drawn up from the supply to balance the amount ejected, whereas with a positive discharge the rate of discharge is so great that fresh solution cannot be drawn up sufficiently rapidly to cope with the loss, and the bubble bursts.

## XIV. *The Charge passing through a Glowing Drop.*

(*a*) *Vertical Field.*—The charge passing through a drop in a vertical field was measured using the apparatus shown in fig. 20. A disc 3·9 cm. diameter, with a central hole of 1·8 cm. diameter, was insulated in the centre of the lower plate and connected to the measuring system as shown. The diameter of the disc was sufficient to contain all the base of the glow in a positive field, and tests with the whole lower plate insulated showed that all the charge was going to the central disc.

---

* Zeleny, 'Proc. Camb. Phil. Soc.,' vol. 18, p. 75 (1915).

The lower plate and disc were connected to earth, and when the field was adjusted as required, the central disc was isolated and the charge passing with one or two drops measured An electrostatic voltmeter was used, and several Leyden jars were added to the capacity as large charges were received.

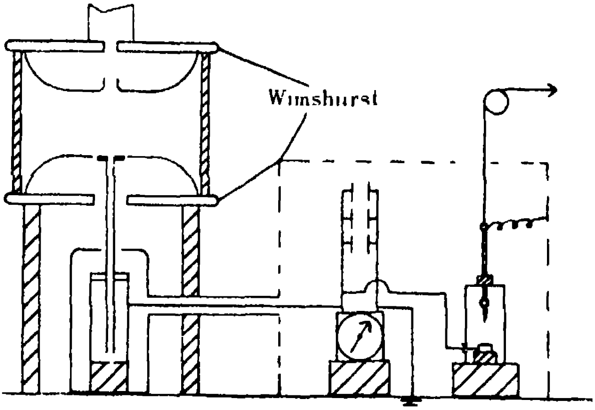

FIG. 20

Careful observations were made to detect the stage at which charging begins, and in every case it was found to coincide with the beginning of instability, with formation of filaments, and a faint glow. In a field which did not cause a glow and yet was within about 2 per cent of that required to do so, no charging at all could be detected ; a charge of 1 per cent. of that given by the smallest glow would have been apparent.

A given size of drop glowing in a definite field gave almost constant values of discharge. It was not possible to determine the charge carried by glows in a negative field as they are far too irregular in occurrence, but there is no reason to suppose that it should be different from the case of a positive field.

The charges which passed through glowing drops of two sizes in various positive fields are given in Table IX.

(*b*) *Horizontal Field.*—To measure the charge passing in a horizontal field one field plate was earthed and connected to the measuring apparatus as before, and arranged so that it could be isolated when desired. Since the field decreased as a result of the passage of the discharge, observations were made on only the first two drops. The values obtained for given drops in a

Table IX.—Charge Passing Through a Glowing Drop in a Positive Vertical Field.

| Radius of drop. | Initial discharge field | Field. | Charge per drop E S.U. |
|---|---|---|---|
| cm. | volts/cm | volts/cm. | |
| 0·136 | 10,500 | 10,550 | $12 \times 10^2$ |
| | | 11,450 | $25 \times 10^2$ |
| | | 11,850 | $37 \times 10^2$ |
| 0 156 | 9,800 | 10,000 | $5 \times 10^2$ |
| | | 10,150 | $9 \times 10^2$ |
| | | 10,500 | $21 \times 10^2$ |
| | | 10,700 | $27 \times 10^2$ |
| | | 10,850 | $33 \times 10^2$ |
| | | 11,200 | $41 \times 10^2$ |
| | | 11,800 | $50 \times 10^2$ |

definite field were not so constant as in the vertical field, and variations up to a factor of two were noted.

The mean values found with three different sizes of drops are given in Table X.

Table X.—Charge Passing Through a Glowing Drop in a Horizontal Field.

| Radius of drop | Initial discharge field. | To positive plate | | To negative plate. | |
|---|---|---|---|---|---|
| | | Field. | E S.U./drop | Field. | E.S U /drop. |
| cm. | volts/cm | | | | |
| 0 128 | 10,900 | 11,250 | $35 \times 10^2$ | 11,000 | $55 \times 10^2$ |
| | | 11,300 | $45 \times 10^2$ | | |
| | | 11,700 | $60 \times 10^2$ | | |
| 0 156 | 9,800 | 9,850 | $50 \times 10^2$ | 10,000 | $45 \times 10^2$ |
| | | 10,000 | $85 \times 10^2$ | 10,150 | $60 \times 10^2$ |
| | | 10,150 | $95 \times 10^2$ | 10,450 | $95 \times 10^2$ |
| 0·225 | 8,350 | 8,760 | $55 \times 10^2$ | 8,900 | $30 \times 10^2$ |
| | | 8,850 | $60 \times 10^2$ | 9,050 | $60 \times 10^2$ |
| | | 9,050 | $75 \times 10^2$ | 9,250 | $65 \times 10^2$ |
| | | 9,250 | $95 \times 10^2$ | 9,400 | $90 \times 10^2$ |

(*c*) *The Current Passing Through a Glowing Drop.*—By calculating the velocity of the drop from its distance of fall, we can estimate the duration of the glows and hence the actual current passing through the drops.

From the above results for a drop of 0·156 cm. radius in a field of 10,000 volts per cm., *i.e.*, 200 volts per cm. above the critical instability field, the current passing was 15 microamperes in a Vertical Field and 30 microamperes in a Horizontal Field. The difference between the two cases is probably due to the errors in estimating the duration of the glows, so it is probable that such a drop, as soon as it begins to glow, will pass a current of the order of 20 microamperes.

It is of interest to compare this figure with results obtained by Zeleny* for a discharge from a water point at the end of a tube. He obtained a current of 2·5 microamperes from a drop of 0·028 cm. radius with a potential 20 per cent. above that required to start a discharge and when the potential was increased to double the starting value a current of 17 microamperes was obtained.

(*d*) *The Charge Acquired by a Drop in an Electric Field.*—An attempt was made to detect any charge carried by the drop, after passing out of the field, by collecting drops in a Faraday cylinder, connected to a measuring apparatus. No charge was ever detected greater than about one E.S.U., and both sign and magnitude of the charge were quite erratic. This is only to be expected when currents of the order found above are passing through the drop and it is obvious that any resultant charge found on the drop is largely fortuitous. Nolan† attempted to measure the charging of drops due to the mechanical disruption when broken in his horizontal fields, and obtained very erratic results. The explanation was almost certainly the same as in the present experiments. Nolan mentions the possibility of a discharge from the drop to one of the field plates, but the fact that he observed the drops only in a bright light probably prevented him detecting any glow discharge.

## XV. *The Field necessary to cause Discharge from a Flat Water Surface.*

To see if a discharge passes more readily from a flat water surface than from a metal one, a sphere 15 cm. diameter was held centrally 2·6 cm. above a flat dish of water and the two connected to opposite poles of the Wimshurst. Whether the sphere was positive or negative there was no glow, and the first discharge was a spark from a flat cone drawn up in the water surface. The appearance is shown in fig. 21, Plate 21. This discharge took place with a potential of 67 kv. and, when a wide metal surface was substituted for the water at the same distance, the discharge passed at 71 kv. Thus the reduction due to the water was only 6 per cent., and it would probably have been less but for small ripples on the water surface, due to vibration from the Wimshurst.

---

* Zeleny, 'Phys. Rev.,' vol. 3, p. 82 (1914).

† *Loc. cit.*, p. 32.

It is interesting to note how the discharge passes over the surface of the water to the electrode at the side of the earthenware vessel.

## XVI. *Some Applications of results to Thundercloud Problems.*

As a result of his experiments, Zeleny* concluded that all the current from a liquid point was carried by small droplets; but Nolan and O'Keeffe† measured the mobility of the ions from a liquid point, and, finding values of one or two cm. per second per volt per cm, concluded that the current is carried by ordinary gaseous ions. The modes of breaking of drops and the luminous discharges observed in the present experiments confirm Nolan's conclusion. Thus, when currents of the order of 20 microamperes are passing from a drop, the amount of ionisation produced by the drop in the air will be very great. It is probable, therefore, that such point discharges from drops will be one of the main sources of ionisation in thunderstorms.

The removal of water by the formation of filaments will set a limit to the size of drops in a thunderstorm. Thus no drops greater than 0·15 cm radius can persist in fields of 9800 volts per cm.

Since the discharge field with drops is independent of the pressure, the field inside thunderstorms will in general rise to a value of the order of 10,000 volts per cm. before a discharge passes. This result is important, as it bears on the production of high energy β-particles, in consequence of the high fields combined with the small loss of energy by collision suffered by electrons at the lower air pressures.

## XVII. *Summary.*

The investigations were concerned with the effect of strong electric fields on water drops ranging in radius from 0·085 to 0·26 cm.

When exposed to increasing fields, a water drop of given radius, $r$ cm. becomes elongated, until at a definite field given in volts per cm. by $F\sqrt{r} = 3875$ it becomes unstable, and filaments are drawn out from the ends.

When instability occurs, a discharge passes through the drop in exactly the same manner as it would through a conductor pointed at both ends, giving the luminous effects characteristic of positive and negative point discharges.

The current through the drop is of the order of 20 microamperes when the critical field is exceeded by a very small amount.

The fields producing discharge through the drops are unaltered by reduction of the air pressure, until the pressure is reached at which the field only slightly exceeds that required to cause a discharge in the absence of the drops.

---

* Zeleny, 'Proc. Camb. Phil. Soc, vol. 18, p. 71 (1915); and 'Phys. Rev., vol. 10 p. 1 (1917).

† Nolan and O'Keeffe, 'Proc. Roy. Irish Acad., A, vol. 39, p. 21 (1929).

A drop is rapidly reduced in size when glowing owing to the removal of water from the filament, this will limit the maximum size of drops which can persist in a strong field

These experiments were carried out at the suggestion of Professor C. T. R. Wilson, and it is a pleasure to acknowledge my great indebtedness to him for his continued interest and advice throughout their progress

---

# *Studies in Membrane Behaviour.* Part* I. *-Equilibrium Conditions with Gelatine Membranes in Acetate Buffer Solutions.*

By W. L. Francis, Laboratory of Physical Chemistry, Cambridge.

(Communicated by E. K. Rideal, F R S —Received June 24, 1931—Revised July 19, 1931 )

## *Introduction.*

The permeability of membranes has been explained in the past either in terms of solution or filtration. In the former case the membrane is considered as a layer of solvent immiscible with the solutions which it separates and the penetrating substance diffuses through by dissolving into the membrane on one side and out of it on the other. In the latter case the membrane is considered as an inert framework filled with the same solvent as that of the solutions it separates and resisting the diffusion of solutes because the dissolved molecules

* It is the aim of this series of papers to extend the knowledge of membrane behaviour in aqueous solutions. The means used are electrical and stoichiometrical. There are three obvious lines of development. The first is to study the influence exerted on the membrane potential by the physical and chemical properties of the substance of the membrane which in turn may be affected by the solutions it separates. This has been done with success by Michaelis and his co-workers (' Bull. Nat. Res Coun. Wash.,' vol. 69) for collodion membranes, and Fujita (' Biochem. Z.,' vol. 162, p. 245 (1925) ) has experimented with protein membranes. The second subject of study is the variation of membrane potential with time during the setting up of the equilibrium value and its readjustment when disturbed. This has not hitherto been attempted. Thirdly, it is intended to determine whether an osmotic gradient can be maintained by artificial membranes which are the seat of chemical action or potential difference.

are blocked by the pores of the membrane material. The same two points of view with regard to membrane potentials lead to their theoretical classification either as phase boundary potentials or as modified diffusion potentials. Phase boundary potentials arise in a system containing immiscible solvents as the result of a tendency for each ionic species to approach a partition equilibrium between the solvents. Because of this tendency a separation of the ions occurs and a double layer of ions is formed at each interface between different solvents. The potential gradient in such a system is therefore sharp at each interface and very gradual within each phase where only small potentials due to diffusion can occur. The mathematical expression of the equilibrium state has been given by Nernst* and Haber.† For a system containing only univalent ions it may be written :—

$$\begin{array}{cc:cc|cc} \text{water} & & \text{oil} & & & \text{water} \\ c_1 & & c_2 & c_3 & & c_4 \\ & \mathrm{E}_1 & & & \mathrm{E}_2 & \end{array}$$

Total e.m.f.

$$\mathrm{E} = \mathrm{E}_1 + \mathrm{E}_2 = \frac{\mathrm{RT}}{\mathrm{F}} \, ln \, \frac{f_1c_1}{f_2c_2} \cdot \frac{f_3c_3}{f_4c_4}, \tag{1}$$

where $c_1$, $c_2$, $c_3$ and $c_4$ are the concentrations (and $f_1$, $f_2$, $f_3$ and $f_4$ the corresponding activity coefficients) of the ion common to all the phases. Beutner‡ verified this equation for a considerable series of oils and electrolytes.

Experiments showed that the maximum e.m.f. obtained in systems of this kind was given by the expression

$$\mathrm{E} = \frac{\mathrm{RT}}{\mathrm{F}} \, ln \, \frac{f_1c_1}{f_4c_4} \tag{2}$$

This occurs when the activity of the common ion is constant throughout the non-aqueous phase and independent of the values of $f_1c_1$ and $f_4c_4$. A specific chemical mechanism is postulated to account for the buffering action of the oil phase. This state of affairs has been realised by Beutner with acid oil membranes and with potassium ferrocyanide precipitation membranes, and by Cremer§ and others with glass membranes. Membranes can thus be reversible to cations in the same way as metal electrodes Whether the reversibility is general for all cations as in a salicylaldehyde oil chain or specific for one ion, *e.g.*, hydrogen ion, as in the glass cell depends on the chemical nature of the membrane.

---

* 'Z. Phys. Chem.,' vol. 9, p. 140 (1892); 'Ann. Physik,' vol. 8, p. 600 (1902).

† 'Ann. Physik,' vol. 26, p. 927 (1908), 'Z. Phys Chem.,' vol. 67, p. 385 (1909).

‡ 'Die Entstehung elektrischer Ströme in lebenden Geweben,' Stuttgart. 1920; also see "Hydrogen Ion Concentration," Michaelis, 1926 (trans.), pp. 192–196.

§ 'Z. Biol.,' vol. 47, p. 1 (1906); Haber and Klemensiewicz, 'Z. Phys. Chem.,' vol. 67, p. 385 (1909); Horovitz, 'Sitzungb. Acad. Wiss.,' A., vol. 134, p. 335 (1925).

Diffusion potentials occur in the simplest cases in free solution in the absence of any membrane. They have been treated mathematically notably by Nernst* and Planck.† For a concentration chain of a uni-univalent electrolyte the e.m.f. is given by

$$E = \frac{u - v}{u + v} \frac{RT}{F} ln \frac{f_1 c_1}{f_2 c_2}, \tag{3}$$

where $u$ and $v$ are the cation and anion mobilities respectively. In the case of two different uni-univalent electrolytes in opposition having the same activities the expression is

$$E = \frac{RT}{F} ln \frac{u_1 + v_2}{u_2 + v_1}, \tag{4}$$

where $u_1$, $v_1$ and $u_2$, $v_2$ are the ionic mobilities of the two electrolytes. This is a simple form of the general equation. In extending this theoretical attitude to membrane measurements, the potentials observed are ascribed to the difference in the velocities of single ions diffusing across the membrane. This involves no sudden jumps in the potential gradient but a zone of transition. The function of the membrane acting as a mass of capillaries is to resist the passage of the ions either by mechanical blocking or preferential adsorption or both. If the ion is large enough, *e.g.*, protein ion or anion of Congo red, Donnan's condition of impermeability is realised as a limiting case.

Considerable experimental illustration has appeared lately of this modified diffusion type of membrane potential.‡ With collodion membranes at least (11, *b*, *d*), the potentials are quantitatively explained by saying that an ion which is adsorbed by the membrane has its mobility reduced with reference to a non-adsorbed ion. An attractive opportunity for testing the scope of this theory is offered by the use of proteins as membranes material since here the sign and extent of ionic adsorption or combination can be governed by the $p_H$ of the system, and the relative ionic mobilities thereby controlled. Fujita (*loc. cit.*) by this means found that the potentials with membranes of hardened gelatine roughly agreed with the theory that on the basic side of the isoelectric point of the protein the anion is retarded and on the acid side of the cation. But his rough determination of the isoelectric point by a flocculation method was done with unhardened gelatine, while all but three of his potential readings in buffered solutions were performed with membranes hardened by tannic acid, potassium dichromate or formaldehyde. These reagents affect the amphoteric properties of gelatine profoundly. It was therefore considered desirable to verify and extend these potential measurements in buffer solutions using unhardened protein, whose isoelectric point was accurately found, and to check the current explanation of the e.m f. values by determinations of the transport number of the ions across the membrane.

---

* 'Z. Phys. Chem.,' vol. 2, p. 611 (1888); vol. 4, p. 129 (1889).

† 'Wied. Annal.,' vol. 40, p. 561 (1890).

‡ (*a*) Prideaux, 'Trans. Faraday Soc.,' vol. 10, p. 160 (1914), vol. 20, p. 37 (1924), vol. 24, p. 11 (1928); (*b*) Michaelis and others, 'Bull. Nat. Res. Coun. Wash.,' No 69; (*c*) Fujita, 'Biochem. Z.,' vol. 162, p. 245 (1925); (*d*) Mond and Hoffman, 'Pflüg. Archiv.,' vol. 220, p. 194 (1928).

## *Preparation and Mounting of the Membranes.*

The preparation of reproducible membranes has always been the first obstacle in osmotic research. As this is particularly true of protein membranes,* the detail is given here of a method used throughout this work, which, besides being satisfactory for proteins, can be applied to study the membrane behaviour of any substance which is adsorbed by unglazed porcelain.

The protein in question was mounted on a porous disc. This avoided the choice of protein being confined only to those that formed gelatinous blocks. Inert material immersed in protein solution adsorbs the protein and takes on its electro-capillary properties.† Loeb‡ used collodion membranes impregnated in this way with gelatine to study anomalous osmosis , he found that the gelatine once absorbed would not wash off. For this work porous discs of sintered Jena glass were first used, but three discs said to be of equal porosity were found to give different e.m.fs. under identical conditions of impregnation. A series of comparable membrane potential readings could thus only be obtained using the one disc. As the impregnation of a disc with protein and the subsequent measurement of the membrane potential-time relation take a day to carry out at each new $p_H$ this time limitation was serious. Speed and uniformity of preparation were attained by the use of two sets each of 12 porous unglazed Berlin porcelain discs which superseded the sintered glass discs. They were made to specification 6 cm. diameter, 0·4 cm. thickness and the two sets were of different pore sizes, namely 0·6 μ and 4·3 μ according to the makers. These figures based on perfusion measurements are only approximate, but accurate relative to one another. These discs are strong and can be washed free of protein by hot dilute acid and then water. They have proved to be thick enough to enable the variation of e.m.f. with time to be followed comfortably, and thin enough for the equilibrium value to be attained within a few hours.

---

* Matsuo, 'Pflüg. Archiv.,' vol. 200, p. 132 (1923); Mond, *ibid.*, vol. 203, p. 247 (1924).

† Abramson, 'J. Amer. Chem. Soc.,' vol. 50, p. 390 (1928); Freundlich and Abramson, 'Z. Phys. Chem.,' vol. 127, p. 25 (1927).

‡ 'J. Gen. Physiol.,' vol. 5, p. 395 (1922–23).

The technique of impregnation was adapted from Bechold's* practice in making gelatinous ultra filters. Zakarias† has stressed the importance of the uniform porosity of the substratum and absence of air bubbles in the preparation of reproducible filters. The following steps were therefore taken. The dry clean disc and the sample of protein solution are each evacuated to 20 mm. Hg in separate vessels and then the solution siphoned on to the disc without the admission of air. When the disc is covered by solution air is admitted and the jar stood overnight. This length of time allows for adsorption equilibrium between the protein and porcelain to be reached. On the morrow the disc is taken out and dried by slow rotation in the air in its own plane which is vertical. The disc is held by three knife edges and drying lasts from 30 to 60 minutes. With gelatine solutions the whole process of impregnation took place in a thermostat at 30° C.

### *Measurement of the Membrane Potential.*

The disc is next mounted with two rubber washers between two flanged glass half cells which are held together by three spring clips. These are more water-tight and less cumbrous than a brass screw collar which was used at first to grip the disc in position. At this stage with non-gelatinous substances on the disc a coating of collodion is run round the rim to prevent lateral leaks from the disc. With gelatine (c. 2 per cent. impregnating solution) on the disc this is unnecessary as lateral diffusion of the solutions does not visibly occur. The solutions are admitted simultaneously from reservoirs via side tubes under their own pressure and left till equilibrium is reached.

The potential is measured by the insertion of the side tubes of saturated calomel electrodes into the vertical limbs of side tubes of the cell, which end in small funnels. This is cleaner than the use of saturated KCl-agar bridges, which were first tried and which have the further disadvantage of contaminating the solutions and breaking down mechanically if the cell is left set up overnight. The calomels are connected to a potentiometer. The accuracy with which the membrane potential can be read varies inversely with the membrane resistance, it is always within 0·2 millivolt, however, in the following experiments.

---

* "Die Kolloide in Biologie und Medizin," 4th ed., 1922.

† 'Koll. Z.,' vol. 37, p. 50 (1925).

### *Materials.*

The gelatine used throughout was an Eastman Kodak ash-free preparation (water 17 per cent., ash 0·02 per cent.). Previous to use it was soaked for an hour in the desired volume of distilled water and then peptised by heating and stirring at 50° C for 10 minutes before transference to the thermostat. The sodium acetate and acetic acid used for the buffer solutions were A.R. reagents.

The buffer solution made up contained sodium acetate and acetic acid in the proportion required to govern the $p_H$. The relative strengths of each pair of solutions used were 10 : 1, the stronger solution being always N/40 with respect to acetate ion.*

### *Isoelectric Point of the Gelatine.*

This was determined by cataphoresis The isoelectric point of the membrane should, ideally, be found *in situ* by electro-osmotic or streaming potential methods. Since, however, in the impregnation of the disc the protein has not been treated with hardening agents which shift the iso-electric point, it is accurate and more convenient to do the determination separately with another

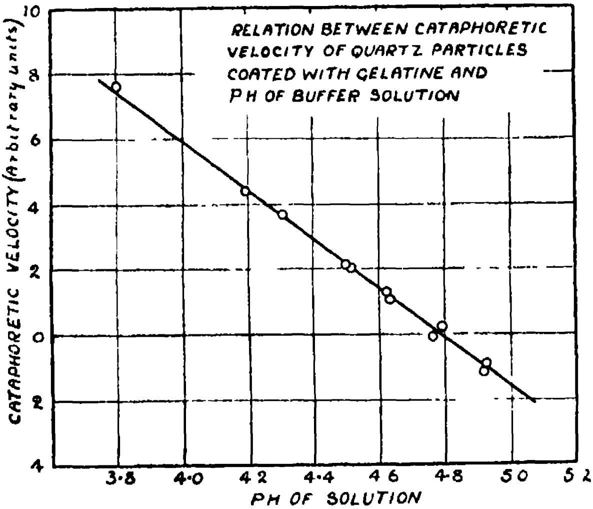

Fig. 1.

---

* Dilution tenfold with distilled water increases the $p_H$ of sodium acetate-acetic acid buffers by 0·06 $p_H$ (Walpole, 1914). $p_H$ readings of the buffer were taken with the N/40 solution and not with the N/400 solution, which gives irregular results when a quinhydrone electrode is used.

sample. The gelatine was adsorbed on quartz particles suspended in N/200 acetate buffer solutions.* The relation between cataphoretic velocity and $p_H$ is shown in fig. 1. Zero velocity corresponds with a $p_H$ of 4·79 which is taken as the isoelectric point.

### *Equilibrium Membrane Potentials with Untreated Discs.*

To determine the magnitude of the potential change due to impregnation by protein, blank experiments were carried out with clean discs. Each disc was evacuated in the impregnated apparatus as if for protein treatment, but water was used instead of protein solution This ensured that air bubbles were removed. The disc while still damp was mounted between the glass half-cells and a coating of collodion in alcohol-ether solution run round the rim to make it water-tight on standing. The opposing solutions were then run in simultaneously, care being taken that the levels on either side of the disc were the same so that diffusion should not be hastened by hydrostatic pressure differences.

Equilibrium was reached using the coarser discs in 30 minutes and maintained several hours. The relation between e m.f. and $p_H$ is shown in fig. 2, curve A. The extreme acid and basic points on the curve were given by acetic acid and

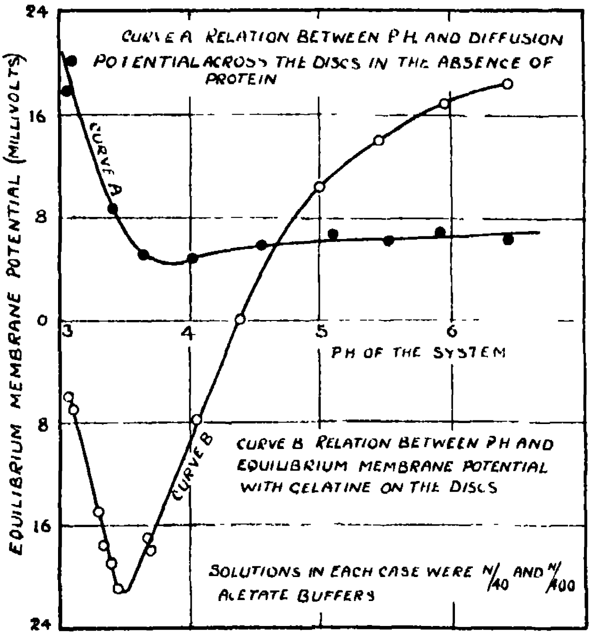

Fig. 2.

---

* I am indebted to Dr. F. P. Bowden for the use of a cataphoresis cell.

sodium acetate solutions respectively. Until highly acid solutions are reached ($p_H$ 3·6, 95 per cent. acid and 5 per cent salt) the liquid junction potential through the disc is practically constant at 6-7 millivolts which, since the $p_H$ is the same on either side, must represent the diffusion potential of sodium acetate in a 10 . 1 gradient. Fujita (*loc. cit.*) found 7·5 millivolts for this value. The theoretical value from Nernst's equation for unimpeded diffusion is 8·9 millivolts using the mobilities of sodium and acetate ion $u_{Na} = 43$ and $v_{Ac} = 35$ taken from conductivity measurements. The porous discs by themselves therefore have little effect on the diffusion potentials of the buffer solutions.

### *Equilibrium Membrane Potentials with Gelatine on the Discs.*

Equilibrium was reached in 4–6 hours and maintained for at least 40 hours longer. The solution of gelatine used for impregnation (17 gm. per litre) was initially at a $p_H$ of 4·8–4·9, *i.e.*, approximately isoelectric. The $p_H$ of the whole system at equilibrium was taken to be that of the buffer solution. The relation between e m.f. and $p_H$ is shown in fig. 2, curve B, where the effect of the gelatine with change in $p_H$ is clearly seen. Each point on the curve was obtained with a separate membrane. It was found, however, that if successive pairs of solutions of varying $p_H$ were put in the cell without changing the membrane the potentials were the same, to within 0·5 millivolt, as if a new membrane had been taken each time The equilibrium membrane potential with buffer solutions therefore varies continuously with the $p_H$ of the system.

The reproducibility of the potentials was ±1 millivolt, which serves as a measure of the reliability of the method of impregnating the discs. The effect of changing the amount of gelatine on the disc was studied by comparing the e.m.fs. obtained when 0·85 per cent. and 1·7 per cent. solutions were used for impregnation. The form of the potential-$p_H$ curve was the same in each case but the stronger gel gave the steeper curve, the respective slopes at the isoelectric point being 11 millivolts per $p_H$ unit for the 0·85 per cent. gel and 13 millivolts per $p_H$ unit for the 1·7 per cent. gel.

### *Discussion*

At first sight it appears that the measurements summarised in fig. 2 agree with the modified diffusion potential theory. The $p_H$'s at which the protein has zero effect on the diffusion potential are 4·73, 4·8 and 4·75 in the separate experiments. The mean of these is 4·76. The isoelectric point of the gelatine was found to be 4·79. The isoelectric point thus almost coincides with the point at which there is no change in the relative mobilities of anion and cation. The change in e.m.f. at increasing $p_H$ distances from the isoelectric point corresponds with the gradual charging-up of the gelatine by anions (on the basic side) or cations (on the acid side) and their consequent retardation. This effect is greater and the gradient of the curve is steeper when the gelatine is more concentrated. This is natural because more ions are then combined.

The mobilities of the sodium and acetate ions with which the potentials found correspond can be calculated from the Nernst equation. To test the values of these mobilities directly and so to justify the consideration of the e.m.fs. as modified diffusion potentials, electric transfer experiments in buffer solutions were carried out. With collodion membranes* this method of checking the diffusion theory gave only a rough agreement with the mobilities calculated from the e.m.f. measurements. The delicacy of the collodion membranes limited the current densities employed so that the ionic transfer was not great enough compared with the experimental error in the analyses of the amount of each ion transferred. With the gelatine membranes, which are far more resistant, larger currents are possible so that changes in concentration are greater and the errors in estimating them far less.

Before these transfer experiments were carried out it was, however, necessary to extend the foregoing membrane potential measurements, using the same buffer mixtures and the same concentration gradient but a higher actual concentration This is required for the following reasons. In comparing the mobilities of sodium and acetate ions through the membrane it is essential that the current passing should be carried by those ions only. In weak solutions of the buffers a considerable part of the current is carried by the hydrions and hydroxyl ions This is shown by the large changes in $p_H$ of the solutions when N/20 buffer solutions are used compared with the corresponding changes with N/2 solutions.

| Solution | N/20 buffer | N/2 buffer |
|---|---|---|
| Original $p_H$ | 4·46 | 4·48 |
| Final cathode $p_H$ | 4 91 | 4 54 |
| Final anode $p_H$ | 4 26 | 4 43 |

These figures were obtained under identical experimental conditions, the quantity of current passed being in each case equivalent to the transference of 1 milli-equivalent of ions. With N/40 solutions the $p_H$ shifts would be even greater. Another advantage of the use of stronger solutions is that, the $p_H$ shifts being small, the $p_H$ of the membrane is constant throughout its thickness and uniform during the course of the experiment. The ionic mobilities determined therefore correspond to one particular $p_H$ which could not be said in the weaker solutions where there is a much greater $p_H$ difference between the opposing solutions at the end of the experiment.

---

* Michaelis, Weech, Yamatori, 'J. Gen. Physiol.,' vol 10, p. 685 (1927).

For these reasons the transfer experiments had to be done with N/2 solutions. The ionic mobilities of sodium and acetate thereby found should not be compared with those calculated from potential measurements given by N/40 and N/400 solutions as the mobilities may change with changing concentration. A better comparison is provided by potential measurements with stronger solutions, viz., N and N/10 in the manner already described. The curve (fig. 3B), although flatter and more extended, shows that the same relation between membrane potential and $p_H$ exists in stronger as in weaker solutions (compare curve B, fig. 2).

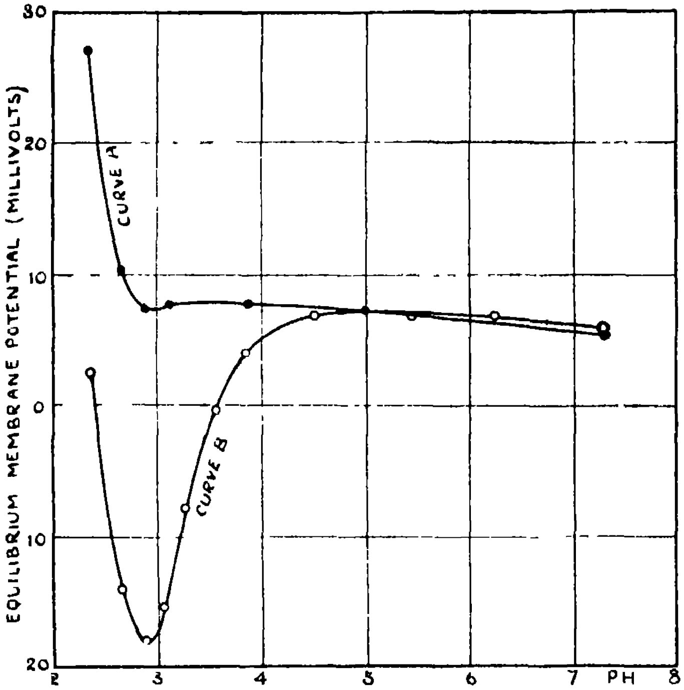

Fig. 3.

It is noticeable that the increase of concentration has removed the difference caused by the presence of gelatine at high $p_H$'s but leaves it unchanged at the acid end of the scale. The mobilities of sodium and acetate ions calculated from this curve in terms of the modified diffusion potential theory are compared with the mobilities directly determined for N/2 solutions in Table A.

Gelatine gels were used as solvent media in early determinations of ionic transport numbers by direct measurements.* Below concentrations of 5 per cent. by weight† the gelatine does not affect the ionic mobilities in aqueous solutions. Above that strength the cation mobility is diminished by the gel though the effect of alteration in $p_H$ was not investigated. Hittorf‡ demonstrated the occurrence of electro-osmosis accompanied by changes in concentration when a current passed across gelatine membranes, and Bethe and Toropoff§ found that with weak solutions of salts a current caused changes in the acidity and basicity on either side of the membrane. It was found, however, in the experiments described below that except when sodium acetate by itself was used, there was no electro-osmosis and the shift in $p_H$ of the solutions did not exceed $0 \cdot 06$ $p_H$.

### *Apparatus and Experimental Method for Transfer Experiments.*

The membranes prepared as before were mounted between specially designed half-cells of the form illustrated (fig. 4). The volumes of the two cells between the taps were 72 c.c. and 74 c.c. and for each experiment the same solution was run into each side, the cells being connected together by a piece of rubber

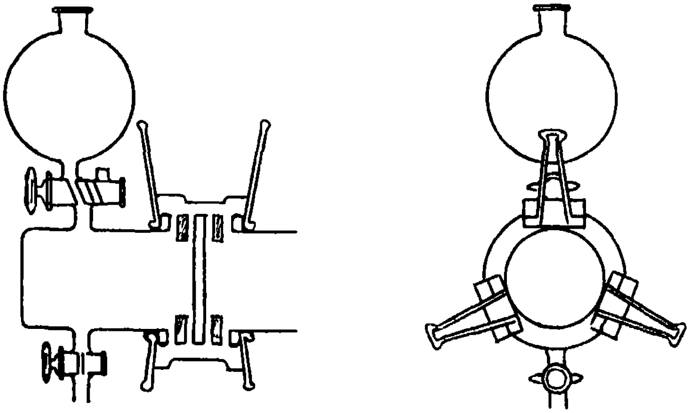

FIG 4

---

* Masson, 'Austral. Ass. Adv. Science,' p. 205 (1901).

† Denison, 'Z. Phys. Chem.,' vol. 44, p. 575 (1903).

‡ 'Z. Phys. Chem.,' vol. 39, p. 613 (1902); vol. 43, p. 329 (1903).

§ 'Z. Phys. Chem.,' vol. 88, p. 686 (1914); vol. 89, p. 597 (1915).

tubing joining the draining tubes for this purpose. When the cells were full, platinum wire electrodes were inserted through the two-way taps from which the gases evolved during electrolysis could escape.

The current was passed from accumulators giving 14 volts with a variable resistance and milliammeter in the external circuit. In the first minute the current fell as the platinum electrodes and membrane became polarised; after that the current remained constant throughout the experiment indicating that the resistance of the membrane was not falling through mechanical breakdown or solution in the electrolyte. The current used was 30–40 milliamperes usually for 40 minutes. As soon as the current was stopped, the electrodes were withdrawn and the solutions run out with shaking into clean dry flasks. A volume of 50 c.c. from each side was then taken for estimation and the remainder used for $p_H$ readings.

### *Estimation of Concentration Changes.*

Sodium acetate-acetic acid buffers were used; the concentration of acetate ion was kept N/2 throughout The sodium present in each specimen of 50 c.c. was estimated by conversion to sulphate by adding excess of sulphuric acid followed by evaporation to dryness and ignition.* Alternatively the acetate was estimated by conversion to carbonate.† The sample of solution was exactly neutralised by caustic soda and evaporated to dryness. The resulting acetate was charred at red heat and on cooling extracted with 40 c c. N sulphuric acid, filtered and the residue washed. After boiling to expel $CO_2$ the filtrate was titrated with N/2 caustic soda solution and the carbonate originally present thus found by difference. These two methods practised on the sodium acetate crystals gave results agreeing within 0·1 per cent. and showing that the acetate crystals ($NaC_2H_3O_23H_2O$) had lost 1 per cent. of their weight by efflorescence. This loss was allowed for in the calculations.

### *Experimental Results.*

(*a*) *Check on the Method.*—The first problem was to check the soundness of the method by proving that the amount of acetate transferred in one direction and sodium in the other were equivalent to the total transfer estimated from the coulombs passed. This is so if the respective transport numbers add up to unity. This check was applied four times, twice at $p_H$ 4·73 and once at $p_H$'s 5·53 and 7·2. The sum of the transport numbers in these cases lay between

---

* Scott, 'Analysis,' 2nd ed., p. 348.

† Sutton. 'Analysis,' 9th ed., p. 91.

0·90 and 0·97 (mean 0·95)* which is satisfactory considering the analytical errors involved. Having shown this, it is justifiable to determine only one of the ions in experiments at other $p_H$'s. The results for two consecutive experiments with the same membrane at $p_H$ 4·73 are shown below. The figures serve to illustrate the order of concentration changes involved In the first table the figures refer to the weight of sodium in 50 c.c. of solution expressed as sodium sulphate. The figure in the first column is calculated from the volume of standard acetate solution used in making up the buffer. This was made by weighing out $NaC_2H_3O_2 . 3H_2O$ crystals whose composition had been checked previously by estimation as sulphate. The volume error in making up the buffer solutions is less than 1 in 1000.

| Solution. | Original sodium | Final sodium. | Difference. | Sodium from coulombs passed. | Transport number. |
|---|---|---|---|---|---|
| I Cathode | 1·024 | 1·0547 | 0·0307 | 0·051 | $\frac{0\cdot0307}{0\cdot0510} = 0\cdot60$ |
| II Anode | 1·024 | 0·9965 | 0·0275 | 0·0436 | $\frac{0\cdot0275}{0\cdot0436} = 0\cdot63$ |

In the next table the acetate concentrations in 50 c.c. of buffer are expressed in cubic centimetres N/2 soda solution which was used in the back titration. The first column figures are calculated from the original concentrations of the acetate and acetic acid solution and the volume compositions of the buffers.

| Solution. | Original acetate | Final acetate. | Difference | Acetate from coulombs passed. | Transport number. |
|---|---|---|---|---|---|
| I Anode | 50·05 | 50·55 | 0·50 | 1·44 | $\frac{0\cdot5}{1\cdot44} = 0\cdot35$ |
| II Cathode | 50·05 | 49·70 | 0·35 | 1·23 | $\frac{0\cdot35}{1\cdot23} = 0\cdot28$ |

For the membrane I $n_{Na} + n_{Ac} = 0\cdot6 + 0\cdot35 = 0\cdot95$

For the membrane II $n_{Na} + n_{Ac} = 0\cdot63 + 0\cdot28 = 0\cdot91$.

The accuracy of the acetate estimations depends on the accuracy of the small volume difference, which can be read to 0·02 c.c. The error in general is therefore ±5 per cent. The error in the sodium estimations is far less, but below $p_H$ 4·5 all the estimations were carried out on the acetate ion. The four checking experiments performed, of which two are quoted above, serve also to show that the loss of one ion in the cathode solution is equal to the gain in the same ion in the anode vessel or *vice versa* to within ±5 per cent. That is, the ions are not absorbed from the solution by the membrane. This is only true if the membrane and solutions have been in contact at least 3 hours and the solutions then rinsed out and renewed before the transport experiment is performed. Otherwise a net loss of electrolyte in the transport membrane is observed.

---

* This figure is less than unity because the current is not all carried by sodium and acetate ions or because part of the concentration difference is lost during the experiment by back diffusion.

(*b*) *Transport Numbers.*—The transport numbers over the range from acetic acid to sodium acetate are summarised in Table A.

## *Discussion.*

A comparison of the figures in columns IV, V and VI indicates no agreement between the ionic mobilities calculated from membrane potential measurements and those found by transfer experiments. $n_{Ac}$ does not show a jump in value towards the acid end to correspond with the dip in the e.m.f. $p_H$ curve in that region The values are roughly steady throughout the $p_H$ range 2·43–7·2 and are uniformly less than $n_{Ac}$ calculated from the concentration chain potentials with or without gelatine on the discs (column VII). A direct test has therefore disproved the validity of the modified diffusion potential method of interpreting equilibrium membrane potentials with protein membranes, although in the cases where the mobilities of both ions were found (experiments 10, 13, 15) their sum (—0·95 av.) indicates that conduction through the membrane is electrolytic and due almost exclusively to sodium and acetate ion. In acid solutions (experiments 1, 2, 3) conduction must be in part due to hydrogen ion, although according to classical theory the salt is more dissociated than the acid and this will compensate in part for the smaller concentration of sodium in the solution. The transition from buffer to complete acid solution is, however, not marked by any sharp change in the value of $n_{Ac}$. If the modified diffusion theory were true it would require the cations to be adsorbed and retarded in acid solutions and the acetate ion mobility to rise progressively as the $p_H$ fell.

It should be noticed that the value of $n_{Ac}$ through the membrane is consistently lower than it is in the free solution (0·32 compared with 0·45) and is equally unaffected by change in $p_H$. The lower mobility through the

Table A.

| Experiment number. | Initial $p_H$. | Final $p_H$ (1) Anode. (2) Cathode | Transport numbers of acetate ions. | | | |
|---|---|---|---|---|---|---|
| | | | Through gelatine membranes. | | | Without gelatine. Calculated from concentration chains. |
| | | | Calculated from concentration chains. | Found by direct experiment in N/2 solutions. | | |
| | | | N–N/10. | Sodium estimation. | Acetate estimation. | N–N/10. |
| I. | II | III. | IV | V. | VI. | VII. |
| 1 | 2·43 | 2·44<br>2·53 | $p_H$ 2·35 0·4 | — | 0·31 | 0·30 |
| 2 | 2·76 | 2·76<br>2·84 | 0·63 | — | 0·29 | 0·43 |
| 3 | 3·10 | 3·11<br>3·20 | 0·61 | — | 0·33 | 0·44 |
| 4 | 3·52 | 3·50 | 0·50 | — | 0·35 | 0·44 |
| 5 | 3·96 | — | 0·45 | — | — | 0·44 |
| 6 | 4·14 | — | 0·44 | — | 0·29 | 0·44 |
| 7 | 4·17 | 4·16<br>4·25 | 0·43 | — | 0·29 | 0·44 |
| 8 | 4·38 | — | 0·43 | — | 0·29 | 0·44 |
| 9 | 4·57 | — | 0·43 | — | 0·35 | 0·44 |

Table A—(continued).

| Experiment number | Initial $p_H$ | Final $p_H$ (1) Anode (2) Cathode | Transport numbers of acetate ions. | | | |
|---|---|---|---|---|---|---|
| | | | Through gelatine membranes. | | | Without gelatine Calculated from concentration chains |
| | | | Calculated from concentration chains | Found by direct experiment in N/2 solutions | | |
| | | | N–N/10 | Sodium estimation | Acetate estimation | N–N/10 |
| 10 | 4·73 | — | 0·42 | 0·40<br>0·37 | 0·35<br>0·28 | 0·44 |
| 11 | 4·78 | 4·77<br>4·81 | 0·42 | 0·42 | — | 0·44 |
| 12 | 5·03 | 5·01<br>5·08 | 0·43 | 0·37 | — | 0·44 |
| 13 | 5·53 | 5·52<br>5·66 | 0·44 | 0·38<br>0·32 | 0·34 | 0·45 |
| 14 | 6·04 | — | 0·45 | 0·35 | 0·30 | 0·45 |
| 15 | 7·2 | 6·55<br>8·87 | 0·45 | 0·38<br>0·40 | 0·29 | 0·45 |

membrane may be ascribed to the greater mechanical opposition offered to the acetate ion compared with the sodium ion, the size of which is less.

It remains now to explain the change in e.m.f. produced by the presence of protein in the disc in terms which do not involve hypothetical ionic mobilities across the membrane. The value of the change in e.m.f. and its dependence on the $p_H$ is shown in fig. 5 for the N/40–N/400 and N–N/10 solutions. If it is assumed that the membrane potential is made up of the liquid junction potential of the opposing solutions and a potential in the reverse direction due to the presence of gelatine, this reverse potential may be considered most simply as due to the differential charging up of the opposite faces of the membrane by ionic adsorption. The sign of this e.m.f. (figs. 2, 3) indicates (1) that the surface of the membrane towards the stronger solution is positively charged, and (2) that the charge increases as the acidity of the system increases, but falls off when basic solutions are approached. This is in agreement with two known facts of the combination of gelatine with ions, namely, (1) that the stronger the electrolyte solutions the more ions combine with a given mass of protein, and (2) that on the acid side of the isoelectric point cations combine more than anions and thereby the protein is positively charged while on the basic side of the isoelectric point the reverse happens. The ratios of the cationic activities just within opposite surfaces of the membrane which are

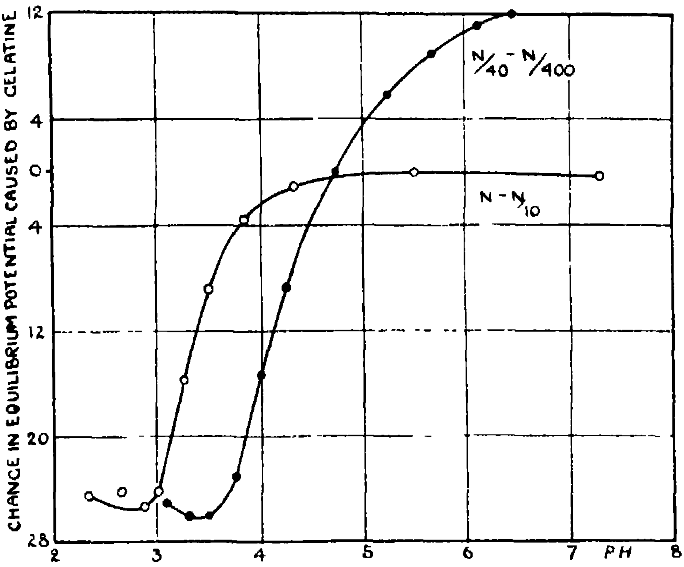

FIG. 5

necessary to account for the observed e.m.fs may be calculated from the equation

$$\text{Reverse e m.f. } E = \frac{RT}{F} \ln \frac{a}{a'}$$

The change in the value of $a/a'$ in the $p_H$ range possible to acetate buffers is from 2·72 to 0·62 for N/40–N/400 solutions and from 2·55 to 0·9 for N–N/10 solutions, the value in extreme acid solutions being written first in each case. Until a means is found of determining the ratio $a/a'$ independently, this view of the membrane potential cannot be confirmed. The only postulate is that different equilibrium concentrations of sodium and acetate ions exist at each membrane-solution interface, which is natural since the solutions differ in concentration by a factor of 10. As diffusion proceeds this difference is flattened down and the reverse e.m.f. accordingly disappears.

## *Summary*

(1) Equilibrium membrane potentials are measured for a buffer concentration gradient of 10 : 1 using N/40–N/400 and N–N/10 solutions. The e.m.fs. with and without gelatine on the membranes are compared over the $p_H$ range 2·35–7·3. The results, more particularly with weaker solutions, appear to support the modified diffusion theory (*i e* , that the anions are retarded in basic solution and the cations in acid solution), which interprets the potential in terms of altered ionic mobilities within the membrane. This evidence is, however, not direct.

(2) Direct evidence, given by determinations of the transport members of the sodium and acetate ions across the membrane in N/2 solution, vetos the modified diffusion potential theory. The value $n_{Ac}$ does not alter systematically with $p_H$ but remains steady throughout between the values 0·29 and 0·37.

(3) The results are discussed and, assuming that the membrane potentials are made up of the ordinary diffusion potential and an opposed e.m.f. due to the combination or adsorption of ions on the protein, an explanation of the variations of the membrane potential with $p_H$ and concentration is suggested which conforms with the known behaviour of gelatine in electrolyte solutions.

I am indebted to Professor T. M. Lowry for his interest in this work. I wish to express my thanks to Professor E. K. Rideal for his constant encouragement and advice and to the Council of King's College, Cambridge, for the award of the Harold Fry Studentship.

# On the Value of the Cosmical Constant.

By Sir Arthur Eddington, F R S

(Received August 11, 1931.)

1. The cosmical constant $\lambda$ occurs in Einstein's law of gravitation $G_{\mu\nu} = \lambda g_{\mu\nu}$. In the resulting equations of motion the term containing $\lambda$ represents a scattering force which tends to make all very remote bodies recede from one another; this phenomenon is the basis of the theories of de Sitter and Lemaître concerning the "expansion of the universe." If the observed recession of the spiral nebulæ is a manifestation of this effect the value of $\lambda$ can be found from the astronomical observations.

In this paper I put forward a simple geometrical interpretation of the term in the wave equation which contains the mass $m$ of an electron; this interpretation provides an alternative expression for the term. The new expression involves $\lambda$, and by equating it to the ordinary expression we find a theoretical value of $\lambda$, viz., $9 \cdot 8 \,.\, 10^{-55}$ cm.$^{-2}$. This agrees satisfactorily with the value found from the observed recession of the spiral nebulæ (§ 8).

The wave equation for an electron moving in the electrostatic field due to a fixed electron is*

$$\frac{ih}{2\pi}\frac{\partial\psi}{\partial t} = c\left\{m^2c^2 + \left(\frac{ih}{2\pi}\right)^2\left(\frac{\partial^2}{\partial x^2} + \frac{\partial^2}{\partial y^2} + \frac{\partial^2}{\partial z^2}\right)\right\}^{\frac{1}{2}}\psi + \frac{e^2}{r}\psi \tag{1}$$

Let

$$\alpha = hc/2\pi e^2, \qquad \gamma = 2\pi mc\alpha/h. \tag{2}$$

Then (1) can be written

$$\left(\alpha\frac{\partial}{c\partial t} + \frac{i}{r}\right)\psi + \left\{\alpha^2\left(\frac{\partial^2}{\partial x^2} + \frac{\partial^2}{\partial y^2} + \frac{\partial^2}{\partial z^2}\right) + (i\gamma)^2\right\}^{\frac{1}{2}}\psi = 0. \tag{3}$$

Following Dirac, we can rationalise (3) by introducing four perpendicular matrices which in my usual notation would be denoted by $E_{14}$, $E_{24}$, $E_{34}$, $E_4$; but I will here write them $i_{14}$, $i_{24}$, $i_{34}$, $i_4$, as a reminder that they are all square roots of $-1$, though they must be distinguished from the ordinary $i$. The resulting linear equation is

$$\left\{i\left(\alpha\frac{\partial}{c\partial t} + \frac{i}{r}\right) + i_{14}\,\alpha\frac{\partial}{\partial x} + i_{24}\,\alpha\frac{\partial}{\partial y} + i_{34}\,\alpha\frac{\partial}{\partial z} + i_4\,(i\gamma)\right\}\psi = 0. \tag{4}$$

---

* Dirac, "Quantum Mechanics," p. 118, equation (5), supplemented by the inclusion of a potential energy $e^2/r$ in the Hamiltonian.

The argument of this paper is that $\gamma$ has the interpretation

$$\gamma = \sqrt{N}/R, \qquad (5)$$

where R is the radius of curvature of the universe in a static state or eigenstate, and N the number of electrons in the universe. It will be seen that there is a suggestive resemblance in the structure of the terms

$$i\left(\frac{i}{r}\right) \quad \text{and} \quad i_4\left(\frac{i\sqrt{N}}{R}\right)$$

in (4), and my theory turns on this similarity. The suggestion is briefly that, if the energy of a specified electron due to a singularity at distance $r$ is $i/r$, the energy of N indistinguishable electrons due to a singularity at distance R (the centre of the spherical universe) will be $i\sqrt{N}/R$.

The suggestion is not based merely on a general analogy. I think I have been able to show that this simple relation of the two terms is definitely demanded by the geometry of the problem (see § 6).

2. In trying to understand the origin of mass we keep in mind the following principles. According to relativity theory, mass is associated with curvature of space-time So long as we keep to the flat space-time ordinarily adopted in wave-mechanics we cannot expect to obtain light on the nature of the term involving the mass ; it must remain an empirical term But by contemplating curved space-time we may hope to assimilate the mass-term into the theory, and see that it arises in a similar manner to the terms involving other energies recognised in quantum theory.

The Machian view that the mass of a body owes its existence to the presence of other bodies was at one time strongly urged by Einstein, and has been more or less recognised in relativity literature. The conceptions of the quantum theory favour it—in particular, the recognition that an electron has no individuality and is not separable from all the other electrons in the universe in the way that the classical picture supposed. I take the view that the mass of an electron is an interchange energy with all the other charges in the universe suitably averaged.

In any problem relating to the actual world we may divide the particles into two groups, (*a*) certain particles specifically mentioned in the problem, and (*b*) the unspecified particles. The unspecified particles are replaced by an averaged distribution of their states which is called the *field*. If the field has directional characteristics this must be definitely stated in the enunciation of the problem, viz , that the specified particles are in a particular gravitational or electromagnetic field, and equation (1) must be modified accordingly.

Otherwise we are entitled to assume that the field is of the most featureless kind possible; it is then in one aspect a pure *inertial field* and in another aspect it is a uniform macroscopic space-time. If we do not take account of (*b*) in our problem there is no inertial field and the specified particles (*a*) are without inertia; they have then no energy other than that of their mutual interaction, and the mass-term will be missing from (1).

3. The physical conception of location in space is inseparable from the conception of interaction; for there is no meaning in saying that a body is located at A rather than at B unless it makes some difference to something that it is at A and not B. The significance of location is that the symbols specifying it (co-ordinates) enter as parameters into the functions describing interaction effects.

If we consider one specified particle in a uniform space so that there is nothing to distinguish one possible position of the particle from another, the interaction of the particle with the space (*i e.*, with the averaged state of the unspecified particles, which the uniform space or inertial field replaces) must be independent of its co-ordinates. At first sight we might think that the interaction must therefore be zero. But we are familiar in dynamics with cases in which the Hamiltonian, whilst not involving a co-ordinate explicitly, involves the corresponding velocity. Such co-ordinates are cyclic, and the energy associated with them must be inserted in the Hamiltonian as shown in the theory of ignoration of co-ordinates. It seems reasonable to think that all terms in (4) of potential energy type, *i e.*, not explicitly involving derivatives, represent energy corresponding to ignored cyclic co-ordinates.

The definition of a cyclic co-ordinate $\theta$ is that by continued application of the change $d\theta$ we reach a state which is counted as identical with the state started from. In flat space-time cyclic co-ordinates can only exist in connection with a singularity; and we see in (4) that corresponding to a specified singularity (electron or proton) a term $(\iota/r)$ appears in the Hamiltonian which presumably represents the energy of the cyclic co-ordinate admitted by it. In a spherical world continued progress in a uniform direction brings us to a state reckoned to be identical with the state started from; I consider that the term $(i\gamma)$ in the Hamiltonian represents the corresponding cyclic momentum.

It is hardly necessary to emphasise that the importance of cyclic transformations is that they are a pitfall for statistical theory. States which are represented as distinct in our continuous analysis are counted as identical for statistical purposes. The primary effect of adopting a curved world in our theory instead of the flat space usually treated is that we introduce a new connectivity which must be allowed for in the statistical theory. The interpretation of irregularities of curvature as gravitational fields is a side development which does not here concern us, and we confine attention to a uniform and therefore spherical space.

4 We now see how material particles " produce " curvature of space-time. As individual singularities they would have cyclic co-ordinates associated with them. In averaging, we may smooth out the singularities and abolish the individual cyclic co-ordinates provided that we furnish an equivalent cyclic co-ordinate in the space which we substitute , and, of course, the space cannot furnish such a cycle unless it is re-entrant. The substituted space is the macroscopic space of which we are aware, which is accessible to experiment and measurement; and we may assume that its dimensions are such as to provide a cyclic co-ordinate dynamically equivalent to the suppressed co-ordinates.

Although only one* particle is specified, the system which we are considering includes all the particles in the universe , for unless we include the unspecified particles the mass of the specified particle is non-existent and we shall not obtain equation (1). The only statical arrangement of N particles is in the form of an Einstein world and we shall deal with this case.

Our " expanding universe " is probably far from the static configuration, and the question arises whether the value of $m$ which we shall deduce for an Einstein universe applies to it. This would be a difficulty if we were attempting to establish equation (1) by a new theoretical argument. That is not our intention. We accept equation (1) as the orthodox wave equation which is supposed to be true whatever the state of the universe,† and apply it to a simple tractable case from which we can obtain a useful result. According to quantum mechanics (1) is satisfied when the specified particle is in an eigenstate whatever the state of the N — 1 unspecified particles, provided that they do not produce an electric or gravitational field ; it is therefore satisfied when the whole N particles are in an eigenstate and form an Einstein world, so that we are at liberty to apply it to this case.

The present radius of our expanding universe is greater than the radius R of the Einstein world ; but, inasmuch as it does not correspond to an eigenstate, it is irrelevant to the theory of the wave equation. That is why the Einstein radius and not the actual radius is given by (5).

---

* Or two, if we count the supernaturally fixed electron which is introduced to provide a convenient comparison term.

† The investigation in § 7 throws some light on the question why (1) continues to hold as the wave equation for a specified electron when the unspecified particles are not in an eigenstate.

5. We know in a general way that the term $(i/r)$ in (4) arises from the interchangeability of the two electrons The line $r$ joining them has a (concealed) way of rotating so that its two ends become interchanged. If $\theta$ is the angular variable measuring this rotation, $\psi$ must contain a factor $e^{i\theta}$, since according to the Fermi-Dirac principle the sign of $\psi$ is reversed when the rotation is through an angle $\pi$ and the two electrons are interchanged. The term $(i/r)\,\psi$ could be written

$$\frac{\partial}{r\,\partial\theta}\psi,$$

so that it is comparable with $\partial/\partial x$, $\partial/c\,dt$, occurring elsewhere in (4). Or we may consider the momentum $p$ associated with a circuit of radius $r$ by the elementary quantum rule $2\pi r\,.\,p = h$, so that

$$p = \frac{h}{2\pi}\;\frac{1}{r},$$

the factor $h/2\pi$ having been removed from the Hamiltonian in (4).*

Our spherical space provides a circuit of radius R, and on the same principles this should furnish a term $(i/\mathrm{R})\,\psi$. There will be N such terms, one for each of the N electrons whose eigenstate is being considered , for, although they are unspecified and their co-ordinates are " ignored " in the Hamiltonian, their cyclic momenta must be included. The question remains whether the N equal terms will compound additively to give a resultant $i\mathrm{N}/\mathrm{R}$ or perpendicularly to give a resultant $i\sqrt{\mathrm{N}}/\mathrm{R}$. Both kinds of combination are exemplified in wave mechanics. It seems clear that one or other of these resultants will appear in the wave equation and the only possible term in (4) with which it can be identified is the mass-term $i\gamma$. The question is whether it is the term $(i\gamma)$ in (4) or the term $(i\gamma)^2$ in (3) which is the simple sum of N elementary terms. In the latter case we can still exhibit the N terms separately in (4) as

$$i_4'\,(i/\mathrm{R}) + i_4''\,(i/\mathrm{R}) + i_4'''\,(i/\mathrm{R}) + \ldots,$$

where $i_4'$, $i_4''$, $i_4'''$, ..., are different anticommuting square roots of $-1$.

In favour of $(i\mathrm{N}/\mathrm{R})$ it may be urged that in the wave equation for two particles the masses are simply added. But that is an altogether different application; the mass term is then doubled, not because there are more particles in the system (for the change is merely that an unspecified particle becomes specified), but because the number of dimensions of the configuration space adopted is doubled A stronger argument is that when there is more than one fixed electron the corresponding terms $(\iota/r)$ are added. But these terms occur linearly both in (3) and (4), so that there is here no suggestion of perpendicular combination. The fact that in the known case of linear composition the equations indicate it unambiguously seems to make it all the more likely that their hint of quadratic composition of $(\iota\gamma)$ is to be accepted.*

---

* It is not necessary to consider here why the potential energy escapes the factor $\alpha$ (= 137) which multiplies the kinetic energy. (I have written on this in other papers.) We shall proceed by comparing potential energy with potential energy, or cyclic energy with cyclic energy, so that the factor (whatever its nature) is eliminated.

If $\psi$ is normalised so as to correspond to one electron in spherical space, $\sqrt{N} \,.\, \psi$ represents the same distribution with density N times greater, corresponding therefore to N electrons in spherical space. I think, therefore, we get a simple view of (4) if we write it as

$$\left\{\iota\left(\alpha\frac{\partial}{c\partial t}+\frac{\iota}{r}\right)+\iota_{14}\,\alpha\frac{\partial}{\partial x}+\iota_{24}\,\alpha\frac{\partial}{\partial y}+\iota_{34}\alpha\frac{\partial}{\partial z}\right\}\psi_1+\left\{\iota_4\left(\frac{i}{R}\right)\right\}\psi_N=0, \qquad (6)$$

where $\psi_N = \sqrt{N} \,.\, \psi_1$ Here the first part, consisting of terms referring to one specified electron, is multiplied by the wave function normalised to represent one electron; and the second part, containing the term common to all the electrons, is multiplied by the wave function normalised to represent N electrons.

Finally, we may perhaps even in the midst of a theoretical discussion not close our eyes altogether to experience and, inasmuch as the two alternative values of the term differ by a factor of about $10^{39}$, there is no doubt that $\sqrt{N}/R$ is the one which accords better with observation.

6. In this section I endeavour to show that the correspondence of $\iota/r$ and $i/R$ is not a vague analogy, but is definitely required by the conditions of the problem.

A difficulty in treating ideally simplified problems is that the equations, if they are to be of practical use, introduce quantities which have no meaning in the ideal conditions and depend on the introduction of some degree of complexity for their physical interpretation. For example, the equations for an unperturbed atom determine quantities which could only have a physical meaning on the assumption that the atom is interacting with its surroundings and therefore not unperturbed. In practice a "simple problem" often means the limit of a more complex problem as the complexity tends to zero. When simplicity is used in this sense, the task of developing a theory by proceeding from the simple to the complex is like developing a theory of number by proceeding from the " simple " conceptions of 0 and ∞.

---

* The singularities are definite centres of rotation, whereas the unspecified electrons are indistinguishable, so that a system of two electrons with one singularity or "fixed" electron is not necessarily equivalent statistically to one electron and two singularities.

In our problem of a fixed and a movable electron in a uniform spherical space, no meaning can be given to co-ordinates or distinctions of position other than those indicated by change of $r$; the equation introduces them in anticipation of approximate application to more complex problems in which space is not so uniform and landmarks less infrequent. We have therefore to distinguish the elements of the problem which are logically simple (and therefore form a suitable starting point for the theory) from those which are simple only as a limiting case of complexity and logically can only be introduced at a later stage. We may regard the problem of which (1) is the solution as gradually taking shape when more and more complexity is introduced; and at each stage we cannot obtain more of the mathematical equation than applies to our partial picture. In the problem stated the first conception to emerge is that of two spherical or hyperspherical loci of radius $r$ and R respectively, expressing that our movable particle is at a distance $r$ from the fixed particle and at a distance R from the centre of the universe. This geometrical picture goes rather too far, for logically we cannot think of a spherical locus before thinking of positional space, and, as already stated, complete distinction of position does not appear until the next stage of complexity is reached; we should rather aim, as best we can, at a pre-geometrical picture of something ready to become a spherical locus when distinction of position is allowed. (In particular, the question of the number of dimensions of these loci would be premature; the conception of connectivity should, I think, precede that of dimensionality in this order of development.) The fact that R will ultimately be treated as a natural constant and $r$ as a variable co-ordinate should be ignored; the difference is only one of degree, for theoretically any alteration of $r$ would slightly alter the equilibrium of the whole universe and increase or decrease R.

Clearly then we must look on equation (1) as developing out of a bipolar problem in which the two radii vectores are denoted by $r$ and R; so that a term $i/r$ must have coupled with it a term $i/\mathrm{R}$. These two terms form the skeleton. We next turn attention to what is supposed to be occupying the two loci. The datum is that just one electron* occupies the sphere of radius $r$, and N indistinguishable electrons occupy the sphere of radius R which constitutes the whole of space. Here the argument of § 5 finds place indicating that a factor $\sqrt{N}$ is introduced, and the coupled terms become $i/r$ and $i\sqrt{N}/R$.

---

* For if there were another electron within range we should not apply equation (1).

It is unnecessary for our purpose to proceed further. The next stage would be to introduce space and time co-ordinates (by treating a rather more complicated problem) and to explain, if we can, why the terms involving these are linked to the skeleton terms in the particular way shown in the equation. I do not profess to have solved this. The point which should be realised is that our view that the terms $i/r$ and $i\sqrt{N}/R$ arise in an identical manner is not shaken by the fact that they appear to be inserted rather unsymmetrically in the wave equation. In a logical development they are not inserted; the wave equation is built up round them. As to why the space-time part of the equation is linked to them unsymmetrically—it could scarcely be otherwise if one locus is to be given the current interpretation as the orbit of an electron and the other as all space

7. When $\psi$ is a simple harmonic function of $t$ so that $\partial\psi/\partial t$ satisfies the same equation as $\psi$, another form of (1), omitting the fixed electron, is

$$\left(\frac{ih}{2\pi}\right)^2 \frac{\partial^2\psi}{\partial t^2} = c^2 \left\{m^2c^2 + \left(\frac{ih}{2\pi}\right)^2 \left(\frac{\partial^2}{\partial x^2} + \frac{\partial^2}{\partial y^2} + \frac{\partial^2}{\partial z^2}\right)\right\}\psi. \tag{7}$$

Reducing as before, this gives

$$\left\{\alpha^2\left(\frac{\partial^2}{c^2\partial t^2} - \frac{\partial^2}{\partial x^2} - \frac{\partial^2}{\partial y^2} - \frac{\partial^2}{\partial z^2}\right) + \gamma^2\right\} \psi = 0. \tag{8}$$

According to our identification

$$\gamma^2 = N/R^2 = N\lambda \tag{9}$$

the cosmical constant $\lambda$ being the inverse square of the radius of the Einstein configuration. Thus (8) becomes

$$(\alpha^2\Box + N\lambda)\,\psi = 0. \tag{10}$$

This may be compared with the equation of propagation of electromagnetic potential $\kappa_\mu$ in curved space satisfying $G_{\mu\nu} = \lambda g_{\mu\nu}$, viz.,*

$$(\Box + \lambda)\,\kappa_\mu = 0. \tag{11}$$

This suggests that there is another equivalent treatment of our problem, depending on the construction of a theoretical proof of (10) analogous to the theory of (11). In one respect this would appear simpler, since the differential properties of curvature are more amenable to analysis than the integral property of connectivity. Moreover (10) and (11) have no special reference to an Einstein world and apply immediately to any state of the universe. But to follow this out we should have to enter into the theory of the factor $\alpha$, the method we have used depends on a comparison in which $\alpha$ is not involved.

---

* Eddington, " Mathematical Theory of Relativity," equation (74.33).

Equation (10) tempts me to a digression. My theoretical investigations of $\alpha$ lead me to think that the circuit corresponding to R needs to be diminished in the ratio of the "packing fraction" 136/137 in order to make it strictly comparable with $r$. I have regarded this correction (if real) as negligible for my purposes, and it is not taken account of elsewhere in the paper. But it has the effect that $\alpha$ in (10) should be taken as 136 (not 137). If protons and electrons are alike except in mass, the equation for the proton will be (10) with $\alpha^2 = 10$ very approximately; that is to say, the equations for free electrons and protons will be respectively

$$(136^2\,\Box + \text{N}\lambda)\,\psi = 0 \qquad (10\,\Box + \text{N}\lambda)\,\psi = 0 \tag{12}$$

the numbers $136^2$ and 10 arising more or less in the way that I have suggested elsewhere.[*]

8. By (2) and (5) we have

$$\frac{2\pi mc\alpha}{h} = \frac{\sqrt{\text{N}}}{\text{R}}. \tag{12}$$

The theory of the Einstein universe gives

$$\text{GM}_0/c^2 = \tfrac{1}{2}\pi\text{R}, \tag{13}$$

where $\text{M}_0$ is the total mass of the universe[†] and G the constant of gravitation. Assuming that the number of protons is equal to the number of electrons, we have approximately

$$\text{M}_0 = \text{N}\textsc{m}$$

where $\textsc{m}$ is the mass of a proton Hence

$$\text{N} = \tfrac{1}{2}\pi c^2\text{R}/\text{G}\textsc{m} \tag{14}$$

so that by (12)

$$\left(\frac{2\pi mc\alpha}{h}\right)^2 = \frac{\tfrac{1}{2}\pi c^2}{\text{G}\textsc{m}}\cdot\frac{1}{\text{R}}. \tag{15}$$

Also in the Einstein world $\lambda = 1/\text{R}^2$, so that

$$\lambda = \left(\frac{2\text{G}\textsc{m}}{\pi}\right)^2\left(\frac{2\pi m\alpha}{h}\right)^4 = 9{\cdot}79\ \ 10^{-55}. \tag{16}$$

---

[*] 'Proc. Camb. Phil. Soc.,' vol. 27, p. 18 (1931).

[†] I adopt spherical (not elliptical) space since the treatment of the semi-circuits in elliptical space is not obvious. I think that it must be impossible to decide experimentally between the two forms of space so that both should give the same result.

This gives

$$R = 1\cdot 01 \,.\, 10^{27} \text{ cm.} = 328 \text{ million parsecs.}$$

$$= 1070 \text{ million light years.}$$

The speed of recession of distant bodies per unit distance is given by $c/R\sqrt{3}$. The result for the above value of R is

528 km. per sec. per megaparsec.

This represents the full effect of cosmic repulsion and would be diminished by any countervailing gravitational attraction between the galaxies. So far as can be judged from estimates of the average density of matter in the universe the reduction, though not entirely negligible, is not likely to be very large.

The observational value according to Hubble is 465 km. per sec. per mp. De Sitter finds nearly the same value; but, owing to the uncertainties of the distance-scale and other causes, the astronomical determination could perhaps be in error by as much as 20 per cent.

9. We have also by (12) and (14)

$$\sqrt{N} = \frac{2\pi mc\alpha}{h} \cdot \frac{2GMN}{\pi c^2},$$

or, since $\alpha = hc/2\pi e^2$,

$$\frac{e^2}{GMm} = \frac{2}{\pi}\sqrt{N}. \tag{17}$$

The left side is the ratio of the electrostatic to the gravitational force between a proton and electron. Denoting this ratio by F, we have

$$N = (\tfrac{1}{2}\pi F)^2 = 1\cdot 29 \,.\, 10^{79}. \tag{18}$$

This is the type of relation which I anticipated in an earlier paper,* but it is reached mainly in a different way. The present investigation is independent of the theory of the proton.

Another formula equivalent to (16) is

$$\lambda = (2mc^2/\pi e^2 F)^2. \tag{19}$$

I have considered the alternative that the value of $\gamma$ might be $\sqrt{2N}/R$, 2N being the number of electrons and protons in the universe. I do not think that this would be in keeping with the general conceptions of the theory. We do not mind whether curved macroscopic space replaces N or 2N singularities; whatever the number and whatever their properties, the observed dimensions of space will be such as to compensate for their abolition. But we are concerned with the fact that in order to make use of this replacement we must consider a system in which our electron is one of N indistinguishable electrons.

---

* 'Proc. Camb. Phil. Soc.,' vol. 27, p. 19 (1931).

### *On the Value of the Cosmical Constant.*

(Abstract.)

It is argued that, owing to the curvature of space, a term $i\sqrt{N}/R$ should appear in the wave equation for an electron, N being the number of electrons in the universe and R the radius of the universe in an eigenstate, and having therefore the dimensions calculated for an Einstein world. The units are here supposed to be such that the electrostatic energy of two electrons at a distance $r$ is simultaneously represented by a term $i/r$ The theoretical term is identified with the term ordinarily attributed to the proper-mass of the electron. From this identification we find the cosmical constant $\lambda = 9{\cdot}79 \, . \, 10^{-55}$, which gives a speed of recession of the spiral nebulæ 528 km. per sec. per megaparsec. The observed speed according to Hubble is 465 km. per sec. per megaparsec

---

# *The Diffraction of Electrons in Gases.*

By F. L. Arnot, Ph.D., Lecturer in Natural Philosophy, The University, St. Andrews

(Communicated by J Chadwick, F R S —Received August 10, 1931.)

## *Introduction.*

The new wave mechanics has been eminently successful in correlating and accounting for the large amount of experimental data on the periodic properties of the atom. The applications of the new theory to aperiodic phenomena, though not nearly so numerous, have been attended with no less success; indeed, it is in these experiments on free electrons, in which diffraction patterns similar to those produced by beams of X-rays and light are obtained, that the wave nature of electrons is so clearly and objectively demonstrated.

Such diffraction effects have been obtained by a number of investigators* by scattering beams of homogeneous electrons in crystals, thin films and by a ruled grating. Similar effects are obtained when electrons are scattered by complex molecules,* owing to the symmetrically situated nuclei in the molecular structure, and when $\alpha$-particles are scattered by helium† owing to interference between the waves of the scattered incident particles and recoiling helium nuclei.‡

---

* Davisson and Germer, G. P. Thomson, Thomson and Reid, Rupp, Kikuchi, Rose, and others. For literature see " The Wave Mechanics of Free Electrons," by G. P. Thomson.

Recently Bullard and Massey§ and the author|| have described a new class of diffraction phenomena which are produced when slow electrons are scattered by single atoms. In these experiments the diffraction patterns observed are due to interference between the secondary wavelets originating from different portions of a single atom, and so may be regarded as the electrical analogue of the diffraction of light by a random distribution of small particles.

In the experiments of the author mercury vapour was used as the scattering gas, and electrons having energies of from 8 to 800 volts, corresponding to wave-lengths of from 4·0 to 0·4 Å.U. were employed. All the scattering curves showed distinct maxima and minima, maxima of four different orders being obtained. Pearson and Arnquist¶ have subsequently published similar results over a smaller range of velocities

The present paper deals with an extension of this work to gases. The angular distributions of the elastically scattered electrons in Xe, Kr, Ar, Ne, $H_2$, $N_2$, $CH_4$ and CO have been measured for several different velocities of the primary beam between 30 and 800 volts, corresponding to wave-lengths of from 2·0 to 0·4 Å.U. The lower velocity curves of the rare gases all show distinct diffraction patterns, but at the higher velocities the maxima and minima in Ar and Ne have completely disappeared.

## *Apparatus.*

The apparatus used in this work was the same as that employed in the work on mercury vapour. Full details of the apparatus and an account of the experimental procedure have been given in two previous papers.** It will be sufficient to reproduce here a diagram of the essential parts, fig. 1.

---

* Mark and Wierl, 'Naturwiss,' vol 18, p. 205 (1930); R. Wierl, 'Ann. Physik,' vol. 8, p. 521.

† Chadwick, 'Proc. Roy. Soc.,' A, vol. 128, p 114 (1930); Blackett and Champion, 'Proc. Roy Soc.,' A, vol. 130, p 380 (1931).

‡ Mott, 'Proc. Roy. Soc.,' A, vol. 126, p. 259 (1930).

§ Bullard and Massey, 'Proc. Roy. Soc.,' A, vol. 130, p. 579 (1931).

|| Arnot, 'Proc. Roy. Soc.,' A, vol. 130, p. 655 (1931).

¶ Pearson and Arnquist, 'Phys. Rev.,' vol. 37, p. 970 (1931).

** Arnot, 'Proc. Roy. Soc.,' A, vol. 130, p. 655 (1931); *ibid*, vol. 129, p. 361 (1930).

These are an electron gun consisting of the tungsten filament, F, entirely enclosed within two cylinders containing two holes, $S_1$ and $S_2$, each of 1 mm. in diameter. The gun could be rotated about the axis, O, through nearly 360° by means of a small ground glass joint.

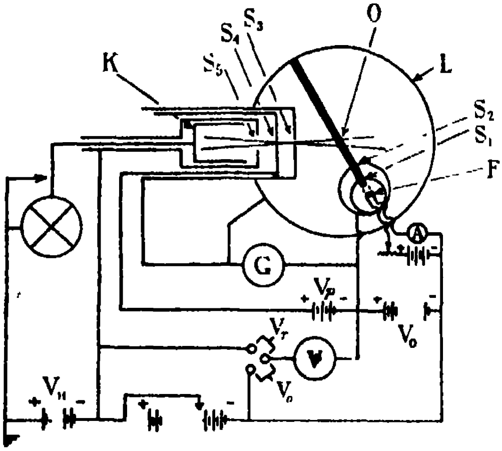

Fig 1.—Diagram of Apparatus.

The receiving system consisted of three concentric cylinders containing the slits, $S_3$, $S_4$, $S_5$, and the concentric Faraday cylinder, K, within the inner shielding cylinder. The dimensions of these slits were respectively 8 mm. × 0·2 mm., 5 mm. × 0·2 mm., 2 mm. × 2 mm., and the three slits were equally spaced 5 mm. apart. The distance of $S_3$ from the scattering point, O, was 12 mm. The inside of the collision chamber was lined with the large nickel cylinder, L.

A small difference of potential, $V_p$, of 9 volts was applied to the first two slits, $S_3$ and $S_4$, to stop positive ions from entering the Faraday cylinder. A potential of $V_r = (V_0 + V_p - 4)$ volts, where $V_0$ is the velocity of the primary electron beam, was applied between the next two slits, $S_4$ and $S_5$, so as to stop all but the elastically scattered electrons from being received. And finally a potential, $V_{II}$, of 12 volts was applied between the slit, $S_5$, and the Faraday cylinder to prevent any secondary emission of electrons from the Faraday cylinder. The glass work was of pyrex and the whole apparatus up to within a few centimetres of the ground glass joints was baked out at a temperature of 500° C., the joints being kept below room temperature by means of water coolers. The apparatus was connected through a liquid air trap to a diffusion pump backed by a Hyvac pump, and a good "sticking vacuum" was obtained on a sensitive McLeod gauge.

The gas was allowed to leak into the apparatus through a fine glass capillary which was internally sealed into the inlet tube. The gas was not circulated, but after passing through the apparatus was pumped off into the atmosphere through another capillary Mercury vapour was excluded from the apparatus by liquid air traps on the inlet and outlet tubes. The gas was contained in a large bulb behind the inlet capillary at a pressure of about 5 mm. This produced a pressure in the apparatus of about 0·003 mm. of Hg which was read on the McLeod gauge. Several runs could be taken without the pressure showing any appreciable decrease When using Xe, Kr and Ne, however, a smaller gas container was used behind the inlet capillary, which resulted in the pressure in the apparatus decreasing by about 10 per cent. during a run. Since the decrease in pressure with time was sensibly uniform, the pressure was read immediately before and after each run, and the readings corrected accordingly. Pressures of from 0·0025 mm to 0·0035 mm. of Hg were used.

The relation between the scattered current and the pressure was measured for several different angles of scattering, and was found to be linear over the above range of pressures. The scattering was therefore due to single collisions. At angles below 30° the linear relationship ceased to hold for pressures above 0·006 mm. in argon, due to the onset of multiple scattering.

## *Results.*

(1) *The Angular Distribution of the Scattered Electrons.*—The results obtained for the monatomic rare gases Xe, Kr, Ar and Ne, are shown in fig. 2. The number at the side of each curve represents the energy in volts of the primary electron beam. I am indebted to Dr. Aston for the loan of the xenon and krypton, both of which gases were at least 99 per cent. pure. The argon and neon were obtained from the British Oxygen Company, the argon being supplied as 99 per cent. pure, and the neon as 98 per cent. pure. The curves for electrons of different velocities in Xe, Kr and Ar have all been displaced in a vertical direction, but the base line for each curve is shown in the figure. In the case of Ne, the curves for the three highest velocities, 205, 412 and 830 volts, are all drawn on the same base line, as are also the curves for the two lowest velocities, 29 and 42 volts.

The results obtained for the diatomic gases $H_2$, $N_2$, CO, and for the more complicated gas, $CH_4$, are shown in fig. 3. The hydrogen, nitrogen, and methane were obtained from commercial cylinders. The methane was subsequently found to contain 15 per cent. of nitrogen, but this should not affect the general shape of the curves. The carbon monoxide was produced by dropping concentrated sulphuric acid on to sodium formate *in vacuo*, the gas being dried by passing through a trap immersed in liquid air. The curves for $N_2$ and CO have all been displaced in a vertical direction by an equal amount,

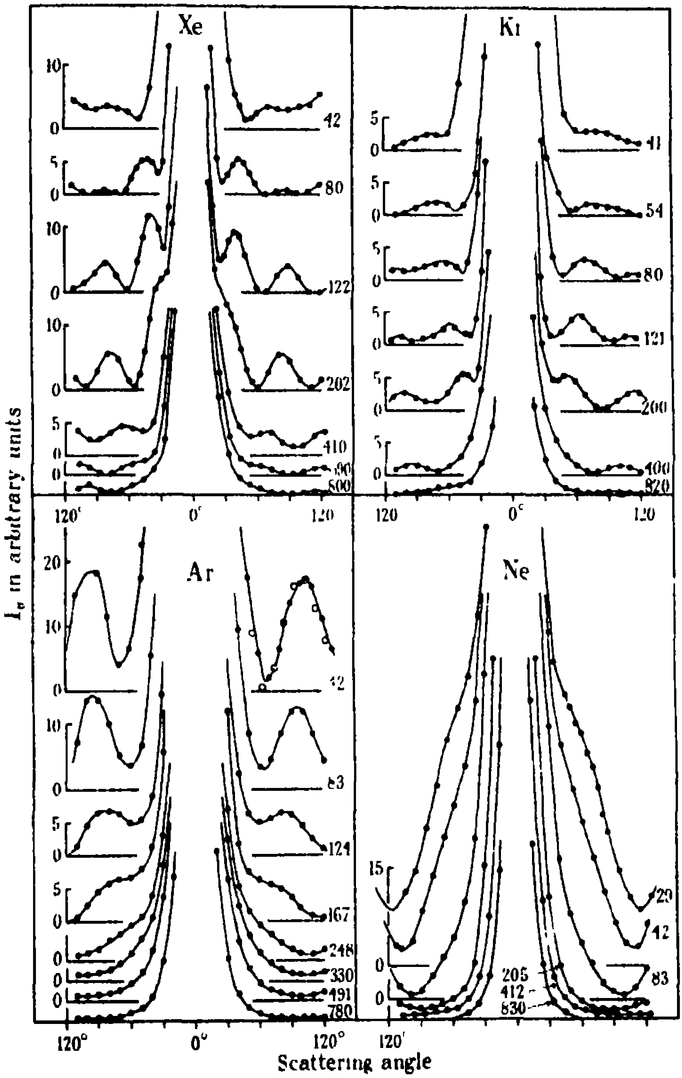

Fig. 2.—Angular Distribution of Scattered Electrons in Xenon, Krypton, Argon and Neon.

the base line of each curve being two units of ordinate above the base line of the curve immediately below it. The curves for $H_2$ and $CH_4$ have not been displaced at all.

All the curves in figs. 2 and 3 have been reduced to a standard pressure of

$10^{-3}$ mm. of Hg at 18° C. and a standard electron beam current of 7·4 micro-amps. The ordinates of both figures represent $I_\theta$ in arbitrary units, where $I_\theta$ is defined thus. If a beam of electrons passes through a gas containing N atoms per unit volume, then $NI_\theta$ is the proportion of the beam elastically scattered

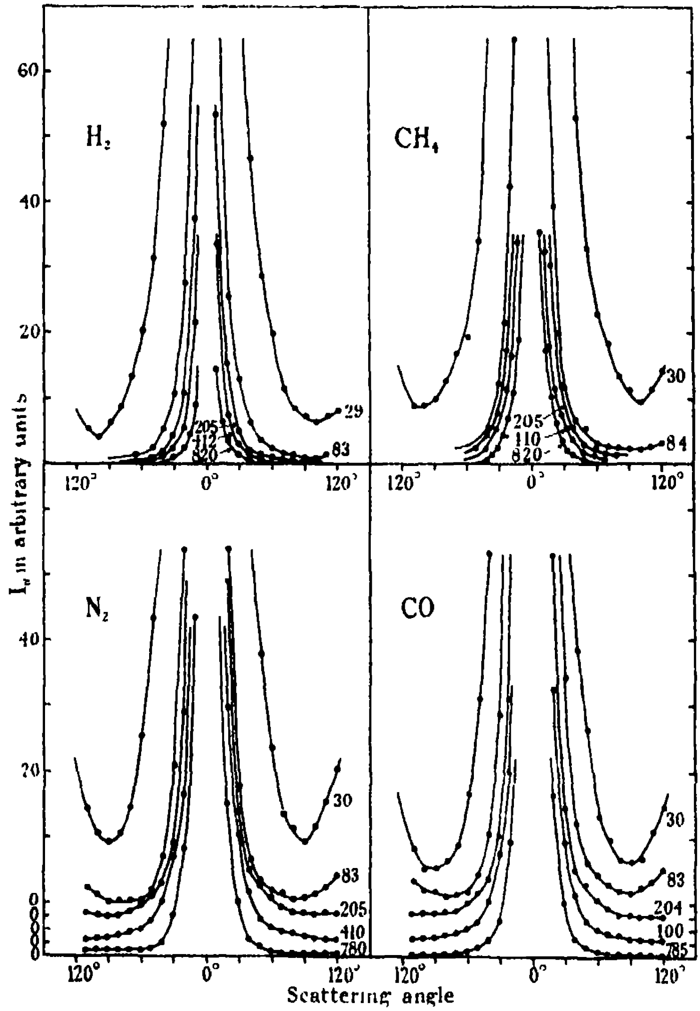

FIG. 3.—Angular Distribution of Scattered Electrons in Hydrogen, Methane, Nitrogen and Carbon Monoxide.

in the direction θ, per unit solid angle and per unit length of the beam. $I_\theta$ has the dimensions of an area.

The experimental points from which the curves in figs. 2 and 3 are drawn are given in Tables I to VI. In using these tables the appropriate angular correction given at the foot of each column must be applied. For example, the values of $I_\theta$ given in the third column of Table I for 80-volt electrons in xenon are for the following angles, 13°, 18°, 23°, 28° and so on to 118°, the angular correction for this column being −2°. This method of tabulating the results has been adopted solely to obviate the necessity of providing a separate column of angles for each velocity.

It will be seen from fig. 2 that the rare gases all show clearly marked diffraction maxima and minima, the angular interval between successive maxima becoming larger as the atomic number of the gas become smaller. As was the case in mercury vapour,* the peaks move in to smaller angles as the velocity of the primary beam is increased. Since the wave-length of the incident electrons varies inversely as their velocity we should expect this to occur on any simple theory of diffraction by rigid spheres. The points denoted by circles on the 42-volt curve in argon are Bullard and Massey's points† for 40-volt electrons in argon fitted to my curve at 103°. The agreement is seen to be very satisfactory. It will be seen that the diffraction maxima and minima have completely disappeared in the higher velocity curves in Ne and Ar. This is due to the refractive index of the atom becoming nearly equal to unity for very short wave-lengths.

Table I.—Xenon.

| $V_0$ | 42. | 80 | 122 | 202 | 410. | 590. | 800 |
|---|---|---|---|---|---|---|---|
| Angle | $I_\theta$. | $I_\theta$ | $I_\theta$ | $I_\theta$ | $I_\theta$ | $I_\theta$ | $I_\theta$. |
| ° | | | | | | | |
| 15 | — | 70·0 | 31·4 | 31·9 | — | — | 24·5 |
| 20 | 80·0 | 22·5 | 13·1 | 18·6 | 22·4 | 15·7 | 15·0 |
| 25 | 41·6 | 5·60 | 4·96 | 13·0 | | — | — |
| 30 | 22·2 | 1·98 | 5·62 | 13·1 | 9·6 | 5·9 | 6·2 |
| 35 | 10·9 | 2·93 | 7·87 | 11·6 | — | — | — |
| 40 | 5·20 | 4·55 | 9·10 | 9·60 | 1·4 | 2·5 | 2·63 |
| 45 | 3·63 | 5·37 | 8·60 | 6·23 | — | — | — |
| 50 | 1·64 | 4·85 | 5·80 | 3·08 | 3·04 | 1·76 | 1·74 |
| 55 | 1·75 | 3·20 | — | 1·17 | — | — | — |
| 60 | 2·60 | 1·79 | 0·80 | 0·60 | 3·46 | 1·39 | 1·04 |
| 70 | 3·40 | 0·00 | 0·00 | 2·75 | 3·57 | 0·86 | 0·50 |
| 80 | 3·11 | 0·51 | 2·64 | 5·40 | 2·02 | 0·32 | 0·31 |
| 90 | 2·89 | 0·71 | 3·96 | 4·36 | 1·44 | 0·13 | 0·20 |
| 100 | 3·55 | 0·22 | 2·17 | 1·70 | 1·60 | 0·56 | 0·32 |
| 110 | 3·85 | 0·56 | 0·0 | 0·53 | 3·00 | 1·08 | 0·53 |
| 120 | 5·36 | 1·48 | 0·0 | 1·74 | 3·70 | 1·12 | 0·18 |
| **Angle correction** | 0° | −2° | −2° | 0° | +2° | +3° | +3° |

---

* Arnot, 'Proc. Roy. Soc.,' A, vol. 130, p. 655 (1931).

† Bullard and Massey, 'Proc. Roy. Soc.,' A, vol. 130, p. 579 (1931).

## Table II.—Krypton.

| $V_0$. | 41. | 54 | | 80 | 121. | 200. | 400 | 820. |
|---|---|---|---|---|---|---|---|---|
| Angle. | $I_\theta$. | $I_\theta$ (Expt ) | $I_\theta$. (Theor.) | $I_\theta$. | $I_\theta$ | $I_\theta$. | $I_\theta$. | $I_\theta$. |
| ° | | | | | | | | |
| 10 | — | — | — | — | — | — | — | 65 |
| 15 | — | 63 | — | — | — | — | — | — |
| 20 | 230 | — | 32·4 | 73 | - - | 47 3 | 24 3 | 13 8 |
| 25 | - | 24 6 | — | - | - | — | — | — |
| 30 | 81 | — | 12 5 | 21 7 | 10 5 | 10 2 | 10 15 | 5 35 |
| 35 | — | 6·3 | — | — | 4 1 | — | — | — |
| 40 | 22 8 | — | 2 04 | 3 65 | 1 64 | 4 84 | 5 33 | 2 12 |
| 45 | — | 1·41 | — | — | — | 4 69 | — | — |
| 50 | 5 73 | — | 0 255 | 0 91 | 2 11 | 5 21 | 3 00 | 1 08 |
| 60 | 3 10 | 1·53 | 1 61 | 2 41 | 3 96 | 4 45 | 1 49 | 0 83 |
| 70 | 3·00 | 1 87 | 2 18 | 3 22 | 4 45 | 2 43 | 0 74 | 0 36 |
| 80 | 3 05 | 1 81 | 1 55 | 2 70 | 2 54 | 0 70 | 0 65 | 0 28 |
| 90 | 2·79 | 0 98 | 0 77 | 1·56 | 0 97 | 0·45 | 1·08 | 0 53 |
| 100 | 2 10 | 0 19 | 0 248 | 0 55 | 0 77 | 1 54 | 1·36 | 0·52 |
| 110 | 1·37 | 0 00 | 0 044 | 0·86 | 1 24 | 2·61 | 1 13 | 0·24 |
| 120 | 1 12 | — | — | 0 85 | 1 13 | 2·66 | 0 48 | 0·15 |
| Angle correction | 0° | 0° | 0° | −2° | −4° | −2° | 0° | 0° |

## Table III.—Argon.

| $V_0$. | 42. | 83 | 124. | 167 | 248 | 330. | 491. | 780. |
|---|---|---|---|---|---|---|---|---|
| Angle | $I_\theta$ | $I_\theta$ | $I_\theta$. | $I_\theta$ | $I_\theta$ | $I_\theta$. | $I_\theta$. | $I_\theta$. |
| ° | | | | | | | | |
| 15 | — | — | — | — | — | — | — | 56 |
| 20 | 160 | 210 | 154 | 114 | 89 | 65 | 50 | 26 |
| 30 | 73 | 65 | 38 | 29 | 23 | 19·5 | 18 | 9 2 |
| 40 | 34 | 24 5 | 12·4 | 11 7 | 11·2 | 10 5 | 9 0 | 4 0 |
| 50 | 17 3 | 8 7 | 6 5 | 7 7 | 7 6 | 6 9 | 5 0 | 2·0 |
| 60 | 5 9 | 3 6 | 5 1 | 6 3 | 5 4 | 4·2 | 2 8 | 1·1 |
| 70 | 2 1 | 4 7 | 5·7 | 5 8 | 4 0 | 2 8 | 1 8 | 0·68 |
| 80 | 6 5 | 8 6 | 6 7 | 5 0 | 2 8 | 1·8 | 1 2 | 0·48 |
| 90 | 13 6 | 11 9 | 6 2 | 3·8 | 1 9 | 1 1 | 0·87 | 0·45 |
| 100 | 16 6 | 11 9 | 4 4 | 2·0 | 1·1 | 1 0 | 0 75 | 0·42 |
| 110 | 16 0 | 8 5 | 2·5 | 0 9 | 1 0 | 1·0 | 0·86 | 0·41 |
| 120 | 11 1 | 4·4 | 1 0 | 0·5 | 1·7 | 1 3 | 1 17 | 0·41 |
| Angle correction | −1° | 0° | −1° | 0° | −1° | 0° | 0° | 0° |

## Table IV.—Neon.

| $V_0$ | 29 | 42 | 83 | 205 | 412 | 830 |
|---|---|---|---|---|---|---|
| Angle. | $I_\theta$ | $I_\theta$ | $I_\theta$ | $I_\theta$ | $I_\theta$. | $I_\theta$ |
| ° | | | | | | |
| 10 | 127 | — | — | 88 | 49 | 26·6 |
| 20 | 81 | 83 | 96 | 55 | 18·0 | 8·2 |
| 30 | 46·4 | 51 | 41·6 | 18·6 | 6·2 | 2·5 |
| 40 | 41·3 | 34 | 21·4 | 8·1 | 3·2 | 1·1 |
| 45 | 39·5 | | — | — | | — |
| 50 | 37·0 | 27 | 13·0 | 4·2 | 1·9 | |
| 55 | 35·5 | — | — | — | — | — |
| 60 | 32·5 | 22 | 8·6 | 2·8 | 1·4 | |
| 65 | 30·2 | — | — | — | — | — |
| 70 | 27·1 | 16·6 | 5·3 | 1·9 | 0·93 | — |
| 75 | 23·1 | | — | — | — | — |
| 80 | 20·4 | 11·2 | 2·6 | 1·6 | 0·87 | — |
| 90 | 14·6 | 6·7 | 1·2 | 1·5 | 0·71 | — |
| 100 | 10·5 | 3·5 | 0·8 | 1·6 | 0·73 | |
| 110 | 8·6 | 3·0 | 1·9 | 2·1 | 0·80 | — |
| 120 | 10·7 | 6·4 | 4·7 | 2·1 | 0·74 | — |
| Angle correction | +6 | +2° | +1 | 0° | +4° | +4° |

## Table V.—Hydrogen and Methane.

| | Hydrogen | | | | | Methane | | | | |
|---|---|---|---|---|---|---|---|---|---|---|
| $V_0$ | 29 | 83 | 205 | 412 | 820 | 30 | 84 | 205 | 410 | 820 |
| Angle | $I_\theta$ | $I_\theta$ | $I_\theta$ | $I_\theta$ | $I_\theta$ | $I_\theta$. | $I_\theta$ | $I_\theta$ | $I_\theta$ | $I_\theta$ |
| ° | | | | | | | | | | |
| 10 | — | (99) | 53·5 | 33·6 | 14·5 | (700) | 178 | (153) | 73 | 35·2 |
| 15 | — | — | — | — | 6·32 | — | 70 | — | 32·5 | 17·2 |
| 20 | 152 | 25·6 | 15·2 | 7·3 | 3·52 | 229 | 40 | 30·5 | 18·0 | 10·2 |
| 25 | — | — | — | — | — | — | 20 | — | 11·6 | 6·2 |
| 30 | 85·3 | 13·0 | 5·0 | 3·0 | 1·30 | 104 | 11·8 | 12·0 | 7·5 | 3·7 |
| 35 | — | — | — | — | — | — | — | — | 5·5 | 2·0 |
| 40 | 46·7 | 6·2 | 2·0 | 1·36 | 0·50 | 53 | 6·8 | 5·8 | 3·7 | 1·3 |
| 50 | 28·8 | 3·6 | 1·3 | 0·72 | — | 33 | 5·6 | 3·0 | 1·9 | 0·8 |
| 60 | 19·9 | 2·2 | 0·87 | — | — | 23 | 3·1 | 2·2 | 1·3 | — |
| 70 | 11·3 | 1·6 | 0·63 | — | — | 18·4 | 2·8 | 1·7 | 0·8 | — |
| 80 | 8·3 | 1·3 | 0·41 | — | — | 13·5 | 2·6 | 1·4 | — | — |
| 90 | 7·1 | 1·0 | 0·38 | — | — | 11·2 | 2·3 | — | — | — |
| 100 | 6·4 | 0·8 | — | — | — | 9·7 | 2·1 | — | — | — |
| 110 | 7·2 | 1·6 | — | — | — | 11·3 | 2·8 | — | — | — |
| 120 | 8·1 | — | — | — | — | 14·2 | 3·1 | — | — | — |
| Angle correction | +1° | 0° | −1° | −1° | −1° | +1° | 0° | −2° | −3° | −2° |

Table VI.—Nitrogen and Carbon Monoxide.

| | Nitrogen | | | | | Carbon monoxide. | | | | |
|---|---|---|---|---|---|---|---|---|---|---|
| $V_0$. | 30. | 83 | 205 | 410. | 780 | 30. | 83 | 204. | 400. | 785 |
| Angle | $I_\theta$ | $I_\theta$ | $I_\theta$ | $I_\theta$. | $I_\theta$ | $I_\theta$ | $I_\theta$. | $I_\theta$ | $I_\theta$. | $I_\theta$ |
| ° | | | | | | | | | | |
| 10 | 660 | 290 | 224 | 137 | 86 | (433) | 350 | 225 | — | — |
| 20 | 243 | 56 | 53 | 35 8 | 23 1 | 152 | 108 | 57 | 38 5 | 24 6 |
| 30 | 118 | 20 | 18 | 16 4 | 8 2 | 75 | 36 2 | 18 5 | 15·4 | 8 1 |
| 40 | 68 | 8 7 | 9 0 | 7 8 | 2 5 | 38 6 | 14·2 | 9 0 | 7 3 | 2 7 |
| 50 | 38 | 5 4 | 6 8 | 3 8 | 1 5 | 26 6 | 8 3 | 7 0 | 3 5 | 1 5 |
| 60 | 23 8 | 4 0 | 4 9 | 2 3 | 0 9 | 13 2 | 6 4 | 4 7 | 2 1 | 0 87 |
| 70 | 13 6 | 3 6 | 3 3 | 1 8 | 0 5 | 9 9 | 5 0 | 3 3 | 1 6 | 0 59 |
| 80 | 11 4 | 2 7 | 2 6 | 1 4 | 0 4 | 6·8 | 3 9 | 2 2 | 1 2 | 0 39 |
| 90 | 9 4 | 2 9 | 2 5 | 1 0 | 0 5 | 6 4 | 3 8 | 2 3 | 0 70 | 0 33 |
| 100 | 11 7 | 3·5 | 2 2 | 0 8 | 0·5 | 6 9 | 4 4 | 2 02 | 0 59 | 0 33 |
| 110 | 15 5 | 4·6 | 2 4 | 0 7 | 0 5 | 11 0 | 5 4 | 2 05 | 0 55 | 0 20 |
| 120 | 20 5 | 6 2 | 2 4 | 0 6 | 0 5 | 14 7 | 7 1 | 2 14 | 0 49 | 0 11 |
| Angle correction | 0° | 0° | −1° | −1° | −1° | +1° | 0° | −1° | −1° | −1° |

Referring now to fig. 3, we see that the molecular gases $H_2$, $CH_4$, $N_2$ and CO all show no diffraction maxima. In the lower velocity curves of each of these gases, however, a minimum occurs in the region of 90° which moves in to smaller angles as the velocity of the electrons is increased, at the same time becoming fainter until it finally disappears altogether, the higher velocity curves falling off monotonically like those of the rare gases. After the minimum is passed the curves probably continue to rise steadily as the angle is increased to 180°, for Ramsauer and Kollath* have recently shown that at much lower velocities the backward scattering may exceed the forward scattering

The similarity of the scattering curves of $CH_4$ to those of $H_2$ is very interesting, for Bullard and Massey† find that at velocities below 30 volts the scattering curves of $CH_4$ resemble those of Ar. It is also well known that the total effective cross section curve for $CH_4$ resembles those of the rare gases for velocities below 30 volts. The similarity of the cross section curves, and also of the scattering curves, of methane and argon for electrons of velocities below about 30 volts can be explained‡ if we assume that the four electrons of the four

---

* Ramsauer and Kollath, 'Ann. Physik,' vol. 10, p. 143 (1931).

† Bullard and Massey, 'Proc. Roy. Soc.,' A, vol. 133, p. 637 (1931).

‡ See Karl Darrow, 'Bell. Tel. System Monograph' B, 527, p. 15 (1930).

H-atoms of the $CH_4$ molecule form with the four outer electrons of the C-atom a closed shell of eight electrons similar to the outer shell of the rare gas atoms. Then, since electrons of less than 30 volts energy will be mainly scattered by this outer shell, we should expect the cross section and angular scattering curves of methane to be similar to those of the rare gases. Electrons of energy greater than 30 volts will, however, penetrate this outer shell without suffering much deflection, and we should, therefore, no longer expect the scattering curves to resemble those of argon, for the inner structure of methane is probably quite different to that of argon It would be possible then to account for the similarity between the angular scattering curves and also the cross section curves (see p 628) of methane and hydrogen by assuming that the electrons are scattered in methane mainly by the four hydrogen nuclei of the $CH_4$ molecule. If this were true we should expect the cross section for $CH_4$ to be about twice that of $H_2$ for electrons of greater than 30 volts energy. It will be shown on p. 628 that this is actually the case

A very interesting idea emerges from the above discussion, namely, that we may be able to examine the structure of complex molecules by analysis of the diffraction patterns exhibited in the angular scattering curves of these molecules in much the same way as the structure of crystals has been determined by analysis of X-ray diffraction patterns By using electrons of increasing velocity we could probe deeper and deeper into the molecule, examining the structure of each successive shell of electrons either by comparing the diffraction patterns obtained with those obtained from simpler atoms of known structure, or, when the theory of electron scattering has been more fully developed, by direct analysis of the diffraction patterns obtained from the molecule alone.

(2) *The Effective Cross Sections for Elastic Collisions.*—If we multiply the ordinates of figs. 2 and 3 by $2\pi \sin \theta$ we obtain curves which represent the proportion of the primary beam scattered in all azimuths per unit angle, as a function of the angle of scattering. The area under these curves,

$$Q = 2\pi \int_0^\pi I_\theta \sin \theta \, . \, d\theta,$$

gives the effective cross section for elastic collisions for electrons of different velocities. The total effective cross section for elastic collisions of all the atoms in a cubic centimetre at 1 mm. pressure and 0° C. is then given by

$$W = \frac{2 \cdot 71 \times 10^{19}}{760} Q \text{ cm}^2 \text{ per cm.}^3.$$

Whereas on the classical theory the scattering per unit solid angle at 0° is infinite, on the quantum theory it is finite, so that the curves representing the scattering per unit angle should all pass through the origin at 0°. When the measurements are taken in to sufficiently small angles these curves do actually bend over so as to extrapolate through the origin. Fig. 4 shows the scattering per unit angle in Ne obtained by multiplying the ordinates of the neon curves in fig. 1 by $2\pi \sin \theta$ This figure clearly shows how the effective elastic cross section decreases as the velocity of the electrons increases.

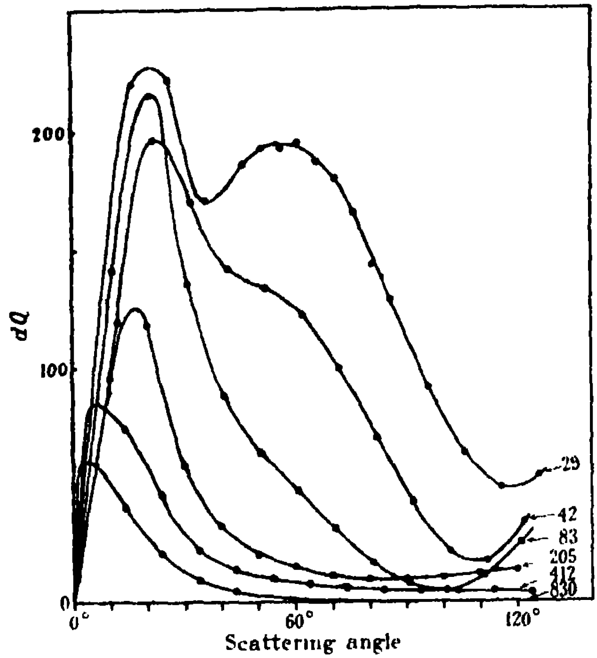

FIG. 4.—Scattering per unit angle in Neon.

In fig. 5 the elastic cross section in arbitrary units is plotted against the velocity of the electrons in $\sqrt{\text{volts}}$. It should be realised that these curves indicate only very roughly the variation of the elastic cross section with velocity for the following reasons :—

(1) The curves representing the scattering per unit angle have only been integrated from 0° to 120° instead of from 0° to 180°, *i.e.*, elastic collisions in which the electrons are scattered through angles greater than 120° are not included.

(2) There is an uncertainty in the extrapolation of some of these curves to 0° owing to readings not having been taken down to sufficiently small angles to determine the point where the curves bend over.

In spite, however, of these defects it appears worth while to consider these cross section curves for elastic collisions in relation to the total effective cross section

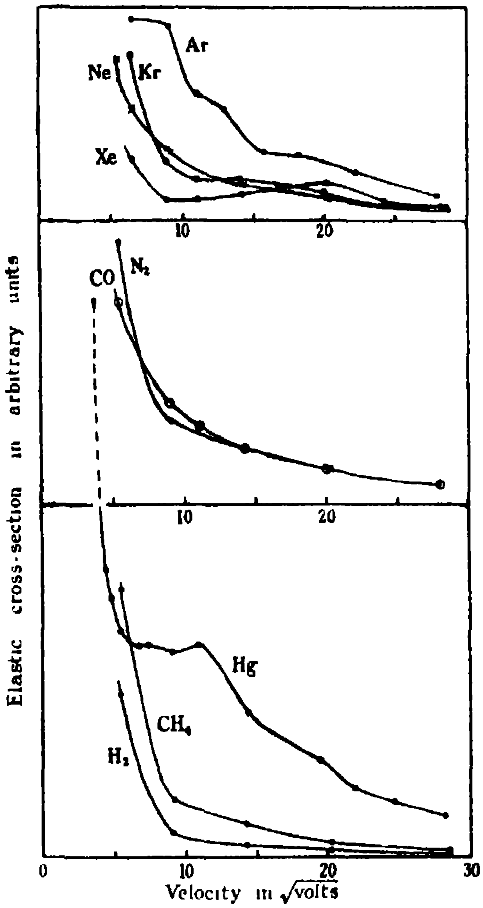

FIG. 5 --The Elastic Cross Section Curves

curves, or absorption coefficient curves, which include both elastic and inelastic collisions.* The latter curves will be referred to briefly as "the total cross section curves," while the former will be called the "elastic cross section curves."

### *Mercury Vapour.*

Fig. 5 also contains the elastic cross section curve for Hg vapour calculated from the author's results for Hg vapour which have already been published.†

---

* For literature and summary of results see Kollath, 'Physik. Z.,' vol. 31, p. 985 (1930).
† Arnot, 'Proc. Roy. Soc.,' A, vol. 130, p. 655 (1931).

The elastic cross section curve shows the slight maximum and steep rise found by Brode* and others for the total cross section. The whole curve is very similar to the total cross section curve, but it appears to be shifted to higher velocities.

### *Hydrogen.*

The elastic cross section curve for $H_2$ is very similar to Normand's curve for the total cross section.† It shows the change in slope observed by Normand at about 81 volts, but this change of slope is far more marked in the elastic cross section curve. As the velocity is increased from 25 volts to 100 volts, the total cross section decreases by a factor of 3 but the elastic cross section decreases by a factor of 9. This means that the proportion of elastic collisions at 100 volts is only one-third of the proportion at 25 volts. Therefore, not more than 33 per cent. of the collisions are elastic at 100 volts. We should expect this large increase in the proportion of inelastic collisions from other considerations; for instance, the efficiency of ionisation increases by a factor of 2·7 when the velocity is increased from 25 volts to 100 volts.‡

### *Methane.*

The elastic cross section curve for $CH_4$ is very similar to that for $H_2$, as are also the respective scattering curves for these two gases (see fig. 3). The elastic cross section for $CH_4$ is roughly about twice that for $H_2$ throughout the velocity range of 25 to 800 volts. The similarity of the elastic cross section curve for $CH_4$ to that of $H_2$ in the velocity range between 25 and 800 volts is especially interesting in view of the fact that for lower velocities the total cross section curve for $CH_4$ closely resembles the total cross section curves of the rare gases. This point has been further discussed on p. 625.

### *Nitrogen and Carbon Monoxide.*

The elastic cross section curves for $N_2$ and CO are both almost identical and are of about the same absolute value, as are also the total cross section curves (Normand, *loc. cit.*). There are not sufficient points on the curve to decide whether the small maximum found by Normand in $N_2$ at 144 volts is due to elastic or inelastic collisions As the velocity is increased from 36 to 400 volts the total cross section decreases by a factor of about 4 and the elastic cross section decreases by a factor of about 5·6. This means that the proportion of elastic collisions at 400 volts is about 71 per cent. of the proportion at 36 volts, *i.e.*, the ratio of elastic to inelastic collisions does not vary very much throughout this range of velocities

---

* Brode, 'Proc. Roy. Soc.,' A, vol. 125, p. 134 (1929).

† Normand, 'Phys. Rev.,' vol. 35, p. 1217 (1930).

‡ Compton and van Voorhis, 'Phys. Rev.,' vol. 27, p. 729 (1926).

### *The Rare Gases.*

The most interesting feature about the elastic cross section curves for the rare gases is the presence of a small maximum (or change of slope) which appears in all the curves between 100 and 400 volts The maximum is most clearly defined in Xe, in which gas it appears at about 400 volts. In Kr it appears at about 144 volts, while in Ar and in Ne its presence is indicated merely by a change in slope of the curve.

Another interesting feature of the elastic cross section curves of the rare gases is that at 50 volts Ar has a greater elastic cross section than Kr, and Kr a greater one than Xe, whereas we know from the results of Ramsauer that where the total cross section curves reach their maximum value, in the neighbourhood of 10 volts, the above order of the gases is reversed, Xe having a greater total cross section than Kr, and Kr a greater one than Ar.

### *Neon*

Dealing now with the rare gases individually we find that for Ne, as the velocity is increased from 36 to 400 volts, the total cross section as found by Normand (*loc. cit* ) decreases by a factor of about 2·7, whereas the elastic cross section decreases by a factor of 5·3 This means that the proportion of elastic collisions at 400 volts is only about 50 per cent of the proportion at 36 volts Therefore not more than 50 per cent. of the collisions are elastic at 400 volts.

### *Argon.*

For Ar we find that, as the velocity is increased from 36 to 400 volts, the total cross section (Normand's curve) decreases by a factor of about 3·5 and the elastic cross section decreases by about the same factor. Thus the ratio of elastic to inelastic collisions does not vary much throughout this range of velocities. Normand's curve also shows the change in slope observed at about 225 volts.

### *Krypton and Xenon.*

I have not been able to find any data on the total cross section for Kr and Xe within the range of 36 to 400 volts, and so no conclusions regarding the proportion of elastic to inelastic collisions can be drawn.

We see from the above that in the two lightest gases used, $H_2$ and Ne, the proportion of elastic collisions decreases considerably as the velocity is increased, while in the heavier gases $N_2$, CO and Ar, the ratio of elastic to inelastic collisions does not vary much throughout the entire velocity range of 36 to 400 volts.

The actual figures given will probably need to be revised when the elastic cross sections have been more accurately determined, but the main features outlined above should not be seriously affected.

Before leaving this subject it may be well to clear up a point which has caused some confusion in the past. It has long been known that remarkably consistent measurements of the total effective cross section, or absorption coefficient, have been obtained with widely different types of apparatus The usual methods involve measuring the decrease in intensity of an electron beam after travelling a fixed distance through the gas. The geometry of the final collecting slits determines the maximum angle through which an electron may be deflected without being measured as absorbed It would be expected, therefore, that measurements made with apparatus having different sized slits would give widely different results if a large fraction of the total number of scattered electrons were deflected through small angles Since, however, consistent results are obtained, it must be concluded that only a small fraction of the scattered electrons are deflected through small angles.* This conclusion has appeared to some writers† to be in direct disagreement with the early measurements‡ made on electron scattering This error has arisen because the results of electron scattering experiments are always plotted so as to show the scattering *per unit solid angle*. When the results are plotted so as to show the scattering between $\theta$ and $\theta + d\theta$, or *per unit angle*, we see that the number of electrons scattered through small angles is only a very small fraction of the total number of scattered electrons. This is clearly shown in fig. 4, which gives the scattering *per unit angle*.

## *Discussion.*

Mott§ has shown that the elastic scattering of electrons by atoms can be treated as the diffraction of de Broglie waves by a static field of force, Huygens' principle being employed to determine the resultant amplitude of the scattered wave. From the amplitude of the scattered wave we can then deduce the number of electrons scattered in any direction. The method employed is to find a solution of the general wave equation of Schrodinger such that the solution represents an incident wave falling on the atom together with a diffracted wave emerging from the atom This solution is in the form of an integral equation. From this equation it is seen that the scattered wave is formed by the interference of secondary wavelets, each of these secondary wavelets orginating from an element of volume ($dx$, $dy$, $dz$) of the atomic field, with an amplitude at a distance R from the scattering centre of

---

* See also M. C. Green, 'Phys. Rev.,' vol. 36, p. 239 (1930).

† Brode, 'Phys. Rev.,' vol. 35, p 504 (1930); Gaertner, 'Ann. Physik,' vol. 8, p. 135, (1931).

‡ *e.g.*, Arnot, 'Proc. Roy. Soc.,' A, vol. 125, p. 660 (1929).

§ Mott, 'Proc. Roy. Soc.,' A, vol. 127, p. 658 (1930).

$$\frac{1}{R}\frac{2\pi m}{h^2} V(xyz)\,\psi(xyz)\,dx\,dy\,dz \tag{1}$$

for an incident wave of unit amplitude

In order to proceed further, Born assumed that the incident wave is not appreciably distorted within the atom With this assumption (1) reduces to

$$\frac{1}{R}\frac{2\pi m}{h^2} V(xyz)\,dx\,dy\,dz. \tag{2}$$

Changing over to spherical polar co-ordinates we find that the amplitude of the resultant wave at a large distance R from the scattering centre, and in a direction making an angle $\theta$ with the direction of the incident wave is

$$\left.\begin{aligned} &R^{-1}f(\theta)\\ \text{where}\qquad &f(\theta) = \frac{8\pi^2 m}{h^2}\int_0^\infty \frac{\sin\mu r}{\mu r} V(r)\,r^2\,dr\\ \text{and}\qquad &\mu = 4\pi\sin\tfrac{1}{2}\theta/\lambda \end{aligned}\right\}, \tag{3}$$

$\lambda$ being the de Broglie wave-length of the incident electrons. The scattered intensity $I_\theta$, defined on p. 620 is then given by

$$I_\theta = [f(\theta)]^2 \tag{4}$$

In order to evaluate the integral in (3), we require to know $V(r)$, which is the potential energy of one of the incident electrons at a distance $r$ from the centre of the field of force of the scattering atom. Approximate expressions for $V(r)$ have been given by Thomas,* Fermi,† and a more accurate one by Hartree ‡ Bullard and Massey,§ using the Thomas-Fermi expression for $V(r)$, have evaluated (3) and so determined $I_\theta$. They have shown that $I_\theta/Z^{2/3}$ is a function of $v \sin \frac{1}{2}\theta/Z^{1/3}$ only, where $v$ is the velocity of the incident electrons and Z the atomic number of the scattering atoms. Thus the scattering produced by all atoms for all velocities and all angles can be represented on a single curve. A table is given from which this curve can be constructed.

---

* Thomas, 'Proc. Camb. Phil. Soc.,' vol. 23, p. 542 (1926).

† Fermi, 'Z. Phys.,' vol 48, p. 73 (1928).

‡ Hartree, 'Proc. Camb. Phil. Soc.,' vol. 24, p. 89 (1928).

§ Bullard and Massey, 'Proc. Camb. Phil. Soc.,' vol. 26, p. 556 (1930).

Born's formula (3) gives a scattering curve for all atomic fields which falls off monotonically with increasing angle, and therefore fails to explain the results given in this paper for low velocities, which show maxima and minima. This failure of Born's formula for low velocities is partly due to the assumption, made in deducing it, that the incident wave is not distorted by the field of the atom.

It will be seen, however, from fig. 2 that as the velocity is increased the maxima and minima gradually disappear, and it might therefore be expected that Born's formula might fit the higher velocity curves of fig. 2. In fig. 6

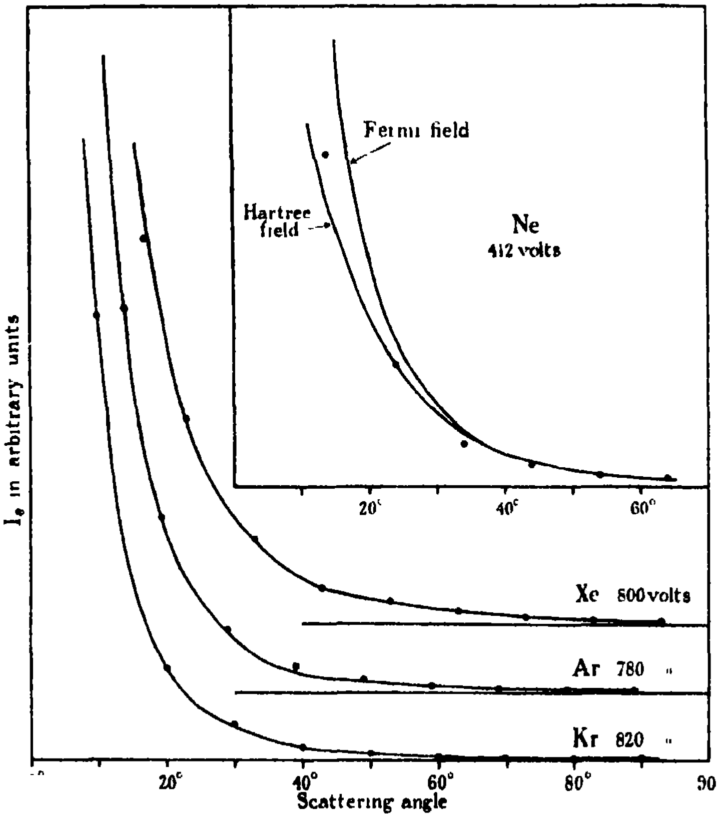

Fig. 6.—Experimental Points fitted to the Born Scattering Curves for Xenon, Krypton Argon and Neon.

the Born scattering curves for 800-volt electrons in Xe, 780-volt electrons in Ar, and 820-volt electrons in Kr, are constructed from the table given in Bullard and Massey's paper. My experimental points have been fitted to each of these curves, and it will be seen that the agreement is remarkably good, especially in view of the fact that in Xe and Kr the maximum beyond 90° has not quite disappeared. It should be mentioned here that the order in which the curves are placed in fig. 6 is not significant, as they are not all drawn to the same scale.

The Born scattering curves, using respectively the Thomas-Fermi and the Hartree fields, have also been drawn in fig 6 for 412-volt electrons in Ne. It will be seen that the experimental points fit the Hartree field curve more closely than they do the Thomas-Fermi field curve This is only to be expected, since the Thomas-Fermi field, though differing only very slightly from the Hartree field for heavy atoms like Xe and Kr, is not at all accurate for light atoms.

The conclusion to be drawn from fig. 6 is that the Born approximation is justified for these relatively high velocities, and consequently that the de Broglie waves of electrons of these velocities are not seriously distorted by the atomic field of the atom.

Massey has applied Born's formula to the case of molecular hydrogen* and nitrogen,† and has informed me that satisfactory agreement is obtained with my experimental curves shown in fig. 3. The calculations, however, are not able to account for the minimum at about 90° observed in the lower velocity curves in these gases.

As has been stated above, Born's formula fails at the lower velocities, and is unable to account for the maxima and minima observed in the scattering curves of the rare gases shown in fig. 2. For the explanation of these curves we must seek a more exact solution of the "integral wave equation" representing the incident and scattered waves Faxen and Holtsmark‡ have given the exact solution of this equation, using, instead of the approximate expression (2), the expression (1) which takes into account the distortion of the incident wave within the atom. By this means Holtsmark§ has successfully accounted for the Ramsauer effect in argon and krypton.

---

* Massey, 'Proc. Roy. Soc.,' A, vol. 129, p. 616 (1930).

† *Unpublished.*

‡ Faxen and Holtsmark, 'Z. Phys.,' vol. 45, p. 307 (1927).

§ Holtsmark, 'Z. Phys.,' vol. 55, p. 437 (1929); *ibid.*, vol. 66, p. 49 (1930).

The expression obtained for the scattered intensity is

$$I_\theta = \frac{a^2}{p^2}\sum_{l=0}^{\infty}\sum_{l'=0}^{\infty}(2l+1)(2l'+1)\cos(\delta_l-\delta_{l'})\sin\delta_l\sin\delta_{l'}P_l(\theta)P_{l'}(\theta), \qquad (5)$$

where

$$p = \frac{2\pi mva}{h}$$

and $a$ is the " radius " of the hydrogen atom $= 0\cdot53 \times 10^{-8}$ cm. Holtsmark,* using the Hartree field with a correction applied for polarisation, has calculated the " phase variations," $\delta$, in Kr for values of $l$ from 0 to 4 for several values of $p$.

The angular scattering curve shown in fig. 7 has been calculated from equation (5) above for a velocity of 54 volts (corresponding to $p = 2\cdot0$) using

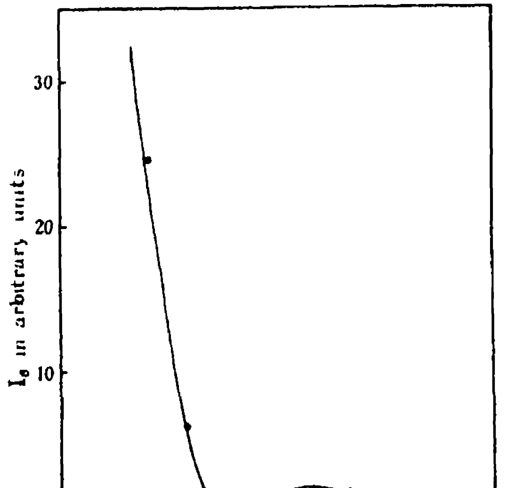

FIG. 7.—Experimental Points fitted to Holtsmark's Theoretical Curve for 54-volt Electrons in Krypton.

the values of $\delta$ from $l = 0$ to $l = 4$ given for the atomic field No. 2 in Table III of Holtsmark's paper. The values of $I_\theta$ from which this curve is drawn are given in Table II, column 4, and Holtsmark's absolute values for I can be obtained by multiplying these values by $33\cdot8 \times 10^{-18}\,\text{cm.}^2$ My experimental points for 54-volt electrons are shown fitted to this curve in fig. 7. The good agreement obtained shows that the experimental results containing maxima and minima, which Born's formula is unable to account for, are satisfactorily explained, at any rate in this particular case, by the exact solution of the wave equation.

---

* Holtsmark, 'Z. Phys.,' vol. 66, p. 49 (1930).

Allis and Morse,[*] using the exact solution of the wave equation and a simplified atomic field in place of the Hartree field, have calculated the total effective cross section for elastic collisions for a number of different atoms. The cross sections are obtained from equation (5) by integrating over the whole sphere Their method, which is much simpler to apply than Holtsmark's owing to the idealised atomic field, gives curves which agree very well with the experimental ones as regards size and form. They have since calculated from equation (5) the angular scattering curves for a number of different voltages in argon. These calculations are not yet published, but they have kindly informed me that satisfactory agreement is obtained with my experimental curves, shown in fig. 2.

It is probable, however, that even the exact solution of the wave equation will fail to account successfully for the experimental results at still lower velocities owing to the electron exchange effect The possibility of interchange between the atomic and colliding electrons has been considered by Oppenheimer[†] and by Mott,[‡] who have shown that interference effects are to be expected, and recently Massey and Mohr[§] have shown that the exchange effect is of fundamental importance in the scattering of electrons of from 4 to 15 volts energy in helium.

When the contributions to the scattering due to the exchange terms have been worked out and included in the expression for the scattering found from the exact solution of the wave equation, and when the Hartree fields have been evaluated for the different atoms, and suitably modified so as to account correctly for the polarisation forces, then we may look with some confidence to a full explanation of the diffraction effects in the monatomic gases described in this paper.

## *Summary.*

The angular distributions of the elastically scattered electrons in Xe, Kr, Ar, Ne, $H_2$, $N_2$, $CH_4$ and CO have been measured for several different velocities of the primary beam between 30 and 800 volts. Diffraction effects are observed in all these gases, the curves of the rare gases showing several maxima and minima, while the lower velocity curves for the molecular gases all have a minimum in the region of 90°.

---

[*] Allis and Morse, 'Z. Phys.,' vol. 70, p. 567 (1931)

[†] Oppenheimer, 'Phys. Rev.,' vol. 32, p. 361 (1928).

[‡] Mott, 'Proc. Roy. Soc.,' A, vol. 125, p. 222 (1929).

[§] Massey and Mohr, 'Proc. Roy. Soc.,' A, vol. 132, p. 605 (1931), and later unpublished work.

In the higher velocity curves the diffraction maxima and minima have practically disappeared in the case of Xe and Kr, and have completely disappeared in the case of the other gases, showing that the refractive index of the atom is practically unity for these short wave-lengths.

The high velocity curves of the rare gases all agree well with the Born scattering formula. The 54-volt curve in Kr is found to be in very good agreement with the theoretical scattering curve calculated from Faxen and Holtsmark's scattering formula.

The effective cross section curves for elastic collisions have been determined by graphical integration of the angular distribution curves. The cross section curves give information concerning the variation with velocity of the proportion of elastic to inelastic collisions. The work is being extended to other gases and vapours, and to smaller and larger scattering angles

This work was carried out during my last year at the Cavendish Laboratory, Cambridge; and it gives me great pleasure to acknowledge here the kindly assistance given me by Professor Lord Rutherford, Mr. P. M. S. Blackett, Dr. J. Chadwick, and other members of the laboratory

# *The Elastic Scattering of Slow Electrons in Gases.—II.*

By E. C. BULLARD, B.A., Denman Baynes Student, Clare College, Cambridge, and H. S. W. MASSEY, B.A., M.Sc., Trinity College, Cambridge, Aitchison Scholar, University of Melbourne

(Communicated by Lord Rutherford, O.M., F.R.S.—Received July 30, 1931.)

## § 1. *Introduction.*

In a previous paper* results of measurements of the angular distributions of slow electrons scattered elastically in argon were described. The appearance of maxima and minima in the curves obtained suggested the analogy of the scattering of electrons by atoms to the scattering of light by small spheres. This idea was given further credence by the results obtained by Arnot† for the angular distributions of electrons scattered elastically in mercury vapour. However, a number of important and interesting phenomena occur in the scattering of electrons by atoms which are not present in the scattering of light by small spheres. Thus there is no optical analogy to the distortion of the de Broglie waves of the electrons by the potential field of the atom, nor to the exchange of electrons between the atoms and the colliding beam. The relative importance of such phenomena in determining the scattering of slow electrons will depend on the properties of the scattering atoms, so we may expect to be able to sort out the individual effects by comparing the results obtained with different atoms in the light of available theory. In order to do this the previous angular distribution measurements have been extended to helium, neon, nitrogen, hydrogen and methane, and as a consequence the interpretation of the phenomena has been much clarified. In this paper the results obtained in the above-mentioned gases are described and discussed.

## § 2. *Method and Results.*

The apparatus used was, except for minor modifications, the same as that described in paper I. Electrons from a tungsten filament were accelerated through a pair of slits by a suitable potential giving a homogeneous beam of known energy. This beam was fired through the gas under investigation at low pressure ($1\cdot5 \times 10^{-3}$ mm. Hg) in a field free space and the scattered electrons collected by a Faraday cylinder. This cylinder could be rotated by a ground joint so enabling the intensity of the scattered beam to be measured at different angles of scattering.

---

* 'Proc. Roy. Soc.,' A vol. 130, p. 579 (1931), referred to throughout as I.

† 'Proc. Roy. Soc.,' A, vol. 130, p. 655 (1931). See also Pearson and Arnquist, 'Phys. Rev.,' vol. 37, p. 970 (1931).

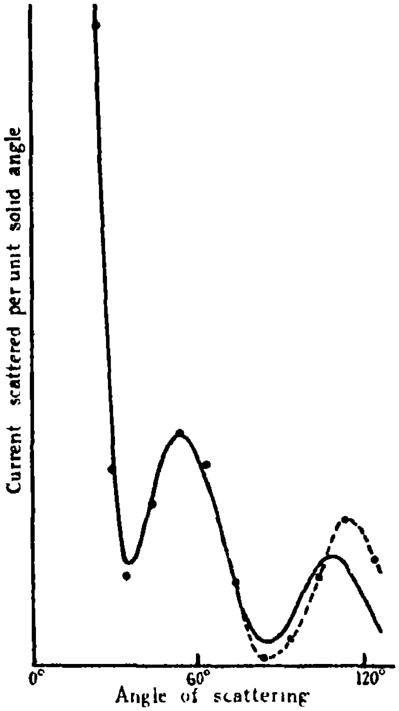

**Fig. 1.**—*Scattering in Mercury at 30 volts, illustrating agreement with Arnot*

- ● Observed points.
- —— Arnot's curve.

It was necessary to establish that the current collected by the Faraday cylinder really consisted of electrons scattered elastically from the main beam after one collision with a gas atom. This was done as described in paper I, by showing the scattered current to be proportional to the gas pressure and the intensity of the main beam, while retarding potential analysis showed the collected electrons to have the same energy as the primary.

In order to obtain an additional check on the consistency of the results obtainable with this type of apparatus the angular distribution of 30-volt electrons, scattered elastically in mercury vapour, was measured. In fig. 1 the results obtained are compared with those obtained by Arnot. The close agreement of the two curves shows that large differences in collecting arrangements and slit widths do not appreciably affect the results.

We now consider the results obtained for the scattering in the different gases.

(*a*) *Methane.*—The results of measurements taken with electrons of 4, 6, 10, 20 and 30 volts energy are tabulated in Table I. In fig. 2 the angular distributions at these different voltages are compared with those obtained in argon (described in paper I). It will be seen that there is a close resemblance between the two sets of curves. This is most noticeable for the low velocity electrons and disappears for electrons with energies greater than 20 volts. This similarity of behaviour of methane and argon towards low velocity electrons has also been observed by Brode* in the close similarity between the effective cross sections which the two gases present to such electrons.

---

* 'Phys. Rev.,' vol. 25, p. 636 (1925).

Table I.—Scattering by Methane.

| Volts \ Angle | 20°. | 30°. | 40°. | 50°. | 60°. | 70°. | 80° | 90°. | 100°. | 110°. | 120°. | 125°. |
|---|---|---|---|---|---|---|---|---|---|---|---|---|
| 4 | 26·4 | 22·6 | 19·7 | 18·1 | 18·3 | 17·8 | 17·6 | 15·2 | 12·1 | 9·4 | — | — |
| 6 | 63·2 | 47·0 | 34·5 | 25·2 | 20·4 | 16·8 | 15·4 | 14·7 | 12·8 | 10·3 | 9·2 | — |
| 10 | 70·2 | 48·1 | 36·3 | 21·2 | 15·9 | 13·5 | 11·0 | 8·6 | 7·5 | 6·8 | 6·82 | 7·85 |
| 20 | 35·3 | 30·2 | 17·5 | 7·76 | 4·82 | 4·52 | 3·74 | 3·32 | 2·78 | 2·80 | 3·01 | — |
| 30 | 17·6 | 10·5 | 4·68 | 3·63 | 2·47 | 1·99 | 1·53 | 1·39 | 1·44 | 1·85 | 2·20 | — |

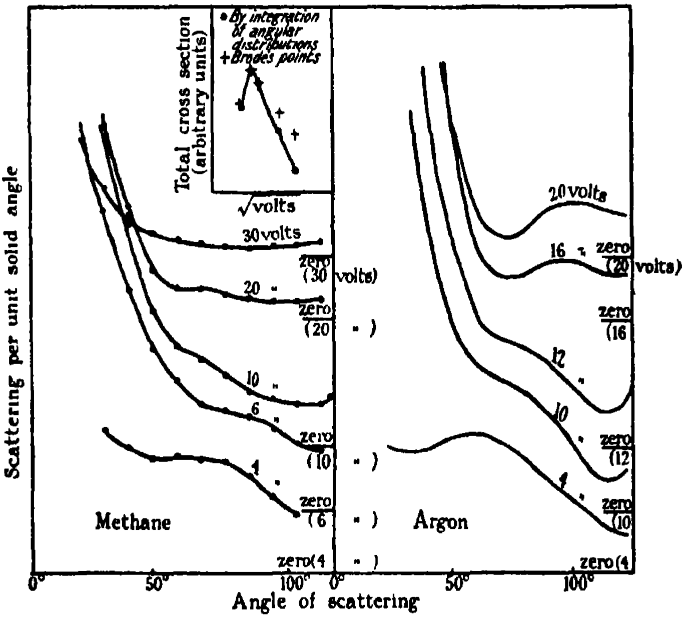

**Fig. 2.**—Scattering in Methane compared with that in Argon (Absolute magnitudes of the two sets of curves are not accurately comparable.)

The methane used was subsequently found by a density determination to contain 15 per cent. nitrogen, but this cannot affect the general agreement with argon, and no correction has been made.

(*b*) *Helium.*—The gas was purified by passage over three charcoal tubes cooled in liquid nitrogen. Spectroscopic examination showed, besides the helium lines, nothing but a trace of H$\alpha$ and an ionisation potential determination by the method described in paper I also showed no appreciable impurity to be present.

The results obtained using electrons of 4, 6, 10, 20, 30 and 50 volts energy are tabulated in Table II and illustrated graphically in fig. 3. It will be seen that the scattering of electrons with energies below 20 volts shows marked peculiarities, a minimum occurring in the angular distribution at quite small angles.

Table II—Scattering by Helium.

| Angle / Volts | 20°. | 30°. | 40° | 50°. | 60°. | 70° | 80°. | 90°. | 100°. | 110° | 120°. | 130°. |
|---|---|---|---|---|---|---|---|---|---|---|---|---|
| 4 | 2·53 | 2·86 | 2·91 | 2·53 | 2·42 | 2·68 | 2·68 | 2·75 | 2·86 | 2·97 | 3·08 | 3·19 |
| 6 | 10·7 | 5·2 | 4·5 | 4·0 | 3·4 | 3·3 | 3·3 | 3·5 | 3·7 | 4·2 | 4·6 | 4·6 |
| 10 | 6·3 | 4·9 | 4·0 | 3·5 | 3·3 | 3·2 | 3·3 | 3·5 | 3·7 | 4·0 | 4·6 | — |
| 20 | 6·0 | 4·2 | 3·12 | 2·50 | 2·20 | 1·99 | 1·85 | 1·80 | 1·75 | 1·75 | 1·77 | — |
| 30 | 17·0 | 5·4 | 4·0 | 3·5 | 2·40 | 1·90 | 1·63 | 1·50 | 1·41 | 1·40 | 1·38 | — |
| 50 | 10·8 | 4·7 | 3·4 | 2·0 | 1·5 | 1·11 | 0·90 | 0·68 | 0·60 | 0·60 | 0·63 | 0·68 |

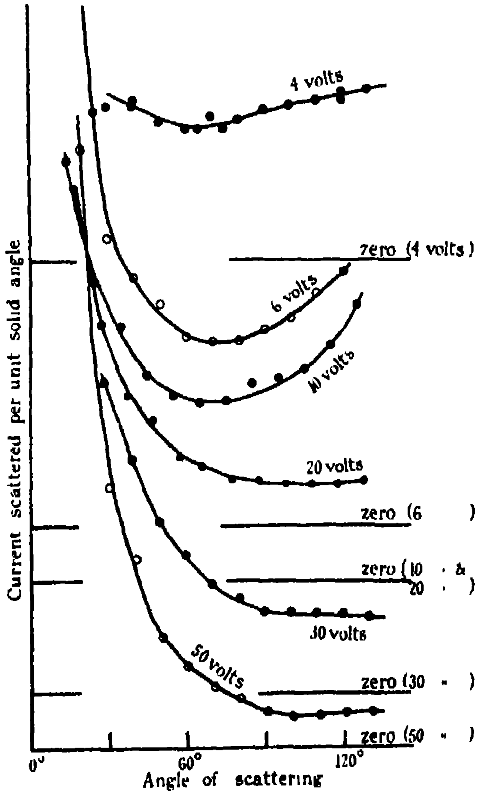

Fig. 3.—Scattering in Helium.

(*c*) *Neon.*—The gas was obtained from the British Oxygen Company and was stated to contain 2 per cent. helium On account of the comparative rarity of this gas, the apparatus was modified to permit the continuous circulation of the gas round the apparatus. A charcoal tube immersed in liquid nitrogen was placed in the circulating system to prevent the accumulation of any gases given off within the system. It was found possible in this way to work with only 3 mm.$^3$ of gas.

The results obtained using electrons of 6, 10, 20 and 30 volts energy are tabulated in Table III and illustrated in fig. 4.

Table III.—Scattering by Neon.

| Angle / Volts | 20°. | 30°. | 40° | 50° | 60° | 70 | 80. | 90° | 100°. | 110° | 120°. | 130°. |
|---|---|---|---|---|---|---|---|---|---|---|---|---|
| 6 | — | 29·0 | 29·3 | 29·8 | 29·5 | 29·3 | 27·0 | 23·5 | 20·6 | 18·4 | 16·3 | 14·7 |
| 10 | — | 27·8 | 27·6 | 27·4 | 27·2 | 24·9 | 23·1 | 16·8 | 13·0 | 9·0 | 6·3 | 5·0 |
| 20 | — | 31·0 | 28·3 | 27·3 | 25·7 | 21·7 | 17·4 | 12·5 | 8·4 | 5·9 | 5·5 | 7·7 |
| 30 | — | 32·8 | 29·7 | 26·9 | 21·3 | 17·4 | 14·4 | 9·4 | 5·4 | 3·4 | 3·6 | 8·4 |

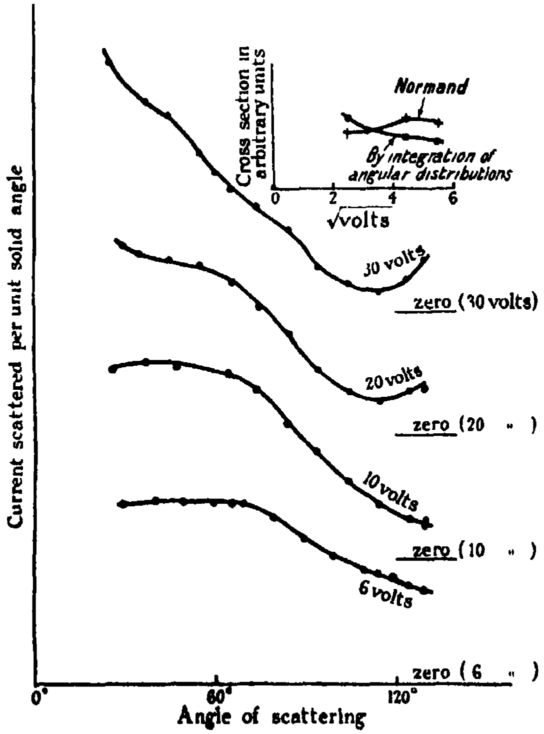

Fig. 4.—Scattering in Neon.

(*d*) *Hydrogen and Nitrogen.*—These gases were obtained from commercial cylinders and were not further purified. The results obtained in hydrogen using 4, 10, 20 and 30 volt electrons are tabulated in Table IV and illustrated in fig. 5, while in Table V the results of measurements in nitrogen using 7, 10, 30 and 60 volt electrons are given. In fig. 6 the nitrogen results are illustrated.

Table IV.—Scattering by Hydrogen.

| Angle / Volts | 20° | 30°. | 40° | 50°. | 60°. | 70°. | 80°. | 90°. | 100°. | 110°. | 120°. |
|---|---|---|---|---|---|---|---|---|---|---|---|
| 4 | 25·0 | 19·4 | 14·8 | 11·9 | 8·0 | 6·8 | 6·4 | 6·2 | 6·4 | 6·8 | 7·1 |
| 10 | — | 29·5 | 19·6 | 14·4 | 10·1 | 7·5 | 6·2 | 5·2 | 4·7 | 4·5 | 4·5 |
| 20 | 23·5 | 13·7 | 7·5 | 4·75 | 3·1 | 2·15 | 1·35 | 1·1 | 1·0 | 1·0 | 1·15 |
| 30 | 14·6 | 7·5 | 3·8 | 2·17 | 1·25 | 0·70 | 0·38 | 0·35 | 0·36 | 0·50 | 0·76 |

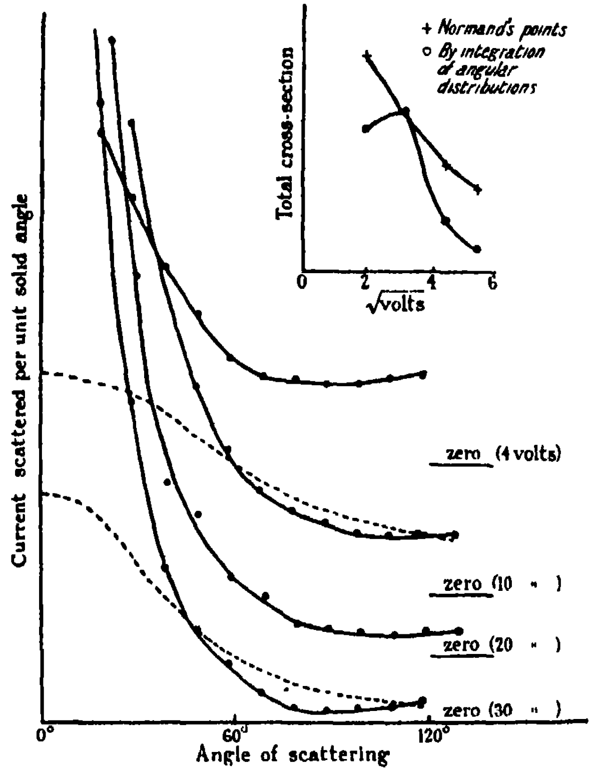

Fig. 5.—Scattering in Hydrogen. Scale of 30 volt curve three times, of 20 volt twice that of 10 volt and 4 volt curves. • • experimental points. — — —, theoretical curve for $H_2$.

Table V.—Scattering by Nitrogen.

| Angle / Volts | 20°. | 30°. | 40°. | 50°. | 60°. | 70°. | 80°. | 90°. | 100°. | 110°. | 120°. | 130°. |
|---|---|---|---|---|---|---|---|---|---|---|---|---|
| 7 | 53·0 | 49·4 | 43·5 | 36·9 | 27·0 | 21·8 | 17·0 | 14·2 | 13·1 | 14·6 | 15·4 | 17·3 |
| 10 | 65·1 | 54·0 | 42·0 | 38·0 | 26·1 | 20·2 | 12·3 | 10·6 | 11·0 | 13·4 | 16·3 | 19·7 |
| 30 | 114·8 | 51·2 | 30·2 | 16·1 | 9·5 | 5·5 | 3·6 | 3·1 | 3·7 | 5·6 | 8·8 | 13·7 |
| 60 | 65·5 | 19·2 | 8·31 | 3·26 | 1·84 | 0·83 | 0·65 | 0·55 | 0·90 | 1·76 | 2·77 | 4·27 |

The most interesting feature of the nitrogen results is the occurrence of a minimum in the angular distributions, the position of which does not vary with the energy of the incident electron beam. The fact that this minimum is at 90° would seem to be significant.

While these measurements were in progress Ramsauer and Kollath* published an account of experiments in which they compared the intensity of the electrons scattered between angles 10° and 65° with that of the electrons scattered between 115° and 170°. They find that for helium the ratio of the forward to the backward scattering falls steadily with decrease of voltage† and at voltages below 10 volts becomes less than unity. This is in agreement with our measurements for helium which, although not extending to such large angles as those in Ramsauer and Kollath's experiments, indicate that for voltages below 10 volts the ratio observed would be less than unity. Similarly in hydrogen the results obtained by us would not indicate a value of the ratio less than unity for electrons of energy greater than 4 volts and actually Ramsauer and Kollath find that for hydrogen the ratio does remain less than unity above 4 volts but decreases rapidly with decrease of voltage and becomes greater than 1 at slightly less than 4 volts.

## § 3. *Discussion.*

The scattering of electrons by atoms is a complicated process involving effects due to the field of the atom, the distortion of the atom by the electron, and the exchange of electrons between the atom and the colliding beam and reactions of all these phenomena with each other. In order to separate these effects it is best to start from the simplest picture and then find how far this will represent the facts before proceeding further.

---

* 'Ann. Physik,' vol. 9, p. 756 (1931).

† Henceforth by voltage is meant the voltage of the incident electron beam.

*Scattering in a Static Field.*—The aperiodic motion of a homogeneous electron beam in an atomic field is represented in quantum mechanics as the diffraction of plane waves by a medium of variable refractive index

$$\mu = \sqrt{\frac{\mathrm{E} - \mathrm{V}}{\mathrm{E}}}. \tag{1}$$

E being the energy of the incident electrons and V the potential of the atomic field acting on the electron. The differential equation for the wave amplitude $\psi$ is then

$$\nabla^2\psi + \frac{8\pi^2 m\mathrm{E}}{h^2}\psi = \frac{8\pi^2 m}{h^2}\mathrm{V}\psi, \tag{2}$$

and use of Green's function shows that $\psi$ must satisfy the integral equation

$$\psi = \mathrm{A}e^{ik\mathbf{n}_0 \cdot \mathbf{r}} + \frac{2\pi m}{h^2}\int \mathrm{V}(r')\frac{e^{ik|\mathbf{r}-\mathbf{r}'|}}{|\mathbf{r}-\mathbf{r}'|}\psi(r')\,dv', \tag{3}$$

where

$$k = \left(\frac{8\pi^2 m\mathrm{E}}{h^2}\right)^{\frac{1}{2}},$$

and $n_0$ is a unit vector in the direction of incidence. We have then as the asymptotic expression for $\psi$

$$\psi \sim \mathrm{A}e^{ik\mathbf{n}_0 \cdot \mathbf{r}} + \frac{2\pi m}{h^2}\frac{e^{ikr}}{r}\int \mathrm{V}(r')\,e^{ik\mathbf{n}\;\mathbf{r}'}\psi(r')\,dv', \tag{4}$$

the first term representing the plane wave incident in the direction of the unit vector $\mathbf{n}_0$ and of amplitude A, the second a scattered spherical wave. Mott* has shown how this method of treatment is equivalent to the use of Huygen's principle, the integral in (3) representing the sum of the contributions from the secondary wavelets at each point in space.

*Born's Approximation.*—The first step toward solving (3) was made by Born† who adopted a method used originally by Huygens and Kirchhoff in considering the scattering of light by obstacles. We assume that the distortion of the incident wave is small and take

$$\psi(r') = \mathrm{A}e^{ik\mathbf{n}_0 \cdot \mathbf{r}'}, \tag{5}$$

giving the well-known Born formula for the ratio of incident to scattered intensity

$$\phi = \left|\frac{2\pi m}{h^2}\int \mathrm{V}e^{ik(\mathbf{n}_0 - \mathbf{n}_1)\cdot \mathbf{r}}\,dv\right|^2 \tag{6}$$

---

* 'Proc. Roy. Soc.,' A, vol. 127, p. 658 (1930).

† 'Z. Physik,' vol. 38, p. 803 (1926).

In attempting to explain the angular distributions obtained the first step is to apply this formula wherever possible and to investigate the conditions under which it is valid. Criteria for its validity have been given by Mott* and Moller,† but it is clear that it will hold best for fast electrons and light atoms as under these conditions there is least distortion. As the angular distribution curves obtained from (6) fall off uniformly with angle for all atomic fields it is clear that the curves obtained for the rare gases are not explicable in this way, though for 50 volt electrons in helium (6) is not far wrong. Below 50 volts the experimental curves down to 10 volts fall off more rapidly initially than the formula (6) would indicate

However, it is possible to calculate (6) for molecular hydrogen, the case in which Born's formula should be most nearly correct. The method of calculation has been given by Massey‡ and has been extended and improved in a paper by Massey and Mohr.§ The results of the calculation are shown in fig 5, and it is seen that the Born formula is not adequate to give the angular distributions in molecular hydrogen down to 30 volts, the experimental curves being much steeper than the calculated, just as in helium

In the case of molecules of nitrogen it is not possible to calculate the molecular field, but a good approximation to the scattering is obtained by taking the system as two scattering centres at a fixed separation, scattering coherently, the fields of each being taken as a nitrogen atomic field. Using the calculations carried out by us‖ for the scattering by the Fermi field of this atom and the nuclear separation as 1·1 Å.U ¶ theoretical curves for the molecule are obtained and are compared with the experimental in fig. 6. It is clear that the Born formula fails below 30 volts in nitrogen as would be expected, but it is surprising that it is so nearly correct for voltages as low as 30. In any case it fails to explain one interesting feature of the experimental results, the rise observed beyond 90° for all voltages. This may be due to the simplified model used for the molecule, but is more likely due to a failure of the Born formula to represent the facts completely

---

* 'Proc Camb Phil. Soc ,' vol. 25, p. 304 (1928).

† 'Z Physik,' vol. 62, p. 54 (1930).

‡ 'Proc. Roy. Soc ,' A, vol 129, p. 616 (1930).

§ 'Proc. Roy. Soc ,' A, vol. 132, p. 605 (1931).

‖ 'Proc. Camb. Phil. Soc.,' vol. 26, p. 536 (1930).

¶ *Vide* P. Debye, 'Phys. Z ,' vol. 31, p. 419 (1930).

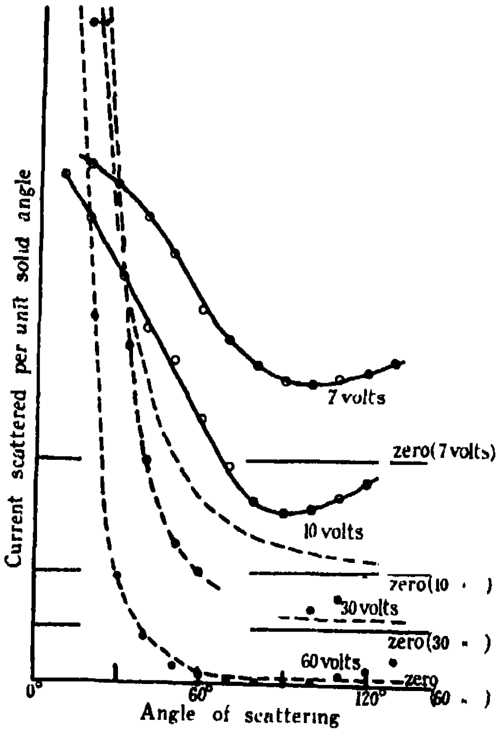

Fig 6.—Scattering in Nitrogen. ● ○ observed points. — — — theoretical.

*Distortion of the Incident Wave.*—Having now applied the simple formula to the cases where it is applicable we must now take into account further approximations. This must take the form of a more exact solution of (3), *i.e.*, to take into account the distortion of the incident wave by the atomic field. This has been done by Faxen and Holtsmark* for spherically symmetrical fields, and a numerical method of solution given. Holtsmark has applied the method to the cases of argon† and krypton‡ and the calculated total cross section presented by these atoms to slow electrons is in good agreement with experiment. His calculations may be used to obtain the angular distributions which are given as a doubly infinite series of spherical harmonics, the coefficients of which have been obtained numerically. In fig. 7 the calculated curves for argon are compared with the experimental. As it is much more difficult to obtain agreement with a curve showing maxima and minima than with a smooth curve the agreement found is probably as good as could be expected, and it would appear that the distortion of the incident wave is of fundamental importance in the scattering of slow electrons by argon

---

* 'Z. Physik,' vol 45, p. 307 (1927).

† 'Z. Physik,' vol. 55, p. 437 (1929).

‡ 'Z. Physik,' vol. 66, p. 49 (1930).

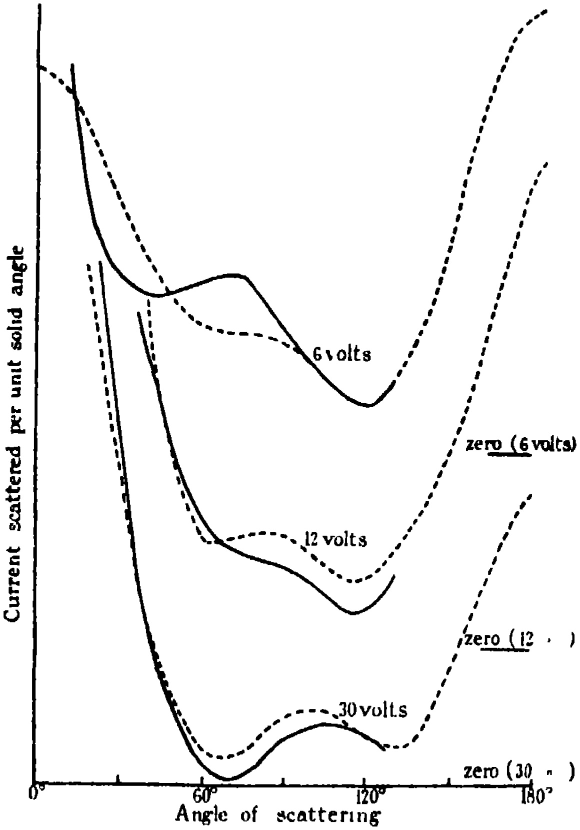

FIG. 7. — Scattering in Argon. ——— experimental curve. — — — calculated from Holtsmark's theory.

Unfortunately, the tedious nature of the numerical calculations necessary in Faxen and Holtsmark's method has restricted its application up to the present to the two cases given above. However, recently, Allis and Morse* have used a simpler atomic model for which the equation (3) can be solved exactly. The atomic field takes the form

$$V = Ze^2\left(\frac{1}{r} - \frac{1}{r_0}\right) \qquad r < r_0$$

$$= 0 \qquad r > r_0$$

---

* 'Z. Physik,' vol. 70, p. 567 (1931).

with Z, $r_0$, given by Slater's rules for atoms.* Using this model it is found possible to explain very well the total cross sections observed for various atoms of the periodic table, in particular the rare gases, the alkali atoms, and the mercury sub-group. This theory should at least give a qualitative idea of the angular distributions.† For helium a uniform distribution in angle is given from 100 volts down to the lowest voltages, while for neon a $\cos^2 \theta$ curve is predicted.‡ Referring to fig. 3 we see that for helium this is not even qualitatively correct, for the angular distribution becomes least normal§ below 10 volts, in agreement also with the results of Ramsauer and Kollath (*loc. cit.*). If the distortion is the predominant feature here, the Morse and Allis theory should hold best at these low voltages, whereas it is worst there. It thus appears necessary to consider the further possibilities due to the non-static nature of the atomic field, in order to explain the helium results. For neon also the agreement is not very good. It appears that the observed displacement of the minimum from 90° outwards is explicable, but not the other irregularity in the observed curves, occurring at smaller angles. Here again it is possible that the electronic (*i.e.*, non-static) nature of the atom is important. We shall now proceed to consider these possibilities.

*Electron Exchange and Polarisation.*—In the previous discussion we have regarded the atom as a structureless field of force and it is now necessary to allow for the electron structure. The presence of the colliding electron produces a disturbance of the atomic system which may result in the exchange of electrons between the atom and colliding beam or in the polarisation of the atom. Both these effects will become largest at low velocities owing to the longer time during which the electron is in the neighbourhood of the atom.

The possibility of electron exchange was first considered by Oppenheimer‖ and later by Mott¶ from somewhat different points of view. Owing to the Pauli principle it was shown that effects are to be expected due to interference of the two waves. Quantitative estimation of the magnitude of this process is more difficult as it necessitates considering a two-body problem instead of the simpler one-body problem of (2). However, Massey and Mohr (*loc. cit.*)

---

* 'Phys. Rev.,' vol. 37, p. 481 (1931).

† In a forthcoming paper by Allis and Morse the agreement of their theoretical curves for argon with the experimental ones will be illustrated.

‡ We are indebted to Drs. Allis and Morse for this information.

§ A normal angular distribution is taken as one showing a uniform decrease of scattering with angle.

‖ 'Phys. Rev.,' vol. 32, p. 361 (1928).

¶ 'Proc. Roy. Soc.,' A, vol. 125, p. 222 (1929).

have recently carried out calculations to a first order approximation for helium in order to obtain a semi-quantitative picture of the effects to be expected. It was found that a minimum is to be expected in the angular distribution moving steadily towards smaller angles with decrease of voltage of the incident beam and eventually disappearing at 0°, leaving for lower voltages a distribution showing a steady increase with angle. This is well illustrated by the 4- and 6-volt curves obtained for helium and shown in fig 3. In the paper cited the voltage at which the minimum first appeared was quite high (70 volts) and disappeared at 8 volts, but these figures are of no quantitative significance. The chief defect of the calculation consisted in the neglect of distortion of the plane incident wave. Since then this has been approximately included* and shown to make the exchange effect much sharper and produce the minima only between 15 and 4 volts, in much better agreement with the above results. It is of interest to notice here that one would expect a similar exchange effect for molecular hydrogen, but it is not observed down to 4 volts. However, as hydrogen is lighter than helium one would expect the effect to occur at lower voltages and actually Ramsauer and Kollath (*loc cit.*) have shown that below 4 volts there is more backward scattering than forward, indicating the effects of exchange. To check this point it will be necessary to carry on the angular distribution measurements with electrons of lower voltages, but it is of interest to notice the striking similarity between the observed curves for hydrogen and curves at higher voltages for helium. Thus we compare 50 volts in helium with 30 volts in hydrogen, 30 in helium with 20 in hydrogen, 20 in helium with 10 in hydrogen. It thus seems very probable that similar exchange effects occur in hydrogen at lower voltages than in helium.

The effect of polarisation is much more difficult to calculate. It corresponds to the effect of the inelastic collisions on the elastic scattering and differs from the exchange effect in that it may be allowed for by modifying the static field of the atom by an amount depending on its polarisability in the field of the incident electron. Holtsmark† has attempted to do this by modifying the static field, assuming the polarisability to be given by its optical value, and the results of his calculation do not indicate any remarkable effect in the angular distribution due to this modification. However, as the optical value is not the correct one to use in the electron case a more detailed treatment is necessary.

From the above discussion of the results it would seem that, for the scattering of slow electrons by heavy atoms, the distortion of the incident wave by the atom is of predominant importance, whereas for light atoms the effect of exchange would seem to be of equal if not greater importance. The validity of the Born approximation seems to extend to lower velocities than would be indicated by the criteria given by Mott and Möller (*loc. cit.*), but whether this is real or accidental (due to cancellation of different forms of correction) is not yet clear.

---

* In a paper to appear shortly.

† 'Z. Physik,' vol. 55, p. 437 (1929).

The results for methane are of interest in another direction. By comparison with the corresponding curves for argon they indicate that, for electron velocities below 30 volts, the electrons of the outer shells of argon and methane must produce the scattering, for the inner shells of the two are in no way similar. The importance of this result is that it leaves open the possibility of considering the scattering by heavy atoms in terms of that by successive electron shells, and may lead to a simplified treatment of the phenomena.

By multiplying the scattering per unit solid angle by the sine of the angle of scattering the scattering per unit angle may be obtained. Classically these curves tend to infinity for zero angle of scattering, on the quantum theory,* however, the scattering per unit solid angle is (except in exceptional cases such as the inverse square law) always finite and is zero at 0°.

Curves were given in paper I illustrating this in the case of argon. Still more definite results have been obtained in the present investigation, some examples of which are given in fig. 8. By integrating these curves the scatter-

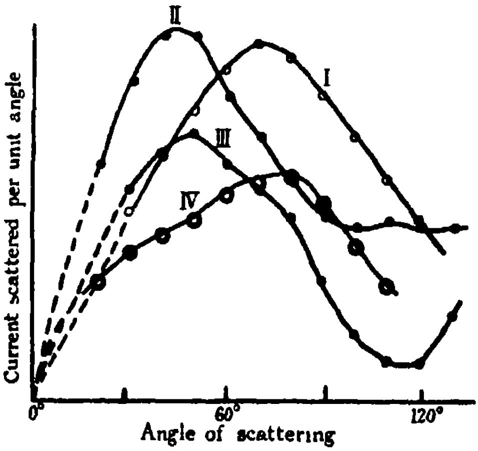

Fig. 8.—Curves illustrating scattering per unit angle for certain voltages and gases. I, neon, 6 volts; II, nitrogen, 7 volts; III, neon, 30 volts; IV, methane, 4 volts.

---

* Mott, 'Proc. Camb. Phil. Soc.,' vol. 25, p. 304 (1928).

ing between any two angles may be obtained. In the inset figures (figs. 2, 4, 5) the results obtained by integrating the results from 0° to 125° are illustrated and compared with those given by Normand for the total cross section. These last should, if fitted to the first below the resonance potential, be greater than them, above the resonance potential, as Normand's measurements include inelastic collisions. No exact comparisons can be made, however, until the angular distribution curves have been extended to 180°. Also it is uncertain how far the effective area of the collecting slit is independent of the velocity of the electrons.*

Although the above results throw considerable light on the processes occurring in the scattering of electrons by atoms, it is obvious that much more remains to be done, and it is hoped to extend the investigations to the vapours of metals, in this way obtaining results for atoms with unclosed shells.

It is a pleasure to express our thanks to Lord Rutherford and Mr. P. M. S. Blackett for their interest and encouragement throughout and to Mr. N. F. Mott for many valuable discussions. One of us is indebted to the Department of Scientific and Industrial Research for a grant.

## *Summary.*

With an apparatus described in a previous paper the angular distributions of slow (4 to 40 volts) electrons scattered elastically in helium, neon, nitrogen, hydrogen, and methane have been investigated from 20° to 125°. The results are described and their interpretation in terms of the quantum theory of electron scattering discussed. Effects due to distortion of the waves by the atoms, the exchange of electrons between atom and incident beam and the diffraction of electrons by the atoms of a diatomic molecule are shown to occur and their relative importance indicated.

---

* This uncertainty is eliminated in Ramsauer's method of measurement of total cross sections.

# *Interpretation of Hyperfine Structure.—Discussion of H.F.S. in Tl II. Relative g (I) factors of Tl, Bi and Pb* (207), *and Nuclear Structure.*

By Professor J. C. McLennan, F.R.S., A. B. McLay,* Ph.D., and M. F. Crawford, M.A.

(Received August 11, 1931.)

## I. *Introduction.*

As the theory of hyperfine structure separations is employed in section II in discussing the hyperfine structure of Tl II,† and again in section III in comparing the Landé $g$ (I) factors of Tl, Pb and Bi, its status is briefly considered in this introduction.

The theory of the interaction of a single valence electron of the $s$ type with a magnetic nucleus is somewhat indefinite, insomuch as it can not be directly verified. The expression for the interaction

$$W = a_{ns} \, \mathrm{I} \, . \, \mathrm{s} \cos (\mathrm{I}s) \tag{1}$$

is undoubtedly correctly formulated, as it has been experimentally verified. The relative hyperfine separations of states of the $6snd$ and the $6snf$ configurations of Tl II, treated in this paper, and of certain configurations in other spectra.‡ in which the interactions with the magnetic nucleus of all the valence electrons except the deeply penetrating $s$ electron are negligible, are in good agreement with the predictions based on this equation. The theoretical expression for the interaction constant, $a_{ns}$,§ which governs the magnitude of the separations, can only be determined by a quantum mechanical treatment of the state of the atom under consideration; and always involves the factor $g$ (I), which as yet has never been determined by other independent methods. Consequently, the validity of the expression for $a_{ns}$ cannot be checked directly. There is, however, the possibility of checking somewhat inexactly the expression for $a_{ns}$ by comparing the value of $g$(I) calculated from the experimental data by the use of the theoretical expression with that expected from our conception of the nucleus. Such comparisons show that $g(\mathrm{I})$ is of the order expected for a spinning proton; but beyond this are, as yet, of little value in checking the formula for $a_{ns}$ since our theory of the nucleus is very uncertain, especially in view of the conclusion expressed in section III.

---

* Assistant Professor of Physics, McMaster University, Hamilton, Canada.

† McLennan and Crawford, 'Proc. Roy. Soc.,' A, vol. 132, p. 10 (1931).

‡ Goudsmit and Bacher, 'Phys. Rev.,' vol. 34, p. 1501 (1929).

§ The subscript "$n$" is the general designation for the principal quantum number of the electron and "$x$" that for the orbital quantum number $l$ ($x = s, p, d$, etc.). The designation $a_{nx}$ ($j$) with the appropriate value of "$j$" is used in place of Goudsmit's $a'$ and $a''$.

For more complex configurations the resultant magnetic interaction of the valence electrons with the nucleus depends on the spectral state of the atom, and is given by the equation

$$\mathrm{W_{IJ}} = \mathrm{A\,(J)} \quad \mathrm{I\,.\,J} \cos \mathrm{(IJ)}. \tag{2}$$

This equation, which is simply the mathematical expression of the hyperfine structure interval rule, in which A (J) is the interval factor of the state considered, has had ample experimental verification. The factor A (J) is composite and involves the interactions of the spin magnetic moments and the orbital magnetic moments of all the valence electrons with the magnetic nucleus. The interval factors of all the states arising from a given configuration, then, should be interrelated; and that of each state expressible in terms of the interaction constants, one for each "*nl*" type of valence electron, and the quantum numbers of the valence electrons of the atom in this state.

An expression has been deduced for the interval factor of a state arising from one valence electron, other than an *s* type, by Fermi, Breit and Casimir, using quantum mechanical methods, and by Goudsmit* using the method of energy sums.

The expression is

$$\mathrm{A\,(J)} = a_{nx} \cdot \frac{l\,(l+1)}{\mathrm{J\,(J+1)}}, \tag{3}$$

where $l$ and J have their usual significance, and $a_{nx}$ is what shall be termed the interaction constant of an $nx$ electron. The value of this constant can be determined rigorously only by a quantum mechanical treatment for the particular state under consideration; but for non-*s* types of penetrating orbits it is expressed approximately in cm.$^{-1}$ by

$$a_{nx} = \frac{\mathrm{R}\alpha^2 \mathrm{Z_i Z_0}^2}{n_e{}^3\, l\,(l+1)\,(l+\frac{1}{2})} \cdot g\,(\mathrm{I}). \tag{4}$$

In this expression $\mathrm{Z_i}$ and $\mathrm{Z_0}$ stand for the effective nuclear charge in the inner and the outer part of the orbit respectively, and $n_e$ for the effective principal quantum number. The other symbols have their usual significance. Equation

---

* Fermi, 'Z Physik,' vol. 60, p. 320 (1930); Breit, 'Phys Rev.,' vol. 37, p. 51 (1931); Pauling and Goudsmit, "Structure of Line Spectra," chap. 11 (McGraw-Hill, New York, 1930); Goudsmit, 'Phys. Rev.,' vol. 37, p. 663 (1931).

(3) expresses the interval factor of each of the two states as a known multiple of a common quantity $a_{n s}$; and consequently predicts a definite relation between them. In the few cases* of one-electron spectra for which the hyperfine structure has been determined, the ratio of the interval factors of the two states is decidedly not in agreement with prediction Two possible causes of this discrepancy have been pointed out: the factor involving the quantum numbers might be incorrect, or the interaction constant, $a_{n x}$, not the same for both states of the doublet. These possibilities have been discussed by Goudsmit (*loc. cit.*) and Breit† respectively, but their conclusions are only qualitative.

Theoretical expressions for the interval factors of the states arising from complex configurations also have been deduced. Goudsmit treated the problem by the method of energy sums. Since the same basic equation which led to equation (3) for a single electron was used in the treatment, the formulæ are expected to be again in disagreement with observation. This anticipated discrepancy has been observed by Goudsmit and Fisher.‡

## II. *Discussion of the Hyperfine Structure of* Tl II.§

Since Tl II is a two-electron spectrum, only the general theory developed by Goudsmit can be applied to its hyperfine structure. In this theory the interactions with the magnetic nucleus of all the valence electrons of a given configuration are treated by the well-known method of energy sums. To obtain useful information by this method the approximation has to be made that the sum rule will hold if applied only over the states arising from this configuration. This approximation may be quite unjustifiable if these states intermix with states of other configurations. From such an application of the rule the interval factors of the states, the J's of which occur only once in the configuration, are completely determined in terms of the interaction constants of the electrons; but for states that have the same J value only the sum of their interval factors is obtained. The individual factors in these sums can be evaluated only for the two cases of extreme coupling. For a configuration exhibiting either of these types of coupling the states are separated into distinct groups, each characterised by a definite value of S and L for Russell-Saunders coupling or by a definite combination of the $j$ values of the electrons for $(jj)$ coupling. For such cases the further approximation that the sum rule will hold over each group is justifiable, and leads to the evaluation of the interval factors of every state of the configuration.

---

* Goudsmit, *loc. cit.*, and Wulff, 'Z. Physik,' vol. 69, p. 70 (1931).

† Breit, 'Phys. Rev.,' vol. 37, p. 1182 (1931).

‡ Fisher and Goudsmit, 'Phys. Rev.,' vol. 37, p. 1057 (1931).

§ McLennan and Crawford, 'Proc. Roy. Soc.,' A, vol. 132, p. 10 (1931).

The applicability of the formulæ deduced by the method of energy sums depends on the justification for the approximations. In the following discussion, in which these formulæ are used, the validity of the approximations is considered for the configurations treated.

*The* 6*sns Configurations.*—The 6*s*7*s* configuration gives rise to two spectral states, $^3S_1$ and $^1S_0$ The $^1S_0$ exhibits *no* hyperfine structure since its J is 0. The $^3S_1$ state, however, is split into two hyperfine levels since I of Tl is $\frac{1}{2}$. The value of the interval factor, A ($^3S_1$), determined from the separation of these levels can be compared with the theoretical expression,*

$$A(^3S_1) = \tfrac{1}{2}(a_{6s} + a_{7s}), \tag{5}$$

which is derivable directly from equation (1) since the quantum orientations of the two vectors in this configuration are known. The validity of the approximations necessary for the application of the sum rule need not be considered in this comparison since equation (5) is independent of the sum rule. Since there is no other interval factor arising from the 6*s*7*s* configuration, equation (5) is the only equation involving the two interaction constants $a_{6s}$ and $a_{7s}$; consequently they can not be determined directly. This case, then, is even less satisfactory for comparison with theory than the $^2S_{\frac{1}{2}}$ state of a single *s* electron, for which the interaction constant could be determined although the theory could not be tested. However, by considering in addition to the hyperfine structure of 6*s*7*s* $^3S_1$ of Tl II, the structure of the 7*s* $^2S_{\frac{1}{2}}$ state of Tl I, the values of $a_{6s}$ and $a_{7s}$ of the 6*s*7*s* configuration can be determined.

The $a_{7s}$ of the 6*s*7*s* configuration of Tl II can be deduced from the known value of the interaction constant of the 7*s* electron of the neutral atom by an application of the approximate expression for the interaction constant. The 7*s* electron of the 6*s*7*s* configuration of Tl II only differs from the 7*s* of Tl I in regard to its effective nuclear charge in the outer part of the orbit and its effective principal quantum number. According to theory the interaction constant depends on these two factors in the following manner:

$$a_{7s} \sim \frac{Z_i Z_0^2}{n_e^3}, \tag{6}$$

where the symbols have the same significance as in equation (4). In passing from the $6s^27s$ $^2S_{\frac{1}{2}}$ state of Tl I to the 6*s*7*s* $^3S_1$ state of Tl II, a 6*s* electron has been removed. The effect of this removal on the 7*s* electron will be to leave $Z_i$ practically unaltered but to increase $Z_0$. Since the screening effect of a 6*s* electron on a 7*s* electron is not perfect, $Z_0$ will be increased by less than one unit. However, following the customary method, $Z_0$ is increased arbitrarily by one unit; and the error so introduced compensated for by increasing $n_e$. Thus, if $n_e$ of the 7*s* electron in the 6*s*7*s* configuration can be determined, its interaction constant $a_{7s}$ can be evaluated. An approximate value of the $n_e$ of the 7*s* of Tl II can be obtained by a comparison of the $n_e$ of the 7*s* of Tl I and the 7*s* of Pb II. Since $Z_0$ of the 7*s* of Tl II is intermediate to the $Z_0$ of the 7*s* of Tl I and the $Z_0$ of the 7*s* of Pb II, the $n_e$ of the 7*s* of Tl II can be taken, as an approximation, equal to the mean of the $n_e$'s of the 7*s* of Tl I and the 7*s* of Pb II.

---

* *Loc. cit.*

$$\left.\begin{aligned} n_e \text{ of } 7s\,{}^2S_{\frac{1}{2}} \text{ of Tl I} &= 2\cdot19 \\ n_e \text{ of } 7s\,{}^2S_{\frac{1}{2}} \text{ of Pb II} &= 2\cdot65 \end{aligned}\right\} \text{mean} = 2\cdot42,$$

$$n_e \text{ of } 7s \text{ of } 6s7s\,{}^3S_1 \text{ of Tl II} \doteqdot 2\cdot42$$

$$a_{7s} \text{ of } 7s\,{}^2S_{\frac{1}{2}} \text{ of Tl I}^* = 0\cdot417 \text{ cm.}^{-1}.$$

$$\text{By equation (6) } a_{7s} \text{ of } 6s7s\,{}^3S_1 \text{ of Tl II} = \frac{0\cdot417 \times (2\cdot19)^3 \times 4}{(2\cdot42)^3} = 1\cdot23 \text{ cm.}^{-1}.$$

Using this value of $a_{7s}$ in equation (5) there results

$$a_{6s} \text{ of } 6s7s\,{}^3S_1 \text{ of Tl II} = 5\cdot40 \text{ cm.}^{-1}.$$

The 6*s*9*s* configuration of Tl II gives rise to two spectral states, ${}^3S_1$ and ${}^1S_0$, which are higher sequence members respectively of the two states arising from the 6*s*7*s* configuration. The interaction constants for this configuration, therefore, can be determined in the same manner as those of the 6*s*7*s* configuration.

$$\left.\begin{aligned} n_e \text{ of } 9s\,{}^2S_{\frac{1}{2}} \text{ of Tl I} &= 4\cdot24 \\ n_e \text{ of } 9s\,{}^2S_{\frac{1}{2}} \text{ of Pb II} &= 4\cdot69 \end{aligned}\right\} \text{mean} = 4\cdot47$$

$$n_e \text{ of } 9s \text{ of } 6s9s\,{}^3S_1 \text{ of Tl II} \doteqdot 4\cdot47$$

$$\text{By equation (6) } a_{9s} \text{ of } 6s9s\,{}^3S_1 \text{ of Tl II} = \frac{0\cdot417 \times (2\cdot19)^3 \times 4}{(4\cdot47)^3} = 0\cdot196 \text{ cm.}^{-1}.$$

Using this value of $a_{9s}$ in equation (5) there results

$$a_{6s} \text{ of } 6s9s\,{}^3S_1 \text{ of Tl II} = 5\cdot82 \text{ cm.}^{-1}.$$

The value of $a_{9s}$, as expected, is much smaller than that of $a_{7s}$, while the higher value of $a_{6s}$ for the 6*s*9*s* configuration shows clearly how the screening effect of the outer electron on the inner $6s$ electron decreases with increasing principal quantum number.

---

* *Loc. cit.*

*The* $6snd$ *Configurations.*—Each of these electronic configurations gives rise to four spectral states, two of which have the same value, 2, for their inner quantum numbers, while the others have J values, 1 and 3 respectively. These states are represented in the tables by $^1D_2$, $^3D_2$, $^3D_1$ and $^3D_3$; but, as the coupling does not conform to the extreme Russell-Saunders type, these quantum descriptions, other than the J values, have little significance. In view of the unusual type of coupling exhibited by these configurations the observed hyperfine structure can be compared only with the theoretical expressions obtained when the first approximation is made in the application of the sum rule. Under these conditions the interval factors A $(^3D_3)$ and A $(^3D_1)$ are each uniquely determined in terms of the two interaction constants $a_{6s}$ and $a_{nd}$, whereas only the sum of A $(^1D_2)$ and A $(^3D_2)$ is expressed in terms of these constants. The formulæ, together with the observed values of the interval factors of the states of these configurations, are listed in Tables I, II and III. The values of the interaction constants, deduced by equating the experimental values to the corresponding theoretical expression, also are given in each table.

Table I —$6s6d$.

| Formula | Observed interval factors | $a_{6s}$. |
|---|---|---|
| | | cm $^{-1}$ |
| (*b*) $A(^3D_3) = \frac{1}{6}a_{6s} + \frac{4}{7}a_{6d}$ | $0·95 \pm 0·01$ | $5·70 \pm 0·06$ |
| (*c*) $A(^3D_2) + A(^1D_2) = \frac{1}{12}a_{6s} + 2a_{6d}$ | $0·22 \pm 0·01 + 0·32 \pm 0·01$ | $6·48 \pm 0·24$ |
| (*d*) $A(^3D_1) = -\frac{1}{4}a_{6s} + 2a_{6d}$ | $-1·41 \pm 0·02$ | $5·64 \pm 0·08$ |

From (*b*) and (*c*) $a_{6s} = 5·56$, $a_{6d} = 0·04$
(*c*) and (*d*) $a_{6s} = 5·85$, $a_{6d} = 0·03$
(*b*) and (*d*) $a_{6s} = 5·68$, $a_{6d} = 0·005$

Table II.—$6s7d$.

| Formula | Observed interval factors. | $a_{6s}$. |
|---|---|---|
| | | cm.$^{-1}$. |
| *b*) $A(^3D_3) = \frac{1}{6}a_{6s} + \frac{4}{7}a_{7d}$ | $0·97 \pm 0·01$ | $5·82 \pm 0·06$ |
| (*c*) $A(^3D_2) + A(^1D_2) = \frac{1}{12}a_{6s} + 2a_{7d}$ | $0·31 \pm 0·01 + 0·25 \pm 0·01$ | $6·72 \pm 0·24$ |
| (*d*) $A(^3D_1) = -\frac{1}{4}a_{6s} + 2a_{7d}$ | $-1·47 \pm 0·01$ | $5·88 \pm 0·04$ |

From (*b*) and (*c*) $a_{6s} = 5·67$, $a_{7d} = 0·05$
(*c*) and (*d*) $a_{6s} = 6·09$, $a_{7d} = 0·03$
(*b*) and (*d*) $a_{6s} = 5·84$, $a_{7d} = -0·005$

Table III.—6*s*8*d*.

| Formula. | Observed interval factors. | $a_{6s}$. |
|---|---|---|
| | | cm.$^{-1}$. |
| $A(^3D_3) = \frac{1}{6}a_{6s} + \frac{4}{7}a_{8d}$ | 0·99±0·01 | 5·94±0·06 |
| $A(^3D_2) + A(^1D_2) = \frac{1}{12}a_{6s} + 2a_{8d}$ | 0·66±0·01+0·0*±0·04 | 7·92±0·6 |
| $A(^3D_1) = -\frac{1}{4}a_{6s} + 2a_{8d}$ | −1·50±0·03 | 6·00±0·12 |

From (*b*) and (*c*) $a_{6s} = 5·61$, $a_{8d} = 0·1$
(*c*) and (*d*) $a_{6s} = 6·48$; $a_{8d} = 0·06$
(*b*) and (*d*) $a_{6s} = 5·90$, $a_{8d} = -0·005$

* $\Delta\nu$ of 6*s*8*d* $^1D_2$ given in reference (1) as 0·1, should be 0·0±0·1.

The formulæ when applied to the observed structure of the states of the 6*s*6*d*, 6*s*7*d* and 6*s*8*d* configurations yield fairly consistent results. In the case of the 6*s*6*d* configuration $a_{6d}$ is 0·04 cm.$^{-1}$ when derived from (*b*) and (*c*), 0·03 cm.$^{-1}$ from (*c*) and (*d*) and negligibly small from (*b*) and (*d*). Little significance can be attached to these values since they are of the order of the errors in the interval factors. The value of $a_{6d}$ derived from (*b*) and (*d*), which are more reliable than (*c*) since they involve terms independent of coupling, indicates that it may be neglected in view of the accuracy of the experimental data. This is anticipated from the fact that no appreciable structure has been observed for the $^2D$ states of single electron spectra. If the value of $a_{6d}$, as indicated, is small enough to be neglected, the numbers listed in column III are the values of $a_{6s}$ computed from (*b*), (*c*) and (*d*) respectively. The values of $a_{6s}$ from (*b*) and (*d*) are in good agreement. The value from (*c*), however, is higher than the other two; and the excess is slightly greater than that expected for the maximum experimental error in the interval factors of (*c*) and for the approximation made in neglecting $a_{nd}$.

The same discussion applies to the 6*s*7*d* and 6*s*8*d* configurations, only the discrepancy between the value of $a_{6s}$ deduced from the equation involving the interval factors A ($^1D_2$) and A ($^3D_2$), and the values deduced from the other equations is slightly more marked in the 6*s*7*d* configuration, and decidedly greater in the 6*s*8*d* configuration. This divergence in the values of $a_{ns}$ cannot be due entirely to neglecting $a_{nd}$ because, if it were, it should decrease for the 6*s*7*d* and 6*s*8*d* configurations instead of increasing, as $a_{7d}$ and $a_{8d}$ are expected to be smaller than $a_{6d}$.

*The 6snf Configurations.*—These configurations are treated in a manner similar to that used for the 6*snd* configurations. Since the coupling is not either of the extreme types, the observed hyperfine structure can be compared only with the formulæ obtained when the first approximation is made in the application of the sum rule. The comparison is made for the states of the 6*s*5*f* and 6*s*6*f* configurations in Tables IV and V respectively.

Table IV.—6*s*5*f*.

| Formula | | Observed interval factors | $a_{6s}$ |
|---|---|---|---|
| | | | cm.$^{-1}$ |
| (*b*) $A(^3F_4^0)$ | $= \frac{1}{8}a_{6s} + \frac{3}{8}a_{5f}$ | $0·735 \pm 0·011$ | $5·88 \pm 0·09$ |
| (*c*) $A(^3F_3^0) + A(^1F_3^0)$ | $= \frac{1}{24}a_{6s} + 2a_{5f}$ | $-0·195 \pm 0·005 + 0·423 \pm 0·005$ | $5·47 \pm 0·24$ |
| (*d*) $A(^3F_2^0)$ | $= -\frac{1}{6}a_{6s} + 1\frac{1}{3}a_{5f}$ | $-0·996 \pm 0·008$ | $5·97 \pm 0·05$ |

From (*b*) and (*c*) $a_{6s} = 5·94$, $a_{5f} = -0·01$
(*c*) and (*d*) $a_{6s} = 5·85$, $a_{5f} = -0·009$
(*b*) and (*d*) $a_{6s} = 5·92$, $a_{5f} = -0·006$

Table V.—6*s*6*f*.

| Formula | | Observed interval factors. | $a_{6s}$. |
|---|---|---|---|
| | | | cm.$^{-1}$. |
| (*b*) $A(^3F_4^0)$ | $= \frac{1}{8}a_{6s} + \frac{3}{8}a_{6f}$ | $0·745 \pm 0·011$ | $5·96 \pm 0·09$ |
| (*c*) $A(^3F_3^0) + A(^1F_3^0)$ | $= \frac{1}{24}a_{6s} + 2a_{6f}$ | $-0·640 \pm 0·014 + 0·843 \pm 0·014$ | $4·80 \pm 0·7$ |
| (*d*) $A(^3F_2^0)$ | $= -\frac{1}{6}a_{6s} + 1\frac{1}{3}a_{6f}$ | $-1·03 \pm 0·02$ | $6·18 \pm 0·12$ |

From (*b*) and (*c*) $a_{6s} = 6·10$, $a_{6f} = -0·02$
(*c*) and (*d*) $a_{6s} = 5·96$, $a_{6f} = -0·02$
(*b*) and (*d*) $a_{6s} = 6·07$, $a_{6f} = -0·01$

The type of discrepancy exhibited in the 6*snd* configurations is also apparent in the 6*snf* configurations. When the formulæ are compared with the experimental data, the values of $a_{6s}$ deduced from the equation involving the sum of the interval factors $A(^1F_3^0)$ and $A(^3F_3^0)$ are smaller, in contrast to the larger values for the 6*snd* configurations, than the values deduced from the other two equations. The discrepancy in the 6*s*6*f* configuration is large, in this respect being analogous to the 6*s*8*d* configuration.

The proximity of levels arising from other electronic configurations is likely the major cause of the discrepancy in the values of $a_{6s}$ deduced from the 6*snd* and 6*snf* states which are dependent on coupling. The formulæ involving the interval factors of states for which the couplings are not known can be derived only by the method of energy sums. The validity of these formulæ depends on the justification for the approximation that limits the summation to the states of a given configuration. This approximation might not be justifiable if these states intermix with the states of other configurations. Formulæ identical with those derived by the sum rule, for the interval factors of the states with known couplings can be obtained, at least in regard to their dependence on $a_{6s}$, equally well by a more direct method which is independent of any approximation as to the proximity of states of other configurations. Thus, in the application of the sum rule to a given configuration it is only necessary to consider intruding states of other configurations when the couplings for these states are indeterminate. In view of these considerations the intermixing of the 6*s*7*d* group with the 6*s*5*f* group and the 6*s*8*d* group with the 6*s*6*f* group does not invalidate the formulæ derived by the method of sums for the individual groups since the coupling for $^3F_2{}^0$, the only state of a 6*snf* configuration that could influence the sum of the 6*snd* $^{1,3}D_2$ interval factors and the coupling for $^3D_3$, the only state of a 6*snd* configuration that could influence the sum of the 6*snf* $^{1,3}F_3{}^0$ interval factors, are both known. The discrepancy, then, is in all probability due to the presence of unidentified states which are dependent on coupling A large number of states arising from configurations involving the $5d^9$ core are expected A few of these already have been identified, and from their position others are predicted in the region of the 6*s*8*d* and 6*s*6*f* groups for which the discrepancy is the greatest.

Although the results are not as conclusive as one would wish, mainly through inability to treat more rigorously such configurations, they show that the interaction constants $a_{8d}$, $a_{7d}$, $a_{8d}$, $a_{5f}$ and $a_{6f}$ are sufficiently small to be neglected in considering the experimental data; and give the value of $a_{6s}$ for each of these configurations These values, with those for the 6*sns* configurations and that for the 6*s* electron of Tl III determined from Arvidson's[‡] results, are summarised in the following table.

Table VI.

| Configuration. | $a_{6s}$ | Configuration | $a_{6s}$. |
|---|---|---|---|
| | cm $^{-1}$. | | cm.$^{-1}$. |
| *6*s*6*p* of Tl II | 4·88 | 6*s*7*d* of Tl II | 5·85 |
| 6*s*7*s* ,, | 5·40 | 6*s*5*f* ,, | 5·93 |
| †6*s*7*p* ,, | 5·52 | 6*s*8*d* ,, | 5·97 |
| 6*s*6*d* ,, | 5·67 | 6*s*6*f* ,, | 6·04 |
| 6*s*9*s* ,, | 5·82 | 6*s* of Tl III | 6·4 |

* Evaluated in treatment of 6*snp* configurations

† Evaluated by same method as used for 6*s*6*p*, $A_{7p}$ ($1\frac{1}{2}$) being negligible.

---

[‡] *Loc. cit.*

These values show clearly the increase of $a_{6s}$ as the outer electron approaches ionisation, and indicate the screening effects of the various outer electron types on the $6s$ electron.

*The 6snp Configurations.*—A survey of the term analysis shows that the $6s7p$ states fall between two states, $^3P_0$ and $^3P_1$, of the $6p^2$ configuration. As no unidentified states are anticipated in this region, these are probably the only intrusions that might invalidate the results of the application of the sum rule to the $6s7p$ group. The effect of these states, however, should be negligible since, first, although the $^3P_0$ and $^3P_1$ fall near the $6s7p$ group, the centres of gravity of the two configurations are remote, and secondly, the interval factors of the $6p^2$ states are small relative to those of the $6s7p$ states, as observed for the $^1D_2$ state and as estimated for the other states from Wulff's (*loc. cit.*) values of A $(6p\,^2P_{1\frac{1}{2}}{}^0)$ and A $(6p\,^2P_{\frac{1}{2}}{}^0)$ for Tl I

Substitution of the values of the interval factors in the expressions obtained by the sum rule, which appear to be applicable to the $6s7p$ group, yields the following equations involving the two interaction constants

$$\mathrm{A}\,(^3P_2{}^0) = \tfrac{1}{4}a_{6s} + \tfrac{2}{5}a_{7p} = 1\cdot38 \qquad (7)$$

$$\mathrm{A}\,(^3P_1{}^0) + \mathrm{A}\,(^1P_1{}^0) = \tfrac{1}{4}a_{6s} + 2a_{7p} = 1\cdot83. \qquad (8)$$

The solution of these equations gives $a_{6s} = 5\cdot06$ cm.$^{-1}$ and $a_{7p} = 0\cdot28$ cm.$^{-1}$. Unfortunately, since one of the states arising from the $6snp$ type has $J = 0$, there are only two equations involving the two constants. The consistency of the theory, consequently, cannot be tested directly. It can, however, be checked indirectly. Table VI gives the values of $a_{6s}$ for various configurations. The value of $a_{6s}$ for $6s7p$ should be intermediate to the values of $a_{6s}$ for $6s7s$ and $6s7d$. The value deduced from equations (7) and (8) is decidedly less than that of $a_{6s}$ for the $6s7s$ configuration.

There is only one possible cause for this inconsistency other than the inapplicability of the results of the sum rule, which has been considered, that possibility is the incorrectness of equations (7) and (8). This is anticipated from the recent results of Goudsmit and Fisher and of Wulff (*loc. cit.*). They found that the theoretical expressions for the interval factors of the two states arising from a single $p$ electron were not in agreement with experiment. The observed value of the ratio A $(^2P_{1\frac{1}{2}}{}^0)$/A $(^2P_{\frac{1}{2}}{}^0)$ was much smaller than the predicted value. Equations (7) and (8) are derived by the use of the same interaction expression for the $p$ electron as employed in the derivation of the interval factors of the $^2P_{\frac{1}{2},1\frac{1}{2}}{}^0$ states, and likewise are expected to be incompatible with observation. Since the $6s7p\,^3P_2{}^0$ state exhibits characteristics of the $^2P_{1\frac{1}{2}}{}^0$ state of the single $p$ electron, especially as the $6s7p$ configuration approaches extreme ($jj$) coupling, and the combination $^3P_1{}^0$ and $^1P_1{}^0$ involves both the states $^2P_{\frac{1}{2}}{}^0$ and $^2P_{1\frac{1}{2}}{}^0$; the value of the second term, $2/5\, a_{7p}$, of equation (7) which involves A ($^3P_2{}^0$) should lead to a smaller value of $a_{7p}$ than the second term, $2a_{7p}$, of equation (8) which involves A ($^3P_1{}^0$) and A ($^1P_1{}^0$). When the mean of $a_{6s}$ for $6s7s$ and $a_{6s}$ for $6s7d$ (Table VI) is substituted in equations (7) and (8) as the value of $a_{6s}$ for the $6s7p$ configuration, the value of $a_{7p}$ derived from equation (7) is $-0 \cdot 05$, from equation (8) $0 \cdot 21$. This is as anticipated, and is further evidence that equation (7) in Goudsmit's paper for the interaction of a single electron, other than an $s$ type, is incorrect. Whether the error is in the bracketed part involving the quantum numbers, as suggested and discussed by Goudsmit, or whether it is in the term $a_{np}$, as suggested by Breit, who pointed out that this value should be different for the two doublet states, the present results do not indicate.

The relative positions of the states of the $6s7p$ group show that for this configuration the coupling approaches the extreme ($jj$) type. The application of the sum rule to configurations with ($jj$) coupling yields unique expressions for each interval factor, and consequently gives for the $6s7p$ configuration three equations.* Two of these equations permit a direct test of the applicability of the interval factor expressions for extreme coupling to the $6s7p$ states. Since the so-called $^1P_1{}^0$ state involves the same state of the $p$ electron as the so-called $^3P_2{}^0$ state, the value of $a_{6s}$ can be determined directly from the expressions for A ($^1P_1{}^0$) and A ($^3P_2{}^0$); and should be independent of any error in the expression for the interaction of the $p$ electron. The value thus obtained can then be compared with the value anticipated from Table VI. Agreement then will be the criterion for extreme ($jj$) coupling. The value, $4 \cdot 72$ cm.$^{-1}$, obtained for $a_{6s}$, assuming the $6s7s$ configuration to be a case of extreme coupling, is much lower than the value of $a_{6s}$ for the $6s7s$ configuration. This result shows that the coupling does not conform closely enough to the extreme ($jj$) type to warrant the application of the corresponding formulæ. This example clearly indicates that caution must be exercised in applying the expressions for extreme couplings since the disposition of states is only a qualitative criterion and in many cases not sufficiently reliable to determine the applicability of these formulæ, especially for states dependent on coupling.

The hyperfine structure of the $6s6p$ configuration cannot be compared with theory since the intervals of all the states are not known, and the coupling is not either of the two extreme types. However, if $a_{6p}$ ($1\frac{1}{2}$) is estimated from

---

* Goudsmit, *loc. cit.*

Wulff's (*loc. cit.*) value, 0·04 cm.$^{-1}$, of $a_{6p}(1\frac{1}{2})$ of Tl I, the $a_{6s}$ of the $6s6p$ configuration can be evaluated from the interval factor of the $^3P_2{}^0$ state. A comparison of the $6p\,^2P^0$ separation of Tl I with the $6s6p\,^{3,1}P^0$ separations of Tl II shows that the value of $Z_0{}^2/n_e{}^3$ for the $6p$ electron is doubled by removing a $6s$ electron in passing from $6s^26p$ of Tl I to $6s6p$ of Tl II. Since $a_{6p}$ also depends on $Z_0{}^2/n_e{}^3$, the value of $a_{6p}(1\frac{1}{2})$ in the $6s6p$ configuration of Tl II will be about twice that of $a_{6p}(1\frac{1}{2})$ in Tl I Using then the value $a_{6p}(1\frac{1}{2}) = 2 \times 0{\cdot}04$ cm.$^{-1}$ in the equation

$$A\,(^3P_2{}^0) = 1{\cdot}28 = \tfrac{1}{4}a_{6s} + \tfrac{3}{4}a_{6p}(1\tfrac{1}{2}),$$

and solving for $a_{6s}$, the value $a_{6s} = 4{\cdot}88$ cm.$^{-1}$ is obtained. This value is lower than the values of $a_{6s}$ for the other configurations, as anticipated, since the screening effect of the $6p$ on the $6s$ electron should be greater than that of an electron with higher principal quantum number.

### III. *Comparison of the* $g$ (I) *Factors of* Tl, Bi *and* Pb.

Certain conclusions regarding nuclear structure, which appear to be independent of any uncertainty that might exist in the theory for $s$ electrons, can be made by comparing the observed values of the interaction constants of certain $s$ electrons of Tl, Bi and Pb. As pointed out, the more exact expression of $a_{ns}$ can be derived only by quantum mechanics; but, as our conclusions are qualitative only, the approximate expression

$$a_{ns} \sim \frac{Z_i\,Z_0{}^2}{n_e{}^3}\cdot g\,(\mathrm{I}) \tag{9}$$

can be used. This expression, in all probability, is valid since any error that might exist would be likely to be in a numerical factor characteristic of the $s$ type electron. As this numerical factor would be the same for all $s$ electrons, it is only necessary to consider the dependency expressed by equation (9) in comparing the values of $a_{ns}$ for different $s$ electrons.

In Table VII the interaction constants of the various $s$ electrons of Tl I and Tl III are compared by the use of equation (9) to illustrate the validity of this approximate formula.

Table VII.

| State. | $a_{ns}$ | $n_e$ | $Z_0$ | $Z_i$ | $a_{ns}\,\frac{n_e{}^3}{Z_i\,.\,Z_0{}^2}$ |
|---|---|---|---|---|---|
| $6s\,^2S_{\frac{1}{2}}$ of Tl III* | 6·4 | 2·02 | 3 | 81 | 0·072 |
| $7s\,^2S_{\frac{1}{2}}$ of Tl III* | 1·37 | 3·12 | 3 | 81 | 0·057 |
| $8s\,^2S_{\frac{1}{2}}$ of Tl III* | 0·606 | 4·15 | 3 | 81 | 0·059 |
| $6s^27s\,^2S_{\frac{1}{2}}$ of Tl I* | 0·417 | 2·19 | 1 | 81 | 0·054 |

* *Loc cit.*

Since $g$ (I) is a nuclear property independent of the extra-nuclear electrons, the product $a_{ns} \,.\, n_e^3/Z_iZ_0^2$, if equation (9) is valid, should be approximately constant for the above states of the Tl atom. The values in column VI of Table VII show that this condition is practically fulfilled. The variations from a constant value indicate the order of the approximation made in equation (9).

Bi III and Bi V furnish additional confirmation of equation (9). About two years ago one of the authors (M. F. Crawford) classified, by an application of the doublet laws to the sequence Au I, Hg II, Tl III, Pb IV and Bi V, the two bismuth lines λ 864 and λ 1139 as $6s^2\,S_{\frac{1}{2}}$—$6p\,{}^2P_{1\frac{1}{2}}{}^0$ and $6s\,{}^2S_{\frac{1}{2}}$—$6p\,{}^2P_{\frac{1}{2}}{}^0$ respectively. The large hyperfine separation observed by Arvidson* for these lines is, as suggested by Fisher and Goudsmit (*loc. cit.*) undoubtedly that of the $6s\,{}^2S_{\frac{1}{2}}$ state of Bi V. The value of $a_{6s}$ determined from this interval and the value of $n_e$ estimated by extrapolation from the values of $n_e$ of the $6s$ of Au I, Hg II and Tl III, permit a comparison of the interaction constants of the $6s$ electrons of Bi III and Bi V. This comparison is made in Table VIII.

Table VIII.

| State. | $a_{ns}$ | $n_e$ | $Z_0$ | $Z_i$ | $a_{ns}\,\frac{n_e^3}{Z_i\,.\,Z_0^2}$ |
|---|---|---|---|---|---|
| $6s^27s\,{}^2S_{\frac{1}{2}}$ of Bi III† | 0.472 | 2.98 | 3 | 83 | 0.0167 |
| $6s\,{}^2S_{\frac{1}{2}}$ of Bi V† | 2.6 | 2.35 | 5 | 83 | 0.016 |

† *Loc. cit.*

The approximate equality of the two values in column VI is further evidence of the applicability of equation (9).

The above examples show clearly the validity of equation (9) for $s$ type electrons of the same atom. The formula should be equally valid for comparing the interaction constants of $s$ electrons having the same principal quantum numbers in iso-electronic configurations of different atoms since the dependency of $a_{ns}$ on the properties of the atoms which are different, namely $Z_i$, $Z_0$, $n_e$ and $g$ (I), is correctly expressed in this formula. The application of this formula to the observed interaction constants of the $s$ electrons of Tl, Bi and Pb enables the relative values of the $g$ (I) factors of these nuclei to be determined.

A comparison of $a_{7s}$ of the $6s^27s\,{}^2S_{\frac{1}{2}}$ state of Tl I with that of the corresponding state of Bi III gives the following value of the ratio of the $g$ (I) factors

---

* Arvidson, 'Nature,' vol. 126, p. 565 (1930).

$$\frac{g\,(\mathrm{I}),\ \mathrm{Tl}}{g\,(\mathrm{I}),\ \mathrm{Bi}} = \frac{0\cdot0541}{0\cdot0167} = 3\cdot2.$$

A similar comparison for the $6s\,^2S_{\frac{1}{2}}$ of Tl III and the $6s\,^2S_{\frac{1}{2}}$ of Bi V gives

$$\frac{g\,(\mathrm{I}),\ \mathrm{Tl}}{g\,(\mathrm{I}),\ \mathrm{Bi}} = \frac{0\cdot0723}{0\cdot0163} = 4\cdot4.$$

These two cases give the extreme values, consequently the $g$ (I) factor of the Tl nucleus is between three and four times that of the Bi nucleus.

During the past year the hyperfine structure of a number of Pb III lines was investigated in this laboratory. The results, which will be published soon, show that $\mathrm{I} = 0$ for Pb (206) and Pb (208), and $\mathrm{I} = \frac{1}{2}$ for Pb (207). Only the states of the Pb (207) isotope exhibit hyperfine structure. The structure is qualitatively similar to that of Tl II, as expected since Pb III is analogous to Tl II and the I values are the same. The magnitude of the structure in Pb (207), III, however, is much smaller than in Tl II. The separation of the $6s7s\,^3S_1$ state of Pb (207) III is only 2·25 cm $^{-1}$ as compared with 4·97 cm. $^{-1}$ of the corresponding state of Tl II.

Since the $6s7s\,^3S_1$ states of both spectra are independent of coupling, the interaction constants of the 6$s$ electrons determined from these states can be compared to determine the ratio of the $g$ (I) factors of Pb (207) and Tl. This determination involves a knowledge of the factors of equation (9) for both Tl II and Pb (207) III The value of $a_{6s}$ of Tl II is 5·40 cm $^{-1}$, as given in Table VI. The $a_{6s}$ of Pb (207) III can be calculated from the value, 1·50 cm.$^{-1}$, of the interval factor of the $^3S_1$ state in a manner similar to that used for the 6$s$7$s$ configuration of Tl II. The relation between the interval factor and the interaction constants is expressed by equation (5). Since the ratio of $a_{7s}$ to $a_{6s}$ for Pb (207) III should be approximately the same as for Tl II, the value, 0·228, of this ratio for Tl II can be used to eliminate $a_{7s}$ from the equation. The value of $a_{6s}$ for Pb (207) III thus obtained is 2·44 cm.$^{-1}$. The factor $Z_i$ is approximately the same for both cases. $Z_0$ is 3 and 2 for Pb (207) III and Tl II respectively. The $n_e$ of the 6$s$ of Pb (207) III will be only slightly greater than the $n_e$ of the 6$s$ of Tl II by approximately the same amount that the $n_e$ of the 6$s$ of Pb IV is in excess of $n_e$ of 6$s$ of Tl III, namely, 0·2. Since the $n_e$ of the 6$s$ of Tl II will be greater than the value, 2·02, of $n_e$ of the 6$s$ of Tl III, the percentage effect of the difference, 0·2, on the relative values of the $n_e$ of Pb (207) III and the $n_e$ of Tl II is such as to place the value of the ratio $n_e^3$ Tl II/$n_e^3$ Pb (207) III between the limits 0·75 and 1·0. From this data by the use of equation (9) the value of the ratio

$$\frac{g\,(\mathrm{I}),\ \mathrm{Tl}}{g\,(\mathrm{I}),\ \mathrm{Pb}}\,(207)$$

is placed between 3·7 and 5.

These results show that the $g$ (I) factors of Bi and Pb (207) are of the same order; whereas that of Tl is unusually large, about four times greater than either.

The result of the comparison of the $g$ (I) factors of Tl and Pb (207) is especially significant. Evidence in general indicates that the resultant nuclear moment of momentum is entirely due to protons. Band spectra, the magnitude of hyperfine structure and the existence of integral I values for atoms with an odd number of particles in the nucleus, all show that the electrons in the nucleus have lost their spins. Moreover, Bartlett* has been able to account for the observed I values on the assumption that protons alone contribute to the resultant moment. The simple assumption that each proton contributes $\pm\frac{1}{2}{}^{h}/2\pi$ to the resultant moment was sufficient to explain the known facts. On this simple theory the resultant moments of the nuclei of Tl and Pb (207), for both of which $\mathrm{I} = \frac{1}{2}$, would be due to one unneutralised spinning proton. The $g$ (I) factors of the two nuclei, then, would be expected to be the same since there is no evidence to indicate why different spinning protons with the same mechanical moment should have widely different magnetic moments. Contrary to this expectation, experiment shows that the $g$ (I) of the Tl nucleus is about four times that of the Pb (207) nucleus. The obvious conclusion is that the moment of at least one of the nuclei is composite and not due simply to a spinning proton. This conclusion invalidates the simple rule that each proton contributes $\pm\frac{1}{2}{}^{h}/2\pi$ to the resultant moment, and necessitates endowing some of the protons in at least one of the nuclei with some property in addition to spin.

Further evidence for this conclusion is obtained from the ratio of $g$ (I) factors for Tl and Bi. Although the I value of Bi is $4\frac{1}{2}$, the $g$ (I) value should be the same as that for Tl if the resultant moments of both nuclei were due to spinning protons only. The observed ratio, however, is about 4 to 1. The approximate equality of the $g$ (I) factors of Pb (207) and Bi indicates that the resultant moment of the Tl nucleus is more complex in its origin.

Although the evidence does not definitely indicate what this additional property is, knowledge of the extra-nuclear electronic structure suggests orbital motion.* This model is not extreme, since the dimensions of a proton relative to a complex nucleus are of the same order as the dimensions of an electron relative to the atom.† Moreover, if the orbital motion of the proton is quantised so that the orbital momentum is an integral multiple of $h/2\pi$, as for extra-nuclear electrons; the simple rule, indicated by experimental evidence, that even numbers of protons imply integral values of I and odd numbers half-integral values, will still be valid.

---

* Bartlett, 'Phys. Rev.,' vol. 37, p. 327 (1931).

Such a model, then, has the possibilities of explaining not only the resultant I values but the nuclear $g$ (I) factors, for which the simple model with spinning protons is now inadequate. A nuclear model composed of protons with spin and orbital moments would be analogous in many features to that for extra-nuclear electrons, and presents the possibility of explaining negative $g$ (I) factors,‡ as suggested for cadmium and lithium. Whether orbital motion of the protons is the correct explanation or not, the observed ratios of the $g$ (I) factors of Tl, Bi and Pb (207) nuclei invalidate the assumption that the resultant moments of momentum of nuclei are entirely due to spinning protons.

---

* This possibility was mentioned by Bartlett (*loc cit.*) but was entirely speculative since at that time there was no experimental evidence demanding a further property of protons in addition to their spins.

† Page and Watson, 'Phys. Rev.,' vol 35, p 1585 (1930)

‡ Goudsmit and Young, 'Nature,' vol. 125, p. 461 (1930)

# *The Significance of the Differences between the Dipole Moments of Saturated and Unsaturated Substances.*

By Leslie Ernest Sutton.

(Communicated by R. Robinson, F R S.—Received May 30, 1931 )

It has long been known that there are generally differences between the electric dipole moments of corresponding saturated and unsaturated compounds,* but the full significance of these has not been realised, and in this communication an attempt has been made to correlate them with the states of the molecule and with the chemical properties of the substances.

Analysis of the available data, which have been supplemented by measurements of the moments of *ortho* and *meta* nitrobenzonitriles, benzyl chloride, benzal chloride, benzotrichloride, and methyl chloroform, does in fact provide definite support for some of the postulates of modern electronic theories of organic reaction.

## *Experimental.*

*Measurement of Electric Dipole Moments.*—The dipole moments herein communicated were measured as before† by the approximate method now most generally used, the non-polar solvent being benzene.

Although the results so obtained contain inherent errors, it is desirable that they should be concordant, and since the main experimental error and cause of existing discrepancies is probably in the determination of the total polarisation of the solute, $P_2$, efforts were made to measure it to within ± 1 per cent. From the actual polarisation/concentration curves it appears that in no case has this limit been exceeded, the accuracy usually being greater. Care, too, was taken to obtain pure substances.

The refractivities, or approximate electron polarisations, were measured for the mercury green line (5461), since these give more correction for the atom polarisation than do those for the sodium D line (the dispersion of most substances being positive) and the source is a very convenient one to use.

*Measurement of Dielectric Constants.*—The apparatus used was of the heterodyne type and differed only in detail from those used by other authors.‡

---

* *E.g.*, Williams, 'Z. Phys. Chem.,' A, vol. 138, p. 75 (1928).

† Hammick, New, Sidgwick and Sutton, 'J. Chem. Soc.,' p. 1876 (1930).

‡ *E.g.*, Williams, 'Fortschr. Chemie, Phys. Phys. Chem.,' vol. 20, No. 5 (1930); Weissberger and Sängewald, 'Phys. Z.,' vol. 30, p. 792 (1929); Müller and Sack, *ibid.*, vol. 31, p. 815 (1930); *cf.* also Bryan and Saunders, 'Phys. Rev.,' vol. 32, p. 302 (1928).

The oscillators, which had common low and high tension supplies to increase constancy of frequency, were shielded from hand capacities as completely as possible, and furthermore had tuned grid circuits so that one set of condenser plates in the measuring system could be conveniently earthed. This system is shown in the following diagram, which includes the valve circuit :—

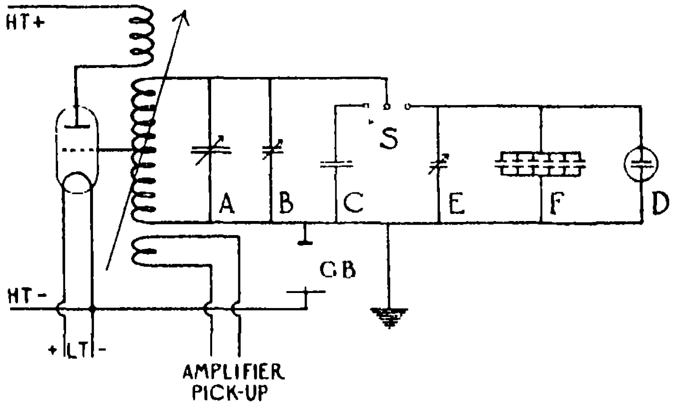

Fig. 1.

A and B were variable condensers, one being for coarse and the other for fine tuning. By means of a two-way switch S it was possible to connect in parallel with them either a condenser C, the capacity of which remained constant during an experiment, or a system consisting of D, wherein were placed the solutions to be examined, a fine variable cylinder condenser E (made after Wulf, 'Phys. Z.' vol. 26, p. 353, by the Leybold Nachfolger A.G ) and F, which was used as a subsidiary to E. It contained six shielded units which could be switched in separately by pushing metal rods through pairs of spring contacts, each unit having a slightly smaller capacity than E and being calibrated against it.

Any capacity changes in the valves of either oscillator could be compensated for by adjusting B, with C, the reference condenser, switched in. The heterodyne note, made audible through a rectifying and amplifying apparatus, was matched to that of a tuning fork with S in either position, so that

$$C_C + C_{\text{leads}} = C_D + C_E + C_F + C'_{\text{leads}} = \text{Constant},$$

D was so designed that practically no lines of force passed through more than one medium when a liquid was placed in it and the following relation therefore held

$$\delta C_D \propto \delta e,$$

$e$ being the dielectric constant of the medium between the plates. E was calibrated for non-linearity by the usual "step" method with a very small fixed condenser, which was built into the apparatus together with its switch, and a corrected scale was calculated so that

$$\delta N \propto \delta C_E, \quad \text{or including} \quad C_F, \ \delta N \propto \delta (C_E + C_F)$$

N being the corrected scale reading. Since $C_D + C_E + C_F$ is kept constant

$$\delta (C_E + C_F) \propto - \delta C_D, \text{ thus } \delta e \propto - \delta N$$

and therefore

$$\frac{\delta e_2}{\delta e_1} = \frac{\delta N_2}{\delta N_1}$$

The dielectric constants of air and benzene were taken to give the standard difference $\delta e_1$* and the difference of scale readings $\delta N_1$ for these media was observed at the beginning of each run. From the difference $\delta N_2$ between benzene and a solution it was possible to calculate $\delta e_2$ and thence the dielectric constant of the solution.

The two-way switch S, which was designed to give accurately reproducible settings, consisted of an aluminium rocker arm, supported in cone bearings, which could be moved by a silk thread passing round a pulley attached to it and made to dip a steel cross-pin into either of two nickel cups containing mercury. It was necessary to clean the metal surfaces and to renew the mercury before each run, but the switch then worked very satisfactorily. A similar one was used in the calibration of E.

Condenser D was so constructed that readings for a series of solutions could be made without disconnecting or dismantling it. There were two earthed cylinders A and B of gold-plated brass, and an insulated one C, of glass heavily silvered on both surfaces except for 5 mm. at each end. B screwed into A by three threaded projections D, and A was fastened to the cover E. Three large openings were cut in the upper part of A, so that the cylinder system was actually supported from a ring by three stiff legs. C rested in slots cut in the projections D, and was clamped in three others cut in spurs on a ring F which was pressed down by a flanged tube G screwing into B. Two platinum ribbons sealed on to C and connected to the insulated terminal H provided contact with the silver films. E was pressed against the ground flange of the glass container J to give an air-tight joint, by screwing it down to a supporting ring K in which J rested on a rubber ring. A slow stream of dry air could be passed through by means of the inlet and outlet tubes L and M to prevent the absorption of moisture by solvent or solute. The condenser was supported in a thermostat at 25·00 ± 0·05° from a tongue on K (not shown).

---

* $e$ benzene = 2·2747 at 25·00°, Hartshorn and Oliver, 'Proc. Roy. Soc.,' A, vol. 123, p. 664 (1929).

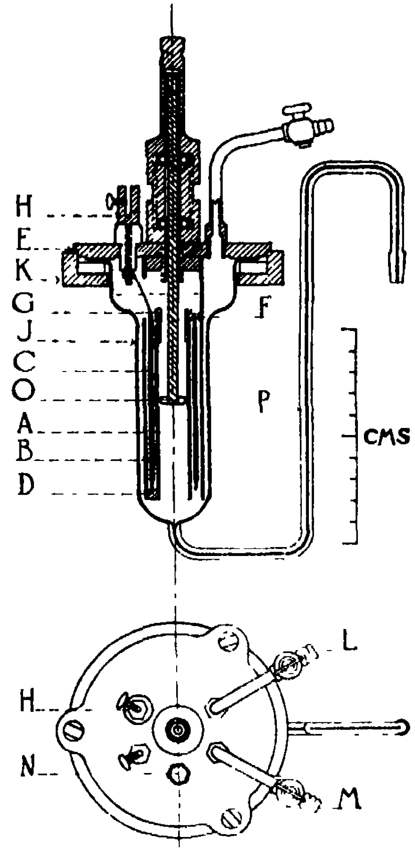

Fig. 2.

The procedure was first to take a reading with air as dielectric (the air capacity was about 60 cms.), then to weigh in some benzene through the aperture N, which could be stoppered, and, by rotating the propeller O, to stir the liquid and bring it to temperature equilibrium so that readings could be taken. It was necessary always to fill the condenser to one definite level, so the benzene was run in until the liquid surface, as seen from below by a mirror, was just broken by a spike projecting from the underside of the lid. To make up a solution, benzene was withdrawn through N or through the capillary P, the level was made up with a solution of known strength (or the solute itself, if liquid) and with benzene, the mixture was stirred and a reading taken. Stirring was repeated until the readings were steady. From the weights of solvent and solution added and subtracted, the strength of the solution within the condenser could be calculated. Readings for three or four solutions were taken in each run, and at least two runs were made with each substance

The readings on the fine condenser could, with care, be obtained constant to ± 1 unit, so the error for the dielectric constant of any solution due to error in setting should be about ± 0·0001, and since the differences between solvent and solution were usually greater than 0·01, these could be measured to at least ± 2 per cent. The real criterion of accuracy was, however, the concordance of the polarisation/concentration points which rarely diverged from the mean curve by so much as 1 per cent. (except for the fourth solutions, which were liable to be affected by cumulative errors).

*Measurements of Refractive Indices.*—These were made with a Pulfrich refractometer (by Hilger) having a separate, centrally divided cell, so that the difference between the emergent angles for the solvent and solution could be measured on the fine adjustment head. Direct heating of the liquids was not possible, as each cell division was covered with a glass plate, and consequently the usual upper jacket was fitted with an extra screen at the back, and the hole in the top was closed, to minimise heat losses. The equilibrium temperature attained by a liquid in the cell when water from a 25° thermostat was circulated in the jackets was found, from the refractive index of a standard oil, to be 24·5°. The values for the refractive indices given below have been corrected to 25·00° by subtracting 0·00027.

*Preparation of Materials.—Benzene.* A.R quality benzene was frozen out four times, dried over calcium chloride, and then refluxed and distilled over sodium: m.p. 5·50° (corr.).

*o- and m-Nitrobenzonitriles*—Laboratory specimens were recrystallised to constant melting-point from ethyl alcohol and animal charcoal: m.p. (ortho) 109·8–110·8° C. corr [*]; m.p (meta) 116–117° C. corr.[†]

*Benzyl Chloride.*—A laboratory specimen was shaken twice with water, dried over anhydrous sodium sulphate, and fractionated *in vacuo* three times, the middle fractions being taken. The product gave no acid reaction with litmus and was used immediately: m.p. –– 37·5°.[‡]

*Benzal Chloride.*—This was prepared by Cahour's method[§]. Benzaldehyde (B.D.H. extra pure) was distilled *in vacuo*, and 53 gms. of the middle fraction was mixed with an equal volume of chloroform and slowly added to 110 gms. of phosphorus pentachloride suspended in chloroform, in a flask with a reflux condenser. The mixture was kept between 25° and 40° during the addition, and was afterwards raised to 50°, to complete the reaction. It was then cooled and poured into one litre of water to which sodium carbonate was slowly added. When the phosphorus oxychloride had hydrolysed, the oily lower layer was separated, washed again with water, twice with sodium bisulphite

[*] 110°, Reissert, 'Ber. Deuts. Chem. Ges.,' vol. 30, p. 1039 (1897); 109·5°, Bogert and Hand, 'J. Amer. Chem. Soc.,' vol. 24, p. 1035 (1902); Gabriel, Meyer, 'Ber. Deuts. Chem. Ges.,' vol. 14, p. 2338 (1881).

[†] 117° to 118° C., Beilstein, Kuhlberg, 'Ann. Chem.,' vol. 146, p. 336 (1868); Minunini, Vassallo, 'Gazz. Chim. Ital.,' vol. 26, p. 458 (1896); 117° to 117·5° C. cor. Bogert and Beans, 'J. Amer. Chem. Soc.,' vol. 26, p. 468 (1904); 118° C., Claus, 'J. Prakt. Chem.,' vol. 51, p. 400 (1850).

[‡] –39·0°, Timmermanns, 'Bull. Soc. Chim. Belg.,' vol. 25, p. 334 (1914); –41·2°, Wroczynski, Guye, 'J. Chim. Phys.,' vol. 8, p. 197 (1910).

[§] 'Ann. Chem.,' vol. 70, p. 39 (1849).

solution, then a third time with water, and, finally, it was dried over calcium chloride. The chloroform was distilled off and the residue fractionated *in vacuo*. The freezing-point of the middle fraction was − 16·2° to − 16·0° (corr.).*

*Benzotrichloride*.—A specimen supplied by Messrs. Hopkins and Williams was treated with lead carbonate, to remove free hydrogen chloride, and was then distilled *in vacuo* until the freezing-point of the middle fraction was constant (three fractionations) m.p − 5·2° to − 5·0° (corr.).†

1, 1, 1-*Trichlorethane* (*Methyl Chloroform*).—This was prepared by chlorinating ethylidene chloride‡ the latter substance being made by a modification of Geuther's method.§ To 450 gms. of phosphorus pentachloride, suspended in dry toluene in a flask with a reflux condenser, 120 gms. of *freshly distilled* paraldehyde was slowly added, the temperature being kept between 10° and 20° as far as possible. The mixture was shaken until all the phosphorus pentachloride had disappeared, and the pale yellow, opalescent liquid produced was roughly fractionated, the portions coming over up to 85° being taken. These were shaken with ice-water until all the phosphorus oxychloride had hydrolysed, then with 10 per cent. sodium hydroxide solution, twice with saturated sodium bisulphite solution, and then once again with water. The product was separated, dried over calcium chloride, and twice fractionated carefully: b.p. 56·9° at 749 mm.||

The ethylidene chloride was boiled in a flask and the vapour, mixed with a slow stream of dry chlorine, allowed to pass up through a quartz tube, packed with calcium chloride and illuminated by a quartz mercury vapour lamp, and to reflux from a condenser cooled with ice-water. To minimise the formation of higher chlorination products an excess of ethylidene chloride vapour was maintained, as judged roughly from the colour. The product was washed with 10 per cent. sodium hydroxide solution, then with water, was dried over calcium chloride, and then fractionated roughly, the lighter fractions

---

* −17·4°, Timmermanns, *loc. cit.*; −16·4°, Hollemann and Vermeulen de Mooy, 'Rec. Trav. Chim.,' vol. 33, p. 21 (1914); −16·1° corr., von Schneider, 'Z. Phys. Chem.,' vol. 22, p. 234 (1897).

† −8·1°, Timmermanns, *loc. cit.*; −5·0°, Hollemann and Vermeulen de Mooy, *loc. cit.*

‡ Regnault, 'Ann. Chem.,' vol. 33, p. 317 (1840); Stadel, *ibid.*, vol. 195, p. 184 (1879).

§ 'Ann. Chem.,' vol. 105, p. 323 (1858); Wurtz, *ibid.*, vol. 108, p. 124 (1858); Wurtz, Frapolli, *ibid.*, vol. 108, p. 223 (1858); Beilstein, *ibid.*, vol. 113, p. 110 (1860).

|| 59·2° at 760 mm., Thorpe, 'J. Chem. Soc.,' vol. 37, p. 185 (1880); 57° to 57·5°, Perkin, *ibid.*, vol. 45, p. 529 (1884), 56·7° to 56·9° at 749 mm., R. Schiff, 'Ann. Chem.,' vol. 220, p. 96 (1883); 57·3°, Timmermanns, 'Chem. Zentr.,' p. 1015 (1911)

being re-chlorinated. Finally, a series of eleven systematic fractional distillations was carried out to remove the ethylidene chloride, and the product distilled over phosphorus pentoxide: b.p. 74·1°–74·5° at 747·5 mm.†

*Dipole Moments*.—The data for the determinations of dipole moments are given in the following table, where :—

$f_2$ = Molecular fraction of the solute.
$e$ = Dielectric constant of the solution, at 25°.
$n$ = Refractive index of the solution at 25°.
$d$ = Density of the solution (those by interpolation*).
$P_2$ = Total polarisation of the solute.
${}_eP_2$ = Electron polarisation of the solute.

### *o*-Nitrobenzonitrile.

| $f_2$. | $d$ | $e$ | $n$. | $P_2$ | ${}_eP_2$ |
|---|---|---|---|---|---|
| 0·009356 | 0·8790 | 2·7859 | 1·50306 | 750·6 | 37·2 |
| 0·006802 | 0·8778 | 2·6464 | — | 771·9 | — |
| 0·004760 | 0·8765* | 2·5325 | — | 790·0 | — |
| 0·003408 | 0·8757 | 2·4601 | — | 799·0 | — |
| 0·007956 | 0·8782 | 2·7104 | — | 764·2 | — |
| 0·005762 | 0·8770* | 2·5903 | — | 782·8 | — |
| 0·00409 | 0·8760* | 2·4993 | — | 801·0 | — |
| 0·00294 | 0·8754* | 2·4364 | — | 810·4 | — |
| 0·02934 | 0·8003 | — | 1·50528 | — | 37·66 |
| 0·01395 | 0·8815 | — | 1·50390 | — | 38·00 |
| 0·00917 | 0·8790 | — | 1·50309 | — | 37·64 |
| 0·00642 | 0·8775 | — | 1·50266 | — | 36·60 |

$P_2$ at infinite dilution = 833 ${}_eP_2$ = 37·6 cm.³
$P_2 - {}_eP_2$ = 795·4 cm.³. $\mu = 6·19 . 10^{-18}$ e.s.u.

---

† 74·9° at 758 mm., Pierre, 'Ann. Chem.,' vol. 80, p. 127 (1851); 74·1° at 760 mm., Städel, 'Ber. Deuts. Chem. Ges.,' vol. 15, p. 2563 (1882); 75·3° to 76·3° corr., Perkin, *loc. cit.*, p. 531.

## *m*-Nitrobenzonitrile.

| $f_2$ | $d$ | $\epsilon$ | $n$ | $P_2$. | $_eP_2$. |
|---|---|---|---|---|---|
| 0·01871 | 0·8839 | 2·6586 | — | 311·5 | — |
| 0·01341 | 0·8810* | 2·5511 | | 319·2 | — |
| 0·00944 | 0·8789 | 2·4676 | — | 321·5 | |
| 0·00689 | 0·8774* | 2·4167 | — | 327·9 | |
| 0·02459 | 0·8874* | 2·7830 | — | 306·3 | — |
| 0·01773 | 0·8835* | 2·6410 | — | 314·3 | — |
| 0·01221 | 0·8803* | 2·5250 | — | 319·2 | — |
| 0·03261 | 0·8920* | — | 1·50497 | — | 36·81 |
| 0·01935 | 0·8844* | — | 1·50367 | — | 36·90 |
| 0·02672 | 0·8886 | | 1·50441 | — | 36·93 |
| 0·01861 | 0·8840 | | 1·50373 | — | 37·18 |
| 0·01272 | 0·8806 | | 1·50321 | — | 37·75 |

$P_2$ at infinite dilution = 334 cm.³ $_eP_2$ = 37·5 cm.³.
$P_2 - {}_eP_2$ = 296·5 cm.³ $\mu$ = 3·78 . $10^{-18}$ e.s.u.

## Benzyl Chloride.

| $f_2$. | $d$ | $\epsilon$ | $n$ | $P_2$ | $_eP_2$ |
|---|---|---|---|---|---|
| 0·05936 | 0·8902* | 2·5675 | — | 103·7 | — |
| 0·04157 | 0·8852* | 2·4792 | | 104·2 | — |
| 0·02949 | 0·8818* | 2·4195 | — | 105·1 | — |
| 0·0114 | 0·8768* | 2·3291 | — | 104·4 | — |
| 0·05258 | 0·8883* | 2·5327 | | 103·55 | — |
| 0·03760 | 0·8841* | 2·4589 | | 104·4 | — |
| 0·01453 | 0·8775* | 2·3419 | | 102·0 | — |
| 0·03554 | 0·8833 | | 1·50372 | — | 36·35 |
| 0·03150 | 0·8826 | — | 1·50357 | | 36·19 |
| 0·02355 | 0·8805 | | 1·50318 | — | 35·96 |
| 0·02060 | 0·8795 | — | 1·50299 | — | 35·92 |
| 0·01647 | 0·8782 | — | 1·50280 | — | 36·32 |

$P_2$ at infinite dilution = 105·0 cm.³. $_eP_2$ = 36·2 cm.³.
$P_2 - {}_eP_2$ = 67·8 cm.³. $\mu$ = 1·82 . $10^{-18}$ e.s.u.

*Cf.* 1·87 . $10^{-18}$ e.s.u., Weissberger and Sängewald, 'Z. Phys. Chem.,' B, vol. 9, p. 133 (1930); 1·84 . $10^{-18}$ e.s.u., Bergmann, Engel and Sandor, *ibid*, vol. 10, p. 397 (1930).

### Benzal Chloride.

| $f_2$. | *d.* | *e.* | *n.* | $P_2$. | ${}_eP_2$. |
|---|---|---|---|---|---|
| 0·02604 | 0·8881 | 2·4330 | 1·50387 | 125·8 | 41·13 |
| 0·01843 | 0·8836 | 2·3861 | 1·50337 | 125·9 | 41·02 |
| 0·01314 | 0·8806 | 2·3534 | 1·50294 | 125·8 | 40·80 |
| 0·04938 | 0·9008 | 2·5726 | 1·50520 | 122·3 | 40·37 |
| 0·03495 | 0·8924 | 2·4859 | 1·50449 | 124·3 | 41·07 |
| 0·02445 | 0·8870 | 2·4229 | 1·50359 | 125·1 | 40·29 |
| 0·01083 | 0·8772 | 2·3309 | 1·50276 | 126·0 | 40·72 |

$P_2$ at infinite dilution = 126 cm.$^3$ ${}_eP_2$ = 40·8 cm.$^3$
$P_2 - {}_eP_2$ = 85·2 cm.$^3$. $\mu$ = 2·03 $10^{-18}$ e.s.u.

### Benzotrichloride.

| $f_2$. | *d.* | *e* | *n.* | $P_2$. | ${}_eP_2$. |
|---|---|---|---|---|---|
| 0·07330 | 0·9298 | 2·7190 | 1·50869 | 126·3 | 46·04 |
| 0·05076 | 0·9132 | 2·5859 | 1·50674 | 128·7 | 45·97 |
| 0·03567 | 0·9016 | 2·4948 | 1·50523 | 130·5 | 45·89 |
| 0·01472 | 0·8851* | 2·3653 | — | 132·4 | — |
| 0·03208 | 0·8988 | 2·4740 | 1·50486 | 131·1 | 45·73 |
| 0·02247 | 0·8914 | 2·4152 | 1·50398 | 132·6 | 45·72 |
| 0·01613 | 0·8863* | 2·3754 | — | 133·5 | — |
| 0·00770 | 0·8796* | 2·3226 | — | 134·0 | — |

$P_2$ at infinite dilution = 135 cm.$^3$. ${}_eP_2$ = 45·8 cm.$^3$.
$P_2 - {}_eP_2$ = 89·2 cm.$^3$. $\mu$ = 2·074 $10^{-18}$ e.s.u

### 1, 1, 1-Trichlorethane (Methyl Chloroform).

| $f_2$ | *d.* | *e.* | *n.* | $P_2$. | ${}_eP_2$. |
|---|---|---|---|---|---|
| 0·01848 | 0·8830 | 2·3435 | 1·50336 | 84·3 | 32·85 |
| 0·01270 | 0·8802 | 2·3219 | 1·50316 | 83·8 | 33·45 |
| 0·00885 | 0·8786* | 2·3076 | 1·50263 | 83·2 | 32·99 |
| 0·04273 | 0·8951 | 2·4341 | 1·50509 | 83·31 | 32·88 |
| 0·02969 | 0·8886 | 2·3850 | 1·50419 | 83·5 | 32·84 |
| 0·02027 | 0·8840* | 2·3500 | 1·50360 | 84·1 | 32·94 |

$P_2$ at infinite dilution = 84·0 cm. ${}_eP_2$ = 33·0 cm.
$P_2 - {}_eP_2$ = 51·0 cm.$^3$. $\mu$ = 1·57 . $10^{-18}$ e.s.u.

### *Discussion of Results.*

As is well known, the properties of substituents in the benzene ring are very different from those exhibited by the same atoms or groups in saturated compounds, and furthermore the substituents have an influence, sometimes a great one, on the properties of the conjugate system of valencies that constitutes the ring; they have, for example, specific effects on the quality, speed, and direction of further substitutions.

Flurscheim* attempted to correlate the chemical facts by the hypothesis that certain atoms, in certain states of combination, could produce changes in covalency which were transmitted along a conjugated system and made alternate carbon atoms active Activating atoms or groups could be classified according to which set of atoms they activated, the odd ones or the even ones.

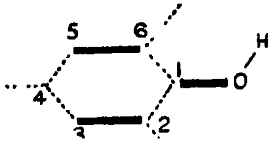

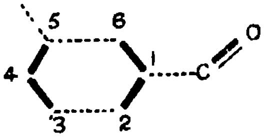

Sir J. J. Thomson,† on the other hand, pointed out that such alternation in activity could be a consequence of the way in which polarisation in a conjugated system must occur, and that dipolar groups with the positive poles nearer the chain or ring would activate the carbon atoms numbered odd, while those groups with the negative pole nearer the chain would activate those numbered even.

Either hypothesis correlates some, but not all, of the facts, and Robinson has suggested‡ that both are in some degree right. He supposes that sometimes only one factor takes effect, sometimes both, and in the latter case that they may either reinforce or oppose one another.

The "electromeric" or "tautomeric" effect, as it is variously called, can be represented as below, where each dot represents a shared electron, and each cross an unshared one. Each atom tends to retain its octet, but the distribution of shared and unshared electrons is altered —

---

* 'J. Prakt. Chem.,' vol. 66, p. 321 (1902).

† 'Phil. Mag.,' vol. 46, p. 497 (1923).

‡ 'J. Soc. Chem. Ind.,' vol. 44, p. 118 (1925); 'J. Chem. Soc.,' p. 401 (1926).

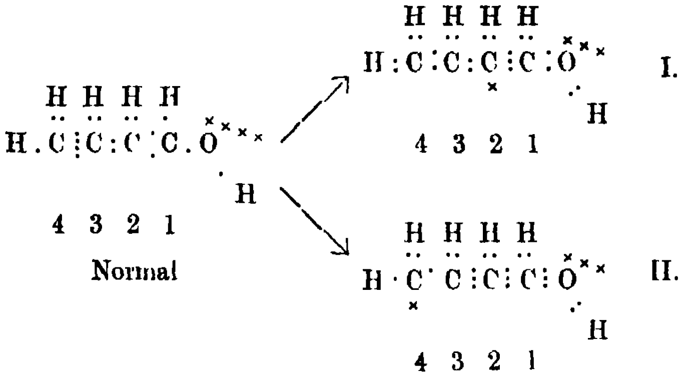

Process I gives atom 2 an unshared electron, and creates a dipole which has its negative pole on this atom, and therefore nearer the hydrocarbon radicle than the positive pole. If the substituted group be written on the right-hand side, as above, then this "electron shift" takes place in a *negative* direction, and therefore the dipole produced may be defined as *positive* Atom 2 is thereby activated towards kationoid reagents, *i.e.*, those which react in a way analogous to kations * Process II activates atom 4 in a similar way.

Certain other groups cause a rearrangement of the electrons in the reverse sense :—

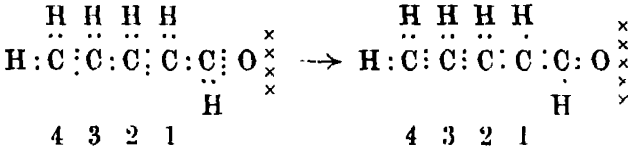

In this case atom 4, which loses an electron and has only a septet of electrons round it, becomes the positive end of the *negative* dipole created by the change, and so is deactivated towards kationoid reagents. Since the tendency to undergo this covalency change probably falls off along the chain, the change in valency 3–4 is less marked than that in valency 1–2, so atom 2 is also deactivated (alternatively the process could be imagined to stop at this atom for part of the time), while atoms 1 and 3, which do not gain or lose by these transfers, are unaffected. They are, therefore, active relative to the others, though not activated relative to those in the unsubstituted hydrocarbon, as were atoms 2 and 4 in the previous type of process. Applied to a benzene ring, the first type of change would activate the ortho and para positions, while the second would deactivate them.

---

* Lapworth, 'Nature,' vol. 115, p. 625 (1925).

The induction effect involves only the distortion of electron orbits, and not the destruction of some and the creation of new ones, as does the electromeric effect. Its action may be illustrated by the following considerations. In a heterogeneous molecule the unlike nuclei will share the covalency electrons unsymmetrically,[*] and, furthermore, the unshared electrons may be unsymmetrically distributed about their nuclei, so unless the molecule has three axes, an alternating axis, or a centre of *permanent* symmetry,[†] it will have a finite dipole moment. The moment of any covalency will depend upon the charges on the two nuclei and upon the effectiveness with which the nuclei are screened by the unshared electrons or by electrons which they are sharing with other nuclei. Thus the dipole moment of any covalency depends upon the molecule as a whole, but it may, for convenience, be regarded as having a primary value, defined for some standard condition of the other valencies, upon which moments due to secondary processes are superimposed. We will, therefore, define the primary moments of the C-H and C-C covalencies as those values which they have in an aliphatic hydrocarbon.

If we take such a hydrocarbon and substitute, say, a chlorine atom for hydrogen, then, since this has a bigger nuclear charge than the carbon atom to which it is attached, the centroid of the shared electrons in the C-Cl link will be nearer the chlorine nucleus, and the carbon nucleus will be less effectively shielded than before the replacement (the shared electron centroid being nearer the carbon nucleus in a C-H link), so it will in turn have a higher effective positive charge, and will cause the electron centroids of its other covalencies to approach closer to it.[‡]

The next carbon atom will be similarly affected and cause similar, though smaller, changes in its other covalencies, and so the effect may be transmitted along the chain for several atoms.[§]

Alternatively, we can consider that when the hydrogen atom is replaced, the secondary effects which arise will be due to the moments *induced* in the other valencies by the moment caused through the replacement. This latter will be the algebraic difference of the moment of C-Cl, which is created, and that of C-H, which is destroyed. The transmission of induced effects along chains producing effects on the atoms which are independent of the configuration of the chain (apart from direct effects through space, which are of secondary importance) indicates that the susceptibility of a link is greater along its length than across it, and is greater than that of the surrounding space, this last conclusion following also from the polarisation theory of dielectrics.

---

[*] See, for example, Niessen, 'Phys. Z.,' vol. 29, p. 52 (1928).

[†] *Cf.* L. Meyer, 'Z. Phys. Chem.,' B, vol. 8, p. 27 (1930).

[‡] Smyth, 'J. Amer. Chem. Soc.,' vol. 51, p. 2386 (1929); Eucken and Meyer, 'Phys. Z.,' vol. 30, p. 398 (1929).

[§] Lewis, "Valence and the Structure of Atoms and Molecules," p. 139.

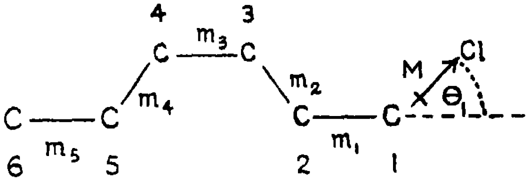

The moment induced in valency 1–2 will be proportional to the component of M, the inducing moment, along its length, and to its longitudinal susceptibility $s_1$, and so it is approximately

$$Ms_1 \cos \theta_1 = m_1 \qquad (\theta_1 = 180 - 109{\cdot}5^\circ = \cos^{-1} 1/3)$$

This induces a moment in valency 2–3 of

$$Ms_1 \cos \theta_1 \,.\, s_1 \cos \theta_1 = m_2$$

and so on along the whole chain.

The induced moment $m$ in any covalency can be considered to confer upon the atoms charges of $\pm\, m/l$, where $l$ is the average length of a covalency, and on this supposition we find that the electron gain on atom 1 is

$$\pm\,\frac{(M - m)}{l} = \pm\,\frac{M\,(1 - s_1 \cos \theta_1)}{l}$$

the sign of this being determined by that of the inducing dipole, a positive one causing electron gain and *vice versa*. The gain or loss by atom 2 is similarly

$$\frac{M\, s_1 \cos \theta_1}{l}\,(1 - s_1 \cos \theta_1)$$

and for the $n$th carbon atom it is

$$\frac{M}{l}\,(s_1 \cos \theta_1)^{n-1}\,(1 - s_1 \cos \theta_1)$$

Moments will also be induced in the C–H valencies and these will tend to reduce the gain or loss of negative charge, caused by the moments in the C–C links, but this effect, together with that of the subsidiary changes of M produced by the induced moments, may be neglected without invalidating the qualitative conclusions. Unless $\cos \theta_1 s_1$ is equal to unity, there will be a steady decrease of the effect on the carbon atoms along the chain, as illustrated by fig. 3.

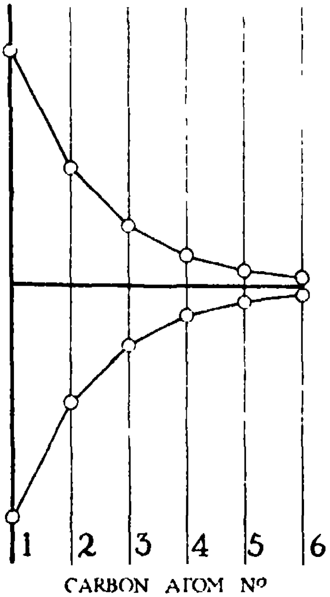

FIG. 3.

The susceptibility of a double bond is greater than that of a single one as shown by the greater refractivity of unsaturated compounds. In a conjugated system the extra allowance per double bond is from 1·7 to 2·58 cm.$^3$ for the $M_D$ values, and if this be attributed to the refractivity of the carbon atom, this latter must be increased from 2·4 to 3·3 or 3·7. As a consequence of this and of the fact that $\theta_2$ ($180° - 125·25° = 54·75°$) is less than $\theta_1$, the effect is transmitted further through such a system.

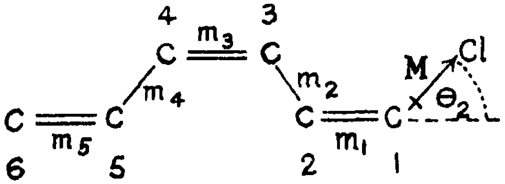

If $s_2$ be the susceptibility of the double bond, the moments induced in the successive valencies will be

$$M\, s_2 \cos\theta_2 \qquad\qquad = m_1$$

$$M\, s_2 \cos\theta_2\ .\ s_1 \cos\theta_2 = m_2$$

and so on. The gain of negative charge by the atoms in the chain will be

$$C_1 = \frac{M}{l}(1 - s_2 \cos \theta_2)$$

$$C_2 = \frac{M}{l} s_2 \cos \theta_2 (1 - s_1 \cos \theta_2)$$

$$C_3 = \frac{M}{l} s_1 s_2 \cos^2 \theta_2 (1 - s_2 \cos \theta_2) \textit{ et seq.}$$

The decrement of the effect along the chain thus alternates, as represented by the curves in fig. 4.

If M is negative, the lower curve of the two will apply, and atoms 2, 4, 6 will be relatively inactive to kationoid reagents, because the decrease in the negative charge is here most marked. The atoms 1, 3, 5, will be more active than the others, but less active than those in the unsubstituted hydrocarbon. If M is positive the upper curve in fig. 4 will apply and atoms 2, 4, 6 are active relative to the others, while all are active relative to those in the unsubstituted hydrocarbon.

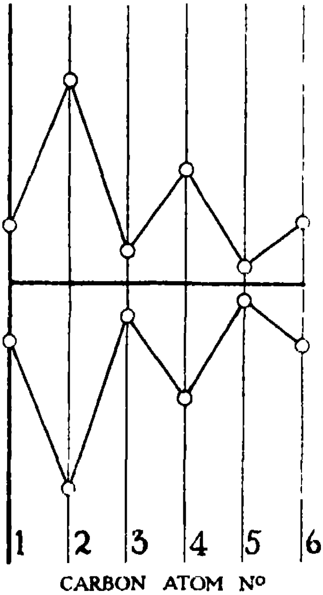

Fig. 4.

Polarisation of the types described above obviously causes a numerical increase in the dipole moment of the whole molecule.

One part of the molecule can also affect others through space, and not through the chain, causing both polarisation and steric effects (*i.e.*, alterations in the angles between covalencies). The polarisations are not usually very large; their chemical effects have been discussed by Lewis.* The steric effects, however, are often important.

If no electromeric effects occurred, groups with positive dipoles (*e.g.*, the methyl group) should be ortho-para directing, while those with negative dipoles should be meta directing (*e.g.*, the nitro, halogen, and carbethoxy groups), and it has previously been pointed out that in several cases, where the sense or direction of the group dipoles has been determined from dipole measurements, this is so (*e.g.*, Ingold, *loc. cit.*). To test Robinson's theory of the dual mechanism it is, however, necessary to separate the effects due to the two processes.

---

* "Valence and Structure of Atoms and Molecules," pp. 139–140; also Bennett and Mosses, 'J. Chem. Soc.,' p. 2366 (1930); Robinson, 'J. Chem. Soc.,' p. 406 (1926); Ingold, 'Rec. Trav. Chim.,' vol. 48, p. 797 (1929).

The total moment of an aliphatic compound can be represented as the vector sum of the primary moments and of the induced moments :—

$$m_{\text{prim}} + m_{\text{ind}}$$

while that of a compound with a conjugated chain or ring is the sum of the primary moments, the induced moments, and possibly of those due to an electromeric effect :—

$$m'_{\text{prim}} + m'_{\text{ind}} + m_e.$$

Thus, if allowance for the first two terms can be made, it is possible to calculate the third one $m_e$.

From the way in which the primary moment is defined it follows that it is equal in corresponding aliphatic and aromatic or chain unsaturated compounds, so long as we may imagine that the latter may be artificially constrained to an " aliphatic state " in which the sharing of electrons in any heterogeneous covalency proceeds as in the former.

Owing to the greater polarisability of the unsaturated compound, $m'_{\text{ind}}$ is greater than $m_{\text{ind}}$, and an attempt to allow for this must be made, and this can be done by taking the moments of the tertiary alkyl compound as the standard of comparison, as will be seen from the following considerations. It is easy to see that the sum of the primary moments of an alkyl derivative is independent of the length of the chain. Since methane has no moment, it follows that the moment of the methyl group is equal and opposite to that of the fourth C-H valency, and if we assume that the primary moment of a C–C link is zero, then in any alkyl group the terminal methyl group or groups are equivalent to single C–H valencies, so far as their contribution to the total primary moment is concerned, and therefore any alkyl group is equivalent to one with one carbon atom less. This is to say, they all have the same effective moment, that of one C–H valency, in the direction of the last, or heterogeneous valency C–X, so the primary moment of the compound is $m_{\text{CX}} - m_{\text{CH}}$ (*cf.* Debye, " Polare Molekeln ").

In most homologous series there is actually a small increase of moment from the methyl derivatives to the ethyl, from the ethyl to the *sec*-propyl and from these to the *tert*-butyl derivatives, as the hydrogen atom near the main dipole is replaced by the more polarisable carbon atoms. Lengthening of the chain by a third atom, however, usually produces no appreciable change, which indicates that very little polarisation occurs after the second atom. Thus, the moment induced in the rest of the molecule by the primary moment is a maximum in the tertiary derivatives. This has already been remarked upon by several authors,* and the relevant data are summarised below in Table I Where several values exist for one substance the arithmetic mean is given, the subscript figure indicating the number of observations. They are all taken from Debye, "Polare Molekeln," Leipzig, 1929, including the supplements published in 1930 and 1931, as are the other moments quoted without authority, and are multiplied by $10^{18}$.

It is therefore possible to calculate $m_e$ approximately from the algebraic difference

$$M_{\text{arom}} - M_{\text{aliph}},$$

taking the *tert*-butyl derivatives for comparison, in order to make the polarisations as nearly alike as possible

Differences in steric effects must also be minimised, and therefore, in the table given below, benzal chloride has been compared with propylidene chloride and benzotrichloride with methyl chloroform

The sense of the dipole of any group X may be determined from the moment of the compound $p$-$C_6H_4XY$, where Y is a group with a moment of known sense, such as the nitro group, which, since it contains the link $N \rightarrow O$, is certainly "negative." If the observed moment is nearer the numerical difference of the moments PhX and PhY than the sum, then the moments of the groups are in the same sense relative to the ring, while if it is nearer the sum than the difference, the groups have moments in opposite senses † It is assumed below that the moment of any group is in the same sense in the aliphatic compounds as in the aromatic.

Although no attempt has been made here‡ to allow for the effect of atom polarisation on the moments of those substances which have been measured in solution at one temperature, no serious difficulties arise from this cause. It happens either that the moments of both the aliphatic and aromatic derivatives are determined from solution measurements, so that both contain errors of the same order, or, where one is from gas or solution measurements at

---

* Höjendahl, 'Phys. Z.,' vol. 30, p. 391 (1929); Williams, *loc. cit.*; K. L. Wolf, 'Z. Phys. Chem.,' B, vol. 2, p. 39 (1929); Parts, 'Z. Phys. Chem.,' B, vol. 7, p. 336 (1930).

† J. J. Thomson, *loc. cit.*; Williams, 'Phys. Z.,' vol. 29, pp. 174, 683 (1928); Höjendahl, *loc. cit.*

‡ See K. L. Wolf, 'Phys. Z.,' vol. 31, p. 227 (1930).

Table I.

| Alkyl group. | Substituted group. | | | | | | | | | | |
|---|---|---|---|---|---|---|---|---|---|---|---|
| | Cl | Br | I. | $NH_2$ | OH | >O | CHO. | CO. | CN. | $CH_3COO$ | $CH_3$. |
| $CH_3$ | $1{\cdot}88_8$ | $1{\cdot}80_2$ | $1{\cdot}63_3$ | $1{\cdot}23_1$ | $1{\cdot}68_3$ | $1{\cdot}29_4$ | $2{\cdot}72_1$ | $2{\cdot}74_6$ | $3{\cdot}34_3$ | $1{\cdot}71_2$ | $0{\cdot}0_1$ |
| $C_2H_5$ | $2{\cdot}03_7$ | $1{\cdot}88_4$ | $1{\cdot}65_7$ | $1{\cdot}31_1$ | $1{\cdot}69_5$ | $1{\cdot}16_{12}$ | — | $2{\cdot}72_1$ | $3{\cdot}47_3$ | $1{\cdot}80_8$ | — |
| $n$-$C_3H_7$ | $2{\cdot}00_7$ | $1{\cdot}79_2$ | $1{\cdot}63_1$ | $1{\cdot}39_1$ | $1{\cdot}65_4$ | $0{\cdot}86_1$ | — | $2{\cdot}73_2$ | $3{\cdot}40_1$ | $1{\cdot}86_1$ | |
| $s$-$C_3H_7$ | $2{\cdot}18_1$ | — | — | — | $1{\cdot}78_1$ | — | — | — | — | — | — |
| $n$-$C_4H_9$ | $1{\cdot}97_4$ | $1{\cdot}88_3$ | $1{\cdot}73_2$ | — | $1{\cdot}67_4$ | — | $2{\cdot}46_1$ | — | — | $1{\cdot}85_1$ | $0{\cdot}0_2$ |
| $s$-$C_4H_9$ | $2{\cdot}09_1$ | $2{\cdot}12_1$ | $2{\cdot}04_1$ | — | $1{\cdot}65_1$ | — | — | — | — | — | — |
| $t$-$C_4H_9$ | $2{\cdot}15_2$ | $2{\cdot}21_1$ | $2{\cdot}13_1$ | — | $1{\cdot}65_1$ | — | — | $2{\cdot}76_1$ | — | — | — |
| iso-$C_4H_9$ | $1{\cdot}96_1$ | $1{\cdot}97_2$ | $1{\cdot}87_1$ | — | $1{\cdot}75_2$ | $1{\cdot}0_1$ | — | — | — | $1{\cdot}87_1$ | $0{\cdot}0_1$ |
| $n$-$C_5H_{11}$ | — | — | — | — | $1{\cdot}63_2$ | — | — | — | — | $1{\cdot}91_1$ | $0{\cdot}0_6$ |
| $s$-$2C_5H_{11}$ | — | — | — | — | $1{\cdot}66_1$ | — | — | — | — | | — |
| $s$-$3C_5H_{11}$ | — | — | — | — | $1{\cdot}64_1$ | — | — | — | — | | — |
| $t$-$C_5H_{11}$ | — | | — | | $1{\cdot}83_1$ | — | — | — | — | | — |
| iso-$C_5H_{11}$ | — | — | | — | $1{\cdot}81_3$ | | — | — | — | | — |
| $n$-$C_6H_{13}$ | — | — | — | — | $1{\cdot}64_1$ | — | — | — | — | — | $0{\cdot}0_3$ |
| $n$-$C_7H_{15}$ | — | $1{\cdot}83_2$ | $1{\cdot}84_1$ | — | $1{\cdot}7_1$ | — | $2{\cdot}56_1$ | — | — | — | $0{\cdot}0_1$ |
| $s$-$2C_7H_{15}$ | $2{\cdot}0_1$ | $2{\cdot}1_1$ | — | — | $1{\cdot}7_1$ | | — | — | — | — | — |
| $s$-$3C_7H_{15}$ | $2{\cdot}1_1$ | $2{\cdot}0_1$ | $1{\cdot}93_1$ | — | $1{\cdot}7_1$ | — | — | — | — | (isomers) | $0{\cdot}0_1$ |
| $s$-$4C_7H_{15}$ | $2{\cdot}0_1$ | $2{\cdot}0_1$ | — | — | $1{\cdot}7_1$ | — | — | — | — | — | — |
| $C_8H_{17}$ | — | — | — | — | $n$ $1{\cdot}67_2$ | — | — | — | — | $s$ $1{\cdot}93_1$ | $n$ $0{\cdot}0_1$ |
| $C_9H_{19}$ | — | —<br>(2-methyl-3-ol) | — | — | $n$ $1{\cdot}60_1$<br>$1{\cdot}62_1$ | — | —<br>— | —<br>— | —<br>— | —<br>— | $n$ $0{\cdot}0_1$<br>— |
| $C_{10}H_{21}$ | | | — | — | $n$ $1{\cdot}61_1$ | — | — | — | — | — | $n$ $0{\cdot}0_1$ |
| $C_{11}H_{23}$ | — | — | — | — | $n$ $1{\cdot}66_1$ | — | — | — | — | — | $n$ $0{\cdot}0_1$ |
| $C_{12}H_{25}$ | — | | | — | $n$ $1{\cdot}62_1$ | — | — | — | — | — | — |
| $C_{16}H_{33}$ | — | — | — | — | $n$ $1{\cdot}66_1$ | — | — | — | — | — | — |

different temperatures and the other from measurements at one temperature, that the former has the greater value, and therefore the error in the latter moment (which is too great), though it affects the magnitude of the difference, does not affect its sign.

Table II.

| Group. | M (arom.). | M (aliph.). | M (ar.) − M (al.) ($m_e$). |
|---|---|---|---|
| $CH_3$ | $+0\cdot 45_3$ | 0·0 | +0·45 |
| $>O$ | $-1\cdot 06_2$ | $-1\cdot 29_4$ | +0·23 |
| $NH_2$ | $+1\cdot 55_3$ | $+1\cdot 23_1$ | +0·32 |
| Cl | $-1\cdot 56_{14}$ | $-2\cdot 15_1$ | +0·59 |
| Br | $-1\cdot 52_5$ | $-2\cdot 21_1$ | +0·69 |
| I | $1\cdot 27_2$ | $-2\cdot 13_1$ | +0·88 |
| $CH_2Cl$ | −1·82* | $-2\cdot 03_7$ | +0·21 |
| $CHCl_2$ | −2·03* | $-2\cdot 06_1$ | +0·0 |
| $CCl_3$ | −2·07* | −1·57* | −0·5 |
| $CO\cdot CH_3$ | $-2\cdot 97_1$ | $-2\cdot 79_1$ | −0·18 |
| CO | $-3\cdot 04_1$ | $-2\cdot 76_1$ | −0·28 |
| $C\equiv N$ | $-3\cdot 89_8$ | $-3\cdot 46_1$ | −0·43 |
| $NO_2$ | $-3\cdot 93_6$ | $-3\cdot 05_1$ | −0·88 |

As in Table I, the subscript figures refer to the number of measurements from which each value is derived, and an asterisk indicates that the value is taken from the experimental section of this communication.

From this table it will be observed that—

(1) the difference $m_e$ is invariably positive for ortho-para directing groups, *i.e.*, those which activate the carbon atoms 2, 4 and 6, indicating a drift of electrons into the benzene ring, and negative for the meta directing groups, indicating a drift from the ring. For the group $-CHCl_2$, which is intermediate in properties, there is no appreciable difference.

(2) The aryl halides have numerically smaller moments than the alkyl halides, which proves that some other process besides polarisation occurs in these.

(3) The differences are of the order $0\cdot 2$ to $1\cdot 0 \, . \, 10^{-18}$ e.s.u., and are therefore much smaller than the moment per molecule produced by a *complete* electromeric process, which can be roughly calculated in the following way.

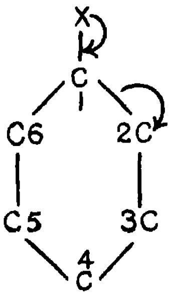

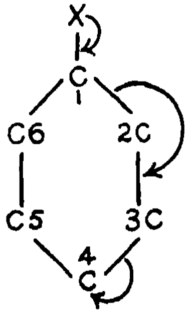

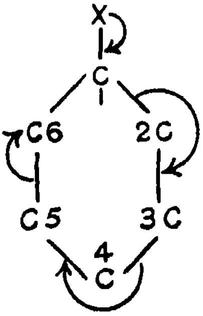

In ortho activation a moment $el/2$ is produced in the $XC_1$ valency ($e$ is the electronic charge and $l$ the average length of a valency), assuming symmetrical sharing as a sufficiently accurate approximation, and another $el/2$ in $C_1C_2$ at 60° to the first, giving a resultant of $\sqrt{3}\ el/2$ or roughly $6 \cdot 10^{-18}$ e.s.u In para activation moments are generated along $XC_1$, $C_1C_2$, $C_2C_3$, and $C_3C_4$, all having the approximate magnitude $el/2$. The vector sum of these is $3\ el/2$, or roughly $11 \cdot 10^{-18}$ e.s.u.

Activation of atom 6 by a further process involving valencies $C_4C_5$ and $C_4C_6$ would also cause a moment $\sqrt{3}\ el/2$.

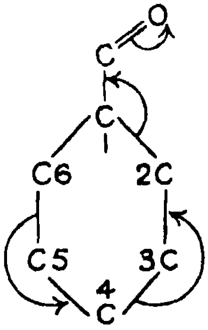

In ortho-para *deactivation*, *e.g.*, by a -CO group, moments are generated along the CO, $CC_1$, $C_1C_2$, $C_2C_3$, $C_3C_4$, $C_4C_5$, $C_5C_6$ valencies, and the vector sum of these is approximately $el$, *i.e.*, $7 \cdot 10^{-18}$ e.s.u.

It is clear, therefore, from the experimental evidence, that these changes cannot occur completely in every molecule at the same instant, and it could be considered either that only a fraction (up to 10 per cent.) of the molecules is fully affected, or that there is a small mean change of dipole moment in each molecule. For most cases either view would be equally satisfactory, but from the fact that there exist ortho-para substitutions which proceed at a much slower rate than substitution into benzene itself, *e.g.*, those into chlorbenzene, it can be shown that the latter view is the more probable. The polarisation produced by the negative moment of the CCl link deactivates all positions, but especially the ortho and para positions, whereas the electromeric effect caused by the chlorine atom tends to activate them. Now the polarisation is a comparatively small effect occurring in every molecule and, therefore, if the electromeric effect were large (about $6–11^{-18}$ e.s.u.) in a few molecules the former would have no appreciable effect in these, indeed the positive "electromeric moment" would be the main polarising influence (Ingold, *loc. cit.*), and consequently the velocity of substitution, being that into activated molecules, would be greater than that into benzene. If, on the other hand, the electromeric effect were small in each molecule, smaller in fact than the polarisation, the ortho and para atoms could be active relative to the meta atoms, but less active than the atoms in unsubstituted benzene, and the substitution would therefore be slower. The latter view, which implies that profound changes in reactivity are associated with only small permanent changes in electron distribution, and therefore of dipole moment, is thus the more probable.* The question of the exact way in which these changes are related to one another is certainly complex. Unless only the molecules of the reagent have to be activated, the reaction is controlled by the production of activated molecules of the benzene derivative and by the nature of their activity. As regards this latter factor, it is possible that in these activated molecules the conditions would be so different that the effects observed from the dipole moments to occur in normal molecules might no longer take place at all, though this view is an extreme one. In any case it is insufficient to consider the changed reactivity as simply a result of the changed electrostatic forces between the reacting molecules. The main point to be made here, however, is that some relation between these electron shifts and the reactivity does exist, whatever its precise origin may be

If it were possible to determine the primary moment $m_{\text{prim}}$, the algebraic sum of the polarisation and the electromeric effect could be calculated, as the latter is equal to the difference between the observed moment and $m_{\text{prim}}$, so the explanation given above of the substitution into chlorbenzene could be tested, but at present it does not appear possible to do this satisfactorily. In brombenzene there is a similar nuclear deactivation, but in iodobenzene there is nuclear activation compared with benzene (Ingold, *loc. cit.*). Furthermore, the ortho-para directing power increases in the order Cl, Br, I, and it is therefore worthy of note that the moment produced by the electromeric effect increases in the same order —Cl (+ 0·59), Br. (+0·69), I (+ 0·88).

The positive difference between the moments of toluene and the paraffins indicates that the method of allowing for the polarisation is inadequate in this particular case, where the aliphatic compound has no moment. Strictly speaking, allowance should have been made for the fact that the benzene CH valency, which we have taken as a standard of reactivity, has a slightly different moment from the aliphatic one, on which we based our definition of primary moment. This difference is, however, less than the moment of toluene, which is in part due to polarisation of the rest of the molecule, and may be about 0·3. An allowance should also be made for the different way in which the aromatic carbon atom and the substituted atom or group will share electrons. These two factors tend to neutralise one another, however, so for this reason, and to avoid complications, no attempt to allow for them was made. As they are probably small, the main deductions would, in any case, still hold good.

---

* See also Robinson, 'J. Chem. Soc.,' vol. 121, p. 429 (1922); 'Trans. Faraday Soc.,' vol. 19, p. 507 (1923); G. N. Lewis, "Valence and the Structure of Atoms and Molecules," pp. 145–146. This view entails some modification of the presentation of the electromeric effect given previously, the precise nature of which is uncertain. The effect may be regarded as an extended alternating disturbance of electron distribution round the carbon atoms in a conjugated system, consequent upon a tendency to reduce local changes in sharing which are caused by an unshared electron tending to become shared or *vice versa*.

In the case of the meta directing groups for which there are data, an electromeric effect would produce a moment of the same sign as that due to polarisation and could not, therefore, be distinguished so sharply as in the phenyl halides. Nevertheless, from the similarity of the differences of moment between the aromatic ketones and either the primary or secondary aliphatic ketones, and from the fact that the differences for the cyano and nitro groups are so large (although, admittedly, data for their tertiary derivatives are lacking), it appears that there is some effect in addition to polarisation. Further reasons in support of this view will be adduced later.

The differences between the ω-chlorinated toluenes and the aliphatic analogues are interesting in that they show an algebraic decrease as the ortho-para directing power of the group on the benzene ring decreases :—

$$-\mathrm{CH_3}\ +0{\cdot}45,\ \mathrm{CH_2Cl}\ +0{\cdot}14\ \text{to}\ +0{\cdot}21,\ \mathrm{CHCl_2}\ 0{\cdot}0,\ \mathrm{CCl_3}\ -0{\cdot}5.$$

It has been recognised that the ortho-para directive powers of the $CH_2Cl$ and $CHCl_2$ groups are difficult to explain, for the moment of the CCl valency is numerically much greater than that of the CH valency, and is opposite in sense,* so the former group should be meta directing. Ingold has suggested

---

* At Dr. Sidgwick's suggestion I have calculated the moments of the C–Cl and C–H covalencies from the observed moments of chloroform and methylene chloride and from the observed angles between the former covalencies (Bewilogua, 'Phys. Z.,' vol. 32, p. 265 (1931) ), assuming (*a*) that the angle between the latter covalencies is the tetrahedral angle 109·5°; or (*b*) that by the spreading apart of the former covalencies the angle between the latter is reduced in the manner suggested by Ingold ('J. Chem. Soc.,' vol. 119, p. 305 (1921) ), an arbitrary value of 100° being taken to test the effect of such changes upon the calculated moments. For M $CHCl_3 = 1{\cdot}0 \,.\, 10^{-18}$ e.s.u. and $\theta = 116°$, M $CH_2Cl_2$ $1{\cdot}6 \,.\, 10^{-18}$ e.s.u. and $\theta = 124°$, I found, on assumption (*a*) $m$ C–Cl $= -1{\cdot}5 \,.\, 10^{-18}$ e.s.u., $m$ C–H $= +0{\cdot}15 \,.\, 10^{-18}$ e.s.u.; on assumption (*b*) $m$ C–Cl $= -1{\cdot}41 \,.\, 10^{-18}$ e.s.u., $m$ C–H $= +0{\cdot}2 \,.\, 10^{-18}$ e.s.u.

The moment of methyl chloride calculated from these values is $1{\cdot}65 \,.\, 10^{-18}$ e.s.u. or $1{\cdot}61 \,.\, 10^{-18}$ e.s.u. (*cf.* $1{\cdot}88 \,.\, 10^{-18}$ e.s.u. observed). The small discrepancies indicate that the covalency moments are not exactly equal in methyl chloride, methylene chloride and chloroform, but that the induction effects between the large C–Cl dipoles produce mutual diminutions of moment, as would be expected from the previous considerations.

(*loc. cit.*) that a weak electromeric effect occurs, though this would be precluded by a strict interpretation of the mechanism, because the chlorine atom is not directly attached to the conjugated system, and it would also be necessary to introduce a hypothesis, to explain why the polarisation effect increases faster than the electromeric on further chlorination. The dipole moments emphasise the anomaly, for benzyl chloride, though it has a more polarisable hydrocarbon radicle than ethyl chloride, actually has a smaller moment, while that of benzal chloride is only just equal to that of ethylidene chloride.

There is one case which is apparently an anomaly. The thio-ether group $C_2S$, though ortho-para directing, appears to cause a negative change of moment from the following data :—*

$$Ph_2S - 1{\cdot}47 \quad (PhCH_2)_2S - 1{\cdot}38 m_e = -0{\cdot}09$$

$$cf\ Ph_2O - 1{\cdot}06 \quad (PhCH_2)_2O - 1{\cdot}38 m_e = +0{\cdot}32.$$

At present no explanation of this is offered †

Other cases which are anomalous, at first sight, are those of the hydroxyl, methoxyl, aldehydo, and ester groups, which, although they have powerful directive properties, appear to cause only small electromeric moments :—

| Group | M (Arom.) | M (Aliph.) | M (Ar.) — M (Al.). |
|---|---|---|---|
| $—OH$ | −1·68 | −1·83 | +0·15 |
| $—OCH_3$ | −1·19 | −1·16 | +0 |
| $—CHO$ | −2·75 | −2·46 | −0·29 |
| $—COCH_3$ | −2·97 | −2·79 | −0·18 |
| $—COOCH_3$ | 1·93 | −1·71 | −0·22 |
| $—COOC_2H_5$ | −1·95 | −1·77 | −0·18 |

None of the benzene compounds containing these groups have any axes of permanent symmetry, however, and the effect of an electron drift in or out of the ring may, therefore, be mainly to alter the direction of the resultant moment relative to the molecule, and not greatly to affect its magnitude.

The observed moment $M_x$ of a compound PhY (where Y is a group of this type) will be, as before, the vector sum of the primary moments, the induced moments, and the electromeric effect, but the two latter components will not now be in the same straight line as the first, and therefore to calculate the moment due to the electromeric effect $m_e$, we need to know the magnitudes and directions relative to the characteristic valencies of the molecule of the vector sum $m_0$ of the other two terms, and of the total resultant moment $M_Y$.

---

* Bergmann, Engel and Sándor, 'Z. Phys. Chem.,' B, vol. 10, p. 397 (1930).

† [*Note added 10th September*, 1931.—In a recent paper Partington and Hunter, 'J. Chem. Soc.,' p. 2062 (1931), give a value of $1{\cdot}57 \,.\, 10^{-18}$ e.s.u. for the dipole moment of di-ethyl sulphide. This substance is more suitable as the aliphatic standard than di-benzyl sulphide is, and since the algebraic difference between the moments of di-phenyl sulphide and it $(-1{\cdot}47 + 1{\cdot}57 = +0{\cdot}1)$ is positive, the anomaly noted above disappears.]

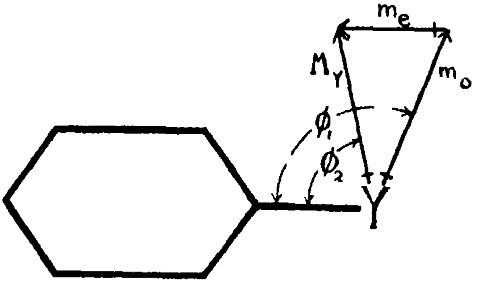

FIG. 5

$m_0$ will be approximately equal in magnitude and direction to the moments of the corresponding alkyl derivatives and these, for the ethers and aldehydes, are as represented below, for, from the conclusions of Niessen (*loc. cit.*) that the centroid of the shared electrons in a covalency is nearer the atom with the bigger nuclear charge (as found to be true for the C $\equiv$ N and C–Cl covalencies), it will be nearer the oxygen atom in the C-O link.

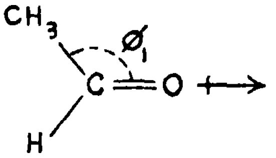

$\phi_1 = 125° \ 16'$

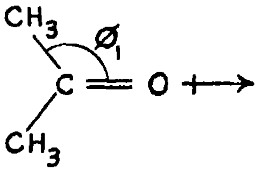

$\phi_1 = 125° \ 16'$

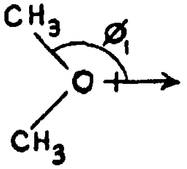

$\phi_1 = 125° \ 16'$

The moment of di-methyl ether is taken as a standard for that of the ether group because, owing apparently to a steric effect, the moments of the higher ethers fall,* and allowance for the polarisation cannot be made as previously. This would cause the value calculated for $m_e$ to be too low, but, on the other hand, a similar steric effect in the phenyl ethers† for which no allowance was made, would cause it to be too great, so the errors tend to compensate. The direction of $m_0$ in the alcohols may be determined by solving a vector triangle ABC in which are known AB, the moment of the OH link (calculated from the moment of water to be $1 \cdot 61 . 10^{-18}$ e.s.u., taking the HOH angle to be 109·5°, see Eucken and Meyer, *loc. cit.*), AC, the moment of the alcohol taken as a standard (*tert*-butyl alcohol M = 1·65 . $10^{-18}$ e.s.u.; *tert*-amyl alcohol M = 1·83 . $10^{-18}$ e.s.u., mean = 1·74 . $10^{-18}$ e.s.u.), and the angle ABC, which is the supplement of that between the CO and OH valencies and is assumed to be 70·5°. $\phi_1$. The obtuse angle between AC and the CO link (the moment being considered to have its positive pole nearer the apex of the angle) is equal to the supplement of the angle ACB and from the above data is found to be 120° (mean).

---

* Sanger and Steiger, 'Helv. Phys. Acta,' vol. 2, p. 136 (1929).

† *Cf.*, however, Weissberger and Sängewald, 'Phys. Z.,' vol. 30, p. 792 (1929).

If the magnitude of the moment $M_Y$ of PhY be known, its direction may

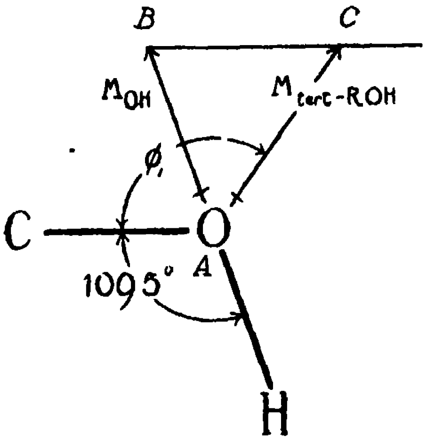

FIG. 6.

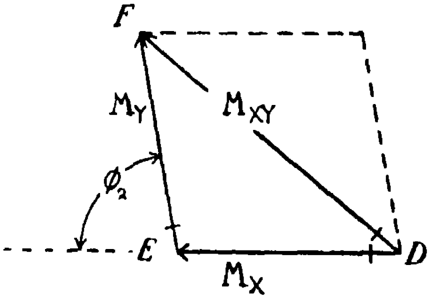

FIG. 7.

be determined from the moment $M_{XY}$ of a compound *p*-$C_6H_4XY$, where X is a simple group such as $CH_3$, Cl, or $NO_2$, whose moment is along the axis of the benzene ring and is of known magnitude, for it is then possible to solve the vector triangle DEF in which all three sides are known—DE, the moment of PhX, EF the moment of PhY, and DF the moment of the para di-substituted compound. $\phi_2$, the angle between the moment $M_Y$ and the CY link, is the supplement of the angle DEF.*

It is immaterial that we know only the total moments of the compounds PhX and PhY, not those of the groups themselves, provided that the moments of the C–H valencies are the same in each and that neither group influences the moment of the other. It was tacitly assumed that this was so, but from the results it is clear, as would indeed be expected, that this is not exactly true. It should be possible, however, to determine the limits within which $\phi_2$ and therefore $m_e$ lie by taking various groups as X, on the one hand the methyl group, which causes a small electron shift into the benzene ring, and on the other, the chlorine and bromine atoms which cause a small nett shift outwards (the nitro group is an extreme case).

---

* *Cf.* Höjendahl, 'Phys. Z.,' vol. 30, p. 391 (1929); Bergmann, Engel and Sandor, 'Z. Phys. Chem.,' B, vol. 10, p. 397 (1930).

From the data assembled by these methods the following values for $m_e$ have been obtained :—

| Y | M(RY). | $\phi_1$. | M(PhY) | X. | $\phi_2$ | $m_e$. |
|---|---|---|---|---|---|---|
| | | ° | | | ° | |
| —OH | $1\cdot74_2$ | 120 | $1\cdot68_4$ | $CH_3$<br>Cl<br>Br<br>$NO_2$ | 87<br>68·5<br>52<br>57 | +0·95<br>+1·5<br>+2·06<br>+1·8 |
| $—OCH_3$ | $1\cdot29_4$ | 125·25 | $1\cdot19_2$ | $CH_3$<br>$NO_2$ | 80·5<br>76 | +0·94<br>+1·04 |
| $—NH_2$ | $1\cdot23_1$ | 100 | $1\cdot55_1$ | Cl<br>$NO_2$<br>$CH_3$ | 39·5<br>0<br>95 | +1·44<br>+2·7<br>+0·34 |
| —CHO | $2\cdot46_1$ | 125·25 | $2\cdot75_1$ | $NO_2$ | 142·5 | −1·05 |

It will be observed that $\phi_2$ is smaller than $\phi_1$ in the case of ortho-para directing groups, so $m_e$ is positive, and that the converse is true for the meta directing group. Furthermore, the $m_e$ values so calculated are as great as, or greater than, those previously found for simple groups.

Effects similar to those in the ring compounds can be shown to occur in the unsaturated open chain compounds :—

| Group. | M (Ethylenic). | M (Aliph.). | M (Eth.) - M (Al.). |
|---|---|---|---|
| Cl | $-1\cdot66_1$ | $-2\cdot15_1$ | +0·49 |
| Br | $-1\cdot48_1$ | $-2\cdot21_1$ | +0·73 |
| $C_2H_5$ | $+0\cdot37_1$ | 0·0 | +0·37 |
| $CH_2Cl$ | $-2\cdot00_2$ | $-2\cdot03_7$ | +0·03 |
| $CH_2Br$ | $-1\cdot93_1$ | $-1\cdot88_4$ | −0·05 |
| $CH_2NH_2$ | $+1\cdot20_1$ | $+1\cdot31_1$ | −0·11 |

From the evidence of organic reactions it would be anticipated that both the inductive and electromeric effects would be greater in open chain conjugated systems than in closed ones.*

Owing to the difficulty of estimating the true primary moments, the former effect cannot be calculated from dipole data and comparisons of its values in different types of compound are therefore not possible. It is, however, extremely probable that they are greater in the open chain compounds because the polarisibility per double bond is greater in these, as shown by the molecular refractivities. Thus, the additional $M_D$ per double bond is 1·7 cc. for benzene, but 2·58 for hexadiene and 2·2 for isoprene, while for the non-conjugated compounds amylene, hexylene and di-allyl, it is 1·69, 1·97 and 1·75 respectively. The electromeric moments above are not greater than those for the benzene derivatives, but none of the compounds have more than one double bond, so the point is not properly tested. Cinnamaldehyde Ph–CH = CH–CHO (M = 3·71 . $10^{-18}$ e.s u.), *mono*-benzol-acetone Ph–CH = CH–CO–$CH_3$, (M = 3·31 . $10^{-18}$ e.s u.), and *di*-benzal-acetone Ph CH = CH–CO–CH = CH–Ph (M = 3·28 $10^{-18}$ e s.u ) (Hassel and Naeshagen, 'Z. Physikal. Chem.,' B, vol. 6, p. 441, vol. 8, p. 357), which have partially open conjugate systems, all have moments numerically bigger, but algebraically smaller than that of benzaldehyde (M = 2·75 $10^{-18}$ e s u ) as anticipated This difference is, moreover, most probably due to an electromeric effect, since the moments of the ketones are numerically smaller than that of cinnamaldehyde, whereas they would be greater if nothing but polarisation occurred, because the hydrogen attached to the CO group is replaced by the more polarisable carbon atoms Allyl chloride differs from benzyl chloride in that the positive difference is smaller, which probably indicates that the inductive effect is greater and the electromeric effect smaller

---

* Robinson, 'J. Chem. Soc.,' p. 403 (1926).

## *Summary.*

The conclusions reached from the foregoing considerations may be summarised as follows. It is possible, by comparing the electric dipole moments of corresponding aliphatic and aromatic compounds, to show that there is an "electron shift" which is towards the benzene ring (positive) when the group substituted is ortho-para directing, and away from the ring (negative) when it is meta directing. In the chlorinated toluenes the shift changes from positive in benzyl chloride to negative in benzotrichloride. These effects occur independently of the polarisation caused by the group dipole and appear to correspond with the electromeric effect postulated in Lapworth's and Robinson's theories of activation in conjugated systems. The mean effect is comparatively small, and it is more probable that there is a small effect in each molecule than that there is a large effect in only a fraction of the molecules. Similar effects occur in unsaturated open chain compounds and, from the available evidence, it appears that they are greater than those in the aromatic compounds if the double bonds are conjugated.

I have great pleasure in taking this opportunity to thank Professor P. Debye, Professor R. Robinson, Mr. D. Ll. Hammick, and especially Dr. N. V. Sidgwick, for their advice, criticism and help, the Department of Scientific and Industrial Research for a grant which enabled me to carry out this work, and, finally, Imperial Chemical Industries, Ltd., for a grant which covered the cost of the apparatus.

---

# *A Simple Method of Measuring Surface Tension.*

By J. H. Gaddum, National Institute for Medical Research, London, N.W.3.

(Communicated by H H Dale, Sec R S —Received June 25, 1931 )

## *Abstract.*

(1) The surface tension of a liquid can be determined in absolute units by measuring the volume of drops by means of the micrometer syringe.

(2) The slow fall of "static" surface tension in the newly-formed surface of a solution of a hydrophilic colloid can be followed by this method.

(3) The apparent viscous-elasticity of the surface of saponin solutions is clearly shown by the changes which occur in the shape of drops. The rapid changes can be explained in terms of the changes which must occur in the concentration of saponin in the surface. It is suggested that the slow changes are due to the diffusion of saponin.

(4) It is suggested that the slow changes which occur in the tension of certain plastic bodies following a strain may also be due to the diffusion of molecules into positions where they affect the tension.

(*The full paper is printed in 'Proceedings,' B, vol.* 109, *pp.* 114–125 )

# OBITUARY NOTICE.

# CONTENTS.

Page

**Herbert Hall Turner** (with portrait) . ..... . .......... ............... ... i

H. H. Turner

# HERBERT HALL TURNER—1861-1930.

Herbert Hall Turner was the son of an artist, John Turner, and was born at Leeds on August 13, 1861. His education began at Leeds, but he passed as a scholar to Clifton College, whence he went as a Major Scholar to Trinity College, Cambridge. He was Second Wrangler in 1882, and gained the second Smith's Prize in 1883. In the following year he was elected a Fellow of Trinity. He had a strong physique that allowed him in those days, as often as he liked, to sit up all night playing whist, evidently without detriment to his studies. He carried this strong physique as well as his devotion to whist all through his life. Another scrap of evidence from this time shows how tenacious were his dominant habits. In the second part of the Tripos, he took "Heat and Electricity." Finding that there was a want of examples for a student to try his teeth on, he searched for and copied out all that had been set in earlier examinations, and so that others should not be put to the same trouble later, he had them published in a little book. His friends will recognise in this the industry, the practical solution of a practical difficulty, and the quite unassuming service for others that gave him a direction all through his life.

W. H. M. Christie became Astronomer Royal in 1881, following Airy's long reign, during which immense expansion of the only national observatory had passed beyond useful consolidation into the stage of crystallisation. Christie determined to infuse some new blood, and selected Turner as his chief assistant. He could hardly have done better. There have been greater astronomers than Turner, and astronomers whom he has not surpassed in industry and scope; there have been men who have originated more, in bringing remote and subtle ideas into use, or in devising new methods of observation; but I have never heard of one who meant more in personal touch. Practically everyone is interested in astronomy, though even at the present day the number of professional astronomers is not large. Whether one belonged to the one class or the other, or to the fluctuating margin between, one was immediately made aware of Turner's unforced, unfeigned sympathy, and to an extraordinary degree of his practical willingness to help at the cost of his own time. He constituted himself that indispensable requisite of modern life—a medium of exchange. It was his practice always and immediately to introduce people to one another if they were working on the same idea He brought a man at once into the ambit of any appropriate organisation. There is almost no living astronomer in this country who is not indebted to him for some service of this kind; nor in this country alone. Late in his life, arriving in Madrid, tired and late, he yet did not fail to pay a visit at once to the astronomers at the observatory, so that they might feel the encouragement of a brother astronomer's interest. I stress this personal element in Turner's character, because I regard it as the dominant one, a voice he never thought of disregarding, and which he could not have disregarded without doing violence to his nature.

Turner had a powerful intellect, though if it were a subtle one he kept that aspect in reserve. He touched a great many interests. Music, drawing, seemed to affect him profoundly. He never spoke about religion. He took his part, however, in "carrying on" during the war—for example, by reading lessons in New College Chapel. He always gave me the impression of putting a bridle on what he said, as a strong man will if he is confident his strength will suffice. Only in minor matters, where he hesitated to hurt somebody's feelings, or in the professional field where he strongly disagreed with some detail of action or policy, was it apparent how strongly he felt, practically on every subject.

At Greenwich Observatory, a young man of 23, he was thrown at once into a very attractive system of routine, which suited his tastes precisely. He had a certain amount of difficulty with those over whom he had been put, and who might have been promoted. His directions were to take general charge in the absence of the Astronomer Royal. As Christie's health was none too good, this occasionally meant considerable responsibility. He took part in all the observers' work in turn. Then as now, carrying on a long tradition, the work of the transit circle gave Greenwich a unique title to regard. Other branches of astronomy, in which Greenwich must compete as one out of a number of observatories, some of them better equipped, had hardly emerged from the laboratory stage. He joined in longitude determinations. He investigated the "R–D Discordance." In those days no one expected astronomers to produce anything more exciting. He partook in the Greenwich expedition to observe the West Indian eclipse in 1886, and thus began the long series of his eclipse expeditions. He went to Japan in 1896, in which he used the cœlostat for the first time, and proved its value, though the eclipse was clouded. He took a major part successfully in three others, travelling to India in 1898, to Algiers in 1900, and to Egypt in 1905, and attended some others as a watcher.

More significant from the point of view of Turner's love of organisation was a project that took shape in 1887. Astronomy is now, through the International Astronomical Union, marked out into sections, each of which is internationally organised. But this is a growth, all dating from the successful organisation of the Astrographic Catalogue and Chart in 1887. It had become visible how greatly photography was destined to assist astronomy. The first of all requisites was to get a map of the sky. It was too large a problem for any one observatory, and besides for geographical reasons no single observatory could carry it out. Acceptors were found, at the Congress at Paris, in 1887, to carry out the whole project. It meant providing special instruments, on a systematic, uniform plan, taking a net of photographs in zones, and most laborious of all, measuring the position and magnitude of each star on them. This was the Catalogue, which was calculated to reach to the 10th or 11th magnitude. Besides this there was the Chart, which went further, with special plates, and was much more costly to produce. After measurement, the catalogue required printing, which was then cheap Not all those who accepted were able to implement their promises, and now after 44 years the position is not likely to change. Wisdom would have completed the project at once, and repeated it at a definite epoch thereafter, say 10 years, as Turner always insisted. In place of that, the organisation was diverted in 1900, when it had just got seriously to work, for an occasion, for which it was indeed very well suited and which no one could have foreseen—determining the distance of the sun by photographs of the newly discovered minor planet Eros. Needless to say, the necessities of the Eros campaign were somewhat different from those of the Catalogue. Very little of the original plan was at that time completed. At first nothing was known of how far registration of stars must go in order to contain matter of new interest. Actually the 10th magnitude hardly reaches beyond the local cluster. The best method of measurement of the plates was not known. In this Turner was very successful and contributed what was, perhaps, his chief permanent mark to astronomy. He devised a scale in the eyepiece, very much reducing the labour of measurement, and he also planned the discussion, showing how a photograph ought to be treated in order to derive positions from it, eliminating the inevitable errors of personality, setting and centering. Greenwich was the first observatory to finish its work, but before that time Turner had already gone to Oxford.

When Turner had been eight years at Greenwich, Professor J. C. Adams died, and the Lowndean Chair became vacant Turner offered himself as a candidate, but was not accepted. Undoubtedly the event was a disappointment to him. But the following year the Savilian Chair of Astronomy at Oxford became vacant and Turner was elected. By the same choice he became a Fellow of New College, and left Greenwich for Oxford, where he remained for the rest of his life. Nor when Christie retired in 1910 was he invited to return to Greenwich. To collect in one place these factual details, at his death he held the degree of D.Sc. at the Universities of Oxford, Sydney, Leeds, Strasbourg, and Wales; D.C.L. of Durham, and LL.D. of California, and was a corresponding member of the Academy of Science of Paris.

As may be supposed, Turner entered at once and whole-heartedly into the intimacies of college life. Before his marriage he lived in college. He became Subwarden in his turn and accompanied the Warden on his " progress " round the college farms. The choir boys came in for his special care. When he required computing boys for the observatory he looked there. For many years the Senior Common Room played the choir boys at cricket, and till the year of his death he never missed a match, playing with zest and compiling respectable scores. He was very proud of his place in New College, and was a loyal son of it, though an adopted one, and in particular was affectionately attached to many of the other Fellows, and to W. A. Spooner, Warden for most of his time. He was always a man of boundless hospitality, instinctively, because he believed profoundly in good personal relations, and the College and its society was a natural outlet for its exercise.

In 1899 he married Agnes Margaret, daughter of Robert Whyte, of Blackheath, who matched his life completely, and who survives him, with their daughter, Dr. Ruth Turner.

The Observatory, under the direction of the Savilian Professor, had been built in the Parks in 1873, after the divergence between the University authorities and the Radcliffe Trustees was judged to be permanent. Like most observatories, the buildings are of a somewhat cramped and unambitious character, as far as the observing sections go, and the position in the Parks was a ready obstacle to any extension. Such as the Observatory was, Turner used it in a way that made its deficiencies forgotten. It had been equipped with one of the astrographic telescopes, and had undertaken the zones from 59° to 65° from the Pole. Turner's first work was to bring this to completion. His guiding note was efficiency. Every use was to be made of the data acquired, but subject to that all should be done in the shortest time, with the least labour and at the least cost. Even so, the first consideration, which was the ruling one, made the task a great one, and enormous when viewed as part of a projected whole. He had no sympathy with those who, feeling they had succeeded in gaining the adhesion of various governments to a world-wide scheme, wished to extend the scope. He considered this a mere exploitation of a favourable position, which would bring its own Nemesis on future schemes of astronomers, in distrust of their undertakings. Before he died he had abundant experience to justify him. At his report to the International Astronomical Union in 1928, 40 years after the commencement, a little more than half was completed, two-thirds of the remainder might be considered on the way, and the rest was quite problematic. Defective though this record is, it would be much more so but for the energy and influence he contributed. What Turner specifically did sounds simple enough—he organised the measurement of the plates with computing boys, who rapidly acquired enormous facility, he cut down the measures by one decimal place, reducing the work and the printing and yet leaving a degree of accuracy superior to that derived from the transit circle, and arranged with the University Press for printing and issuing it promptly. When his own share was done, he found himself able to assist others, and in succession the zones undertaken by the Vatican Observatory and also those at Hyderabad he helped to bring to completion.

The Observatory in the Parks had no house attached to it, and suffered in efficiency accordingly. Almost at once Turner tried to get the University to build one, or to permit the building. He was unsuccessful. He tried again, with varied suggestions, for he was very tenacious. The matter became one of those *causes célèbres* to which the older Universities are particularly subject, because of the close quarters at which people live and the peculiarly developed powers of expression and criticism that are found there. At this distance of time most people will be content to regard the matter as a storm in a teacup that only wants forgetting. Suffice it to say that there is still no house attached to the Observatory, though in the interval the sacrosanctity of the Parks has changed very much

Before quitting the question of the Observatory and the Astrographic Catalogue, one very curious incident deserves to be recorded. The photographic plates are set with certain chosen eighth magnitude stars near the centre of the field, and these are used for the purposes of guiding. Under Turner's examination one plate appeared to have been guided on the wrong star. On pushing the puzzle home, the star in question turned out to be a new star. A Nova had appeared just at that point and of about the right magnitude, and had tripped the observer up. Novæ are now regarded as very numerous, but they were not so regarded then, and in any case those that are bright enough to be detected at the time are very rare. It was so strange an accident that it would have been improbable as an invention.

It was Turner's continual study to get the maximum out of the material at hand. The point of interest of the stellar problem has now definitely shifted beyond the Astrographic Catalogue, even if completed. It is now clear that we must go to much fainter stars, and that it is hopeless to deal with any except selected areas, which may be studied intensively, and treated as representative samples of the whole. But the Astrographic Catalogue being there, it was a definite problem what to do with it. Turner devoted many a paper to this, analysing the magnitudes, the distribution of stars, the proper motions, in fact everything he could get from it. The outcome was perhaps not much, but we could not have known that it would not be much, had the work not been done.

Another great and most opportune service of Turner's must now be mentioned. It was undertaken at first temporarily and because no other person was willing to be so unselfish. The science of seismology is now fairly on its feet, but 25 to 30 years ago it was a different story. Milne had indeed succeeded by his great energy and largely at his personal cost in planting a network of observing stations at many widely separated points in the British Empire. This is not the place to revise Milne's work and to weigh its excellences and defects, or to assess it in comparison with others. As Prince Galitzin wrote: "I entertain the most sincere hope that the great work of Milne will be continued, taken up by others, and developed in accordance with the necessities of modern investigation. This would be the best monument to his memory." On his death in 1913 there was a serious risk that it might all collapse. Milne had been a close friend of Turner's, and Turner consented to carry it on temporarily Once it was in his hands, others did nothing to take it out. The work grew continually in spite of compression to significant points and organisation, in which he was most loyally helped by his permanent assistant at the Observatory, F. A. Bellamy, with his niece. Fortunately it grew in interest also The organisation was at first centred at Shide, Isle of Wight, where Milne had lived, but was gradually transferred to Oxford.

Another man with whom seismology brought Turner into long and tried connection was Mr. J. J. Shaw. Mr. Shaw had made an improvement in the Milne instrument. He had added the features it wanted most, while preserving its lightness, cheapness and sensitivity It was so distinct an improvement that Turner, with Mr. Shaw as maker, set about replacing all the Milne instruments by the Milne-Shaw pattern, and at the time of his death many had been so replaced.

Milne's work was that of a pioneer and Turner's first duty was to consolidate it. This meant rejecting and altering some of it, reconsidering a great deal and extending it. The tentative character of the numerical analysis of the united records of any great earthquake offered just the task in which he was most skilled. He continued all his life to revise, and re-revise, the indication of the speed of the different waves, which included the determination of the latitude and longitude of the exact spot where the earthquake had originated, and in addition the third co-ordinate of the depth below the surface, which is by no means always negligible. A good record at any place is a fairly detailed document. The collected records of any great earthquake become voluminous. Turner bent all his powers of organisation, by card catalogues and the like, to get the maximum out of them with the minimum of waste effort. He made the International Seismological Summary a model of clearness and compression. Most of the work was done by J. S. Hughes of New College and Miss Bellamy, but he added revision, direction, and discussions of such points of interest as the particulars suggested.

Milne was not the first to investigate earthquakes, nor when he died was he by any means the sole worker. After the war, when scientific organisations were collected into International Unions, the various workers in seismology were united in a Commission of the International Union of Geodesy and Geophysics, which received a subvention for publications and for the maintenance of a central observatory. Turner became President of the Commission, and retained the work he had performed, while the observing station was located at Strasbourg. Thus for the moment were removed the difficulties of finance, which from the beginning had been not the least troublesome of Turner's problems, and one which Milne had solved roughly by paying out of his own pocket. Milne had worked as secretary of a committee of the British Association. The cost of the organisation was very substantial. Slowly and inadequately and by the help of private benefactors the British Association was able to support it. And very soon the money granted by the Union of Geodesy and Geophysics shrunk in effectiveness in a notable way when the franc began to depreciate The financial side became again a continual anxiety to Turner, and he, like Milne, often solved it by recourse to his own pocket.

As he was led to take up seismology almost by an accident, so by little more, discharging a useful work because no one else was available, he took up variable stars; editing for the Royal Astronomical Society the accumulated observations made by Mr George Knott (1899), and later, in response to a special request, those made by Mr. Grover under the direction of Sir Cuthbert Peek, Bt. (1904). He was not a superficial editor. One is aware that any work to which his name is attached will have the stamp of experience, with economy in presentation and no point missed. Once engaged, he continued to be interested, and to devote his skill in numerical analysis to the great variety of problems that variable stars present.

One recognises a necessary thread of theory in all Turner's main work. A large proportion of the regularities of nature are offered to us mixed with irrelevancies. Anyone can see that the regularities exist, but in most cases we should not hope to reduce them to any fundamental "law." But there is the difficult, preliminary, middle region of separating the wheat from the chaff. Turner loved this work and was continually at it; his methods were rough and practical, such as simple harmonic analysis by grouping, and the easier applications of the periodogram. Possibly in some cases his judgment was led astray, since a first hypothesis of this work is that the material is representative, which may not be true. None the less it was useful to try, and much more so because it bears the stamp of his experience.

In passing Turner's life in review, the question arises whether more selfishness, such as most men show, in choosing for themselves a preferential line of study and leaving those that originate others to carry their own burdens, would have been better. One recognises that his action was the expression of his character, in which intellectual curiosity was strong, but not nearly so strong as the personal, practical instincts of utility. An unanswered question is perhaps the most interesting one On the one side is the knowledge that most discussions are inadequately done. It is of great value to a future user of the work to be sure that neither competence nor labour has been spared. Then there is a great deal to be said for examining things at an early stage. One can never foresee the requirements of a problem beyond the next discovery. Very often a large accumulated mass proves to be a mere repetition of some unessential point, while a vital consideration, that might have been elucidated, has been passed by. Perhaps it was Turner's experience in discussing varied accumulations of others that led to his statement that no one should amass observations without printing them for more than two years, or for more than five years without discussing them. In these days of rapid movement this sounds a less surprising dictum than it did at the time. We have now grown used to large blocks of study being rendered obsolete by an unexpected consideration. Under such circumstances the sensible thing to do is to work from hand to mouth, even though it may mean that life-long devotion to one master idea is a thing of the past, suitable only for a museum.

Turner was an incessant worker, on every railway journey writing or correcting proof sheets, a habit that allowed him to accomplish easily what others would have found an impossible amount of work. He wrote upwards of 180 papers for the 'Monthly Notices.' In other matters, of which there is no permanent record, such as lectures to a popular audience, his idea appears to have been to put the maximum amount of work into the preparation. Whether he regarded it as work or not, he never missed supplying each month to the 'Observatory' magazine some pages "From an Oxford Note Book"—containing comments serious and humorous on any matter that turned up touching astronomy, and a good many that did not. The store seemed endless; the matter was not exactly witty, but humorous, and quite unforced. Later, anyone who had a good thing and wanted it published, sent it to Turner, who could nearly always add some pertinent coda. It was significant of the unique place that Turner filled, that after his death there was not so much as a question of continuing these comments in any form at all. He was in addition a frequent writer of letters to *The Times*, all of them marked by cogent good sense and some very interesting. He was an advocate of Mr. Willet's project of "Summer Time" long before it was adopted. He took endless trouble in connection with the Workers' Education Association. The social side of Turner's nature became almost an international asset. It was expressed, perhaps at its best in his bonds with American astronomers. There is a dining club as old as the Royal Astronomical Society, to which he was greatly attached. It is very methodical in its records, and keeps a tally of the number of times each member attends. At the time of his death Turner had reached the unequalled total of 339. The club is also very hospitable and during the last 12 years when he was President, and before that, Turner made a point of introducing as guests men of mark of all kinds, especially those whose mark was out of the way, proposing their health in genial form, from which all trace of conflict was banished. It is to such a group as this that the direction in his will must be understood as addressed, "I venture to hope there may be some who will care to drink a glass to my memory; . . . if anyone should desire to know my preference, then I say 'let it be strong ale.'"

Turner died at Stockholm on August 20, 1930. He was presiding at a meeting of the International Commission on Seismology; he leaned forward on his hand and was found to have lost consciousness; he never recovered it. Following his practical bent, and with the knowledge and concurrence of his family, he was found to have bequeathed his body as a gift to a hospital.

R. A. S.

# INDEX TO VOL. CXXXIII. (A).

Absorption coefficient, stellar (Chandrasekhar), 241.
Actinium C, analysis of alpha-particles (Rutherford), 351.
Air, specific heat from 20° C. to 370° C. (Henry), 492.
Alkyl halides, absorption spectra (Iredale and Mills), 430.
Allin (E. J.) *See* McLennan and others.
Allsopp (C. B.) *See* Lowry and Allsopp.
Alpha-particles emitted from Thorium C and Actinium C (Rutherford and others), 351.
Arnot (F. L.) The Diffraction of Electrons in Gases, 615.
Atomic weight of thallium (Briscoe and others), 440.

Beta-particle emission of radium D (Richardson), 367.
Bingham (R. T. W.) A Vacuum Spectrometer for Long Wave-length X-Rays, 266.
Bingham (R. T. W.) *See also* Laby and Bingham.
Bismuth, discontinuities at melting-point (Webster), 162.
Briscoe (H. V. A.), Kikuchi (S.) and Peel (J. B.) A Revision of the Atomic Weight of Thallium, 440.
Bullard (E. C.) and Massey (H. S. W.) The Elastic Scattering of Slow Electrons in Gases, II, 637.

Cataphoresis, new experimental method (Sumner and Henry), 130.
Cataphoresis of suspended particles (Henry), 106.
Chandrasekhar (S.) The Stellar Coefficients of Absorption and Opacity, 241.
Cosmical constant, value (Eddington), 605.
Crawford (M. F.) *See* McLennan and others.

Dipole moments between saturated and unsaturated substances (Sutton), 668.
Dirac (P. A. M.) Quantised Singularities in the Electromagnetic Field, 60.
Distance in curved space (Whittaker), 93

Eddington (Sir Arthur) The Properties of Wave Tensors, 311; on the Value of the Cosmical Constant, 605.
Electric discharges, gaseous combustion (Finch and Mahler), 173.
Electrolytes, adsorption by pure charcoal (Phelps), 155.
Electromagnetic field, quantised singularities (Dirac), 60.
Electronic semi-conductors, theory (Wilson), 458.
Electrons, diffraction by single crystals (Thomson), 1.
Electrons, diffraction in gases (Arnot), 615.
Electrons in gases, elastic scattering (Bullard and Massey), 637.
Evans (S. F.) The Arc Spectrum of Iodine, 417.

Finch (G. I.) and Mahler (E. A. J.) Gaseous Combustion in Electric Discharges, VIII, 173.
Fowler (A.) The Spectrum of the Hydrogen-Nitrous Oxide Flame, 325.
Francis (W. L.) Studies in Membrane Behaviour, I, 587.

Gaddum (J. H.) A Simple Method of Measuring Surface Tension (Abstract), 695.
Gamma-rays, photoelectric effect (Hulme), 381.
Gaseous compounds, refraction and dispersion (Lowery), 188.

Hall (K. E.) *See* McLennan and others.
Harvey (A.) Interpretation of the Spectra of CaF and SrF, 336.
Henry (D. C.) The Cataphoresis of Suspended Particles, I, 106.
Henry (D. C.) *See also* Sumner and Henry.
Henry (P. S. H.) The Specific Heats of Air, Oxygen, Nitrogen from 20° C. to 370° C., 492.
Hitchen (C. S.) *See* Twyman and Hitchen.
Hulme (H. R.) The Photoelectric Effect for $\gamma$-Rays, 381.
Hydrogen, chemical constants of vapours (Stern), 303.
Hydrogen chloride, chemical constants of vapours (Stern), 303.
Hydrogen-ion concentration (Peters), 140.
Hydrogen-ion concentration and adsorption (Phelps), 155.
Hydrogen-oxygen mixtures, cathodic combustion (Finch and Mahler), 173.
Hydrogen, sorption on copper (Ward), 506.
Hyperfine structure, interpretation (McLennan and others), 652.

Iodine, arc spectrum (Evans), 417.
Indium atom, nuclear moment (McLennan and others), 333.
Iredale (T.) and Mills (A. G.) Absorption Spectra of the Alkyl Halides, 430.

Jackson (C. V.) Interferometric Measurements in the Spectrum of the Iron Arc in Air in the Region $\lambda$ 3100–$\lambda$ 3500, 553.
Johnson (L. W.) and Johnson (R. C.) The Band Spectrum of Yttrium Oxide, 207.
Johnson (R. C.) *See* Johnson and Johnson.

Kikuchi (S.) *See* Briscoe and others.
Kronig (R. de L.) The Quantum Theory of Dispersion in Metallic Conductors, II, 255.

Laby (T. H.) and Bingham (R. T. W.) The Reflection and Diffraction of X-Rays, 274.
Lewis (W. B.) *See* Rutherford and others.
Lonsdale (K.) An X-Ray Analysis of the Structure of Hexachlorobenzene, using the Fourier Method, 536.
Lowery (H.) The Refraction and Dispersion of some Gaseous Compounds, 188.
Lowry (T. M.) and Allsopp (C. B.) Refractive Dispersion of Organic Compounds, I, II, III, 26.

Macky (W. A.) Some Investigations on the Deformation and Breaking of Water Drops in Strong Electric Fields, 565.
Mahler (E. A. J.) *See* Finch and Mahler.
Massey (H. S. W.) *See* Bullard and Massey.
McLay (A. B.) *See* McLennan and others.
McLennan (J. C.), Allin (E. J.) and Hall (K. E.) The Nuclear Moment of the Indium Atom, 333.
McLennan (J. C.), McLay (A. B.) and Crawford (M. F.) Interpretation of Hyperfine Structure, 652.
Membrane behaviour in aequeous solutions (Francis), 587.
Metals in solution, estimation by spark spectra (Twyman and Hitchen), 72.
Mills (A. G.) *See* Iredale and Mills.
Mohr (C. B. O.) The Reflection of Long X-Rays, 292.
Mott (N. F.) The Theory of the Effect of Resonance Levels on Artificial Disintegration, 228.

Nitrogen, specific heat from 20° C. to 370° C. (Henry), 492.

Obituary Notice :—Turner, H. H., i.
Opacity coefficient, stellar (Chandrasekhar), 241.
Organic compounds, refractive dispersion (Lowry and Allsopp), 26.
Oxygen, specific heat from 20° C. to 370° C. (Henry), 492.

Paramagnetic substances, gyromagnetic effect (Sucksmith), 179.
Peel (J. B.) *See* Briscoe and others.
Penney (W. G.) The Photoelectric Effect in Thin Metallic Films, 407.
Peters (R. A.) Interfacial Tension and Hydrogen-ion Concentration, 140.
Phelps (H. J.) The Influence of Hydrogen-ion Concentration upon the Adsorption of Weak Electrolytes by Pure Charcoal, II, 155.
Photoelectric effect for γ-rays (Hulme), 381.
Photoelectric effect in thin metallic films (Penney), 407.

Radium D, β-particle emission (Richardson), 367.
Rao (K. R.) The Spark Spectra of Tellurium, 220.
Refractive dispersion of organic compounds (Lowry and Allsopp), 26.
Resonance levels, effect on artificial disintegration (Mott), 228.
Richardson (H O. W.) The β-Particle Emission of Radium D, 367.
Rutherford (Lord), Wynn-Williams (C. E.) and Lewis (W. B.) Analysis of the α-Particles Emitted from Thorium C and Actinium C, 351.

Sorption of hydrogen on copper (Ward), 506.
Spark spectra, estimation of metals in solution (Twyman and Hitchen), 72.
Specific heats of air, oxygen, nitrogen (Henry), 492.
Spectral lines of distant sources, displacement (Whittaker), 93.
Spectra of alkyl halides (Iredale and Mills), 430.
Spectra of CaF and SrF (Harvey), 336.
Spectra of tellurium (Rao), 220.
Spectrometer for long wave-length X-rays (Bingham), 266.
Spectrum of hydrogen-nitrous oxide flame (Fowler), 325.
Spectrum of iodine (Evans), 417.
Spectrum of iron arc, interferometric measurements (Jackson), 553.
Spectrum of yttrium oxide (Johnson and Johnson), 207.
Spectrum, theory of dispersion in metallic conductors (Kronig), 255.
Stern (T. E.) The Chemical Constants of the Vapours of Hydrogen and of Hydrogen Chloride, 303.
Sucksmith (W.) The Gyromagnetic Effect for Paramagnetic Substances, II, 179.
Sumner (C. G.) and Henry (D. C.) Cataphoresis, II, 130.
Sutton (L. E.) The Significance of the Differences between the Dipole Moments of Saturated and Unsaturated Substances, 668.

Tension, interfacial (Peters), 140.
Thallium, atomic weight (Briscoe and others), 440.
Thomson (G. P.) The Diffraction of Electrons by Single Crystals, 1.
Thorium C, analysis of alpha-particles ((Rutherford and others), 351.
Turner (H. H.), obituary, i.
Twyman (F.) and Hitchen (C. S.) Estimation of Metals in Solution by means of their Spark Spectra, 72.

Ward (A. F. H.) The Sorption of Hydrogen on Copper, I, II, 506.
Water drops, investigations on deformation and breaking (Macky), 565.
Wave Tensors, properties (Eddington), 311.
Webster (W. L.) Discontinuities at the Melting-point of Bismuth, 162.
Whittaker (E. T.) On the Definition of Distance in Curved Space, and the Displacement of the Spectral Lines of Distant Sources, 93.
Wilson (A. H.) The Theory of Electronic Semi-Conductors, 458.
Wynn-Williams (C. E.) *See* Rutherford and others.

X-ray analysis of hexachlorobenzene (Lonsdale), 536.
X-rays, reflection (Mohr), 292.
X-rays, reflection and diffraction (Laby and Bingham), 274.
X-rays, vacuum spectrometer (Bingham), 266.

END OF THE ONE HUNDRED AND THIRTY-THIRD VOLUME (SERIES A).

I. A. R. I. 75

IMPERIAL AGRICULTURAL RESEARCH
INSTITUTE LIBRARY
NEW DELHI.

| Date of issue. | Date of issue. | Date of issue. |
|---|---|---|
| 19.1.42 | ~~27 FEB 1986~~ | |
| 19.1.42 | | |
| 18.8.52 | 28 FEB 1986 | |
| 4.1.62 | | |
| | | |
| | | |
| | | |
| | | |
| | | |
| | | |
| | | |
| | | |
| | | |
| | | |